

PROGRESS IN FLAVOUR RESEARCH 2021



Proceedings
of the
16th Weurman Flavour Research Symposium

**Weurman
Dijon 2020**

**16th Weurman
Online
May 4-6, 2021**

Edited by

**Elisabeth Guichard
and Jean-Luc Le Quéré**





Weurman
Dijon 2020



Proceedings of the 16th Weurman Flavour Research Symposium

Edited by

Elisabeth Guichard

Jean-Luc Le Quéré

National Research Institute for Agriculture, Food and Environment (INRAE)

Centre for Taste, Smell and Feeding Behaviour
Centre des Sciences du Goût et de l'Alimentation (CSGA)
Dijon, France

INRAE



Scientific Committee

Dr. Loïc Briand (CSGA, INRAE Dijon)
Dr. Francis Canon (CSGA, INRAE Dijon)
Dr. Pascale Chalier (Montpellier University)
Prof. Philippe Darriet (Bordeaux University)
Dr. Erwan Engel (INRAE, Theix)
Prof. Xavier Fernandez (Nice University)
Dr. Elisabeth Guichard (CSGA, INRAE Dijon)
Dr. Sophie Landaud-Liautaud (INRAE, Grignon)
Dr. Jean-Luc Le Quéré (CSGA, INRAE Dijon)
Prof. Carole Prost (ONIRIS, Nantes)
Dr. Thierry Thomas-Danguin (CSGA, INRAE Dijon)
Dr. Nadine Vallet (ISIPCA, Versailles)

PROGRESS IN FLAVOUR RESEARCH 2021

Proceedings of the 16th Weurman Flavour Research
Symposium e-book (pdf); ISBN: 978-2-7592-3622-0
<https://www.zenodo.org/communities/weurman2021/>
DOI: 10.5281/zenodo.6600605

Preface

Since 1975, the Weurman Flavour Research Symposia held every three years in different European countries have been unique opportunities for scientists from academia and industry, from different disciplines, and from all over the World, to discuss trends and new paradigms in the field of flavour research. It would have been a great honour for us to host the 16th edition of this internationally recognised Symposium, scheduled in September 2020 in Dijon. Unfortunately, the pandemic COVID-19 that spread out over the World from the beginning of 2020, and the resulting ongoing pandemic crisis constrained us to postpone the symposium and to finally hold this edition online in May 2021.

This e-book is organised in five sections, reflecting the structure of the Symposium held online from 4th to 6th May, 2021, and attended by 423 registered participants from 28 countries in Europe (16), Asia (7), Americas (2), Oceania (2) and Africa (1). This highly international attendance resulted in 194 presentations (44 lectures and 150 posters) as well as four workshops dedicated to (i) chemistry and biochemistry of flavour compounds in the mouth, (ii) flavour perception: from molecules via bioreceptors to physiological functions, (iii) in vivo flavour release and perception by time resolved sensory and instrumental methods, and (iv) perceptual interactions in flavour perception. This e-book contains 104 contributions of the initial 194, and we warmly thank the volunteers who send their manuscripts in order to maintain the tradition of the Weurman symposia for publishing a Proceedings book. All the contributed manuscripts have already received a DOI number and are accessible on the Zenodo platform at <https://www.zenodo.org/communities/weurman2021/>. Minutes of the fourth workshop dedicated to perceptual interactions in flavour perception are also included.

We thank the members of the Scientific Committee for their advices during the initial discussions to settle the symposium programme, and for choosing and reviewing the numerous abstracts and manuscripts. We are grateful to all our generous sponsors who allowed us to propose low registration fees, especially for PhD students and young post-docs who registered massively. We hope that their participation in the symposium will encourage them to continue their research activities in the exciting domain of flavour. Thanks to our sponsors' support, it was also possible to set awards for best poster presentations in each poster session that could be presented during an online award ceremony.

Before letting you discover the content of this e-book, we want to express our gratitude to the CSGA members Véronique Ponchelet and Laurence Petit, Symposium Secretaries, who managed all the registration fees, Olivier Lalouette and Eurélie Cachon for their advices on the administrative part, and to the successive CSGA directors Lionel Brétilon and Loïc Briand for their unshakeable support. Our gratitude also to Amaury Chouzenoux from 'Live! by GL events' for the very efficient set-up of the online website, as we know it was appreciated by all the participants.

Elisabeth Guichard
Jean-Luc Le Quéré

Dijon, February 2022

Sponsors

Platinum



MARS
Advanced Research
Institute

Gold



Givaudan



Silver



Nestlé Good food, Good life

Bronze

Eat Well, Live Well!



AJINOMOTO



Institutional Support



Contents

Section 1: Sensory interactions	1
The question of Organic Unity in Flavour: The whole is not equal to the sum of the parts <i>Thierry Thomas-Danguin</i>	3
Partitioned glass, a new practical tool to evaluate the origins of perceptive interactions in wine <i>Margaux Cameleyre, Georgia Lytra, Jean-Christophe Barbe</i>	9
Odour-Induced Taste Enhancement in normal-weight and obese people <i>Christopher Aveline, Cécile Leroy, Thierry Thomas-Danguin, Charlotte Sinding</i>	15
Section 2: Flavour analysis and analytical tools	21
NMR based studies on odorant melanoidin interactions in coffee beverages <i>Michael Gigl, Oliver Frank, Thomas Hofmann</i>	23
Unified mint quantitation: Development of a high-throughput analysis for the quantitation of key aroma compounds in mint <i>Verena Christina Tabea Peters, Andreas Dunkel, Oliver Frank, Brian McCormack, Eric Dowd, John Didzbalis, Corinna Dawid, Thomas Hofmann</i>	29
Pinellic acid generation in whole wheat products: Impact of linoleic acid content and lipoxygenase activity <i>Wen Cong, Eric Schwartz, Devin G. Peterson</i>	35
Towards cooked meat less loaded in heterocyclic aromatic amines but sensorially acceptable! <i>Maia Meurillon, Chloé Anderson, Magaly Angénieux, Frédéric Mercier, Nathalie Kondjoyan, Erwan Engel</i>	41
Fruity expression of red wines resulting from varieties adapted to climate change. A comparative study with the "traditional" grape varieties planted in Bordeaux <i>Justine Garbay, Margaux Cameleyre, Nicolas Le Menn, Jean-Christophe Barbe, Georgia Lytra</i>	47
Climate change and cocoa flavour quality: analytical investigations to identify off-odour in cocoa products <i>Erica Liberto, Chiara Cordero, Pamela Perotti, Cristian Bortolini, Carlo Bicchi</i>	53
Microwave sensor based on molecularly imprinted silica for the detection of phenylacetaldehyde in wine <i>Elias Bou-Maroun, Jérôme Rossignol, Didier Stuerga, Philippe Cayot, Régis D. Gougeon</i>	59

Impact of processing and storage on changes in the volatile compounds of whole chickpeas: an untargeted headspace fingerprinting study <i>Laura E. C. Noordraven, Carolien Buvé, Chao Chen, Marc E. Hendrickx, Ann M. Van Loey</i>	63
Assessment of champagne glass geometries - Dynamic head space sampling of champagne aromas <i>Per Malmberg, Jan Olof Svensson</i>	67
Untargeted or targeted analysis? Application to craft beer and gin <i>Cody Williams, Mpho Mafata, Astrid Buica</i>	71
Unravelling the typicity of 17 rum terroirs by GC-FID and aroma compound mapping <i>Nicolas Malfondet, Fannie Thibaud, Alexandre Gabriel</i>	75
Extended volatile range PTR-MS setup for real-time puff-by-puff analysis of electronic nicotine delivery systems <i>Andreas Mauracher, Bea Rosenkranz, Rene Gutmann, Markus Müller, Andreas Klinger, Philipp Sulzer</i>	79
Identification and semi-quantification of sesquiterpenes and sesquiterpenoids from Chamomile, Hop, Lavender, Basil and Lemon balm <i>Benedikt Slavik, Julian Nehr, Helene M. Loos, Andrea Buettner</i>	83
Changes in the aroma profile during thermal processing and storage of strawberry purees originating from different cultivars <i>Natalia Teribia, Carolien Buvé, Daniel Bonerz, Julian Aschoff, Marc Hendrickx, Ann Van Loey</i>	87
The volatile constituents and key character impact compounds of two different commercial dark chocolates, each containing 64% of cocoa from different origins <i>Catherine Vermeulen, Julien Simonis, Léonor Bonnafous, Cécile Petit, Filip Arnaut</i>	91
Chemical and physical stability of soluble coffee stored in different packaging materials <i>Josephine Charve, Nicolas Antille, Moritz Kindlein, Luigi Poisson, Jan Engmann</i>	95
Dual-fibre solid-phase microextraction coupled with gas chromatography - mass spectrometry for the analysis of volatile compounds in traditional Chinese dry-cured ham <i>Shui Jiang, Huan Liu, Junlong Huang, Qingkun Hu, Yan Ping Chen, Keqiang Lai, Jianqiao Xu, Gangfeng Ouyang, Yuan Liu</i>	101
Biomimetic Approach towards Filbertone <i>Michael Backes, Jekaterina Ongouta, Egon Gross, Sina Bruns, Uwe Schäfer, Lars Meier, Gerhard Krammer</i>	105
Identification of odour-active compounds in a paste of roasted hazelnut from Piedmont Tonda Gentile Trilobata <i>Claudia Geyer, Sophie Kemmer, Petra Steinhaus, Eashwari Shanmugam, Alexander Hässelbarth, Valentina Bongiovanni, Andrea Cavallero</i>	109
A new approach for the sensitive detection of thiols in food by affinity solid phase extraction and GC-MS <i>Stephan Neumann, Egon Gross, Stephanie Korte, Birgit Kohlenberg, Melanie Esselen, Hans-Ulrich Humpf, Johannes Kiefl</i>	115

Giffonins as contributors to the bitter off-taste in hazelnuts <i>Jekaterina Ongouta, Michael Backes, Anastasia Albrecht, Katharina Hempel, Gerhard Krammer, Uwe Schäfer, Susanne Paetz, Peter Winterhalter, Andreas Kirschning</i>	119
Differential effects of cryo-concentration on volatiles in apple juice <i>Mikael Agerlin Petersen, Pernille Nygaard Kristensen, Sophia Maria Odorico Gormsen, Mette Fangel Juda, Torben Bo Toldam-Andersen</i>	123
Effect of polyols on the release and on the self-diffusion coefficient of sweet aroma compounds in soda beverages <i>Carmen Barba, Juan Ignacio Maté, Alfonso Cornejo</i>	127
Characterisation of key aroma compounds in Burgundy truffle <i>Isabelle Andriot, Karine Gourrat, Rémy Reynaud, Sylvie Cordelle, Caroline Peltier, Olivier Berdeaux, Géraldine Lucchi</i>	131
Developing methods for characterising flavour compounds in distilled spirits: Application to gin, rum and whisky <i>Quentin Barnes, Marie-Anne Contamin, Nicolas Papaiconomou, Xavier Fernandez</i>	135
Impact of non-volatile compounds on volatiles perception: How proanthocyanidic tannins affect red wine fruity aroma? <i>Margaux Cameleyre, Georgia Lytra, Jean-Christophe Barbe</i>	139
Characterisation of key aroma compounds in foods containing vegetable proteins <i>Karine Gourrat, Marine Voisine, Andreas Redl, Olivier Berdeaux</i>	143
A new trend in aromatic sample preparation: Vacuum Assisted Sorbent Extraction (VASE) applied to pet food aroma analysis <i>Gautier Le Guillas, Cécile Marzin, Karine Hanaoka, Marion Guilloux, Cécile Pétel, Laurence Callejon, Angélique Villière, Carole Prost, Laurent Lethuaut</i>	147
Comparison of three ionisation methods - electron ionisation, chemical ionisation and atmospheric pressure photoionisation - for the characterisation of volatile organic compounds (VOCs) <i>Géraldine Lucchi, Jean-Luc Le Quéré, Karine Gourrat, Marine Crépin</i>	151
Aromatic profile of wheat flour and bran fractions <i>José Daniel Wicochea Rodríguez, Cécile Barron, Valérie Lullien-Pellerin, Peggy Rigou, Pascale Chalier</i>	155
Methoxypyrazines as a potential “green” off-odour in wine distillates <i>Panagiotis Stamatoopoulos, Xavier Poitou, Sandrine Weingartner</i>	159
Modelling of essential oils kinetics release from encapsulation matrix <i>José Daniel Wicochea-Rodriguez, Thierry Ruiz, Emmanuelle Gastaldi, Pascale Chalier</i>	163
Characterisation of the volatile sensometabolome in human breath of cigarette smokers, electronic cigarette users and non-smokers by Aroma Extract Dilution Analysis <i>Freya Grondinger, Georgina Wright, Theresa Stolle, Steven Coburn</i>	167
Understanding flavour isolation: Aroma analysis <i>Katrin Pechinger, Sam Wordsworth, Lewis L. Jones</i>	171

Characterisation of Piemonte peppermint essential oil by gas chromatography-olfactometry (GC-O) and identification of trace key-odorants contributing to the sweet and round flavour by comprehensive two dimensional gas chromatography coupled to time-of-flight mass spectrometry <i>E. Gabetti, B. Sgorbini, F. Stilo, C. Bicchi, P. Rubiolo, F. Chialva, S.E. Reichenbach, V. Bongiovanni, C. Cordero, A. Cavallero</i>	175
Analysis of retro-nasal flavour of beef pate using a chewing simulator <i>Kazuhiro Hayashi, Yuji Nakada, Etienne Semon, Christian Salles</i>	179
Studies on the enantiomers of dehydrorose oxide (4-methylene-2-(2-methylprop-1-enyl)oxane) <i>Shunsuke Takishima, Yasuhiro Fukui, Shunsuke Konishi, Kenji Haraguchi, Yuichiro Ohmori</i>	183
The taste of future foods: molecular insight into plant protein and flavour binding <i>Cristina Barallat, Teresa Oliviero, Hans-Gerd Janssen, Sara I.F.S. Martins, Vincenzo Fogliano</i>	187
Comparison and optimisation of headspace methods for the analyses of oxidation related off-flavour compounds in plant protein concentrates and infant formula <i>Catrienus de Jong, Cornelis van Kekem, M. L. Ondino Azario, Frank Koudijs, Naem Babae, Wibke S. U. Roland</i>	191
Most popular odours in food products in March 2021 according to VCF-online.nl <i>William van Dongen, Bert Wiggers</i>	195
Identification of odour-important norisoprenoids in <i>Arbutus pavarii</i> honey <i>Nagiat T. Hwisa, Keith R. Cadwallader</i>	199
Aroma variations of mid-Atlantic hops driven by growing regions and postharvest practices <i>Xueqian Su, Ken Hurley, Laban Rutto, Holly Scoggins, Yixiang Xu, Sean O'Keefe, Yun Yin</i>	203
Aroma-Active Compounds Contributing to Aged Riesling Character <i>Melissa Dein, Trenton Kerley, John P. Munafo, Jr.</i>	209
Asparagus waste streams to aroma-rich vegetable flavourings (The effect of partial replacement of maltodextrin with vegetable fibres in spray-dried white asparagus on its aroma properties) <i>Eirini Pegiou, Joanne W Siccama, Nienke M. Eijkelboom, Lu Zhang, Roland Mumm, Maarten A.I. Schutyser, Robert D. Hall</i>	213
Volatile aroma and bioactive compounds diversity in wild populations of rosemary (<i>Salvia rosmarinus</i> Schleid.) from Italy cultivated under homogeneous environmental conditions <i>Antonio Raffo, Irene Baiamonte, Elisabetta Lupotto, Nicoletta Nardo, Flavio Paoletti, Claudio Cervelli</i>	217
Volatile compounds contributing to the odour of oats <i>Sari A. Mustonen, Oskar Laaksonen, Kaisa M. Linderborg</i>	221

Section 3: Flavour perception	225
New insights on olfactory priming effects on the cerebral processing of food pictures in normal-weight, overweight, and obese adults <i>Isabella Zsoldos, Charlotte Sinding, Ambre Godet, Stéphanie Chambaron</i>	227
Understanding the effect of saliva composition depending on gender and age on wine aroma perception: oral aroma release, dynamics of sensory perception and consumer preferences and liking <i>Celia Criado, María Pérez-Jiménez, Carolina Muñoz-González, Maria Angeles Pozo-Bayon</i>	233
Tracing odour- and taste-active compounds in human milk <i>Marcel Debong, Roman Lang, Katharina N'Diaye, Andrea Buettner, Thomas Hofmann, Helene M. Loos</i>	239
Do space conditions change flavour perception and decrease food intake by astronauts? <i>Andrew Taylor, Scott McGrane, Martina Heer, Jonathan Beauchamp, Loic Briand</i>	245
Receptomics: Tongue-on-a-chip with novel opportunities for food screening <i>Margriet Roelse, Maurice G.L. Henquet, Maarten A. Jongsma</i>	251
Development of a purification protocol guided by bitter taste receptor activation and sensory analysis to isolate new taste-active compounds in barrel-aged wines <i>Delphine Winstel, Christine Belloir, Pierre Waffo-Téguo, Loic Briand, Axel Marchal</i>	257
Molecular triggers of post-COVID-19 parosmia in grilled chicken <i>Jane K. Parker, Christine E. Kelly, Simon Gane</i>	263
Identification of odour-active trace compounds in toasted oak wood: impact on wines and spirits aroma <i>Marie Courregelongue, Svitlana Shinkaruk, Philippe Darriet, Alexandre Pons</i>	267
Understanding flavour release and sensory perception of composite foods by combining dynamic sensory methods with in vivo nose space analysis <i>Karina Gonzalez-Estanol, Iuliia Khomenko, Danny Clicerì, Markus Stieger, Franco Biasioli</i>	273
Impact of capsaicin on salt release and salt perception during consumption of salt and salt-capsaicin solutions <i>Ni Yang, Qian Yang, Jing Zhao, Xiaolei Fan, Jianshe Chen, Ian Fisk</i>	279
Impact of smoked water on umami and salt taste <i>Kanokkan Panchan, Stella Lignou, Huw D. Griffiths, David A. Baines, Jane K. Parker</i>	285
Volatile compounds in the vehicle-interior: Odorants of an aqueous cavity preservation and beyond <i>Florian Buchecker, Helene M. Loos, Andrea Buettner</i>	289
An oenological approach to increase the consumer acceptability of black chokeberry (<i>Aronia melanocarpa</i> L.) juice <i>Sarah Ziermann-Österreicher, G. Thünauer, Barbara Siegmund</i>	293

Perception and sensory acceptance of salty taste by individuals who work/study on different shifts <i>Ana Carolina Bom Camargo, Ana Carolina Conti-Silva</i>	297
Effects of salt and monosodium glutamate on the sensory acceptance of low-sodium cheese-flavoured corn grits expanded snacks <i>Aline Catharina Panzarini, Michele Eliza Cortazzo Menis-Henrique, Ana Carolina Conti-Silva</i>	301
Characterisation of the key-aroma compounds among the volatile constituents in different hemp strains (<i>Cannabis sativa</i> L.) <i>Markus Kneubühl, Amandine André, Irene Chetschik</i>	305
Using the Check-All-That-Apply (CATA) methodology to evaluate the flavour of foreign global and domestic Chinese coffee products <i>Yan Ping Chen, Xiayidan Julaiti, Chenyang Guo, Imre Blank, Disheng Zhou, Lingxiao Yu, Yuan Liu</i>	309
Correlation between volatile aroma compounds and sensory changes during storage of heat processed beef flavour <i>Zeyu Zhang, Bei Wang, Imre Blank, Yanping Cao</i>	313
Investigation of the amino acid derivatives and small peptides profile in culinary bases <i>Benedikt Stiglbauer, David Komarek, Maria Monteiro de Araújo Silva, Timo D. Stark, Thomas Hofmann</i>	319
Understanding sweetness of dry wines: First evidence of Astilbin isomers in red wines and quantitation in a one-century range of vintages <i>Marie Le Scanff, Syntia Fayad, Axel Marchal</i>	323
Gluten-free breads: a response to a technological challenge <i>Lidwine Grosmaire, Lan Lin, Isabelle Maraval</i>	327
Oral astringency: effect of ageing and role of saliva <i>Mei Wang, Chantal Septier, Hélène Brignot, Christophe Martin, Francis Canon, Gilles Feron</i>	331
Impact of ingredient composition on sensory properties of powdered cocoa malted beverage <i>Ruo Xin Chan, Yi-Xin Seow, Florian Viton, Weibiao Zhou</i>	335
Section 4: Flavour generation	339
Furfuryl alcohol confirmed as key intermediate for furfurylthiol in coffee <i>Christoph Cerny, Hedwig Schlichtherle-Cerny, Romelo Gibe, Yuan Yuan</i>	341
Odour compounds in thermo-mechanically processed food based on pulse ingredients <i>Svenja Krause, Anahita Hashemi, Séverine Keller, Catherine Bonazzi, Barbara Rega</i>	347
Methods for predicting and assessing flavour evolution during white wine ageing <i>Josh Hixson, Lisa Pisaniello, Mango Parker, Yevgeniya Grebneva, Eleanor Bilogrevic, Robin Stegmann, Leigh Francis</i>	353

Genetic bases of fruity notes (fresh and dried) of the Nacional cocoa variety <i>Kelly Colonges, Juan-Carlos Jimenez, Alejandra Saltos, Edward Seguin, Rey Gastón Loor Solorzano, Olivier Fouet, Xavier Argout, Sophie Assemat, Fabrice Davrieux, Eduardo Morillo, Renaud Boulanger, Emile Cros, Claire Lanaud</i>	359
Generation of bitter blocker Maillard-dietary phenolic compound reaction products <i>Adeline Bonneau, Edison Tello, Devin G. Peterson</i>	365
Occurrence of (suspected) genotoxic flavouring substances in Belgian alcohol-free beers <i>Alexandre Dusart, Birgit Mertens, Els Van Hoeck, Margaux Simon, Séverine Gosciny, Sonia Collin</i>	369
Supplemental study on acetals in food flavourings <i>Jan Petka, Johann Leitner</i>	373
Investigating the flavour development of scab-resistant Crimson Crisp apples <i>Niklas Pontesegger, Thomas Ruehmer, Barbara Siegmund</i>	377
Enzymatic release of flavour compounds from Heritage apple varieties <i>Valerie Ruppert, Georg Innerhofer, Jörg Voit, Peter Hiden, Barbara Siegmund</i>	381
Lactic acid bacteria used to produce natural flavour compounds from whey and castor oil <i>Alejandro Álvarez, Alejandra Gutiérrez, Frank Cuenca, Cristina Ramírez, Germán Bolívar</i>	385
Flavour enhancement of beer and related beverages by increasing flavour precursors in raw materials by enzymes <i>Claire Lin Lin, Mikael Agerlin Petersen Andrea Gottlieb</i>	389
Evaluation of methodology to follow volatile composition over time <i>Lena Charlotte Ströhla, Mikael Agerlin Petersen</i>	393
Generation of meaty flavour compounds from Maillard origin under mild conditions simulating the dry curing process <i>Lei Li, Carmela Belloch, Monica Flores</i>	397
How do oxidoreduction conditions affect the balance of volatile compounds produced by lactic acid bacteria in a curd-based medium? <i>Solange Buchin, Sabrina Jeannin, Céline Arnould, Romain Palme, Franck Dufrene, Eric Beuvier</i>	401
The role of diketopiperazines in cooked cheese flavour <i>Rosa C. Sullivan, Colette Fagan, Maria Oruna-Concha, Jane K. Parker</i>	405
Identification of key volatiles in boiled chicken aroma <i>H.Q. Yeo, D.P. Balagiannis, J.H. Koek, J.K. Parker</i>	409
Identification of a key odorant contributing to Muscat aroma of Darjeeling black tea <i>Yasuhiro Fukui, Shunsuke Konishi, Kazuya Kawabata, Kenji Haraguchi, Yuichiro Ohmori, Akira Nakanishi, Susumu Ishizaki</i>	413
Meaty flavour tonalities by Maillard reaction <i>Jan H. Koek, Cathy De Sousa Ferreira</i>	417

Effect of malt kilning temperature on the concentration of (E)- β -damascenone in malt, mashing and wort boiling in the brewing process	421
<i>José A. Piornos, Jean-Philippe Kanter, Dimitrios P. Balagiannis, Elisabeth Koussissi, August Bekkers, Johan Vissenaekens, Bert-Jan Grootes, Eric Brouwer, Jane K. Parker</i>	
Section 5: Flavour perception/modelling	425
Effects of fat and coffee concentration on aroma compounds and their intensity in formulated iced-coffee beverages	427
<i>M M Chayan Mahmud, Russell Keast, Robert A Shellie</i>	
The bitter taste of vitamins is mediated by human TAS2R activation	435
<i>Thomas Delompré, Christine Belloir, Christian Salles, Loïc Briand</i>	
Sensory analysis, aroma compounds and flavour modulation of rapeseed oil: A review	439
<i>Youfeng Zhang, Yuqi Wu, Sirui Chen, Binbin Yang, Hui Zhang, Xingguo Wang, Michael Granvogl, Qingzhe Jin</i>	
3D live cell imaging: study of inter- and intracellular signalling induced by bitter molecules in tongue cell spheroids	443
<i>Elena von Molitor, Elina Nürnberg, Torsten Fauth, Paul Scholz, Katja Riedel, Michael Krohn, Mathias Hafner, Rüdiger Rudolf, Tiziana Cesetti</i>	
A receptor-based assay to study the bitterness masking effect of yeast extracts	447
<i>Christine Belloir, Antoine Thomas, Rudy Menin, Loïc Briand</i>	
Impact of ageing on pea protein volatile compounds and correlation with odour	451
<i>Estelle Fischer, Rémy Cachon, Nathalie Cayot</i>	
Fat-salty sensory interactions in model cheeses: multivariate analysis of a compilation of data from different projects organised in the BaGaTeL database	455
<i>Elisabeth Guichard, Thierry Thomas-Danguin, Hervé Guillemin, Bruno Perret, Solange Buchin, Caroline Pénicaud, Christian Salles</i>	
Is there a role for salivary detoxification enzymes in taste perception?	459
<i>Mathieu Schwartz, Hélène Brignot, Evelyne Chavanne, Gilles Feron, Thomas Hummel, Yunmeng Zhu, Dorothee von Koskull, Jean-Marie Heydel, Loic Briand, Francis Canon, Fabrice Neiers</i>	
Oxidation markers of premature ageing in Chardonnay wine: Combined use of GC-MS/MS, GC-O/Olfactoscan and sensory analysis for their characterisation	463
<i>Marie Simon, Amandine Vessot, Jérôme Mallard, Rémy Romanet, Noëlle Béno, Markus Lübke, Jordi Ballester, Maria Nikolantonaki, Régis Gougeon, Thierry Thomas-Danguin, Yves Le Fur</i>	
Exploring the odorant and molecular characteristics of molecules sharing the odour notes of an aroma blending mixture	467
<i>Anne Tromelin, Florian Koensgen, Marylène Rugard, Karine Audouze, Thierry Thomas Danguin, Elisabeth Guichard</i>	

SketchOscent: towards a knowledge-based model and interactive visualisation of the odour space <i>Angélique Villière, Catherine Fillonneau, Carole Prost, Fabrice Guillet</i>	471
Coffee sensory properties: a complementary data fusion to simulate odour and taste integration by instrumental approach. Possibilities and limits <i>Giulia Strocchi, Erica Liberto, Gloria Pellegrino, Manuela R. Ruosi, Carlo Bicchi</i>	475
Flavour profiling and sensory acceptance of <i>Premna cordifolia</i> Roxb. functional drink: comparison of different sample preparation methods <i>Farah Nini Liyana Mohamad Zuhaidi, Nurul Hanisah Juhari</i>	479
Minutes of the Workshop ‘Perceptual interactions in flavour perception’, organised by <i>Charlotte Sinding and Thierry Thomas-Danguin</i>	483

Section 1

Sensory interactions

The question of Organic Unity in Flavour: The whole is not equal to the sum of the parts

THIERRY THOMAS-DANGUIN

Centre des Sciences du Goût et de l'Alimentation, INRAE, Université Bourgogne Franche-Comté, CNRS, Institut Agro Dijon, France
thierry.thomas-danguin@inrae.fr

Abstract

The Flavour of food is a multimodal perception that involves at least the chemical senses. Therefore, Flavour is the result of the processing of complex mixtures of chemical compounds reaching the receptors of the senses of smell, taste, and chemesthesis and the further integration by the brain of the corresponding sensory information. How these sensory cues are processed in the brain, stored, combined with visual or auditory perceptions, and related to a given food object to provide a whole perceptual picture of food is still to be fully discovered. However, recent findings indicated that all the components of flavour are not independent, which suggests that there is an organic unity of food flavour. In this lecture, I first consider the organic unity of the olfactory dimension of food flavour leading to examining odour object as the cornerstone of food perception. The demonstration is supported by studies demonstrating that the components of an odour object are so closely connected that the transposal or withdrawal of any one of them can disjoin and dislocate the whole. In contrast, other studies showed that not all the components are of the same importance thus underlying the concept of key compounds or key associations in the configural processing of complex mixtures of odorants. Then, I consider smell-taste cross-modal interactions as the support of the whole flavour percept consolidation. The specificity and non-reciprocity of such interactions are examined to understand how smell and taste cues are bound in the context of flavour unity. Finally, I discuss the implications of such a view in terms of Flavour analysis and the need to develop innovative tools and methodologies to analyse flavour in its entirety, but also in terms of healthier and sustainable food development for which flavour is likely a key to ensure consumer acceptability.

Keywords: flavour, food, odour objects, taste, interactions

The Flavour of food

Flavour may have several definitions. One of the most explicit and complete ones has been provided by Jeanine Delwiche [1], who proposed a definition in line with the International Standard Organization [2]. In this definition, Flavour is considered to be the combination of taste, aroma (or smell), and irritation (or Chemesthesis) perceived in the mouth and nose during in-mouth food or beverage tasting. Flavour can thus be considered as the brain representation of all the multisensory information elicited by this complex chemical mixture released by food in the mouth and detected by the receptors of the senses of smell, taste, and chemesthesis, and the subsequent cerebral integration processes [3]. Flavour might be influenced or completed by several other perceptual dimensions such as texture, visual cues, or temperature.

Despite its obvious multimodality, Flavour can be considered as an *organic unity*, in line with the discussion of the philosopher Aristotle, for whom organic unity reflects “a complete whole, with its several constituting parts so closely connected that the transposal or withdrawal of any one of them will disjoin and dislocate the whole”. Therefore, Flavour, as it is represented in the brain, may be more than the sum of the parts, that are the percepts of each of its molecular constituents. Within this conceptual framework, the elements, which constitute the whole, are important; some might be key for the representation, but also, they can be interdependent meaning that the organisation of the elements is critical to reveal the overall configuration. In that sense, the whole flavour is more than the simple sum of its part. Such a view is in line with several other theoretical holistic approaches of perception such as in the Gestalt Theory for instance.

In this lecture, I brought several pieces of experimental evidence that could support the conceptual view of food flavour as an organic unity.

The smell dimension in Flavour

The smell dimension of flavour is critical for the food identity as highlighted in experiments in which beverage-like samples were submitted to an identification task performed with or without odour cues [4, 5]. The results of these experiments have shown that the identification scores with odour cues were much higher than the scores without odour, which fell below 50% (except for water). These reports confirmed that odour or aroma are critical sensory dimensions of food identity.

Food odour and aroma result from the processing of complex mixtures of odorants. The mechanisms underpinning the efficient analysis of odour mixtures support the idea that olfaction, as vision and audition, relies on a configural encoding of the sensory information. If configural processing of complex stimuli is well known in the visual and auditory modalities, for smell, very few studies reported data on the perception of odour whole and odour elements [6]. Our research group performed a study to test the configural hypothesis of odour perception using a binary mixture of A (ethyl isobutyrate) and B (ethyl maltol). This mixture, in a specific ratio, was expected to evoke a pineapple odour, whilst the single components evoke a fruity-strawberry odour and a caramel odour, respectively [7]. Following a typicality rating task, it was shown that the binary mixture was more typical of the pineapple target odour compared to the single components (**Figure 1**), thus supporting the configural processing of this mixture.

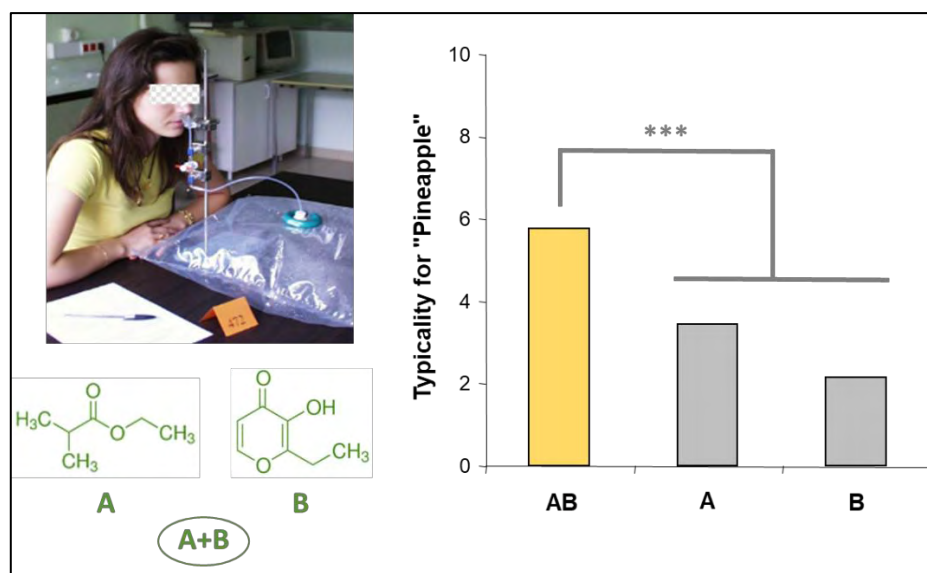


Figure 1: Typicality rating scores towards the odour of pineapple of a binary mixture AB (A: ethyl isobutyrate, and B: ethyl maltol) and its single components. *** means $p < 0.001$.

The configural processing of odours, highlighting that the odour of the mixture is qualitatively different from the odour of the odorants, has been extended to odour mixtures of higher complexity. A model odour mixture called RC was formulated on the basis of 6 pure odorants [8]. Naive subjects performed a sorting task on a set of 7 odour samples made of the RC mixture and the 6 single components. The major result of this experiment was that the RC mixture was not significantly grouped with the components supporting the idea that the mixture evokes an odour quality different from its components. In a follow-up experiment based on the same 6-component odour mixture RC, a group of naive subjects had to compare two odour samples in a pair in terms of their odour similarity. One odour in the pair is a constant reference RC and the other sample is a sub-mixture of RC including from one to 5 odorants [9]. Overall, the results showed that the 6-component RC mixture is processed in a configural way so that its odour quality is different from the quality of its components. Moreover, the perceptual weight of each component in the configuration is not the same. Indeed, it has been found that the mixture included a specific association between at least two of the odorants, which likely constitutes the core of the configuration.

All these results pointed to the configural processing of certain odour mixtures in which a few (key) elements might play a critical role. The proposed view is that, in a mixture, odorants may keep their characteristic odour, which could be still identifiable within the mixture. In that case, the mixture would be perceived as a collection of distinguishable odours carried by some of the odorants, which can be qualified as key odorants. Conversely, odorants may lose some of their characteristic odour when mixed and create meaningful associations that strongly contribute to the mixture's odour quality. These associations can be considered as key associations. This would be the case for the configurally perceived mixture RC, in which the binary association of two odorants produced an odour that differed from the odours of the two single components. Such a view is illustrated in **Figure 2**, showing the concept of key compounds in analytically perceived odour mixtures and the concept of key association at the basis of the configural perception of odour mixtures. Following this conceptualisation, the arrangement or the association between elements is coded as a piece of supplementary information on top of the addition of the elements so that the overall smell might be considered an organic unity.

The organic unity nature of odour mixtures representation has been demonstrated following a combined pharmacological and behavioural approach in animal studies [10]. It was especially shown that, after learning of a mixture, there was a coexistence of a specific memory of the mixture's component odour, but also of an independent memory of the mixture's odour itself. This result demonstrates the existence of configurations in odour mixtures and their representation as unique perceptual objects.

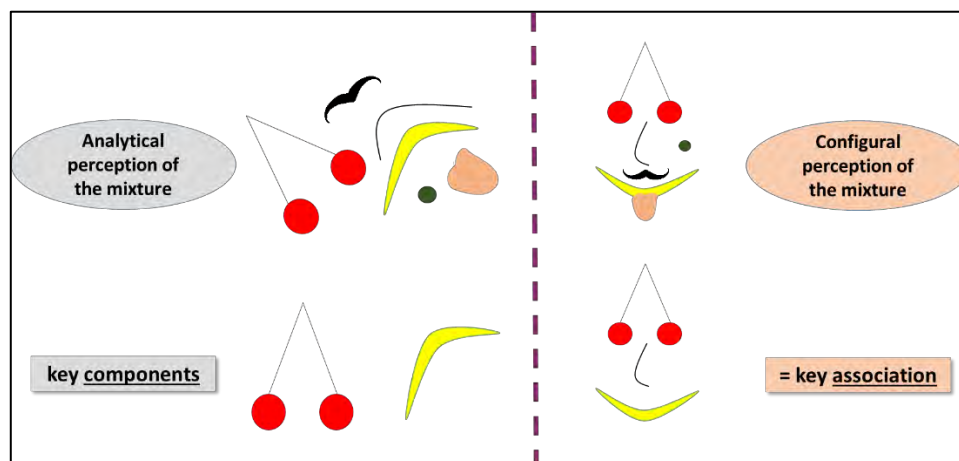


Figure 2: Illustration of the perception of key elements and key associations regarding elemental or configural processing of chemosensory mixtures (adapted from Romagny et al., 2018 [9]).

Flavour is more than smell

If smell is critical to the perceptual identity of edible objects, Flavour especially involves the taste dimension. Therefore, it is likely that odour-taste interactions might be involved in the perception of flavour. Odour-taste interactions have been studied for several years. For instance, in a seminal experiment, Franck and Byram [11] studied the sweetness of whipped cream samples with various sucrose levels. They showed that when a strawberry aroma was added to the samples, the sweet taste intensity was higher compared to the no-odour-added samples. In contrast, when a peanut butter odour was added, no such sweet taste enhancement was observed. These results demonstrated that only specific odours can contribute to taste dimension and that these odours have to be associated with the taste, which is the case of the strawberry odour with the sweet taste. Several other studies indeed confirmed that the so-called odour-induced taste enhancement [12] is a result of co-exposure between taste and aroma during food tasting and that associative learning plays a major role in the acquisition of taste-like properties by odours [13].

Odour-Taste associations have been further demonstrated in several experiments. For instance, our group studied the association between food odours and salty taste in an experiment in which a panel of subjects rated the taste and odour intensity of a series of water solutions containing various tasteless odour composition [14]. The results highlighted that several odours such as sardine, bacon, or peanuts were rated as salty. Overall, the acquisition of taste properties by odours suggests a configural encoding of flavour including at least smell and taste, but also trigeminal cues. These results support the idea that flavour is more than the sum of unimodal perception because of certain dependencies (associations) between chemosensory information. This advocated for the organic unity of flavour that has for consequence that certain aromas can contribute to taste dimension and thus enhance taste perception. One can thus consider the overall sweetness of e.g. pineapple flavour that includes sweet taste *per se* but also the smell contribution to sweetness. Nevertheless, there is no reciprocity in these interactions since the sweet taste of sugar cannot induce a perception of a smell, which advocates for key smell-taste associations that deserve further research.

Analysing Flavour considered as an organic unity

The classical path in flavour analysis is to establish the most exhaustive list of chemosensory-active compounds contained in a food sample. This approach is based on the separation, identification, and quantification of these compounds. However, if one considers the organic unity of flavour, the question is, how can we imagine innovative tools to study flavour as a whole and for instance uncover the key associations between odours (odorants), or between odours and tastes (odorants and tastants).

In the case of odour-active compounds analysis, a few methods have been proposed to consider not only separated odorants but also their mixtures that could carry a specific configural odour [15–18]. Moreover, to consider odour-taste associations, we recently proposed a screening method based on a GC/O design: the GC/O-AT, namely the Gas Chromatography / Olfactometry – Associated Taste [19]. This method relies firstly on a classical GC/O run in which a trained panel qualified the odour of the odour-active compounds found in a food extract injected in the GC. In that case, we obtain a classical aromagram. Then a second GC run is performed, in which panellists have to provide a taste descriptor to the odour they perceive, this is the taste-associated GC/O run. In that case for each peak, we obtained a descriptor such as sweet, salty, sour, or bitter. In our study, following the detection frequency method, it was possible to construct such a taste-associated aromagram that helped identify the compounds that are for instance the most associated to sweet taste in a fruit juice.



Figure 3: A: Schematic representation of the Olfactoscan device (adapted from Barba et al., 2018 [19]); B: Picture of the experimental setup at the ChemoSens platform of CSGA.

In order to check whether the compounds identified by GC/O-AT have the potency to contribute to the overall sweet dimension within the juice flavour, we used the olfactoscan method first introduced by Burseg and De Jong [20]. This method is based on the functional coupling of a GC/O and an olfactometer that can deliver a background odour of a real food product, for instance, a fruit juice (**Figure 3**). Using olfactoscan, we were able to construct odour mixtures that combine, one by one, the odorants eluted from the GC at the olfactory port with the mixture of odorants in the headspace of the fruit juice and that can be adjusted in terms of intensity owing to the olfactometer. Using this technical setup, we compared the level of sweetness of the fruit juice odour with the level of sweetness of the juice odour spiked with one odorant expected to contribute to the sweet flavour. The results pointed toward four odour-active compounds that contributed significantly to the perceived sweetness of the fruit juice odour, namely involved in the overall sweet flavour of the juice.

A final step consisted in a sensory experiment in which a sensory panel compared the sweet taste of a sugar-reduced fruit juice and the same juice that contained a candidate odorant. We especially found that an odorant (ethyl-2- methyl butanoate) can significantly enhance sweet taste in the sugar-reduced fruit juice.

Conclusion

It is proposed here to conceive the flavour of food as an organic unity, namely a complete whole, with its several constituting parts closely connected to form the configuration of a perceptual object. In such a view, the perceptual features of flavour might be considered in its entirety. For instance, sweetness should be considered not only to result from the input of the taste system but also from the contribution of the olfactory system, and likely from other sensory inputs. Therefore, it becomes obvious that odour can be bound to taste after associative learning, and thus odour can enhance taste perception. It is now needed to develop innovative tools to study and analyse flavour through this conceptual prism. It is expected that such innovative approaches would contribute to developing flavour-guided formulations for sustainable and healthy foods and beverages while maintaining taste and acceptability for consumers.

Acknowledgements

The author thanks all his collaborators who contributed to this work during the past 15 years, especially the Ph.D. students and Postdoctoral fellows who were involved. The work received financial support from INRAE, ANR, MESRI, Institut Carnot Qualiment, EU-FEDER, EU-MSCA, and the Region Bourgogne Franche Comté.

References

1. Delwiche, J. The Impact of Perceptual Interactions on Perceived Flavor. *Food Qual Prefer.* 2004;15(2):137–146.
2. ISO 5492:2008(en), Sensory analysis — Vocabulary <https://www.iso.org/obp/ui#iso:std:iso:5492:ed-2:v1:en> (accessed 2022 -05 -04).
3. Thomas-Danguin, T. Flavor. In *Encyclopedia of Neuroscience*; Binder, M. D., Hirokawa, N., Windhorst, U., Eds.; Springer-Verlag Berlin and Heidelberg GmbH & Co. K: Berlin Heidelberg, Germany, 2009; pp 1580–1582. https://doi.org/10.1007/978-3-540-29678-2_1772.
4. Mozell, M. M.; Smith, B. P.; Smith, P. E.; Sullivan, R. L.; Swender, P. Nasal Chemoreception in Flavor Identification. *Arch Otolaryngol.* 1969;90(3):367–373. <https://doi.org/10.1001/archotol.1969.00770030369020>.
5. Hornung, D. E.; Enns, M. P. Separating the Contributions of Smells and Tastes in Flavor Perception. In *Perception of complex smells and tastes*; Laing, D. G., Cain, W. S., McBride, R. L., Ache, B., Eds.; Academic Press: Sydney, Australia, 1989; pp 285–296.
6. Thomas-Danguin, T.; Sinding, C.; Romagny, S.; El Mountassir, F.; Atanasova, B.; Le Berre, E.; Le Bon, A.-M.; Coureaud, G. The Perception of Odor Objects in Everyday Life: A Review on the Processing of Odor Mixtures. *Front Psychol.* 2014;5(June):504. <https://doi.org/10.3389/fpsyg.2014.00504>.
7. Barkat, S.; Le Berre, E.; Coureaud, G.; Sicard, G.; Thomas-Danguin, T. Perceptual Blending in Odor Mixtures Depends on the Nature of Odorants and Human Olfactory Expertise. *Chem Senses.* 2012;37(2):159–166. <https://doi.org/10.1093/chemse/bjr086>.
8. Sinding, C.; Thomas-Danguin, T.; Chambault, A.; Béno, N.; Dosne, T.; Chabanet, C.; Schaal, B.; Coureaud, G. Rabbit Neonates and Human Adults Perceive a Blending 6-Component Odor Mixture in a Comparable Manner. *PloS One.* 2013;8(1):e53534. <https://doi.org/10.1371/journal.pone.0053534>.
9. Romagny, S.; Coureaud, G.; Thomas-Danguin, T. Key Odorants or Key Associations? Insights into Elemental and Configural Odour Processing. *Flavour Frag J.* 2018;33(1):97–105. <https://doi.org/10.1002/ffj.3429>.
10. Coureaud, G.; Thomas-Danguin, T.; Wilson, D. A.; Ferreira, G. Neonatal Representation of Odour Objects: Distinct Memories of the Whole and Its Parts. *Proc R Soc B-Biol Sci.* 2014;281(1789):20133319–20133319. <https://doi.org/10.1098/rspb.2013.3319>.
11. Frank, R. A.; Byram, J. Taste-Smell Interactions Are Tastant and Odorant Dependent. *Chem Senses.* 1988;13(3):445–455. <https://doi.org/10.1093/chemse/13.3.445>.
12. Djordjevic, J.; Zatorre, R. J.; Jones-Gotman, M. Odor-Induced Changes in Taste Perception. *Exp Brain Res.* 2004;159(3):405–408. <https://doi.org/10.1007/s00221-004-2103-y>.
13. Stevenson, R. J.; Prescott, J.; Boakes, R. A. The Acquisition of Taste Properties by Odors. *Learn Motiv.* 1995;26(4):433–455. [https://doi.org/10.1016/S0023-9690\(05\)80006-2](https://doi.org/10.1016/S0023-9690(05)80006-2).
14. Lawrence, G. Physicochemical and Perceptual Interactions between Composition/Texture, Taste and Odour: A Way to Enhance Saltiness in Low-Salt Content Foods, Université de Bourgogne, 2009.
15. Hallier, A.; Courcoux, P.; Sérot, T.; Prost, C. New Gas Chromatography–Olfactometric Investigative Method, and Its Application to Cooked *Silurus Glanis* (European Catfish) Odor Characterization. *J Chromatogr A.* 2004;1056(1–2):201–208. <https://doi.org/10.1016/j.chroma.2004.06.044>.
16. Burseg, K.; de Jong, C. Application of the Olfactoscan Method To Study the Ability of Saturated Aldehydes in Masking the Odor of Methional. *J Agric Food Chem.* 2009;57(19):9086–9090. <https://doi.org/10.1021/jf9016866>.
17. Hattori, S.; Takagaki, H.; Fujimori, T. Identification of Volatile Compounds Which Enhance Odor Notes in Japanese Green Tea Using the OASIS (Original Aroma Simultaneously Input to the Sniffing Port) Method. *Food Sci Technol Res.* 2005;11(2):171–174. <https://doi.org/10.3136/fstr.11.171>.
18. Williams, R. C.; Sartre, E.; Parisot, F.; Kurtz, A. J.; Acree, T. E. A Gas Chromatograph–Pedestal Olfactometer (GC–PO) for the Study of Odor Mixtures. *Chemosens Percept.* 2009;2(4):173–179. <https://doi.org/10.1007/s12078-009-9056-2>.
19. Barba, C.; Beno, N.; Guichard, E.; Thomas-Danguin, T. Selecting Odorant Compounds to Enhance Sweet Flavor Perception by Gas Chromatography/Olfactometry-Associated Taste (GC/O-AT). *Food Chem.* 2018;257:172–181. <https://doi.org/10.1016/j.foodchem.2018.02.152>.
20. Burseg, K. M. M.; de Jong, C. The Olfactoscan: In-Vivo Screening for Off-Flavour Solutions. In *Weurman Symposium*; Yeretizian, C., Ed.; Zurich University: Interlaken, Switzerland, 2008.

Partitioned glass, a new practical tool to evaluate the origins of perceptive interactions in wine

MARGAUX CAMELEYRE, Georgia Lytra and Jean-Christophe Barbe

Unité de recherche *Enologie*, EA 4577, USC 1366 INRAE, ISVV, Université de Bordeaux, F33882 Villenave d'Ornon France

margaux.cameleyre@wanadoo.fr

Abstract

Examples of perceptive interactions effects among volatiles on the fruity aromatic expression of wines have been previously highlighted. It was also shown that non-volatile molecules, such as tannins, impact fruity pool both at sensory and physicochemical level. Perceptive interactions have been described as occurring at four different levels: the first as a pre-sensory one, whereas the three others referred to interactions in the peripheral and central nervous system, at the receptor surface or in the olfactory bulb. An original protocol has been conceived to evaluate the odour modulation in binary mixtures: each compound was placed in a separate bottle, the two bottles being individually and simultaneously placed in a larger container, whose odour was evaluated. Thus, the resulting odour came from a mixture of these compounds in gaseous phase and not from the mixture in liquid phase, thus avoiding physico-chemical effects linked to physical mixture.

Inspired by this work, an innovative methodological tool was developed to study if perceptive interactions were only due to headspace phase modifications after components mixture. An ISO wine glass with two identical compartments at the filling part was conceived. Such a glass, which is used like a conventional ISO wine glass by the taster, allowed to compare the perceived odour resulting from the mixture or not of the components in each compartment.

Triangular tests were conducted to validate if the orientation of the wall separating the two compartments in the horizontal plane was perceived by the panel (4 positions evaluated: N-S, NE-SW, E-W and SE-NW). For each glass, fruity pool and tannins were added separately in each compartment. No significant difference was observed, indicating that the orientation of the glass had no effect on the global perception of the mixture. Various concentrations of fruity pool were also tested, between 25 and 200% of average concentrations found in wine. Finally, triangular tests were again conducted: the odour of a mixture of tannins and the fruity pool in both compartments was compared to the odour of tannins and the fruity pool separated in each compartment. The panel was able to significantly differentiate them. This data proved the existence of pre-sensory interaction between tannins and the fruity pool, thus permitting to understand results observed in a previous study with conventional ISO glass.

This new sensory tool was also used to characterise further perceptive interactions we have previously identified, thus revealing additional highlights to physico-chemical changes observed with analytical tools and permitting to elucidate interaction origins.

Keywords: red wine, fruity aroma, perceptive interaction origin

Introduction

Each foodstuff has its own sensory characteristics and specificities, generally due to particular products and techniques used for their elaboration and conditioning their composition. Pineau et al. [1] showed that at least a part of Bordeaux red wine fruity aroma results from perceptive interactions between several aromatic compounds [1]. Many examples of perceptive interactions impacting the fruity aromatic expression of wine have previously been highlighted [2]. The perception of volatiles during sensory analysis is strongly related to the distribution of aromas between the matrix and the gas phase, and may be related to perception during food consumption [3].

Describing the perception mechanism, Berglund et al. [4] suggested that perceptive interactions occur on four different levels [4]. The first is described as pre-sensory interactions, such as chemical or physicochemical interactions in the gas phase or in the nasal pathway and mucosa. The three others refer to interactions in the peripheral and central nervous system, at the receptor surface or in the olfactory bulb. A recent work using an analytical approach and partition coefficient calculation highlighted that pre-sensory modification explains the masking effect of commercial proanthocyanidic tannins on fruity perception [5].

In order to study masking phenomena in binary mixtures, Barkat [6] placed each odorant in separate flasks, themselves put into a bigger flask. This experimental design allowed Barkat to study an odorant vapour mixture and not a mixture in liquid phase, and thus to olfactorily appreciate an overall odour which is not impacted by the interactions taking place in solution between its components [6].

In this global context, this work aims to understand if only pre-sensory origin explain sensory effects observed thanks to a new sensory tool. This new tool was developed in accordance with the work of Barkat [6] and consisted in a double compartment glass. The validation of this new tool will be also described.

Experimental

Matrices

The tannins were added at 5 g/L into a dilute alcohol solution (12% vol. (v/v) and then evaporated using a Rotavapor to 1/3 of the initial volume (Laborota 4010 digital Rotary Evaporator, Heidolph, Germany) with a 20°C bath temperature. The liquid was then mixed with ethanol and microfiltered water to reproduce the alcohol concentration and volume of the original solution. Then, 5 g/L of tartaric acid were added and pH was adjusted to 3.5 with sodium hydroxide. The solution was then supplemented with 5 g/L LiChrolut EN resin (40–120 µm), stirred for 12h to eliminate all traces of volatile compounds, and filtered twice. The resulting solution, called tannin solution (TS) did not contain any trace of volatile compounds.

Dilute alcohol solution (DAS) was prepared with ethanol and microfiltered water to obtain an ethanol level of 12% vol. (v/v) and 5 g/L of tartaric acid (pH adjusted to 3.5 with sodium hydroxide).

Aromatic reconstitutions

The fruity aromatic reconstitution (FAR) was prepared in DAS or TS, with esters added at the average concentrations found in red wines (Table 1) [7].

Table 1: Ethyl esters and acetates concentrations (µg/L) used.

C ₃ C ₂	C ₄ C ₂	C ₆ C ₂	C ₈ C ₂	2MeC ₃ C ₂	(2S)-2MeC ₄ C ₂	(2S)- and (2R)- 2OH4MeC ₅ C ₂ (95/5, m/m)	C ₂ C ₄	C ₂ C ₆	C ₂ iC ₄	C ₂ iC ₅	3OHC ₄ C ₂	3MeC ₄ C ₂
150	200	200	200	250	50	400	10	2	50	250	300	50

C₃C₂, ethyl propanoate; C₄C₂, ethyl butanoate; C₆C₂, ethyl hexanoate; C₈C₂, ethyl octanoate; 2MeC₃C₂, ethyl 2-methylpropanoate; (2S)-2MeC₄C₂, (S)-ethyl ethyl (2S)-2-methylbutanoate; (2S)- and (2R)-2OH4MeC₅C₂, ethyl (2S)- and (2R)-2-hydroxy-4-methylpentanoate; C₂C₄, butyl acetate; C₂C₆, hexyl acetate; C₂iC₄, 2-methylpropyl acetate; C₂iC₅, 3-methylbutyl acetate; 3OHC₄C₂, ethyl 3-hydroxybutanoate; 3MeC₄C₂, ethyl 3-methylbutanoate.

ISO glass

A part of sensory evaluations was performed in ISO glasses, coded by a three-digit random number. Each glass contained about 50 mL liquid.

Double glass compartment

Double compartment glasses were also used (Figure 1). There were built from ISO glasses by a glassmaker (Atelier Prémont, Bordeaux, France) by first separating the foot and the balloon from the glass. The flask was then cut into 2 identical parts and a glass plate fixed with a polymer (Rubson FT101, Henkel). The glass was then reassembled with the different elements being fixed together using the same polymer as before. These double compartment glasses were coded by a three-digit random number. Each glass contained about 50 mL liquid, with 25 mL solution in each compartment.

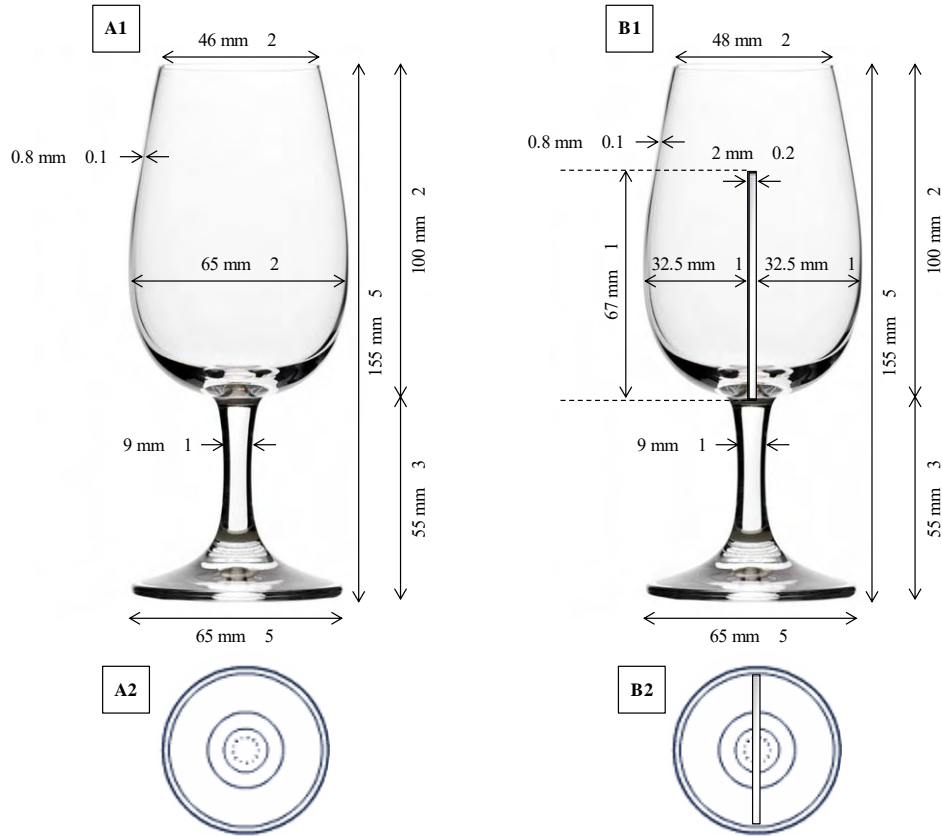


Figure 1: Representation of glasses used for sensory analysis. Frontal (A1) and transverse (A2) cross-sections of ISO glass, and frontal (B1) and transverse (B2) cross-sections of double compartment glass.

Sensory analysis

The panel consisted of 38 judges, 15 males and 23 females, aged 25.5 ± 8.6 (mean \pm SD) years. All panellists were research laboratory staff at ISVV, Bordeaux University, selected for their experience.

To validate the use of double compartment glasses, triangle tests were conducted. These tests were realised in order to determine whether the orientation of the wall separating the two compartments in the horizontal plane impacted the perception (4 orientations evaluated: N-S, NE-SW, E-W and SE-NW, Figure 2).

First, the position of the odorant in the glass for the same orientation was studied: in the first compartment, DAS alone was added, and in the second compartment DAS was supplemented with FAR (Figure 2, tests 1 to 4).

The impact of the orientation of the double compartment glass was then tested (Figure 2, tests 5 to 10).

A last triangle test was realised comparing a double compartment glass, in which the first compartment was filled with TS and the second with FAR in DAS, to another double compartment glass where both compartments contained FAR in TS.

Each judge used direct olfaction to identify the sample perceived as different in each test and gave an answer, even if they were not sure. Each participant was asked not to touch or swirl the glass during all the sessions. Each sample was assessed in duplicate.

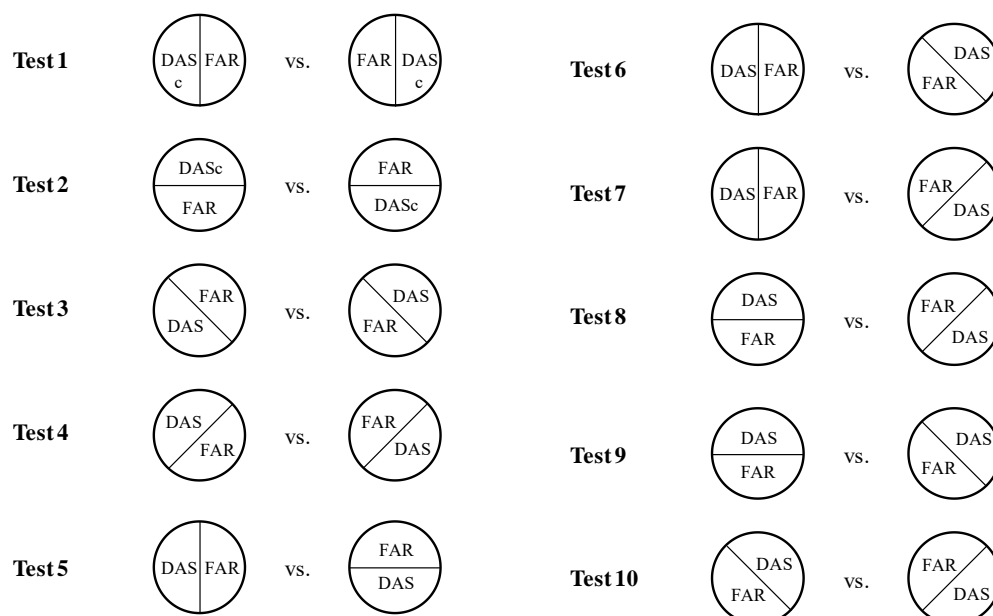


Figure 2: Triangle test realised for double compartment glass validation. DAS, dilute solution; FAR, fruity aromatic reconstitution in dilute alcohol solution.

Results and discussion

A new glass was designed using an ISO glass separated into two compartments (Figure 1). This new tool was called “double compartment glass”. Thanks to this glass, it was possible to put in mixture, or not, different molecules in order to study whether the sensory modifications classically observed were also observed when these molecules were not in mixture in solution.

First of all, validation experiments were performed thanks to triangle tests. First, the impact of the odorant stimulus’s position in the glass on perception was evaluated (Figure 2, tests 1 to 4). For all the odorant positions tested in the glass, no significant difference between samples was observed ($p > 0.05$). Therefore, the position of the odorant in the double glass compartment has no impact on overall perception.

The impact of the position of the double compartment glass was also evaluated (Figure 2, tests 5 to 10). As observed for the odorant position, the orientation of the double compartment glass has no significant impact on overall perception ($p > 0.05$).

Thanks to sensory and physico-chemical analysis, it was recently demonstrated that the presence of commercial proanthocyanidic tannins in dilute alcohol solution led to a masking effect of fruity aroma, but also in a decrease in ester release in the headspace when the matrix was supplemented with tannins [5]. This fact highlights the involvement of pre-sensory modifications in the fruity character modulation observed through sensory analysis, and, via physico-chemical approaches, shows that the olfactory receptors of the taster may be less stimulated in presence of tannins in the matrix. This model of volatile/non-volatile mixture was used to practically validate the double glass compartment.

A triangle test was carried out comparing a double compartment glass where the first compartment was filled with TS and the second with FAR in DAS, to another double compartment glass with FAR in TS in both compartments. These two modalities were significantly differentiated ($p < 0.001$). This result revealed that the panel was able to discriminate the smell of the mixture produced in solution from the one resulting from its two constituents. This fact corroborates results observed during the triangle test in classical ISO glass previously performed, but also the results observed through the ester partition coefficient evaluation.

Then, sensory profile was performed on the same modalities in order to evaluate the potential modification of perception of overall aroma, fresh- and jammy-fruit, red- and black-berry-fruit notes.

As presented in Figure 3, a decrease in the perception of overall aroma, red-berry- and fresh-fruit notes was observed when FAR was in TS in both compartments, compared to the glass where FAR was separated from TS. This result on sensory profile was the same as the result observed with the ISO glass. This data revealed that the double glass compartment may be used in order to establish the origin of perceptive interaction, *i.e.* pre-sensory or sensory origin.

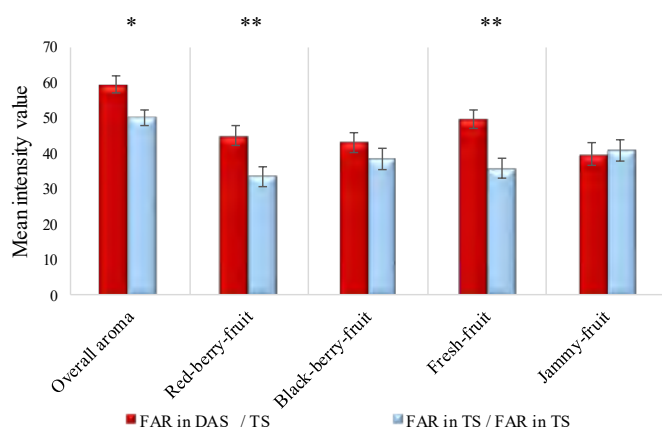


Figure 3: Effect of the mixture or not of the fruity aromatic reconstitution and the tannin solution in the double compartment glass on the perception of the fruity aromatic reconstitution. *, $p < 0.05$; **, $p < 0.001$; FAR, Fruity Aromatic Reconstitution; DAS, dilute alcohol solution; TS, tannin solution. FAR in DAS/TS, fruity aromatic reconstitution in dilute alcohol solution in the first compartment, and tannin solution alone in the second compartment. FAR in TS/ FAR in TS, fruity aromatic reconstitution in tannin solution in both compartments. Error bars indicate standard error deviation.

Conclusion

Previous work has highlighted that pre-sensory effects explained alone sensory masking effect observed, with a decreased in molecules released from matrix, and thus an attenuation in taster olfactory receptors stimulation.

A new sensory tool was developed, based on Samy Barkat's thesis work [6]. It consisted in an adaptation of ISO glass containing two compartments separated by a glass wall. This tool allowed to place in each compartment one of the components of the mixture, and thus compare the perceived odours according to whether the components of the mixture were physically mixed together or not.

The use of this double compartment glass was validated, and more precisely the absence of impact of odorant position in the glass, but also the double glass position. Next, further triangle tests and sensory analyses were carried out in order to evaluate whether there was a difference when the fruity aromatic reconstitution was in the mixture, or not, with proanthocyanidic tannins.

Sensory analysis using this double compartment glass showed the same results as with the classical ISO glass, *i.e.* a masking effect of red-berry- and fresh-fruit. This highlights that only pre-sensory modification explains the sensory effects observed and validates the use of the double compartment glass to investigate the origins of perceptive interaction.

This new sensory tool might be applied to other examples of perceptive interactions already described in the literature in order to elucidate their potential origins.

References

1. Pineau, B.; Barbe, J.-C.; Van Leeuwen, C.; Dubourdieu, D. Examples of Perceptive Interactions Involved in Specific "Red-" and "Black-Berry" Aromas in Red Wines. *J Agric Food Chem.* 2009;57(9):3702–3708.
2. Pozo-Bayón, M. Á.; Reineccius, G. Interactions Between Wine Matrix Macro-Components and Aroma Compounds. In *Wine Chemistry and Biochemistry*; Moreno-Arribas, M. V., Polo, M. C., Eds.; Springer New York, 2009; pp 417–435.
3. Cameleyre, M.; Lytra, G.; Barbe, J.-C. Static Headspace Analysis Using Low-Pressure Gas Chromatography and Mass Spectrometry, Application to Determining Multiple Partition Coefficients: A Practical Tool for Understanding Red Wine Fruity Volatile Perception and the Sensory Impact of Higher Alcohols. *Anal Chem.* 2018;90(18):10812–10818.
4. Berglund, B.; Berglund, U.; Lindvall, T. Psychological Processing of Odor Mixtures. *Psychol Rev.* 1976;83(6):432–441.
5. Cameleyre, M.; Monsant, C.; Tempere, S.; Lytra, G.; Barbe, J.-C. Towards a better understanding of perceptive interactions between volatile and non-volatile compounds. The case of proanthocyanidic tannins and red wine fruity esters: Methodological, sensory and physico-chemical approaches. *J Agric Food Chem.* 2021;69(34):9895–9904.
6. Barkat, S. *La Qualité Perçue Des Mélanges Odorants : Analyses Psychophysiologiques*, Université de Lyon.; 2005.
7. Lytra, G.; Tempere, S.; de Revel, G.; Barbe, J.-C. Distribution and Organoleptic Impact of Ethyl 2-Methylbutanoate Enantiomers in Wine. *J Agric Food Chem.* 2014;62(22):5005–5010.

Odour-Induced Taste Enhancement in normal-weight and obese people

CHRISTOPHER AVELINE, Cécile Leroy, Thierry Thomas-Danguin, Charlotte Sinding

Centre des Sciences du Goût et de l'Alimentation, AgroSup Dijon, CNRS, INRAE, Université Bourgogne Franche-Comté, F-21000 Dijon, France

christopher.aveline@inrae.fr; charlotte.sinding@inrae.fr

Abstract

The Odour-Induced Taste Enhancement (OITE) phenomenon allows, by addition of odorants in food or beverages, to enhance the perception of taste. To the best of our knowledge, only Proserpio *et al.* [1] studied OITE in obese people. Interestingly, in this study, the addition of butter aroma in custard dessert produced OITE only in obese and not in normal-weight people. Here we extended this result by comparing Odour-Induced Sweetness and Saltiness Enhancement in normal-weight and obese peoples using a ranking task on beverages. Forty-three normal weight (NW: $20 < \text{BMI} < 25 \text{kg/m}^2$) and 28 obese participants (OB: $\text{BMI} > 30 \text{kg/m}^2$) took part in the sensory evaluation of 2 sweet solutions and 2 salty solutions. The sweet base solutions were apple juice (Aj) and water and the added odorant was vanillin. The salty base solutions were a green-pea soup and water and the added odorant was a bacon aroma. For the ranking task, three additional solutions with increasing concentrations of either sucrose or sodium chloride (S1 to S3) were prepared for each base. Each solution was tested in a dedicated ranking trial. Subjects received four bottles in a given trial, the three sweet or salty concentrations of the base solution (e.g. AjS1, AjS2, and AjS3) and one of the odorant-added solutions (e.g. AjS1+vanillin). Participants had to rank the 4 bottles according to sweetness or saltiness intensity. The results showed that OITE occurred for all the solutions but differently according to the group and the complexity of the beverage base. In the sweet complex beverage (Aj), only OB perceived a sweet taste enhancement whereas in the green-pea soup OB and NW perceived a salty taste enhancement. OB and NW participants ranked the water-based solutions in a similar way, independently of taste, but with a lower effect size compared with the complex solutions. The highest OITE was observed for the sweet Aj+vanillin and the salty Wsa+bacon samples (sweetness and saltiness increased by at least 50% and 75%, respectively) in OB. To conclude, we showed that the OITE phenomenon significantly differed between NW and OB. Only OB experienced OITE in the sweet complex beverage, while OB and NW experienced OITE in the salty soup. Both groups experienced OITE in the sweet water solutions but with a lower effect size compared with the complex solution (Aj). Our results also demonstrated that the ranking task is efficient to assess OITE and to highlight OITE differences between groups and solutions.

Keywords: ranking task, flavour, OITE, perception, food, obesity, salty, sweet.

Introduction

During food consumption, tastants and odorants are released in the mouth. While odorants reach olfactory receptors in the nose through the retronasal pathway, tastants directly activate taste receptors on the tongue. The activation of these different receptors allows respectively odour and taste perceptions. When taste and odour perceptions co-occur repeatedly, our brain unifies the perceptions into a single holistic food percept called flavour perception. The integration of odour and taste into flavour also transfers a taste property to the odour. After which, the odorant can enhance a taste perception. This phenomenon called “Odour-Induced Taste Enhancement” (OITE) has been largely described in sweet [2] and salty simple beverages [2, 4] as water.

The study of this phenomenon in more complex beverages is challenging because multiple perceptual interactions occur between tastes, odours, and textures, which complicates the identification of taste-enhancing odorants. Therefore, few studies showed this phenomenon in complex beverages [5] or food [3, 6]. However, more studies on this topic are needed to understand if the strategy that aims to reduce salt and sugar while compensating taste loss with aroma would be effective in reducing salt and sugar intake. This strategy is promising in a society where the prevalence of obesity and food-related diseases is increasing.

While the study of the food base is of interest to delineate how OITE could be used in food, physiological factors like BMI should also be considered. Proserpio and collaborators assessed OITE between normal-weight (NW) and obese (OB) population [1]. Interestingly, they found that only obese participants presented a sweet enhancement when butter aroma was added to a custard dessert. Therefore, it seems that obese participants are more sensitive to this butter-induced sweetness effect. We wished to replicate and extend these results by comparing sweet and salty enhancements in OB and NW within a simple (water) and a complex (apple juice or green-pea soup) base. We hypothesized that OITE will occur in the normal-weight and the obese populations for sweet and salty tastes, but we expected that OB would find the OITE solution as more sweet/salty than NW.

We used a ranking task instead of intensity visual analogue scales traditionally used to assess the OITE. Sweet or salty intensity scales are often difficult to use and produce a large interindividual variability that includes bias

linked to the scale use. It often necessitates training or at least references to delineate the scale's anchors or the intensity of the middle of the scales [7]. Compared to taste intensity scales, the ranking task is easily assimilated by participants and does not require training or references. Indeed, the ranking task was effectively used by children [8] or elderly [9]. It is also less prone to inter-individual variability and provides a direct measure of consensus across participants. Former studies showed that the ranking task was efficient to assess differences in taste intensities from different solutions [10] and it was previously used to measure OITE in water [11]. In this experiment, the participants had to rank 14 solutions containing different concentrations of sugar with and without the addition of the vanillin aroma. We simplified the ranking task design of Nguyen [11] and used three levels of concentrations among which the aroma-added and tastant-reduced solution had to be positioned to highlight the level of OITE.

Materials and Methods

Participants

We recruited 43 normal-weight (NW: $20 < \text{body mass index} < 25 \text{kg/m}^2$) and 28 obese (OB: $\text{body mass index} > 30 \text{kg/m}^2$) French participants. The sweet and salty solutions were evaluated in different sessions. The participants were scaled and weighed at the end of the first session. They should not eat, drink or smoke at least 1 hour 30 min before the sessions. The experimental procedure was explained to each participant before recruitment and again before each test session. Participants signed an informed consent form to participate in the study. They received 10€ compensation for each hour spent performing evaluations. The study was conducted following the Helsinki Declaration and was approved by the ethics committee CPP EST I #19.04.26 (ID RCB #2019-A00120-57).

Solutions

To study the odour-induced sweetness enhancement, two bases were used: Apple juice (Aj) and sweet Water (Wsw). The Aj base was constituted of apple juice (Carrefour, France) initially containing 10% of sugars that was diluted at 4% (w/w) with water (Evian, France). We selected vanillin (Sigma Aldrich, CAS: 121-33-5) as a potential sweet enhancer for both Aj and Wsw. The odorant was dissolved in Evian water at 4000 ppm and diluted in Aj at 300 ppm and in Wsw at 600 ppm. To study the odour-induced saltiness enhancement, two bases were used: Green-pea soup (Gp) and salty water (Wsa). The Gp base was prepared by extracting the supernatant of an unsalted green-pea puree (Bledina, France). A bacon complex (Firmenich, Switzerland) was chosen as a potential saltiness enhancer for both Gp and Wsa. The Gp and aroma solution were not diluted before mixing. For the ranking task, three solutions with increasing concentrations of either sucrose or sodium chloride (S1 to S3) were prepared for each food base. A fourth solution was prepared, containing the aroma diluted in the S1 solution (Table 1).

Table 1: Concentration (w/w) of each solution by food base used during the ranking task.

Beverage base	Aroma	S1	S2	S3	S1 + Aroma
Apple Juice (Aj)	Vanillin	4%	6%	8%	4% + 0.03%
Sweet Water (Wsw)	Vanillin	4%	7%	10%	4% + 0.06%
Green-pea soup (Gp)	Bacon	0.25%	0.50%	0.75%	0.25% + 0.005%
Salt Water (Wsa)	Bacon	0.10%	0.18%	0.25%	0.10% + 0.005%

Sensory procedure

The ranking task instructions and sensory data collection were monitored with Fizz software (Biosystèmes, Couternon, France). Each food base was tested in a dedicated ranking task (4 ranking tasks in total). Participants received three sweet or salty concentrations of the base solution (e.g. AjS1, AjS2, and AjS3) and one of the odorant-added solutions (e.g. AjS1+vanillin); they were asked to rank the 4 bottles according to the increasing sweetness or saltiness intensity. The ranking tasks' and solutions' orders were counterbalanced among participants. The solutions were delivered using spray bottles, which avoid orthonasal smelling before tasting. At the beginning of the session, participants were trained to use the spray bottles. To perform a ranking task, the panellist had to spray two pulses of each solution in the mouth, swallow and rank the bottles accordingly to their salty/sweet intensity; equally ranked were not allowed. When necessary, they could rinse their mouth. After a preliminary ranking, they were instructed to confirm their choice by testing once again each solution from the lowest to the highest salty/sweet intensity and register their ranking. Between two rankings, the subjects had to rinse their mouth with lukewarm Evian© water (40°C).

Data analysis

For each solution, the distribution of the participants that have ranked in the first, second, third, or fourth position was calculated. The position of the ranking (2nd, 3rd, and 4th positions) represented the strength of OITE. For each ranking task, a first Wilcoxon test was done to check whether the ranking was correct for each base solution ($S1 < S2 < S3$). Another Wilcoxon test was done to compare the ranking of the beverage with the aroma against the base solutions with different levels of sugars/salt ($S1 + \text{aroma}$ vs $S1$, $S2$, or $S3$). A between-group Wilcoxon test was performed to compare the ranking of the aroma-added solution in each food base to assess whether the enhancement is similar between groups. Finally, a within-group Wilcoxon test was performed to compare the ranking of the aroma-added solution between the salty and sweet bases for the water and the complex bases. The Wilcoxon tests were corrected with a False Discovery Rate (FDR) correction; a comparison was considered as significant for $p < 0.05$ (*), $p < 0.01$ (**), and $p < 0.001$ (***)

Results

OITE in complex beverages

In the apple juice, 83% of OB ranked AjS1+vanillin at least in the second position, whose 33% in the third position and 17% in the fourth. By contrast, only 61% of NW people ranked AjS1+vanillin at least in the second position whose only 6% in the third position (Figure 1A). Therefore, AjS1+vanillin was ranked as significantly higher than AjS1 by OB ($W = 156$, $p = 0.003$) but not by NW ($W = 316$, $p = 0.14$). The distribution of the ranking is significantly different between the groups ($W = 144$, $p = 0.003$). These results showed an OITE in the apple juice for OB but not for NW. Interestingly, OB perceived AjS1+vanillin as sweet as AjS2 ($W = 85.5$, $p = 1$) while NW perceived AjS1+vanillin as less sweet than AjS2 ($W = 20$, $p < 0.0001$). Therefore, the solution AjS1+vanillin was perceived as sweeter than AjS2 in the OB group but not in the NW group.

Different results were found with the green-pea soup, 80% of OB ranked GpS1+bacon at least in the second position whose 5% in third, and 5% in fourth. By contrast, 62% of NW ranked GpS1+bacon at least in second position, whose only 8% in third and 5% in fourth (Figure 1B). Therefore, GpS1+bacon was ranked as significantly higher than GpS1 by OB ($W = 172$, $p = 0.007$) and by NW ($W = 472$, $p = 0.05$). Even if a higher number of OB rated the aroma-added solution in the second position, the ranking was not significantly different between the groups ($W = 320.5$, $p = 0.36$). Both groups evaluated the GpS1+bacon as less salty than GpS2 (OB: $W = 26$, $p = 0.003$; NW: $W = 92$, $p < 0.0001$). Therefore, the solution GpS1+bacon was perceived as saltier than GpS1 but less than GpS2 in NW and OB and ranking was similar between the groups.

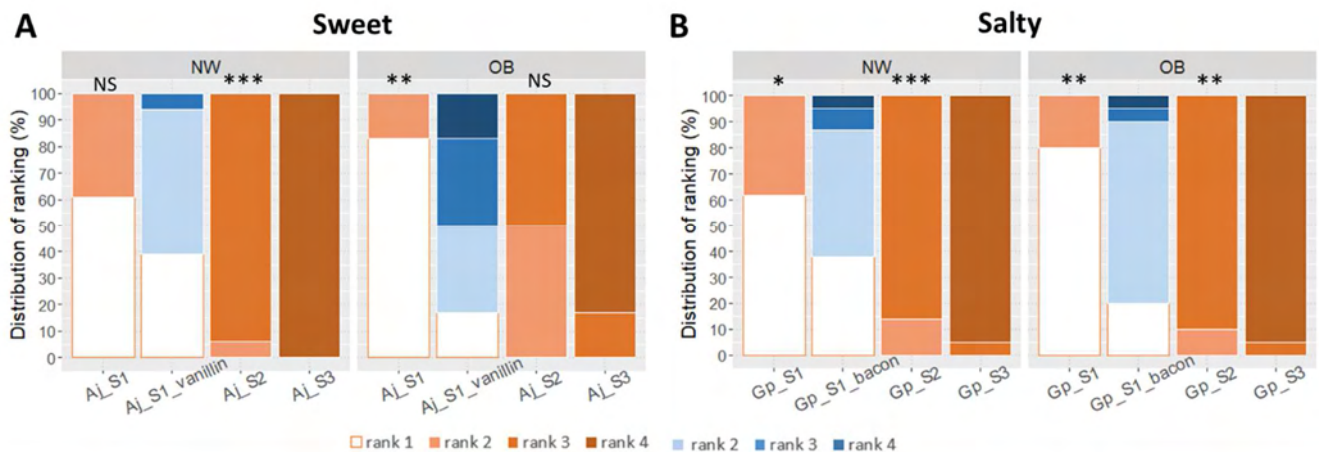


Figure 1: Distribution of the participants who ranked in 1st, 2nd, 3rd and 4th position the A) three sweet levels of an Apple juice (AjS1, AjS2, and AjS3) and B) three salty concentrations of a Green-pea soup (GpS1, GpS2, and GpS3) and an odorant-added solution (AjS1+vanillin or GpS1+bacon). The colour gradient corresponds to the distribution of the participants who ranked in positions 1, 2, 3, or 4. The orange colours correspond to the solutions without aroma and the blue colours to the ranking of the odorant-added solutions. The stars indicate that the solution is significantly different from the solution containing the aroma at respectively: ***: $p < 0.001$; **: $p < 0.01$; and *: $p < 0.05$ (Wilcoxon test).

OITE in water base beverage

In the sweet water, 89% of OB ranked WswS1+vanillin at least in the second position, whose 12% in third and 4% in fourth position. In contrast, 75% of NW people ranked WswS1+vanillin at least in second position, whose only 8% in third and 3% in fourth position (Figure 2A). Therefore, WswS1+vanillin was ranked as significantly sweeter from WswS1 by OB ($W=316.5$, $p=0.0002$) and by NW ($W=600$, $p=0.001$). These results correspond to an OITE for both groups in the sweet water. Both groups evaluated the WswS1+vanillin as less sweet than WswS2 (OB: $W=59$, $p=0.002$; NW: $W=77.5$, $p<0.0001$). Therefore, the solution WswS1+vanillin was perceived as sweeter than WswS1 but less than WswS2 in NW and OB and ranking was similar between the groups.

Similar results were found in the salted water (Figure 2B), 85% of OB ranked WsaS1+Bacon at least in second whose 10% in third, and 25% in fourth. In contrast, 77% of NW people ranked WsaS1+Bacon at least at the second position whose only 31% at the third position and 3% at the fourth. Therefore, WsaS1+bacon was ranked as significantly saltier than WsaS1 for the OB group ($W=189$, $p=0.002$) and the NW group ($W=566$, $p=0.0002$). These results correspond to an OITE for both groups in the salty water. Interestingly, WsaS1+Bacon was not ranked differently from WsaS2 for the OB group ($W=95.5$, $p=0.73$). Comparatively, WsaS1+bacon was not ranked differently from WsaS2 for the NW group ($W=186$, $p<0.02$). OB and NW both perceived OITE in salty water plus bacon, but the enhancement was higher in OB than in NW.

Within-group comparison between salty and sweet enhancements

In NW, the comparison between sweet and salty taste enhancements revealed no difference of ranking of the aroma-added solutions in the simple bases Wsw and Wsa ($W=564$, $p=0.11$) as well in the complex bases (Aj vs Gp: $W=542$, $p=0.67$). However, in OB even if no difference was found between the simple bases Wsw and Wsa ($W=216$, $p=0.26$), OITE tended strongly to be higher in the AjS1+vanillin than in the GpS1+bacon solutions ($W=241.5$, $p=0.052$). To conclude, it is not possible to say that differences between OB and NW are solely based on the type of OITE (salty or sweet).

Within-group comparison between complex and simple beverages

In OB, the complex AjS1+vanillin was ranked higher than the simple water solution WswS1+vanillin ($W=9$, $p=0.03$). No significant differences of ranking between the sweet beverages WswS1+vanillin and AjS1+vanillin in NW ($W=102.5$, $p=0.45$) were found. However, in the salty beverages, the NW group tended to rank higher WsaS1+bacon in comparison to the GpS1+bacon ($W=828.5$, $p=0.054$) and the same trend was observed in the OB group ($W=62$, $p=0.07$). Therefore, the complexity of the base solution alone cannot explain the differences of OITE observed in OB and NW.

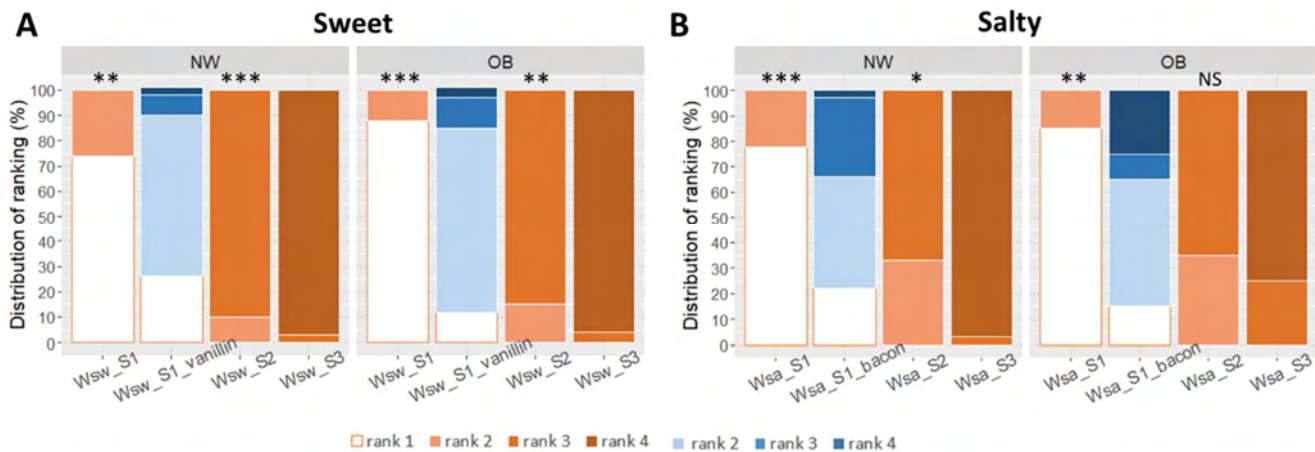


Figure 2: Distribution of the participants who ranked in 1st, 2nd, 3rd, and 4th position the A) three sweet levels of a sweet water (WswS1, WswS2, and WswS3) and B) three salty concentrations of a salty water (WsaS1, WsaS2, and WsaS3) and an odorant-added solution (WswS1+vanillin or WsaS1+bacon). The colour gradient corresponds to the distribution of participants who ranked in positions 1, 2, 3, or 4. The orange colours correspond to the solutions without aroma and the blue colours to the odorant-added solutions.

Discussion and Conclusion

The study aimed to determine odour-induced taste enhancement differences between obese and normal-weight populations on salty and sweet tastes. We hypothesized that OITE will occur in the normal-weight and in the obese

population for sweet and salty tastes, but we expected that OB would find the OITE solution as more sweet/salty than NW.

We found a large consensus among OB participants (83%) concerning the OITE induced by vanillin in the apple juice. This OITE was not found in NW. In the sweet water solution, OITE was observed in both groups but did not differ between groups. In OB, sweetness enhancement is so high that it would allow decreasing sugar content by 33% while 50% of the participants still perceived it as sweet as before reduction. For the green-pea soup, the OITE was rather low in both groups. However, it was much higher in salty water. OB perceived a high salty enhancement, with a large consensus among participants (85%) in water solution with bacon although it was not significantly higher than NW. In the OB group, saltiness enhancement in water is so high that it would allow decreasing salt content by 75%, and 35% of the tasters would still perceive it as salty as before reduction. The OITE difference between OB and NW was explained neither by the complexity of the solution nor by the taste modality (salty or sweet).

The strong OITE observed in the apple-juice with vanillin in OB and the absence of OITE in NW is congruent with the results found by Proserpio and collaborators [1]. They showed an increase of the sweetness with a butter aroma added in a custard dessert only in the obese group. This result could be explained by differences in food habits between the groups. Obese people are generally more exposed to sweet drinks [12] and probably to sweet desserts with vanillin. The repeated exposure to this odorant in sweet desserts could lead to stronger associative learning between sweetness and vanillin [13]. This associative learning results in the unification of taste and odorant into a single perception (configuration) called flavour perception. This configural process follows integratory neuronal rules [14]. The subsequent experiences of this odour in food or beverage reactivate the configural encoding which leads to the perception of an odour as a taste [15-17].

We did not find clear OITE differences between salty and sweet beverages, more solutions should be tested in order to clarify the results. However, we should consider that sweet and salty solutions target differently the reward system, which may then modify OITE. The sweet perception involves the whole reward system while the salty perception targets only the amygdala [18]. Therefore associative learning effects might be less pronounced for saltiness than for sweetness. Because the apple juice is more caloric than the green-pea soup, the higher enhancement observed in the apple juice could also be due to a reinforcement of the association between the sweet taste and the aroma perception due to the caloric load.

Similarly, concerning the “complexity” effect (water vs complex base), while the OITE was more effective in the complex base for sweetness, the salty OITE was more effective in the simple water base. It is possible that an interaction between “taste” (salty or sweet), and “complexity” occurred. Therefore, here again, more solutions should be tested to ascertain the effect of complexity on OITE. Nevertheless, we should notice that tendencies for higher OITE with the bacon in water solution compared with the green-pea soup were found in both groups. This result could be explained by taste-taste interaction. Indeed, green peas are naturally sweet, therefore, the saltiness brought by the bacon could be reduced by the sweetness of the green peas leading to a lower OITE. As in the green-pea soup, the taste-taste interaction could also be present in the apple juice. Indeed, the typical apple juice flavour consists in a balance between the sweet and the sour tastes. Finally, the bacon-induced saltiness enhancement and the vanillin-induced sweetness enhancement in complex bases could be modulated by these taste-taste interactions.

Our results showed that the ranking task is an efficient method to highlight OITE. To our knowledge, only Nguyen [11] used this sensory procedure to assess odour-taste interactions. However, in that study the ranking task was rather complex due to a high number of solutions. Here, we simplified the task using only three levels of sweet or salt concentrations and one concentration of odorant. The results were contrasted in terms of OITE, some odorants did not produce OITE, and some odorants produced OITE with different strengths depending on the group, which validate the methodology.

To conclude, as a main result, we showed that the OITE phenomenon is present in obese and normal-weight people for sweet and salty tastes, but with stronger OITE in OB for vanillin in apple juice and bacon in salty water. As flavour perception is a non-conscious brain construction, it would be interesting to go further in the understanding of the OITE phenomenon by investigating the brain mechanisms that underlie odour-taste interactions in normal-weight and obese people in different food bases.

Acknowledgements

This work was supported by the French “Investissements d’Avenir” program, project ISITE-BFC (contract ANR-15-IDEX-0003) awarded to C. Sinding for the EATERS project, and by Firmenich, Geneva, Switzerland. We would like to thank Dr. Marie Claude Brindisi as the medical investigator of the study. We would like to thank for their technical and logistical support on the experiment: Noëlle Béno, and Françoise Durey from the ChemoSens platform, and Chantal Septier, Claire Follot, Gaia Maillard, Marianela Santoyo Zedillo, Marie Simon and Yue Ma from the FFOPP team of CSGA.

References

1. Proserpio, C., Laureati, M., Invitti, C., Cattaneo, C., and Pagliarini, E., "BMI and gender related differences in cross-modal interaction and liking of sensory stimuli," *Food Qual. Prefer.* 2017;56:49–54. doi: 10.1016/j.foodqual.2016.09.011.
2. Djordjevic, J., Zatorre, R.J., and Jones-Gotman, M., "Odor-induced changes in taste perception," *Exp. Brain Res.* 2004;159(3):405–408. doi: 10.1007/s00221-004-2103-y.
3. Frank, R.A. and Byram, J., "Taste-smell interactions are tastant and odorant dependent," *Chem. Senses* 1988;13(3):445–455. doi: 10.1093/chemse/13.3.445.
4. Lawrence, G., Salles, C., Septier, C., Busch, J., and Thomas-Danguin, T., "Odour-taste interactions: A way to enhance saltiness in low-salt content solutions," *Food Qual. Prefer.* 2009;20(3):241–248. doi: 10.1016/j.foodqual.2008.10.004.
5. Barba, C., Beno, N., Guichard, E., and Thomas-danguin, T., "Selecting odorant compounds to enhance sweet flavor perception by gas chromatography / olfactometry-associated taste (GC / O-AT)," *Food Chem.* 2018;257:172–181. doi: 10.1016/j.foodchem.2018.02.152.
6. Lawrence, G., Salles, C., Palicki, O., Septier, C., Busch, J., and Thomas-Danguin, T., "Using cross-modal interactions to counterbalance salt reduction in solid foods," *Int. Dairy J.* 2011;21(2):103–110. doi: 10.1016/j.idairyj.2010.09.005.
7. Depled, F., "Evaluation sensorielle Manuel méthodologique," in *SSHA 3rd edition*, 2009, p. 146.
8. Liem, D.G., Mars, M., and de Graaf, C., "Consistency of sensory testing with 4- and 5-year-old children," *Food Qual. Prefer.* 2004;15(6):541–548. doi: 10.1016/j.foodqual.2003.11.006.
9. Barylko-Pikielna, N., Matuszewska, I., Jeruszka, M., Kozłowska, K., Brzozowska, A., and Roszkowski, W., "Discriminability and appropriateness of category scaling versus ranking methods to study sensory preferences in elderly," *Food Qual. Prefer.* 2004;15(2):167–175. doi: 10.1016/S0950-3293(03)00055-7.
10. Carabante, K.M. and Prinyawiwatkul, W., "Serving Duplicates in a Single Session Can Selectively Improve Sensitivity of Duplicated Intensity Ranking Tests," *J. Food Sci.* 2018;83(7):1933–1940. doi: 10.1111/1750-3841.14194.
11. Nguyen, H.D., "Contribution à l'étude des interactions entre entrées sensorielles : l'effet de la présence d'un arôme sur la perception d'une saveur," PhD thesis, Université de Bourgogne, 2000.
12. Morenga, L. Te, Mallard, S., and Mann, J., "Dietary sugars and body weight: Systematic review and meta-analyses of randomised controlled trials and cohort studies," *BMJ-British Medical Journal* 2013;346:e7492. doi: 10.1136/bmj.e7492.
13. Stevenson, R.J., Boakes, R.A., and Prescott, J., "Changes in Odor Sweetness Resulting from Implicit Learning of a Simultaneous Odor-Sweetness Association: An Example of Learned Synesthesia," *Learn. Motiv.* 1998;29(2):113–132. doi: 10.1006/lmot.1998.0996.
14. Wilson, D.A. and Stevenson, R.J., *Learning to smell: Olfactory perception from neurobiology to behavior*. Baltimore, Maryland (USA): The Johns Hopkins University Press, 2006.
15. Stevenson, R.J., Prescott, J., and Boakes, R.A., "Confusing tastes and smells: How odours can influence the perception of sweet and sour tastes," *Chem. Senses* 1999;24(6):627–635. doi: 10.1093/chemse/24.6.627.
16. Stevenson, R.J., Prescott, J., and Boakes, R.A., "The Acquisition of Taste Properties by Odors," *Learn. Motiv.* 1995;26(4):433–455. doi: 10.1016/S0023-9690(05)80006-2.
17. Stevenson, R.J., Boakes, R.A., and Wilson, J.P., "Counter-conditioning following human odor-taste and color-taste learning," *Learn. Motiv.* 2000;31(2):114–127. doi: 10.1006/lmot.1999.1044.
18. Spetter, M.S., Smeets, P.A.M., de Graaf, C., and Viergever, M.A., "Representation of Sweet and Salty Taste Intensity in the Brain," *Chem. Senses* 2010;35(9):831–840. doi: 10.1093/chemse/bjq093.

Section 2

Flavour analysis and analytical tools

NMR based studies on odorant melanoidin interactions in coffee beverages

MICHAEL GIGL, Oliver Frank and Thomas Hofmann

Chair of Food Chemistry and Molecular Sensory Science, Technical University of Munich, michael.gigl@tum.de

Abstract

Freshly brewed coffee is appreciated by consumers all over the world because of its stimulating effect, its characteristic taste centring on sourness and pleasant bitterness and its alluring aroma with characteristic “roasty/sulphurous” odour notes, culminating in the unique flavour sensation of coffee. The molecules responsible for the olfactory sensation of roasted coffee beans and percolated coffee beverages, analysed by means of the molecular sensory science approach are well understood. With previous studies providing qualitative and quantitative data, using aroma extract dilution analysis (AEDA), gas chromatography-olfactometry (GC-O) and headspace GC-MS techniques resulting in comprehensive aroma recombinates consisting of not more than 30 odorants [1-3]. Although the aroma of coffee can be reconstituted rather well, the impact of the melanoidin containing high molecular weight fractions (HMW) on the sensory quality of coffee beverages, is still mostly unclear on a molecular basis. Whereas former studies clearly indicated that especially odour active thiols exhibit high binding affinity to high molecular weight melanoidin fractions of coffee, only covalent interactions have been considered so far. The impact of non-covalent π - π interactions on coffee flavour is still completely unclear [4, 5]. To get detailed insight into the molecular phenomenon of odorant polymer interactions and the sensory impact on coffee flavour perception, a quantitative ¹H-NMR based screening approach was developed, which allowed the direct and non-invasive analysis of molecular interactions between key coffee odorants, like 2-furfurylthiol and high molecular weight melanoidin polymers (>10 kDa). A clear distinction between covalent and non-covalent interactions was achieved by monitoring time dependency of odorant polymer interactions, with 2-furfurylthiol exhibiting π - π interactions as well as covalent bindings. In contrast, pyrazines and hydroxyphenols showed only non-covalent π - π stacking, whereas aldehydes incubated with HMW material showed only covalent interactions at prolonged incubation times. Furanones, as well as diketones showed no interactions with the HMW. Human sensory experiments with isolated HMW material >10 kDa and a full aroma recombine of coffee were well in the line with the findings from the NMR based approach. A drastic reduction of “roasty/sulphurous” aroma notes in combination with a decrease in overall coffee-like odour quality, as well as an increased “sweetish/caramel-like” flavour was perceivable upon incubation of coffee melanoidins with the aroma recombine. The lack of binding affinity of the sweetish/caramel smelling 4-hydroxy-2,5-dimethyl-3(2H)-furanone in combination with the high binding affinity of coffee thiols provides explanation of the sensory evaluation and might be the reason for the fast disappearance of the “roasty/sulphurous” aroma impressions of a freshly prepared coffee brew.

Keywords: NMR, coffee aroma staling, sensory experiments, covalent interactions, π - π interactions

Introduction

Unfortunately, the aroma of a freshly prepared coffee beverage is very unstable and deteriorates within minutes after the preparation of the brew [5]. Molecular reactions taking place during storage of coffee beverages were analysed in previous studies with the aim of clarifying the reasons for the unstable nature of the coffee aroma on a molecular basis. A drastic influence of storage on the concentrations of the “roasty/sulphurous” smelling thiols 3-methyl-2-butene-1-thiol, 3-mercapto-3-methylbutyl formate, 2-methyl-3-furanthiol, methanethiol, and, the major key aroma compound of roasted coffee 2-furfurylthiol (FFT) could be shown in the literature after keeping a freshly brewed coffee warm in a thermos flask. A biomimetic in-bean model roasting approach clearly demonstrated the high thiol binding affinity of low molecular weight (LMW) compounds derived from chlorogenic acid degradation [6]. Consequently, the conjugation of FFT with di- and trihydroxybenzenes was confirmed using LC-MS and NMR techniques [7, 8]. Furthermore, furan derivatives, like furfuryl alcohol, were shown to interact with dihydroxy- and trihydroxybenzenes and lead to the detection of numerous (furan-2-yl)methylated benzene diols and triols in brewed coffee [9]. Recently, an untargeted UPLC-TOF-MS screening approach in combination with statistical S-plot analysis was used to identify reaction products formed between Strecker aldehydes, present in the coffee aroma and chlorogenic acid, quinic acid and a quinic acid lactone [10].

Additionally, besides adducts formed between LMW coffee compounds and odorants during roasting and/or storage of the percolated brew, the effect of HMW coffee melanoidins was evaluated regarding their influence on the aroma staling phenomenon [4, 5]. These brown coloured macromolecules are generated by thermal processing of foods, like the roasting of coffee and embody a very heterogeneous compound class [11–15].

These melanoidin populations contain a plethora of reactive compounds and/or side-groups (i.e. phenols), and were shown to exhibit high binding affinities to odour active thiols, like 2-furfurylthiol by means of gas chromatography(GC) -mass spectrometry (MS) and human sensory experiments [5]. Using coffee-like model

systems, it could be demonstrated, that odour-active thiols can react with pyrazinium di-cations, the oxidation products of the "CROSSPY" radicals. These radical species were reported to be key intermediates in melanoidin formation [4, 16, 17].

However, the discovery of molecular interaction between volatile and non-volatile coffee constituents was restricted mainly to the occurrence of covalent reactions as a result of the analytical methods that were used. Interactions such as complex formation by e.g. non-covalent (π - π), dipole-dipole or van der Waals interactions were revealed to be disbanded during liquid chromatography because of the dynamic equilibrium between lightly associated complexation partners [18]. Thus, bound and unbound states of the ligands could not be differentiated, and state of the art GC or UHPLC analysis remains not suitable for observing dynamic non-covalent interactions. To overcome these challenges, NMR-based methodologies were developed to enable the investigation of binding affinities of selected LMW ligands, by monitoring their specific resonance signals with regards to signal shape, multiplicity, and chemical shift.

In the literature non-covalent interactions were reported to influence proteins and ligands [19-22], the oral astringency of polyphenols [18], as well as the co-pigmentation of anthocyanins [23].

Specifically, for coffee, a π - π complex encompassing chlorogenic acid and caffeine is known from literature, signifying the possibility of π - π stacking to occur in percolated coffee [24-26]. In order to study the influence of non-covalent interactions on aroma active compounds, an NMR based approach was shown to yield promising results for red wine aroma perception. It was reported, that the 2-methylpyrazine and vanillin showed a high binding affinity to red wine polyphenols like gallic acid and naringin [27]. So far, non-covalent interactions were not discussed in the context of olfactory perception of coffee brew and the loss of the characteristic "roasty/sulphurous" aroma impressions during storage of coffee beverages. Thus, the object of the current study is to obtain comprehensive and detailed understanding of the interaction between key coffee odorants and the melanoidin containing fraction of coffee, as well as to depict the sensory impact on coffee aroma perception.

First, human sensory experiments were performed, in order to assess the effects of melanoidin addition on the aroma profile of coffee, followed by a qualitative and quantitative $^1\text{H-NMR}$ based approach to further evaluate and classify these interactions on a molecular basis.

Experimental

Preparation of coffee beverages

A single-dose capsule machine (De'Longhi Nespresso Inissa EN 80.B) was used to percolate commercially available coffee capsules. The coffee Capsa Lungo Mild Roast (Dallmayr Capsa, Munich, Germany) was brewed with water (104 mL water/capsule), resulting in standard coffee beverages with concentrations of 5.4 g/100 mL. After rapidly cooling to room temperature in an ice bath, five freshly prepared standard coffee beverages were pooled (n=5, 520 mL) and submitted to the ultrafiltration process.

Isolation and purification of HMW material from coffee by means of ultrafiltration

Isolation of high molecular weight (HMW) material from coffee was achieved with a crossflow ultrafiltration system (Sartorius Stedim Biotech, Göttingen, Germany) and a molecular weight cut-off filter (10 kDa, Sartorius Stedim Biotech, Göttingen, Germany) resulting in a HMW fraction >10 kDa, which was used for the present studies. The HMW fraction was purified by washing with water (5 L) and the cleansing progression was checked by acquiring $^1\text{H-NMR}$ spectra after each flushing period (1 L).

Nuclear Magnetic Resonance (NMR) Spectroscopy

$^1\text{H-NMR}$ measurements were performed on a Bruker AVANCE III 500 MHz system equipped with a cryo-TCI Probe at 300 K in 5 mm \times 7" NMR tubes (Z107374 USC tubes, Bruker, Faellanden, Switzerland). Data handling was done using the Topspin software version 3.1 and 4.0.

Quantitative NMR spectroscopy (qHNMR) was achieved with the ERETIC 2 procedure, based on the PULCON methodology, according to literature [28]. Spectrometer calibration was done via L-tyrosine (5.21 mmol/L) as the external reference, integrating the specific proton resonance signal at 7.10 ppm (m, 2H).

Reference compounds were weighed in volumetric flasks and filled with water, giving concentrations of 2-25 mmol/L. Before NMR measurements, solutions of reference compounds and isolated HMW fractions (540 μL) were spiked with a NMR buffer (60 μL , pH 5.5). The buffer contained potassium dihydrogen phosphate (10.2 g), potassium hydroxide (1.5 g), trimethylsilyl propionic acid (50 mg) and sodium azide (5 mg) dissolved in D_2O (40 mL). Then, a deuterium chloride solution (4.0 mol/L in D_2O) was used to adjust the pH value to 5.5 and made up to 50 mL with D_2O .

Sensory experiments

Human sensory experiments were carried out as described in the literature [1]. Samples (20 mL) were prepared in phosphate buffered water (0.1 mol/L, pH 5.5) and transferred to glass beakers (diameter 45 mm, capacity 45 mL). Odourless sugar colour was used to negate to optical differences in samples in combination with red lighting in the sensory booths. Sensory analyses were carried out in a sensory panel room with individual cabins at 22-25 °C.

Panellists (8 females, 7 males; 23–32 years in age) were requested to assess the intensities of the aroma attributes “sweetish/caramel-like”, “earthy”, “roasty/sulphurous” and “smoky”, “seasoning-like” and “fruity” on a scale from 0 (absent) to 3 (very strong). Additionally, the following reference compounds were presented to the panellists: 4-hydroxy-2,5-dimethyl-3(2H)-furanone for “sweetish/caramel-like”, 2,3-diethyl-5-methoxypyrazine for “earthy”, a mixture of 2-furfurylthiol, 3-mercapto-3-methylbutanol and 3-mercapto-3-methylbutyl formate representing “roasty/sulphurous”, 2-methoxyphenol for “smoky”, 3-hydroxy-4,5-dimethylfuran-2(5H)-one for “seasoning-like” and a mixture of β -damascenone and acetaldehyde for “fruity”.

Results and discussion

First, the high molecular fraction (HMW) of a coffee beverage was isolated via a crossflow ultrafiltration system using a cut-off membrane (10 kDa). In order to verify the purification of the HMW and to ensure that all small molecules were flushed out, ¹H NMR spectra were recorded after each washing cycle with water (1 L). Aliquots of the isolated and purified HMW fraction >10 kDa were used for human sensory experiments and NMR studies.

To evaluate the role of HMW coffee melanoidins on coffee aroma perception, first, a basic aroma recombine was prepared consisting of 25 aroma active compounds displayed in Figure 1 [1]. With this recombine, aroma profiles of the aqueous coffee aroma recombine, and the aroma recombine with the HMW fraction >10 kDa added in original concentration were determined. All samples were incubated for 60 min at room temperature, to allow possible interactions between odorants and high molecular weight coffee melanoidins.

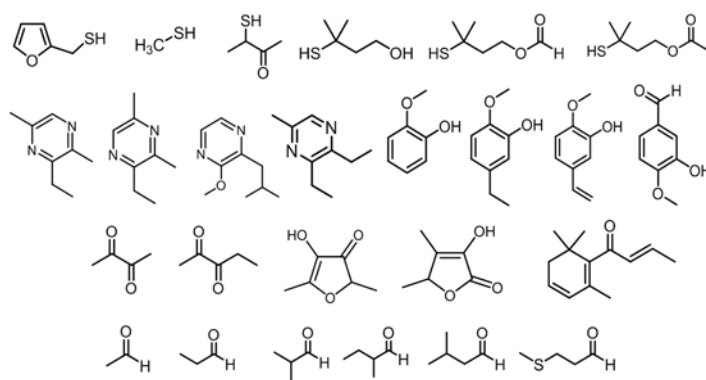


Figure 1: Structures of odorants present in the coffee aroma recombine.

The resulting aroma profiles showed a major influence of added melanoidins to the aqueous aroma recombine. The attributes “roasty/sulphurous”, “earthy”, and “smoky” were reported to be less prominent in the samples containing added melanoidins (Figure 2). The intensity of “roasty/sulphurous” aroma notes of the samples with added HMW fraction were rated with 1.6 and were substantially reduced, compared to the recombine without added melanoidins (rated 2.2). A similar trend could be shown for the aroma attributes earthy and smoky. On the other hand, the aroma intensity of “sweetish/caramel-like” aroma notes was rated with 1.9 in the samples with added HMW fraction and was therefore perceived stronger compared to the samples without HMW, which were rated with just 1.5 by the panellists. These findings are well in line with the literature, where storage time [3] and melanoidin addition severely influenced the rated aroma intensities of coffee aroma attributes [4, 5].

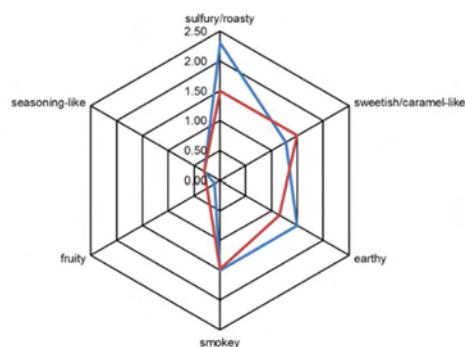


Figure 2: Aroma profiles of the aqueous aroma recombine (blue) and the aroma recombine with added melanoidins (red) in original coffee concentration.

In order to elucidate the molecular mechanisms involved in the aroma staling phenomenon, observed between the HMW fraction of coffee and key odour compounds an $^1\text{H-NMR}$ based approach was used. NMR spectroscopy is a suitable method to investigate non-covalent interactions on a molecular level [19]. The NMR based method principally makes use of $^1\text{H-NMR}$ signal attenuation as well as chemical shift difference of low molecular weight ligands due to interactions with HMW compounds. The resonance signal of interacting ligands shows reduced intensity and consequently a smaller integral. Comparing the integral of samples with HMW material to aqueous isomolar references without added HMW fraction enables the evaluation binding ratios of the respective odorants.

Consequently, the odorants 4-hydroxy-2,5-dimethyl-3(2H)-furanone, 2,3-butanedione, 3-methylbutanal, 3-mercapto-3-methylbutyl formate, 2-furfurylthiol, 2,3-diethyl-5-methylpyrazine, 2-methoxyphenol and (E)- β -damascenone as representatives of each compound class (furanones, diketones, aldehydes, non-aromatic thiols, aromatic thiols, pyrazines, methoxyphenols, and terpenes) were used for the NMR studies. Solutions of the respective aroma compounds were prepared, and the exact concentration was quantified in a buffered system representing coffee conditions via qHNMR. Samples for NMR analyses were prepared by adding odorants (5 mmol/L) to the HMW fraction (>10 kDa) in native coffee concentration. As a reference, all odorants were prepared without HMW addition. After incubating the samples for 60 min at room temperature quantitative $^1\text{H-NMR}$ spectra were acquired. To avoid chemical shift differences caused by the pH value, all solutions were buffered at pH 5.5. The NMR spectra of odorants with the added HMW fraction were evaluated in comparison to the aqueous reference.

NMR based screening clearly showed the influence of melanoidin addition on aroma active compounds. For example, the representative substances for the odorant classes pyrazines (2,3-diethyl-5-methylpyrazine), and aromatic thiols (FFT) were highly influenced by addition of the HMW fraction. The signal shape as well as the signal width, measured as the full width at half maximum (FWHM), indicated high binding affinity to macromolecular coffee melanoidins (Figure 3). The FWHM of 2,3-diethyl-5-methylpyrazine changed from 2.02 Hz in the aqueous reference to 4.16 Hz in the sample with added melanoidins and therefore led to significant signal broadening of 2.14 Hz and was shifted to higher frequencies by 1.42 Hz, which is supported by literature, where it is reported that compounds exhibiting non-covalent π - π interactions studied by NMR spectroscopy often show line broadening and shift of resonances to higher frequencies [36, 37, 18]. In comparison, the aroma active compounds 4-hydroxy-2,5-dimethyl-3(2H)-furanone and 2,3-butanedione, representing furanones and diketones are mostly unaffected by the addition of the HMW fraction >10 kDa. The resonance signal of 4-hydroxy-2,5-dimethyl-3(2H)-furanone showed matching chemical shift, signal shape and FWHM compared to the aqueous reference, well in the line with the observations from the sensory analysis, that no interaction with coffee melanoidins takes place. The aroma active compounds 3-methylbutanal and 3-mercapto-3-methylbutylformate were analysed exemplary for aldehydes and non-aromatic thiols. Evaluation of the signal shape of the methyl protons of 3-methylbutanal showed reduced signal intensity after 60 min of incubation with the HMW fraction of coffee, suggesting potential interactions with melanoidins.

The coffee melanoidins revealed a drastic influence on pyrazine, methoxyphenol, terpene and aromatic thiol. While the aldehyde and non-aromatic thiol were only slightly influenced by the addition of melanoidins, furanones and diketones were unaffected by the presence of HMW material.

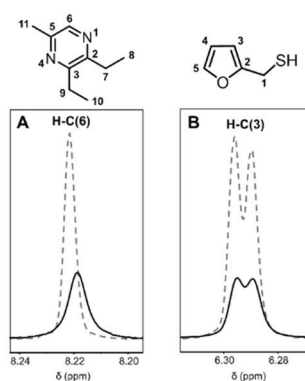


Figure 3: Excerpts of qHNMR spectra (500 MHz; H₂O/D₂O, 9/1, v/v, pH 5.5; 300 K) of the two key coffee odorants 2,3-diethyl-5-methylpyrazine (A) and 2-furfurylthiol (B) with (black line) and without (dotted grey line) added melanoidin fraction >10 kDa in original coffee concentration.

Since these model studies with selected odorants and melanoidins were able to confirm the results of the human sensory experiments, a coffee brew in its entirety was analysed regarding the occurrence of aroma binding interaction. Therefore, a coffee beverage was freshly brewed, cooled to room temperature and an aliquot spiked directly with 2,3-diethyl-5-methylpyrazine. The mixture was incubated for 60 min at room temperature and subjected to NMR measurement. In comparison to an aqueous reference solution without coffee, the pyrazine resonance signal of H-C(6) displayed significant line broadening, reduced intensity and a shift to higher frequencies, unequivocally demonstrating a reduction of free pyrazine upon the incubation with coffee brew from 47.8 mmol/L (reference solution) to 24.4 mmol/L resulting in a recovery rate of 51%, revealing the same interaction behaviour as demonstrated in the model experiments shown above. Consequently, the non-covalent interactions could also be observed in a real coffee beverage, validating the suitability of the NMR based approach to determine binding activities of key coffee odorants to the macromolecular melanoidins.

Conclusion

In summary the quantitative qHNMR based approach allowed the evaluation of binding affinities and the characterization of interactions between LMW and HMW coffee constituents. Results from the qHNMR experiments revealed structure activity relationships between the chemical structure of the odour active compounds and their interaction activity. In addition, the conclusions drawn from model systems were effectively confirmed to occur in freshly prepared coffee beverages. In addition, the human sensory experiments were in good agreement with the NMR data and provided explanation of the described interactions. The overall aroma of coffee was shifted to less "roasty" and more "sweet/caramel-like" aroma notes, by selectively interacting with "roasty" smelling thiols, like FFT as well as the absence of interactions with "caramel-like" odour compounds, i.e. 4-hydroxy-2,5-dimethyl-3(2H)-furanone.

References

1. Mayer F, Czerny M, Grosch W. Sensory study of the character impact aroma compounds of a coffee beverage. *Eur Food Res Technol.* 2000;211(4):272–276.
2. Semmelroch P, Grosch W. Analysis of roasted coffee powders and brews by gas chromatography-olfactometry of headspace samples. *LWT-Food Sci Technol.* 1995;28(3):310–313.
3. Semmelroch P, Grosch W. Studies on Character Impact Odorants of Coffee Brews. *J Agric Food Chem.* 1996;44(2):537–543.
4. Hofmann T, Schieberle P. Chemical Interactions between Odor-Active Thiols and Melanoidins Involved in the Aroma Staling of Coffee Beverages. *J Agric Food Chem.* 2002;50(2):319–326.
5. Hofmann T, Czerny M, Calligaris S, Schieberle P. Model Studies on the Influence of Coffee Melanoidins on Flavor Volatiles of Coffee Beverages. *J Agric Food Chem.* 2001;49(5):2382–2386.
6. Müller C, Hofmann T. Screening of raw coffee for thiol binding site precursors using "in bean" model roasting experiments. *J Agric Food Chem.* 2005;53(7):2623–2629.
7. Müller C, Hofmann T. Quantitative studies on the formation of phenol/2-furfurylthiol conjugates in coffee beverages toward the understanding of the molecular mechanisms of coffee aroma staling. *J Agric Food Chem.* 2007;55(10):4095–4102.
8. Müller C, Hemmersbach S, Slot G, Hofmann T. Synthesis and structure determination of covalent conjugates formed from the sulfury-roasty-smelling 2-furfurylthiol and di- or trihydroxybenzenes and their identification in coffee brew. *J Agric Food Chem.* 2006;54(26):10076–10085.
9. Kreppenhof S, Frank O, Hofmann T. Identification of (furan-2-yl)methylated benzene diols and triols as a novel class of bitter compounds in roasted coffee. *Food Chem.* 2011;126(2):441–449.

10. Gigl M, Frank O, Barz J, Gabler A, Hegmanns C, Hofmann T. Identification and Quantitation of Reaction Products from Quinic Acid, Quinic Acid Lactone, and Chlorogenic Acid with Strecker Aldehydes in Roasted Coffee. *J Agric Food Chem.* 2021;69(3):1027–1038.
11. Nunes F, Coimbra M. Chemical Characterization of the High-Molecular-Weight Material Extracted with Hot Water from Green and Roasted Robusta Coffees As Affected by the Degree of Roast. *J Agric Food Chem.* 2002;50(24):7046–7052.
12. Moreira A, Nunes F, Domingues M, Coimbra M. Coffee melanoidins. Structures, mechanisms of formation and potential health impacts. *Food Funct.* 2012;3(9):903–915.
13. Bekedam E, Schols H, van Boekel M, Smit G. Incorporation of chlorogenic acids in coffee brew melanoidins. *J Agric Food Chem.* 2008;56(6):2055–2063.
14. Bekedam E, Loots M, Schols H, van Boekel M, Smit G. Roasting effects on formation mechanisms of coffee brew melanoidins. *J Agric Food Chem.* 2008;56(16):7138–7145.
15. Bekedam E, Schols H, van Boekel M, Smit G. High molecular weight melanoidins from coffee brew. *J Agric Food Chem.* 2006;54(20):7658–7666.
16. Hofmann T; Bors W; Stettmaier K.: CROSSPY. A Radical Intermediate of Melanoidin Formation in Roasted Coffee. *Free Radicals in Food.* 2002: 49–68.
17. Hofmann T, Bors W, Stettmaier K. Radical-assisted melanoidin formation during thermal processing of foods as well as under physiological conditions. *J Agric Food Chem.* 1999;47(2):391–396.
18. Delius J, Frank O, Hofmann T. Label-free quantitative ¹H NMR spectroscopy to study low-affinity ligand-protein interactions in solution. A contribution to the mechanism of polyphenol-mediated astringency. *PLoS One.* 2017;12(9):e0184487.
19. Burley S K, Petsko G A, Aromatic-aromatic interaction. A mechanism of protein structure stabilization. *Science (New York, N.Y.).* 1985;4708(229):23–28.
20. Wang Z-X, Ravi Kumar N, Srivastava D K. A novel spectroscopic titration method for determining the dissociation constant and stoichiometry of protein-ligand complex. *Anal Biochem.* 1992;206(2):376–381.
21. Marsili S, Chelli R, Schettino V, Procacci P. Thermodynamics of stacking interactions in proteins. *Phys Chem Chem Phys.* 2008;10(19):2673–2685.
22. Wilson K A, Kellie J L, Wetmore S D. DNA-protein π -interactions in nature. Abundance, structure, composition and strength of contacts between aromatic amino acids and DNA nucleobases or deoxyribose sugar. *Nucleic Acids Res.* 2014;42(10):6726–6741.
23. Mistry T V, Cai Y, Lilley T H, Haslam E. Polyphenol interactions. Part 5. Anthocyanin co-pigmentation. *J Chem Soc.* 1991;2(8):1287–1295.
24. Sondheimer E, Covitz F, Marquisee M J. Association of Naturally Occurring Compounds, the Chlorogenic Acid-Caffeine Complex. *Arch Biochem Biophys.* 1961;93:63–73.
25. Horman I, Viani R. The Nature and Conformation of the Caffeine-Chlorogenate Complex of Coffee. *J Food Sci.* 1972;37(6):925–927.
26. Martin R, Lilley T H, Falshaw C P, Haslam E, Begley M J, Magnolato D. The Caffeine-Potassium Chlorogenate Molecular Complex. *Phytochemistry.* 1987;26:273–279.
27. Jung D M, de Ropp J S, Ebeler S E. Study of Interactions between Food Phenolics and Aromatic Flavors Using One- and Two-Dimensional ¹H NMR Spectroscopy. *J Agric Food Chem.* 2000;48(2):407–412.
28. Frank O; Kreissl J; Daschner A; Hofmann T.: Accurate determination of reference materials and natural isolates by means of quantitative (¹H) NMR spectroscopy. *J Agric Food Chem.* 2014;62(12):2506–2515.

Unified mint quantitation: Development of a high-throughput analysis for the quantitation of key aroma compounds in mint

VERENA CHRISTINA TABEA PETERS¹, Andreas Dunkel², Oliver Frank¹,
Brian McCormack³, Eric Dowd³, John Didzbalis⁴, Corinna Dawid¹ and Thomas Hofmann¹

¹ Chair of Food Chemistry and Molecular and Sensory Science, Technical University of Munich, Lise-Meitner-Str. 34, D-85354 Freising, Germany

² Leibniz-Institute for Food Systems Biology at the Technical University of Munich, Lise-Meitner-Str. 34, D-85354 Freising, Germany

³ Flavor/Mint Science, Mars Wrigley, 1132 W. Blackhawk St., Chicago, IL 60642, United States

⁴ Mars, Incorporated, Mars Advanced Research Institute, McLean, VA 22101, United States
verena.peters@tum.de

Abstract

Essential oils of the genus *Mentha* are extensively used as flavour ingredients in the food, cosmetic and pharmaceutical industry. To avoid the very time and labour-intensive traditional flavour analysis comprising isolation by solvent assisted flavour extraction and comprehensive GC-MS analysis, a new high-throughput approach based on a bead-beater homogenisation followed by SIDA-LC MS/MS has been developed. While terpenes could be directly detected using atmospheric pressure chemical ionisation (APCI), alcohols and carbonyls compounds were quantified following specific derivatisations. For example, the reaction of carbonyl compounds such as menthone and (*R,S*)-carvone with 3-nitrophenylhydrazine [1] enabled their highly sensitive detection by means of electrospray ionisation. In total, over 50 odour-active analytes responsible for the characteristic flavour of mint could be quantified using fast and robust UHPLC-MS/MS methods in small sample amounts such as a single mint leaf. Application of this procedure to more than 150 different genotypes of the genus *Mentha* enabled the mapping of flavour alterations depending on e.g. growth stages or environmental conditions.

Keywords: mint, aroma, unified flavour quantitation, high-throughput analysis, UHPLC-MS/MS

Introduction

Due to the characteristic aroma, the Genus *Mentha* is a well-known member of the *Lamiacea* family and enjoying a great popularity in the food, cosmetic and pharmaceutical industry. In general, in total 18 species and 11 natural hybrids are known, and due to natural hybridisation of this genus, there are hundreds of hybrids, representing a huge aromatic diversity. For the industry primary the species Peppermint (*Mentha x piperita*), Cornmint (*Mentha arvensis*) and Spearmint (*Mentha spicata*) are of particular importance due to the very popular and characteristic aroma composition [1].

In recent years, many research groups have studied the aromatic composition of individual mint varieties by identifying and characterizing hundreds of aroma-active compounds. The first step of these scientific studies always included a time and labour-intensive sample workup of a few grams of mint material by means of solvent assisted flavour evaporation (SAFE) extraction or simultaneous distillation extraction (SDE) to separate the volatile from the non-volatile compounds. Identification and quantification of the aroma compounds was performed by gas chromatography-olfactometry (GC-O), GC with flame ionisation detection (GC-FID) and GC-mass spectrometry (GC-MS), whereas analytics of non-volatile compounds, as e.g. polyphenols was achieved by means of liquid chromatography-tandem MS (LC-MS/MS). Through applications of these techniques, it has been decoded that compounds such as menthol, menthone, 1,8-cineole and (+)-menthofuran are responsible for the cool and refreshing aroma of Peppermint and Cornmint, while compounds as (*R,S*)-carvone, limonene and myrcene are representative for Spearmint.

However, in the past it has been shown that for the sensory perception of food not only odorants, but also non-volatile tastants are of importance. Out of the over 10,000 identified volatile food compounds, only ~ 230 odorants stood out as key aroma compounds and through precise combination of no more than 3-40 key food odorants and 15-40 key tastants the authentic flavour of a food item was mimicked [2]. Due to the importance of the aroma compounds and taste-active compounds, Hofstetter *et al.* [3] made it his task to develop an approach that covers analytically the entirety of a food item. By selective derivatisation and enrichment of aroma compounds through stir-bar sorptive extraction, a unified high-throughput quantitation approach was developed, that enables to quantify both volatile compounds and non-volatile tastants in apple juice by means of ultra high performance LC-MS/MS (UHPLC-MS/MS) [3]. For accurate quantitation of the aroma compounds stable isotope dilution analysis (SIDA) based on addition of stable isotope (¹³C, ²H)-labelled analogue molecules of the aroma compounds was performed, which has proven to be a reliable method in gas and liquid chromatography in recent years [4]. This

unified flavour approach enabled therefore for the first time a quantitation of sugars as e.g. fructose and glucose as well as aroma compounds such as e.g. hexanal and β -damascenone in one run by means of UHPLC-MS/MS [3].

Due to sustainability, innovation and the desire to replace synthetic ingredients with natural options, the demand for natural products such as mint and mint oils is increasing more and more every year. Consequently, it is crucial to ensure the demand for such a natural substance. However, properties and characteristics of the mint plant are influenced by many various factors, as e.g., species, growing stages, environmental conditions, changing climate and diseases. Therefore, it is more important than ever, to enable a high-throughput quantitation of the valuable volatile aroma compounds in mint after a minimal sample workup of a very small amount of samples material, in the shortest possible time to understand which effects the various factors have on the flavour composition, thus ensuring an ongoing quality of this natural product.

Experimental

Sample workup

After addition of stable isotope labelled compounds, mint leaves were extractive grinded by means of a bead-beater homogeniser (Precellys evolution, Homogeniser, Bertin Technologies, Montigny Le Bretonneux, France) using ceramic beads. After equilibration and centrifugation using an Eppendorf Centrifuge Minispin (Eppendorf, Hamburg, Germany) the extracts were used for derivatisation and analysis. Due to the high concentrations of the aroma compounds in mint oils, this type of sample material required only a dilution step before derivatisation and analysis. For derivatisation of the aroma compounds, like carbonyl compounds and alcohols, the mint extract and diluted mint oils were mixed and modified with the appropriate derivatisation reagents.

For calibration curves, stock solutions of each compound were prepared, and concentrations were determined by means of quantitative proton NMR spectroscopy (qHNMR) on a 400 MHz Avance III spectrometer (Bruker, Rheinstetten, Germany).

UHPLC-MS/MS

Separation of samples was achieved by means of an ExionLC (Sciex, Darmstadt, Germany), consisting of two LC pump systems ExionLC AD Pump, an ExionLC degaser, an ExionLC AC column oven and an ExionLC controller. Detection of derivatised carbonyl compounds and alcohols was achieved using an ESI source, while detection of terpenes was ensured using an APCI source of a QTRAP 6500+ mass spectrometer (Sciex, Darmstadt, Germany) controlled by the Analyst software (version 1.6.3, Sciex, Darmstadt, Germany). Data interpretation was performed using MultiQuant software (version 3.0.2, Sciex, Darmstadt, Germany).

Statistical Analysis

Data analysis was performed within the programming and visualisation platform R (version 4.0.3) and the pheatmap package (version 1.0.12). Clusters were formed according to Ward's minimum variance method, while for clustering Euclidean distance were applied as distance measurement. From the pairwise similarity matrix the chemical similarity network was calculated based on PubChem Fingerprints [5] and the Tanimoto similarity coefficient and visualised by Gephi (version Gephi 0.9.3-SNAPSHOT 202004172136) [6].

Results and discussion

Through the preliminary work of many research groups, the most important aroma compounds that make the odour of mint so special and unique have already been decoded. The only common feature of all aroma compounds in mint is the volatility, apart from that they are very different from a chemical point of view. The aroma compounds present in mint differ mainly in their structures, functional groups, polarities, and odour qualities, mainly caused by different formation pathways. Non-polar terpenes, as limonene (53), myrcene (50) and α -pinene (47), formed exclusively from isopentenyl pyrophosphate (IPP) via the characteristic terpene biosynthesis pathway, make up a very high percentage of the aroma compounds present in mint. Through enzymatic formation these terpenes are formed into carbonyl compounds and alcohols as e.g. (*R,S*)-carvone (12), menthone (13), menthol (21) and linalool (31), which are representing two further compound classes in mint. However, the aroma compound diversity of the genus *Mentha* is not only formed by the terpene biosynthesis pathway, compounds like hexanal (11), 2-phenylethanol (23) and 3-methylbutanal (9) are completing the comprehensive odour impression of mint.

To be able to analyse and quantitate compounds accurately and precisely by means of UHPLC-MS/MS, on the one hand a liquid chromatographic separation and on the other a mass spectrometric ionisation of the compounds are required. These two parameters are mainly influenced and controlled by the chemical properties of the analytes mentioned above. In total 59 aroma compounds were selected, playing an important role for the aroma of the genus *Mentha*. Based on their chemical properties they were divided into three groups, visualised in a chemical similarity

network in Figure 1. On this basis, appropriate conditions and parameters for a quantitation by means of UHPLC-MS/MS methods were developed.

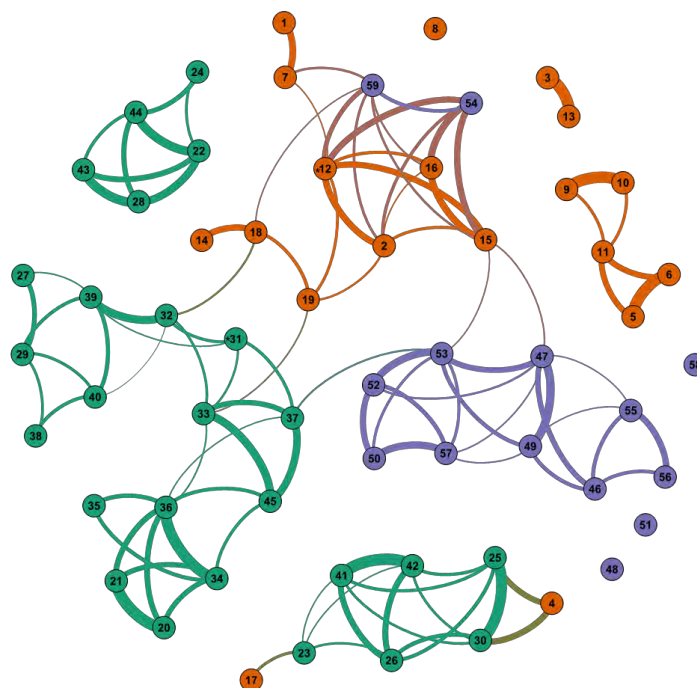


Figure 1: Method network of 59 aroma compounds in mint detected by means of UHPLC-MS/MS. Thickness of connecting lines is representing the size of the correlation coefficient between the chemical similarity of the structures and each colour represents the analytes covered by a method.

Method development

To avoid the time and labour-intensive workup of mint leaves by means of solvent assisted flavour evaporation (SAFE) extraction, simultaneous distillation extraction (SDE) or steam distillation, a bead-beater extraction approach was implemented in order to extract in total 59 aroma compounds of hundreds of mint leaves in a reasonable period of time. By extraction of one single mint leaf, sufficient amounts of volatile compounds were obtained to ensure identification and quantification by means of UHPLC-MS/MS. Mint oils solely required a dilution step.

For appropriate MS/MS detection, the ionisation parameters were optimised by continuous infusion of solution of the reference compounds and stable isotope labelled standards to enable the analysis of the aroma compounds by using the multiple reaction monitoring (MRM) mode. Terpenes, as e.g. myrcene (50), limonene (53) and α -pinene (47) were ionised by atmospheric pressure chemical ionisation (APCI) whereas for aroma compounds containing a functional group, as menthol (21), (*R,S*)-carvone (12) and menthone (13) appropriate derivatisation enabled a liquid chromatographic separation, reduction of the volatility and an improvement of electrospray ionisation (ESI). To ensure precise and accurate quantification results, (^{13}C , ^2H) labelled molecules were used as internal standards to compensate for workup losses based on the molar ratio and through quantitative determination of the calibration standards using qHNMR technique [7] a great linearity and precision of the linear regressions for all 59 aroma compounds was achieved.

To assure the quality of the methods, the validation of the analytical methods was an important aspect. The subsequent validation experiments, such as e.g. recovery experiments and determination of limit of detection (LoD) and limit of quantitation (LoQ) verified the precise functionality of the UHPLC-MS/MS methods.

In total 59 aroma compounds, as e.g. menthone (13), (*R,S*)-carvone (12), hexanal (11), menthol (21), limonene (53), myrcene (50), α -pinene (47) and linalool (31) (Figure 2), could be quantitated in mint leaves as well as in mint oils by means of UHPLC-MS/MS.

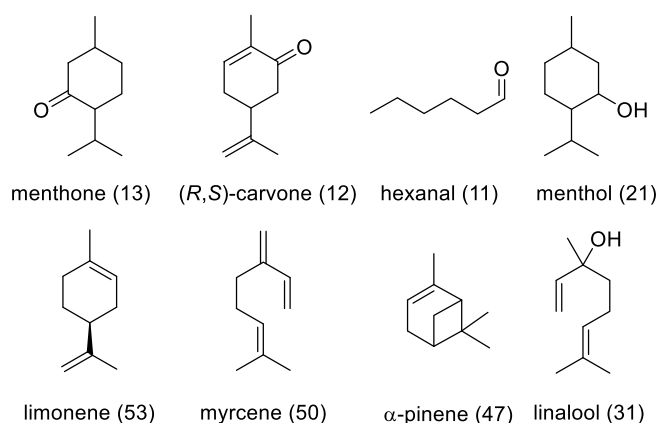


Figure 2: Chemical structures of selected compounds (13, 12, 11, 21, 53, 50, 47 and 31) analysed by UHPLC-MS/MS.

Quantitation of 59 aroma compounds in mint leaves and mint oils of different *Mentha* species

The aim of this high-throughput approach by means of a bead-beater homogenisation and UHPLC-MS/MS was to enable an extraction and quantification of the for mint valuable aroma compounds in different samples like single mint leaves and mint oils of various *Mentha* species in a short time. In this study, mint leaves and mint oils of the for the industry important species Black Mitcham (*Mentha x piperita*), Arvensis (*Mentha arvensis*), Scotch and Native Spearmint (*Mentha spicata*) were analysed by means of this newly developed high-throughput approach. To visualise the quantitative data of these samples, a heatmap was generated and combined with hierarchical agglomerative clustering (Figure 3).

The peculiarity of the genus *Mentha* is that the varieties are showing great differences in the composition of aroma compounds. While menthol (21), menthone (13) are characteristic compounds for Black Mitcham and Arvensis, high amounts of (R,S)-carvone (12) and limonene (53) are characterizing Scotch and Native Spearmint. Apart from high concentration up to 300000 $\mu\text{g/mL}$ in mint oils and 3000 $\mu\text{g/g}$ in mint leaves for e.g. menthol (21), the UPHLC-MS/MS methods enabled furthermore also the quantitation of minor compounds like hexanal (11) with concentrations up to 1.9 $\mu\text{g/g}$ in the mint leaves and up to 214.8 $\mu\text{g/mL}$ in mint oils without workup of different sample volumes or injection of different dilution of the samples. 59 aroma compounds were quantitated in several mint species over a concentration range of 6 orders of magnitude by means of UHPLC-MS/MS and enabled therefore a comprehensive characterisation of the aroma composition of the mint leaves and mint oils of the four commercially important species Black Mitcham, Arvensis and Native and Scotch Spearmint.

The mint oils showed compared to the mint leaves in total higher concentration of the aroma compounds, due to the concentrations process of the aroma compounds during the distillation. Menthol (21) and menthone (13) were the most abundant compounds in Black Mitcham and Arvensis mint leaves and mint oils, whereas (R,S)-carvone (12) was the dominating aroma compound in Native and Scotch Spearmint.

The compound (+)-menthofuran (48), which is enzymatically formed through oxidation of (+)-pulegone (2) and formed during blooming of the mint plant, was characteristic for mint leaves of the species Black Mitcham. Furthermore, high concentration of 1,8-cineole (51), neomenthol (20), α -humulene (57) and α -pinene (47) were detected in the mint leaves and oils of this species. The aroma composition of the analysed Arvensis mint leaves and mint oils was very similar to Black Mitcham, but showed rarely greater differences in the concentration of single compounds as e.g. menthol (21) and menthone (13).

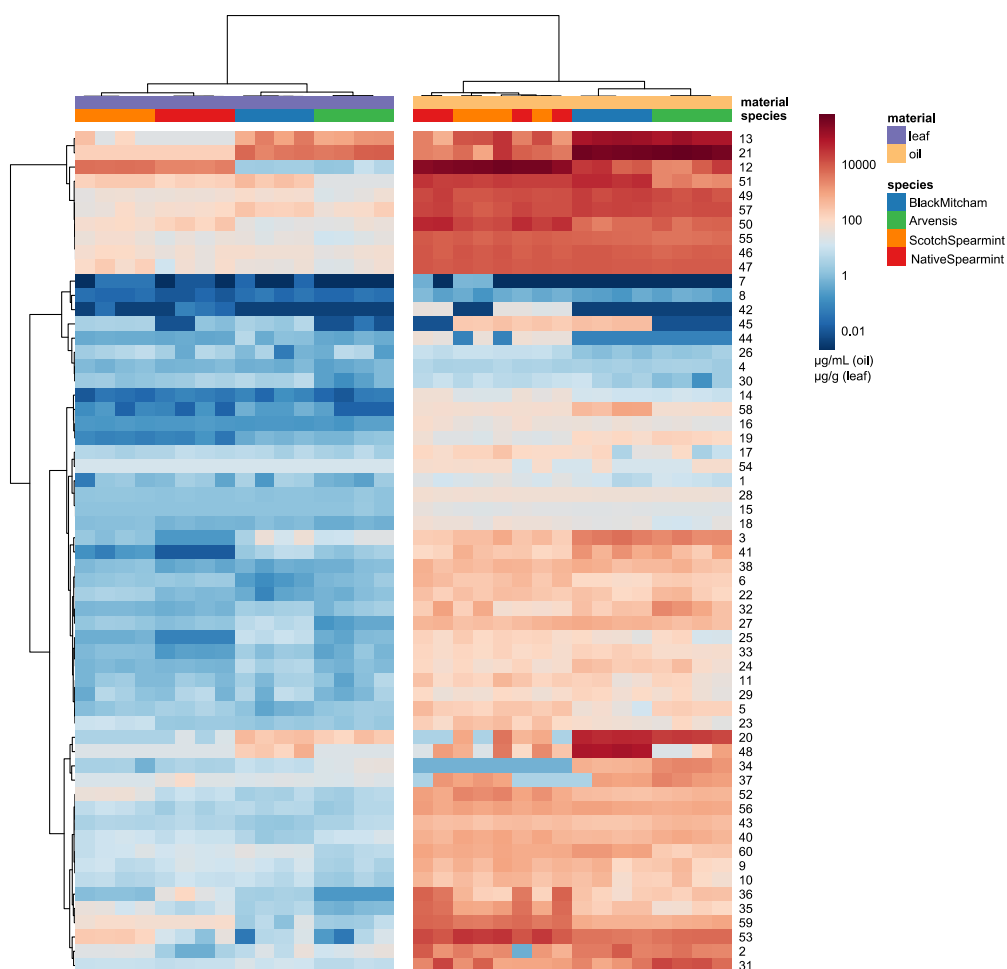


Figure 3: Heatmap showing the concentrations of the aroma compounds quantified by means of UHPLC-MS/MS in mint leaves and the corresponding mint oils of the *Mentha* species Black Mitcham, Arvensis, Native and Scotch Spearmint.

On the other side, in addition to high amounts of (R,S)-carvone (12), leaves and oils of the species Native and Scotch Spearmint revealed high concentrations of limonene (53), 1,8-cineole (51) and myrcene (50). (R,S)-carvone (12) and limonene (53) showed in comparison of these two Spearmint species higher amounts in mint leaves and oils of Native Spearmint, whereas Scotch Spearmint contained higher amounts of myrcene (50).

Compounds like (R,S)-carvone (12) and menthone (13) were consequently characteristic for a species, whereas some compounds as α -pinene (47), β -pinene (46), limonene (53) and myrcene (50) occurred regardless of the species in high concentration in mint leaves and mint oils. Further, a similar aroma composition of *Mentha* varieties indicated a biological relationship, as demonstrated in this study for Native and Scotch Spearmint.

Conclusion

In summary in this study, a high-throughput approach for aroma compounds in mint was developed. By skilful extraction of one single mint leaf by means of a bead-beater homogeniser a sufficient amount of aroma compounds was extracted in a short period of time, whereby the time and labour-intensive SAFE extraction or steam distillation process could be avoided. Through rapid appropriate derivatisation of the aroma compounds and optimisation of ionisation parameter, 59 aroma compounds in mint leaves and mint oils could be quantitated by means of UHPLC-MS/MS. To compensate for workup losses stable isotope labelled standards were used.

This new approach enables a high-throughput analysis of hundreds of different samples independent of the sample material as mint leaves or mint oil and regardless of the mint variety in a short time without laborious sample workup in order to map flavour alterations depending on e.g. growing stages, environmental conditions to sustain mint as valuable natural product for the industries.

References

1. Lawrence BM. *Mint: the genus Mentha*: CRC Press; 2006.
2. Dunkel A, Steinhaus M, Kotthoff M, Nowak B, Krautwurst D, Schieberle P, et al. Nature's chemical signatures in human olfaction: a foodborne perspective for future biotechnology. *Angew Chem -Int Edit*. 2014;53(28):7124-43.
3. Hofstetter CK, Dunkel A, Hofmann T. Unified Flavor Quantitation: Toward High-Throughput Analysis of Key Food Odorants and Tastants by Means of Ultra-High-Performance Liquid Chromatography Tandem Mass Spectrometry. *J Agric Food Chem*. 2019;67(31):8599-608.
4. Schieberle P, Grosch W. Quantitative analysis of aroma compounds in wheat and rye bread crusts using a stable isotope dilution assay. *J Agric Food Chem*. 1987;35(2):252-7.
5. Kim S, Thiessen PA, Bolton EE, Chen J, Fu G, Gindulyte A, et al. PubChem substance and compound databases. *Nucleic acids research*. 2016;44(D1):D1202-D13.
6. Bastian M, Heymann S, Jacomy M, editors. *Gephi: an open source software for exploring and manipulating networks*. Proceedings of the International AAAI Conference on Web and Social Media; 2009.
7. Frank O, Kreissl JK, Daschner A, Hofmann T. Accurate determination of reference materials and natural isolates by means of quantitative ¹H NMR spectroscopy. *J Agric Food Chem*. 2014;62(12):2506-15.

Pinellic acid generation in whole wheat products: Impact of linoleic acid content and lipoxygenase activity

Wen Cong, Eric Schwartz, and DEVIN G. PETERSON

Department of Food Science and Technology, 317 Parker Food Science & Technology Building, The Ohio State University, 2015 Fyffe Rd., Columbus, OH 43210; E-mail: peterson.892@osu.edu

Abstract

The impact of linoleic acid concentration (precursor) and lipoxygenase activity in whole wheat flour on the biosynthesis of the bitter compound pinellic acid in dough were investigated. Utilizing wheat knock out (KO) lines for lipase (LIP), lipoxygenase (LOX) and a double lip/lox KO, the LOX variant was reported to significantly reduce pinellic acid formation in comparison to their wild-type controls. Further mapping of two hundred and twenty US hard wheat varieties indicated there was no correlation between the linoleic acid concentration (or lipoxygenase activity) and pinellic acid generation in the dough. However, differences in lipoxygenase activity were evident between Hard Red Winter (HRW) and Hard White Winter (HWW) wheat classes. These findings indicated that lipoxygenase is a key enzymatic step in the generation of pinellic acid in commercial wheat samples however biosynthesis is impacted by other enzymatic steps or factors.

Keywords: pinellic acid, linoleic acid, lipoxygenase activity, bitterness, whole wheat bread

Introduction

Whole grains are rich in vitamins, minerals, antioxidants, and health-promoting fibres. Health benefits associated with whole-grain intake have been linked to a reduction of chronic pathological conditions including heart disease, cancer, diabetes, and a reduced risk of weight gain [1]. The U.S. Department of Agriculture USDA recommends that at least half of all grain intake should be from whole grain sources [2]. Based on the data obtained from the 2001-2004 National Health and Nutrition Examination Survey (NHANS), nearly everyone (96.2% to 99.9%) in each sex-age group failed to meet the recommendations for whole-grain [3]. Aversive flavour attributes, such as bitterness, challenge the development of high quality products, limiting whole-grain consumption [4]. Bitterness from added germ extract during bread making has been shown to decrease consumer liking of whole wheat bread. In addition, previous studies have reported that some oxylipins, like pinellic acid, are the most influential bitter compounds in whole wheat bread crumb [5] and also one of the most predictive compounds of dislike in whole wheat bread [6]. Moreover, pinellic acid is generated more than 30-fold upon flour hydration and is thought to be produced primarily through the lipid oxidation pathway (LOX) [7].

Oxylipins, in plants, have an important signalling function that regulates developmental processes, such as pollen formation or mediation of environmental responses that include healing and defensive reactions (antimicrobial). They are usually biosynthesized by the oxidation of polyunsaturated fatty acids (PUFAs) by different enzymes at different positions of the fatty acid backbone. Trihydroxy oxylipins, including pinellic acid, were initially characterized by Graveland [8] through the study of enzymatic (lipoxygenase) conversion of linoleic acid in dough and flour-water suspensions to oxidized fatty acid isomers. This pathway in plants plays an important role in response to stress and innate immunity [9]. Further, pinellic acid is recognized as a bioactive molecule with antifungal [10] and potent adjuvant activities [11], as well as a bitter taste in aqueous bran and whole meal suspensions [12, 13]. Thus, the understanding of the chemistry which influences the production of pinellic acid, and the mechanism of formation is valuable to develop a strategy to control bitter off-flavour.

Experimental

Chemicals and reagents

Ethanol (absolute, HPLC grade), MeOH (HPLC grade), isopropanol (Optima, LC/MS grade), formic acid (Optima, LC/MS), acetic acid (Optima, LC/MS), acetonitrile (Optima, LC/MS grade) were purchased from Fisher Scientific (Fair Lawn, NJ, USA). Water was purified through a Barnstead Nanopure Diamond water purification system (Thermo Scientific, Dubuque, IA). Quick Start™ Bovine Serum Albumin (BSA) Standard Set and Quick Start™ were purchased from Bio-Rad (Berkeley, CA, USA). 3-(di-methylamino) benzoic acid (DMAB), 3-Methyl-2-benzothiazolinone (MBTH), the haemoglobin from bovine blood, Tween 20, Sodium dodecyl sulphate (SDS) solution, linoleic acid, and ¹³C-linoleic acid were purchased from Sigma Aldrich (St. Louis, MO, USA). Internal reference compound Leucine-enkephalin was purchased from Waters (Waters Co.). Schaftoside standard

was purchased from BOC Sciences (Shirley, NY, USA). Prostaglandin F2 α (purity \geq 98%) was purchased from Cayman Chemical (Ann Arbor, MI, USA).

Whole wheat flour samples

Two hundred and twenty whole wheat varieties developed in the USA from 1873 to 2016 were provided by the Poland Lab and Wheat Genetics Resource Center at Kansas State University (WGRC), one of the world's most comprehensive collections of wheat germplasm. All seeds analysed were sourced from wheat grown in 2016, from the same growing region. Seed samples were ground to fine homogenous flour in 4 mL reinforced PE vials containing one 3/8" stainless steel grinding ball using GenoGrinder (1300 rpm, 150 seconds) for further analysis. Additionally, HRS lipoxygenase knockout (Lpx KO), lipase knockout (Lip KO), and double knockout of lipoxygenase and lipase (Lip*Lpx KO), as well as their corresponding wild-type HRS control wheat lines were sourced from Arcadia Biosciences (Davis, CA) and milled by Ardent Mills.

Quantification of Pinellinic Acid and Linoleic Acid by Ultra Performance Liquid Chromatography-Tandem Mass Spectrometry (UPLC/MS/MS)

For the analysis of pinellinic acid in dough samples, 15 mg of flour was first transferred to a 2 mL Eppendorf tube followed by the addition of one 1/4 inch stainless steel mixing ball, then 12 μ L (4:5 water/flour ratio) was added to the flour and dough formation was carried out through mixing using GenoGrinder at 1000 rpm for 5 min. Then, an extraction mixture of 1 mL of solvent (1:1 IPA/H₂O, v/v) spiked with internal standard (prostaglandin-F2 α (PGE-f2 α), 1 μ g/mL) was added to the dough for solvent extraction. Samples were sonicated for 10 min followed by shaking using the GenoGrinder at 1000 rpm for 10 min. Samples were then diluted 1:50 and sample clean-up was carried out using a 96-well Oasis PRiME HLB plate (1 cc, 30 mg sorbent). After sample loading (250 μ L) and washing (750 μ L, 10% acetonitrile (aq.) with 0.1% formic acid) steps, the retentate was eluted with 500 μ L 90% acetonitrile (aq.) with 0.1% formic acid. Samples were further diluted to 2 mL using water with 0.1% formic acid. The quantification was made by the standard addition method using a 6-point calibration curve. Concentrations ranged from 0.24 - 500 μ g/mL.

For the analysis of linoleic acid in flour, 50 mg was transferred into 2 mL Eppendorf tubes (triplicate for each variety), followed by the addition of one 1/4 inch stainless steel ball. An extraction solvent mixture (2:1 MeOH:DCM, v/v) was added followed by the addition of 50 μ L of ¹³C₁₈-linoleic acid as an internal standard (10 μ g/mL final concentration). The mixture was homogenized using a GenoGrinder at 1000 rpm for 10 min. Samples were then centrifuged at 12,000 rpm for 5 min. An aliquot (100 μ L) of the supernatant was diluted 1:10 with MeOH, and sample clean-up was carried out using a 96-well Oasis PRiME HLB plate (1 cc, 30 mg sorbent) utilizing a pass-through method (200 μ L load followed by elution with 500 μ L of MeOH). Samples were further diluted with 300 μ L of water. An external standard calibration curve was prepared using 7-points ranged g from 31 - 2000 ng/mL.

LC/MS/MS analysis was conducted using a Waters ACQUITY H-class UPLC system coupled with a Xevo TQ-S mass spectrometer (Waters Co.). Quantitative analysis was conducted using MRM acquisition mode. MS conditions employed included a capillary voltage of 2.2 kV, sample cone voltage of 50V, ESI⁻, a source temperature of 150°C, and a desolvation temperature of 550 °C. Chromatographic separation was performed on an ACQUITY UPLC BEH C18 1.7 μ m column (2.1 mm \times 50 mm) (Waters Co.) kept at 40 °C. Nanopure water with 0.1% formic acid (solvent A) and 9:1 acetonitrile/isopropanol with 0.1% formic acid (solvent B) were used as mobile phase. Flow rate was set to 0.5 mL/min and a solvent gradient program of 25% B (0.0 - 1.0 min), 25-95% B (1.0 - 8.0 min), 95% B (8.0 - 8.5 min), 25% B (8.5 - 10.0 min) was employed. The MS/MS transitions and collision energy used for the analysis of the compounds were as follows: pinellinic acid m/z 329 \rightarrow 211 (22 eV), and internal standard PGE-f2 α m/z 353 \rightarrow 193 (22 eV). The MS/MS transitions for linoleic acid used were ESI⁻ m/z 279 \rightarrow 58 and m/z 279 \rightarrow 261 (20 eV), and internal standard ¹³C₁₈-linoleic acid ESI⁻ m/z 297 \rightarrow 60 and m/z 297 \rightarrow 279 (22 eV).

Lipoxygenase activity

Twenty-five mg of flour was suspended in 1.5 mL of 50 mM potassium phosphate buffer (pH 6.6) in 2 mL Eppendorf tubes. The samples were vortexed and incubated in an ice-water bath for 1 h, followed by vortexing for 1 min at 15-minute intervals. The samples were then centrifuged at 15,000 rpm for 20 min. The supernatant was collected as the crude enzyme solution and stored over an ice-water bath and used within 12 hours. The amount of crude enzyme was determined through the Bradford method utilizing bovine serum albumin (BSA) as a standard for the calibration curve.

Total lipoxygenase activity in whole grain wheat flour was measured using a modified colorimetric assay using the coupled reaction of 3-(di-methylamino) benzoic acid (DMAB) and 3-Methyl-2-benzothiazolinone (MBTH) as described by Anthon and Barrett [14]. The analysis was performed on 2 μ g of the crude enzyme as determined from the Bradford method. Stock solutions of 10 Mm MBTH in water, 5 mg/kg haemoglobin in water, 20 mM DMAB, 100 mM phosphate buffer solution (pH 6.0) were prepared and stored at 4 C. A solution of linoleic acid

stock was also prepared to contain 140 mg linoleic acid, 280 mg Tween 20, 0.6 mL of 1 N NaOH, and all diluted to a final volume of 20 mL with water.

The assay was performed at room temperature and two working solutions were prepared from the solutions listed above, working solution A (10 mL of 20 mM DMAB, 100 mM phosphate buffer solution (pH 6.0), 0.4 mL of 25 mM linoleic acid stock, and 9.6 mL water) and working solution B (0.4 mL of 10 mM MBTH, 0.4 mL 5 mg/mL haemoglobin, and 19.2 mL water). Sample (2 µg crude enzyme, about 5 µL sample) was incubated in 100 µL of solution A for 15 min. Then 100 µL solution B was added and samples were incubated for 10 min. The reaction was terminated by the addition of 100 µL of a 1 % (w/v) SDS. Negative controls were prepared by inactivation of the crude enzyme by heat treatment at 100 °C for 20 min. Blanks were prepared by an initial spike of 1% (w/v) SDS. Lipoxygenase activity was defined as the absorbance value at 598 nm per µg of protein times 1000.

Results and discussion

Lipoxygenase (LOX) plays an important role in biosynthetic pathways catalysing stereo-specific peroxidation of polyunsaturated fatty acids containing *cis,cis*-1,4-pentadiene systems to their corresponding hydroperoxy derivatives, e.g., linoleic acid, to a hydroperoxide intermediate [15, 16]. To investigate the dependence of pinellic acid formation on lipoxygenase enzyme, wheat knockout lines (KO) were analysed. In addition to a LOX KO sample, a Lipase (LIP) KO sample was also analysed (linoleic acid formation); as well as a double LOX/LIP KO line. Figure 1 shows the LOX activity of the three KO samples compared to their wild sibling control samples. As expected, the LOX activity was significantly lower in the LOX and LIP/LOX KO samples, reporting a 96.4 and 94.1% lower activity, respectively, than the corresponding wild sibling controls.

The generation of pinellic acid in the dough samples made from the KOs and their wild sibling control wheat samples is reported in Figure 2. During bread making, pinellic acid is generated upon flour hydration [7,8]. The LOX and LIP/LOX KO significantly reduced the generation of pinellic acid, resulting in an 87.5 and 91.1% reduction in the compound concentration, respectively, then the corresponding wild sibling controls. The LIP KO had no significant impact on pinellic acid formation, indicating lipase activity did not impact the formation of this compound.

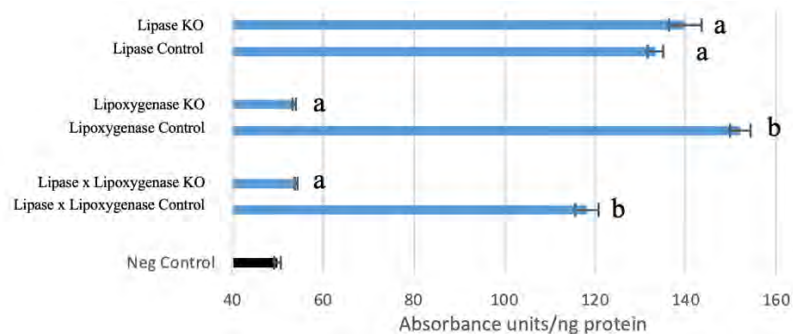


Figure 1: Comparison of flour lipoxygenase activity in lipase KO, lipoxygenase KO, and double KO of lipase and lipoxygenase vs their corresponding wild-type control; different letters indicate significant differences between wild sibling and KO ($p < 0.05$) according to Tukey's HSD; error bars represent standard errors.

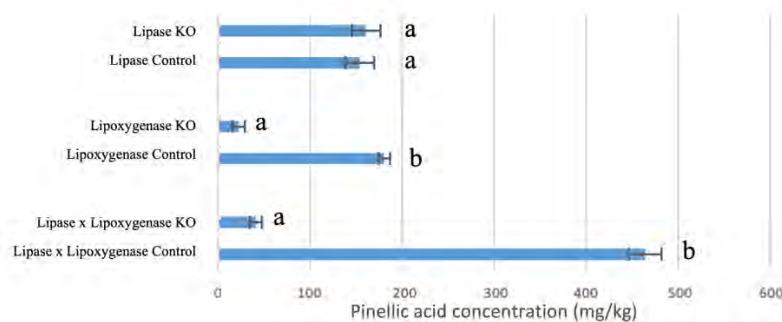


Figure 2: Comparison of dough pinellic acid concentration in lipase KO, lipoxygenase KO and double lipase and lipoxygenase KO vs their corresponding wild-type control; different letters indicate significant ($p < 0.05$) according to Tukey's HSD; error bars represent standard errors.

While the analysis of the KO wheat samples indicated LOX as a key enzyme for pinellic acid formation, further analysis of a large wheat panel consisting of commercial samples was investigated to understand if lipoxygenase activity and linoleic acid (precursor) were predictive of product formation in the dough. Two hundred and twenty wheat different commercial variety samples developed over the past 140 years in the USA and grown in the same calendar year at the Wheat Genetic Resource Center at Kansas State University were analysed. The samples consisted of two wheat classes, hard red winter wheat (HRW) vs hard white winter wheat (HWW).

Analysis of the wheat panel reported the linoleic acid concentration in the flour ranged approximately 4-fold (363 to 1419 mg/kg) whereas the pinellic acid concentration in the dough ranged about 3-fold (97.9 to 304.4 mg/kg), however, no correlation was reported $R^2 = 0.018$ (Figure 3). These findings suggested the amount of the precursor, linoleic acid, was sufficient in whole wheat flour (in excess) and did not have a significant influence on the formation of pinellic acid in whole wheat dough samples.

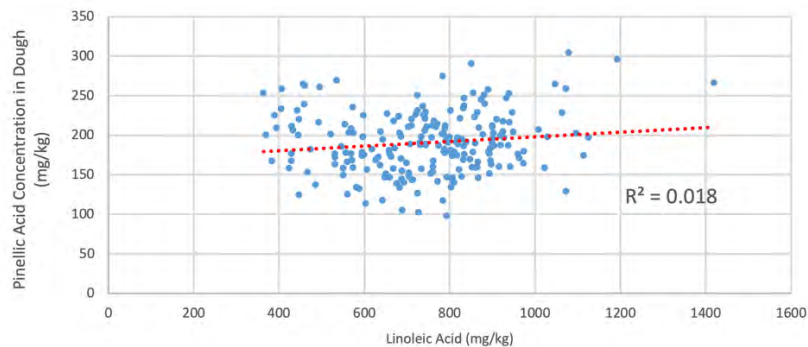


Figure 3: Scatter plot of flour linoleic acid content versus dough pinellic acid concentration across 220 US hard wheat varieties.

Further analysis of the lipoxygenase activity across the wheat panel (ranged 4.2-fold) revealed no significant correlation with pinellic acid concentration ($R^2 = 0.0004$) (Figure 4). These results indicated the complex nature of the biosynthesis of this compound and the need for more understanding about the mechanisms, enzymes, and intermediate products involved, as multiple factors are likely implicated in the regulating flux of this pathway. Hamberg and Hamberg [17] outlined multiple oxidative enzymes involved in the biosynthetic route of linoleic acid to pinellic acid (LOX, peroxygenase, and epoxide hydrolase), thus provide other possible enzymatic ‘bottlenecks’ for product formation. Furthermore, wheat compounds could also modulate the activities of these key oxidative enzymes. Recently Cong et al. [18] reported an endogenous wheat compound schaftoside (apigenin di-C-glycoside) reduced the generation of pinellic acid during bread manufacture and decreased the perceived bitterness of whole wheat bread. They suggested schaftoside functioned as an allosteric inhibitor of lipoxygenase or epoxide hydrolase and suppressed the formation of hydroxylated fatty acids, such as pinellic acid.

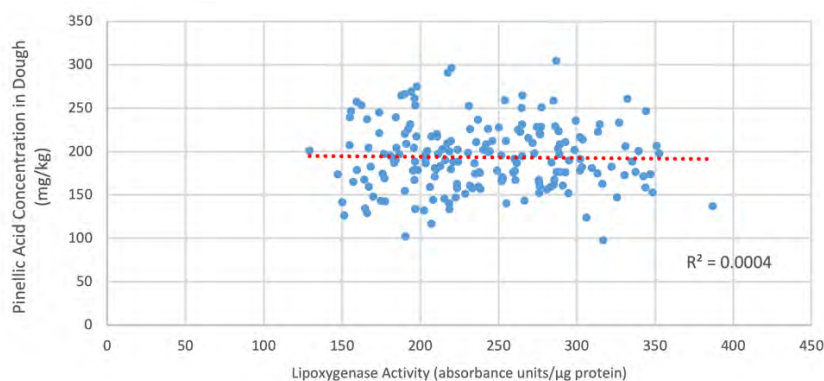


Figure 4: Scatter plot of flour lipoxygenase activity versus dough pinellic acid concentration across 220 US hard wheat varieties.

Quantitative differences in the flour linoleic acid content and lipoxygenase activity, as well as the pinellic acid concentration in the dough, between the two wheat classes of hard red winter (HRW) and hard white winter (HWW) varieties were also evaluated and shown in Figures 5-7. No significant differences in concentration of linoleic acid were shown between red and white varieties (Figure 5) whereas the LOX activity was significantly higher in the HRW samples (Figure 6). However, no significant difference was reported in the pinellic acid

concentration reported in the dough (Figure 7), as expected from the lack of correlations reported between linoleic acid (Figure 3) and LOX activity (Figure 4).

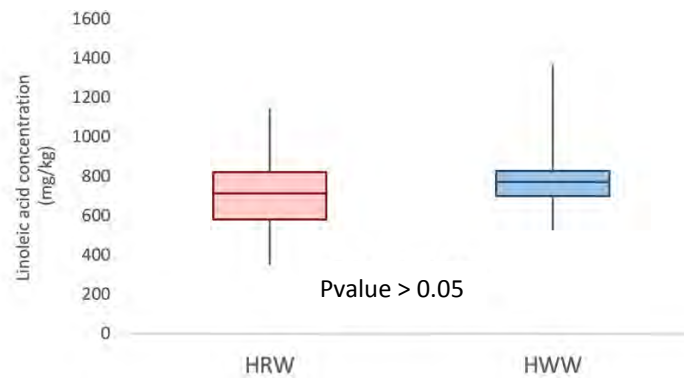


Figure 5: Box plot of flour linoleic acid concentration in hard red winter wheat (HRW) vs hard white winter wheat (HWW) across 220 US wheat varieties.

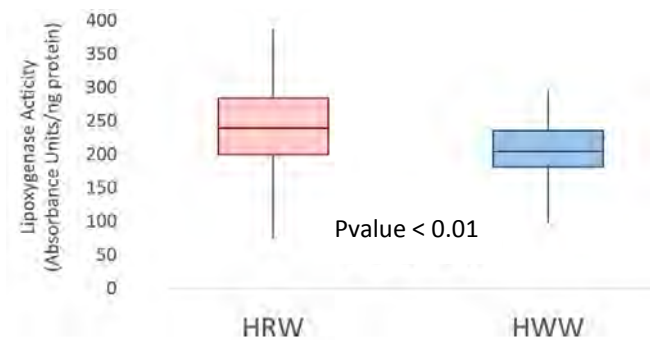


Figure 6: Box plot of flour lipoxygenase activity in hard red winter wheat (HRW) vs hard white winter wheat (HWW) flour across 220 US wheat varieties.

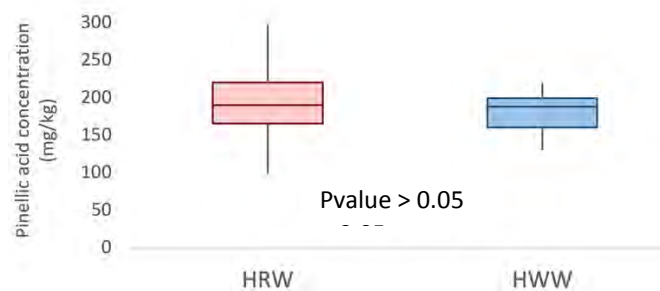


Figure 7: Box plot of dough pinellic acid concentration in hard red winter wheat (HRW) vs hard white winter wheat (HWW) across 220 US wheat varieties.

Conclusion

Lipoxygenase was reported as a key enzymatic step in the formation of pinellic acid during bread making. However, variation in linoleic acid content (precursor) or lipoxygenase activity in commercial US wheat flour samples were not predictive of the pinellic acid content, indicating the other enzymatic steps (i.e. peroxygenase and epoxide hydrolase) or enzymatic modulation (i.e. allosteric inhibitors) impacted the generation of the bitter compound pinellic acid in wheat food products.

References

- 1 M. P. McRae, "Health Benefits of Dietary Whole Grains: An Umbrella Review of Meta-analyses," *J. Chiropr. Med.* 2017;16(1):10–18. doi: 10.1016/j.jcm.2016.08.008.
- 2 S. Kranz, K. W. Dodd, W. Y. Juan, L. A. K. Johnson, and L. Jahns, "Whole grains contribute only a small proportion of dietary fiber to the U.S. diet," *Nutrients* 2017;9(2):1–8. doi: 10.3390/nu9020153.
- 3 S. M. Krebs-Smith, P. M. Guenther, A. F. Subar, S. I. Kirkpatrick, and K. W. Dodd, "Americans Do Not Meet Federal Dietary Recommendations," *J. Nutr.* 2010;140(10):1832–1838. doi: 10.3945/jn.110.124826.
- 4 E. McMackin, M. Dean, J. V. Woodside, and M. C. McKinley, "Whole grains and health: Attitudes to whole grains against a prevailing background of increased marketing and promotion," *Public Health Nutr.* 2013;16(4):743–751. doi: 10.1017/S1368980012003205.
- 5 A. Bakke and Z. Vickers, "Effects of bitterness, roughness, PROP taster status, and fungiform papillae density on bread acceptance," *Food Qual. Prefer.* 2011;22(4):317–325. doi: 10.1016/j.foodqual.2010.11.006.
- 6 W. Cong, E. Schwartz, E., E. Tello, and D. G. Peterson. Identification of Compounds that Negatively Impact Whole Wheat Bread Flavor Liking. *Food Chem.* 2021; Accepted.
- 7 Q. Bin and D. G. Peterson, "Identification of bitter compounds in whole wheat bread crumb," *Food Chem.* 2016;203:8–15. doi: 10.1016/j.foodchem.2016.01.116.
- 8 A. Graveland, "Enzymatic oxidations of linoleic acid and glycerol-1-monolinoleate in doughs and flour-water suspensions," *J. Am. Oil Chem. Soc.* 1970;47(9):352–361. doi: 10.1007/BF02639001.
- 9 N. A. Eckardt, "Oxylipin signaling in plant stress responses," *Plant Cell* 2008;20(3):495–497. doi: 10.1105/tpc.108.059485.
- 10 C. Toc and Y. S. Tis, "An Antifungal Compound , 9 , 12 , 13-Trihydroxy- (E) - 10-Octadecenoic Acid , From *Colocasia antiquorum* inoculated with *Ceratocystis Fimbriata*," *Phytochemistry* 1989;28(10):2613–2615.
- 11 T. Sunazuka et al., "Total synthesis of pinellic acid, a potent oral adjuvant for nasal influenza vaccine. Determination of the relative and absolute configuration," *Tetrahedron Lett.* 2002;43(7):1265–1268. doi: 10.1016/S0040-4039(01)02348-6.
- 12 T. Galliard and D. M. Gallagher, "The effects of wheat bran particle size and storage period on bran flavour and baking quality of bran/flour blends," *J. Cereal Sci.* 1988, doi: 10.1016/S0733-5210(88)80025-0.
- 13 U. Biermann, A. Wittmann, and W. Grosch, "Occurrence of Bitter Hydroxy Fatty Acids in Oat and Wheat," *Fette, Seifen, Anstrichm.* 1980;82(6):236–240. doi: 10.1002/lipi.19800820607.
- 14 G. E. Anthon and D. M. Barrett, "Colorimetric method for the determination of lipooxygenase activity," *J. Agric. Food Chem.* 2001;49(1):32–37. doi: 10.1021/jf000871s.
- 15 A. Graveland, "Analysis of lipooxygenase nonvolatile reaction products of linoleic acid in aqueous cereal suspensions by urea extraction and gas chromatography," *Lipids* 1973;8(11):599–605. doi: 10.1007/BF02533141.
- 16 D. M. Pereira, P. Valentão, and P. B. Andrade, "Lessons from the sea: Distribution, sar, and molecular mechanisms of anti-inflammatory drugs from marine organisms," *Stud. Nat. Prod. Chem.* 2013;40:205–228. doi: 10.1016/B978-0-444-59603-1.00007-2.
- 17 M. Hamberg, and G. Hamberg. "Peroxygenase-Catalyzed Fatty Acid Epoxidation in Cereal Seeds (Sequential Oxidation of Linoleic Acid into 9(S),12(S),13(S)-Trihydroxy-10(E)-Octadecenoic Acid)," *Plant Physiology* 1996;110(3):807–815. doi.org/10.1104/pp.110.3.807.
- 18 W. Cong, E. Schwartz, and D. G. Peterson, "Identification of Inhibitors of Pinellic Acid Generation in Whole Wheat Bread," *Food Chem.* 2021;351:129291. doi.org/10.1016/j.foodchem.2021.129291.

Towards cooked meat less loaded in heterocyclic aromatic amines but sensorially acceptable!

MAIA MEURILLON, Chloé Anderson, Magaly Angénieux, Frédéric Mercier,
Nathalie Kondjoyan and Erwan Engel

INRAE, QuaPA unit, Microcontaminants, Aroma & Separation Science group, Clermont-Ferrand, France
maia.meurillon@inrae.fr

Abstract

Formulation by adding antioxidants is a promising lever for reducing the formation of heterocyclic aromatic amines (HAAs), incriminated in the development of colorectal cancers. A unique and original method based on medicinal chemistry approaches was thus developed and permitted to select antioxidants best suited to inhibit HAA formation in meat: caper, oregano, red wine and green tea. The aim of the present work is to evaluate the sensory acceptability of the formulations tested for their HAA content and determine the odour-active compounds incriminated in the potential differences, in order to select formulations representing the best compromise between mitigation solution for process-induced toxicants and sensory acceptability. Firstly, a hedonic study was done to determine which formulations among the 4 tested were the most appreciated by consumers. Then non-verbal analyses were done to assess to what extent these hedonic differences were attributable to sensory differences. To characterize these differences, a fast sensory profiling was done followed by gas-chromatography-olfactometry (GC-8O) to identify the odour-active compounds responsible for these differences. This paper permitted to evidence the best balance between health benefit and sensory inconvenience and to assess the best option of formulation.

Keywords: hedonic rating, non-verbal analysis, fast sensory profiling, gas-chromatography-olfactometry

Introduction

In 2015, the consumption of red meat has been classified as probably carcinogenic (group 2A) for Human by the International Agency for Research on Cancer [1] and heterocyclic aromatic amines (HAAs) have been identified among the process-induced toxicants responsible. Mitigation strategies to reduce HAA impact on human health were proposed and one of the most promising was the addition of natural antioxidants to limit HAA formation [2]. But to date there is no method for making a reasoned choice of antioxidants. Therefore, in the first part of this work [3] a unique and original method based on medicinal chemistry approaches was developed to select antioxidants best suited to inhibit HAA formation in meat. This method allowed a rationalization of the choice of antioxidants to optimize meat chemical safety but it would only be admissible if these antioxidants are sensorially validated as the addition of antioxidants should in no way modify the sensory acceptance of the product or be subject to its rejection by consumers. Previous works studying the sensorial effect of the addition of antioxidants in meat often used descriptive analysis [4, 5] but such method is long and expensive as it requires a deeply trained panel. To circumvent these issues the present work develops an original strategy using hedonic studies, non-verbal and quantitative descriptive analyses and gas-chromatography-olfactometry (GC-8O) in order to determine what drives consumer's acceptance and to identify the sensory determinants that are at the origin of the latter. This strategy is implemented to compare the sensory effects of the addition of the 4 natural ingredients rich in phenolic antioxidants evidenced by the first part of this work [3]: caper, oregano, red wine and green tea.

Experimental

Hedonic scoring

Fifty-nine meat consumers were recruited to participate in two sessions over a period of two weeks. For each session the samples formulations were composed of two different natural products rich in antioxidants at two concentrations and a standard. The samples were coded with a 3-digit number and given in a monadic way to be rated on a 9-point hedonic scale (1, dislike extremely; 5, neither like nor dislike; 9, extremely pleasant).

Direct dissimilarity assessment

The non-verbal procedures used in this research work were directly inspired by Bonaïti et al. [6]. Fifteen selected panellists were instructed to estimate the overall dissimilarity between samples by positioning them in a square paper map of 60 x 60cm. This part was divided into two sessions in the same week. The first session only assessed overall dissimilarity while the second assessed olfactive and gustative dissimilarity. Samples were presented in the centre of the paper and panellists were allowed to smell and/or taste the samples as many times as

they wanted without respecting any specific order. In this non-verbal analysis, panellists were asked to place the formulations on a white sheet of paper based on their dissimilarities in terms of flavour and odour. Coordinates were calculated for each sample and each assessor. The largest between-sample distance was used to normalize distances that were obtained from each panellist. Normalized distances were then compiled to obtain an average distance matrix. The results were analysed through multidimensional scaling (MDS).

Fast sensory profiling

The panellists from the previous step were trained during an orientation session and came back two days later to evaluate the samples based on the training session instructions. The aim of the first session was to develop descriptive terms that could describe each sample and agree on the definition of each term. The session was monitored in order to agree on a consensual vocabulary. The final list was composed of 16 terms describing taste (4), texture (2) and aroma (10). In the second session, semi-trained panellists received the concentrations chosen in the hedonic step, including two standards (unmarinated and water marinated) and were instructed to rate the intensity of each term using a 10 cm unstructured linear scale from 'no perception' to 'strong perception'. For this session, the samples were presented in a monadic way to balance report and position effects.

Gas Chromatography/Mass spectrometry – olfactometry

Beef patties (four formulations rich in antioxidants, one standard and one water-marinated standard) were prepared and stored at -80°C. The day before the analyses, the samples were thawed at -4°C overnight. The next morning, they were cooked under same conditions than previous samples [3]. Ten grams of cooked sample were taken, 5 g from the centre of the steak and 5 g from the edge with some juice to be representative of the whole sample. Condensed volatile compounds were analysed by GC-O (model 6890; Hewlett-Packard, Avondale, PA). The volatile compounds were extracted by dynamic headspace (Tekmar, Cincinnati, OH, USA) coupled to gas chromatography (GC 4890D, Agilent Technologies) according to Giri et al. [7]. The sample was purged with helium (purity 99.995%) at 30°C for 1h with a flow rate of 40 mL.min⁻¹ using a Tenax trap. After injection, volatiles were separated and smelled according to Berdagué et al. [8]. The unique GC-8O system accumulates the performance of 8 judges simultaneously on the same sample to detect what are the most significant odour zones in the chromatogram. The selected sniffers were non-smokers with no known health disorders and with tested sensitivity and ability to detect and consistently describe a wide range of odours. They were advised to stay away from coffee or food 3 hours prior to the manipulation. The sniffers were asked to signal each odorous passage and provide one descriptor and its corresponding intensity on a five-level scale (1, very weak; 3, moderate; 5, very strong) [8]. This manipulation took place over 6 sessions of 35 min with the first one using water-marinated sample to familiarise the panellists and to give them a baseline. Olfactometric data were acquired and processed with the AcquiSniff® software [9]. Coupled with mass spectrometry, the GC-8O enables to identify the odour-active compounds and to assess their contribution to the overall odour/aroma of the product.

Data analysis

Data were analysed using Statistica software 10.0 (Statsoft, Maisons-Alfort, France) and AcquiSniff® software (INRA, Clermont-Ferrand, France). Hedonic mean scores were compared using Duncan's test. Direct dissimilarity assessment data were analysed by MDS mapping as proposed by Bonaïti et al. [6].

Results and discussion

Acceptability of the different formulations: Hedonic rating

This first part of the study aimed at determining the most preferred formulations among the panellists and permitted to guide the following sensory experiments. The four formulations (caper, oregano, green tea and wine) at two different concentrations were tested by the panellists along with a standard. The results displayed in figure 1 showed a great disparity of the hedonic scores between the formulations. The standard was the most preferred with respect to food neophobia often reported for novel foods [10]. Interestingly, two formulations, caper 0.5% and oregano 0.25 %, were non-significantly different from the standards. This can be due to the relative congruence of capers and oregano with ground beef patties. From Figure 1, wine and tea did confer a change that was noticeable by consumers as they rated those formulations as the least preferred. Our findings are in accordance with the results of Melo et al. [4] showing that longer marinating time in wine (4 to 6h) would generate unpleasant wine aroma, strong red colour and poor overall quality, contrary to 2h marinating time which resulted in no to little notable differences in sensorial perceptions [4, 5]. Moreover, the low hedonic scores of wine and tea formulations can again be related to the food neophobia phenomenon as those products are not usually used for ground beef preparations in our occidental countries.

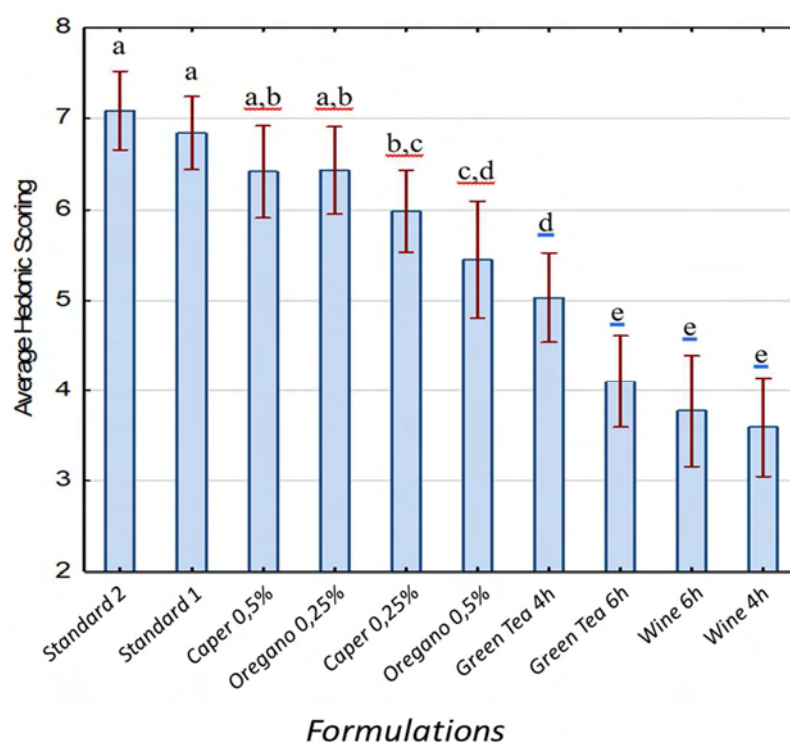


Figure 1: Mean values obtained for the 8 formulations by hedonic rating using a 9-point hedonic scale.

Given the results of hedonic scoring, the formulations chosen for the next part of the work were the less concentrated in order to be as close as possible of household practices.

Sensory dimensions responsible for the differences of acceptability

- Non-verbal dissimilarity rating

In order to explain the hedonic scoring of our formulations, non-verbal analysis was used to make the link between the odorous compounds and the acceptance. The results of MDS are displayed in figure 2.

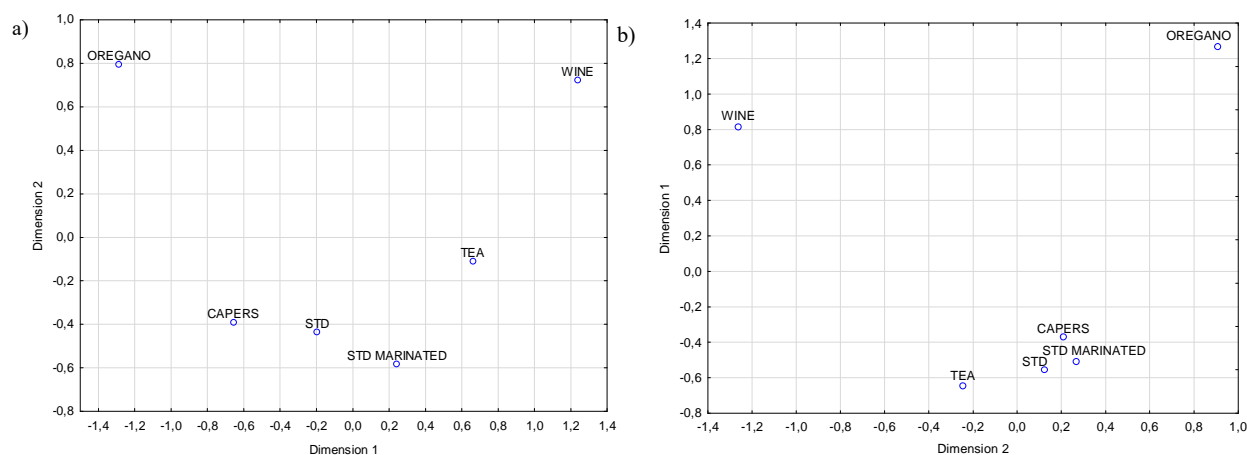


Figure 2: Positioning of the 4 formulations and 2 standards according to their flavour or odour: a) 2-D multidimensional scaling of the average distance matrix based on 2D flavour dissimilarity assessment; b) 2-D multidimensional scaling of the average distance matrix based on 2D odour dissimilarity assessment.

A MDS mapping of flavour dissimilarities was undertaken (Figure 2a) to determine if flavour plays an important role in the differentiation of the formulations. A similar non-verbal analysis focused on the smell was also produced (Figure 2b) to know if the smell plays a key role in the differentiation on the flavour, as understanding the contribution of the odour on the discrimination is essential. The MDS map of the flavour

dissimilarity profile (Figure 2a) clearly showed that wine and oregano formulations were different between themselves (dimension 1) and to the others (dimension 2). Caper formulation, marinated standard and standard were closely related in the second dimension and tea preparation, although close to this second group, was slightly different in the second dimension. Similar results were found for odour dissimilarity profile (Figure 2b). Non-verbal results highlighted the dissimilarity between oregano and standard formulations but as oregano is congruent with meat preparation, these sensorial differences didn't result in consumer rejection. On the contrary, as wine and to a lesser extent tea are not congruent with meat preparation, the sensory differences highlighted in the non-verbal results could explain their low acceptability (as shown by the hedonic rating). It seems that the other two chemical senses contributing to flavour (gustatory and trigeminal) contribute little to the differences in flavour profiles evidenced by non-verbal analysis. As a result, this research will focus on the olfactive dimension to find the molecular determinants responsible for the difference of acceptability.

- Fast sensory profiling

Table 1: Comparison of the attribute intensities measured by fast sensory profiling for the 2 standards and 4 formulations according to the 2-way ANOVA. The table presents only the attributes for which the p-value of the product effect is <0.01 or <0.005 and the relative judge effect is not significant.

	<i>Standard</i>	<i>Marinated Standard</i>	<i>Green Tea formulation</i>	<i>Caper formulation</i>	<i>Oregano formulation</i>	<i>Wine formulation</i>
<i>Grilled</i>	$4.0 \pm 2.8^{a,b}$	$4.9 \pm 2.4^{a,b}$	$2.9 \pm 2.1^{b,c}$	5.7 ± 3.1^a	$4.8 \pm 2.2^{a,b}$	1.8 ± 2.1^c
<i>Aromatic Plants</i>	0.3 ± 0.6^b	0.2 ± 0.3^b	0.3 ± 0.8^b	0.5 ± 1.0^b	7.8 ± 2.2^a	0.7 ± 1.8^b
<i>Winy</i>	0.1 ± 0.2^c	1.2 ± 2.5^c	2.8 ± 3.4^b	0.3 ± 0.6^c	0.3 ± 0.6^c	8.2 ± 2.0^a
<i>Juiciness</i>	5.3 ± 2.8^a	2.6 ± 2.0^b	2.4 ± 1.8^b	$3.9 \pm 2.5^{a,b}$	$3.9 \pm 2.7^{a,b}$	4.9 ± 2.7^a

The results from the sensory profiling (Table 1) permitted to evaluate the nature of the differences highlighted by non-verbal analyses. Based on this fast sensory profiling, the winy attribute, not congruent for proteinaceous foods, explained the result of the non-verbal analysis and permitted to discriminate wine and to a lesser extent green tea formulation from the others. In contrast, the aromatic plant note, which is congruent with meat products, permitted to differentiate oregano formulation from the others.

Odour-active drivers of the acceptability differences between the studied formulations

- Qualitative comparison of the aromagrams of the different formulations

When comparing the different aromagrams (Figure 3), the wine and oregano formulations showed the highest variation with the standard which explained the differences observed in MDS analyses. The “green/aromatic plant” note at 950s present in the aromagram of the standard was absent in both wine and oregano formulations. This peak corresponds to hexanal which is an oxidation product. Its disappearance in both formulations can be related to the antioxidant activities of wine and oregano. The wine formulation was distinguished by a strong contribution of fruity/floral notes which could be related to esters, benzaldehyde or linalool previously reported in Pinot Noir [11]. These differences observed in the aromagrams of wine formulation and standard were consistent with the fast sensory profiling results showing more important fruity and wine attributes in wine formulation. The oregano aromagram was differentiated by high intensity poles (>3.5) “butter/lactic/cheese” and “vegetable”.

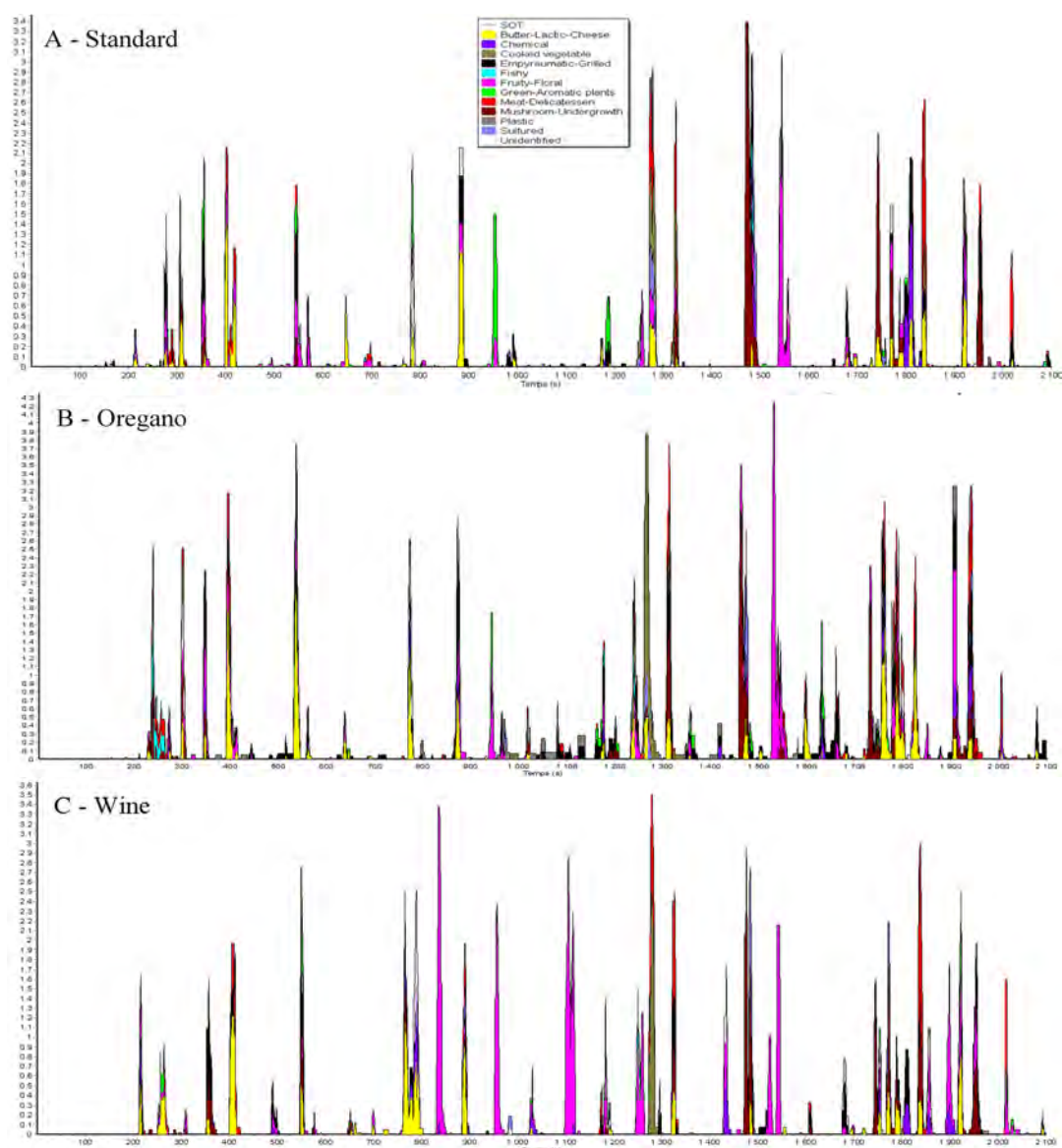


Figure 3. Mean aromagrams of (A) Standard (B) Oregano (C) Wine calculated from 8 individual sniffing sessions. The breakdown of the signal into twelve odour classes shows the odorant zones belonging to a given olfactory class.

- Identification of discriminant volatile compounds for each formulation

Table 2 presents the main distinctive peaks of the different formulations obtained by coupling GC-O and GC/MS data. The matching of the resulting candidate compounds and the odour descriptors generated by the trained panellists was assessed thanks to a library of aroma descriptors and retention time found at thegoodsentcompany.com and the nature of the peaks was proposed (Table 2).

Table 2. Nature of the significant peaks of the different formulations obtained by coupling GC-O and GC/MS data with LRI: Linear Retention Indices; S: standard formulation; W: wine formulation; O: oregano formulation; C: caper formulation; T: green tea formulation.

Peak	LRI	Chemical Name	Odour Descriptor	Formulations				
				S	W	O	C	T
3	829	Ethyl isobutyrate	Fruity, strawberry candy, citrus		X			
6	1002	Ethyl-2-hydroxypropanoate	Caramel, bread crust, grilled beef				X	
7	1099	Ethyl-2-methylbutanoate	Strawberry, sour candies		X			
9	1308	2,3-dimethyl-pyrazine	Cold cuts, peanut, ham, mushroom			X		X
11	1428	4-methyl-cyclohexanone	Mint, sulfur, chemical, fruity		X			
		heptanol						
		benzaldehyde						

14	1626	1,8-cineole	Grass, caramel, mint					
16	1755	Ethyl heptanoate	Sausage, fermented grass, butyric acid, floral, rind, mustiness			X		X
		3-ethyl-2,5-dimethyl pyrazine						
		2-nonanone						
17	1819	Unknown	Grilled meat, sausage, grilled peanut, butter			X		X
18	1824	Dimethyltrisulfide isomer	Sausage, ham butter sandwich, smoked lard, roasted, broth, pizza, warm chicken, mustiness	X	X		X	
		2-Phenylethanol						
19	1904	Methyl-2-methyl-3-furyl-disulfide	Green leaf, burnt paper, fermented grass, vegetable, floral			X		X
20	2001	Ethyl octanoate	Sausage, ham, potato, coffee, broth					

Peaks 3 and 7, both described with fruity descriptors and found in wine formulation, seemed distinctive from the other formulations. Ethyl isobutyrate (peak 3) and ethyl-2-methylbutanoate (peak 7) confirmed the strong contribution of fruity/floral notes previously observed in figure 3. Their presence in wine formulation was coherent with previous studies as they resulted from the fermentation process [11]. Peak 18 distinguished wine from oregano and green tea formulations. Peaks 9, 16, 17 and 19 found in oregano and green tea seemed distinctive from standard formulation. The presence of 2,3-dimethylpyrazine (peak 9) explained the overexpression of the vegetable note at 1280s in oregano and green tea aromagrams compared to standard and is consistent with the work of Zhu et al. [12] who detected several pyrazines in green tea samples. Peak 6 found in caper formulation seemed distinctive from the other formulations. The presence of ethyl-2-hydroxypropanoate (peak 6) was therefore a marker for this formulation as evidenced by the overexpression of the “butter/lactic/cheese” note at 1000-1030 s in caper aromagram compared to the standard.

Conclusion

Based on this work, we could now determine that oregano would be the best choice as at medium concentration it displays a strong congruence with ground beef patties and presents an acceptability comparable to that of the target product, as to know cooked meat. The approach proposed here made it possible to select among 4 formulations the one which was the most realistic from the point of view of sensory acceptability. These data will allow the oregano model, or in any case its active principle, to be used to subsequently elucidate the mechanism of inhibition of the formation of HAAs and the impact of this formulation on colorectal carcinogenesis in connection with exposure to HAAs.

References

1. Bouvard, V., Loomis, D., Guyton, K. Z., Grosse, Y., Ghissassi, F. E., Benbrahim-Tallaa, L., & et al. Carcinogenicity of consumption of red and processed meat. *Lancet Oncol.* 2015; Published online, October 26, 2015.
2. Meurillon, M., & Engel, E. Mitigation strategies to reduce the impact of heterocyclic aromatic amines in proteinaceous foods. *Trends Food Sci Technol.* 2016;50:70-84.
3. Meurillon, M., Angénioux, M., Mercier, F., Blinet, P., Chaloin, L., Chevolleau, S., Debrauwer, L., Engel, E. Mitigation of heterocyclic aromatic amines in cooked meat Part I: Informed selection of antioxidants based on molecular modeling. *Food Chem.* 2020;331:127264.
4. Melo, A., Viegas, O., Petisca, C., Pinho, O., & Ferreira, I. M. Effect of beer/red wine marinades on the formation of heterocyclic aromatic amines in pan-fried beef. *J Agric Food Chem.* 2008;56(22):10625-10632.
5. Quelhas, I., Petisca, C., Viegas, O., Melo, A., Pinho, O., & Ferreira, I. M. Effect of green tea marinades on the formation of heterocyclic aromatic amines and sensory quality of pan-fried beef. *Food Chem.* 2010;122:98-104.
6. Bonaiti, C., Irlinger, F., Spinnler, H.E., Engel, E. An iterative sensory procedure to select odor-active associations in complex consortia of microorganisms: Application to the construction of a cheese model. *J Dairy Sci.* 2005;88(5):1671-1684.
7. Giri, A., Khummueng, W., Mercier, F., Kondjoyan, N., Tournayre, P., Meurillon, M., Ratel, J., & Engel, E. Relevance of two-dimensional gas chromatography and high resolution olfactometry for the parallel determination of heat-induced toxicants and odorants in cooked food. *J Chromatogr A* 2015;1388:217-226.
8. Berdagué, J. L., Tournayre, P., & Cambou, S. Novel multi-gas chromatography-olfactometry device and software for the identification of odour-active compounds. *J Chromatogr A* 2007;1146(1):85-92.
9. Tournayre, P., & Berdagué, J. L. AcquiSniff® Software. In U. Q. T. A. Distributed by INRA, F-63122 Saint Genès Champanelle, France (Ed.), 2003;(Vol. IDDN FR.001.210006.000R.P.2003.000.30000).
10. Raudenbush, B., & Frank, R. A. Assessing food neophobia: The role of stimulus familiarity. *Appetite* 1999;32(2):261-271.
11. Fang, Y., & Qian, M. Aroma compounds in Oregon Pinot Noir wine determined by aroma extract dilution analysis (AEDA). *Flavour Fragr J.* 2005;20(1):22-29.
12. Zhu, J., Niu, Y., Xiao, Z. Characterization of the key aroma compounds in Laoshan green teas by application of odour activity value (OAV), gas chromatography-mass spectrometry-olfactometry (GC-MS-O) and comprehensive two-dimensional gas chromatography mass spectrometry (GC × GC-qMS). *Food Chem.* 2021;339:128136.

Fruity expression of red wines resulting from varieties adapted to climate change. A comparative study with the "traditional" grape varieties planted in Bordeaux

JUSTINE GARBAY, Margaux Cameleyre, Nicolas Le Menn, Jean-Christophe Barbe and Georgia Lytra

Unité de recherche OEnologie, EA 4577, USC 1366 INRAE, ISVV, Université de Bordeaux, F33882 Villenave d'Ornon France, justine.garbay@u-bordeaux.fr

Abstract

Currently, one of the major issues for the wine sector is the impact of climate change linked to the increasing temperatures recorded and expected in the upcoming years. The vegetative cycle of the grape varieties authorised and planted in the Bordeaux wine region is tending to shorten, affecting the physicochemical parameters of the grapes and, consequently, the quality of the wines. In some varieties, the attenuation of their fresh fruity character is accompanied by the accentuation of dried-fruit notes [1]. As of today, winegrowers must implement adaptive strategies to continue producing high quality wines in a climate that is becoming warmer and drier. Some winegrowers have initiated changes in the mix of vine varieties [2].

This study intends to explore the fruitiness in wines produced from grape varieties adapted to the future climate of Bordeaux. Indeed, Bordeaux wines currently have a recognized fruity typicity [3], that it is imperative to preserve to maintain its reputation and avoid economic and, therefore social consequences.

For that, commercial single-variety wines from 2018 vintage made from the main grape varieties grown in the Bordeaux region (Merlot and Cabernet-Sauvignon) as well as from indigenous grape late-ripening varieties from the Mediterranean basin were collected, such as France (Cabernet-Franc, Cabernet-Sauvignon, Merlot and Syrah), Greece (Agiorgitiko, Xinomavro), Portugal (Touriga Nacional) and Spain (Garnacha and Tempranillo). Wines were evaluated sensorially: a sorting task was instructed to the panel and descriptive analyses of all wines were recorded with descriptors related to the fruity character of each wine. To study their fruity aroma expression, samples were prepared from wine, using an HPLC method which preserves wine aroma and isolates fruity characteristics in 25 specific fractions [3]. A trained panel evaluated sensorially the fractions. The descriptors characterising each wine matched those attributed to the different fractions. Then all fractions with intense fruity notes were selected for each wine and the comparative study of their fruity expression highlighted some fractions of interest. Aromatic reconstitutions were realised by mixing fractions with a fruity aroma ("fruity pool") in ethanol and microfiltered water to obtain an ethanol level of 12% (v/v). By comparing the fruity expression of each fruity aromatic reconstitution (FAR) made from the different late-grape varieties previously selected, 3 distinct groups were highlighted. FAR of wines made from late-grape varieties from Spain (Garnacha and Tempranillo) were gathered into the group 1 with the FAR of the wine made from a grape variety from France (Syrah). The group 1 was characterised by "red-berry", "black-berry" and "exotic" fruits notes. The group 2 was composed by FARs of wines made from two grape-varieties from France (Cabernet-Sauvignon and Merlot) and two grape-varieties from Greece (Agiorgitiko and Xinomavro). This second group was mainly described as "red-berry", "black-berry", "candy", "amylic" and "artificial" fruits notes. Finally, FAR of the wine made from grape variety from Portugal (Touriga Nacional) was classified into the group 3 with the FAR of the wine made from the last grape variety from France (Cabernet-Franc). The group 3 was mainly characterised by "freshness", "mint" and "eucalyptus" notes.

These results open up new prospects for the preparation of aromatic reconstitutions [4] from several fractions in order to study the impact of perceptive interactions on wine fruity aroma expression after the integration of wines from "new" late-ripening varieties in Bordeaux blends.

Keywords: red wine, fruity notes, fractionation, climate change, late-ripening varieties

Introduction

In the Bordeaux vineyards, the climatic conditions of recent vintages have led to a great heterogeneity in grape ripening. Various parameters, such as the variety mix, have affected the wines' aromatic expression. These climatic variations have resulted in higher quality wines made from late-ripening varieties, such as Cabernet-Sauvignon. From a sensory standpoint, oenologists have noted a strong influence of climate change on the aromatic quality and typicality of red wines. Among the multiple sensory characteristics involved in judging wine quality, olfactory notes are the most affected [5]. Thus, today, the fruity character of red wines, typical of a particular region, is considered synonymous with quality and highly sought-after by consumers. The work of Pineau [3] highlighted the existence of a fruity aroma, specific to Bordeaux red wines, marked by notes of "black-berry" and "jammy" fruit. Therefore, adapting the variety mix by (re-)introducing more suitable, late-ripening varieties seems essential to avoid a radical change in the fruity expression of Bordeaux wines [2].

Climate change is tending towards warmer, drier conditions, increasing the risk that, in the medium term, grape varieties that currently produce satisfactory results in the various production regions, and more precisely Merlot, will no longer be adapted in the future. Therefore, it makes sense to research the possibility of modifying the blend and (re-)introducing grape varieties adapted to the future climate. In order to preserve the fruity typicality of Bordeaux region wines after the introduction of these “new” grape varieties in the vineyards, the sector wishes to evaluate their aromatic potential by comparing them to the main grape varieties currently grown in the Bordeaux region (Merlot, Cabernet-Sauvignon, and Cabernet franc). The aim is to evaluate wines made from indigenous grape varieties from the Mediterranean basin (France, Greece, Italy, Spain, Portugal, etc.) planted in areas with hot climates (simulating the future climate of Bordeaux), and compare them with wines made from the main grape varieties currently grown in the Bordeaux region.

Experimental

Acquisition of wines

Nineteen commercial single-varietal red wines made from late-ripening grape varieties planted in a region with a high-temperature climate (Mediterranean basin) were collected (Table 1). These wines were from the 2018 vintage, as red wines express their typical fruity aroma, distinguishable from the fermentation aromas, after at least 2 years of ageing [6].

Table 1: 19 commercial single-varietal red wines collected from the Mediterranean basin.

Country	Grape varieties
France	Cabernet franc, Cabernet-Sauvignon, Carmenere, Cinsault, Malbec, Merlot, Sciaccarello and Syrah
Greece	Agiorgitiko, Kotsifali and Xinomavro
Cyprus	Giannoudi and Mavro
Italy	Aglianico and Nebbiolo
Portugal	Touriga Nacional
Spain	Garnacha and Tempranillo

The aromatic properties of all the red wines were established using a sensory analysis methodology, exclusively via orthonasal perception. Wines were evaluated at the controlled room temperature (20 °C) of ISVV, in individual booths, using covered ISO glasses (ISO 3591:1977, 1977) containing about 50 mL liquid, coded with three-digit random numbers.

The panel consisted of five judges from the research laboratory staff at ISVV, Bordeaux University, and all experts in assessing fruity aromas in red wines. Two questions were addressed to the panel to evaluate the fruity aromatic quality of each of the presented wines: “Does this wine have one or more defects? If yes, please specify which defect(s) you have detected” and “Among the wines sorted as “defect-free wines”, please perform a generation of descriptors (maximum 5) related to the fruitiness of the wine (if fruitiness is perceived)”. This acquisition phase consisted of discussing the fruity characteristic descriptors for the whole panel (NF ISO 11035: 1995) and selecting the wines with qualitative fruity descriptors, marked by black-berry, red-berry, fresh and jammy fruit notes and excluding those with dried-fruit notes.

Realisation of Aromatic Reconstitutions (AR)

Samples were prepared from 9 single-varietal red wines, using a methodology optimised by Lytra et al. [4]. A 500 mL wine sample was extracted successively using 80, 80 and 40 mL of dichloromethane, with a separatory funnel for 10 min. The organic phases were collected, blended, dried over sodium sulphate, and concentrated under nitrogen flow (100 mL/min) to obtain 1.25 mL of wine extract. Aroma extract of wines were eluted with a Reversed-Phase (RP) High-Performance-Liquid-Chromatography (HPLC) methodology, developed by Ferreira et al. [7]. The HPLC fractionation was realised by using a Nova-Pak C18 column (300 × 3.9 mm i.d., 4 µm, 60 Å, Waters, Saint-Quentin, France), without a guard cartridge [3]. The HPLC system consisted of an L-6200A pump (Merck-Hitachi, Germany). Chromatographic conditions were as optimised by Pineau [3]: 20 flow rate, 0.5 mL/min; injection volume, 250 µL wine extract; program gradient, phase A, water, phase B, ethanol; 0–2 min, 100% A, linearly programmed until 100% B at minute 50. The effluent was collected in 1 mL fractions.

This methodology was used to isolate fractions with intense fruity notes (fractions 17–21), thus creating a fruity pool. For fruity AR (FAR), fractions of the fruity pool (fractions 17–21) were blended together to reproduce the initial concentrations in the original wines, adding ethanol and microfiltered water to obtain an ethanol level of 12% (v/v) [4].

Sensory analysis of Aromatic Reconstitutions

Nine FAR were all presented randomly to the panel to compare the fruitiness of samples. A free sorting task was applied to explore perceptive similarities among FAR [8]. Assessors were instructed to classify each FAR according to their similarities or dissimilarities. No constraints were required for this test and assessors had the possibility to do the number of groups they wanted (with the minimum of 2 groups) and to put as many samples they considered important into each group. Then, participants were asked to generate some descriptors to describe each group.

Results and discussion

Acquisition of wines

Three wines that presented aromatic defects (notes of reduction, vegetal and horsy notes) were eliminated. Sixteen wines were characterised as “defect-free wines”, but 8 of them were marked by a non-typical fruit (dried fruit notes). Finally, 8 wines described with a typical fruit (red-berry, black berry, fresh and jammy fruit notes) were collected for this study. The single-variety red wines presenting the most qualitative typical fruity aroma were: Garnacha (Spain), Tempranillo (Spain), Touriga Nacional (Portugal), Xinomavro (Greece), Agiorgitiko (Greece), Cabernet-Franc (France), Cabernet-Sauvignon (France) and Syrah (France). The Merlot wine (from France) was kept for further analysis, even if its fruity character was not typical, with the aim to compare its fruity expression to the fruity expression of other single-variety wines.

Data collection and analysis: Free sorting task test

A total of 25 fractions (fractions 1-25) with various flavours were obtained and evaluated by the panel using a free sorting task test. The descriptors characterising each wine matched those attributed to the different fractions and the fruity character of each selected wine (marked by black-berry, red-berry, fresh and jammy fruits) was preserved into the fruity pool (fractions 17-21).

Data collected from the free sorting task test were organised into a dissimilarity matrix (Table 2) [9]. Then, a Hierarchical Cluster Analysis (HCA) was performed on the dissimilarity matrix to obtain a dendrogram (Figure 1). Samples were gathered according to their similarities or dissimilarities comparing their fruity expression.

Statistical analysis highlighted the existence of 3 distinct groups constituted by different FAR made from different single-variety red wines (Figure 1). The first group in green colour was composed by the FAR of the two single-variety red wines from Spain, Garnacha (A) and Tempranillo (B), and the single-variety red wine from France, Syrah (G). Regarding the second group in orange colour, FAR of the two grape varieties from France, Cabernet-Sauvignon (E) and Merlot (I), were classified with the FAR of the two grape varieties from Greece, Xinomavro (C) and Agiorgitiko (D). Finally, the third group in violet colour was composed by the single-variety red wines from France, Cabernet-Franc (F) and from Portugal, Touriga Nacional (H).

Table 2: Dissimilarity matrix on data generated by the free sorting task test (A: Garnacha; B: Tempranillo; C: Xinomavro; D: Agiorgitiko; E: Cabernet-Sauvignon; F: Cabernet-Franc; G: Syrah; H: Touriga Nacional; I: Merlot).

	AR - A	AR - B	AR - C	AR - D	AR - E	AR - F	AR - G	AR - H	AR - I
AR - A	0	4	3	4	5	5	2	3	3
AR - B	4	0	5	5	4	4	3	5	4
AR - C	3	5	0	3	4	4	4	3	4
AR - D	4	5	3	0	3	5	5	4	3
AR - E	5	4	4	3	0	4	5	5	4
AR - F	5	4	4	5	4	0	5	2	5
AR - G	2	3	4	5	5	5	0	4	5
AR - H	3	5	3	4	5	2	4	0	4
AR - I	3	4	4	3	4	5	5	4	0

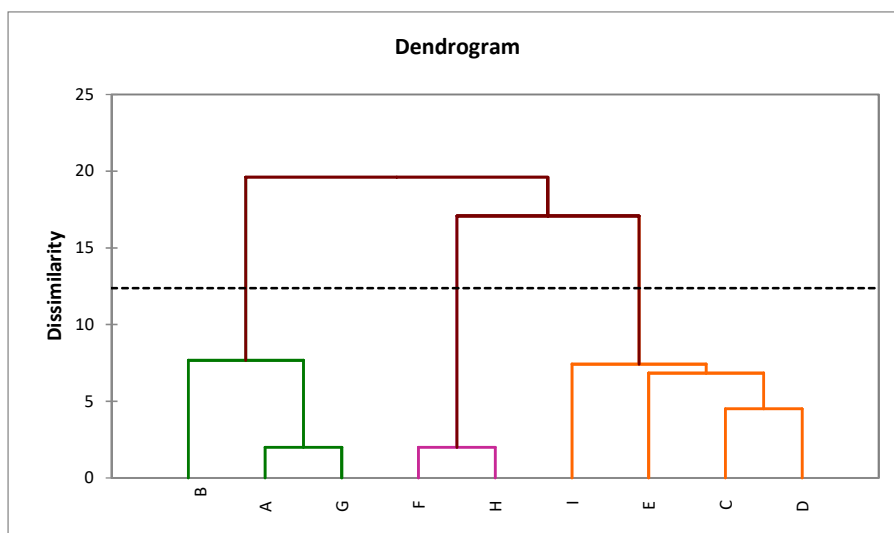


Figure 1: Dendrogram obtained using a dissimilarity matrix applied on free sorting data (A: Garnacha; B: Tempranillo; C: Xinomavro; D: Agiorgitiko; E: Cabernet-Sauvignon; F: Cabernet-Franc; G: Syrah; H: Touriga Nacional; I: Merlot).

Data collection and analysis: Generation of descriptors based on citation frequencies

Ten descriptors were generated by the panel, and were gathered into 5 groups according to their olfactory similarities: “black-berry and red-berry fruits”, “exotic fruits”, “mint, eucalyptus and freshness notes”, “spicy” and “candy, amylic and dark fruits”. The citation frequency of descriptors for each group was calculated using the number of time a word is cited in each group divided by the total number of time the word is cited.

Citations frequencies of various descriptors for each group were represented on a histogram (Figure 2). Participants selected “black-berry” and “red-berry” descriptors for all the 3 groups with a higher citation frequency for the group 2, composed by FAR from the 2 single-varietal red wines from Greece (Agiorgitiko and Xinomavro) and from France (Cabernet-Sauvignon and Merlot).

The first group was mainly characterised by “black-berry”, “red-berry” and “exotic” fruits. The second group was mainly characterised by “candy, amylic, artificial fruits” and “spicy” notes, as well as “exotic”, “black-berry and red-berry” fruits. Finally, the third group was mainly described as “mint, eucalyptus and freshness” notes, as well as “exotic”, “black-berry” and “red-berry” fruits.

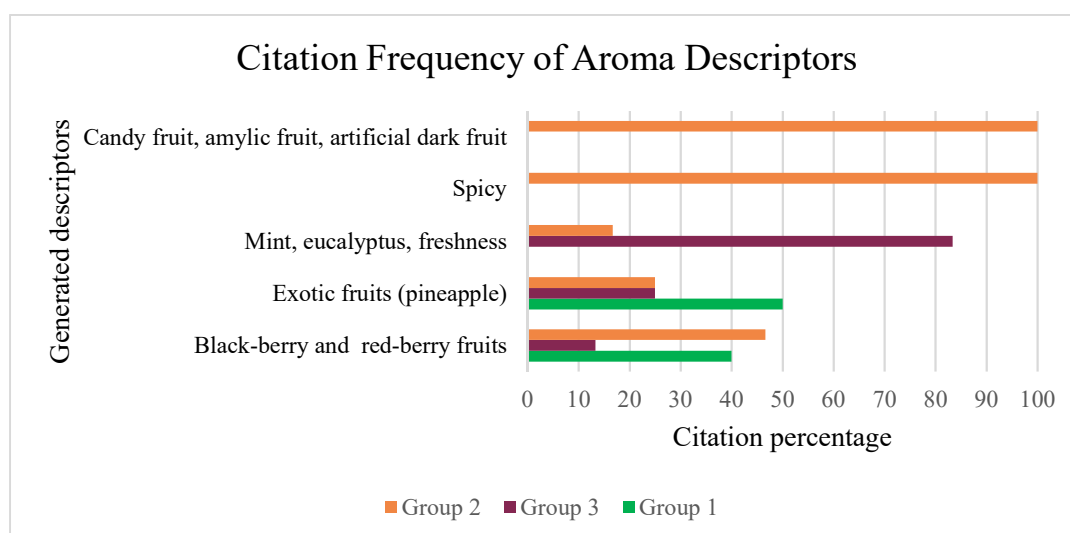


Figure 2: Histogram obtained using citation frequencies of each generated descriptors (Group 1: Garnacha, Tempranillo, Syrah; Group 2: Cabernet-Sauvignon, Merlot, Agiorgitiko, Xinomavro; Group 3: Cabernet-Franc and Touriga Nacional).

Conclusion

Qualitative descriptors, marked by “black-berry” and “red-berry” fruits, were found in several single-varietal red wines made from late-grape varieties from the Mediterranean basin, opening perspectives for their addition to Bordeaux traditional blend. Different groups of similarity were formed. FAR of Cabernet-Sauvignon, Merlot, Agiorgitiko and Xinomavro were gathered together, highlighting their similar fruitiness and the possible replacement of Merlot by these varieties in the Bordeaux traditional blend. The aromatic reconstitution of the “fruity pool” of Merlot red wine was finally characterised with a qualitative fruity expression suggesting that the fruity character of the overall aroma of Merlot red wines may be affected by other compounds in wine.

As a future perspective, sensory analyses will be coupled with instrumental analysis to understand how aromatic composition and variation of some compounds may influence the fruity expression in samples. Moreover, investigating new perceptual interactions due to the presence of some aroma compounds responsible for the mint and freshness notes in FAR, remains an interesting study. Further sensory analyses need to be performed to extend and validate these results using other experimental conditions such as panel, wine references, grape-varieties diversity and wine vintage.

References

1. Pons A, Allamy L, Schüttler A, Rauhut D, Thibon C, Darriet P. What is the expected impact of climate change on wine aroma compounds and their precursors in grape? *OENO One*. 2017;51(2):141-146.
2. Van Leeuwen C, Destruct-Irvine A, Dubernet M, Duchêne E, Gowdy M, Marguerit E, Ollat N. An update on the impact of climate change in viticulture and potential adaptations. *Agronomy*. 2019;9(9):514.
3. Pineau B. Contribution à l'étude de l'arôme fruité spécifique des vins rouges de *Vitis vinifera* L. cv. Merlot noir et Cabernet-Sauvignon. Ph.D. Thesis. 2007, University of Bordeaux 2.
4. Lytra G, Tempere S, De Revel G, Barbe J.C. Impact of perceptible interactions on red wine fruity aroma. *J. Agric. Food Chem*. 2012;60(50):12260-12269.
5. Van Leeuwen C, Barbe J.C., Darriet P, Gomès E, Guillaumie S, Thibon C. Recent advancements in understanding the terroir effect on aromas on aromas in grapes and wines. *OENO One*. 2020;54(4):985-1006.
6. Lytra G, Franc C, Cameleyre M, Barbe J.C. Study of substituted ester formation in red wine by the development of a new method for quantitative determination and enantiomeric separation of their corresponding acids. *J. Agric. Food Chem*. 2017;65(24):5018-5025.
7. Ferreira V, Hernandez-Orte P, Escudero A, Lopez R, Cacho J. Semipreparative reversed-phase liquid chromatographic fractionation of aroma extracts from wine and other beverages. *J. Chromatogr., A*. 1999;864:77-88.
8. Maître I, Symoneaux R, Jourjon F, Mehinagic E. Sensory typicality of wines: How scientists have recently dealt with this subject. *Food Qual. Prefer*. 2010;21:726-731.
9. Faye P, Courcoux P, Qannari E.M., Giboreau A. Méthodes de traitement statistique des données issues d'une épreuve de tri libre. *Revue MODULAD*. 2011;43.

Climate change and cocoa flavour quality: analytical investigations to identify off-odour in cocoa products

ERICA LIBERTO^{1*}, Chiara Cordero¹, Pamela Perotti¹, Cristian Bortolini² and Carlo Bicchi¹

¹Dept. of Drug Science and Technology, University of Turin, Turin, Italy; erica.liberto@unito.it

²Soremartec Italia Srl (Ferrero Group) P.le P. Ferrero 1, 12051 Alba (CN), Italy

Abstract

Cocoa smoky off-flavour is due to inappropriate post-harvest processing and cannot be removed in the subsequent chocolate-manufacturing steps. To date, no reliable analytical method to detect key-analytes responsible for smoky off-flavour in incoming raw material is available and the sensory tests are time-consuming. This study aims to develop an analytical method to detect smoky markers, suitable for quality control. A top-down procedure was applied: the cocoa volatilome was first profiled by headspace solid phase microextraction (HS-SPME) combined with comprehensive two-dimensional gas chromatography-mass spectrometry (GCxGC-TOF-MS) from a set of representative smoky and non-smoky samples; advanced fingerprinting revealed the chemicals responsible for the off-flavour. The results served to develop a 1D-GC method suitable for routine application. Ten identified smoky markers were subjected to accurate quantification, thereby defining operative ranges to accept/reject incoming bean samples. A step ahead was devoted to automatically speeding up the controls through a MS-enose platform coupled with suitable chemometric modelling to classify smoky and non-smoky samples and cross-validated by the confirmatory quantitative method through HS-SPME-GC-MS. Thus, it was successfully developed an objective and automatic analytical decision maker suitable for the control at multistep level on the chocolate production chain.

Keywords: Cocoa volatilome, smoky off-flavour, GCxGC-TOF-MS, HS-SPME-GC-MS, MS-enose

Introduction

Climate change is heavily conditioning the agricultural productions. Cocoa growing in a rainfall area will also affect the choice of the methods of drying that when improperly conducted can develop a typical smoky off-flavour thereby strongly influencing the flavour quality of the finished product [1]. Chocolate manufacturer therefore need informative, practical and cost-effective methods to identify off-flavour to evaluate the quality of the in-coming raw material. Sensomics is the gold standard in the definition for the aroma blue print of a food as well as for off-flavours characterization [2, 3], but it is too time consuming. Modern analytical techniques combined with chemometric methods enables to speed-up the chemical characterization and the definition of quality marker as well as to model and implement analytical decision maker (ADM) tools to apply in routine controls [4].

Experimental

The sample set included beans (n= 65) and liquors (n= 176) of cocoa samples from different origins and harvested in different years. Rejected and accepted samples analysed have been selected based on the sensory tests carried out from the industrial panel. All samples were of commercial grade and compliant with the industrial quality control of Soremartec Italia srl (Alba, Italy).

HS-SPME-GC×GC-TOF-MS and HS-SPME-GC-MS and instrument set-up and analytical conditions

Optimised extraction conditions: 5.0 µL of internal standard (ISTD) (n-C17 at 1000 mg/L) was pre-loaded onto the SPME device (DVB/CAR/PDMS) df 50/30 µm - 2 cm length at 80°C for 20 min. 1 g of cocoa powder was sampled for 40 min at 80° at a shaking speed of 350 rpm. Multiple headspace extraction (MHE) quantification was by the External Standard approach; an aliquot of 0.100 g, to achieve headspace linearity for target analytes, was submitted to multiple consecutive extractions at the same sampling conditions. A series of calibrating solutions of reference compounds in cyclohexane, ranging from 0.1 to 50 mg/L, were used in full evaporation for MHE external calibration. Suitable volumes of standard solutions at different concentrations were submitted to multiple consecutive extractions (as for the cocoa samples).

GC-MS analysis-Chromatographic conditions: analyses were run on a Shimadzu QP2010 GC-MS system, Injector temperature: 240°C, injection mode: splitless; helium, flow rate: 1 mL/min; column: SolGelwax 30 m x 0.25 mm dc x 0.25 µm df (Trajan Analytical Science - Ringwood, Australia). Temperature program, from 40°C (2 min) to 200°C at 3.5°C/min, then to 240°C (5 min) at 10°C/min.

GC×GC-TOF-MS analysis-Chromatographic conditions: GC×GC analyses were run on an Agilent 7890 GC unit coupled with a Markes BenchTOF-Select and Select-eV® option (Markes International Ltd, Llantrisant UK)

operating in the EI mode at 70eV. The transfer line was set at 250°C. TOF acquisition was set at m/z 35–350 with 100 Hz sampling frequency. The GC system was equipped with a two-stage KT 2004 loop thermal modulator (Zoex Corporation, Houston, TX) cooled with liquid nitrogen and controlled by Optimode™ V.2 (SRA Instruments, Cernusco sul Naviglio, MI, Italy). Hot jet pulse time was set at 250 ms, modulation time was 3.5 s and cold-jet total flow progressively reduced with a linear function from 40% of Mass Flow Controller (MFC) at initial conditions to 8% at the end of the run.

SPME thermal desorption into the GC injector port was in split mode, split ratio 1:20, Tinj: 250°C. Carrier gas was helium at a constant flow of 1.3 mL/min. The oven temperature program was from 40°C (2 min) to 200°C at 3.5°C/min and to 240°C at 10°C/min (10 min). The column set was configured as follows: 1D SolGel-Wax column (100% polyethylene glycol) (30 m × 0.25 mm dc, 0.25 µm df) from SGE Analytical Science (Ringwood, Australia) coupled with a 2D OV1701 column (86% polydimethylsiloxane, 7% phenyl, 7% cyanopropyl) (2m × 0.1 mm dc, 0.10 µm df), from J&W (Agilent, Little Falls, DE, USA).

HS-SPME-MS-enose instrument set-up

Cocoa powder (1.00 g) was equilibrated for 5 min at 80°C and then sampled using HS-SPME for 10 min shaking speed of 350 rpm. Analysis were carried out on a MPS-2 multipurpose sampler controlled by Gerstel Maestro software (Gerstel, Mülheim a/d Ruhr, Germany), which was combined on-line with an Agilent 7890A GC coupled to a 5975B MS detector (Agilent, Little Falls, DE, USA). The GC oven and injector were maintained at 250 °C; injection mode, split; split ratio, 1/10; carrier gas, helium; flow rate, 0.4 mL/min; fibre desorption time and reconditioning, 3 min. The transfer column was uncoated deactivated fused silica tubing (dc = 0.10 mm, length = 6.70 m) from MEGA (Legnano, Italy). MSD conditions: EI ionisation mode at 70 eV; temperatures: ion source: 230 °C, transfer line: 280°C. Standard tuning was used and the scan range was set at m/z 35–350 with a scanning rate of 1,000 amu/s.

Data acquisition and processing

GC×GC-TOF MS data were acquired by TOF-DS software (Markes International, Llantrisant, UK) and processed using GC Image GC×GC Software, version 2.8 (GC Image, LLC, Lincoln NE, USA). GC-MS data were collected by GCMS Solution 2.5SU1 software (Shimadzu, Milan, Italy). MS-enose Data were acquired and processed using an Agilent MSD Chem Station ver. E.02.01.1177 (Agilent, Little Falls, DE, USA). Raw data were transformed using RapidDataInterpretation software by Gerstel (Gerstel, Mülheim a/d Ruhr, Germany). Targeted analysis was focused on about 70 compounds identified by matching their EI-MS fragmentation patterns (NIST MS Search algorithm, version 2.0, National Institute of Standards and Technology, Gaithersburg, MD, USA, with Direct Matching threshold 900 and Reverse Matching threshold 950) with those stored in commercial (NIST2014 and Wiley 7n) and in-house databases. Linear retention indices (ITS) were taken as a further parameter to support identification, and experimental values were compared to tabulated units.

Chemometric analyses, Principal component analysis (PCA), SIMCA (Soft-Independent modelling of Class Analogy) and Partial Least Square Discriminant Analysis (PLS-DA) were carried out using Pirouette® (Comprehensive Chemometrics Modelling Software, version 4.5-2014) (Infometrix, Inc. Bothell, WA).

Results and discussion

A subset of cocoa samples between good and defective beans and liquors were investigated. HS-SPME-GC×GC-TOF-MS analysis provided 2D fingerprints mined by pattern recognition tools (i.e. template matching fingerprinting and scripting) which resulted in highly informative chemical signatures for quality assessment (Figure 1) [3]. 231 target analytes were identified and matched through the sample set; Fisher ratio found that about 60 of them, belonging to different chemical classes: esters, branched alcohols, carbonyls and phenolic and aromatics derivatives, showed to be discriminative between defective and good quality cocoa samples.

When the 2D GC×GC method was transferred to 1D-GC to screen these components, potential smoky markers gave poor signals due to their chemical-physical characteristics, their high retention in the matrix because of both their relatively low volatility and the high percentage of fat in cocoa. A careful set-up of the analytical conditions and approaches were tested to improve the recovery of these compounds from the cocoa samples always taking into account the need of automation of the analytical process. The final sampling conditions are reported in the experimental.

Unsupervised pattern recognition through heatmap and PCA showed groups related to smoky and non-smoky samples and evidenced 10 compounds that significantly correlated with smoky note (p-values <0.001 in the non-parametric Kruskal-Wallis test with $\alpha=0.05$), both for beans and liquors and not affected by the different origins of the samples: naphthalene (*pungent*), guaiacol (*smoky/phenolic/spice*), 2-methoxy-4-methylphenol (*sweet/smoky/medicinal*), phenol (*phenolic/rubbery*), 1H-pyrrole-2-carboxaldehyde (*musty*), p-ethylguaiacol (*smoky/phenolic/spice*), p-cresol (*phenolic/pungent*), 3-ethylphenol (*musty*), 2,6-dimethoxyphenol (*sweet/smoky/medicinal*), 4-methyl-2,6-dimethoxyphenol (*sweet/smoky/medicinal*) (Figure 2).

Quantitation of selected target smoky compounds was then performed in order to define an operative range in acceptance of samples. But a confirmatory method that is based on a reference standard material is not feasible due to the lack of a cocoa smoky reference standard. Furthermore, several smoky volatiles are also endogenous components in beans and even more so in liquors. On the other hand spiking methods, performed via the standard addition, would falsify the quantitation due to their non-homogeneous distribution in the cocoa products, because of the heterogeneous nature of the solid matrix. Therefore a Multiple headspace extraction (MHE) approach to quantify potential markers was applied. MHE consists in a stepwise quantitative approach based on dynamic gas extraction enabling to quantify the total amount of an analyte in a matrix and to overcome the matrix effect [5, 6].

Quantitation of the selected markers afforded to effectively define an acceptance operative range of 10 and 100 ng/g respectively for beans and liquors.

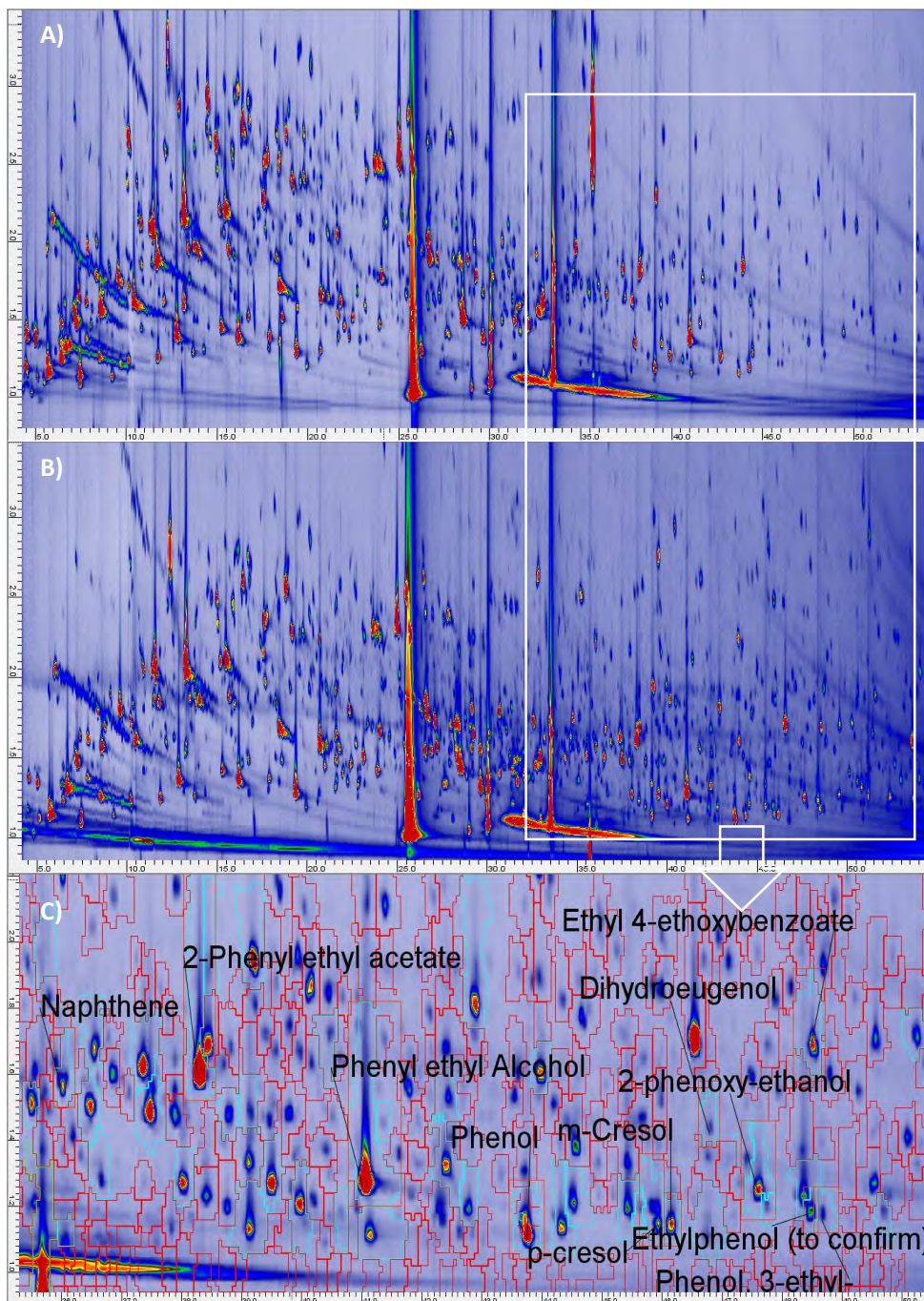


Figure 1: GCxGC-TOF-MS patterns of volatiles for non-smoky A) and smoky samples B); C) zoom of the aromatic and phenol region, with tentative identification.

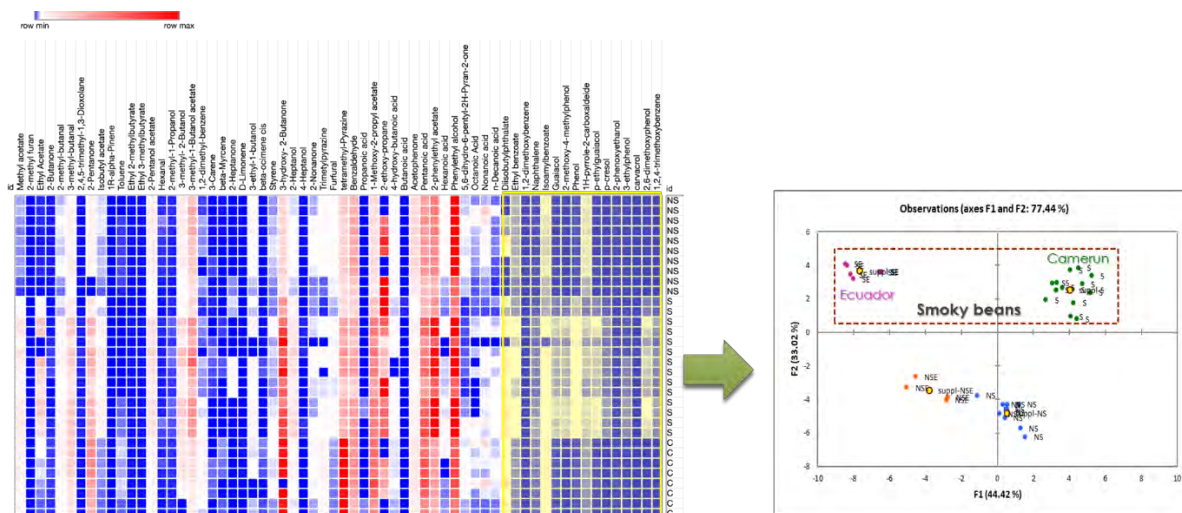


Figure 2: Heat-map of the HS-SPME-GC-MS volatile profiling of beans clustering by Spearman rank correlation, with the average linkage method. PCA scores plot of bean samples. Data matrix was transformed by Log10 and pre-processed through auto scaling both in PCA and in PLS-DA. SE: Smoky Ecuador, NSE: Non-smoky Ecuador; SC: Smoky Cameroon; NSC: Non-smoky Cameroon.

To meet the industry needs, in order to speed up the decision maker in quality control, a faster analytical procedure by MS-enose was applied. This strategy is based on the informative power of the diagnostics mass spectral fingerprints method, which, coupled with a suitable data mining, is exploited in developing an objective instrumental prediction tool useful for high throughput controls. But due to the low concentration of the smoky markers compared to the major volatiles, and the possible co-contribution of several different analytes to the fragment intensities in so complex fingerprints, the ability of the MS-enose in samples discrimination may not be so obvious.

We would like to verify whether the contribution of spectral masses of smoky volatiles is of sufficient diagnostic value to discriminate samples and whether this analytical approach, combined with mathematical model, can effectively be exploited as an analytical decision maker (ADM).

Different classification model algorithms were tested to classify beans and liquor samples. The evaluation in their prediction ability in discriminating smoked from non-smoked samples was performed on an external test set. From the confusion matrices, SIMCA models showed higher global prediction classification rate. In addition, the class specificity was very good and the sensitivity of the model for both classes was above 90% (Figure 3).

Ion fragments with higher discriminant power for smoky samples were m/z 152 and 154, which represent *p*-ethyl guaiacol ($m/z=152$) at 96% and 2,6-dimethoxyphenol ($m/z=154$) at 81% on the 1D-GC-MS chromatographic profile. The same variables and the additional m/z 107, 123, 137, 138 were diagnostic ions for isomers of phenol, methyl phenols (cresol isomers) and *p*-ethylguaiacol, whose abundance in the 1D-GC-MS chromatographic pattern of liquors for the above-cited volatiles was 62%. This means that class modelling is robust, and that only a very low percentage of samples should be investigated further by a confirmatory method or by a sensory panel to verify their acceptability.

External Test set misclassification: SIMCA				External Test set misclassification: PLS-DA			
	PredSmo@5	PredNoSmo@5	No match		PredSmo@5	PredNoSmo@5	No match
Actual Smo	9	0	1	ActualSmo	8	2	0
ActualNoSmo	0	13	1	ActualNoSmo	1	12	1
Unmodeled	0	0	0	Unmodeled	0	0	0
	<i>Sensitivity</i>	<i>Specificity</i>	<i>Total</i>		<i>Sensitivity</i>	<i>Specificity</i>	<i>Total</i>
Smo	90.0	100	91.6%	Smo	80.0	89	83.3
NoSmo	92.8	100		NoSmo	85.7	86	

External Test set misclassification: SIMCA				External Test set misclassification: PLS-DA			
	PredSmo@5	PredNoSmo@5	No match		PredSmo@6	PredNoSmo@6	No match
ActualSmo	8	0	0	ActualSmo	6	2	0
ActualNoSmo	1	31	0	ActualNoSmo	1	31	0
Unmodeled	0	0	0	Unmodeled	0	0	0
	<i>Sensitivity</i>	<i>Specificity</i>	<i>Total</i>		<i>Sensitivity</i>	<i>Specificity</i>	<i>Total</i>
Smo	100	89	97.5	CS1	75.0	86.0	92.5
NoSmo	96.8	100		NoSmo	96.8	94.0	

Figure 3: Confusion matrices of bean and liquor classification in prediction on an external test set, respectively for SIMCA and PLS-DA, together with sensitivity, specificity and correct classification rate values.

Conclusion

The top-down procedure applied afforded to define smoky cocoa markers exploiting the high informative power of the analytical approaches used combined with chemometrics. Sample preparation requires sensitivity and selectivity for the compounds responsible for the off-note. Several compounds related to the smoky off-note were identified and quantified to define an operative acceptance ranges for cocoa products. The MS-enose offers a further gain in time despite the compositional complexity of the cocoa volatiles. Based on a sensory-driven approach, an Artificial Smelling Machine [6] as an objective tool used as ADM in the rejection of smoky cocoa products was developed. Furthermore, the exploited system is versatile since it can be used for both a conventional setting for 1D-GC-MS and a MS-enose mode, and is therefore suitable for a high throughput, objective, and cost-effective multi-steps analytical control on the manufacturing chain of chocolate.

References

1. CABISCO/ECA/FCC. [http://www.cocoaquality.eu/data/Cocoa Beans Industry Quality Requirements Apr 2016_En.pdf](http://www.cocoaquality.eu/data/Cocoa%20Beans%20Industry%20Quality%20Requirements%20Apr%202016_En.pdf).
2. Frauendorfer F, Schieberle P. Identification of the key aroma compounds in cocoa powder based on molecular sensory correlations. *J Agric Food Chem.* 2006;54:5521
3. Magagna F, Guglielmetti A, Liberto E, Reichenbach S E, Allegrucci E, et al. Comprehensive chemical fingerprinting of high-quality cocoa at early stages of processing: effectiveness of combined untargeted and targeted approaches for classification and discrimination. *J Agric Food Chem.* 2017;65(30):6329–6341.
4. Bressanello D, Liberto E, Cordero C, Sgorbini B, Rubiolo P, Pellegrino G, Ruosi MR, Bicchi C. Chemometric Modeling of Coffee Sensory Notes through Their Chemical Signatures: Potential and Limits in Defining an Analytical Tool for Quality Control. *J Agric Food Chem.* 2018;66:7096–7109.
5. Sgorbini B, Cagliero C, Liberto E, Rubiolo P, Bicchi C, Cordero C. Strategies for Accurate Quantitation of Volatiles from Foods and Plant-Origin Materials: A Challenging Task. *J Agric Food Chem.* 2019;67:1619-1630.
6. Nicolotti L, Mall V, Schieberle P. Characterization of Key Aroma Compounds in a Commercial Rum and an Australian Red Wine by Means of a New Sensomics-Based Expert System (SEBES)-An Approach To Use Artificial intelligence in Determining Food Odor Codes. *J Agric Food Chem.* 2019;67:4011–4022.

Microwave sensor based on molecularly imprinted silica for the detection of phenylacetaldehyde in wine

ELIAS BOU-MAROUN¹, Jérôme Rossignol², Didier Stuerger², Philippe Cayot¹ and Régis D. Gougeon¹

¹ Univ. Bourgogne Franche-Comté, AgroSup Dijon, PAM, UMR A 02.102, Dijon, France
elias.bou-maroun@agrosupdijon.fr

² Univ. Bourgogne Franche-Comté, ICB, Dept Interface, GERM, CNRS UMR 6303, Dijon, France

Abstract

In this work, a microwave sensor having a molecularly imprinted silica (MIS) as sensitive material was developed to detect phenylacetaldehyde (PAA), a chemical indicator of wine oxidation. This real time method does not require any sample preparation and represents an alternative to expensive and tedious chromatographic methods. The methodology used to achieve this goal begins with the synthesis of several imprinted and non-imprinted silica (NIS). These MIS and NIS have been tested on their ability to extract PAA from hydro alcoholic medium and finally their selectivity toward PAA in the presence of competing molecules. The selected MIS was deposited on the surface of a microwave antenna and was used to detect PAA in red wine. The detection limit of the sensor is near the $\mu\text{g}\cdot\text{L}^{-1}$ level below the off-flavour threshold of PAA.

Keywords: Molecularly imprinted silica, microwave sensor, wine oxidation, phenylacetaldehyde, fast analysis

Introduction

Off-flavours, related to wine oxidation generate wine rejection and cause a significant economic loss in wine production. Aldehydes constitute a known family of aroma compounds associated with wine oxidation. Phenylacetaldehyde (PAA) can be considered as a chemical indicator of the oxidation level of a given wine [1]. Its odour threshold varies between 1 and 25 $\mu\text{g}\cdot\text{L}^{-1}$ depending on the matrix. It is important to have analytical tools able to detect PAA at a concentration below its odour threshold. The most used technics are gas chromatography coupled to mass detection. These targeted technics are highly efficient but relatively expensive, require a tedious sample preparation step and need high technical experience for the lab staff. A rapid, cheap and real-time analytical tool is essential to assess the level of wine oxidation.

Molecularly imprinted materials (MIM) are one of the most specific and selective materials used in analytical chemistry. They are biomimetic synthetic materials able to mimic the specific interactions between antigens and antibodies, hormones and receptors or substrates and enzymes. MIM have the big advantage of being stable in extreme conditions of pH and temperature in comparison with biological materials [2]. MIM have a low cost of production. They are used in this study to interact specifically with PAA. The use of microwave sensing in a broad range of frequency (10 Mhz to 20 GHz) provides a rich-information spectrum, allowing easy quantification of the target molecule in complex matrices such as wine [3].

In a previous work, we demonstrated the feasibility of such a MIS-sensor to detect a fungicide in wine model solution down to 0.33 $\text{ng}\cdot\text{L}^{-1}$ [4]. We present in this work the strategy used to develop a microwave sensor, having molecularly imprinted silica (MIS) as a sensitive material, able to detect PAA in wine below 1 $\mu\text{g}\cdot\text{L}^{-1}$ without any sample preparation.

Experimental

To select a molecularly imprinted silica (MIS) in order to integrate it in a microwave sensor, the following strategy was used: 1) Synthesis of five different MIS and their corresponding control, non-imprinted silica (NIS). 2) Batch extraction studies of PAA in hydro alcoholic medium by the five MIS and NIS in order to assess the sorption ability of the polymers. 3) Batch selectivity studies in hydro alcoholic medium where the MIS and NIS are contacted with PAA and other competing molecules.

Molecularly imprinted silica synthesis

MIS polymers were prepared at 40 °C in a thermostatic water bath under magnetic stirring. The template molecule was first solubilised in the solvent. Then, water was added, followed by the functional monomer and the crosslinker TEOS. Finally, NH_4OH or HCl was introduced. The reaction mixture was left under stirring for 20 h. The polymers were separated from the liquid phase by centrifugation at 10 000 g for 10 min at room temperature. In order to eliminate the template, polymers were washed several times with ethanol until it was no longer detectable by chromatography in washing solvents. After washing, polymers were dried for 6 h at 60 °C. In parallel,

NIS were synthesised under the same synthesis conditions as those of MIS, but without PAA, the template molecule. NIS served as control polymers.

Batch extraction studies of PAA in hydro alcoholic medium

The tested polymers were suspended in water/EtOH (90/10; v/v). A stock solution of water/ethanol with PAA was prepared at 400 mg.L⁻¹. Three concentrations were studied: 20, 80 and 200 mg.L⁻¹. Tests were done in 2 mL Eppendorf tubes in triplicate. In each tube, 1 mg of polymer (MIS or NIS) was contacted with PAA solutions at room temperature. The tubes were agitated in an orbital shaker for 2 hours at 20 rpm, then centrifuged 10 min at 15 000 g. 500 µL of supernatant was mixed with 500 µL of 1-octanol internal standard solution and analysed by Gas Chromatography Mass Spectrometry (GC-MS).

Batch selectivity studies in hydro alcoholic medium

The selectivity studies were performed the same way as the batch extraction study. PAA was replaced by a mixture of competing molecules: phenylacetaldehyde (PAA), Benzaldehyde (BA), 1-octen-3-one (1o3o) and 2-aminoacetophenone (AAP). The initial concentration of each of these molecules was 400 mg.L⁻¹. The partition coefficient (K_p) of each compound between the polymer and the hydro alcoholic medium was used to assess the selectivity. It was calculated using the following equation:

$$Kp = \frac{C_i - C_f}{C_f} \times \frac{V}{m}$$

Where C_i is the initial concentration of the target compound, C_f the concentration at equilibrium, V the solution volume and m the polymer mass.

Microwave sensor measurement

The microwave transduction is based on the electromagnetic wave excitation in a sensitive material inside a propagative structure (coplanar sensor) in the range of microwave (between 1 GHz and 8 GHz). The reflected and transmitted waves are determined using a Vector Network Analyser (VNA). The experimental setup (Figure 1) includes a portable VNA connected to a computer. The VNA and its cable (including the phase of calibration) are mechanically stable to avoid perturbations of the signal. The sensor was immersed in 100 mL of red wine alone (blank) or red wine supplemented with PAA. The concentration of PAA was varied using the standard addition method. The stock solution was prepared in water/EtOH (90/10; v/v) and was at 10 mg.L⁻¹.

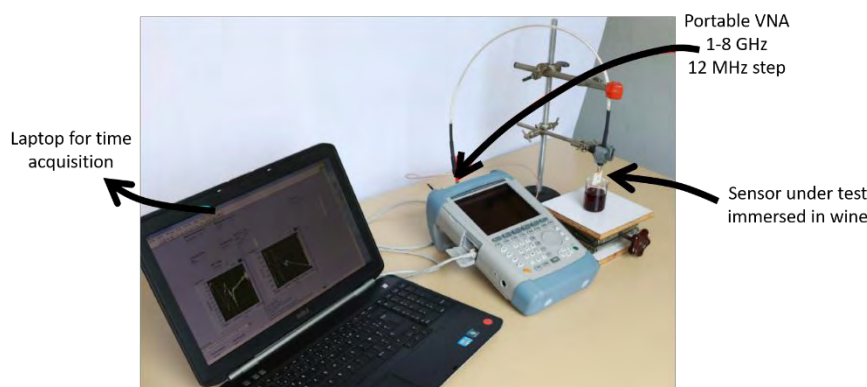


Figure 1: *Experimental setup of the microwave measurement test bench.*

After deposition of the MIS and the NIS on the microwave antenna using spin coating, the microwave sensor response at a specific frequency (f) was characterised by the reflection coefficient $\Gamma(f) = \text{Re}(f) + i\text{Im}(f)$. Re represents the real part of the coefficient and Im the imaginary part. The exploited signals were obtained from the relative variation of the reflection coefficient during the immersion in a sample, in comparison with the immersion in a reference blank solution (without target compounds). It was calculated from the following equation:

$$\frac{\Delta\Gamma}{\Gamma} = \frac{\Gamma(\text{sample}) - \Gamma(\text{blank})}{\Gamma(\text{blank})}$$

Transformation and logarithmic scaling was implemented on $\Gamma(f)$ coefficient giving:
 $A = 20\log(\sqrt{Re^2 + Im^2})$ where A represents the amplitude in dB.

Results and discussion

The synthesised polymers are presented in table 1.

Table 1: Experimental design for the synthesis of the five MIS/NIS.

	MIS1	MIS2	MIS3	MIS4	MIS5
FM	PATMS	APTMS	PATMS	PTMS	APTMS
C	TEOS	TEOS	TEOS	TEOS	TEOS
I	NH ₄ OH	NH ₄ OH	NH ₄ OH	NH ₄ OH	HCl
S	W/EtOH 50/50	W/EtOH 90/10	W/EtOH 90/10	W/EtOH 90/10	W/EtOH 90/10
Polymerisation	no	yes	yes	yes	yes

FM = functional monomer, C = Crosslinker, I = Initiator, S = Solvent, W/EtOH = Water/Ethanol, PATMS = Propylaniline trimethoxysilane, APTMS = Aminopropyl trimethoxysilane, PTMS = phenyl trimethoxysilane, TEOS = Tetraethoxysilane.

MIS1 was eliminated because polymerization did not occur. MIS2 was eliminated because parasitic reaction occurred between the amine group of APTMS and the aldehyde function of phenylacetaldehyde.

A batch extraction of phenylacetaldehyde by all the polymers was done in hydro alcoholic medium. The selectivity study was done in hydro alcoholic medium in the presence of phenylacetaldehyde and 3 competing molecules. Results of the batch extraction and the selectivity study are shown in figure 2A and figure 2B respectively.

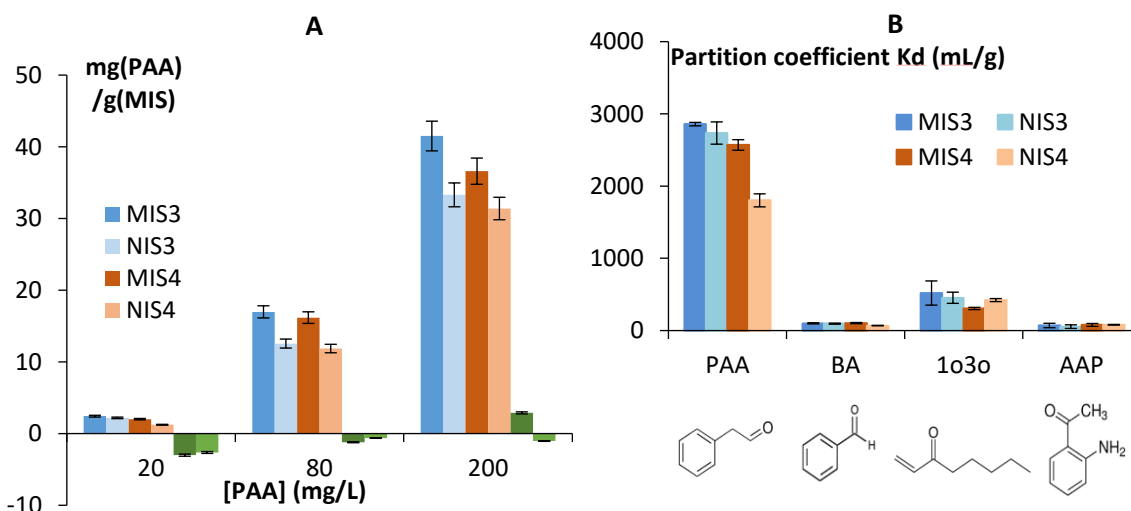


Figure 2: A) Adsorbed PAA/g of polymer vs initial concentration in water/EtOH (90/10; v/v). B) Partition coefficient in water/EtOH (90/10; v/v). Phenylacetaldehyde (PAA), Benzaldehyde (BA), 1-octen-3-one (1o3o) and 2-aminoacétophenone (AAP).

In figure 2A, the quantity of adsorbed phenylacetaldehyde is expressed as a function of the initial concentration. Polymer 5 was eliminated because it gave the smallest adsorption of phenylacetaldehyde. Polymers 3 and 4 were kept for the selectivity study. The values of partition coefficient between the initial solution and the polymer are presented in figure 2B. Both MIS3 and MIS4 gave high partition coefficient for PAA in comparison with competing molecules. They are then selective to PAA. In the case of PAA, the difference between MIS4 and NIS4 was higher than the one between MIS3 and NIS3. MIS4 was selected in order to be used in the microwave sensor.

After the deposition of the imprinted and the non-imprinted polymers (MIS4 and NIS4) on the surface of the microwave sensor, the microwave signal was measured at different concentrations of phenylacetaldehyde in hydro alcoholic medium (Figure 3A) and in red wine (Figure 3B).

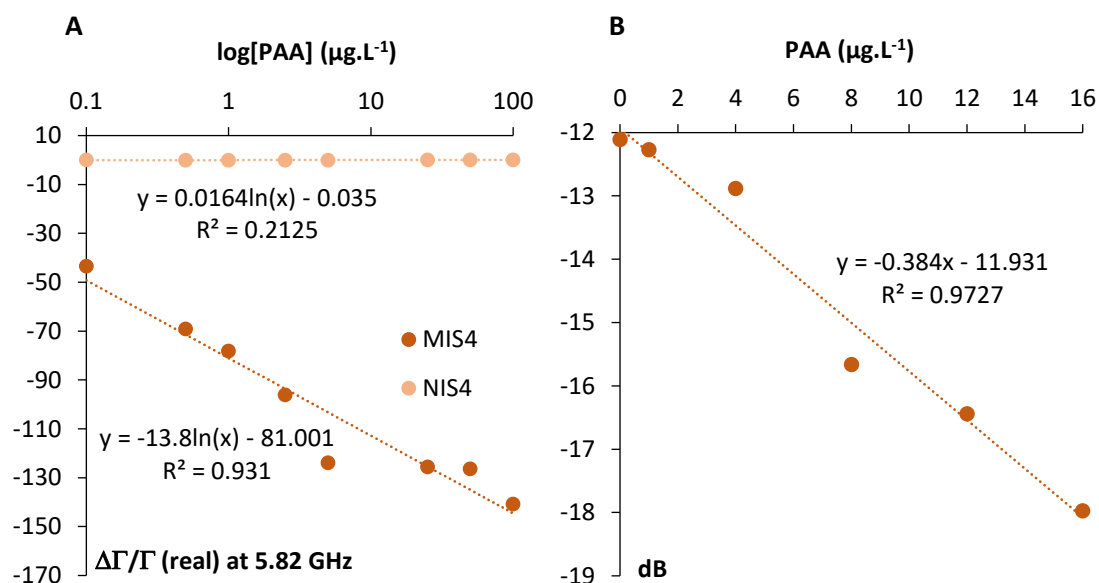


Figure 3: A) Effect of PAA concentration on the response of the MIS/NIS-microwave sensor in water/EtOH (90/10; v/v). Uncertainty on $\Delta\Gamma/\Gamma = 0.1\%$. B) Effect of PAA concentration on the response of the MIS-microwave sensor in red wine. Uncertainty on dB = 1%. The correlation coefficients for linear correlation in A and B are over the critical values of the Pearson's correlation coefficient in a one-tailed test at the level of significance of 1%. For A (8 points, 6 degree of freedom), $R_{\text{critical value}} = 0.789 < R_{\text{observed}} = 0.965$; for B (6 points, 4 degree of freedom), $R_{\text{critical value}} = 0.882 < R_{\text{observed}} = 0.986$.

The MIS based sensor shows a linear response in hydro alcoholic medium for PAA concentrations between 0.1 and 100 $\mu\text{g.L}^{-1}$. The NIS based sensor response is independent of phenylacetaldehyde concentration. This result shows that the molecular imprinting was efficient. In red wine, the microwave signal (amplitude) is proportional to PAA concentration between 1 and 16 $\mu\text{g.L}^{-1}$. Molecularly imprinted based sensors are thus able to detect phenylacetaldehyde in red wine at the $\mu\text{g.L}^{-1}$ level below the off-flavour threshold.

Conclusion

One of the main organoleptic defect in wine is oxidation. Phenylacetaldehyde is a good chemical indicator of the oxidation level. Its odour threshold varies between 1 and 25 $\mu\text{g.L}^{-1}$. The classical method of phenylacetaldehyde assessment is gas chromatography coupled to mass spectrometry. GC-MS is time consuming and expensive. In this work, a microwave sensor having as sensitive material a molecularly imprinted silica was developed as a fast and cheap method for the analysis of PAA. The developed microwave sensor was able to detect PAA in red wine at the $\mu\text{g.L}^{-1}$ level.

References

1. Bueno M, Culleré L, Cacho J, Ferreira V. Chemical and sensory characterization of oxidative behavior in different wines. *Food Res Internat.* 2010;43(5):1423-8.
2. Svenson J, Nicholls IA. On the thermal and chemical stability of molecularly imprinted polymers. *Anal Chim Acta.* 2001;435(1):19-24.
3. Rossignol J, Dujourdy L, Stuerger D, Cayot P, Gougeon RD, Bou-Maroun E. A First Tentative for Simultaneous Detection of Fungicides in Model and Real Wines by Microwave Sensor Coupled to Molecularly Imprinted Sol-Gel Polymers. *Sensors.* 2020;20(21):6224.
4. Bou-Maroun E, Rossignol J, De Fonseca B, Lafarge C, Gougeon RD, Stuerger D, Cayot P. Feasibility of a microwave liquid sensor based on molecularly imprinted sol-gel polymer for the detection of iprodione fungicide. *Sens Actuators B.* 2017;244:24-30.

Impact of processing and storage on changes in the volatile compounds of whole chickpeas: an untargeted headspace fingerprinting study

LAURA E. C. NOORDRAVEN, Carolien Buvé, Chao Chen, Marc E. Hendrickx and Ann M. Van Loey

KU Leuven, Laboratory of Food Technology, Leuven Food Science and Nutrition Research Centre (LForCe), Department of Microbial and Molecular Systems (M²S), Leuven, Belgium, laura.noordraven@kuleuven.be

Abstract

In the present research the impact of processing (soaking, cooking and sterilisation) and oxygen availability during storage (up to 40 weeks at 20 °C) on the volatile compounds in whole chickpeas was investigated. Volatile profiles of the differently processed chickpeas were obtained and compared. Soaking resulted in an increased number of aldehydes and alcohols, while thermal processing (e.g. cooking and sterilisation) originated compounds like furan derivatives, sulphur compounds and aromatic compounds. More hydrocarbons, ketones and sulphur compounds were formed in sterilised chickpeas after storage at higher oxygen availability, while more alcohols were present in the chickpeas stored at lower oxygen availability. The results showed that both processing and oxygen availability during storage significantly affected the volatile profile of intact chickpeas.

Keywords: *Cicer arietinum L.*, volatile analysis, HS-SPME-GC-MS, untargeted fingerprinting approach, MVDA

Introduction

Aroma is an important attribute that can partly determine the sensory shelf life of shelf-stable food products and thus can influence their marketability. Legumes, such as chickpeas, have become increasingly important in the last few years but are often associated with an unfamiliar and unpleasant ‘beany’ aroma. The volatiles classified as contributing to this ‘beany’ aroma can be formed at different stages in the pulse processing chain. Chickpeas are most commonly available as processed ready-to-eat chickpeas. Yet, the volatile compounds in whole processed chickpeas and their evolution during storage are only very scarcely described in scientific literature. Therefore, in this study the headspace volatile components in differently processed chickpeas as well as in chickpeas stored between 0 and 40 weeks, in different packaging materials, were investigated.

Experimental

Preparation of soaked and cooked chickpeas

Dried kabuli chickpeas were soaked for 16 hours in an excess of demineralised water to obtain the ‘raw, soaked chickpeas’. These chickpeas were cooked in semi-closed recipients in a water bath at 95 °C for 40 min to obtain the ‘home-cooked chickpeas’. In order to obtain the industrially ‘sterilised chickpeas’, the same chickpeas were soaked in standardised production water and consecutively sterilised at 116 °C in a Steriflow pilot retort (Barriquand, Paris, France) to obtain a F₀-value of 15.6 min. Two types of pouches were used during sterilisation, aluminium and plastic pouches, with an oxygen permeability of 0.05 and 1 cm³/(m²day.bar), respectively. The sterilised chickpeas were stored at 20 °C and samples were taken at 12 time points between 0 and 40 weeks (sampling weeks: 0, 1, 2, 3, 4, 8, 12, 16, 20, 24, 28, 32, 40). At the specific sampling points, pouches were opened and chickpeas (without aquafaba) were transferred into odourless tubes, frozen and stored at -40 °C until analysis.

HS-SPME-GC-MS fingerprinting

All samples were analysed using an untargeted headspace solid-phase micro extraction-gas chromatography (HS-SPME-GC-MS) fingerprinting approach, adapted from Kebede *et al.* [1] and Vervoort *et al.* [2].

Chickpeas were mashed with demineralised water (ratio dry chickpea to water 1:3.4) using an Ultra-Turrax T25 (Janke & Kunkel, IKA Labortechnik, Staufen, Germany) at 8000 rpm for 1 min. 3 ± 0.05 g chickpea puree and 3 ml saturated NaCl solution were added to amber glass vials (20 ml, Macherey-Nagel, Düren, Germany). A GC (Agilent Technologies, Santa Clara, CA, United States) coupled to an MSD 5977A (Agilent Technologies, Santa Clara, CA, United States) was used to analyse the volatiles and six replications per sample were analysed. Samples were incubated and extracted at 40°C for 30 and 40 minutes, respectively, under 500 rpm agitation. Desorption took place at 230 °C for 2 minutes at the GC inlet where a splitless injection was performed. The GC was equipped with a capillary HP Innowax column (60 m x 250 µm x 0,25 µm, Agilent Technologies, Santa

Clara, CA, United States) with helium as the carrier gas at a constant flow of 1.1 ml/min and a pressure of 124.9 kPa. The temperature profile of the GC oven consisted of a holding step (40 °C, 2 min), a first heating ramp (40 °C to 80 °C at 3 °C/min), a second holding step (80 °C, 1 min), a second heating ramp (80 to 220 °C at 6 °C/min) and a final heating ramp (220 to 250 °C at 50 °C/min). MS detection was obtained in electron ionisation mode at 70 eV with a scanning range of 35 – 400 m/z and a scanning speed of 3.8 scans per second. The MS ion source and quadrupole were 230 °C and 150 °C, respectively.

Data analysis

GC-MS fingerprinting data were analysed using the multivariate data analysis (MVDA) approach as described by Kebede *et al.* [1] and Vervoort *et al.* [2], to obtain PLS and PLS-DA models and to calculate variable identification coefficients (VID). Depending on the volatile data, volatiles with an |VID| value between 0.7 or 0.8 to 1.0 were considered as discriminant components for a certain class of samples (PLS-DA models) or to be significantly changing over shelf life (PLS models). To identify the volatile components, the spectral library of NIST (NIST14, version 2.2, National Institute of Standards and Technology, Gaithersburg, MA, USA) was used as well as comparison of retention indices to those reported in literature or obtained by analytical standards.

Results and discussion

Impact of processing method on chickpea volatiles

A total of 121, 72 and 109 volatiles were found in the headspace of the soaked, cooked and sterilised chickpeas, respectively. A PLS-DA model with 2 LVs was obtained, explaining 99.8% of the Y-variance. In Figure 1, a biplot of this PLS-DA model explaining the difference between the three processing conditions on the volatile compounds is shown. In this biplot the differently processed samples are denoted as the coloured objects, the volatile compounds as the open circles. The vectors represent the correlation loadings of the classes (processing conditions). From the biplot it is clear that processing conditions significantly impacted the volatile profile of chickpeas, as the three different classes are clearly separated.

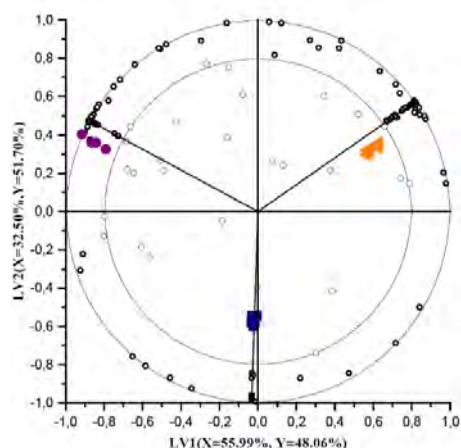


Figure 1: Biplot (LV axes 1 vs 2) of the PLS-DA conducted on the volatile profile of raw (soaked) (●), cooked (■) and sterilised (▲) chickpeas. Volatile components are represented as open circles and markers with |VID|>0.8 are represented in bold. The vectors represent the correlation loadings for the Y-variables (classes). The outer and inner circles on the biplot represent the correlation coefficient of 1.0 and 0.8 respectively, indicating the area where the volatiles that are characteristic for a certain class are present.

Discriminant compounds were determined for the different classes using the VID criterion (|VID|>0.8), indicating that these compounds were present in higher (positive value) or lower (negative value) concentration in a certain class compared to the other classes. These discriminant compounds are presented as the bold open circles in Figure 1. For the soaked, cooked and sterilised chickpeas, 66, 13, and 53 discriminant components with a positive and 2, 12, and 5 discriminant components with a negative VID coefficient were found, respectively. Of these components, 43, 5, and 31 of the discriminant components with a positive and 2, 7, and 2 of the discriminant components with a negative VID coefficient could be (tentatively) identified, respectively.

In raw, soaked chickpeas the identified discriminant components with a positive VID coefficient consisted mainly of aldehydes (45%) and alcohols (30%). Possibly, these compounds resulted from enzymatic lipid breakdown in the chickpeas during the soaking step or at the beginning of the supply chain, prior to drying of the chickpeas. In raw chickpeas, aldehydes and alcohols have previously been described to be the most abundant volatile classes [3] and these types of compounds can potentially be associated with a ‘beany’ type of aroma [4].

In contrast, in the thermally processed chickpeas (i.e. cooked and sterilised), other volatile classes were present at higher concentrations. In the cooked chickpeas, two sulphur compounds, a furan derivative, an organic compound and an alcohol were found. High intensity processing (sterilisation) mainly resulted in more aromatic compounds (23%) and furan derivatives (19%). The sulphur compounds potentially resulted from degradation of sulphur containing amino acids during cooking, the aromatic compounds from lipid oxidation or degradation of aromatic amino acids, while furan derivatives potentially formed during the early stages of Maillard reactions [5].

Impact of oxygen availability during ambient storage on chickpea volatiles

Headspace volatiles of the sterilised chickpeas stored in both aluminium and plastic pouches were analysed at several time points between 0 and 40 weeks. PLS models with 3 and 4 LVs were obtained, explaining 94.7% and 96.3% of the Y-variance for chickpeas stored in the aluminium and plastic pouches, respectively. Biplots of the first two LVs of the PLS models on the volatile profile of these samples are shown in Figure 2. In these biplots, the samples stored at different time points are presented as the coloured objects, the volatiles as the open circles and the volatiles significantly changing over time are presented as the bold open circles. The vectors represent the correlation loading for the Y-variables (time). In total, 121 volatiles were found in the chickpeas stored in the aluminium pouches, 156 in the chickpeas stored in the plastic pouches. The higher number of volatiles formed in the plastic pouches is probably caused by an increased amount of oxidation reactions during storage due to the higher oxygen permeability of this packaging material.

Comparing the two biplots, some differences can be observed. In the biplot of the aluminium pouches (Figure 2A), the first LV is explaining the major part of the effect of storage time, as a clear chronological trend is found from the left to the right in the biplot. In this biplot, most of the volatile compounds were located closer to the centre of the biplot. This indicates that most volatiles did not significantly change during the storage period of 40 weeks. In the biplot of the chickpeas stored in plastic pouches, a less clear chronological trend is observed in the biplot, indicating that the volatile profile of the chickpeas stored in the plastic pouches were not largely affected by storage time either. However, based on the VID criterion ($|\text{VID}| > 0.7$), in both chickpeas stored in the different packaging materials, some compounds were found to be significantly changing during storage time.

At lower oxygen availability, acetyl thiazole significantly decreased during storage time, while ethyl acetate significantly increased. At higher oxygen availability, different changes took place. Methyl benzaldehyde decreased over time and methyl cyclohexane increased over time. This indicates that the oxygen availability related to packaging permeability during storage not only changed the amount of chemical reactions, but also the type of chemical reactions taking place.

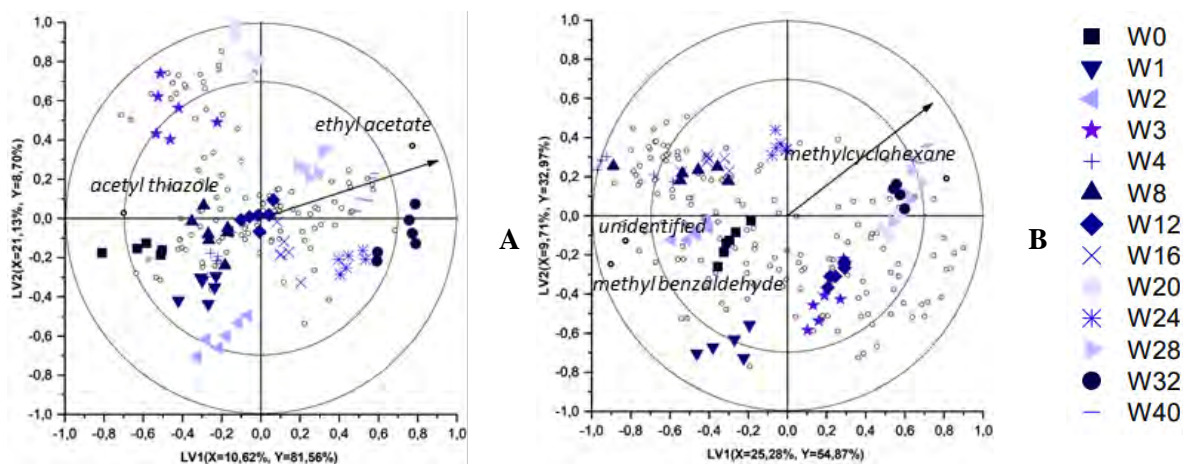


Figure 2: Biplots (LV axes 1 vs 2) of the PLS models representing volatile changes of chickpeas stored in aluminium (A) and plastic (B) pouches. Volatile components are represented as open circles and markers with $|\text{VID}| > 0.7$ are represented in bold. The vectors represent the correlation loadings for the Y-variable (time). The outer and inner circles on the biplot represent the correlation coefficient of 1.0 and 0.7 respectively, indicating the area where volatiles changing significantly during storage are present. W=weeks of storage.

In order to investigate the differences in the volatile changes at different oxygen availability in more detail, the headspace volatiles of chickpeas stored in aluminium and plastic pouches for 0 weeks and 40 weeks were compared. A PLS-DA model with 4 LVs, explaining 95.9% of the Y-variance was obtained. A biplot of the first two LVs of the PLS-DA model is presented in Figure 3. Four classes can be seen in this biplot. In the chickpea samples at the beginning of storage (0 weeks), for the aluminium and plastic pouches, 12 and 3 discriminant compounds with a positive and 5 and 7 discriminant compounds with a negative VID coefficient were found, respectively ($|\text{VID}| > 0.7$). These compounds consisted of an aromatic compound and an aldehyde for the plastic pouches, and for the aluminium pouches, they mostly consisted of aromatic compounds (40%) and of sulphur

compounds (30%) formed during the sterilisation process. These results indicate that, even though the samples had undergone the same sterilisation process, the oxygen permeability of the pouches impacted the volatile profile of the sterilised chickpeas during the process. After a 40-week storage period, the volatiles profiles of the chickpeas stored in the different packaging materials were more different from each other. In the plastic pouches, the discriminant compounds present in higher concentrations were mainly hydrocarbons (33%), ketones (22%) and sulphur compounds (22%), the former two probably resulting from lipid oxidation during storage at higher oxygen availability. In contrast, the chickpeas stored in the aluminium pouches showed a higher concentration of alcohols (33%) compared to the other samples. Probably more alcohols were found in these samples, because less oxidation of alcohols to other compounds, like ketones, took place at lower oxygen availability [6]. This figure also confirms the storage effect for a given packaging.

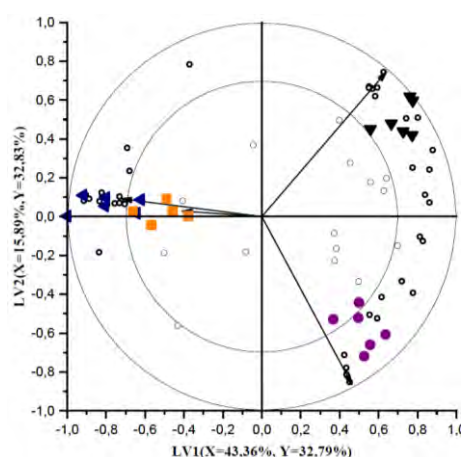


Figure 3: Biplot (LV axes 1 vs 2) of the PLS DA-model on the volatile profile of chickpeas sterilised and stored for 0 weeks (plastic (■), aluminium (◄)) and 40 weeks (plastic (▼), aluminium (●)). Volatile components are represented as open circles and markers with $|VID| > 0.7$ are represented as bold circles. The vectors represent the correlation loadings for the Y-variables (classes). The outer and inner circles on the biplot represent the correlation coefficient of 1.0 and 0.7 respectively, indicating the area where the volatiles that are characteristic for a certain class are present.

Conclusion

It was concluded that processing conditions significantly influence the volatile profile of whole chickpeas. Since the soaked chickpeas were found to contain more ‘beany’ related compounds, it could be stated that thermal treatment can potentially be used to contribute to a more pleasantly perceived chickpea aroma. However, additional sensory testing needs to be performed to confirm which processing conditions give the most desirable aroma.

Moreover, it was concluded that oxygen availability, depending on permeability of the packaging material, significantly impacts the volatile profile of chickpeas during a 40-week storage period at 20 °C. However, additional sensory testing is required to understand if these volatile differences are actually observed by the consumer and if so, which packaging material is most desirable.

Acknowledgement

This research project is part of the FOODENGINE project and has received funding from the European Union’s Horizon 2020 Research & Innovation Programme under the Marie Skłodowska-Curie Grant Agreement No. 765415.

References

1. Kebede B. T., Grauwet T., Palmers S., Vervoort L., Carle R., Hendrickx M., & Van Loey A. Effect of high pressure high temperature processing on the volatile fraction of differently coloured carrots. *Food Chem.* 2014;153:340-352.
2. Vervoort L., Grauwet T., Kebede B. T., Van der Plancken I., Timmermans R., Hendrickx M. & Van Loey A. Headspace fingerprinting as an untargeted approach to compare novel and traditional processing technologies: A case-study on orange juice pasteurisation. *Food Chem.* 2012;134(4):2303-2312.
3. Khrisanapant P., Kebede B., Leong S. Y. & Oey I. A comprehensive characterisation of volatile and fatty acid profiles of legume seeds. *Foods.* 2019;8(12):651.
4. Vara-Ubol S., Chambers E. & Chambers D. H. Sensory characteristics of chemical compounds potentially associated with beany aroma in foods. *J Sens Stud.* 2004;19(1):15-26.
5. Diez-Simon C., Mumm R. & Hall R. D. Mass spectrometry-based metabolomics of volatiles as a new tool for understanding aroma and flavour chemistry in processed food products. *Metabolomics.* 2019;15(3):1-20.
6. Taylor A. J., Linforth R. S. T. *Food Flavour Technology*; 2004; Vol. 23.

Assessment of champagne glass geometries - Dynamic head space sampling of champagne aromas

Per Malmberg and JAN OLOF SVENSSON

Analytical Chemistry, Division of Chemistry and Biochemistry, Chalmers University of Technology, Gothenburg, Sweden, jansvens@chalmers.se

Abstract

Enjoying a glass of champagne where the evolution of aromas is carried by the wine's effervescence in a process changing over time is a challenging phenomenon to characterise using instrumental analysis.

A time-resolved instrumental analysis set-up using desorption liners in combination with gas chromatography-mass spectrometry (GC-MS) was successfully used to characterise aroma evolution from different champagne glass geometries as a function of time.

The present work showed that by using thermal desorption technique it is possible to characterise aroma evolution from different champagne glass geometries as a function of time.

Keywords: wine aroma, champagne, aroma release, dynamic sampling

Introduction

Glass vessels for drinking have been used and discussed at least since the days of Pliny (23-79 AD), but the importance of glass geometries for the hedonistic enjoyment of wine has been out of focus until rather recently. Most research activities have been assessing orthonasal olfaction using trained or untrained sensory panels [1, 2], and only a limited amount of research has been focusing on the chemical composition of the headspace in a wineglass using chemical analysis [3].

Many identifications and quantifications have been based on a steady state sampling situation, often using Solid Phase Micro Extraction (SPME) techniques with long sampling times. This will assess a situation far from the real-life situation when enjoying a glass of champagne, where the evolution of aromas is carried by the wine's effervescence in a process changing over time. Hence a dynamic analytical approach is needed to evaluate the evolution over time.

Experimental

Material and method

Champagne *Duménil Brut Premier Cru*, 2008 (part 1) and *Veuve Clicquot Brut NV* (part 2).

Glass Richard **Juhlin** champagne glass (*Reijmyre, Sweden*), **Grand Cru** champagne (*Skruf, Sweden*), both of flute shape and **ICA** supermarket champagne glass, of cylinder shape without tapered opening.

Equipment and method The aroma air samples (240 mL) were collected at the mouth of the champagne glasses onto desorption liners for a Thermal Desorption Unit (*Gerstel, Mülheim an der Ruhr, Germany*) packed with Carboxen 100 and Carbosieve III of 4 mm inner diameter, using a plastic syringe.

The adsorbed aroma components were subsequently thermally desorbed by heating the liner (30 to 285 °C (120 °C/min), 10 min hold) into a cryo-cooling trap (-30 °C) using Tenax TA liner and then rapidly heated (to 275 °C, 12 °C/sec) hold 4 sec) to inject the sample into a gas chromatograph (Agilent 7890B, *Agilent Technologies Inc. USA*) equipped with a HP-5MS UI column (*Agilent J&W*, 30 m x 0.25 mm x 25 µm), He carrier gas at 1 mL/min, temperature program from 35 to 210 °C (4 /min) then to 275 °C (20.0 °C/min) connected to a QTOF mass spectrometer operated in EI mode (70 eV), scan range 35-500, 200 ms/spectrum using a solvent delay of 3 min, using quench gas (He) and collision gas (N₂). The data were analysed using Masshunter software (*Agilent Technologies Inc. USA*) and NIST/EPA/NIH EI-MS library.

Experimental

The investigations presented were performed in subsequent steps, in order to refine the experimental set-up and to study different aspects of aroma evolution.

Part 1. An initial comparison was performed using **ICA** and **Juhlin** glasses (n=1). Aliquots of champagne were poured, and headspace air samples (240 mL at a sampling rate of approx. 120 mL/min) were withdrawn after 30

and 90 minutes. In order to facilitate the data evaluation some aroma marker compounds were selected and monitored (ethyl acetate, 3-methyl-butanol, ethyl hexanoate, ethyl octanoate).

Part 2. In the subsequent part, the temporal evolution, shortly after pouring, was studied using the **Grand Cru** glass (n=1) in order to illustrate the role of the effervescence as an aroma carrier. Two minutes after pouring, four samples were withdrawn directly after each other using same volume but at a slower flow rate as compared to study part 1 (240 mL at a sampling rate of approx. 60 mL/min). By the time of withdrawing the fourth sample, the initially brisk effervescence had ceased considerably.

The aroma marker compounds ethyl butanoate, ethyl hexanoate, ethyl octanoate, and ethyl decanoate were selected and monitored.

Results and discussion

Part 1. It was found that the flute shaped champagne glass gave slightly higher amounts of some selected aroma components as compared to the basic supermarket cylindrical shaped champagne glass, see Figure 1.

The time-resolved air sampling indicated that the two glasses gave rise to somewhat different aroma development. This illustrates possible effects of glass shapes on the aroma development over time in a poured glass of champagne.

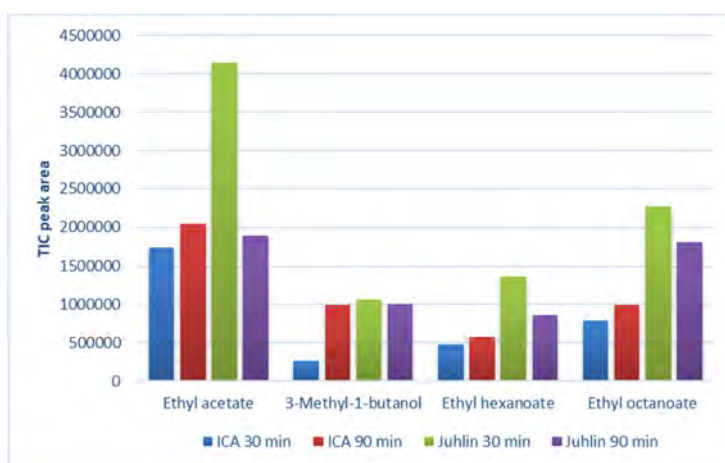


Figure 1. Aroma evolution in ICA and Juhlin champagne glasses, sampled at 30 and 90 minutes after pouring.

Part 2. The four consecutive samples showed a decay of the selected aroma components after an initial partial increase, see Figure 2.

The overall aroma decay coincided with the effervescence decay, thus indicating the role of effervescence as aroma carrier. A blank sample from ambient atmosphere was also collected, showing no detectable levels of aroma components.

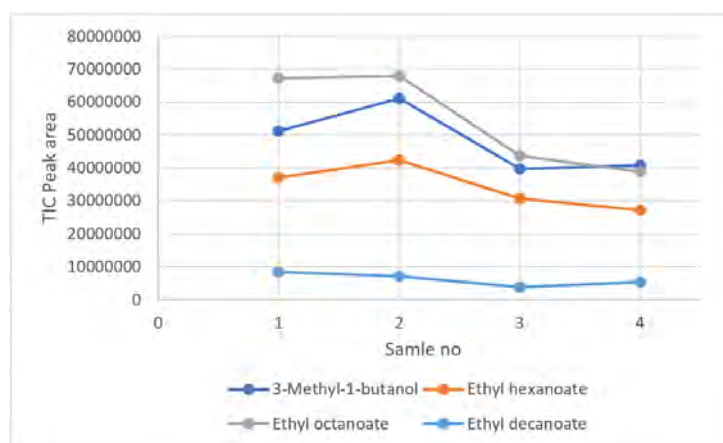


Figure 2: Aroma evolution in *Grand Cru* champagne glass over time.

Considerations

The variability of the results found during method development indicates that an improved sampling procedure would be beneficial. By slightly increasing the diameter of the sampling tube (i.e., the desorption liner opening) a sampling set-up closer to the human orthonasal olfaction situation could be obtained. In combination with a further reduced sampling flow rate and sampling volume, the risk of local depletion of analytes during the air sampling would be reduced. In order to obtain more robust datasets and to draw more firm conclusions, automating the air sampling and thus increasing the number of samples withdrawn would be beneficial.

Conclusion

Enjoying a glass of champagne where the evolution of aromas is carried by the wine's effervescence in a process changing over time is a challenging phenomenon to characterise using instrumental analysis. The concentration levels of the relevant aroma compounds are challengingly low and the available air volume to sample is limited.

However, the presented work indicates that by using thermal desorption technique in combination with GC/MS it is possible to characterise aroma evolution from different champagne glass geometries as a function of time.

References

1. Cliff A M. Influence of wine glass shape on perceived aroma and colour intensity in wines. *J Wine Res.* 2001;12(1):39-46.
2. Delwiche J and Pelchat M. Influence of glass shape on wine aroma. *J Sens Stud.* 2002;17:19-28.
3. Hirson G, Heymann H, & Ebeler S. Equilibration time and glass shape effects on chemical and sensory properties of wine. *Am J Enol Vitic.* 2012;63:515-521.

Untargeted or targeted analysis? Application to craft beer and gin

Cody Williams^{1,2}, Mpho Mafata^{1,3} and ASTRID BUICA¹

¹South African Grape and Wine Research Institute, Department of Viticulture and Oenology, Stellenbosch University, Stellenbosch 7600, South Africa, abuica@sun.ac.za, astrid.buica@gmail.com

²Department of Biochemistry, Stellenbosch University, Stellenbosch, 7600, South Africa

³School for Data Science and Computational Thinking, Stellenbosch University, Stellenbosch, 7600 South Africa

Abstract

Terpenoids represent an important class of aroma compounds present in beer and gin. The complexity of terpenoids and the variable nature of craft beer and gin makes the analysis of these matrices challenging. This is corroborated by the lack of literature for these applications and provides rationale for the current investigation. A novel terpenoid method for the analysis of beer and gin by online HS-SPME-GC-MS was developed. To the best of our knowledge, this method contains the highest number of terpenoids quantified in a single method (*i.e.* 53 compounds). In addition, a non-targeted online HS-SPME-GC-MS method was developed and applied to the same samples to fingerprint their volatile profiles. Unsupervised multivariate analysis (PCA and HCA) was applied to both targeted and non-targeted datasets, while heatmaps were used to illustrate a snapshot of the terpenoid analysis results. The work presented is part of a larger study evaluating the chemical spaces created through targeted and non-targeted analyses and comparing if there is any loss of significant information when using targeted vs non-targeted strategy for beer and gin aroma profiling.

Keywords: terpenoids, beer, gin, metabolomics, multivariate statistics

Introduction

Classically, targeted analysis have been used to quantify specific analytes of interest, but this approach may result in loss of potentially important information. In order to compensate, non-targeted analysis is often used to profile the sample and obtain more information. However, the process of acquiring more information also results in more chemical noise. Both targeted and non-targeted strategies are subject to their own limitations.

Terpenoids are by nature isoprenoids and further classified into monoterpenoids, sesquiterpenoids or norisoprenoids based on their chemical structure. Terpenoids and their oxygenated derivatives are either derived from biosynthetic pathways or via oxidative degradation of diterpenes and carotenoids [1, 2]. The vast array of these compounds, their low concentration and complex matrices, make the extraction and analysis of terpenoids particularly challenging. Previous work looked at the comparison of two sample preparation methods for the extraction of terpenoids in wine [3]. To extend the scope of this study further and to test its applicability, gin and beer were selected as matrices and a modified method was applied to quantify the terpenoids present. In addition, a non-targeted screening headspace-solid phase microextraction-gas chromatography-mass spectrometry (HS-SPME-GC-MS) method was applied to the same beer and gin samples. The results were subjected to unsupervised multivariate analysis to understand the chemical space obtained through non-targeted and targeted analysis. The aim of this work was to explore the information related to the aroma space configuration when using the targeted vs non-targeted strategy as applied to craft beer and gin.

Experimental

General

Commercially available craft beer ($n = 34$, of which 19 ale-style and 15 lager-style according to the labels) and gin samples ($n = 21$, of which 14 produced in South Africa, 4 in Italy, and 3 in the USA) were used in this pilot study. Gin samples were diluted 5-fold with deionised water before analysis using either targeted or non-targeted HS-SPME-GC-MS methods. Beer samples were analysed without any sample pre-treatment unless stipulated. All chemicals, standards and materials used were according to the literature [3]. Beer samples are coded as (producer code)_(product name code) and gin samples as (producer code)_(country of origin)_(product name code). For example DP_IPA stands for the Imperial Pale Ale produced by DP, while SGB_SA_OF stands for Original Fynbos gin from South Africa, produced by Sugarbird (SGB).

Targeted - Terpenoids

To a 20 mL headspace vial, 2g NaCl were added. Either 10 mL of beer or 2 mL gin (with 8 mL deionised water) were added, followed by 100 μ L of internal standard solution (10 mg/L of 3-octanol and 2,6-dimethyl-6-hepten-2-ol). Samples were hermetically sealed, vortexed until NaCl dissolution before analysis by HS-SPME-GC-MS. GC-MS instrument parameters and extraction conditions were according to the literature [5].

Non-Targeted - Screening

The screening method [6] was used with some modifications to allow for the analysis of the volatile profile of the respective matrices. Extracted data were converted to AIA format and analysed using an online metabolomics platform, XCMS online. Normalised and retention time aligned data were extracted from this platform and subjected to multivariate analysis.

Data Analysis

The data from targeted and non-targeted analysis were analysed using MassHunter qualitative (B.07.00) and quantitative (B.07.01) workstation software. In addition, XLSTAT 2019 (Addinsoft SARL, New York, NY, USA) was used to generate the principal component analysis (PCA), hierarchical cluster analysis (HCA) and corresponding heatmaps for the beer and gin data sets.

Results and discussion

In order to establish a comparison between the chemical spaces of non-targeted vs targeted methodologies, two proprietary analytical methods were developed [5, 6]. The targeted terpenoid method quantified 53 terpenoids in a single method; based on their chemical structure, the compounds were monoterpene hydrocarbons, monoterpene carbonyls, monoterpene alcohols, sesquiterpenes, sesquiterpene oxides, cineoles, aryl terpenes, and norisoprenoids. The total terpenoid concentrations for gin ranged from 149 – 192083 μ g/L. Notably, MFY and BLM gins contained the highest concentrations of total terpenoids at 69715 μ g/L and 48711 μ g/L respectively. In contrast, the INR and LGN contained the lowest concentrations at 8260 and 15658 μ g/L, respectively. For the MFY, BLM, INR and LGN samples, the highest contributors to the total terpenoid concentrations were the monoterpene carbonyls (main compounds *cis*-rose oxide and citronellol) and sesquiterpenes (main compound valencene) (Figures 1 and 2). Linking these results to the literature is challenging as for these matrices only 10 or so terpenoids are reported, so the main contributors are not a true reflection due to the limited number of compounds quantified.

Beer total terpenoid concentrations were expectedly much lower than for gin. Gin is based on the extraction of volatiles from botanicals using alcohol via distillation for example. In contrast, beer is a fermentation product which yields predominantly more esters, alcohols, and fatty acids in comparison to terpenoids [4]. The total terpenoid concentration in beer ranged from 72 – 5513 μ g/L. The classification into ales and lagers used in this study was derived from the description provided by the supplier. Notably, ales yielded a higher average terpenoid concentration (4.5 fold) in comparison to the lagers. Main contributors to the total terpenoid concentrations in lagers were monoterpene carbonyls, monoterpene alcohols, and sesquiterpene oxides. In contrast, the ales' total terpenoid concentration were dominated by monoterpene carbonyls, monoterpene alcohols, and monoterpene hydrocarbons. Citronellol and geraniol (carbonyls), linalool and α -terpineol (alcohols), β -myrcene and α -phellandrene (hydrocarbons) were the dominating monoterpenes (Figures 1 and 2).

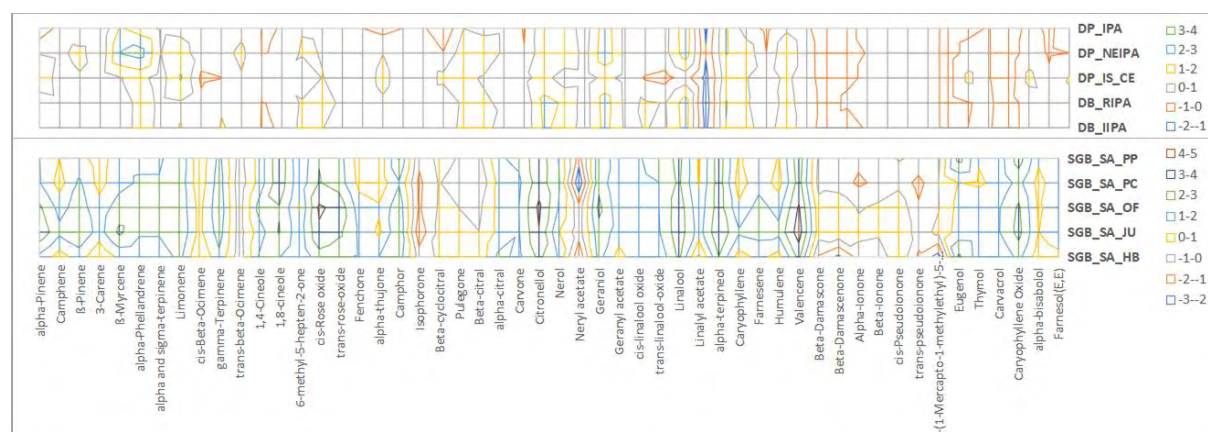


Figure 1. Contour map representation of the terpenoid concentration of a subset of beers (top) and gins (bottom). Values transformed using log 10 for scaling. Samples chosen to illustrate the terpenoid levels variability.

For gin terpenoids results, the most distinct grouping was attributed to the INR and BLM samples (*i.e.* by producer), even though the gins have different aroma profiles according to the tasting notes. SGB samples (sharing a producer) were split: three grouped together (Original Fynbos/OF, Juniper Unfiltered/JU and Pino and Pelargonium/PP), while two others were separate from the group and each other (Protea and Cucumber/PC and Hibiscus/HB). This was more in line with expected results according to the production similarities; the first three samples contain Fynbos as one of the main ingredients, while the latter two have other aromatics added. The analysis of the aroma fingerprints, the BLM samples were still closely clustered, while the INR samples showed a much higher dissimilarity. In the case of SGB samples, only HB was dissimilar from the rest.

For the beer datasets, moderate clustering was observed for the ale in comparison to the lager for both terpenoids and fingerprinting data sets. (As all the samples were craft beers, a clear classification according to production is not always possible.) Notably the IPA beer styles clustered, which suggests that there may be certain characteristics, which are unique to the IPA class; this will be explored further in a forthcoming paper. Further analysis by HCA revealed that the IPA and Imperial Stout/IS samples exhibited some degree of similarity. When comparing the respective producers, moderate similarity was observed for the HJ, DB and FB producers, which may suggest that the production processes may have some degree of similarity.

In order to identify the degree of correlation between the non-targeted and targeted datasets, the RV-coefficients were calculated. For the gin and beer data sets, RV coefficients were only 0.29 and 0.14, respectively, for the first two principal components. The RV coefficient values for both gin and beer outlined that the chemical spaces were different when comparing targeted vs non-targeted analysis. This observation suggests that there may be additional compounds detected in the non-targeted analysis, which significantly contribute to the aroma profiles (expected for beer). Even though the chemical spaces for targeted vs non-targeted for gin were more similar than beer as terpenoids are the predominant class of analytes in gin, the RV value was very low. This could be due to the profile obtained from the untargeted analysis (which was optimised for general profiling and not specifically for terpenoids) or the sample set size (small) and variability (large, as it could be seen already from this set of only 21 samples).

Conclusion

Methods for the targeted and non-targeted analysis of beer and gin were established. A total of 53 compounds were quantified in the targeted terpenoid method, which to the best of the authors knowledge is the most terpenoids quantified in a single method using authentic standards. Unsupervised multivariate analysis of the results from craft gin and beer samples revealed moderate clustering based more on producers than styles. The chemical spaces for non-targeted and targeted analysis were calculated using RV coefficients; their values indicated low similarities between product configurations. As the work presented here is a subset of a larger sample set, the exploration of the craft gins and beers chemical spaces is ongoing. The results should clarify what are the drivers for the chemical spaces of the products and styles.

References

1. Câmara JS, Arminda Alves M, Marques JC. Development of headspace solid-phase microextraction-gas chromatography-mass spectrometry methodology for analysis of terpenoids in Madeira wines. *Anal Chim Acta*. 2006;555:191-200.
2. Serra S. Recent advances in the synthesis of carotenoid-derived flavours and fragrances. *Molecules*. 2015;20:12817-12840.
3. Williams C, Buica A. Comparison of an offline SPE–GC–MS and online HS–SPME–GC–MS method for the analysis of volatile terpenoids in wine. *Molecules*. 2020;25:657.
4. Bettenhausen HM, et al. Variation in Sensory Attributes and Volatile Compounds in Beers Brewed from Genetically Distinct Malts: An Integrated Sensory and Non-Targeted Metabolomics Approach. *J Am Soc Brew Chem*. 2020;78:136–152.
5. Williams C, Medvedovici AV, Stander MA, Buica A. Analysis of 53 terpenoids in beer and gin. *In preparation*.
6. Williams, C., Mafata, M., Medvedovici, A.V., Sarbu, C., Mokwena, L. & Buica, A. Strategies for sample preparation and data handling in GC-MS wine applications, 11th International Symposium of Oenology/ 11th In Vino Analytica Scientia (*Oeno/IVAS*). 2019; Bordeaux, France.

Unravelling the typicity of 17 rum terroirs by GC-FID and aroma compound mapping

NICOLAS MALFONDET, Fannie Thibaud and Alexandre Gabriel

MAISON FERRAND R&D Department, Châteaubernard, France, nmalfondet@maisonferrand.com

Abstract

The flavour composition of a large number of rum samples coming from different terroirs has been analysed by GC-FID. A graph (called the “aroma compound mapping”) has been drawn using the quantitative data of esters and higher alcohols contained in the rums. The samples plotted on the mapping allow to explain the differences in their making processes, which symbolises the typicity of each rum terroir. This methodology represents a useful tool to highlight and better understand the specificities of rum production among the terroirs and their impact in the flavour composition of the final product.

Keywords: rum, terroirs, typicity, GC-FID, aroma compound mapping

Introduction

Rum is one of the most consumed spirit drinks around the world. It is produced in many countries, thereafter referred to as terroirs. A terroir is defined by the OIV as “a concept which refers to an area in which collective knowledge of the interactions between the identifiable physical and biological environment and applied vitivicultural practices develops, providing distinctive characteristics for the products originating from this area” [1]. In the case of rum, each terroir has its own typicity related to the making process, resulting in as many flavour profiles of rum as there are terroirs. It starts from the type of raw material used, which can be either sugarcane juice or molasses. The fermentation of these raw materials is also a key step in the generation of flavours in rum. Two main styles exist: the “short and clean” fermentation which lasts for one or two days, featuring *Saccharomyces cerevisiae* yeast only, and the “long and complex” fermentation which lasts for weeks, featuring several yeasts but also bacteria species. After fermentation, the distillation is a crucial stage. Here also two main possibilities co-exist: the continuous column still and the batch pot still. The ageing process in wooden barrels is however relatively similar between the terroirs, generally occurring in 200 L American oak casks. Nevertheless, climate here plays an important role, with temperature and humidity content impacting the evolution of rum during its ageing. Every stage of the rum making process contributes to the flavour typicity of rums according to their terroir or origin [2, 3]. In this work, we aimed to understand and highlight these typicalities, by analysing the flavour composition of a great number of samples coming from several terroirs.

Experimental

One hundred and seventy-eight rum samples coming from 17 terroirs have been selected within the Maison Ferrand stock. Their technical characteristics are presented in Table 1.

Samples have been analysed by Gas Chromatography-Flame Ionization Detector after direct injection on a polar column. In each sample, 10 esters and 6 higher alcohols were quantified (Table 2). The followed procedure is based on the OIV method for the determination of the principal volatile substances of spirit drinks [4].

The quantitative data allow a graph – a mapping – to be created, with the sum of the 6 higher alcohols studied representing the x-axis, and the sum of the 10 esters, the y-axis. Thus, the different rum samples are plotted on this mapping according to their content in these flavour compounds.

Table 1: Technical characteristics of the rum samples.

Raw Material	Sugarcane juice		Sugarcane molasses
	Réunion, Martinique, Haiti (<i>a.k.a. Agricoles rums</i>)		All the other terroirs
Fermentation	“Short and clean”	“Intermediate”	“Long and complex”
	Trinidad, Panama, Porto Rico, Guatemala, Dominican Republic, Cuba, Nicaragua, Belize	<i>Agricoles rums</i> , Barbados, Peru, Fiji	Jamaica, Saint Lucia, Guyana
Distillation	Continuous column still	Blends of column and pot stills	Batch pot still
	Trinidad, Panama, Porto Rico, Guatemala, Dominican Republic, Cuba, Nicaragua, Belize, <i>Agricoles rums</i>	Barbados, Peru, Fiji	Jamaica, Saint Lucia, Guyana

Table 2: Compounds quantified in the rum samples.

Esters	ethyl formate, ethyl acetate, ethyl 2-hydroxypropanoate, ethyl butanoate, 3-methylbutyl acetate, ethyl hexanoate, ethyl octanoate, diethyl butanedioate, ethyl decanoate, ethyl dodecanoate
Higher alcohols	propan-1-ol, 2-methylpropan-1-ol, butan-1-ol, butan-2-ol, 2- & 3-methylbutan-1-ol

Results and discussion

On the mapping, the rums originate from the same terroir are plotted close to each other. Then, ellipses can be schematically drawn around the group of samples to visualise the terroir locations on the graph (Figure 1). The making process specificities of terroir are then highlighted.

Rum made from sugarcane juice (*Agricoles rums*) are richer in esters but generally poorer in higher alcohols than molasses rums.

Concerning fermentation: The longer it is, the more flavour compounds (especially esters) are produced, as for Jamaican rums. An extreme example being the aptly named “high ester” rums, also from Jamaica. Those are produced with extremely “long and complex” fermentations that last for weeks, featuring bacteria beside yeasts and also the addition of sugarcane vinegar, leading to extremely concentrated rums with strong fruity notes [5]. On the other side of the mapping are rums made from “short and clean” fermentations, such as Trinidadian, Panamanian or Cuban rums among others. In between, with “intermediate” fermentations, we find for instance the terroirs of Barbados, Peru or Fiji.

Concerning distillation: Continuous column still gives overall lighter rums than batch pot still. This is due to the higher rectification of the first compared to the latter. Some terroirs usually blend rum made from column with rum made from pot stills (e.g., Barbados), resulting in a richer product. Very aromatic rums rich in higher alcohols, like St Lucian or Guyanese rums, can be related to their long fermentation process. This time, the differences with Jamaica can be linked to the type of pot still being different between the 3 terroirs: Its shape and its size truly impact the aromatic profile of the distillate [3].

Finally, during ageing in wooden casks, all the spirits are gaining flavour compounds as already shown in the literature [6]. Aged rums are richer in higher alcohols and esters than younger, or even unaged rums.

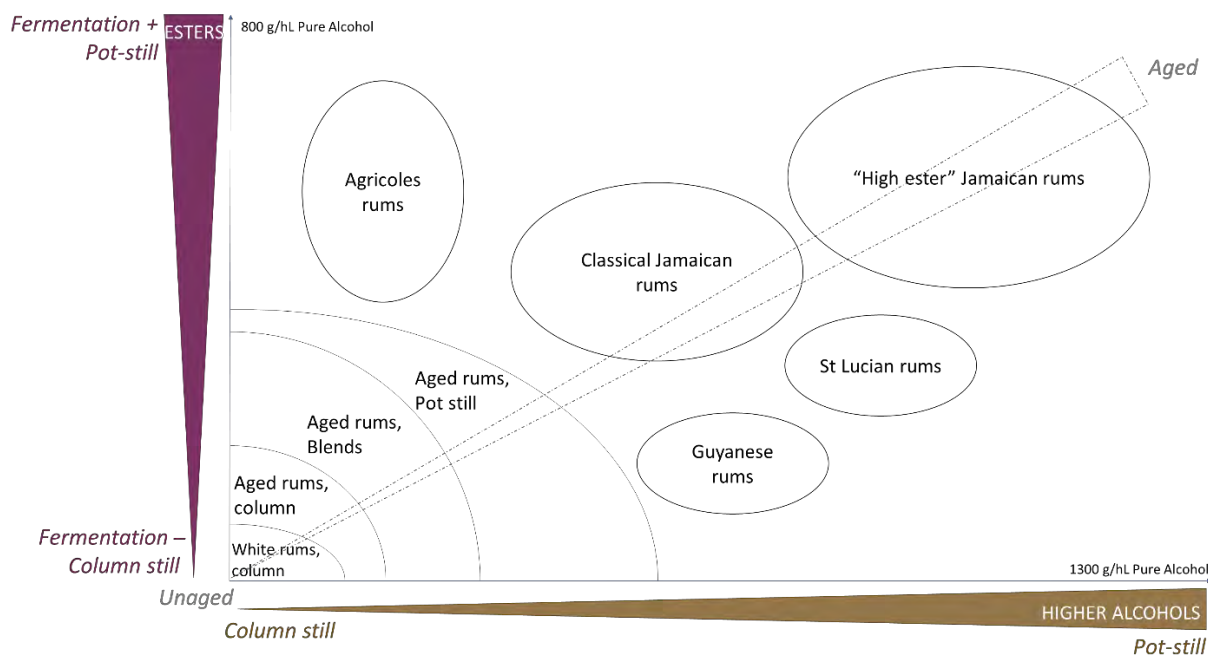


Figure 1: Aroma compound mapping: Classification of rum terroirs by the concentrations of esters & higher alcohols in 178 samples. Ellipses are drawn around the groups of samples to simplify the visualisation.

Conclusion

The different rums are plotted among the aroma compound mapping so that the specificities of their terroirs (and making processes) can be emphasised. Indeed, according to the raw material, throughout fermentation, distillation and ageing, the flavour composition of the rum differs substantially. Sugarcane juice produces rum with more esters compared to molasses. Also, the longer the fermentation, the richer the rum, especially in esters. Continuous column still produces lighter rums compared to batch pot stills, with blended rums in between. There is also a crucial impact of the still itself, its shape and size. Lastly, ageing in wooden casks gives a richer overall spirit.

The variety of rum is so wide that many terroirs exist, with as much typicities. Some have been highlighted in this work. Sensory data (not shown) allowed to find cause and effect links between chemical and organoleptic profiles of the samples.

This analytical tool – this aroma compound mapping – contributes to better understand the impact of the rum making processes. The methodology will now be submitted to other spirits such as cognac, brandy or whisky. Also, a third axis will be added to the graph, expressing the concentration in wood compounds such as vanillin, syringaldehyde or whisky lactones, in order to better explain the flavour complexity of alcoholic beverages, especially the one gained during ageing in casks.

References

1. OIV. Definition of terroir. 2010.
2. Malfondet N, Galais B, Gabriel A. Rum and cognac aroma characterization by GC-FID and PCA for products comparison purpose and deeper understanding of the compositions of both spirits. Presented at the 11th Oeno-Ivas Symposium, Bordeaux. 2019.
3. Coelho C, Brottier C, Beuchet F, Elichiry-Ortiz P, Bach B, Lafarge C, Tourdot-Maréchal R. Effect of ageing on lees and distillation process on fermented sugarcane molasses for the production of rum. *Food Chem.* 2020;303:125405.
4. OIV. Determination of the principal volatile substances of spirit drinks of viti-vinicultural origin. 2014.
5. Fahrasmene L, Ganou-Parfait B. Microbial flora of rum fermentation media. *J Appl Microbiol.* 1998;84:921-928.
6. Puech J-L, Leauté R, Clot G, Nomdedeu L, Mondié H. Evolution of volatile and phenolic constituents of cognac during ageing. *Sci Aliment.* 1984;4:65-80.

Extended volatile range PTR-MS setup for real-time puff-by-puff analysis of electronic nicotine delivery systems

Andreas Mauracher, Bea Rosenkranz, Rene Gutmann, Markus Müller, Andreas Klinger and PHILIPP SULZER

IONICON Analytik GmbH, Eduard-Bodem-Gasse 3, 6020 Innsbruck, Austria, philipp.sulzer@ionicon.com

Abstract

The popularity of Electronic Nicotine Delivery Systems (ENDS) has led to an increase in interest in characterising the aerosol produced by these devices. So far, most published studies utilise traditional offline methods (e.g. GC-MS) which only give information on the average concentrations / amounts of compounds delivered by ENDS over a series of puffs. In order to be able to carry out detailed studies, there is a high demand for scientific data obtained with online methods that allow true puff-by-puff analysis. Proton Transfer Reaction – Time-Of-Flight – Mass Spectrometry (PTR-TOF-MS) with its real-time quantification capability is well-established in food and flavour science and therefore ideally suited for this task. However, there are several difficulties to overcome, for example the enormous concentration differences between the mainstream aerosol and the residual compounds in exhaled breath and the highly condensable nature of the aerosol, leading to extended retention times in mass spectrometric devices.

Here, we present a newly developed PTR-TOF-MS multipurpose sampling setup with a well-defined three-stage dilution system that can shift the instrument's dynamic range by more than four orders of magnitude. All surfaces that come in contact with the sample air are specially coated and heated to considerably reduce retention effects. We show results from a proof-of-concept study on exhaled air before, during and after the use of an ENDS. Our results demonstrate the ability of our system to perform highly time-resolved puff-by-puff characterisation of ENDS mainstream aerosol as well as in exhaled breath after ENDS consumption.

Keywords: ENDS, PTR-MS, real-time, puff-by-puff analysis, breath analysis

Introduction

Electronic devices that deliver nicotine via inhalation have been introduced already in the 1960s [1] and are nowadays commonly known as electronic cigarettes, e-cigarettes, electronic vaping devices or Electronic Nicotine Delivery Systems (ENDS). However, they were only successfully commercialised in the early 2000s [2]. Especially in the last decade, ENDS have achieved widespread use [3, 4]. It seems understandable that the rapid growth of the ENDS market increased the attention of the public, the media and regulatory authorities [5], particularly as ENDS have often been promoted as a safer alternative to conventional tobacco cigarettes because no combustion products are inhaled [6]. However, a systematic review of the existing literature on the health effects of ENDS shows that no firm statements can be made about the safety of ENDS [7] and that there is a lack of online data during product consumption, particularly on puff-by-puff variations. This is because mostly offline methods are used where, for example, the subjects exhale into a Tedlar bag immediately after smoking or vaping [8] and the contents of the bags are subsequently analysed.

One of the first studies using Proton Transfer Reaction - Mass Spectrometry (PTR-MS) to investigate exhaled air was conducted as early as 1995 to investigate time-dependent concentrations of benzene and acetonitrile in the breath of smokers and non-smokers [10]. In 2009, the advantages of using PTR in combination with Time-Of-Flight (TOF) analysers instead of quadrupole mass filters for online breath analysis were demonstrated [11]. In the context of e-cigarettes, the nicotine retention time of e-cigarette aerosols inhalation was determined by GC coupled with a flame ionisation detector and PTR-TOF-MS. Since the total Volatile Organic Compound (VOC) concentration was higher than the upper limit of the dynamic range of the PTR-TOF-MS device, a single-stage dilution system was developed [5]. More recently, a two-stage dilution system has been used to investigate both mainstream aerosols and exhaled breath [12]. The two-stage dilution system was necessary to achieve coverage of the concentration ranges in these two scenarios. With the growing interest in this field and the increasing demand for high-end studies, some shortcomings in this setup have become apparent.

Herein we present a proof-of-concept study of a fundamentally revised experimental setup to directly quantify the high concentrations in the ENDS mainstream aerosol of up to 10,000 ppmv as well as pptv-level concentrations in exhaled air tens of minutes after product use.

Experimental

In this study, we employed a PTR-TOF 6000 X2 (IONICON Analytik GmbH, Innsbruck, Austria). The technical specifications of this instrument are: Limit of Detection (LOD) < 10 pptv (1 s integration time), sensitivity > 2000 cps/ppbv, response time < 100 ms, mass resolution > 6000 m/Δm [13]. Details on the components and principles of PTR-MS instruments as well as established fields of application have already been described in detail in the book by Ellis and Mayhew [14]. In principle, the apparatus consists of two main parts, the ionisation section, where VOCs are ionised by chemical ionisation, and the detection section, where the ionised species are analysed according to their mass-to-charge (m/z) ratio by means of TOF-MS. The PTR-TOF 6000 X2 is equipped with the recently introduced Extended Volatility Range (EVR) technology [16]. That is, the inlet line and the PTR reaction region, and in general all other surfaces that come in contact with the sample air, are covered with a sophisticated coating and heated, avoiding any cold spots.

Although this instrument is equipped with Selective Reagent Ion Mass Spectrometry (SRI-MS) technology, which allows the use of H_3O^+ , NO^+ , O_2^+ , Kr^+ , and NH_4^+ as primary ions, we only use H_3O^+ ions for this proof-of-concept study.

Concentration calibration

Based on basic principles of ion chemistry and certain approximations, PTR-MS allows quantification without external calibration for most compounds [14]. The two main constituents of e-liquids used in ENDS, Propylene Glycol (PG, $\text{C}_3\text{H}_8\text{O}_2$) and (Vegetable) Glycerol (VG, $\text{C}_3\text{H}_8\text{O}_3$), are among the very few molecules that show strong fragmentation in soft PTR ionisation. Thus, we used a liquid calibration unit (LCU, IONICON Analytik GmbH, Innsbruck, Austria [15]) to transfer aqueous solutions of PG and VG in well-defined concentrations into the gas phase and carefully calibrated the instrument. Additionally, a calibration measurement was carried out for the e-liquid constituent nicotine ($\text{C}_{10}\text{H}_{14}\text{N}_2$). However, since nicotine nearly exclusively forms the protonated molecule after PTR from H_3O^+ , the calibrated results showed excellent agreement with the calculated values, thus confirming the initiatory statement.

Sampling setup

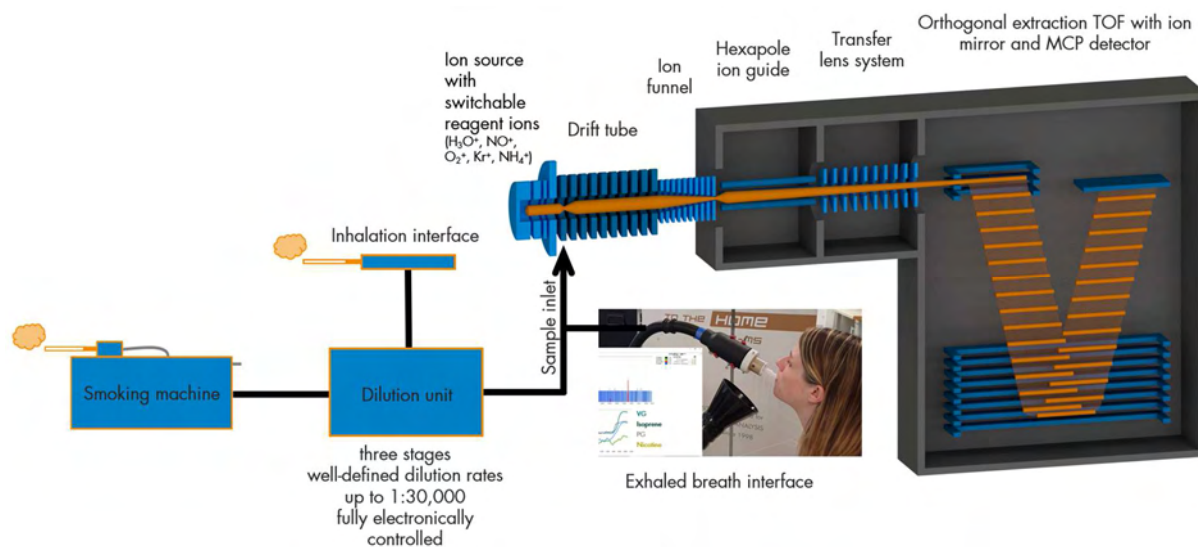


Figure 1: Schematic view of the newly developed PTR-TOF-MS multipurpose sampling setup (see text for details).

Based on the experiences obtained with a previous sampling setup [12], we constructed a completely revised sampling setup to enable comprehensive ENDS studies with extremely high time resolution and thus the possibility of online puff-by-puff analysis of mainstream aerosols as well as exhaled breath with a single PTR-MS instrument (see Figure 1). The novel inlet system consists of three main parts:

(i) A port for connecting a common smoking machine. With such a device, standardised puff volumes, durations and profiles can be selected. Thus, puff-by-puff variations of the constituents of mainstream aerosol can be analysed in real time.

(ii) An inhalation interface to quantify the actual concentrations of compounds during consumption of ENDS. That is, the subject inhales *ad libitum* via the interface connected to any ENDS.

(iii) An exhaled breath interface. After using an ENDS, the exhaled breath can be analysed to monitor metabolic processes in the human body and retention rates of inhaled or mouth-held compounds.

The new dilution system can achieve dilution rates up to 1:30,000 via a fully electronically controlled three-stage dilution, which provides high sample gas flow rates in all stages for improved response times. Furthermore, all surfaces that come into contact with sample air (dilution system, sample gas lines, EVR PTR-TOF-MS instrument [16]) are specially coated in order to prevent adsorption effects already at moderate temperatures (120°C).

Results and discussion

PTR-TOF-MS enables the acquisition of a complete mass spectrum with high mass resolution and time resolution and therefore the identification of a wide range of VOCs. The integration time in our experiments was 0.5 s for each data point. Three of the most common constituents present in ENDS aerosol are VG, PG and nicotine. Particularly gaseous VG and nicotine are known for their condensable or "sticky" nature causing memory effects and thus pose a challenge for online analysis techniques. As nicotine is present in detectable concentrations (pptv range) only in exhalations immediately following inhaling the ENDS aerosol, the results are not shown here.

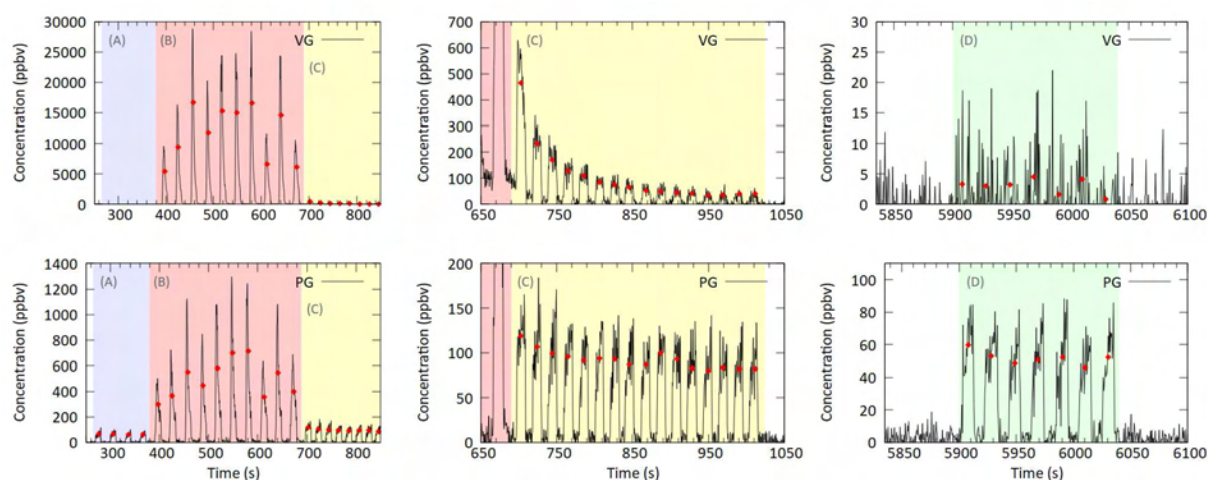


Figure 2: Concentration (in ppbv) as a function of time (in s) for glycerol (VG) and propylene glycol (PG) in the top and bottom row, respectively. Four different time-frames were chosen: (A, blue background) prior to and (B, red background) immediately following inhalation of ENDS aerosol, (C, yellow background) immediately after stopping the use of ENDS and (D, green background) approximately one hour after the last inhalation of an ENDS. The red dots indicate average values of concentration of respective exhalations. See text for further explanations.

Figure 2 shows the results of the proof-of-concept study for concentrations of VG and PG (in ppbv) in the top and bottom rows, respectively, as a function of time (in s). Note that the scale of the y-axes varies for each panel, while the time range is the same for each column for better comparability of relative VG and PG concentrations in exhaled air. In addition, an average value for each exhalation is indicated by a red dot. This value was determined as an average value within the time window where the concentration is always above 20% of the maximum concentration of the corresponding exhaled breath. The value of 20% was chosen to be clearly above the background noise.

In order to obtain "blank" concentrations, the test subject first exhaled into the novel breath interface after a period of fasting of several hours (prior to about 390 s). While there is no trace of VG in these four exhaled breaths, there is a distinct presence of PG in the subject's breath, ranging from an average value of 59 to 67 ppbv.

Subsequently, the test subject performed a deep inhalation of the ENDS' aerosol and exhaled into the breath interface. This process was repeated ten times with about 20 s in between each repetition and is also shown in the first column of Figure 2 (red background). Remarkably, considerable puff-by-puff concentration variations are visible. This is most likely the result of individual ENDS use and inhalation manoeuvres, but could also be due to a certain degree to variations in the aerosol production of the utilised device. Either way, the findings underline the importance of puff-by-puff resolved studies for further investigations. The measured concentration range is from 5448 to 16591 ppbv and 299 to 712 ppbv in the case of VG and PG, respectively. However, the variations of the concentrations of VG and PG are correlated, as can be seen in the first column of Figure 2.

After the ten exhalations following inhalation of the aerosols of an ENDS, we recorded the washout phase of these compounds in the subject's breath. In the second column, the concentrations and the respective time frame, i.e. up to 1050 s, are shown. Note that the first high signal region in the time from approximately 666 to 680 s (red background) belongs to the series of the ten exhaled breaths after using an ENDS. In the second panel of the first row, an exponential-like decrease in the mean value of the VG concentration can be observed (yellow background).

The mean value is only 40 ppbv after 5 min. In the case of PG (second panel in the second row, yellow background), on the other hand, a fairly constant concentration can be seen, ranging from 80 to 119 ppbv. This is about twice as high as directly before the use of an ENDS.

After 87 min since the last use of an ENDS, we recorded again seven exhaled breaths. In the case of PG, see Figure 2 right panel in the bottom row (green background), the average concentration has decreased to a comparable range like before the use of an ENDS (46 to 52 ppbv). In the case of VG, see Figure 2 right panel in the top row (green background), there is hardly any concentration above the background noise level present. Since it was difficult to define borders for the calculation of the average values per exhaled breath in this case, we used the time windows determined from the PG concentration. We find average concentration values only below 5 ppbv.

Conclusion

We presented results obtained with a novel PTR-TOF-MS inlet system that enables the online analysis of ENDS mainstream aerosol and exhaled breath in real-time with high time resolution. As a first proof-of-concept, concentrations of VG and PG in exhaled breath were shown before, during and after using an ENDS. During the use of an ENDS, we find that the concentrations of both VG and PG can vary quite substantially, i.e. by a factor of about 3, which underlines the importance of puff-by-puff resolved studies.

The concentration of VG in exhaled breath decreases in an exponential-like fashion immediately after the end of the use of the ENDS. About one and a half hours after the use of the ENDS, there is hardly any trace of VG detectable. In the case of PG, we find a certain background in the exhaled breath of the subject (about 60 ppbv) before the use of the ENDS. Immediately after the end of consumption, the concentration values drop and remain at an almost constant value, which is about twice as high as in blank breath. One and a half hours later, the concentration of PG has reached about the same level as before the inhalation of the ENDS' aerosol.

With these results, we demonstrated the capability of our setup for online monitoring of ENDS inhalation and exhalation, which allows comprehensive studies to quantitatively investigate the concentrations of constituents of ENDS aerosols. Furthermore, our findings indicate that the setup is perfectly suitable for studies on the human metabolism of compounds ingested via ENDS use.

References

1. Gilbert H A. Smokeless non-tobacco cigarette. 3,200,819 United States Patent Office 1965; Filed April 17, 1963.
2. Sleight, V J. A brief history of the electronic cigarette. *J Lung Pulm Respir Res.* 2016;3(5):135–136.
3. Laverty A A, Filippidis F T, Vardavas C I. Patterns, trends and determinants of e-cigarette use in 28 European Union Member States 2014–2017. *Prev. Med.* 2018;116:13-18.
4. Papaefstathiou E, Stylianou M, Agapiou A. Main and side stream effects of electronic cigarettes. *J Environ Manage.* 2019;238:10-17.
5. O'Connell G, Colard S, Breiev K, Sulzer P, Biel S S, Cahours X, et al. An experimental method to determine the concentration of nicotine in exhaled breath and its retention rate following use of an electronic cigarette. *J Environ Anal Chem.* 2015,2:5.
6. Pepper J K, Brewer N T. Electronic nicotine delivery systems (electronic cigarette) awareness, use, reactions and beliefs: a systematic review. *Tob Control.* 2014,23:375-384.
7. Pisinger C, Døssing M. A systematic review of health effects of electronic cigarettes. *Prev Med.* 2014;69:248-260.
8. Papaefstathiou E, Stylianou M, Andreou C, Agapiou A. Breath analysis of smokers, non-smokers, and e-cigarette users. *J Chromatogr B.* 2020;1160:122349
9. Wagner K A, Higby R, Stutt K. Puff-by-puff analysis of selected mainstream smoke constituents in the Kentucky Reference 2R4F cigarette. *Beitr Tabakforsch Int.* 2014;21(5):273-279.
10. Jordan A, Hansel A, Holzinger R, Lindinger W. Acetonitrile and benzene in the breath of smokers and non-smokers investigated by proton transfer reaction mass spectrometry (PTR-MS). *Int J Mass Spectrom Ion Processes.* 1995;148:L1-L3.
11. Herbig J, Müller M, Schallhart S, Titzmann T, Graus M, Hansel A. On-line breath analysis with PTR-TOF. *J Breath Res.* 2009;3:027004-10.
12. Breiev K, Bursev K M M, O'Connell G, Hartungen E, Biel S S, Cahours X, et al. An online method for the analysis of volatile organic compounds in electronic aerosol based on proton transfer reaction mass spectrometry. *Rapid Commun Mass Spectrom.* 2016;30:691-697.
13. <https://www.ionicon.com/products/details/ptr-tof-6000-x2> (30.04.2021)
14. Ellis A M, Mayhew C A. Proton transfer reaction mass spectrometry: principles and applications. John Wiley & Sons Ltd. West Sussex (UK). 2014. 978-1-405-17668-2.
15. Fischer L, Klinger A, Herbig J, Winkler K, Gutmann R, Hansel A. in 6th International Conference on Proton Transfer Reaction Mass Spectrometry and its Applications, (Eds: Hansel A, Dunkl J). Innsbruck University Press, Innsbruck. 2013;192-195.
16. Piel F, Müller M, Winkler K, Skytte af Sätra J, Wisthaler A. Introducing the extended volatility range proton-transfer-reaction mass spectrometer (EVR PTR-MS). *Atmos Meas Tech.* 2021;14:1355-1363.

Identification and semi-quantification of sesquiterpenes and sesquiterpenoids from Chamomile, Hop, Lavender, Basil and Lemon balm

BENEDIKT SLAVIK¹, Julian Nehr¹, Helene M. Loos^{1,2}, Andrea Buettner^{1,2}

¹ Chair of Aroma and Smell Research, Friedrich-Alexander-Universität Erlangen-Nürnberg (FAU), Germany, benedikt.slavik@fau.de

² Fraunhofer Institute for Process Engineering and Packaging IVV, Germany

Abstract

Sesquiterpenes are naturally occurring compounds with 15 carbon atoms and are formally composed of three isoprene units. Together with their derivatives, the sesquiterpenoids represent one of the major substance classes of essential oils. As essential oils are often attributed with positive effects on human health, these compounds are interesting targets for physiological and biochemical investigations. The here investigated chamomile (*Matricaria chamomilla* L.), hop (*Humulus lupulus*), lavender (*Lavandula angustifolia*), basil (*Ocimum basilicum*) and lemon balm (*Melissa officinalis*) are famous members of plants with highly acknowledged beneficial health effects. To study these effects, sesquiterpenes and sesquiterpenoids (SQTs) as major constituents need to be studied more intensely. The here described tentative identification and quantification complement the existing literature by adding a concrete quantitative dimension to these valuable substances in the five plants, and help to further elucidate the contribution of SQTs to the overall properties of essential oils.

Keywords: GC-MS, solvent assisted flavour evaporation, internal standard, isolation, essential oils

Introduction

Essential oil-bearing plants are popular remedies used in traditional medicine. As they often have fewer complications compared to modern pharmaceutical drugs, they are very commonly applied. Many psycho- and physiological effects have been discovered, and the quest for new naturally occurring bioactive substances is still ongoing. Furthermore, we could recently show that sesquiterpenes and sesquiterpenoids (SQTs) can have a high influence on the overall aroma of natural materials [1], revealing the ability of SQTs to have a huge impact even at trace levels. For biochemical and physiological investigations, often the whole essential oil is administered. This may, however, obscure the effects of single compounds. Additionally, as naturally occurring substances like the SQTs are structurally very demanding, only few are synthetically accessible, and are therefore not investigated so far. In this study, we want to complement the research on SQTs and on their identification and semi-quantification. Most investigations only consider a comparison of the peak areas determined by gas chromatography – mass spectrometry (GC-MS), and utilise these for an approximated quantification. Here we report the tentative identification together with semi-quantification based on internal standards.

Experimental

Plant materials and chemicals

Dried chamomile flower heads, dried hop cones and dried lavender flower heads were obtained from a local store (Erlangen, Germany). Fresh samples of basil and lemon balm were purchased from Bioland Kräuter Gut Dworschak-Fleischmann (Nürnberg, Germany). Dichloromethane (DCM, purified by distillation before usage) and sodium sulphate were purchased from VWR (VWR International Radnor, PA, USA). α -Bisabolol, α -humulene, (+)-nootkaton and the series of *n*-alkanes were purchased from Sigma-Aldrich (Sigma-Aldrich Corporation, St. Louis, MO, USA).

Extraction and distillation

The dried plant materials were finely chopped (Kenwood mini chopper CH180, 300 W, Kenwood Limited, Havant, United Kingdom) until a powder or fine needles, respectively, were obtained. The leaves of the fresh samples were cut into small pieces. Subsequently, dependent on the plant material, different amounts (ranging from 0.5 g to 5.0 g) of the samples were extracted with DCM (50 mL, 30 min) and were dried over sodium sulphate. The resulting extracts were applied for solvent assisted flavour evaporation (SAFE) [2] at 60 °C under vacuum. Finally, the distillates were reduced by Vigreux and micro distillation to 100 μ L (250 μ L for lavender and 200 μ L for hop) [3].

Analysis by GC-MS

The analyses for the identification and quantification were performed on a GC 6890 coupled with a 5973 MSD (Agilent Technologies, Santa Clara, CA, USA). The system was equipped with a Multipurpose Sampler 2 and a CIS 3 injection system (GERSTEL GmbH & Co. KG, Mülheim an der Ruhr, Germany). A DB-5 capillary column was used (30 x 0.25 mm, film thickness 0.25 μ m), connected to an uncoated fused silica capillary pre-column (3 m x 0.53 mm; Agilent J&W Scientific, Santa Clara, CA, USA). The following oven temperature program was used following the instructions by Adams [4]: 60 °C until 246 °C with a temperature ramp of 3 °C/min. A split of 20:1 was used to apply 2.0 μ L of sample (for the dried samples a 1:10 dilution of the original distillate was prepared for the measurements). The helium carrier gas stream was set to 1 mL/min. EI mass spectra were recorded at 70 eV in TIC mode (40-400 amu).

Tentative identification of SQTs

The tentative identification was based on the following criteria: The comparison with the linear retention index (RI) on a DB-5 capillary column and the matching with literature mass spectra. For both, the literature [4] or the NIST mass spectral library (version 2.0, National Institute of Standards and Technologies, Gaithersburg, MD, USA) were consulted. For the RI a difference lower than 15 (value compared to literature values) was required for the tentative identification. For the matches with the NIST a value of >800 was taken as criterion. The following SQTs could not be identified and remain unknown: Chamomile RIs: 1388, 1410, 1479, 1506, 1554, 1580, 1583, 1587, 1590, 1605, 1608, 1614, 1630, 1646, 1659, 1674 and 1718; hop RIs: 1382, 1507 and 1629; lavender RIs: 1443, 1498, 1542, 1589, 1620, 1668 and 1692; basil RIs: 1418 and 1482.

Semi-quantification of SQTs

For the semi-quantification, an internal standard (ISTD, (+)-nootkaton) was used to cover the loss during the workups and measurements. Additionally, two calibration standards (CSTD) were used for the calculation of the concentration of sesquiterpenes (α -humulene) and sesquiterpenoids (α -bisabolol). A 5-point calibration curve was prepared for both CSTDs by plotting the peak area CSTD/ISTD against the concentration of the respective CSTD, while varying the concentration of the CSTD and keeping constant the concentration of the ISTD (α -humulene: $y = 0.0422x + 0.0097$, $R^2 = 0.9992$, α -bisabolol: $y = 0.0297x - 0.0935$, $R^2 = 0.9985$). Each sample was worked up twice and the final values were obtained by calculating the mean value.

Results and discussion

In Table 1, the results of the tentative identification and semi-quantification are summarised. In total 52 SQTs could be tentatively identified in the investigated plant materials. Our findings show that the volatile fractions, especially for the dried samples, reveal high concentrations of SQTs. In contrast, the fresh samples contained a lower amount, which can be explained by the higher content of water. Our findings are in line with earlier reported values from the literature. Interestingly, within the individual plant materials many SQTs are related in terms of their structure. For instance, chamomile contains several SQTs which are derived from α -bisabolol, e.g., α -bisabolol oxide B, α -bisabolone oxide A or α -bisabolol oxide A. In contrast, there are also SQTs which could be tentatively identified in several of the investigated plant materials, e.g., β -caryophyllene, α -humulene or γ -muurolene, which are well researched members of the SQTs family.

Table 1: Compounds tentatively identified (RI: retention index on DB-5) and semi-quantified in the investigated plants; values of the semi-quantification are given in ppm; tr = traces.

N°	RI (DB-5)	Compound	Chamomile	Hop	Lavender	Basil	Lemon balm
1	1345	α -Cubebene		6.3			
2	1348	α -Longipinene	tr				
3	1368	α -Ylangene		28.3			
4	1374	Cedrene	tr				
5	1374	α -Copaene		99.0		0.1	
6	1380	Modhephene	0.2				
7	1405	α -Gurjunene	tr				
8	1416-18	β -Caryophyllene	0.5	1786.1	190.5		3.7
9	1427	β -Gurjunene		72.3			
10	1428	β -Copaene	tr				

Table 1 (cont.)

11	1431	α -trans-Bergamotene				6.9	
12	1436	Aromadendrene	tr				
13	1452	(<i>E</i>)- β -Farnesene	260.9		47.7	6.6	
14	1453-54	α -Humulene		4950.0		tr	0.1
15	1457-58	Alloaromadendrene	0.6				tr
16	1470	(<i>E</i>)-Cadina-1(6),4-diene		tr			
17	1473-79	γ -Muurolene	tr	176.2	26.1	2.5	
18	1477	α -Amorphene		18.4			
19	1488-1506	Valencene	0.3			0.3	
20	1493	Bicyclogermacrene	13.6			0.5	
21	1494	α -Selinene		41.6			
22	1496	α -Muurolene		36.7			
23	1499	α -Bulnesene				0.2	
24	1504	(<i>E,E</i>)- α -Farnesene	tr				
25	1510-11	γ -Cadinene	tr	223.3	134.2	0.2	
26	1515-17	δ -Cadinene	tr	321.4			
27	1520	Zonarene		48.6			
28	1521-23	β -Sesqui-phellandrene	tr			0.1	
29	1530	(<i>E</i>)-Cadina-1,4-diene		34.2			
30	1534	α -Cadinene		39.3			
31	1539	α -Calacorene		18.3			
32	1556	Germacrene B		tr			
33	1574	Spathulenol	140.1				
34	1579	Caryophyllene oxide		151.8	573.3		
35	1585	Gleenol		10.8			
36	1602	Globulol	7.0				
37	1606	Humulene epoxide II		570.5			
38	1612	1,10-di-epi-Cubenol		24.9			
39	1613	Cubenol			23.2		
40	1625	1-epi-Cubenol		32.3			
41	1632	(<i>Z</i>)-Cadin-4-en-7-ol		87.2			
42	1639-41	epi- α -Cadinol	8.2	83.8	145.2	1.1	
43	1645	α -Muurolol		12.8			
44	1653	α -Eudesmol				0.8	
45	1653	α -Bisabolol oxide B	464.7				
46	1654	α -Cadinol		55.8			
47	1679	α -Bisabolone oxide A	317.0				
48	1682	cis-14-nor-Muuro-5-en-4-one			26.9		
49	1684	α -Bisabolol	29.3				
50	1688	Eudesma-4(15),7-dien-1 β -ol	10.5				
51	1709	(<i>Z</i>)- β -Santalol			40.6		
52	1746	α -Bisabolol oxide A	622.5				

Conclusion

SQTs are important compounds present in foods, plants and essential oils and thereby contribute to their respective properties. Chamomile, hop, lavender, basil and lemon balm were chopped and extracted with DCM. After solvent assisted flavour evaporation, the distillates were investigated by means of GC-MS. For the semi-quantification, an ISTD was used and CSTDs enabled the calculation of the respective amounts. The highest amounts of SQTs were detected for the dried samples; especially, hop was found to be rich in α -humulene (4950.0 ppm) and β -caryophyllene (1786.1 ppm). Both compounds were recently characterised to undergo structural changes during digestion in the human body [5]. For chamomile and lavender, the highest amounts were found for α -bisabolol oxide A (622.5 ppm) and caryophyllene oxide (573.3 ppm) respectively. The here reported values complement existing literature and may help to promote research dealing with single administered SQTs in biochemical and physiological assays. We aim to test several of the here investigated SQTs in terms of their neurotropic interaction on the human GABA_A Receptor [6].

References

1. Niebler J, Zhuravlova K, Minceva M, Buettner A. Fragrant Sesquiterpene Ketones as Trace Constituents in Frankincense Volatile Oil of *Boswellia sacra*. *J Nat Prod*. 2016;79(4):1160-4.
2. Engel W, Bahr W, Schieberle P. Solvent assisted flavour evaporation - a new and versatile technique for the careful and direct isolation of aroma compounds from complex food matrices. *Eur Food Res Technol*. 1999;209(3-4):237-41.
3. Bemelmans JMH. Review of Isolation and Concentration Techniques. *Progress in Flavour Research*, Applied Science Publisher, London. 1979:79-98.
4. Adams RP. Identification of Essential Oil Components by Gas Chromatography/Mass Spectrometry, 4th Edition. Kozłowski AC, editor. Carol Stream, IL, USA: Allured Business Media; 2012.
5. Heinlein A, Buettner A. Monitoring of biotransformation of hop aroma compounds in an in vitro digestion model. *Food Funct*. 2012;3(10):1059-67.
6. Kessler A, Sahin-Nadeem H, Lummis SC, Weigel I, Pischetsrieder M, Buettner A, et al. GABA(A) receptor modulation by terpenoids from *Sideritis* extracts. *Mol Nutr Food Res*. 2014;58(4):851-62.

Changes in the aroma profile during thermal processing and storage of strawberry purees originating from different cultivars

NATALIA TERIBIA^{1,2}, Carolien Buvé¹, Daniel Bonerz², Julian Aschoff², Marc Hendrickx¹ and Ann Van Loey¹

¹ KU Leuven, Laboratory of Food Technology, Leuven, Belgium, nataliamar.teribiacasado@kuleuven.be

² Döhler GmbH, Darmstadt, Germany

Abstract

Changes in the volatile fraction of strawberry purees prepared from five single cultivars (i.e. 6082, Honeoye, Lola, Rendezvous and Senga Sengana) during pasteurisation (95 °C, 1 min) and subsequent accelerated storage (35 °C, 14 days) were studied using an untargeted HS-SPME-GC MS fingerprinting approach. The application of multivariate data analysis on the untargeted data showed three distinctive clusters in the fresh purees. Rendezvous, Lola and 6082 appeared to be similar in the volatile fraction whereas Senga Sengana and Honeoye were not grouped together confirming their distinctive aroma profile with more than 20 and 8 markers, respectively. Thermal processing generally decreased the amount of aldehydes (hexanal), higher alcohols and increased acetate esters content. Subsequent accelerated storage resulted in the degradation of esters, aldehydes (hexanal), some terpenes (trans-nerolidol) and the formation of sulphur compounds (dimethyl sulphide), hydrocarbons, benzene derivatives and α -terpineol. Furthermore, the PLS-DA models showed that despite the initial differences on the volatile fraction among the cultivars, these differences remain similar throughout the processing chain and subsequent storage. The present study highlights the importance of adequate raw material selection for processing purposes as the cultivar strongly influences the aroma profile of the final product.

Keywords: strawberry, volatiles, cultivar, processing, storage

Introduction

Strawberries are the most consumed berries worldwide. Although the majority of the produced strawberries are used for the fresh market there is a growing interest for their use as a food ingredient (e.g. puree) in beverages, dairy and bakery products due to their unique flavour characteristics, which are the combination of aroma, taste and mouthfeel sensations. The attractive aroma is derived from a complex mixture of volatiles that include esters, aldehydes, alcohols, ketones and sulphur compounds (among others) and this aroma profile is known to be highly dependent on the cultivar [1]. Next to this, processing and subsequent storage can result in drastic changes of the aroma, as the characteristic fruity and fresh odour is replaced by unpleasant flavours (e.g. off-flavours) [2]. However, limited information from the effect of cultivar on the flavour stability during the processing chain of strawberry products has been described in the literature. Therefore, five different strawberry cultivars (i.e. 6082, Honeoye, Lola, Rendezvous and Senga Sengana) were selected and the changes in the volatile fraction of strawberry puree during pasteurisation (95 °C, 1 min) and subsequent storage (35 °C, 14 days) were studied using an untargeted HS-SPME-GC-MS approach.

Experimental

Puree processing and storage

Frozen strawberries of the cultivars 6082, Honeoye, Lola, Rendezvous and Senga Sengana were thawed overnight (4 °C) and subsequently blended in a Thermomix. The resulting puree was passed through a 500 μ m sieve to remove seeds. Pasteurisation was performed in a UHT Tubular Heat Exchanger at 95 °C for 1 min. Pasteurised strawberry purees were filled manually in polypropylene (PP) containers and stored at accelerated conditions (35 °C) for 14 days with two sampling times after pasteurisation (0 day), 4 and 14 days of storage. After sample collection, purees were frozen and stored at -20 °C until analysis. Applying elevated storage temperatures could result in a larger impact of storage on the concentration (i.e. faster change) of some volatiles as previously described by Buvé et al. [2] in strawberry juice. Yet, it has been shown in previous research that reactions were merely accelerated, and generally no new reaction pathways were induced. Next to storage temperature, the packing material is an important factor that can negatively affect the aroma of a food product through the scalping phenomena. The use of polypropylene compared to polystyrene packages during the storage of strawberry yogurt, resulted in greater losses of fruity odours due to the degradation of esters (ethyl esters) and γ -decalactone [3].

Untargeted GC-MS analysis & Data analysis

Volatile compounds were analysed in sextuplicate in a HS-SPME-GC-MS using the previous method developed by Buvé et al. [2]. The obtained chromatogram data was further analysed using first an Automated Mass Spectral deconvolution and Identification system (AMDIS) and further a Mass Profile Professional software. The resulting dataset (i.e. peak areas) was used for the multivariate data analysis (MVDA). To study the effect of treatment (i.e. fresh, pasteurised, 4- and 14-day storage) as well as the cultivar a PLS-DA model was applied. Y-variables corresponded to the treatment or cultivars, whereas X-variables were the volatile compounds. The outcome of the analysis i.e. scores and correlation loadings describing the first two latent variables (LV) were plotted in a biplot. In addition, to select those volatiles characteristic of a class, variable identification coefficients (VIDs) were calculated and those with a value above $|0.80|$ were selected and identified by comparison of the deconvoluted mass spectrum with the reference mass spectra from NIST spectral library (NIST14) as well as by composition of the experimentally determined retention index with literature data.

Results and discussion

The differences between the cultivars on the volatile fraction of strawberry puree for each treatment were described employing PLS-DA models. Four LVs were chosen to describe each model but only the first two LVs are plotted in the biplot (they explained in total 50% of the Y-variance). In the present study, the effect of cultivar on namely fresh, pasteurised and 14-day-stored samples are discussed.

Effect of cultivar on the volatile fraction

The differences in the volatile profile of the fresh samples can be seen in Figure 1A. There is a clear separation between the cultivars indicating differences in the volatile fraction among these five cultivars. Honeoye and Senga Sengana appeared far from each other and from the other cultivars in the biplot, suggesting that the volatile profile of these two cultivars are very different from each other and from the others.

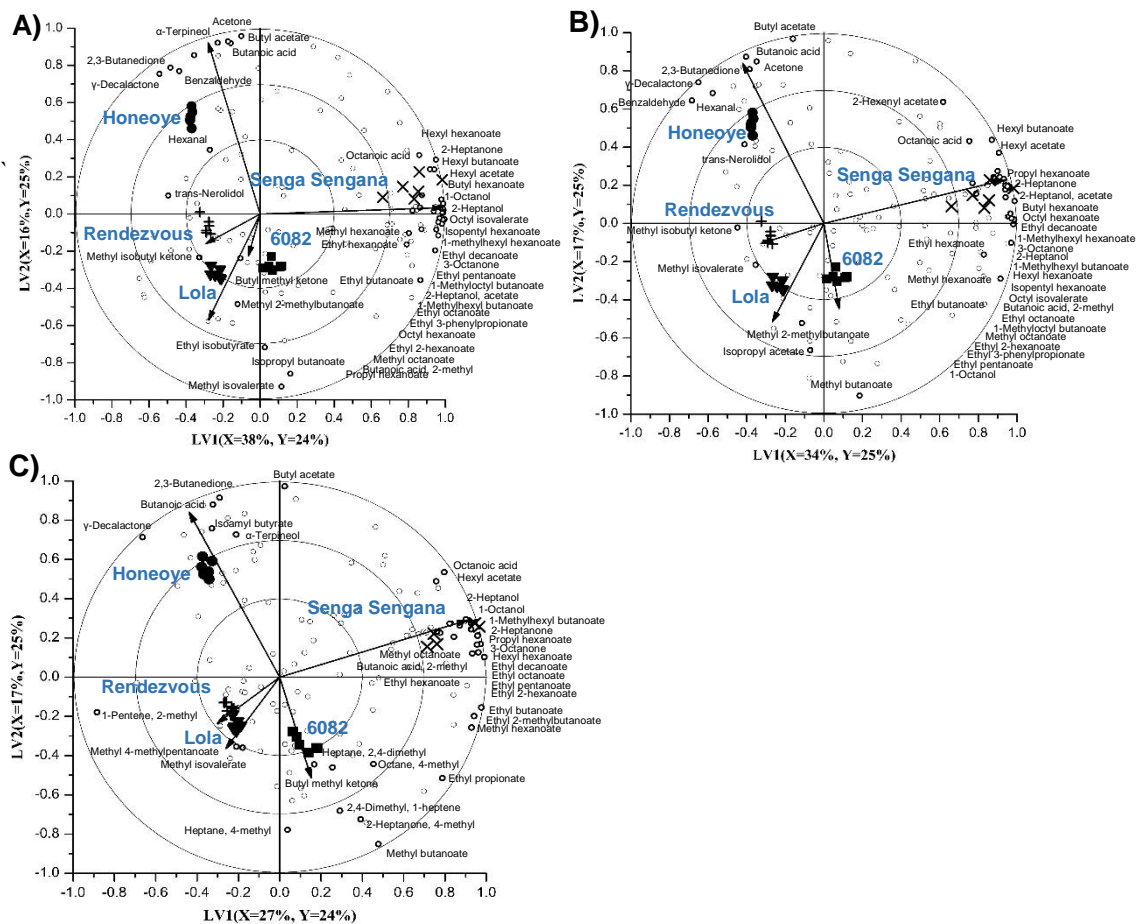


Figure 1: PLS-DA biplots showing the volatile changes of (A) fresh, (B) pasteurised and (C) 14-day stored purees (at 35 °C) originated from five single cultivars. The percentages X- and Y- variances described by the first two LVs. The vectors represent the correlation loadings for the Y-variables. Those volatiles with a VID $> |0.80|$ are marked in with an open bold circle and referred to as discriminative markers.

Twenty-seven markers were found for Senga Sengana, the majority belonging to the ester class (e.g. octyl hexanoate, 1-methyloctyl butanoate, hexyl hexanoate, etc.) whereas Honeoye exhibited a more diverse profile with 8 markers being terpenes (α -terpineol), esters (butyl acetate), lactone (γ -decalactone) and aldehydes (hexanal and benzaldehyde). Isopropyl butanoate and methyl butanoate (with negative VIDs, data not shown) were either not present or present in low concentrations, respectively, in Honeoye cultivar. Rendezvous, 6082 and Lola exhibited a more similar volatile fraction with 3, 2 and 1 discriminative markers, respectively. Our results are in agreement with Zhao et al. [1] who observed that alcohols, esters, aldehydes and acids were the volatile classes affecting the most the cultivar separation.

After thermal processing (Figure 1B), the different cultivars were separated in a similar way in the biplot meaning that after pasteurisation, the differences on the volatile profile among the cultivars remained largely unchanged. Similar results were observed during storage (Figure 1C), but the differences between Rendezvous and Lola became smaller after 14 days of storage. With regard to the markers, storage had a negative impact on some selected volatiles. For example, in Senga Sengana esters such as octyl hexanoate, octyl isovalerate, 1-methyloctyl butanoate, butyl hexanoate, etc. decreased during storage. Hexanal and trans-nerolidol were also negatively affected by the storage. New volatile markers (with positive VIDs) appeared next to the 6082 indicating that the concentration of these volatiles increased during storage. The majority of them belong to the hydrocarbon class (e.g. 2,4-methylheptane, 4-methyloctane, etc.). Increasing concentrations of hydrocarbons could be associated with the oxidation of unsaturated fatty acids [4].

Effect of pasteurisation and storage on the volatile fraction

In the present manuscript, only the results from the Honeoye cultivar are shown. A PLS-DA model with three LVs (explained 95% of the total Y-variance) was chosen to better describe the effect of pasteurisation and storage on the volatile fraction of strawberry puree (cv. Honeoye). In the biplot (Figure 2), it can clearly be seen the separation of the four classes (i.e. fresh, pasteurised, 4- and 14-day stored samples) indicating that thermal processing and subsequent storage had an impact on the volatile fraction. Fresh purees from Honeoye cultivar exhibited high contents (positive VID) of aldehydes (hexanal) and esters (methyl isovalerate, ethyl butanoate, ethyl octanoate, ethyl isovalerate) which provide green-fresh, sweet and fruity odours, respectively. Alcohols such as 1-pentanol and 1-hexanol were also present in freshly prepared purees. Pasteurisation resulted in the formation (positive VIDs) of acetate esters such as butyl acetate, hexyl acetate isoamyl acetate and 2-hexenyl acetate as these volatiles were located close to the pasteurised class. Acetate esters are associated with banana, apple and glue-like odours.

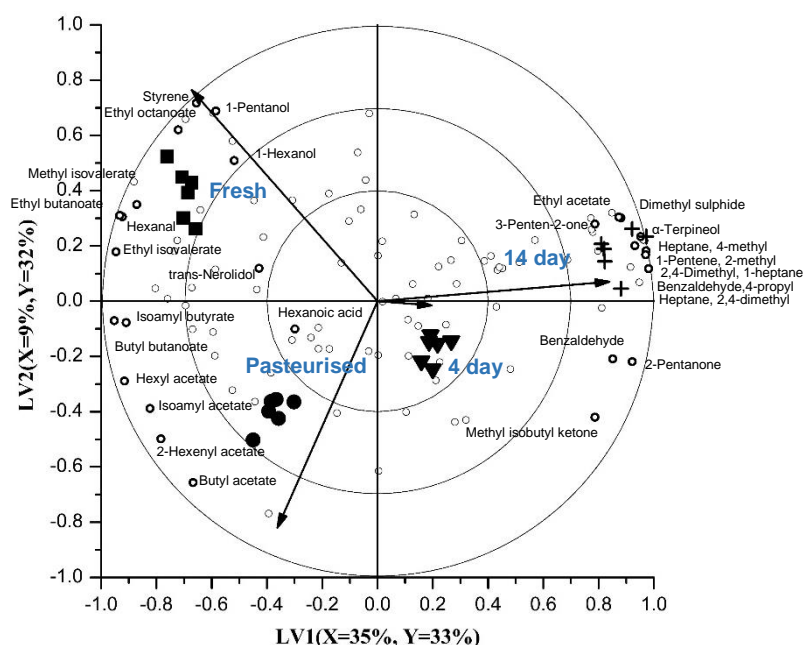


Figure 2: PLS-DA biplots showing the volatile changes in strawberry purees from the Honeoye cultivar upon thermal processing and subsequent accelerated storage at 35 °C. The percentages X- and Y variances described by the first two LVs. The vectors represent the correlation loadings for the Y-variables. Those volatiles with a VID > |0.80| are marked in with an open bold circle.

During storage the volatile fraction of strawberry puree underwent some changes as the two classes (4- and 14-day) were located on the right side of the biplot, far from fresh and pasteurised samples. Storage led to the formation of new volatile compounds and/or degradation of the volatiles. This can be observed based on the position of the volatile in the biplot and the VID coefficient (data not shown). For example, dimethyl sulphide (sulphur compounds), α -terpineol (terpene alcohol), benzaldehyde 4-methyl (benzene derivative) and hydrocarbons (alkanes and alkenes) increased (positive VIDs). The increase in dimethyl sulphide can be attributed to the Strecker degradation of methionine which can lead to the formation of off-flavours [5]. Furthermore, the formation of α -terpineol during accelerated storage has been previously reported in strawberry juice and it can be related to the acid-catalysed hydration of linalool into α -terpineol [2, 6].

Conclusion

An untargeted HS-SPME-GC-MS approach followed by a multivariate data analysis successfully evaluated the impact of cultivar, thermal processing and accelerated storage on the volatile fraction of strawberry puree. The PLS-DA models showed the differences between the five cultivars in which Senga Sengana and Honeoye exhibited the most distinctive volatile profiles. After thermal processing and storage the differences on the volatile constituents of the different cultivars remained similar. This highlights the importance of adequate raw material selection for processing purposes as the cultivar strongly influences the aroma profile of the final product. Moreover, thermal processing but especially storage in PP packaging had a negative impact on the aroma of strawberry puree.

References

1. Zhao J, Liu J, Wang F, Wang S, Feng H, Xie X. et al. Volatile constituents and ellagic acid formation in strawberry fruits of selected cultivars. *Food Res Int.* 2020;138:109767.
2. Buvé C, Neckebroek B, Haenen A, Kebede B, Hendrickx M, Grauwet T, Van Loey A. Combining untargeted, targeted and sensory data to investigate the impact of storage on food volatiles: A case study on strawberry juice. *Food Res Int.* 2018;113:382–391.
3. Saint Eve A, Lévy C, Le Moigne M, Ducruet V, Souchon I. Quality changes in yogurt during storage in different packaging materials. *Food Chem.* 2008;110:285–293.
4. Azarnia S, Boye J.I, Warkentin T, Malcolmson L. Changes in volatile flavour compounds in field pea cultivars as affected by storage conditions. *Int J Food Sci Tech.* 2011;46:2408-2419.
5. Perez-Cacho P. R, Mahattanatawee K, Smoot J. M, Rouseff R. Identification of sulfur volatiles in canned orange juices lacking orange flavor. *J Agric Food Chem.* 2007;55:5761–5767.
6. Haleva-Toledo E, Naim M, Zehavi U, & Rouseff R L. Formation of α -terpineol in citrus juices, model and buffer solutions. *J Food Sci.* 1999;64:838–841.

The volatile constituents and key character impact compounds of two different commercial dark chocolates, each containing 64% of cocoa from different origins

CATHERINE VERMEULEN, Julien Simonis, Léonor Bonnafous, Cécile Petit and Filip Arnaut

Puratos NV, Groot-Bijgaarden, Belgium, cvermeulen2@puratos.com

Abstract

The composition in flavouring substances and the sensorial profile of chocolate are known to be influenced by many parameters: the cocoa variety, the cocoa geographical origin, the cocoa fermentation and roasting conditions but also the chocolate recipe itself and its manufacturing. In this study, we analysed by SAFE-GC-MS/O (AEDA) two commercial dark chocolates, each containing 64% of cocoa from different origins: Peru and Costa Rica. While more than 10 components had a same and very high odour dilution factor respectively in both chocolates (e.g. vanillin, acetic acid, methional, furaneol, 2-phenylethyl acetate, 2-methoxyphenol), a higher impact of the 2/3-methylbutyl acetate and the delta-octalactone could be observed in the “Peru-chocolate”, explaining its typical fruitiness. The “Costa Rica-chocolate” with a more complex sensorial profile, reminiscent of olive, seemed for its part to be richer in 2,3,5-trimethylpyrazine, octanal and isovaleric acid to name a few.

Keywords: flavouring substance, aroma, sensorial characteristic, dark chocolate, cocoa origin

Introduction

The world of cocoa and chocolate is really fascinating. Today, by sharing their passion, knowledge and expertise, cocoa farmers and chocolate manufacturers or chocolatiers are able to offer a huge diversity of taste experiences to consumers, fulfilling their greatest need [1].

Many parameters are known to influence the final sensorial profile of chocolate: the variety of cocoa tree that is cultivated, the origin of this cocoa, the way the cocoa beans are fermented or roasted and the chocolate manufacturing processes that are applied. By combining and playing with these parameters, the possibilities to create something unique or characteristic are endless.

Obviously, chocolate is a very complex matrix, which contains hundreds of different flavouring substances. They all come indirectly from the ingredients that are used to make chocolate. Some of them or their precursors are generated by the yeasts and bacteria during the fermentation step of the cocoa beans. Others are issued from chemical reactions like the Maillard reactions during the roasting of these beans or from additional reactions during the conching of the chocolate itself, etc. Finally, along the way or over time, due to their high volatility or reactivity, some of these components also get lost or further transformed [1-3].

Because of this molecular complexity and the presence of fats or other foodstuffs, thorough and instrumental analyses of chocolate can be quite challenging and time-consuming. However, the most difficult part of this kind of studies very likely lies in making the links between these instrumental data and the consolidated input of a sensorial expert panel [4].

In this case, we analysed by the combined techniques solvent assisted flavour evaporation (SAFE) and gas chromatography-mass spectrometry/olfactometry (GC-MS/O) using the aroma extract dilution analysis (AEDA) olfactometric methodology two commercial dark chocolates, each containing 64% of cocoa from two different origins (Peru, Costa Rica) and we tried to correlate those results with their respective sensorial description.

Experimental

All the experiments were conducted separately by an external research institute (GC analyses) or a partner (sensorial analyses) and run as a proof of concept to determine which future investments would be the most relevant to make in our own analytical laboratory.

Extraction and concentration – SAFE + distillations

The extraction of the flavouring substances was done by putting 20 g (\pm 0.1 g) of dark chocolate in ~150 mL of dichloromethane (freshly distilled), stirring it all vigorously for 30 minutes at room temperature. The extract was then filtered and, afterwards, the volatiles were separated from the non-volatiles by means of the SAFE technique. The distillates were dried over anhydrous sodium sulphate, filtered, concentrated at 50 °C to ~3 mL using a Vigreux column and finally concentrated to ~100 μ L by micro-distillation.

Separation and identification – GC-O (AEDA) & GC-MS

The separation and sniffing of the flavouring substances via GC-O was performed using a TRACE GC (Thermo Fisher Scientific Inc., MA, United States) equipped with a DB-FFAP fused silica capillary column (30 m × 0.32 mm i.d., 0.25 µm film thickness). Aliquots (2 µl) of the SAFE-extract were injected manually by the cold on-column technique (40 °C). After 2 min, the temperature was raised at 8 °C/min to 235 °C (DB-FFAP), and held for 5 min. The flow rate of the carrier gas helium was 2.2 mL/min. At the end of the column, the effluent was split 1:1 by a Y-splitter. Two deactivated fused silica capillaries of the same length (30 cm × 0.32 mm i.d.) led either to a FID (250 °C) or to an Odour Detection Port (ODP, 250 °C). Linear retention indices (RIs) of the compounds were calculated by a homologous series of n-alkanes (C6–C26). AEDA with determination of flavour dilution (FD) factors was done by two trained panellists by diluting the distillate stepwise with dichloromethane (1+2 by volume). Each dilution step (1:3; 1:9; 1:27; 1:81; 1:243; v/v) was then analysed by GC-O. The highest dilution at which an odour of an individual compound was detectable was defined as the flavour dilution factor for that odorant. Detection in the undiluted extract corresponds to FD 1, detection in higher dilutions corresponds to higher FDs.

The separation and identification of the flavouring substances by GC-MS was performed using a GC-O/MS system consisted of a Thermo GC Ultra coupled to a DSQ II mass spectrometer (both: Thermo Fischer Scientific, Dreieich, Germany), equipped with the same capillary column as the one described above. Aliquots (2 µL) of the SAFE-extracts were injected at 40 °C using the cold on-column technique by a Multi-Purpose-Autosampler (Gerstel, Mülheim an der Ruhr, Germany), following the same temperature program than the one mentioned above. The flow rate of the carrier gas helium was 2.3 ml/min. Mass spectra were generated in the positive electron impact (EI) ionisation mode at 70 eV (scan 25-350 m/z).

Description – Sensorial analysis

The sensorial analyses (conventional profiling and quantitative descriptive analyses) were performed by seven expert panellists, exploiting the XLSTAT software.

Results and discussion

More than 65 different smells were detected by GC-O in these two dark chocolates. Those with the highest FD factors or with significantly different FD factors for each chocolate were identified based on their retention index, mass spectra, etc. (Table 1).

Dimethyl trisulphide, acetic acid, 2-ethyl-3,6-dimethylpyrazine, methional, 3-isobutyl-2-methoxypyrazine, 2-phenyl ethyl acetate, 2-methoxyphenol, ethyl-3-phenylpropionate, 2-phenylethanol, δ-octalactone, furaneol, γ-decalactone / ethyl cinnamate (co-eluting), (R)-5,6-dihydro-6-pentyl-2H-pyran-2-one and vanillin, commonly present in both analysed chocolates and characterised by FD factor ≥81, actively contribute to the overall sensorial profile of dark chocolate.

Table 1: The most odour-active or differentiating molecules in the two analysed dark chocolate extracts (1st part).

RI ^a	Flavouring substance ^b	Smell description ^c	FD factor ^d	
			Costa Rica	Peru
1121	2/3-methylbutyl acetate ^e	banana-like	1	27
1231	(Z)-4-heptenal ^e	fishy, cod liver oil-like	81	9
1275	octanal	citrus-like	81	9
1288	1-octen-3-one ^e	mushroom-like	243	27
1356	dimethyl trisulphide	sulphury, cabbage-like	243	243
1394	2,3,5-trimethylpyrazine	earthy	243	27
1427	acetic acid	vinegar-like	81	81
1433	2-ethyl-3,6-dimethylpyrazine ^e	earthy	81	81
1440	methional ^e	cooked potato-like	243	243
1500	3-isobutyl-2-methoxypyrazine	bell pepper-like	243	243
1636	2-methyl(3-methyldithio)furan ^f	fatty, broth-like	243	27
1657	2/3-isovaleric acid	sweaty	243	81
1664	2-acetyl pyrazine ^f	fatty, roasty	243	81

Table 1: The most odour-active or differentiating molecules in the two analysed dark chocolate extracts (2nd part).

RI ^a	Flavouring substance ^b	Smell description ^c	FD factor ^d	
			Costa Rica	Peru
1679	3-methyl-2,4-nonanedione ^f	sweaty, herbal	243	81
1785	2-phenyl ethyl acetate	flowery, rose-like	243	243
1842	2-methoxy phenol	ham-like	243	243
1858	ethyl-3-phenylpropionate	flowery	243	243
1883	2-phenylethanol	flowery, rose-like	243	243
1975	δ -octalactone	flowery, coconut-like	9	81
2017	4-hydroxy-2,5-dimethyl-3(2H)furanone (furanol) ^e	roasty, caramel-like	81	81
2100	γ -decalactone / ethyl cinnamate	coconut-like, cinnamon-like	243	243
2205	(R)-5,6-dihydro-6-pentyl-2H-pyran-2-one	peach/coconut-like	243	243
2530	vanillin	vanilla-like	243	243
2585	3-phenylpropanoic acid ^e	beeswax-like	243	81

^a Linear retention index (DB-FFAP) ; ^b Molecule identified based on its smell, retention index (DB-FFAP) and mass spectra (EI mode) ; ^c Smell perceived by GC-O ; ^d Flavour dilution factor determined by GC-O (AEDA) ; ^e No mass spectrum for this molecule ; ^f No mass spectrum for this molecule and no reference substance available to validate/check its RI

The higher impact of the 2/3-methylbutyl acetate in the “Peru-chocolate” correlates very well with the differentiating and subtle notes of banana spotted by the sensorial expert panel in this chocolate (Figure 1).

The “Costa Rica-chocolate” with its complex profile, described by the expert panel as more intense in hay and dried fruit notes (Figure 1) or by some of our chocolatiers as reminiscent of olives, has many molecules with a significantly higher FD factor than the one obtained for the same molecule in “Peru-chocolate”: (Z)-4-heptenal, octanal, 1-octen-3-one, 2,3,5-trimethylpyrazine, 2-methyl(3-methylthio)furan, 2/3-isovaleric acid, 2-acetyl pyrazine, 3-methyl-2,4-nonanedione, 3-phenylpropanoic acid.

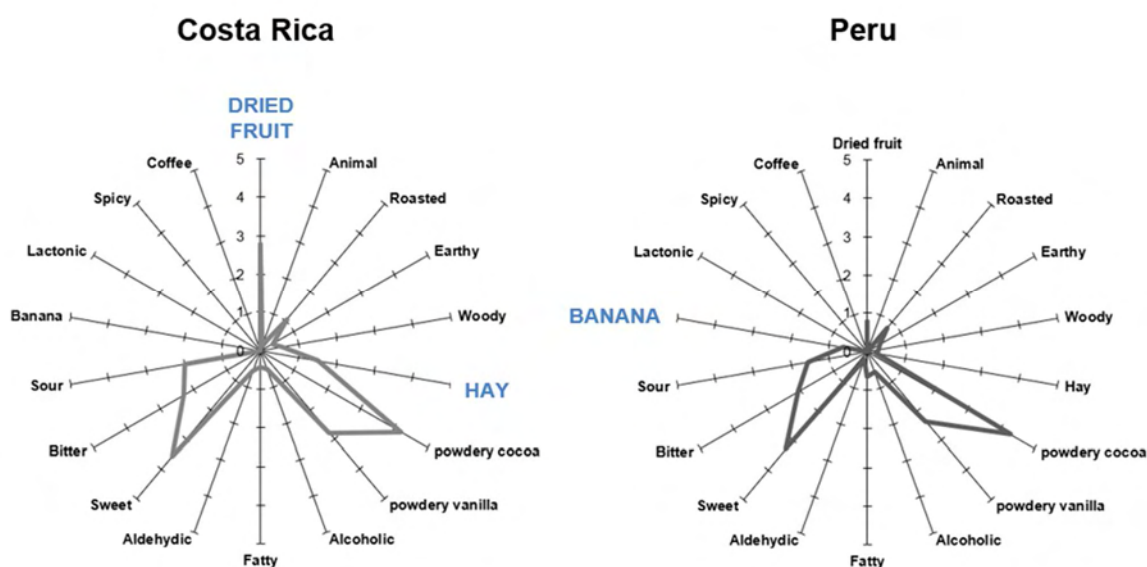


Figure 1: Sensorial description of the “Costa Rica-chocolate” and “Peru-chocolate” with their respective and differentiating sensorial characteristics highlighted in blue.

Conclusion

It is nice to observe that the organoleptic impacts of the delta-octalactone and more especially of the 2/3-methylbutyl acetate, which are suspected to be higher in the “Peru-chocolate” based on the instrumental analyses and FD factors, are indeed very likely contributing to its typical and mild fruitiness.

The “Costa Rica-chocolate”, in which multiple and very diverse components like pyrazines, furans, organic acids and other carbonylated molecules seem to play a more discriminant role, has a different sensorial profile, which is also much more difficult or less straightforward to describe. Further and deeper analyses would be needed to highlight which molecules are the most critical and differentiating in this “Costa Rica-chocolate”. Nevertheless, thanks to these first and indicative results, the components to focus on in the future have been identified.

Finally, as an extra insight, please note that, with the same purpose, other instruments and methodologies (e.g. electronic nose or SPME(HS)-GC-O) were investigated in this study but the SAFE-GC-MS/O (AEDA) turned out to be the most appropriate and comprehensive approach.

References

1. Afoakwa E O, et al. Flavor Formation and Character in Cocoa and Chocolate: A Critical Review. *Crit Rev Food Sci Nutr.* 2008;48(9):840–857.
2. Aprotosoiaie A C, et al. Flavor Chemistry of Cocoa and Cocoa Products—An Overview. *Compr Rev Food Sci Food Saf.* 2016;15:73-91.
3. Muñoz M S, et al. An overview of the physical and biochemical transformation of cocoa seeds to beans and to chocolate: Flavor formation. *Crit Rev Food Sci Nutr.* 2020;60(10):1593-1613.
4. Lemarcq V, et al. Assessing the flavor of cocoa liquor and chocolate through instrumental and sensory analysis: a critical review. *Crit Rev Food Sci Nutr.* 2021; DOI: 10.1080/10408398.2021.1887076.

Chemical and physical stability of soluble coffee stored in different packaging materials

JOSEPHINE CHARVE¹, Nicolas Antille¹, Moritz Kindlein¹, Luigi Poisson² and Jan Engmann¹

¹ Société des Produits Nestlé SA, Nestlé Research, Route du Jorat 57, 1000 Lausanne 26, Switzerland

² Société des Produits Nestlé SA, Nestlé Product Technology Center Beverage, Route de Chavornay 3, 1350 Orbe, Switzerland

Josephine.Charve@rdls.nestle.com

Abstract

Using recyclable packaging such as paper-based materials raises challenges in terms of barrier performance compared to materials with very strong barrier performance such as plastic laminates. Dry products are at higher risk to experience physical and chemical changes during shelf-life, especially in tropical climates. Quantitative understanding of the mechanisms contributing to the quality losses is needed to address this challenge. This work addresses the stability of soluble coffee during short-term storage (20 days) under different storage conditions (20 °C/ 20 % RH, 50 °C/ 20 % RH, 20 °C/ 70 % RH) in sachets made from different packaging materials (OSPET-PE, PET-PE, high barrier metallized paper). The moisture uptake of the powders was tracked, and comparative descriptive sensory analysis was performed to evaluate differences when compared to fresh samples. Changes in key volatile compounds were monitored by headspace solid phase microextraction gas chromatography-mass spectrometry. Additionally, a predictive model accounting for the packaging barrier quality and physical properties of the ingredients was used to estimate moisture sorption and powder stability under different storage conditions. Elevated storage temperature had a stronger effect on aroma stability than humidity, independently of the tested package. Compounds with high and medium volatilities were the most affected (up to 55 % losses). Sulphur compounds illustrated oxidative reactions occurring during storage at 50 °C in all packaging materials. Aldehydes, diketones, and N-methylpyrrole revealed important degradation at 50 °C and at high environmental humidity in one type of packaging material; this indicates chemical reactions occurring and likely triggered by the transition from solid to rubbery state and resulting increased molecular mobility above the glass transition temperature. Sensory evaluation showed that samples stored at high temperature deviated the most from the fresh reference, with higher oxidized notes.

Keywords: recyclable packaging, aroma losses, soluble coffee, physical/chemical stability, shelf-life prediction

Introduction

Using recyclable packaging such as paper-based materials raises challenges in terms of barrier performance compared to materials with very strong barrier performance like plastic laminates. Dry products are at higher risk to experience physical and chemical changes during shelf-life, especially in tropical climates [1]. For soluble coffee, powder agglomeration (caking) and decrease in aroma quality (aroma fading and formation of off-notes) are the main risks. The objective of the present study was to determine the influence of storage conditions (temperature, relative humidity, and packaging material) on aroma losses in soluble coffee and the impact on sensory perception.

Experimental

An overview of the experimental set-up is provided in Figure 1. Soluble coffee was stored for 20 days in different packaging materials under various climatic conditions (temperature and relative humidity). Remaining aroma levels, moisture uptake and sensory deviations were examined.

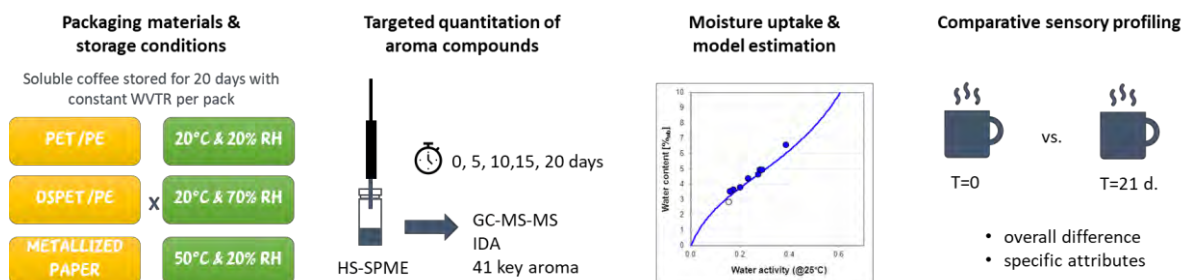


Figure 1: Experimental set-up for the study of chemical and physical stability of soluble coffee stored in different packaging materials.

Soluble coffee samples, packaging materials and storage conditions

All samples were prepared in the laboratory at the beginning of the study with two sets of sachets per sampling point for analytical and sensory analyses (in triplicate). The packaging materials included sheets of polyethylene terephthalate-polyethylene (PET-PE), oxygen scavenger polyethylene terephthalate-polyethylene (OSPET-PE), and a high barrier metallized paper. Those materials were chosen for their differences in water vapour transmission rates (WVTR) and oxygen transfer rates (OTR). Soluble coffee (100% Robusta) was manually filled in the pre-formed hand-made sachets. The sachets were heat-sealed on four sides to prevent moisture exchanges from the edges. All samples were placed vertically in climatic chambers to allow proper air and moisture exposure for 20 days at three storage conditions: 20 °C/ 20 % RH, 20 °C/ 70 % RH and 50 °C/ 20 % RH. Samples were collected on day 0, 5, 10, 15 and 20 and kept frozen (-40°C) until analysis at the end of the study.

Aroma analysis

Quantification of key aroma compounds was performed by Isotope Dilution Assay (IDA) in combination with the aroma isolation by Solid Phase Micro Extraction (SPME). The volatile compounds were separated by gas chromatography and detected by mass spectrometry (GC-MS/MS). In total, 41 volatile compounds were quantitatively assessed and subdivided in groups based on chemical class (e.g., aldehydes, furans, sulphides, ethyl esters, diketones, thiols, alkyl pyrazines, phenols, cyclic enolones, N-methylpyrrole) and volatility (based on Henry's law constant). The compounds were chosen based on their impact on coffee aroma and/ or as key markers for the shelf-life status of a coffee [2-4].

Water content analysis and predictive model

Water activity was measured with an AquaLab 4TE Decagon (Decagon Devices Inc., US) instrument. The measurement is based on the detection of dew point when the sample and the headspace are in chemical (moisture) and thermal equilibrium. The measurements were performed at 25 °C for all samples and determined in duplicates with a precision of ± 0.007 . Water content was calculated from the measured water activity using the sorption isotherm of coffee, which had been determined independently.

The kinetics of externally driven changes in coffee moisture content were modelled by a mass balance for water between atmosphere, packaging barrier, product headspace, and product. For the packaging materials used in our study, moisture diffusion through the barrier is rate-limiting, i.e., slow enough to neglect diffusion lag inside powder particles and the powder is always considered in thermodynamic equilibrium with regards to moisture content, i.e., the sorption isotherm provides a relation between moisture content and water activity. Glass transition temperature of the coffee was calculated according to the present water content, using a Gordon-Taylor model with parameters previously determined for the soluble coffee under consideration.

Sensory analysis

Only samples stored for 20 days were sensorially evaluated by comparative descriptive analysis. Prior to the session, samples were reconstituted in hot water (Acqua Panna water, 85 °C). The beverages were kept at serving temperature (60 °C) and served to the panellists (30 mL) just before tasting. The sensory evaluation was carried out with an untrained panel (n=8) and consisted in comparing each stored sample to the reference (fresh sample at T=0 day which was kept frozen until analysis). The panellists were asked to rate the differences between stored and fresh samples 1) for overall aroma above the cup and flavour intensity using a 10-point structured scale (0= No difference; 10= Extreme difference); and 2) for specific flavour attributes related to the coffeeness and off-notes using a structured scale (anchored with "much less" (-3), "much more" (+3) and "no difference" (0)).

Data analysis

For each sample, the absolute concentration of the individual volatile compounds (in mg/kg soluble coffee powder) were expressed as a percentage of the initial concentration (T0 set as 100 %) to get a measure of the remaining aroma after storage. The total aroma remaining was calculated as the geometrical mean of the remaining levels of the 41 compounds. Obtained values were processed individually for each compound using a two-way analysis of variance to assess the significance of the effect of the storage conditions and packaging material of the remaining aroma.

A two-way analysis of variance (with "sample" as a fixed factor and "panellist" as a random factor) was performed for each sensory attribute and global differences scores (aroma above the cup and flavour) to calculate the Fisher's Least Significant Difference (LSD). In parallel, individual sensory scores were averaged across all panellists to obtain a mean sensory profile for each sample. Then, the mean sensory intensity of each attribute for calculated storage conditions and packaging material, and obtained values were compared using the previously calculated LSD divided by the square root of 3 (the number of samples featuring each storage condition and packaging material) to assess the significance of the effect of the storage conditions and packaging material [5]. All analyses were performed with R 4.0.2 (www.R-project.org) and with a 95% confidence level for statistics.

Results and discussion

This work addresses the stability of soluble coffee during short-term storage (20 days) under different storage conditions in sachets made from different packaging materials. The influence of storage conditions on powder stability, aroma losses and the impact on sensory perception are reported here.

Aroma evolution during storage

During storage of coffee, aroma fading and the formation of off-notes can alter the complex balance of coffee aroma and hence its quality. Evaporation, oxidation, and reactivity of some coffee aroma compounds are the main mechanisms involved [6]. Changes in key volatile compounds used as markers for coffee shelf-life status were monitored by headspace solid phase microextraction gas chromatography-mass spectrometry.

In this study, storage temperature had a stronger effect on coffee aroma stability than humidity across all packaging materials. Samples stored at 50 °C resulted in the lowest total aroma remaining [%]. Storage temperature is known as an important factor determining the shelf life duration of soluble coffee. In general, soluble coffee can be stored for 24 to 36 months at 20 °C before getting into a critical sensorial zone whereas shelf-life timespan drastically reduces at temperatures above 30 °C [7]. Here, compounds with high and medium volatilities were the most affected with remaining levels between 64 and 46 % of their initial quantities at day 20 (Figure 2).

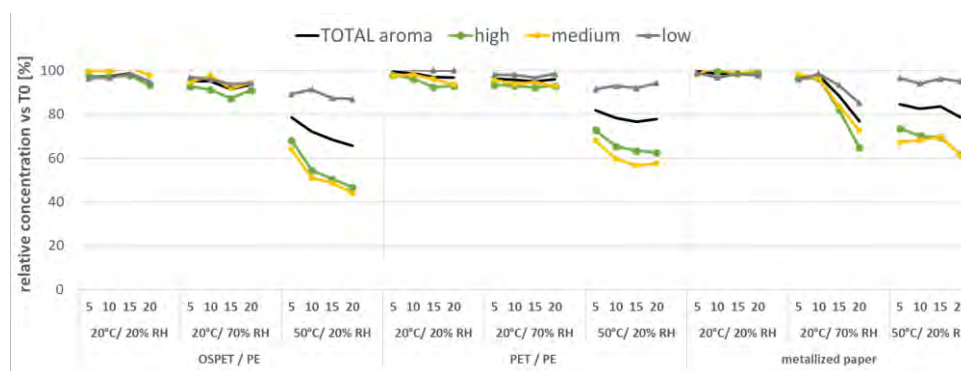


Figure 2: Remaining aroma levels [%] compared to T0 at 5, 10, 15 and 20 days in soluble coffee samples stored under different conditions. Aroma compounds shown as total aroma (geometrical mean of all compounds) and sub-split in three classes according to their volatilities (high, medium and low volatiles).

The increased mobility of molecules due to higher temperature also resulted in crucial acceleration of the chemical reactivity: oxidative and non-oxidative reactions were observed when looking more in details at the different chemical classes (Figure 3).

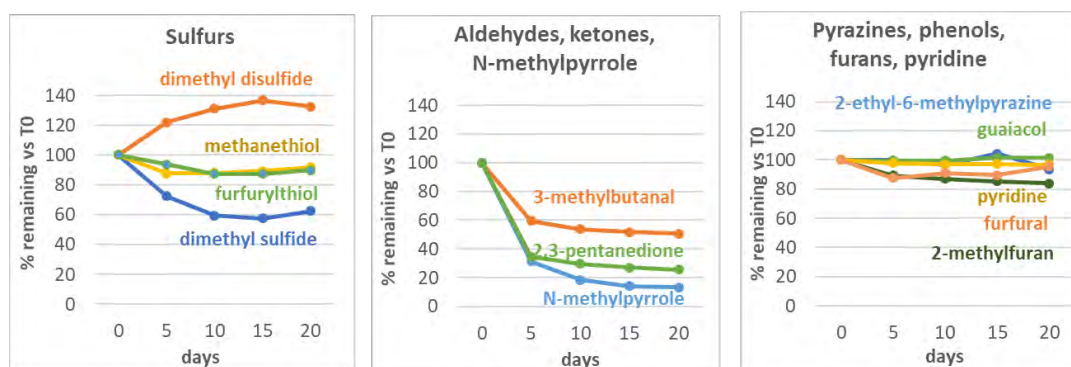


Figure 3: Evolution of specific aroma compounds during storage of soluble coffee samples stored in PET- PE sachets at 50°C/20% RH. Aroma levels expressed as [%] compared to T0.

Sulphur compounds illustrated oxidative reactions occurring during storage at 50 °C in all packaging materials (Figure 3, left). The degradation of odour impact sulphur compounds is well known and occurs instantly if the coffee is not well protected against oxidation. Best reported case is the oxidative degradation of thiols like methanethiol or 2-furfurylthiol forming disulphides by dimerization [8]. The formed dimethyl disulphide can further disproportionate to dimethyl sulphide and dimethyl trisulphide. Yeretziyan et al. [6] formulated the relationship between the degradation of methanethiol and the formation dimethyl disulphide as ratio index for the

definition of coffee freshness. Lipid oxidation did not seem to play an important role in soluble coffee as no increase of the lipid oxidation marker hexanal was noticed. Contrary to roast and ground coffee, oxygen has only a small influence on shelf life of soluble coffee [7]. Aldehydes, α -diketones, and N-methylpyrrole revealed important degradation at 50 °C in all packaging materials (Figure 3, middle) and at high environmental humidity for the metallized paper. Short-chain aldehydes are the most electrophilic molecules present in the coffee aroma. Therefore, they are highly susceptible to many kinds of chemical reactions (e.g., aldol condensation, addition to N-alkylpyrroles). On the other hand, compounds usually considered as stable (e.g., furans, alkyl pyrazines and phenols in Figure 3, right) remained at constant levels.

Powder stability

When using packaging materials with a low vapour barrier performance, the critical moisture level (~8%) at which time powder agglomeration (caking) occurs could be reached much more rapidly. In the present study, the moisture uptake of the soluble coffee powders was tracked. The moisture content remained essentially constant around 3.5 % during storage at 20°C/ 20 % RH and increased up to 6.8 % in samples stored at 70 % RH, whereas it slightly decreased (ca. 2.4%) in samples stored under high temperature/ dry environmental humidity (50 °C/ 20 % RH). No powder caking was observed in any stored samples. If kept under dry conditions (i.e., moisture level in the product < 4-5%), the shelf-life of soluble coffee is commonly between 18-36 months.

A Gordon-Taylor model, based on independent measurements of glass transition temperature as a function of moisture content, showed that samples stored at high temperature (50 °C) were exposed to temperatures above their glass transition temperature (T_g) considerably longer than samples stored at high environmental humidity (70 % RH). As previously discussed, the samples stored at 50 °C had higher aroma losses compared to the other conditions (Figure 2). Thus, it is argued that glass transition of the amorphous solid coffee matrix plays a key role in aroma stability and aroma loss, respectively. Volatiles become more mobile in the “rubbery” state, enhancing both diffusion out of the coffee particles (driven by the concentration gradient) and chemical reactions [8].

Sensory analysis

As for volatiles, sensory shifts were driven by humidity and temperature as all stored samples were scored as significantly different from the reference regarding the overall flavour. Differences due to the packaging material were smaller than those due to storage conditions although sensory deviations were minimized overall with OSPET-PE. Significant differences were also found between stored samples, with those stored at 50 °C being the most different from the reference (Figure 4, left). Data collected at the sensory attribute level confirmed that storing samples at high temperature was the most detrimental to the aroma/ flavour profile: samples were characterized with higher oxidized notes (Figure 4, right), and a slightly lower roasty intensity compared to samples stored at 20 °C (data not shown).

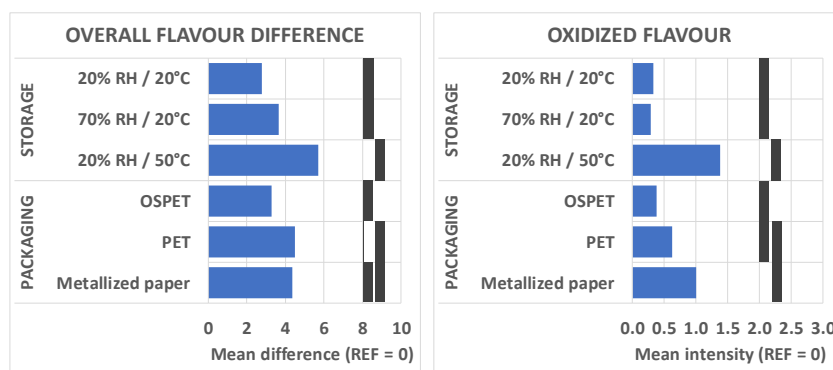


Figure 4: Mean sensory deviations for stored soluble coffee samples (day 20) compared to fresh. Conditions with overlapping black bars are not significantly different (storage and packaging to be looked at separately).

Conclusion

The study showed on the one hand that the tested packaging materials did not influence much the aroma and sensory profile of stored coffees. On the other hand, it demonstrated that storing pure soluble coffee at 50 °C (vs. 20 °C) was more detrimental to the aroma and sensory profile than storing it at 70% RH (vs. 20% RH). Main sensory changes - induced by a high temperature storage - included the development of oxidized notes and a decrease of important coffee signature notes (e.g. roasty). Those samples were exposed to temperatures above their glass transition temperature (T_g) considerably longer than samples stored at high environmental humidity. It

confirms the key role of glass transition of amorphous solid matrices for aroma loss as molecules become more mobile in the “rubbery” state, enhancing both diffusion and chemical reactions.

References

1. Manzocco L. The acceptability limit in food shelf life studies. *Crit Rev Food Sci.* 2016;56(10):1640-6.
2. Kerler J, Poisson L. Understanding coffee aroma for new product development. *New Food Magazine.* 2011;14(6):39-43.
3. Mestdagh F, Davidek T, Chaumonteuil M, Folmer B, Blank I. The kinetics of coffee aroma extraction. *Food Res Int.* 2014;63:271-4.
4. Mestdagh F, Thomas E, Poisson P, Kerler J, Blank I. Learning from other industries – Insights from coffee on advanced sensory-analytical correlations. *Proc 15th Austral Wine Ind Techn Conf, Sydney.* 2013. p. 102-6.
5. Pineau N, Moser M, Rawyler F, Lepage M, Antille N, Rytz A. Design of experiment with sensory data: A pragmatic data analysis approach. *J Sensory Stud.* 2019;34(2):e12489.
6. Yeretian C, Blank I, Wyser Y. Chapter 14 - Protecting the Flavors—Freshness as a Key to Quality. In: Folmer B, editor. *The Craft and Science of Coffee: Academic Press;* 2017. p. 329-53.
7. Nicoli MC, Manzocco L, Calligaris S. Packaging and the shelf life of coffee. In: Robertson GL, editor. *Food packaging and shelf life : a practical guide.* Boca Raton, FL, USA: CRC Press/Taylor & Francis Group; 2010. p. 199-214.
8. Karel M, Lund DB. *Physical Principles of Food Preservation. Revised and Expanded (2nd ed)* Marcel Dekker, Inc., New York; 2003. p. 451-6.

Dual-fibre solid-phase microextraction coupled with gas chromatography - mass spectrometry for the analysis of volatile compounds in traditional Chinese dry-cured ham

SHUI JIANG¹, Huan Liu², Junlong Huang², Qingkun Hu², Yan Ping Chen¹, Keqiang Lai², Jianqiao Xu³, Gangfeng Ouyang³, Yuan Liu^{1*}

¹ School of Agriculture & Biology, Shanghai Jiao Tong University, Shanghai, 200240, China

² College of Food Science & Technology, Shanghai Ocean University, Shanghai 2001306, China

³ School of Chemistry, Sun Yat-sen University, Guangzhou 510275, China

Abstract

The multiple intelligent sensory technologies including the electronic nose (E-nose), electronic tongue (E-tongue), and computer vision were applied to evaluate the sensory properties of Jinhua dry-cured hams. The back propagation neural network (BPNN) models exhibited satisfying performance on simultaneously predicting different sensory attributes ($R^2 > 0.935$). The dual-fibre solid-phase microextraction (SPME) combined with gas chromatography-mass spectrometry (GC-MS) was used to analyse the volatile compounds of Jinhua dry-cured hams. The total number (72) of volatile compounds identified by the dual-fibre SPME were larger than those identified by the mono-fibre SPME method using a single fibre. The Jinhua dry-cured hams with the different storage times could successfully be distinguished based on the dual-fibre SPME. This study suggests that data fusion of multiple intelligent sensory technologies and the dual-fibre SPME are promising methods for flavour evaluation of Jinhua dry-cured hams.

Keywords: Jinhua dry-cured ham, Electronic nose, Electronic tongue, Computer vision, Dual-fibre SPME

Introduction

Chinese dry-cured hams are increasingly popular in the world because of the unique flavour. Jinhua dry-cured ham is one of the most famous dry-cured hams in the world. The traditional processing of Jinhua dry-cured ham consists of green ham preparation, salting, washing, sun-drying and shaping, ripening, and post-ripening. The sensory properties of Jinhua dry-cured hams changed significantly when the storage time increase during the post-ripening procedure [1]. The multiple intelligent sensory technologies including the electronic nose (E-nose), electronic tongue (E-tongue), and computer vision could be applied to evaluate Jinhua dry-cured hams [2]. To further explore the volatile compound profiles of Jinhua dry-cured hams, the solid-phase microextraction (SPME) fibres coated with different stationary phases could be used. The types and extraction parameters could be optimized for the implementation of dual-fibre SPME to distinguish Jinhua dry-cured hams.

Experimental

Sample preparation

Jinhua dry-cured hams were supplied by Jinhua Jinzi Ham Co., Ltd. (Jinhua, Zhejiang province, China, 119.65 E, 29.08 N). A total of 18 hams were divided into 3 groups (6 hams/group) according to the storage time (1 year, 2 years, and 3 years) that were defined as J1, J2, and J3, respectively. The *biceps femoris* muscle parts of hams were cut into cubes (1 cm×1 cm×1 cm) for the detection of computer vision. Afterwards, these cubes were ground into powder, and 10 g powder was used for E-nose detection. Finally, 5 g powder was added into 20 mL deionized water and kept still for 2 h. The centrifugation of the sample solution was performed for 30 min on the condition of 9500 r/min. The supernatants were processed through the 0.45 μ m aqueous microporous membrane, and the filtrate was diluted in a ratio of 1:15. The finally obtained solution was used for E-tongue detection. The *biceps femoris* muscle was ground with a grinder. Then, 4 g of minced muscle and 7 g of distilled water saturated with NaCl were put into the 20 mL headspace vial for the detection of SPME.

Detections based on intelligent sensory technologies

The E-nose (SuperNose, Isenso Intelligent, Shanghai, China) equipped with 14 sensors, the E-tongue (Astree II, Alpha MOS Company, Toulouse, France) equipped with 7 sensors, and the computer vision system (Shenzhen Jingtuoyoucheng Technology Co., Ltd) were applied. For E-nose detection, the ham powder (10 g) was put into a 100 mL head-space vial which was sealed with the plastic wrap, and was kept still for 30 min, and the detecting time was 60 s. For E-tongue detection, the solution was put into an 80 mL glass beaker, and the detection lasted

for 120 s. The computer vision system consisted of a complementary metal-oxide semiconductor (CMOS) camera (1/2.33 inch, Panasonic Electric Works, Ltd.), two light sources (natural-light LEDs, 5500 K), a zoom lens with an eyepiece lens (0.5 \times) and an objective lens (0.7 \times -4.5 \times), a height-adjustable platform and a soft light box (400 mm \times 400 mm \times 400 mm). All images were saved as the JPG format with a size of 640 \times 480 pixels. Then, a 300 \times 300 pixel region of interest (ROI) which focused on the centre of the original image was extracted for the following analysis. For each ham, 5 replicates were conducted, and 90 data sets (5 replicates/ham \times 6 hams/category \times 3 categories) were obtained from E-nose, E-tongue, and computer vision, respectively. All the experiments were conducted at the room temperature of 20 $^{\circ}\text{C} \pm 1$ $^{\circ}\text{C}$.

Features extraction methods

The peak values of E-nose data and the signals of E-tongue at 120 s were extracted as the features for the modelling. For the computer vision data, the mean values and the standard deviations of redness (R), greenness (G), and blueness (B) were extracted from each image as the features.

Dual-SPME combined with GC-MS

50/30 μm DVB/CAR/PDMS and 85 μm Carboxen/PDMS were used as the dual-SPME. After extraction the fibre was immediately introduced into a 7890B GC coupled with a 5977A MS (Agilent technologies, CA, USA) for about 5 min in splitless mode. GC oven program was 40 $^{\circ}\text{C}$ for 2 min, ramped at 4 $^{\circ}\text{C}/\text{min}$ to 70 $^{\circ}\text{C}$, and then ramped at 1 $^{\circ}\text{C}/\text{min}$ to 80 $^{\circ}\text{C}$ and ramped at 3 $^{\circ}\text{C}/\text{min}$ to 100 $^{\circ}\text{C}$, ramped at 7 $^{\circ}\text{C}/\text{min}$ to 240 $^{\circ}\text{C}$, holding for 3 min. Chromatographic separation was performed with a HP-5ms (30 m \times 0.25 mm I.D. \times 0.25 μm thickness) fused silica column from Agilent and ultra-high purity helium was used as the carrier gas. Electron-impact mass spectra was generated at 70 eV with m/z scan range from 35 to 550 amu. The ion source temperature was 230 $^{\circ}\text{C}$ [3].

Results and discussion

A total of 27 features were extracted from the intelligent sensory technologies data that could reflect different characteristics of Jinhua dry-cured hams. The response values obtained from the E-nose, E-tongue, and computer vision were shown in Figure 1. Several values such as S2, S4, S6 in E-nose, and S2 S6 in E-tongue, and R value in computer vision were significant different among the different Jinhua dry-cured hams. The results demonstrated that the intelligent sensory technologies could characterize the Jinhua dry-cured hams from different angles. Furthermore, the principal component analysis (PCA) and linear discriminant analysis (LDA) were applied to perform the dimensionality reduction and data visualization. The PCA is the unsupervised dimensionality reduction method, while the LDA is the supervised one which takes full advantage of the label information of different samples. Normally, the distribution of different sample groups in the LDA plot exhibits the larger distances among different groups and the smaller ones within one group. The two-dimension visualization plots of PCA and LDA were shown in Figure 2. The spatial distribution of sample points exhibited a clustering phenomenon of different groups. The sum of PC1 and PC2 contained 49.44% variance information of original data. The LD1 and LD2 contained almost 100% variance information. The result indicated that the LDA could classify different Jinhua dry-cured hams better than PCA. The fusion data was further used for BPNN modelling for simultaneously predicting sensory attribute results. The BPNN model exhibited good performance both in calibration set ($R^2 > 0.974$) and validation set ($R^2 > 0.935$).

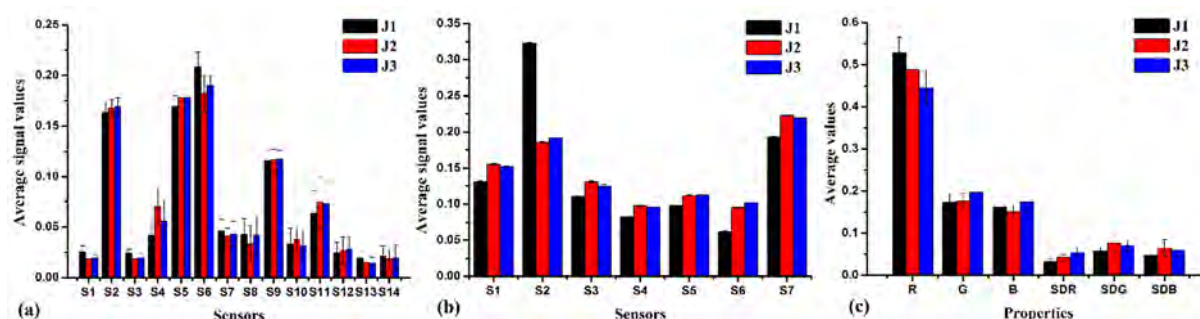


Figure 1: Response values obtained from the E-nose (a), E-tongue (b), and computer vision (c).

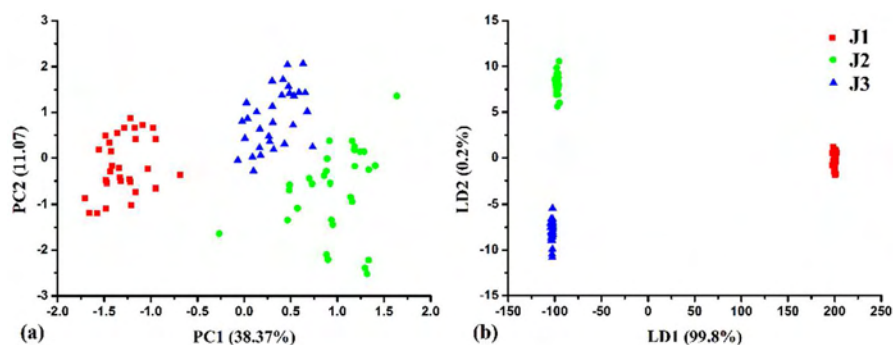


Figure 2: PCA (a) and LDA (b) results based on the fusion data of E-nose, E-tongue, and computer vision.

The fibres of DVB/CAR/PDMS and Carboxen/PDMS were applied for the dual-fibre SPME. A total of 80 volatile compounds were identified by the dual-fibre and the mono-fibre SPME. The Venn diagram of volatile compounds identified by the dual-fibre SPME and mono-fibre SPME was shown in Figure 3. Among them, 72 volatile compounds were identified by the dual-fibre SPME, which demonstrated that the dual-fibre SPME could identify more volatile compounds than mono-fibre SPME (63 compounds by the DVB/CAR/PDMS SPME and 53 compounds by the Carboxen/PDMS SPME). In addition, a total of 14 volatile compounds were only identified by the dual-fibre SPME method, which indicated that the dual-fibre SPME method was more efficient to extract more volatile compounds in Jinhua dry-cured hams. The dual-fibre SPME method was applied to analyse the three Jinhua dry-cured hams (J1, J2 and J3), and the result was shown in Figure 4. In the following work, the correlation analysis between the dual-fibre SPME method and E-nose will be conducted to verify the superiority.

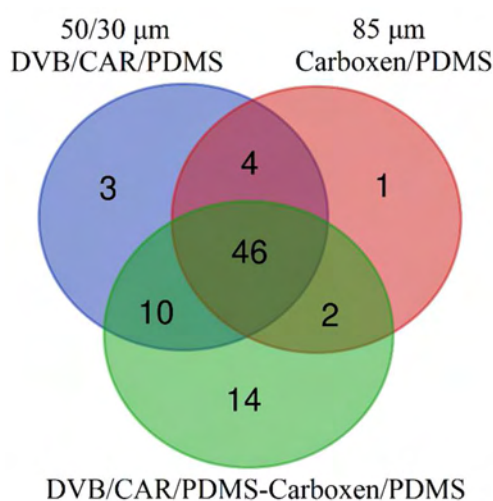


Figure 3: Venn diagram of volatile compounds identified by the dual-fibre SPME and mono-fibre SPME.

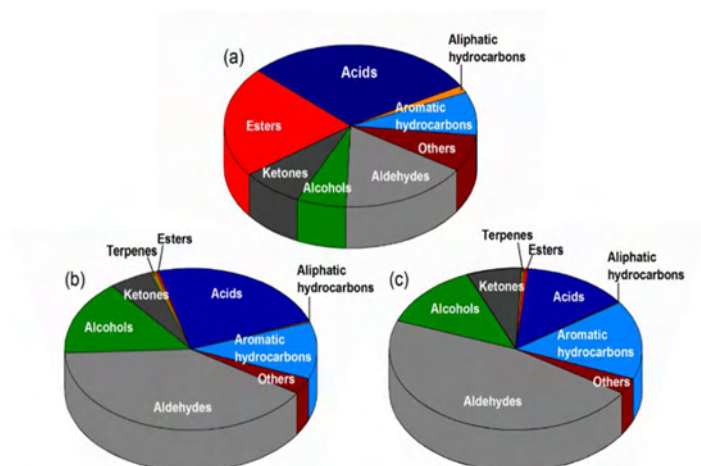


Figure 4: The types and proportions of volatile compounds identified in (a) J3, (b) J2, (c) J1 by the dual-fibre SPME method.

Conclusion

The different Jinhua dry-cured hams could be successfully classified based on the fused data of multiple intelligent sensory technologies, and the BPNN model could simultaneously predict sensory attributes scores of Jinhua dry-cured hams. The developed dual-fibre SPME method exhibited better coverage and higher extraction capacity than the conventional mono-fibre SPME.

References

1. Liu D, Bai L, Feng X, Chen Y, Zhang D, Yao W, et al., Characterization of Jinhua ham aroma profiles in specific to aging time by gas chromatography-ion mobility spectrometry (GC-IMS). *Meat Sci.* 2020;168: 108178.
2. Jiang S, Liu Y. Gas sensors for volatile compounds analysis in muscle foods: A review. *TrAC-Trends Anal. Chem.* 2020;126: 115877.
3. Liu H, Huang J, Hu Q, Chen Y, Lai K, Xu J, Ouyang G, Liu Y. Dual-fibre solid-phase microextraction coupled with gas chromatography-mass spectrometry for the analysis of volatile compounds in traditional Chinese dry-cured ham. *J. Chromatogr. B.* 2020;1140: 121994.

Biomimetic Approach towards Filbertone

MICHAEL BACKES, Jekaterina Ongouta, Egon Gross, Sina Bruns, Uwe Schäfer, Lars Meier and Gerhard Krammer

Symrise AG, Flavor Division, Mühlenfeldstraße 1, 37603 Holzminden

Abstract

Within this study, we would like to present a different approach from commercially available natural starting materials towards filbertone. In a three step procedure, combining Aldol chemistry and fermentation, we are able to realize this reaction without using any inorganic reagents or catalysts. The required stereochemistry should be introduced during the fermentative reduction of (*E*)-3-methylpent-3-en-2-one employing commercially available baker's yeast. This reaction could be accomplished in good yield and, provided access to the enantiomerically enriched intermediate (3*S*)-3-methylpentan-2-one. The obtained enantiomeric excess of 70 % *ee* correlates very well with the observed value of filbertone isolated from raw hazelnuts. Unfortunately, the reaction conditions of the second acid catalysed Aldol condensation to furnish filbertone proved to be too harsh to preserve the installed stereocenter and resulted in complete racemization of the obtained filbertone.

Keywords: filbertone, fermentation, Aldol condensation, enantiomeric excess

Introduction

Since its first publication as flavour material in 1985 [1] and subsequent identification in raw and roasted hazelnuts in 1989 [2] filbertone (**5**) is known as the character impact compound in hazelnuts and has been extensively studied during the last decades [3]. Whereas the enantiomeric excess of the (*S*)-enantiomer in raw hazelnuts is found to be quite constant around 70 % *ee*, it drops remarkably during roasting. Considering the observed increase of the total amount of filbertone during roasting, this could be attributed to a release of racemic material from a precursor. Alternatively, partial racemization while heating has also been observed, depending on the matrix [4]. Despite the obvious tendency for racemization, the detected enantiomeric excess is used as one potential marker to identify adulteration in hazelnut products [5].

The general trend towards natural and sustainable flavours poses an enormous task for the industry, especially in the case of filbertone (**5**), as the commercial isolation from hazelnuts is hardly viable due to the low amounts present. Several routes to filbertone (**5**) are described in the literature; however they still require inorganic reagents and catalysts. In addition, the so far described approaches towards enantiomerically enriched filbertone are all relying on starting materials from the chiral pool [3, 6].

Experimental

The baker's yeast used for these experiments was purchased from UNIFERM GMBH & CO. KG, all other chemicals and solvents were obtained from MERCK KGAA. Optical rotation was measured on a UniPol 1000 (SCHMIDT & HAENSCH), chiral GC experiments were carried out on an Agilent GC 7890 system employing a Hydrodex- β -TBDAC column (25 m, 0.25 mm i.d.). The conditions for the analysis were: split injection (split ratio 1:50), injector temperature 60 °C – 12 °C/sec – 220 °C; oven temperature 40 °C – 2 °C/min – 180 °C. Hydrogen was used as the carrier gas and the flow rate was 2.0 mL/min.

(*E*)-3-methylpent-3-en-2-one (**3**)

30.0 g (1.0 eq.) of 2-butanone (**1**) was treated under stirring with 15.0 g water, 60.6 g (1.0 eq.) of tartaric acid and subsequently with 33.8 mL (1.5 eq.) of acetaldehyde (**2**). The resulting reaction mixture was heated to 120 °C for 16 h in a closed autoclave, which resulted in an inherent pressure of 6 bar. Subsequently, the reaction mixture was cooled to room temperature and washed with water and NaOH solution (5%) to remove the acid. The product was extracted with 200 mL methyl *tert*-butyl ether (MTBE). Finally, the organic phase was concentrated under reduced pressure and the obtained product was distilled (at 30 mbar, at 90 °C) to give 21.6 g of (*E*)-3-methylpent-3-en-2-one (**3**). The analytical data was comparable to that found in literature [7]. Yield: 55 %.

3-methylpentan-2-one (**4**)

To a baker's yeast solution (750 mL of a 200 mM potassium phosphate buffer (pH 7.0), containing 235 g/L yeast) 1.5 g of (*E*)-3-methylpent-3-en-2-one (**3**) were added. The resulting reaction mixture was stirred at room temperature for 24 h. Subsequently, the reaction mixture was steam distilled at 120 °C under normal pressure.

The resulting water-product mixture was extracted with MTBE. After removal of the solvent, the product was distilled under reduced pressure (at 400 mbar, at 80 °C) to give 0.56 g of 3-methylpentan-2-one (**4**). $[\alpha]_D^{26} = 8.0^\circ$, ($c = 0.18$ g/L, $\text{CH}_3\text{CH}_2\text{OH}$); literature: $[\alpha]_D^{25} = +8.0^\circ$ ($c = 1.0$, CHCl_3); 70 % *ee* in favour of the (*S*)-enantiomer. Other analytical data was comparable to that found in literature [7] as well. Yield: 37 %.

Filbertone

20.0 g (1.0 eq) of 3-methylpentan-2-one (**4**) was treated under stirring with 19.2 g (0.5 eq) of citric acid and subsequently with 16.9 ml (1.5 eq) of acetaldehyde. The resulting reaction mixture was then heated to 120 °C for 10 h in an autoclave. The reaction mixture was cooled to room temperature and treated with 19.2 g (0.5 eq) of citric acid and subsequently with 16.9 ml (1.5 eq) of acetaldehyde. The resulting reaction mixture was then heated to 120 °C for another 15 h in an autoclave. The reaction mixture was cooled to room temperature and washed with water and a 10 % KOH solution to remove the organic acid. The product was extracted with 400 mL MTBE. Finally, the organic phase was concentrated under reduced pressure and the resulting product was distilled under reduced pressure (at 10 mbar, at 90 °C) to give 2.77 g of filbertone (**5**). The analytical data was comparable to those found in literature [2]. Yield: 11 %.

Results and discussion

Inspired by the synthetic strategy chosen by Cheng [8], we envisaged to employ only sustainable organic starting materials and reagents to furnish the first truly green and enantioselective synthesis of filbertone not relying on starting materials from the chiral pool.

Acid catalysed Aldol reaction to (*E*)-3-methylpent-3-en-2-one (**3**)

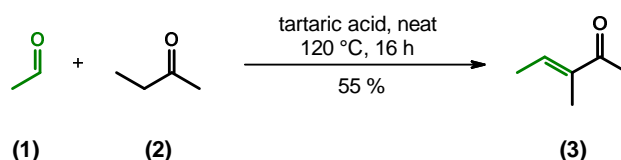


Figure 1: Aldol Reaction of 2-butanone (**2**).

In a first step – the condensation reaction of acetaldehyde (**1**) and butanone (**2**) – the hydrochloric acid could be replaced by tartaric acid without observing a significant drop in yield (Figure 1). Due to the high volatility the reaction is conducted in a stainless steel autoclave at an inherent pressure of 6 bar. The reaction also proceeds employing other natural acids like formic acid or citric acid, however, the yield drops dramatically.

Fermentation employing Baker's Yeast

The subsequent reduction of 3-methylpent-3-en-2-one (**3**) should be achieved by replacing the palladium catalyst by commercially available baker's yeast (Figure 2).

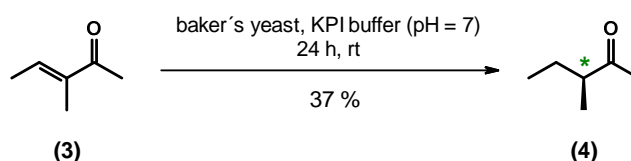


Figure 2: Reduction of 3-methylpent-3-en-2-one (**3**).

As the consumer is very conscious about the use of genetically modified organisms for the production of flavourings, the use of traditional baker's yeast can be regarded as favourable. However, due to the low conversion rate towards the used substrate, the concentration of the yeast is very high, which adds additional complexity to the downstream processing, especially as the product is highly volatile. It is expected, that the isolated yield of the 3-methylpentan-2-one (**4**) could be improved further by adapting the isolation and purification conditions. The configuration of the newly generated stereocenter was determined as (*S*) *via* comparison of the optical rotation to the existing literature [7]. The enantiomeric excess was determined as 70 % *ee* *via* chiral GC analysis, which correlates very well with the observed value of filbertone isolated from raw hazelnuts.

Acid catalysed Aldol reaction to Filbertone

In the final step, Cheng used zinc acetate which could be again replaced by natural organic acids with good selectivity albeit obtaining only low conversion (Figure 3).

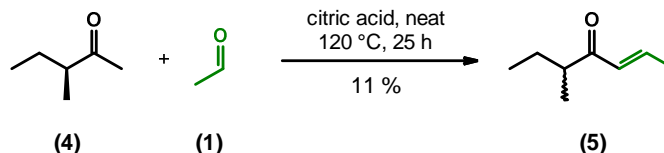


Figure 3: Acid catalysed Aldol reaction to filbertone.

Interestingly, citric acid instead of tartaric acid proved to be especially beneficial for this transformation, which has to be carried out in a stainless steel autoclave due to the high volatility for the reagents which resulted in an inherent pressure of 6 bars. A larger excess of citric acid and acetic aldehyde (1) and a prolonged reaction time are necessary compared to the first aldol reaction, due to the lower reactivity of the 3-methylpentan-2-one (4) in this reaction. Albeit the yield of 11 % is rather poor, the reaction is quite selective, as 70 % of the starting material could be re-isolated, which results in a conversion-adjusted yield of 37 %. Unfortunately, the reaction conditions are too harsh to preserve the parent stereocenter and the starting material undergoes complete racemization which consequently leads to racemic filbertone (5) as well.

Conclusion

Filbertone (5) was generated in a three step procedure by using only natural and sustainable raw materials, reagents and processes. The reduction employing non-genetically modified baker's yeast furnished an enantiomerically enriched intermediate. Unfortunately, complete racemization occurs during the final step, which again underlines tendency of filbertone to racemise under various conditions.

References

1. Emberger R, Köpsel M, Brüning J, Hopp R, Sand T Verwendung von 5-Methyl-2-hepten-4-on als Riech- und/oder Aromastoff sowie diesen Stoff enthaltende Riech- und oder Aromastoffkompositionen 1985, DE3345784.
2. Jauch J, Schmalzing D, Schurig V, Emberger R, Hopp R, Köpsel M, Silberzahn W, Werkhoff P, Isolation, Synthesis, and Absolute Configuration of Filbertone – the Principal Flavor Component of the Hazelnut. *Angew. Chem. Int. Ed. Engl.* 1989;28(8):1022.
3. Eva Puchl'ová E, Szolcsányi P, Filbertone: A Review. *J. Agric. Food Chem.* 2018, 66(43): 11221.
4. Blanch G P, Jauch J Enantiomeric Composition of Filbertone in Hazelnuts in Relation to Extraction Conditions. Multidimensional Gas Chromatography and Gas Chromatography/Mass Spectrometry in the Single Ion Monitoring Mode of a Natural Sample. *J. Agric. Food Chem.* 1998;46(10):4283.
5. Ruiz del Castillo M L, Gómez Caballero E, Blanch G P, Herraiz M, Enantiomeric composition of filbertone in hazelnuts and hazelnut oils from different geographical origins. *J. Am. Oil Chem. Soc.* 2002;79(6):589.
6. Puchl'ová E, Dendys M, Špánik I, Szolcsányi P, Scalable Preparation of Enantioenriched (S)-5-methylhept-2-en-4-one. Synthesis and Aroma Properties of Achiral Analogues Thereof. *Molecules* 2019,24(24):4497.
7. Peters B B C, Jongcharoenkamol J, Krajangsri S, Andersson P G, Highly Enantioselective Iridium-Catalyzed Hydrogenation of Conjugated Trisubstituted Enones. *Org. Lett.* 2021,23(1):242.
8. Cheng C, Method for synthesizing filbertone. 2009 CN101597223.

Identification of odour-active compounds in a paste of roasted hazelnut from Piedmont Tonda Gentile Trilobata

CLAUDIA GEYER¹, Sophie Kemmer¹, Petra Steinhaus¹, Eashwari Shanmugam¹,
Alexander Hässelbarth¹, Valentina Bongiovanni² and Andrea Cavallero²

¹ Flavologic GmbH, Dompfaffweg 15, D-85591 Vaterstetten, Germany; Claudia.geyer@flavologic.com

² SOREMARTEC ITALIA SRL, P. Le P. FERRERO 1, I-12051 Alba, Italy

Abstract

Application of gas chromatography-olfactometry on the volatiles isolated from roasted Tonda Gentile Trilobata (TGT) hazelnut paste by means of solvent extraction and solid phase extraction revealed 129 odour-active areas. Besides known hazelnut odorants, 24 components have been identified for the first time as odour-active compounds in roasted hazelnuts, namely 3-methylbutyl acetate, ethyl hexanoate, methyl phenylacetate, 3-methyl-2,4-nonandione, α -phellandrene, isoeugenol, 2-vinyl-3,5-dimethylpyrazine, 2-acetyl-2-thiazoline, 3-methyl-2-buten-1-thiol, 3-mercapto-3-methylbutyl formate, methyl-3-(methylthio)furan, furfuryl methyl sulphide, δ -nonalactone, γ -decalactone, δ -decalactone, massoia lactone, γ -dodecalactone, δ -dodecalactone, 3-hydroxy-4,5-dimethyl-2(5H)-furanone, 3-hydroxy-2-methylpyran-4-one, methyl cyclopentenolone, 2-aminoacetophenone, 3- and/or 4-ethylphenol and 3-methylindole.

Keywords: roasted hazelnut paste, solid phase extraction, gas chromatography-olfactometry, 3-hydroxy-4,5-dimethyl-2(5H)-furanone, TGT/TGL

Introduction

The principal countries producing hazelnut are Turkey, Italy, Spain, USA and Greece (<http://www.fao.org/docrep/>) [1]. Italy is the second worldwide hazelnut producer with 132,700 t (<http://dati.istat.it/>) [2]. The 98% of Italian producing surface is located in four regions: Campania, Latium, Piedmont and Sicily.

Nut production in Piedmont is very variable among the years and, in 2018, was 36 477 tons (<http://dati.istat.it/>). It is based on a single cultivar: Tonda Gentile delle Langhe (TGL) or also known, since the end of XIX century, as “Tonda gentile del Piemonte” or “Tonda gentile trilobata (TGT)” that has been investigated since the 1950s [3, 4]. TGL was selected directly by farmers for its good environmental adaptability to Piedmont climate and for the excellent quality of the kernel [5]. Another important characteristic of this hazelnut is the high degree of peelability after roasting.

Roasting is the key technological process in hazelnut industrial transformation. The main purpose of roasting is to improve colour, crispiness and crunchiness of the product but beside all these aspects, the principal reason of roasting is to improve the flavour.

The unique pleasant aroma of roasted hazelnuts has been the topic of several investigations in recent years. In 1972, Kinlin et al. [6] were the first to investigate the volatile fraction of roasted hazelnuts and identified over 200 volatile compounds using various extraction methods and packed column gas chromatography.

However, only few groups undertook efforts to distinguish the odour-active compounds from the bulk of odourless volatile compounds identified in raw or roasted hazelnuts by application of gas chromatography-olfactometry on the volatile fraction of hazelnuts so far [7-13].

Several different extraction methods have been studied on different hazelnut samples in the past to identify new aroma compounds. During the present study, a combination of solvent extraction followed by Solid Phase Extraction (SPE) was applied as sample preparation method the first time.

SPE as sample preparation procedure offers the advantage of being proceeded at low temperatures. Moreover, the aqueous conditions often used resemble the conditions during consumption of food and thus mimic the aroma release from the hazelnut paste matrix during natural consumption conditions. Additionally, using SPE as sample preparation approach, we expected to find further odour-active compounds particularly among the low volatile compounds as reported by Engel et al. [10]. In their study, quantitative data obtained by mixtures of n-alkanes (C-10 to C-26) distillates by means of the SAFE technique at 35 °C showed that the yields for n-alkanes up to a chain length of 14 (n-tetradecane, boiling point: 252 °C) were 100%, while the yield of n-hexadecane (boiling point: 284 °C) and n-octadecane (boiling point: 317 °C) was only 59 and 12 %, respectively [10].

In order to include also the polar compounds among the low volatile components in the work-up procedure, solvent extraction prior to SPE was performed using water as a polar solvent. A portion of 10 % ethanol was added to provide a reasonable efficient extraction of nonpolar compounds as well. The use of this water/ethanol mixture

(90/10; w/w) should on one hand guarantee an extraction of the low volatile compounds including the polar compounds, and on the other hand prevent the extraction of fat.

The aim of the present study was, therefore, to use a combination of solvent extraction followed by solid phase extraction as sample preparation method in order to identify the odour-active compounds of a roasted TGT hazelnut paste and characterise them by means of gas chromatography-olfactometry (GC-O), gas chromatography-mass spectrometry (GC-MS) and heart-cut gas chromatography-gas chromatography-olfactometry-mass spectrometry (GC/GC-O/MS).

Experimental

Roasted hazelnut paste

The roasted hazelnut paste under investigation was provided by Soremartec Italy Srl. Commercial sample of hazelnut *Corylus avellana* L. TGT, harvested in 2017 in Piedmont area. In order to get a representative sample, 2 tons of hazelnuts (calibre ranging from 12 to 14 mm) have been roasted following industrial roasting process protocol. After roasting the hazelnuts have been grinded to obtain a paste that was stored in fridge (4°C, controlled humidity) until the time of extraction.

Isolation of volatiles

A mixture of 180 g tap water (40 °C) and 20 g ethanol (96 vol%) was added to the hazelnut paste under investigation (40 g) and stirred vigorously with an Ultraturrax T18 (IKA GmbH, Staufen, Germany) for 2 minutes. The mixture was centrifuged for 30 min at 4 °C and 13000 RPM (UniCen MR, Herolab GmbH, Wiesloch, Germany). Then the aqueous phase was decanted cautiously and filtered through a coffee filter. Another portion of water/ethanol as described above was added to the centrifuge tube containing the remaining sediment and fat and the mixture was again stirred, ultrafiltrated and the aqueous phase decanted, filtered and combined with the first aqueous phase (extraction cycle 1). This procedure was repeated for five times taking portions of fresh hazelnut paste (40 g) each time (extraction cycles 2 to 6). Finally, all six portions of aqueous filtrate were combined. The combined aqueous phases now contained the ingredients of 240 g hazelnut paste and each portion of hazelnut paste (40 g) was extracted twice.

Solid Phase Extraction (SPE)

An SPE cartridge containing 2 g of Chromabond HR-P (Macherey-Nagel GmbH, Düren, Germany) was activated with ethanol (96 vol%, 12 mL) and rinsed with tap water (12 mL). The combined aqueous phases obtained as described above were adsorbed on the SPE cartridge with minimum pressure using a SPE vacuum manifold and rinsed with tap water (12 mL). Then the SPE cartridge was turned around and desorbed with ethanol in the opposite direction of the adsorption one. The aqueous phase (approximately 1.5 mL) was discarded and the ethanolic phase (4 mL) was collected and dried over sodium sulphate.

Gas chromatography-Olfactometry (GC-O)

Gas chromatography-olfactometry was performed by means of a gas chromatograph GC 2010 (Shimadzu, Duisburg, Germany) with Helium serving as carrier gas at a pressure of 70 kPa. Samples were injected by the split/splitless-injection onto capillaries DB-5 or DB-FFAP (both 30 m, 0.25 mm i.d., 0.25 µm film thickness; J&W, Agilent Technologies, Waldbronn, Germany). The end of the capillary was connected to a deactivated Y-shaped glass splitter dividing the effluent of the column into two equal parts, which were then transferred via two deactivated but uncoated fused silica capillaries (30 cm x 0.25 mm i.d.) to a sniffing port and a FID, respectively. The sniffing port which was mounted on a detector base of the GC was heated to 230 °C, the FID was operated at 240°C. Split/splitless-injection of the samples (1.0 µL) was performed at an oven temperature of 30°C. After 2 min, the temperature was raised by 10°C per min to 60°C and then by 6°C per min to 240°C (DB-FFAP) or 250°C (DB-5). The final temperature was held for 10 min. During a GC run, the panellist placed his/her nose closely above the top of the sniffing port and evaluated the odour of the chromatographic effluent. Sniffing was performed by three trained sniffers. Linear retention indices (RI) of the compounds were calculated from the retention times of n-alkanes.

Gas chromatography-Mass Spectrometry (GC-MS)

Gas chromatography-mass spectrometry was performed by means of a Shimadzu GC-MS QP2010 (Shimadzu, Duisburg, Germany) with the quadrupole mass spectrometer running in the electron ionization mode (EI) at 70 eV. Samples were injected by the split/splitless-injection onto capillaries DB-5 or DB-FFAP (both 30 m, 0.25 mm I.D., 0.25 µm film thickness; J&W, Agilent Technologies, Waldbronn, Germany) with helium serving as carrier gas at a pressure of 70 kPa. Temperature programs were the same as used for GC-O.

Heart Cut Gas chromatography- Gas chromatography-Olfactometry-Mass spectrometry (GC/GC-O/MS)

Heart-cut GC/GC-O/MS was performed using a GC2010 (Shimadzu, Duisburg, Germany) connected to a GC-MS QP2020 (Shimadzu, Duisburg, Germany). In the first dimension, the separation of the extract was achieved on a DB-FFAP column (30 m x 0.25 mm fused silica capillary DB-FFAP, 0.25 μ m, J&W, Agilent Technologies, Waldbronn, Germany). The elution range containing the selected odorants was transferred to a second capillary column by means of a Multi-Deans Switch system. The second capillary column was a DB-5 (30 m x 0.25 mm fused silica capillary, 0.25 μ m, J&W, Agilent Technologies, Waldbronn, Germany). For mass chromatography, the second column was connected to a quadrupole mass spectrometer QP 2020 (Shimadzu, Duisburg, Germany) running in the electron ionization mode (EI) at 70 eV.

For simultaneous GC/GC-O/MS, the effluent of the first column was divided by means of the Multi-Deans Switch system and was then transferred to the second capillary column. Furthermore, the end of the second capillary column was connected to a deactivated Y-shaped glass splitter dividing the effluent of the column into two equal parts, which were then transferred via two deactivated but uncoated fused silica capillaries (30 cm x 0.25 mm i.d.) to a sniffing port and the mass spectrometer, respectively. The sniffing port which was mounted on a detector base of the second GC was also heated to 230 °C.

Results and discussion

Application of gas chromatography-olfactometry on the ethanolic roasted hazelnut extract revealed 129 odour-active areas showing a high variety of odour qualities such as malty, fruity, roasted, hazelnut-like, earthy, popcorn-like, sweet and fatty. The flavour extract was evaluated by sniffing the effluent eluting from two capillary columns of different polarity. While most of the odour impressions were instrumentally detected on both capillary columns, some of them were perceived by sniffing on only one of them – likely due to either coelution of aroma impressions or varying elution characteristics resulting of the different polarities of the compounds.

The calculation of retention indices and their comparison with data of an in-house database and literature data was used to determine compounds for the odour-active areas.

These structures were finally confirmed by comparing the mass spectra of the analytes as well as their odour qualities and odour potencies with those of the respective authentic reference compounds.

However, for several odour-active areas, no unequivocal mass spectra could be obtained by one-dimensional GC-MS. Using a two-dimensional GC/GC-MS system, the interesting elution range was transferred from the first column (DB-FFAP) to a second capillary column (DB-5) by means of a heart-cut Deans Switch System. The compounds eluting from DB-5 were also evaluated by means of simultaneous GC-O and GC-MS.

Corroboration of formerly identified odour-active compounds in hazelnuts

Several of the odour-active compounds detected in this study have already been reported as potent odorant in roasted hazelnut paste before. 3-Methylbutanal with its malty odour has already been reported by Burdack-Freitag and Schieberle as odorant in roasted hazelnut paste [9]. The same was true for the fruity smelling ethyl 2-methylbutanoate, the fruity, hazelnut-like smelling 3-methyl-4-heptanone, the also fruity, hazelnut-like smelling 5-methyl-(E)-2-hepten-4-one and 5-methyl-(Z)-2-hepten-4-one, octanal (fatty, green), 2-acetyl-1-pyrroline (popcorn), dimethyl trisulphide (onion, sulphury), (Z)-2-octenal (green, fatty), 2-propionyl-1-pyrroline (popcorn), 3-(methylthio)propanal (cooked potato), γ -heptalactone (fruity, honey, floral), (E,E)-2,4-decadienal (fatty, fishy, metallic), 2-methoxyphenol (smoky, vanilla, phenolic), and 4-hydroxy-2,5-dimethyl-3(2H)-furanone (caramel, cotton candy). Ethyl 2-methylbutanoate, (E,E)-2,4-decadienal, and (E)- β -damascenone had already been reported as potent odorants in hazelnut oil by Matsui et al. before [8].

Additionally, multiple compounds which had already been identified or identified tentatively before as volatile compounds in hazelnuts, but without evaluation of their odour quality, have now been characterised as odour-active compounds by means of GC-O.

Newly identified odour-active compounds in hazelnut paste

In this study, 24 components have been identified for the first time as odour-active compounds in roasted TGT hazelnut paste, namely 3-methylbutyl acetate, ethyl hexanoate, methyl phenylacetate, 3-methyl-2,4-nonanedione, α -phellandrene, isoeugenol, 2-vinyl-3,5-dimethylpyrazine, 2-acetyl-2-thiazoline, 3-methyl-2-buten-1-thiol, 3-mercapto-3-methylbutyl formate, methyl-3-(methylthio)furan, furfuryl methyl sulphide, δ -nonalactone, γ -decalactone, δ -decalactone, massoia lactone, γ -dodecalactone, δ -dodecalactone, 3-hydroxy-4,5-dimethyl-2(5H)-furanone, 3-hydroxy-2-methylpyran-4-one (maltol), methyl cyclopentenolone, 2-aminoacetophenone, 3- and/or 4-ethylphenol and 3-methylindole. Table 1 summarises the newly identified odour-active compounds, their retention indices, odour description as well as their mode of identification.

Unknown compounds

Various compounds which were detected sensorially during sniffing remained unidentified. Many of these still unknown compounds showed relatively high retention indices on either or both capillary columns and, according to their odour qualities, some of them might significantly contribute to the overall aroma of the roasted hazelnut paste. The retention indices of the unknowns are given in Table 1. The identification of these compounds will be the task for further studies.

Table 1. Newly identified and unknown odour-active compounds in hazelnut paste.

No.	Odorant ^a	Odour quality ^b	RI ^c	
			DB-FFAP	DB-5
1	3-methylbutyl acetate ^{d, e}	fruity, banana	1144	
2	3-methyl-2-buten-1-thiol ^d	beer, sulphur	1156	690
3	α -phellandrene ^d	fir needle, green, floral	1238	995
4	ethyl hexanoate ^{d, e}	fruity, floral, herbal	1251	
5	3-mercapto-3-methylbutyl formate ^d	cassis, roasted	1533	1030
6	2-vinyl-3,5-dimethylpyrazine ^{d, e}	earthy, roasted, green	1556	1121
7	unknown	bread, popcorn, roasted	1577	
8	3-methyl-2,4-nonandione ^{d, e}	floral, green	1723	
9	2-methyl-3-(methylthio)furan ^d	sulphury, coffee	1736	
10	methyl phenylacetate ^d	fruity, medical	1752	
11	2-acetyl-2-thiazoline ^{d, e}	nutty, roasted	1774	
12	unknown	citrus, smoky, fruity	1859	
13	methyl cyclopentenolone ^{d, e}	Sweet, maple, meaty, savoury	1936	
14	unknown	savoury, sulphury	1964	
15	unknown	violet, phenolic	1972	
16	3-hydroxy-2-methylpyran-4-one ^{d, e}	sweet	2040	
17	unknown	fir needles, fruity	2055	
18	isoeugenol ^d	clove	2098	
19	unknown	fruity, creamy, chocolate	2107	
20	unknown	goat shed, leather, animal	2175	
21	γ -decalactone ^{d, e}	waxy, fruity	2182	1470
22	3-/ 4-ethylphenol ^d	animal, cow shed	2222	
23	δ -decalactone ^{d, e}	waxy, fruity	2229	1507
24	aminoacetophenone ^{d, e}	sweaty, floral	2238	
25	unknown	clove, faecal, flowery	2247	
26	massoia lactone ^d	peach, waxy	2269	
27	unknown	fruity, musty	2283	
28	unknown	herbal, clove	2299	
29	3-hydroxy-4,5-dimethyl-2(5H)-furanone ^{d, e}	savoury, Maggi	2302	1105
30	γ -dodecalactone ^d	peach, waxy, fruity	2450	1670
31	unknown	nutty, earthy, musty	2467	
32	δ -dodecalactone ^{d, e}	coconut, creamy	2480	1712
33	3-methylindole ^d	faecal, bad breath	2568	
34	furfuryl methyl sulphide ^e	onion, meaty		1000
35	δ -nonalactone ^d	coconut		1436

^a Structure assignment of each odorant was based on the comparison of the compound's retention indices on FFAP and/or DB-5. ^b Odour quality as perceived at the sniffing port during GC-O. ^c Retention index calculated from the retention time of the compound and the retention times of adjacent n-alkanes by linear interpolation. ^d Confirmation by odour quality of reference compound as perceived at the sniffing port during GC-O and retention index on FFAP and/or DB-5. ^e Confirmation by mass spectrum obtained by GC-MS or GC-GC-MS of sample extract.

Conclusion

In summary, this study successfully characterised the odour-active compounds in hazelnut. Owing to its variety, geographical sourcing and controlled roasting conditions, Piedmont hazelnut (TGT) paste has a complex aroma, containing a high number of odorants. Twenty-four of them have been identified for the first time in roasted hazelnut paste. Some of these newly identified compounds are well known to be high impact odorants, which probably contribute to the characteristic profile of the TGT roasted hazelnuts.

Their presence in other hazelnut varieties/origins could be the objective of further studies.

Most of the newly identified compounds are polar and low volatile. This result meets the expectations of our study as the design of the work-up procedure including the application of aqueous extraction conditions, low temperatures and solid phase extraction was developed to include particularly the polar, low volatile compounds in the hazelnut paste aroma extract.

Therefore, extraction of aroma material with a polar solvent followed by solid phase extraction should be considered as versatile method for the identification of polar low volatile odour-active compounds.

References

1. Food and Agriculture Organization of the United Nations (2018). <http://www.fao.org/>
2. Statistiche ISTAT (Agriculture-Crops & livestock – fruit plantation) <http://dati.istat.it/>
3. Carlone, R.; Il nocciuolo nell'Alta Langa. *Il Coltivatore e Giornale Vinicolo Italiano*, 1957;9.
4. Romisondo, P.; La coltura del nocciuolo in Piemonte. *Frutticoltura XXII*, 1960;2:127-135.
5. Valentini, N.; Calizzano, F.; Boccacci, P.; Botta, R.; Investigation on clonal variants within the hazelnut (*Corylus avellana* L.) cultivar 'Tonda Gentile delle Langhe'. *Sci Hortic.* 2014;165:303-310.
6. Kinlin, T.E.; Muralidhara, R.; Pittet, A.O.; Sanderson, A.; Walradt, J. P. Volatile components of roasted filberts. *J Agric Food Chem.* 1972;20:1021-1028.
7. Langourieux, S.; Perren, R.; Escher, F. Influence of processing parameters on the aroma of dry-roasted hazelnuts. In: *Frontiers of Flavour Science*; Schieberle, P.; Engel, K.H. (Eds.) Deutsche Forschungsanstalt für Lebensmittelchemie, Garching, Germany ; 2000;527-535 (ISBN 3-00-005556-8).
8. Matsui, T.; Guth, H.; Grosch, W. A comparative study of potent odorants in peanut, hazelnut, and pumpkin seed oils on the basis of aroma extract dilution analysis (AEDA) and gas chromatography-olfactometry of headspace samples (GCOH). *Fett-Lipid.* 1998;100:51-56.
9. Burdack-Freitag, A.; Schieberle, P. Changes in the key odorants of Italian hazelnuts (*Coryllus avellana* L. Var. Tonda Romana) induced by roasting. *J Agric Food Chem.* 2010;58:6351-6359.
10. Engel, W.; Bahr, W.; Schieberle, P. Solvent assisted flavour evaporation – a new and versatile technique for the careful and direct isolation of aroma compounds from complex food matrices. *Eur Food Res Technol.* 1999;209:237-241.
11. Burdack-Freitag, A.; Schieberle, P. Characterization of the key odorants in raw Italian hazelnuts (*Coryllus avellana* L. Var. Tonda Romana) and roasted hazelnut paste by means of molecular sensory science. *J Agric Food Chem.* 2012;60:5057-5064.
12. Kiefl, J.; Schieberle, P. Evaluation of process parameters governing the aroma generation in three hazelnut cultivars (*Corylus avellana* L.) by correlating quantitative key odorant profiling with sensory evaluation. *J Agric Food Chem.* 2013;61:5236-5244.
13. Kiefl, J.; Pollner, G.; Schieberle, P. Sensomics analysis of key hazelnut odorants (*Corylus avellana* L. 'Tonda Gentile') using comprehensive two-dimensional gas chromatography in combination with time-of-flight mass spectrometry (GCxGC-TOF-MS). *J Agric Food Chem.* 2013;61:5226-5235.

A new approach for the sensitive detection of thiols in food by affinity solid phase extraction and GC-MS

Stephan Neumann^{1,2}, Egon Gross², Stephanie Korte², Birgit Kohlenberg², Melanie Esselen¹, Hans-Ulrich Humpf¹ and JOHANNES KIEFL²

¹ Institute of Food Chemistry, University of Muenster, Corrensstrasse 45, 48149 Muenster, Germany;

² Symrise AG, Muehlenfeldstrasse 1, 37603 Holzminden, Germany; johannes.kiefl@symrise.com

Abstract

Sulphur containing volatile molecules belong to the most aroma active components in food with reported concentrations below 1 µg/L. Various extraction methods have been developed in the past to enrich thiols and improve detectability [1-4]. Here, we describe the development of a new extraction protocol using 2-thiopyridyl disulphide activated agarose gel (known as thiopropyl-sepharose 6B, TPS) commonly used for protein analysis [5]. Primary, secondary and tertiary thiols namely 1-hexanethiol, 2-furfurylthiol, 2-phenylethanethiol, pentane-2-thiol, 3-mercaptohexyl acetate, 2-methyltetrahydrofuran-3-thiol, 4-methoxy-2-methyl-2-butanethiol, 4-mercapto-4-methyl-2-pentanone, 1-p-menthene-8-thiol and p-mentha-8-thiol-3-one were used to study the binding affinity of the stationary phase. The optimization of the overall extraction parameters was performed by a design of experiment (DOE) approach. A selective enrichment and concentration was achieved by factor up to 70 for primary thiols on TPS and by an additional factor up to 5000 for stir bar sorptive extraction (SBSE) of the ethanolic extract obtained after elution of bound thiols with tris(2-carboxyethyl)phosphine. Limit of detection levels less than 1 µg/L could be achieved by combining TPS based extraction with SBSE-gas chromatography-mass spectrometry (GC-MS).

Keywords: thiols, enrichment, thiopropyl-sepharose, aroma, affinity solid phase extraction

Introduction

Extraction and derivatization of thiols with reagents such as 4-vinylpyridine [1], ebselen [2] and disulphide reagents such as 6,6'-dithiodinicotinic acid [3] and 4,4'-dithiodipyridine [4] are used to sensitively analyse known thiols with liquid chromatography mass spectrometry. In the contrary, fewer methodologies for affinity based solid phase extraction such as mercuric benzoate linked agarose gel are reported [6]. An alternative protocol was developed for the mercuric benzoate based method for occupational safety reasons using 2-thiopyridyl-disulphide activated agarose gel by a covalent chromatography based on thiol-disulphide exchange reaction [5] for enrichment of free thiols. The latter is used for protein analysis but was so far not adopted for extraction of aroma-active thiols in food.

Experimental

The following reference compounds were obtained in the highest available grade of purity: 2-pentanethiol, 1-p-menthene-8-thiol, 2-methyltetrahydrofuran-3-thiol, 2-furfurylthiol, 4-mercapto-4-methyl-2-pentanone, p-mentha-8-thiol-3-one (ThermoFischer Scientific, Karlsruhe, Germany); 4-methoxy-2-methyl-2-butanethiol, 2-phenylethanethiol, 3-mercaptohexyl acetate, 1-hexanethiol (Sigma-Aldrich, Steinheim, Germany). A 1000 mg/kg stock solution of the references in ethanol was freshly prepared and further diluted with deionized water (Arium mini, Sartorius, Germany) to 100 mg/kg (model stock solution) prior use. Further, a coupling buffer was prepared by solubilizing 18.61 mg ethylenediaminetetraacetic acid disodium salt dehydrate (EDTA-Na₂ H₂O) (1 mmol/L) and 1.46 g sodium chloride (NaCl) (0.5 mol/L) in 50 mL phosphate buffer (67 mmol/L, pH 7.5). To release thiols bound on TPS resin (thiopropyl-sepharose 6B, Sigma-Aldrich, Steinheim, Germany), the disulphide bridge was reduced with a solution of tris(2 carboxyethyl)phosphine hydrochloride (TCEP HCl) (100 mmol/kg). Therefore, 710 mg of TCEP HCl and 9.3 mg EDTA-Na₂ H₂O were sonicated in 12.5 g phosphate buffer (67 mmol/L, pH 7.5) followed by addition of sodium hydroxide solution (1 mol/L) for pH readjustment (pH = 7.5) and finally 12.5 g ethanol. It is important to keep the order of dissolution to pre-dissolve TCEP HCl in water.

Extraction protocol

Enrichment of free thiols was performed by using a thiol-affinity and cross-linked TPS resin with reactive 2-thiopyridyl disulphide groups linked to hydroxypropanol via ether bonds (Figure 1). Free thiols are bound and released by thiol-disulphide exchange reaction referred to as covalent chromatography. The freeze-dried resin was rehydrated by weighing 150 mg TPS resin in a 2 mL safe-lock tube, adding 1.5 mL deionized water and incubating it at room temperature for 15 min. Subsequently, sedimented resin was homogenized gently by using a 1000 µL pipette and left at room temperature for additional 15 min.

The settled resin was transferred to a 2 mL empty SPE-cartridge with an integrated frit and was connected to a SPE-Baker-Box by a Lure-lock valve. Excessive water was removed under reduced pressure. The gel was gently washed with 9 mL deionized water followed by gently washing with 6 mL of coupling buffer. In the next step an aliquot of 1000 μ L of the free thiol containing model solution (120 mL) was added to the prewashed resin and was then quantitatively transferred to a 200 mL Erlenmeyer flask. This suspension was shaken on an IKA shaker (KS 130 basic, IKA Works, Inc., Wilmington, USA) for 6 hours at 400 rpm and room temperature. After shaking, the suspension was transferred back to the previous used SPE-cartridge, left to settle down and washed by adding 40 mL EtOH followed by 40 mL EtOH/H₂O (1+1, w/w).

After washing, the valve was closed and 1 g of the prepared TCEP solution (100 mmol/kg) was added followed by gentle homogenization and incubation at room temperature for 20 min. Finally, the solution was eluted in a 2 mL auto sampler vial followed by addition of 100 μ L hydrochloric acid (1 mol/L) to prevent possible side reactions like thiol disulphide exchange reactions and dimerization.

To achieve a further enrichment of thiols, the stir bar sorptive extraction (SBSE) was used. Therefore, 200 mg of eluate and 800 mg water were combined in a 2 mL auto sampler vial, the stir bar (PDMS Twister with 1 mm layer thickness and 10 mm length, Gerstel, Muelheim, Germany) was added, the vial sealed with a cap and stirred on a magnetic stirrer for 1 hour at 600 rpm and room temperature. The stir bar was removed after this extraction and gently rinsed with few millilitres of deionized water and carefully dried with clean paper towels and transferred to a thermal desorption unit for measurement (TDU, Gerstel, Muelheim, Germany).

GC-MS/FID analysis

Sample volatiles were transferred to the GC by desorbing the Twister at 280 °C for 10 min in the Gerstel thermal desorption unit, then the analytes were cryo-focussed at -30 °C in the cooled injection system inlet containing a Tenax filled glass liner and then desorbed at 280 °C for 10 min onto the GC column, where the analytes were separated on an Agilent Technologies DB-1ms (60 m x 0.32 mm, 0.25 μ m, Agilent, Waldbronn, Germany) placed in an Agilent 7890A gas chromatograph (Waldbronn, Germany) using helium as the carrier gas. A constant flow of 2 mL/min was applied. The GC temperature was programmed starting at 40 °C, held for 2 min, then raised at 4 °C/min to 300 °C, and held for 75 min. Retention indices were calculated by chromatography of a homologous series of n-alkanes from C6 to C30. The effluent was split and transferred to the FID set at 300 °C and MS set in scan mode (EI ionization 70 eV, m/z 33 – 450, 3.4 scans/sec). The yield of recovered primary, secondary and tertiary thiols was determined by extracting model solution with 100 mg/kg of each thiol with TPS and dividing the analysed concentration (using external calibration) by expected 100 mg/kg. External calibration with internal standard 1-hexanethiol and GC-FID was used for quantitation and assessment of validation parameters. Recovery rate was determined by division of quantitated amount and spiked amount of thiol times 100. Data were acquired by Agilent MSD ChemStation version E.02.02.

Design of experiments (DOE)

A sequential approach using DOE principles was set up to study sample preparation parameters on thiol recovery rates. After preliminary trials, a rotatable Central Composite Design (CCD) with three continuous factors and six centre points was designed. The parameters and their maximum border values were binding time (29.6 – 120 min), sample volume (19.5 – 500 ml) and desorption time (9.6 – 90.4 min). The composition of the sample itself was kept constant comprising a predefined mixture of reference thiols.

In a second generally comparable CCD-attempt, the objective was to investigate the influence of the factors (i) thiol concentration (5 – 50 μ g/kg), (ii) amount of TPS (mg) and (iii) pH-value (3 – 9) on recovery rates at 6-hour constant exposure time.

The results from both designs were modelled using the standard least square approach while fitting and optimizing all models simultaneously to enable a simultaneous interpretation of the independent factors obeying the heredity. This more general modelling approach was chosen in order to get an overall describing model for all occurring effects. Due to the high skewness of the analytical results, a log₁₀-transformation was necessary to overcome the non-normal distribution prior to the modelling procedure.

Results and discussion

The goal of this study was to develop an alternative sample preparation protocol to mercury based thiol extraction. This protocol uses covalent chromatography based on thiol-disulphide exchange reaction [5] for enrichment of free thiols in liquid food samples on the TPS solid phase. Free thiols were bound on this commercially available activated agarose resin with 2-thiopyridyldisulphide as the active group (Figure 1) and with a binding capacity of 18 to 31 μ mol/ml of resin.

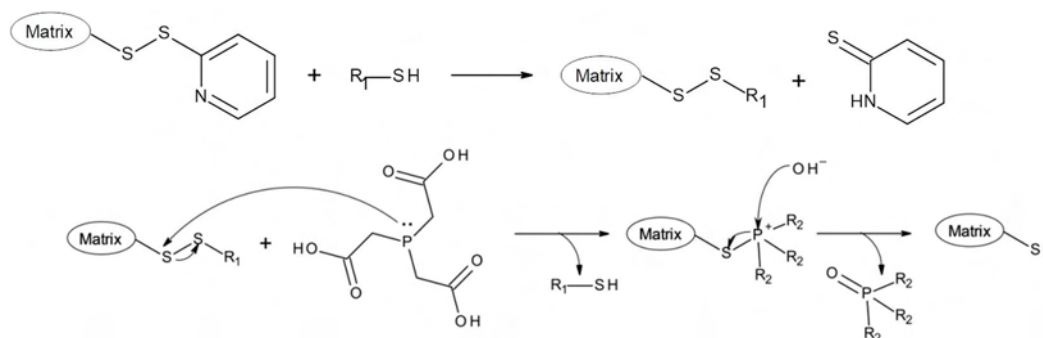


Figure 1: Mechanism of covalent binding of free thiol (R_1 -SH) with 2-thiopyridyldisulphide activated agarose.

In a first step, a free nucleophile thiolate attacks the sulphur atom next to the 2-thiopyridine leaving group to perform a new disulphide bond under release of 2-thiopyridone. 2-Thiopyridone exists in a thiol-thione tautomeric form and reacts under oxidative autocatalysis to 2,2'-dithiodipyridine [7]. The matrix bound thiols are then released by reduction with tris(2-carboxyethyl)phosphine (TCEP).

The principle of binding free thiols to disulphide reactants such as 6,6'-dithiodinicotinic acid [3] and 4,4'-dithiodipyridine [4] is well known and was early adapted for aroma analysis. However, these reactants have been developed to measure the degree of reaction by photometry or liquid chromatography of derivatized thiols. The analysis of derivatization products aims at increasing sensitivity by reacting analytes with highly detector responsive groups, which is useful for detection and quantitation of known thiols. However, derivatized thiols cannot be sniffed by GC-Olfactometry, the lack of mass spectrometric information especially EI-MS fragmentation pattern limits the identification and the derivatization process does not include a concentration step. In contrast, thiols derivatized with agarose bound 2-thiopyridyldisulphide can be released after concentration and analysed by GC-MS/O.

Initial optimisation trials with TPS revealed a binding capacity of 2.5 μmol per 35 mg resin, tested with model solutions of 2-furfurylthiol at different concentrations. Next, the binding of the thiols in a continuous flow mode was tested by transferring the resin to the empty SPE-cartridge and slowly passing 250 mL of model solution under reduced pressure for 82 min. The yield of recovered thiols showed that the contact time was too short to quantitatively bind free thiols (data not shown). Therefore, the washed resin was transferred from the SPE-cartridge to a flask and reacted under static condition. Dithiothreitol and TCEP were tested as reducing agent and TCEP was found to give higher yields (data not shown). Finally, liquid injection (GC-MS/FID), dynamic headspace (DHS)-GC-MS/FID and SBSE-GC-MS/FID were tested to analyse the eluate and SBSE-GC-MS/FID technique with a polydimethyl siloxane (PDMS) coated Twister (Gerstel) was chosen.

The extraction of free thiols in liquid samples by using TPS resin causes a structure-dependent enrichment. A design of experiment (DOE) approach was conducted to systematically study the effect of pH value, concentration of educts, exposure time and release with TCEP on the yield of recovered primary, secondary and tertiary thiols in model solution. The exposure time was set to 6 hours yielding the best overall thiol recovery ($p < 0.001$). The DOE data further show that the pH-value affects the binding of primary, secondary and tertiary thiols alike ($p < 0.001$). The greater the pH value the higher the reactivity of free thiols with an observed optimum of pH 7.5. Furthermore, the amount of TPS and thiol concentration was identified as significantly impacting the recovery of primary and secondary thiols ($p < 0.007$ and $p < 0.007$) although no saturation of active sides could take place. Primary thiols like 2-phenylethanethiol (75% yield, enrichment factor of 70) and also secondary thiols like 3-mercaptohexyl acetate (in average 80% yield, enrichment factor 25) achieve a higher recovery than tertiary thiols like *p*-mentha-8-thiol-3-one (in average 30% yield, enrichment factor 10).

This extraction leads to a selective depletion of non-sulphurous flavour compounds facilitating mass spectrometric identification of unknown thiols in complex matrices. For example, a Scheurebe white wine from Franconia has been spiked with sulphur compounds (no. 1-8) at 10 $\mu\text{g}/\text{kg}$ and was measured before enrichment (A) and after thiol enrichment (B) (Figure 2).

This new methodology was validated by external calibration with 1-hexanethiol internal standard (100 $\mu\text{g}/\text{kg}$, Table 1) in white wine conducting TPS based extraction. Recovery rates were calculated as average of measurements at concentration levels of 0.5 $\mu\text{g}/\text{kg}$, 5 $\mu\text{g}/\text{kg}$ and 50 $\mu\text{g}/\text{kg}$.

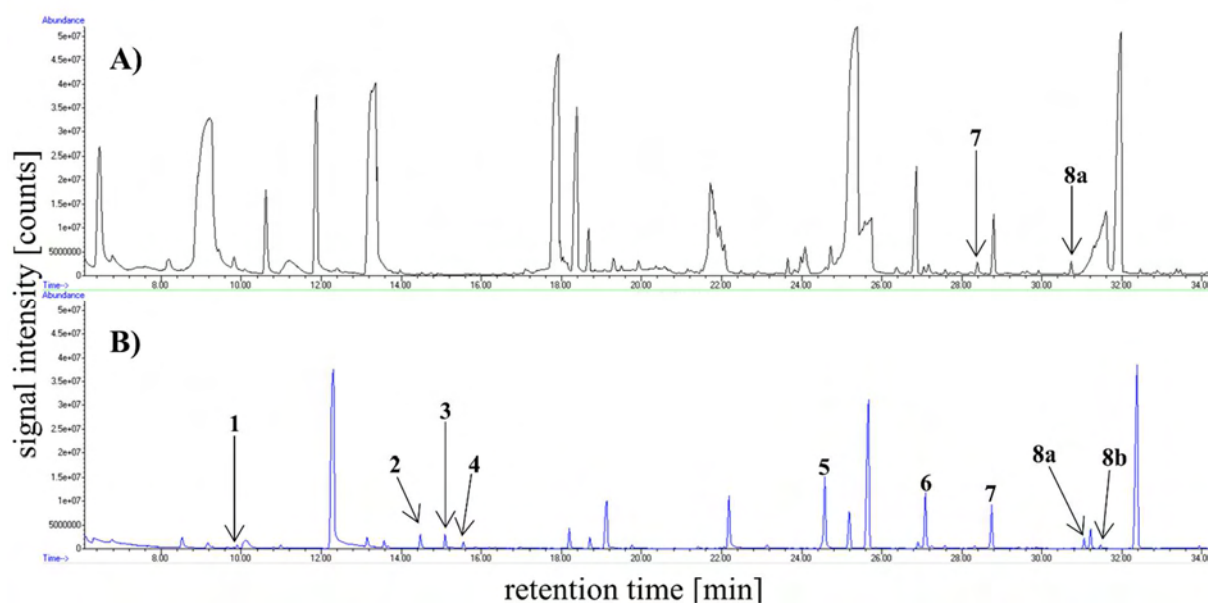


Figure 2: Comparison of two SBSE-GC-MS-chromatograms before enrichment (A) and after thiol enrichment (B) of a Scheurebe white wine from Franconia spiked with thiol model solution at 10 $\mu\text{g}/\text{kg}$ (no. 1-8).

Table 1: Summary of validation results for spiked Franconin white wine.

no	compound	calibration curve			sensitivity				
		R ²	slope	intercept	linearity [$\mu\text{g}/\text{kg}$]	LOD [$\mu\text{g}/\text{kg}$]	LOQ [$\mu\text{g}/\text{kg}$]	recovery [%]	RSD [%]
1	pentane-2-thiol	0.9992	0.0473	-0.03	52 - 520	33.2	52.0	110.0	5.3
2	2-furfurylthiol	0.9989	0.2228	0.06	58 - 1154	15.3	57.7	132.7	1.7
3	4-methoxy-2-methylbutane-2-thiol	0.9958	0.6592	0.23	4.9 - 491	0.50	4.93	62.1	11.7
4	4-mercapto-4-methylpentane-2-one	0.9946	0.3577	0.13	5.0 - 496	0.98	4.98	144.5	11.1
5	2-phenylethanethiol	0.9999	1.1025	-0.05	5.3 - 524	5.10	5.26	93.8	0.6
6	3-mercaptohexyl acetate	0.9985	0.8291	0.22	5.5 - 547	2.52	5.49	115.7	1.5
7	1- <i>p</i> -menthene-8-thiol	0.9992	0.6874	-0.12	5.3 - 529	4.06	5.31	157.5	2.3
8	<i>p</i> -mentha-8-thiol-3-one ¹	0.9958	0.6687	0.20	6.6 - 656	0.66	6.59	47.9	9.9

¹ *trans* and *cis* form.

TPS based extraction combined with SBSE-GC-MS/FID achieved low LOD values like 0.5 $\mu\text{g}/\text{kg}$ for 4-methoxy-2-methylbutane-2-thiol, mostly quantitative recovery and relative standard deviation of mostly < 10%.

References

- Katritzky, A. R.; Takahashi, I.; Marson, C. M., 2-(4-Pyridyl)ethyl as a protecting group for sulfur functionality, *Org Chem.* 1986;51(25):4914-4920.
- Vichi, S.; Cortés-Francisco, N.; Romero, A.; Caixach, J., Determination of volatile thiols in virgin olive oil by derivatisation and LC-HRMS, and relation with sensory attributes *Food Chem.* 2014;149:313-318.
- Nishiyama, J.; Kuninori, T., Assay of biological thiols by a combination of high-performance liquid chromatography and postcolumn reaction with 6, 6'-dithiodinicotinic acid, *Anal Biochem.* 1984;138(1):95-98.
- Capone, D. L.; Ristic, R.; Pardon, K. H.; Jeffery, D. W., Simple quantitative determination of potent thiols at ultratrace levels in wine by derivatization and high-performance liquid chromatography-tandem mass spectrometry (HPLC-MS/MS) analysis, *Anal Chem.* 2015;87(2):1226-1231.
- Brocklehurst, K.; Carlsson, J.; Kierstan, M. P. J.; Crook, E. M., In *Methods in Enzymology*, Kaplan, N. P.; Colowick, N. P.; Jakoby, W. B.; Wilchek, M., Covalent chromatography by thiol-disulfide interchange, Eds. Academic Press: 1974; Vol. 34, pp 531-544.
- Full, G.; Schreier, P., A valuable method for the aroma analysis of thiols at trace levels, *Lebensmittelchemie* 1994;48:1-4.
- Stoyanov, S.; Petkov, I.; Antonov, L.; Stoyanova, T.; Karagiannidis, P.; Aslanidis, P., Thione-thiol tautomerism and stability of 2- and 4-mercaptopyridines and 2-mercaptopyrimidines, *Can J Chem.* 1990;68(9):1482-1489.

Giffonins as contributors to the bitter off-taste in hazelnuts

JEKATERINA ONGOUTA¹, Michael Backes¹, Anastasia Albrecht², Katharina Hempel³, Gerhard Krammer¹, Uwe Schäfer¹, Susanne Paetz¹, Peter Winterhalter² and Andreas Kirschning³

¹Symrise AG, Holzminden, Germany, jekaterina.ongouta@symrise.com

²Technical University of Braunschweig, Institute of Food Chemistry, Braunschweig, Germany

³Leibniz University Hannover, Institute of Organic Chemistry, Hannover, Germany

Abstract

Hazelnuts are important raw materials for the bakery and confectionary industry, due to their highly appreciated nutty, roasted, cocoa and buttery taste profile. However, in recent years an intensive, long lasting bitter off-taste of hazelnuts was reported. Cyclic diarylheptanoid natural products were identified as putative inducers of this bitter off-taste. In order to get a deeper knowledge about the natural products that are responsible for this bitter off-taste, the access to such compounds via isolation from ‘cimiciato’-defected hazelnuts or total synthesis was investigated. The key steps of the synthesis include ALDOL-reaction to construct the heptanoid-chain and a metal-assisted coupling to close the 13-membered ring.

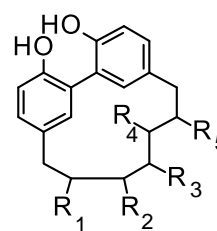
Keywords: diarylheptanoid, hazelnut, bitter off-taste

Introduction

The taste of raw hazelnuts is described as nutty, oily, fruity, sweet and caramel-like with a lasting desirable after taste, whereas roasted hazelnuts are dominated by a roasted and coffee-like aroma. However, in the last years a bitter off-taste in hazelnuts has been reported. This off-taste is still detectable after roasting and therefore also noticeable in finished products leading to consumer complaints and economic losses for the food industry. Activity-guided fractionation and taste dilution analysis of hazelnut kernel (*Corylus avellana L.*) extracts led to the identification of cyclic diarylheptanoid natural products, as putative inducers of this bitter off-taste [1]. Amongst others, Giffonin O (**3**) was identified as one of the candidates for this taste defect. Since 2015 different diarylheptanoids (Giffonins A-V, Carpinontriol B (**5**)) were isolated from the leaves, flowers and shells of hazelnuts [2] (Table 1). For most of them no sensory properties are known.

Table 1: Diarylheptanoids isolated from the leaves, flowers and shells of hazelnuts.

	R ₁	R ₂	R ₃	R ₄	R ₅
Giffonin L (1)	OH	H	OH	OH	OH
Giffonin M (2)	OH	H	OH	=O	H
Giffonin O (3)	OH	OH	=O	H	OH
Giffonin P (4)	OH	OH	OH	OH	OH
Carpinontriol B (5)	OH	OH	OH	=O	H



In order to get a deeper knowledge about sensory properties of these cyclic diarylheptanoids, the access to such compounds is highly relevant, as larger amounts of reference samples would be needed to explore effective masking solutions for mitigating these taste defects.

Within this study the isolation of cyclic diarylheptanoids from ‘cimiciato’-defected hazelnuts was accomplished. In addition we focussed on the development of a synthetic strategy towards these natural products. The key steps of the synthesis include an ALDOL-reaction to construct the heptanoid-chain followed by a metal-assisted coupling to close the 13-membered ring.

Experimental

The ‘cimiciato’-defected hazelnuts were selected from the hazelnut harvest of 2017 in Italy. The solvents and chemicals for the synthesis were purchased from HONEYWELL, SIGMA ALDRICH or ALFA AESER.

The measured NMR data of the isolated cyclic diarylheptanoid natural products matched the published data [2, 3].

Preparation of the ketone **20**: *n*-BuLi (0.13 mL, 0.33 mmol, 2.5 M solution in THF) was added dropwise to a solution of anhydrous *i*-Pr₂NH (50 µL, 0.33 mmol) in Et₂O (10.0 mL) at -20 °C under nitrogen atmosphere. The

mixture was stirred for 20 min at -20 °C and then cooled to -78 °C. Then, the solution of ketone **18** (100 mg, 0.22 mmol) in Et₂O (3 mL) was added dropwise and the resulting solution was stirred for 30 min at -78 °C. Subsequently, the solution of aldehyde **19** (66 mg, 0.44 mmol) in Et₂O (1 mL) was added dropwise and the resulting solution was stirred for 90 min at -78 °C. The reaction was terminated by the addition of saturated NH₄Cl (25 mL) and vigorously stirred at room temperature (rt) for 10 min. The product was extracted with Et₂O. The organic phase was dried over Na₂SO₄ and concentrated. The resulting crude material was purified by column chromatography on silica (hexane/EtOAc = 4:1) to give 105 mg (0.17 mmol) of ketone **20**. Yield: 79 %. ¹H-NMR (400 MHz, C₆D₆) δ -0.2 (s, 3H), -0.07 (s, 3H), -0.03 (s, 3H), 0.16 (s, 3H), 0.86 (s, 9H), 0.99 (s, 9H), 2.71 (dd, *J* = 18.65, 9.28 Hz, 1H), 2.72 (dd, *J* = 13.53, 7.24 Hz, 1H), 2.82 (dd, *J* = 13.53, 6.06 Hz, 1H), 2.88 (dd, *J* = 18.25, 2.71 Hz, 1H), 2.95 (dd, *J* = 13.48, 6.14 Hz, 1H), 3.02 (dd, *J* = 13.53, 8.65 Hz, 1H), 3.32 (s, 3H), 3.34 (s, 3H), 4.13 (d, *J* = 1.75 Hz, 1H), 4.23 (ddd, *J* = 8.25, 6.24, 1.75 Hz, 1H), 4.35-4.45 (m, 1H), 6.72-6.82 (m, 4H), 7.02-7.12 (m, 2H), 7.14-7.24 (n, 2H); ¹³C-NMR (101 MHz, C₆D₆) δ 214.04 (C), 159.07 (C), 158.90 (C), 131.37 (CH), 130.88 (CH), 130.58 (C), 130.11 (C), 114.26 (CH), 81.24 (CH), 79.36 (CH), 69.05 (CH), 54.81 (CH₃), 54.76 (CH₃), 46.00 (CH₂), 42.80 (CH₂), 39.51 (CH₂), 26.28 (CH₃), 26.02 (CH₃), 18.43 (C), 18.34 (C), -4.12 (CH₃), -4.58 (CH₃), -4.88 (CH₃), -5.31 (CH₃). HRMS (ESI) *m/z* for C₃₃H₅₄O₆Si₂Na [M+Na]⁺ calc. 625.3351, found 625.3352.

Preparation of the ketone **21**: TBSOTf (60 μL, 0.25 mmol) was added dropwise to a solution of ketone **20** (100 mg, 0.17 mmol) and 2,6-lutidine (50 μL, 0.42 mmol) in anhydrous CH₂Cl₂ (20 mL) at 0 °C under nitrogen atmosphere. The resulting mixture was stirred for 1 h at 0 °C and for 1 h at rt. The reaction was terminated by the addition of saturated NaHCO₃ (25 mL) and vigorously stirred at room temperature for 10 min. The product was extracted with CH₂Cl₂. The organic phase was dried over Na₂SO₄ and concentrated. The resulting crude material was purified by column chromatography on silica (hexane/EtOAc = 10:1) to give 110 mg (0.15 mmol) of TBS protected ketone. To the solution of this intermediate (50 mg, 0.07 mmol) in CH₂Cl₂ (5 mL) silver trifluoroacetate (46 mg, 0.21 mmol) was added. Subsequently, a solution of I₂ (53 mg, 0.21 mmol) in CH₂Cl₂ (10 mL) was added dropwise and the resulting suspension was stirred for 30 min at rt. The yellow suspension was filtered through Celite and the filtrate was concentrated. The resulting crude material was purified by column chromatography on silica (hexane/EtOAc = 10:1) to give 50 mg (0.05 mmol) of ketone **21**. Yield: 75 %. ¹H-NMR (400 MHz, CDCl₃) δ 7.61 (d, *J* = 2.1 Hz, 1H), 7.58 (d, *J* = 2.1 Hz, 1H), 7.13 (dd, *J* = 8.4, 2.1 Hz, 1H), 7.12 (dd, *J* = 8.3, 2.1 Hz, 1H), 6.72 (d, *J* = 8.4 Hz, 2H), 4.30 (p, *J* = 6.0 Hz, 1H), 4.03 (td, *J* = 7.0, 1.7 Hz, 1H), 3.92 (d, *J* = 1.8 Hz, 1H), 3.84 (s, 6H), 2.79 (dd, *J* = 19.1, 6.4 Hz, 1H), 2.68 (dd, *J* = 19.0, 5.7 Hz, 1H), 2.69 - 2.63 (m, 2H), 2.60 (dd, *J* = 13.6, 4.9 Hz, 1H), 2.58 (dd, *J* = 13.6, 4.9 Hz, 1H), 0.87 (s, 9H), 0.85 (s, 9H), 0.83 (s, 9H), 0.01 (s, 3H), 0.01 (s, 3H), -0.01 (s, 3H), -0.09 (s, 3H), -0.12 (s, 3H), -0.21 (s, 3H). ¹³C-NMR (101 MHz, CDCl₃) δ 211.24 (C), 156.76 (C), 156.72 (C), 140.63 (CH), 140.60 (CH), 133.18 (C), 132.71 (C), 131.10 (CH), 130.74 (CH), 110.67 (CH), 85.72 (C), 85.63 (C), 81.52 (CH), 77.70 (CH), 68.67 (CH), 56.42 (CH₃), 47.20 (CH₂), 42.58 (CH₂), 37.96 (CH₂), 26.07 (CH₃), 25.90 (CH₃), 25.88 (CH₃), 18.25 (C), 18.16 (C), 17.99 (C), -4.33 (CH₃), -4.38 (CH₃), -4.70 (CH₃), -4.92 (CH₃), -5.22 (CH₃), -5.24 (CH₃). HRMS (ESI) *m/z* for C₃₉H₆₆I₂O₆Si₃Na [M+Na]⁺ calc. 991.2149, found 991.2152.

Results and discussion

Isolation of diarylheptanoids from hazelnuts

The analysis of the methanol extracts of ‘cimiciato’-defected hazelnuts identified several diarylheptanoids. Due to very small concentrations of these natural products only three diarylheptanoids could be isolated and characterised by NMR: giffonin P (**4**), carpinontriol B (**5**) and betulatetraol (**6**) (Figure 1). As the main diarylheptanoid carpinontriol B (**5**) was isolated. The concentration of this compound in ‘cimiciato’-defected hazelnut paste was determined to be 136 ppm.

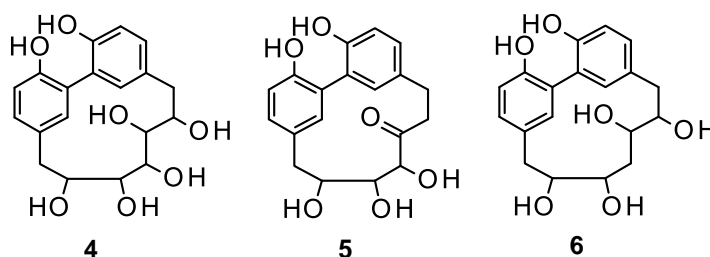


Figure 1: Diarylheptanoids isolated from ‘cimiciato’-defected hazelnut.

The sensory evaluation of carpinontriol B (**5**) confirmed the bitter off-taste (25 ppm solution is equally bitter to a 250 ppm solution of salicin). The other two natural products could be obtained only in very small amounts (concentration in hazelnut paste < 1 ppm), which were not sufficient for the sensory evaluation.

Synthetic strategy towards diarylheptanoid natural products

In order to get access to other diarylheptanoids a variable synthetic strategy was developed. For example, Giffonin O (**3**) was dissected retro synthetically into three fragments: the western fragment (in green), the eastern fragment (in red) and the southern fragment (in blue). A metal-assisted biaryl-coupling is intended to be the key step to close the 13-membered macrocycle. The precursor for this cyclization is envisaged to be prepared by an aldol reaction between the eastern fragment **8** and the coupling product of the western fragment **9** and southern fragment **10** (Figure 2).

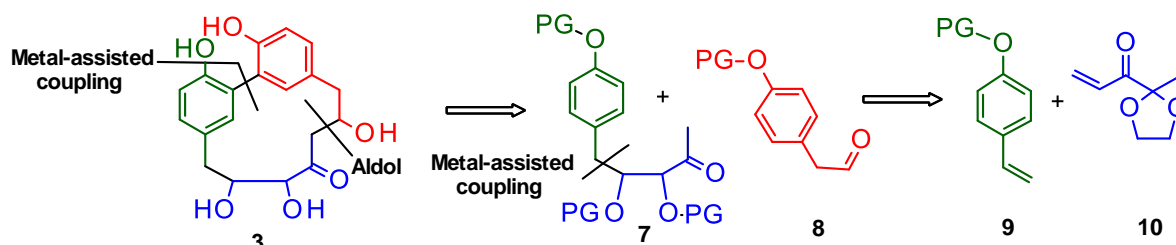


Figure 2: Retrosynthesis of Giffonin O (**3**).

The starting point for the synthesis was the preparation of the southern fragment **10** from ethyl pyruvate (**11**). After the protection of the ketone functionality of **11** with ethylene glycol under acidic conditions, the corresponding Weinreb amide **13** was generated. The formation of Weinreb amide was necessary for the GRIGNARD addition to obtain ketone **10**, since the direct alkylation of ester **11** provided mainly the double alkylated product (Figure 3).

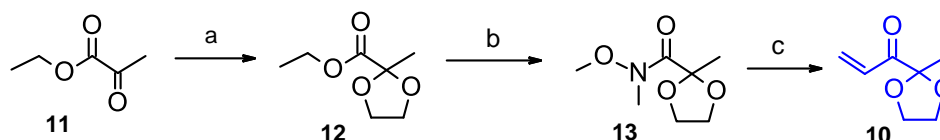


Figure 3: Synthesis of the southern fragment. Reaction conditions: a) 1,2-Ethanediol, TFA, PTSA, toluene, reflux, 5 h, 29 %; b) *n*-BuLi, MeNHOMe · HCl, THF, -78 °C, 12 h, 42 %; c) VinylMgBr, THF, -78 °C, 3.5 h, 85 %.

Ruthenium catalysed cross-metathesis between the southern fragment **10** and the western fragment **14** yielded the corresponding ketone **15** in very good yield. To avoid the dimerization of the fragments, the commercially available western fragment **14** was used in excess. By using three equivalents of 4-methoxy-styrene (**14**) full conversion of the southern fragment **10** could be achieved. The resulting α,β -unsaturated ketone **15** was then transferred to the epoxide **16** via 1,4-hydride addition using WILKINSON procedure [4], followed by epoxidation of the resulting enol ether with *m*-CPBA. Subsequent reductive opening of the epoxide with diisobutylaluminum hydride provided the TES-protected diol **17**. During the FeCl₃ catalysed deprotection of the ketone functionality, the TES-protecting group was also cleaved. In the next step the hydroxyl functions were again protected with TBS to obtain the ketone **18**. The following aldol reaction with *para*-methoxyphenyl acetaldehyde (**19**) provided the open chain diarylheptanoid (**20**) in 79 % yield (Figure 4).

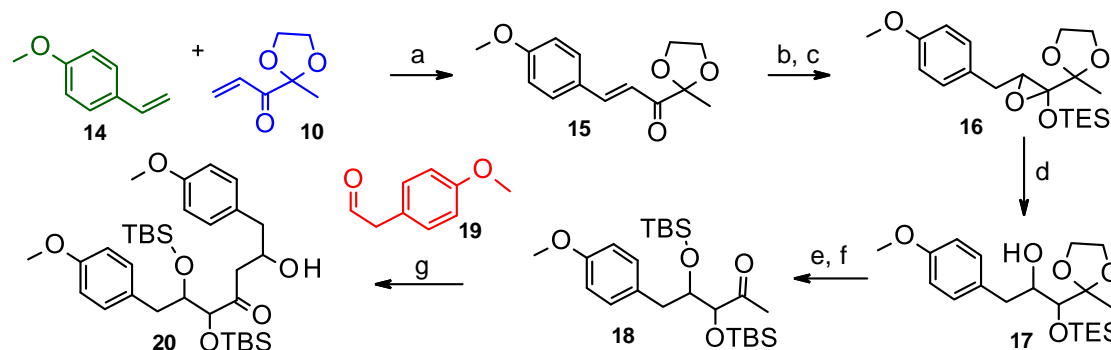


Figure 4: Coupling of the fragments. Reaction conditions: a) Hoveyda-Grubbs 2nd gen., CH₂Cl₂, 40 °C, 10 h, 99 %; b) Et₃SiH, RhCl(PPh₃)₃, toluene, 65 °C, 5 h, 95 %; c) *m*-CPBA, NaHCO₃, CH₂Cl₂, 0 °C, 4 h, 78 %; d) DIBAL-H, CH₂Cl₂, -78 °C, 6 h, 43 %; e) FeCl₃·6H₂O, CH₂Cl₂, 0 °C, 2 h, rt, 1 h, 66 %; f) TBSOTf, 2,6-Lutidine, CH₂Cl₂, rt, 2 h, 80 %; g) (*i*-Pr)₂NH, *n*-BuLi, **19**, -78 °C, Et₂O, 2 h, 79 %.

The TBS-protection, followed by iodination using silver trifluoroacetate and iodine gave the open chain intermediate **21** which was then used as substrate for the metal-assisted macrocyclisation. Macrocyclisation of highly functionalized and rigid precursors is challenging and the conversion of such macrocyclisations is usually poor. Palladium catalysed SUZUKI-coupling was not effective for the desired transformation. The successful formation of the protected Giffonin O (**22**) could be achieved using activated copper or Ni(PPh₃)₄ (Figure 5). However, only small amounts of the desired macrocycle **22** could be isolated. In order to proceed with the synthesis the macrocyclisation has to be optimized further.

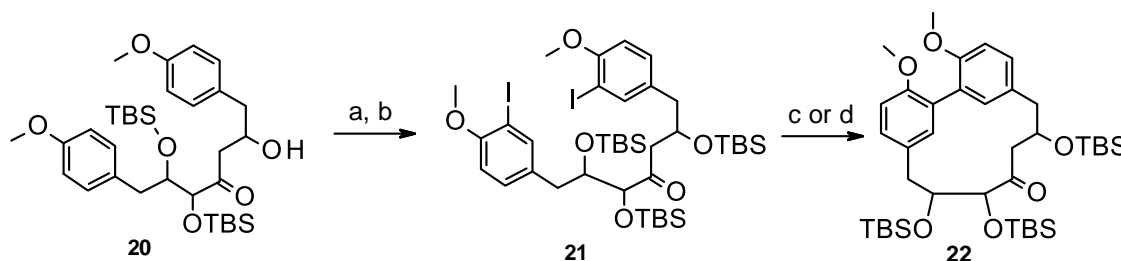


Figure 5: Final cyclisation. Reaction conditions: a) TBSOTf, 2,6-Lutidine, CH₂Cl₂, rt, 2 h, 92 %; b) CF₃COOAg, I₂, CH₂Cl₂, rt, 0.5h, 75 %; c) Cu, DEF, 150-180 °C, 4 h; d) Ni(PPh₃)₄, DEF, 110-150 °C, 30 h.

Conclusion

Three cyclic diarylheptanoids from 'cimiciato'-defected hazelnuts were isolated and characterised. The sensory evaluation of carpinontriol B (**5**) confirmed the bitter off-taste. In addition, the synthetic strategy towards the protected Giffonin O (**22**) could be developed. The removal of all remaining protection groups should lead to the target molecule **3**. In addition, the reduction of the ketone and subsequent deprotection should furnish the second diarylheptanoid Giffonin L (**1**) (Figure 6).

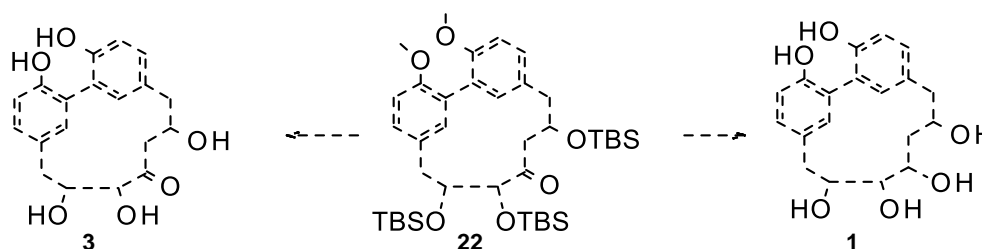


Figure 6: Final deprotection.

This variable synthetic strategy should also allow the synthesis of further diarylheptanoid natural products with different substitution pattern. In addition, the stereoselective epoxidation of compound **15** should provide access to enantiomerically pure diarylheptanoids.

The sensory evaluation of the diarylheptanoids could provide valuable information about structure activity relationships of the cyclic diarylheptanoids as contributors to the bitter off-taste in hazelnuts. This is highly relevant to explore effective masking solutions for these taste defects.

References

1. Singldinger B, Dunkel A, Hofmann T, The Cyclic Diarylheptanoid Asadanin as the Main Contributor to the Bitter Off-Taste in Hazelnuts (*Corylus avellana* L.). *J Agric Food Chem.* 2017;65:1677; Singldinger B, Dunkel A, Bahmann D, Bahmann C, Kadow D, Bisping B, Hofmann T. New Taste-Active 3-(O-β-D-Glucosyl)-2-oxoindole-3-acetic Acids and Diarylheptanoids in Cimiciato-Infected Hazelnuts. *J Agric Food Chem.* 2018;66:4660.
2. Masullo M, Cerulli A, Olas B, Pizza C, Piacente S, Giffonins A-I, antioxidant cyclized diarylheptanoids from the leaves of the hazelnut tree (*Corylus avellana*), source of the Italian PGI product "Nocciola di Giffoni", *J Nat Prod.* 2015;78:2975; Masullo M, Mari A, Cerulli A, Bottone A, Kontek B, Olas B, Pizza C, Piacente S. Quali-quantitative analysis of the phenolic fraction of the flowers of *Corylus avellana*, source of the Italian PGI product "Nocciola di Giffoni": Isolation of antioxidant diarylheptanoids, *Phytochemistry* 2016;130:273–281; Cerulli A, Lauro G, Masullo M, Cantone V, Olas B, Kontek B, Nazzaro F, Bi-fulco G, Piacente S. Cyclic Diarylheptanoids from *Corylus avellana* Green Leafy Covers: Determination of Their Absolute Configurations and Evaluation of Their Anti-oxidant and Antimicrobial Activities, *J Nat Prod.* 2017;80(6):1703–1713.
3. Lee M.-W, Tanaka T, Nonaka G.-I, Hahn D.-R. Phenolic compounds on the leaves of *Betula platyphylla* var. *latifolia*, *Arch Pharm Res.* 1992;15(3):211–214.
4. Heinrich E. B, Sowell G, Little D. Electrolyte-assisted stereoselection and control of cyclization vs saturation in electroreductive cyclizations. *Tetrahedron Lett.* 1990;31:2525–2528.

Differential effects of cryo-concentration on volatiles in apple juice

MIKAEL AGERLIN PETERSEN¹, Pernille Nygaard Kristensen¹, Sophia Maria Odorico Gormsen¹, Mette Fangel Juda¹ and Torben Bo Toldam-Andersen²

¹Department of Food Science, University of Copenhagen, Frederiksberg, Denmark

²Department of Plant and Environmental Sciences, University of Copenhagen, Frederiksberg, Denmark
map@food.ku.dk

Abstract

Cryo-concentration of apple juice shows that concentration of esters increases proportionally with increasing Brix value while the concentration of furan compounds has an irregular but in some cases close to exponential increase during the concentration process. Some furans have pleasant caramel-like odours, which have been reported in apple wine from cryo-concentrated apple juice. It is therefore concluded that cryo-concentration introduces an opportunity to produce richer apple wine not just due to concentration but most likely also due to formation of pleasantly smelling aroma compounds such as furans.

Keywords: cryo-concentration, furans, fruit wine, de novo synthesis

Introduction

New ways of utilizing Danish apples are of interest in order to prevent food waste and loss of this Danish cultural heritage [1]. In earlier projects conducted by University of Copenhagen in collaboration with Cold Hand Winery (Randers, Denmark) it was found that several apple cultivars produced in Denmark are highly suitable for wine production [2]. However, due to the low sugar content of plain apple juice, regular wine of good quality, as known from grapes, is difficult to achieve. To prepare an apple juice, which is more suitable for wine production, cryo-concentration of the juice prior to fermentation can be done [3]. Cryo-concentration is a gentle process where sugars, acids and volatiles are efficiently concentrated with low losses of both volatiles and solids. The concentrated juice – and the wine produced from it – is generally intensified. However, it has been an experience that the cryo-concentration does not equally affect all volatiles. This study shows the differential effects of cryo-concentration on two groups of aroma compounds: esters and furans in apple juice made from ‘Bramley’ and ‘Graasten’ cultivars.

Experimental

Materials

Apple juice was freshly prepared from ‘Graasten’ (90%) and ‘Bramley’ (10%) cultivars harvested at the Pometum, which is University of Copenhagen’s orchard.

Method

Juice was frozen at -18°C in two 10L plastic containers (A and B) and kept frozen for four months. The juice was thawed slowly (at 0.0 ± 0.5°C for five days) following the method of complete block cryo-concentration inspired by Aider & Hallux [3] (Figure 1). Samples (n=17) of individual thawed fractions were collected throughout the melting process and content of soluble solids was measured as °Brix. Volatile profile was analysed by dynamic headspace sampling (DHS) and gas chromatography mass spectrometry (GC-MS) as described in [4]. The objective was to measure juice composition at approximately every 200 mL of thawed must. A control was thawed completely over six days at 5°C.



Figure 1: Left: frozen apple juice before thawing. Right: remaining ice block with little dry matter left after thawing.

Results and discussion

During thawing, °Brix decreased from 49 in the first fraction to 9 in the last, when collection was terminated. By DHS-GC-MS analysis, a total of 88 volatiles were identified reflecting the common composition found in apples: esters (n=27), alcohols (n=15), aldehydes (n=15), acids (n=11), furans (n=8), ketones (n=7), and terpenes (n=5).

Esters

Figure 2 illustrates how the concentration of esters was proportional to Brix values, thus the concentrations followed a linear tendency with R^2 close to 1. This development in volatile compounds is anticipated upon cryo-concentration and indicates that esters are concentrated and not lost nor formed during the thawing process.

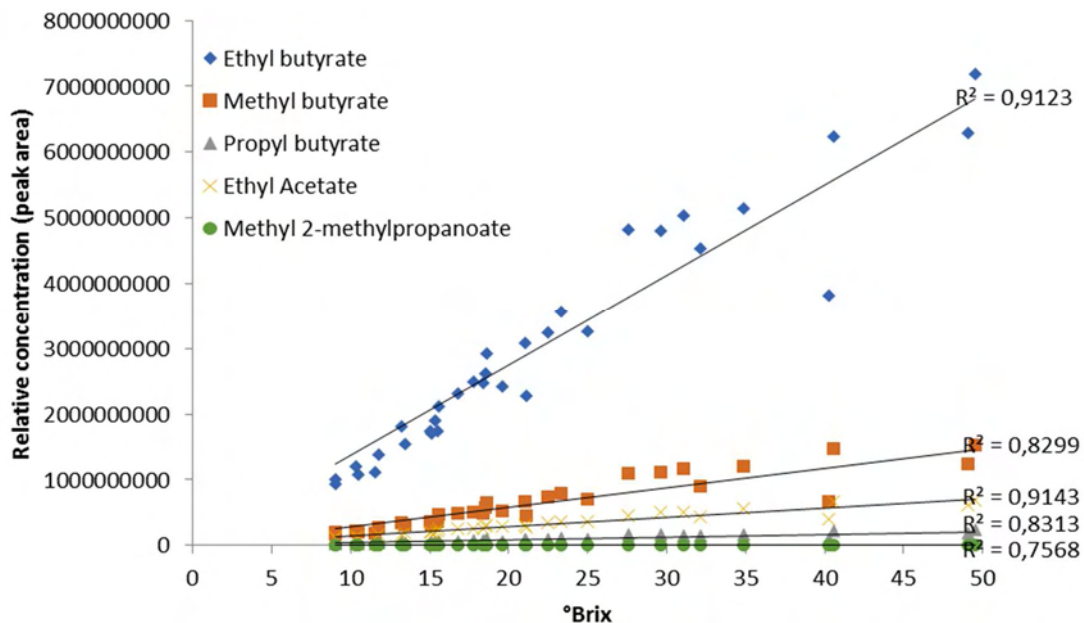


Figure 2: Concentration of esters in thawed fractions with different °Brix. The plot includes all measurements from container A and B.

Furans

High Brix samples of cryo-concentrated apple juice also contained high concentrations of furans. The development was, however, very irregular and it was not possible to fit a common model to all samples. If data from the two biological replicates (A and B) were analysed separately, it appeared that they behaved very differently. Figure 3 shows data for three furans in container B, and here the development was well described by power functions. The development in container A could not be described by power functions or any other standard

functions. It should be noted, that container A and B were treated the same way, and that data for the esters (Figure 2) showed identical patterns in the two containers.

Comparison of the development in concentrations of esters and furans shows that the increase in furans is not only due to the concentration effect. Furans are possibly also formed de novo during cryo-concentration.

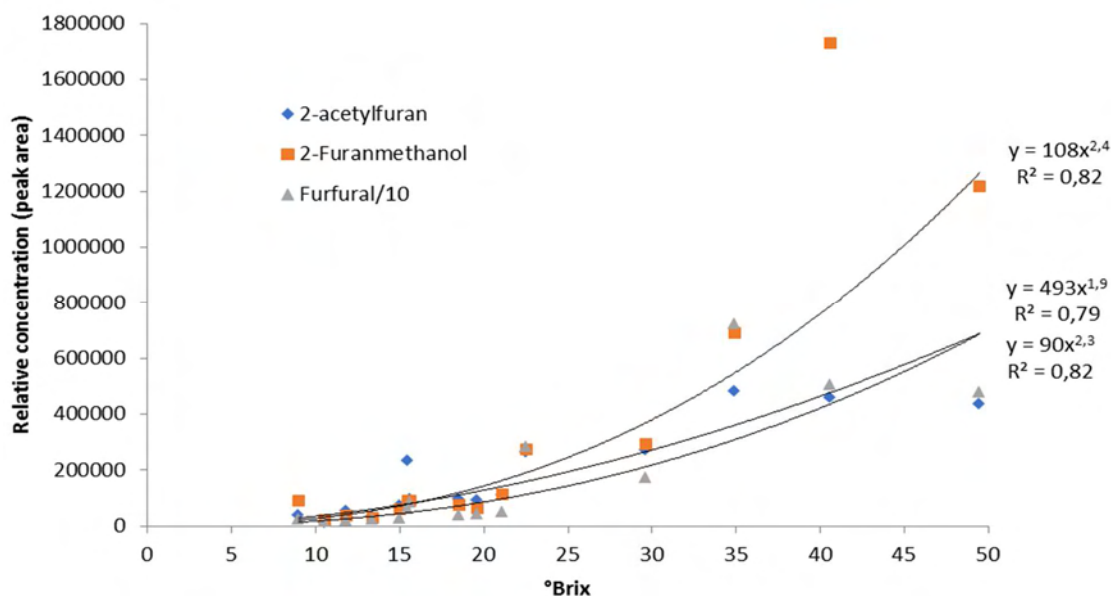


Figure 3: Concentration of furans in thawed fractions with different °Brix. The plot includes only measurements from container B.

Microenvironments and acid-catalysed caramelisation

The formation of furans is often associated with heat treatment. However, even at low temperatures, the reaction mechanisms of caramelisation can be considered identical to those at high heat, if the sugar solution is very concentrated and the pH is low [5]. In the present study, pH varied from 3.37 in the most concentrated fractions to 3.52 in the least concentrated.

During cryo-concentration, high concentrations of solids, such as sugars and acids are achieved. As the freezing point decreases with high concentrations of these compounds, a part of the juice will remain unfrozen even at temperatures below -7°C [6], which provides the opportunity of microenvironments to arise, which is favourable for the formation of furans by caramelisation reactions. It can be hypothesised that these microenvironments are a part of the reason for formation of furans as well as the reason for irregularity of formation.

Formation of furans during storage of cryo-concentrated apple juice

A sample of cryo-concentrated apple juice (19.5°Brix) was kept stored at 0°C for 14 days. This was done in order to investigate whether the high sugar and acid levels in the cryo-concentrated apple juice can lead to formation of aroma compounds during storage. Compared to the control, cryo-concentrated juice had 27% higher level of total furans while stored cryo-concentrated juice had 71% more. The samples of cryo-concentrated juice and stored cryo-concentrated juice had the same °Brix (19.5°Brix). The difference between these two samples was 35% which indicates a tendency that storage of the cryo-concentrated apple juice results in formation of furans. The increase was primarily due to 2-furanmethanol, 5-ethyl-2(5H)-furanone, 2(5H)-furanone and furfural. This supports the hypothesis that microenvironments with high sugar/acid concentrations might enable formation of furans. Due to lack of replicates, significance testing could not be performed. Nonetheless, a three-fold increase was seen for 2-furanmethanol in stored samples compared to non-stored.

Tadao Kurata and Yosito Sakurai [7] found that ascorbic acid degrades to furfural under acidic conditions during storage or cooking of foods (Figure 4). It is hypothesised that this could be part of the reason for the increase in furans after storage of the cryo-concentrated apple juice.

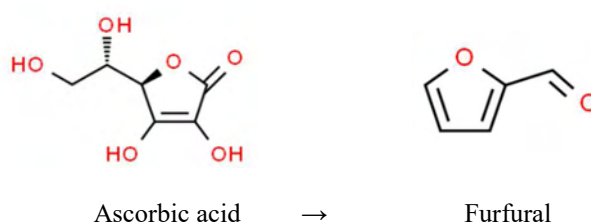


Figure 4: Degradation reaction of ascorbic acid to furfural under acidic conditions.

Conclusion

Cryo-concentration of apple juice affects volatiles such as furans and esters in different ways. While esters were found to concentrate proportionally to °Brix, furans had a different and very irregular development during the concentration process, most probably due to de novo synthesis even at the low temperatures applied. This finding supports previous findings from University of Copenhagen where a higher level of furans was found in cryo-concentrated sparkling apple wine compared to non-cryo-concentrated apple wine. It is therefore concluded that cryo-concentration introduces an opportunity to produce richer apple wine not just due to a general concentration of the soluble solids but most likely also due to formation of new aroma compounds with caramel-like or other pleasantly smelling qualities. This presents an innovative way of using surplus apples as well as specially produced high quality apples, and could lead to new and interesting products from local produce with a sensory profile, which differentiates them from other apple products.

References

1. CONCITO. Det skjulte madspild - Kortlægning og handlingskatalog. Report from CONCITO and the Danish Ministry of Food 2011. Available from <https://concito.dk/udgivelser/skjulte-madspild>.
2. Toldam-Andersen TB. Kryo-koncentrerede frugtvine. Resultater fra et 4 årigt udviklingsprojekt. *Vinpressen* 2018;6:16-21.
3. Aider M, de Halleux D. Cryoconcentration technology in the bio-food industry: Principles and applications. *LWT-Food Sci Technol.* 2009;42(3):679-685.
4. Zhang S, Petersen MA, Liu J, Toldam-Andersen TB. Influence of Pre-fermentation Treatments on Wine Volatile and Sensory Profile of the new Disease Tolerant Cultivar Solaris. *Molecules* 2015;23(2):357.
5. Quintas M, Fundo J, Silva C. Sucrose in the concentrated solution or the supercooled "state": A review of caramelisation reactions and physical behaviour. *Food Eng Rev.* 2010;2(3):204-215.
6. Auleda J, Raventos M, Sanchez J, Hernandez E. Estimation of the freezing point of concentrated fruit juices for application in freeze concentration. *J Food Eng.* 2011;105(2):289-294.
7. Kurata T, Sakurai Y. Degradation of L-Ascorbic Acid and Mechanism of Nonenzymic Browning Reaction, *Agric Biol Chem.* 1967;31(2):170-184.

Effect of polyols on the release and on the self-diffusion coefficient of sweet aroma compounds in soda beverages

CARMEN BARBA¹, Juan Ignacio Maté¹, Alfonso Cornejo²

¹ISFOOD - Institute for Innovation & Sustainable Development in Food Chain, Public University of Navarre, Campus de Arrosadía, 31006, Pamplona, Spain, carmen.barba@unavarra.es

²INAMAT- Institute for Advanced Materials and Mathematics, Public University of Navarre, Campus de Arrosadía, 31006, Pamplona, Spain

Abstract

The overall objective of this study was to investigate the effect of polyols on the release of an aroma compound named 2-phenylethanol in solution. The first set of experiments evaluated the effect of three polyols named erythritol (MW=122.12), D-mannitol (MW=182.17) and maltitol (MW=344.31) on the concentration of 2-phenylethanol in the headspace. The headspace concentration of aroma compounds was analysed by headspace solid-phase microextraction gas chromatography (HS-SPME-GC). In the second set of experiments, self-diffusion coefficient of 2-phenylethanol was calculated in presence of polyols by diffusion ordered spectroscopy-nuclear magnetic resonance (DOSY NMR). Results showed that the structures of all polyols had a relevant effect on the headspace volatility of 2-phenylethanol. The “salting-out effect” was slightly increased with the molecular weight of the polyol. The aroma self-diffusion coefficient of 2-phenylethanol was not affected with the presence of polyols at low concentration (10%, w/w). Both methods provide complementary information on flavour-food matrix interactions, which it is critical for the selection of aroma compounds to formulate new soda beverages with polyols. This study provides a new insight about how one may combine aroma and polyols to formulate soda beverages when replacing sucrose.

Keywords: polyols, 2-phenylethanol, release, self-diffusion coefficient, HS-SPME-GC

Introduction

Polyols are molecules able to modulate sweet perception and they are used as sweeteners. Their similarities to sugars, both in sweet flavour and physical properties, have resulted in using them as low-calorie sweeteners and bulk sugar replacement. Moreover, polyols intake are not linked with obesity, diabetes and caries. The microbial production of polyols and the current regulation have been recently reviewed [1]. Due to the industrial impact that may have this sucrose alternative, its use is controversial in food industry. Polyols are used generally in combination with other high intensity sweeteners to avoid high concentrations while keeping a high sweet perception.

Flavour release during consumption is an important aspect because of its influence on flavour perception and on the acceptability of food or beverage products [2]. The study of the interactions that may occur with flavour compounds contributes to understand flavour release. Interactions of flavour compounds with other food matrix compounds such as proteins, carbohydrates and lipids have been well studied as they have a strong influence on the release of flavour compounds from foods [3, 4]. However, the literature contains only a few examples of the impact of polyols on flavour release in food and beverage products [5-8]. Another approach, much less explored in the industry and in the literature, is to reduce polyols concentration from food and beverage products using odour associated to sweet taste compounds, based on the fact that an odour may evoke a taste [9].

The aims of this work were: i) to evaluate the effect of polyols (erythritol, D-mannitol and maltitol) on the headspace concentration of a flavour compound, namely 2-phenylethanol, by HS-SPME; ii) to quantify the self-diffusion coefficients of 2-phenylethanol by DOSY NMR to explore mechanism of interactions between polyols and 2-phenylethanol.

Experimental

Samples and chemicals

Erythritol (C₄H₁₀O₄, MW=122.12 g/mol), D-mannitol (C₆H₁₄O₆, MW=182.17 g/mol) and maltitol (C₁₂H₂₄O₁₁, MW=344.31 g/mol) were provided by Cargill (Minnesota, USA). The volatile compound 2-phenylethanol was provided by Merck (Darmstadt, Germany). Solutions of 2-phenylethanol were prepared in deionized water (reference solution) at 100 mg/L. Solutions of each polyol 10% (w/w) with 2-phenylethanol (100 mg/L) were stirred at 200 rpm for 40 minutes and sonicated for 30 minutes at room temperature (19 ± 1 °C).

HS-SPME

Although experimental conditions used for the HS-SPME procedure were initially set as suggested by other authors [10, 11] slight variations were introduced in the present work with a view to the specific requirements of the proposed objectives. Different parameters were tested to optimize this method: absorption of two fibres from the same batch, two different type of fibres (DVB/CAR/PDMS and Carboxen/PDMS) and sample volume in the vial (1, 3 and 5 mL). Finally, a Supelco (Bellefonte, PA, USA) holder and a SPME Stableflex 2 cm-50/30 DVB/CAR/PDMS fibre was employed to retain 2-phenylethanol. According to the recommendations of the manufacturer, prior to its use the fibre was conditioned for 60 min in the GC injector port maintained at 270 °C. Before each analysis, the fibre was cleaned at 250 °C for 5 minutes. 3 mL of each sample was placed in a 10 mL vial and sealed with parafilm. In all cases samples were placed in a bath at 25 °C for 1 h. Volatile compound was extracted at different extraction times (1, 5, 30, 60, 80, 120, 140 and 180 min). Volatile compounds were desorbed by inserting the fibre into the GC injector set at 250 °C for 5 min. HS-SPME analysis were done in triplicate RSD value were less 5%.

GC-FID analysis

An Agilent 8860 equipped with split/splitless injector and a FID detector was used. A 30 m × 0.32 mm I.D. fused silica capillary column coated with a 0.5 mm layer of polyethylene glycol (DB-Wax, Agilent) was employed. The carrier gas was He at 30 cm/s. The oven temperature was held at 40 °C for 5 min, increased to 220 °C at 5 °C/min and then held at 220 °C for 10 min. The temperature of injector and detector were 250 °C and 300 °C, respectively.

DOSY NMR

Diffusion coefficients of erythritol, D-mannitol and maltitol were measured at 10 % w/w whereas 2-phenylethanol was measured at 100 mg/L in D₂O. Samples combining polyol and 2-phenylethanol were prepared at 10 % w/w and 2-phenylethanol at 100 mg/L, respectively. NMR measurements were made at 25 °C on a Bruker Ascend III spectrometer equipped with a PABBO 5 probe, at 400 MHz and 101 MHz for ¹H and ¹³C respectively and were processed using Bruker Topspin 3.2 software. NMR samples were prepared in D₂O and residual H₂O signal referenced at 4.7 ppm as reported by Savary et al. [4]. DOSY was run using *stebpgp1s* pulse program in QF acquisition mode. Diffusion delay (*d20*) in *stebpgp1s* was optimized using residual H₂O signal keeping gradient pulse length (*p30*) constant at 1000 μs, resulting in 160-170 ms. Each pseudo-2D experiment consisted on a series of 16 or 32 spectra. DOSY experiments were made in DMSO-*d*₆ at 300 K and at fixed low concentrations, 1 % w/v. The accuracy of the gradient was previously checked by the determination of the diffusion coefficient of residual DMSO in DMSO-*d*₆. DOSY analysis were processed using TOPSPIN 3.2 software from Bruker. Once F2 were phased, automatic baseline correction was run using a 5th grade polynomial function. Using the T1/T2 relaxation module installed in the module permitted FID for the first spectrum (2 % gradient) to be extracted and to perform manual integration. The integration regions were exported to the relaxation module where decay values were fitted by area using the *vargrad* preinstalled function using a 5.35 G/mm as gradient calibration constant. Graphical processing was run using 'Dynamic Center v. 2.6.1' software from Bruker. Unless otherwise stated, Stejskal-Tanner equation was fitted using the intensity obtained after the peak picking of the first spectrum corresponding to 2% gradient. DOSY NMR analyses were done in duplicate.

Results and discussion

The influence of the addition of polyols on aroma release depends on aroma compound and the type of polyol studied. HS-SPME allowed us to determine that erythritol, D-mannitol and maltitol induce a greater increase in the release of 2-phenylethanol. Figure 1 shows kinetics of adsorption of 2-phenylethanol on the SPME fibre. After equilibrium time of the sample (60 min) at 25°C, SPME fibre was introduced into sample headspace and held for different times periods (1, 5, 30, 60, 80, 120, 140 and 180 min) before analysis by GC. The adsorption rate of 2-phenylethanol increases when a polyol was added. Kinetics of 2-phenylethanol in water was linear ($y = 9.62 \cdot 10^5 x + 4.70 \cdot 10^5$ $R^2 = 0.9929$) for 80 min sampling. The linear behaviour was reduced to 30 minutes sampling when erythritol, D-mannitol and maltitol was added. The adsorption rate was $1.79 \cdot 10^5 \text{ min}^{-1}$, $1.83 \cdot 10^5 \text{ min}^{-1}$ and $1.98 \cdot 10^5 \text{ min}^{-1}$ for erythritol, D-mannitol and maltitol, respectively. This result can be explained by the "salting-out effect" that polyols produce on 2-phenylethanol. Erythritol, D-mannitol and maltitol are highly polar molecules that keep in the sample (water); hence, the less polar component (2-phenylethanol) is forced to be in the vapour phase (headspace). The alteration of 2-phenylethanol concentration in the headspace increases as the molecular weight of the polyol increases. This slightly difference may be due to the fact that the solubility of polyol decreases as molecular weight increases and this forces the 2-phenylethanol to the headspace. For ease of comparison, the extent of release of 2-phenylethanol in the presence of polyols was expressed in a normalized ion response related

to the response for water (100%). Changes in flavour headspace concentration with addition of erythritol, D-mannitol and maltitol increase 6, 9 and 10%, respectively. This data suggests that at low polyol concentration the volatility of aroma primarily controls 2-phenylethanol release. The present study corroborates previous published results [5].

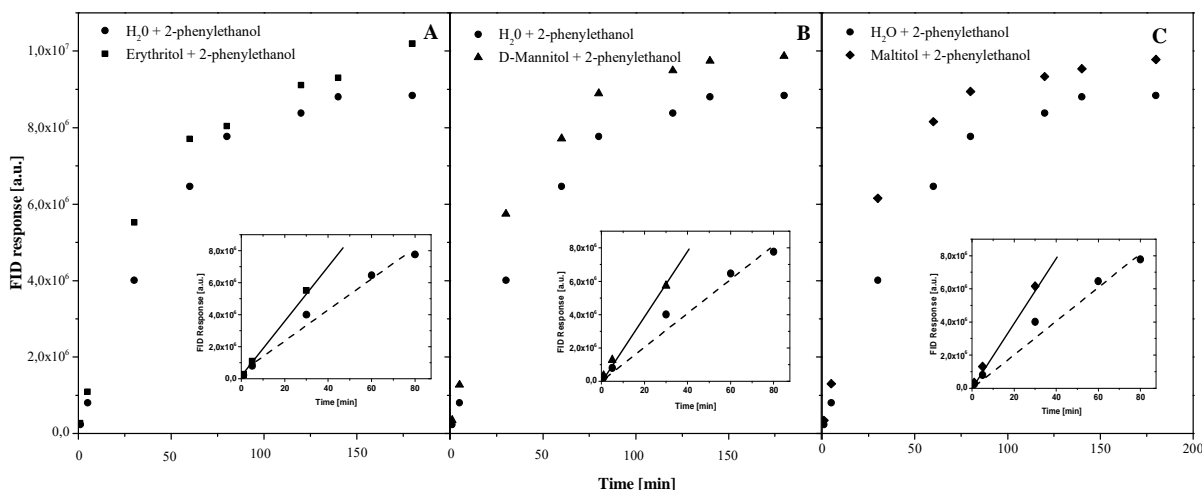


Figure 1: Kinetics of adsorption of 2-phenylethanol in H_2O (reference solution) and with: (A) erythritol; (B) D-mannitol; and (C) maltitol. Linear regression adjustment is shown in the insert of panel A), B) and C).

Figure 2 illustrates DOSY spectrum of 2-phenylethanol at 100 mg/L in D_2O (reference solution) and with erythritol, D-mannitol and maltitol (10%, w/w). The DOSY spectrum of 2-phenylethanol in D_2O shows three signals corresponding to the three proton groups of the molecule, CH₂ (1) at 2.85 ppm, CH₂ (2) at 3.83 and CH (4-8) at 7.40-7.26 ppm. The diffusion coefficient of 2-phenylethanol was calculated using the integration for each of the three signals and the average of the value was $7.33 \cdot 10^{-10} \text{ m}^2/\text{s}$. In the DOSY spectrum of erythritol two sets of signals to the protons of the molecule, CH₂ (2), CH (3), CH (4), CH (5) at 3.79-3.66 ppm and 3.66-3.50 ppm were used for the calculation of the diffusion coefficient. These signals were highly affected for the four -OH electronegative groups of the molecule. The diffusion coefficient of erythritol was calculated with this signal and the value was $5.62 \cdot 10^{-10} \text{ m}^2/\text{s}$. In the DOSY spectrum of D-mannitol three sets of signals, CH₂ (1, 6), CH (2, 5) and CH (3, 4), 3.87-3.78 ppm, 3.78-3.67 ppm and 3.66-3.58 ppm were used. The diffusion coefficient of D-mannitol was calculated with these sets of signals and the value was $4.48 \cdot 10^{-10} \text{ m}^2/\text{s}$. The DOSY spectrum of maltitol presented three sets of signals, 5.13-5.04 ppm, 4.00-3.72 ppm and 3.72-3.34 that were used in the calculation of the diffusion coefficient, $3.47 \cdot 10^{-10} \text{ m}^2/\text{s}$. These results indicate that 2-phenylethanol, erythritol, D-mannitol and maltitol diffuse more slowly as the molecular weight increases and the hydrophobicity character decreases ($\log P_{\text{erythritol}} = 1.36 > \log P_{\text{D-mannitol}} = -3.10 > \log P_{\text{maltitol}} = -4.67$).

The impact of the nature of the polyol on the 2-phenylethanol diffusion was evaluated. This was done by comparing the diffusion coefficient calculated using the integration of the signal corresponding at the aromatic hydrogen atoms of 2-phenylethanol, 7.47-7.26 ppm. The influence of the addition of polyol on aroma release presents similar effects for the three polyols studied. The diffusion coefficient was $7.33 \cdot 10^{-10} \text{ m}^2/\text{s}$ and slightly decreases at $5.78 \cdot 10^{-10} \text{ m}^2/\text{s}$, $6.44 \cdot 10^{-10} \text{ m}^2/\text{s}$ with erythritol, D-mannitol and maltitol, respectively. The mobility of 2-phenylethanol is not affected by the presence of polyol at low concentration (10%). Moreover, there was no difference between chemical shift of 2-phenylethanol, erythritol, D-mannitol and maltitol alone and in the different media with polyols. This data suggests that there is not interaction between 2-phenylethanol and the polyols studied. These results were consistent with the indirect macroscopic information of mass transfer given by HS-SPME GC showed in Figure 1.

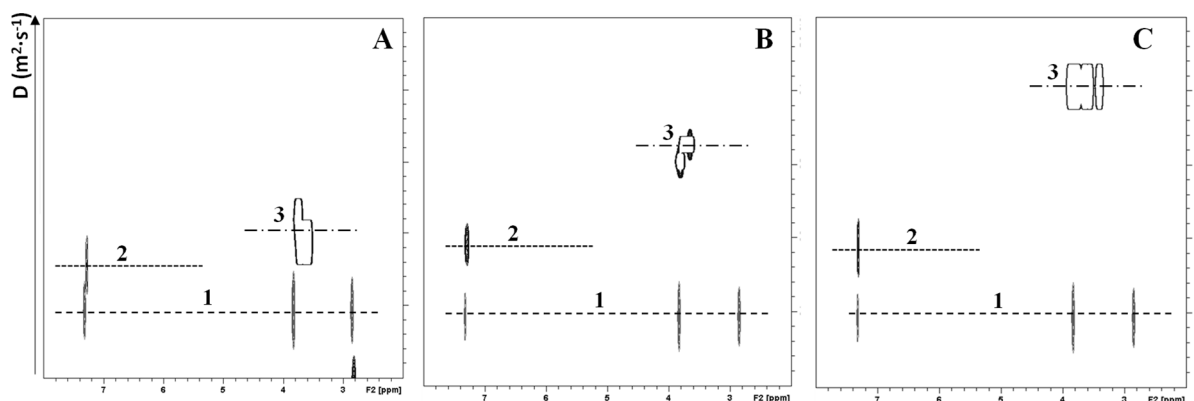


Figure 2: ¹H NMR DOSY spectra of 2-phenylethanol at 100 ppm (1), 2-phenylethanol with erythritol 10% (w/w) (2), erythritol 10% (3) (A); and 2-phenylethanol at 100 ppm (1), 2-phenylethanol with D-mannitol 10% (w/w) (2), D-mannitol 10% (3) (B); and 2-phenylethanol at 100 ppm (1), 2-phenylethanol with maltitol 10% (w/w) (2) and maltitol (3) (C).

Conclusion

HS-SPME-GC results show that the use of polyols causes a “salting-out effect” on 2-phenylethanol release. NMR DOSY results confirm that there is no chemical interaction between 2-phenylethanol and polyols. The diffusion coefficients were $7.33 \cdot 10^{-10}$ m²/s, $5.78 \cdot 10^{-10}$ m²/s, $6.44 \cdot 10^{-10}$ m²/s with erythritol, D-mannitol and maltitol, respectively. The mobility of 2-phenylethanol is not affected by the presence of polyol at low concentration (10%). Both methodologies (HS-SPME-GC and DOSY NMR) provide complementary information on flavour-food matrix interactions, which is critical for the selection of aroma compounds to formulate new soda beverages with polyols replacing sucrose. Other experiments will be conducted to understand how concentration and other volatile compounds are affected by the presence of polyols.

References

1. Rice T, Zannini E, Arendt E K, Coffey A. A review of polyols - biotechnological production, food applications, regulation, labeling and health effects. *Crit. Rev. Food Sci. and Nutr.* 2020;60(12):2034-2051.
2. Taylor A J. Release and transport of flavors in vivo: physicochemical, physiological, and perceptual considerations. *Comp. Rev. Food Sci. Food Saf.* 2002;1(2):45-57.
3. Guichard E. Interaction of aroma compounds with food matrices. In *Flavour Development, Analysis and Perception in Food and Beverages*, Woodhead Publishing Series in Food science, technology and nutrition. 2014; 273-295.
4. Savary G, Guichard E, Doublier JL, Cayot N, Moreau C. Influence of ingredients on the self-diffusion of aroma compounds in a model fruit preparation: an nuclear magnetic resonance-diffusion-ordered spectroscopy investigation. *J. Agric. Food Chem.* 2006;54(3):665-671.
5. Siefarth C, Tyapkova O, Beauchamp J, Schweiggert U, Buettner A, Bader S. Influence of polyols and bulking agents on flavour release from low-viscosity solutions. *Food Chem.* 2011;129(4):1462-1468.
6. Siefarth C, Tyapkova O, Beauchamp J, Schweiggert U, Buettner A, Bader S. Mixture design approach as a tool to study in vitro flavor release and viscosity interactions in sugar-free polyol and bulking agent solutions. *Food Res. Int.* 2011; 44(10):3202-3211.
7. Raithore S, Peterson D G. Delivery of Taste and aroma components in sugar-free chewing gum: mass balance analysis. *Chemosens. Percept.* 2016;9(4):182-192.
8. Raithore S, Peterson D G. Effects of polyol type and particle size on flavor release in chewing gum. *Food Chem.* 2018; 253(1):293-299.
9. Guichard E, Barba C, Thomas-Danguin T, Tromelin A. Multivariate statistical analysis and odor-taste network to reveal odor-taste Associations. *J. Agric. Food Chem.* 2020;68(38):10318-10328.
10. Fabre M, Aubry V, Guichard E. Comparison of different methods: static and dynamic headspace and solid-phase microextraction for the measurement of interactions between milk proteins and flavor compounds with an application to emulsions. *J. Agric. Food Chem.* 2002;50(6):1497-1501.
11. Jung DM, Ebeler E. Headspace solid-phase microextraction method for the study of the volatility of selected flavor compounds. *J. Agric. Food Chem.* 2003;51(1):200-205.

Characterisation of key aroma compounds in Burgundy truffle

ISABELLE ANDRIOT, Karine Gourrat, Rémy Reynaud, Sylvie Cordelle, Caroline Peltier, Olivier Berdeaux and Géraldine Lucchi

Centre des Sciences du Goût et de l'Alimentation (CSGA), ChemoSens Platform, AgroSup Dijon, CNRS, INRAE, University of Bourgogne Franche-Comté, Dijon, France, isabelle.andriot@inrae.fr

Abstract

Burgundy truffle plays an important role in the region's economic market. One of the objectives of this project is to better understand the origin and diversity of Burgundy truffle aromas.

Aroma compounds of Burgundy truffles were investigated with sensory evaluation (Quantitative Descriptive Analysis, QDA) and two physical-chemical methods:

- An analysis by Dynamic HeadSpace (DHS) coupled with Gas Chromatography - Mass Spectrometry (GC-MS) for volatile organic compounds (VOCs) identification,
- A new *in vitro* analytical method by Proton Transfer Reaction - Time of Flight - Mass Spectrometry (PTR-ToF-MS) to obtain an aroma mass fingerprint of all the samples.

With these different methods, we showed that aroma compounds of truffles are different according to varieties, harvests places and seasons.

Keywords: Burgundy truffles, sensory analysis, GC-MS, PTR-ToF-MS

Introduction

Truffles have an important economic value due to their gastronomic qualities appreciated in “grande cuisine”. While Périgord (*Tuber melanosporum*) and White Alba (*Tuber magnatum pico*) truffles are well-valued, Burgundy truffle (*Tuber uncinatum*) is not well-characterised in its production area.

INRAE is involved to help producers to better characterise these truffles through different research axes, especially the influence of ripeness and geographical origin on aromatic composition [1]. For this purpose, we had first to define an analytical strategy to better characterise aroma compounds in this noble fungus, and secondly, to compare aroma truffles from Burgundy and Lot regions respectively.

Experimental

Truffles

Twenty-eight truffles were analysed in this study. Burgundy truffles were harvested by truffle farmers in different places in Burgundy, but also in Lot to study aroma compounds from 2 varieties (Burgundy, *Tuber uncinatum* and Lot, *Tuber aestivum*) (Table 1).

Table 1: Characteristics of analysed truffles.

Truffles numbers	Harvest dates	Harvest places
221 to 227 (7 truffles)	5 th June (Summer)	Lot
228 to 234 (7 truffles)	23 th June (Summer)	Burgundy, Vaubarden
238 to 244 (7 truffles)	5 th October (Autumn)	Burgundy, Vaubarden
245, 246, 249, 250 (4 truffles)	22 th November (Autumn)	Burgundy, Daix
247, 248, 251 (3 truffles)	22 th November (Autumn)	Burgundy, Bonniere

Aroma compounds analyses were realised on fresh truffles. After deliveries, truffles were cleaned, diced, frozen quickly with liquid nitrogen and finally grinded (grinding AICOK, model CG9100). Diced truffles (0.5 g) were transferred in amber vials for sensory analysis, while grinded truffles (1 g) were placed in 20 mL vials for GC-MS analysis. Twenty-five mg of grinded truffles were also used for PTR-ToF-MS analysis. Physical-chemical analyses were performed in triplicate.

Sensory analysis

Sixteen panellists were trained during 8 sessions to recognise odour descriptors established by experts' panel. Fresh truffles were evaluated only by olfaction, during different periods (June to November). A classical descriptive profile (QDA) was made, using a continuous linear scale (noted weak to strong). The evaluated

descriptors were: button mushroom, cep, chanterelle (girolle) mushroom, undergrowth, earthy, mouldy, nut, alcohol-pharmaceutical, spicy, smoked, animal, pungent, pepper, fruity, vanilla, bread.

PTR-ToF-MS analysis

All the experiments were conducted with a PTR-ToF-MS instrument (PTR-ToF 8000, Ionicon Analytik GmbH, Innsbruck, Austria) with H_3O^+ as reagent ion in funnel mode. The drift-tube parameters were fixed as follows: $P_{\text{drift}} 2.3 \text{ mbar}$, $T_{\text{drift}} 80^\circ\text{C}$, $U_{\text{drift}} 390 \text{ V}$ resulting in an E/N value of 92 Td ($1 \text{ Td} = 10^{-17} \text{ V}\cdot\text{cm}^2$). Mass spectra were acquired at a scan speed of 0.5 s for the mass range m/z 1-227.

Truffle vials were equilibrated at 36°C during 2 hours. The setup (Figure 1) was adapted from [2]. The truffles were rich in aroma compounds and induced a depletion of reactant ions. Hence, truffle headspace was diluted with pure air prior to be analysed with the PTR-ToF-MS.

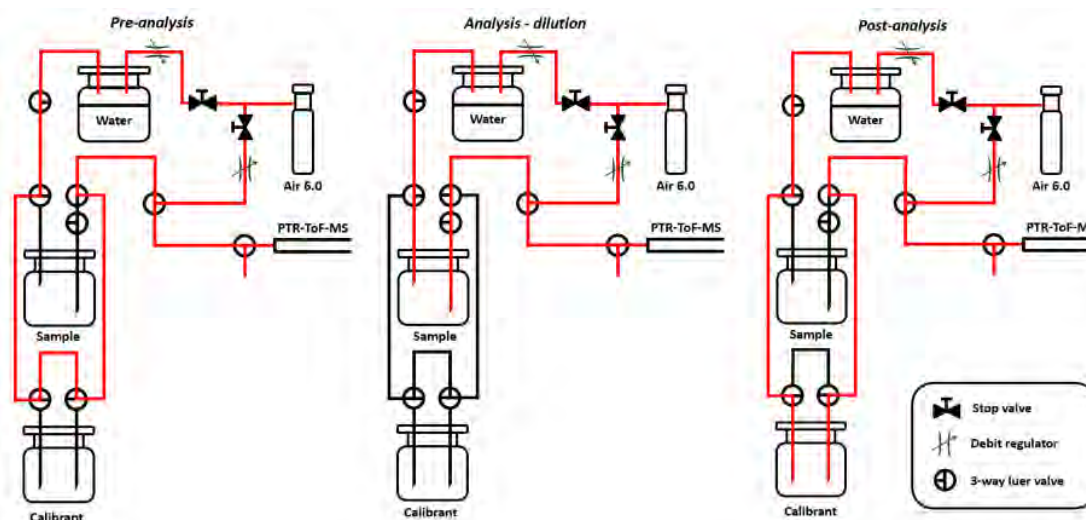


Figure 1: Experimental setup connected to the transfer line of the PTR-ToF-MS instrument.

GC-MS analysis

GC-MS analyses were conducted with only 14 truffles (7 Burgundy truffles, June and 7 Burgundy truffles, November) for practical reasons (low quantity available). Dynamic HeadSpace analyses (Table 2) were carried out with an automatic autosampler (Gerstel, MPS 2; Gerstel Inc., Mülheim an der Ruhr, Germany) coupled with a Gas Chromatography-Mass Spectrometer (7890A-8975c TAD Agilent Technologies, Inc., Palo Alto, CA, U.S.A). Aroma compounds released in the vapour phase were trapped on Tenax tube for DHS analyses. The aroma compounds were separated with a column DB-HeavyWax (30m, 0.25mm, 0.5 μm , Agilent) with helium as carrier gas (velocity of 40 $\text{cm}\cdot\text{s}^{-1}$). The identification of aroma compounds was validated thanks to retention index (RI) and electron ionisation (EI) mass spectrum. RI values were calculated using the Van den Dool and Kratz formula [3] from retention times of n-alkanes (C_{10} - C_{30}) on the same column, then compared with RIs from the literature and the following databases (NIST, INRAMass home database and Wiley11N17).

Table 2: DHS parameters.

	DHS
Incubation	36°C , 15 min
Extraction / Trapping	20°C , 675 mL, 45 mL/min
Drying	20°C , 1500 mL, 100 mL/min
Thermal desorption	30°C , $100^\circ\text{C}/\text{min}$, 270°C during 5 min
Injection	CIS, -100°C , $12^\circ\text{C}/\text{s}$, 280°C during 5 min

Results and discussion

Sensory analysis

A canonical variable analysis (Figure 2) and a hierarchical classification (Figure 3) on QDA data showed sensory differences between truffles. Burgundy truffles (summer) were weakly odorant, Lot truffles were characterised by forest odours (mushroom, undergrowth, earthy) and sweet odours (fruity, bread, vanilla, nut) whereas Burgundy truffles (autumn) were characterised by negative odours (animal, mouldy, undergrowth, earthy) and spicy odours (alcohol, smoked, spicy, animal).

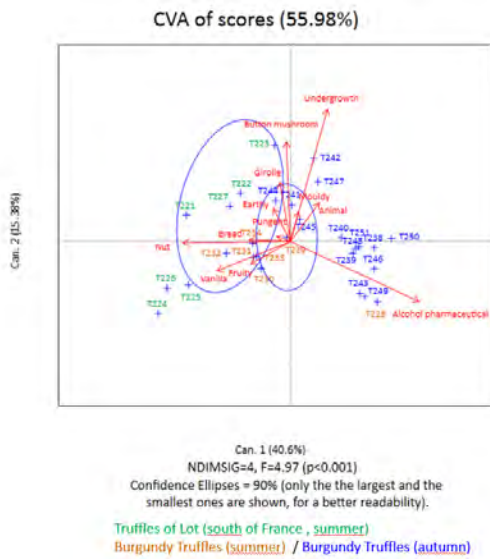


Figure 2: Canonical variables analysis of truffles (QDA).

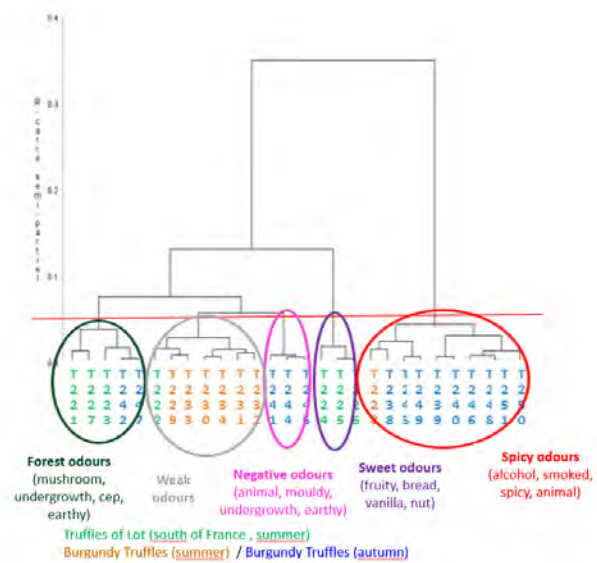


Figure 3: Hierarchical classification analysis of truffles (QDA data).

PTR-ToF-MS analysis

A principal component analysis (Figure 4) on intensities and a hierarchical clustering (Figure 5) showed that truffles were separated according to places and seasons [1, 4, 5]. However, analyses of frozen mix truffles as a control showed a sample dispersion according to time from June to November (data not shown). We consequently suspected truffle conservation problems and/or an instrumental bias, and considered these results very cautiously.

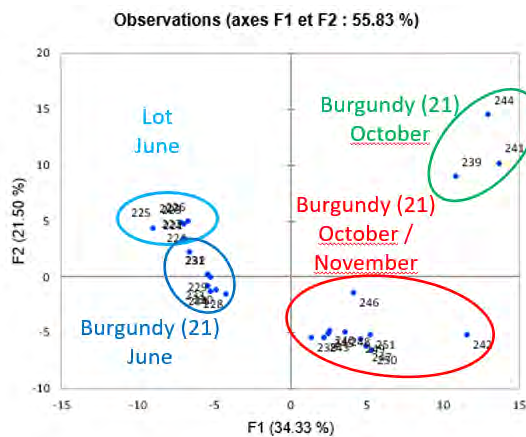


Figure 4: PCA (PTR-MS intensities) of truffles from different harvests and places.

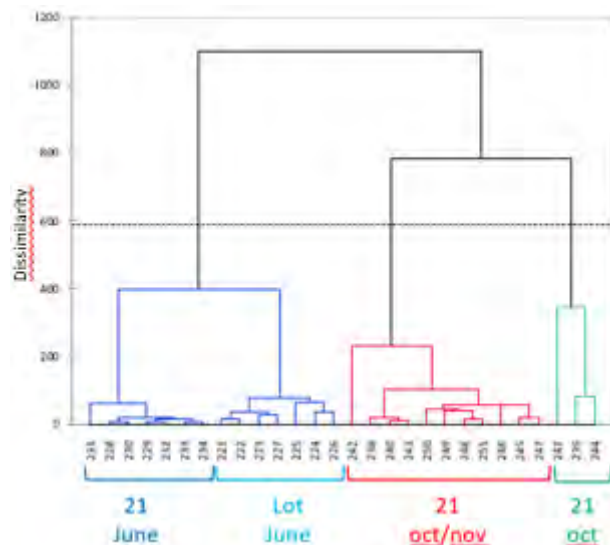


Figure 5: Dendrogram of truffles (the same truffles as PCA-Figure 4).

GC-MS analysis

Results obtained by GC-MS confirmed the results obtained by PTR-ToF-MS and sensory analyses. Truffles were separated according to harvest places and seasons (Figure 6). Unfortunately, Lot truffles could not be analysed by GC-MS due to an insufficient sampling.

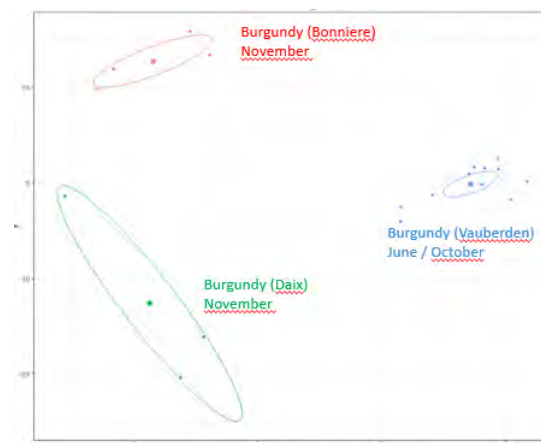


Figure 6: PCA of truffles from different places in Burgundy (GC-MS data; same truffles analysed by sensory analyses and PTR-ToF-MS analyses).

GC-MS peak areas were calculated for each ion in the total ion chromatogram (TIC), for each sample, then ions of interest were highlighted, by considering a fold change higher than 3 and a p -value $< 10^{-5}$. These results are presented in Table 3.

Table 3: Compounds over-expressed, and corresponding truffles.

Over-expressed compounds	Truffles
Butan-2-one	Burgundy (Bonnieres and Daix) / November
Butan-2-ol	Burgundy (Bonnieres and Daix) / November
Pentane-2,3-dione	Burgundy (Bonnieres and Daix) / November
3-hydroxypentan-2-one	Burgundy (Bonnieres and Daix) / November
2-hydroxypentan-3-one	Burgundy (Bonnieres and Daix) / November
4-hydroxyhexan-3-one	Burgundy (Vauberden) / June

Pentane-2,3-dione and butan-2-one were characteristic of truffle freshness [6]. The same results were found with the PTR-ToF-MS for the truffles harvested in October and November. The odour description of butan-2-ol is alcohol. This compound was over-expressed in GC-MS analyses of truffles from Bonnieres and Daix. These truffles were also described by the descriptor alcohol in sensory analysis.

Conclusion

Sensory analyses, PTR-ToF-MS and GC-MS succeeded in differentiating truffles according to harvest places and seasons. Burgundy truffles harvested in summer were less odorant than Burgundy truffles harvested in autumn. These results will be combined to microbiota data and genetic analyses and will bring a scientific contribution to the creation of an IGP (Indication Géographique Protégée) request.

This study is part of the research project BIJOU, supported by FEADER and Bourgogne Franche-Comté Region.

References

- Vita F, Taiti C, Pompeiano A, Bazihizina N, Lucarotti V, Mancuso S, et al. Volatile organic compounds in truffle (*Tuber magnatum Pico*): comparison of samples from different regions of Italy and from different seasons. *Sci Rep.* 2015;5:12629.
- Deuscher Z, Andriot I, Semon E, Repoux M, Preys S, Roger JM, et al. Volatile compounds profiling by using proton transfer reaction-time of flight-mass spectrometry (PTR-ToF-MS). The case study of dark chocolates organoleptic differences. *J Mass Spectrom.* 2019;54(1):92-119.
- van Den Dool H, Dec. Kratz P. A generalization of the retention index system including linear temperature programmed gas-liquid partition chromatography. *J Chromatogr A.* 1963;11(C):463-71.
- Gioacchini AM, Menotta M, Bertini L, Rossi I, Zeppa S, Zambonelli A, et al. Solid-phase microextraction gas chromatography/mass spectrometry: A new method for species identification of truffles. *Rapid Commun Mass Spectrom.* 2005;19(17):2365-70.
- March RE, Richards DS, Ryan RW. Volatile compounds from six species of truffle - head-space analysis and vapor analysis at high mass resolution. *Int J Mass Spectrom.* 2006;249:60-7.
- Vahdatzadeh M, Deveau A, Splivallo R. Are bacteria responsible for aroma deterioration upon storage of the black truffle *Tuber aestivum*: A microbiome and volatilome study. *Food Microbiol.* 2019;84:103251.

Developing methods for characterising flavour compounds in distilled spirits: Application to gin, rum and whisky

QUENTIN BARNES^{1,2}, Marie-Anne Contamin², Nicolas Papaiconomou¹ and Xavier Fernandez¹

¹ ICN, UMR Université Côte d'Azur - CNRS 7272, Nice, France, quentin.barnes@univ-cotedazur.fr

² Comte de Grasse, Grasse, France

Abstract

In order to develop an analytical technique to study aroma compounds applicable to all kinds of liquors, a model mixture embodying a theoretical distilled spirit was developed. This solution contains 25 of the most frequent flavour compounds found in these alcoholic drinks, classified in 15 chemical classes, at their mean concentrations. Liquid-liquid extraction (LLE), solid phase extraction (SPE), solid phase microextraction (SPME) and stir bar sorptive extraction/headspace sorptive extraction (SBSE/HSSE) were tested on the model mixture before analysis by gas chromatography-mass spectrometry/flame ionisation detection (GC-MS/FID). HS-SPME appeared to be the best compromise between efficiency, time and ease of use. The HS-SPME method optimised to the model mixture was successfully applied to 3 commercial samples.

Keywords: distilled spirit, analytical technique, model mixture, extraction, flavour compound

Introduction

The number and the popularity of craft distilleries has considerably increased over the last decade, resulting in a surge of innovative production processes offering new aromas and flavours for distilled spirits [1]. In order to characterise trials as part of research and development studies and to ensure batch-to-batch reproducibility through quality control processes, efficient, reliable, and fast analytical methods are needed.

Comte de Grasse is a company producing premium distilled spirits inspired by the extraction techniques used in perfumery. They intend to develop innovative and sustainable processes for the fermentation, distillation and ageing of liquors. With the aim of describing the flavour profile of their alcoholic drinks, analytical techniques applicable to all kinds of spirits are required.

Gas chromatography is the most frequently used method for the analysis of distilled spirits because it enables the identification of a large number of analytes and can be coupled to various detectors [2]. Some of the substances found in alcoholic beverages present at very low levels contribute significantly to the aroma profile of the beverage. When a classic chromatographic system is used (GC-FID or single quadrupole GC-MS), a concentration of the volatile fraction prior to analysis is necessary for their detection [3]. Thus, the selection and the optimization of an appropriate extraction method is critical.

To that end, a model mixture embodying a theoretical distilled spirit was developed. The model mixture was therefore submitted to 4 extraction techniques frequently described in literature for the concentration of flavour compounds in distilled spirits: liquid-liquid extraction (LLE), solid phase extraction (SPE), solid phase microextraction (SPME) and stir bar sorptive extraction/headspace sorptive extraction (SBSE/HSSE).

Experimental

Commercial samples of distilled spirits and chemicals

The rum (Diplomático Selección de Familia) and whisky (Glenfiddich 14 year bourbon barrel reserve) were bought at a local store. The gin sample (Comte de Grasse 44°N) was provided by Comte de Grasse. The compounds used to make the model mixture were obtained from commercial sources. Dichloromethane and acetonitrile (Merck) were freshly distilled prior to use. Ethanol (96% purity) was obtained from Isnard (Grasse, France).

Liquid-liquid extraction

The model mixture (50 mL) was mixed with deionised water (150 mL) and NaCl (20 g). Dichloromethane was added and it was put under stirring (500 rpm) for 10 min. at room temperature (3 x 60 mL). The organic phases were gathered, dried on MgSO₄, filtrated with a Büchner funnel and evaporated to 500 µL with a Kuderna-Danish concentrator. The extract was filtrated on a 0.22 µm syringe filter and stored at -18°C before analysis. Each trial was carried out in triplicate.

Solid phase extraction

The model mixture (12,5 mL) was mixed with deionised water (37,5 mL) and percolated through a Lichrolut EN 500 mg SPE cartridge (Merck) after conditioning with acetonitrile and equilibrating with an ethanol/water 9:1 (v/v) solution. Compounds of interest were eluted with dichloromethane (2 x 4 mL) which was evaporated to 500 μ L with a Kuderna-Danish concentrator.

Solid phase microextraction

Fibres and a manual SPME device were obtained from Supelco Co. (Bellefonte, PA). Fibres tested for extraction of the volatile components were as follows: poly(dimethylsiloxane) (PDMS) 100 μ m, carboxen/PDMS (CAR/PDMS) 85 μ m and divinylbenzene/CAR/PDMS (DVB/CAR/PDMS) 50/30 μ m. Before use, fibres were conditioned as recommended by the manufacturer. If necessary, the model mixture was diluted with deionised water to reduce the EtOH content. When needed, 1.3 g NaCl were added. 13 mL of a sample was then placed in a 40 mL amber vial closed by a PTFE/silicone septum (Supelco). Before extraction, the vial headspace was let to reach equilibrium for 24h at 25°C and 300 rpm. When extraction was not carried out at 25 °C, a water bath was used to control the temperature and the sample was conditioned during 5 minutes before extraction. Each analysis was carried out in triplicate. After exposure, the fibre was thermally desorbed into a GC and left in the injection port (equipped with a 0.75 mm i.d. inlet liner) for 5 min. The injector was set at the temperature recommended by the manufacturer and operated in splitless mode for 5 min.

Stir bar sorptive extraction / headspace sorptive extraction

Extractions were carried out with PDMS commercial stir bars (10mm length \times 0.5mm film thickness), supplied by Gerstel (Mülheim a/d Ruhr, Germany) as follows: a volume of 3.25 mL of sample and 9.25 mL of deionised water were placed in a 40 mL amber vial. The stir bar was then added to the flask or placed in the headspace. The vial was closed by a PTFE/silicone septum. The PDMS stir bar (or a standard stir bar for HSSE) was stirred at 800 rpm at 25°C for 60 min. After removal from the sample, PDMS stir bar was washed for a few seconds in distilled water and gently dried with a lint-free tissue. It was then transferred into a thermal desorption tube for thermal desorption. Before each extraction, the stir bar was conditioned at 300°C for 60 min.

Apparatus

LLE, SPE and SPME: These analyses were carried out using a 7820A/5977B GC-MS/FID (Agilent, Little Falls, DE, USA) equipped with an HP-5ms capillary column (30 m \times 0.25 mm \times 0.25 μ m, Agilent). The temperature program was as follows: 40°C for 4 min, 40 to 220 °C at 2°C/min, 220 to 270°C at 8°C/min, holding for 7.25 min. The detection by the mass spectrometer was performed in the electron ionisation (EI) mode (70 eV ionisation energy). The acquisition was performed in scanning mode (mass range m/z 35–350 u). Identification of the aroma compounds was achieved by comparing the retention indices (RI) and mass fragmented patterns with those of reference compounds or with mass spectrums in commercial and homemade libraries and previously reported RI in the literature. Some of the identifications were confirmed by the injection of the chemical standards. Linear retention indices of the compounds were calculated using an n-alkane series.

SBSE/HSSE: The coated stir bars were thermally desorbed using an ATD-350 thermodesorption system (Perkin Elmer, Waltham, MA, USA) at 250°C for 15 min under a helium flow (50 mL min⁻¹) and the desorbed analytes were focused on a trap at -35°C. Finally, the trap was programmed from -35°C to 300°C (held for 3 min) at 20°C s⁻¹ for analysis by GC-MS. Capillary GC-MS analyses mode were performed using an Clarus 680 - SQ 8T system (Perkin Elmer), equipped with an Elite-5ms capillary column (30 m \times 0.25 mm \times 0.25 μ m, Perkin). The temperature program was as follows: 40 to 220 °C at 2°C/min, 220 to 270°C at 8°C/min, holding for 6.25 min. The detection by the mass spectrometer was performed in the electron ionisation (EI) mode (70 eV ionisation energy). The acquisition was performed in scanning mode (mass range m/z 35–350 u). Identification of the aroma compounds was achieved by comparing mass fragmented patterns with mass spectrums in commercial and homemade libraries.

Results and discussion

Model mixture

A literature study led to the identification of 15 chemical classes usually found in liquors. For each class, at least one of the most recurrent compounds was chosen and put in the mixture at its mean concentrations in distilled spirits. Additional compounds were added in order to study the influence of the chemical structure on the extraction (chain length, aromaticity, presence of a cycle). An important ratio (x20000) was noticed between the extreme concentration values (sotolon – 0.00093 mg L⁻¹, furfural – 18.2 mg L⁻¹).

Table 1: Composition of the model mixture.

Compound	Concentration (mg/L)	Mean odour threshold in water (mg/L)*
hexanal	0.132	0.0501
furfural	18.2	9.602
o-xylene	0.313	0.45
α -pinene	4.02	0.296
benzaldehyde	7.98	1.72
dimethyl trisulfide	0.0595	0.00003
2-octanone	0.261	0.0418
ethyl hexanoate	17.4	0.00186
trimethylpyrazine	0.154	0.216
hexanoic acid	1.39	4.145
1,1,3-triethoxypropane	0.103	3.70 ^a
linalool	5.28	0.0108
2-phenylethanol	7.31	1.331
sotolon	0.000938	0.00565
diethyl succinate	3.78	353 ^a
2-phenylethyl acetate	0.457	0.249
decanol	0.114	0.047
<i>cis</i> -whiskey lactone	0.69	0.035 ^b
<i>trans</i> -whiskey lactone	0.31	0.05 ^c
decanoic acid	5.56	5.464
(E)- β -damascenone	0.0469	0.00125
ethyl decanoate	7.45	1.299
vanillin	2.86	0.301
β -caryophyllene	0.679	0.461
<i>cis</i> -nerolidol	0.0387	0.1

*from van Gemert, L.J. et al (2011)

Extraction technique comparison

A pre-optimisation study identified dichloromethane as the most efficient solvent for LLE (with NaCl addition), and ethylvinylbenzene-divinylbenzene copolymer as the most suitable sorbent for SPE. Among the four tested extraction techniques, LLE gave the best results as it enabled to detect 23 out of the 25 compounds in the mixture. Two compounds were not detected because of either a low concentration (sotolon – 0.000938 mg/L) or a poor response with apolar columns (hexanoic acid). This technique is however significantly time, solvent and sample consuming. The efficiency of SPE in terms of compounds detected was lower than that of LLE. SBSE and HSSE gave slightly better results (22 compounds detected) than SPME (21 compounds detected), which could be explained by the fact that stir bars have a larger coating volume than SPME fibres. However, SPME can be fully automated while the stir bar extractions have to be carried out manually [4]. SPME was thus chosen as the preferred method of extraction and was further optimised.

Table 2: Results obtained by applying different extraction techniques to the model mixture.

Extraction technique	Detected compounds (/25)	Handling time	Sample amount	Solvent amount
LLE	23	3 h	50 mL	200 mL
SPE	17	1 h	13 mL	10 mL
SPME	21	0.2 h	3 mL	-
SBSE	22	0.2 h	3 mL	-
HSSE	22			

SPME condition optimisation

DVB/CAR/PDMS in headspace mode was more efficient than CAR/PDMS (headspace) and PDMS (headspace and immersion) fibre types. Reducing the ethanol strength from 40 to 10% volume increased the number of compounds detected, a result in agreement with previous reports [5]. The addition of sodium chloride led to better results, which could be explained by the salting-out effect. Optimal time and temperature conditions were determined by studying specifically the peak area of furfural, α -pinene, (E)- β -damascenone and β -caryophyllene, four compounds of the model mixture covering a fairly wide range of polarities and volatilities. A kinetic monitoring showed that at least 1 hour extraction was necessary to get a satisfactory signal to noise ratio for (E)- β -damascenone, and to reach equilibrium for α -pinene and furfural. Varying the temperature between room

temperature and 45 °C revealed that except for (E)- β -damascenone, all peak areas were highest at a temperature of 30 °C. Because the largest peak area for (E)- β -damascenone was found to be slightly higher at 45 °C than at 30 °C, the optimum value for the temperature was set to 35°C.

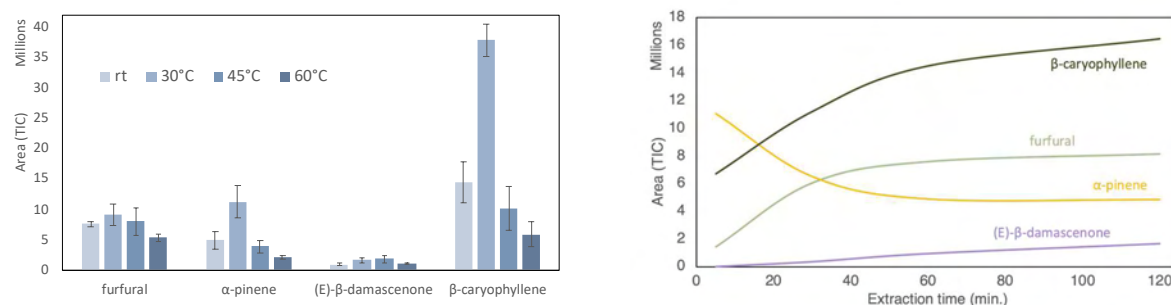


Figure 1: SPME time and temperature optimisation.

Analysis of gin, rum and whisky samples by HS-SPME-GC-FID/MS

The optimised SPME method was then applied to 3 commercial samples which were analysed with a GC-MS/FID. Most compounds identified in the gin sample were terpenes, which utterly reflects the production process as this product was obtained by maceration and distillation of 13 botanicals in a water/ethanol mixture. The analysis of the rum and whisky samples enabled to identify 32 and 43 esters respectively which are quality markers in distilled spirits [6]. On the other hand, a higher number of phenols and furans was somehow expected as these 2 spirits have been oak-aged for several years, but this could be solved by the use of a polar column.

Table 3: Number of volatile compounds by chemical class identified in 3 commercial liquors analysed by HS-SPME-GC-MS/FID.

Chemical classes	44*N gin	Diplomatico rum	Glenfiddich whisky
alcohols	0	5	9
esters	10	32	43
lactones	0	1	2
carbonyls	3	4	7
acetals	1	2	2
acids	1	0	2
phenols	1	3	0
furans	1	1	2
aromatics	4	2	4
monoterpenes	19	1	1
oxygenated monoterpenes	26	1	0
sesquiterpenes	30	1	0
oxygenated sesquiterpenes	17	1	1
others	9	7	1
Total	122	61	74

Conclusion

The use of a model mixture allowed for the development of an analytical method applicable to three different kinds of distilled spirits. It enabled the comparison of four extraction techniques and the optimisation of SPME conditions which were successfully applied to commercial samples. Dynamic headspace method (Purge and Trap) will soon be developed and compared to the other four concentration methods.

References

1. Panda, S.K. et al. Innovations in Technologies for Fermented Food and Beverage Industries. 2018;1:7.
2. Wiśniewska, P. et al. Application of Gas Chromatography to Analysis of Spirit-Based Alcoholic Beverages. Crit Rev Anal Chem. 2015;45:3:201-225.
3. Buglass, A.J. Handbook of Alcoholic Beverages: Technical, Analytical and Nutritional Aspects. 2011;4(2):648.
4. Ebeler, S.E. Analysis of brandy aroma by solid-phase microextraction and liquid-liquid extraction. J Sci Food Agric. 2000;80:625-630.
5. Padilla-Sanchez, J.A. et al. Applications and Strategies Based on Gas Chromatography– Low-Resolution Mass Spectrometry (GC–LRMS) for the Determination of Residues and Organic Contaminants in Environmental Samples. Compr Anal Chem. 2013;8:187.
6. Spaho, N. Distillation: Innovative Applications and Modeling. 2017;6:142.

Impact of non-volatile compounds on volatiles perception: How proanthocyanidic tannins affect red wine fruity aroma?

MARGAUX CAMELEYRE, Georgia Lytra and Jean-Christophe Barbe

¹Unité de recherche Œnologie, EA 4577, USC 1366 INRAE, ISVV, Université de Bordeaux, F33882 Villenave d'Ornon France

margaux.cameleyre@wanadoo.fr

Abstract

Previous research on the fruity character of red wines highlighted that the perception of a “fruity pool” of esters was modified by the presence of fruity or non-fruity compounds with synergistic and/or masking effects. Moreover, some works described that non-volatile compounds may have an important impact on wine perception, but also on odorant compounds volatility. The goal of this work was to assess the olfactory consequences of a mixture between esters and proanthocyanidic tannins, through sensory and physico-chemical approaches.

Sensory analyses including triangle tests, detection thresholds, and sensory profiles, were conducted in order to evaluate the sensory impact of pure tannins on red wines “fruity pool” perception. Then, the impact of these non-volatile molecules on esters volatility, and thus taster stimulation, was evaluated thanks to the determination of partition coefficients.

Triangular test revealed a significant difference on global perception between the fruity pool containing esters and the same fruity pool in mixture with proanthocyanidic tannins. Sensory profiles evaluation showed fruity notes perception were significantly lower for the fruity pool supplemented with tannins compared to the fruity pool alone in dilute alcohol solution. These results confirmed the sensory importance of some non-volatile compounds on odour perception. Finally, esters partition coefficient evaluation revealed a decrease of the volatility of esters when tannins were present in the matrix, thus corroborating sensory evaluation results.

Proanthocyanidic tannins decrease esters volatility when they are added in the matrix, thus reducing orthonasal taster stimulation and consequently reducing red wine fruity notes perception. Such a study should be extended to other wine tannins and anthocyanins, including their concentration ranges, to assess the impact of the phenolic matrix on red wines aroma perception.

Keywords: red wine, fruity aroma, non-volatile matrix, perceptive interaction

Introduction

Wine is a very complex aromatic matrix, composed of more than a thousand volatile compounds. This diversity of chemical families gives wine its tremendous aromatic complexity [1]. In red wines, Pineau et al. (2009) showed that at least part of the fruity aroma of red wines resulted from perceptive interactions between several aromatic compounds, particularly ethyl esters and acetates, even if they were present at concentrations below their olfactory thresholds [2]. Thus, these authors identified a 13-ester fruity pool that characterized Bordeaux red wine aromas. Many other examples of perceptive interactions have been highlighted, with synergistic or masking effects on the fruity aromatic expression of wines [3, 4].

The perception of volatiles during sensory analysis is strongly related to the distribution of aromas between the matrix and the gas phase, and may be related to perception during food consumption; thus, the composition of the matrix may considerably influence the rate of release to the gas phase [5, 6]. Various studies have shown the impact of wine compounds on global perception. However, to date, no study has elucidated the role of polyphenols in the fruity perception of red wines, nor in the fruity compounds released from the matrix to the gas phase.

Describing the perception mechanism, Berglund et al. (1976) suggested that perceptive interactions occur at four different levels [7]. The first is described as pre-sensory interactions, such as chemical or physicochemical interactions in the gas phase or in the nasal pathway and mucosa. The three others refer to interactions in the peripheral and central nervous system, at the receptor surface or in the olfactory bulb. A recent work using an analytical approach and partition coefficient calculation highlighted that pre-sensory modification may explain, at least partly, the masking effect of higher alcohols on fruity perception [5].

In this global context, the aim of this work was to provide a global overview on the impact of proanthocyanidic tannins on the aroma of a 13-ester mixture representative of Bordeaux red wines fruity aroma. The sensory consequences of the mixture were studied as well as the presence of tannins on ester volatility, which was measured by calculating their partition coefficients, thus allowing us to evaluate the involvement of pre-sensory changes.

Experimental

Matrices and aromatic reconstitutions

The tannins were added at 5 g/L into a dilute alcohol solution (12% vol. (v/v)) and then evaporated using a Rotavapor to 1/3 of the initial volume (Laborota 4010 digital Rotary Evaporator, Heidolph, Germany) with a 20°C bath temperature. The liquid was then mixed with ethanol and microfiltered water to reproduce the alcohol concentration and volume of the original solution. Then, 5 g/L of tartaric acid were added and pH was adjusted to 3.5 with sodium hydroxide. The solution was then supplemented with 5 g/L LiChrolut EN resin (40–120 µm), stirred for 12h to eliminate all traces of volatile compounds, and filtered twice. The resulting solution, called tannin solution (TS) did not contain any trace of volatile compounds.

Dilute alcohol solution (DAS) was prepared with ethanol and microfiltered water to obtain an ethanol level of 12% vol. (v/v) and 5 g/L of tartaric acid (pH adjusted to 3.5 with sodium hydroxide).

The fruity aromatic reconstitution (FAR) was prepared in DAS or TS, with esters added at the average concentrations found in red wines (Table 1).

Table 1: Ethyl ester and acetate concentrations (µg/L) used.

C ₃ C ₂	C ₄ C ₂	C ₆ C ₂	C ₈ C ₂	2MeC ₃ C ₂	(2S)-2MeC ₄ C ₂	(2S)- and (2R)- 2OH4MeC ₅ C ₂ (95/5, m/m)	C ₂ C ₄	C ₂ C ₆	C ₂ iC ₄	C ₂ iC ₅	3OHC ₄ C ₂	3MeC ₄ C ₂
150	200	200	200	250	50	400	10	2	50	250	300	50

C₃C₂, ethyl propanoate; C₄C₂, ethyl butanoate; C₆C₂, ethyl hexanoate; C₈C₂, ethyl octanoate; 2MeC₃C₂, ethyl 2-methylpropanoate; (2S)-2MeC₄C₂, (S)-ethyl ethyl (2S)-2-methylbutanoate; (2S)- and (2R)-2OH4MeC₅C₂, ethyl (2S)- and (2R)-2-hydroxy-4-methylpentanoate; C₂C₄, butyl acetate; C₂C₆, hexyl acetate; C₂iC₄, 2-methylpropyl acetate; C₂iC₅, 3-methylbutyl acetate; 3OHC₄C₂, ethyl 3-hydroxybutanoate; 3MeC₄C₂, ethyl 3-methylbutanoate.

Sensory analysis

The panel consisted of 38 judges, 15 males and 23 females aged 25.5 ± 8.6 (mean ± SD) years. All panellists were research laboratory staff at ISVV, Bordeaux University, selected for their experience.

First, triangle test was performed by comparing the perception of FAR in DAS or in TS.

Next, sensory profiles using continuous line scale were carried out. Various reconstitutions were presented to the panel to evaluate sensory profiles for overall aroma, fresh- and jammy-fruit, red- and black-berry-fruit notes. FAR in DAS at the concentrations indicated in Table S1 was compared to FAR in TS. Each sample was assessed in duplicate.

Partition coefficient calculation

The chromatographic conditions for the partition coefficient calculation were developed by Cameleyre et al. [5]. The partition coefficients were evaluated using static headspace coupled to low-pressure GC-MS (SHS-LP-GC/MS) under equilibrium conditions at 20°C.

Results and discussion

A set of triangle tests was performed by the panel, evaluating FAR in DAS or in TS at concentrations indicated in Table 1.

The presence of tannins induced a change in the perception of the FAR ($p = 0.013$), revealing that even though they had no odour, proanthocyanidic tannins modified the overall perception of the FAR.

Next, sensory profile was realised. As presented in Figure 1, adding FAR into TS led to significant changes in the perception of various descriptors, compared to FAR in DAS. The presence of tannins at 5 g/L in the matrix led to an attenuation of the perception of overall aroma ($p < 0.05$), red-berry- and fresh-fruit ($p < 0.01$). These results were in agreement with those observed in the triangle tests, with a significant difference between the perception of FAR in DAS and in TS.

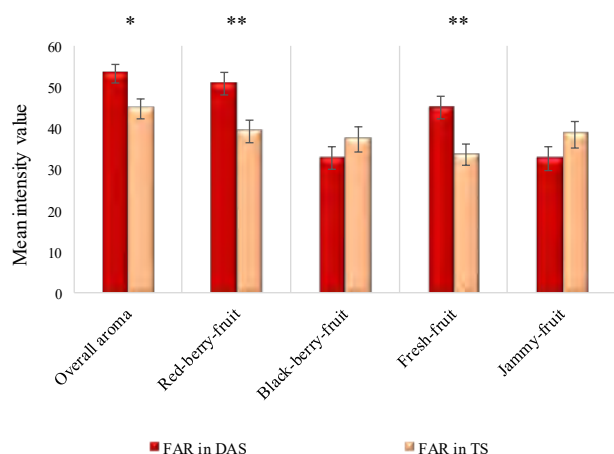


Figure 1: Aromatic impact of the matrix (dilute alcohol solution coloured or tannin solution) on the fruity aromatic reconstitution perception. *, $p < 0.05$; **, $p < 0.001$; FAR, Fruity Aromatic Reconstitution; DAS, dilute alcohol solution; TS, tannin solution. Error bars indicate standard error deviation.

In order to evaluate whether ester release between the matrix and the headspace was affected by the presence of tannins, partition coefficients were determined for nine esters in DAS and in TS, as shown in Figure 2. A significant difference in partition coefficient was observed for seven of the nine esters tested ($p < 0.05$). The presence of proanthocyanidic tannins did not affect the partition coefficient of higher alcohol acetates (2-methylpropyl acetate and 3-methylbutyl acetate, $p > 0.05$). For the other molecules, the partition coefficient was higher in DAS than in TS, revealing that the esters were more volatilised from the matrix in DAS than in TS.

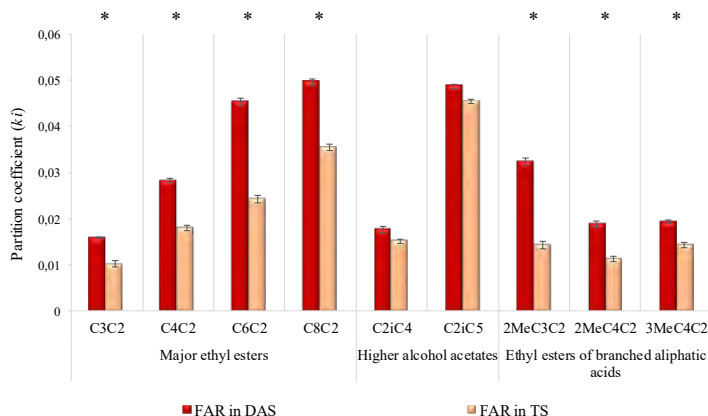


Figure 2: Impact of the matrix (dilute alcohol solution coloured or tannin solution) on the partition coefficients of ethyl esters and acetates. *, $p < 0.05$; Error bars indicate standard deviation. FAR, Fruity Aromatic Reconstitution; DASc, dilute alcohol solution coloured; TS, tannin solution; k_i , partition coefficient between gas and liquid phase; C3C2, Ethyl propanoate; C4C2, Ethyl butanoate; C6C2, Ethyl hexanoate; C8C2, Ethyl octanoate; 2MeC3C2, Ethyl 2-methylpropanoate; 2MeC4C2, Ethyl 2-methylbutanoate; C2iC4, 2-methylpropyl acetate; C2iC5, 3-methylbutyl acetate; 3MeC4C2, Ethyl 3-methylbutanoate.

Our results may be correlated with those obtained with sensory analysis approaches. If fewer esters are present in the TS headspace, it is highly probable that fewer esters are able to reach the nasal cavities of the taster when he smells, and this may explain the masking effect of fruity aromas observed when proanthocyanidic tannins were present in the matrix. This fact highlights that proanthocyanidic tannins lead to perceptual modification via pre-sensory changes.

Conclusion

The impact of commercial proanthocyanidic tannins on fruity pool of esters, representing the fruitiness of Bordeaux red wines, was assessed in model solutions. It was shown that the presence of tannins in the matrix significantly attenuated perception of fruity notes. Physico-chemical analysis demonstrated that the presence of proanthocyanidic tannins in dilute alcohol solution resulted in a decrease in ester partition coefficients and thus in a decrease in ester contents in the headspace. This fact highlighted pre-sensory changes.

References

1. Etievant, P. X. Wine. In *Volatile Compounds of Food and Beverages*; H. Maarse: New-York, 1991; pp 483–546.
2. Pineau, B.; Barbe, J. C.; Leeuwen, C. V.; Dubourdieu, D. Examples of Perceptive Interactions Involved in Specific “Red-” and “Black-Berry” Aromas in Red Wines. *J Agric Food Chem.* 2009;57(9):3702–3708.
3. Lytra, G.; Tempere, S.; Zhang, S.; Marchand, S.; De Revel, G.; Barbe, J.-C. Olfactory Impact of Dimethyl Sulfide on Red Wine Fruity Esters Aroma Expression in Model Solution. *J Int Sci Vigne Vin.* 2014;48:75–85.
4. Cameleyre, M.; Lytra, G.; Tempere, S.; Barbe, J.-C. Olfactory Impact of Higher Alcohols on Red Wine Fruity Ester Aroma Expression in Model Solution. *J Agric Food Chem.* 2015;63(44):9777–9788.
5. Cameleyre, M.; Lytra, G.; Barbe, J.-C. Static Headspace Analysis Using Low-Pressure Gas Chromatography and Mass Spectrometry, Application to Determining Multiple Partition Coefficients: A Practical Tool for Understanding Red Wine Fruity Volatile Perception and the Sensory Impact of Higher Alcohols. *Anal Chem.* 2018;90(18):10812–10818.
6. Guth, H.; Rusu, M. Food Matrices – Determination of Odorant Partition Coefficients and Application of Models for Their Prediction. *Food Chem.* 2008;108(4):1208–1216.
7. Berglund, B.; Berglund, U.; Lindvall, T. Psychological Processing of Odor Mixtures. *Psychological Rev.* 1976;83(6):432–441.

Characterisation of key aroma compounds in foods containing vegetable proteins

KARINE GOURRAT¹, Marine Voisine¹, Andreas Redl² and Olivier Berdeaux¹

¹ Centre des Sciences du Goût et de l'Alimentation (CSGA), ChemoSens Platform, AgroSup Dijon, CNRS, INRAE, University of Bourgogne Franche-Comté, Dijon, France, karine.gourrat@inrae.fr

² TEREOS, Marckolsheim, France

Abstract

The aroma profile of foods containing vegetable proteins is complex due to the presence of a large number of compounds belonging to different chemical classes. The manufacturing process use many parameters of which temperature plays a role in the generation of volatile compounds. The flavour profiles of two vegetable proteins samples (high and low thermal processing) were studied. GC-MS analyses detected and identified 71 aroma compounds (pyrazines, alcohols, ketones, aldehydes) in the two samples. Quantification showed a difference between the two thermal treatments. GC-O analysis described 70 olfactive areas, 39 of which attributed to a chemical compound.

Keywords: Vegetable proteins, Food, SAFE, GC-O, GC-MS

Introduction

For several years, vegetable proteins have been the subject of particular attention. Considered by many people as the food of the future, they are more and more popular within consumers.

The project GenVie aimed to develop new foods based on vegetable protein in order to obtain a good digestibility and acceptability by the consumer [1, 2]. To better characterize the taste of these products, we conducted experiments to identify the flavour compounds in two samples produced at different thermal processes. The two vegetable protein samples (high and low thermal processing) [3] were submitted in triplicate to Solvent Assisted Flavour Evaporation (SAFE) [4]. The aroma compounds present in the resulting aqueous distillate were extracted with dichloromethane. The identification and quantification of the aroma compounds were performed by Gas Chromatography–Mass Spectrometry (GC-MS). The odorant compounds were detected by Gas Chromatography–Olfactometry (GC-O) with a panel of ten assessors.

Experimental

The manufacture of vegetable meats consists of producing protein fibres from an extract of concentrate and giving them a structure similar to that of meat. Depending on the product, the addition of flavour, fats, colourings, nutritional additives and coagulable proteins is possible. The two vegetable proteins samples (high-GV1 and low-GV3 thermal processing) studied are developed and produced by Tereos, they contain about 50 to 70% water.

Extraction of volatile compounds (Solvent Assisted Flavour Evaporation)

Each vegetable proteins sample (50 g) was crushed and mixed with 60 ml of ultra-pure water. Three hundred microliters of butan-1-ol solution (124 ng/μl in water) were added for internal standardisation. This mixture was stirred, introduced into the SAFE apparatus and vacuum distillation was performed for two hours. The thermostat of the head and legs of the apparatus was fixed at 37°C. The same temperature was used to heat the distillation vessel by means of a water bath. The aqueous distillate was then extracted with dichloromethane (1 x 20 ml then 2 x 10 ml). After liquid-liquid separation, the organic phase was collected and filtered through glass wool and dried over anhydrous sodium sulphate. The extract was concentrated to 400 μl with a Kuderna-Danish apparatus in a 70°C water bath.

Gas Chromatography-Mass Spectrometry (GC-MS)

GC-MS analyses were performed using a 7890A series GC-5975C quadrupole MSD (Agilent Technologies, Santa Clara, USA) equipped with a DB-WAX column (30 m length x 0.32 mm i.d., 0.5 μm film thickness; Agilent J&W). One microliter of each extract was injected in splitless mode. The oven temperature was held at 40°C, raised to 240°C at 4°C/min and then held at 240°C for 10 min. Helium, as the carrier gas, was run at a constant flow rate of 1.5 ml/min. (velocity 44 cm/s). The injector and detector transfer line temperatures were both maintained at 250°C. Mass spectra were obtained in the electron ionisation mode with an energy voltage of 70eV. Acquisitions were achieved in scan mode (mass range m/z 29-350 uma, 4 scans/s).

The compounds were identified based on their retention indices (RIs) and mass spectra. RI values were calculated using the Van den Dool and Kratz formula from the retention times of *n*-alkanes (C₁₀-C₃₀) on the same column. RI values were compared with RIs from the literature. The mass spectra were compared with those from databases: NIST, WILEY and INRAMASS (internal database achieved using standard compounds).

Gas Chromatography-Olfactometry (GC-O)

GC-O analyses were performed using an HP 6890A GC (Agilent Technologies, Santa Clara, USA) coupled to a flame ionisation detector (FID) and an olfactometric detection port (ODP, Gerstel sniffing, Gerstel Mülheim an der Ruhr, Germany). This system was used with a DB-Wax column, (30 m length x 0.32 mm i.d 0.5 µm film thickness; Agilent J&W). The chromatographic conditions were the same as for GC-MS analysis. The column was equipped with a Y-splitter dividing effluent between the FID and the ODP (ratio1:1). Each analysis was carried out with a panel of ten assessors, a total 10 analyses per extract. During a 40 min analysis, the assessors were asked to describe the odour perceived using their own words. Odour descriptions and times were recorded using Olfactory Recorder software (Gerstel). The data were processed using the detection frequency method. Odorant zones (OZ) were characterised by the number of assessors detecting an odour active compound at the ODP simultaneously (detection frequency, odour descriptions by the whole panel and the retention index on the DB-Wax column). One OZ was taken into consideration if the detection frequency was higher than 4/10 (40%) for at least one extract.

Results and discussion

The combination of GC-MS and GC-O analysis provided the identification of volatile compounds and the odour associated with some of them (Table 1). Seventy-four volatile compounds were identified and semi-quantified with the internal standard (butan-1-ol). Seventy odorant zones (OZ) were selected four or more times in at least one sample and thirty-nine OZ were attributed to a chemical compound.

We observe that the amounts of pyrazines (written in orange) and ketones (written in purple) are more intense in GV1 sample (High thermal processing) than in GV3 sample (Low thermal processing). In contrast, the amounts of alcohols (written in green) decreased in GV1 compared to GV3.

For pyrazines classes, the detection frequency is greater in GV1 in accordance with the quantity. The odour description were noted as grilled, peanuts, earth, and cabbage.

Most of the aldehydes (written in blue) are detected by the panel with two categories of descriptors: vegetable, fruity, floral for the saturated aldehydes and grilled, cereals, spicy, popcorn, and oil for the unsaturated ones. Only some ketones and alcohols have been described as fruity, floral, solvent, and chemical.

The compounds oct-1-en-3-one (11), oct-1-en-3-ol (26), and furaneol (69) were detected in GCO analysis but they were not detected in GC-MS analysis. The identification was based on odour descriptors and on retention indices (experimental and literature).

Table 1: Identification of volatile compounds by GCMS and associated odours by GCO

Peak Number	Compounds Identification	Retention Index		Standard Equivalent Concentration (µg/kg)		Odour Description
		RI _{Exp}	RI _{Lit}	GV1	GV3	Detection frequency (/10) [GV1/GV3]
1	Hexanal	1080	1078	1275	2465	cut grass, vegetable [7/8]
2	Heptan-2-one	1180	1184	237	151	fruity, sweet [3/4]
3	Heptanal	1183	1185	176	135	
4	Limonene	1198	1189	91	107	
5	2-pentylfuran	1230	1230	718	615	
6	Pentan-1-ol	1249	1251	137	543	
7	2-methylpyrazine	1262	1264	120	22	
8	3-hydroxybutan-2-one	1278	1280	107	215	
9	Octan-2-one	1283	1287	66	41	
10	Octanal	1286	1289	128	104	lemon, fruity, citrus [5/6]
11	Oct-1-en-3-one	1304	1298	nd	nd	mushroom [10/8]
12	1-hydroxypropan-2-one	1292	1290	232	53	
13	2,5-dimethylpyrazine	1320	1323	497	336	
14	2,6-dimethylpyrazine	1326	1328	205	88	

Key aroma compounds in foods containing vegetable proteins

15	Ethylpyrazine	1331	1333	19	trace	grilled, toast, peanuts [9/4]
16	6-methylhept-5-en-2-one	1334	1339	13	trace	
17	Hexan-1-ol	1352	1352	340	3000	
18	2-ethyl-6-methylpyrazine	1383	1385	59	20	rotten, gas, cabbage [9/8]
19	Nonan-2-one	1386	1390	40	23	
20	Nonanal	1390	1392	376	266	fruity, candy [4/0]
21	Trimethylpyrazine	1402	1406	230	77	mushroom [8/5]
22	Oct-3-en-2-one	1403	1414	trace	trace	spicy, burnt, dust [6/3]
23	5-ethylformylcyclopent-1-ene	1412	-	103	103	
24	(E)-Oct-2-enal	1425	1437	116	129	wine stopper, chemical [9/7]
25	3-ethyl-2,5-dimethylpyrazine	1443	1447	131	49	asparagus, earth, potato [8/6]
26	Oct-1-en-3-ol	1450	1456	nd	nd	vegetal, earth, cardboard [7/3]
27	Methional (ion 104)	1447	1443	6,2E+04	1,4E+04	potato [9/8]
28	Oct-1-en-3-ol	1448	1451	229	400	
29	Furfural	1454	1460	241	73	
30	Heptan-1-ol (ion 70)	1454	1453	1,3E+05	6,5E+05	
31	2-ethyl-3,5-dimethylpyrazine	1460	1460	65	9	dust, earth, vegetable [7/3]
32	2-ethylhexan-1-ol (ion 57)	1488	1484	3,2E+05	3,3E+05	
33	Decan-2-one (ion 58)	1490	1489	3,4E+05	1,6E+05	floral, vegetal [7/3]
34	Decanal (ion 112)	1495	1495	2,9E+05	1,0E+05	floral, vegetal [7/6]
35	Acetylfurane (ion 95)	1499	1501	1,4E+06	3,2E+05	
36	Non-3-en-2-one	1507	1506	29	27	
37	Benzaldehyde	1514	1528	480	362	
38	(E)-Non-2-enal	1530	1532	104	79	dust, mothballs, cardboard [10/8]
39	Octan-1-ol	1556	1550	104	148	
40	Undecan-3-one	1561	1555	58	48	
41	5-methyl-2-furfural (ion 110)	1564	1567	1,1E+05	4,0E+04	
42	2-pentylpyridine	1573	1572	69	27	anise, mint [10/7]
43	β -caryophyllene (ion 93)	1594	1597	8,2E+04	1,0E+05	
44	Undecan-2-one (ion 58)	1594	1598	2,0E+05	1,5E+05	
45	Butyrolactone	1615	1617	196	78	toasted, hazelnut, burnt [10/5]
46	6-Dodecanone	1625	-	57	46	floral, animal [8/3]
47	Phenylacetaldehyde (ion 91)	1633	1648	6,6E+05	3,1E+05	
48	2-acetylthiazole	1638	1644	62	77	grilled, hazelnut, popcorn [5/7]
49	2-Furanmethanol	1653	1659	704	178	
50	(E,Z)-Nona-2,4-dienal	1659	1650	trace	trace	grilled, popcorn, cooked rice [10/5]
51	6(5)-methyl-2-acetylpyrazine	1674	-	29	trace	
52	γ -hexalactone	1690	1694	39	49	
53	(E,E)-Nona-2,4-dienal	1693	1702	27	49	grilled, cereals, spicy [10/8]
54	4-ethylbenzaldehyde (ion 134)	1698	1752	5,7E+04	1,0E+05	anise, fruity, mint [8/7]
55	Δ -Carvone	1727	1728	73	120	
56	2(5H)-Furanone	1739	1745	265	90	plant, bug [8/5]
57	Undecen-2-al	1746	1755	217	154	grilled, hazelnut, popcorn [8/6]
58	(E,Z)-deca-2,4-dienal	1757	1753	353	388	oil, grilled, vegetable [8/6]
59	(E,E)-deca-2,4-dienal	1807	1805	3281	2856	oil, spice, burnt, toasted [9/5]

60	3-methyl-6-propylphenol	1836	-	265	486	
61	Benzyl alcohol	1867	1867	150	215	pharmacy, synthol, solvent, clove, chemical [10/6]
62	2-phenylethanol (ion 91)	1902	1902	7,3E+05	1,6E+06	floral, solvent, coconut [10/7]
63	2-acetylpyrrole	1960	1952	104	21	
64	Maltol (ion 126)	1961	1931	7,1E+06	1,5E+06	sweet, vanilla, caramel [7/3]
65	Phenol (ion 94)	1994	-	2,6E+05	2,0E+05	paint, metallic, vegetal [9/7]
66	2-formylpyrrole	2011	2009	101	trace	floral, vegetal, anise, pepper, vanilla, gingerbread [5/5]
67	γ -nonalactone	2017	2023	288	361	coconut, fruity, sweet [7/7]
68	Octadecanal	2022	2020	116	163	
69	Furaneol	2033	2033	nd	nd	cotton candy, caramel, vanilla [8/4]
70	5-pentyl-5(H)-furan-2-one	2063	-	192	170	sweet, vanilla, coconut, woody, pine, vegetal [7/6]
71	2-phenoxyethanol	2131	2139	127	64	sweet, fruity, lactone [7/5]
72	Caprolactam	2173	-	353	194	
73	2-methoxy-4-vinylphenol	2182	2181	61	28	Spices, chorizo, cabbage [9/3]
74	Indole	2428	2435	83	33	

RI Exp: experimental retention indices on DB-Wax column. RI Litt: literature retention indices on DB-Wax column

Text in grey: volatile compounds coelution. Ion specific area

n.d: not detected by GC-MS

Trace: not quantified

Conclusion

The results of this study constitute a first step in the knowledge of volatile compounds in foods made with vegetable proteins. GC-MS and GC-O data showed a large spectrum of identified compounds (pyrazines, alcohols, ketones, aldehydes) and associated descriptors (roasted, vegetal, fruity...) contributing to the richness and complexity of the sample flavours. The chromatographic profile of the two samples is the same while the quantities of compounds are different between the two thermal treatments. The amounts of pyrazines and ketones are higher in GV1 sample (high temperature) while the amounts of alcohols are higher in sample GV3 (low temperature).

References

1. Deureuder A. Tereos se lance dans les analogues de viande, Process Alimentaire 2015.
2. Amanda Gomes Almeida Sá et al. Food processing for the improvement of plant proteins digestibility, Crit. Rev. Food Sci. Nutr. 2020;60:3367-3386.
3. Ma Z, Boye JI, Azarnia S, Simpson B K. Volatile flavor profile of Saskatchewan grown pulses as affected by different thermal processing treatments. Int. J. Food Prop. 2016, 19, 2251– 2271.
4. Engel W, Bahr W, Schieberle P. Solvent assisted flavour evaporation—a new and versatile technique for the careful and direct isolation of aroma compounds from complex food matrices. Eur. Food Res. Technol. 1999;209(3):237–241.

A new trend in aromatic sample preparation: Vacuum Assisted Sorbent Extraction (VASE) applied to pet food aroma analysis

GAUTIER LE GUILLAS¹, Cécile Marzin¹, Karine Hanaoka², Marion Guilloux², Cécile Pétel², Laurence Callejon², Angélique Villière¹, Carole Prost¹ and Laurent Lethuaut¹

¹ Oniris, Nantes University, CNRS, GEPEA MA(PS)2 team and Flavour Research Group, UMR 6144, rue de la Géraudière, 44322 Nantes, France, gautier.le-guillas@oniris-nantes.fr

² Diana Pet Food, ZA du Gohélis, 56250 Elven, France

Abstract

Aroma compounds extraction remains challenging to ensure a proper detection of volatile compounds when determination of the overall composition of the aroma is needed. Recently emerged, the Vacuum Assisted Sorbent Extraction (VASE) strives for a wider range of detection of the food aroma composition by combining high sensitivity traps and the benefits of a vacuumed environment. The present work aimed to compare abilities of three different available adsorbent phases combined to VASE technic on the extraction of volatile compounds from a meat flavoured extruded dry pet food. Two extraction times under vacuum (4h and 24h) were also compared for each adsorbent phase to highlight the importance of an appropriate extraction time. A higher extraction time enabled a significantly better volatile compounds detection (higher number of compounds and higher mean peak areas; p-value < 0.001) as well as an improvement of repeatability, reducing by more than half the coefficient of variation. A relevant impact of the adsorbent phase has also stood out (p-value < 0.001) and specificities were spotted. Whatever adsorbent type, a common pattern composed of 33 compounds, on a total of 100 identified, was extracted, probably due to the Tenax[®] TA contained by the three adsorbent phases. The Carboxen 1000 supplemented Tenax TA adsorbent trap favoured extraction of additional nitrogen and carbonyl compounds whereas the Carbopack[™] X supplemented one ended up to be the less efficient except for low boiling point (<100°C) volatile compounds. Therefore, the adsorbent phase should be carefully selected depending on the nature of the volatile compounds suspected in the product.

Keywords: aroma compounds, vacuum extraction, sorbent pen, sample preparation, extruded pet food

Introduction

Beyond sensitivity and accuracy of GC/MS, sample preparation and extraction remain critical steps to untargeted aroma compounds analysis. Requiring a good compromise between sensitivity, reproducibility and selectivity, the extraction technique has to be carefully chosen and optimised to meet the accuracy of expected results. Vacuum Assisted Sorbent Extraction (VASE) emerged recently to extend high concentrative extraction techniques to a vacuumed environment favouring release of VOC in headspace of the sample without heating. It results in a specifically designed device called Headspace Sorbent Pen[™] (SP), containing a large amount of adsorbent (approx. 500 times the volume typically used for SPME) [1] and enabling the creation of a vacuumed environment. The SP is inserted into the top of the sample vial, which is then brought under reduced pressure. Thereby, combined with appropriate extraction conditions, VASE coupled to SP could allow the detection of a wide range of compounds without sample heating.

According to literature, different application areas could be concerned by this new trend (food as beer and coriander cold pressed oil, environment, microbiology). To our knowledge, only few works applying this technique to volatile compounds extraction were published up to now and no publication has been dedicated to pet food matrix [1-4]. All these works used a SP containing Tenax[®] TA. However, new adsorbent phase combinations are now available which could be interesting given chemical property diversities of volatile compounds in aroma composition. Dealing with extraction conditions, no consensus on extraction time could be established in literature, varying from minutes to days according to the matrix used.

The aims of this work were then to compare the efficiency of three different adsorbents (Tenax[®] TA, Tenax[®] TA + Carboxen 1000 and Tenax[®] TA + Carbopack[™] X) and to determine the impact of extraction time (4 hours versus 24 hours) on volatile compounds detection. A commercial meat flavoured extruded dry pet food was chosen because of its aroma complexity and to explore a new application area.

Experimental

Materials

The meat flavoured extruded dry pet food was commercially available and purchased in a local supermarket. For the extraction step, SPs with three different adsorbent phases were used: Tenax[®] TA (35/60) (TA), Tenax TA

coupled with Carboxen 1000 (TA-CBX) and Tenax TA coupled with CarboxenTM X (TA-CPK) (Entech Instruments, Simi Valley, CA, USA).

Sample preparation and Vacuum Assisted Sorbent Extraction (VASE)

One hundred grams of the product were directly weighted in a 1 L vial, sealed up with a specific lid and cap enabling the insertion of a SP (Entech Instruments, Simi Valley, CA, USA). Vacuum was performed through the SP with a pump until reaching 29 mmHg (Vacuubrand GmbH + Co, Wertheim, Germany). The vial-SP system was placed at 30°C for a 4-hour or a 24-hour extraction. At the end of the extraction time, the vacuum inside the vial was controlled to ensure that the vacuum lasted the whole time of the extraction. For each condition, experiment was performed in triplicate.

GC/MS-FID analysis

All experiments were conducted on a GC/MS coupled to a Flame Ionisation Detector (FID) (6890/5973 Agilent GC/MS Agilent Technologies, Santa Clara, CA, USA) and equipped with a DB-WAX column (30 m x 250 µm x 0.5 µm; Agilent Technologies, Santa Clara, CA, USA). The SP was desorbed 20 min at 280°C using a SPDU, Sorbent Pen Desorption Unit (Entech Instruments, Simi Valley, CA, USA). Helium thermal desorption flow was fixed at 24 mL/min. The extract was then transferred inside the capillary column thanks to a Helium carrier gas at a 1 mL/min flow. The initial oven temperature was 35°C held five minutes, followed by a customised temperature ramp to 230°C, held five minutes.

Data Analyses

Chromatograms were analysed with MSD Chemstation Data Analysis software (Agilent Technologies, USA). The MS signal chromatograms permitted to suggest hypotheses on the nature of each volatile compound using the combined Wiley Registry 11th Edition / NIST 2017 mass spectral library. Minimum similarity match value between experimental and database mass spectra was fixed at 80% to assign a name. Identification was confirmed by comparison of experimental LRI to literature LRI or validated by injection of chemical standard compounds. FID area of each peak was considered as quantitative data.

A 2-way ANOVA with interactions and LSD test were conducted on the mean total peak area of each condition. Mean total areas and standard deviations of the three replicates enabled to calculate a coefficient of variation in percentage to evaluate the repeatability of each condition. A normalised Principal Component Analysis (PCA) was generated on area measurements of individual identified aroma compounds to highlight the effect of each condition on the individual compounds. All statistical analyses were conducted using the XLStat software (Addinsoft, Paris, France).

Results and discussion

A total number of 100 volatile compounds were identified with all of the six conditions used. Among these compounds, 33 compounds formed a common pattern that neither depended on the extraction time nor the adsorbent phase, and which might be linked to the presence of TA in each adsorbent trap (Table 1). Increasing the extraction time from 4 hours to 24 hours enabled to identify a higher total number of compounds for each adsorbent phase without losing the compounds originally identified after the 4h extraction. Concerning the different adsorbent phases, TA and TA-CBX were able to extract a similar total number of compounds that was also higher than the total number of compounds extracted by TA-CPK. However, specificities appeared depending on the adsorbent phase used.

Considering 24 h extractions, TA specifically extracted 12 compounds, mostly alkanes, aldehydes and nitrogen compounds plus few other compounds (2-methyloctane, nonane, 3-methylnonane, hexadecane, 4-pentanal, octanal, 2,5-dimethylpyrazine, 2(1H)-pyridinone, 2-pyrrolidinone, 2-penten-1-ol (Z), hexyl acetate, 2-ethyl-1-hexene). TA-CBX specifically extracted 17 compounds which were mostly nitrogen compounds and some carbonyl compounds (2-ethyl-5-methyl-pyrazine, N,N-dimethylacetamide, 3-ethyl-2,5-dimethyl-pyrazine, 1-methyl-2-pyrrolidinone, acetamide, 2-butanal, 2-pentanal (E), pentylcyclopentane, 2-acetylfuran, acetone, acetoin, 2-methylthiophene, sulphur dioxide, 2-thiophene carboxaldehyde, 1,3-pentadiene, 3-ethyl-1-pentene). As observed in literature, addition of CBX in SPME fibres enabled a better detection of nitrogen compounds, such as pyrazines, and carbonyl compounds [5-7]. TA-CPK specifically extracted 12 compounds: 7 compounds from diverse chemical classes (butanal, ethanol, 3-methylfuran, 2,3-butanedione, trimethylamine, ethylbenzene and dimethyl sulfone) and 5 alkanes with a low boiling point (BP<100°C) (pentane, 2-methylpentane, 3-methylpentane, methyl-cyclopentane and cyclohexane). According to literature, CarboxenTM X might be a suitable choice for highly volatile compounds with low BP [8, 9]. We may hypothesise that CarboxenTM X was added to TA to fill its deficiency to extract low BP compounds [9]. This was emphasised by the fact that TA and TA-CBX respectively extracted 12 and 15 compounds with a BP under 100°C, while TA-CPK achieved to extract 20 of them.

Among the additional compounds shared by some of the conditions, 15 compounds were exclusively shared by TA and TA-CBX and 6 compounds by TA and TA-CPK, while only 1 was exclusively shared by TA-CBX and TA-CPK. The presence of TA in each SP probably explains why all these compounds were shared, but the differences could be explain by the different proportions of adsorbent phases for each combination.

Table 1: Number of shared and specific compounds according to adsorbent phases and extraction times.

Volatile compounds shared:	TA 4	TA 24	TA-CBX 4	TA-CBX 24	TA-CPK 4	TA-CPK 24
by the 3 adsorbents and the 2 extraction times	33	33	33	33	33	33
by the 3 adsorbents and at least 1 extraction time	2	4	3	4	2	4
with TA	-	-	14	15	6	6
with TA-CBX	14	15	-	-	1	1
with TA-CPK	6	6	1	1	-	-
// Specific compounds //	11	12	13	17	9	12
Total number	66	70	64	70	51	56

Dealing with mean total peak areas, significant effects of extraction time and of adsorbent phase (both p -value < 0.001) were evidenced without any interaction between these 2 parameters (p -value = 0.229). A 24 h extraction enabled a significantly higher mean total peak area compared to a 4 h extraction (Figure 1A). This was in accordance with [4] who concluded to a major influence of time. Moreover, increasing extraction time resulted in reducing by more than half the CV%, i.e. offering better repeatability. Independently of extraction time tested, the adsorbent phases TA and TA-CBX resulted to a higher mean total peak area than TA-CPK. The three adsorbent phases showed similar mean repeatability.

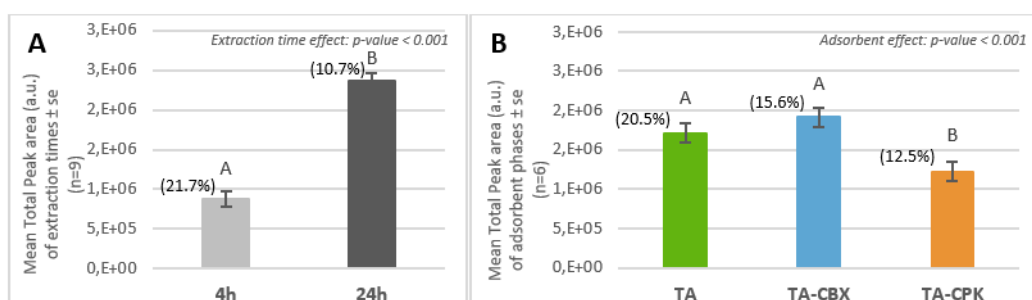


Figure 1: Mean total peak area of extraction times (A) and the three adsorbent phases (B). Different letters indicate a significant difference determined by a LSD test ($\alpha=5\%$). Numbers in brackets represent the CV%.

Concerning the individual peak areas, three principal components are needed to restore 94% of the variability (Figure 2A & 2B). F1, F2 and F3 represented respectively 47.77%, 29.19% and 17.03% of the total variation. The first component (F1) was mainly composed by the compounds from the common pattern, the compounds shared by TA & TA-CBX and the compounds specific to TA. The second component (F2) was defined by compounds shared by TA & TA-CPK, compounds specific to TA-CBX and the common compound of TA-CBX & TA-CPK. The third component (F3) was interesting to study as it was almost only defined by the specific compounds of TA-CPK.

The two biplots showed discrimination of the three different SP. Increasing the extraction time enhanced the discrimination pattern of the three different SP types. Figure 2A highlighted discrimination of the 4 h extractions and Figure 2B emphasised the discrimination between a 4h extraction and 24 h extraction. Values of the compounds defining the axes of the biplots were under the mean value with a 4-hour extraction compared to a 24-hour extraction. Moreover, these biplot enabled to emphasise that TA 24 drawn most of compounds from the common pattern as well as compounds specific to TA & TA-CBX and TA & TA-CPK. It could be attributed to a more abundant Tenax[®] TA proportion inside the SP compared to the dual-phase SP. In other words, this probably led to the lower detection of some of these compounds when extracted by TA-CBX and TA-CPK compared to TA alone.

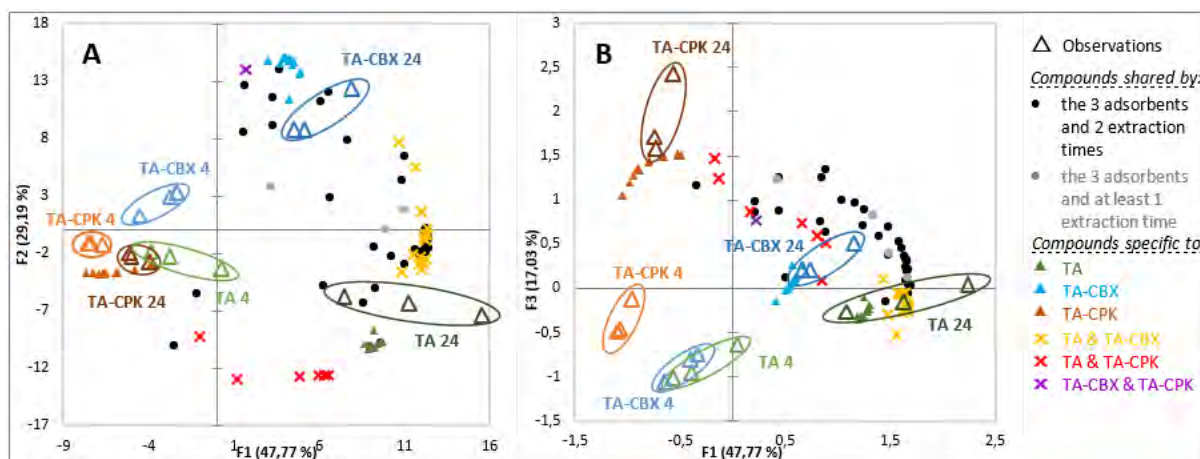


Figure 2: Biplots of principal components F1 and F2 (A) and principal components F1 and F3 (B) of a normalised PCA on area of individual compounds.

Conclusion

Dealing with optimisation of VASE conditions, results demonstrated significant effects of extraction time and adsorbent phase. Whatever adsorbent phase used, a longer extraction time should be favoured to screen a larger number of volatile compounds in a higher concentration. A long extraction time would also enable a better repeatability. The adsorbent phase should be carefully selected depending on the nature of the volatile compounds suspected in the product. When nitrogen and carbonyl volatile compounds are targeted, TA-CBX should be favoured while TA should be recommended when alkanes or aldehydes are targeted. If an aroma is mainly composed of highly volatile compounds with low boiling point, TA-CPK might be considered. Comparing VASE to well-known technics like SPME, many adsorbent phases and coatings remain to be developed and studied to widen the range of SP. Dual or triple phases like CAR/PDMS or DVD/CAR/PDMS of SPME fibres could be adapted to SP. Moreover, to go further on the evaluation of VASE technic, it should be useful to compare it to usual extraction technic like SPME or other high adsorbent capacity technics as SBSE or HSSE.

References

1. Trujillo-Rodríguez M.J., Anderson J.L., Dunham S.J.B., Noad V.L., Cardin D.B. Vacuum-assisted sorbent extraction: An analytical methodology for the determination of ultraviolet filters in environmental samples. *Talanta*. 2019; doi: <https://doi.org/10.1016/j.talanta.2019.120390>.
2. Jeleń H.H., Marcinkowska M.A., Marek M. Determination of Volatile Terpenes in Coriander Cold Pressed Oil by Vacuum Assisted Sorbent Extraction (VASE). *Molecules*. 2021;26:884. doi: <https://doi.org/10.3390/molecules26040884>.
3. Phan J., Kapsia III J., Rodriguez C. I., Vogel V.L., Dunham S.J.B., Whiteson K. Capturing actively produced microbial volatile organic compounds from human associated samples with vacuum assisted sorbent extraction. *BioRxiv*. 2021; doi: <https://doi.org/10.1101/2021.02.16.431476>.
4. Jeleń H.H., Gaca A., Marcinkowska M. Use of Sorbent-Based Vacuum Extraction for Determination of Volatile Phenols in Beer. *Food Anal Methods*. 2018; doi: <https://doi.org/10.1007/s12161-018-1277-z>.
5. Slaghenaufi D., Tonidandel L., Moser S., Villegas T.R., Larcher R. Rapid Analysis of 27 Volatile Sulfur Compounds in Wine by Headspace Solid-Phase Microextraction Gas Chromatography Tandem Mass Spectrometry. *Food Anal Methods*. 2018; doi: [10.1007/s12161-017-0930-2](https://doi.org/10.1007/s12161-017-0930-2).
6. Bingman M., Stellick C., Pelkey J., Scott J., Cole C. Monitoring Cider Aroma Development throughout the Fermentation Process by Headspace Solid Phase Microextraction (HS-SPME) Gas Chromatography–Mass Spectrometry (GC-MS). *Beverages*. 2020; doi: [10.3390/beverages6020040](https://doi.org/10.3390/beverages6020040).
7. Yang Y., Zhang M., Hua J., Deng Y., Jiang Y., Li J., Wang J., et al. Quantitation of pyrazines in roasted green tea by infrared-assisted extraction coupled to headspace solid-phase microextraction in combination with GC-Qq-MSMS. *Food Res. Int.* 2020; doi: <https://doi.org/10.1016/j.foodres.2020.109167>.
8. Qin Y., Pang Y., Cheng Z. Needle Trap Device as a New Sampling and Preconcentration Approach for Volatile Organic Compounds of Herbal Medicines and its Application to the Analysis of Volatile Components in *Viola tianschanica*. *Wiley Online Library*. 2016; doi: [10.1002/pca.2636](https://doi.org/10.1002/pca.2636).
9. Sunesson A.-L., Greenwood R., Mills G., Vrana B. Passive sampling in combination with thermal desorption and gas chromatography as a tool for assessment of chemical exposure. *Compr. Anal. Chem.*, vol. 48, Elsevier. 2007; pp. 57-83.

Comparison of three ionisation methods - electron ionisation, chemical ionisation and atmospheric pressure photoionisation - for the characterisation of volatile organic compounds (VOCs)

GERALDINE LUCCHI¹, Jean-Luc Le Quééré², Karine Gourrat¹, Marine Crépin¹

¹ CSGA, ChemoSens Platform, AgroSup Dijon, CNRS, INRAE, Université Bourgogne Franche-Comté, Dijon,

² CSGA, AgroSup Dijon, CNRS, INRAE, Université Bourgogne Franche-Comté, Dijon, France

geraldine.lucchi@inrae.fr

Abstract

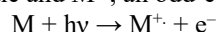
Different chemical classes of VOCs were analysed by three ionisation methods: the oldest gold standard, the electron ionisation (EI), was compared to chemical ionisation (CI) and to atmospheric pressure photoionisation (APPI), a more recent and rarest one. Methodological development on the APPI source coupled to an Orbitrap Fusion, was able to set the best parameters for VOCs high-resolution analysis. LODs calculation has shown a good sensitivity for EI and CI when methane was used as a reagent gas, but APPI, despite in-source fragmentation, is a promising technique for co-elution resolution problems.

Keywords: EI, CI, APPI, high-resolution, in-source fragmentation

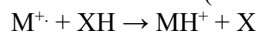
Introduction

Gas chromatography (GC) is a reproducible, robust, selective, sensitive method to analyse volatile compounds and thermo-stable molecules in a wide range of applications. The separated analytes are generally analysed by mass spectrometry (MS) under vacuum conditions. The main ionisation method is the electron ionisation (EI). High kinetic energy (70eV) is commonly used. The electrons pass through the ionisation chamber by cutting the perpendicular flow of analytes. Energy exchanges occur causing molecular fragmentations [1]. CI is another ionisation method. A reactive gas, for instance, methane (CH₄) or ammonia (NH₃), is introduced into the source and is ionised by electron ionisation to form reactant ions that react with the analytes by proton transfer [2]. This type of ion-molecule reaction is less energetic than the electron ionisation. Thus, it limits fragmentations, however, it reduces sensitivity.

GC-MS can also be used coupled to Atmospheric Pressure Ionisation (API) conditions. The most recent API source is the APPI source. Photoionisation of molecules occurs if their ionisation potential is lower than the energy of the photons. APPI was introduced by Revel'skii [3]; the absorption of a photon by the molecule leads to the reaction below, where M is an ionisable molecule and M⁺, an odd-electron radical cation:



Moreover, hydrogen atom abstraction by the molecular radical cation frequently occurs during in-source collisions and produces a large quantity of protonated molecules (MH⁺):



In our research platform, we recently coupled a GC to a High Resolution Mass Spectrometer (HRMS) with an APPI source developed by Mascom (Bremen, Germany). In this work, first, we present a general overview of the technical developments carried out on 13 VOCs with the GC-APPI-HRMS hyphenated technique. Secondly, we compare the three ionisation methods listed above. For this purpose, we used 6 VOCs of different chemical classes to determine the Limit of Detection (LOD) for each ionisation mode.

Experimental

Standards

Thirteen aroma compounds from different chemical classes (butanoic acid, 2-methylbutanoic acid, heptan-2-ol, 2-methylbutan-1-ol, 3-methylbutan-1-ol, 2-phenylethanol, linalool, heptanal, heptan-2-one, diacetyl, ethyl butanoate, isoamyl acetate) were purchased from Sigma Aldrich (Sigma Aldrich, France). They were chosen as representative key-aroma compounds in food. Concentrated solutions of each aroma compound were prepared in 99% dichloromethane (Fisher Scientific, France). For the evaluation of ionisation, each individual compound was prepared at various final concentrations from 0.1 to 200 ng/μL.

Gas chromatography-Mass spectrometry

Chromatographic separation was performed on a DB-Wax capillary column (30 m x 0.25 mm x 0.5 μm , Agilent Technologies, USA) with the following temperature program : 40°C to 240°C (held for 10 min), 4°C/min. The carrier gas (He) velocity was 40 $\text{cm}\cdot\text{s}^{-1}$. Splitless mode at 240°C was used in the injection port (1 μL). GC-EI-MS and GC-CI-MS were conducted on a GC 7890A coupled to a quadrupole MS 5973 (Agilent Technologies, USA). The EI operating conditions were as follow: ion source at 230°C, electron ionisation mode at 70 eV, scan range from 29 to 350 m/z. For the CI operating conditions: ion source at 250°C, electron ionisation mode at 128 eV, chemical ionisation with ammonia and methane successively, scan range from 70 to 400 m/z. Data were recorded with MSD ChemStation (Agilent Technologies, USA). GC-APPI-HRMS was conducted on a GC Trace 1310 (ThermoScientific, USA) with the same above chromatographic conditions. Acquisitions in full scan and MS2 mode were performed on an Orbitrap Fusion instrument (ThermoScientific, USA) equipped with an APPI source developed by Mascom (Germany). The operating conditions were as follow: ion spray at 3500 V, scan range from 50 to 250 m/z. Data were recorded with Xcalibur.

Data analysis

Each compound was validated by its identification based on its retention index (RI) and EI mass spectrum. RI values were calculated using the Van den Dool and Kratz formula [4] from the retention times of n-alkanes (C10-C30) on the same column. RI values were compared with RIs from the literature. The mass spectra were compared with those from databases: NIST, WILEY and INRAMASS (internal database achieved using standard compounds). For LOD comparison, standard solutions were analysed in triplicate. 4 to 7 points were chosen in the compound linearity domain and 1 to 3 ions were selected for each ionisation method. The sum of the abundances of these ions, for each triplicate and each solution, was calculated first, then the average and the standard deviation. LOD calculation was used to determine the minimal concentration detectable for each ionisation method and each compound.

Results and discussion

After analysis by GC-APPI-HRMS, adducts at + 27.959 Da were detected for each n-alkanes used to calculate RIs, without any molecular ion being observed. For example, the undecane, with a $\text{C}_{11}\text{H}_{24}$ raw formula and a theoretical mass MH^+ at m/z 157.195, was detected at m/z 185.154 with a $\text{C}_{11}\text{H}_{21}\text{O}_2$ suggested raw formula (Figure 1). The same phenomenon was observed in the troposphere, alkanes coming from engines and industrial combustions react by photooxidation with OH radical at atmospheric pressure to form, for instance, + 27.959 Da adducts (ketone or furfural chemical classes have been suggested) [5].

Methodological development was performed on 13 VOCs of different chemical classes (acids, alcohols, aldehydes, pyrazines, ketones and esters); the goal was to adjust several instrument parameters to get the best sensitivity in our mass spectra. Critical parameters for the 13 VOCs studied were, first of all, the source parameters. Sheath gas flow needed to be very low to avoid dispersion of the molecules at the entry of the mass spectrometer. The transfer tube temperature was set to 150°C; higher temperatures gave rise to molecular dissociations while lower temperatures decreased sensitivity. Secondly, full scan mass parameters were investigated. Positive scan mode allowed the sensitivity to be doubled compared to negative mode. The Automatic Gain Control parameter (AGC) of the C-Trap was tested from 2E5 to 1E6 and the best performances were obtain with a low AGC value. Indeed, AGC regulates the ion stacks stored in the C-Trap before being shot into the Orbitrap. Large ion stacks lead to collisions between molecules, and dissociations occur. Resolution was set to 15,000. This resolution setting enabled to distinguish two ions separated by 0.006 Da, at m/z 89. A Radio Frequency (RF) Lens parameter from 20 to 40 % was optimal to promote the transmission of our low m/z ratio ions. Thirdly, MS^n parameters like fragmentation energies in CID (Collision-Induced Dissociation) and HCD (High-Collision Dissociation) were adjusted. HCD was more informative than CID, and low collisional energies were necessary to perform MS^n experiments on VOCs.

Despite these methodological developments, in-source fragmentation was observed on such chemical classes (Figure 2). 2,3-dimethylpyrazine spectrum presented a unique and intense protonated molecular ion. MH^+ butanoic acid ion remained the most intense peak in the full scan mass spectrum, but fragment ions started to be observed in the background. The parent ion of 2-methylbutanoic acid was under-detected compared to fragment ions while MH^+ heptan-2-ol was undetectable in the mass spectrum. Ionisation energy of oxygenated molecules is relatively low. The radical cation of the linear oxygenated aroma compounds is subject to rearrangements that require very little activation energy, and give rise to *in fine* fragmentation. When photoionisation occurs, the aroma compound recovers energy from the photons to lose its electron, and the difference is converted into internal energy which is available for the rearrangement and fragmentation processes.

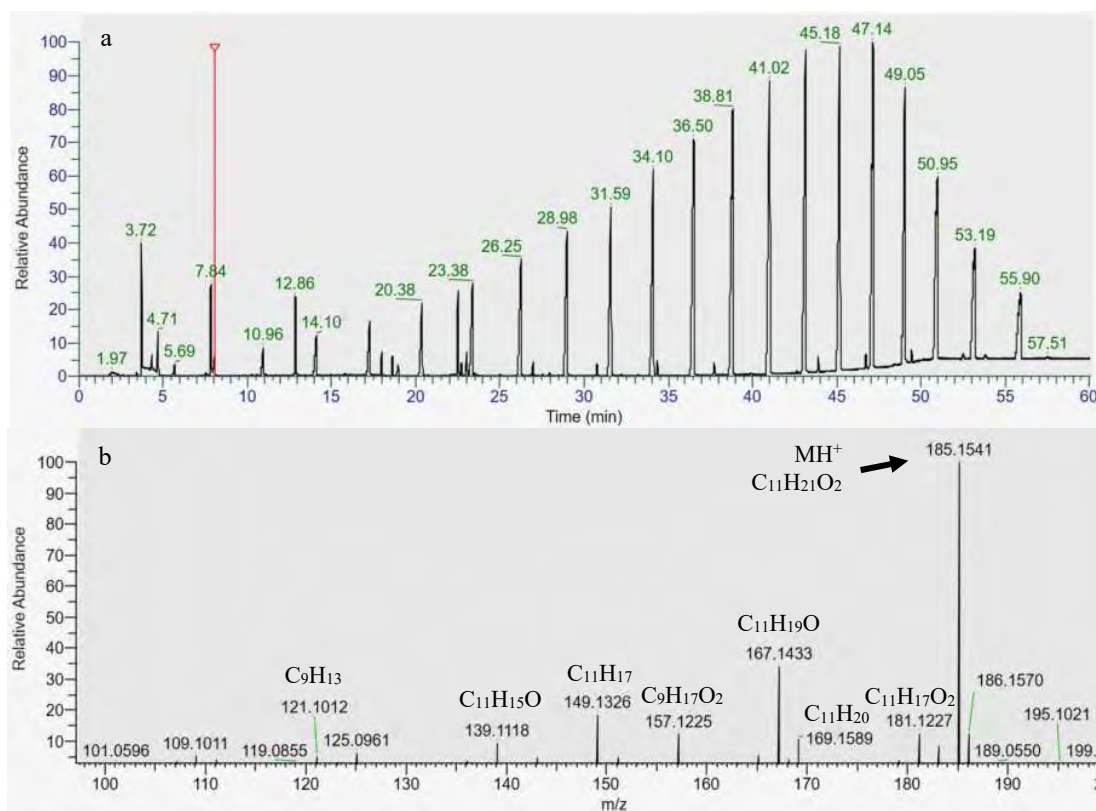


Figure 1: (a) Total ion chromatogram of the *n*-alkanes. The red line is the undecane retention time. (b) Full scan mass spectrum of the undecane with a $C_{11}H_{24}$ raw formula and a theoretical mass MH^+ at m/z 157.195. Elemental compositions are calculated by the FreeStyle software (ThermoScientific).

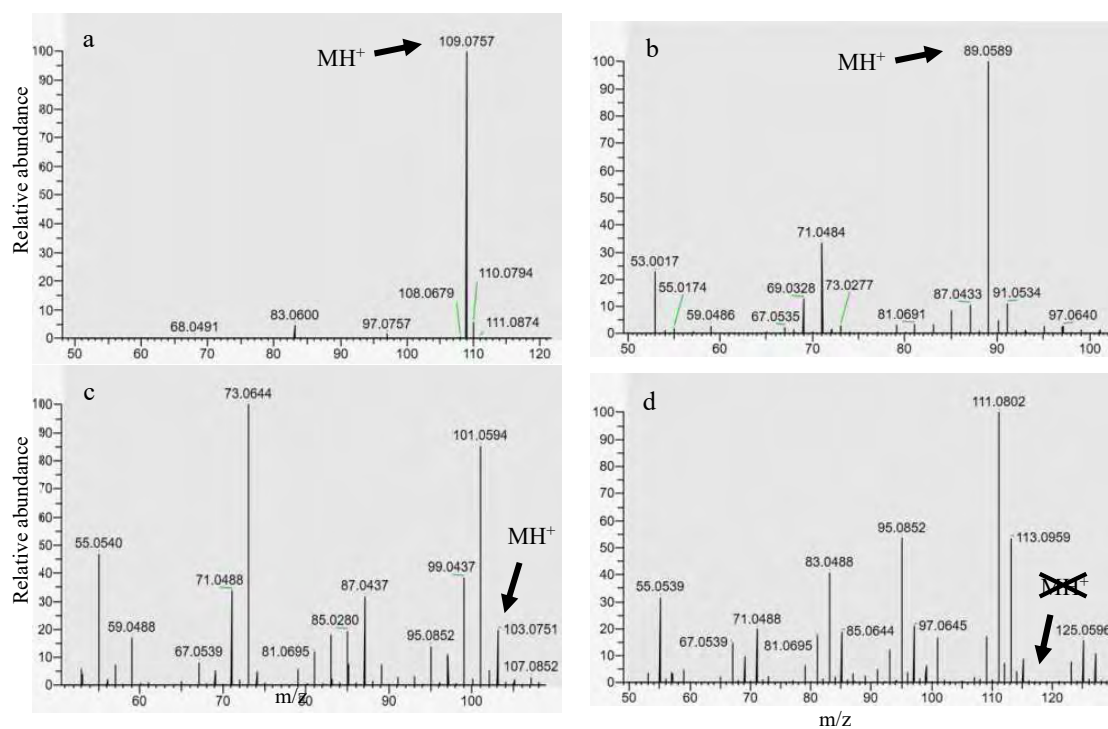


Figure 2: Full scan mass spectra of (a) 2,3-dimethylpyrazine (b) butanoic acid (c) 2-methylbutanoic acid and (d) heptan-2-ol. The arrows highlight the parent ion of each compound. Fragment ions appear for butanoic acid and are very abundant in the 2-methylbutanoic acid and heptan-2-ol mass spectra.

Six COVs were chosen to compare LODs in GC-APPI-HRMS with the two standard ionisation methods, EI and CI (methane and ammonia as reagent gas). Table 1 lists the minimal concentration detected for each aroma compound and each technique. A great disparity in sensitivity was observed according to the chemical classes and the ionisation method. EI and CI (CH₄) were usually the most sensitive ionisation methods for the studied VOCs. The bad sensitivity obtained in CI (NH₃) could be explained by a relatively high background noise in the spectra compared to CH₄, which makes data processing more complex and consequently, gives higher LODs. Moreover, ionisation of molecules occurs if their proton affinity is lower than that of the reagent gas (204 Kcal/mol for NH₃ and 129 Kcal/mol for CH₄). Except 2,3-dimethylpyrazine, whose proton affinity is around 219 Kcal/mol, our other VOCs are not able to give rise to MH⁺ ions in CI NH₃. However, adduct ions [M+NH₄]⁺ were systematically present in their spectra, the abundance of which was considered for LODs determination. The studied pyrazine is the best-detected molecular species for the four considered methods, maybe because of the good stability of the nitrogen cycle and its proton affinity very favourable. Even if APPI is not the most sensitive method in this experiment, APPI LODs are better than those described in the literature where the limit of detection in GC-APPI-MS is between 1 and 100 ng/μL [6].

Table 1: Minimal concentration detected (ng/μL) for each volatile organic compound and each ionisation method. (EI) Electron Ionisation, (CI) Chemical Ionisation, (CH₄) methane as reagent gas, (NH₃) ammonia as reagent gas and (APPI) Atmospheric Pressure PhotoIonisation.

VOCs	Ionisation method			
	EI	CI (CH ₄)	CI (NH ₃)	APPI
2-methylbutanoic acid	0.029	0.038	2.706	0.331
heptan-2-ol	0.006	0.028	0.719	0.165
heptanal	0.023	0.008	6.872	0.052
2,3-dimethylpyrazine	0.002	0.002	0.005	0.004
heptan-2-one	0.003	0.004	0.052	0.020
Isoamyl acetate	0.003	0.009	0.064	0.223

Conclusion

These preliminary results allowed to set up optimised parameters to characterise VOCs better by GC-APPI-HRMS. LODs were calculated for different chemical classes and compared to other ionisation methods. EI remains the most appropriate one to identify chemical compounds in databases, while CI (CH₄) could provide supplementary information for molecular characterisation. APPI, a promising technique to resolve co-elution problems, has to be improved, especially to reduce in-source fragmentation and enhance the efficiency of ion formation. Robb et al. [7] developed the use of a photo-ionisable dopant, working as an intermediate between the analytes and the photons; thereby, a reactant ionises the analytes by charge exchange or proton transfer, allowing a greater detection sensitivity. Acetone (m/z 59) as a dopant gas should be a good candidate for our applications, its low molecular weight being below the mass of interest of the VOCs.

References

1. Märk T, Dunn G. Electron Impact Ionisation. Springer. 1985.
2. Harrison AG. Chemical Ionisation Mass Spectrometry. CRC Press. 1992.
3. Revel'skii IA, Yashin YS, Voznesenskii VN, Kurochkin VK, Kostyanovskii RC. Mass Spectrometry with Photoionization of n-Alkanes, Alcohols, Ketones, Esters, and Amines at Atmospheric Pressure. Russian Chemical Bulletin. 1986;35(9):1806-1810.
4. Van den Dool H, Kratz PD. A generalization of the retention index system including linear temperature programmed gas-liquid partition chromatography. J Chromatogr. 1963;11:463-71.
5. Lamkaddam H, Gratien A, Pangui E, David M, Peinado F, Polienor JM, Jerome M, Cazaunau M, Gaimoz C, Picquet-Varrault B, Kourtchev I, Kalberer M, Doussin JF. Role of Relative Humidity in the Secondary Organic Aerosol Formation from High-NOx Photooxidation of Long-Chain Alkanes: n-Dodecane Case Study. ACS Earth Space Chem. 2020;4(12):2414-2425.
6. Revel'skii IA, Yashin YS, Revel'skii IA. Atmospheric Pressure Photoionization Mass Spectrometry: New Capabilities for the Determination of the Numbers of Components in Complex Mixtures and Their Identification. J Anal Chem. 2019;74(2):192-197.
7. Robb DB, Covey TR, Bruins AP. Atmospheric Pressure Photoionisation: An Ionization Method for Liquid Chromatography-Mass Spectrometry. Anal. Chem. 2000;72(15):3653-3659.

Aromatic profile of wheat flour and bran fractions

José Daniel Wicochea Rodríguez¹, Cécile Barron¹, Valérie Lullien-Pellerin¹, Peggy Rigou² and PASCALE CHALIER¹

¹ IATE, Univ. Montpellier, INRAE, Institut Agro, Montpellier, France, pascale.chalier@umontpellier.fr

² SPO, Univ. Montpellier, INRAE, Montpellier, France

Abstract

The major output of milling process of wheat grains is flour, bran represents the most important fraction of all by-products. Its content in fibres and micro-nutrients makes its enrichment interesting in breads and cereals products if no unfavourable changes in the sensorial properties are induced. In this research, we proposed to compare the volatile components of flour, fine and coarse brans to evaluate the potential impact of addition of bran in flour. The three fractions were obtained by using a micro-mill and the aromatic profile was characterized by GC-MS after SPME extraction. Numerous compounds due to lipid oxidation such as hexanal, 1-octen-3-ol, nonanal, 2-heptanone were found in the three fractions. Limonene, a terpenic compound, characterized by sweet, citrus and peely odour was identified in the three fractions. This unexpected compound was already identified in flour. Eugenol, a phenolic compound, with spicy, clove like, woody odour and phenolic savour was only identified in the brans fraction. This compound is formed via the general phenylpropanoid pathway, including the conversion of coniferyl alcohol and specific enzyme. It could provide a specific marker of bran addition in flour.

Keywords: aroma profile, bran, flour, marker, SPME, wheat

Introduction

Wheat grain is an indehiscent dry fruit consisting of a single seed intimately welded to different envelopes or layers. The seed was constituted of the starchy endosperm and the aleurone layer, embryonic axis and the scutellum and the nucellar epidermis and the testa. Each of these tissues has a particular structure and composition [1]. The milling process has for aim to recover the major part of the starchy endosperm into flour, a rich source of starch and proteins that is used to make cereal-based foods products. The flour extraction rate varies classically between 70 and 77%. Other fractions obtained by milling are coarse, fine brans and shorts. Wheat bran is composed with the pericarp, testa, hyaline and aleurone layer but also contains part of the peripheral starchy endosperm. Bran represents the most important fraction of overall by-products accounting for around 15-25% of the grain weight. It contains dietary fibres (45-55%), proteins (13-18%), minerals (ash 3.4-8%), lipids (3-4%) and micro-nutrients as antioxidant component and therefore its addition could improve breads and cereals products nutritional values if potential contaminants (heavy metals, pesticides, mycotoxins) are carefully checked and conform to the prevailing legislation limits [2]. However, bran addition in the consumable products can also induce changes in the sensorial properties such as texture of the dough or undesirable taste and flavour. In this research, we proposed to compare the volatile components of flour, fine and coarse brans to evaluate the potential impact of addition of bran in flour. Indeed, if the volatile compounds of flour have already been identified, few data exist about the volatile compounds present in the brans fractions after milling.

Experimental

Materials

Common wheat (*Triticum aestivum* L.) grown in organic conditions was purchased from Salvagnac Agribio Union (Salvagnac, France).

Milling

The wheat grains were tempered to reach 16.5 % (w/w) of moisture content. A micro-mill was used to simulate the industrial milling process. The process of milling is divided in four steps including two breaking stages, one sizing and one reduction stage leading to 4 fractions; flour, fine bran, coarse bran and shorts. Each step consisted of a size reduction phase and a sieving phase. For the last two phases, the flour obtained after milling was processed with a bran finisher (CHOPIN S.A) for 1.5 min. The total flour obtained corresponds to an extraction rate higher than 70%.

Extraction and analysis

Headspace Solid Phase Micro-Extraction (HS-SPME) was used to analyse the different fractions obtained after milling. Samples of 0.5 g were deposited in 20 ml vial. For semi-quantification, 5 μ l of internal standard solution was added (0.2 g/l of 2-heptanol in distilled water). Each sample was pre-incubated for 5 min at 50°C and extracted during 30 min at 50°C using fibre (30/50 μ m DVB/CAR/PDMS, stableflex 2 cm 23 Ga). The desorption was carried out for 5 min at 250°C in the automatic Combipal injector. Between each measurement the fibre was baked-out for 30 min at 270°C.

GC-MS ISQ (ThermoScientific, Austin, Texas, USA) equipped with a DB-WAX polar capillary column (30 m, 0.25 mm i.d. x 0.25 μ m of thickness) and a quadrupole detector was used for identification. Helium was used as carrier gas with a flow rate of 1.2 ml/min. The oven temperature was kept at 40°C for 5 min and programmed to 250 °C at a rate of 2°C/min. Spectra were obtained in the electron impact mode with 70 eV. The full scan mode was used, and the range of scans was between 40-500 amu. Compounds were identified by using different libraries (INRA, NIST, Wiley) and linear retention indices calculation.

Results and discussion

First, it is important to highlight that the HS-SPME method allowed to well extract the most volatile compounds compared to liquid-liquid extraction (data not shown).

Numerous compounds due to lipid oxidation such as 1-pentanol, hexanol, 1-octen-3-ol, 2-heptanone, hexanal and nonanal were present in the 3 fractions (Table 1) but in different rather high amounts.

Table 1: Aroma compounds of wheat grains milling fractions and their semi-quantification estimated using 2-heptanol as internal standard.

Aroma Compound (mg/kg dry basis)	LRI	Flour	Fine bran	Coarse bran	Odour quality ^a
Hexanal	1106	0.094± 0.003	0.057±0.009	0.093±0.009	Fresh green
2-Heptanone	1220	0.110±0.075	0.64±0.09	1.37±0.20	Cheese,fruity,
(R)-Limonene	1227	0.504±0.135	4.93±0.55	4.64±0.44	Citrus, peely
3-Methyl-1-Butanol	1254	ND	ND	0.127±0.004	Pleasant, fruity, brandy
2-Pentyl-furan	1263	ND	0.679±0.027	0.427±0.015	Beany, nut
1-Pentanol	1288	0.086±0.028	0.057±0.020	ND	Pungent, bready
1-Hexanol	1388	0.441±0.063	0.905±0.039	0.936±0.033	Pungent, fruity
Nonanal	1417	0.262±0.079	0.035±0.006	0.017±0.003	Aldehydic, citrus
Acetic Acid	1481	0.049±0.005	0.090±0.004	0.066±0.003	Sour, acetic
1-Octen-3-ol	1487	0.051±0.006	0.104±0.007	0.059±0.004	Earthy, fungal
2-Ethylhexanol	1525	0.089±0.012	ND	ND	Citrus fresh floral
Hexanoic Acid	1889	tr	0.156±0.009	0.087±0.005	Sour, fatty, cheese
Benzyl Alcohol	1919	0.052±0.009	0.051±0.007	ND	Sweet, floral, fruity
Eugenol	2229	ND	0.134±0.008	0.120±0.005	Spicy, clove like, wood
Total		1.799±0.521	7.843±0.845	7.944±0.738	

^aAll odour qualities collected at: <http://www.thegoodscentscompany.com/>. ND non detected

Quantitatively, the flour was less rich in volatile compounds (around to 2mg/kg dry basis) than fine and coarse brans (around 8mg/kg dry basis). As derived product of lipid represented the major part of volatiles components, it can be related to the lowest lipid content of flour compared to fine and coarse brans, 1.6, 5.3 and 4.7 %, respectively.

In the flour, the more represented compounds were limonene, 1-hexanol and nonanal followed by 2-heptanone. In the brans, limonene is clearly the major compound, but 1-hexanol and 2-heptanone were also identified. In general, the main contributors to the wheat flour aroma are the compounds derived from lipid peroxidation [3] and the amount of these compounds changed with the progress of reaction: the longer the time before analysis, the greater the risk of oxidation causing volatile profile modification. In their study Xu et al. [3] found that 1-hexanol was the major compound of the flour produced from common wheat grains followed by hexanal, and nonanal. Hexanol is produced by the action of alcohol dehydrogenase from hexanal. This latter is the main volatile product from the lipoxygenase activity and autooxidation degradation of linoleic acid. Nonanal is produced mostly from oleic acid and was strongly represented in flour. A high quantity of these compounds (aldehydes and alcohols) is an indication of major extend of lipid oxidation. In our fractions, their amounts remain relatively low suggesting a good preservation of the fractions.

2-Heptanone is formed by β -oxidation from octanoic acid in mitochondria of entire cell plants or by the action of fungi as *Penicillium* sp. Its higher presence in coarse brans could be due to the less intensive cell degradation. This hypothesis agrees with the presence of hexanoic acid, another product of β -oxidation of octanoic acid mainly in brans fractions.

2-Pentylfuran was only detected in brans but was not specific of these fractions because it has been already found in flour [3]; this component is formed via auto-oxidation of linoleic acid.

The strong amount of (R)-limonene specifically in the brans (50% of volatile compounds) was unexpected. However, limonene and other terpenes were evidenced in flour [3] and in derived product as bread. Their presence could be explained by the contamination by other plants which could be cropped with wheat grains. Limonene is also the major component of insecticide, fungicide and acaricide used in organic farming for vegetables. Then, a cross over contamination could be also evocated to explain the high amount of this compound in the flour and particularly in the bran fractions which are constituted to the more external layer of grains. It is important to highlight that the studied wheat was cultivated in organic conditions. Another hypothesis was the contamination by fungi able to produce terpene compounds.

In flour, three other compounds previously detected [3], were formed by other ways than lipid oxidation. Acetic acid can be a sign of natural grain contamination by acetic bacteria or other microorganisms. Benzyl-alcohol could occur from phenylalanine via benzaldehyde either by β -oxidative pathway and non-oxidative way. This compound was present in flour and in fine bran but not in coarse bran indicating potential difference in enzymes equipment or protein amount (e.g., more germ in fine than in coarse).

While the presence of 2-ethylhexanol has been already detected in flours, its origin requires further investigations. Indeed, it is known as an indoor air pollutant with human toxicity [4]. Its detection in flour only is surprising and could be problematic.

In bran fractions, two specific compounds were identified 3-methyl-1-butanol and eugenol. The former resulted from reduction of 3-methylbutanal which can be synthesized from leucine via Ehrlich pathway or Strecker degradation. The presence of alcohol indicates strong activity of alcohol-dehydrogenase [5]. The aldehyde and its corresponding alcohol were already identified in sourdough or bread and alcohol formation is considered as the result of yeast action.

Eugenol is a simple phenolic compound, formed via the general phenylpropanoid pathway, including the conversion of coniferyl alcohol and the action of specific enzymes [6]. The richness in lignin of bran suggested a possible deviation of the general way toward eugenol. It is possible that its formation is a defence mechanism due to pathogens attack. Other compounds like acetophenone and derived components have been found in brans (data not shown) with feruloyl-coA as a precursor and their presence was also described in a context of plant defence. The production of eugenol is positive because it shows antimicrobial activity against fungi (*Fusarium*, *Penicillium* or *Aspergillus* sp) contaminating wheat. Moreover, as this compound, is found only in bran, it can play the role of a marker of bran addition in flour.

Concerning the odour quality of compounds present in all fractions, the majority was characterized by green, vegetal aroma and are rather pleasant with the exception of acetic acid, 1-pentanol and 1-hexanol that are perceived as pungent. The presence of limonene can improve the sensorial attribute with citrus odour. The addition of bran in flour should not have a detrimental influence because numerous compounds are common to the flour and the two specific compounds have a pleasant odour. However, the oxidation reaction could be more important during storage in relation to the higher lipid content of brans and shelf life of product reevaluated in functions of bran addition.

Conclusion

Numerous volatile compounds coming from lipid oxidation are present in all milling fractions. The amount of volatile components is higher in brans than in flour in relation to the strongest lipids content of bran. Limonene is found in great quantity, surpassing all the other components, in particular in brans. Its origin should be investigated. The specific bran compounds are pleasant and should positively impact flour sensory properties. Moreover, eugenol may provide a specific marker of bran addition into flour. Its presence or that of other phenylpropanoids need to be checked on a large number of samples.

References

1. Hemery Y., Rouau, X., Lullien-Pellerin V., Barron, C., Abecassis, J. Dry processes to develop wheat fractions and products with enhanced nutritional quality. *J. Cereal Science*. 2007;46(3):327–347.
2. Apprich, S., Ö. Tirpanalan, J. Hell, M. Reisinger, S. Böhmendorfer, S. Siebenhandl-Ehn, S. Novalin and W. Kneifel. Wheat bran-based biorefinery 2: Valorization of products. *LWT - Food Science and Technology*.2014;56(2): 222-231.
3. Xu, J., Zhang, W., Adhikari, K., & Shi, Y. C. Determination of volatile compounds in heat-treated straight-grade flours from normal and waxy wheats. *J. Cereal Science*. 2017;75: 77–83.
4. Wakayama T., Ito Y., Sakai K., Miyake M., Shibata E., Ohno H. et al Comprehensive review of 2ethyl-hexanol as an indoor pollutant. *J. Occup Health*. 2019;61:19–35.
5. Smit B. A., Engel W.J.M., Smit G. 2009, Branched chain aldehydes: production and breakdown pathways and relevance for flavor in foods, *Applied Microbiol. Biotechnol*. 2009;81:987-999.
6. Vogt T. Phenylpropanoid Biosynthesis. *Molecular Plant*, 2010;3(1):2-20.

Methoxypyrazines as a potential “green” off-odour in wine distillates

PANAGIOTIS STAMATOPOULOS, Xavier Poitou and Sandrine Weingartner

*Hennessy, rue de la Richonne-CS 20020, 16101 Cognac-Cedex, France
pstamatopoulos@moethennessy.com*

Abstract

Aroma is one of the main quality parameters of wine distillates. Avoiding generation of off-odours is therefore an issue of great concern in the industry and consequently numerous studies have investigated to identify off-odours using a variety of different approaches. Different wine distillates were studied for the expression of “green-earthy” notes by means of TD-MDGC-MS/O and two odoriferous zones were identified. The compounds identified were 3-isopropyl-2-methoxypyrazine (IPMP) for the first odoriferous zone with intense earthy note and 3-isobutyl-2-methoxypyrazine (IBMP) for the second odoriferous zone with intense green note. The quantification experiments showed high concentrations of IPMP and IBMP for an average of 46.2 and 51 ng/L respectively, with some extreme levels of 178 ng/L for IPMP and 126 ng/L for IBMP. Further experiments showed different kinetics for the extraction of methoxypyrazines during distillation process. Thus, extraction of IPMP is more pronounced in the first fractions, contrary of IBMP which is more present in the last fractions of distillation process. Moreover, the sensory impact of the methoxypyrazines was confirmed.

Keywords: Methoxypyrazines, IPMP, IBMP, Off-odour, wine distillates.

Introduction

Methoxypyrazines, naturally present in plants, are derived from amino acid metabolism. They are potent aroma-active components found in some *Vitis vinifera* grapes and their wines, particularly Sauvignon Blanc and Cabernet Sauvignon. Their low levels may contribute to the expected varietal aroma and flavour, while elevated concentrations can be unpleasant and often associated with “green-unripe” or “earthy” characteristics [1]. 3-Isobutyl-2-methoxypyrazine (IBMP) and 3-isopropyl-2-methoxypyrazine (IPMP) are very powerful aromatic compounds with very low detection thresholds of 2 ng/L and 1 ng/L respectively [2, 3]. These compounds have a vegetal-green odour with a more “earthy” notes for IPMP. The goal of this study is to quantitate methoxypyrazines content in a selection of wine distillates presenting “green/cooked vegetables” characteristics during sensory evaluation. Furthermore, the sensory impact of the methoxypyrazines in wines distillates was studied.

Experimental

Wine distillate samples

A panel of six experienced assessors selected a set of 30 wine distillates. Through sensory evaluation, 14 of them were evaluated with a “green/cooked vegetables” off-odour and the other 16 were evaluated as standard examples of wine distillates. In addition, 5 distillation fractions were evaluated through quantitation experiments.

Sample preparation and selectable MDGC TOF-MS/O

For identification and quantitation of methoxypyrazines the different samples were analysed by an adaptation of a previously published method [4], as follows. Briefly, 1 mL of wine distillate and 9 mL of Milli-Q water were transferred to a 10 mL headspace vial. A stir bar was added, and the vial was sealed with a screw cap. Stir bar sorptive extraction (SBSE) of several samples was performed simultaneously at room temperature (24 °C) for 60 min while stirring at 900 rpm. After extraction, the stir bar was removed with forceps, dipped briefly in Milli-Q water, dried with a lint-free tissue, and placed in a glass thermal desorption liner. The glass liner was placed in the thermal desorption unit. No further sample preparation was necessary. The stir bar was then desorbed using a thermal desorption unit (TDU) and a cryo-cooled injection system (CIS 4) with a programmable temperature vaporization (PTV) inlet (Gerstel, Müllheim an der Ruhr, Germany) equipped with a MPS auto-sampler from Gerstel (Müllheim an der Ruhr, Germany). The stir bar was thermally desorbed in the TDU in splitless mode.

A selectable one-dimensional (1D) or two-dimensional (2D) gas chromatography-mass spectrometry (selectable 1D/2D GC-MS) (Agilent 7890B) system with selective detection (TOF-MS/O) was developed by using capillary flow technology and low thermal mass GC (LTM-GC). The advantages of this system are the simple and fast selection of 1DGC-MS or 2DGC-MS operation without any instrumental set-up change and simultaneous mass spectrometric and olfactometry detection for both 1D and 2D separation to assure selection of a heart-cut

region and correct identification of compounds of interest. In this study, the separations were performed on a DB-Wax fused silica capillary column with 30 m, 0.25 mm i.d., 0.25 μm film thickness (Agilent) as the 1D column and a DB-5MS fused silica capillary column with 30 m, 0.25 mm i.d., 0.25 μm film thickness (Agilent) as the 2D column. The GC oven was used as a host system and was kept at a constant temperature of 240 $^{\circ}\text{C}$.

Sensory evaluation

A solution of IPMP and IPMP 1/1 (v/v) was added at different concentrations (10, 20, 40, 80 and 160 ng/L) in a control wine distillate, in order to evaluate their sensory impact. The evaluation was performed using a 0 to 10-point non-structural scale were 0=no aroma perceived and 10=high intensity of “green” aroma.

Results and discussion

Using MDGC technology for the analysis of the “green” wine distillates two odoriferous zones were targeted for their olfactory characteristics on the 1D olfactometry port. Then, an adequate 1 min “heart cut” was performed for each odoriferous zone. The separation on the analytical column (2D, DB-5MS capillary) coupled with both the olfactometry port and the TOF-MS detector, revealed the presence of two odoriferous zones related with “earthy” and “green/bell pepper” odours. On the basis of the TOF-MS data obtained and the associated chromatographic peaks, the two odoriferous zones were identified as 3-isopropyl-2-methoxypyrazine (IPMP) for the first odoriferous zone with intense earthy note and 3-isobutyl-2-methoxypyrazine (IBMP) for the second odoriferous zone with intense green note (Table 1).

Table 1 : Detected compounds responsible for the distinctive “green” aroma of wine distillates.

Odoriferous zone	Odorant	Odour quality	Retention Index	
			DB-Wax	DB-5MS
1	IPMP	Earthy	1442	1101
2	IBMP	Green	1553	1191

IPMP and IBPM were then quantitated in a selection of 30 wine distillates, 14 of which presenting a “green” off-odour. The quantification experiments showed high concentrations of IPMP and IBMP (Figure 1) for the “green” wine distillates, with some extreme levels of 178 ng/L for IPMP and 126 ng/L for IBMP.

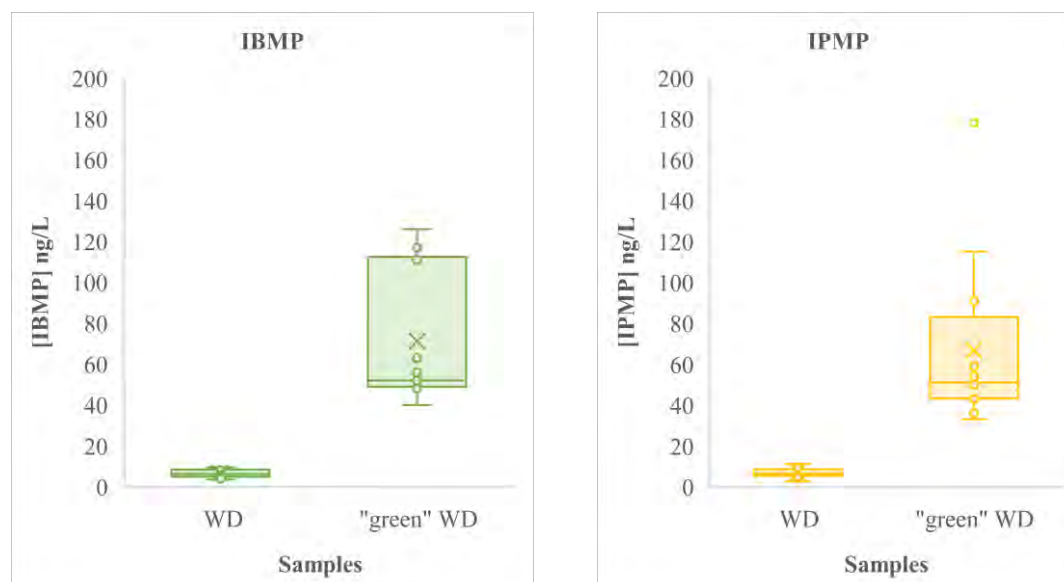


Figure 1 : Distribution of IBMP and IPMP concentration in the control wine distillates (WD) and the wine distillates presenting the “green” off-odour (“green” WD).

All the “green” wine distillates present concentrations well above the rejection threshold for the methoxypyrazines in wine distillates which is estimated around 20 ng/L. Contrary, the totality of the control wine distillates present concentration under 15 ng/L. The results confirmed the hypothesis that IPMP and IBPM were responsible for the “green” off-odour with very high content for both IPMP and IBPM.

Further quantitation experiments through distillation showed different kinetics for the extraction of methoxypyrazines during distillation process. Thus, extraction of IPMP is more pronounced in the heads and heart with 540 ng/L in heads and 280 ng/L in heart, contrarily to IBMP which is more present in the last fractions of the

distillation process, with 38 ng/L in the end of heart and 57 ng/L in the seconds (Figure 2). The difference between the boiling points of the molecules, IPMP presenting a lower boiling point than IBMP, may explain the different kinetics through the distillation process.

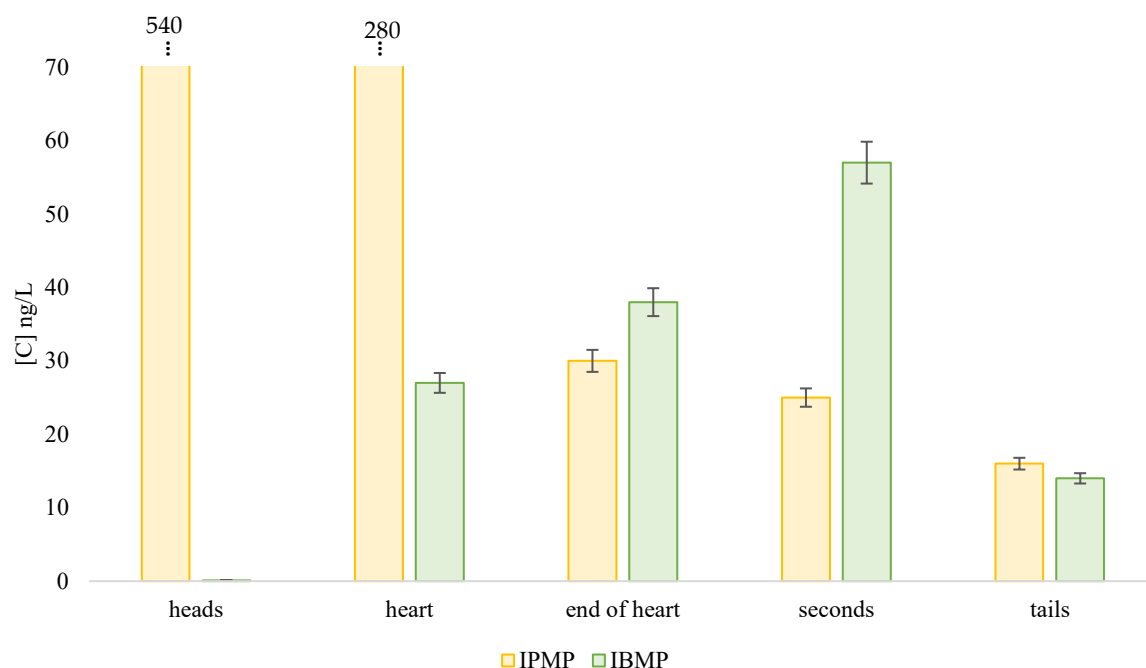


Figure 2 : Concentration of IPMP and IBMP through distillation process.

Finally, the supplementation of a mixture of IPMP and IBPM (1/1 v/v) in a control wine distillate was studied. The results showed a clear impact of the addition of the mixture even in 20 ng/L with a mean notation of the green intensity at 3.4, confirming the impact of the methoxy pyrazines in concentration around 20 ng/L. When the concentration of the mixture is 40 ng/L, the green intensity was noted at 6.4, which is already considered as an off-odour. While the rejection threshold was estimated at 20 ng/L, higher concentrations of methoxy pyrazines are considered as an off-odour that alters the sensory qualities of the wine distillates.

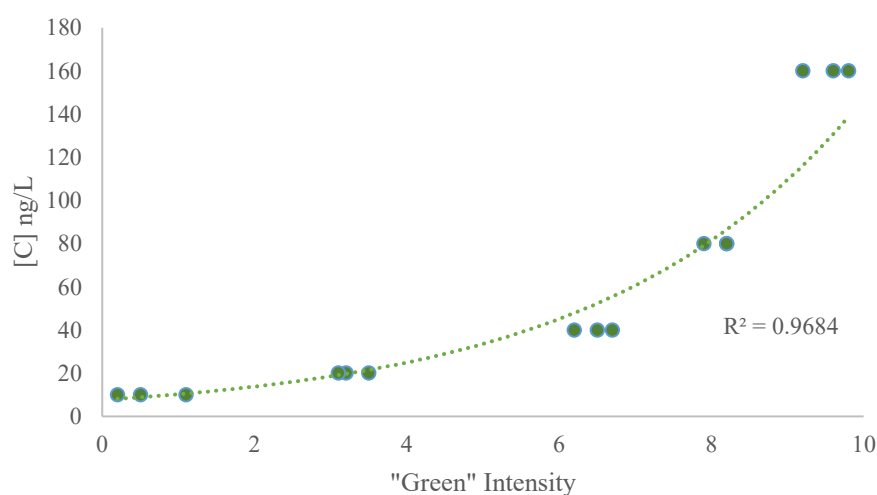


Figure 3 : Green intensity of wine distillates in relation with the concentration of mixture of IPMP and IBMP.

Conclusion

This study concerning the “green” off-odour in wine distillates revealed the presence of the methoxypyrazines IPMP and IBMP in concentrations well above their rejection thresholds. Moreover, the concentration of methoxypyrazines were below 10 ng/L in control wine distillates. Although the methoxypyrazines are naturally present in vine grapes, their high content in the “green” wine distillates suggests the contamination of the grapes at harvest or the wines, even though the distillation acts as a concentration factor. The study of the distillation fractions clearly shows that a contaminated wine can produce a contaminated wine distillate, as IPMP and IBPM showed different kinetics through distillation. Hence, any manipulation of the distillation process cannot influence the methoxypyrazines content. As the methoxypyrazines were already identified in Cognac spirits [5], this is the first time, to our knowledge, that they were reported as off-odour compounds in wine distillates. Moreover, experiments will be carried out in order to identify the origins of the over expression of methoxypyrazines in wine distillates. Identifying the pathway of their formation will be a key step to preserve the quality of the produced wine distillates.

References

1. Allen MS, Lacey MJ. Methoxypyrazines of grapes and wines. 1998; *Chemistry of Wine Flavor*, 3, 31.
2. Buttery RG, Seifert RM, Guadani DG, Ling LC. Characterization of some volatile constituents of bell peppers. *J Agric Food Chem*. 1969;17(6):1322-1327.
3. Seifert RM, Buttery RG, Guadani DG, Black DR, Harris JG. Synthesis of some 3-methoxy-3-alkylpyrazines with strong bell pepper-like odors. *J Agric Food Chem*. 1970;18(2):246-249.
4. Wen Y, Ontañón I, Ferreira V, Lopez, R. Determination of ppq-levels of alkylmethoxypyrazines in wine by stir bar sorptive extraction combined with multidimensional gas chromatography-mass spectrometry. *Food Chem*. 2018;255:235-241.
5. Uselmann V, Shieberle P. Decoding the combinatorial aroma code of a commercial Cognac by application of the sensomics concept and first insights into differences from a German brandy. *J Agric Food Chem*. 2015;63(7):1948-1956.

Modelling of essential oils kinetics release from encapsulation matrix

JOSÉ DANIEL WICOCHEA-RODRÍGUEZ¹, Thierry Ruiz², Emmanuelle Gastaldi¹ and Pascale Chalier¹

¹ UMR IATE, Univ. Montpellier, INRAE, Agro Institute, Montpellier, France, danielwicochea@gmail.com

² UMR Qualisud, Univ. Montpellier, CIRAD, Montpellier, France

Abstract

Essential oils (EO) contain active agents (AA) possessing repellent, antimicrobial and insecticidal properties. Encapsulation is a way to control their release and increasing the AA activity. The release kinetic from the matrix in a controlled environment can be interpolated by the solution of a zero-, half- or first-order differential equation. Even if in practical the release rate might be more complicated, their parameters provide pertinent information about the processes. Several models exist to fit the experimental data and also to describe the release mechanisms such as Avrami, Korsmeyer-Peppas or Higuchi. In the field of controlled release, the Avrami's equation was generally used to describe the dissolution of a drug in a liquid. Indeed, Avrami's equation considers several phenomena that may occur simultaneous such as the diffusion of the penetrant into the matrix, the potential swelling of matrix and the release of drug. The objective of this study was to use these three different models to evaluate the release in atmosphere of two different essential oils from an organic matrix. The two essential oils: spearmint and sweet orange, are characterised by varied properties, the former being less volatile, more polar and more viscous than the latter. Moreover, limonene was present in both oils but in higher concentration in one of them. As expected, Avrami's model leads to the best fit of the experimental kinetic data. The identification of the exponent of Avrami's model: n , varying between 0.40 and 0.75, indicates that the prevailing release mechanism is diffusional for both essential oils. The usefulness and relevance of the other models will be discussed taking into account the essential oil nature and the envisaged practical applications.

Keywords: release, EO, encapsulation, model

Introduction

Aroma compounds are efficient active agents for a broad range of applications (flavouring, antimicrobial, anti-oxidant, repellent, insecticide...). Their high volatility and reactivity provoke their losses or transformation during processing and storage. Their encapsulation in a protective matrix is a way to prevent these losses. Moreover, by the optimal choice of the matrix, the release of the aroma compound can be controlled depending on the initial concentration but also the environmental conditions like open or closed system, the nature of solutions, the temperature, the relative humidity ...etc. In an idealised system, the release of the active agent from the matrix can follow a zero-, half- or first-order kinetic. In practical, the release rate of the active agent might be more complicated and dependent on the physicochemical and thermodynamical properties of the systems [1]. Moreover, the initial active agent concentration in the matrix is generally considered as uniform which is not always the case [2]. Several models exist to fit the experimental data and to propose an interpretation of the release mechanisms such as Higuchi (square root law) Korsmeyer-Peppas (power law) and Avrami (stretched exponential law) [2, 3]. These models allow to describe the apparent drug release in a liquid for different shape materials (film, tablet, and cylinder). The Avrami's equation was first used to the crystallisation phenomena, however, its usage in the field of the controlled release for various application such as encapsulated aroma compound has been developed with success [1]. Indeed, Avrami's equation considers several phenomena that may occur simultaneously such as the diffusion of the penetrant into the matrix, the potential swelling of matrix and the release of drug. The objective of this study was to use the above-mentioned three different models to evaluate the release of two different essential oils from an encapsulating organic matrix. The two essential oils: spearmint and sweet orange, are characterised by varied properties, the former being less volatile, more polar and more viscous than the latter. Moreover, limonene was present in both oils but in higher concentration in one of them.

Experimental

Materials

Spearmint (*Mentha spicata*) essential oil from India, and sweet orange (*Citrus sinensis* (L) Persoon CH essential oil from Mexico were purchased from Golgemma (Esperza, France). The major components of spearmint EO was (*R*)-Carvone (49%) and (*R*)-Limonene (25%) followed by menthol, β -myrcene, β -

caryophyllene, β -bourbonene, β -phellandrene. The major components of sweet Orange EO were (*R*)-limonene (96.8%) and β -myrcene (2.8%).

Methods

The encapsulating system is a porous matrix shaping with a cylinder form and obtained from a specific process. The release experiments were carried out in controlled environmental conditions (70% RH and T = 25°C). At selected times, the EO from the matrix was extracted by liquid–liquid extraction using hexane as solvent and quantified by GG-FID using 2-heptanol as internal standard. The dimensionless release rate: $\frac{M_t}{M_0}$ of the whole components (above-mentioned) was estimated with M_0 , the initial amount in the matrix and M_t , the amount released at time t. M_t was deducted from the residual amount in the matrix. The kinetic release was made in duplicate and the reported data are the average of the two experiments.

Models

For all models, “n” indicates the nature of the mechanism of release and “k” is linked to the apparent release rate constant.

The Higuchi model is based on a fixed value of n equals to 0.5:

$$\frac{M_t}{M_0} = kt^{0.5} \quad \text{Equation 1}$$

The Korsmeyer-Peppas describes the kinetic by a power law where n needs to be adjusted:

$$\frac{M_t}{M_0} = kt^n \quad \text{Equation 2}$$

For a cylinder when n = 0.45, the mechanism of release is considered as diffusive.

The Avrami model is based on a Weibull distribution:

$$\frac{M_t}{M_0} = 1 - (\exp^{-kt^n}) \quad \text{Equation 3}$$

By taking a double logarithm of both sides of Eq. (3) that yields to Eq. (4) allowing to determine n and k by a simple linear regression to adjust the best fit:

$$\ln \left[-\ln \left(1 - \frac{M_t}{M_0} \right) \right] = \ln k + n \ln t \quad \text{Equation 4}$$

Results and discussion

In table 1 the values of n and k are reported. The values of k are presented with the unit imposed by their respective equation: h^{-n} . We have also reduced them to: h^{-1} in order to be able to compare them. In each case, they were determined considering the entire set of data. As the nature and the texture of the matrix is identical for both EOs, the variations of n and k are only dependent on the EOs properties and on their affinity with the matrix. Whatever the model, the values of release rate constant expressed in h^{-1} were always higher for sweet orange EO than for spearmint EO. The former is more volatile, less viscous and more apolar than the latter. This means that EO can be less retained by the matrix in relation to weak affinity and/or more easily driven in liquid and gaseous phases in the porous matrix. Clearly, the physicochemical properties of EO influence the release but it was not possible to conclude about the discriminant parameter.

The simplest model is those of Higuchi, as n is fixed, only one parameter, k, can vary with EO. For this model k is described depending on the diffusion coefficient and the area of specific surface of the matrix. As the surface area of matrices is unchanged for both EO, the determinant parameter was the diffusion coefficient which would be higher for Sweet Orange oil compared to Spearmint EO. The R^2 was higher than 0.9 but was the lowest of the three models. The comparison between experimental data and fitting for Spearmint EO showed clearly that this model allows to predict only the first part of the kinetic data (Figure 1). After 70% of release, a strong deviation was observed. This bad fitting at the end of kinetic release is also observed for both Korsmeyer-Peppas models reflecting the fact that a power law model cannot describe a saturating phenomenon. The values of n were close to 0.4 and imposing n=0.45 increased the R^2 indicating that the prevailing mechanism is Fickian diffusion for the two EOs.

Table 1: The parameters and R2 of the fitting by the three models (after linearization) to the release of Spearmint EO and sweet Orange EO from encapsulating matrix.

Model and parameters	Spearmint EO				Sweet Orange EO			
	k (h ⁻ⁿ)	n	k (h ⁻¹)	R ²	k (h ⁻ⁿ)	n	k (h ⁻¹)	R ²
Higuchi	0.0785	0.50	0.280	0.92	0.197	0.5	0.443	0.93
Korsmeyer-Peppas	0.147	0.36	0.499	0.94	0.264	0.39	0.594	0.94
	0.099	0.45†	0.353	0.95	0.227	0.45†	0.513	0.96
Avrami	0.113	0.56	0.293	0.97	0.232	0.73	0.344	0.97

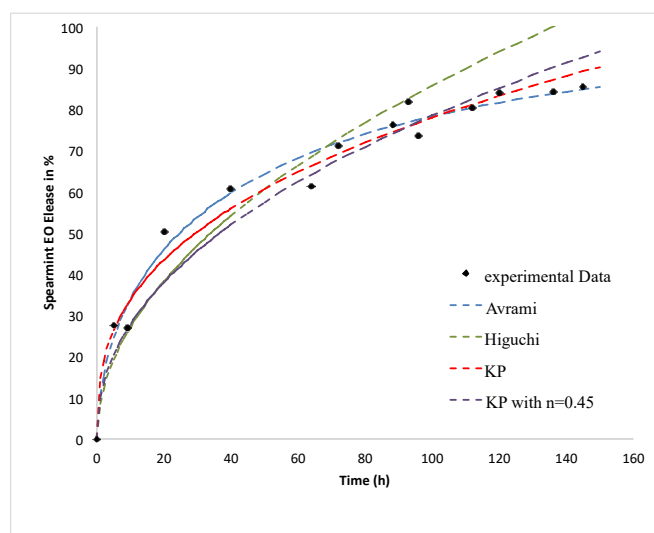


Figure 1: Release kinetic of spearmint EO under controlled conditions ($T=25^{\circ}\text{C}$ and $\text{RH } 70\%$): Experimental data and fitting by the different mode.

Avrami’s model leads to the best fit of the entire dataset for both EOs. The sigmoidal shape of the stretched exponential function being, a priori, able to describe a saturating phenomenon which is initiated by a latent phase. The model well characterised the entire set of data compared to the others as already described in literature [3]. The values of k reflected always the fast release of sweet orange compared to spearmint EO. However, due to the more accentuated difference between n values, the release rate constants were closer than for the other models.

A value of 0.73 was identified to characterise the release for sweet orange oil and corresponds to a diffusion mechanism for a cylinder as previously described [3, 4]. For a cylinder form system, the release is considered as a Fickian diffusion if n lies in the range of 0.69-0.75. When n was between 0.39 and 0.69, the diffusion mechanism is considered to take place in a fractal or disordered substrate different from percolation cluster [3, 4]. It is important to highlight that the models were always established for the release of monomolecular liquid.

For Spearmint EO, the value of n is lower than 0.69 and could be indicative of different behaviours of the EO molecules. Indeed, the global kinetic corresponded to the release of 7 molecules together ((R)-carvone, (R)-limonene, menthol, β -myrcene, β -caryophyllene, β -bourbonene and β -phellandrene). By comparison, the data used to follow the Sweet Orange oil release corresponded only to 2 molecules (R)-limonene and β -Myrcene with one major. The values of n and k considering only (R)-limonene were not significantly different from those

found for sweet orange EO. For the spearmint, the values of k and n calculated for (*R*)-carvone were slightly different from those found for the global ($n=0.567$ and $k = 0.257 \text{ h}^{-1}$) but varied values were observed for the other compounds which influenced the final values.

It was also demonstrated a correlation between the n values found both Avrami and KP models: when $n=0.45$ which indicates pure diffusion for the KP model, n is in a range of 0.69-0.75 for Avrami [3]. This correlation is not clearly evidenced because we considered the entire set of data. If we only considered spearmint EO, the 60% first release for the KP model, the R^2 was increased but the n remained unchanged. For sweet orange oil, the R^2 increased and n was approaching 0.45. This report confirmed that the characterization of EO transfer with numerous molecules is more complicated than for EO with a major component.

Conclusion

All models allow to differentiate the behaviour of each EOs: the values of k indicating that the release being slower for Spearmint EO which is less volatile, more polar and more viscous than sweet Orange EO. Avrami model allows to fit the entire set of data while the other model gives a good correlation only for the first kinetic data. Diffusion is clearly the main mechanism for Sweet Orange EO which is characterised by a major component. For Spearmint EO, the presence of numerous components seems to induce a more complex mechanism. The release of aroma compounds is complex and several mechanisms of mass transfer but also the interactions between matrix and aroma compounds or between aroma compounds into the matrix can occur limiting the completely understanding of a mixture of aroma compounds such as essential oils behaviour.

References

1. Pothakamury, U. R.; Barbosa-gnovas, G. V. Fundamental Aspects of Controlled Release in Foods. *Trends Food Sci Technol.* 1995;61(12):397-406.
2. Ritger, P. L.; Peppas, N. A. A Simple Equation for Description of Solute Release I. Fickian and Non-Fickian Release from Non-Swellable Devices in the Form of Slabs, Spheres, Cylinders or Discs. *J Control Release.* 1987;5(1):23-36.
3. Papadopoulou, V.; Kosmidis, K.; Vlachou, M.; Macheras, P. On the Use of the Weibull Function for the Discernment of Drug Release Mechanisms. *Int J Pharm.* 2006;309(1-2):44-50.
4. Kosmidis, K.; Macheras, P. Monte Carlo Simulations of Drug Release from Matrices with Periodic Layers of High and Low Diffusivity. *Int J Pharm.* 2003;354(1-2):111-116.

Characterisation of the volatile sensometabolome in human breath of cigarette smokers, electronic cigarette users and non-smokers by Aroma Extract Dilution Analysis

FREYA GRONDINGER, Georgina Wright, Theresa Stolle and Steven Coburn

British American Tobacco Ltd., Regents Park Road, Southampton, SO15 8TL, UK; freya_grondinger@bat.com

Abstract

Smokers are known to have a characteristic smelling and long-lasting breath after the consumption of a cigarette. However, the responsible compounds for this malodour have not been fully explored yet. Therefore, the aim of the present study was to characterise key aroma compounds in the breath of cigarette smokers and compare the resulting aroma profile to electronic cigarette (EC) users' and non-smokers' (NS) breath before and after product consumption by application of aroma extract dilution analysis (AEDA) in combination with gas chromatography olfactometry (GC-O).

Interestingly, the breath of cigarette smokers revealed a significantly higher intensity in the overall aroma, resulting in higher flavour dilution factors, in comparison to the breath of non-smokers or electronic cigarette users. This was predominantly caused by a high number of aroma-active pyrazines. Exhibiting an earthy, musty smell, these combustion products can still be found in breath one hour after smoking and are hypothesised to be responsible for the characteristic 'ashtray' smell. These findings align well with results of a study on cigar smokers' breath by Bazemore et al. who suggest that due to their structure, pyrazines are trapped in both mucosa and saliva leading to a long-lasting 'smokers-breath'. In comparison, the breath of EC users revealed similar aroma profiles to the ones of NS even immediately after consumption. In doing so, these data suggest that EC use may have personal and social consideration benefits.

Keywords: Aroma, GC-O, Breath, Vaping, Smoking

Introduction

Tobacco is a stimulant which was known to the inhabitants of Mesoamerica long before it was first described in literature over 400 years ago [1]. The reason for the enduring popularity of the tobacco plant (*Nicotiana Tabacum*) is its high content of nicotine, a highly addictive drug exhibiting positive psychological effects [2]. Today, the most common form of tobacco consumption is as cigarette, with more than one billion cigarette smokers worldwide [3].

Cigarette combustion is a complex process, which leads to a vast spectrum of chemical compounds in the aerosol of smoked tobacco [4]. In fact, more than 5000 substances have been identified in cigarette smoke [5]. It is common knowledge that cigarette aerosol contains a high number of harmful substances, however, pyrolysis of tobacco also leads to large variety of aroma active compounds that can be found in cigarette smoke.

Some of these substances cause an undesired malodour in the breath of smokers after the consumption of a cigarette which is long-lasting and often described as 'ashtray-like' or 'smokers' breath'. Bazemore et al. identified several pyridines and pyrazines in the saliva of cigar smokers, which may contribute to the characteristic breath odour [6].

In recent years, a new technology for nicotine consumption by inhalation was developed [7]. Electronic cigarettes (or e-cigarettes) are electronic nicotine delivery systems (ENDS) that do not contain tobacco, nor undergo combustion [8, 9]. E-cigarettes have become increasingly popular over the past decade as alternative to conventional tobacco smoking [9, 10]. Instead of pyrolysing natural material, these battery-operated devices heat up a cartridge which typically but not exclusively contains nicotine, humectants and a flavour mixture to create an aerosol that is chemically very different to tobacco smoke [9, 10]. Even though e-cigarette users do not seem to exhibit a characteristic aroma profile in their breath such as smokers, no scientific data have been reported to date to verify this hypothesis.

Therefore, the aim of the present study was to identify differences in the aroma profiles of breath in e-cigarette users (EC) and cigarette smokers (CS) by gas-chromatography-olfactometry (GC-O) and compare them to non-smokers (NS) who do not use either of both products.

When it comes to the sampling of volatiles in human breath, several methods have been deployed. Breath volatile organic compounds (VOC) are commonly present in very low levels, and thus, efficient sampling and concentration is crucial [11]. A frequently reported method to collect and concentrate breath VOCs describes exhalation into polymer bags with consequent trapping of volatiles onto thermal desorption (TD) tubes [11]. This approach, however, is not suitable for most GC-O instruments, which are not commonly set up with a thermal desorption unit. A different methodology that has been described to identify aroma active compounds in human

breath by GC-O used nylon mesh coated swabs on the subject's tongue surface, which was consequently concentrated via solid phase micro extraction (SPME) [6]. While this approach is simple and fast, substances that are not trapped in the saliva or the mucosa of the tongue may be neglected.

Thus, a new method involving the trapping of breath VOCs on SPE cartridges with consequent elution, concentration and GC-O analysis has been developed for the aim of the present study.

Experimental

Panellist Recruitment

A group of nine healthy individuals, both male and female between 26 – 52 years old, three of each group: non-smokers (NS), electronic cigarette users (EC) and cigarette smokers (CS) were recruited to participate in the study. Panellists were asked to use their own preferred product for the study. Furthermore, they were asked not to use their product, eat or drink anything apart from water within 60 min prior to breath sampling.

Prior to the study, participants gave their informed consent for participation.

Sample Preparation

Breath samples were taken at time points T_0 (prior to consumption), T_1 (5 minutes post consumption) and T_2 (60 minutes post consumption), with NS following the same sampling pattern without consuming a product. After the first sampling step, participants were asked to consume their product in an allocated testing room for 10 minutes.

In order to trap the volatile fraction in breath samples volunteers were asked to breathe normally for 10 minutes and exhale during this period into a Teflon mouthpiece that was connected to an S15 sorbent cartridge (FlavoLogic, Germany). The cartridge was connected via tubing to a vacuum pump. A constant flow rate of 1.6 ml/min was maintained and controlled with a flowmeter that was connected between pump and cartridge.

Following volatile trapping, the compounds were eluted off the sorbent cartridge using 10 ml methylene chloride (p.A., Merck, Germany) and dried over sodium sulphate (anhydrous, Sigma Aldrich, Germany). Samples were transferred into a pointed flask, and individual samples per consumer group and time point were pooled to eliminate inter-subject variability. Finally, the sample extracts were concentrated to 250 μ l via gentle distillation at 50 °C. Consequently, the concentrate was diluted in 1:1 steps with methylene chloride. Breath extracts were stored at -16 °C and analysed within 48h of sampling.

Each dilution was assessed at the olfactory detection port (ODP) of the gas chromatograph by two trained assessors in altering order until no smell could be perceived anymore.

Gas Chromatography-Olfactometry/Mass spectrometry

Chromatography was performed using an Agilent 7890 Gas chromatograph fitted with a low thermal mass (LTM Series II) column module coupled to an Agilent 5977 A mass spectrometer (MSD) and a Gerstel olfactory detection port (ODP 3). Liquid samples volumes of 1 μ l were injected in splitless mode and the inlet was held at 250 °C. Helium was used as carrier gas with a constant flow rate of 1.5 ml/min. Separation of compounds was achieved using a DB-FFAP fused silica capillary column with the following dimensions: 30 m x 0.25 mm i.d. x 0.25 μ m film thickness. The column module was programmed to run the following temperature gradient: 40 °C (1 min), with 6 °C/min to 200 °C (0.1 min), then with 10 °C/min to 250 °C (6.5 min). MSD source was held at 230 °C, ODP and GC oven holding uncoated fused silica capillaries were held at 250 °C and the split ratio between the two detectors was 1:1. The MSD was operated in electron impact ionizing mode with an ionizing energy of 70 eV.

Identification of compounds was achieved by matching odour quality and retention index with an internal standard database, at a minimum. Additionally, all aroma active compounds were checked for their mass spectrum and optionally identified using MS NIST library. Compounds that only matched odour quality and a hit within the NIST library were marked as 'tentatively identified'.

Results and discussion

The developed method for breath sample collection in combination with GC-O was efficient for the purpose of the present study. The breath odour of three consumer groups at three different time steps has been assessed.

In total, 113 compounds have been identified as aroma active across samples. A range of compounds have been detected with similar flavour dilution (FD) factors in all samples, such as 3-Ethylphenol, 3-Phenylpropionic acid as well as a range of 'earthy' smelling pyrazines, thus suggesting that these compounds are present in human breath naturally.

Interestingly, all three groups also exhibited differences in aroma profiles in their unstimulated breath, most of which can be explained as individual biological variability in combination with a low number of participants. Though, it is remarkable that CS exhibited a differentiated control breath compared to EC and NS, showing a higher variety in substances with 'earthy' odour characteristics.

Figure 1 shows, however, that key driver for differentiation between samples is stimulation, with the largest shift within CS at T₁, immediately after product consumption. Interestingly, this shift is predominantly caused by high FD factors as well as higher numbers of ‘earthy’ and ‘roasted’ smelling compounds, thus exhibiting the same odour impression as the previously mentioned unique compounds of CS T₀. Additionally, some ‘creamy’ and ‘savoury’ smelling substances were perceived at the ODP that could not be detected pre cigarette consumption, nor in any other consumer group.

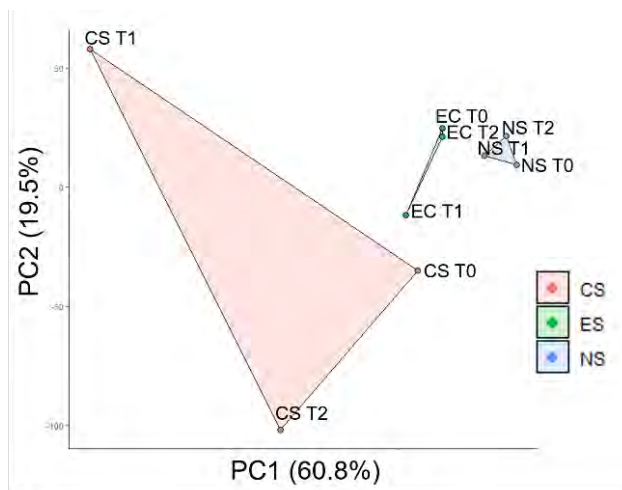


Figure 1: PCA Score Plot of all samples based on compounds flavour dilution factors.

The shift observed in EC at T₁ was less prominent. Apart from a ‘fruity’ smelling compound with an FD factor of 32 that was not found in any other samples, the aroma profile showed only minor changes compared to T₀, which can be explained by the biological variability of assessing sniffers.

The compounds with the highest impact towards the aroma profiles of breath samples in T₁ across groups are listed in Table 1.

Table 1: Key compounds (FD >16) in T₁ across groups.

Compound	RI (FFAP)	Perceived Odour quality	FD in T ₁ samples		
			CS	EC	NS
2-Ethyl-3-methylpyrazine	1424	Roasted, Earthy	128	n.d.	n.d.
3-Ethylphenol	2204	Phenolic	64	64	32
Unknown	1118	Earthy	64	n.d.	n.d.
Ethyl Lactate ¹	1237	Creamy, Fruity	64	1	n.d.
4-Methylphenol	2092	Faecal, Horse	n.d.	n.d.	64
2-Isobutyl-3-Methoxypyrazine	1536	Green bell pepper, Earthy	32	32	4
Unknown	2773	Earthy	32	n.d.	n.d.
Unknown	2044	Sweet, Fruity	n.d.	32	n.d.
2-Ethyl-3,5/6-dimethylpyrazine	1442	Earthy	8	32	2

¹ Tentatively identified

While in EC no major difference could be detected at T₂ anymore, CS still show a differentiation to T₀, as seen in Figure 1. The reason for this is again persisting ‘earthy’ smelling compounds, many of which have been identified as various pyrazines. Compounds of this chemical class have previously shown potential for repartition in the mucosa of the upper airways [12] and they may also be retained by lipocalins in saliva, proteins which have been proven to bind small hydrophobic molecules [13].

Their physicochemical properties, as well as the fact that pyrazines are vastly found in cigarette smoke, are in accordance with the increased detection as well as the elongated duration in CS breath. Additionally, these findings align well with the initially mentioned study, which also suggested pyrazines to have a major impact on the aroma of cigar smokers’ breath [6].

Some pyrazines exhibit an extremely low odour perception threshold, such as the in CS identified 2-Isobutyl-3-methoxypyrazine with a threshold of 0.002 ppb in water [14], which may ultimately lead to olfactory detection in the exhaled breath of smokers over time, even at low retention and release levels in the oral cavity.

Finally, it is worth noting that none of the in literature described as ‘bad breath’ causing sulphur-containing volatiles could be detected. These compounds have extremely low boiling points and therefore, the described method may not be suitable for their detection.

Conclusion

The aroma profile in cigarette smokers’ breath showed alterations within at least the first hour of smoking. Most of these changes resulted in an increase of ‘earthy’ smelling compounds which may lead to the distinctive ‘smokers’ breath’. Neither electronic cigarette users, nor non-smokers exhibited those long-lasting changes. However, the panel of participants in the study was rather small and changes in breath aroma could be detected even in non-consumers. Furthermore, some unique compounds were seen in each group, which leads to the conclusion that the biological inter-subject variability is large.

In addition, GC-O methods are strongly dependent on the individual perception and performance of sniffers, which leads to large error margins. Though, GC-O is crucial for the identification of aroma active compounds and the present study led to the identification of chemical classes that play a role in the breath aroma of the three consumer groups, which delivers the basis to further targeted investigations with a larger cohort of participants as well as a robust quantitation method that includes volatile sulphur compounds to provide detailed aroma profiles across consumers.

References

1. Schadewaldt H. Kultur- und Medizingeschichtliches ueber den Tabak (I), *Med Welt*. 1967;36:2140-2148.
2. Lagrue G. Le bicentenaire de la nicotine. *Presse Med*. 2012;41:1031-1034.
3. World Health Organisation. Tobacco; retrieved 21.04.2021; URL:<https://www.who.int/news-room/fact-sheets/detail/tobacco#:~:text=Tobacco%20kills%20more%20than%208,%2D%20and%20middle%2Dincome%20countries>.
4. Centers for Disease Control and Prevention (US); National Center for Chronic Disease Prevention and Health Promotion (US); Office on Smoking and Health (US). *How Tobacco Smoke Causes Disease: The Biology and Behavioral Basis for Smoking-Attributable Disease: A Report of the Surgeon General*. Atlanta (GA): Centers for Disease Control and Prevention (US). 2010;3, *Chemistry and Toxicology of Cigarette Smoke and Biomarkers of Exposure and Harm*.
5. Rodgman A, Perfetti T. *The Chemical Components of Tobacco and Tobacco Smoke*, CRC Press, 2013;(2):42.
6. Bazemore R, Harrison C, Greenberg M. Identification of Components Responsible for the Odor of Cigar Smoker’s Breath. *J Agric Food Chem*. 2006;54:497-501.
7. Lik H. A Flameless Electronic Atomizing Cigarette. 2006; European Patent Specification EP1618803 (A1).
8. Murphy J, Gaca M, Lowe F, Minet E. et al. Assessing modified risk tobacco and nicotine products: Description of the scientific framework and assessment of a closed modular electronic cigarette. *Regul Toxicol Pharmacol*. 2007;90:342-357.
9. Pepper J, Brewer N. Electronic Nicotine Delivery System (Electronic Cigarettes) Awareness, Use, Reactions and Beliefs: A Systematic Review. *Tob Control*. 2014;23(5):375-384.
10. Margham J, McAdam K, Forster M, Liu C, Wright C, Mariner D, Procter C. Chemical Composition of Aerosol from an E-Cigarette: A Quantitative Comparison with Cigarette Smoke. *Chem Res Toxicol*. 2016;29:1662-1678.
11. Lawal O, Ahmed W, Nijsen T, Goodacre R, Fowler S. Exhaled breath analysis: a review of ‘breath-taking’ methods for off-line analysis. *Metabolomics*. 2017;13(110).
12. Berger R. *Flavours and Fragrances*. Springer Berlin; 2007;pp.372.
13. Ployon S, Morzel M, Canon F. The role of saliva in aroma release and perception. *Food Chem*. 2017;226:212-220.
14. Belitz H, Grosch W, Schieberle P. *Food Chemistry*. Springer Berlin; 2009;pp.340.

Understanding flavour isolation: Aroma analysis

Katrin Pechinger¹, Sam Wordsworth² and LEWIS L. JONES¹

¹ Sensient Technologies Corporation, Bletchley, United Kingdom, lewis.jones@sensient.com

² University of Nottingham, Nottingham, United Kingdom

Abstract

Flavour isolation is critical for the flavour industry. Isolation methods, such as extraction, are used to prepare samples for chemical analysis, ensuring a product's safety and authenticity. Extraction is also used to create natural flavourings that are used to impart an enjoyable smell and taste to foods. This work evaluates the extraction efficiency (EE) of two small-scale sample preparation techniques. Using this data, a machine learning model predicting the extraction efficiency of odorants was built using their physical-chemical properties, i.e. vapour pressure (VP) and the octanol:water partition coefficient (LogP), as well as the sample matrix composition. The model gives the analyst the ability to select the most appropriate extraction technique for their purpose. Historical work showed that there is no one perfect technique for flavour extraction [1]. This conclusion still holds true for the more modern techniques investigated here. For example, there is a considerable decrease in extraction efficiency for Solvent Assisted Flavour Evaporation (SAFE) when lipid is present in the extraction matrix. In fact, SAFE and Solid Phase Microextraction (SPME) both have low recoveries for volatile, hydrophilic compounds when used for sample preparation. Adapting the machine learning workflow to predicting the extraction efficiency of – potentially – any raw material would be a useful tool for the flavour industry. To test the application of this model to real-world raw material analysis, data on the extraction efficiency of ginger root using one of three isolation methods (CO₂ extraction, vacuum distillation, percolation) is currently being gathered.

Keywords: Sample Preparation, Flavour Manufacture, Extraction Efficiency, Modelling, Prediction

Introduction

Flavour analysis is carried out using a multitude of extraction techniques to isolate odorants (aroma-active volatile organic compounds, VOCs) before analysis; these techniques include SAFE and SPME. Ideally, isolation techniques remove all VOCs present in an unbiased manner, however, no available technique is currently able to achieve this. Therefore, the first objective of this study is to understand the bias associated with SAFE and SPME. This was achieved by calculating extraction efficiency of odorants from model matrices. Odorants were selected across a broad range of volatility and hydrophobicity with the model matrix comprising a mixture of water and oil. The second aim of this study is to determine whether extraction efficiency could be predicted using supervised machine learning. If successful, the prediction algorithm could be used to pre-select the best extraction method for a given raw material, saving valuable analysis time and money.

Experimental

Calculating Extraction Efficiency

A total of 21 odorants were selected (Table 1) from a comprehensive database [2] to cover a broad range of volatility (VP) and hydrophobicity (LogP). The odorants were subjected to stability testing to ensure stability over the experimental period. Odorant concentrations for the test mixture were set within the linear dynamic range of analytical instrumentation. The test mixture was then dosed into one of three matrices, i.e. 100% MCT, 10% MCT:90% water or 100% water, and extracted using SAFE and SPME. The test mixture itself and isolates from SAFE and SPME were analysed by Gas Chromatograph – Flame Ionization Detection (GC-FID), with EE calculated by comparison of peak areas [3].

For SAFE, a mixture of test matrix (50 g) and test mixture (200 µl) was extracted twice with diethyl ether (100 ml, 50 ml). The extract was then vacuum distilled [4], concentrated by Vigreux column (2 ml) and micro-distillation [5] to exactly 200 µl, allowing for direct comparison of test mixture to isolate by injection of 1 µl onto the GC.

For headspace SPME, a mixture of test matrix (6 g) and test mixture (2.4 µl) was equilibrated in a 22 ml headspace vial for 5 min at 40°C and then exposed to a 50/30 µm DVB/CAR/PDMS SPME fibre at 40°C for 35 min. The fibre was desorbed into the inlet of a GC-MS-FID and the results compared to an injection volume of 2.4 µl of test mixture, thus allowing direct comparison of test mixture and isolate.

An Agilent 7890 GC fitted with a Phenomenex FFAP column (30 m, 0.25 mm, 0.25 µm) was used to carry out all analyses. Post column the eluent was split at a 1:1 ratio to a FID and MS (Agilent 5975). GC column conditions

were as follows: 30°C for 1 min, 3°C/min to 60°C, 6°C/min to 250°C. Helium was used as a carrier gas (flow rate 3 ml/min). All injections were splitless.

Table 1: Model test mixture compounds, their CAS numbers, LogP and VP values. Trimethylamine and dimethyl sulphide were selected for the test mixture but subsequently excluded because they co-eluted with the solvent (diethyl ether) during GC [3].

Chemical Name	CAS	LogP	VP (mm Hg, 25°C)
Butan-2-one	000078-93-3	2.60E-01	9.85E+01
Dimethylfuran	000625-86-5	2.46E+00	4.94E+01
Ethyl octanoate	000106-32-1	4.27E+00	4.02E+00
2,3-butanedione (diacetyl)	000431-03-8	-1.34E+00	7.02E+01
1-(1,3-thiazol-2-yl)-1-ethanone	024295-03-2	-6.00E-02	9.66E+00
Dimethyl sulfoxide	000067-68-5	-1.22E+00	6.22E-01
Undecalactone	000104-67-6	6.70E-01	1.85E-01
Hydroxymethylfurfural	000067-47-0	4.14E+00	3.25E-03
Phenylacetic acid	000103-82-2	5.76E+00	1.11E-02
Pyrazine	000290-37-9	3.00E-01	1.45E-04
Undecen-1-ol	000112-43-6	2.61E+00	1.04E-01
Alpha-pinene	000080-56-8	3.85E+00	1.24E-02
Xylenol	000105-67-9	3.06E+00	4.09E-03
2,4-Dibromoanisole	021702-84-1	2.98E+00	4.12E-04
Androstrenone	018339-16-7	-9.00E-02	5.28E-03
Ethyl maltol	004940-11-8	1.55E+00	2.93E-04
Ethyl vanillin	000121-32-4	1.43E+00	3.86E-03
Hedione	024851-98-7	2.12E+00	4.87E-04
4-Chlorophenylacetic acid	001878-66-6	4.39E+00	3.17E-05
5-methyl-hexan-2-one	000110-12-3	2.60E-01	9.85E+01
1,10-Dichlorodecane	002162-98-3	2.46E+00	4.94E+01

Prediction of Extraction Efficiency by Machine Learning

To predict EE from our dataset with 126 observations, three machine learning models were built using R version 3.6.1: linear regression, Random Forest (RF) and Gradient Boosting Machine (GBM). The prediction variables were as follows: LogP, LogVP, sample preparation method and sample matrix. The models were trained and evaluated using the *caret* package [6]; the *ranger* method was used to train the RF model. To evaluate the performance of the models 5-fold cross-validation with 5 repeats was used. The performance metrics used to select the best model for prediction were root mean square error (RMSE), R^2 and mean absolute error (MAE). The four predictor variables were checked for collinearity and variable importance calculated using permutation (RF and GBM models only).

Results and discussion

Calculating Extraction Efficiency

Neither SPME nor SAFE resulted in unbiased extraction. SAFE was vastly more successful at extracting VOCs from all three matrices compared to SPME (Figure 1). For SAFE the extraction efficiency of VOCs from water exceeds 90% for VOCs with a VP of 1×10^{-4} to 0.1 mm Hg (25°C). However, when extracting from a mixture of water and MCT (10% w/w) the extraction efficiency of these VOCs reduces to less than 20%. In fact, both SAFE and SPME have low recoveries for very volatile (VP > 10 mm Hg, 25°C) and hydrophilic compounds (LogP < 0). Interestingly, neither of the methods was able to extract alpha-pinene from any of the matrices. This could be due to a number of reasons, e.g. co-elution or thermal degradation, and should be investigated further. Although the extraction efficiency of SPME is low, this does not generally result in smaller chromatographic peaks compared to SAFE isolates. This is due to the whole SPME isolate being injected onto the GC column during analysis as opposed to only a fraction of the isolate being injected during SAFE.

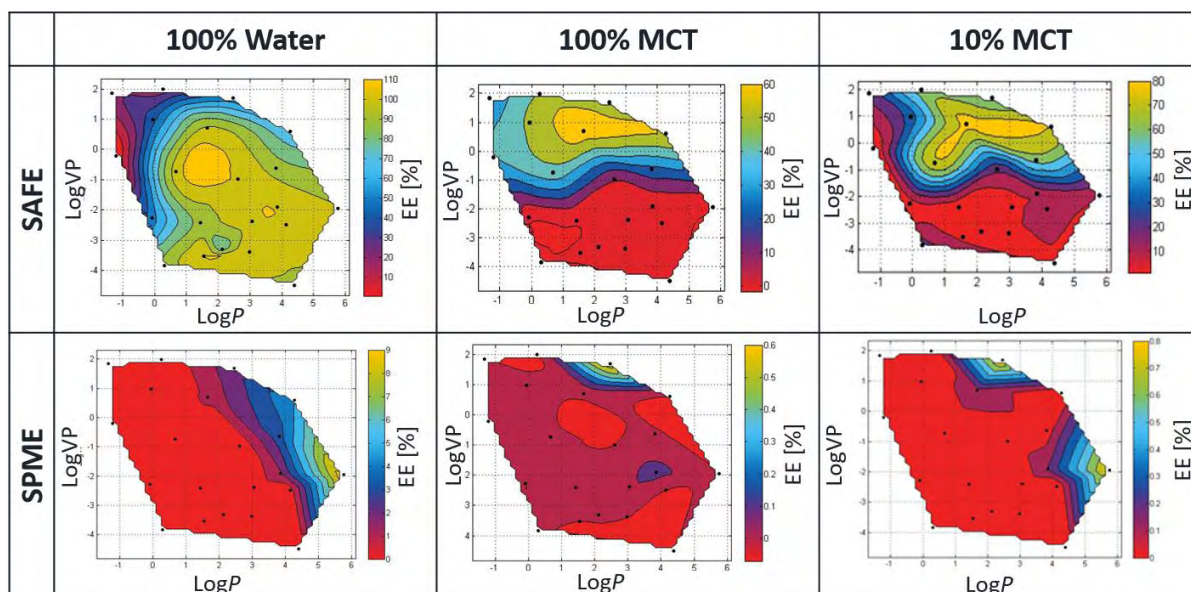


Figure 1: Contour plots showing extraction efficiency (EE) of chemicals across a range of $\text{Log}P$ and $\text{Log}VP$ values using SAFE or SPME in three different matrices, i.e. 100% water, 100% MCT or 10% MCT/90% water. Black points represent compounds in the test mixture. Contour plots were created using cubic interpolated surface plots in Matlab®.

Prediction of Extraction Efficiency by Machine Learning

Of the three models built to predict EE from $\text{Log}P$, $\text{Log}VP$, sample preparation method and sample matrix, the random forest model was best able to predict EE. The RF model outperformed the linear regression and GBM machine models on all metrics, i.e. RMSE, R^2 and MAE (Table 2). The final hyperparameters for the RF model were $mtry = 3$, $splitrule = variance$ and $min.node.size = 5$ (held constant).

Table 2: Performance metrics for three 5-fold cross-validated machine learning models.

Model	RMSE	R^2	MAE
Linear regression	25.76	0.47	19.96
Gradient Boosting Machine	21.69	0.61	17.16
Random Forest	13.89	0.83	7.70

The most important feature in the RF model was the sample preparation method followed by the make-up of the matrix and $\text{Log}VP$. It is to be noted though that the overall drop in accuracy was nearly 5 times as high for the most important feature (method) compared to the least important feature (vapour pressure). Interestingly, $\text{Log}P$ had an importance score of zero and therefore had no influence on the accuracy of predictions made by the model.

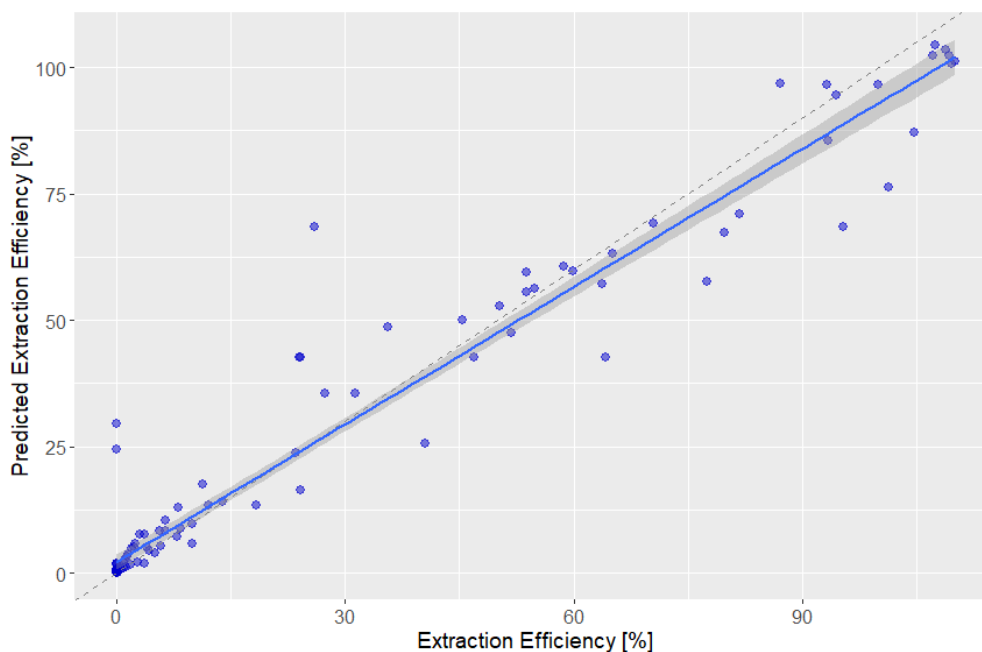


Figure 2: Measured extraction efficiency vs predicted extraction efficiency for 126 compounds predicted by the Random Forest machine learning model.

Conclusion

Neither SPME nor SAFE result in unbiased extraction of odorants. There is no one perfect sample preparation technique; neither SPME nor SAFE were able to efficiently extract volatile hydrophilic VOCs. To achieve holistic extraction, methods have to be combined and extraction techniques targeting volatile hydrophilic VOCs found. Extraction efficiency can be predicted using a Random Forest machine learning model. Of all the features considered, the extraction method had the greatest impact on EE. The physical-chemical properties did not have a significant effect on the prediction accuracy of the model; $\text{Log}P$ could be removed from the model and prediction accuracy would not change. Applying this machine learning model to raw materials, i.e. ginger root, is currently being explored.

References

1. Reineccius G. Flavor Chemistry and Technology: CRC Press; 2005.
2. Linforth R. University of Nottingham, personal communication. 2012.
3. Wordsworth S. Aroma Analysis Extraction Techniques Examined and Modelled to Show the Inherent Bias Towards Certain Physical and Chemical Properties.
4. Engel W, Bahr W, Schieberle P. Solvent assisted flavour evaporation – a new and versatile technique for the careful and direct isolation of aroma compounds from complex food matrices. *Eur Food Res Technol.* 1999;209(3):237-41.
5. Bemelmans J. Review of isolation and concentration techniques. *Progress in Flavour Research.* 1979;8:79-98.
6. Kuhn M. Building predictive models in R using the caret package. *J Stat Softw.* 2008;28(5):1-26.

Characterisation of Piemonte peppermint essential oil by gas chromatography-olfactometry (GC-O) and identification of trace key-odorants contributing to the sweet and round flavour by comprehensive two dimensional gas chromatography coupled to time-of-flight mass spectrometry

E. GABETTI¹, B. Sgorbini², F. Stilo², C. Bicchi², P. Rubiolo², F. Chialva³, S.E. Reichenbach⁴, V. Bongiovanni¹, C. Cordero² and A. Cavallero¹

¹ Soremartec Italia srl (Alba, Cuneo Italy)

² Università degli Studi di Torino, Dipartimento di Scienza e Tecnologia del Farmaco (Turin, Italy)

³ Azienda agricola Chialva, Pancalieri, Turin, Italy

⁴ University of Nebraska (Lincoln NE USA)

elena.gabetti@ferrero.com

Abstract

Peppermint essential oil (EO) is obtained by the steam distillation of the *Mentha × piperita* L. aerial parts; it is widely used in several fields including chewing gums, confectionary, oral hygiene products, pharmaceuticals and liquors.

Most peppermint EO is nowadays produced in United States but Italy has maintained a commercial production of peppermint EO confined to a restricted area in Piedmont (Torino and Cuneo Province) dated from the 18th century. Piedmont peppermint EO is produced from a single mint variety, i.e., the *Mentha × piperita* L. var. Italo-Mitcham (black mint), it is considered of very high quality and characterised by freshness and long lasting sweetness.

In this study, peculiar flavour characteristics of peppermint EO have been investigated by Gas Chromatography-Olfactometry (GC-O) using the Aroma Extraction Dilution Analysis (AEDA) approach. Among the compounds responsible for intense sweet, coconut, coumarin-like notes, the most intense odorant was menthofuroolactone (i.e., 3,6-Dimethyl-4,5,6,7-tetrahydro-benzo[b]-furan-2(3H)-one – CAS [16642-41-4]). This trace odour-active compound belongs to *p*-menthane lactones family that represents a class of minor components in peppermint EO although they highly affect the overall flavour profile. The presence of menthofuroolactone and related compounds (i.e., chemical signature) in different samples was confirmed by combining bi-dimensional retention data and spectral data collected at 70 and 12 eV by Comprehensive Two-Dimensional Gas Chromatography coupled to Time-of-Flight Mass Spectrometry (GC×GC-TOF MS) featuring tandem ionisation.

A selection of raw peppermint EOs from different geographic origin were accurately profiled by GC×GC-TOF MS to further investigate the distribution of these key-aroma compounds and reveal diagnostic signatures of *p*-menthane lactones family.

Piedmont peppermint EOs showed a diagnostically higher amount of this trace-odorant, and related compounds, compared to the other commercial EOs, as an evidence of its contribute to Piedmont EO rich and round flavour profile. A dedicated fingerprinting approach based on diagnostic signatures of potent odorants within specific retention windows, validate this correlation and poses solid foundation to an objective qualification of this highly valuable product.

Keywords: *Mentha × piperita* L. var. Italo-Mitcham, Piemonte peppermint, GC-O AEDA, GC×GC-TOF MS and tandem ionisation, fingerprinting

Introduction

The rationale of the work was to combine Comprehensive Two-Dimensional Gas Chromatography coupled to Time-of-Flight Mass Spectrometry (GC×GC-TOF MS) featuring Tandem Ionisation™ with off-line Gas Chromatography-Olfactometry GC-O/AEDA to capture the unique *signature* of Piemonte peppermint essential oil (EO), appreciated for its high quality due to sweet and rich profile [1, 2]. Moreover, chromatographic fingerprinting and accurate profiling of target components were exploited to characterise chemical features of peppermint EOs of different geographical areas.

The strategy of combining analytical data with sensory screening was applied to discriminate high-quality products out of the existing standard ISO compositional markers (ISO 856:2006 [3]).

GC×GC-TOF MS provides a greater sensitivity and separation power enhancement compared to mono-dimensional (1D)-GC, resulting in suitability for the analysis of highly complex matrices as essential oils. [4-10].

GC-O technique was used to orient data processing towards odour active regions locked by linear retention index (*I'*) of the GC×GC chromatographic space to discriminate samples connoted by different organoleptic profiles.

Experimental

EOs from *Mentha x piperita* L. var. Italo-Mitcham (formerly var. officinalis sole, species rubescens Camus), also known as Mitcham Mint from Pancalieri (PDO essential oil Menta di Pancalieri) of 2015-2019 harvest years were provided by Dr Franco Chialva (ChialvaMenta, Pancalieri, Turin, Italy).

Commercial samples of *Mentha x piperita* L. (var. Black Mitcham) representative of USA production regions: Idaho, Kennewick, Midwest, Northern California, Willamette, and Yakima from different harvest years were kindly provided by WILD Flavors Inc. (previously A.M. Todd ADM, Kalamazoo, USA).

A reference mixture of menthofurolactones (3,6-dimethyl-4,5,6,7-tetrahydro-benzo[b]-furan-2(3H)-one) for identity confirmation was kindly provided by Dr Eric Frérot (Firmenich, SA, Geneva, Switzerland).

Pure standards of *n*-alkanes (*n*-C9 to *n*-C25) for linear I^T calibration and internal standards 1,4-dibromobenzene, *n*-C13, and *n*-C17 were from Merck (Milan, Italy).

GC×GC-TOF MS featuring Tandem Ionisation™ setting and method parameters

GC×GC analyses were performed by an Agilent 7890B GC (Agilent Technologies, Santa Clara, CA, USA) coupled to a Bench TOF-Select™ system (Markes International, Llantrisant, UK) featuring Tandem Ionisation™: ionisation at 70 eV was used for identity confirmation and ionisation at 12 eV was set to obtain complementarity information from spectral signatures.

The system was equipped with a two-stage KT 2004 loop thermal modulator (Zoex Corporation, Houston, TX, USA) cooled with liquid nitrogen controlled by Optimode™ V.2 (SRA Instruments, Cernusco sul Naviglio, MI, Italy). The modulation period was set at 3 s and the hot-jet pulse time was 350 ms.

The column set-up consisted in the combination of a first-dimension (¹D) DB-5 column (30 m × 0.25 mm *d_c*, 0.25 μm *d_f*) coupled with a second-dimension (²D) OV1701 column (2 m × 0.1 mm *d_c*, 0.10 μm *d_f*), from Agilent J&W by a silTite μ-union (Trajan Scientific and Medical, Ringwood, Victoria, Australia). The first 0.80 m of the 2D column were wrapped in the modulator slit and used as loop-capillary for cryogenic modulation. Helium at a constant flow of 1.3 mL/min was used as carrier gas. The oven temperature program was: 40°C (1 min) to 280°C (5 min) at 3°C/min.

Peppermint EOs solutions (2.0 μL) at 5 g/L and 20 g/L were analysed in split mode, with a split ratio of 1:20.

GC-MS and GC-O/FID for Aroma Extract Dilution Analysis (AEDA)

GC-MS analyses of peppermint EOs were performed by an Agilent 7890B GC coupled to an Agilent 5977B MS detector with High Efficiency Source (HES) in EI mode at 70 eV. A DB-5 column (30 m × 0.25 mm *d_c*, 0.25 μm *d_f*) from Agilent J&W was used. The oven temperature program was 40°C (1 min) to 180°C at 3°C/min then to 280°C at 15°C/min (5 min). Peppermint EOs solutions (2.0 μL) at 5 g/L and 20 g/L were analysed in split mode, a split ratio 1:20.

GC-O/FID experiments were performed by an Agilent 7890A GC unit equipped with a FID and an olfactory detection port ODP 3 (Gerstel GmbH & Co., Mülheim an der Ruhr, Germany) on two different stationary phases, a Stabilwax-DA (30 m × 0.25 mm *d_c*, 0.50 μm *d_f*) and a Sil-5MS column (30 m × 0.25 mm *d_c*, 0.25 μm *d_f*) both from Restek Corporation (Bellefonte, Pennsylvania, USA). Samples were injected by split/splitless injection in splitless mode with the following oven temperature program: 33°C (1.5 min) to 230°C (15 min) at 6°C/min.

Peppermint EO (1 μL) was injected and the effluent was split to both the FID and the sniffing port-ODP 3 (1:3 split ratio). Sniffing was performed by six assessors within the flavour team of the Soremartec Italia Company. The EOs were stepwise diluted with ethanol (1:3 v/v) up to 729 times dilution and all the six dilutions (1:3, 1:9, 1:27, 1:81, 1:243, 1:729) were again evaluated by the whole panel Aroma Extract Dilution Analysis (AEDA) approach was applied to determine the flavour dilution (FD) factors [11] of the perceived odorants.

Data acquisition and data processing

GC×GC data were acquired by Markes TOF-DS software (Markes International) and processed by GC Image GC×GC Edition, ver. 2.9 (GC Image LLC, Lincoln, Nebraska, USA); GC-MS/FID data were acquired and processed by Agilent Enhanced MassHunter software (Agilent Technologies) and GC-O data were acquired by Agilent ChemStation software integrated with Gerstel's ODP Recorder 3.

Results and discussion

Comprehensive chromatographic fingerprinting on peppermint EOs samples

The GC×GC-TOF MS data elaboration workflow consisted in a comprehensive chromatographic fingerprinting based on template matching algorithms to extract metadata information (retention times, MS fragmentation patterns, and detector responses) from analysed samples, including both untargeted and targeted components (UT fingerprinting approach) [12].

Metadata extracted for 2D peaks and peak-regions were used to establish correspondences across multiple chromatograms by applying a spectral similarity threshold of 750 for direct match factor (DMF) and reverse match factor (RMF).

Peppermint samples showed a medium-complexity composition, more than 350 peak-regions were detected in peppermint EOs, among the 95 targeted compounds, 35 belonged to the *p*-menthane class.

Several minor components mono and sesquiterpenoids hydrocarbons rarely reported in literature were identified in all samples: α -thujene, (average 0.08% response), camphene (0.09%), alloaromadendrene (0.09%), α -terpinolene (0.198%), bicycloelemene (0.145%), and 1,5-di-epi- β -bourbonene (0.02%).

Potent odorants in Piemonte peppermint EOs

In the AEDA GC-O study, 35 odorants were perceived in Piemonte peppermint EO and 1,8-cineole (eucalyptus, fresh, camphoraceous), menthone (minty, herbaceous) and menthofuran (minty, musty, petroleum-like) showed the highest LogFD values (i.e., 8.11).

Some creamy and coconut-like sniffing impressions were detected until the last step dilution of AEDA, localised in the odour zone characterised by I^T range 1353-1356 on apolar column and by I^T range 2385-2386 on the polar one in the GC-O analyses.

A trace compound belonging to *p*-menthane lactones family with a very low odour-threshold (4.0×10^{-5} $\mu\text{g/L}$ air) [13] was identified as 3,6-dimethyl-4,5,6,7-tetrahydro-benzo[b]-furan- 2(3H)- one (i.e., menthofurolactone) by combining analytical data (I^T and EI-MS fragmentation pattern at 70 eV and 12 eV), olfactory profile, information reported in literature [13] and lastly the analysis of a reference mixture of menthofurolactones.

Menthofurolactone was mapped in all analysed peppermint EO samples but Piemonte EOs showed a higher relative abundance, 3.7 fold, compared to US samples; this suggests likely the contribution of this *p*-menthane lactones to the creamy and round flavour of Piemonte peppermint EO profile.

Data processing: combination of GCxGC chromatographic fingerprinting and GC-O results

The rationale adopted to drive data processing was to locate retention regions of the 2D retention space at which the most potent odorants perceivable at the third dilution of AEDA eluted. All the targeted and untargeted components eluting in odour active regions (within a ± 10 units 1D I^T) were selected and further processed (Figure 1). By prioritizing the investigation of volatiles on GC-O odour active regions, including targeted compounds and untargeted ones, Piemonte peppermint EOs were separately clustered from US samples.

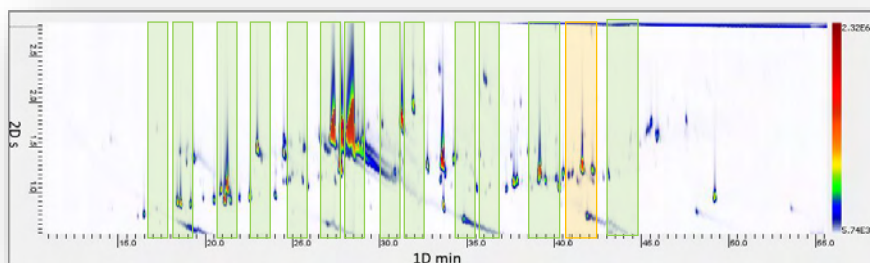


Figure 1: Retention regions (green rectangles) of the GCxGC 2D chromatogram at which the most potent odorants perceivable at the third dilution of AEDA of Piemonte peppermint EO eluted. Yellow rectangle highlights retention range in which creamy and coumarinic note was perceived.

Figure 2 illustrates the results of a hierarchical clustering (HC) on % Responses from 131 UT compounds perceivable at the third dilution of AEDA; HC was based on Pearson correlation values after Z-score data normalization. Among the most discriminant components highlighted by the Variable Importance in the Projection (VIP) derived from partial least-squares discriminant analysis (PLS-DA) on Piemonte vs. US EOs, targeted analytes were: 4-methyl-2-propan-2-yl-1,3-thiazole, *p*-cymene, (*E*)- β - caryophyllene, *p*-cymenene, menthofurolactone isomer II, 2-methylbutyl 3-methylbutanoate, 2,5- diethyltetrahydrofuran, isomenthone, β -myrcene, (*E*)-6,10-dimethylundeca-5,9-dien-2-one, oct-1-en-3-ol, pulegone, and camphene, with most of them already detected by GC-O.

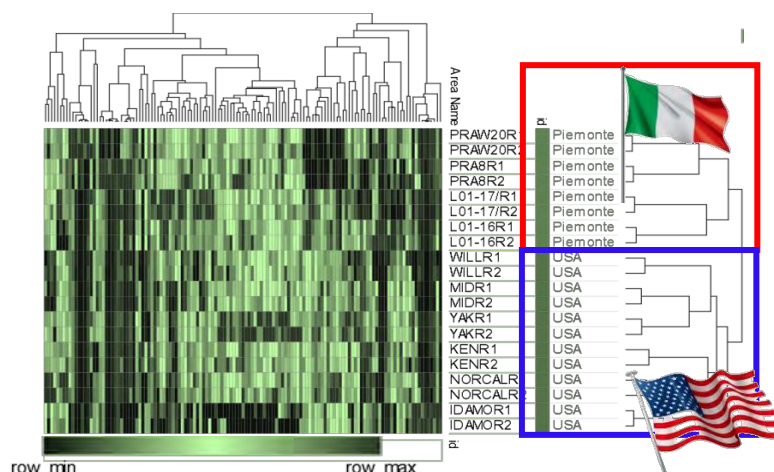


Figure 2: Hierarchical Clustering on % Responses from 131 UT compounds perceivable at the 3rd dilution of AEDA in Piemonte peppermint EO.

Conclusions

Chromatographic fingerprinting by GC×GC-TOF MS combined to AEDA GC-O data results in a successful strategy to capture characteristic odorant patterns of Piemonte peppermint EO [14].

Odour-driven data processing helps to identify volatile/odorant components and peak-regions diagnostic of the composition of Piemonte peppermint achieving an efficient discrimination between Piemonte and US peppermint samples.

References

1. Lawrence B.M., The composition of commercially important mints, in: *Mint Genus Mentha*, Taylor & Francis, 2006:217–319.
2. Näf R., Velluz A. Phenols and lactones in Italo-Mitcham peppermint oil *Mentha x piperita* L. *Flavour Fragr J.* 1998;13:203–208.
3. ISO International Organization for Standardization, ISO 856:2006 Oil of peppermint (*Mentha x piperita* L.). 2006:18.
4. Cordero C., Kiefl J., Reichenbach S.E., Bicchi C. Characterization of odorant patterns by comprehensive two-dimensional gas chromatography: A challenge in omic studies. *Trends Anal Chem.* 2019;113:364–378.
5. Adahchour M., Beens J., Vreuls R.J.J., Brinkman U.A.T., Recent developments in comprehensive two-dimensional gas chromatography (GC x GC). IV. Further applications, conclusions and perspectives. *Trends Anal Chem.* 2006;25:821–840.
6. Adahchour m., van Stee L.L.P., Beens J, Vreuls R.J.J., Batenburg M.A., Brinkman U.A.T., Comprehensive two-dimensional gas chromatography with time-of-flight mass spectrometric detection for the trace analysis of flavour compounds in food. *J Chromatogr A.* 2003;1019:157–172.
7. Cordero C., Kiefl J., Schieberle P., Reichenbach S.E., Bicchi C., Comprehensive two-dimensional gas chromatography and food sensory properties: Potential and challenges. *Anal Bioanal Chem.* 2015;407:169–191.
8. Tranchida P.Q., Donato P., Cacciola F., Beccaria M., Dugo P., Mondello L., Potential of comprehensive chromatography in food analysis. *Trends Anal Chem.* 2013;52:186-205.
9. Tranchida P.Q, Franchina F.A., Dugo P., Mondello L., Comprehensive two-dimensional gas chromatography-mass spectrometry: Recent evolution and current trends, *Mass Spectrom Rev.* 2016;35:524–534.
10. Stilo F., Bicchi C., Jimenez-Carvelo A.M., Cuadros-Rodríguez L., Reichenbach S.E., Cordero C., Chromatographic fingerprinting by comprehensive two-dimensional chromatography: Fundamentals and tools. *Trends Anal Chem.* 2021;134:116-133.
11. Belitz H.D., Grosch W., Schieberle P., *Food Chem.* 2013; doi: 10. 1017/CBO9781107415324.004.
12. Magagna F., Valverde-Som L., Ruíz-Samblás C., Cuadros-Rodríguez L., Reichenbach S.E., Bicchi C., Cordero C., Combined untargeted and targeted fingerprinting with comprehensive two-dimensional chromatography for volatiles and ripening indicators in olive oil. *Anal Chim Acta.* 2016;936:245–258.
13. Frérot E., Bagnoud A., Vuilleumier C. Menthofurocatone: a new p-menthane lactone in *Mentha piperita* L.: analysis, synthesis and olfactory properties, *Flavour Fragr J.* 2002;17:218–226.
14. Gabetti E., Sgorbini B., Stilo F., Bicchi C., Rubiolo P., Chialva P., Reichenbach S.E., Bongiovanni V., Cordero C., Cavallero A., Chemical fingerprinting strategies based on comprehensive two-dimensional gas chromatography combined with gas chromatography-olfactometry to capture the unique signature of Piemonte peppermint essential oil (*Mentha x piperita* var Italo-Mitcham). *J Chromatogr A.* 2021;1645:462101.

Analysis of retro-nasal flavour of beef pate using a chewing simulator

KAZUHIRO HAYASHI¹, Yuji Nakada¹, Etienne Semon² and Christian Salles²

¹ Institute of Food Sciences & Technologies, Ajinomoto Co. Inc., Japan, kazuhiro_hayashi@ajinomoto.com

² CSGA, AgroSupDijon, CNRS, INRAE, Université Bourgogne Franche-Comté, 17 rue Sully, 21000, Dijon, France

Abstract

In the case of retro-nasal aroma, since the aroma compounds released from the food during chewing are targeted, the change of the food structure during chewing (crushing, grinding, disintegration, melting, dilution by saliva, etc.) strongly influences the release and thus the perception. In this study, the relation between retro-nasal flavour and food deliciousness based on the physicochemical properties of flavour was examined. Beef pate was used as a model to study flavour release under controlled in vitro mastication and salivation conditions considering the consumption of solid foods and elderly people, using a chewing simulator. In addition, with the recent aging society, the number of elderly people who cannot enjoy eating due to the deterioration of eating function has been increasing. The decrease in masticatory ability, muscle weakness of the swallowing muscles, and changes in saliva composition and secretion volume contributed to a decrease in taste, smell, and other perceptions. Also, in this study, the effect of these oral parameters on flavour release under controlled chewing and saliva conditions considering the eating of the elderly person was further examined by the utilization of the chewing simulator. Through these studies, it was found that the effect of coexisting ingredients such as beef fat on the time course behaviour of aroma release, it was confirmed that the release curve of middle and last type aromas in particular changed depending on the strength of chewing and fat content. Considering the model saliva of the elderly, it is presumed that the lowering of the flavour sensation in the elderly is also caused by the change of the saliva composition.

Keywords: aroma release, pate, chewing simulator, fat content, elderly

Introduction

Olfactory sensation is the sensation produced by the interactions of aroma compounds with receptors of the olfactory cells on the olfactory epithelium at the top of the nasal cavity. It is also possible to feel the flavour when eating and drinking food by putting it in your mouth. This is called a retro-nasal aroma, aroma compounds radiated from the food in the oral cavity reaching the nasal cavity through the respiratory tract to be sensed. In the case of retro-nasal aroma, since the aroma compounds released from the food during chewing are targeted, the change of the food structure during chewing (crushing, grinding, disintegration, melting, dilution by saliva, etc.) strongly influences the release and thus the perception. In this study, the relation between retro-nasal flavour and food deliciousness based on the physicochemical properties of flavour was examined. Beef pate was used as a model to study the flavour release under controlled in vitro mastication and salivation conditions considering the consumption of solid foods and elderly people, using a chewing simulator [1] to analyse multiple samples without individual differences in the contribution of flavour during mastication of solid materials. In this presentation, the effect of these oral parameters on flavour release under controlled chewing and saliva conditions considering the eating of the elderly person was further examined by the utilization of the chewing simulator.

Experimental

Materials

Beef pate was prepared as follow. Minced beef lean meat 50g was placed in a mould and shaped. Then, it was grilled with a 180-degree Celsius hot plate for 3 minutes in the front and 2 minutes in the back. Crushed pate with added aroma compounds was placed in a mould and shaped. High-fat samples in which 10% and 20% of bovine fat were added, were also prepared and examined.

Each aroma compound was added such as the final concentration was 0.1% (1000ppm) as shown in Table 1.

The standard artificial saliva [2, 3] was dissolved by blending NaHCO₃: 5.20g, K₂HPO₄: 1.36g, NaCl: 0.88g, KCl: 0.48g, CaCl₂: 0.44g, Mucin (M1778-10g, from porcine stomach) 2.16g into 1L of milli-Q water.

PTR-TOF-MS

The drift tube of a PTR-TOF 8000 (Ionicon, Innsbruck, Austria) was kept under controlled conditions of pressure (2.3 mbar), temperature (50° Celsius) and voltage (480 V) resulting in a field density ratio (E/N) of 110

Td (E being the electric field strength and N the gas number density; $1 \text{ Td} = 10^{-17} \text{ V cm}^2$). Detected aroma compounds and ions were as shown in Table.1

Table 1: PTR-MS detected compounds and ions.

Compounds name	m/z	Log ow	Log aw
methanethiol (MeSH)	49.011	0.78	-0.89
butanoic acid	89.0597	0.79	4.66
furfural	98.0318	0.41	3.81
dimethyl trisulfide (DMTS)	128.966	1.87	1.12
nonanal	143.143	4.79	1.52

Log ow: oil-water partition coefficient; Log aw: air-water partition coefficient

Chewing Simulator

The samples used were 5g pate pieces. The operating condition of the chewing simulator was basically Force: 25daN and Share Angle: 2 degrees unless otherwise stated. The influx of artificial saliva into chewing simulator was carried out at a setting of 1ml/min. The data were run in n=5 and averaged. Nitrogen flow to chewing simulator was carried out at 70 ml/min. Varying chewing simulator operation conditions was as follows. Force: 25daN, Share Angle: 2 degrees (weak chewing), and Force: 30daN, Share Angle: 3 degrees (normal chewing)

Data Processing

PTR-MS flavour release curves were processed in the following manner. Slope of the Nth chewing: Relative peak intensity of the Nth mastication/peak intensity of the first mastication, I_{max}: Maximum peak intensity, T_{max}: Number of mastication showing maximal peak intensity

Results and discussion

Using PTR-MS, we examined the aroma release behaviour of the samples for which the chewing strength and fat content in the pate were changed. From T_{max} results shown in Figure 1a, the flavour release became faster when the strength of chewing was increased (T_{max} decrease) and became slower when the lipid content was increased (T_{max} increase) The flavour release tended to be faster for 20% of lipids. I_{max} results showed that the release amount increased when the strength of mastication increased, and the release amount decreased when the lipid content increased. Figure.1b showed that the flavour release became faster when the strength of mastication increased, and the flavour release became slower when the lipid content increased.

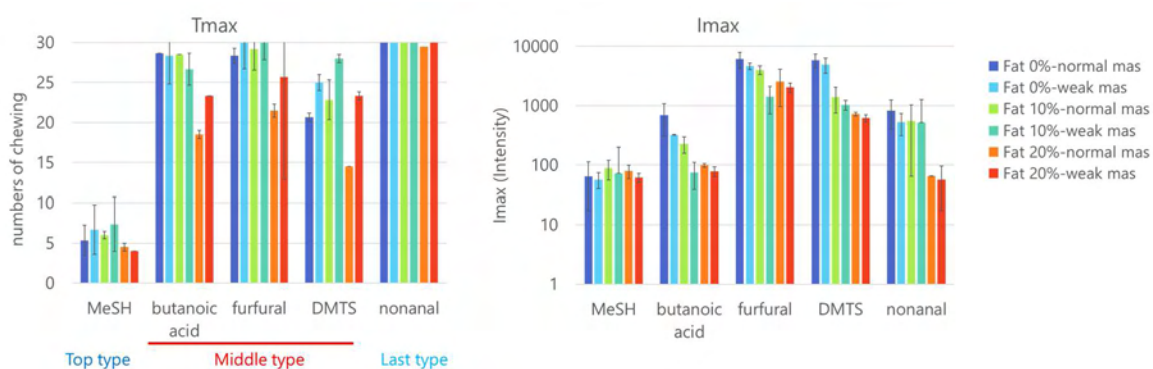


Figure 1a: Changes in aroma release due to differences in the strength of mastication and the amount of fat.

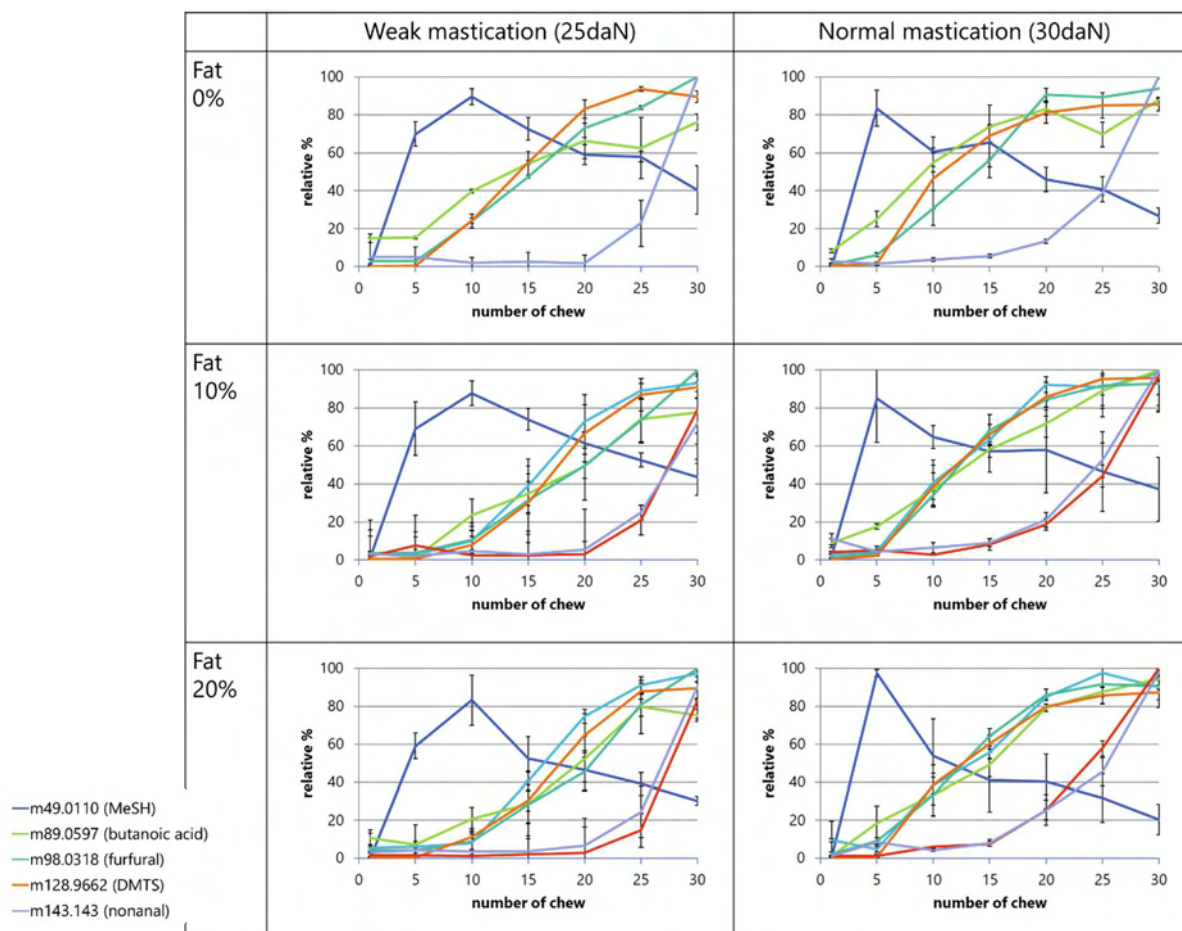


Figure 1b: Changes in aroma release due to differences in the strength of mastication and the amount of fat.

Confirmation based on the saliva composition and saliva flow rate of the elderly people as shown in Table 2 were used to model elderly flavour release. As a result of Figure 2, in salivary compositions 2 and 3, the flavour release of all compounds was delayed due to the increase in Tmax, and the decrease in I_{max} was also observed, thereby confirming the tendency of the intensity to be suppressed. In addition, it was confirmed that a change in the saliva flow rate influences a change in the flavour release more than a change in the mucin amount. It is presumed that these are largely due to the decrease in the salting-out effect including inorganic salts contained in artificial saliva. It was presumed that it was one of the causes which made it difficult to feel the flavour of the elderly people.

Table 2: Elderly artificial saliva composition and flow.

(g)	1. Std	2.High concentration (30%), half flow (50%)	3. 2 & half mucin
Water	1000	1000	1000
NaHCO ₃	0.397	0.567	0.567
K ₂ HPO ₄	0.645	0.921	0.921
NaCl	0.067	0.0957	0.0957
KCl	0.774	1.11	1.11
CaCl ₂	0.205	0.293	0.293
Mucin	2.16	3.09	1.54
flow rate	1ml/min	0.5ml/min	0.5ml/min

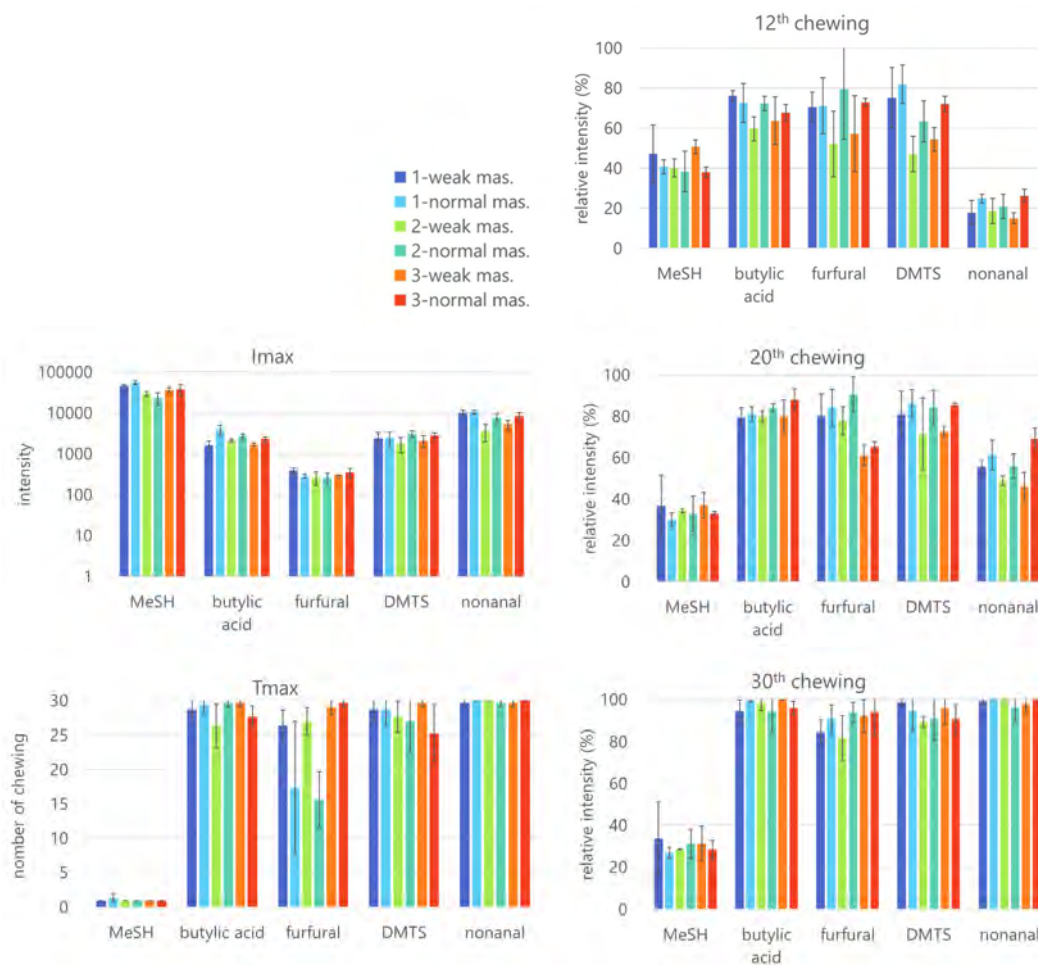


Figure 2: Changes in aroma release due to differences in the strength of mastication, saliva composition and flow.

Conclusion

Studying the effect of coexisting components on the time course behaviour of aroma releases using PTR-MS, it was presumed that there were three major patterns of "top type", "middle type", and "last type" and that they were related to the physicochemical properties of the aroma compounds. In addition, the degree of mastication and lipid content changed, especially the release curves of middle and last type compounds were delayed and suppressed, and it was speculated that mastication degree and matrices including lipids strongly affected flavour release.

As a result of the examination using the elderly person model saliva, the suppression of the aroma release was confirmed by the decrease of the saliva flow rate. The decrease of the salting-out effect was presumed to be a factor, and the decrease of the flavour sensation in the elderly was presumed to be a consequence of the change of the saliva composition.

References

1. Salles C, Tarrega A, Mielle P, Maratray J, Gorria P, Liaboef J, Liodenot J.-J. Development of a chewing simulator for food breakdown and the analysis of in vitro flavor compound release in a mouth environment. *J Food Eng.* 2007;82:189-198.
2. Nagler R.M, Hershkovich O. Relationships between age, drugs, oral sensorial complaints and salivary profile. *Arch. Oral Biol.* 2005;50(1):7-16.
3. Vissink A, Spijkervet F.K.L, Amerongen A.V.N. Aging and saliva: A review of the literature. *Special Care in Dentistry.* 1996;16(3):95-103.

Studies on the enantiomers of dehydrorose oxide (4-methylene-2-(2-methylprop-1-enyl)oxane)

SHUNSUKE TAKISHIMA, Yasuhiro Fukui, Shunsuke Konishi, Kenji Haraguchi and Yuichiro Ohmori

R & D Center, T. Hasegawa Co., Ltd., Kariyado, Nakahara-ku, Kawasaki-shi. 211-0022, Japan, shunsuke_takishima@t-hasegawa.co.jp

Abstract

Dehydrorose oxide (4-methylene-2-(2-methylprop-1-enyl)oxane) (DHRO) is mainly responsible for the Muscat-like aroma of Darjeeling black tea. To reveal the characteristics of the enantiomers in DHRO as flavour components, pure enantiomers of DHRO were obtained by optical resolution through chiral high-performance liquid chromatography. (*R*)-DHRO has green, metallic, and oily notes, whereas (*S*)-DHRO has a juicy Muscat-like aroma. The odour thresholds of both enantiomers are almost identical. In multidimensional chiral gas chromatography/mass spectrometry analysis, DHRO was identified as a racemate in Darjeeling black tea. When the enantiomers were added to a model black tea, (*R*)-DHRO enhanced the feeling of tea leaves, whereas (*S*)-DHRO enhanced the Muscat-like aroma.

Keywords: 4-methylene-2-(2-methylprop-1-enyl)oxane, dehydrorose oxide, optical resolution, Darjeeling black tea, Muscat-like aroma

Introduction

Our company has discovered the main ingredient that gives Darjeeling black tea its unique Muscat-like aroma [1, 2]: dehydrorose oxide (4-methylene-2-(2-methylprop-1-enyl)oxane) (DHRO) (refer the proceeding written by Fukui et al. entitled “Identification of a key odorant contributing to Muscat aroma of Darjeeling black tea”). As the DHRO molecule contains an asymmetric carbon atom, it has two enantiomers. The enantiomers of DHRO were reported as synthetic products [3, 4], but their odours were not described in detail, so their characteristics as flavour components remain unknown. The present study aims to ascertain the difference in the odour of the enantiomers of DHRO, measure the optical isomer ratio of DHRO in Darjeeling black tea, and determine the effect the addition of these isomers has on a model black tea.

Experimental

Synthesis of racemic DHRO

KHSO₄ (1.09 g, 8.00 mmol) and toluene (380 g) were heated to an azeotropic temperature and a mixture of 3-methyl-3-buten-1-ol (172 g, 2.00 mol) and 3-methyl-2-butenal (168 g, 2.00 mol) was added dropwise for 3 hours. After 2 hours of azeotropic dehydration, the reaction mixture was cooled to 80 °C, and 10% aq. NaOH (300 g) was added and refluxed for 30 minutes. After cooling to room temperature, the organic layer was isolated, washed with brine, concentrated in vacuo. The concentrate was distilled to obtain DHRO (85.5 g, 28.1% yield).

Optical resolution by chiral HPLC

Synthesised racemic DHRO was injected into a chiral high-performance liquid chromatography (HPLC) instrument (Shimadzu, Japan). The separation was performed on CHIRALPAK[®] IG 5 μm (4.6 mm I.D. × 250 mm, DAICEL, Japan) filled with polysaccharide-derived stationary phases (amylose tris-(3-chloro-5-methylphenylcarbamate) immobilised on silica gel). The mobile phase was 99.9/0.1 hexane/ethanol (isocratic) and the column oven was set to 25 °C. DHRO was detected by ultraviolet absorbance (210 nm). Under the analytical condition, the flow rate was 1.0 mL/min and the sample load was 10 μg racemic DHRO. In chiral HPLC preparation, the inner column diameter, flow rate, and sample load were scaled up to 20 mm, 19.0 mL/min, and 7.5 mg, respectively. After 130 cycles of HPLC preparation and distillation, approximately 300 milligrams of both enantiomers were obtained. The enantiomers were dissolved in CHCl₃ and their optical rotations were measured using a P-2300 polarimeter (Jasco, Japan). Their enantiomeric excess (ee) were calculated from the areas under the peaks in the chiral HPLC chromatogram. (*R*)-DHRO: retention time 6.7 min, yield 349 mg, [α]_D²⁰ +31.5° (*c* = 1.03, CHCl₃), >99% ee; (*S*)-DHRO: retention time 8.0 min, yield 274 mg, [α]_D²⁰ -31.7° (*c* = 1.01, CHCl₃), >99% ee.

Preparation of the Darjeeling black tea infusion and chiral multidimensional GC/MS

Darjeeling second-flush black tea (GOOMTEE MUSCATEL VALLEY, FTGFOP1, 2016-DJ19) was purchased from a local shop (LUPICIA, Japan). Hot water (300 g) was added to the tea leaves (3 g) and tea was extracted for 5 minutes. After extraction, the tea leaves were separated and the infusion was immediately cooled to 25 °C. Sodium chloride (15 g) was added to the obtained infusion (100 g) and the flavour components of the Darjeeling second-flush black tea infusion were extracted using the stir bar sorptive extraction (SBSE) method with a TWISTER® (Gerstel, Germany) magnetic stir bar coated with polydimethylsiloxane. The flavour components were injected into a multidimensional gas chromatography (GC) through a thermal desorption unit (TDU) instrument. The GC/mass spectrometry (MS) system comprised a GC-MSD 1D/2D LTM system (Agilent, USA) with TD3.5+ (Gerstel). The first column was a DB-WAX (30 m × 0.25 mm × 0.25 μm, Agilent) and the second column was an InertCap CHIRAMIX® (30 m × 0.25 mm × 0.25 μm, GL Sciences, Japan) [5]. The heart cut was performed at 18.8–19.8 min (established by the synthesised DHRO) in the first separation polar column, and the flavour components (including DHRO) were installed in the second separation chiral column. The optical ratio was calculated from the peak areas in the GC/MS extracted ion chromatogram (m/z 85).

Sensory evaluation

All panellists were trained assessors from the R&D Centre of T. Hasegawa Co., Ltd.

The odour thresholds of DHRO in water were determined by 20 assessors (14 males and 6 females; age range 20–50 years). The assessment method was reported elsewhere [6].

The effect of DHRO on a model black tea was assessed in a descriptive analysis by 12 assessors (8 males and 4 females; age range 20–50 years). (*R*)-DHRO, (*S*)-DHRO, and racemic DHRO were added (0.5 μg/kg each) to an aroma recombinant solution. The composition of this solution was based on the quantitative values of the aroma compounds in Darjeeling black tea [7], and its orthonasal aroma was subjected to sensory evaluations.

Results and discussion

Synthesis of racemic DHRO

DHRO was synthesised via Prins cyclization reaction of 3-methyl-3-buten-1-ol and 3-methyl-2-butenal in the presence of an acid catalyst. The formed DHRO was obtained as a mixture with nerol oxide (Figure 1). After distillation, pure DHRO (>99%) was obtained (28.1% yield).

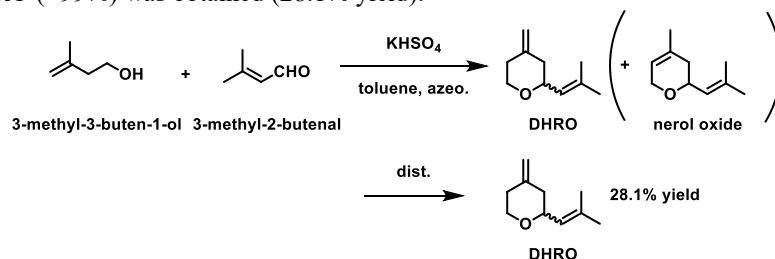


Figure 1: Synthesis scheme of DHRO.

Optical resolution of DHRO

The optical resolution of the synthesised racemic DHRO was conducted using chiral HPLC with polysaccharide-derived chiral stationary phases (Figure 2). After many cycles of HPLC preparation and distillation of peaks (1) and (2), hundreds of milligrams of both enantiomers were obtained. The enantiomers were extremely chemically pure with high enantiomeric excess (Figure 3). Their absolute configurations were previously identified through optical rotation [3]. The (*R*)-enantiomer is dextrorotatory (+) while the (*S*)-enantiomer is levorotatory (−).

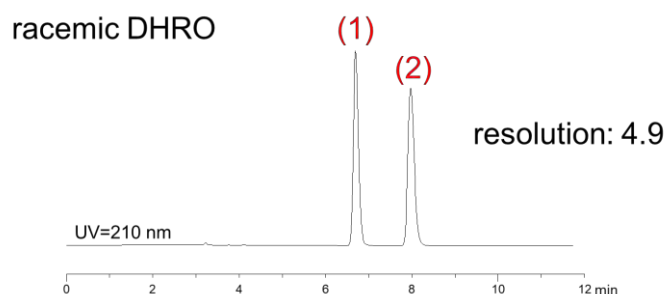


Figure 2: Chiral HPLC chromatogram of racemic DHRO.

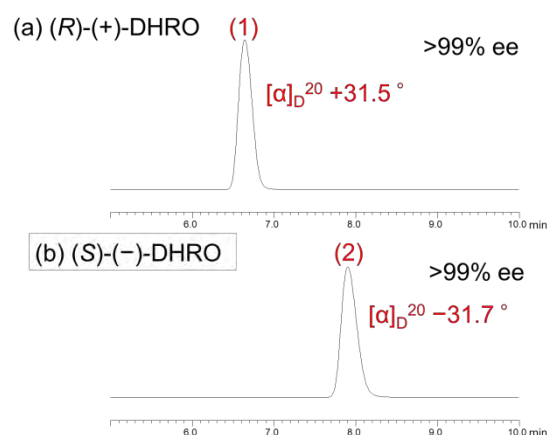


Figure 3: Chiral HPLC chromatogram of the prepared DHRO: (a) (*R*)-DHRO [peak (1)] and (b) (*S*)-DHRO [peak (2)].

Olfactory properties and odour thresholds of pure DHRO enantiomers

(*R*)-(+)-DHRO has green, metallic, and oily notes, whereas (*S*)-(-)-DHRO has a juicy Muscat-like aroma. On average, the odour thresholds of the (*S*)-enantiomer and (*R*)-enantiomer were almost identical (Table 1). However, the (*S*)-enantiomer was rated as much more odorous than the (*R*)-enantiomer by some assessors, who could detect the odour at the sub-ppt level.

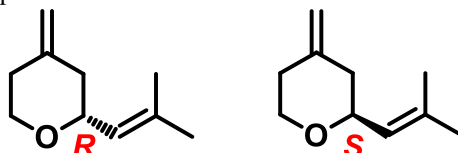


Figure 4: Structures of (*R*)-(+)-DHRO and (*S*)-(-)-DHRO.

Table 1: Olfactory properties and odour thresholds of pure DHRO enantiomers.

	(<i>R</i>)-(+)-DHRO	(<i>S</i>)-(-)-DHRO
olfactory property	green, metallic, oily	juicy Muscat-like
odour threshold	0.2 µg/kg (in water)	0.1 µg/kg (in water)

※The odour threshold of racemic DHRO is 0.2 µg/kg.

Optical isomer ratio of DHRO in Darjeeling black tea

The optical isomer ratio of DHRO in nature was determined using chiral GC/MS (Figure 5). The flavour components of the Darjeeling black tea infusion (GOOMTEE farm, FTGFOP1) were extracted using the SBSE method. The flavour components were injected into the multidimensional GC through a TDU instrument. In the chromatogram of Darjeeling black tea, the peak areas corresponding to (*S*)- and (*R*)-DHRO were the same, affirming that DHRO exists as a racemate (Figure 6).

Different types of Darjeeling black tea (the first, second, and third flush from another farm) were also analysed using chiral GC/MS. Although the DHRO in these variants differed in content, it was always racemic (data not shown).

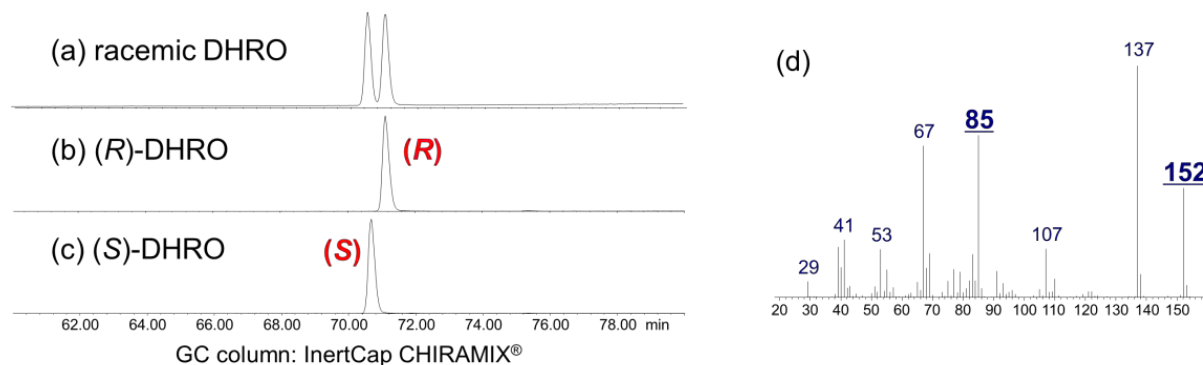


Figure 5: Chiral GC/MS chromatograms of (a) synthesised racemic DHRO, (b) (*R*)-DHRO, and (c) (*S*)-DHRO; (d) mass spectrum of DHRO.

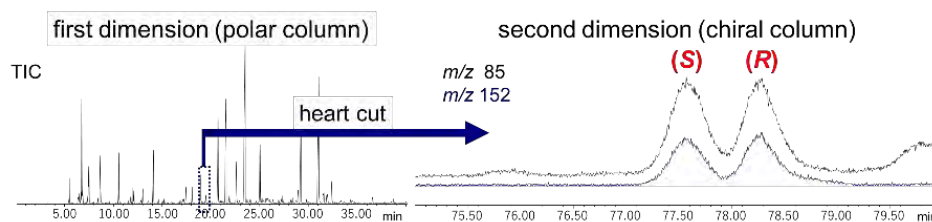


Figure 6: Multidimensional GC/MS chromatogram of Darjeeling black tea (GOOMTEE farm, FTGFOP1).

Effect of DHRO on a model black tea

(*R*)-DHRO, (*S*)-DHRO, and racemic DHRO were added (0.5 µg/kg each) to an aroma recombinant solution. The components of this solution were based on the quantitative values of aroma compounds in Darjeeling black tea [7]. In sensory evaluations of their orthonasal aromas (Figure 7), it was found that (*R*)-DHRO enhanced the feeling of tea leaves, whereas (*S*)-DHRO enhanced especially the Muscat-like aroma (Table 2).

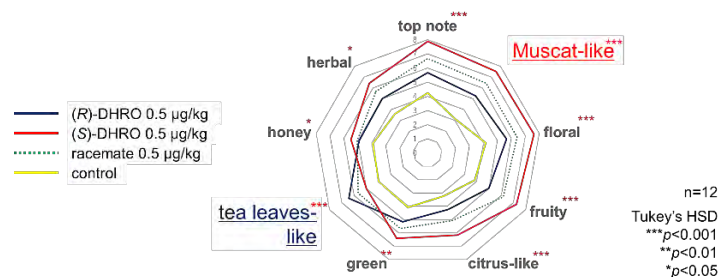


Figure 7: Sensory evaluation of the model black tea (orthonasal).

Table 2: Summary of effect of DHRO on a model black tea.

Added DHRO	Effect on the model black tea
(<i>R</i>)-DHRO	Enhances the feeling of tea leaves strongly.
(<i>S</i>)-DHRO	Enhances many features, especially the Muscat-like aroma.
Racemic DHRO	All scores are intermediate between those of (<i>R</i>)- and (<i>S</i>)-DHRO.

Conclusion

The enantiomers of DHRO obtained by chiral HPLC optical resolution have almost identical odour thresholds [(*R*): 0.2 µg/kg, (*S*): 0.1 µg/kg] and different odour characteristics. (*R*)-DHRO has green, metallic, and oily notes, whereas (*S*)-DHRO has a juicy Muscat-like aroma. Multidimensional chiral GC/MS analysis revealed that DHRO exists as a racemate in Darjeeling black tea. When the enantiomers were added to a model black tea, and subjected to sensory evaluations by 12 assessors, (*R*)-DHRO enhanced the feeling of tea leaves, whereas (*S*)-DHRO enhanced the Muscat-like aroma. In fact, the (*S*)-enantiomer was mainly responsible for the Muscat-like aroma of Darjeeling black tea. Therefore, using the (*S*)-DHRO as a flavour compound should be effective in increasing the palatability of the black tea flavourings.

References

- Kawakami, M., Ganguly S. N., Banerjee, J., Kobayashi, A. Aroma Composition of Oolong Tea and Black Tea by Brewed Extraction Method and Characterizing Compounds of Darjeeling Tea Aroma. *J Agric Food Chem.* 1995;43(1):200-207.
- Baba, R., Nakamura, A., Kumazawa, K. Identification of the Potent Odourants Contributing to the Characteristic Aroma of Darjeeling Tea Infusion. *J Jpn Soc Food Sci Technol.* 2017;64(6):294-301.
- Ohloff, G., Giersch, W., Schulte-Elte, K. H., Enggist, P., Demole, E. Synthesis of (*R*)- and (*S*)-4-Methyl-6-2'-methylprop-1'-enyl-5,6-dihydro-2*H*-pyran (Nerol oxide) and Natural Occurrence of its Racemate. *Helv Chim Acta.* 1980;63(6):1582-1588.
- Liu, L., Kaib, S. J. P., Tap, A., List, B. A General Catalytic Asymmetric Prins Cyclization. *J Am Chem Soc.* 2016;138(34):10822-10825.
- Tamogami, S., Awano, K., Amaike, M., Takagi, Y., Kitahara, T. Development of an efficient GLC system with a mixed chiral stationary phase and its application to the separation of optical isomers. *Flavour Fragr J.* 2001;16(5):349-352.
- Meilgaard, M., Civille, G. V., Carr, B. T. *Sensory Evaluation Techniques* (5th edition). Boca Raton, FL, CRC Press 2016;pp. 153-163.
- Schieberle, P., Schuh, C. Characterization of the Key Aroma Compounds in the Beverage Prepared from Darjeeling Black Tea: Quantitative Differences between Tea Leaves and Infusion. *J Agric Food Chem* 2006;54(3):916-924.

The taste of future foods: molecular insight into plant protein and flavour binding

CRISTINA BARALLAT¹, Teresa Oliviero¹, Hans-Gerd Janssen^{1,2}, Sara I.F.S. Martins^{1,2}, Vincenzo Fogliano¹

¹Wageningen University & Research, Food Quality and Design Group, Wageningen, The Netherlands

²Unilever Research & Development, Wageningen, The Netherlands
cristinal.barallatperez@wur.nl

Abstract

Plant proteins have gained attention to be used as healthier ingredients in new food applications. However, indigenous off-flavours, such as bitterness and astringency, reduce consumer liking and acceptability of plant-based food products. To tackle this concern often flavour addition is seen as a solution. Nevertheless, proteins can interact extensively with flavour molecules that can bind the protein's binding sites, thus affecting their release. As a result, overall flavour perception is disrupted. Therefore, this study aims to unravel the drivers of the binding mechanism at the molecular level, and determine how the chemical structure of both aroma molecules and proteins has an impact on the interactions with plant proteins and thus, on aroma release and retention. Hence, we hypothesize that size and shape of aroma molecules may influence the strength, nature and behaviour of these interactions. In the current preliminary study, binding to PPI (1%) capacity increased by enlarging the chain length of ketones, which is related to hydrophobic interactions. Exponential growth by 1.5% is observed when adding an extra carbon atom to the ketone molecules. A flavour chemical structure with an extensive number of carbon atoms and thus, long carbon chains, will lead to the existence of more binding sites and lastly, to a higher binding tendency. Besides, binding to PPI (1%) decreased in the following order: *trans*-2-nonenal (95%)>nonanal (85%)>2-nonanone (52%). The location of the functional group at the end of nonanal resulted in a higher binding as compared to the functional group located more in the middle of the structure (2-nonanone). This is partly explained by an occurring reaction of the alkenal double bond with lysine and histidine residues. Sensory studies will be carried out to investigate the impact of aroma retention on the dynamics of *in-vivo* aroma release, thus to acquire a complete picture of the flavour molecules engaged in the binding mechanism.

Keywords: flavour, protein, binding, chemical structure, retention, interactions, release.

Introduction

Aroma compounds are known to interact with other food nutrients of the food matrix such as lipids, carbohydrates and proteins by molecular interactions [1, 2]. Hydrophobic interactions, hydrogen bonds, van der Waals, ionic and electrostatic linkages and covalent bonds are the major categories reported [3-5]. Proteins can interact with flavour molecules by reversible or irreversible binding [6]. When binding mechanism occurs, the flavour is retained since the available binding pockets of the protein are occupied by flavour molecules, hindering its release while food consumption. This issue reduces the consumer acceptability of such products. Therefore, this preliminary study aims to determine if the ability of a flavour compound to bind to the protein is influenced by aroma molecule's structure, but also to confirm, the fact that retention of flavours to protein increases with increasing carbon chain length of the flavour molecules [7, 8]. As plant food ingredients, in particular pulses proteins, are one of the most promising food components regarding the development of novel high protein food products, pea protein was selected.

Experimental

To assess the binding behaviour between plant protein and aroma compounds, headspace analysis was carried out through GC-MS/MS (AGILENT- 7890A GC coupled with an AGILENT 5975C with triple-axis detector MS). It operated in split mode 1:10 and 8 mL/min split flow. Samples were incubated and shaken for 14 min at 40°C. 1 mL of sample headspace was injected into the GC injector. A DB-WAX 121-7023 column (20 m*180 µm* 0.3 µm) run at 0.8 mL/min constant flow. The temperature was programmed by heating the GC column at a rate of 40°C/min to 240°C.

Plant protein stock solutions

Plant protein solutions were prepared using Pea Protein Isolate (PPI) EMSLAND E86 F30 (Emlichheim, Germany) at an initial concentration of 2% (w/v) in sodium phosphate as buffer solution 0.01 M (pH 7.85). Subsequently, samples were placed into a multipoint stirrer (Variomag Multipoint magnetic stirrer, Sigma-Aldrich, St. Louis, MO, USA) for 1.5 h to ensure complete dispersion of the protein isolates.

Flavour stock solutions

Each volatile flavour compound was prepared in sodium phosphate buffer solution at an initial concentration of 10.0 mg/kg. Aroma stock solutions were placed in an ultrasonic water bath (Elma, Elma Schmidbauer GmbH, Singen, Germany) to ensure a proper mixture of the flavour. Opaque 100 mL vessels (Pyrex, Sigma-Aldrich, St. Louis, MO, USA) were used to protect them from the light. Stock solutions were kept in the fridge after each use.

GC-MS/MS samples

In order to determine the binding, each aroma and PPI stock solutions were mixed in a specific ratio. 1 mL of 2% (w/v) PPI stock solution was loaded into a 20 mL GC-MS/MS vial followed by the addition of 1 mL of flavour stock solution. Thus, a final protein solution of 1% (w/v) and 5.0 mg/kg flavour concentration was produced. The reference sample was 1 mL of PPI stock solution in 1 mL of buffer, without the addition of flavour. The vials were then closed and introduced in a water bath shaker (SW22, Julabo GmbH, Seelbach, Germany) at 30°C and 125 rpm for 3 h before headspace sampling.

Binding calculation

To determine the binding percentage of flavours to PPI, retention was calculated as followed (adapted from [8])

$$\text{Binding (\%)} = 1 - \frac{\text{Peak area (protein solution+aroma)} - \text{Peak area (protein solution+buffer)}}{\text{Peak area (aroma solution+buffer)}} \times 100$$

Results and discussion

Several authors have noted that by increasing the carbon chain length within the same chemical family, the binding effect becomes stronger regardless of the chemical class or type of protein [8-12]. To confirm this fact, a homologous series of ketones at 5.0 mg/kg was investigated (Figure 1). Overall, it was demonstrated that lengthy flavour molecules are retained to a greater extent than when compared to shorter chain flavour molecules. Binding increased from 9.6% for the 2-hexanone to 73.94% for 2-decanone, showing an exponential growth of 1.5% when adding an extra carbon atom to the flavour structure. These results are in line with previous research works [10, 13, 14].

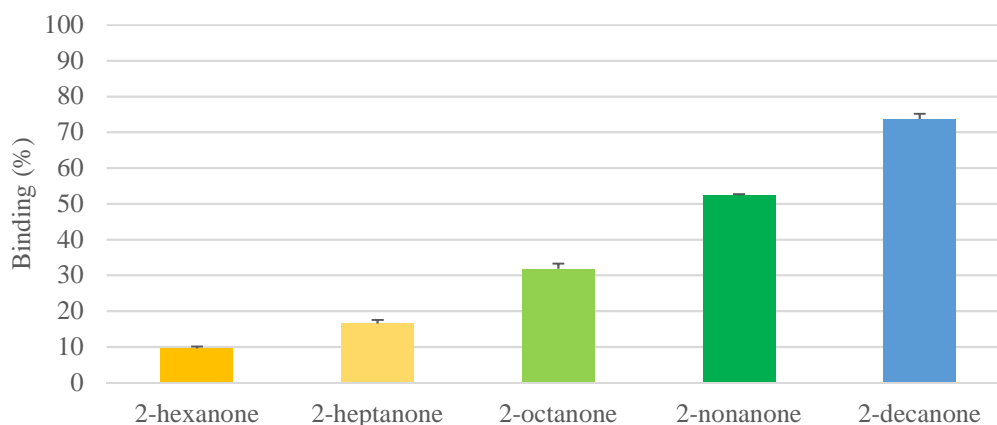


Figure 1. Binding of a homologous series of ketones (5.0 mg/kg) to PPI (1%).

Binding capacity increased by enlarging chain length. The affinity of the longer carbon chain structures of the ketones to proteins is linked to hydrophobic interactions [4]. A chemical structure with an extensive number of carbon atoms and hence, long structures, leads to the existence of more binding sites and thus, a higher adsorption ability and binding tendency [15].

To evaluate the effect of both the location of the radical group and the unsaturation on the retention mechanism with PPI, flavour compounds built up of nine carbon atoms were used. They differed on the number of double bonds and the position of the functional group. At the flavour concentration of 5.0 mg/kg, binding to PPI (1%) decreased in the following order: trans-2-nonenal (95%) > nonanal (85%) > 2-nonanone (52%) (Figure 2). Even though, trans-2-nonenal is less hydrophobic than nonanal (logP values 3.1 and 3.3, respectively) bound more to the PPI. However, when compared to 2-nonanone with the same logP of 3.1, trans-2-nonenal showed a

considerable higher binding. The presence of more double bonds seems to influence and enhance the binding to the protein [9].

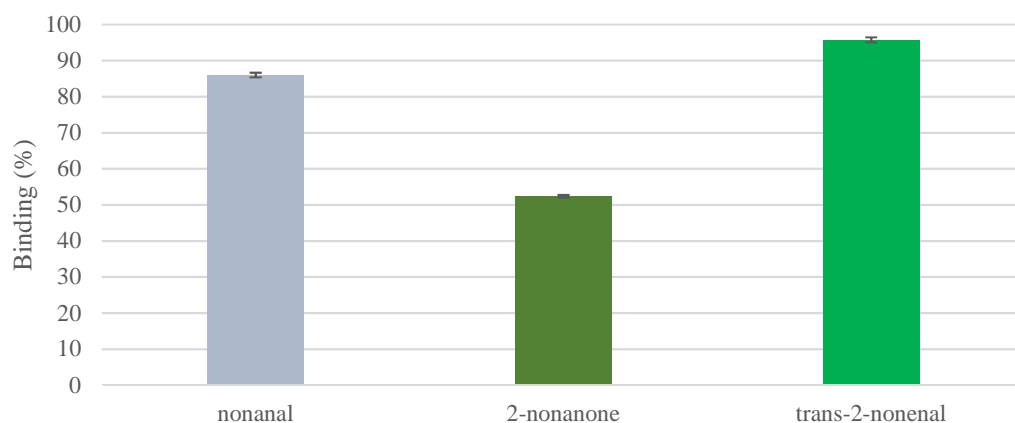


Figure 2. Binding of C9 flavour compounds (5.0 mg/kg) to PPI (1%).

The presence of the keto group (-CHO) located at the end of nonanal derived in a greater binding (85%) as compared to the keto group positioned more into the middle of the structure (2-nonanone) (52%). This is partly explained by an occurring reaction of the alkenal double bond with lysine and histidine residues. There is less binding when incorporating unsaturation more into the middle of the chain. The keto group at the 2-position in ketones may limit hydrophobic interactions and thus, intercept these hydrophobic flavours from binding to the protein. This effect was already explained and observed by Kühn et al., 2008 [9] when studying Whey Protein Isolate (WPI) at 0.5% and C9 flavour compounds at 1.0 mg/kg.

Conclusion and future research

The molecular behaviour of protein-flavour interactions is a complex mechanism where several parameters are involved. From the current preliminary results, it can be concluded that the location of the radical group, number of double bonds and chain length affects the retention phenomena to industrialized PPI.

To further unravel the drivers of the molecular retention phenomena between protein and flavour molecules, headspace measurements will be conducted using advanced methods such as Proton-Transfer-Reaction Mass-Spectrometry (PTR-MS, Ionicon, Austria). Different plant protein will be assessed.

In addition, a flow of sensory studies will be foreseen to study the repercussion of flavour retention on the dynamics on in-vivo aroma release. By combining analytical and sensory methodologies, would be possible to acquire a complete picture of the flavour molecules involved in the overall binding mechanism.

References

1. Reineccius. G. *Flavour Chemistry and Technology*. Taylor & Francis, Boca Raton, FL. 2006.
2. Archunan. G. Odorant binding proteins: a key player in the sense of smell. *Bio information*, 2018;14(01):036-037.
3. Greml. H. Interaction of flavour compounds with soy protein. *J. Amer. Oil Chem. Soc.*, 1974; 51(1):95A-97A.
4. Andriot. I, Marin. I, Feron. G, Relkin. P, Guichard. E. Binding of benzaldehyde by β -lactoglobulin, by static headspace and high-performance liquid chromatography in different physicochemical conditions. *Dairy Sci. Technol. Le Lait* 1999;79(6):577-586.
5. Zhou. Q, Lee. S-Y, Cadwallader. K.R. Inverse Gas Chromatographic evaluation of the influence of soy protein on the binding of selected butter flavour compounds in a wheat soda cracker. *J. Agric. Food Chem.* 2006; 54(15):5516-5520.
6. Guichard. E. Interactions between flavour compounds and food ingredients and their influence on flavour perception. *Food Rev. Int.* 2002;18(1):49-70.
7. Damodaran. S and Kinsella. L.E. Interaction of carbonyls with soy protein: Thermodynamic effects. *J. Agric. Food Chem.* 1981;29(6):1249-1253.
8. Wang. K and Arntfield. S.D. Binding of carbonyl flavour to canola, pea and wheat proteins using GC/MS approach. *Food Chem.* 2014;157:364-372.
9. Kühn. J, Considine. T, Singh. H. Binding of flavour compounds and whey protein isolate as affected by heat and high-pressure treatments. *J. Agric. Food Chem.* 2008;56(21):10218-10224.
10. Andriot. I, Harrison. M, Fournier. N, Guichard. E. Interactions between methyl ketones and β -lactoglobulin: Sensory analysis, headspace analysis, and mathematical modelling. *J. Agric. Food Chem.* 2000;48(9):4246-4251.

11. Pelletier, E, Sostman, K, Guichard, E. Measurement of interactions between β -lactoglobulin and flavour compounds (esters, acids and pyrazines) by affinity and exclusion size chromatography. *J. Agric. Food Chem.* 1998;46(4):1506-1509.
12. Viry, O, Boom, R, Avison, S, Pascu, M, Bodnár, I. A predictive model for flavour partitioning and protein-flavour interactions in fat-free dairy protein solutions. *Food Res. Internat.* 2018;109:52-58.
13. Heng, L, van Koningsveld, G.A, Gruppen, H, van Boekel, M.A.J.S, Vincken, J.P. Protein-flavour interactions in relation to the development of novel protein foods. *Trends Food Sci. Technol.* 2004;15(3-4):217-224.
14. Naknean, P and Meenune, M. Factors affecting retention and release of flavour compounds in food carbohydrates. *Int. Food Res. J.* 2010;17(1):23-34.
15. Tan, Y and Siebert, J.K. Modeling bovine serum albumin binding of flavour compounds (alcohols, aldehydes, esters, and ketones) as a function of molecular properties. *J. Food Sci.* 2008;73(1):56-63.

Comparison and optimisation of headspace methods for the analyses of oxidation related off-flavour compounds in plant protein concentrates and infant formula

CATRIENUS DE JONG¹, Cornelis van Kekem¹, M. L. Ondino Azario¹, Frank Koudijs², Naem Babae² and Wibke S. U. Roland¹

¹ Wageningen Food & Biobased Research (WUR), Wageningen, The Netherlands, catrienus.dejong@wur.nl

² Interscience, Breda, The Netherlands

Abstract

The aim of this study was to develop an effective and fast method for key-marker compound analysis of available oxidation related off-flavours, both in dry protein powder and in protein powder dispersed in water. Four different headspace techniques (static headspace (HS), dynamic headspace (DHS-ITEX), and solid phase microextractions (HS-SPME, HS-Arrow)) were compared under different extraction conditions. HS-Arrow in combination with true capillary cold trapping showed to be most sensitive and an efficient extraction technique for a wide range of oxidation related HRGC-MS analyses. Although HS-Arrow in combination with GC-MS is a relative fast technique for the analyses of the key aroma compounds of plant protein related products and infant formula, still some key aroma compounds could not be detected. Especially 2,4,7-decatrienal, an important key compound to detect “fishy” off-flavours in products with added DHA like infant formula, is missed by these four headspace techniques.

Keywords: headspace extraction, GC-MS, Arrow, off-flavours, oxidation, plant proteins, infant formula

Introduction

The growing world population demands new sustainable sources of protein and a transition from animal to plant based protein foods. Most crop varieties currently available in the market are primarily designed for high yield and other agriculturally important aspects, instead for optimal flavour when used as ingredients in new food applications [1].

Many volatile compounds in plant protein concentrates that lead to sensory off-flavour attributes, such as “beany”, “green”, “oily”, are formed by oxidation, mainly due to the action of lipoxygenases (LOX) [2]. The same group of compounds are found in food and nutritional products such as infant formula with added polyunsaturated fatty acids (PUFAs). In the case of docosahexaenoic acid (DHA) and arachidonic acid (ARA), oxidation leads to “painty”, “tallowy”, “metallic”, and “fishy” off-flavours. Often, the sensory attributes are not caused by one single compound but are the result of a certain balance between different oxidation compounds. Sensory omission experiments with the Composent (a preparative GC with omission feature) showed that for the typical “cod-liver” / “fishy” off-flavour found in “oxidised” infant formula not one but a balance of four compounds is responsible ((E,E)-2,4-heptadienal, (E,E)-3,5-octadien-2-one, (E,Z,Z)-2,4,7-decatrienal and (E,E)-4,5-epoxy-2-decenal) [3].

The aim of this study was to develop an effective and fast method for key-marker compound analysis of available oxidation related off-flavours, both in dry protein powder and in protein powder dispersed in water.

Four different headspace techniques (static headspace (HS), dynamic headspace (DHS-ITEX), and solid phase microextractions (HS-SPME, HS-Arrow)) were compared under different extraction conditions. Beside plant protein concentrates, also an infant formula and a flavour standard were used in this study.

Experimental

Sample preparation

The samples analysed were a flavour mixture (STD), a pea protein concentrate (PPC), a soy protein concentrate (SPC) and a 1st age infant formula (IF). The STD consisted of 26 volatile compounds namely: diacetyl, hexanal, octanal, nonanal, 2,4-decadienal, 2,6-nonadienal, benzaldehyde, 3-methylbutanal, 2-methylfuran, 2-pentylfuran, hexanol, 3-methylbutanol, 1-octen-3-ol, 2-heptanone, 2-nonanone, pyrrole, 2-ethyl-3-methoxypyrazine, 2-ethylpyrazine, dimethyl sulphide, dimethyl disulphide, δ -decalactone, δ -dodecalactone; internal standards: propyl acetate, undecane, dodecane, d12-hexanal.

The headspaces of the proteins (PPC & SPC) were analysed above the dry powder (2 g) and above a dispersion in water (2.5%). The headspace above the IF was analysed above the dry powder (2 g) and above a dispersion in water (12.5%).

Gas chromatography-mass spectrometry (GC-MS)

The gas chromatograph (HRGC) consisted of a Thermo Trace 1300 GC equipped with a SSL injector (250°C) in combination with true capillary (in column) cryogen cold trapping (-120°C) and fitted with a capillary column Rxi-5Sil MS, 30 m × 0.25 mm I.D. × 1.0 µm df. The HRGC was connected with a Single quad-MS ISQ7000 (Thermo Scientific™) using Advanced Electron Ionisation (AEI) and robotics to execute the different extraction and HRGC-injection techniques.

The operating conditions were:

- GC Tx program: 40°C (3 min)—8°C/min—140°C—25°C/min—240° (5 min)
- GC flow: 1.5 ml/min (constant flow)
- Split mode: SSL; 6 min; 30 ml/min
- Cold trap: -120°C/260°C, 0.53 mm fused silica capillary
- MS scan: 35-250 amu

Extraction techniques

1. Static Headspace (HS)

2. Dynamic Headspace (DHS-ITEX)

Parameter	Setting	Parameter	Setting
Analysis time	35 min	Adsorbent	Tenax TA 80/100 mesh
Sample draw	1.5 mL	Analysis time	35 min
Agitator temp	40-60°C	Sampling volume	1000 µL
Incubation time	10-40 min	Agitator temp	40-60°C
Agitator on	10 sec	Incubation time	10-40 min
Agitator off	2 sec	Agitator on	10 sec
Syringe temp	70°C	Agitator off	2 sec
Filling volume	1-2 mL	Sampling depth mode	Standard
Pre-inj. syringe flush	5 sec	Extraction volume	1000 µL
Post-inj. syringe flush	30 sec	Aspirate/Dispense flow	100 µL/s
Filling speed	20 mL/min	Number of strokes	5-25
Injection speed	5 mL/min	Prefill ratio	40%
Injection depth	45 mm	Syringe temp	65°C
Penetration speed	25 mm/s	Trap pre cleaning temp	250°C
Pre-inj. Delay	0 sec	Trap pre cleaning time	120 sec
Post inj. Delay	0 sec	Trap extraction temp	35°C
		Trap purge time	10 sec
		Trap post cleaning temp	250°C
		Trap post cleaning time	120 sec
		Injection depth	35 mm
		Injection speed	80 µL/s
		Injection temp	250°C

3. Headspace Solid Phase Micro Extraction (SPME & Arrow)

Parameter	Setting	Parameter	Setting
Fibre SPME	50/30 µm, 1 cm, DVB/CAR/PDMS	Analysis time	35 min
Fibre Arrow	120µm, 2cm, DVB/CWR/PDMS	Injection depth	70 mm
Temp incubation/extraction	40-60°C	Penetration speed	40 mm/sec
Agitator speed	750 -1200rpm	Desorption time	2 min
Incubation time	2- 5 min	Start mode	At injection
Extraction stirrer speed	700-1200 rpm	Pre desorb time	1.0 min
Extract time	10-40 min	Post desorb time	1.0 min
Needle speed /depth in vial	20 mm/s / 20mm	Conditioning temp	250°C

Results and discussion

Several analysis experiments were carried out with varying parameters regarding sample incubation (volume, temperature, time, mixing) and injection/desorption (temperature, time, strokes, speed). The results were compared in order to find optimum conditions for the different analysis techniques in which as much as possible (PPC, SPC

and IF) key aroma could be analysed with a simple and fast method. Special attention was paid to the oxidation related compounds. A summary of the outcome of this large analysis experiment is shown in Table 1.

Table 1: Optimal extraction and injection conditions for the HRGC-MS analyses of oxidation compounds in PPC, SPC and IF.

Extraction technique	HS	DHS	SPME	ARROW
Extraction mode	HS	HS	HS	HS
Incubation time (min)	20	20	12	12
Incubation temp (°C)	60	60	40	40
Extraction volume (ml)	2	1	x	x
Strokes (#)	x	15	x	x
Agitator on fixed/Arrow (rpm)	on	on	on	750
Desorption time (min)	x	12.5	2	2

In Figure 1, as an example, a part of the GC-MS chromatogram of a pea protein concentrate is shown, obtained with a HS-Arrow extraction executed with the parameters shown in Table 1.

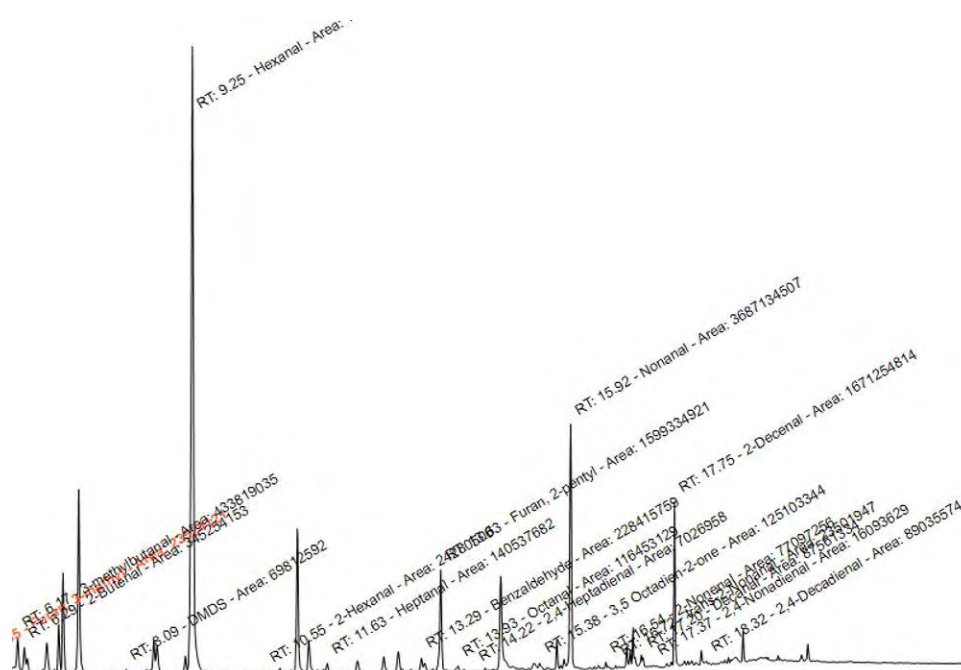


Figure 1: HRGC-MS chromatogram obtained after a HS-Arrow extraction in the headspace above a 2.5% dispersion of PPC in water.

A comparison of the headspace extraction techniques tested in both the dry product and in aqueous dispersion showed that HS-Arrow is the most efficient for effective analysis of the key oxidation related compounds. Also, HS-SPME and HS-Arrow extraction allow for lower (40°C) operational incubation temperature compared to HS-DHS (60°C) to detect the most relevant key aroma compounds. When higher incubation temperatures are used for the SPME and Arrow extractions, compounds as hexanal and 2-pentylfuran are overloaded for most samples.

At the other hand, DHS is more effective for very volatile compounds compared to HS and SPME. In Figure 2 the extraction efficiency is shown for some key oxidation related compounds in IF.

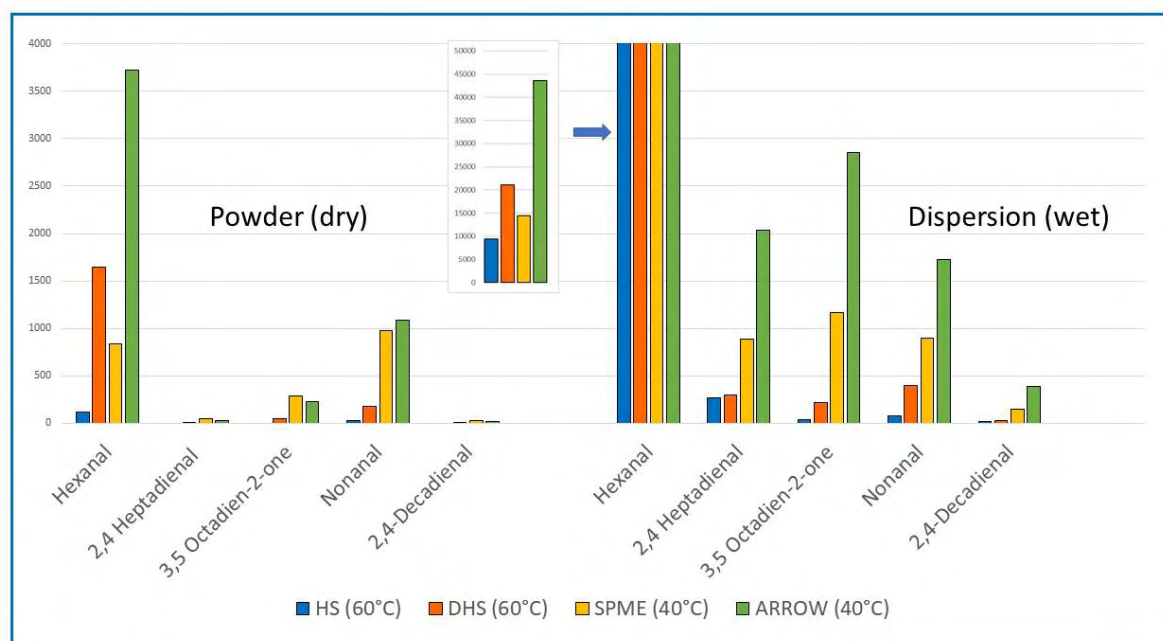


Figure 2: Example of extraction efficiency comparison for an infant formula 1st age sample with added fish oil PUFA's like DHA and ARA.

Besides the extraction efficiency of different techniques tested, Figure 2 also shows a difference in concentration in the headspace between the powder analyses and the analyses of the dispersions. The difference in flavour compound balance (e.g. 3,5-octadien-2-one, 2,4-heptadienal) will most probably lead to a different sensory perception. Similar observations were made for PPC and SPC. This means that the (off-) flavour quality of the protein powder as such and the (off-) flavour quality of the protein in application can be different, and it should be kept in mind that sensory evaluation of protein powder by smell only could lead to misinterpretation of the (off-flavour) perception when the intention is to use the protein powder in a moist product. Furthermore, some important and interesting compounds like lactones and 2,4,7-decatrional were still difficult to detect using the headspace techniques studied. Stir Bar Sorptive Extraction (SBSE) could give possibilities here [4].

Conclusion

Headspace Solid Phase Micro Extraction using Arrow (HS-Arrow) in combination with true capillary cold trapping is the most sensitive and efficient extraction technique of the four tested techniques for a wide range of oxidation related HRGC-MS analyses. Although HS-Arrow in combination with HRGC-MS is a relative fast technique for the analyses of the key aroma compounds of plant protein related products and infant formula still some key aroma compounds could not be detected. Especially 2,4,7-decatrional, an important key compound to detect “fishy” off-flavours in products with added DHA like infant formula, is missed by these four headspace techniques.

References

1. Roland WSU, Pouvreau L, Curran J, Van de Velde F, De Kok PMT. Flavor aspects of pulse ingredients. *Cereal Chem.* 2017;94(1):58–65.
2. Rackis JJ, Sessa DJ, Honig DH. Flavor problems of vegetable food proteins. *J Am Oil Chem Soc.* 1979;56(3):262-271.
3. De Jong C, Rippen M, Van Hijum SAFT, Koudijs F. Study on the impact of individual key compounds on the flavour perception in complex product aroma mixtures. Poster presentation, 12th Wartburg Symposium. 2019.
4. High R, Bremer P, Kebede B, Eyres GT. Comparison of four extraction techniques for the evaluation of volatile compounds in spray-dried New Zealand sheep milk. *Molecules* 2019;24(10):1917.

Most popular odours in food products in March 2021 according to VCF-online.nl

WILLIAM VAN DONGEN and Bert Wiggers

VCF-online, Reeuwijk, The Netherlands

Abstract

The Volatile Compounds in Food (VCF) database contains compounds that contribute to the flavour and odour of food. Descriptors, concentration ranges and analytical methods to determine them are listed in the VCF database. Subscribers to the database can search and consult the VCF-online data to look for compounds that contribute to the odour and flavour quality of food products. The most popular flavours and odours based on the use of the VCF database during March 1 – April 4, 2021 were: 1. α -terpineol, 2-phenylethanol and phenylethanal. The most popular food products and their odour and flavour compounds were allium species (garlic, leek, onion, scallion, and shallot), citrus fruit and milk products (including cheeses).

Keywords: VCF-online, odour, food products

Introduction

The Volatile Compounds in Food (VCF) database [1] contains an excess of 9300 volatile compounds that contribute to the odour and taste of food and food ingredients. The volatile compounds are listed by 571 food products and grouped in 18 chemical classes, such as hydrocarbons, aldehydes, esters, acids, etc. Also, flavour descriptors, concentration ranges and analytical methods to determine them are listed in the VCF database. The database is based on scientific literature, and only compounds that have been identified by at least two independent analytical methods are listed. The VCF database is covered by total more than 6000 literature references.

Presently, more than 100 food-oriented companies have a subscription to the VCF database. From monitoring keyword searches and the use of the database, trends can be identified.

This poster presentation will give and discuss observations and trends of the most popular flavours and odours in food products based on the use of the VCF database during March 1 – April 4, 2021.

Experimental

The use of the VCF-online [1] database was monitored in the period of March 1- April 4, 2021 with regards to the number of times subscribers viewed certain food products and odour compounds. The number of views (or hits) was recorded during 5 weeks in this period. The top 10 mostly viewed food products and odour compounds are listed.

Results and discussion

The ten most popular food products in the period of March 1-April 2021 were (total observations 9656):

1. allium species (garlic, leek, onion, scallion, shallot): 474 times observed
2. citrus fruit: 311
3. milk products (including cheeses): 225
4. tea: 200
5. capsicum (bell peppers, cayenne, paprika and jalapeños): 193
6. chamomile: 189
7. lemon peel oil: 164
8. satsuma mandarin: 162
9. tomato: 159
10. coffee: 146

Figure 1 gives the number of views of the 10 most popular food products according to the use of the VCF database on a weekly basis in weeks 9-13 of 2021.

It is apparent that spices and condiments such as allium and capsicum species had a lot of attention. Also, citrus fruit and milk products (including cheeses) had a lot of attention.

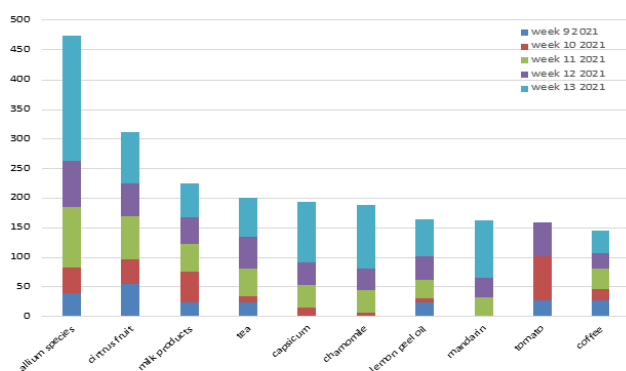


Figure 1: Number of views of the 10 most popular food products according to the use of the VCF database in the period March 1 - April 4, 2021 (weeks 9-13).

The ten most popular odour compounds in the period of March 1-April 2021 were (total observations 2632):

1. α -terpineol: 105 times observed
2. 2-phenylethanol: 81
3. phenylethanal: 71
4. endo-borneol: 70
5. phenylacetic acid: 67
6. L-borneol: 66
7. furaneol: 62
8. eugenol: 57
9. citronellal: 56
10. vanillin: 55

Table 1 lists the ten mostly viewed odour compounds, together with their presence in food products, threshold data and odour descriptors. Moreover, the number of views of these popular odour compounds according to the use of the VCF database on a weekly basis in weeks 9-13 of 2021 is presented in Figure 2.

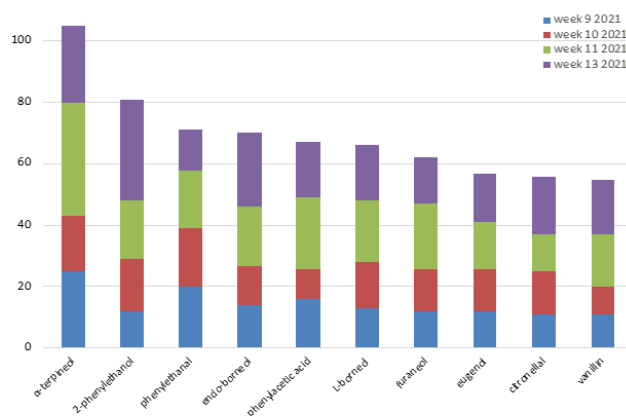


Figure 2: Number of views of the 10 most popular odour compounds according to the use of the VCF database in the period March 1 - April 4, 2021 (weeks 9-13).

The majority of the top-10 viewed compounds has an odour profile of sweet, floral, honey, fruit (6 out of 10) and to a lesser extent an odour profile of pungent, camphor, burnt (3 out of 10).

Conclusion

The mostly viewed food products in the period of March 1-April 2021 were spices and condiments such as allium and capsicum species.

The odour profiles of the most popular compounds looked at during March 1-April 2021 were in the quadrant sweet, floral, honey and fruit (6 out of 10) and to a lesser extent pungent, camphor, burnt (3 out of 10).

References

1. <https://www.vcf-online.nl/>; VCF Volatile Compounds in Food: database / Van Dongen, W.D.; Donders, J.J.H. [eds]. – Version 16.8 – Reeuwijk (The Netherlands): BeWiDo B.V., 1963-2021.

Table 1: The ten mostly viewed odour compounds are listed, together with their amount in food products, threshold data and odour descriptors.

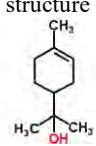
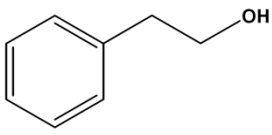
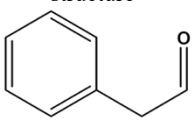
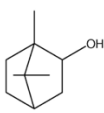
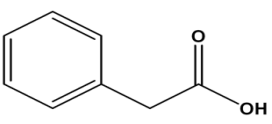
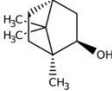
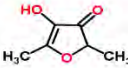
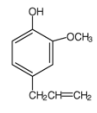
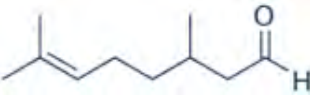
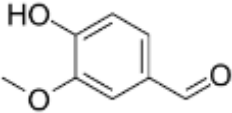
1. α -terpineol: 105 times viewed				
top 5 presence in products (ppm)		threshold data		odour
all products (n=543)	0 — 113300	air (mg/m ³)	water (mg/L)	mint
citrus fruits	133000	-	0,33	lily
pistacia	96000	structure 		fresh
ginger	60000			oil
laurel	60000			sweet
cardamom (ginger)	43000			
2. 2-phenylethanol: 81 times viewed				
top 5 presence in products (ppm)		threshold data		odour
all products (n=355)	0 — 122000 ppm	air (mg/m ³)	water (mg/L)	fruit
chestnut	122000	0,015	1,0	honey
meadowsweet flower oil	28000	structure 		rose
mustard	23000			sweet apple
cinnamomum	4000			wine
wine	200			
3. phenylethanal: 71 times viewed				
top 5 presence in products (ppm)		threshold data		odour
all products (n=185)	0 — 55000	air (mg/m ³)	water (mg/L)	berry
wormwood oil	55000	0,0012	0,004	geranium
lemon balm	16000	structure 		honey
mustard	12000			nut
salvia species	11000			pungent
maize	2000			
4. endo-borneol: 70 times viewed				
top 5 presence in products (ppm)		threshold data		odour
all products (n=144)	0 — 436500	air (mg/m ³)	water (mg/L)	camphor
thyme	436500	-	0,14	fragrant
rosemary	155600	structure 		green
ginger	54000			polis
pistachio	29000			
coriander	20000			
5. phenylacetic acid: 67 times viewed				
top 5 presence in products (ppm)		threshold data		odour
all products (n=80)	0-978	air (mg/m ³)	water (mg/L)	beeswax
honey	978	0,00003	2	caramel
milk products	75	structure 		floral
cocoa	8			honey
wine	7			urine
sugar molasses	3			

Table 1 (cont.): The ten mostly viewed odour compounds are listed, together with their amount in food products, threshold data and odour descriptors.

6. L-borneol: 66 times viewed				
top 5 presence in products (ppm)		threshold data		odour
all products (n=1)	9000 ppm	air (mg/m ³)	water (mg/L)	camphor pungent
lemon grass oil	9000	-	-	
black pepper	qual	structure 		
fennel (venkel)	qual			
-	-			
-	-			
7. furaneol: 62 times viewed				
top 5 presence in products (ppm)		threshold data		odour
all products (n=111)	0 — 131 ppm	air (mg/m ³)	water (mg/L)	burnt caramel honey strawberry sweet
coffee	131	0,001	0,05	
beef	9	structure 		
cocoa	6			
milk products	4			
beer	3			
8. eugenol: 57 times viewed				
top 5 presence in products (ppm)		threshold data		odour
all products (n=199)	0 — 886000	air (mg/m ³)	water (mg/L)	burnt clove smoke spice
cinnamomum	886000	0,0002	0,01	
pimento (all spice)	870000	structure 		
cloves (kruidnagel)	848200			
lemon balm (plant)	45000			
laurel	44500			
9. citronellal: 56 times viewed				
top 5 presence in products (ppm)		threshold data		odour
all products (n=123)	0-390000	air (mg/m ³)	water (mg/L)	citrus fat leaf
lemon balm	390000	0,005	0,05	
citrus fruits	168000	structure 		
lemon grass oil	10200			
ginger	2900			
black pepper	1000			
10. vanillin: 55 times viewed				
top 5 presence in products (ppm)		threshold data		odour
all products (n=151)	0 — 96000	air (mg/m ³)	water (mg/L)	chocolate sweet vanilla
maize	96000	0,08	0,058	
vanilla	23187	structure 		
cinnamomum	23100			
pork	23			
coffee	16			

Identification of odour-important norisoprenoids in *Arbutus pavarii* honey

NAGIAT T. HWISA and Keith R. Cadwallader*

University of Illinois, Department of Food Science & Human, University of Illinois, Urbana, Illinois. USA, email *cadwlldr@illinois.edu

Abstract

Arbutus pavarii honey is a rare and expensive honey derived from the floral nectar of the wild strawberry tree *Arbutus pavarii* pamp. This study focused on the identification and characterisation of norisoprenoids responsible for its unique savoury, saffron-like aroma. Volatile components (from honey samples collected over three years 2015, 2016, 2017) were isolated by continuous liquid-liquid extraction (cLLE) combined with solvent-assisted flavour evaporation (SAFE) and the potent odorants determined by GC-olfactometry, aroma extract dilution analysis (AEDA) and GC-MS. Seventeen norisoprenoids and two additional isophorone derivatives were detected, 14 of which were positively identified and their concentrations determined by stable isotope dilution analysis (SIDA)-HS-SPME-GC-(TOF)MS. Results indicated that lanierone (1) was the most important odorant, while α -isophorone (4) was the most abundant norisoprenoid in *Arbutus pavarii* honey.

Keywords: honey, *Arbutus pavarii*, odorants, norisoprenoids, lanierone

Introduction

Monofloral honeys often possess unique volatile fingerprints that distinguish them from other honeys, especially multifloral types. A type of monofloral honey produced in Libya, known locally as honnoon or bitter honey, is derived from the flower nectar of the wild strawberry or shmary tree (*Arbutus pavarii* pamp., family Ericaceae) [1]. This tree is endemic to Libya but is scarce and vulnerable to potential extinction [2], which in turn causes *A. pavarii* honey to be quite rare and expensive. This honey is characterised by its bitter taste and its unique savoury saffron-like aroma. Although various qualitative criteria have been established for *A. pavarii* honey, there are no published reports regarding its characteristic aroma constituents. Therefore, the purpose of this study was to identify and characterise the odorants responsible for the savoury aroma in *A. pavarii* honey.

Experimental

Aroma profiling of one representative sample of *A. pavarii* honey (sample 2017) was carried out by descriptive sensory aroma analysis according to the method described by Zhou et al. (2002) [3] using a 9-member trained panel (4 female and 5 male, university students and staff, age 20 to 58 years).

The volatile components of *A. pavarii* honey samples were isolated by continuous liquid-liquid extraction (cLLE) combined with solvent-assisted flavour evaporation (SAFE).

GC-O analysis of the concentrated cLLE/SAFE extracts and serial dilutions of each extract was performed using a 6890N GC (Agilent Technologies Inc., Santa Clara, CA) equipped with a flame ionization detector (FID), a sniff port (DATU Technology Transfer, Geneva, NY) and a cool on-column injector (+3 °C oven tracking mode). Separations were performed on either RTX®- Stabilwax or RTX®-5 GC column (30 m x 0.25 mm i.d. x 0.25 μ m film thickness; Restek, Bellefonte, PA).

A GC-MS-O system consisted of an olfactory detector (ODP2, Gerstel, Germany) and a 6890 GC/5973N mass selective detector (Agilent Technologies, Inc). cLLE/SAFE extracts were injected (2 μ L) by cold splitless injection mode using a CIS4 inlet (Gerstel). Separations were performed on either a Stabilwax-DA® or Rxi-5ms-sil (30 m x 0.25 mm i.d. x 0.25 μ m df; Restek, Bellefonte, PA) capillary column. Column effluent was split between the MS detector and olfactory detection port. The mass spectra were recorded in full scan mode (35-300 amu, scan rate 5.27 scans/s, interface temperature 250°C, and ionization energy 70 eV.).

Quantitation of selected odorants was performed by SIDA combined with HS-SPME, and GC-(TOF)MS. Samples (0.1 to 1 g) in 22-mL vials were spiked with appropriate levels of labelled internal standards (IS) before analysis using a CombiPal autosampler (Leap Technologies, Inc., Fort Lauderdale, FL) connected to a 7890A GC (Agilent Technologies, Inc.) time-of-flight mass spectrometer [(TOF)MS; Pegasus 4D; LECO®, St. Joseph, MI]. Sample vial was pre-incubated at 60 °C for 10 min at an agitator speed of 250 rpm. A 2 cm, 50/30 μ m DVB/CAR/PDMS SPME fibre (Supelco Co., Bellefonte, PA, USA) was then exposed to the headspace of the sample vial for 30 minutes at the same temperature. The SPME fibre was inserted into the GC injector for desorption, hot splitless mode, at 260 °C with 4 min. valve delay, then kept in the inlet for an addition 20 min for post injection fibre conditioning. Analysis was carried out using a Stabilwax® GC column (30 m x 0.25 mm

id \times 0.25 μm film thickness; Restek). Mass spectra were acquired at m/z range of 35 to 300 amu; electron multiplier voltage, Autotune + 200 V; and a scan rate of 50 scans/s. Peak areas for selected ions of target analytes/IS were determined using Leco Chroma TOF software (version 3.34).

Odour-activity values (OAVs) for potent odorants were calculated by dividing their concentrations by their odour detection thresholds (ODTs) in water.

Results and discussion

To characterise the aroma profile of *A. pavarii* honey, the overall aroma and 4 defined aroma attributes of *A. pavarii* honey were evaluated; namely, saffron-like, phenolic, caramellic and raisin-like aroma. Results indicated that savoury, saffron-like aroma was the predominant aroma attribute of this honey (Figure 1).

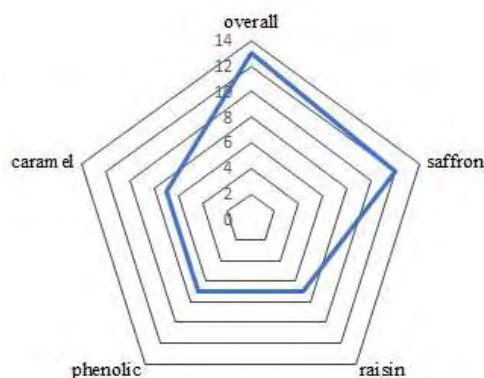


Figure 1: Sensory descriptive aroma profile of *Arbutus pavarii* honey (sample 2017).

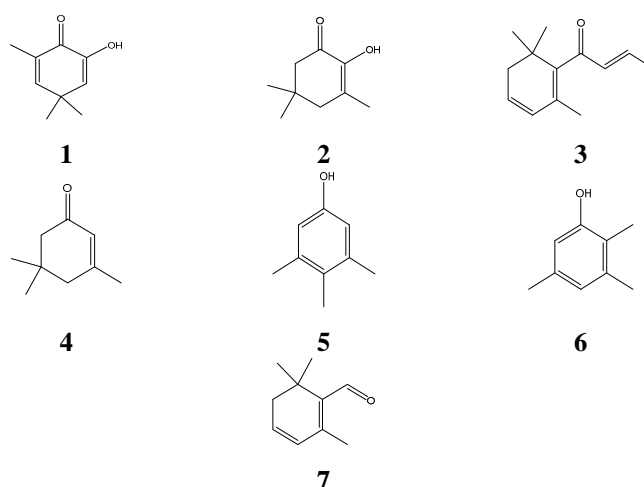


Figure 2: Structures of selected norisoprenoids identified in *A. pavarii* honey (Compound numbers correspond to those in Table 1).

Sixty-nine aroma-active compounds were detected by GC-O and GC-MS. AEDA results indicated that the predominant odorants were norisoprenoids. A total 16 were norisoprenoids were detected along with two trimethylphenols which are known to be derived from isophorone. Twelve of the norisoprenoids and the two trimethylphenols (**5** and **6**) were positively identified and their concentrations and OAVs in *A. pavarii* honey determined (Figure 2, Table 1). Both FD factors and OAVs ranked lanierone (**1**) as the most potent odourant among all other volatile constituents of *A. pavarii* honey, followed by 2-hydroxyisophorone (**2**) (indicated only by its high FD factor since its OAV could not be calculated due to lack of an ODT). In addition, the results showed that α -isophorone was the most abundant volatile component of this honey. Some of the identified norisoprenoids, such as lanierone (**1**), 2-hydroxyisophorone (**2**), 4-hydroxyisophorone, 4-oxoisophorone, levodione and the two trimethylphenols (**5** and **6**) may exist either naturally in *A. pavarii* honey or could possibly be generated from α -isophorone (**4**) through chemical reactions [4] or through microbial conversions [5].

Table 1: FD Factors and OAVs of selected norisoprenoids in *A. pavarii* honey.

No.	Compound	FD ^a			OAV ^b		
		2015	2016	2017	2015	2016	2017
1	2-hydroxy-4,4,6-trimethylcyclohexa-2,5-dienone (lanierone)	59049 (19683)	59049 (19683)	59049 (19683)	6320	5680	6700
2	2-hydroxy-3,5,5-trimethylcyclohexa-2-enone (2-hydroxyisophorone)	2187 (2187)	2187 (2187)	2187 (2187)	NA	NA	NA
3	1-(2,6,6-trimethyl-1,3-cyclohexadien-1-yl)-2-buten-1-one (β -damascenone)	729 (2187)	729 (2187)	2187 (2187)	187	238	118
4	3,5,5-trimethylcyclohexa-2-enone (α -isophorone)	81 (729)	81 (729)	243 (729)	35	29	27
5	3,4,5-trimethylphenol	729 (81)	729 (81)	729 (243)	NA	NA	NA
6	2,3,5-trimethylphenol	729 (ND)	729 (ND)	729 (ND)	NA	NA	NA
7	2,6,6-trimethylcyclohexa-1,3-dienecarbaldehyde (safranal)	243 (27)	729 (27)	729 (27)	0.9	1.6	0.9

^a Average of three replications; FD values on Rtx-Wax (FD values on Rtx-5 column are given in parenthesis);

^b Odour-activity values (OAV) calculated by dividing average concentration by the odour detection threshold (ODT); ND: not detected; NA: not available due to lack of ODT values in literature.

Conclusion

This research represents the first to comprehensively characterise norisoprenoids in *A. pavarii* honey. GC analysis results of this study showed that norisoprenoids are the main attributors of *A. pavarii* honey aroma with lanierone being the most important odorant and α -isophorone the most abundant odorant among other odour-active constituents of this honey. Twelve norisoprenoids were positively identified in this study, some of them, such as, 2-hydroxy-4,4,6-trimethylcyclohexa-2,5-dienone (lanierone), 3,5,5-trimethyl-4-methylene-2-cyclohexene-1-one (4-methylene isophorone), have not been reported earlier in any other type of honey.

References

1. Elabidi N, Elshatshat S. Qualitative criteria of the endemic *Arbutus pavarii* pamp. Libyan honey. EPRA International Journal of Research and Development. 2017;2(1):132-135.
2. IUCN. (1998). International Union for Conservation of Nature red list of threatened species. Date accessed: May 2015. <https://www.iucn.org>
3. Zhou Q, Wintersteen, C-L, Cadwallader, K-R. Identification and quantification of active-aroma components that contribute to the distinct malty flavor of buckwheat honey. J. Agric. Food Chem. 2002;50:2016-2021.
4. Vidal, D. M., Moreira, M. A. B., Coracini, M. D. A., and Zarbin, P. H. G. Isophorone derivatives as a new structural motif of aggregation pheromones in Curculionidae. Sci. Rep. 2019;9(776):1-12.
5. Joe Y-A, Goo Y-M, Lee Y-Y. Microbiological oxidation of isophorone to 4-hydroxyisophorone and chemical transformation of 4-hydroxyisophorone to 2,3,5-trimethyl-p-benzoquinone. Arch. Pharm. Res. 1989;12(2):73-78.

Aroma variations of mid-Atlantic hops driven by growing regions and postharvest practices

XUEQIAN SU¹, Ken Hurley¹, Laban Rutto², Holly Scoggins³, Yixiang Xu², Sean O’Keefe¹ and Yun Yin^{1*}

¹ Department of Food Science and Technology, Virginia Tech, Blacksburg, VA, USA

² College of Agriculture, Virginia State University, Petersburg, VA, USA

³ Department of Horticulture, Virginia Tech, Blacksburg, VA, USA

Abstract

Hop (*Humulus lupulus* L.) is an indispensable raw material with unique bitterness and pleasant aroma in the brewing industry. Recently, hop has become an emerging specialty crop in Mid-Atlantic regions due to the unprecedented development of the craft brewing. However, the aroma characteristics of these region-specific hops are not yet available. This study explored the aroma profiles of hops harvested from multiple mid-Atlantic locations and experienced various postharvest practices by use of headspace-solid-phase microextraction-gas chromatography-mass spectrometry-olfactometry (HS-SPME-GC-MS-O). Results showed that β -myrcene, geraniol, linalool and methyl octanoate with respective herbal, citrus and floral notes were predominant compounds in all fresh and dried hops. Fresh Cascade and Chinook from Meadowview contained significantly higher concentrations for most aroma compounds comparing to the ones harvested from other locations. Dehydrator drying could effectively preserve aroma compounds in both varieties, especially when compared to oven drying. Additionally, freeze-drying maximally retained the original hop colour.

Keywords: hops, aroma, quality, growing regions, drying

Introduction

Hop plant is a vigorous, climbing and herbaceous perennial. It is primarily used as an imperative brewing ingredient due to its unique bitterness and pleasant aroma [1, 2]. The distinguishing bitterness mainly derives from the α -acids and β -acids from the lupulin glands of female hop cones. The “hoppy” aroma, however, is far away from being fully understood due to its extremely complicated composition. The unique aroma in hops is a result of the interaction among hundreds of volatile compounds, which are collectively known as hop essential oil [3]. The complexity behind hop essential oil has made aroma characterisation in hops a really challenging task.

Several Pacific Northwest states, like Washington, Oregon and Idaho, are the leading hop producers in US for decades. The hop production in mid-Atlantic regions has always been minor due to climate challenges like shorter day length and high heat and humidity [4, 5]. However, in recent years, following the fertiliser recommendations for economic hop production and the increasing consumer interest in locally-sourced ingredients, regional craft brewing industry is continuously blooming and hop has become an emerging specialty crop in mid-Atlantic states. Cascade and Chinook have been reported as the dominant hop varieties due to their resilient adaptability to the regional environment. Despite this, the aroma characteristics of region-specific hops are still unavailable.

Drying is the most commonly-used postharvest practice for hops to prevent the spoilage. It is well known that the temperature and oxygen levels involved in the drying process could greatly affect the aroma generation routes through oxidation, polymerization and Maillard reaction [6]. Therefore, understanding the influences of different drying practices on hop aroma behind these chemical transformations is of vital importance for the selection of appropriate postharvest applications for enhanced final quality of hop products.

This study aimed to investigate the aroma characteristics of Cascade and Chinook hops harvested from various mid-Atlantic locations and assess the impact of different postharvest practices on their aroma profiles by combined use of headspace-solid-phase microextraction-gas chromatography-mass spectrometry-olfactometry (HS-SPME-GC-MS-O) and meticulous quantitation approaches.

Experimental

Sample preparation

Fresh Cascade hops were harvested from three farms located at Meadowview (MDV), Petersburg (PTB) and Blacksburg (BKB) in Virginia, US, respectively. Fresh Chinook hops were collected from the first two growing regions mentioned above. Both hop varieties were harvested at their optimal maturities during the 2019 harvesting season. Dehydrator drying, oven drying and freeze-drying were applied as three different postharvest practices to Meadowview Cascade and Chinook hops. All samples were dried down to a final moisture content between

8%~10% (wet basis). Dried hop cones were cooled at room temperature, transferred into odour-free sealing bags, sealed with a vacuum sealer (KOIOS Vacuum Sealer Machine, California, USA) and finally stored in a freezer (-80°C) until further analysis.

HS-SPME sampling

Frozen fresh and dried cones were ground for 1 min with a blender (Vitamix Explorian blender, Ohio, USA) prior to aroma analysis. Forty mg of fresh hop powder or 10 mg of dried hop powder were placed in a 20-mL amber SPME vial (Supelco, Bellefonte, PA, USA). The vials were sealed with a PTFE-lined cap (Supelco, Bellefonte, PA, USA) and equilibrated in the autosampler agitator (Leap Technologies Inc., Carrboro, NC, USA) for 10 min at 50°C with a stirring speed of 250 rpm. A preconditioned 1-cm 50/30 divinylbenzene/Carboxen/PDMS fibre (Supelco, Bellefonte, PA) was exposed to the headspace of the vial for an additional 30 min at 50°C prior to GC injection.

GC-MS-O analysis

The GC-MS-O system equipped with a 6890N GC (Agilent Technologies Inc., Santa Clara, CA, USA), an 5975B MSD and a PHASER Olfactory Detection Port (GL Sciences, Eindhoven, The Netherlands) was used to analyse the aroma composition in hops. Separations were performed on a DB-WAX capillary column (30 m × 0.32 mm i.d., 0.25 µm film thickness) (Supelco, Bellefonte, PA, USA). Oven temperature was programmed from 40°C to 150°C at 5°C/min and then to 225°C at 20°C/min with an initial and final holding time of 5 and 20 min, respectively. Helium was used as the carrier gas at a constant flow rate of 2 ml/min. Conditions for the MSD were as follows: interface temperature, 230°C; ionization energy, 70 eV; mass range, 40~500 amu; EM voltage, Autotune +165 V; scan rate, 4.45 scans/s.

Three panellists (aged from 25 to 45) were selected to perform olfactometry analysis. All panellists have received at least 20 h of GC-O training by sniffing 25 aroma standards commonly found in hops. The retention time, odour descriptors, and intensities of all the perceivable odorants were recorded.

Quantitation

Stable isotope dilution analysis (SIDA) and standard addition method (SAM) were used for the quantitation of aroma-active compounds in hops. Isotopically labelled standards including 1.20 µg/µL [²H₂]-β-myrcene, 0.10 µg/µL [²H₃]-linalool, 0.10 µg/µL [²H₆]-geraniol, 0.05 µg/µL [²H₆]-geraniol acetate, 0.05 µg/µL [²H₁₅]-methyl octanoate and 0.01 µg/µL [²H₂]-cis-3-hexen-1-ol in methylene chloride were employed for accurate quantitation, with response factors of 0.9389, 1.0274, 0.8576, 1.2723, 1.3879 and 1.5775, respectively. The mixture of 0.73 µg/µL decane and 0.48 µg/µL 2-octanol in methanol was used as the internal standard for SAM. Peak area ratio and mass ratio of targeted aromas to internal standard were obtained to build calibration curves, which can be further applied for calculating the final concentrations of analytes.

Colour evaluation

Parameters relating to the colour of dried hops were determined using a hand-held colorimeter (Minolta Co., Ltd., Chiyoda, Tokyo, Japan) according to the International Commission on Illumination (CIE) colour coordinates *L**, *a** and *b**. Browning index, which is a reflection of the brown colour purity in hops, can be further calculated using the following equation:

$$\text{Browning index (BI)} = \frac{100 \times \left(\frac{a^* + 1.75 \times L^*}{5.645 \times L^* + a^* - 3.012 \times b^*} \right) - 0.31}{0.17}$$

Results and discussion

A total of 33 aroma-active compounds were identified in five fresh Cascade and Chinook hops using HS-SPME-GC-MS-O. Tables 1 and 2 show the odour attributes and concentrations of selected aroma-active compounds in five fresh hop samples, respectively. Most of these aroma compounds exhibited fruity, sweet, floral and citrus notes except α-pinene and β-myrcene, which possessed piney, woody and herbal notes. All five samples expressed complex profiles with varied concentrations of aroma constituents. In general, both Meadowview Cascade and Meadowview Chinook contained significantly higher aroma concentrations for most of the compounds compared to their counterparts from other growing regions, which might be attributed to the advantageous climate condition, soil or agronomic practices from that particular growing site. In addition, L-calamenene and germacrene B were characteristic aroma compounds unique to Cascade and Chinook hops, respectively.

Table 1: Odour attributes of selected aroma-active compounds in fresh Cascade and Chinook hops.

No.	Aroma compounds	Odour description
1	2-Methylbutyl isovalerate	floral, fruity, berry, apple
2	Methyl octanoate	sweet, fruity, waxy, herbal, plastic
3	Methyl (4E)-4-nonenoate	fruity, citrus, lemon
4	α -Pinene	cedarwood, piney
5	β -Myrcene	balsamic, woody, herbal
6	trans- α -Bergamotene	sweet, floral, citrus
7	L-Calamenene	rosy, sweet, cinnamon
8	Germacrene B	rosy, sweet
9	Linalool	sweet, floral, orange
10	Geraniol	orange, citrus

Table 2: Concentrations of selected aroma-active compounds in fresh Cascade and Chinook hops¹.

No. ²	Concentration (μ g/g hops dry basis)				
	Ca-MDV	Ca-PTB	Ca-BKB	Ch-MDV	Ch-PTB
1	5.59 \pm 0.31 ^a	2.92 \pm 0.13 ^c	3.52 \pm 0.23 ^b	25.38 \pm 0.67 ^a	2.66 \pm 0.22 ^b
2	3.85 \pm 0.77 ^a	1.80 \pm 0.21 ^b	2.35 \pm 0.14 ^{ab}	11.36 \pm 2.21 ^a	5.46 \pm 0.17 ^a
3	5.02 \pm 0.07 ^a	2.41 \pm 0.08 ^c	3.10 \pm 0.21 ^b	5.36 \pm 0.06 ^a	1.93 \pm 0.17 ^b
4	2.79 \pm 0.29 ^a	2.82 \pm 0.13 ^a	2.70 \pm 0.25 ^a	4.36 \pm 0.67 ^a	1.04 \pm 0.04 ^b
5	1872.01 \pm 108.10 ^a	1384.89 \pm 151.81 ^a	1473.63 \pm 143.92 ^a	2121.68 \pm 101.56 ^a	418.79 \pm 31.61 ^b
6	54.98 \pm 3.66 ^a	35.27 \pm 0.74 ^b	38.97 \pm 7.99 ^b	132.33 \pm 9.78 ^a	11.57 \pm 1.92 ^b
7	0.15 \pm 0.01 ^b	0.19 \pm 0.00 ^a	0.17 \pm 0.02 ^{ab}	ND	ND
8	ND ³	ND	ND	308.57 \pm 37.70 ^a	23.74 \pm 5.34 ^b
9	25.24 \pm 0.74 ^a	17.10 \pm 1.43 ^b	18.61 \pm 0.35 ^b	23.29 \pm 0.99 ^a	11.08 \pm 0.54 ^b
10	9.65 \pm 0.02 ^a	6.48 \pm 0.45 ^b	8.44 \pm 0.30 ^a	44.52 \pm 1.49 ^a	3.35 \pm 0.30 ^b

¹ Ca: Cascade; Ch: Chinook; MDV: Meadowview; PTB: Petersburg; BKB: Blacksburg;

² The number is corresponding to the aroma compounds in Table 1;

³ ND: Not detected;

Within the same hop variety, values of concentration followed by same superscript letter in the same row were not significantly different ($p < 0.05$).

According to the HS-SPME-GC-MS-O results, a total of 35 aroma-active compounds were identified in dried Meadowview Cascade and Chinook hops. Table 3 exhibited the odour characteristics of the 9 most important compounds in dried hops. In addition to β -myrcene and β -ocimene that were perceived as woody, herbal, smoky and earthy notes, other aroma compounds possessed typical floral, fruity, sweet and citrus odour impressions. The concentrations of the above-mentioned aroma-active compounds were shown in Table 4. The dehydrator-dried hops showed significantly higher aroma concentrations for most of the compounds in both varieties, followed by freeze-dried hops and then oven-dried ones. Linalool and geraniol were two exceptions in Meadowview Chinook hops, in which significantly higher contents of these two compounds were observed after freeze-drying. Freeze-drying is usually considered as a reliable approach to circumvent thermal degradation and achieve excellent aroma retention in food products. However, in this study, freeze-drying only led to intermediate content levels for most aromas among three drying practices. This might be ascribed to the pressure reduction in the drying chamber that might have led to considerable loss of volatile compounds with low-boiling points to the environment [7].

Table 3: Odour attributes of selected aroma-active compounds in dried Cascade and Chinook hops.

No.	Aroma compounds	Odour description
1	Methyl octanoate	floral, sweet, fruity
2	Geranyl propionate	floral, rose, waxy
3	β -Myrcene	balsamic, woody, herbal
4	β -Ocimene	earthy, smoky, green
5	trans- α -Bergamotene	sweet, floral, citrus
6	Germacrene B	rose, sweet
7	L-Calamenene	rose, sweet, cinnamon
8	Linalool	sweet, floral, orange
9	Geraniol	orange, citrus

Table 4: Concentrations of selected aroma-active compounds in dried Cascade and Chinook hops¹.

No. ²	Ca-MDV			Ch-MDV		
	DD	OD	FD	DD	OD	FD
1	8.10±0.07 ^a	6.11±0.38 ^a	7.02±0.78 ^a	20.70±0.76 ^a	19.13±1.17 ^b	30.42±0.85 ^b
2	9.83±0.07 ^a	8.12±0.86 ^b	8.11±0.75 ^b	8.59±0.75 ^a	7.09±0.89 ^{ab}	6.82±0.28 ^b
3	2333.52±110.53 ^a	1750.02±141.12 ^b	2069.47±129.80 ^{ab}	3122.19±105.82 ^a	2839.74±195.33 ^a	2678.52±232.53 ^a
4	13.94±0.46 ^a	11.83±0.54 ^b	12.35±1.00 ^{ab}	15.28±0.62 ^a	12.28±0.60 ^b	13.17±0.48 ^b
5	37.23±1.53 ^a	30.73±1.24 ^b	30.98±2.06 ^b	104.41±7.06 ^a	82.41±6.07 ^b	82.59±1.57 ^b
6	ND ³	ND	ND	77.46±5.53 ^a	53.70±5.05 ^b	63.65±1.05 ^b
7	0.12±0.00 ^a	0.11±0.00 ^a	0.11±0.00 ^a	ND	ND	ND
8	16.68±1.77 ^a	10.89±0.23 ^b	15.53±0.12 ^a	18.45±0.56 ^b	16.70±0.75 ^c	26.26±0.77 ^a
9	9.65±0.44 ^a	7.39±0.37 ^a	9.10±1.00 ^a	74.49±2.66 ^b	53.79±4.43 ^c	98.71±0.18 ^a

¹ Ca: Cascade; Ch: Chinook; MDV: Meadowview; PTB: Petersburg; BKB: Blacksburg; DD: Dehydrator drying; OD: Oven drying; FD: Freeze-drying

² The number is corresponding to the aroma compounds in Table 3;

³ ND: Not detected

Within each hop variety, values of concentration followed by same superscript letter in the same row were not significantly different ($p < 0.05$).

Principal component analysis was applied in this study to further understand the difference in aroma profiles of fresh and dried hops. Figure 1a shows the score plot for all fresh hops in triplicates. The only overlap observed were Blacksburg and Petersburg Cascade hops, suggesting certain similarity in their aroma profiles. Both Meadowview Cascade and Chinook hops were well separated from their counterparts, demonstrating their unique aroma characteristics. This is in agreement with the quantitation results. According to the score plot for dried hop samples (Figure 1b), different drying techniques resulted in dissimilarity of aroma compositions in hops. Dehydrator-dried hops could be clearly discriminated from corresponding oven-dried and freeze-dried ones, whereas the latter two were overlapped for both hop varieties. This indicated the distinguishing aroma profile in dehydrator-dried hops.

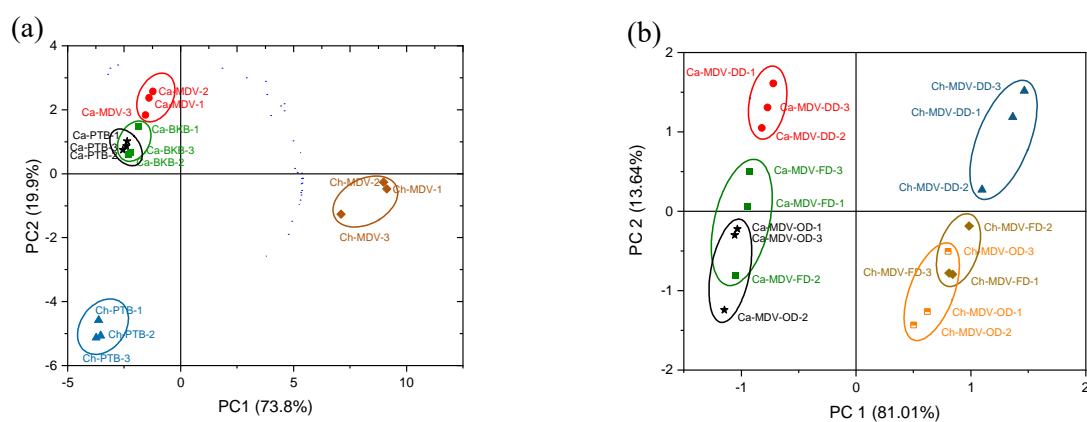


Figure 1: Principal component score plot of (a) five fresh hops and (b) dried hops based on the concentrations of selected aroma-active compounds. Ca: Cascade; Ch: Chinook; MDV: Meadowview; PTB: Petersburg; BKB: Blacksburg; DD: Dehydrator drying; OD: Oven drying; FD: Freeze-drying.

From a consumer-acceptance point of view, colour is an important attribute to determine the quality of dried products, therefore the colour of dried hops was also evaluated (Table 5). As expected, freeze-drying could provide both varieties with the highest L^* and b^* and the lowest a^* and BI values, followed by dehydrator drying and then oven drying. In other words, among all the drying practices, freeze-drying could minimise the green colour degradation and retain the original hues of hops most effectively. The reason for the better performance of freeze-drying might be ascribed to its lower possessing temperature, which can prevent the nonenzymatic browning and provide the maximum retention of chlorophyll in hops [8]. However, freeze-drying is a costly process and its operation requires high-energy consumption. To this end, dehydrator drying is an overall appropriate drying practice for small-size hop growers due to its decent aroma and colour retention as well as low initial investment and energy consumption.

Table 5: Colour evaluation of dried Cascade and Chinook hops¹.

Colour Attributes ²	Ca-MDV			Ch-MDV		
	DD	OD	FD	DD	OD	FD
<i>L</i> [*]	15.18±0.30 ^b	13.30±0.45 ^c	17.87±0.15 ^a	13.02±0.31 ^b	12.86±0.21 ^b	17.34±0.26 ^a
<i>a</i> [*]	-2.28±0.28 ^b	-0.15±0.07 ^a	-4.23±0.17 ^c	-0.90±0.05 ^b	1.10±0.08 ^a	-3.55±0.10 ^c
<i>b</i> [*]	16.27±0.40 ^a	15.68±0.15 ^a	16.53±0.49 ^a	16.56±0.15 ^a	16.47±0.14 ^{ab}	16.16±0.11 ^b
BI	233.41±14.34 ^b	309.45±21.58 ^a	157.27±8.89 ^c	385.41±21.58 ^a	395.42±27.36 ^a	162.87±5.37 ^b

¹ Ca: Cascade; Ch: Chinook; MDV: Meadowview; PTB: Petersburg; BKB: Blacksburg; DD: Dehydrator drying; OD: Oven drying; FD: Freeze-drying

² *L*^{*}: 0 (black) to 100 (white); *a*^{*}: +60 (red) to -60 (green); *b*^{*}: +60 (yellow) to -60 (blue); BI: Browning Index, brown colour purity; Within each hop variety, values with same superscript letter in the same row were not significantly different ($p < 0.05$).

Conclusion

All fresh samples investigated in this study exhibited distinctive aroma profiles, which might have been attributed not only to varietal difference, but also to other environmental and agronomical factors at different growing sites. Predominant components detected were responsible for typical herbal, sweet and citrus notes. Both varieties from Meadowview farm exhibited the highest concentrations for most aroma compounds, indicating a potential location advantage. Dehydrator drying was able to retain higher aroma concentrations compared to oven and freeze-drying, therefore was considered as a desirable drying practice for small-size hop growers to enhance the quality of final hop products.

References

1. Steenackers B, De Cooman L, De Vos D. Chemical transformations of characteristic hop secondary metabolites in relation to beer properties and the brewing process: A review. *Food Chem.* 2015;172:742-756.
2. Hieronymus, S. Growing hops. In: Hieronymus S, editors. *For the love of hops: the practical guide to aroma, bitterness and the culture of hops.* Boulder, CO, USA: Brewers Publications; 2012. p. 87-112.
3. Almaguer C, Schönberger C, Gastl M, Arendt E-K, Becker T. *Humulus lupulus*—a story that begs to be told. A review. *J Inst Brew.* 2014;120(4):289-314.
4. Garber B, Morgan K-L, Scoggins H, Seigle L. An overview of small-scale commercial hops production in Virginia. *J Food Distrib Res.* 2019;50(1): 89-92.
5. Judd B-D. Hops production in Virginia: nutrition, fungal pathogens, and cultivar trials. Degree of Master of Science. Virginia Polytechnic Institute and State University, Blacksburg, VA; 2018.
6. Tressl R, Friese L, Fendesack F, Koppler H. Studies of the volatile composition of hops during storage. *J Agric Food Chem.* 1978;26(6):1426-1430.
7. Ca Lin-Sanchez A, Szumny A, Figiel A, Jalszynski K, Adamski M, Ca Rbonell-Barrachina A-A. Effects of vacuum level and microwave power on rosemary volatile composition during vacuum-microwave drying. *J Food Eng.* 2011;103(2):219-227.
8. Guiné, R-P-F, Barroca M-J. Effect of drying treatments on texture and colour of vegetables (pumpkin and green pepper). *Food Bioprod Process.* 2012;90(1):58-63.

Aroma-Active Compounds Contributing to Aged Riesling Character

MELISSA DEIN, Trenton Kerley, John P. Munafo, Jr.

Department of Food Science, University of Tennessee, Knoxville, TN, United States, mfoley9@vols.utk.edu

Abstract

The Riesling varietal, which originates from the Rhine region of Germany, is globally one of the most popular white wine grapes. Young Riesling wines are favoured for their fruity and floral character; however, lesser-known aged Rieslings possess a more complex aroma profile with notes of sherry, maple, and a balanced petrol character. Several fruity esters and alcohols are known to contribute to the tropical fruit and floral character of young Rieslings, but the odorants that contribute to the complexity of aged Rieslings are not well characterised. Thus, the goal of this study was to employ aroma extract dilution analysis (AEDA) and stable isotope dilution assays (SIDA) to identify and quantitate the key odorants that contribute to the aroma of a ten-year-old Joh. Jos. Prüm Riesling. This study afforded 34 odorants with flavour dilution (FD) factors greater than 1, with 2-phenylethanol (floral, rose) and ethyl butanoate (fruity) having the highest FD factor of 1024. Upon quantitation by SIDA, the odorant with the highest odour activity value (OAV) was wine lactone (coconut, OAV 460) followed by ethyl octanoate (fruity, OAV 240) and ethyl hexanoate (fruity, OAV 97). Other odorants with OAVs greater than 1, which may contribute to the complex aroma of the aged Riesling, included 5-ethyl-3-hydroxy-4-methyl-(5H)-furan-2-one (sherry, OAV 33), 1,1,6-trimethyl-1,2-dihydronaphthalene (petrol, OAV 6.4), and 3-methylbutan-1-ol (malty, OAV 3.6). This study has provided a comprehensive evaluation of key odorants contributing to the characteristic aroma of a bottle-aged Riesling and provides a foundation for future studies to probe the influence of each odorant in the overall aroma of aged Riesling.

Keywords: aged Riesling, aroma extract dilution analysis, stable isotope dilution assays

Introduction

The Riesling varietal originates from a region of south-western Germany surrounding the Rhine River and is the most commonly grown variety in Germany. The varietal has gained global popularity for its refreshing fruity and floral character and is now grown in cool climates throughout the world. The aroma of young Riesling is described as having a predominant fruity and floral character with notes of citrus, tropical fruit and even honey. Previous studies have shown that several esters and alcohols are responsible for the aroma of young Riesling [1, 2]. However, the odorants that contribute to the more complex aroma profile of bottle-aged Riesling, which include notes of sherry, maple, and petrol, are not fully understood.

Experimental

To characterise the aroma of a bottle aged Riesling the wine was extracted with organic solvent and distilled by solvent assisted flavour evaporation (SAFE) to isolate the volatile compounds. Aroma extract dilution analysis (AEDA) of the SAFE isolate was employed to identify which volatile compounds were aroma-active and stable isotope dilution assays (SIDA) were used to quantitate aroma-active compounds.

Selected Wine

The bottle aged Riesling selected for this study was a 2009 Riesling Kabinett produced by Joh. Jos. Prüm. The wine was purchased from a local distributor and maintained at 2 °C prior to analysis.

Extraction and Isolation of volatile compounds by solvent assisted flavour evaporation (SAFE)

Volatile compounds were extracted from the wine with distilled diethyl ether (Honeywell Burdick and Jackson, Muskegon, MI) and distilled by SAFE. Wine (50 mL), NaCl (5 g), and diethyl ether (100 mL) were combined and extracted by manual shaking (5 min). The aqueous phase was re-extracted with additional diethyl ether (50 mL) and the organic phases combined. The organic extract was then washed with saturated NaCl solution two times (2 x 50 mL) and then dried over anhydrous Na₂SO₄. The volatile compounds were distilled from the organic extract by SAFE with the apparatus maintained at 41 °C and under vacuum (10⁻³ mbar). The SAFE isolate was dried over anhydrous Na₂SO₄ and condensed to 200 µL with a Vigreux column followed by a gentle stream of N₂.

Aroma Extract Dilution Analysis (AEDA)

The SAFE isolate was serially diluted with diethyl ether to generate eleven samples decreasing in concentration and designated as flavour dilution 1 (FD 1) to flavour dilution 1024 (FD 1024). Each sample was individually

analysed by gas chromatography-olfactometry (GC-O) beginning with FD 1 (the undiluted SAFE isolate) and ending with FD 1024. Each aroma detected by GC-O was assigned an odour quality and the highest flavour dilution that each aroma could be perceived was determined. The identity of each odorant was determined through a combination of odour quality, retention index, and mass spectrum.

GC-O was carried out on an Agilent 7820A GC system with a flame ionization detector (FID) (Agilent Technologies, Santa Clara, CA) fitted with a Zebtron ZB-FFAP GC column (30 m length, 0.32 mm i.d., 0.25 µm film thickness) from Phenomenex (Torrance, CA). A 1 µL sample was injected on column and carried by helium gas (1.5 mL/min) and separated with the following temperature program: initial temperature of 35 °C was held for 1 minute, ramp to 60 °C at 60 °C/min, ramp to 240 °C at 6 °C/min, and a final hold time of 10 minutes at 240 °C. At the end of the chromatographic column the effluent was split with a Y-splitter and half the effluent was channelled to a heated nose cone (250 °C) and the other half was channelled to the FID detector (250 °C, 40 mL/min hydrogen gas, 450 mL/min air, and 45 mL/min makeup gas).

Stable Isotope Dilution Assays (SIDA)

To quantitate each analyte, an isotopically labelled analogue was used as an internal standard. The isotopically labelled standards were acquired from commercial suppliers or synthesized in house, and a response factor for each analyte/standard pair was determined by GC-MS (Table 1). The isotopically labelled standards were volumetrically added to the wine prior to being extracted with diethyl ether, subjected to SAFE, and condensed according to the method described above. The resulting SAFE isolate was analysed by GC-MS and the odorants were quantitated using the previously determined response factors.

GC-MS was carried out on an Agilent 7820A GC system coupled to an Agilent 5977B mass spectrometer (Agilent Technologies, Santa Clara, CA). A Zebtron ZB-FFAP GC capillary column (30 m length, 0.25 mm i.d., 0.25 µm film thickness) from Phenomenex (Torrance, CA) was used for chromatographic separation. A 1 µL sample was injected on column (35 °C) and carried by helium gas (1.5 mL/min). The following temperature program was used to achieve chromatographic separation: initial temperature of 35 °C was held for 1 minute, ramp to 60 °C at 60 °C/min, ramp to 250 °C at 6 °C/min, and a final hold time of 5 minutes at 250 °C. The MS detector was operated in electron impact ionization mode (70 eV), the MS source was held at 230 °C, and the MS quadrupole at 150 °C.

Table 1: Ions and response factors of odorants and labelled isotopes used for stable isotope dilution assays.

no.	odorant	labelled standard	ion (<i>m/z</i>)		
			analyte	standard	RF
1	ethyl isobutyrate ^a	ethyl isobutyrate-d2 ^d	116	118	0.98
2	ethyl butanoate ^a	ethyl butanoate-d3 ^e	116	119	0.96
3	(<i>S</i>)-ethyl 2-methylbutanoate ^a	(<i>S</i>)-ethyl 2-methylbutanoate-d9 ^e	102	107	0.86
4	ethyl 3-methylbutanoate ^a	ethyl 3-methylbutanoate-d2 ^d	85	87	0.58
5	2-methylpropan-1-ol ^a	2-methylpropan-1-ol-d7 ^f	74	81	1.66
7	2- and 3-methylbutan-1-ol ^a	3-methylbutan-1-ol-d4 ^e	70	74	1.22
8	ethyl hexanoate ^a	ethyl hexanoate-d11 ^e	99	110	0.83
11	cis-rose oxide ^a	cis-rose oxide-d2 ^f	139	141	0.62
13	ethyl octanoate ^a	ethyl octanoate-d15 ^e	127	142	0.80
14	acetic acid ^a	acetic acid- ¹³ C1 ^a	60	61	1.13
15	3-(methylsulphanyl)propanal ^a	3-(methylsulfonyl)propanal-d3 ^d	104	107	1.21
16	linalool ^a	linalool-d3 ^e	93	96	0.85
17	2-methylpropanoic acid ^a	2-methylpropanoic acid-d7 ^e	88	95	1.14
18	butanoic acid ^a	butanoic acid-d7 ^e	73	77	0.89
19a	2-methylbutanoic acid ^a	2-methylbutanoic acid-d9 ^e	57	66	1.05
19b	3-methylbutanoic acid ^a	3-methylbutanoic acid-d9 ^e	60	63	1.02
21	1,1,6-trimethyl-1,2-dihydronaphthalene ^b	1,1,6-trimethyl-1,2,3,4-tetrahydronaphthalene-d4 ^f	157	162	0.73
22	(<i>E</i>)-β-damascenone ^a	(<i>E</i>)-β-damascenone-d4 ^d	69	73	0.92
23	2-phenylethyl acetate ^a	2-phenylethyl acetate-d5 ^f	104	109	1.25
27	2-phenylethanol ^a	2-phenylethanol-d5 ^e	122	127	0.99
29	HDMF ^a	HDMF- ¹³ C2 ^a	128	130	0.96
31	wine lactone ^c	wine lactone-d3 ^d	166	169	0.94
32	5-ethyl-3-hydroxy-4-methyl-(5 <i>H</i>)-furan-2-one ^a	3-hydroxy-4,5-dimethylfuran-2(5 <i>H</i>)-one - ¹³ C2 ^d	142	130	1.29
33	2-phenylacetic acid ^a	2-phenylacetic acid-d5 ^g	91	96	0.90
34	4-hydroxy-3-methoxybenzaldehyde ^a	4-hydroxy-3-methoxybenzaldehyde-d3 ^e	152	155	0.21

^a reference standard purchased from Millipore Sigma (St. Louis, MO). ^b reference standard purchased from MuseChem (Fairfield, NJ). ^c reference standard purchased from eNovation Chemicals LLC (Green Brook, NJ). ^d labelled standard purchased from aromaLAB (Planegg, Germany). ^e labelled standard purchased from C/D/N Isotopes Inc. (Pointe-Clair, Quebec, Canada). ^f labelled standard synthesized in house. ^g labelled standard purchased from Cambridge Isotope Laboratories, Inc. (Tewksbury, MA).

Results and discussion

To gain insight into the odorants that may be indicative of aged Riesling character, an individual wine that embodied these aged qualities was selected for a full aroma characterisation. The selected wine was a 2009 Riesling Kabinett produced by Joh. Jos. Prüm, a winery highly regarded for producing some of the highest quality Rieslings in Germany. The aroma of this wine is described as having prominent fruity, floral and citrus character with balanced acidity and more subtle notes of vanilla, coconut, caramel, sherry, maple, and petrol.

AEDA was employed to determine the odorants that were present in the aged Riesling, which could be perceived by GC-O, and the relative impact of each odorant. As a result, 34 odorants were identified with FD factors ≥ 1 (Figure 1). Ethyl butanoate and 2-phenylethanol, which exhibit fruity and rose odour characteristics respectively, had the highest FD factor (FD 1024). Other odorants with fruity and floral odour characteristics were identified with an FD factor of 256, namely (*S*)-ethyl 2-methylbutanoate, ethyl 3-methylbutanoate, ethyl hexanoate, ethyl octanoate, and (*E*)- β -damascenone. However, 2 and 3-methylbutan-1-ol (malty), HDMF (caramel), and 5-ethyl-3-hydroxy-4-methyl-(5*H*)-furan-2-one (sherry) also had FD factors of 256 and thus may be contributing to the complexity of aged Riesling aroma beyond the fruity and floral qualities.

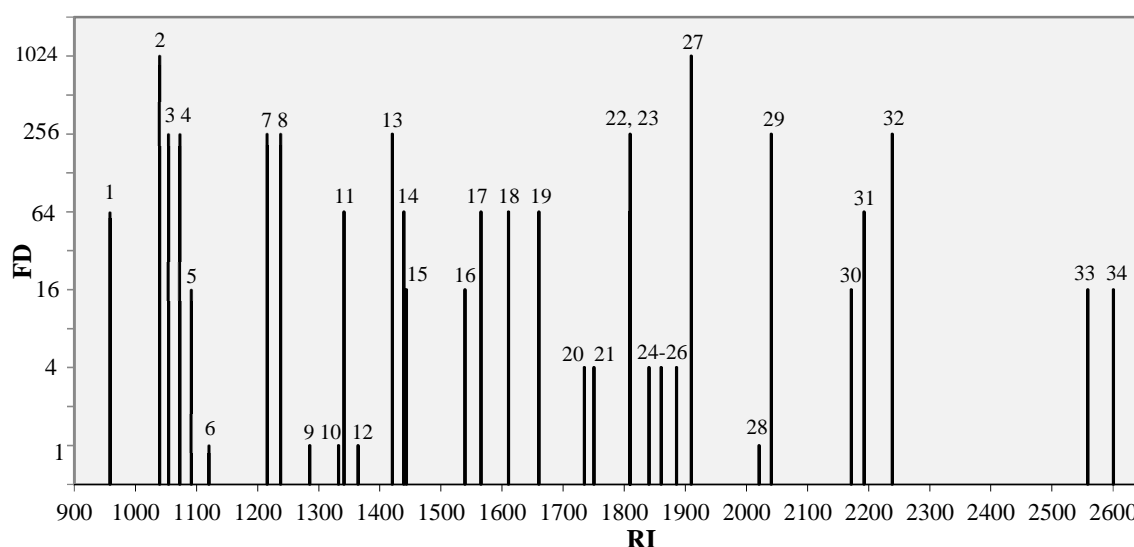


Figure 1. Flavor dilution chromatogram of odorants identified in bottle aged Riesling wine by aroma extract dilution analysis. (1) ethyl isobutyrate; (2) ethyl butanoate; (3) (*S*)-ethyl 2-methylbutanoate; (4) ethyl 3-methylbutanoate; (5) 2-methylpropan-1-ol; (6) 3-methylbutyl acetate; (7) 2 and 3-methylbutan-1-ol; (8) ethyl hexanoate; (9) 1-octen-3-one; (10) hexanol; (11) cis-rose oxide; (12) (*Z*)-3-hexenol; (13) ethyl octanoate; (14) acetic acid; (15) 3-(methylsulphonyl)propanal; (16) linalool; (17) 2-methylpropanoic acid; (18) butanoic acid; (19) 2- and 3-methylbutanoic acid; (20) pentanoic acid; (21) 1,1,6-trimethyl-1,2-dihydronaphthalene; (22) (*E*)- β -damascenone; (23) 2-phenylethyl acetate; (24) hexanoic acid; (25) geraniol; (26) 2-methoxyphenol; (27) 2-phenylethanol; (28) γ -nonalactone; (29) HDMF; (30) sotolon; (31) wine lactone; (32) 5-ethyl-3-hydroxy-4-methyl-(5*H*)-furan-2-one; (33) 2-phenylacetic acid; (34) 4-hydroxy-3-methoxybenzaldehyde.

To further probe the relative impact of each odorant in the matrix of the aged Riesling, odorants were accurately quantitated and odour activity values calculated. The odorants with high FD factors ($FD \geq 64$ and other selected odorants) were quantitated through the application of SIDAs, resulting in 14 quantitated odorants having OAVs ≥ 1 (Table 2). The odorants with the highest OAVs were wine lactone (coconut, OAV 460), ethyl octanoate (fruity, OAV 240), ethyl hexanoate (fruity, OAV 97), and (*E*)- β -damascenone (cooked apple, OAV 60). In addition to these and other fruity and floral odorants, some odorants that are not traditionally found in young Riesling wines also had OAVs ≥ 1 . 5-ethyl-3-hydroxy-4-methyl-(5*H*)-furan-2-one, which has not been previously identified in young Rieslings, was determined to have a relatively high OAV of 33. This compound imparts a sherry odour quality, which can be associated with aged Riesling. Likewise, 1,1,6-trimethyl-1,2-dihydronaphthalene (petrol) was determined to have an OAV of 6.4. The importance of this compound to the aroma of aged Riesling is supported by previous findings that this odorant is generated during bottle aging and imparts a petrol-like note to Riesling [3, 4]. Similarly, 3-methylbutan-1-ol (malty) was determined to have an OAV of 3.6. This compound has been previously identified as important to the aroma of sherry [5], another aged wine, and may also contribute to the malty notes associated with aged Riesling. This analysis has indicated several key odorants that exhibit odour qualities associated with aged Riesling character. Though these findings provide insight into odorants that may contribute to the unique aroma profile of aged Riesling, additional sensory experiments are needed to fully understand the complexity of aged Riesling aroma.

Table 2: Odorant concentrations, odour thresholds, and odour activity values of key odorants in bottle aged Riesling.

no.	odorant	odour quality	concentration ($\mu\text{g/L}$) ^a	odour threshold ($\mu\text{g/L}$) ^b	OAV ^d
31	wine lactone	coconut	4.59	0.010	460
13	ethyl octanoate	fruity	481	2.0	240
8	ethyl hexanoate	fruity	483	5.0	97
22	(<i>E</i>)- β -damascenone	cooked apple	3.00	0.050	60
32	5-ethyl-3-hydroxy-4-methyl-(5 <i>H</i>)-furan-2-one	sherry	163	5.0	33
3	(<i>S</i>)-ethyl 2-methylbutanoate	fruity	21.6	1.0	22
15	3-(methylsulphanyl)propanal	cooked potato	8.55	0.43 ^c	20
1	ethyl isobutyrate	fruity	142	15	9.5
2	ethyl butanoate	fruity	141	20	7.1
21	1,1,6-trimethyl-1,2-dihydronaphthalene	petrol	12.9	2.0	6.4
11	cis-rose oxide	floral	1.18	0.20	5.9
7b	3-methylbutan-1-ol	malty	109000	30000	3.6
27	2-phenylethanol	rose	31000	10000	3.1
4	ethyl 3-methylbutanoate	fruity	6.85	3.0	2.3
5	2-methylpropan-1-ol	malty	32600	40000	<1
16	linalool	floral	9.99	15	<1
23	2-phenylethyl acetate	floral	139	250	<1
14	acetic acid	vinegar	94300	200000	<1
34	4-hydroxy-3-methoxybenzaldehyde	vanilla-like	89.5	200	<1
18	butanoic acid	sweaty	1390	10000	<1
19b	3-methylbutanoic acid	sweaty, rancid	239	3000	<1
19a	2-methylbutanoic acid	sweaty, rancid	174	3000	<1
7a	2-methylbutan-1-ol	malty	76.2	3700 ^c	<1
33	2-phenylacetic acid	honey	69.9	6100 ^c	<1
29	HDMF	caramel	2.62	500	<1
17	2-methylpropanoic acid	sweaty	857	200000	<1

^a mean of at least three data points. ^b odour thresholds determined in water/ ethanol (90/10, w/w) reported in [6]. ^c odour threshold determined in water reported in [7]. ^d odour activity value (concentration/odour threshold).

Conclusion

As a result of this study, 34 odorants with FD factors ≥ 1 were identified from an aged Riesling by AEDA and 26 of the odorants were quantitated by SIDAs. Several key odorants with OAVs ≥ 1 exhibited odour qualities such as coconut, sherry, petrol, and malty suggesting these odorants may be influential to the aroma of the bottle aged Riesling. Future studies, such as aroma recombination and omission experiments, are needed to further probe the impact of each odorant on the aroma of the aged Riesling.

References

1. Chisholm MG, Guiher LA, Vonah TM, Beaumont JL. Comparison of some French-American hybrid wines with White Riesling using gas chromatography-olfactometry. *Am J Enol Vitic.* 1994;45(2):201-12.
2. Bowen AJ, Reynolds AG. Odor potency of aroma compounds in Riesling and Vidal blanc table wines and icewines by gas chromatography-olfactometry-mass spectrometry. *J Agric Food Chem.* 2012;60(11):2874-83.
3. Winterhalter P. 1, 1, 6-Trimethyl-1, 2-dihydronaphthalene (TDN) formation in wine. 1. Studies on the hydrolysis of 2, 6, 10, 10-tetramethyl-1-oxaspiro [4.5] dec-6-ene-2, 8-diol rationalizing the origin of TDN and related C13 norisoprenoids in Riesling wine. *J Agric Food Chem.* 1991;39(10):1825-9.
4. Winterhalter P, Gök R. TDN and β -Damascenone: Two important carotenoid metabolites in wine. *Carotenoid Cleavage Products: ACS Publications;* 2013. p. 125-37.
5. Marcq P, Schieberle P. Characterization of the key aroma compounds in a commercial amontillado sherry wine by means of the sensomics approach. *J Agric Food Chem.* 2015;63(19):4761-70.
6. Guth H. Quantitation and sensory studies of character impact odorants of different white wine varieties. *J Agric Food Chem.* 1997;45(8):3027-32.
7. Czerny M, Christlbauer M, Christlbauer M, Fischer A, Granvogl M, Hammer M, et al. Re-investigation on odour thresholds of key food aroma compounds and development of an aroma language based on odour qualities of defined aqueous odorant solutions. *Eur Food Res Technol.* 2008;228(2):265-73.

Asparagus waste streams to aroma-rich vegetable flavourings (The effect of partial replacement of maltodextrin with vegetable fibres in spray-dried white asparagus on its aroma properties)

EIRINI PEGIOU^{1,a}, Joanne W Siccama^{2,a}, Nienke M. Eijkelboom², Lu Zhang², Roland Mumm³, Maarten A.I. Schutyser² and Robert D. Hall^{1,3}

1 Wageningen University & Research, Laboratory of Plant Physiology, Wageningen, The Netherlands

2 Wageningen University & Research, Laboratory of Food Process Engineering, Wageningen, The Netherlands

3 Wageningen University & Research, Bioscience, Wageningen, The Netherlands

^a Shared first authorship: these authors contributed equally.

eirini.pegiou@wur.nl

Abstract

White asparagus (*A. officinalis*) is a popular vegetable consumed worldwide and its cooked spears are appreciated for their distinct flavour profile. During asparagus harvesting, around one-third of the total material is usually discarded. This significant waste stream partially consists of the stem bases which are cut off to produce spears with the same desired length for delivery to the supermarket. This waste stream could become a valuable resource of food ingredients. Asparagus waste was used to generate an asparagus concentrate, and this was spray-dried in different carrier formulations in which maltodextrin was partially replaced by cellulose-based carriers, i.e. asparagus fibre, citrus fibre or microcrystalline cellulose. Powders obtained from feed solutions with an initial solids content of 40 % w/w showed better physical properties and aroma retention than 30 % w/w. Partial replacement of maltodextrin by cellulose-based carriers resulted in powders with similar physical properties to the control and did not detrimentally influence the aroma profiles as analysed by headspace solid-phase microextraction and gas chromatography-mass spectrometry. Aroma analysis was focused on asparagus key volatiles based on previous studies. This research showed that fibre obtained from asparagus waste streams could potentially be used as a carrier to produce spray-dried asparagus powder with retained key asparagus odorants such as 2-methoxy-3-isopropyl pyrazine. Valorisation of these materials could reduce the amount of agricultural waste while generating aroma-rich natural food products.

Keywords: asparagus aroma, volatile retention, GC-MS, asparagus fibre

Introduction

White asparagus (*A. officinalis*) is a globally popular vegetable, of which the cooked spears are appreciated for their distinct flavour profile which is perceived as being slightly more bitter and less sweet than its green counterpart [1]. Vegetables, including asparagus, often have rich aroma profiles which are also influenced by their processing history (e.g. fresh, cooked, dried, etc.). The aroma profile of cooked white asparagus has been studied in the past [2,3], and these studies have indicated its complexity as it consists of volatile compounds from diverse chemical classes, including aldehydes, pyrazines and sulphur compounds (Figure 1).

Asparagus is known for its limited harvest season, which in Europe is between March until June. Unfortunately, after harvest, ca. one third of the collected crop is discarded as waste for the following reasons; the bottom parts are cut off to create spears of the same length and some harvested spears are bent, broken or slightly purple/green-pigmented, and thus do not fit the strict market requirements.

Asparagus waste streams are being used for the production of dry powders as ingredients for soups and sauces in the food industry. However, currently available asparagus powders are considered inferior to the quality of the fresh material in terms of flavour, as the retention of key aroma components is poor. Ideally, the food ingredient industry requires a powder which has the maximum levels of key flavour and fragrance components typifying the freshly – cooked vegetable, and which meets clean-labelling and sustainability requirements without the need for any ‘artificial’ additives. The objective of this study was to evaluate the aroma profile of dried asparagus powders that were produced with the suggested split-stream processing strategy (Figure 2) [4]. This strategy aims for the optimal exploitation of the generated asparagus waste streams to produce a dried powder with the maximum possible retention of key aroma compounds. The aroma profiles of the dried powders were analysed using a headspace solid phase microextraction gas chromatography mass spectrometry method (HS-SPME GC-MS).

USA). All extractions were performed by the MPS2 autosampler robot (Gerstel, the Netherlands). For the GC-MS analysis, an Agilent GC7890A coupled to a 5975C quadrupole mass spectrometer was used, and the column was a Zebron ZB-5MSplus with dimensions 30 m × 0.25 mm id × 1 µm film thickness (Phenomenex, the Netherlands). The analysis settings were as described previously [4, 5]. The GC oven temperature was programmed to start at 45 °C for 2 min, then increased at a rate of 8 °C/min to 250 °C, then at a rate of 15 °C/min to 280 °C and then held at 280 °C for 3 min. The carrier gas was helium, at a constant flow rate of 1 ml/min. The column effluent was ionised by electron impact at 70 eV, in the scan range m/z 33–330. The MS interface temperature was set to 280 °C. For calculating retention indices (RIs) for the identification of the compounds, a series of *n*-alkanes (C7-C21) was injected and analysed using the same method as for the samples and as part of the same sample series.

Statistical data analysis

Processed GC-MS data were subjected to Principal Component Analysis (PCA) and Hierarchical Clustering Analysis (HCA), after log10 transformation and Pareto-scaling using SIMCA 15.0.2. software (Umetrics, Sartorius Stedim Data Analytics AB, Umeå, Sweden). Additional uni- and multi-variate statistical analyses were performed using RStudio with R version 4.0.3 (2020–10-10). Graphs were also produced using Microsoft Office Excel.

Results and discussion

We aimed to investigate the influence of the carrier agent concentration used for the spray drying of asparagus concentrate on the volatiles profile of the obtained spray-dried powders, as this influenced the total solids content. Maltodextrin (MD) is a commonly-used spray drying carrier agent, and in the case of asparagus concentrate, it has been showed to lead to powders with acceptable physical properties (e.g. moisture content, particle size) [5]. In this study, we also investigated the effect of partially replacing MD by cellulose-based carriers, such as microcrystalline cellulose (MCC), citrus fibre (CF) and the AF that was pressed out of the asparagus juice during the processing. All spray-dried powder samples contained the same amount of asparagus solids to enable the direct comparison of the samples. However, the total solids content varied, and we also studied this effect. The effect of both the total solids content and the type of the cellulose-based carrier replacing MD was evident (Figure 3). The clustering of the analysed spray-dried powders is based on the carrier composition; powders with CF formed one cluster (yellow box), the AF-containing powders formed a second cluster (green box) and the powders with MD and MD + MCC formed a third cluster (black box). The grouping of the samples in the third cluster (black box) implies that there is only a minor effect of partially substituting MD with MCC. Moreover, the other two clusters suggest the potential contribution of unique compounds from CF and AF matrix to the volatile profile of the final spray-dried powders, which is expected as CF and AF are fibres from vegetables with distinct aroma profiles. In the same dendrogram, within each cluster, the powders with the same total solids content also cluster close together, implying that their profiles are similar and suggesting the impact of the total solids content on the retention of volatile components. The two powders with 30% w/w total solids content, and 10% MCC, are clustered separately and distant from all other samples (Figure 3). This deviation of the volatile profiles between the powders with 10% MCC and the rest may be linked to the fact that the MD + MCC 30–10% powders were collected from the drying chamber, instead of the collection vessel, and there the temperature is slightly higher, which can influence the volatile profile. However, this requires further investigation.

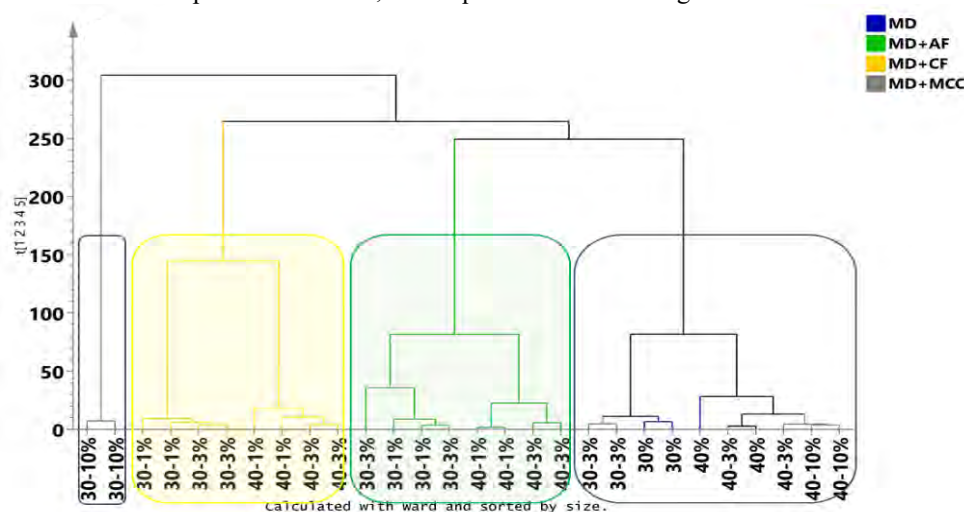


Figure 3: Hierarchical clustering analysis on the 221 volatiles detected in 28 spray-dried asparagus powders with different carrier agents (MD: maltodextrin, MCC: microcrystalline cellulose, AF: asparagus fibre, CF: citrus fibre) and carrier concentrations (total solids content 30% or 40%). Figure reproduced with permission from [4].

In addition, we calculated the retention of a selection of specific aroma compounds under different spray drying conditions (solids content and carrier types), on the basis of the ratio of the peak intensity in the spray-dried powder to that in the mixture before spray drying [5]. The retention of volatiles was higher in the samples with a total solids content of 40% w/w, regardless of carrier type (Figure 4). This was in agreement with the previous study where a higher MD concentration led to higher retention of important asparagus alcohols (e.g. 1-octen-3-ol) [5]. A partial replacement of MD with the cellulose-based carriers led to lower retention of the volatiles, as compared to the powders containing only MD. However, the retention of important volatiles e.g. 2-methoxy-3-isopropyl pyrazine in the AF-containing powders was ca. 80% and thus, at an acceptable level (Figure 4).

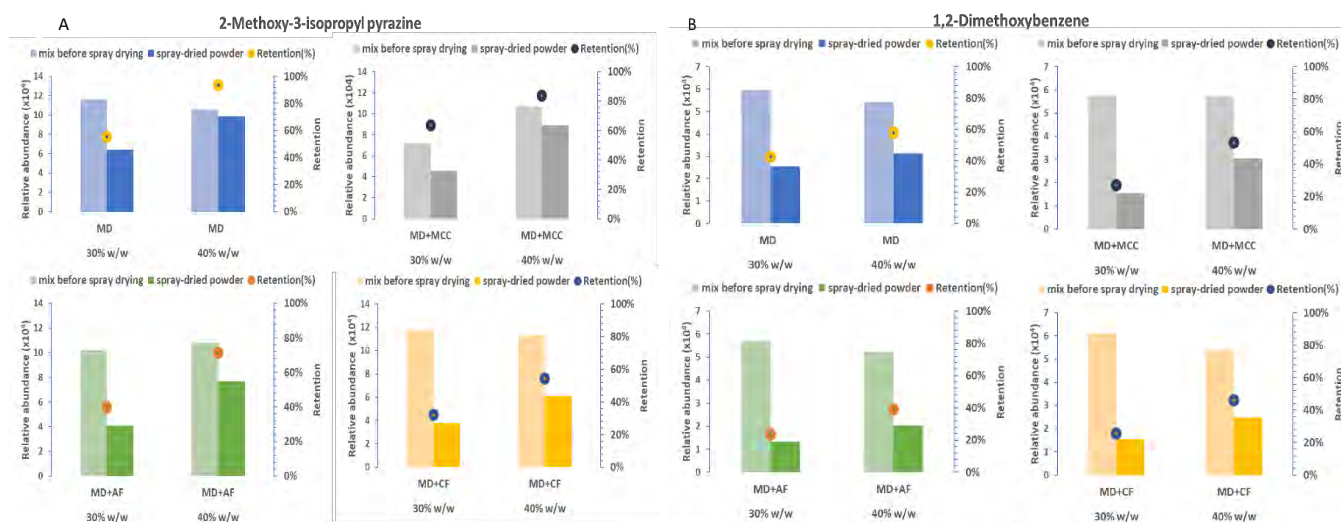


Figure 4: Relative abundance of two selected aroma compounds in the mix before and after spray drying, and the retention% in the samples with 30 % and 40 % w/w total solids content and the different carrier agents (MD: maltodextrin, MCC: microcrystalline cellulose, AF: asparagus fibre, CF: citrus fibre). Figure reproduced with permission from [4].

Conclusion

Asparagus waste streams can be used to produce aroma-rich spray-dried powders. Higher total solids (40% w/w) led to improved aroma retention, and in addition, low maltodextrin replacement did not strongly affect the volatile profile of the powders. Further optimization of the split-stream processing technique will lead to the effective exploitation of the asparagus waste stream to produce high-quality natural food ingredients.

Acknowledgements

This study is part of the Waste2Taste project (Projectnumber:TKITOEDR-20-11), which is cofunded by TKI Energy with the supplementary grant 'TKI-Toeslag' for Top consortia for Knowledge and Innovation (TKI's) of the Ministry of Economic Affairs and Climate Policy.

References

- Pegiou E., Mumm R., Acharya P., de Vos R.C.H. and Hall R.D. Green and White Asparagus (*Asparagus officinalis*): A Source of Developmental, Chemical and Urinary Intrigue. *Metabolites*. 2020;10:17-40.
- Hoberg E., Ulrich D. and Wonneberger C. Proposal for a Flavour Standard - Sensory Profiles of European White *Asparagus officinalis* L. Cultivars. *Acta Horticulturae*. 2008;776:239-245.
- Ulrich D., Hoberg E., Bittner T., Engewald W. and Meilchen K. Contribution of volatile compounds to the flavor of cooked asparagus. *Eur Food Res Technol*. 2001;213(3):200-204.
- Siccama J.W., Pegiou E., Eijkelboom N.M., Zhang L., Mumm R., Hall R.D. and Schutyser M.A.I. The effect of partial replacement of maltodextrin with vegetable fibres in spray-dried white asparagus powder on its physical and aroma properties. *Food Chem*. 2021;356:129567.
- Siccama J.W., Pegiou E., Zhang L., Mumm R., Hall R.D. and Schutyser M.A.I. Maltodextrin improves physical properties and volatile compound retention of spray-dried asparagus concentrate. *LWT - Food Sci Technol*. 2021;142:111058.

Volatile aroma and bioactive compounds diversity in wild populations of rosemary (*Salvia rosmarinus* Schleid.) from Italy cultivated under homogeneous environmental conditions

ANTONIO RAFFO¹, Irene Baiamonte¹, Elisabetta Lupotto¹, Nicoletta Nardo¹, Flavio Paoletti¹ and Claudio Cervelli²

¹ CREA-Research Centre for Food and Nutrition, Via Ardeatina, 546, 00178 Rome, Italy

² CREA-Research Centre for Vegetable and Ornamental Crops, Corso Inglese, 508, 18038 Sanremo, Italy
antonio.raffo@crea.gov.it

Abstract

Current and potential uses of Rosemary (*Salvia rosmarinus* Schleid.) in the food, cosmetic and pharmaceutical industry are based on the sensory properties and biological activities related to Volatile Organic Compounds (VOCs) and non-volatile bioactive compounds, such as phenolic diterpenes and acids. Fifty-six rosemary plants from the CREA germplasm collection, representing 14 wild populations (4 plants for each population) collected in different geographical areas across Italy, were characterised for VOCs and phenolic diterpenes and acids. Three chemotypes were identified and associated to different geographical areas, with marked differences in the levels of key odorants, such as 1,8-cineole, verbenone and camphor, and key antioxidant compounds, such as carnosic acid. Genotypes characterised by potentially better flavour profile seemed also to be associated with enhanced level of bioactive compounds and related functional properties. This diversity can be exploited to design specific products for the food and flavouring industry, with improved flavour quality and functional properties.

Keywords: Rosmarinus officinalis, aroma compounds, essential oil, antioxidants, biodiversity

Introduction

Rosemary (*Salvia rosmarinus* Schleid.) is an aromatic plant native of the Mediterranean basin which is traditionally used for culinary and medicinal purposes, but also increasingly used nowadays in the food and cosmetic industry. Key chemical constituents for such uses are volatile organic compounds (VOCs), which form the essential oil, and non-volatile bioactive compounds, such as phenolic diterpenes and acids, which attract increasing interest related to their potential health-protecting properties and application as food additive [1]. While VOCs play a main role in determining rosemary flavour, also phenolic diterpenes and acids may contribute to it, by imparting a mild bitter taste and by preventing the formation of off-flavours due to their strong antioxidant activity [2].

A germplasm collection of rosemary has been established at the CREA-Research Centre for Vegetable and Ornamental Crops (Sanremo, Italy), where spontaneous plants collected across the Mediterranean basin are maintained ex situ and are available to investigate genetic and phenotypic biodiversity within the species [3, 4]. The purpose of the collection is to preserve and study the biodiversity within the species, also in view of promoting its conservation through use. The aim of the present study was to characterise the chemical composition of rosemary plants from 14 wild populations collected in Italy and conserved in such germplasm collection, by analysing both VOCs, by GC-MS, and phenolic diterpenes and acids, by HPLC-DAD.

Experimental

Plant material

Rosemary plants belonging to wild populations collected in 14 natural areas distributed across Italy (Figure 1) and conserved ex situ at the CREA-Research Centre for Vegetable and Ornamental Crops (Sanremo, Italy) were tested in the present study. All plants were cultivated for four years at the CREA-Research Centre under similar environmental conditions, climate and substrate, in order to minimise environmental influences and highlight genetic related differences in chemical composition. For each population 4 individual plants, for a total of 56 plants, were characterised for VOCs and phenolic diterpenes and acids content in the dried leaves.

Chemical analyses

For VOCs determination a 0.5-g sample of powdered dried rosemary leaves was extracted by 5 mL of tert-butyl methyl ether solution containing 0.25 µL/mL butyl benzene as internal standard, for 24 h at ambient temperature, and then filtered through anhydrous Na₂SO₄ and silica gel 60. Quantification of VOCs was carried out by a GC-

MS analytical system (6890-5973N Agilent Technologies, Palo Alto, CA, USA) according to the following conditions: analytical column, Rxi-5Sil MS (30m, 0.25 mm, 0.25 μm); temperature ramp: 50 (1 min), 5°C/min to 250°C, then 20°C/min to 315°C (15 min); He, carrier gas at 43 cm/s; 1 μL of extract injection; split injection, with 5:1 split ratio, at 250°C; transfer line at 325°C; MS spectrometer operating by the EI mode at 70 eV with a scan range of 30-250 amu. The identification of VOCs was based on comparison of mass spectra with NIST/Wiley libraries, and retention indices. Quantification data were calculated as percentage of total VOCs content.



Figure 1: map of Italy indicating the collection sites of the 14 wild populations of rosemary plants. Red points: North Western Italy; green points: Sardinia; blue points Central and Southern Italy.

For determination of phenolic diterpenes and acids, 200 mg of powdered rosemary dried leaves were dissolved in a 70% ethanol extracting solution, stirred and then sonicated for 30 minutes. After centrifugation and filtration, 10 μL were injected into an Agilent 1100 HPLC system, the column used being a Zorbax XDB C18 (25cm x 4.6 mm x 5 μm) thermostated at 30 °C. HPLC conditions: gradient elution with soln. A (H_2O acidified with 1% v/v of acetic acid) and soln. B (methanol) as mobile phases; readings at 280 and 330 nm. Quantification was carried out by using calibration curves obtained by standard solutions of pure compounds; results were expressed as mg/g of dry matter.

Statistical analyses

Principal Components Analysis (PCA) and Agglomerative hierarchical clustering (AHC) analyses were performed by the XLStat software package (2020.4.1 version). AHC analysis was performed on average data (n=4) obtained on each population.

Results and discussion

As regards VOCs, 32 individual compounds were quantified, belonging to the following groups: 11 monoterpene hydrocarbons, 7 oxygenated monoterpenes, 6 sesquiterpenes, 2 oxygenated sesquiterpenes and 6 from other minor groups. Carnosic acid and carnosol were determined for phenolic diterpenes and rosmarinic acid for phenolic acids. AHC analysis grouped all populations into three clusters representing different chemotypes, as shown by the dendrogram reported in Figure 2: populations from Sardinia (green) with high verbenone levels, from Central and Southern Italy (blue) with high 1,8-cineole levels, and from North Western Italy (red) with relatively high camphor levels. Populations assigned to the three clusters seemed to belong to the three main chemotypes previously described in the literature, the verbenoniferum, the cineoliferum and the camphoriferum [3]. The profile plot also suggested that the verbenone level is particularly low in the cluster from Central and Southern Italy and in that one from North Western Italy. Average level of verbenone in populations from Sardinia amounted to 30.5%, whereas in the cluster from North Western Italy it reached 5.5% and in the third cluster its content was very low (<0.1%). This point could be of particular interest, because high levels of verbenone have been reported to be associated with better flavour properties [2]. Moreover, the cluster from Sardinia was also characterised by the highest content of carnosic acid, with an average content of 55 mg/g d.m., followed by the North Western Italy cluster with an average level of 41 mg/g d.m. One particular population, SPIE, showed an average carnosic acid level of 77 mg/g d.m., higher than in accessions previously selected for high level in carnosic acid [5]. As a whole, classification of the examined populations according to VOCs and bioactive compounds reflected results from a previous genetic characterisation of the same populations [4].

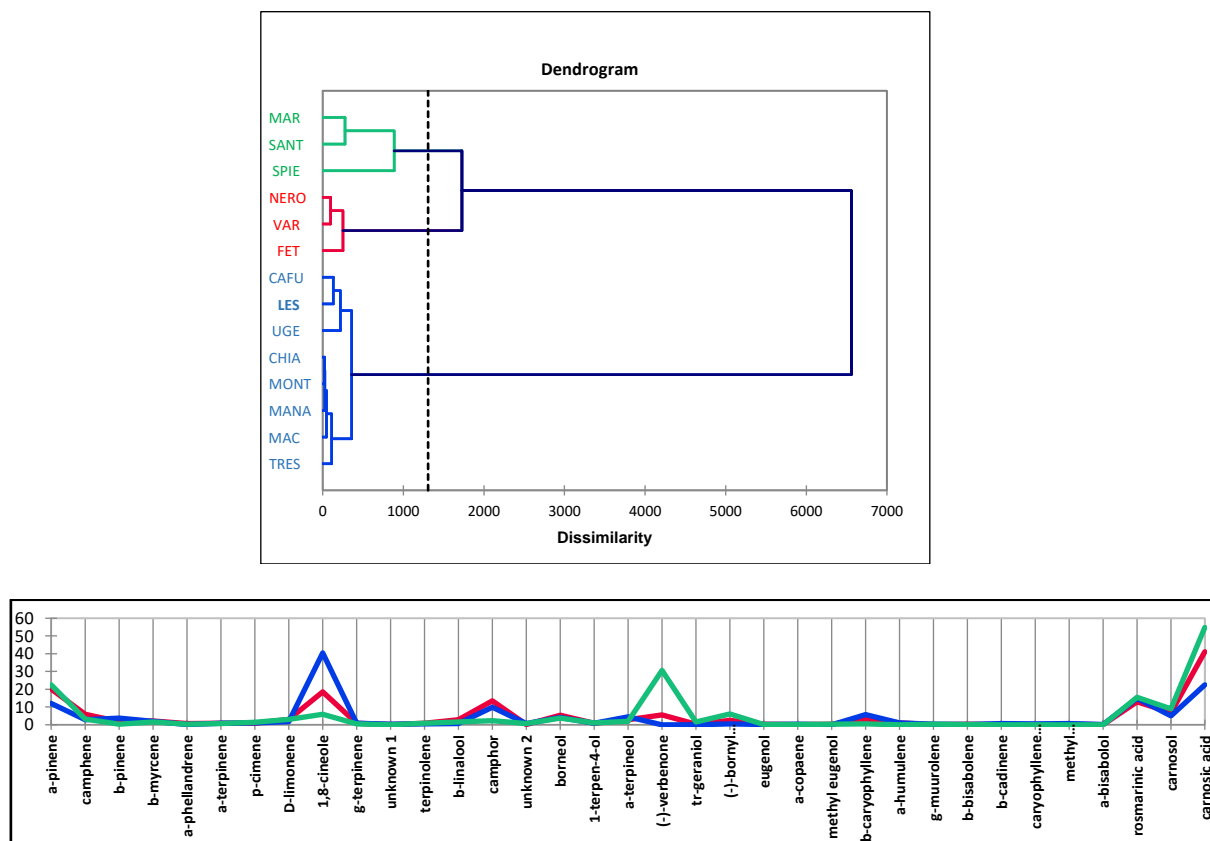


Figure 2: Dendrogram and profile comparing the means of the different classes that have been created, as obtained by Agglomerative Hierarchical Clustering (AHC) analysis.

PCA analysis further supported the chemotype classification highlighted by the AHC analysis (Figure 3). All plants from the Central and Southern Italy cluster (blue labels), were associated with positive values of the first PC, whereas at negative values of the first PC, plants from the two other clusters (North Western Italy in red and Sardinia in green) tended to group apart from each other, with minor exceptions (Figure 3: Observations). Interestingly, the plot of variables also showed that levels of the bioactive phenolic diterpenes carnosic acid and carnosol are high in genotypes characterised by high verbenone and a-pinene content as main VOCs (Figure 3: Variables), suggesting that the accumulation of both group of compounds seemed to be controlled in a similar way by genetic factors. Pearson's correlation coefficients highlighted significant (at $p < 0.05$) linear correlation between verbenone and carnosic acid content ($R = 0.768$) and inverse correlation between 1,8-cineole and carnosic acid content ($R = -0.778$).

Conclusion

The highlighted chemical diversity can be usefully exploited to improve the flavour of rosemary based products and to design specific products for the food industry, such as essential oils for flavourings, characterised by geographically distinctive aroma notes, thus providing flavour diversity. Interestingly, genotypes characterised by potentially better flavour profile seemed also to be associated to enhanced level of bioactive compounds and related functional properties.

(Funding: Project: PRO-ORG: Code of Practice for organic food processing. CORE Organic Cofund).

References

1. Ribeiro-Santos R, Carvalho-Costa D, Cavaleiro C, Costa H S, Albuquerque T G, Castilho M C, Ramos F, Melo N R, & Sanches-Silva A. A novel insight on an ancient aromatic plant: The rosemary (*Rosmarinus officinalis* L.). *Trends Food Sci Technol.* 2015;45(2):355-368. <https://doi.org/10.1016/j.tifs.2015.07.015>.
2. Chadwick M. Optimising flavour in rosemary. Technical review, AHDB Horticulture, <https://ahdb.org.uk/knowledge-library/optimising-flavour-in-rosemary>. 2018 (accessed on May 24, 2021).
3. Li G, Cervelli C, Ruffoni B, Shachter A & Dudai N. Volatile diversity in wild populations of rosemary (*Rosmarinus officinalis* L.) from the Tyrrhenian Sea vicinity cultivated under homogeneous environmental conditions. *Ind Crop Prod.* 2016;84:381-390. <https://doi.org/10.1016/j.indcrop.2016.02.029>.

4. Nunziata A, De Benedetti L, Marchioni I, & Cervelli C. High throughput measure of diversity in cytoplasmic and nuclear traits for unravelling geographic distribution of rosemary. *Ecol Evol.* 2019;9(7):3728-3739. <https://doi.org/10.1002/ece3.4998>.

5. Wellwood C R L, & Cole R A. Relevance of Carnosic Acid Concentrations to the Selection of Rosemary, *Rosmarinus officinalis* (L.), Accessions for Optimization of Antioxidant Yield. *J Agric Food Chem.* 2004;52(20):6101-6107. <https://doi.org/10.1021/jf035335p>.

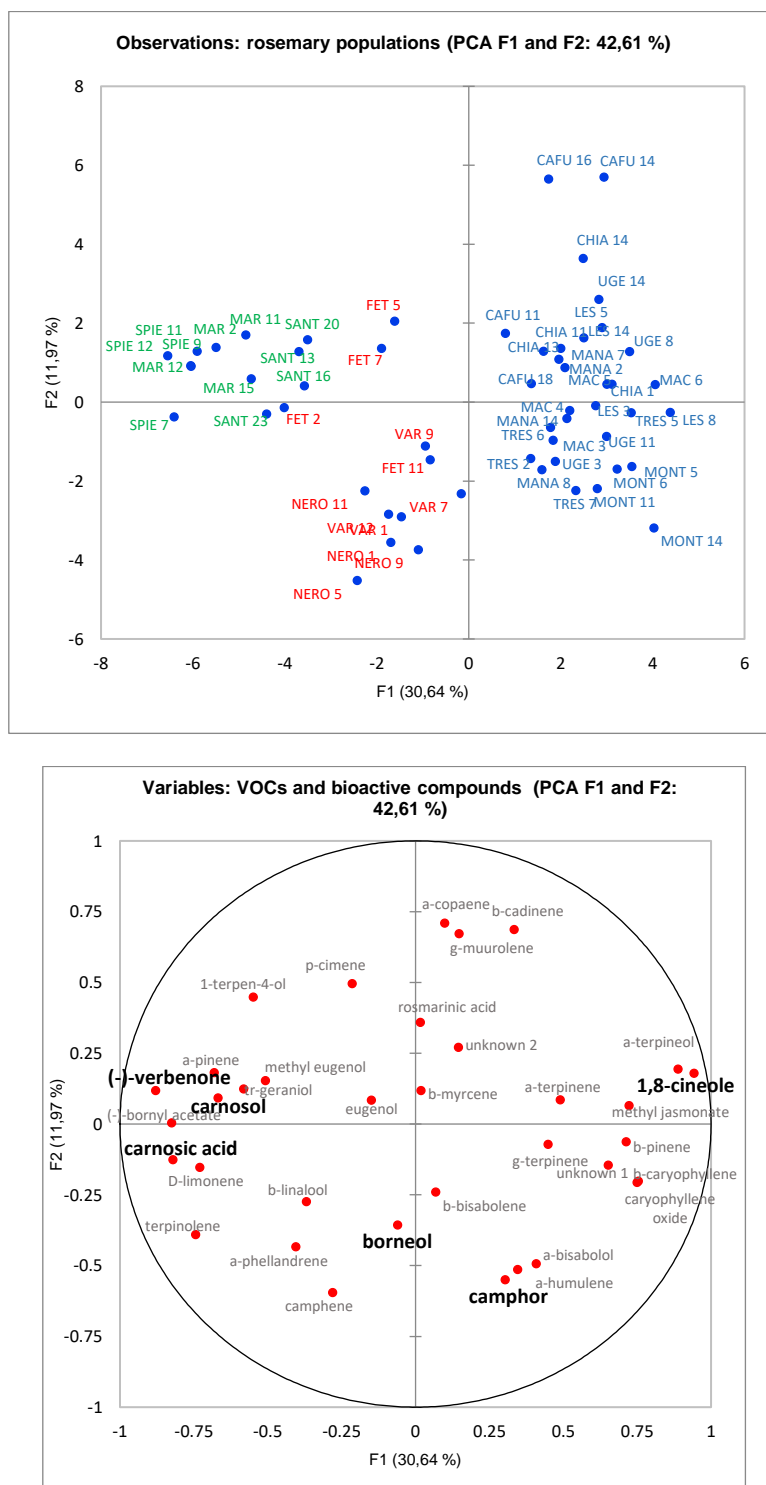


Figure 3: Score plot (*Observations: rosemary populations*) and loadings plot (*Variables: VOCs and bioactive compounds*) of the PCA analysis: PCs 1 and 2. PCA was carried out on the dataset formed by experimental data of 32 VOCs and 3 bioactive compounds determined on 56 individual rosemary plants. In the score plot the label denotes a single plant (acronym: population; number: individual plant within the population).

Volatile compounds contributing to the odour of oats

Sari A. Mustonen, OSKAR LAAKSONEN and Kaisa M. Linderborg

Food Chemistry and Food Development, Department of Life Technologies, University of Turku, Finland
oskar.laaksonen@utu.fi

Abstract

Oats are increasingly popular due to their healthiness, and the number of new different types of oat products on the market is constantly increasing. Oats have higher content of lipids compared to many other grains and therefore their quality and volatile compound profile is susceptible to changes. In this study, selected oat samples were investigated using HS-SPME-GC-O panel and trained sensory panel in order to identify the compounds contributing to the odour characteristics. GC-O panel was trained to describe odours and to evaluate odour intensities of oat samples as flour-water mixtures. The odour and flavour characteristics of the same oat samples were characterised using a sensory panel using generic descriptive analysis. The GC-O panel detected 30 odour-active compounds. The most often described compounds were aldehydes, such as hexanal described as 'green' and 'grassy', or 3-methylbutanal described as 'chemical' and 'pungent'. At the same time, little differences were observed in 'green odour' by the sensory panel, whereas more differences were observed in bitter taste and odour and flavour intensities.

Keywords: oat, volatile compounds, odour, flavour, sensory analysis

Introduction

The importance of oats is increasing globally due to the need for a shift to plant-based diet and public health concerns. A variety of oat products and fractions are available for use as such and as oat-containing foods, and the number of different types of oat products on the market is constantly increasing. Due to the extensive exploitation of oats in food industry, there are interests and concerns among oat producers, industry and researchers to better understand the factors affecting the quality of oats. Oats have higher content of lipids compared to many other grains and therefore their characteristics including the quantity and quality of volatile compounds is susceptible to changes, and certainly affected by processing [1,2]. Many of the compounds formed during processing are derived from oxidation of oat lipids [1-3]. At the same time, the odour of unprocessed oats is mild, and the typical odour characteristics are formed in various processes, such as heat treatment during milling [3].

The study was conducted as part of a larger OatHow research consortium in Finland aiming to investigate and define quality factors of oats. In this study, selected oat flour samples of Finnish origin were investigated using HS-SPME-GC-O panel and trained sensory panel in order to identify the compounds contributing to the odour characteristics of oats. The selected samples originated from a single crop year (either 2017 or 2018 and a known cultivar, and were industrially dehulled, heat-treated and milled from flakes.

Experimental

Gas chromatography olfactometry (GC-O)

GC-O analyses were performed with a Hewlett-Packard HP6890 Series GC system (Agilent Technologies Inc., CA, USA) coupled with a flame ion detector (FID) and an olfactometry port (ODP-1, Gerstel GmbH & Co. KG, Germany). A portion of 12 g of sample was mixed with MQ water (1:2.5, w/w) and placed in a 50 mL Erlenmeyer flask with 10% NaH₂PO₄. The sample was equilibrated and stirred thoroughly using a magnetic stirrer at 50 °C for 10 min. The SPME fibre (DVB/CAR/PDMS, 2 cm; Supelco, USA) was exposed to the headspace of the sample vial for 45 min at 50 °C. A medium polar capillary column (DB-624, 60 m×0.25 mm×1.4 µm, Agilent Technologies Inc., USA) was used to separate the compounds. The oven temperature-program was 40 °C held for 6 min, increased at 25 °C/min to 100 °C and then 7 °C/min to 220 °C and held 10 min at the final temperature. The injector temperature was set to 240 °C, and splitless injection was used. Helium was used as a carrier gas with linear velocity of 38 cm s⁻¹. Temperature of FID was set to 290 °C, and sampling rate to 20 Hz. Identification of compounds was performed using the retention indices and standard compounds. Chromatographic data were collected using GC ChemStation software (Rev. A.09.01, Agilent Technologies Inc., CA, USA) and olfactometric data using mp3DirectCut freeware (version 2.22).

The panel (n=5) was first trained to describe odours and to evaluate odour intensities (on scale 1-5; 1 = no odour, 2 = barely detectable, 3 = detectable, barely recognisable, 4 = recognisable, 5 = recognisable, strong) with odour bottles and then in GC-O with mixtures of standard compounds, and later with oat sample. The panel

continued to evaluate four oat samples as flour-water mixtures (40 weight-% flour / 60 weight-% water) in duplicate.

Sensory evaluation

The odour and flavour characteristics of the oat samples were characterised using a sensory panel (n=11) using generic descriptive analysis. Sensory attributes (four odour attributes: ‘oat’, ‘roasty’, ‘sweet’ and total intensity; five flavour attributes: ‘green’, ‘oat’, total intensity and bitter and sweet tastes) were evaluated on line scales (0-10) with a help of reference compounds in triplicate by the panel. Oat flour-water mixture samples were prepared as described above. Samples (ca. 2.5g) were presented in 4 cL transparent plastic cups with glass lids in randomised order. Data was collected using Compusense Cloud software version 21.0 (Compusense Inc., Guelph, Ontario, Canada) in controlled sensory laboratory conditions.

Statistical analysis

Principal component analysis (PCA) models were used to investigate correlations between oat samples and perceived compound intensities by the GC-O panel (as mean-centred and unit-variance scaled as X-data) or sensory attributes (as mean-centred X-data). PCA models were created using Unscrambler (version 11, Camo Inc., Norway). Rated intensities for samples in GC-O analyses were compared using oneway-ANOVA (SPSS version 27, SPSS Inc., Chicago IL).

Results and discussion

The GC-O panel (n=5 in duplicate) detected 30 potentially odour-active compounds from the oat flour-water mixture samples (Table 1). Eighteen compounds were detected at least five times or more often. The most often described compounds were aldehydes, for example hexanal (9) described as ‘green’ and ‘grassy’, or 3-methylbutanal (6) described as ‘chemical’ and ‘pungent’. Hexanal, 1-octen-3-ol (with typical ‘mushroom’ descriptor) and 2,3-butanedione (commonly referred as diacetyl; with fatty, popcorn and sweet descriptors) were among the compounds rated as most intense on the scale. Aldehydes and ketones are among the typically detected compounds in oat samples (e.g. in review article by McGorin [1]). Schuh and Schieberle (2004) reported a nonatrienal compound ((*E,E,Z*)-2,4,6-nonatrienal) being the key compound contributing to aroma of oats already in low concentrations. This compound was not detected in this study due to lack of standard. Potentially, it may be one of the unidentified compounds with number 25, 26 or 27. Many other compounds that were not detected in this study, have been reported in oats, especially compounds that are formed in further processing of the oats [1-3].

Only three compounds (7, 16, 20) differed statistically significantly in their intensities in oneway-ANOVA (Table 1). The intensity of compound 7 (2-methylbutanal with ‘sweaty’, ‘fatty’ and ‘chemical’ descriptors) was rated significantly lower in sample Oat3, compound 16 (unidentified) was lowest in sample Oat2 and compound 20 (nonanal with ‘sweet’ and ‘fresh’) was not detected in Oat4. At the same time, several compounds, such as 2-methylbutanal (7) with ‘sweaty’ and ‘fatty’ descriptors and the unidentified compound (25) with ‘oat’, ‘roasty’ and ‘chemical’, were observed differently among the oat samples in a PCA model in Figure 1.

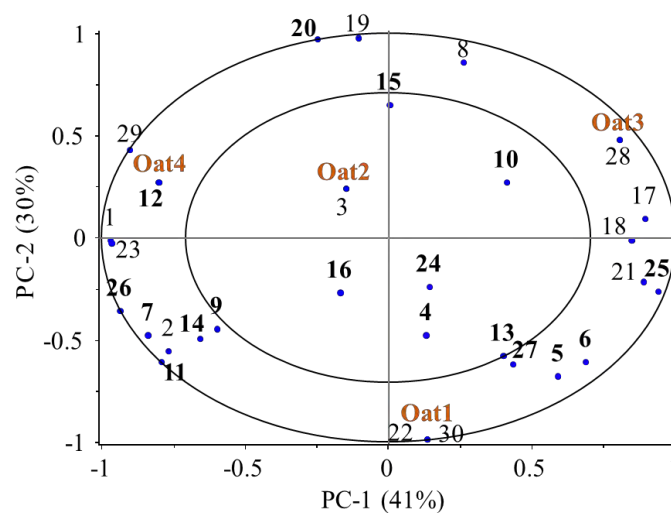


Figure 1: PCA correlations loadings plot (PCs 1 vs 2) with four oat flour-water mixture samples (Oat1-4, brown font; included as dummy variables) and 30 compound variables from GC-O analysis (as average rated intensities on scale 1-5). Variable numbers and bolded variables refer to Table 1.

Sample Oat1 was characterised by lacking nonanal (20) along the PC2, whereas the samples Oat3 and Oat 4 were separated on the first PC.

Table 1: Volatile compounds, their retention indices, odour descriptors and averaged rated intensities (on a scale 1-5 in duplicate) detected by the GC-O panel (n=5).

Compound number	RI (DB-624)	Compound	Descriptors by GC-O panel	Oat1	Oat2	Oat3	Oat4
1	<590	-	fusty, rancid, sweaty	3.8	3.3	3.0	3.3
2	<590	-	meat, rotten, pungent	3.0	3.0	1.0	3.2
3	591	-	-	1.0	2.0	1.0	1.0
4	596	2-methylpropanal	solvent, fusty, sweet	2.9	3.4	3.0	3.3
5	634	2,3-butanedione	fatty, popcorn, sweet	3.6	3.5	3.9	4.1
6	696	3-methylbutanal	pungent, chemical, sweet	3.3	3.5	3.5	3.6
7	705	2-methylbutanal	sweaty, fatty, chemical	3.2^{ab}	3.0^{ab}	1.0^a	3.1^b
8	738	Pentanal	green, rancid, fatty	2.6	2.5	2.7	2.4
9	842	Hexanal	green, grass	4.2	4.4	3.9	4.3
10	876	-	sweet, flowery, fruity	2.6	3.3	3.0	2.8
11	909	Furfural	oat, flour, roasty	3.2	3.0	2.7	3.2
12	935	2-heptanone	mushroom, flour	2.0	1.0	1.0	1.0
13	948	Heptanal	mushroom, flour, fusty	3.1	2.9	3.2	3.3
14	980	-	mushroom, potato, fusty	3.6	3.1	3.1	3.5
15	1026	1-octen-3-ol	mushroom	4.1	3.9	4.1	3.9
16	1036	-	pungent, fatty, spicy, roasty	4.4^b	2.8^a	4.2^{ab}	4.3^{ab}
17	1051	Octanal	green, fresh	1.0	3.0	3.5	2.5
18	1127	(<i>E</i>)-2-octenal	sweaty, rancid, roasty	1.0	3.3	3.5	2.8
19	1144	-	sweet, chemical, dusty	2.8	2.3	2.8	1.0
20	1153	Nonanal	sweet, fresh	2.5^{ab}	2.3^b	2.3^b	1.0^a
21	1162	-	hay, mould, medicinal	1.0	1.0	2.7	2.2
22	1179	-	sweet, roasty, toffee	1.0	1.0	1.0	2.5
23	1213	-	green, citrus	3.0	2.7	1.0	2.0
24	1232	(<i>E</i>)-2-nonenal	oat, flour, green, fresh	3.4	3.1	3.4	3.4
25	1247	-	oat, roasty, chemical	2.8	3.3	3.6	3.5
26	1302	-	oat, roasty	3.5	3.2	2.8	3.3
27	1368	-	fusty, spoiled, oat	2.9	2.6	3.1	3.3
28	1415	-	flour, dusty	1.0	1.0	2.3	1.0
29	1443	-	flour, fresh, roasty	3.0	2.3	1.0	1.0
30	1471	-	chocolate, vanilla	1.0	1.0	1.0	3.0

Compounds with bold font detected in at least 50% of GC-O panel evaluations. Statistically significant differences between rated intensities is based on oneway-ANOVA and Tukey's HSD test and shown with letters a-b.

Only little differences were observed between samples by the sensory panel in odour characteristics, whereas more differences were observed in bitter taste and total odour and flavour intensities. Sample Oat4 had the most intense odour, flavour and bitterness based on the PCA model in Figure 2. At the same time, Oat2 had milder odour and flavour with some positive correlation with 'oat odour' along the first PC. Sample Oat3 correlated with 'oat flavour' along the PC2. This sample also correlated with compound 25 (with descriptor 'oat') in the Figure 1.

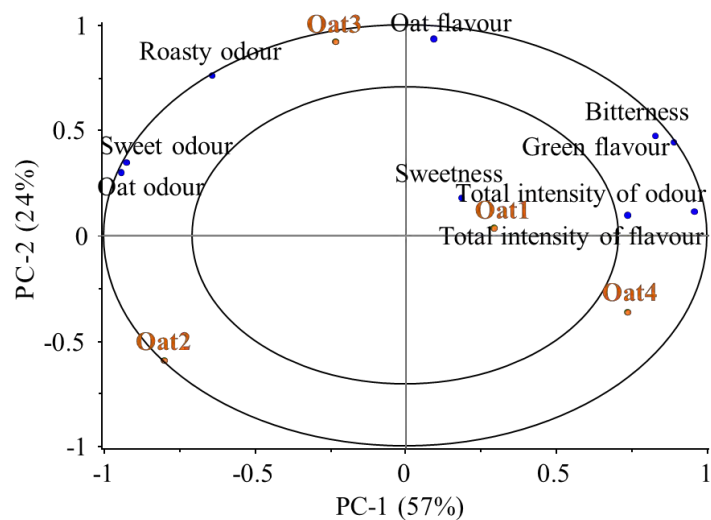


Figure 2: PCA correlations loadings plot (PCs 1 vs 2) with four oat flour-water mixture samples (Oat1-4, brown font; included as dummy variables) and nine sensory variables from the generic descriptive analysis (as mean rated intensities on scale 0-10).

Conclusion

Oat flour samples in this study had generally mild odour and flavour properties, and its odour was contributed by multiple volatile compounds. Only a part of the compounds described in literature, primarily aldehydes, were detected in this study. Oat flour samples selected to this study differed from one another in terms of the perceived odour as flour-water mixtures, especially those described as “sweaty”, “fatty” or with bitter taste. In subsequent studies, more oat samples with varying origins are investigated and the odour-active compounds will be studied in detail with GC-MS analyses. Additionally, a storage test of these flours will be carried out, as well as, certain concept products will be prepared from the flours in order to further investigate the suitability of different oat flours for different end-products.

References

1. McGorin, R.J. Key aroma compounds in oats and oat cereals. *J Agric Food Chem.* 2019;67:13778–13789.
2. Schuh, C., Schieberle, P. Characterization of (*E,E,Z*)-2,4,6-nonatrienal as a character impact aroma compound of oat flakes. *J Agric Food Chem.* 2005;53:8699–8705.
3. Heiniö, R.-L.; Kaukovirta-Norja, A.; Poutanen, K. Flavor in processing new oat foods. *Cereal Foods World* 2011;56(1):21–26.

Section 3

Flavour perception

New insights on olfactory priming effects on the cerebral processing of food pictures in normal-weight, overweight, and obese adults

Isabella Zsoldos, CHARLOTTE SINDING, Ambre Godet and Stéphanie Chambaron

Centre des Sciences du Goût et de l'Alimentation (CSGA), AgroSup Dijon, CNRS, INRAE, University of Bourgogne Franche-Comté, Dijon, France, charlotte.sinding@inrae.fr

Abstract

The cerebral activity associated with attentional processes may differ between individuals with different weight statuses in the presence of food stimuli (e.g. odours, pictures). The objective of the present study was to test the influence of non-attentively perceived food odours on the cerebral activity underlying the processing of food pictures, in normal-weight, overweight, and obese adults. To do so, we used an implicit olfactory priming paradigm with a pear odour and a pound cake odour as primes, respectively priming sweet low-energy-density foods and sweet high-energy-density foods. Event-related potentials were recorded while the participants passively watched pictures of sweet low- and high-energy-density foods, under the two priming conditions plus an odourless control condition. The amplitude of the P100 and the P200 peaks were measured. The results suggest that the cerebral activity underlying the processing of food cues differs depending on weight status, from early and non-conscious stages of attentional processing.

Keywords: food odour, priming, obesity, event-related potentials, electroencephalography

Introduction

As obesity rate keeps increasing worldwide [1], a better understanding of the mechanisms underlying food choices and weight gain is needed to improve people's diet. Automatic and non-conscious processes, including cognitive and cerebral functioning, play a major role in our food choices [2]. There is evidence that the cerebral activity underlying attentional processes may differ as a function of body mass index (BMI), starting from the early stages of the perception of food cues in the environment [3, 4]. In particular, studies using electroencephalography (EEG) to record event-related potentials (ERPs) reported a greater amplitude of the P200 peak elicited by visual food stimuli in obese individuals, compared with normal-weight individuals [5, 6]. The P200 is a mid-latency component of the ERP waveform peaking around 200 ms after stimulus presentation, reflecting preconscious attentional processing: the greater its amplitude, the greater the involvement of automatic attentional resources to process the stimuli. Thus, individuals with higher BMIs may allocate more cerebral resources to process food cues, at early and automatic stages of attention orientation. It has been suggested that such a phenomenon may contribute to overeating and weight gain [4].

An interesting method to study automatic attentional processes toward food cues in individuals with different weight statuses is the priming paradigm. It consists in exposing individuals to one stimulus (called the prime) to influence a response to a subsequent stimulus (the target), without conscious guidance. The target can be either congruent (related) or incongruent (unrelated) to the prime. Such a paradigm activates the pre-wired brain pathways that have been previously associated with the prime. In the context of food-related cognition, a recent study using an olfactory priming paradigm showed that obese adults directed their attention more toward food pictures (vs. non-edible objects) in presence of a fatty-sweet odour (pound cake), compared to normal-weight adults [7]. This result was observed only when the obese adults did not attentively perceive the odour (vs. an explicit condition where the participants were informed about the presence of odours). Obese individuals may thus be particularly reactive to non-attentively perceived food odours from the environment, which may automatically direct their attention toward available foods. However, little is known about the brain mechanisms involved in these odour priming processes and whether odour primes already affect food perception at non-conscious levels.

Based on these observations, we made the hypothesis that non-attentively perceived food odours may influence the cerebral activity underlying the processing of food pictures, and this effect may differ between normal-weight, overweight, and obese adults. We used an implicit olfactory priming paradigm with two odours as primes: 1/ a pear odour, priming sweet low-energy-density (LED) foods, and 2/ a pound cake odour, priming sweet high-energy-density (HED) foods. We used pictures of sweet low- and high-energy-density foods as targets, congruent to either one of the odours (e.g., fruits, cakes). ERPs were recorded while the participants passively watched the food pictures on a computer screen (passive viewing task), under the two priming conditions plus an odourless control condition. We measured the amplitude of two ERP peaks elicited by the pictures: 1/ the P100, because it reflects early perceptive and pre attentive sensory processing [3], and 2/ the P200, because it is associated with

automatic attentional processes [5, 6]. For all participants and both peaks, we expected a greater amplitude for congruent odour-picture pairs (e.g., pound-cake odour and HED food pictures). Considering the increased reactivity for food cues in obese subjects, we expected this effect to be more pronounced with increasing BMI, and particularly in the presence of the pound cake odour.

Experimental

For a more detailed description of the experimental procedure, see Zsoldos, Sinding, Godet, & Chamberon, 2021 [8].

Participants

The study was conducted in accordance with the Declaration of Helsinki and was approved by the Comité d'Evaluation Ethique de l'Inserm (CEEI, File number IRB 0000388817-417). All participants provided written informed consent and received a 20 euros voucher in return for their participation. All participants were French speakers, right-handed, aged between 20 and 50 years old, non-smokers and free from known psychiatric or neurological conditions and metabolic diseases associated with excess weight (diabetes, cardiovascular diseases). The other exclusion criteria were: past or current eating disorders (anorexia, bulimia), food allergies, bariatric surgery, pregnancy, or a vegan diet. Sixty-two participants were included and split in three groups based on their BMI: 23 normal-weight (NW; BMI between 18.5 and 25 kg/m²), 19 overweight (OW; BMI between 25 kg/m² and 30 kg/m²) and 20 obese adults (OB; BMI >30 kg/m²).

Pictures

Based on a pilot study, we selected 12 HED food pictures (e.g. cookies, chocolate) and 12 LED food pictures (e.g. various whole and sliced fruits) from the FoodPics database [8]. All pictures had a mean liking score above 6, and liking was statistically equivalent between the LED and HED categories ($p > .05$). Pictures from both categories were similar according to object size, brightness, contrast, visual complexity, spatial frequencies, and familiarity ($p > .05$).

Olfactory priming device

The olfactory priming device used in the current research was based on the method developed by Marty and collaborators [9] and successfully used in other studies since [7, 10]. In these studies, the participants successively wore different headsets, whose microphone foams had been odourised beforehand. Three odours were used as primes: a pear odour (fruity odour, priming LED foods), a pound cake odour (fatty-sweet odour, priming HED foods), and a control condition (no odour). For the olfactory primes, we selected a pear aroma and a pound cake aroma (Meilleur du Chef, Bassussarry, France), because they have proven to be efficient as implicit olfactory primes in the previously cited studies. Both odours were also rated as equivalent in terms of liking ($t(40)=1.14$, $p=.26$) and hedonicity ($t(40)=0.38$, $p=.70$) [9]. In a pilot study including 10 adults, the pure pear odour and the 1/25 diluted pound cake odour (in dipropylene glycol) were rated as isointense and were therefore selected for the study. For the olfactory priming, we placed 15 μ L of each dilution (pear, pound cake) inside disposable microphone foams. For the non-odourised control condition, we used 15 μ L of dipropylene glycol. The microphone was cleaned with ethanol between participants and the foams were changed.

Procedure and passive viewing task

The participants were invited to the laboratory under a false pretext that did not mention food odours, in order to keep the olfactory priming implicit. They were instructed not to eat anything during the 3 hours before the session, and not to wear perfume and hair products. To ensure the absence of residual odours, the sessions took place in a positive pressure room, which allowed the complete renewal of the air every two minutes.

After giving her/his informed consent, the participant was seated in front of the computer and the EEG electrodes were installed by the experimenter. A first headset microphone, odourised according to one of the three priming conditions (pear, pound cake, none), was placed above the EEG cap. To control for hunger levels, the participant indicated the time of her/his last meal and the intensity of her/his hunger on a scale going from 1–*not hungry at all* to 10–*very hungry*. Then, the EEG recording started and the participant completed a passive viewing task.

The passive viewing task was programmed with Eprime 2.0 (Psychology Software Tools). The participants were instructed to pay close attention to the pictures that would be presented on the computer screen (passive viewing without responses). One trial consisted of a fixation cross (presented for 1600 ± 100 ms) followed either by a LED or HED food picture (presented for 200 ms) on a silver-grey background (see Figure 1, A). The task was divided into three identical blocks, each one corresponding to a different olfactory priming condition. The twelve

LED food pictures and the 12 HED food pictures were presented 8 times by block in a randomised order, resulting in 192 trials by block (96 LED and 96 HED trials; see Figure 1, B).

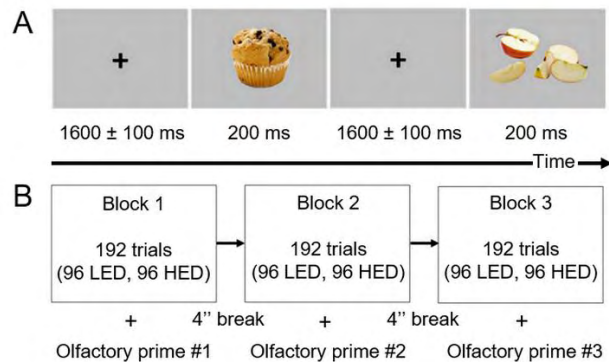


Figure 1: (A) Example of a “HED” trial followed by a “LED” trial; (B) Design of the passive viewing task and the olfactory priming paradigm.

Between the blocks, the participants had 4-minute breaks where they were offered to do a “connect-the-dots” game on a sheet of paper. The purpose of these breaks was to distract the participants while the experimenter switched the odourised headset microphones out of their sight, in order to alternate the three olfactory priming conditions. All participants did the three priming conditions in a counterbalanced order. During the blocks, a white noise was continuously played in the headset, and the participants were instructed to use the microphone to call the experimenter when the words “break time” would appear on the screen at the end of each block. These two aspects justified the presence of the headset microphone. EEG was continuously recorded during each block.

After the last block, the participants indicated again their level of hunger on the 10-points scale, and the EEG cap was removed. To control that all participants had a proper sense of smell and that olfactory capacities did not differ between BMI groups, the participants performed The European Test of Olfactory Capabilities [11]. All included subjects had a total score above 80% and were considered normosmic. They also answered an investigation questionnaire, in which they had to indicate whether they noticed anything particular during the task that could have influenced their performance. This step ensured that no odour was perceived, validating the implicit quality of the priming. Participants reporting odours of headsets were excluded from the study ($N = 14$). Finally, anthropometric measurements were conducted by the experimenter to calculate BMI (weight in kg/height in m^2).

EEG recording

Visual ERPs, time-locked to picture onset, were recorded using a 32-channel EEG with Ag–AgCl active electrodes. ERPs were recorded with a 24-bit resolution and a sampling rate of 1000 Hz running AcqKnowledge 4.1 software, and the signal was amplified using an Active Two amplifier system (BioSemi, Amsterdam, Netherlands). Reference electrodes were fixed on the left and right earlobes, and ground electrodes on the left and right mastoids. Two additional electrodes were placed above and below the right eye to record the vertical electro-oculogram, and two other electrodes were placed on the outer corners of the left and right eyes to record the horizontal electro-oculogram. Electrode impedance was kept below 5 $k\Omega$ with the help of a saline gel. Throughout the experiment, triggers were sent with Eprime 2.0 (Psychology Software Tools) and recorded as events on the EEG signal at the onset of each food picture.

ERP pre-processing

Offline data analysis was performed with Letswave 6 implemented in MATLAB R2018b. For drift correction, the EEG data were first offline filtered with a 0.1-Hz low cutoff filter. Data were then epoched starting at 200 ms before picture onset and ending 1000 ms after picture onset. They were filtered (Butterworth, bandpass filter: 0.01–30 Hz, filter order 4) and baseline corrected [$y_i = x_i - \text{mean}(b_l)$] using the 200 ms before the stimulus. The epochs contaminated by eye blinks, eye movements, or any peaks exceeding $|90| \mu V$ at any electrode were automatically excluded from the average. Each subject’s dataset was also visually inspected. After removal of the artefacts, participants who presented fewer than 10% valid trials for at least two conditions were excluded from further analysis ($N=8$). The remaining epochs were then averaged for each participant and each electrode, by priming condition (control, pear, pound cake) and type of food picture (HED, LED), resulting in six conditions (control-HED, control-LED, pear-HED, pear-LED, pound cake-HED, pound cake-LED). Grand-average waveforms were generated by group. Based on the literature and for all conditions, we extracted amplitude values (μV) in a 10–100 ms window for the P100 peak, and a 130–230 ms window for the P200 (see Figures 2 and 3 for the grand-averages

highlighting the measured peaks). To simplify the statistical model, we selected subsets of homogeneous electrodes for further analysis of each peak (see [8] for the detail of the statistical procedure for electrode selection). We kept two occipital electrodes for the analysis of the P100 peak (O1, O2), and three centro-parietal electrodes for the analysis of the P200 (CP1, CP2, Cz).

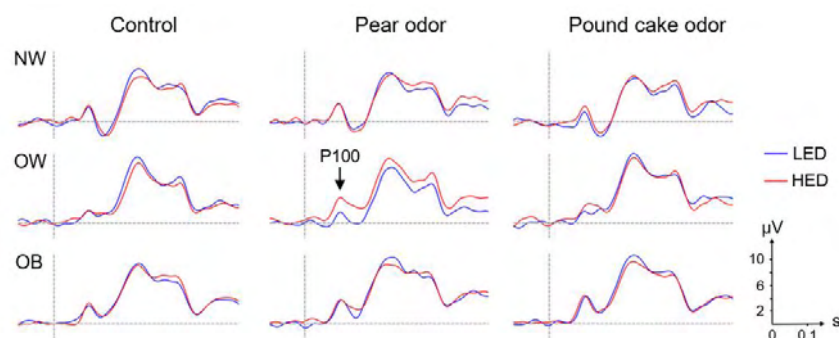


Figure 2: Grand-average ERP highlighting the P100 peak at the O1 electrode, by group (NW, OW, OB), priming condition (control, pear odour, pound cake odour), and type of food picture (LED, HED).

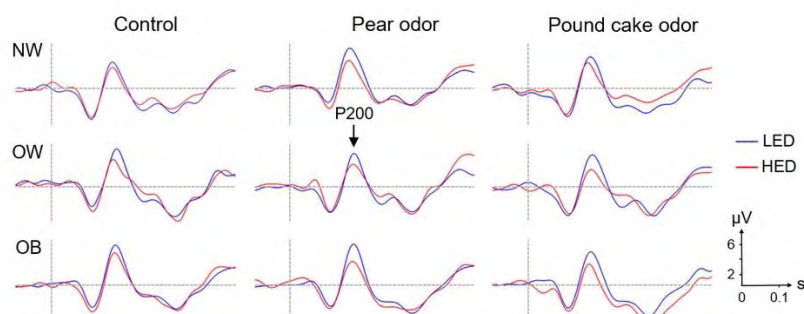


Figure 3: Grand-average ERP highlighting the P200 peak at the Cz electrode, by group (NW, OW, OB), priming condition (control, pear odour, pound cake odour), and type of food picture (LED, HED).

ERP data analysis

To study the impact of food odours on the cerebral processing of food pictures in individuals with different BMIs, we used a linear mixed-effects model (LME model; “lme” function in the R package “nlme”, R-3.6.3 software, R Development Core Team) to analyse the amplitude of each peak, calculated on the individual averages. For each subject and condition, these measures were weighted by the number of trials included in individual averages. The model included the *group* (NW, OW, OB) as a between-subjects factor, the *priming condition* (pear odour, pound cake odour, no odour) and the *type of food picture* (HED, LED) as within-subjects factors. The subjects were added as a random factor. All datasets presented normal distributions and equal variances ($p > .05$). Main effects and interactions are detailed below and were considered as significant for $p < .05$. When significant interactions were found, the data were split based on levels of one or two factors and tested independently with the LME model ($p < .05$).

Results

P100 amplitude. The interaction between group, priming condition, and type of food picture was significant ($F(4, 659) = 2.56, p = .04$; see Figure 4). In NW subjects, P100 amplitude was larger for HED than LED food pictures when they were primed with the pound cake odour ($F(1, 65) = 4.61, p = .04$). The difference in P100 amplitude by type of food picture was not significant when NW subjects were primed with the pear odour ($F(1, 68) = 0.34, p = .56$) or in the odourless control condition ($F(1, 68) = 0.01, p = .94$). In OW subjects, P100 amplitude was larger for HED than LED food pictures in the presence of the pear odour ($F(1, 56) = 22.34, p < .001$), but no significant differences were observed with the pound cake odour ($F(1, 54) = 0.10, p = .76$) or in the control condition ($F(1, 56) = 0.08, p = .77$). OB individuals presented no differences in P100 amplitude by type of food pictures when primed with the pear odour ($F(1, 58) = 0.34, p = .56$), the pound cake odour ($F(1, 59) = 1.61, p = .21$), and in the non-odourised condition ($F(1, 58) = 0.73, p = .40$).

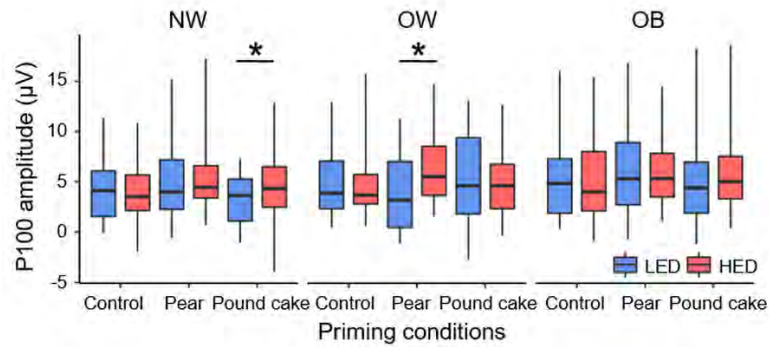


Figure 4: P100 amplitude (mV) by group (NW, OW, OB), priming condition (control, pear, pound cake), and picture type (LED, HED). The significant differences are represented with a threshold set to $*p < .05$.

P200 amplitude. Results showed a higher amplitude of the P200 for LED than HED food pictures, independently from group and priming conditions (main effect of food pictures: $F(1, 1036)=54.93, p < .001$). The interaction between group, priming condition, and type of food picture was also significant ($F(4, 1036)=2.99, p = .02$). Similarly to the P100, independent LME models were performed to test the differences in amplitude between LED and HED food pictures, for each priming condition by group separately (see Figure 5). In NW individuals, the P200 amplitude was greater for LED than HED food pictures in the control condition ($F(1, 114)=4.53, p = .03$), and when they were primed with the pear odour ($F(1, 114)=6.81, p = .01$). NW subjects presented no differences in P200 amplitude by type of food picture when they were primed with the pound cake odour ($F(1, 114)=2.21, p = .14$). OW individuals presented a greater P200 amplitude for LED than HED food pictures in all conditions: without odours ($F(1, 94)=21.70, p < .001$), when primed with the pound-cake odour ($F(1, 94)=10.65, p = .001$), and with the pear odour ($F(1, 94)=13.46, p < .001$). OB individuals had a greater P200 amplitude for LED than HED food pictures when primed with the pear odour ($F(1, 96)=26.56, p < .001$), and also with the pound cake odour ($F(1, 99)=34.01, p < .001$). In the non-odourised condition, we observed no differences in amplitude by type of food picture ($F(1, 99)=0.03, p = .86$).

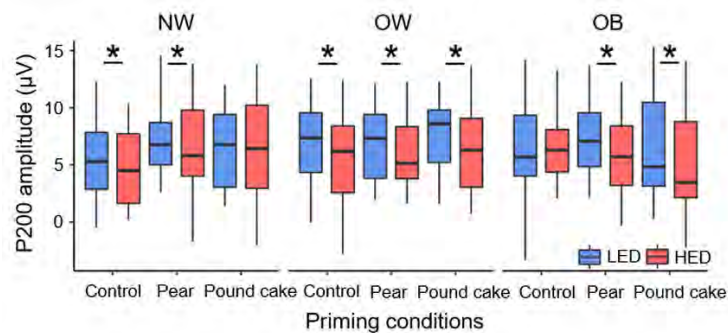


Figure 5: P200 amplitude (mV) by group (NW, OW, OB), priming condition (control, pear, pound cake), and picture type (LED, HED). The significant differences are represented with a threshold set to $*p < .05$.

Discussion

The main objective of the current study was to assess the effect of non-attentively perceived food odours on the ERPs elicited by HED and LED food pictures in NW, OW, and OB individuals. Overall, the results suggested significant differences between groups with different BMIs on the amplitude of the P100 and P200 peaks.

The P100 reflects the early cerebral activity associated with pre-attentive sensory processing. Cerebral differences between the groups were not observed on the P100 in the odourless condition, but only in the presence of the olfactory primes. A larger P100 amplitude for HED than LED food pictures was observed: 1/ in NW subjects when they were primed with the pound cake odour, and 2/ in OW subjects when they were primed with the pear odour. These results suggest that the initial sensory processing of food cues can be enhanced in favour of HED food pictures in the presence of food odours, at least in NW and OW individuals, even when the odours are not consciously perceived. This effect does not seem to depend on a specific food odour, as both the congruent odour (pound cake) and the incongruent odour (pear) led to an increased processing of HED food pictures. However, the subjects reacted to one type of odour or the other depending on their BMI, suggesting an influence of weight status on the reactivity to specific food odours. The fact that the early cerebral processing increased specifically for HED food pictures rather than LED food pictures may be partly explained by the more appealing nature of HED foods, which makes them more salient in the environment [12]. OB adults presented no significant differences in P100

amplitude between the two categories of food pictures, in any of the priming conditions. Therefore, food odours seem to have little impact on the P100 peak in OB individuals but do have an impact on the early cerebral processing in OW and NW individuals.

The P200 peak is thought to reflect automatic attentional processes [5, 6]. A significant main effect of the type of food pictures showed that the P200 was generally larger for LED than HED food pictures. The OW subjects presented a larger P200 for LED food pictures in all priming conditions, suggesting that these subjects tend to automatically engage more attentional resources toward LED food pictures, whether olfactory cues are present or not. In parallel, OB adults presented a larger P200 for LED food pictures in the presence of odours, but not in the odourless control condition. This result suggests that OB adults automatically engage more attention toward one type of food stimuli in the presence of olfactory cues. Thus, environmental food odours may be a greater source of influence for OB individuals (at least on attentional processes), compared with OW or NW individuals. In OW and OB subjects, the presence of the HED food odour led to an increased attentional processing of the incongruent LED food pictures. This could be explained by the fact that attentional resources orient toward the most appropriate choice based on each person's motivations [13]. As our experimental sessions took part in summer, fruits may have been more attractive than fatty-sweet foods, leading to a larger P200 amplitude for LED foods in presence of any food odour. The hypothesis of such a "seasonality effect" depending on the energy density of the foods remains to be tested.

Conclusion

For the first time, our study showed that non-attentively perceived food odours can influence the cerebral activity associated with the perception and attentional processing of food pictures. Moreover, this influence is modulated by the weight status of the subjects and the energy density of the food stimuli. BMI effects were observed early on the ERP, starting from the P100 peak. The food odours influenced the cerebral activity of NW and OW adults earlier (P100) than OB adults. This early perceptive processing was mainly enhanced for HED food pictures in the presence of both odours. This trend reversed over the time course of the ERP, as the results on the P200 peak showed an increased involvement of attentional resources for LED compared with HED food pictures. The P200 of OW and OB subjects was modulated by both odours, while it was not modulated by the pound cake odour in NW subjects, suggesting an enhanced reactivity to odours in persons with higher BMIs. Our results support the idea that weight status influences the cerebral activity underlying the processing of food cues outside of consciousness, as early as the first detectable P100 peak. Further research should be pursued to characterise the cerebral and cognitive features of individuals with different weight statuses, to better understand how these features may influence the subsequent food choices.

References

1. World Health Organization data: <https://www.who.int/topics/obesity/en/>
2. Jacquier C, Bonthoux F, Baciu M, Ruffieux B. Improving the effectiveness of nutritional information policies: assessment of unconscious pleasure mechanisms involved in food-choice decisions. *Nutr Rev.* 2012;70(2):118-131.
3. Carbine KA, Rodeback R, Modersitzki E, Miner M, Lecheminant JD, Larson MJ. The utility of event-related potentials (ERPs) in understanding food-related cognition: A systematic review and recommendations. *Appetite.* 2018;128:58–78.
4. Hendrikse JJ, Cachia RL, Kothe EJ, McPhie S, Skouteris H, Hayden MJ. Attentional biases for food cues in overweight and individuals with obesity: a systematic review of the literature. *Obes Rev.* 2015;16(5):424–432.
5. Nijs IMT, Franken IHA, Muris P. Food-related Stroop interference in obese and normal-weight individuals: behavioral and electrophysiological indices. *Eat Behav.* 2010;11(4):258–265.
6. Hume JD, Howells FM, Rauch HGL, Kroff J, Lambert VE. Electrophysiological indices of visual food cue-reactivity. Differences in obese, overweight and normal weight women. *Appetite.* 2015;85:126–137.
7. Mas M, Brindisi MC, Chabanet C, Nicklaus S, Chamberon S. Weight status and attentional biases toward foods: impact of implicit olfactory priming. *Front Psychol.* 2019;10:1–14.
8. Zsoldos I, Sinding C, Godet A, Chamberon S. Do Food Odours Differently Influence Cerebral Activity Depending on Weight Status? An Electroencephalography Study of Implicit Olfactory Priming Effects on the Processing of Food Pictures. *Neuroscience.* 2021;460:130-144.
9. Marty L, Bentivegna H, Nicklaus S, Monnery-Patris S, Chamberon S. Non-conscious effect of food odours on children's food choices varies by weight status. *Front Nutr.* 2017;4:16.
10. Mas M, Brindisi MC, Chabanet C, Chamberon S. Implicit food odour priming effects on reactivity and inhibitory control towards foods. *PLoS One.* 2020;15(6):e0228830.
11. Thomas-Danguin T, Rouby C, Sicard G, Vigouroux M, Farget V, Johanson A, Dumont JP. Development of the ETOC: a European test of olfactory capabilities. *Rhinology.* 2003;41:142–151.
12. Alonso-Alonso M, Woods SC, Pelchat M, Grigson PS, Stice E, Farooqi S, Khoo CS, Mattes RD, Beauchamp GK. Food reward system: current perspectives and future research needs. *Nutr Rev.* 2015;73(5):296–307.
13. Vuilleumier P. Affective and motivational control of vision. *Curr Opin Neurol.* 2015;28(1):29–35.

Understanding the effect of saliva composition depending on gender and age on wine aroma perception: oral aroma release, dynamics of sensory perception and consumer preferences and liking

Celia Criado, María Pérez-Jiménez, Carolina Muñoz-González and MARIA ANGELES POZO-BAYÓN

Instituto de Investigación en Ciencias de la Alimentación (CIAL) (CSIC-UAM) C/Nicolás Cabrera, 9, 28049, Madrid (Spain), m.delpozo@csic.es

Abstract

In order to determine the relationship between saliva composition depending on age and gender on wine oral aroma release and the impact this might have on aroma perception over consumption and on consumer preferences and liking, a large study comprising three different approaches was performed based on (a) determining oral aroma release during wine intake; (b) rating the perceived retronasal aroma intensity over wine consumption by time-intensity assays and (c) checking the consumer's hedonic and emotional response to wines. Participants belonged to two different age groups (younger (18-35 y.o.) and seniors (>55 y.o)) and they were gendered balanced. Their saliva samples were collected in order to relate saliva composition to instrumental and sensory measurements. Significant differences ($p < 0.05$) on aroma release and aroma perception between age-gender groups were found, which also depended on the wine type. Total protein content and salivary flow were the two salivary parameters more related with this. Additionally, differences in some emotional response among groups were found, which will be explored in future works in the aim to elaborate more personalised wines for target consumers in order to increase their acceptance of wine.

Keywords: wine, retronasal aroma release, saliva, aroma perception, consumer hedonic and emotional response

Introduction

Spain is the third largest wine producer country in Europe, behind France and Italy [1], however, the consumption of wine compared to other alcoholic beverages (such as beer or spirits) is considerably lower in Spain (28 %) compared to France (59%) or Italy (65%). Indeed, the consumption of wine in the Spanish households has decreased by over 60% in the last two decades [2]. Additionally, a large difference in wine consumption patterns depending on age has been also noticed. While seniors (55 years and above) consume more than 73 % (total litres of wine consumed in households), the consumption of youngsters (under 35 years old) is clearly lower (4.5 %) [3].

Furthermore, differences in wine liking and emotions considering a group of consumers of different ages have recently been observed [4]. Interestingly, a relationship between wine liking, emotions and sensory characteristics have also been shown [5]. Therefore, although the reasons driving wine consumption could be of different nature and linked to intrinsic factors (e.g. label, wine name, shape of the bottle, etc.), there is certainly an impact of wine sensory characteristics on consumer's choice that are directly dependent on the wine chemical composition.

In this sense, aroma has been one of the most important sensory attributes for driving consumer's preference and choice, and although the olfactory cues can give us an idea or expectation of wine liking, wine acceptability and the repeated purchase of a wine can be only assessed during wine tasting. During wine intake, aroma molecules are released in the oral and throat cavities where they can interact with saliva. Different effects such as aroma dilution, interaction with proteins or even metabolism have been described in the literature, which might affect the amount and type of the aroma molecules that could finally reach the olfactory receptors, therefore with a putative effect on aroma intensity and aroma quality [6].

On the other hand, different works have also shown that saliva composition can change through lifespan [7]. This invites us to hypothesize that changes in saliva composition depending on age could also affect aroma release and perception and therefore wine aroma liking.

Therefore, the aim of this work has been to evaluate the effect of saliva composition depending on age (and gender) on wine oral aroma release, aroma perception over consumption and on consumer's preference (hedonic and emotional response).

Experimental

Three independent studies aimed at determining (a) oral aroma release during wine intake, (b) aroma intensity over wine consumption and (c) the consumer's hedonic and emotional response to wine were performed. In all of them, saliva samples were collected and their composition determined. All the participants in this study received pertinent information about it and they signed the approval consent for their participation. The Bioethical Committee of the Spanish National Council of Research (CSIC) also approved the experimental procedure. The experimental approaches are described here in.

Oral aroma release during wine intake

For this study, 32 individuals belonging to two different age groups: younger (<35 y.o.) and senior (>55 y.o.) were recruited and grouped accordingly to their age-gender in: (YF) Young-Female (n=8), (YM) Young-Male (n=8); (SF) Senior-Female (n=7); (SM) Senior-Male (n=9). Stimulated saliva was collected before the assays and pH, salivary flow, viscosity, minerals (Zn, Na, K, Ca, Mg), total protein content (TPC), and some enzymatic activities (total salivary esterase activity (TSEA) and α -amylase) were determined using procedures previously described [8]. For this study we used two types of wines, a red one and a white one. To monitor oral aroma release we used the in mouth Head Space Stir Bar Sorptive extraction followed by GC-MS analysis (in mouth-HS SBSE-GC-MS) as previously described [9]. The procedure consisted in a gentle mouth rinsing with the wine for 30 s, and three in-mouth samplings after spatting the wine off: immediately (0 s), at 60 s and at 120 s. Each sampling was for 30 s with a different twister. All the analyses were done in triplicates. Before each sampling, the oral cavity was also sampled to check for the absence of typical wine volatiles. All the twistors were desorbed in the TDU and trapped in the CIS of the GC-MS in the conditions described by Pérez-Jiménez and Pozo-Bayón [9] to build the release curves of each volatile compound identified in the mouth.

Aroma intensity over wine consumption

This study aimed to know if there were also differences on aroma perception between age groups over wine consumption. For this, we recruited 22 volunteers from both genders, eleven were from the senior group (> 55 y.o.) and the other eleven were young individuals (between 18 and 35 years old). Although most of them already participated in the first study (n=18), four new participants belonging to the younger group were exclusively recruited for this study. Two wines, a red and a white wine, were used. In previous trials, some characteristic wine aroma attributes, such as apple and pineapple in the white wine; and smoky and black pepper in the red wine were selected for the Time-Intensity (T-I) study. Before the sample analysis, volunteers were trained in the recognition of the selected aroma descriptors and in the T-I methodology by using tablets and the Compusense software. For the sensory evaluation, volunteers rated the variation in the intensity of the above mentioned attributes over 2 minutes after wine intake and expectoration (15 mL). T-I parameters (Imax, TImax, Tend and AUC) were extracted from the T-I curve and they were correlated with salivary parameters. For the latest, the same procedure already described was employed and the salivary composition was also determined [10].

Consumer's hedonic and emotional response to wine

For this study we recruited 105 consumers, 45 of them were seniors and 58 of them were within the younger group. Two wines, a red and a white wine with *black pepper* and *pineapple* notes as dominant descriptors, respectively, were used for this study. Consumer tests were performed by using the Compusense software. Volunteers were asked to rate aroma intensity, wine liking and their emotional response considering 15 emotional terms from the lexicon recently published for the Spanish wine consumer [5]. A saliva sample was always collected prior to the sensory test as previously described [10]. Two measurements, salivary flow and total protein content were performed in this sample, since they were the most correlated salivary parameters to aroma perception from the T-I study [10].

Results and discussion

In order to determine the relationship between age and oral aroma release during wine intake, the oral aroma release after wine tasting was assessed at three different times, immediately, 60 s and 120 s after wine expectoration using a white and a red wine. A total of 24 and 23 aroma compounds were identified in the oral cavity after the white and red wine intake, respectively. After application of different statistical tests (ANOVA and stepwise linear discriminant analysis) it was possible to confirm differences in oral aroma release among the four age-gender groups (YF, YM, SF, SM), which also depended on the aroma compound and wine type. These results can be shown in the PCA depicted in Figure 1, where it is also possible to check the relationship between oral aroma release and saliva composition. As it can be seen, the higher release of furanic compounds and C13-norisoprenoids in senior groups after red wine tasting could be related to some differences in their saliva

composition (higher TPC and α -amylase activity). On the contrary, the effect of gender on aroma release was larger in younger individuals. YM group showed a higher release of esters and alcohols regardless the type of wine (white and red) (Figure 1). On the contrary, the YF group showed the lowest oral aroma release in both wines from the four age-gender groups; but this did not seem to be explained by saliva composition. Overall, differences in oral aroma release among gender groups were more evident in younger than in seniors.

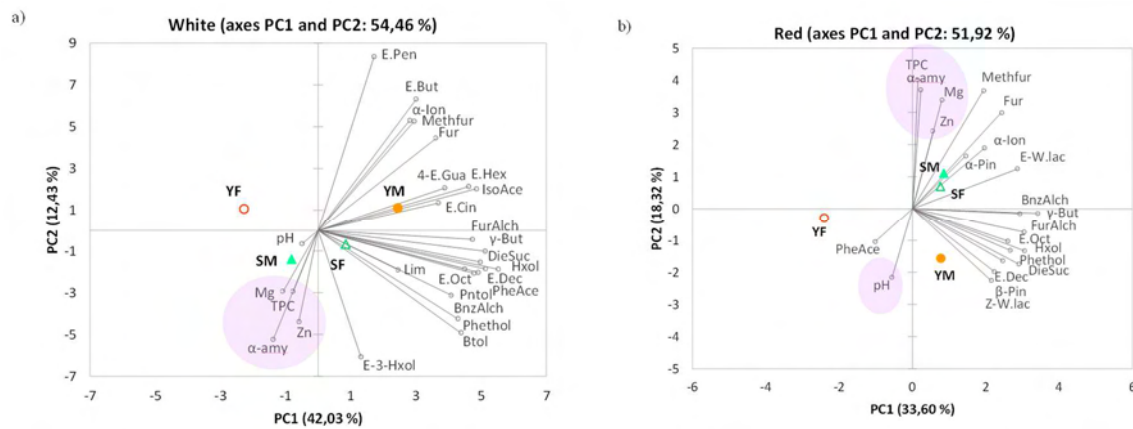


Figure 1: Graphical projection of the two firsts components obtained after the application of PCA to oral aroma release data after white wine (a) and red wine tasting (b) and saliva composition in the four age-gender groups. Only those variables that showed significant differences among groups ($p < 0.05$) have been included. For each age-gender groups only the centroids are represented.

The results from the T-I study also revealed differences in aroma perception depending on the age. Interestingly, results only showed an effect of the age group in the intensity perception of the two aroma attributes in the red wine (smoky and black pepper aroma) but not in the perception of any of the aroma attributes considered in the white wine (apple and pineapple). In the red wine significant differences ($p < 0.005$) in most parameters extracted from the T-I curve (Imax, Tend and AUC) were found. For instance, senior individuals showed the highest values of Imax, Tend and AUC of smoky aroma (Figure 2). Similar results were found for black pepper and the highest Tend and AUC values were found in senior compared to the younger individuals. These results are in agreement with the higher oral aroma release of certain compounds (e.g methyl fufural, furfural) in the senior group in the previous study (Figure 1), which might be associated to these aroma attributes in red wines. Additionally, the Pearson correlation analysis showed that the salivary total protein content (that was significantly higher in the senior group) was positively and significantly related to Imax (0.406) while the salivary flow (significantly lower in the senior compared to the younger group) was negatively related to Imax (-0.444).

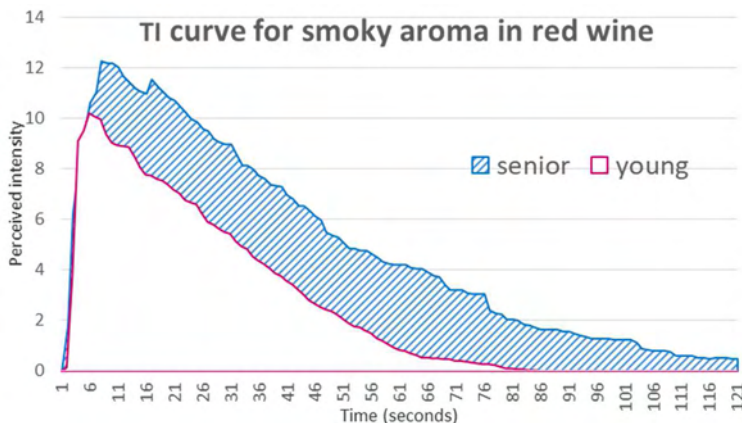


Figure 2: T-I profile (average values) for the smoky aroma rated by senior and younger participants.

Finally, results from the consumer study also showed an impact of the age-gender groups, but only in the black pepper attribute in red wine. Nonetheless, there was no significant effect in the perceived intensity of pineapple aroma (Figure 3). Interestingly, senior women rated the lowest aroma intensity of black pepper, which is not in agreement with results from the T-I, in which seniors showed the highest perception of smoky and black pepper aroma. Nonetheless, differences in the type of volunteers, trained in the case of T-I, or untrained

consumers, more focused on hedonics than in descriptive traits, could be the reason for this disparity, which has also been noticed in previous studies [11].

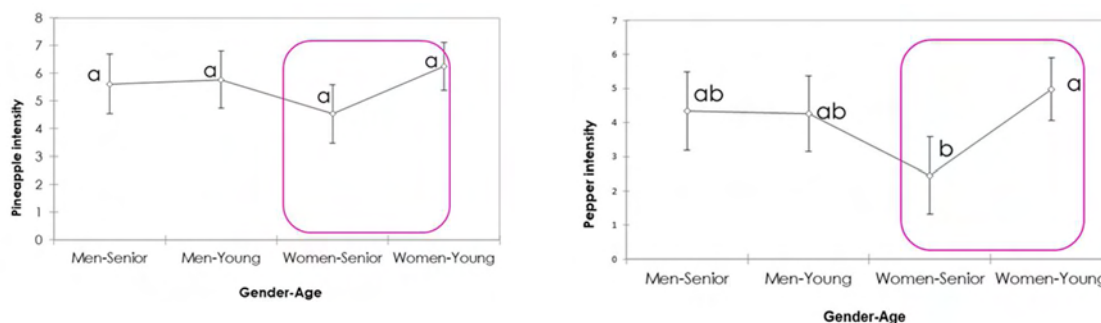


Figure 3: Scores of the pineapple and pepper intensity in the red wine considering the four age-gender groups of consumers.

Interestingly, the salivary analysis in such large population was quite in agreement with previous results, and seniors showed the highest TPC and senior women the lowest salivary flow. On the contrary, younger men showed the highest salivary flow and lowest TPC. The Pearson correlation analysis also revealed some interesting facts. For instance, a positive and significant ($p < 0.05$) correlation between black pepper aroma and salivary flow (0.218) and between liking and TPC (0.211) was found. This result could be related to the intensity of the astringency perceived by the consumer (that was not measured in this study), which is often linked with lower wine acceptability. This sensation is associated with the capacity of tannins to bind some salivary proteins, which can affect the oral mucosal pellicle reducing the lubricity of the oral cavity. However, if the total protein content is higher there could be still salivary proteins to keep this lubricity and therefore, the astringency perceived should be lower [12]. Nonetheless, this hypothesis should be confirmed in further studies, which also must include the score of this orosensory perception.

Regarding the emotional response, which could provide additional information to liking, there were only significant differences by age-gender groups in one of the 15 emotional terms. Specifically, the emotion *curious* was rated with the lowest intensity in the case of senior women and only in red wines. Some other differences in the emotional response were also found, depending on the wine type. For instance *nostalgic* was higher in red wines, while *refreshed* was higher in white wines. On the other hand, and interestingly, a positive correlation between liking and positive emotions was confirmed. Some examples of these emotions included *satisfied* (0.70), *joyful* (0.54), *desirous* (0.54), *lucky* (0.53) and *cheerful* (0.51) among others. On the contrary, correlations with liking were negative for negative emotions such as *displeased* (-0.46), *sadness* (-0.25), or *sleepy* (-0.22).

Conclusions

Overall, this study has confirmed differences in aroma release and aroma perception between age-gender groups, which were more pronounced during red wine than during white wine consumption. Additionally, saliva composition, and specifically salivary total protein content and flow (which were inversely related) were related to aroma release and perception in a compound dependent manner. Finally, the age-gender groups also had an effect on consumer's aroma perception in red wines, but it did not affect the liking. Nonetheless, a positive correlation between red wine liking and salivary total protein content was found. Finally, the differences found in the emotional response in some groups (senior-women, younger-women), could be interesting for targeting new types of products, able to elicit specific positive emotions in these consumer groups increasing their acceptance of wine.

References

1. OIV. OIV assessment of the world wine situation. 2019 [Press release].
2. OeMv. Consumption of wine and other beverages in the Spanish food channel. 2018. Retrieved from www.oemv.es.
3. MAPA. Annual Food Consumption Report in Spain 2018. 2019. Retrieved from www.mapa.gob.es: <http://publicacionesoficiales.boe.es>
4. Mora, M., Urdaneta, E., & Chaya, C. Emotional response to wine: Sensory properties, age and gender as drivers of consumers' preferences. *Food Qual. Prefer.* 2018;66:19-28.
5. Mora, M., de Matos, A. D., Fernández-Ruiz, V., Briz, T., Chaya, C. Comparison of methods to develop an emotional lexicon of wine: Conventional vs Rapid-method approach. *Food Qual. Pref.* 2020;83:10392
6. Muñoz-González, C., Feron, G., Canon, F. Main effects of human saliva on flavour perception and the potential contribution to food consumption. *Proc. Nutr. Soc.* 2018;77(4):423-431.

7. Muñoz-González, C., Feron, G., & Canon, F. Physiological and oral parameters contribute prediction of retronasal aroma release in an elderly cohort. *Food Chem.* 2021;342:128355.
8. Criado, C., Chaya, C., Fernández-Ruiz, V., Álvarez, M. D., Herranz, B., Pozo-Bayón, M. Á. Effect of saliva composition and flow on inter-individual differences in the temporal perception of retronasal aroma during wine tasting. *Food Res. Int.* 2019;126:108677.
9. Pérez-Jiménez, M., Pozo-Bayón, M. Á. Development of an in-mouth headspace sorptive extraction method (HSSE) for oral aroma monitoring and application to wines of different chemical composition. *Food Res. Int.* 2019;121:97-107.
10. Criado, C., Muñoz-González, C., & Pozo-Bayón, M. Á. Differences in salivary flow and composition between age groups are correlated to dynamic retronasal aroma perception during wine consumption. *Food Qual. Pref.* 2021;87:104046.
11. Sáenz-Navajas, M. P., Avizcuri, J. M., Ballester, J., Fernández-Zurbano, P., Ferreira, V., Peyron, D., & Valentin, D. Sensory-active compounds influencing wine experts' and consumers' perception of red wine intrinsic quality. *LWT.* 2015;60(1):400-411.
12. Crawford, C. R., & Running, C. A. Addition of chocolate milk to diet corresponds to protein concentration changes in human saliva. *Physiol. Behav.* 2020;225:113080.

Tracing odour- and taste-active compounds in human milk

MARCEL DEBONG^{1*}, ROMAN LANG^{2,3*}, Katharina N'Diaye², Andrea Buettner^{1,4},
Thomas Hofmann^{2,3} and Helene M. Loos^{1,4}

¹ Friedrich-Alexander-Universität Erlangen-Nürnberg, Chair of Aroma and Smell Research, Erlangen, Germany

² Technical University of Munich, Chair of Food Chemistry and Molecular Sensory Science, Freising, Germany

³ Leibniz-Institute for Food Systems Biology at Technical University of Munich, Freising, Germany

⁴ Fraunhofer Institute for Process Engineering and Packaging IVV, Freising, Germany

*These authors contributed equally to this publication.

marcel.debong@fau.de ; r.lang.leibnitz-lsb@tum.de

Abstract

Scope

The alteration of the flavour of human milk by the maternal diet and thereby the possibility of sensory programming of the infant has been reported in several studies. The objective of this study was to exemplarily illustrate and compare the simultaneous transition of odour- and taste-active compounds from a customary curry dish into milk.

Methods and Results

A standardised curry dish was prepared and its flavour-active compounds were characterised. This dish was used in an intervention study with lactating mothers who donated four milk samples, one before and three after the intervention. These samples were used to quantify the transition of flavour-active compounds from the curry dish into milk via GC-MS and LC-MS. The concentration courses of linalool, 1,8-cineole and piperine are illustrated here for the milk samples of three exemplary test persons. These courses demonstrate a transition after the intervention as well as interindividual variations regarding transition time and amounts.

Conclusion

Flavour-active substances can migrate from the maternal diet into human milk. The transferred compounds do not necessarily reach concentrations perceivable by adults. Though, even at below threshold concentrations, the transferred compounds can interact with the nurslings' receptors and induce physiological changes in the chemosensory system.

Keywords: curry, metabonomics, piperine, linalool, 1,8-cineole

Note: Our use of the term "flavour" relates to compounds, which contribute to the overall oral impression and thus includes aroma-, taste- and trigeminal-moderated sensations.

Introduction

The fact that the interplay of smell, taste and trigeminally moderated oral impressions has more effect on our perception of food than the sum of its parts is the subject of current research in the field of sensory science [1-4]. For instance, a citrus flavouring is perceived as more intense when it is presented in a sugar solution than without the tastant [1]. The concept of multisensory integration encompasses all those sensory impressions whose combination is matched and harmonised as a pattern in the human brain [5]. Multisensory experiences and expectations develop in the course of life. During breastfeeding, infants already experience first flavour impressions, which can provide the basis for flavour learning [6-8]. The flavour of breast milk can be influenced by maternal nutrition [8-11], and for many odorants, the transition of dietary aroma into milk has been demonstrated on a molecular level [10, 12, 13]. For tastants and trigeminally active compounds, however, there are only a few indications of a transfer into breast milk. Up to now, only a transfer of alkaloids such as caffeine [14] has been demonstrated, and a general connection between a diet rich in bitter substances and bitterness of breast milk has been observed [15]. However, an investigation of the interplay of odorants and tastants from an everyday multi-component dish has not yet taken place. This is where our work comes in, in which we set ourselves the goal of characterising the transition of flavour compounds in parallel from a standardised curry dish into breast milk. For this purpose, breastfeeding mothers gave milk samples before and after curry consumption as part of an intervention study to determine the temporal course of the possible transition of flavour-active substances.

Experimental

Curry dish

The basis of our intervention study was the usage of a standardised curry dish. The curry spice powder used for this dish comprised coriander seeds, cumin seeds, turmeric powder, dried red chilies, fenugreek, black

peppercorns, cinnamon sticks, green cardamom, curry leaves and cloves. For the preparation of the dish, the curry powder was mixed with coconut milk, water, salt and fresh ginger to prepare a curry sauce which was then served with rice. The detailed recipe is available from Dehong et al. and N'Diaye et al. (2021, submitted).

Intervention study

For the intervention study, nursing mothers were asked to donate milk samples following a specific procedure. This procedure, illustrated in Figure 1, started with a two-day washout phase during which the mothers refrained from the intake of certain food and kept a nutrition diary. On the study day, the mothers first donated a blank milk sample, then consumed the curry dish and subsequently donated further milk samples (for the detailed procedure see Dehong et al. and N'Diaye et al., 2021, submitted). The samples were then aliquoted for the determination of odorants as well as tastants. The study was performed in agreement with the Declaration of Helsinki and approved by the Ethical Committee of the Friedrich-Alexander-Universität Erlangen-Nürnberg (registration number 24_16 B).

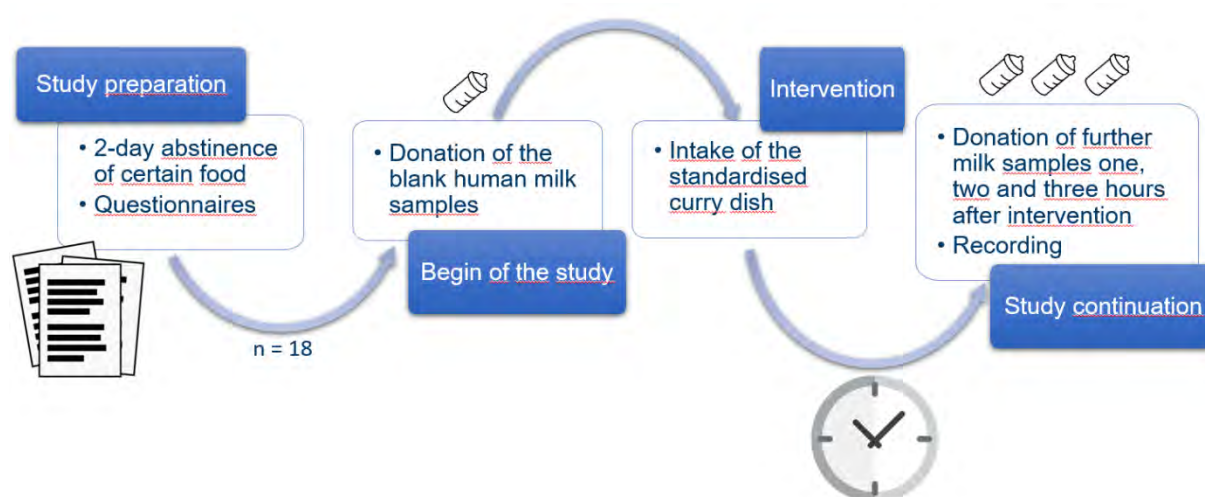


Figure 1: Scheme of the intervention study procedure.

Characterisation of the curry dish

To gain dosage information on the odour- and taste-active compounds we performed a targeted quantification of the compounds which were determined as the most relevant flavour-active compounds in the curry dish. These comprised, amongst others, the odorants 1,8-cineole and linalool, on which we will focus here. Those substances were quantified using a stable isotope dilution assay (SIDA) approach in combination with solvent assisted flavour evaporation (SAFE) and GC-MS with internal calibration. Detailed information is provided in Dehong et al. (2021, submitted). The pungent oral sensation of the curry dish suggested pungent compounds as additional target analytes. These comprised, amongst others, piperine. Piperine was quantified by LC-MS/MS using an in-house synthesised d_{10} -piperine standard for an internal calibration. Detailed information is provided in N'Diaye et al. (2021, submitted).

Detection of odorants and tastants in milk and estimation of their sensory relevance

An instrumental-analytical approach was utilised to characterise the transfer of odorants and tastants from the curry dish into milk, analogously to the determination of the target compounds in the curry dish. In addition to that, odour and taste activity values (OAVs and TAVs) were calculated to evaluate the relevance of such flavour transition. Therefore, a trained panel determined the odour/taste thresholds of the target compounds in a cow-milk based substitution matrix (for details see Dehong et al., N'Diaye et al., submitted). The OAVs and TAVs were then calculated as quotients of the flavour compound concentration in a sample and the odour/taste threshold of the respective compound.

Results and discussion

Flavour transition into milk

On average, the absolute dosages of the odorants linalool and 1,8-cineole were 224 μmol and 2.6 μmol per serving, respectively. The dosage amount of piperine was 32 μmol per curry dish. Exemplary transition courses of three milk sets are illustrated in Figure 2 and will be discussed in the following sections.

Considering the here illustrated examples, the concentrations of linalool in the milk samples donated before the intervention were about 1 nmol/L. Within one hour after the intervention the concentrations rose to values between 6 nmol/L (course A) and 22 nmol/L (course C). The concentrations of 1,8-cineole in the milk samples obtained before the intervention ranged between 2 nmol/L (course C) and 16 nmol/L (course A). Within one hour after the intervention the concentrations rose to values between 3 nmol/L (course C) and 22 nmol/L (course A). The piperine concentrations in the initial samples before the intervention ranged between 0.4 nmol/L (course A) and 102 nmol/L (course C). They rose to 26 nmol (courses A and B) and 135 nmol/L (course C) within one hour after the intervention.

Linalool, the compound with the highest dosage in the curry dish, had a transition rate of $2-4 \times 10^{-4}$ % during the sampling period after intervention in the illustrated sample sets. 1,8-cineole had a transition rate of about $0.4-8 \times 10^{-2}$ % and piperine of about $0.5-2 \times 10^{-2}$ %. Due to these low transition rates, it can be expected that the substances underlie vast metabolization processes, which might have transformed their structure in phase I-reactions or conjugated them e.g. with glucuronic acid in phase II-reactions, and/or that they were eliminated via other pathways like urine, breath or faeces. The transition rates furthermore reveal substance-specific as well as interindividual differences. The transition amount can vary strongly, as can be seen by the comparison of course B to C. In course B the piperine maximum concentration is about five times lower and the 1,8-cineole maximum concentration about five times higher than in course C. Metabolic or other individual factors might explain such differences.

Additionally, the three exemplary transition courses reveal that interindividual differences can play a significant role with regard to temporal aspects of the transition of flavour-active substances. While the concentration courses of linalool in course A and C were similar – starting from a low initial level of linalool of around 1 nmol/L, rising to about 10 nmol/L within one hour after intervention and then continuously declining in the following samples – the linalool concentration in course B rose again in the last sample, obtained three hours after the intervention. For the transition courses of 1,8-cineole similar variations occurred. Basically, the 1,8-cineole concentration rose within one hour after intervention, but in course A the 1,8-cineole concentration increased again three hours after the intervention, similar to the linalool concentration in course B. For piperine such second maxima appeared in all of the three exemplary courses. The occurrence of these second transition maxima have recently been reported for ramson-derived metabolites in milk [13].

The three participants also differed in their basis levels of the investigated flavour-active compounds, despite the instruction of avoiding certain food during the wash-out phase. Especially for piperine and 1,8-cineole comparatively high basis levels were detected in some participants. Non-compliance might be one explanation, but also unintentional uptake of flavour compounds via products like tooth paste or chewing gums, which might contain 1,8-cineole. For the case of the high piperine basis level, the provided nutrition diary of the test person revealed that a dish seasoned with pepper was consumed on the evening before the intervention. This is especially interesting as it shows that the transition of flavour compounds apparently influences the composition of human milk not just in the first hours after intake but for a prolonged time. Such transitions could even cumulate, especially for those substances which occur in a diet very often. Pepper is one of the world's most consumed spices and contains piperine as well as linalool. The fact that pepper is often consumed all over the day during breakfast, lunch and supper could lead to a continuous and cumulated transition into milk.

On the basis of our results, the transition of flavour-active compounds is compared in terms of transition time and transition rate. The concentrations of all of the three target compounds rose within 1 h after the curry consumption, which demonstrates the possibility of a simultaneous transfer of both odour- and trigeminally-active substances into milk. The transition rates during the first three hours after intervention were $2-4 \times 10^{-4}$ % for linalool, $0.4-8 \times 10^{-2}$ % for 1,8-cineole and $0.5-2 \times 10^{-2}$ % for piperine in the three exemplary milk sets. Therefore, it is suggested that 1,8-cineole and piperine have a similar and stronger tendency to migrate into human milk than linalool.

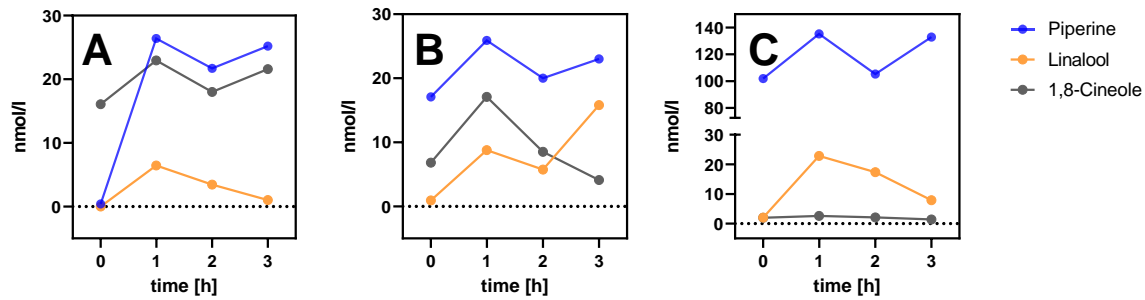


Figure 2: Concentration course of piperine, linalool and 1,8-cineole before (0h) and after the intervention (1-3h) for three exemplary milk sets.

Estimation of the sensory relevance of flavour transfer

The odour thresholds of linalool and 1,8-cineole were 4 nmol/L and 21 nmol/L, respectively. The threshold for pungency of piperine in milk matrix was 17500 nmol/L. Linalool reached OAVs > 1 in all three exemplary courses and even in seven of the nine illustrated samples after intervention. For 1,8-cineole, OAVs > 1 were calculated for the first and third sample after the intervention in course A. The piperine concentrations resulted in TAVs < 1 in all samples. Compounds with OAVs or TAVs > 1 are suggested to potentially alter the overall flavour of a milk sample, because their concentrations exceed their threshold levels. Accordingly, for linalool it can be argued that its ingestion with the curry dish leads to an impact on the overall aroma of the milk. For 1,8-cineole this might only be the case for few participants. Piperine can, based on its TAVs, not be suggested to have an impact on the overall flavour of the human milk.

The OAVs and TAVs were calculated based on average threshold levels of adult panellists. Odour perception of nurslings might be more sensitive [16] compared with adults. Moreover, retronasal odour perception is in general more intense [17-19]. Accordingly, the transition of 1,8-cineole, and possibly also of piperine, might lead to a sensory effect in the infant perception during nursing. Additionally, it is important to consider that early exposure could also impact later preferences towards, or tolerance of, the respective flavour substances when being below perception threshold. Finally, cross-modal summation, which is the concept that mixtures of e.g. odour- and taste-active substances can be perceived even if both stimuli are below their perception threshold, could lead to an actual perception of the given odour-taste mixture [20]. This effect has been shown in several current studies in which the intensity of taste impressions could be increased by flavourants [21-23] and as shown by Sinding et al. (2021), this could even lower the perception threshold of certain compounds [4].

Conclusion

A simultaneous transition of odour- and trigeminally-active substances from a curry dish into milk could be outlined in this work. This transition can be described as fast but marginal with an average maximum in milk samples donated one hour after the intervention and a rate of about 2×10^{-4} - 0.08 % of the initial dosage within the here considered sampling period. While the transfer did not seem to have an impact on the overall flavour of the milk in the case of piperine, for the investigated odorants that was at least partly the case. Additional evidence reported in Debong et al. (2021, submitted) and N'Diaye et al. (2021, submitted) suggests that not all flavour-active substances migrate from the curry dish into milk. As shown here, among those substances for which a transfer takes place not all might be perceivable. But some of them might be perceived or activate the nurslings' receptors and thus provide the basis for an early flavour learning and the creation of multisensory associations.

References

1. Lim J, Fujimaru T, Linscott TD. The role of congruency in taste-odor interactions. *Food Qual Prefer.* 2014;34:5-13.
2. Liu J, Wan P, Xie C, Chen DW. Key aroma-active compounds in brown sugar and their influence on sweetness. *Food Chem.* 2021;345.
3. Fondberg R, Lundström JN, Blöchl M, Olsson MJ, Seubert J. Multisensory flavor perception: The relationship between congruency, pleasantness, and odor referral to the mouth. *Appetite.* 2018;125:244-52.
4. Sinding C, Thibault H, Hummel T, Thomas-Danguin T. Odor-Induced Saltiness Enhancement: Insights Into The Brain Chronometry Of Flavor Perception. *Neuroscience.* 2021;452:126-37.
5. Freiherr J, Lundström J, Habel U, Reetz K. Multisensory integration mechanisms during aging. *Front Hum Neurosci.* 2013;7(863).

6. Loos HM, Reger D, Schaal B. The odour of human milk: Its chemical variability and detection by newborns. *Physiol Behav.* 2019;199:88-99.
7. Mennella JA, Beauchamp GK. The human infants' response to vanilla flavors in mother's milk and formula. *Infant Behav Dev.* 1996;19(1):13-9.
8. Mennella JA, Beauchamp GK. Maternal Diet Alters the Sensory Qualities of Human Milk and the Nursling's Behavior. *Pediatrics.* 1991;88(4):737.
9. Scheffler L, Sauer mann Y, Zeh G, Hauf K, Heinlein A, Sharapa C, et al. Detection of Volatile Metabolites of Garlic in Human Breast Milk. *Metabolites.* 2016;6(2).
10. Kirsch F, Horst K, Röhrig W, Rychlik M, Buettner A. Tracing Metabolite Profiles in Human Milk: Studies on the Odorant 1,8-Cineole Transferred into Breast Milk after Oral Intake. *Metabolomics.* 2013;9(2):483-96.
11. Dehong MW, Loos HM. Diet-Induced Flavor Changes in Human Milk: Update and Perspectives. *J Agric Food Chem.* 2020;68(38):10275-80.
12. Hausner H, Bredie WLP, Mølgaard C, Petersen MA, Møller P. Differential transfer of dietary flavour compounds into human breast milk. *Physiol Behav.* 2008;95(1-2):118-24.
13. Scheffler L, Sharapa C, Amar T, Buettner A. Identification and Quantification of Volatile Ramson-Derived Metabolites in Humans. *Front Chem.* 2018;6(410).
14. Escuder-Vieco D, Garcia-Algar Ó, Joya X, Marchei E, Pichini S, Pacifici R, et al. Breast Milk and Hair Testing to Detect Illegal Drugs, Nicotine, and Caffeine in Donors to a Human Milk Bank. *J Hum Lact.* 2016;32(3):542-5.
15. Mastorakou D, Ruark A, Weenen H, Stahl B, Stieger M. Sensory characteristics of human milk: Association between mothers' diet and milk for bitter taste. *J Dairy Sci.* 2019;102(2):1116-30.
16. Loos HM, Doucet S, Védrières F, Sharapa C, Soussignan R, Durand K, et al. Responses of Human Neonates to Highly Diluted Odorants from Sweat. *J Chem Ecol.* 2017;43(1):106-17.
17. Czerny M, Christlbauer M, Christlbauer M, Fischer A, Granvogl M, Hammer M, et al. Re-investigation on odour thresholds of key food aroma compounds and development of an aroma language based on odour qualities of defined aqueous odorant solutions. *Eur Food Res Technol.* 2008;228(2):265-73.
18. Cartwright LC. Vanilla-like Synthetics, Solubility and Volatility of Propenyl Guaethyl, Bourbonal, Vanillin, and Coumarin. *J Agric Food Chem.* 1953;1(4):312-4.
19. Rychlik M, Schieberle P, Grosch W, Deutsche Forschungsanstalt für L, Universität M, Institut für Lebensmittelchemie der T. Compilation of odor thresholds, odor qualities and retention indices of key food odorants. Garching: Deutsche Forschungsanstalt für Lebensmittelchemie and Institut für Lebensmittelchemie der Technischen Universität München; 1998.
20. Delwiche JF, Heffelfinger AL. Cross-modal additivity of taste and smell. *J Sens Stud.* 2005;20(6):512-25.
21. Velázquez AL, Vidal L, Varela P, Ares G. Cross-modal interactions as a strategy for sugar reduction in products targeted at children: Case study with vanilla milk desserts. *Food Res Int.* 2020;130.
22. Hartley L, Russell CG, Liem DG. Addition of a visual cue to rice increases perceived flavour intensity but not liking. *Food Res Int.* 2021;139.
23. Alcaire F, Antúnez L, Vidal L, Giménez A, Ares G. Aroma-related cross-modal interactions for sugar reduction in milk desserts: Influence on consumer perception. *Food Res Int.* 2017;97:45-50.

Do space conditions change flavour perception and decrease food intake by astronauts?

ANDREW TAYLOR¹, Scott McGrane², Martina Heer³, Jonathan Beauchamp⁴ and Loic Briand⁵

¹ Flavometrix Limited, Long Whatton, United Kingdom

² Waltham Petcare Science Institute, Waltham-on-the-Wolds, United Kingdom

³ International University of Applied Sciences, Bad Honnef, Germany

⁴ Fraunhofer Institute for Process Engineering and Packaging IVV, Freising, Germany

⁵ Centre for Taste, Smell and Feeding Behaviour, Dijon, France

flavometrix@btconnect.com

Abstract

Several hundred astronauts have experienced spaceflight for periods of up to 15 months on visits to the International Space Station (ISS). Each astronaut's health is monitored and there is clear evidence that their calorie intake only meets around 80% of the recommended daily allowance. There is concern that this underconsumption may have negative consequences on astronauts' mental and physical health during the planned interplanetary missions which will last about three years. There are many hypotheses for the calorie deficit and we have focused on just one; the concept that chemical contaminants in recycled air and water could change the flavour quality of meals during spaceflight and therefore affect food intake. Using detailed NASA data on the composition of ISS recycled air and water, we applied the Dose-over-Threshold (DoT) concept to identify contaminants that might be odour active and could change the perceived overall food flavour. However, because of the large variation in published odour threshold values, the DoT concept delivered inconclusive results. The limitations of the DoT concept and ways to improve it are discussed.

Keywords: space food, odour interaction, flavour perception

Introduction

The welfare of astronauts is a key factor in space exploration. Since the first human spaceflight in 1961, and the launch of the International Space Station (ISS) over two decades ago, much has been learnt about the changes that occur to the human body during spaceflight over periods of three months to one year. One factor that is still not explained is why astronauts only consume around 80% of their daily calorie needs [1, 2]. While this seems to be tolerable for (short) visits to the ISS, the proposed crewed mission to Mars will take around three years and the weight loss could be detrimental to astronauts' physical health and mental wellbeing. Although there could be many reasons for underconsumption, one hypothesis is that the conditions onboard the spacecraft alter the perceived flavour of food [3] and Earth-based studies have established that flavour quality is linked to palatability of food, as well as food intake [4, 5].

Within the ISS, air and water are extensively recycled to make the ISS more self-sufficient. Close monitoring of recycled air and water quality is carried out to ensure these supplies are safe for the astronauts [6, 7]. However, the recycled air and water contain contaminants, some of which could affect the flavour perception of food in space and decrease food intake. For example, NASA has identified certain contaminants that reduce water consumption (RWC) due to poor taste at very high levels, but that are acceptable at the levels reported by the regular analyses [8]. Further, ISS air contains a range of volatile compounds and a ten-fold higher carbon dioxide concentration compared to the levels found on Earth. Detailed analyses of ISS air and water samples from different missions are available from the NASA archives [9-12], where the concentrations of a wide range of contaminants (several hundred) are reported. The data published by NASA has focused primarily on safety but it is well-documented that some contaminants in potable water are detectable by smell and taste, well below the safety levels set for health reasons (see Table 9 in [13]). Despite the detailed chemical analyses of ISS air and water, our search of the space literature found no systematic studies on the potential taste activity, or odour activity, of these contaminants.

Current methods to relate the perceived intensity of taste and aroma compounds with their concentrations are limited to Stevens Law and the Dose-over-Threshold (DoT) concept (concentration of a compound divided by its odour threshold). Stevens law states that perceived intensity is related to concentration through a power law function, with different flavour compounds having different exponents; unfortunately, there are limited data available on the values of these exponents. In contrast, threshold data on a range of taste and odour compounds are available, through experimental [13, 14] or calculated values [15]. Therefore, the DoT concept is really the only way to assess the potential flavour intensity of the compounds listed in the NASA analyses. Experimental values of odour threshold (OT) range over several orders of magnitude, apparently due to variation in odour

presentation to panellists, as well as the difference between human assessors [16], so a mean or median value is usually taken when calculating the DoT value, where values >1 indicate detectable odour or taste intensity while values <1 indicate a lack of detectable odour/taste.

A limitation of the DoT concept is that it considers each flavour compound individually, whereas there is a considerable amount of data that inter- and intra-actions between taste and odour compounds can deliver detectable odour when one or more of the compounds is below its individual taste/odour threshold. Studies in the 1960s measured the odour intensity of sub-threshold mixtures using sensory analysis and showed that there were some “additive” effects. More recently, the published data has been reviewed [17, 18] and it is clear that sub-threshold interactions do occur, not just in fundamental studies using model mixtures, but also in real food and beverage products.

Therefore, assessing the potential odour/taste activity within the ISS air and water supplies is severely limited due to the following factors:

1. The DoT concept relies on the availability and accuracy of odour and taste threshold data.
2. The threshold data in compilations and individual publications cover a few hundred compounds only and time-intensive sensory analysis is the primary method to obtain threshold values.
3. Data are recorded as the detection and/or recognition threshold concentrations.
4. Published odour threshold values vary significantly due to differences in methodology as well as human variation and it is difficult to decide which value to use.
5. The DoT concept treats each flavour compound as a discrete entity and ignores the well-documented interactions between flavour compounds.
6. There is strong evidence of interactions between odour compounds that change perception.

Experimental

Data sources

Literature searches covered the mainstream food and flavour journals as well as journals associated with space travel (for example, *Aviation Space and Environmental Medicine*, *New Space*, *Advances in Space Research*) and publications from the American Institute of Aeronautics and Astronautics. In the absence of science-based information on astronauts’ perception of space food, anecdotal information was obtained by a web search. The NASA archives contain reports, presentations and policy documents, which can be found at <https://ntrs.nasa.gov/>. There are also datasets that can be downloaded from <https://nasa.github.io/data-nasa-gov-frontpage/>. Data from the European Space Agency can be found at [https://www.esa.int/About_Us/ESA_Publications/\(archive\)](https://www.esa.int/About_Us/ESA_Publications/(archive)).

Results and discussion

The RWC compounds identified by NASA as potentially flavour-active in the ISS water supply are shown in Table 1, along with their concentrations in samples of potable ISS water. Values vary across the different samples taken, so high and low levels are quoted in Table 1.

Table 1. Estimation of the sensory effect of RWC compounds in ISS potable water supplies

Compound	Lowest level ^a	Highest level ^a	OT in water ^b	DoT level/OT	DoT level/OT
	µg/L (ppb)	µg/L (ppb)	µg/L (ppb)	Low	High
Methylethylketone	5	20	8400	0.0006	0.024
Dichloromethane	5	20	9100	0.0005	0.0022
Chloroform	5	20	2400	0.0021	0.0083
Ammonia	2	34	1500	0.0013	0.022
Acetone	3	34	20000	0.0002	0.00017
Methylamine	125	125	2400	0.052	0.052
Trimethylamine	125	125	0.20	625	625
2-Mercaptobenzothiazole	40	320	1760 ^c	0.0227	0.182
Phenol	4	20	790	0.0005	0.0025

- a) Data taken from Appendix 4 in Straub *et al.* [9]. The data in the reference are quoted in increments e.g., <5 or <20 µg/L but, to calculate DoT values they have been quoted in the Table as discrete values.
- b) Odour threshold values [19] were determined in drinking water as the concentration in water that would elicit a detectable odour in the headspace.
- c) The odour threshold (water) of 2-mercaptobenzothiazole is taken from Nielsen [20].

Table 1 uses OT data from a single source [19] (with the exception of 2-mercaptobenzothiazole, taken from [20]) to calculate the DoT values, in an attempt to produce DoT values that could be compared with each other. On this basis, only trimethylamine shows a DoT >1, however, the OT value for trimethylamine in Table 1 (0.2 µg/L; [19]) is much lower than the values quoted elsewhere (500 and 1700 µg/L; [14]), so it is debatable whether trimethylamine is perceivable at the concentrations present in ISS water. Given the use of chlorine to disinfect drinking water, there are limited data on the flavour thresholds values of some organochlorine compounds [13]. Using the Amoore & Hautala OT data, neither of the organochlorine compounds in Table 1 will be perceivable at their concentrations present in ISS water, and even using the lowest reported OTs, only dichloromethane has a DoT >1 if the OT is taken as 4.5 µg/L. A study of other compounds in ISS water depends on the availability of odour threshold data, requiring searches on individual compounds to establish the OT ranges. Our experience is that a web search can identify OT values in various scientific and commercial web sources although the units used vary. It is not always apparent whether the values are quoted as the OT in air or the OT above aqueous solutions and further searching and calculation is required to validate the values.

The examples given above illustrate the difficulty when applying DoT values to evaluate whether a contaminant could change the flavour of ISS water. A similar situation is found when examining the contaminants in air. Air circulation within the ISS lacks the convection element found on Earth (cold air cannot sink to the ground in microgravity!), so fans are used to circulate air and it is acknowledged that this is partially successful, but does lead to higher localised concentrations of contaminants in certain areas of the ISS. The stand out difference is that CO₂ levels in ISS air are around 0.4%, 10-fold greater than on Earth. In humans, gaseous CO₂ is not detected at concentrations up to 30% [21], but the presence of CO₂ in carbonated beverages suggests its detection is through the conversion of CO₂ into carbonic acid by the enzyme carbonic anhydrase (Figure 1).

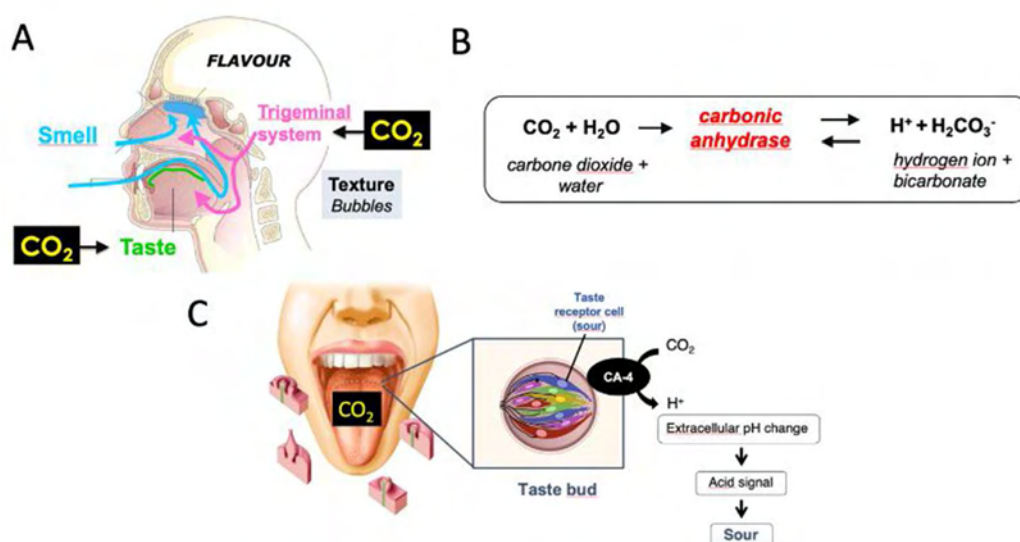


Figure 1: Schematic representation of carbonation perception. (A) CO₂ is odourless to human but activates the taste and trigeminal systems. (B) The reaction catalysed by carbonic anhydrase (CA). (C) CA operates in CO₂ sensing and provokes a taste response to acidity. Reproduced from [3].

Carbonic acid has been reported to activate not only the TRPA1 but also the sour taste receptors. Most published work on the effects of CO₂ on flavour perception comes from studies on carbonated beverages where decreases in sweetness and increases in bitter after-taste have been noted [3]. Recirculated ISS air also contains numerous other volatile organic compounds (Figure 2) that are derived from two main sources: the metabolic products from the astronauts and “off-gassing” of volatile compounds from the construction materials used within the ISS [22]. Depending on the level of physical activity by the astronauts, and the nature of the payloads that are uploaded to carry out different types of scientific experiments, the concentrations of airborne contaminants can vary from day to day, although CO₂ levels are kept fairly constant by the recycling plant because elevated levels are known to adversely affect astronauts [23].

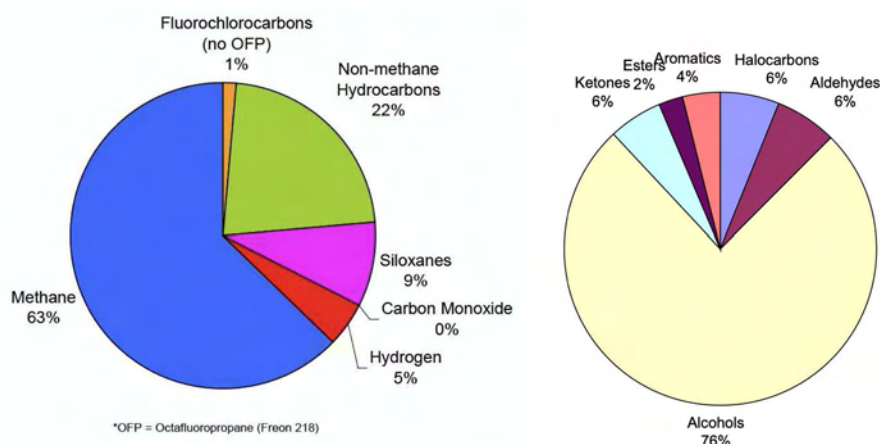


Figure 2: Composition of volatile compounds in ISS air (volume basis). Left hand pie chart shows composition excluding nitrogen and oxygen, right hand chart shows breakdown of non-methane hydrocarbons [22].

In Figure 2, siloxanes are a class of compounds released through off-gassing, while methane, ketones, alcohols and aldehydes are produced by human (or microbial) metabolism [22]. DoT analysis of the volatile compounds listed by NASA suggests that only the C2 to C7 aldehydes and n-butanol are potentially odour active [3], while methane is described in the literature as odourless. Although the data on chemical analysis of ISS water and air is detailed and robust, systematic information on astronauts' perception of the odour inside the ISS or the taste of food in space was not found in our literature search. The anecdotal information from astronauts during debriefing or during public interviews is also scarce and variable (see [3] for more information). Carrying out conventional sensory tests in orbit is currently restricted, due to the small numbers of participants available, as well as the difficulty in delivering odours or tastes under microgravity conditions.

Conclusion

Our attempts to use the DoT concept to identify compounds that might cause changes in flavour quality during spaceflight have led to inconclusive results and there are many reasons for this. Obviously, the factors described in the Introduction play a role (variation in odour threshold values, potential odour interactions) and this is not helped by the lack of sensory data from space-based experiments. To make further progress, it is possible to design Earth-based experiments to reproduce some of the conditions on the ISS and test whether they affect flavour perception of food samples. For example, the effect of higher CO₂ levels on flavour perception of a test food could be assessed by a sensory panel, while exposed to atmospheres containing 0.04 and 0.4% CO₂, providing a suitable ventilation system could be designed and the safety of the panellists could be ensured. Designing Earth-based experiments to determine whether the levels of odour-active contaminants found on the ISS could affect the perceived flavour of food are possible, but could not easily reproduce the effects of microgravity nor the composition of the ISS atmosphere. For contaminants found in the ISS potable water supply, it is technically feasible to add selected contaminants to food and drink samples and test whether their addition causes a significant sensory change. The potential sticking point is the sheer number of compounds found in the ISS air and water supplies, as well as the need to obtain permission from the safety and ethical perspectives. The situation may be made easier by the extensive testing that has been carried out to assess the safe levels of contaminants for astronauts over extended exposure periods. Space-based experiments are possible but there are restrictions on the weight, size and time needed to set up and execute experiments. Sensory experiments would have to be longitudinal-type studies since the number of participants during any one mission is limited to two to three astronauts. Studies would involve choosing odour or taste stimuli that could be measured in individual astronauts before, during and after the spaceflight, and repeated over several missions to get sufficient data that could be statistically analysed. The stimulus would have to be light, easy to use and reproducible, so the options are really limited to using something like odour pens as the stimuli. In turn, these experimental design choices restrict the results that could be obtained and only simple measures could be studied, such as determining odour intensity or odour threshold of single compounds. Both outputs are far away from the ultimate goal of determining whether a contaminant can alter the flavour of a space food to such an extent that it is under-consumed.

The other conclusion of this work is to question whether the DoT concept is a useful and valid tool to identify odour-active compounds. The wide variability of odour thresholds reported in the literature means that compounds may, or may not be odour active, depending on which OT value is to be believed. Genetic variability in the human taste and odour receptors is well known [24], and accounts for some of the variation, while anatomical and physiological differences can affect the degree to which flavour stimuli are transferred to the receptors [25].

Therefore, it could be argued that any sensory panel will produce a different set of threshold values due to genetic and physiological differences. It is difficult to see how an “average” panel could be convened to provide a set of benchmark threshold values. Could molecular biology help by assembling odour and taste receptors that are representative of the general population and determining threshold values using EC₅₀ data? This is possible, but it still does not address the strong evidence that some flavour compounds can affect flavour perception below their odour thresholds. The evidence for odour-odour interactions is compelling [17]. Psychophysical data from the 1960s, showed that subthreshold levels of one odorant could change the perception of another odorant (see, for example, [26]) and more recent work has found similar interactions in a vodka-based beverage [27]. Besides the psychophysical effects, interactions may occur at other stages in the flavour perception process. For example, competition for enzymes at the peri-receptor level can change the odour profile reaching the odour receptors and therefore change perception [28]; some compounds appear to modulate the signal from the receptors [29], while others act as antagonists at the odour receptors [30]. There are also taste-odour interactions at subthreshold levels that alter the sensory properties [31] or the neural coding patterns [32]. Given the complexity of the data, Artificial Intelligence (AI) is a potential tool to analyse the data available. AI studies have focused on the link between odour structure and odour quality through the DREAM project [33] and similar work on bitterness has also been reported [34, 35]. These reports do not consider the intensity of the odour or bitter compound, nor do they calculate thresholds. A method to calculate odour thresholds based on physicochemical properties was proposed in 2002 [36] and a recent publication described the use of machine learning to predict odour-odour interactions [37]. AI is a powerful tool but, for a successful outcome, high-quality data is still needed and it is unclear how and where this data will come from. Identifying the problems in using DoT values is simple, but finding a solution to provide flavour researchers with a more sophisticated tool to understand how interactions affect flavour perception is a massive task and will require a truly multidisciplinary effort to obtain quality data from sensory, genetic and physicochemical sources, then combine the datasets to investigate the overall effect of odour-odour, taste-taste and taste-odour interactions. Until progress is made in these areas, it is difficult to test the hypothesis that contaminants in the recycled air and water of spacecraft can alter the flavour of food and decrease food intake during spaceflight. Spiking some food samples with known levels of contaminants is theoretically possible but raises ethical and safety issues, and deciding which of the several hundred contaminants to use makes experimentation more trial and error than sharply focused.

Acknowledgements

The European Space Agency funded two meetings of the team through a Topical Team award (Contract # 4000125158). Victor Demaria Pesce (INSERM, ESA) and Ines Antunes (ESA) are thanked for their support of the project. We appreciate constructive discussions on this topic with further members of the Topical Team, namely Thomas Hummel, Christian Margot, Paola Pittia, Charles Spence and Serge Pieters. We are grateful to Neil DaCosta (IFF) for organising the 2019 ACS Orlando meeting on “Food for Space Travel & Extreme Environments” and connecting researchers from different backgrounds.

References

1. Heer M, Boerger A, Kamps K, Mika C, Korr C, Drummer C. Nutrient supply during recent European missions. *Pflügers Archiv-European Journal of Physiology*. 2000;441(2-3):R8-R14.
2. Smith SM, Zwart SR, Heer M. Evidence report: Risk factor of inadequate nutrition. 2015. Report No.: JSC-CN-32587 Contract No.: 20150000512
3. Taylor AJ, Beauchamp JD, Briand L, Heer M, Hummel T, Margot C, et al. Factors affecting flavor perception in space: Does the spacecraft environment influence food intake by astronauts? *Critical Reviews in Food Science and Food Safety*. 2020;19:3439-75.
4. Yeomans MR. Taste, palatability and the control of appetite. *Proc Nutr Soc*. 1998;57(4):609-15.
5. Yin W, Hewson L, Linforth R, Taylor M, Fisk ID. Effects of aroma and taste, independently or in combination, on appetite sensation and subsequent food intake. *Appetite*. 2017;114:265-74.
6. National Academies of Sciences Engineering And Medicine. Refinements to the methods for developing spacecraft exposure guidelines. Washington, DC: The National Academies Press.; 2016.
7. National Research Council. Spacecraft maximum allowable concentrations for selected airborne contaminants: Volume 5. Washington, DC: The National Academies Press; 2008. 406 p.
8. Ryder VA, McCoy T, Hayes JC, Koerner CA. Spacecraft water exposure guidelines (SWEGs). Lyndon B. Johnson Space Center, Houston, Texas, USA: NASA; 2017. Report No.: JSC 63414.
9. Straub II J, Plumlee DK, Schultz JR, editors. ISS expeditions 16 thru 20: Chemical analysis results for potable water. 40th International Conference on Environmental Systems; 2012 16 November 2012 American Institute of Aeronautics and Astronautics.
10. Straub II J, Plumlee DK, Schultz JR, McCoy JT, editors. Chemical analysis results for potable water from ISS expeditions 21 through 25. 41st International Conference on Environmental Systems; 2011 17 - 21 July 2011; Portland, Oregon.

11. Straub II J, Plumlee DK, Schultz JR, McCoy JT, editors. International space station potable water quality for expeditions 26 through 29. 42nd International Conference on Environmental Systems; 2012 16 November 2012 San Diego, California: American Institute of Aeronautics and Astronautics.
12. Straub II J, Plumlee DK, Schultz JR, McCoy JT, editors. Potable water quality for International Space Station expeditions 30-33. 43rd International Conference on Environmental Systems; 2013 14-18 July 2013 Vail, Colorado: American Institute of Aeronautics and Astronautics.
13. Young WF, Horth H, Crane R, Ogden IT, Arnott M. Taste and odour threshold concentrations of potential potable water contaminants. *Water Research*. 1996;30(2):331-40.
14. Van Gemert LJ, Nettenbreijer AH. Compilation of odor threshold values in air and water. Voorburg, The Netherlands: National Institute for Water Supply; 1977.
15. Abraham MH, Sánchez-Moreno R, Cometto-Muñiz JE, Cain WS. An algorithm for 353 odor detection thresholds in humans. *Chem Senses*. 2011; 37(3):207-18.
16. Schmidt R, Cain WS. Making scents: Dynamic olfactometry for threshold measurement. *Chem Senses*. 2010;35(2):109-20.
17. Ferreira V. Revisiting psychophysical work on the quantitative and qualitative odour properties of simple odour mixtures: A flavour chemistry view. Part 1: Intensity and detectability. A review. *Flav Frag J*. 2012;27(2):124-40.
18. Ferreira V. Revisiting psychophysical work on the quantitative and qualitative odour properties of simple odour mixtures: A flavour chemistry view. Part 2: Qualitative aspects. A review. *Flav Frag J*. 2012;27(3):201-15.
19. Amore JE, Hautala E. Odor as an aid to chemical safety: Odor thresholds compared with threshold limit values and volatilities for 214 industrial chemicals in air and water dilution. *Journal of Applied Toxicology*. 1983;3(6):272-90.
20. Nielsen E. 2-mercapto-benzothiazole (MBT). ISBN 978-87-93026-84-1. 2014.
21. Shusterman D. Review of the upper airway, including olfaction, as mediator of symptoms. *Environmental Health Perspectives*. 2002;110:649-53.
22. Macatangay A, Bruce R. Impacts of microbial growth on the air quality of the International Space Station. 40th international conference on environmental systems. International conference on environmental systems (ICES): American Institute of Aeronautics and Astronautics; 2010.
23. Law J, Van Baalen M, Foy M, Mason SS, Mendez C, Wear ML, et al. Relationship between carbon dioxide levels and reported headaches on the International Space Station. *Journal of Occupational and Environmental Medicine*. 2014;56(5):477-83.
24. Trimmer C, Keller A, Murphy NR, Snyder LL, Willer JR, Nagai MH, et al. Genetic variation across the human olfactory receptor repertoire alters odor perception. *Proceedings of the National Academy of Sciences*. 2019;116(19):9475.
25. Salles C, Chagnon M-C, Feron G, Guichard E, Laboure H, Morzel M, et al. In-mouth mechanisms leading to flavor release and perception. *Crit Rev Food Sci Nutr*. 2011;51(1):67-90.
26. Guadagni DG, Burr HK, Buttery RG, Okano S. Additive effect of sub-threshold concentrations of some organic compounds associated with food aromas. *Nature*. 1963;200(491):1288-&.
27. Niu Y, Wang P, Xiao Q, Xiao Z, Mao H, Zhang J. Characterization of odor-active volatiles and odor contribution based on binary interaction effects in mango and vodka cocktail. *Molecules*. 2020;25(5):1083.
28. Hanser H-I, Faure P, Robert-Hazotte A, Artur Y, Duchamp-Viret P, Coureaud G, et al. Odorant-odorant metabolic interaction, a novel actor in olfactory perception and behavioral responsiveness *Scientific Reports*. 2017;7:10219.
29. Xu L, Li W, Voleti V, Zou D-J, Hillman EMC, Firestein S. Widespread receptor-driven modulation in peripheral olfactory coding. *Science*. 2020;368(6487):eaaz5390.
30. Zak JD, Reddy G, Vergassola M, Murthy VN. Antagonistic odor interactions in olfactory sensory neurons are widespread in freely breathing mice. *Nature Communications*. 2020;11(1):3350.
31. Dalton P, Doolittle N, Nagata H, Breslin PaS. The merging of the senses: Integration of subthreshold taste and smell. *Nat Neurosci*. 2000;3(5):431-2.
32. De March CA, Titlow WB, Sengoku T, Breheny P, Matsunami H, McClintock TS. Modulation of the combinatorial code of odorant receptor response patterns in odorant mixtures. *Molecular and Cellular Neuroscience*. 2020;104.
33. Keller A, Gerkin RC, Guan Y, Dhurandhar A, Turu G, Szalai B, et al. Predicting human olfactory perception from chemical features of odor molecules. *Science*. 2017;355:820-6.
34. Dagan-Wiener A, Nissim I, Abu NB, Borgonovo G, Bassoli A, Niv MY. Bitter or not? Bitterpredict, a tool for predicting taste from chemical structure. *Scientific Reports*. 2017;7.
35. Margulis E, Dagan-Wiener A, Ives RS, Jaffari S, Siems K, M.Y N. Intense bitterness of molecules: Machine learning for expediting drug discovery. *Computational and Structural Biotechnology*. 2021;19:568-76.
36. Abraham MH, Gola JMR, Cometto-Muniz JE, Cain WS. A model for odour thresholds. *Chem Senses*. 2002;27(2):95-104.
37. Yan L, Wu C, Liu J. Visual analysis of odor interaction based on support vector regression method. *Sensors*. 2020;20:1707.

Receptomics: Tongue-on-a-chip with novel opportunities for food screening

MARGRIET ROELSE, Maurice G.L. Henquet, and Maarten A. Jongsma

BU Bioscience, Wageningen University and Research, The Netherlands
Margriet.roelse@wur.nl

Abstract

Within the food and flavour industry it is considered a “holy grail” to measure the sensory aspects of taste and aroma quantitatively and independent from a taste panel. A microfluidic tongue- or nose-on-a-chip platform could be a system to emulate sensory perception into an instrument by monitoring the activation of specific taste and olfactory receptors in response to food samples. The complexity of food matrices, however, presents a large hurdle for the development and practical application of such systems. The issues are related to the frequent occurrence of (i) sample fluorescence, and (ii) non-specific host cell responses. In this paper we outline how we tackled these two issues with some practical examples; the sample fluorescence of coffee and the host cell response to bitter gourd and tomato juice. With the microfluidic receptor array developed in our lab, we were able to extract specific signals despite the sample fluorescence and host cell response effects. Reliable results could be obtained from these samples based on internal calibrations on-chip and sample controls. The fluidic measurement setup allows repeated exposures of the entire cell array to contrasting samples. With this strategy we could extract receptor-specific response trends to samples independent from generic host cell responses and sample fluorescence artefacts.

Keywords: taste receptors, biosensor, microfluidics, receptomics

Introduction

The term receptomics was first coined in 2004 to describe the systematic study of the receptorome, i.e. the collection of receptors and ligand-gated ion channels that control many physiological processes by serving as sensors for the cells and tissues that make up a specific organism [1, 2]. The class of G protein-coupled receptors (GPCRs) alone makes up an estimated 8% of the total human genome and represents an important target for food and drug research. The function(s) and ligand-specificity of many GPCRs of the human receptorome are still unknown [3, 4]. Additionally, the large number of single nucleotide polymorphisms (SNPs) and splicing variants of the receptor or ion-channel genes further increases their diversity for potential ligands, as well as the potential to couple to different G protein complexes [5-7]. As a consequence, the number of potential receptor conformations is remarkably high, and, therefore, a receptomics approach may promote the systematic screening of large compound libraries or complex natural food or health samples.

Receptomics requires an effective and efficient screening approach, but the conventional well-based, single use assays are notoriously costly especially for screening hundreds of receptors in parallel. Miniaturization and fluidics (sequential assays) potentially offer large advantages there. We used reverse transfection as method to make a live cell array on a carrier surface by simply printing a receptor DNA pattern on a slide and overlaying it with a cell line [8]. The expression of GPCRs in a cell array format was previously done by printing DNA arrays inside multi-well plates [9] or in fabricated micro reaction wells [10]. Combination with microfluidics, however, is considered the most promising road towards reducing the cost and increasing the throughput of screening receptor libraries [11].

The most fundamental difference between receptomics assays and end-point assays is the implementation of a microfluidic system and sequential exposures of the receptor cell array. While in an end-point assay the reagent and test mixture remain in the assay well, the receptomics cell array is exposed to the samples for a controlled period of time by the microfluidic system which sends a continuous flow of assay buffer across the cell array intermitted with injections of specific sample volumes from a sample loop [12, 13].

The microfluidic receptor cell array assay which was set up in our lab [14, 15] involves, in short, the expression of (taste) receptors in HEK293 cells co-expressing the Gα₁₆GUSTDUCIN44 chimera to target the signalling pathway towards intracellular calcium responses. Co-expression of the FRET-based calcium probe, Twitch2B [16], allows the live monitoring of changes in intracellular calcium levels resulting from specific receptor activations.

Taste receptors are located in specialized taste cells of the tongue and their specific activation in response to ingested food is interpreted by the brain. Bitter taste is recognized by the TAS2R receptor family for which 25 GPCRs have been identified in humans [17]. The ability to taste bitter substances is considered as an evolutionarily-developed mechanism that allows mammals to recognize toxins in plants. Since toxins are structurally very diverse, a wide range of bitter receptors have evolved to cover different classes of compounds. These bitter taste receptors have evolved into either broadly-tuned ones or more-specialized ones. Three TAS2R

members (TAS2R10, -R14 and -R46) have a broad spectrum of agonists while TAS2R members R3, R5, R8, R13, R49, R50 and R9 are activated by only a few agonists known so far. While most bitter receptors have been orphanised, meaning that at least one agonist has been found, there are still a few orphan bitter receptors with unknown ligands, in particular TAS2R19, -R42, -R45, and -R60.

In this article we explore the potential of receptomics technology for analysing the bitter taste of coffee and bitter gourd and we explore the ability to identify bitter compound spikes in tomato juice. In whole food sample analysis we encounter two main bottlenecks: the effect of sample fluorescence in fluorescence measurements and the induction of a non-specific host cell calcium response after exposure to the food samples. In this article we show these effects, ways to compensate them, and we propose solutions to overcome the challenges to enable complex food receptomics studies.

Experimental

The cell culture conditions, receptomics setup, experimental condition, data analysis and statistical calculations were performed as previously described [14, 15, 18].

The coffee sample was prepared fresh on the day of measurement (45 grams of fine grounded coffee with 1L tap water), cooled to room temperature and diluted in assay buffer (NaCl 130 mM, KCl 5 mM, Glucose 10 mM, CaCl₂ 2 mM, HEPES 10 mM at pH 7.4). The bitter gourd fruit and tomato fruits were flash frozen in liquid nitrogen and grinded. The powder was defrosted and centrifuged to separate the insoluble fraction from the water fraction. The water fraction or juice was diluted in assay buffer. The tomato juice was spiked with Chloramphenicol 300 μM, D-Salicin 2 mM, Picrotoxinin 300 μM, Denatonium Benzoate 300 μM, Aristolochic acid 30 nM and PROP 10 μM.

Results and discussion

Sample fluorescence of food samples

When samples are fluorescent to the extent that it interferes with a fluorescence-based receptor cell assay one solution is to dilute the sample until the sample fluorescence is low enough, although this will also dilute the sample's bioactivity. We tested this approach using coffee as a pilot experiment. Coffee contains alkaloids which contribute to a high level of fluorescence [19], that is detected by the CFP and YFP emission filters (Em 480/40 and 535/30 respectively) of the FRET based calcium sensor Twitch2B. We used 8x diluted coffee in assay buffer as optimum to balance the high levels of sample fluorescence while maintaining detectable bitterness in the sample.

An array of bitter taste receptors was exposed to a series of injections of 8x diluted Arabica and Robusta (light roast, AL and RL respectively) coffee. A set of 23 bitter taste receptors was assayed including 2 polymorphisms for R4 and R46 together with a mock control. To monitor any effects on the fluorescence caused by the sample we included a fluorescence control (YC-). This is a modified version of the calcium sensor where a deletion in the calmodulin and M13 domain makes the protein inactive for sensing calcium. This allows the monitoring of any sample effects on the baseline fluorescence. Samples that display fluorescence at CFP excitation wavelengths usually give increasing signals in both the CFP and YFP emission channels.

To separate sample fluorescence from the ratiometric FRET signal, our current solution is a computational method to separate background from actual signal. Using the ratiometric properties of the probe it is possible to separate the sample fluorescence –a signal that increases in both CFP and YFP channels- from a signal that originates from the ratiometric calcium probe - a FRET signal that decreases in the CFP channel and increases in the YFP channel. This method is still under development, but could efficiently eliminate sample fluorescence from a fluorescein control and from 8x diluted coffee. Figure 1 shows the raw FRET ratio signals and sample fluorescence or background (BG) corrected signals of a measurement series for 11 sample injections. The charts show signal curves for the controls Mock and YC- and one of the 23 bitter taste receptors; TAS2R16. The injection series is measured with an injection interval of 5 minutes and an exposure time to the samples of 30 seconds. The fluorescein injection serves as a control injection for auto-fluorescence background. At a concentration of 1 μM the fluorescein dye results in a fluorescence signal in both emission channels, but it does not elicit a cellular calcium response. The ATP injection is a control which triggers a host cell calcium response [20] and the D-salicin injection is a control bitter compound for TAS2R16 ensuring a response from transiently expressed bitter receptor on the cell array.

After the computational separation of signal and background the resulting signal remains for ATP and the D-salicin sample for TAS2R16. The YC- control line is clean of the sample fluorescent background signal. The coffee sample still shows fluctuations in intracellular calcium which indicates that even at 8x dilution the coffee still triggers a non-specific host cell calcium response in the HEK293 cells.

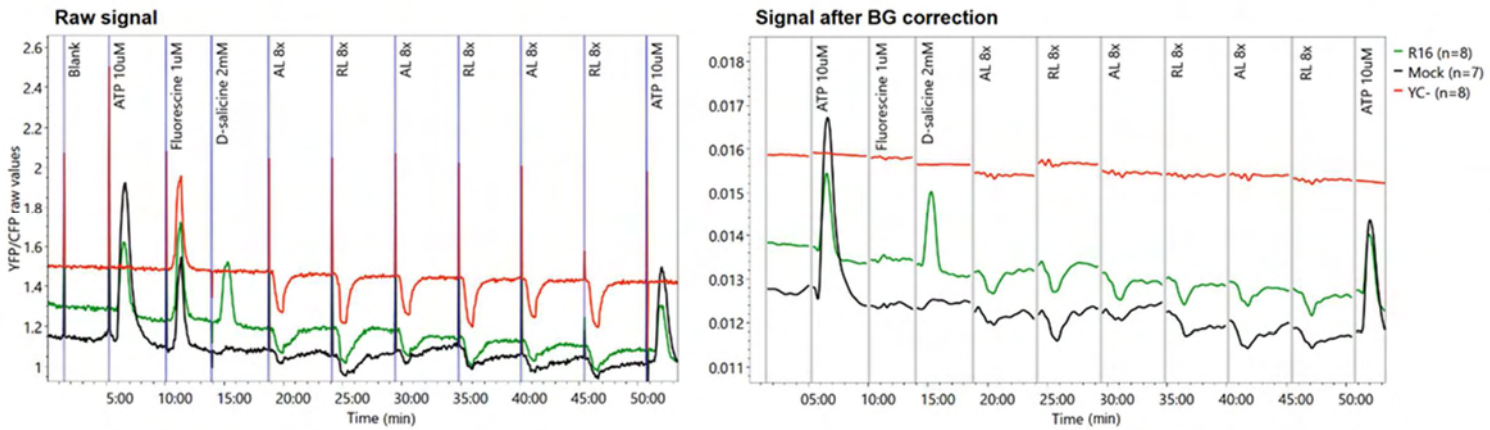


Figure 1: Raw YFP/CFP ratio curves (left) and background (BG, right) corrected curves for an injection series of coffee samples Arabica and Robusta light roast (AL and RL) 8x diluted in assay buffer. Curves are showing for controls Mock and YC- and TAS2R16 bitter taste receptor. In brackets are the number of spots on the cell array.

To detect specific signals for any of the bitter receptors we analysed the signals of all 23 bitter taste receptors coded on the cell array. The Arabica and Robusta light roasted (AL and RL) samples were injected sequentially in alternating order and in three replications. With several alternating and repeated injections, a spot-based response trend can be determined showing inter-sample differences based on a linear mixed model [18]. This spot-based data analysis considers each spot as a separate measurement. Because each spot is serially exposed, this allows us to draw conclusions about differences between samples and eliminate the variability between spots. In this way we can separate the considerable biological variability between spots of the same type from the relevant information, that is, the variation in responses between the two samples. This statistical analysis is shown in Figure 2. Bitter taste receptor TAS2R8 is the only receptor displaying a clear specific response to the Robusta coffee sample relative to the blank injection. However, focusing statistically on inter sample differences, comparing AL to RL, the contrast shows a higher bitter receptor activation in Robusta coffee for TAS2R8, R14 and R50.

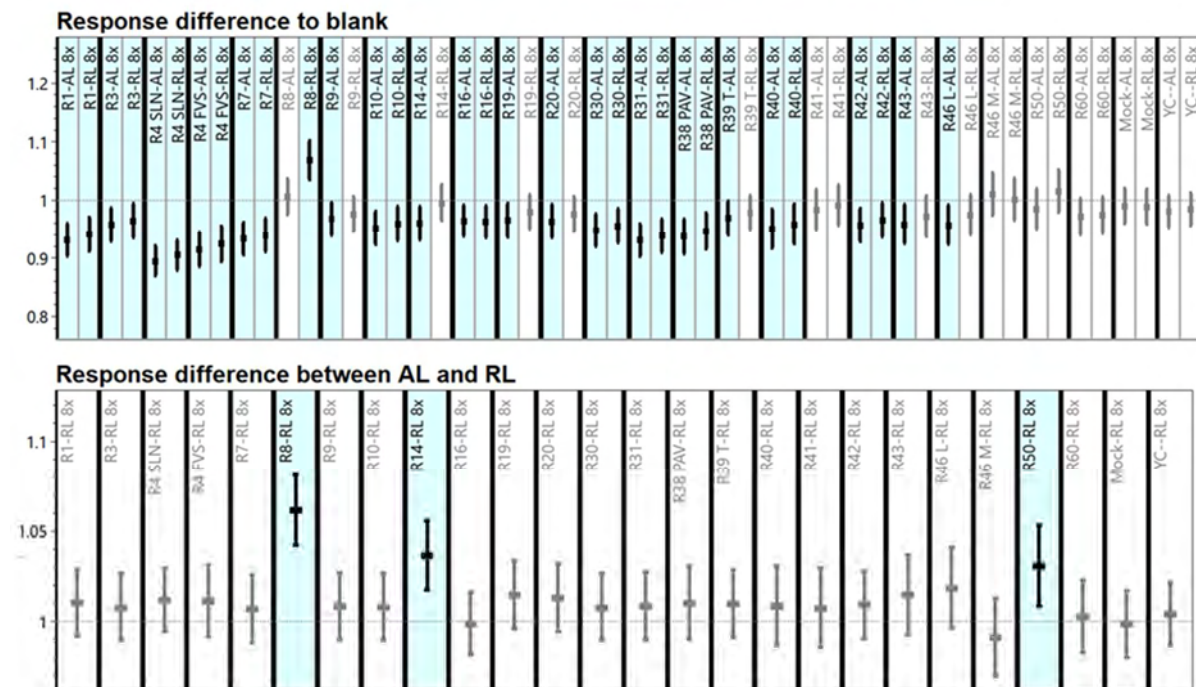


Figure 2: Statistical comparison of Arabica and Robusta light roast (AL and RL) 8x diluted in assay buffer to the blank (top) and an inter-sample difference (bottom). In both analysis the responses are normalized to the Mock.

In conclusion, although the signals in the analysis of 8x diluted coffee were low, some sample differences based on bitter receptor activations were detectable. However, overall, the bitter response fingerprint may not be complete due to the dilution. The fluorescence-based detection method, even with smartly designed computational methods, may not be very suitable for the measurement of undiluted samples like coffee because the dynamic range for measuring receptor activation becomes comparatively smaller resulting in noisier signals. A way to counter the problem of sample fluorescence may be to switch to the use of bioluminescent probes and detection systems that do not depend on external excitation light. Suitable sensors would be the bioluminescence calcium sensor $\text{GeNL}(\text{Ca}^{2+})$ 60-520 based on split NanoLuc [21] or the use of a BRET based calcium sensor CalfluxVTN [22].

Host cell responses of complex samples

One advantage of the microfluidic receptomics platform is that it enables sequential injection of samples and determination of differences between samples. But when these samples are complex mixtures, extracts or even food products, there can be non-specific host cell calcium responses triggered in the cell that bear no relation to the specific receptor activations of interest. These endogenous host cell responses may be caused by pH or salt perturbations in the samples, but usually these parameters can be minimized by adjusting the conditions of the assay. However, samples may also contain compounds that activate a host cell receptor or contain toxic compounds, and then the assay will measure a positive or negative host cell response in the mock transfected spots (spots without recombinant receptor). One straightforward solution is to dilute the sample until the host cell response is below threshold. This solution will not be applicable to all types of samples, but if bioactivity is stronger than the host cell response a sample dilution may help to separate specific responses from host cell responses. This was shown earlier for a crude chilli pepper extract that was measured for bioactivity with the TRPV1 ion channel [13]. At a 300-fold dilution of the extracts, there was no generic host cell response to the extract anymore, but there was still a clearly specific TRPV1 ion channel activation.

Similarly, here we show results with bitter gourd juice. This bitter gourd sample was diluted 30-180-fold in assay buffer and exposed to the array of bitter taste receptors, see Figure 3. The sample did not display sample fluorescence, but there was a considerable concentration dependent nonspecific host cell response in the Mock spots. Superimposed on this host cell response, however, the spots coding bitter taste receptors TAS2R16 and TAS2R8 show additional strong calcium activation peaks that become more distinct from the host cell response at the higher dilutions. The TAS2R14 shown in Figure 3 along with the other 21 bitter taste receptors on the array did not show a specific response. Thus by analysing this crude vegetable extract, we can pinpoint specific bioactivity to TAS2R16 and TAS2R8. Follow-up studies may be conducted to identify the metabolites responsible for this strong bitter taste.

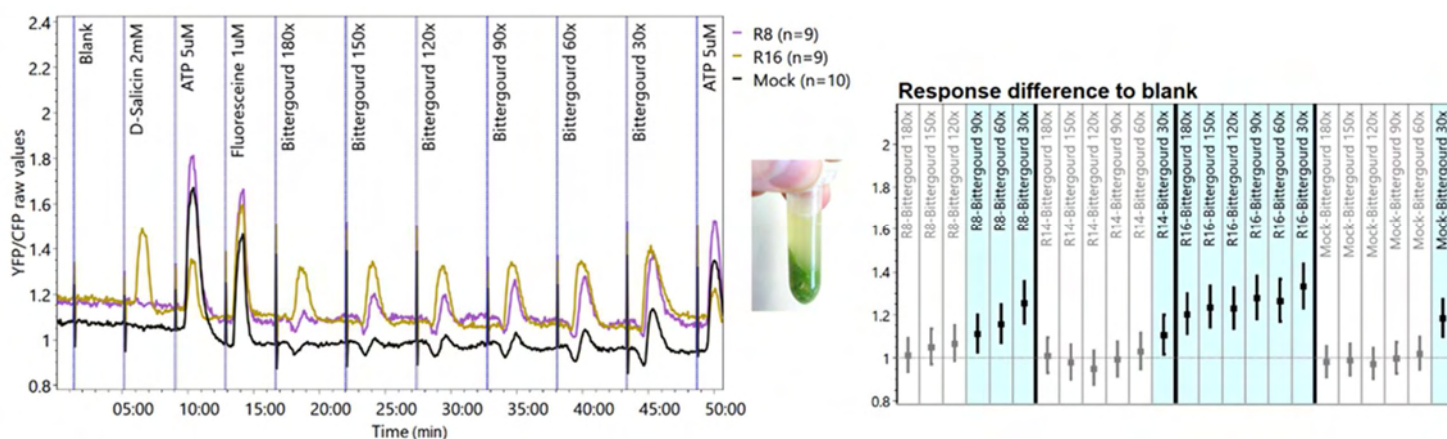


Figure 3: Raw YFP/CFP ratio curves (left) and statistical comparison (right) of bitter gourd fruit juice diluted in assay buffer. Showing responses for TAS2R8, TAS2R16 and Mock and including TAS2R14 as reference in the statistical analysis.

Unfortunately, it is not always possible to sufficiently dilute a sample to keep the host cell response within acceptable limits, without losing the bioactivity as well. However, we found that with the aid of a simulated host cell response –a host cell response to ATP- the response can be normalized in a spot-dependent manner using the ATP injections as a reference in a two sample contrast [18]. Bitter receptor spikes were retrieved from the sample comparison even though the host cell response was considerable and variable between spot types. This approach was demonstrated using tomato juice samples spiked with bitter compounds as shown in Figure 4 (ECRO 2018

conference poster [23]). This result showed that a receptor-specific calcium response may be cumulative to a host cell response. In a direct contrast of 5-fold diluted tomato juice with and without bitter compound spikes and using the ATP response to normalize the responses, 6 out of 8 bitter spikes were recovered. However, the approach of using an ATP host cell response correction only works when it accurately mimics the host cell response. This can be determined in a response correlation between the ATP responses and sample host cell responses. Other sources of intracellular calcium modulation, like the activation of ion-channels for example, may potentially introduce artefacts.

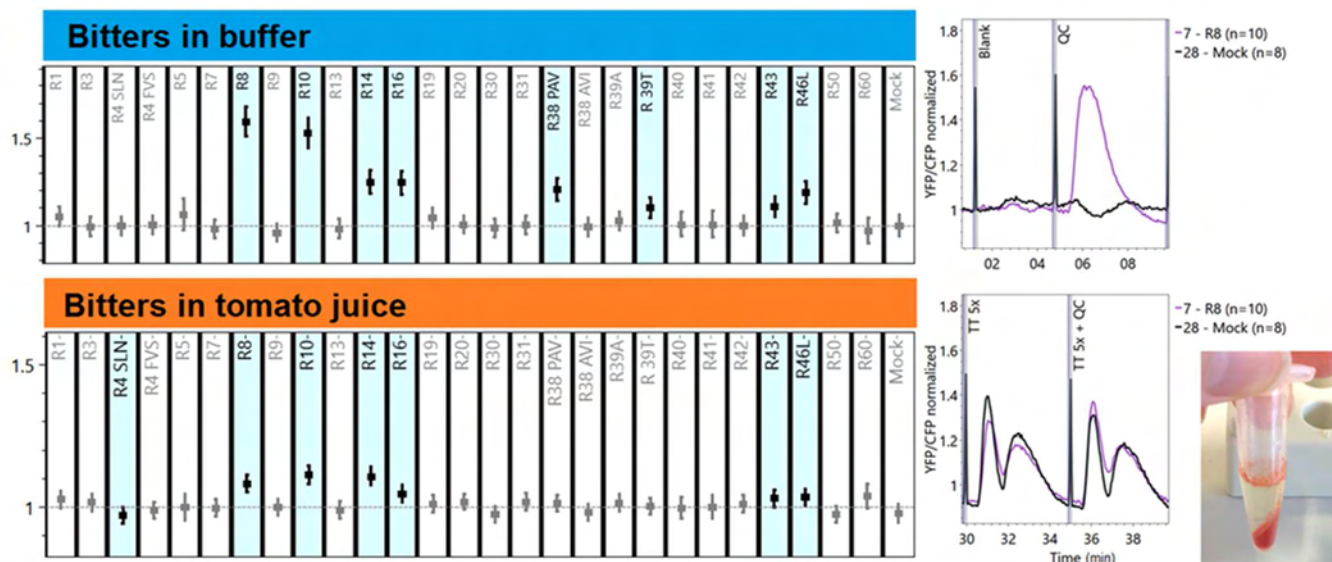


Figure 4: Statistical comparison of bitter compounds in buffer (top) and a comparison of tomato juice diluted 5x in assay buffer with and without bitter compounds (bottom). Bitter compounds Chloramphenicol 300 μ M, Denatonium Benzoate 300 μ M, Picrotoxinin 300 μ M, D-Salicin 2 mM, PROP 10 μ M and Aristolochic acid 30 nM were used which activate TAS2R8, R10, R14, R16, R38PAV and R43 respectively. TAS2R46 is activated by several compounds. The response of TAS2R8 to Chloramphenicol in buffer (QC) and in 5x diluted tomato juice (TT) is displayed in the small graphs on the right.

As long as a calcium read out system is used to detect receptor activation of complex samples, the host cell response remains something that must always be considered. There is a need, therefore, for a different read-out system that is receptor-specific and not based on second messengers like calcium or cAMP. An example is the miniG system introduced by Wan in 2018 [24]. Both the receptor and G protein are fused to parts (Smbit and Lgbit) of a split nanoluciferase. Only when the receptor-Smbit is activated and the Lgbit-miniG protein binds the receptor the luciferase is reconstituted and starts to emit light. This system promises to offer an elegant way of eliminating host cell response interference by literally keeping those responses in the dark. Pilot results show that this system is applicable and detectable in a cell array format as well.

Conclusion

For taste and flavour research the most promising feature of the receptomics platform is the possibility of screening and comparing complex samples (matrices). In product development or crop breeding, subtle sample differences in taste are difficult to measure using taste panels where subjectivity can be an issue. If this receptomics platform could provide an efficient means of pre-screening samples/varieties this could become a valuable tool. Preliminary results have indicated that indeed the receptomics platform is able to measure sample differences in vegetable extracts and beverages despite the complexity of the samples if appropriate dilutions are chosen (sample fluorescence and host cell responses). Bioluminescent assays promise to bridge the step to undiluted samples.

References

1. Roth BL, Lopez E, Beischel S, Westkaemper RB, Evans JM. Screening the receptorome to discover the molecular targets for plant-derived psychoactive compounds: a novel approach for CNS drug discovery. *Pharmacol Ther.* 2004;102(2):99-110.
2. Kroeze WK, Roth BL. Screening the receptorome. *J Psychopharmacol.* 2006;20(4 Suppl):41-6.
3. Bjarnadottir TK, Gloriam DE, Hellstrand SH, Kristiansson H, Fredriksson R, Schiöth HB. Comprehensive repertoire and phylogenetic analysis of the G protein-coupled receptors in human and mouse. *Genomics.* 2006;88(3):263-73.
4. Stockert JA, Devi LA. Advancements in therapeutically targeting orphan GPCRs. *Front Pharmacol.* 2015;6:100.

5. Iida A, Saito S, Sekine A, Kataoka Y, Tabei W, Nakamura Y. Catalog of 300 SNPs in 23 genes encoding G-protein coupled receptors. *J Hum Genet.* 2004;49(4):194-208.
6. Iida A, Nakamura Y. Identification of 156 novel SNPs in 29 genes encoding G-protein coupled receptors. *J Hum Genet.* 2005;50(4):182-91.
7. Hayes JE, Feeney EL, Allen AL. Do polymorphisms in chemosensory genes matter for human ingestive behavior? *Food Qual. Prefer.* 2013;30(2):202-16.
8. Ziauddin J, Sabatini DM. Microarrays of cells expressing defined cDNAs. *Nature.* 2001;411(6833):107-10.
9. Mishina YM, Wilson CJ, Bruett L, Smith JJ, Stoop-Myer C, Jong S, et al. Multiplex GPCR assay in reverse transfection cell microarrays. *J. Biomol. Screen.* 2004;9(3):196-207.
10. Oh EH, Lee SH, Lee SH, Ko HJ, Park TH. Cell-based high-throughput odorant screening system through visualization on a microwell array. *Biosens. Bioelectron.* 2014;53:18-25.
11. Martins SA, Trabuco JR, Monteiro GA, Chu V, Conde JP, Prazeres DM. Towards the miniaturization of GPCR-based live-cell screening assays. *Trends Biotechnol.* 2012;30(11):566-74.
12. Roelse M, de Ruijter NC, Vrouwe EX, Jongsma MA. A generic microfluidic biosensor of G protein-coupled receptor activation-monitoring cytoplasmic $[Ca^{2+}]$ changes in human HEK293 cells. *Biosens. Bioelectron.* 2013;47:436-44.
13. Henquet MG, Roelse M, de Vos RC, Schipper A, Polder G, de Ruijter NC, et al. Metabolomics meets functional assays: coupling LC-MS and microfluidic cell-based receptor-ligand analyses. *Metabolomics.* 2016;12:115.
14. Roelse M, Henquet MGL, Verhoeven HA, de Ruijter NCA, Wehrens R, van Lenthe MS, et al. Calcium Imaging of GPCR Activation Using Arrays of Reverse Transfected HEK293 Cells in a Microfluidic System. *Sensors.* 2018;18(2).
15. Roelse M, Wehrens R, Henquet MGL, Witkamp RF, Hall RD, Jongsma MA. The effect of calcium buffering and calcium sensor type on the sensitivity of an array-based bitter receptor screening assay. *Chem. Senses.* 2019.
16. Thestrup T, Litzlbauer J, Bartholomaeus I, Mues M, Russo L, Dana H, et al. Optimized ratiometric calcium sensors for functional in vivo imaging of neurons and T lymphocytes. *Nat. methods.* 2014;11(2):175-82.
17. Chandrashekar J, Mueller KL, Hoon MA, Adler E, Feng L, Guo W, et al. T2Rs function as bitter taste receptors. *Cell.* 2000;100(6):703-11.
18. Wehrens R, Roelse M, Henquet M, van Lenthe M, Goedhart PW, Jongsma MA. Statistical models discriminating between complex samples measured with microfluidic receptor-cell arrays. *PLoS one.* 2019;14(4):e0214878.
19. Yisak H, Redi-Abshiro M, Chandravanshi BS. New fluorescence spectroscopic method for the simultaneous determination of alkaloids in aqueous extract of green coffee beans. *Chem Cent J.* 2018;12(1):59.
20. Jacobson KA, Ivanov AA, de Castro S, Harden TK, Ko H. Development of selective agonists and antagonists of P2Y receptors. *Purinergic Signal.* 2009;5(1):75-89.
21. Suzuki K, Kimura T, Shinoda H, Bai G, Daniels MJ, Arai Y, et al. Five colour variants of bright luminescent protein for real-time multicolour bioimaging. *Nat. commun.* 2016;7:13718.
22. Yang J, Cumberbatch D, Centanni S, Shi SQ, Winder D, Webb D, et al. Coupling optogenetic stimulation with NanoLuc-based luminescence (BRET) Ca^{++} sensing. *Nat. commun.* 2016;7:13268.
23. Roelse M, Henquet M, Jongsma M. Receptomics: Calcium imaging of sensory receptor cell arrays in a microfluidic system and novel applications for food screening. *Chem. Senses.* 2019;44(3):E33-E4.
24. Wan Q, Okashah N, Inoue A, Nehme R, Carpenter B, Tate CG, et al. Mini G protein probes for active G protein-coupled receptors (GPCRs) in live cells. *J. Biol. Chem.* 2018;293(19):7466-73.

Development of a purification protocol guided by bitter taste receptor activation and sensory analysis to isolate new taste-active compounds in barrel-aged wines

DELPHINE WINSTEL¹, Christine Belloir², Pierre Waffo-Téguo¹, Loïc Briand² and Axel Marchal¹

¹ Unité de recherche Œnologie, EA 4577, USC 1366 INRAE, ISVV, Université de Bordeaux, F33882 Villenave d'Ornon, France, delphine.winstel@u-bordeaux.fr

² Centre des Sciences du Goût et de l'Alimentation, AgroSup Dijon, CNRS, INRAE, Université de Bourgogne Franche-Comté, 21000 Dijon, France

Abstract

Wine sensory quality is strongly dependent on oak wood ageing, as it can occasionally increase the perception of bitterness. This sensory phenomenon is due to the release of non-volatile molecules from wood. The search for such bitter compounds, requires both reliable purification tools and powerful identification techniques. The aim of this work was to propose the development of an original inductive approach, using separative techniques, sensory analysis and human bitter taste receptor activation, to discover new taste-active molecules. This new methodology was implemented on oak wood extracts to isolate and purify bitter compounds. By using High Resolution Mass Spectrometry (HRMS) and Nuclear Magnetic Resonance (NMR), a new galloyl glucopyranosyl compound, named GG-DMC, was elucidated for the first time. Its bitter properties were validated by receptor activation and sensory analysis in two matrices. These findings demonstrated the relevance and the effectiveness of the developed strategy.

Keywords: bitterness, taste-guided purification, taste, TAS2R, receptors

Introduction

During barrel ageing, wines and spirits undergo organoleptic changes caused by the release of aroma and taste molecules. While the key aromatic compounds released from oak wood have been identified, the bitter and sweet molecular determinants remain largely unknown. A gain in sweetness is frequently observed during ageing [1], that can be explained by the release of sweet triterpenoids from oak wood [2, 3]. Ageing in barrels can sometimes increase the perception of bitterness in wines, which has a negative impact on their value. This phenomenon has been widely attributed to ellagitannins, whose bitter characteristics have been suggested [4]. However, results showed that the detection thresholds of the main ellagitannins were significantly higher than their concentrations in wines, suggesting their low influence on wine bitterness [5]. More recently, the bitter properties of lyoniresinol, a lignan extracted from oak wood, have been demonstrated [6]. Despite these significant acquisitions, these compounds cannot explain the gustatory importance of oak ageing. Consequently, a large number of non-volatile molecules released by the oak remain to be identified, as well as their sensory contribution. To isolate these bitter molecules, an inductive approach with a fractionation protocol guided by gustatometry has been implemented in our laboratory for over 10 years [2, 7-8]. The success of this approach is based on the choice of raw extract, the reliability of the sensory test, and on the access to various complementary analytical techniques. In order to improve the search for taste-active compounds, new methodologies could be used. In an attempt to overcome the masking phenomena occurring during tasting, the fractions, obtained with the fractionation protocol, were screened by measuring the activation of human bitter taste receptors (TAS2Rs). Therefore, this work aims at proposing a complementary strategy for the discovery of taste-active compounds.

Experimental

Samples

Oak wood used for this study was supplied by the cooperage company Seguin-Moreau (Merpins, France). It was sampled in April 2017 from a batch of staves used to make barrels. The three levels of toasting corresponded to untoasted wood (UW), to toasted wood (TW) under the same conditions as those for "bousinage" of the barrels (around 180° C for a few minutes) and to heavy toasted wood (HTW) (200°C for 4 hours). The botanical species was assigned to *Quercus petraea* according to the method described by Marchal et al [9].

Liquid Chromatography High Resolution Mass Spectrometry (LC-HRMS) analysis

The LC-HRMS platform consisted of a Vanquish system (Thermo Fisher Scientific, Les Ulis, France) with binary pumps, an autosampler and a heated column compartment and with an Exactive Orbitrap mass spectrometer, equipped with a heated electrospray ionization (HESI-II) probe (both from Thermo Fisher Scientific). Liquid chromatography separation was performed on a C18 column (Hypersil Gold 2.1mm × 100 mm, 1.9 µm particle size, Thermo Fisher Scientific) with water containing 0.1% of formic acid (A) and acetonitrile with 0.1% of formic acid (B) as mobile phases. The flow rate was 600 µL/min and eluent B varied as follows: 0 min, 10%; 1.0 min, 10%; 5.0 min, 50%; 5.3 min, 98%; 6.0 min, 98%; 6.15 min, 10%; 7 min, 10%. Optimization of voltages, gas values, and temperatures applied for ion transfer and ionization was performed in negative mode.

Extraction of oak wood

The three modalities of sessile oak wood (600 g) were macerated in 6 L of H₂O/EtOH solution (50:50; v/v), for 2 weeks and under an inert atmosphere. Filtration (0.45 µm) was used to remove wood sawdust and particles. The three solutions containing soluble wood compounds were evaporated *in vacuo*, suspended in water, and freeze-dried to obtain brownish powders.

Liquid-liquid extractions

The powder of untoasted wood extract was dissolved in 450 mL of water and was washed twice with 450 mL of *n*-heptane. This aqueous layer was then extracted successively with methyl *tert*-butyl ether (MTBE) (6×500 mL), ethyl acetate (EtOAc) (5×800 mL) and with water-saturated butan-1-ol (BuOH) (4×800 mL). The combined organic layers were evaporated *in vacuo*, suspended in water, and freeze-dried to get powders of MTBE (1.5 g), EtOAc (1.6 g), BuOH (3.6 g) and aqueous (14.6 g) pre-purified extracts.

Centrifugal partition chromatography (CPC)

CPC was performed on a Spot prep II LC coupled with a SCPC-100+1000 (Armen Instrument, Saint-Avé, France), both controlled by Armen Glider Prep V5.0 software. A 1 L rotor was employed. The choice of an appropriate biphasic system of solvents was based on the study of the partition of extract compounds in both phases following the procedure described by Marchal et al [2]. The partition coefficient, *K_d*, was calculated as the ratio of the solute area in each phase. On this basis, various systems were tested, and the BuOH extract was fractionated using the ternary biphasic system EtOAc/propan-2-ol/H₂O (5:1:5, v/v). Separation was performed by one CPC run of 3.6 g injection. Six fractions F1 to F6 were constituted on the basis of their similar chromatographic profile, after being combined, evaporated *in vacuo*, suspended in water and freeze-dried.

Preparative liquid chromatography

Preparative HPLC analyses were performed using a Waters Prep 150 LC including a 2545 Quaternary Gradient Module, a 2489 UV/Visible detector and a 2424 ELSD detector (Waters, Guyancourt, France). Separations were performed using a SunFire Prep C18 OBD (19 mm × 250 mm, 5 µm particle size, Waters) equipped with a SunFire preparative C18 guard cartridge (20 × 19 mm, 5 µm particle size, Waters). The mobile phase was a mixture of ultrapure water and acetonitrile, both containing 0.1% of formic acid. UV detection was carried out at 280 nm and chromatographic peaks were collected manually just after the detector. Samples obtained after successive injections were pooled, evaporated *in vacuo* to remove acetonitrile and freeze-dried twice.

Nuclear Magnetic Resonance (NMR) experiments

NMR experiments were conducted on a Bruker UltraShield® System Avance 600 NMR, spectrometer (¹H at 600.27 MHz and ¹³C at 150.95 MHz) equipped with a 5 mm TXI probe. All 1D (proton) and 2D (¹H-¹H COSY, ¹H-¹H ROESY, ¹H-¹³C HSQC, and ¹H-¹³C HMBC) spectra were acquired at 300 K in methanol-*d*₄.

Sensory analysis

Taste evaluation was performed in a dedicated room, under normal daylight, at room temperature (around 20°C) and with normalized glass. Fractions or pure compounds were tasted by five experts in wine tasting. They were asked to give their written consent to participate and instructed to spit out the samples after tasting. They described the gustatory perception (bitterness, sourness, sweetness, astringency) of each glass using the vocabulary of wine tasting and were asked in particular to evaluate the bitterness intensity on a scale from 0 (not detectable) to 5 (strongly detectable). The newly identified compounds, named GG-DMC, was tasted at 5 mg/L in water (eau de source de Montagne, Laqueuille, France), as well as in a non-oaked white wine (Bordeaux 2013).

Measurement of the activation of the TAS2Rs by calcium-mobilization assays

To measure the activation of 25 human TAS2Rs, two preliminary steps were necessary. Seeding on 96-well microtiter plates, lasting 24 hours, on HEK293 cell lines stably transfected with the Ga16-gust44 protein (gustducin) was first carried out. The next step, transient transfection with one of the TAS2R expression plasmid was performed and promoted by a common transfection reagent, lipofectamine 2000™ (Thermo Fisher Scientific). Mock cells were also transfected with empty expression vector. Subsequently, transfected cells were loaded with the calcium fluorescent probe, Fluo4-AM (Molecular Probes). Cells were then stimulated with oak wood extracts at increasing concentrations: from 0.1 to 10 mg/mL for the sessile oak wood extract, from 0.0003 to 1 mg/mL for the UW, TW and HTW extracts, from 0.0033 to 3.3 mg/mL for the MTBE, EtOAc, BuOH and aqueous phase extracts of UW, and from 0.001 to 1 mg/mL for the first CPC fractionation of the UW_extract. The changes of fluorescence of TAS2R-expressing cells were recorded using a fluorometric imaging plate reader (Flexstation®, Molecular Devices) at 510 nm following excitation at 488 nm. All the measurements were carried out in duplicate.

Results and discussion

To isolate new bitter molecules, an inductive approach with a fractionation protocol guided by gustatometry has been implemented in our laboratory. This approach involves an extraction step followed by the development of a fractionation protocol implemented using various separation techniques such as liquid/liquid extractions, centrifugal partition chromatography (CPC), and preparative-HPLC. After each fractionation step, sensory analysis was used to select relevant fractions. However, masking phenomena between compounds of a same fraction can occur during tasting and could affect the efficiency of this approach. Consequently, a complementary strategy was implemented by coupling the sensory analysis to measurement of the activation of the human bitter taste receptors. After each fractionation step, the extracts obtained were tested for their ability to activate functionally expressed TAS2Rs using *in vitro* calcium imaging assay on the 25 human TAS2Rs (Figure 1).

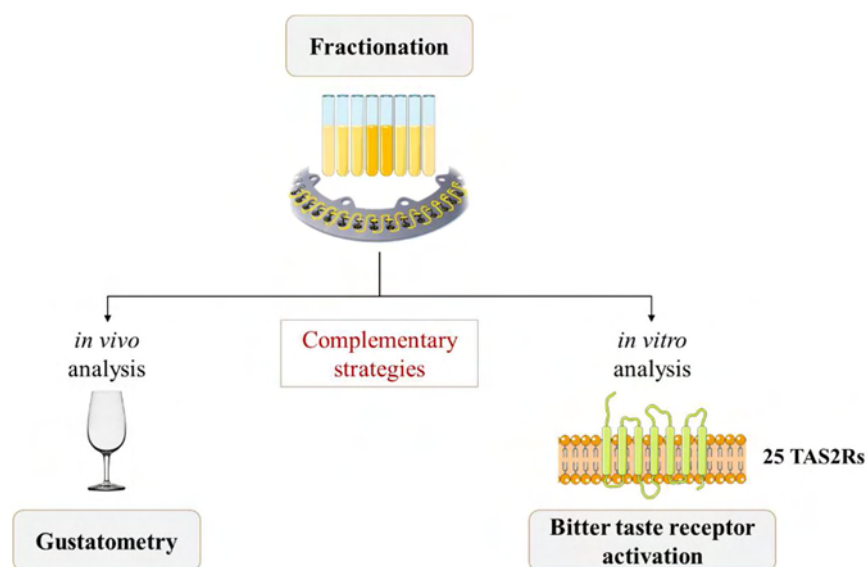


Figure 1: Fraction screening strategies during the fractionation protocol.

TAS2Rs activation test by an extract of sessile oak wood

To begin this new approach, a preliminary test was performed on a sessile oak wood extract. A screening of the different bitter taste receptors was carried out in order to identify the best activated TAS2R receptor by the oak wood. The receptor activations following stimulation with increasing concentrations of extract were measured. Fluorescence changes were compared to a control well, i.e. a well without addition of extract, and responses of mock-transfected cells were subtracted. The results showed that cells expressing five of the twenty-five TAS2Rs responded to an oak wood extract (Figure 2). The best response was obtained for TAS2R7, followed by TAS2R4, TAS2R16, TAS2R38, and TAS2R43 receptors. For TAS2R7, fluorescence increased with concentration then decreased from 3 g/L. Indeed, at too high concentrations, the environment could become toxic to the cells, which would lead to a decrease in the cell response. To continue this approach, we focused on the TAS2R7 receptor, which induced robust cellular response.

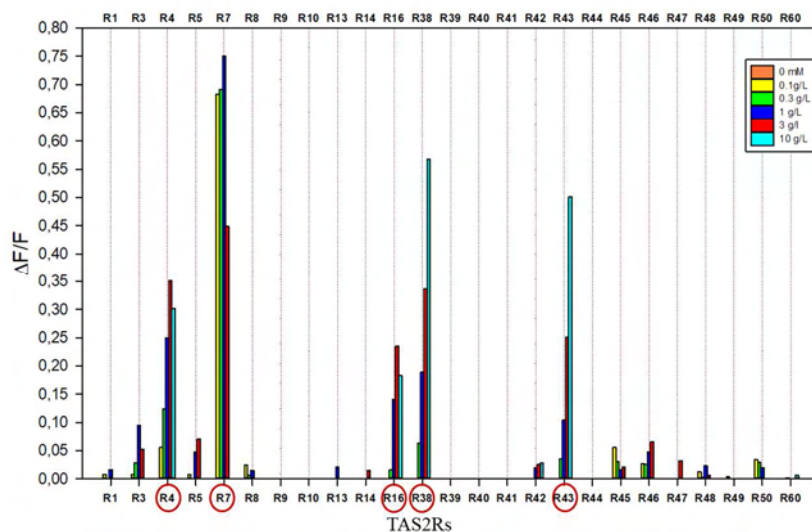


Figure 2: Activation of TAS2R receptors by an extract of sessile oak wood.

TAS2R7 activation test by UW, TW, HTW extracts

The same protocol was performed on three different extracts, which corresponded to different toasting levels of sessile oak wood extracts: heavy toasted wood (HTW), toasted wood (TW) and untoasted wood (UW). In order to analyse the ability of the fractions to activate bitter taste receptors, a dose-response curve was established, which allowed the calculation of the half maximal effective concentration (EC_{50} value). This value reflects the taste potency of a substance: the lower the EC_{50} value obtained, the greater the potency of the substance. Solutions of increasing concentrations of these extracts were added to the cells, then the activation of the TAS2R7 receptor was measured (Figure 3).

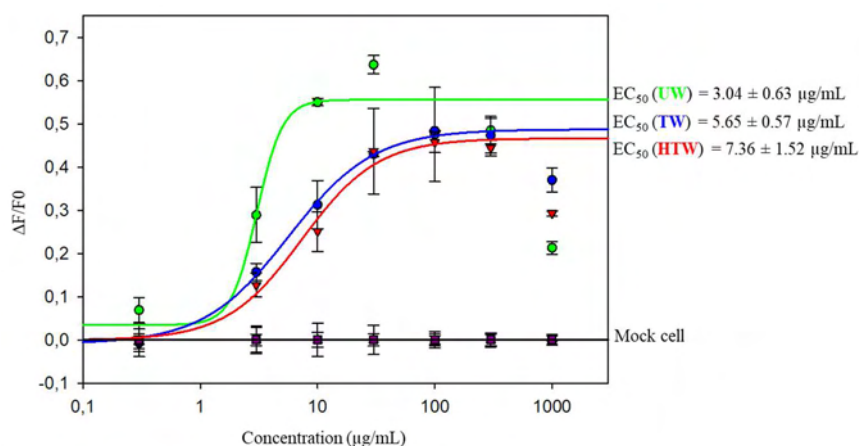


Figure 3: Activation of TAS2R7 by UW, TW, HTW extracts.

For all three extracts, we found that the TAS2R7 receptor was activated. Nevertheless, a better dose-response was observed for UW extract leading to an EC_{50} value of $3.04 \pm 0.65 \mu\text{g/mL}$. Conversely, the dose-response of HTW was half that of UW, with an EC_{50} value of $7.36 \pm 1.52 \mu\text{g/mL}$. These results are consistent with the empirical observations of coopers and winemakers, and confirmed that untoasted wood brings more bitterness than heavy toasted wood. So, this UW extract was selected for further fractionation.

TAS2R7 activation test by extracts of MTBE, EtOAc, BuOH and aqueous phase of UW

To begin the purification protocol, successive liquid-liquid extractions of UW have been carried out with solvents of increasing polarity. Four extracts were subsequently obtained and corresponded to MTBE, EtOAc, BuOH extracts and the aqueous phase. Increasing concentrations of these fractions were added to the cells expressing the bitter taste receptors and the activation of the TAS2R7 receptor was measured (Figure 4). The best responses were obtained for the aqueous phase and the butanol extract.

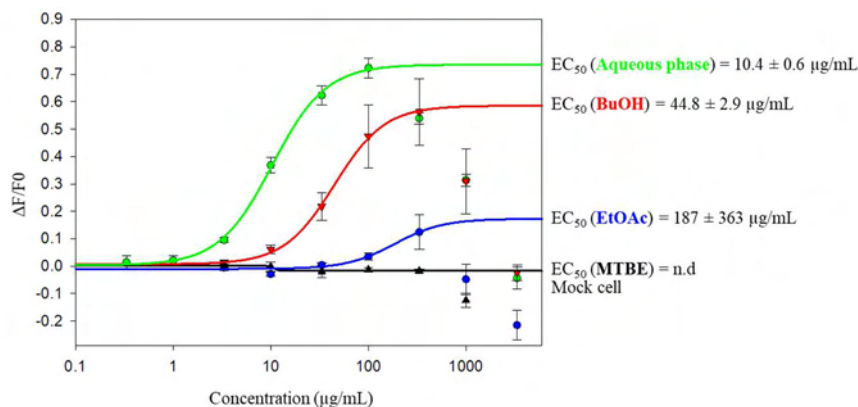


Figure 4: Activation of TAS2R7 by extracts of MTBE, EtOAc, BuOH and aqueous phase of UW.

LC-HRMS analysis of the aqueous phase showed that this extract mainly contained ellagitannins. However, a previous study showed that the TAS2R7 receptor was activated by these hydrolysable tannins [10]. Thereby, it was possible that the measured signal for the aqueous phase was due to these compounds. Further studies will aim at validating this hypothesis. In order to search for new compounds, we only focused on butanol extract. The chemical complexity of the enriched BuOH extract required a further fractionation by CPC.

Activation of TAS2R7 by CPC fractions of UW_BuOH extract

A ternary biphasic system EtOAc/propan-2-ol/H₂O (5:1:5, v/v) allowed the best partition of the BuOH extract between the two phases. At the end of this experiment, the tubes were analysed by LC-HRMS and pooled according to their composition to give fractions. After solvent evaporation and freeze-drying, 6 fractions (noted F1 to F6) were obtained as powder in variable quantities. Increasing concentrations of these fractions were added to the cells and the activation of the TAS2R7 receptor was measured (Figure 5).

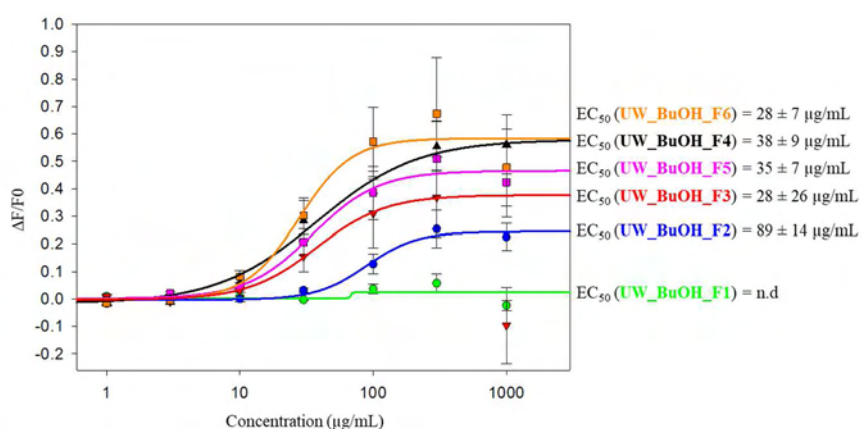


Figure 5: Activation of TAS2R7 by six CPC fractions (F1 to F6) of UW_BuOH extract

No signal was detected for F1, suggesting that TAS2R7 was not activated. Fraction F2 had the highest EC₅₀ of the other fractions. Fraction 6 obtained the best dose response with an EC₅₀ of 28 ± 7 μg/mL, followed by fraction F4 then F5 and F3. Then, tasting of the CPC fractions made it possible to distinguish a bitter fraction, the F5, which was in agreement with the positive response of the receptor to its contact. So, to continue this inductive approach, fraction F5 was selected. Its simplified chromatographic profile allowed us to perform a Preparative-LC.

Activation of TAS2R7 by compound of *m/z* 539

To see which molecules were responsible for activating TAS2R7, fraction F5 was submitted to preparative HPLC with UV detection. A preliminary injection showed that the chromatograms presented a refined profile with only a few peaks detected both in ELSD and in UV a 280 nm. Thus, an appropriate gradient was chosen and the entire was fractionated by successive injections. The main components of fraction F5 were purified, including one compound of *m/z* 539. Its HRMS spectrum exhibited a deprotonated [M - H]⁻ ion at *m/z* 539.1411. Given the isotopic ratio and the experimental mass of the deprotonated ion, the empirical formula C₂₄H₂₈O₁₄ was assigned to

this compound. Before proceeding to its structural characterization, increasing concentrations of this unknown compound were added to the cells expressing the bitter receptor TAS2R7 (Figure 6). Results showed a robust dose-response of m/z 539 on TAS2R7 leading to an EC_{50} value of 8 $\mu\text{g/mL}$ or approximately of 15 μM . By comparison, magnesium sulphate, which is known as a bitter agonist of TAS2R7, presents an EC_{50} on the order of 15 mM [11]. Measuring the activation of TAS2R7 helped to guide the fractionation to the isolation of a new bitter compound. Then, its structure was elucidated by using HRMS and NMR. To our knowledge, this compound, belonging to the galloyl glucopyranosyl family, had never been described in the literature previously, so we named it GG-DMC. This molecule was also tasted at 5 mg/L in water and in a unoaked white wine. It was perceived as bitter in these two matrices, which confirmed the results obtained during the activation of the bitter TAS2R7 receptor. By LC-HRMS screening, GG-DMC was also identified in several spirits.

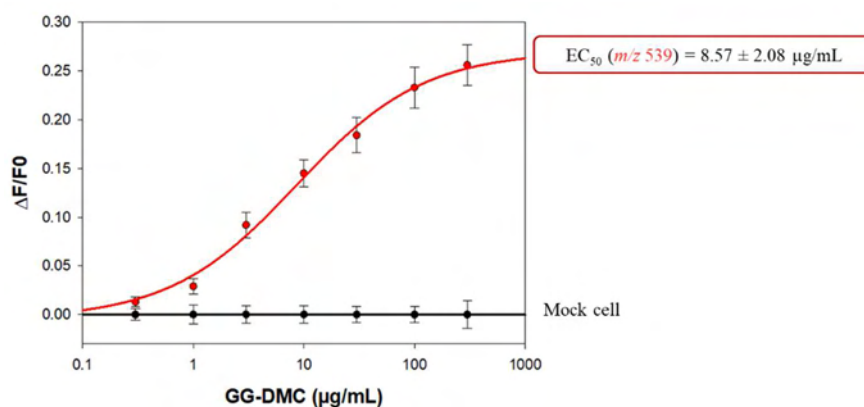


Figure 6: Activation of TAS2R7 by compound of m/z 539 (GG-DMC).

Conclusion

The aim of this work was to propose an efficient methodology for discovering new taste-active compounds in oak wood. The results demonstrated the relevance and the effectiveness of combining separative techniques, sensory analysis and receptor activation to identify and purify bitter compounds. This purification protocol guided by *in vitro* and *in vivo* analysis led to the isolation of a new bitter compound, a galloyl glucopyranosyl derivative called GG-DMC. Its structural elucidation was carried out by high resolution mass spectrometry and nuclear magnetic resonance, and will be detailed in a forthcoming publication. Its bitter taste was validated by sensory analysis and receptor activation. These studies provide promising perspectives for a better understanding of the molecular markers responsible for the taste of foods and beverages such as wine.

References

1. Marchal, A.; Pons, A.; Lavigne, V.; Dubourdieu, D. Contribution of Oak Wood Ageing to the Sweet Perception of Dry Wines: Effect of Oak Ageing on Wine Sweetness. *Aust J Grape Wine Res.* 2013;19:11–19.
2. Marchal, A.; Waffo-Téguo, P.; Génin, E.; Méridon, J.-M.; Dubourdieu, D. Identification of New Natural Sweet Compounds in Wine Using Centrifugal Partition Chromatography–Gustatometry and Fourier Transform Mass Spectrometry. *Anal Chem.* 2011;83:9629–9637.
3. Gammacurta, M.; Waffo-Teguo, P.; Winstel, D.; Cretin, B.N.; Sindt, L.; Dubourdieu, D.; Marchal, A. Triterpenoids from *Quercus Petraea*: Identification in Wines and Spirits and Sensory Assessment. *J Nat Prod.* 2019;82:265–275.
4. Quinn, M.K.; Singleton, V.L. Isolation and Identification of Ellagitannins from White Oak Wood and an Estimation of Their Roles in Wine. *Am J Enol Vitic.* 1985;36:8.
5. Glabasnia, A.; Hofmann, T. Sensory-Directed Identification of Taste-Active Ellagitannins in American (*Quercus Alba* L.) and European Oak Wood (*Quercus Robur* L.) and Quantitative Analysis in Bourbon Whiskey and Oak-Matured Red Wines. *J Agric Food Chem.* 2006;54:3380–3390.
6. Marchal, A.; Cretin, B.N.; Sindt, L.; Waffo-Téguo, P.; Dubourdieu, D. Contribution of Oak Lignans to Wine Taste: Chemical Identification, Sensory Characterization and Quantification. *Tetrahedron* 2015;71:3148–3156.
7. Cretin, B.N.; Waffo-Teguo, P.; Dubourdieu, D.; Marchal, A. Taste-Guided Isolation of Sweet-Tasting Compounds from Grape Seeds, Structural Elucidation and Identification in Wines. *Food Chem.* 2019;272:388–395.
8. Sindt, L.; Gammacurta, M.; Waffo-Teguo, P.; Dubourdieu, D.; Marchal, A. Taste-Guided Isolation of Bitter Lignans from *Quercus Petraea* and Their Identification in Wine. *J Nat Prod.* 2016;79:2432–2438.
9. Marchal, A.; Prida, A.; Dubourdieu, D. New Approach for Differentiating Sessile and Pedunculate Oak: Development of a LC-HRMS Method To Quantitate Triterpenoids in Wood. *J Agric Food Chem.* 2016;64:618–626.
10. Soares, S.; Silva, M.S.; García-Estevéz, I.; Großmann, P.; Brás, N.; Brandão, E.; Mateus, N.; de Freitas, V.; Behrens, M.; Meyerhof, W. Human Bitter Taste Receptors Are Activated by Different Classes of Polyphenols. *J Agric Food Chem.* 2018;66(33):8814–8823.
11. Behrens, M.; Redel, U.; Blank, K.; Meyerhof, W. The Human Bitter Taste Receptor TAS2R7 Facilitates the Detection of Bitter Salts. *Biochem Biophys Res Commun.* 2019;512:877–881.

Molecular triggers of post-COVID-19 parosmia in grilled chicken

JANE K. PARKER¹, Christine E. Kelly² and Simon Gane³

¹Department of Food and Nutritional Sciences, University of Reading, UK, j.k.parker@reading.ac.uk

²AbScent, 14 London Road, Andover, Hampshire, UK

³Royal National Ear, Nose and Throat and Eastman Dental Hospitals, University College London Hospital, UK

Abstract

Since the onset of the COVID-19 pandemic, incidences of loss of smell and taste have increased substantially and, whereas many of these recover within a few weeks, in about 5% of all cases of COVID-19, olfactory dysfunction persists for many months or years. During the recovery process, many experience parosmia, which is a condition in which everyday aromas become distorted and usually evoke a sense of disgust. Previous work has shown that a set of highly potent odorants in coffee can trigger these distortions. They fall into clusters of thiols, disulphides and pyrazines, and many (but not all) of these compounds are products of the Maillard reaction. In this work, we investigated another Maillard system and asked whether any of the Maillard-derived trigger molecules from coffee were also reported to be triggers in grilled chicken. GC-olfactometry was carried out by four participants and one non-parosmic expert to assess all the odour-active compounds in grilled chicken. Results revealed that indeed six triggers were found in common with coffee – all derived from the Maillard reaction. We postulate that the same few compounds may be responsible for distortions in many roasted, grilled and fried foods, and recommend that those suffering from parosmia avoid highly cooked foods.

Keywords: parosmia, anosmia, COVID-19, GC-Olfactometry, chicken, molecular triggers, olfactory dysfunction

Introduction

The impact of smell loss on quality of life is underestimated. Inability to smell gas or burnt food, or to smell intimate partners or the sufferer's own body odour, causes significant stress and anxiety, to the point where those who suffer can become clinically depressed [1]. Never have there been so many cases of anosmia (loss of sense of smell) as during the COVID-19 pandemic, when loss of “smell and taste” was recognised as an official symptom [2]. In fact, sudden loss of sense of smell [3] is so characteristic of SARS-CoV-2 infection, that it is by far the best predictor of COVID-19 [4], with an odds ratio (in the UK) of it being linked to COVID-19 of 6.5, whilst the odds ratio for all other symptoms was <2.5. Parma et al [5] showed that there was a mean drop of 89% in self-reported sense of smell, 76% in taste and 46% in chemesthesis during SARS-CoV-2 infection compared to before onset. Sudden onset of anosmia has been estimated to occur in about 50-60% of all cases of COVID-19 [6] but fortunately it is estimated that up to 80% of these will recover their sense of smell and taste within a few weeks [7]. Whilst the SARS-Cov-2 virus causes inflammation in the support cells in the olfactory epithelium [8], it is believed that for the majority of cases, the olfactory neurons remain intact and normal olfaction returns when the inflammation subsides. For the unfortunate 20% who do not recover their sense of smell within a few weeks, the problem is persistent and can last for many months or years and can be considered part of the Long-Covid suite of symptoms. This type of post-infectious anosmia is not new and is known to occur in other infections of the upper respiratory tract (influenza, common cold and sinus infections) but, until now, has been largely under-researched.

Recovery from post-infectious anosmia often starts 2-3-months after the initial loss of smell, when everyday smells become distorted and objectionable. These distortions can arise from foods, beverages, fragrances in personal care or household items, environmental aromas or even water [9]. This is known as parosmia, and those severely affected start to reject food, lose or gain weight, leading to clinical depression [9, 10]. Little is known about the underlying mechanisms, but it is generally believed that the virus causes widespread destruction of the olfactory sensory neurons, which need to regenerate before any sense of smell can return. The prevailing hypothesis for return of a distorted sense of smell is a random mis-wiring of the olfactory sensory neurons in the olfactory bulb, as they regenerate from the olfactory epithelium [11], sending unrecognised signals to the brain.

Several studies have collated lists of foods, drinks and personal care items that tend to trigger distortions [9, 12], and these indicate that coffee, meat, onions, garlic, egg, chocolate, toothpaste and shower gel are among the most frequently reported. Recently, Parker et al [11] proposed that many of the foods in question contained some of the most powerful odorants known, and set out to test the hypothesis that these potent odorants may be the origin of the distortions. Rather than using a time-consuming approach to determine individual molecular thresholds of a set of molecules selected by intelligent guesswork, GC-olfactometry was used to expose parosmic

participants (N=29) and non-parosmic participants (N=15) to a much wider selection of aroma compounds during a 30 min run time. Coffee was selected as a stable and convenient source of potent odorants, as it had the additional advantage that it is widely consumed and is one of the most frequently mentioned triggers. Parker et al. [11] showed that the parosmic group detected between them 30 different compounds at the odour port compared to the non-parosmic group who detected 60, and on average, each parosmic participant detected only 19 aroma compounds at the odour port, whereas the non-parosmic group detected twice as many (37). Of these 19 aroma compounds, on average only six were reported as being triggers. This finding was important as it demonstrated for the first time that the origin of the distortions was in the olfactory epithelium, indicating (at least in part) a peripheral mechanism rather than a purely central mechanism based in the integrative centres on the brain. Furthermore, the fact that two-thirds of the aroma compounds detected by the parosmic group were perceived as normal places constraints on the prevailing mis-wiring theory.

The most frequently reported trigger compounds identified in coffee fell into four different groups (Table 1). The most commonly reported (20/29) was 2-furanmethanethiol which has an exceptionally low threshold (0.005 µg/L) and is a character impact compound in coffee. The second most frequently reported compound was 2-ethyl-3,6-dimethylpyrazine which was reported 18/29 times as a trigger and has an odour threshold of 0.01 µg/L. The other 12 confirmed triggers were all known potent aroma compounds in coffee. Interestingly 4-ethylguaiacol and (E)-β-damascenone, which are also potent odorants in coffee, were perceived by some of the parosmic group but always with their characteristic descriptors (spicy and fruity respectively).

Table 1: Trigger compounds detected in coffee headspace by parosmic participants.

Thiols	Tri-substituted pyrazines	Disulphides	Methoxypyrazines
2-furanmethanethiol	2-ethyl-3,6-dimethylpyrazine	2-furanmethyl methyl disulphide	2-ethyl-3-methoxypyrazine
2-methyl-3-furanthiol	2,3-diethyl-5-methylpyrazine	2-methyl-3-furyl methyl disulphide	2-isobutyl-3-methoxypyrazine
3-methyl-2-butene-1-thiol	2-ethyl-3,5-dimethylpyrazine		2-isopropyl-3-methoxypyrazine
3-mercapto-3-methylbutanol	trimethylpyrazine		
3-mercapto-3-methylbutyl formate			

Sorted in decreasing order according to the number of times each compound was reported as a trigger.

Although coffee was selected for the initial study, in an analysis of parosmia social media groups [9], both onions and meat (which included beef, pork, chicken and lamb, but excluded bacon and sausages) were reported as frequently. Recognising that meat contains many of the compounds reported in Table 1, the aim of this experiment was to determine whether the same molecules triggered distortions in both coffee and grilled chicken.

Experimental

Ethics

This study (No 22/19) was approved by the University of Reading Research Ethics Committee.

Preparation of grilled chicken

A lean skinless chicken breast fillet was purchased at a local supermarket. Slices of 1 cm thickness were grilled for 3 min on both sides using a Cuisinart grill (Stamford, CT) set on high.

GC-Olfactometry and GC-MS of grilled chicken

Finely chopped grilled chicken (3 g) was placed in an SPME vial, equilibrated for 20 min at 55 °C, and the headspace extracted onto a triple phase SPME fibre (50/30 µm divinylbenzene/carboxen on polydimethylsiloxane (Supelco, Poole, UK)) for 20 min at 55 °C. After extraction, the volatiles were desorbed in a split/splitless injection port (280 °C) of an HP7890 GC from Agilent Technologies (Santa Clara, CA, USA) equipped with an Agilent HP-5 MSUi capillary (30 m, 0.25 mm i.d., 1.0 µm df) non-polar column, and coupled to a Series II ODO 2 GC-O system (SGE, Ringwood, Victoria, Australia). The temperature program was 40 °C for 2 min, then a rise of 5 °C/min up to 200 °C and 15 °C/min from 200 °C to 300 °C and the final temperature held for a further 19 min. Helium was used as carrier gas (2 mL/min). At the end of the column, the flow was split 1:1 between a flame ionisation detector (kept at 250 °C) and a sniffing port using two untreated silica-fused capillaries of the same

dimensions (1 m, 0.32 mm i.d.). The flow to the odour-port was diluted with a moist make up gas. One sample was also analysed on an Agilent 7890A Gas Chromatograph coupled to a 5975C series GC/MSD using the same column and a similar temperature program.

All the participants had already assessed coffee and were familiar with the procedure previously reported [11]. Four participants who had expressed their disgust for cooked chicken were invited to carry out the GC-Olfactometry procedure on grilled chicken. They were asked to describe the aromas as they eluted from the column, score their intensity on a general labelled magnitude scale (gLMS) and indicate whether the aroma was one that triggered parosmic distortions. One expert assessor also assessed a similar sample.

Results and discussion

Table 2: Trigger compounds detected in grilled chicken headspace by parosmic participants.

LRI ^a	Compound	Participant A	Participant B	Participant C	Participant D
674	unknown				parosmic meat (6)
867	2-methyl-3-furanthiol	onion (54* ^b)	rancid mouldy (25)		toast parosmic (6*)
906	methional (tentative)				parosmic lime (6)
912	2-furan-methanethiol	vegetable, terrible (35*)		cooked chicken (17*)	
1003	trimethylpyrazine			unpleasant (1*)	
1080	2-ethyl-3,6-dimethyl-pyrazine	not nice, lingers (35*)		popcorn unpleasant (9*)	
1088	2-ethyl-3,5-dimethyl-pyrazine		not nice cats pee (17*)	unpleasant (9*)	
1097	2-isopropyl-3-methoxy-pyrazine		not nice cats pee (17)		
1157	2,3-diethyl-5-methyl-pyrazine (and/or 3,5-dimethyl-1,2,4-trithiolane)	cats pee chocolate (51)			
1241	unknown	off veg (6)			

*Compounds that were reported as triggers for 4 different participants: participant A's combined gLMS score was the greatest and participants D's was the least. ^aLRI on a DB5 column, all compounds were detected by the expert assessor and have been reported in cooked chicken previously. ^bScore on a gLMS scale where 0 = no sensation, 1.4 = barely detectable, 6 = weak, 17 = moderate, 35 = strong, 51 = very strong and 100 = strongest imaginable sensation of any kind. *Compounds that were also reported as triggers by that participant in coffee.*

There was a significant overlap with coffee in the trigger compounds reported in grilled chicken. The two furanthiols, four trisubstituted pyrazines and one of the methoxypyrazines were all reported as triggers in both coffee and grilled chicken. Six of these are products of the Maillard reaction, and we anticipate that these compounds may also be responsible for the distortions experienced by many people with parosmia from anything roasted, grilled or fried (e.g. crisps, cocoa, peanut butter, marmite, toast).

Participant A reported the two furanthiols and one pyrazine as triggers, which had been previously reported as triggers in coffee. Interestingly participant A also reported a compound at LRI 1157 as cats pee, chocolate and very different to the descriptor at LRI 1088. It is possible that in grilled chicken, participant A was detecting 3,5-dimethyl-1,2,4-trithiolane which elutes at a similar LRI and has been reported in chicken previously as well 2,3-diethyl-5-methyl-pyrazine. The cyclic sulphur compound is more likely to give a cats pee note whereas the pyrazine would give a chocolate note. Further work needs to be carried out to carefully verify the identity of this trigger in grilled chicken for participant A. Participant B did not detect 2-methyl-3-furanthiol in coffee but did in chicken. We suggest that the higher concentrations present in meat, where it is a character impact compound, may

mean that this compound is above threshold in meat but not in coffee (for B). For participant C, all triggers reported for grilled chicken were also triggers in coffee. For participant D, all triggers were weak, but 2-methyl-3-furanthiol was reported as a trigger as it had been in coffee. The aroma at LRI 906 eluted a little early to be 2-furanmethanethiol, but may be methional, but this compound has not previously been reported as a trigger.

Although it is not the Maillard reaction per se which triggers distortions, it certainly generates many of the highly potent thiols and pyrazines which have been shown to be triggers in coffee and grilled chicken.

Conclusion

Many of the molecules that have previously been identified in coffee as triggers of the distortions, experienced by those with parosmia, were also identified as triggers in the headspace of grilled chicken. They are typical products of the Maillard reaction, whereas those compounds which are more specific to coffee were not found in chicken. It is likely that these Maillard-derived compounds may also act as triggers in other roasted, grilled or fried foods.

References

1. Croy I, Nordin S, Hummel T. Olfactory Disorders and Quality of Life-An Updated Review. *Chem. Senses* 2014;39(3):185-94.
2. Hopkins C. Loss of sense of smell as marker of COVID-19 infection. *ENT UK*; 2020.
3. Gane SB, Kelly C, Hopkins C. Isolated sudden onset anosmia in COVID-19 infection. A novel syndrome? *Rhinology* 2020;58(3):299-301.
4. Menni C, Valdes AM, Freidin MB, Sudre CH, Nguyen LH, Drew DA, et al. Real-time tracking of self-reported symptoms to predict potential COVID-19. *Nat Med.* 2020;26(7):1037-1040.
5. Parma V, Ohla K, Veldhuizen MG, Niv MY, Kelly CE, Bakke AJ, et al. More than smell - COVID-19 is associated with severe impairment of smell, taste, and chemesthesis. *Chem. Senses* 2020;45(7):609-622.
6. Boscolo-Rizzo P, Polesel J, Spinato G, Menegaldo A, Fabbris C, Calvanese L, et al. Predominance of an altered sense of smell or taste among long-lasting symptoms in patients with mildly symptomatic COVID-19. *Rhinology* 2020;58(5):524-5.
7. Hopkins C, Surda P, Whitehead E, Kumar BN. Early recovery following new onset anosmia during the COVID-19 pandemic - an observational cohort study. *J Otolaryngol-Head N.* 2020;49(26).
8. Brann DH, Tsukahara T, Weinreb C, Lipovsek M, Van den Berge K, Gong B, et al. Non-neuronal expression of SARS-CoV-2 entry genes in the olfactory system suggests mechanisms underlying COVID-19-associated anosmia. *Sci Adv.* 2020;6(31).
9. Parker JK, Kelly CE, Smith B, Hopkins C, Gane S. An analysis of patients' perspectives on qualitative olfactory dysfunction using social media. *MedRxiv* 2020.12.30.20249029.
10. Burges Watson DL, Campbell M, Hopkins C, Smith B, Kelly C, Deary V. Altered Smell and Taste: anosmia, parosmia and the impact of long Covid-19. *MedRxiv.* 2020.11.26.20239152.
11. Parker JK, Kelly CE, Kirkwood AF, Gane S. Identification of Molecular Triggers for Parosmia. *MedRxiv* 2021.02.05.21251085.
12. Keller A, Malaspina D. Hidden consequences of olfactory dysfunction: a patient report series. *BMC ear, nose, and throat disorders.* 2013;13(1):8.

Identification of odour-active trace compounds in toasted oak wood: impact on wines and spirits aroma

MARIE COURREGELONGUE^{1,2}, Svitlana Shinkaruk^{1,3}, Philippe Darriet¹, Alexandre Pons^{1,2}

¹ Unité de recherche Œnologie, EA 4577, USC 1366 INRAe, ISVV, Université de Bordeaux, Villenave d'Ornon, France, marie.courregelongue@u-bordeaux.fr

² Tonnellerie Seguin Moreau, Cognac, France

³ Institut des Sciences Moléculaires, UMR 5255 CNRS, Université de Bordeaux, Talence, France

Abstract

The aging of wine in oak barrels is an important step in the maturation of quality wines. The oak toasting process generates several nuances that can be released into the wine. Significant research has been devoted to identifying the wood-derived volatile compounds that influence wine aromas [1, 2] (e.g., whisky-lactone, maltol, eugenol, guaiacol, vanillin). However, these compounds only partially explain oak wood aromas and their effect on wine complexity. The purpose of our research was to gain a greater understanding of toasted oak aromas. To achieve this, we used a sensory-guided approach based on the purification of organic extracts of crude oak wood using a preparative high-performance liquid chromatography (HPLC) technique and gas chromatography analysis paired with olfactometry and high-resolution mass spectrometry (GC-O-TOF MS). This approach revealed odorous zones in oak wood extracts with reminiscence of metal and pastry aromas. The odorous zone with metallic aroma was attributed to (*E*)-4,5-epoxy-(*E*)-2-decenal, while the one with pastry aroma was attributed to 2,4,6-nonatrienal isomers. The injection of standard confirmed the identification of (*E*)-4,5-epoxy-(*E*)-2-decenal. Two isomers were detected for the 2,4,6-nonatrienal compound (*E,E,Z* and *E,E,E*). We used a chemical organic synthesis method (Wittig reaction) to synthesize the isomers. An additional purification step using semi-preparative HPLC allowed us to isolate the (*E,E,Z*) isomer with 99% purity. These compounds were identified for the first time in wood, wine and spirits by using SPE extraction and optimized GC-MS NCI (NH₃) separation and detection. Furthermore, their very low olfactory-detection threshold in a hydro-alcoholic model solution demonstrated their impact on the aroma of these beverages. Their quantitation in numerous samples of oak wood also revealed the influence of toasting intensity on their formation. Additional results on their precursors in oak and wine were also discussed.

Keywords: toasted oak wood, (*E*)-4,5-epoxy-(*E*)-2-decenal, 2,4,6-nonatrienal, sensory impact, chemical synthesis

Introduction

Oak barrel aging has been recognized as an important step in the production of quality wines and spirits. Among the 250 species of the genus *Quercus*, empirical selection by wine industry professionals in recent oenological history has revealed that only three species produce quality wood suitable for oenological use: two European oak species, sessile oak (*Quercus sessilis* or *petrae*) and pedunculate oak (*Quercus robur*), and an American oak species called white oak (*Quercus alba*). Oak barrel production involves many steps, including the important toasting process. The wood is first subjected to high temperatures (160 °C - 210 °C) to facilitate bending. Heat is then applied a second time to produce a variety of volatile compounds through the thermal-degradation of oak wood components. The second heating is called oenological heating or *bousinage*. Coopers possess the expertise needed to carry out this process, which is the source of a true olfactory fingerprint. When oak wood is subjected to toasting, its odour changes. Its aromas can be reminiscent of a mix of coconut, vanilla and pastry aromas in the case of light to medium heating and produce aromas reminiscent of toasted bread, roasting, spices and even smoke aromas when heated to the highest temperatures.

Over the last 30 years, many studies have been conducted to characterize these aromas. A literature review allowed us to list around 350 volatile compounds in oak wood. These compounds belong to different chemical families, including alcohols, aldehydes, ketones, carboxylic acids, esters and lactones. The organoleptic impact has only been identified for certain compounds. For example, the two isomers of β-methyl-γ-octalactone (whisky lactone, [1]) with coconut notes, vanillin with vanilla odours [3], the Maillard derivative compounds as maltol, furfural, 5-methylfurfural with caramel notes [4, 5], and eugenol, isoeugenol, guaiacol and its derivatives with spicy aromas, leather and smoky notes [1, 6]. These compounds are produced by the thermal-degradation of the three main components of oak wood: cellulose (40-50 %), hemicellulose (28 %) and lignin (16-25 %). On the other hand, toasting can lead to volatile compound degradation, such as *trans*-2-nonenal, which is associated with a sawdust odour [7]. Therefore, although many oak wood-derived volatile compounds had been identified and studied in toasted oak wood, there was a need to identify others in order to enrich our understanding of oak wood quality for oenological use. For example, certain aromas observed in wine and wood, such as pastry, roasted and

smoky notes, had not yet been explained from a molecular standpoint. The goal of this study was to identify the volatile compounds associated with these aromas in toasted oak wood.

Experimental Methods

Samples of oak wood, wine and spirits

For the identification work, oak wood samples (*Q. sessilis*) were provided by Seguin Moreau cooperage (Merpins, France). During this first step, three commercial samples were selected with different aromas and toasting intensities, referred to respectively as vanilla, toasted and smoked. As its name suggests, the first sample was reminiscent of vanilla. The second had a complex mixture of toasted bread, pastry, and coconut aromas. The third had smoke aromas. The cooper performed additional toasting experiments involving different time and temperature combinations. Several species were selected for use in the quantitation experiments, including sessile, pedunculate, American, Caucase, chestnut, acacia and cherry wood species.

In addition, the wines (red and white) and spirits (Cognac, whisky, rum, brandy) studied were produced using different grape varieties and winemaking or aging processes. They were either supplied by winemakers, Seguin Moreau cooperage, or purchased from stores.

Sample preparation and GC-O-TOF MS experiments

GC-O-MS analysis was performed on organic extracts of oak wood solution (50 g/L, EtOH 12%, 7 days), obtained from three successive liquid-liquid extractions (100 mL of oak wood solution, 3x5 mL of dichloromethane). In order to purify the matrix and target the odorous zones (OZ), a semi-preparative HPLC fractionation was performed on these organic extracts. Reversed-phase (RP) HPLC was performed on the raw organic extract, using a Novapak C18 column (300 × 7.8 mm internal diameter (i.d.), 6 μm, Waters, Saint Quentin, France) with a guard column of the same phase. The Ultimate 3000 semi-preparative HPLC system was from Dionex (Courtaboeuf, France). The chromatographic conditions were as follows: flow rate, 1 mL/min; injection volume, 250 μL; eluent A, microfiltered water, eluent B, ethanol; gradient, 0–2 min, 0% B, 2–50 min, 0–100% B. Fifty effluent fractions of 1 mL were collected. Each fraction was diluted into 12% ethanol, then poured into normalized glasses for sensory evaluation by a panel of four experts who were asked to describe them. Among fractions, some were selected as fractions of interest based on their sensory descriptors. These selected fractions were extracted by liquid-liquid extraction (same protocol) and then injected into an Agilent 7890A gas chromatograph (Agilent Technologies, Santa Clara, CA) on a BP20 capillary column (50 m x 0.22 mm (i.d.), 0.25 μm, SGE) and a DB5 capillary column (50 m x 0.22 mm (i.d.), 0.25 μm, Agilent) coupled to an ODP-3 olfactometric port (Gerstel, Mülheim an der Ruhr, Germany) and a JMS-T100GC time-of-flight mass spectrometer (JEOL Ltd, Akishima, Tokyo, Japan).

Synthesis and purification of 2,4,6-nonatrienal isomers

Inspired by the work of Schuh and Schieberle [8], the organic synthesis of (*E,E,Z*)-2,4,6-nonatrienal was optimized. This involves adding double bonds to (*Z*)-2-penten-1-ol via a Wittig reaction, while avoiding isomerization during the six steps required to add three conjugated double bonds in the molecule. Next, a semi-preparative HPLC purification using a ChiralPak IA column (25 cm, 1 cm (i.d.), 5 μm particle size, Chiral Technologies Inc., West Chester, PA, USA) was performed to isolate and characterize each synthesized isomer by ¹H NMR (300 MHz).

Development and validation of a quantitative method

A quantitative method using solid-phase extraction (SPE) was developed and validated to quantify 2,4,6-nonatrienal isomers and (*E*)-4,5-epoxy-(*E*)-2-decenal in oak wood, wines and spirits. Quantitation was performed on a Trace GC Ultra system coupled to a mass spectrometer DSQ II (Thermo Fisher Scientific, Waltham, MA) using negative chemical ionization with ammonia (NCI).

*Organoleptic impact of (*E,E,Z*) 2,4,6-nonatrienal and (*E*)-4,5-epoxy-(*E*)-2-decenal*

Olfactory detection thresholds (ODT) were evaluated according to the ISO standard (ISO 13301:2018) in a model wine solution (ethanol 12 % vol., L(+)-tartaric acid 5g/L, pH 3.5). In order to confirm the sensory impact of the volatile compounds, concentrations were compared to ODT (ratio concentration/ODT). If the ratio was above 1, we could conclude that the compound had a direct sensory impact.

Results and discussion

Identification of the volatile compounds responsible for toasted oak wood aromas by GC-O-TOFMS

The first step in this process was the comparison of aromagrams of oak wood extracts, with differentiated aromas, obtained by GC-O-MS analysis. The aromagrams revealed the complexity of these samples, in which more than 60 OZ were detected. Comparison of aromagrams from the three commercial oak samples showed three intense and unknown OZ, specific to one particular toasting intensity and sensory profile: two with pastry odours (LRI 1839 and 1928, OZ1 and OZ1') and the other with a metallic odour (LRI 1932, OZ2) (Table 1).

Table 1: Example of aromagram illustrating odorous zones detected and identified by GC-O-TOF MS analysis of three toasted oak wood extracts (Vanilla, Toasted and Smoked).

LRI ¹	Odorous zone	Identified compound	Vanilla	Toasted	Smoked
1822	apple sauce	β -damascenone	+	+	+
1839	puff pastry	unknown	+	+	-
1847	coconut	(Z)-whisky lactone	+	+	+
1861	caramel	cyclotene	-	+	-
1868	wine vinegar, acid	unknown	+	+	+
1875	coconut	γ -octalactone	+	-	-
1894	curry, sweet	unknown	+	+	+
1906	vanilla, almond, chocolate, sweet, prune	unknown	+	+	+
1913	coconut	(E)-whisky lactone	+	+	+
1917	caramel, cooked strawberry	maltol	+	+	+
1928	puff pastry	unknown	+	+	-
1932	metallic, fatty	unknown	-	+	+

¹Linear retention indices on BP20 (50 m; 0.22 mm, 0.25 μ m, SGE)

However, this analytical approach did not enable identification of a peak on the chromatogram based on the retention times of these OZ. This may be due to co-elution issues, since oak wood is a complex matrix, or it could be related to detection and sensitivity issues. A semi-preparative HPLC fractionation was therefore performed. Similar fractions were gathered and analysed by GC-O-TOFMS. Both OZ were detected in the same gathered fractions (F3) (Table 2).

Table 2: GC-O analysis on gathered fractions (F3) of different toasted oak wood extracts (Vanilla, Toasted and Smoked).

LRI		Sensory descriptors (N=4)			Odorous zones
BP20	DB5	Vanilla	Toasted	Smoked	
1839	1278	puff pastry, cereal	puff pastry, cereal	-	OZ1
1928	1392	puff pastry, cereal	puff pastry, cereal	-	OZ1'
1953	1453	metallic (fatty, butter)	metallic (fatty, butter)	metallic (fatty, butter)	OZ2

One compound, 2,4,6-nonatrienal, was suggested for association with OZ1 based on similar LRI on polar and non-polar columns and sensory descriptors similar to those cited in the literature. Schuh and Schieberle [8] identified this compound as the key odorant in oat flakes, with an oatmeal-like and sweet odour. Since the standard is not commercially available, organic synthesis was performed (Figure 1).

The organic synthesis resulted in the formation of a mixture of four isomers of 2,4,6-nonatrienal, with two major compounds in a 6:4 ratio corresponding to the E,E,Z and E,E,E isomers, respectively, according to GC-MS and ¹H NMR analysis. Isomerization occurred during the second Wittig reaction. In fact, based on ¹H NMR data, there were two compounds for methyl-2,4,6-nonatrienoate, which is an intermediate product of the reaction. J_{6-7} coupling constant revealed a *trans* configuration (14.85 Hz) and a *cis* configuration (11.1 Hz) at the double bonds at C-6. Furthermore, specific multiplicity profiles were observed between E,E,E and E,E,Z isomers. 2,4,6-nonatrienal showed the same constants and multiplicity profiles, which allowed for well-characterized isomers.

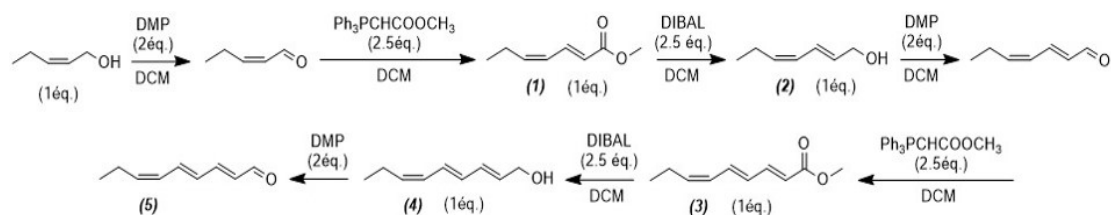


Figure 1: Synthetic route used in the synthesis of (*E,E,Z*)-2,4,6-nonatrienal. (DMP: Dess-Martin periodinane; DIBAL: diisobutylaluminium hydride).

Semi-preparative HPLC purification was performed to isolate each isomer and (*E,E,Z*)-2,4,6-nonatrienal was obtained with 99 % purity. The compound was co-injected with an oak wood extract to confirm its identification using GC-O-TOF MS (Figure 2A).

In addition, the characteristic odour of OZ1' led to identify 2,4,6-decatrienal as responsible of this OZ. In fact, in literature this compound is also described in oat with an oat-like odour [9]. Moreover, its LRI on polar (1984) and non-polar (1376) correspond to our [9,10]. As 2,4,6-nonatrienal, this compound present different isomers, but the (*E,E,Z*) and (*E,E,E*)-2,4,6-decatrienal are the most abundant.

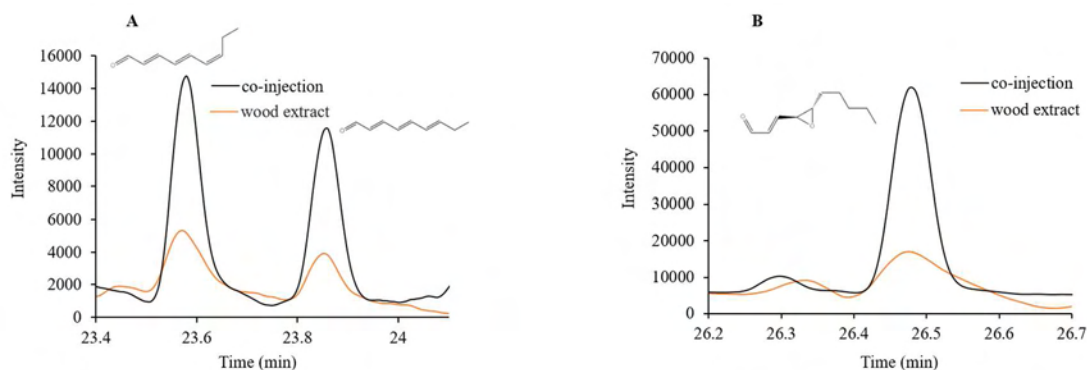


Figure 2: GC-MS NCI analysis of oak wood extract with (black) and without (orange) standard: synthesised 2,4,6-nonatrienal isomers (A) and (*E*)-4,5-epoxy-(*E*)-2-decenal (B). ($m/z=136$ and $m/z=97$, respectively).

Regarding OZ2, its specific odour enabled identification of (*E*)-4,5-epoxy-(*E*)-2-decenal, which was confirmed by its LRI, mass spectrum and the injection of its standard (Figure 2B). In the literature, studies have shown that (*E*)-4,5-epoxy-(*E*)-alk-2-enals are responsible for this characteristic metallic odour [11,12], particularly the (*E*)-4,5-epoxy-(*E*)-2-decenal which is the most odorant of these compounds.

These compounds were identified in oak wood for oenological use for the first time.

Distribution of 2,4,6-nonatrienal isomers and trans-4,5-epoxy-(E)-2-decenal during toasting

Quantitation experiments were conducted using oak wood samples heated with different time and temperature combinations to understand the formation of these two new compounds. Different species were also studied (sessile, pedunculate, American, Caucase). This study detected 2,4,6-nonatrienal in non-toasted oak woods. Optimum treatment was achieved with medium heating (180°C for 30 min) and, in general, high temperatures were not conducive to the formation of the *E,E,Z* isomer (Figure 3). On the other hand, toasting was conducive to the formation of the *E,E,E* isomer (Figure 3), except in extreme conditions (240 °C for 30 min). These observations were consistent with the sensory perceptions. The expert panel described the lightly toasted oak wood samples as having brioche, pastry and sweet notes, which were not cited in the descriptions of highly toasted oak wood.

High temperatures are conducive to the formation of (*E*)-4,5-epoxy-(*E*)-2-decenal (Figure 4). It was present in non-toasted oak wood, but in small amounts compared to the other conditions, in which it can reach ten times its initial concentration.

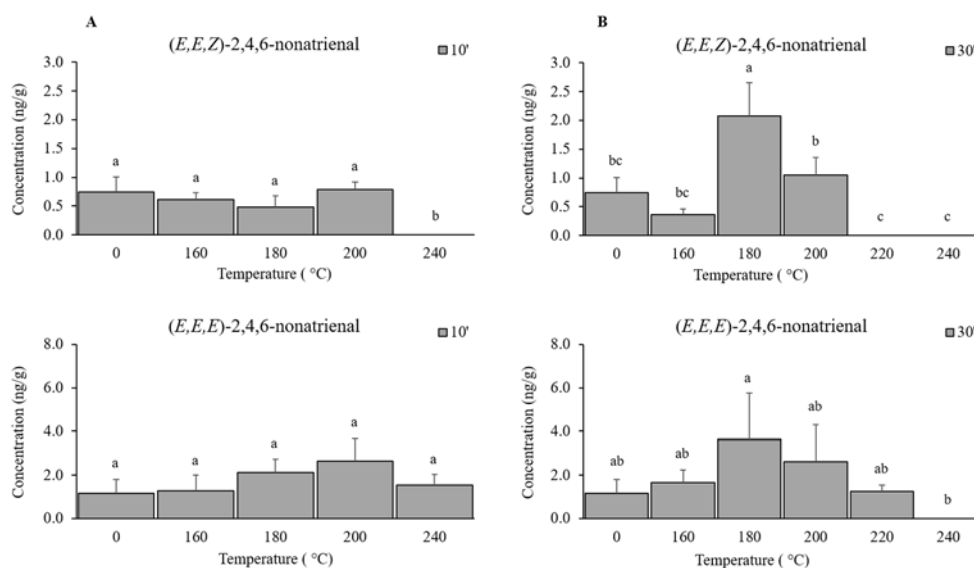


Figure 3: Distribution of (E,E,Z) and (E,E,E)-2,4,6-nonatrienal during temperature increases with the same heating time: 10 min (A) or 30 min (B). (n=3; Different letters correspond to significant differences according to one way ANOVA at p-value<0.05).

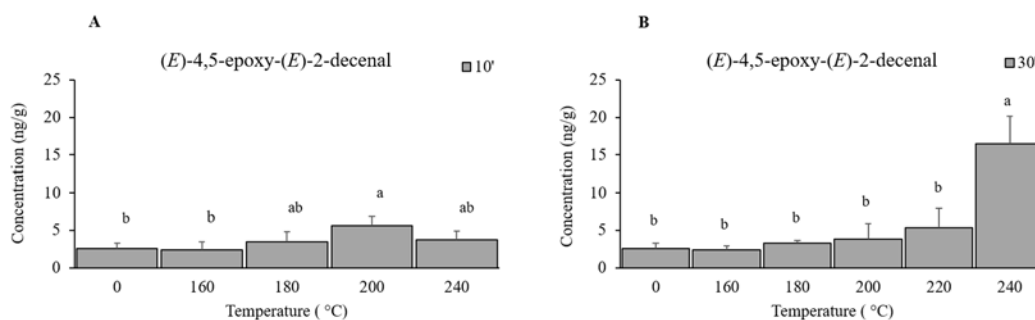


Figure 4: Distribution of (E)-4,5-epoxy-(E)-2-decenal during temperature increases with the same heating time: 10 min (A) or 30 min (B). (n=3; Different letters correspond to significant differences according to one way ANOVA at p-value<0.05).

Fatty acids, specifically linoleic and linolenic acids, had already been described in oat, butterfat and beans as precursors of (E)-4,5-epoxy-(E)-2-decenal and 2,4,6-nonatrienal, respectively [8, 11, 13, 14] based on an oxidation mechanism. It is therefore likely that, in our experimental conditions, the association between heat stress and oxidative stress caused fatty acid degradation and aldehyde production, and, depending on the chemical structure of the compounds, their degradation or volatilization at higher temperatures.

Impact of 2,4,6-nonatrienal and trans-4,5-epoxy-(E)-2-decenal on the aromas of wines and spirits

The two isomers of 2,4,6-nonatrienal were identified in red wine and quantitated. Concentrations of the most odorous isomer were generally higher (441.3 ng/L) than concentrations of the E,E,E isomer (178.2 ng/L) (Table 3). However, in some red wines, only the E,E,E isomer was present. Moreover, 2,4,6-nonatrienal is not exclusively present in red wines aged in barrels. Quantitation revealed that 2,4,6-nonatrienal can also be present in red wines not aged in barrels (Table 3). However, concentrations in red wines aged in barrels are higher (441.32 ng/L) than those observed in red wines not aged in barrels (275.84 ng/L). These observations led to the conclusion that this compound can be released through contact with oak wood and/or produced during grape ripening or winemaking. In the case of (E)-4,5-epoxy-(E)-2-decenal, its distribution differs from one wine to another. First, concentrations are higher in red wines not aged in barrels (24.3 ng/L in average). Furthermore, few red wines aged in barrels contain (E)-4,5-epoxy-(E)-2-decenal, but concentrations of this compound can reach 56.3 ng/L (66.7 ng/L) in red wines not aged in barrels. Like 2,4,6-nonatrienal, (E)-4,5-epoxy-(E)-2-decenal can be released through contact with oak wood and/or during grape ripening and winemaking.

When we compare the results obtained for the two new compounds in red wines, we observe a noticeable difference in their distribution. They are not necessarily present in the same samples.

Table 3: Distribution (ng/L) of (E,E,Z)-2,4,6-nonatrienal (1), (E,E,E)-2,4,6-nonatrienal (2) and (E)-4,5-epoxy-(E)-2-decenal (3) in several red wines aged (OB) or not (NOB) in oak barrels. (n= number of samples, SD=standard deviation, Q1=quartile 1 and Q3=quartile 3).

Compounds		n	Average	SD	Median	Min.	Max.	Q1	Q3
(1)	OB	11	146.5	160.1	80.4	3.6	441.3	32.3	254.2
	N-OB	24	88.5	72.7	64.0	12.3	275.8	44.1	115.6
(2)	OB	17	54.4	55.1	47.3	2.7	169.6	10.7	66.7
	N-OB	37	59.0	38.8	44.9	10.9	178.2	29.6	79.5
(3)	OB	5	22.7	19.4	17.3	6.4	56.3	14.0	19.4
	N-OB	37	24.3	10.3	23.4	8.5	66.7	18.2	27.6

To determine their organoleptic impact, ODT were evaluated by experts. The ODT of *trans*-4,5-epoxy-(*E*)-2-decenal was evaluated at 43 ng/L in model wine solution (n=17). The ODT of (E,E,Z)-2,4,6-nonatrienal was evaluated at 16 ng/L in model wine solution (n=10). Both have a very low ODT and are among the most odorous compounds found in wines. Based on its concentrations in red wine, which are much higher than its individual ODT, (E,E,Z)-2,4,6-nonatrienal directly affects the aroma of red wine. (E)-4,5-epoxy-(E)-2-decenal, on the other hand, affects the aroma of certain red wines.

Conclusion

Oak wood barrels have been known and used for many years, but some of the volatile compounds responsible for their aromas remain unknown. In this study, two new compounds were identified and characterized: 2,4,6-nonatrienal and (E)-4,5-epoxy-(E)-2-decenal. They are responsible for puff pastry and metallic odours, respectively. Quantitation in oak wood revealed the influence of toasting intensity on their formation. In red wines, both have a direct organoleptic impact on the aroma due to their low ODT. Additional sensory analysis will be needed to determine how they modulate the aroma of wine and spirits. Quantitation in other wines (red and white) and spirits is currently underway. The initial results reveal the presence of 2,4,6-nonatrienal in some spirits.

References

1. Chatonnet, P. Incidence Du Bois de Chêne Sur La Composition Chimique et Les Qualités Organoleptiques Des Vins. Applications Technologiques. *Thesis Univ. Bordx. II* 1991.
2. Jarauta, I.; Cacho, J.; Ferreira, V. Concurrent Phenomena Contributing to the Formation of the Aroma of Wine during Aging in Oak Wood: An Analytical Study. *J. Agric. Food Chem.* 2005;53:4166–4177.
3. Sefton, M.A.; Francis, I.L.; Pocock, K.F.; Williams, P.J. The Influence of Natural Seasoning on the Concentrations of Eugenol, Vanillin, and Cis- and Trans- β -Methyl- γ -Octalactone Extracted from French and American Oakwood. *Sci. Aliments* 1993;13: 629–643.
4. Cutzach, I.; Chatonnet, P.; Henry, R.; Dubourdieu, D. Identification of Volatile Compounds with a “Toasty” Aroma in Heated Oak Used in Barrelmaking. *J. Agric. Food Chem.* 1997;45:2217–2224.
5. Cutzach, I.; Chatonnet, P.; Henry, R.; Dubourdieu, D. Identifying New Volatile Compounds in Toasted Oak. *J. Agric. Food Chem.* 1999;47:1663–1667.
6. Cerdán, T.G.; Goñi, D.T.; Azpilicueta, C.A. Accumulation of Volatile Compounds during Ageing of Two Red Wines with Different Composition. *J. Food Eng.* 2004;65:349–356.
7. Chatonnet, P.; Dubourdieu, D. Identification of Substances Responsible for the ‘Sawdust’ Aroma in Oak Wood. *J. Sci. Food Agric.* 1998;76:179–188.
8. Schuh, C.; Schieberle, P. Characterization of (E,E,Z)-2,4,6-Nonatrienal as a Character Impact Aroma Compound of Oat Flakes. *J. Agric. Food Chem.* 2005;53:8699–8705.
9. Dach, A.; Schieberle, P. Characterization of the Key Aroma Compounds in a Freshly Prepared Oat (*Avena Sativa* L.) Pastry by Application of the Sensomics Approach. *J. Agric. Food Chem.* 2021;69:1578–1588.
10. Dach, A.; Schieberle, P. Changes in the Concentrations of Key Aroma Compounds in Oat (*Avena Sativa*) Flour during Manufacturing of Oat Pastry. *J. Agric. Food Chem.* 2021;69(5):1589–1597.
11. Buettner, A.; Schieberle, P. Aroma Properties of a Homologous Series of 2,3-Epoxyalkanals and *Trans*-4,5-Epoxyalk-2-Enals. *J. Agric. Food Chem.* 2001;49:3881–3884.
12. Gassenmeier, K.; Schieberle, P. Formation of the Intense Flavor Compound *Trans*-4,5-Epoxy-(*E*)-2-Decenal in Thermally Treated Fats. *J. Am. Oil Chem. Soc.* 1994;71:1315–1319.
13. Guth, H.; Grosch, W. Comparison of Stored Soya-Bean and Rapeseed Oils by Aroma Extract Dilution Analysis. *Lebensm. Wiss. Technol.* 1990;23:59–65.
14. Buttery, R.G. Nona-2,4,6-Trienal, an Unusual Component of Blended Dry Beans. *J. Agric. Food Chem.* 1975;23:1003–1004.

Understanding flavour release and sensory perception of composite foods by combining dynamic sensory methods with *in vivo* nose space analysis

KARINA GONZALEZ-ESTANOL^{1,2,3}, Iuliia Khomenko¹, Danny Clicerì¹, Markus Stieger² and Franco Biasioli¹

¹ Department of Food Quality and Nutrition, Edmund Mach Foundation, San Michele all'Adige (TN), Italy

² Food Quality and Design, Wageningen University, Wageningen, The Netherlands

³ Department of Agri-food and Environmental Sciences, Trento University, Trento, Italy.

karina.gonzalezestanol@fmach.it

Abstract

The aim of the study was to investigate the effect of food structure and composition on aroma release and sensory perception of composite foods. Dynamic sensory perception was assessed with Temporal-Check-All-That-Apply (TCATA) (n=72) while quantification of aroma release was done with *in vivo* nose space analysis using a commercial PTR-ToF-MS (Proton Transfer Reaction Time-of-Flight Mass Spectrometer, Ionicon Analytik, Innsbruck, Austria) (n=8, in triplicate).

Six composite foods were prepared by combining two carriers (bread and wafer) with three formulations of chocolate-hazelnut spreads varying in fat and sugar content (high fat/high sugar; high fat/low sugar; low fat/high sugar). The spreads were spiked with a known quantity of 5 aroma compounds. Evaluations of the hazelnut spreads without carriers and for the carrier-spread combinations were performed.

In general, fat and sugar content had little effect on flavour release and sensory perception of chocolate hazelnut spread. Addition of carriers increased aroma release and decreased flavour perception.

We conclude that *in vivo* nose space analysis by direct injection mass spectrometry (PTR-MS) and dynamic sensory method (TCATA) allowed to investigate aroma release and perception of real food matrices (spreads and composite foods). Flavour release and sensory perception of hazelnut chocolate spreads is strongly affected by addition of carriers. However, it seems that sensory perception of composite foods is modulated by cognitive mechanisms.

Keywords: Temporal-Check-All-That-Apply (TCATA), Aroma release, Proton Transfer Reaction–Time of Flight–Mass Spectrometry (PTR–ToF–MS), Composite food

Introduction

Even though the practice of eating is well known to all of us, the fundamental principles involved in flavour release and sensory perception of foods are not as obvious as they are normally perceived. For instance, they are both complex dynamic processes that depend on different variables. First, they depend on the aroma compounds that are released from the food matrix into the olfactory receptors located in the human nasal cavity through retronasal pathway [1]. Moreover, they will also be influenced by food composition, food structure and dynamic changes thereof during oral processing [2-4].

In the past years, studies have focused on the relationship between aroma release and perception by coupling *in vivo* flavour release analysis and dynamic sensory methods [5-10]. *In vivo* nose space analysis provides information on the molecules that are interacting with our receptors by analyzing the air coming out of the nostrils [11]. Because of its high resolution, the Proton-Transfer Reaction Mass-Spectrometry equipped with a Time of Flight Mass Analyzer (PTR-ToF-MS) can be used for breath analysis and nose space measurement during consumption of food [5, 12]. To better understand flavour perception, PTR-ToF-MS is often coupled with sensory methodologies such as Time Intensity (TI) methodology or Temporal Dominance of Sensations (TDS). Nevertheless, the selection of a single attribute at a time might give rise to dumping effects [13]. Temporal Check-All-That-Apply (TCATA) extends Check-All-That-Apply (CATA) to provide a more complete description of the dynamics of the sensory characteristics of a product. The assessors' task is to indicate and continually update the attributes that apply to the sample moment to moment. Multiple attributes from different modalities (e.g. taste and texture), can be selected simultaneously, which permit the description of sensations that arise concurrently, decreasing the chance for a dumping effect [14].

However, while most of the studies involve single or model foods that do not represent the real eating context, little is known about the flavour release and sensory perception of composite foods, even though they are commonly consumed. For example, bread, or wafer biscuits (carrier foods) are commonly consumed in combination with spreads. Composition, mechanical properties, and sensory characteristics of the carrier foods differ considerably from the spreads [15, 16]. Thus, the flavour release and sensory perception of the composite

food will be different from that of the single foods as the characteristics of one component will influence the flavour release and perception of the other components [16, 17]. For example, Van Eck et al. demonstrated that the carrier tends to dominate texture perception, whereas the condiment topping dominates flavour perception [17].

Characterizing composite foods is gaining interest not only because of the increased sensory complexity but also because they are more representative of the natural consumption context. Moreover, since flavour perception plays a key role in the liking of food and depends on different variables, a better understanding of how the release and fading of flavour compounds is perceived and how it contributes to liking, is needed. Thus, the aims of this study were (i) to investigate the effect of carrier addition on the flavour release and sensory perception of chocolate-hazelnut spread and (ii) to investigate the effect of fat and sugar content of chocolate-hazelnut spread on flavour release and sensory perception of a composite food using *in vivo* nose space analysis with PTR-ToF-MS and TCATA sensory analysis.

Experimental Design

Samples

Three chocolate hazelnut spreads varying in fat and sugar content (high fat/high sugar (control); high fat/ low sugar (15% reduction); low fat (15% reduction)/ high sugar), were used. All formulations were spiked with 0.2% (w/w) of an aroma solution containing 5 compounds: Benzaldehyde, Filbertone, delta-Dodecalactone, Isovaleraldehyde, and 2-Methylpyrazine (Table 1). These molecules were chosen because they present a rather wide range of chemical classes, and because their sensory properties are in line with chocolate-hazelnut spread.

Table 1. Characteristics of selected compounds used to spike the chocolate hazelnut spreads

Compound	Chemical formula	Sensory Attributes	Fragmentation pattern by PTR-MS:
Benzaldehyde	C ₇ H ₇ O	Similar to bitter almond	107.05
Filbertone	C ₈ H ₁₄ O	Hazelnut aroma	127.112
delta-Dodecalactone	C ₁₂ H ₂₂ O ₂	creamy, milky, buttery	199.1727/ 85.0683
Isovaleraldehyde	C ₅ H ₁₀ O	Chocolate, nutty, cocoa	87.077
2-Methylpyrazine	C ₅ H ₆ N ₂	Cocoa, nutty, roasted	95.0572

Composite foods were formed by combining all spreads with two different carriers (bread and wafer). Evaluations of the chocolate-hazelnut spreads without carriers and for the carrier-spread combinations were performed (n=9). All samples consisted of 6 grams of spread. The spreads evaluated alone were served on a plastic spoon. For the spread-wafer samples, wafer biscuits were pre-cut in the form of a shell with dimensions of 3cm*4cm (mean weight 1.56 ± 0.10 g), filled with the spread and packed. For the spread-bread combinations, bread (Morato Bruschelle, Italy) was cut in squares of 3cm*3cm without crust (mean weight 2.23 ± 0.50 g), and spread was served on top.

Subjects

Eight women (mean age 34.2 ± 7.4 years) were recruited for the nose space analysis and 72 (mean age 22.6 ± 2.0 years) for the sensory evaluation. Both cohorts consisted of volunteers from Edmund Mach Foundation (San Michele all'Adige (TN), Italy) and Wageningen University (Wageningen, The Netherlands), respectively. All participants were Caucasian women that consume hazelnut spread on regular basis. Other inclusion criteria were the following: not to have any dietary restrictions, non-pregnant, non-smoking, with no history of oral perception disorders or olfactory impairments (self-reported), no intolerance/allergy to any ingredient in chocolate-hazelnut spread. Participants gave a written informed consent before the start of the study.

In vivo nose space analysis

As part of a bigger project, the selected 8 panellists went through four training sessions of 60 min each. The experimental set up was adapted from previous PTR-ToF-MS nose space studies [6, 7]. A commercial PTR-ToF-MS 8000 instrument (Ionicon Analytik GmbH, Innsbruck, Austria) was used for the *in vivo* nose space analysis. The ionization conditions, with H_3O^+ to trace panellist breath [9], were the following: drift voltage 628V, at 110°C, and pressure of 2.80 mbar. Acquisition was set to 1 mass spectrum per second. Nose space sampling was carried out via two Teflon tubes placed in both nostrils of the assessors and connected to a heated device (N.A.S.E, IONICON at 110°C) which was directly connected into the inlet of the PTR-ToF-MS system. Evaluations took place in a laboratory with filtered air. Panellists were asked to insert the Teflon tubes in their nostrils and to start breathing normally through the nose keeping their mouth closed. Their breath was sampled for 60 s after which they were instructed to put the entire sample in their mouth and chew normally with their mouth closed. The time of the swallowing was standardized to 15 seconds for the spread served on its own, and 20 seconds for the bread and wafer combinations. Nose space data were acquired for 1 minute and 45 seconds. Between each sample, panellists were asked to clean their mouth with warm water. Panellists' breath was retested before each new measurement.

Sensory evaluation

Sensory evaluations took place in a testing room at Centrum voor Smaak Onderzoek, (Wageningen, The Netherlands), under normal light conditions at room temperature. Panellists evaluated the nine samples in one session of 60 minutes with short breaks in between. They received a pre-made attribute lists with definitions by email and were instructed to familiarize themselves with them. They were also asked not to smoke, eat, drink, and use any persistent-flavoured product for at least one hour before their session. Subjects seated individually and were provided with a tablet which the test was displayed on. For each sample, subjects were instructed to click on a start button concurrently with taking the whole sample in their mouth, and to immediately start tracking sensory changes. At any time between clicking start and the end of the evaluation time, they were free to check the terms that applied to describe the sensory characteristics of the sample at each moment and to uncheck the terms when they were no longer applicable. Just as in the nose space assessment, precise instructions were given regarding the moment at which assessors should swallow the sample and the total duration of the evaluation (1 minute and 45 seconds).

Results and discussion

In vivo nose space analysis

Mean time of maximum aroma concentration (Tmax) and area under the curve (AUC) were calculated for each compound separately. To test how these parameters differed across formulas and carriers, mixed model ANOVA was performed on Tmax and AUC, with formula, carrier and their interaction as fixed factors and subject as random one. Upon significance of the ANOVA, Tukey's HSD pairwise comparison was performed. Tmax was not affected by neither formula nor carrier, except for Isovaleraldehyde (m/z 87.0811), where there was a significant effect in the interaction between formula and carrier ($p < 0.05$). AUC of all compounds was significantly affected by the addition of carrier ($p < 0.05$). In general, when bread and wafer were added to the spread, there was an increase of the AUC. For example, in case of delta-Dodecalactone (m/z 85.0683), AUC increased of 165.8% on average after addition of bread across all formulations ($p < 0.05$) (Figure 1A). The same was observed for Filbertone (m/z 127.1140), where there was a significant increase of AUC of 14.0% and 12.9% in average across all formulations, with the addition of bread and wafer, respectively ($p < 0.05$). Finally, Isovaleraldehyde showed as well a significant increase of 53.1% and 56.8% with bread and wafer addition, respectively ($p < 0.05$). Overall, fat and sugar content did not affect flavour release significantly ($p > 0.05$), except for Isovaleraldehyde, where there was a significant decrease of AUC of 10.6% with the low sugar formulation, across all carriers.

Dynamic Sensory Perception

The addition of carrier (bread and wafer) influenced the sensory perception of the different spreads. For instance, citation proportion of the attribute *Milky*, which could be partly related with the release of delta-Dodecalactone, decreased significantly ($p < 0.05$) when bread and wafer were added, especially in the beginning of the consumption (Figure 1B). This was clearly observed in the control formulation and to a lesser extent in the low fat and low sugar formulations. Similar trends were observed for the attributes *Hazelnut* and *Cocoa*, which could be partly related to the release of Filbertone and Isovaleraldehyde, respectively. In both cases, the addition of a carrier led to a significant decrease ($p < 0.05$) in the perception of the attributes across the three formulations, in the beginning of the consumption time. Overall, fat and sugar content had little effect on the sensory perception of spreads ($p > 0.05$).

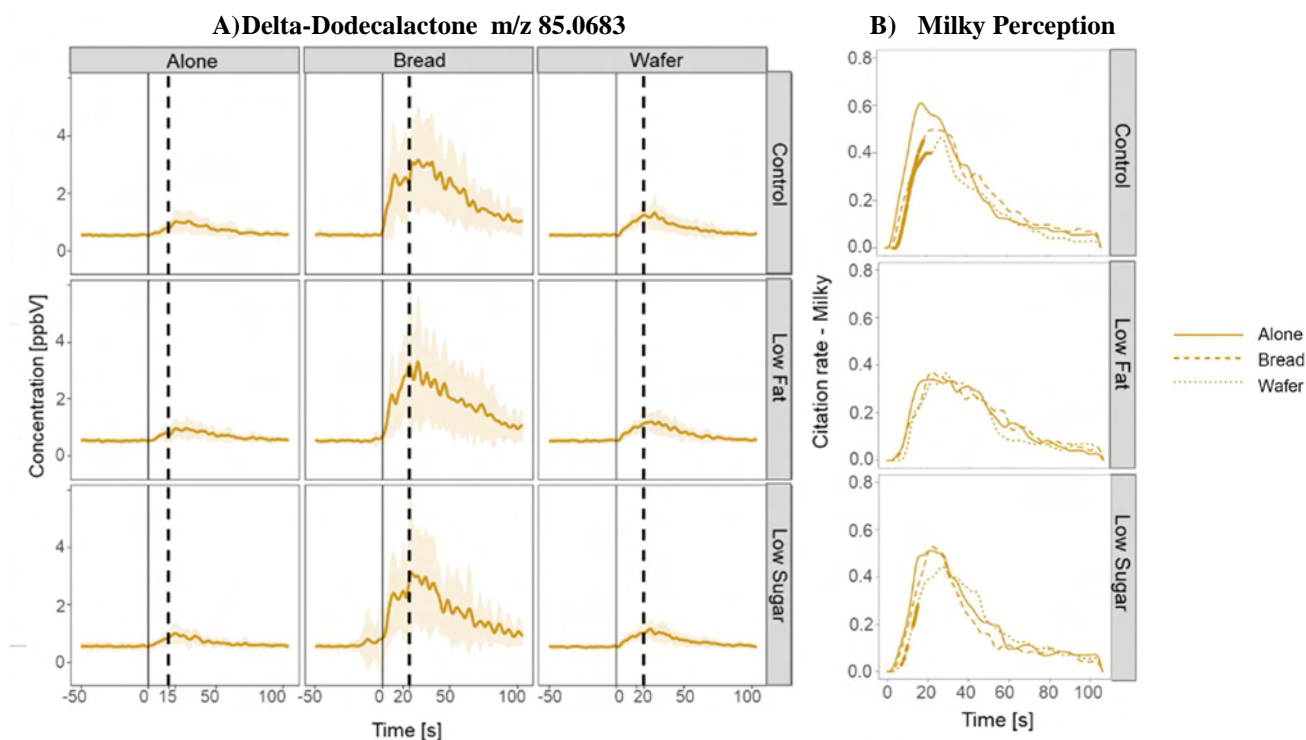


Figure 1: Averaged in-nose release ($n=8$ subjects in triplicate) of delta-Dodecalactone (a) and smoothed TCATA curves ($n=72$) for the attribute Milky (b). Black continuous and dotted lines represent moment when samples are put in the mouth, and swallowing moment, respectively. Shaded areas represent standard error of the mean. Periods of significant differences ($p < 0.05$) in proportion of citations in TCATA curves, compared to Spread Alone are indicated by highlighted thick sections.

To summarize, neither the composition nor the addition of carrier influenced time of maximum aroma concentration of any of the aroma molecules used to spike the spreads. Fat and sugar content had little effect on flavour release and sensory perception. When chocolate-hazelnut spreads were combined with a carrier (bread or wafer) aroma release was enhanced. This may be partly attributed to the difference of oral processing time between spreads alone (15 seconds) and spreads in combination with a carrier (20 seconds). In addition, spreads alone do not require chewing and they are just swirled around the mouth, while spread/carrier combinations require more chewing to breakdown the food, thus, inducing more aroma release. Besides, because of chewing and mixing, the surface area of spread-carrier combinations probably increased, allowing a higher transfer of aroma compounds from the spread into to the vapour phase [19]. Instinctively, it would be expected that this increase would also increase the sensory perception. However, the addition of a carrier, led to a decrease in sensory perception. This decrease is in line with previous studies where flavour intensity of a sauce/topping decreased with the addition of a solid food [19,18]. This reduction in perception is not due to a lower release of aromatic compounds into the nose space, but rather other factors may play a role. It has been suggested that cognitive effects play a role in the modulation of condiment-carrier perception, *i.e.* consumers pay more attention to texture and/or chewing with the presence of carriers [19].

Conclusion

We conclude that *in vivo* nose space analysis by direct injection mass spectrometry (PTR-ToF-MS) and dynamic sensory methods (TCATA) allowed to investigate aroma release and perception of real food matrices which not only increases the complexity of the food consumed, but also is more representative of the common consumption context. Moreover, coupling nose space with TCATA analysis, underlined the presence of cross modal associations between food texture and aroma perception in complex, real food matrices. Flavour release and sensory perception of hazelnut chocolate spreads is strongly affected by addition of carriers such as bread and wafer. Finally, it seems that perception of composite foods is modulated by cognitive effects.

References

1. Robert-Hazotte, A., et al., Ex vivo real-time monitoring of volatile metabolites resulting from nasal odorant metabolism. *Scientific Reports* 2019;9(1):1-13.
2. Tournier, C., C. Sulmont-Rossé, and E. Guichard, Flavour perception: aroma, taste and texture interactions. 2007, Global Science Books.
3. Buettner, A. and J. Beauchamp, Chemical input–Sensory output: Diverse modes of physiology–flavour interaction. *Food Quality and Preference* 2010;21(8):915-924.
4. Pointot, P., et al., How can aroma–related cross–modal interactions be analysed? A review of current methodologies. *Food Quality and Preference* 2013;28(1):304-316.
5. Heenan, S., et al., PTR-TOF-MS monitoring of in vitro and in vivo flavour release in cereal bars with varying sugar composition. *Food Chemistry* 2012;131(2):477-484.
6. Pedrotti, M., et al., Ethnicity, gender and physiological parameters: Their effect on in vivo flavour release and perception during chewing gum consumption. *Food Research International* 2019;116:57-70.
7. Charles, M., et al., Understanding flavour perception of espresso coffee by the combination of a dynamic sensory method and in-vivo nosespace analysis. *Food Research International* 2015;69:9-20.
8. Déléris, I., et al., The dynamics of aroma release during consumption of candies of different structures, and relationship with temporal perception. *Food Chemistry* 2011;127(4):1615-1624.
9. Weel, K.G., et al., Flavor release and perception of flavored whey protein gels: Perception is determined by texture rather than by release. *Journal of Agricultural and Food Chemistry* 2002;50(18):5149-5155.
10. Mesurolle, J., et al., Impact of fruit piece structure in yogurts on the dynamics of aroma release and sensory perception. *Molecules* 2013;18(5):6035-6056.
11. Biasioli, F., et al., PTR-MS monitoring of VOCs and BVOCs in food science and technology. *TrAC Trends in Analytical Chemistry* 2011;30(7):968-977.
12. Déléris, I., et al., Comparison of direct mass spectrometry methods for the on-line analysis of volatile compounds in foods. *Journal of Mass Spectrometry* 2013;48(5):594-607.
13. Varela, P., et al., What is dominance? An exploration of the concept in TDS tests with trained assessors and consumers. *Food Quality and Preference* 2018;64:72-81.
14. Castura, J.C., et al., Temporal Check-All-That-Apply (TCATA): A novel dynamic method for characterizing products. *Food Quality and Preference* 2016;47:79-90.
15. de Lavergne, M.D., et al., Dynamic texture perception, oral processing behaviour and bolus properties of emulsion-filled gels with and without contrasting mechanical properties. *Food Hydrocolloids* 2016;52:648-660.
16. Scholten, E., Composite foods: from structure to sensory perception. *Food & Function* 2017;8(2):481-497.
17. van Eck, A., et al., Oral processing behavior and dynamic sensory perception of composite foods: Toppings assist saliva in bolus formation. *Food Quality and Preference* 2019;71:497-509.
18. Cherdchu, P. and E. Chambers IV, Effect of carriers on descriptive sensory characteristics: A case study with soy sauce. *Journal of Sensory Studies* 2014;29(4):272-284.
19. van Eck, A., et al., What drives in vivo aroma release and perception of condiments consumed with carrier foods?, submitted.

Impact of capsaicin on salt release and salt perception during consumption of salt and salt-capsaicin solutions

NI YANG¹, Qian Yang¹, Jing Zhao¹, Xiaolei Fan¹, Jianshe Chen², and Ian Fisk¹

¹ Division of Food, Nutrition and Dietetics, School of Biosciences, University of Nottingham, U.K.

² Laboratory of Food Oral Processing, School of Food Science and Biotechnology, Zhejiang Gongshang University, Hangzhou, China. ni.yang@nottingham.ac.uk

Abstract

The mechanism on how capsaicin could affect salt release in the mouth and its saltiness perception was unknown. This is the first study designed to investigate the impact of capsaicin on salt release in the tongue and correlate with its perception during and after consumption. A simple 1% NaCl solution was used without or with 5 ppm capsaicin as CTR or CAP solution, respectively. Thirty panellists were recruited and trained to score salt and spicy intensity when holding the sample in the mouth for 10 s, then for every 10 s after swallowing till 60 s. Swab analysis was used to investigate the level of salt released after consumption of CTR or CAP solution every 10 s till 60 s. The results indicated that the saltiness rating was significantly reduced by 13% as the result of capsaicin ($P < 0.05$), which could be due to the dilution effect by extra capsaicin-stimulated saliva. Individual panellists varied on their saltiness and spiciness scores, but there was a positive Pearson's correlation between saltiness and spiciness scores ($P < 0.05$), that is, the higher the spiciness ratings, the higher the saltiness ratings. This indicated a potential multimodal interaction between trigeminal and taste sensation.

Keywords: chilli, spicy, capsaicin, salt, perception

Introduction

Excessive salt intake in our diet has been linked with the onset of hypertension and its cardiovascular complications [1], and a large cohort study (over 13,000 Chinese adults followed for 9 years) revealed that chilli intake was inversely associated with the risk of developing hypertension [2]. Another study [3] indicated that enjoyment of spicy food may significantly reduce individual salt preference, daily salt intake and blood pressure by modifying the neural processing of salt taste in the brain. However, the mechanism on how spicy food could affect salt release in the mouth and its saltiness perception was unknown. Capsaicin, as one of the major functional components in spicy food, is known to trigger the trigeminal sensation in the mouth [4]. This study was designed to investigate the impact of capsaicin on salt release and perception from a simple matrix- 1% sodium chloride solution.

Experimental

Sample solution preparation

Capsaicin stock solution (1%) was prepared by dissolving capsaicin (0.1 g) with food-grade ethanol (10 g). Salt stock solution (1 L) of 1% NaCl was prepared with pure water (Purite Ltd, Oxon, UK), then half of the stock solution (0.5 L) was used as control solution (CTR), and 250 μ L of 1% capsaicin was added to another 0.5 L to make 5 ppm capsaicin solution (CAP).

Panel recruitment

Thirty panellists (age 22-35, 8 males, 22 females) at the University of Nottingham were recruited. The frequency of their chilli consumption was recorded and varied between 0-7 times per week (37% consumed less than 3 times, 43% had 3-5 times, and 27% more than 5 times). Every panellist attended two separate sessions: one for salt release analysis, and another for sensory analysis.

Swab analysis

According to an established protocol [4], every panellist firstly rinsed their mouth with 10 mL water, and swab at the top of their tongue with a pre-weighted cotton bud (regard at 0 s). Then they received a randomised sample solution (10 mL) with a 3-digital code, and they swallowed the solution after holding for 10 s, the second swab was taken at 10 s, and they swabbed every 10 s till 60 s. They took 5 min break between samples to rinse their mouth with water, and triplicates samples were given for each solution. All the swabs were extracted by 10 mL of methanol/water (50/50) solution, and their sodium levels were measured by Flame Photometry (Sherwood Scientific Ltd., Model 410, Cambridge, UK), followed a standard method [5].

Sensory analysis

Sequential profiling in this study used a similar protocol as the previous chilli study [6], and the perceived intensity of saltiness and spiciness was recorded by Compusense™ (Guelph, Canada). A training session was given for every panellist to practice the scoring method using trial samples following a similar procedure as swab analysis: i) holding 10 mL of solution for 10 s, scoring its salty and spicy intensity; ii) swallowing at 10 s, and scoring salty and spiciness every 10 s till 60 s. There was 5 min break between samples to rinse their mouth with water and each solution was measured in triplicates with a randomised order.

Data analysis

A total of 1260 data were collected from swab analysis (30 pp x 3 reps x 7 time-points x 2 solutions), and sensory analysis collected 2520 data (30 pp x 3 reps x 7-time points x 2 solutions x 2 attributes). All the statistical data analysis was done by SPSS (IBM® SPSS® Statistics version 25) and XLSTAT Software ©-Pro (2020.1.3, Addinsoft, Inc). Analysis of variance analysis (ANOVA) was conducted to confirm any significant differences ($P < 0.05$).

Results and discussion

The average sodium level during the 60 s observation period was calculated for both CTR and CAP solutions (Figure 1a). The results indicated that there was a 14% lower level in CAP than CTR, which could be due to the saliva dilution effect. It was reported that 5 ppm capsaicin solution could stimulate an extra 92% saliva over 60 s period [6], so additional saliva could dilute any salt on the tongue before and after swallowing the solution.

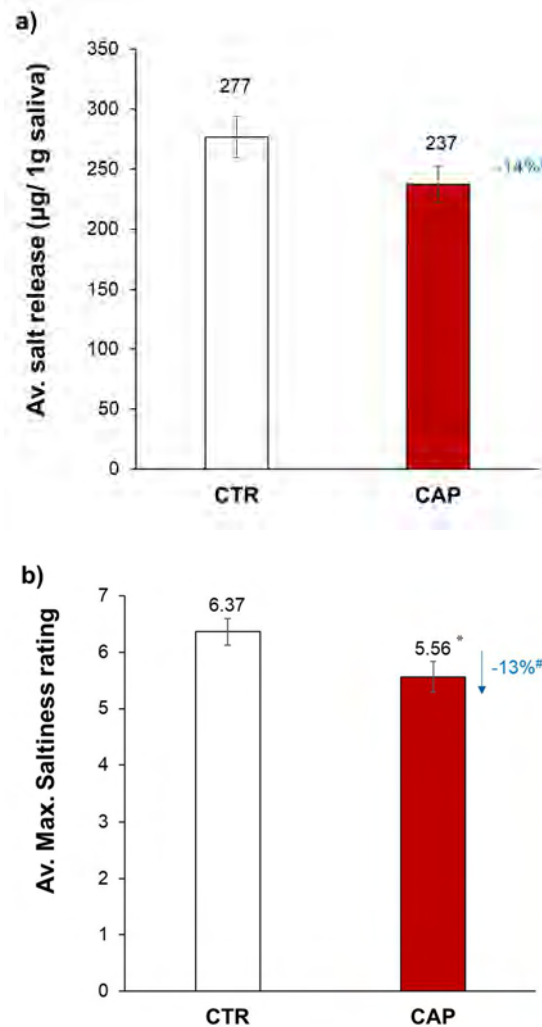


Figure 1: a) average salt release ($\mu\text{g}/1\text{g}$ saliva) and b) average of the maximum saltiness rating for CTR (white bar) and CAP (red bar) with standard error bars (30 panellists, 3 reps, 7-time points). # indicated % change as $(\text{CAP}-\text{CTR})/\text{CAP} * 100\%$; * indicated a significant difference at $p < 0.05$.

Additionally, the maximum saltiness rating was averaged between all the panellists (Figure 1b). A similar reduction of 13% in saltiness perception was found, which might correlate to the lower level of salt released during this period. Statically, there is a significant reduction in saltiness perception for CAP, compared to the CTR ($p < 0.05$).

Dynamic profile for salt release was summarised in Figure 2a). The maximum sodium level was reached at 10 s immediately after swallowing the solution, and then the level decreased with time. Generally, CAP had a lower level than CTR after swallowing, which might be caused by the dilution effect by extra saliva secreted by capsaicin.

The perceived saltiness also decreased with time (Figure 2b), and the maximum saltiness perception for CTR reached 10 s when swallowing, but the maximum salty perception for CAP was at 0 s when holding the solution. Saltiness ratings were significantly lower in CAP than in CTR ($p < 0.05$), so capsaicin in salt solution significantly reduced its saltiness perception.

The spiciness rating over 60 s (Figure 2c) illustrated a significant difference between CTR and CAP ($p < 0.05$). Spiciness rating for CAP reached its maximum at 20 s, that is, 10 s after swallowing the solution, so the results illustrated the delayed effect of spiciness perception. Then the spiciness perception reduced gradually with time till 60 s, but the rating at 60 s remained much higher than the maximum spicy rating for CTR, which indicated a long-lasting spicy sensation by capsaicin stimulation. Interesting, CTR solution without any capsaicin had an average spiciness score ~ 2 at 0 s, which may be due to the panellists were forced to make a choice and some of them might consider 1% salt solution as irritation and scored its spiciness when holding the salt solution. There might also be a “halo” effect as both attributes (spiciness and saltiness) were scored at the same time, so some panellists were likely to rate spiciness the same way as they rated saltiness.

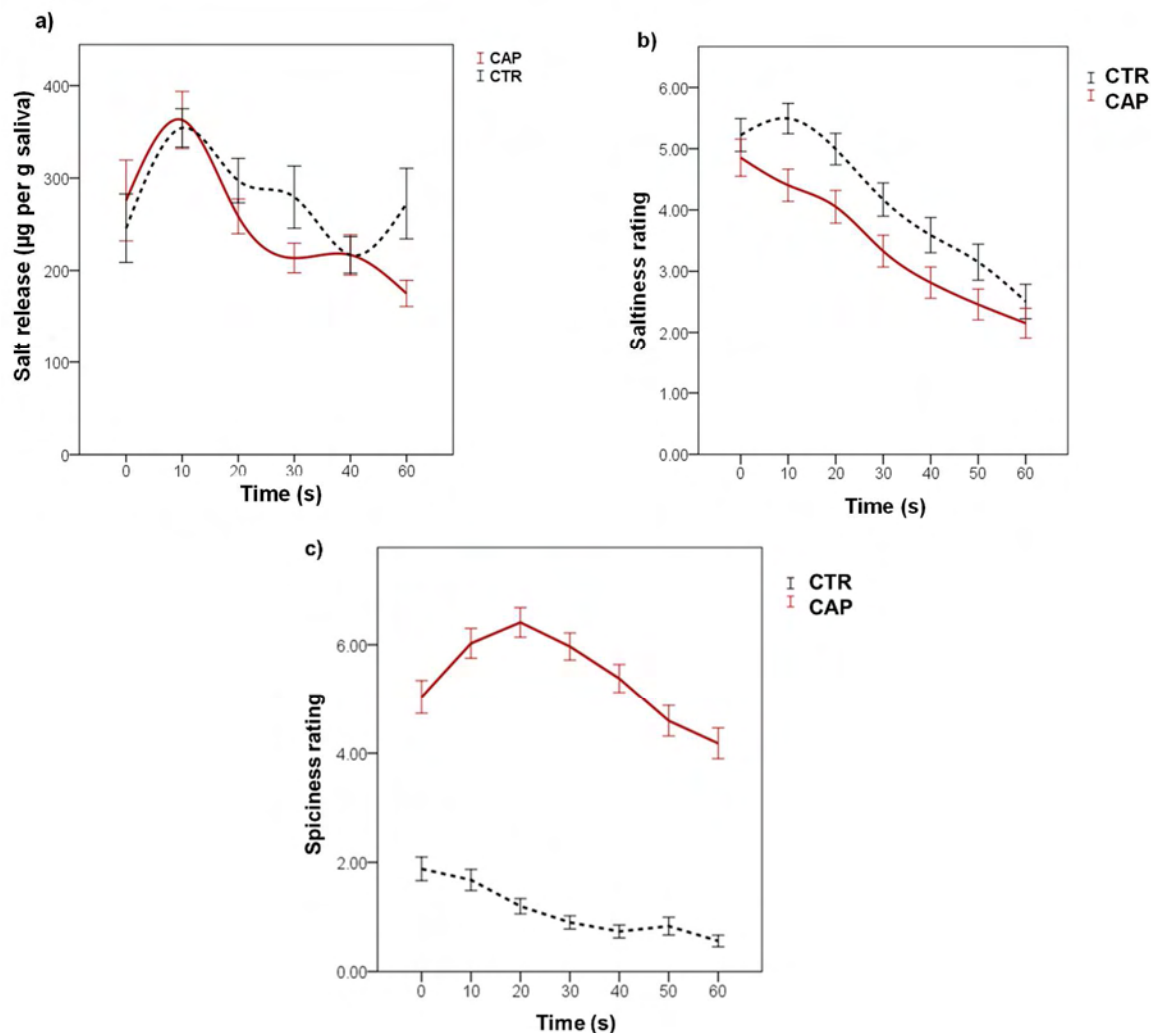


Figure 2: a) salt release ($\mu\text{g}/ 1\text{g saliva}$), b) saltiness rating, and c) spiciness rating over 60 s for CTR (black dashed line) and CAP (red solid line) when solutions were held in the mouth for 10 s and swallowed after 10 s till 60 s. The standard error is shown as \pm error bar (30 panellists, 3 reps).

The average spiciness and saltiness scores for every panellist were calculated and plotted in Figure 3. The control samples (Figure 3a) indicated that the range of average saltiness ratings (y-axis) was from 1 to 8, so there was an individual difference in their saltiness perception. However, without adding any capsaicin, most people gave a relatively low spiciness rating (< 3). The spiciness scores (x-axis) of CAP samples (Figure 3b) illustrated a wide rating range (1-8), and there was a significant Pearson's correlation ($p < 0.05$) between spiciness and saltiness ratings, i.e., the higher the spiciness rating, the higher the saltiness rating. This might indicate a multimodal interaction between trigeminal and taste sensation, as a recent study also reported a potential multisensory interaction between capsaicin-triggered trigeminal sensation and aroma perception [6].

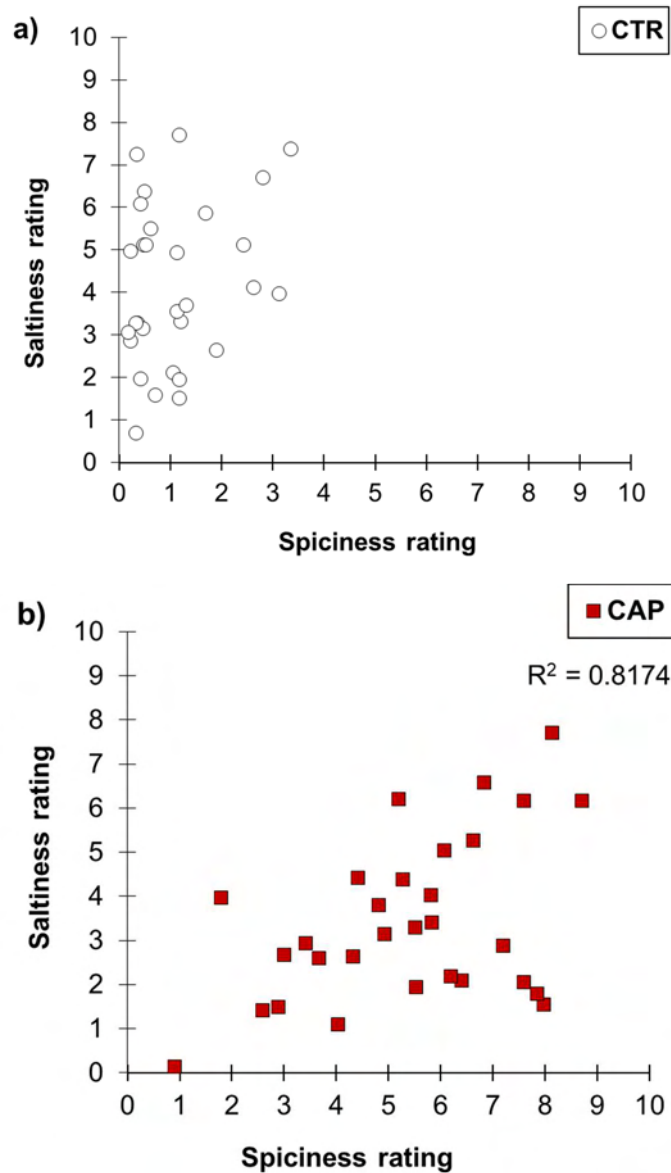


Figure 3: Scatter plot of maximum spiciness rating against maximum aroma perception for CTR (white dot) and CAP (red square). R^2 value is the coefficient of determination based on Pearson's correlation ($p < 0.05$).

Conclusion

This study first demonstrated that capsaicin caused a significant reduction in saltiness perception by 13%, and this could be due to the dilution effect by extra saliva with capsaicin stimulation. The individual variations were observed on the saltiness and spiciness ratings, but saltiness ratings were found to be positively correlated with spiciness ratings, so there might be a multimodal interaction between trigeminal and taste sensation. The swab analysis and sensory methods established in the simple salt solution can be further applied into other matrices,

such as more complicated dry food systems, which would allow capsaicin-stimulated saliva to penetrate the matrix and release the embedded salt to the tongue more effectively and lead to a more significant impact on its release and perception.

References

1. WHO. (2012) Guideline: Sodium intake for adults and children. <https://www.who.int/publications-detail/sodium-intake-for-adults-and-children>
2. Shi Z, Riley M, Brown A, Page A. Chilli intake is inversely associated with hypertension among adults Clin. Nutr. ESPE. 2018;23: 67-72.
3. Li Q, Cui Y, Jin R, Lang H, Yu H, Sun F, et al. Enjoyment of Spicy Flavor Enhances Central Salty-Taste Perception and Reduces Salt Intake and Blood Pressure. Hypertension. 2017;70(6):1291-1299.
4. Rama R, Chiu N, Carvalho Da Silva M, Hewson L, Hort J, Fisk I. Impact of Salt Crystal Size on in-Mouth Delivery of Sodium and Saltiness Perception from Snack Foods. J Texture Stud. 2013;44(5):338-345.
5. Chiu N, Hewson L, Yang N, Linforth R, Fisk I. Controlling salt and aroma perception through the inclusion of air fillers. Lebensm-Wiss Technol-Food Sci Technol. 2015;63(1):65-70.
6. Yang N, Yang Q, Chen J, Fisk I. Impact of capsaicin on aroma release and perception from flavoured solutions. Lebensm-Wiss Technol-Food Sci Technol. 2021;138:110613.

Impact of smoked water on umami and salt taste

KANOKKAN PANCHAN¹, Stella Lignou¹, Huw D. Griffiths², David A. Baines³ and Jane K. Parker¹

¹ Department of Food and Nutritional Sciences, University of Reading, UK, k.panchan@pgr.reading.ac.uk

² Besmoke Ltd. Unit B1, Ford Airfield Industrial Estate, Arundel BN18 0HY, UK

³ Baines Food Consultancy Ltd., 22 Elizabeth Close, Thornbury, Bristol, BS35 2YN, UK

Abstract

The aim of this study was to investigate whether the use of smoked ingredients could enhance either salty or umami taste, whether any enhancement was due to taste-active or taste-enhancing compounds, and whether smoky aroma induced taste enhancement. A trained sensory panel (n=12) performed three-Alternative Forced Choice (3-AFC) discrimination tests with nose clips on to assess taste-active and taste-enhancing compounds in smoked water. The first set of 3-AFC discrimination tests investigated whether there were any tastes, particularly salty or umami, in water with addition of 1% of a commercial smoked water. The second set of 3-AFC tests investigated whether the smoked water contained umami-enhancing compounds when mixed with various concentrations of MSG and /or ribonucleotides in water. Set 3 was similar but was carried out in a model chicken soup containing MSG with or without ribonucleotides. Our data show that the addition of smoked water can increase the umami taste in aqueous solutions, but this is masked in more complex matrices. This means we can investigate odour-induced taste enhancement of smoked water, in the knowledge that there will be minimal contribution to the umami and salty taste from the smoked water.

Keywords: smoked water, taste, umami, salty, discrimination tests, 3-AFC

Introduction

The reduction in sodium content in order to comply with recent regulations [1] is often linked to a decrease in the consumer acceptance due to the loss of saltiness and the taste of food products. The use of a flavour enhancer to enhance saltiness or umami through multi-sensory integration of cross-modal odour-taste interaction has been shown to be an effective and promising method to compensate for the loss of salty taste when salt reduction strategies are implemented [2, 3]. Typically, flavour enhancers such as the amino acid L-glutamate and/or 5'-ribonucleotides are used to enhance the savoury flavour of food products; besides, it can also be used to enhance other fundamental tastes, such as saltiness or sweetness [4]. Smoked ingredients are renowned for their aromatic character and we suggest that they play a part in improving the perception of taste, especially salty and umami taste. The aim of this study was to investigate the three possible mechanisms for taste enhancement that may arise from incorporation of smoked ingredients such as smoked water into simple mixtures and real food products. The smoke may contain tastants or taste enhancers, or the enhancement could be due to cross-modal interactions. Two different smoked waters were tested: traditional apple-wood smoked water (TRAD) and apple-wood water prepared using PureSmoke Technology (PST) [5] which is a patented process to remove carcinogens (polyaromatic hydrocarbons) from the smoke [6].

Experimental

Preliminary screening with fresh soup samples

For initial screening, a commercial ASDA chicken and vegetable broth (Asda Stores Ltd., Leeds, UK) was passed through a kitchen sieve to remove the chunks prior to addition of the smoked water. Sieved fresh commercial soup with or without 1% TRAD smoked water was presented to 11 panellists, once for each taste modality. The panellists wore nose clips and were asked to choose the sample with the strongest taste (sweet, sour, salty, umami and bitter).

Determination of appropriate MSG concentration

Nine serial dilutions of MSG were used to select the appropriate concentration for the discrimination tests. For the serial dilution, MSG (4.65 g) was dissolved in filtered tap water (Maxtra MicroFlow Technology, Germany) and made up to 500 mL (concentration = 9300 mg/L) corresponding to MSG level 9. Eight serial dilutions of MSG were prepared using a ratio of 60 mL MSG: 120 mL water. Each MSG dilution (15 mL) was presented in disposable cups, labelled number 1-9, respectively and presented to the sensory panellists who rated their perception of intensity on a general labelled magnitude scale (gLMS).

Preparation of the aqueous model solutions

Filtered tap water with or without 1% smoked water was used to investigate taste-active compounds. For the investigation of taste-enhancing compounds, four concentrations of MSG determined as above (0, 0.004, 0.012, and 0.034%) were prepared with or without the addition of a 1:1 mix of disodium inosine-5'-monophosphate (IMP) and disodium guanosine-5'-monophosphate (GMP) each at 0.007% (Ribo).

Preparation of model chicken soup

A chicken soup powder base comprised of corn flour, creamer, whole milk powder, granulated sugar, onion powder, ground sage, parsley flakes, pepper extract, turmeric extract, salt and chicken flavourings (free from MSG and ribonucleotides). This instant chicken soup powder (26 g) was made up with 250 mL boiling filtered tap water to make a standard 0.50% NaCl model soup.

Sensory evaluation

A screened and trained sensory panel (n = 12; 1 male and 11 female) was used, each member with a minimum of 1 years' experience and with expertise in discrimination techniques. Sensory evaluation was carried out in individual booths and the soup served at 75-80 °C in 20 mL tasting cups. The panellists wore nose clips for all discrimination tests. Full-fat natural set yogurt, cucumber slices, and filtered tap water were provided as palate cleansers between samples and during an enforced break. All tests were performed in duplicate and a 2-min rest was imposed between duplicates.

Taste and taste-enhancing activity of smoked water

The 3-AFC discrimination test was used to determine whether panellists could discriminate between samples. To see whether the smoked water contained any taste-active compounds, tests were conducted in water. Tests carried out in monosodium glutamate (MSG) and/or ribonucleotides solutions and in model chicken soups were used to check for any taste-enhancing activity. For all experiments, two control samples without smoked water and one sample containing smoked water at 1% were prepared. Approximately 15 mL of each sample was poured into a tasting cup labelled with a random three-digit numbers and served to the panellists in a balanced order. Panellists wore a nose clip during tasting. They were presented with three samples, asked to taste all three samples in the order presented and to identify the sample that was the saltiest or had the most umami taste.

Data collection and analysis

All data obtained from the discrimination testing by the three-Alternative Forced Choice (3-AFC) method were analysed using the Thurstonian model in XLSTAT Version 2018.5 (Addinsoft, New York, USA) to determine if a significant difference existed between the samples. In all cases, the samples were considered significantly different if $p < 0.05$.

Results and discussion

Preliminary screening with fresh soup samples

Screening for different taste modalities in fresh soup showed that 8/11 panellists selected the sample with smoke as the saltiest, 7/11 as the most umami, 5/11 for sweetness, 3/11 for bitterness and 2/11 for sourness. This indicated that salty and umami should be monitored in discrimination tests to investigate taste-active and taste-enhancing compounds in smoked water.

Determination of appropriate MSG concentration

To investigate the potential taste-enhancing properties of smoked water when incorporated with MSG and/or ribonucleotides, the acceptable concentrations of MSG for each panellist was first evaluated (shown in Figure 1). Level 5 was ideal for 9/12 panellists who rated the umami intensity between 10 and 50 on the gLMS scale, but level 6 was also included in order for panellists F and K to perceive the umami taste. Level 4 was also included to see if smoke aroma could boost umami levels in MSG close to threshold. Levels 4, 5 and 6, corresponding to 38, 115, 344 mg/L respectively (or 0.004, 0.012 and 0.038% as used in Table 1), were selected based on the concentrations that most of the panellists could detect, but was not overly strong. These results are consistent with the published average detection threshold for MSG, which is 0.03% [7].

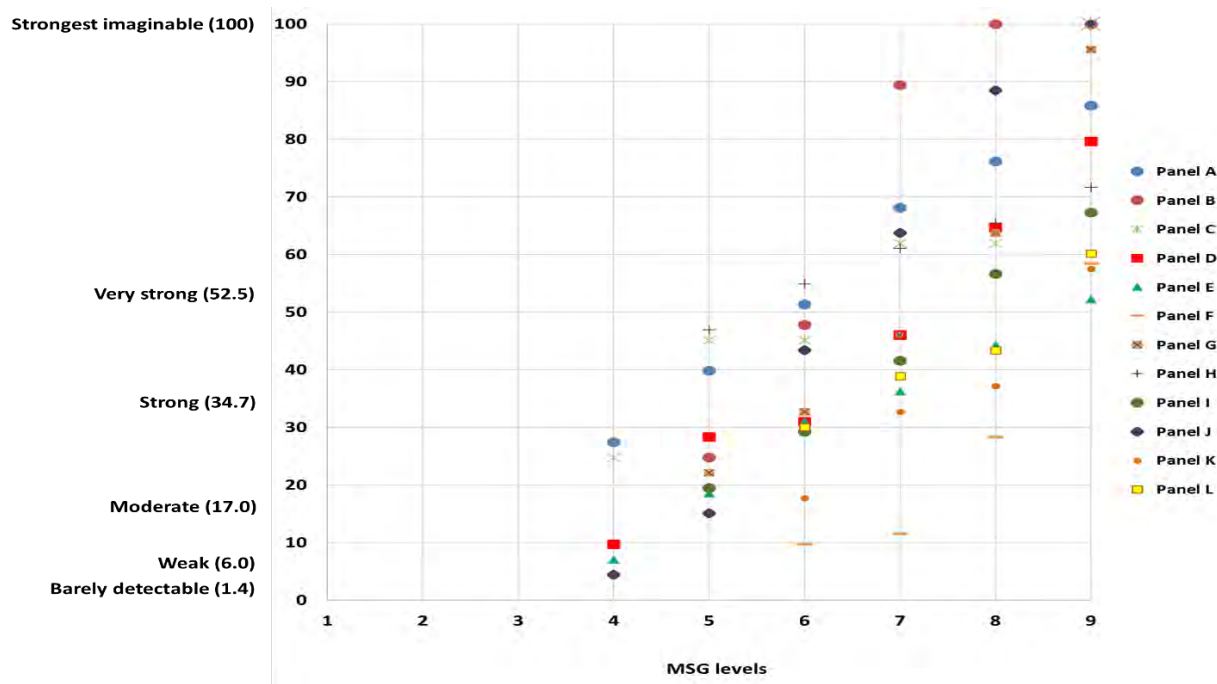


Figure 1: Ratings of umami intensity on a general labelled magnitude scale (0-100) from the preliminary study to determine acceptable concentrations of MSG for the panel ($n=12$; Panel A-L) using serial dilutions of MSG (levels 1-9; 1.42, 4.25, 12.76, 38, 115, 344, 1033, 3100, and 9300 mg/L, respectively).

Taste and taste-enhancing activity of smoked ingredient

The results of the discrimination tests are shown in table 1. The results show that there was a significant increase in umami taste when 1% smoked water was added to tap water (both TRAD and PST smoke) (experiment 1b), but no significant difference in salty taste (experiment 1a). These results suggest that there may be non-volatile taste-active compounds in these smoked waters, which elicit an umami taste.

There was also a significant increase in umami taste when 1% smoked water was added to water containing 0.007% ribonucleotides (subthreshold) for both TRAD and PST (experiment 2e), and in the case of PST, the larger d' may indicate a synergy between the nucleotides and the components in the smoked water. However, in the model soup (experiments 3a and 3e), the increase in umami was only found in TRAD (with ribonucleotides) and not in PST, and differences may have been masked by the other components of the soup.

In the presence of low levels of MSG (Level 4) (experiments 2b, 2f, 3b, 3f), where the MSG was subthreshold for 7/12 panellists, one might still expect panellists to observe the umami taste in the smoked water, however the results were a bit inconclusive. In three out of the eight discrimination tests at level 4 MSG, there was a significant increase in umami when smoked water was added, but there was no consistency. One discrimination test was significant in water but two in soup, two in TRAD and one in PST, and two with ribonucleotides and one without. In water with TRAD, there was a significant umami increase with smoked water, that was not observed when the ribonucleotides were also present (experiments 2b vs 2f). In the model soup, the pattern was different with both TRAD and PST showing significant differences for level 4, only if the ribonucleotides were present (experiment 3b vs. 3f). In the presence of Levels 5 and 6 MSG, only one out of the eight discrimination tests was significant.

Conclusion

We can conclude that, in the absence of MSG, the panel perceived an umami taste when the smoked water was present. At peri-threshold levels of MSG, the panel may detect an increase in umami taste, but there was no evidence of any synergy. At suprathreshold levels of MSG, any additional enhancement from the smoked water was insignificant. The data were not entirely consistent but suggest that the smoked water may contribute an umami taste when not overwhelmed by MSG or other components in the food. This gives us confidence to proceed with investigating odour-induced taste enhancement in model soups, knowing that any enhancements observed will not be due to taste properties of smoked water.

Table 1: Results of 3-AFC tests.

Expt ^a No	Sample base	MSG (%)	Ribo ^b (%)	TRAD ^c smoke p-value ^e	TRAD ^c smoke <i>d'</i> ^f	PST ^d smoke p-value ^e	PST ^d smoke <i>d'</i> ^f
Set 1a Tastant properties (salty)							
1a	Water	0	0	0.108	0.559	0.453	0.148
Set 1b Tastant properties (umami)							
1b/2a	Water	0	0	0.004	1.116	0.004	1.191
Set 2 Taste-enhancing properties in water (umami)							
2b	Water	0.004	0	0.003	1.010	0.092	0.559
2c	Water	0.012	0	0.638	nd	0.339	0.232
2d	Water	0.034	0	0.079	0.559	0.521	0.061
2e	Water	0	0.007	0.017	1.032	<0.001	1.710
2f	Water	0.004	0.007	0.895	nd	0.453	0.148
2g	Water	0.012	0.007	0.149	0.559	0.453	0.148
2h	Water	0.034	0.007	0.310	0.327	0.263	0.356
Set 3 Taste-enhancing properties in model soup (umami)							
3a	Model soup	0	0	0.293	0.262	0.068	0.559
3b	Model soup	0.004	0	0.263	0.356	0.339	0.232
3c	Model soup	0.012	0	0.092	0.559	0.108	0.559
3d	Model soup	0.034	0	0.191	0.397	0.521	0.061
3e	Model soup	0	0.007	0.019	1.116	0.263	0.356
3f	Model soup	0.004	0.007	0.004	1.432	0.004	1.191
3g	Model soup	0.012	0.007	0.019	1.116	0.263	0.356
3h	Model soup	0.034	0.007	0.178	0.559	0.016	0.971

^aIn all experiments, the panellists were asked to select the sample with the greatest umami taste, except in experiment 1a where they selected the sample with the greatest salty taste; ^bRibo = addition of a 50:50 mix of 5'IMP and 5'GMP each at 0.007%; ^cTRAD is the smoked water which had been prepared using a traditional smoking method; ^dPST is the smoked water which had been treated with the PureSmoke™ Technology to remove PAHs; ^ep-values were generated using the Thurstonian model, the samples were considered significantly different at the 5% significance level; ^f*d'* is the distance in perceptual standard deviations between sample pairs used for each sample, as determined by Thurstonian calculations; numbers in bold represent a significant p-value; nd = value for *d'* could not be determined.

References

1. World Health Organization. Reducing salt intake in populations. Report of a WHO forum and technical meeting 5-7 October 2006. Paris, France, 2007.
2. Lawrence G, Salles C, Septier C, Busch J, Thomas-Danguin T. Odour-taste interactions: A way to enhance saltiness in low-salt contents solutions. *Food Qual Prefer.* 2009;20:241-248.
3. Thomas-Danguin T, Guichard E, Salles C. Cross-modal interactions as a strategy to enhance salty taste and to maintain liking of low-salt food: a review. *Food Funct.* 2019;10:5269-5281.
4. Methven, L. Natural food and beverage flavour enhancer. In: Baines DA and Seal R, editors. *Natural food additives, ingredients and flavourings.* Woodhead Publishing; 2012. p. 76-99.
5. Parker JK, Lignou S, Shankland K, Kurwie P, Griffiths HD, Baines DA. Development of a zeolite filter for removing polycyclic aromatic hydrocarbons (PAHs) from smoke and smoked ingredients while retaining the smoky flavor. *J Agric Food Chem.* 2018;66:2449-2458.
6. Baines DA, Griffiths HD, Parker JK. Puresmoke Ltd. (2014). *Smoked Food, method for smoking food and apparatus therefor.* WO2015007742 A1.
7. Baines D, Brown M. Flavor enhancers: characteristics and uses. *Encyclopedia of Food and Health, Elsevier.* 2016:716-723.

Volatile compounds in the vehicle-interior: Odorants of an aqueous cavity preservation and beyond

FLORIAN BUCHECKER^{1,2}, Helene M. Loos^{1,3} and Andrea Buettner^{1,3}

¹ Friedrich-Alexander-Universität Erlangen-Nürnberg, Erlangen, Germany

² BMW Group, Munich, Germany

³ Fraunhofer Institute for Process Engineering and Packaging IVV, Freising, Germany

Florian.Buecheker@bmw.de

Abstract

The smell of the vehicle-interior of cars, especially new cars, can be very distinct. Amongst other sources, we here discuss one material aspect that has hitherto not been further considered: the odour of an aqueous cavity preservation may be perceived in the vehicle interior as volatile compounds of the anti-corrosion agent can easily penetrate the vehicle cabin. To investigate the respective odour-active compounds, an automotive wax-based aqueous cavity preservation was analysed by extracting the volatiles with dichloromethane, followed by isolation of volatiles via solvent-assisted flavour evaporation. Screening via gas chromatography-olfactometry revealed eleven odour-active compounds, of which γ -lactones and carboxylic acids exhibited high odour potency. The results are discussed in relation to other studies focusing on the odorants of materials in the vehicle-interior, where mainly plastics and seat covers have been investigated so far. It is interesting to note that γ -lactones like γ -nonalactone and carboxylic acids like butanoic acid have also been reported in these studies, suggesting that, due to their diverse material sources, these substance classes generally contribute to the odour of the vehicle-interior.

Keywords: cavity wax, vehicle-interior, odour, gas chromatography, olfactometry

Introduction

An aqueous cavity preservation is used in vehicles as a rust prevention agent. It is applied as a liquid to the inner part of the vehicle body and hardens by evaporation of water. Environmental influences such as rain, coastal climate with high salt content or intrusion of road salt into the cavities of a vehicle body favour corrosion in uncoated areas [1]. A cavity preservation consists of waxes which protect the structural parts of the car as a barrier through their hydrophobicity, and thus prevent metal corrosion. Cavity preservations exhibit a typical odour. Negative pressure in a vehicle-interior, caused by an open sunroof or window [2], can thus result in the transfer of this typical odour into the vehicle-interior.

Instrumental analyses of vehicle manufacturers and suppliers mainly target the identification of substances by gas chromatography-mass spectrometry (GC-MS) and human sensory evaluation is often only performed by rating the overall odour of the car. Thereby, general emissions of single volatile organic compounds into the vehicle-interior have been intensively studied, with the aim of elucidating their impact on the air quality of the indoor air of the passenger cabin [3]. However, sound knowledge with respect to the odour-contributing substances, especially those that are present at trace level, is not yet at hand, especially with respect to aqueous cavity preservations.

To fill this gap, we designed an experimental set-up to first simulate the hardening of an aqueous cavity preservation, and then characterize the odour-active compounds by using GC-O (gas chromatography-olfactometry) and 2D-GC-MS/O (two-dimensional gas chromatography mass-spectrometry/ olfactometry). We then relate the obtained results to previous reports of odorous substances in the car interior and we further discuss potential sources of odorants in the vehicle-interior. Additionally, we provide an overview of the most potent odorants of the materials in the vehicle-interior which have been investigated by GC-O so far.

Experimental

Material

The wax-based aqueous cavity preservation was provided by a paint shop in a vehicle assembly plant of the BMW Group and was obtained as a bulk liquid. Nine g of the liquid aqueous cavity preservation were applied on a 0.05 m² metal sheet ensuring equal distribution and afterwards, the metal sheet was stored in a darkened room with air exchange at ambient temperature to simulate hardening. After seven days, the sample was further investigated.

Sample workup

Solvent extraction was accomplished by stirring 0.68 g of the hardened aqueous cavity preservation in 200 mL dichloromethane (DCM) for 1 h. Subsequently, non-volatile compounds were removed from the volatiles by means of the solvent-assisted flavour evaporation (SAFE) technique [4]. The DCM distillate containing the volatile fraction was then dried, filtered, and concentrated to a total volume of 100 μ L at 50°C by using Vigreux and microdistillation according to Bemelmans [5]. The main odorants detected were identified as described in the following section.

Identification with gas chromatography-olfactometry (GC-O) and two-dimensional gas chromatography with mass spectrometry and olfactometry (2D-GC-MS/O)

The identification of the odour-active compounds was based on the comparison of odour quality, retention indices on two capillaries with different polarities and mass spectra with those of authentic reference compounds. GC-O was performed using a gas chromatograph (TRACE GC Ultra; Thermo Fischer Scientific, Waltham, USA) equipped with a cold on column injector on a DB-5 or DB-FFAP capillary column, respectively (both 30 m x 0.32 mm, film thickness 0.25 μ m; J & W Scientific Agilent Technologies, Santa Clara, USA). At the end of the capillary, the effluent was split into two equal parts and transferred to a sniffing port and a flame ionization detector (FID). Retention indices were calculated for each odour-active compound by means of a reference series of homologous alkanes (C₆-C₃₀) [6].

Mass spectra were obtained with a 2D-GC-MS/O system (two Agilent 7890B GC and Agilent 5977B MS; Agilent Technologies, Santa Clara, US). The first GC was equipped with a cold on column injector and a DB-FFAP capillary column, the second GC was coupled to the first oven with a cryo-trap system and contained a DB-5 capillary column (column details see GC-O). After one part of the effluent was transferred onto the second oven and was injected by thermodesorption, the effluent of the first GC was split again into a sniffing port and an FID. The effluent of the second GC was split by transferring the compounds to a mass spectrometer as well as to a sniffing-port. Mass spectra were generated at 70 eV ionization energy in the electron impact mode with a m/z range from 35 to 400.

Results and discussion

Identification of odorants of the aqueous cavity preservation

Analysis via GC-O revealed a series of odour-active compounds that clearly belonged to a set of substance groups that were primarily dominated by lactones and acids. Representative substances of both groups are displayed in figure 1. Eleven of these substances were successfully identified according to the above-mentioned identification criteria. Primarily the coconut-like, fruity and peach-like smelling homologous series of γ -lactones from γ -octalactone to γ -undecalactone and the cheesy, musty, coriander-like and soapy smelling carboxylic acids butanoic acid, octanoic acid, decanoic acid and undecanoic acid and vanillin are, to the best of our knowledge, reported here for the first time as odorous constituents of an aqueous cavity preservation for usage in cars.

The identified substances have already been reported as odorants in non-food materials, especially in waxes [7]. The formation of lactones could be explained by reactions initiated by environmental factors, e.g. heat, light, or radiation [8, 9], and the same formation process can, accordingly, be suspected for the formation of the identified δ -nonalactone. In addition, generation of the carboxylic acids is also supported by heat, light, or radiation, and potential formation pathways have already been suggested [7]. Consequently, odorous acids are also likely to be found in different olefins and waxes. Vanillin is also a well-known odorant and has already been reported in diverse non-food materials [7, 10].

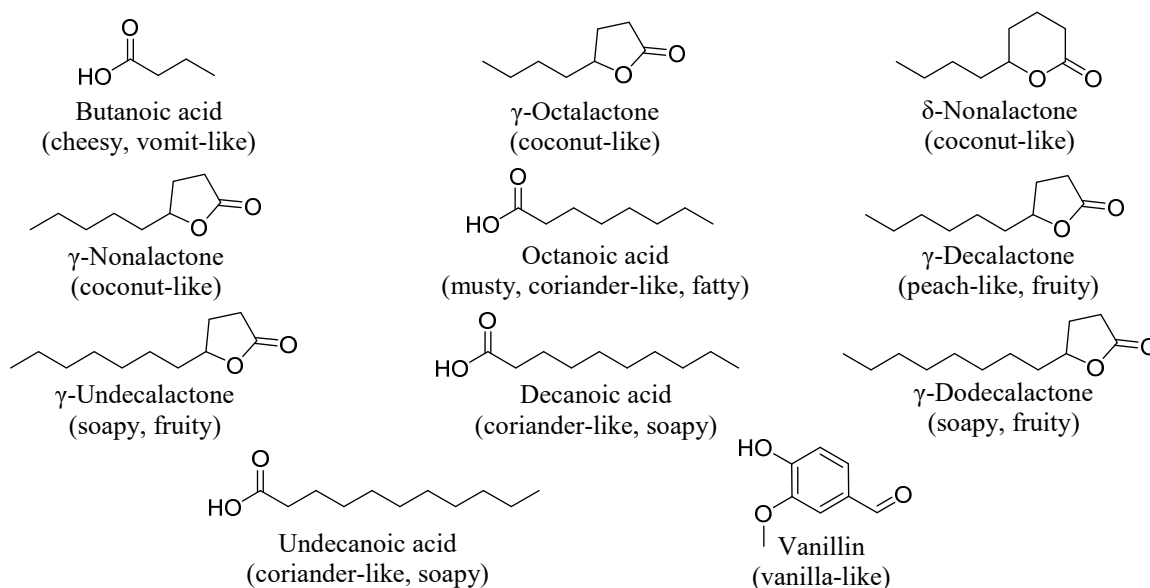


Figure 1: Identified odorants and their odour qualities in the hardened aqueous cavity preservation.

Odorants of the cavity preservation in the context of previously reported odorants of the vehicle-interior

To date, the odorants of only a few materials of the vehicle-interior have been investigated by olfactometric techniques, namely plastic and leather materials. In Table 1 we provide an overview of the predominantly investigated materials together with their prominent odorants. All in all, mainly plastics and seat covers have been investigated so far by means of GC-O, based on the consideration that these materials exhibit a large surface area and could, as a result, strongly contribute to the interior odour of a car. In addition to the visible construction materials of the vehicle-interior, however, other aids such as lubricants and adhesives are used in vehicle construction and could also contribute to the overall smell in the passenger cabin [11]. In this respect, we were the first to investigate one of these materials.

When comparing the most potent odorants of the investigated materials of the vehicle-interior, it becomes evident that 1-hexen-3-one has been repeatedly observed as one of the main odorants in three different plastic materials. Despite the noticeable prevalence of this plastic-like smelling and pungent compound, the formation of 1-hexen-3-one is still unknown [10]. The fatty, cardboard-like smelling aldehydes (*E*)-2-nonenal and (*Z*)-2-nonenal, on the other hand, are likely to be formed via oxidation of unsaturated fatty acids [12]. Besides their occurrence in foods, these compounds have also been detected in various non-food materials. Trace remnants of fats in thermoplastic polyolefin and leather could lead to the formation of these potent odorants [11]. The third group of potent odorants in the materials were the substituted phenols, like the phenolic smelling 2-*tert*-butylphenol and smoky smelling 2-methoxyphenol. Degradation of phenolic antioxidants like butylated hydroxy toluene can be proposed as precursors forming such odorants in materials of the vehicle-interior [11].

Table 1: Overview of materials of the vehicle-interior investigated by GC-O.

Material	Most potent odorants	Reference
Polyvinylchloride based artificial leather	1-hexen-3-one, acetophenone, 1-octen-3-one	[13]
Polypropylene materials	1-hexen-3-one, butanoic acid, 4-methylphenol, 1-butanol, 2- <i>tert</i> -butylphenol	[10]
Thermoplastic polyolefin	2,3-butanedione, 1-hexen-3-one, methional, (<i>Z</i>)-2-nonenal, (<i>E</i>)-2-nonenal, 2-acetyl-1-pyrroline	[11]
Polyurethane foam	2-ethyl-3,5-dimethylpyrazine	[11]
Polyphenyloxide material	2-methoxyphenol, methyl phenols, dimethyl, phenols	[11]
Leather	γ -nonalactone, vanillin, (<i>E</i>)-2-nonenal, 4-ethyl-2-methoxyphenol, 4-chloro-3-methylphenol	[14, 15]

When comparing the odorants of the aqueous cavity preservation with the common odorants of the investigated materials of the vehicle-interior it becomes evident that carboxylic acids and lactones have already previously been reported. Butanoic acid was identified in polypropylene materials [10] whereas γ -nonalactone and vanillin were detected in leather [14, 15], leading to the suggestion that these substance classes generally contribute to the smell of the passenger cabins.

The aqueous cavity preservation is of especially high interest here as it comes directly into contact with air that can pass to a relevant extent into the vehicle-interior. Future studies of our group will therefore target the question, which compounds exert the main impact on car smell, and which sources are the most prominent with respect to smell. This will be the basis for optimizing materials for technical applications, or to develop the respective substitutes.

Conclusion

For the first time, an anti-corrosion agent for an automotive application was investigated regarding its odour. As odorants, γ -lactones and carboxylic acids were identified as characteristic odorous constituents of the aqueous cavity preservation. The successful identification of potent odorants in this agent encourages further investigations on materials that are used in the vehicle interior, and to optimize their composition regarding a future avoidance of odour generation. In other fields, such approaches are already successfully implemented into the design and development of odour-optimized products, examples are plastic and leather [15, 16]. Nevertheless, to achieve a comprehensive smell optimization, all materials used in car production need to be taken into consideration.

References

1. Akafuah N, Poozesh S, Salaimeh A, Patrick G, Lawler K, Saito K. Evolution of the Automotive Body Coating Process - A Review. *Coatings*. 2016;6(2):1–22.
2. Talay E, Altinisik A. The effect of door structural stiffness and flexural components to the interior wind noise at elevated vehicle speeds. *Appl Acoust*. 2019;148(4):86–96.
3. Xu B, Chen X, Xiong J. Air quality inside motor vehicles' cabins: A review. *Indoor Built Environ*. 2018;27(4):452–465.
4. Engel W, Bahr W, Schieberle P. Solvent assisted flavour evaporation – a new and versatile technique for the careful and direct isolation of aroma compounds from complex food matrices. *Eur Food Res Technol*. 1999;209:237–241.
5. Bemelmans JMH. Review of Isolation and Concentration Techniques. In: Land DG, Nussten HE, editors. *Progress in Flavour Research*. London: Applied Science Publishers; 1979. p. 79–98.
6. van den Dool H, Kratz PD. A generalization of the retention index system including linear temperature programmed gas-liquid partition chromatography. *J Chromatogr A*. 1963;2:463–471.
7. Denk P, Ortner E, Buettner A. Characterization of odorants in waxes for hot melt adhesives using sensory and instrumental analyses. *Int J Adhes Adhes*. 2019;95(4):102406.
8. Lacoste J, Carlsson DJ. Gamma-, photo-, and thermally-initiated oxidation of linear low density polyethylene: A quantitative comparison of oxidation products. *J Polym Sci Pol Chem*. 1992;30(3):493-500.
9. Tyapkova O, Czerny M, Buettner A. Characterisation of flavour compounds formed by γ -irradiation of polypropylene. *Polym Degrad Stabil*. 2009;94(5):757–769.
10. Frank S, Reglitz K, Mall V, Morgenstern U, Steinhaus M. Molecular background of the undesired odor of polypropylene materials and insights into the sources of key odorants. *Indoor Air*. 2021;00:1–12.
11. Mayer F, Breuer K. Material odor-odoractive compounds identified in different materials - the surprising similarities with certain foods, possible sources and hypotheses on their formation. *Indoor Air*. 2006;16(5):373–382.
12. Ullrich F, Grosch W. Identification of the most intense volatile flavour compounds formed during autoxidation of linoleic acid. *Z Lebensm Unters Forsch*. 1987;184:277–282.
13. Reglitz K, Steinhaus M. Key odorants in the artificial leather of car interiors. In: Siegmund B, Leitner E, editors. *Flavour Science*. Technische Universität Graz; 2018. p. 389–394.
14. Schroeffer M, Czerny M, Schulz H, Schieberle P. The Odor of Leather. *J Am Leather Chem As*. 2013;108:94–107.
15. Czerny M, Schieberle P. Identification of intense odorants in leathers produced by different tanning systems. In: Hofmann T, Meyerhof W, Schieberle P, editors. *Recent highlights in flavor chemistry and biology*. Garching; 2008. p. 351–355.
16. Strangl M, Ortner E, Fell T, Ginzinger T, Buettner A. Odor characterization along the recycling process of post-consumer plastic film fractions. *J Clean Prod*. 2020;260(1):121104.

An oenological approach to increase the consumer acceptability of black chokeberry (*Aronia melanocarpa* L.) juice

Sarah Ziermann-Österreicher¹, G. Thünauer² and BARBARA SIEGMUND¹

¹ Graz University of Technology, Institute of Analytical Chemistry and Food Chemistry, Austria

² Styrian Chamber of Agriculture and Forestry, Austria Affiliation

barbara.siegmund@tugraz.at

Abstract

The black chokeberry (*Aronia melanocarpa* L.) is a berry with exceptionally high concentrations of phenolic compounds with high antioxidative potential as well as high amounts of minerals, trace elements and vitamins. The health beneficial effect of aronia consumption was shown in several studies. Recently, these properties have made aronia a new domestic and, thus, sustainable 'superfood'. However, in contrast to other products aronia juice lacks pronounced fruitiness, but shows distinct bitterness and astringency. These sensory properties are the limiting factors for a high consumer acceptability of aronia juice. In this study, we investigated the applicability of fining technologies to aronia juice with the aim to reduce the astringency and bitterness. Commercially available fining agents that are well established in wine technology were selected for these experiments. The effect of these measures was investigated by (i) HS SPME GC-MS to investigate the impact on volatile compounds, (ii) and UV-Vis spectrophotometry to follow the colour changes upon fining (iii) sensory analysis to evaluate the bitterness and astringency. Fining of aronia juice leads to a significant change in the aronia volatilome and a reduction of the monomeric polyphenols. Hence, fining results in changes on odour- as well as taste-active compounds and causes multimodal changes in the sensory perception.

Keywords: black chokeberry juice, fining, volatiles, bitterness, astringency

Introduction

The black chokeberry (*Aronia melanocarpa* L.) has gained increasing popularity during the last years as a domestic 'superfood'. The cultivation areas have been continuously enlarged in Austria. The berry is well known due to its exceptionally high content of polyphenolic substances (i.e., anthocyanins, pro-anthocyanidins, flavonols and phenolic acids) with the highest content of total phenolics compared to most other berry species [1]. The consumption of polyphenolic compounds is assumed to have beneficial health effects. Their antioxidative potential, anti-cancer, cardioprotective, and anti-diabetic effects as well as other advantages were subject of many investigations [2-4, 6-7].

In contrast to other products, aronia juice is lacking pronounced fruitiness, but shows distinct bitterness and astringency which is a major limitation for its consumption for most consumers [5]. Due to the young history of chokeberry juice, only little research has been performed with the aim to reduce its bitterness and astringency. However, there is vast knowledge and experience from oenology on how to cope with bitterness and astringency in red wines. Fining is a well-established technological measure in winemaking, which is used to reduce astringency and bitterness by removing polyphenols and tannins. Therefore, in this study we investigated the effects of fining on not-from-concentrate chokeberry juice. Six different commercially available fining agents were applied on chokeberry juices. The effects were evaluated using (i) headspace SPME-GC-MS to investigate the impact on aronia volatiles, (ii) UV-Vis spectrophotometric methods to investigate the impact on the colour of the juices and (iii) sensory methods to investigate the impact of fining on the overall flavour with a focus on bitterness and astringency.

Experimental

Material

Not-from-concentrate chokeberry juice was prepared from approximately 400 kg fully ripe aronia berries that were harvested in the South of Austria (variety Nero, harvest year 2019). The berries were processed by a local fruit processing company immediately after the harvest. The pasteurized juices were stored in the dark at 5°C in 3 L polyethylene bags until further use. Fining was performed with six different commercially available fining agents (A - Degustin, B - ErbiGel Bio, C - Erbslöh Mostgelatine, D - Vinpur Special, E - LittoFresh Liquid, F - ErbiGel Liquid; all provided by Erbslöh Austria GmbH). The fining agents were applied in the highest dosage recommended for the fining of red wine and let react over night at 4°C. After coagulation took place, filtration or decantation was used to separate the clear juice from the precipitate.

Gas chromatography-mass spectrometry (GC-MS) analysis of the volatile compounds

An aliquot of 100 μL of chokeberry juice (untreated or fined juices) was transferred into 20 mL headspace vials with the addition of 50 mg NaCl. 2-Octanol was added as an internal standard (100 ng absolute). The extraction/enrichment of the volatiles was performed by headspace solid-phase-microextraction (HS-SPME; 2 cm stable flex fibre, 50/30 μm DVB/Car/PDMS fibre) for 20 minutes at 40°C. Samples were stirred thoroughly during the enrichment process. The GC-MS analysis was conducted on a non-polar column (Shimadzu GC-2010 Plus, MS QP 2020, Shimadzu Europa GmbH; Rxi-5ms 30 m \times 0.25 mm \times 1 μm , Restek Corporation, USA; EI 70 eV, scan range 35 - 350 amu). The samples were analysed in triplicate in randomized order. The identification of the volatiles was based on probability-based matching of their mass spectra with those from MS libraries, authentic reference compounds and linear temperature-programmed retention indices. Retention indices were calculated by measuring the homologous series of *n*-alkanes (C5-C26) using the same GC-MS conditions as for the samples. Data deconvolution and integration was done with the PARADISE software, based on the PARAFAC2 model [8]. Semi-quantification was done via the internal standard (2-octanol) assuming a response factor of 1 for all compounds.

Monomeric index

The determination of the monomeric index was performed according to Bonerz et al., 2006 [9]. The monomeric index was calculated as the ratio of the absorption of the monomeric and polymeric anthocyanins ($A_{\text{mono}}/A_{\text{poly}}$) at $\lambda=520$ nm after discolouration of the monomeric anthocyanins upon a reaction with $\text{K}_2\text{S}_2\text{O}_5$.

Sensory evaluation

Sensory evaluation of the juices was performed with a well-trained expert panel, experienced in analysing chokeberry products (14 members) under standardized conditions in the sensory laboratory. Descriptive analysis as well as discrimination tests were applied. Sensory data were recorded using Compusense sensory software (Compusense Inc., Guelph, Canada).

Statistical evaluation of the results

Statistical analysis was performed using one-way analysis of variance (ANOVA) to identify statistically significant differences between the samples as well as principal component analysis (PCA), using Pearson correlation to find correlations between volatiles and samples. For statistical analysis, the MS excel add-in XLSTAT was used (Addinsoft 2020, Long Island, NY, USA).

Results and discussion

In this study, we evaluated the impact of fining on not-from-concentrate aronia juice with the aim to reduce the pronounced astringency and bitterness of the products. It is well known from oenology, that fining does not only impact the concentrations of phenolic compounds of the product. Depending on the selected fining agent, interaction with volatile compounds may be observed and may, thus, lead to alterations of the overall flavour of the product. As a consequence, we investigated aronia volatiles, the overall flavour of the juices as well as the so-called monomeric index as a measure for anthocyanins as a major group of phenolic compounds in chokeberry juice.

Headspace SPME-GC-MS was used to analyse the volatile compounds of aronia juice. A total of 74 volatile compounds could be identified in the aronia juice. As reported in a previous study [5], in contrast to other fruit juice types, only very few fruit esters are present in aronia juice; on the other hand, we identified a long list of alcohols, aldehydes and ketones, some free short-chain fatty acids as well as some terpenes and terpenoids. The results from HS-SPME-GC-MS analysis showed a significant reduction of many volatiles upon the fining process. Mainly low-molecular weight esters and ketones, which are generally made responsible for fruitiness, were significantly decreased in their concentrations. Terpenes were hardly affected by the fining process; free fatty acids did not show a clear trend, neither did alcohols. To better visualize the effect of fining on the volatiles of aronia juice, we performed multivariate data analysis in terms of principal component analysis.

Figure 1 gives the biplot showing the correlations of aronia volatiles and the juices treated with different fining agents in comparison to the non-treated juice. The effect of fining on the aronia volatiles can be seen clearly. The untreated juice is the only product located in quadrant IV and shows a high correlation with a large number of volatiles, specifically with esters, some alcohols and ketones. The biplot also demonstrates the different interactions of the selected fining agents with volatile compounds. Whereas the juice fined with the fining agent A is centred in quadrant I and highly correlates with a high number of C6 'green leaf' aldehydes and alcohols, the juices fined with fining agents B and C are located at the border of quadrant I and II and only correlate with few compounds from different compound classes. On the contrary, juices treated with the fining agents D, E and

F show high correlations to one another; interestingly, high correlations were observed with the 2- and 3-methyl-branched butanoic acids. Having in mind the rather unpleasant sensory properties and the low odour threshold values of these acids, this finding might be an indication for a negative impact of the fining procedure on the flavour of the juices.

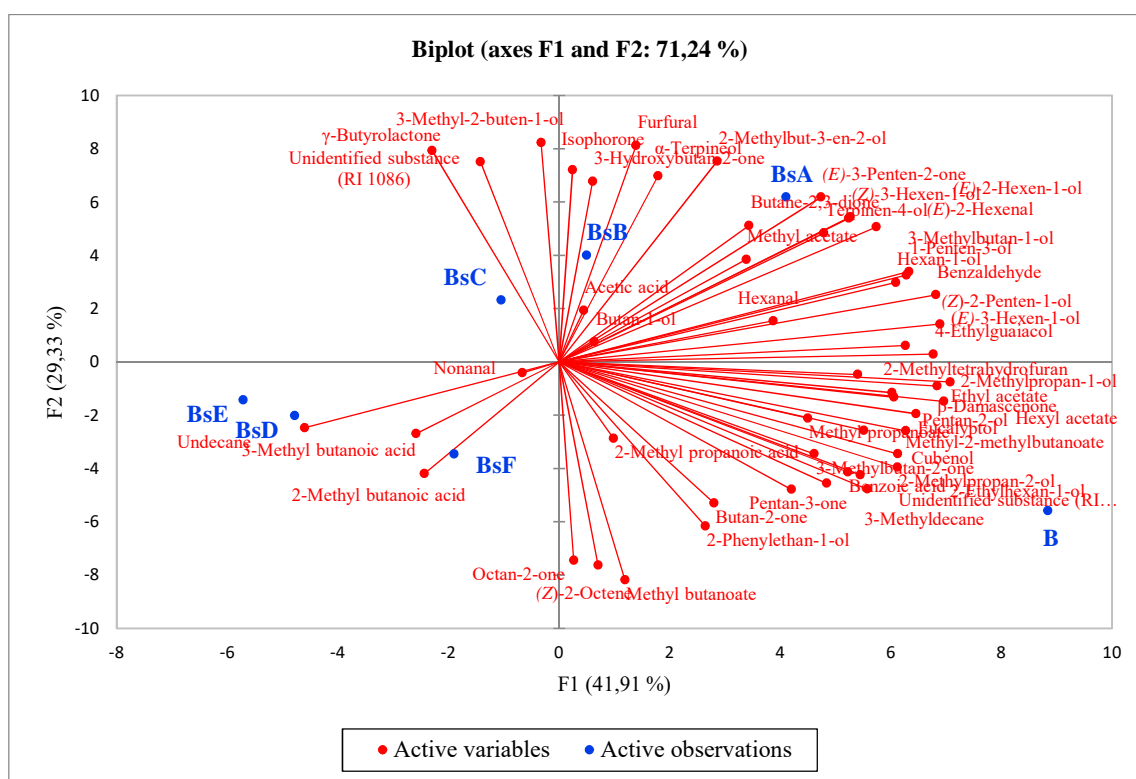


Figure 1: Biplot of the PCA analysis (Pearson correlation) of the volatile compounds of the untreated aronia juice B in comparison to juices that were fined with commercially available fining agents (BsA Degustin, BsB ErbiGel Bio, BsC Erbslöh Mostgelatine, BsD Vinpur Special, BsE LittoFresh Liquid, BsF ErbiGel Liquid).

Phenolic compounds that are present in high concentrations in aronia juice are made responsible for the bitterness and the pronounced astringency of the products. Thus, in addition to the analysis of the volatile compounds, we followed the fining process by analysing the so-called monomeric index as a measure of the total content of anthocyanins in the juice. This was done to evaluate if the use of fining agents designed for oenological practices might also work for the treatment of aronia juice. The results of the fining experiments with respect to the monomeric index are given in Table 1. Fining with four out of six fining agents resulted in a low, however, significant decrease of the monomeric index as a result of the fining process. These results – in combination with the formation of a highly coloured precipitate – show that the selected fining agents interact and reduce the phenolic components of aronia juice. The decrease in the monomeric index indicates a stronger reduction of monomeric phenolic compounds (i.e., anthocyanins) in comparison to the polymeric phenols.

Preliminary results from sensory evaluation demonstrate a change in the sensory properties of the fined juices in comparison to the unfined reference juice. Results from descriptive analysis demonstrate that bitterness was reduced by almost all fining agents, whereas the perceived astringency remained unchanged upon fining with fining agents A and C, for example, while fining agent D also reduced astringency. It is also worthwhile to note that the reduction of bitterness and/or astringency led to an overall change of the perceived flavour; fining with fining agent A led to a reduced perception of bitterness with a simultaneous increase in perceived fruitiness, while fining with fining agent F led to an increase in the perceived astringency and sourness. Monomeric flavon-3-ols as well as dimers and trimers are described to be bitter, but not astringent [10]. Thus, the reduced bitterness-intensity indicates a reduction of monomeric anthocyanins upon the fining process, rather than a reduction of the condensed polyphenols.

These findings correlate well with the values for the monomeric index that also show a reduction of monomeric polyphenols due to the fining process. These preliminary results from sensory evaluation combined with the results obtained from GC-MS analysis of the aronia volatilome and colour measurements indicate, that complex interactions take place between the juice and the respective fining agent leading to multimodal sensory effects that are specific for each fining agent.

Table 1: Monomeric index of the unfined and fined juices (n=3).

Sample	Monomer index	Sig [§]
Unfined juice	12,60 ± 1,1	-
Fined juice (Degustin)	11,52 ± 0,7	ns
Fined juice (ErbiGel Bio)	10,17 ± 0,5	*
Fined juice (Erbslöh Mostgelatine)	13,55 ± 1,9	ns
Fined juice (Vinpur Special)	11,39 ± 0,2	*
Fined juice (LittoFresh Liquid)	11,04 ± 0,9	*
Fined juice (ErbiGel Liquid)	10,78 ± 0,6	*

[§]significance of difference between the unfined juice and the fined juices FJ
 ns = no significant difference between means (p > 0.05); * significant at the 5% level

Conclusion

The results of this study show that fining of aronia juice might be a suitable oenological practice to specifically reduce its pronounced bitterness. The findings from the analysis of the aronia volatillome, UV-Vis spectrophotometry on polyphenols and the sensory evaluation indicate that different fining agents do not interact in a uniform way with the juice components. This specific behaviour results in different multimodal effects on the sensory perception of the fined product. The preliminary results from this study may serve as a good basis for further investigations to identify the most appropriate fining agent and its optimum dosage for the specific composition of aronia juice. With this and the follow-up experiments, we hope to successfully contribute to improve the sensory properties of this highly valuable domestic product and to increase the consumer acceptability of aronia juice.

Acknowledgement: The authors are grateful to the members of the sensory test panel for evaluating the samples and to Erbslöh Austria for providing the fining agents.

References

1. Mikulic-Petkovsek M, Schmitzer V, Slatnar A, Stampar F, Veberic R. Composition of sugars, organic acids, and total phenolics in 25 wild or cultivated berry species. *J Food Sci.* 2012;77:C1064-70.
2. Kulling S E; Rawel H M. Chokeberry (*Aronia melanocarpa*) - A review on the characteristic components and potential health effects. *Planta medica* 2008;74:1625–1634.
3. Jakobek L, Drenjančević M, Jukić V, Šeruga M. Phenolic acids, flavonols, anthocyanins and antiradical activity of “Nero”, “Viking”, “Galicianka” and wild chokeberries. *Sci. Hortic.* 2012;147:56–63.
4. Olas B. Role of Black Chokeberries in Breast Cancer: A Focus on Antioxidant Activity. In: *Cancer: Oxidative Stress and Dietary Antioxidants*; Preedy VR (ed.); Academic Press: London. 2014;p.151–157.
5. Robert S, Siegmund B. *Aronia melanocarpa* - the Styrian ‘super berry’: a flavour characterisation of black chokeberry juice. In: *Flavour Science: Proceedings of the XV Weurman Flavour Research Symposium*; Siegmund B, Leitner E (eds.); Verlag der Technischen Universität Graz. 2018;p.139–142.
6. Denev PN, Kratchanov CG, Ciz M, Lojek A, Kratchanova MG. Bioavailability and Antioxidant Activity of Black Chokeberry (*Aronia melanocarpa*) Polyphenols: in vitro and in vivo Evidences and Possible Mechanisms of Action: A Review. *Compr Rev Food Sci Food Saf* 2012;11:471–489.
7. Sidor A, Drożdżyńska A, Gramza-Michałowska A. Black chokeberry (*Aronia melanocarpa*) and its products as potential health-promoting factors - An overview. *Trends Food Sci Techn.* 2019; 89: 45–60.
8. Johnsen LG, Skou PB, Khakimov B, Bro R. Gas chromatography - mass spectrometry data processing made easy. *J Chromatogr A.* 2017;1503:57–64.
9. Bonerz D, Würth K, Patz CD, Dietrich H. The "Monomeric Index" method: A rapid and cheap screening method regarding the colouring pigments in red fruit juices and concentrates. *Dtsch Lebensmittel Rundsch* 2006;102:195–202.
10. Peleg H, Gacon K, Schlich P, Noble AC. Bitterness and astringency of flavan-3-ol monomers, dimers and trimers. *J Sci Food Agric.* 1999:1123-1128.

Perception and sensory acceptance of salty taste by individuals who work/study on different shifts

Ana Carolina Bom Camargo and ANA CAROLINA CONTI-SILVA

São Paulo State University (Unesp), Institute of Biosciences, Humanities and Exact Sciences (Ibilce), Campus São José do Rio Preto, Department of Food Engineering and Technology, São José do Rio Preto, SP, Brazil, conti.silva@unesp.br

Abstract

Night activity, whether at work or in teaching, has been increasing significantly in recent years. However, the human being has a daytime nature and sleep restriction that can influence the modulation of various situations managed by the circadian cycle, such as eating behaviour. Thus, we evaluated the perception and sensory acceptance of salty taste by individuals who work/study in different shifts. Three groups of individuals were recruited: Control group (individuals that study during the day and do not work at night), Group 1 (individuals that study in the evening) and Group 2 (individuals that work overnight). The individuals were submitted to a detection threshold test using sodium chloride solutions and to a sensory acceptance test using a structured hedonic scale and a Just-About-Right scale for salty taste in meatball. Sleep time decreased significantly from the Control group to Group 1, and then even more to Group 2. The detection threshold of Group 2 was significantly higher than the other groups. Nevertheless, few statistical differences were found between the three groups in terms of sensory acceptance of salty taste. Concluding, the change in the sleep pattern, either due to a shift change or in the amount of sleep time, influences the salty taste sensory perception.

Keywords: circadian cycle, nightshift workers, night-school students, detection threshold test, sensory acceptance

Introduction

Night activity, both work and study, has been increasing significantly in recent years and, although there has been an increase in night activity, human beings are diurnal by nature and their sleep-wake pattern is determined by the light/dark cycle. This phenomenon, called the circadian cycle [1], is regulated by a central clock in the brain and corresponds to a physiological cycle with periodicity of approximately 24 hours. In 2017, researchers won the Noble Prize in Medicine for discovering the molecular mechanisms that control the circadian rhythm [2] and demonstrating that the internal clock of plants, animals and human beings is responsible for readapting the physiology with high precision to the different phases of the day, regulating critical functions, such as behaviour, hormone levels, sleep, body temperature and metabolism. Consequently, circadian desynchrony is involved in several pathological conditions. Nevertheless, no studies in the literature that have evaluated the relationship between changes in sleeping patterns and sensibility to basic tastes and the sensory acceptance of food were found. Thus, we aimed to evaluate the perception and sensory acceptance of salty taste by individuals that work/study on different shifts.

Experimental

Three groups of individuals were recruited: Control group (individuals that study during the day and do not work at night); Group 1 (individuals that study in the evening); and Group 2 (individuals that reverse the shifts, i.e., that work overnight). Each group was composed by thirty-seven individuals, who were characterised regarding the usual bedtime and sleep time. Moreover, the individuals were only included in each group if they had been in the same 'routine' for at least one year to guarantee their adjustment to those sleeping/waking and working/studying patterns [3].

The individuals were submitted to a detection threshold test (in two repetitions) using sodium chloride solutions (Table 1). Samples of sodium chloride were presented in pairs (distilled water and solution), from the most diluted concentration to the more concentrated. The panellist should indicate whether there was any difference between the two samples (distilled water and solution). In the case of a negative answer (no difference detected), the next plastic cup with solution along with one of distilled water were offered. The pairs of plastic cups were offered until the panellist detected a difference between the samples in two successive concentrations of sodium chloride. When this occurred, the analysis was stopped, and the mean of these two successive concentrations was taken as the detection threshold for that panellist [4]. The panellists were also submitted to a sensory acceptance test using a structured hedonic scale and a Just-About-Right scale (both of nine points) for salty taste in meatballs with different sodium chloride concentrations (Table 1).

Table 1: Sodium chloride concentrations for the detection threshold test and acceptance of salty taste of meatballs.

Detection threshold (g sodium chloride/L*)	Acceptance test (g sodium chloride/kg meat)
2.00	32.60
1.40	22.80
0.98	15.84
0.69	11.08
0.48	7.60
0.34	5.32
0.24	4.08
0.16	2.88
R = 0.7	R = 0.7

*ISO 3972:2011 [5]

R = geometric proportion (ISO 3972:2011).

The means of usual bedtimes were compared using the Student's t test for independent variables, while the analysis of variance followed by the Tukey test were performed for sleep time and detection threshold. Moreover, the general linear model having sample and group as factors, as well as the interaction between such factors, was applied to the sensory acceptance data, and the means were compared through the Tukey test. These analyses were performed using the Minitab 17 (Minitab Inc.) software and the 0.05 significance level. Moreover, the linear regression analysis between the results from the Just-About-Right scale as a function of sodium chloride concentrations was performed using the Excel 2013 program.

Results and discussion

When asked about their usual bedtime (Table 2), individuals of the Control group and Group 1 had a clear pattern in their answers, i.e., the individuals slept at different times, but always at the same time every night. However, individuals of Group 2 did not have any pattern to their answers, once people who work overnight often work a shift scheme called 12/36 h, in which they work for 12 h overnight and rest for 36 h before the next shift. When they work the night shift, they sleep during the day, and this may begin at 4 h or 8 h or even as late as 15 h. However, when they do not work and have a day's rest, they sleep during the night. Regarding the sleep time, there was a decrease significantly from the Control group to Group 1 and then even more for Group 2 (Table 2).

Table 2: Characterization of individuals (mean \pm SD; n = 37).

Group	Usual bedtime	Sleep time (min)
Control	23h18min \pm 48min ^a	431.4 \pm 50.7 ^c
1	00h12min \pm 56min ^b	376.2 \pm 77.0 ^b
2	-	319.5 \pm 91.7 ^a

Different letters for usual bedtime indicate significantly different means by Student's t test ($p \leq 0.05$).Different letters for sleep time indicate significantly different means by Tukey test ($p \leq 0.05$).

The detection thresholds between the Control group and Group 1 did not differ significantly for the salty taste. However, both were significantly lower than Group 2 (Table 3). This shows that a change in the sleep pattern, whether it be in the change of shifts or in the number of hours slept, influences the salty taste sensory perception. The individuals that work overnight are less sensitive to the salty taste than individuals that study in the evening or do not have changes in their sleep pattern.

Table 3: Detection threshold (average \pm SD; n = 37) for sodium chloride by different groups.

Group	Sodium chloride concentration (g/L)
Control	0.34 \pm 0.16 ^a
1	0.42 \pm 0.28 ^a
2	0.63 \pm 1.88 ^b

Different letters indicate significantly different means by the Tukey test ($p \leq 0.05$).

The sensory acceptance of the salty taste of meatballs was affected only by sample and group. Regarding samples, as the sodium chloride concentration increased, the degree of liking and the ideal of intensity also

increased up to certain concentrations (Figure 1). At the last concentration of sodium (32.60 g sodium chloride/kg meat, sample 8), there was a significant decline in the degree of liking (Figure 1A; statistic result not shown). However, from the concentration of 22.80 g sodium chloride/kg meat (sample 7), there was a significant change in the ideal of intensity of salty taste (statistic result not shown) because it stops being 'ideal intensity', when the average reaches a value close to 5, reaching 'more intense than ideal' (means higher than 6) (Figure 1B). Such results indicate that the increase in the sodium chloride concentration from certain concentrations had become prejudicial to the sensory acceptance.

Comparing the degree of liking between the different groups, the Control group showed a significantly higher degree of liking for samples regarding the salty taste in comparison to the others (Figure 1A; statistic result not shown), while the ideal of intensity was significantly higher than Group 1 (Figure 1B; statistic result not shown), although the three means are near to 5, which represents the 'ideal intensity' of salty taste. These last results are corroborated by the linear regression analysis (Figure 2), which shows concentrations of sodium chloride close to each other for an ideal intensity of salty taste ($y = 5$): 14.65 g sodium chloride/kg meat, 16.68 g sodium chloride/kg meat and 14.93 g sodium chloride/kg meat for the Control group, Group 1 and Group 2, respectively.

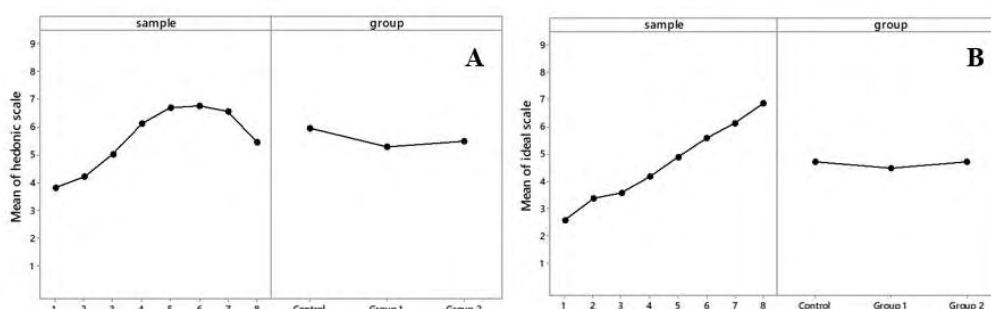


Figure 1: Salty taste acceptance through hedonic (A) and JAR (B) scales of the beef meatballs by sample (averages from $n = 111$) and group (averages from $n = 296$). Legend for samples: 1) 2.88, 2) 4.08, 3) 5.32, 4) 7.60, 5) 11.08, 6) 15.84, 7) 22.80, and 8) 32.60 (values in g sodium chloride/kg meat). Legend for groups: Control group: individuals who study during the day and do not work at night, Group 1: individuals who study in the evening, and Group 2: individuals who reverse the shift (work overnight).

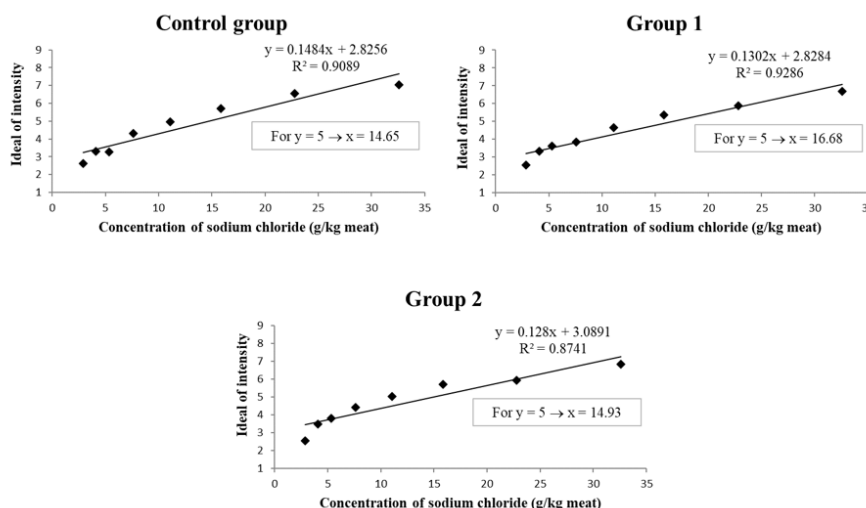


Figure 2: Ideal of intensity of salty taste in function of the sodium chloride concentration in the meatballs. Legend: Control group: individuals who study during the day and do not work at night, Group 1: individuals who study in the evening, and Group 2: individuals who reverse the shift (work overnight).

The average daily salt consumption varies among different populations. Salt can be found in a lot of daily intake food and it is difficult to calculate the total daily consumption because the preference and evaluation of salt consumption in such studies is usually self-referred. Thus, methods for measuring salt intake may not be reliable. On the other hand, the detection threshold test can reflect indirectly on the daily salt consumption because an increased salt taste sensitivity threshold score was associated with salted food intake and salty taste preference [6].

In this way, individuals from Group 2 could need more salt to detect the salty taste, contributing to their higher salt consumption. However, considering the different tests for characterizing the taste function in humans, the detection threshold test for salty taste is not as efficient as a suprathreshold test (stimuli concentrations between the recognition threshold and the terminal threshold) for reflecting the liking of individual for such taste [7, 8]. Thus, other analyses should be performed in the future, providing new complementary results, for example, an investigation of the total daily consumption of salt through individual food intake survey methods.

Conclusion

The detection threshold of Group 2 was higher than the other groups, indicating that a change in the sleep pattern, either due to a shift change or in the amount of sleep time, influences the salty taste sensory perception. Nevertheless, changes in sleep pattern did not have important influences on the salty taste acceptance. Deeper studies need to be performed to better understand relationships between circadian cycle and sensory perception and acceptance of foods.

References

1. Harthoorn LF, Sañé A, Nethé M, Heerikhuizen JJ. Multi-transcriptional profiling of melanin-concentrating hormone and orexin-containing neurons. *Cell Mol Neurobiol.* 2005;25(8):1209-1223.
2. The Nobel Prize in Physiology or Medicine. 2017. (<https://www.nobelprize.org/prizes/medicine/2017/summary/>). Accessed October 1 2020.
3. Silva RM, Beck CLC, Magnago TSBS, Carmagnani MIS, Tavares JP, Prestes FC. Night shift and the repercussion in nurses' health. *Esc Anna Nery.* 2011;15(2):270-276.
4. Meilgaard M, Civille GV, Carr BT. *Sensory Evaluation Techniques* (3rd ed.). Boca Raton, Florida: CRC Press. 1999.
5. ISO 3972:2011, Sensory analysis - Methodology - Method of investigating sensitivity of taste. Geneva: International Organization for Standardization. 2011.
6. Yang WG, Chen CB, Wang ZX, Liu YP, Wen XY, Zhang SF, et al. A case-control study on the relationship between salt intake and salty taste and risk of gastric cancer. *World J Gastroenterol.* 2011;17(15):2049-2053.
7. Bartoshuk LM. The psychophysics of taste. *Am J Clin Nutr.* 1978;31(6):1068-1077.
8. Webb J, Bolhuis DP, Cicerale S, Hayes JE, Keast R. The relationships between common measurements of taste function. *Chemosens Percept.* 2015;8:11-18.

Effects of salt and monosodium glutamate on the sensory acceptance of low-sodium cheese-flavoured corn grits expanded snacks

Aline Catharina Panzarini, Michele Eliza Cortazzo Menis-Henrique and ANA CAROLINA CONTI-SILVA

São Paulo State University (Unesp), Institute of Biosciences, Humanities and Exact Sciences (Ibilce), Campus São José do Rio Preto, Department of Food Engineering and Technology, São José do Rio Preto, SP, Brazil, conti.silva@unesp.br

Abstract

The reduction of salt content in foods is not a simple task because sodium compounds play an important role in the flavour of foods. Thus, we evaluated the effects of salt and monosodium glutamate on the sensory acceptance of cheese-flavoured corn grits expanded snacks, looking at reducing sodium content of these products. The addition of salt and monosodium glutamate was performed based on the Response Surface Methodology, having the addition of salt (0.20, 0.35, 0.70, 1.05 and 1.20%) and addition of monosodium glutamate (0.18, 0.30, 0.60, 0.90 and 1.02%) as independent variables. The snacks were evaluated through the Just-About-Right scale and the structured hedonic scale (both of nine points). An increase in the percentage of salt increased the ideal of intensity of salty taste, the degree of liking of salty taste and the degree of liking of flavour, while an increase in the monosodium glutamate percentage increased only the first two previous sensory responses. No interactions were observed between salt and monosodium glutamate. Among the snacks studied, that with 1.2% salt and 0.6% monosodium glutamate stands out, since it was sensorially accepted and still had estimated sodium content below the average for commercial snacks. Concluding, our results are relevant for providing alternatives for reducing the sodium content on products; the reduction, however, must be gradual so as not to negatively affect consumer acceptance.

Keywords: thermoplastic extrusion, sensory acceptance, sodium

Introduction

The reduction of sodium content in foods is not a simple task because sodium ions play an important role in the flavour of foods. Among products with high salt content, expanded snacks often spring to mind. Such products have both high fat and salt content, being regarded as highly energetic and nutritionally poor [1], reasons because they are highly criticized [2]. Despite this, the snack market has been gaining prominence due to the consumer search for practical and fast food. The thermoplastic extrusion is used for many varied products in the food industry because of its high versatility and flexibility, with expanded corn snacks standing out. The combination of practicality and the tendency to consume healthier foods leads to the need to increase the production of snacks with lower sodium content. Therefore, we aimed to assess the effects of salt and monosodium glutamate on the sensory acceptance of cheese-flavoured corn grits expanded snacks, aiming to reduce the sodium content of these products.

Experimental

Corn grits with 15% moisture (wet basis) were extruded in an RXPQ Labor 24 single screw extruder (INBRAMAQ, Ribeirão Preto, Brazil) with five independent heating zones. The extrusion conditions were: three helicoidally grooved barrel; screw with a large step of one exit with a compression ratio of 2.3:1 and length-to-diameter ratio of 15.5:1; pre-die extruder with holes of 3.01 mm; extruder die with a diameter of 2.93 mm (round hole); feed rate of 265 g/min; screw speed at 237 rpm; temperatures in zones 1 to 5: off (around 25 °C), 70 °C, 90 °C, 140 °C and 140 °C respectively.

A mixture of 6% of sunflower oil, 1.5% of cheese aroma, salt and monosodium glutamate was used for extrudate flavouring. The sunflower oil quantity was defined based on a previous study [3], while the quantity of cheese aroma was recommended by the donor company of the aroma. The addition of salt and monosodium glutamate was performed based on the Response Surface Methodology, through a rotational central composite design for two independent variables with five levels each: addition of salt (0.20, 0.35, 0.70, 1.05 and 1.20%) and addition of monosodium glutamate (0.18, 0.30, 0.60, 0.90 and 1.02%), both in percentages related to 100 g of extrudate. Twelve assays were performed: four assays of factorial points (2²), four assays of axial points and four repetitions of the central point. The dependent variables were: 1) acceptance of cheese odour, salty taste and cheese

flavour using the Just-About-Right scale of nine points, and 2) acceptance of odour, salty taste, and flavour, as well as overall acceptance, using the nine-point structured hedonic scale. Sixty-three consumers were recruited.

Linear and quadratic models were tested to explain the influence of the independent variables on the dependent variables using the Minitab 17 software (Minitab Inc.). The results were then subjected to multiple regression analysis and coefficients of the model with p-values ≤ 0.05 were considered significant. Analysis of variance was applied and p-values ≤ 0.05 and > 0.05 were considered to evaluate the significance of regression and the lack of fit, respectively. Only models that were significant, with no lack of fit, and with R^2 higher than or equal to 70% are presented in this paper. The response surfaces were plotted using the Statistica 7.0 software (StatSoft Inc.).

Results and discussion

The intensity was 'slightly less than ideal' (means around 4) for cheese odour and between 'slightly and moderately less than ideal' for the salty taste and cheese flavour (means between 4 and 3, respectively) (Table 1). Moreover, the means of the degree of liking of odour, salty taste, flavour and overall acceptance of the snacks ranged from 'neither liked nor disliked' (score 5) to 'I liked it slightly' (score 6).

Table 1: Sensory acceptance of cheese-flavoured corn grits expanded snacks (mean \pm SD; n = 63).

assay	salt (%)	MSG (%)	JAR scale			hedonic scale			
			cheese odour	salty taste	cheese flavour	odour	salty taste	flavour	overall
1	0.35	0.30	4.0 \pm 1.4	3.3 \pm 1.5	3.4 \pm 1.4	5.9 \pm 1.8	5.1 \pm 1.9	5.3 \pm 1.9	5.4 \pm 1.7
2	1.05	0.30	4.3 \pm 1.3	3.6 \pm 1.3	3.8 \pm 1.3	6.3 \pm 1.8	5.6 \pm 1.8	6.1 \pm 1.7	6.0 \pm 1.7
3	0.35	0.90	4.3 \pm 1.5	3.9 \pm 1.6	4.1 \pm 1.8	6.3 \pm 1.6	5.3 \pm 1.8	5.7 \pm 1.8	5.9 \pm 1.6
4	1.05	0.90	4.1 \pm 1.3	3.9 \pm 1.4	3.9 \pm 1.5	6.0 \pm 1.9	5.6 \pm 1.8	6.0 \pm 2.0	6.0 \pm 1.9
5	0.20	0.60	4.0 \pm 1.5	3.2 \pm 1.5	3.3 \pm 1.6	5.8 \pm 1.8	4.8 \pm 1.8	5.0 \pm 1.7	5.2 \pm 1.7
6	1.20	0.60	4.1 \pm 1.5	3.9 \pm 1.6	3.7 \pm 1.6	6.1 \pm 1.7	5.8 \pm 1.9	5.9 \pm 1.7	6.0 \pm 1.6
7	0.70	0.18	4.1 \pm 1.5	3.5 \pm 1.5	3.6 \pm 1.6	6.0 \pm 1.8	5.0 \pm 1.7	5.4 \pm 1.8	5.5 \pm 1.7
8	0.70	1.02	4.3 \pm 1.2	4.2 \pm 1.5	4.0 \pm 1.5	6.4 \pm 1.7	5.7 \pm 1.8	5.9 \pm 1.7	6.0 \pm 1.5
9	0.70	0.60	3.9 \pm 1.5	3.7 \pm 1.5	3.6 \pm 1.5	5.8 \pm 1.7	5.3 \pm 1.8	5.6 \pm 1.8	5.5 \pm 1.7
10	0.70	0.60	4.0 \pm 1.5	3.7 \pm 1.7	3.7 \pm 1.7	6.1 \pm 2.1	5.3 \pm 2.0	5.5 \pm 2.1	5.5 \pm 2.0
11	0.70	0.60	4.1 \pm 1.3	3.7 \pm 1.4	3.5 \pm 1.6	6.0 \pm 1.6	5.7 \pm 1.6	5.7 \pm 1.7	5.8 \pm 1.5
12	0.70	0.60	4.2 \pm 1.6	3.7 \pm 1.6	3.5 \pm 1.6	6.0 \pm 1.8	5.4 \pm 1.9	5.6 \pm 1.9	5.8 \pm 1.7

MSG = monosodium glutamate.

The independent variables influenced the ideal of intensity of salty taste and the degrees of liking of salty taste and flavour (Table 2). The increase in the salt percentage or the increase in the monosodium glutamate percentage increased the ideal of intensity of salty taste and the degree of liking of the salty taste. Only the response surface for the ideal of intensity of salty taste is presented here (Figure 1), since the surfaces for ideal of intensity of salty taste and for degree of liking of salty taste are all similar. The increase in the salt percentage increased the degree of liking of flavour (Table 2 and Figure 2).

Table 2: Models and goodness of fit for the dependent variables.

Dependent variable	Model	R^2 adjusted (%)	p-value	p of lack of fit
Ideal of intensity of salty taste	$Y_{IIST} = 6.0423 + 0.2662X_1 + 0.2466X_2$	77.48	<0.001	0.332
Degree of liking of salty taste	$Y_{DLST} = 5.3730 + 0.2724X_1 + 0.1616X_2$	70.04	0.002	0.568
Degree of liking of flavour	$Y_{DLF} = 5.6217 + 0.2825X_1$	69.86	0.002	0.157

X_1 = salt (%), X_2 = monosodium glutamate (%).

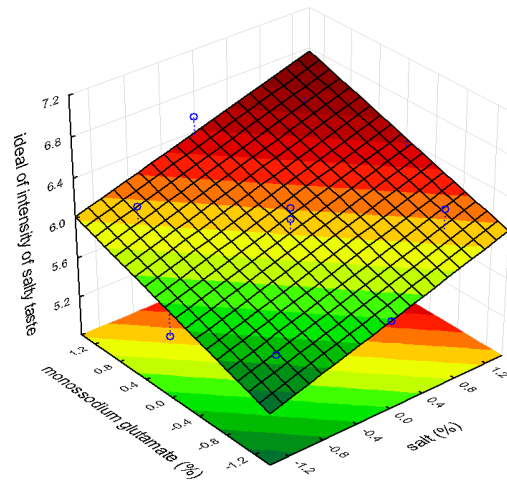


Figure 1: Ideal of intensity of salty taste in function of the addition of salt or the addition of monosodium glutamate (both independent variables are as coded variables).

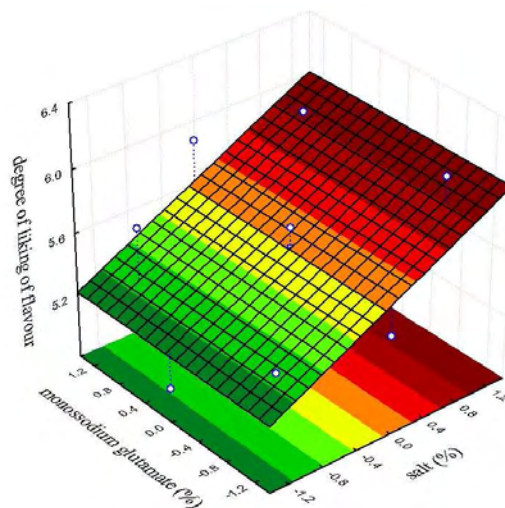


Figure 2: Degree of liking of flavour in function of the addition of salt (both independent variables are as coded variables).

The most interesting result and different from the expected is that there was no interaction between the independent variables; that is, the long-awaited 'flavour enhancing' effect of monosodium glutamate was not observed. Some authors [4] described that the ability of monosodium glutamate to be a flavour enhancer may be dependent on the particular flavour of interest. Additionally, we may raise a hypothesis that probably interaction between salt and monosodium glutamate and their effects on the sensory characteristics may be dependent also on the food matrix and the kind of food.

The monosodium glutamate did not have an effect on the degree of liking of flavour, although had affected the acceptance of salty taste as well as the salt (Table 2). Considering that monosodium glutamate has less sodium than salt (approximately 123 mg and 393 mg of sodium, respectively) [5], this can be a way of reducing sodium in this type of product, and monosodium glutamate is scientifically recognized as safe [6, 7].

Among the snacks studied, that with 1.2% salt and 0.6% monosodium glutamate (assay 6 of Table 1) stands out, once it is in the regions of higher acceptance both in Figures 1 and 2, is sensorially accepted (6.0 in the nine-point hedonic scale for overall liking; Table 1) and still has estimated sodium content below (123.9 mg Na/25 g snack) the average for commercial snacks available in the local market (from 87 to 298 mg Na/25 g snack).

Conclusion

The increase in the salt percentage increased the ideal of intensity of salty taste, the degree of liking of the salty taste and the degree of liking of flavour, while the increase in the monosodium glutamate percentage increased only the first two sensory responses. No interactions were observed between salt and monosodium glutamate considering results from Response Surface Methodology. Our results are relevant for providing alternatives for

reducing the sodium content on expanded snacks. Nevertheless, the reduction must be gradual so as not to negatively affect consumer acceptance.

References

1. Brennan MA, Derbyshire E, Tiwari BK, Brennan CS. Ready-to-eat snack products: the role of extrusion technology in developing consumer acceptable and nutritious snacks. *Int J Food Sci Technol*. 2013;48(5):893-902.
2. Moubarac JC, Martins APB, Claro RM, Levy RB, Cannon G, Monteiro CA. Consumption of ultra - processed foods and likely impact on human health. Evidence from Canada. *Public Health Nutr*. 2012;16(12):2240-2248.
3. Menis-Henrique MEC, Janzanti NS, Andriot I, Semon E, Berdeaux O, Schlich P, et al. Cheese-flavored expanded snacks with low lipid content: Oil effects on the in vitro release of butyric acid and on the duration of the dominant sensations of the products. *LWT-Food Sci Technol*. 2019;105:30-36.
4. Niimi J, Eddy AI, Overington AR, Silcock P, Bremer PJ, Delahunty CM. Cross-modal interaction between cheese taste and aroma. *Int Dairy J*. 2014;39(2):222-228.
5. Maluly HDB, Ariseto-Bragotto AP, Reyes FGR. Monosodium glutamate as a tool to reduce sodium in foodstuffs: Technological and safety aspects. *Food Sci Nutr*. 2017;5(6):1039-1048.
6. Beyreuther K, Biesalski HK, Fernstrom JD, Grimm P, Hammes WP, Heinemann U, et al. Consensus meeting: Monosodium glutamate - An update. *Eur J Clin Nutr*. 2007;61(3):304-313.
7. Henry-Unaeze HN. Update on food safety of monosodium L-glutamate (MSG). *Pathophysiol*. 2017;24(4):243-249.

Characterisation of the key-aroma compounds among the volatile constituents in different hemp strains (*Cannabis sativa* L.)

Markus Kneubühl, Amandine André and IRENE CHETSCHIK

ZHAW - Zurich University of Applied Sciences, Institute of Food and Beverage Innovation, Wädenswil, Switzerland, irene.chetschik@zhaw.ch

Abstract

The key-aroma compounds and the volatile constituents of the flowers of three different industrial hemp varieties (KC Virtus, Felina 32 and Santhica 70) grown during a field study in Switzerland, have been analysed by means of Gas Chromatography-Olfactometry (GC-O) and Gas Chromatography – Mass Spectrometry (GC-MS) in fresh flower samples at different time points of plant growth. The GC-O analysis revealed 33 different odour-active compounds, whereas most of these compounds were detectable in all three hemp cultivars, with different odour intensities. Not only terpenes but also compounds from other substance classes were detected as odour-active constituents. The GC-MS analysis of the terpene constitution in the same samples revealed cultivar-specific differences among the main volatile constituents. Furthermore, changes in the terpene profile could be observed during plant growth. Overall, it could be shown that the flowers of industrial hemp varieties can be regarded as a valuable source of aroma compounds for future food and beverage applications.

Keywords: key-aroma compounds, volatiles, industrial hemp varieties, gas chromatography-olfactometry, gas chromatography-mass spectrometry

Introduction

Hemp (*Cannabis sativa* L.) has been cultivated and used in folk medicine and for textile production since ancient times [1]. After its recent revival as a plant for medical and recreational purposes [2], the attention of the food industry towards industrial hemp with low contents of Δ -9-tetrahydrocannabinol (0.2 % w/w) is growing, due to its high contents in unsaturated fatty acids, proteins, antioxidants and, last but not least, aromatic substances such as terpenes [3-5]. The volatile composition of different *Cannabis sativa* species was studied intensively in many previous investigations by methodologies such as gas chromatography–mass spectrometry (GC-MS) [4, 6-8]. However, studies analysing the odour-active constituents in the aroma profiles of hemp, especially in industrial hemp varieties, by methodologies such as gas chromatography–olfactometry (GC-O), are scarcely available in literature. Therefore, the aim of this investigation was to characterise the key-aroma compounds among the volatile constituents in different industrial hemp varieties (cultivated in Switzerland, containing less than 0.2 % w/w of Δ -9-tetrahydrocannabinol) in the freshly harvested materials, by methodologies such as GC-O and GC-MS. Furthermore, the evolution of some selected volatile marker compounds during plant growth was investigated.

Experimental

The industrial hemp varieties KC Virtus, Felina 32, Santhica 70 (all cultivated in Switzerland, each containing less than 0.2 % w/w of Δ -9-tetrahydrocannabinol) were analysed for their odour-active constituents by GC-O analysis in the fresh flower samples harvested at the end of flowering or the full flowering stage. For this analysis, the hemp flowers were directly frozen in liquid nitrogen after harvest and ground into a fine powder; 25 g of the obtained hemp flower powder was immediately extracted with 250 ml freshly distilled dichloromethane for 2 hours. The extracted volatiles were separated from the non-volatiles by means of the solvent assisted flavour evaporation (SAFE) [9]. The obtained aroma distillate was concentrated and analysed by GC-O, applying the instrumental settings as previously reported [10]. Furthermore, the major terpene compounds in the flowers of the above-mentioned hemp samples were identified by GC-MS and quantified by gas chromatography with flame ionization detection (GC-FID) as previously described [8]. Additionally, the evolution of the terpene profile during the plant growth was studied as recently described [8].

Results and discussion

The GC-O analysis revealed 33 odour-active compounds in the flowers of three different hemp cultivars, in the fresh materials after harvest. Most of the odorants were detectable in all three hemp cultivars. However, differences in the intensities of the odorants were perceivable among the samples. Interestingly, not only terpenes but also compounds from other odour classes such as lipid degradation products, methoxy-pyrazines, sulphur

compounds, one ester and even one pyrroline could be detected among the odour-active constituents during the GC-O analysis.

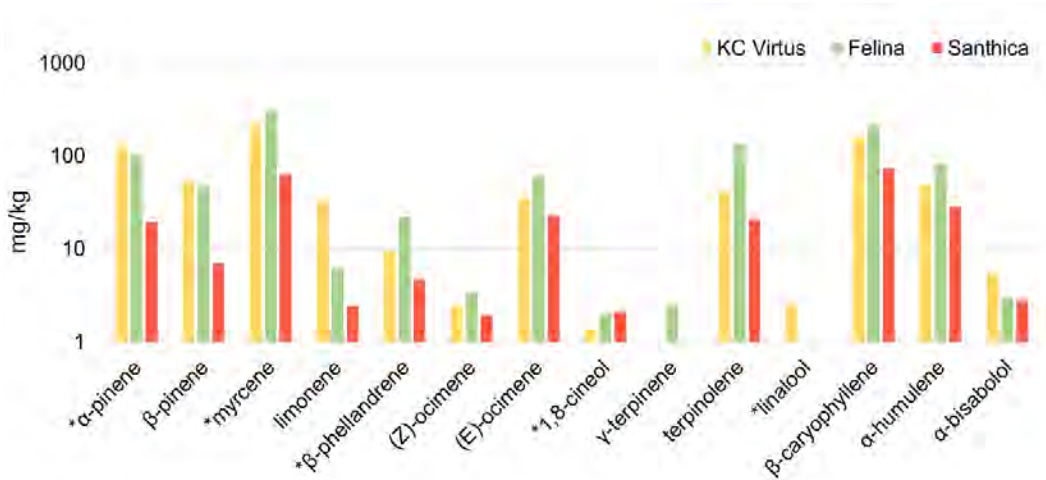
Table 1: Odour-active compounds determined by GC-O analysis in the flowers of three different hemp cultivars (fresh material).

no.	compound	odour-quality	RI- FFAP	odour intensity perceived during GC-O		
				KC Virtus	Felina	Santhica
1	α -pinene ^a	pine-like	1035	++	++	+
2	3-methyl-2-butene-1-thiol ^b	sulphury	1102	++	++	++
3	(Z)-3-hexenal ^{b*}	green	1138	++	++	++
4	α -pinene ^a	metallic	1156	+++	+++	++
5	1,8-cineol ^a	eucalyptus-like	1215	+	+	+
6	(Z)-4-heptenal ^{b*}	biscuit-like, fatty	1236	-	-	++
7	β -phellandrene ^a	terpene-like	1243	+	++	+
8	1-octen-3-one ^b	mushroom-like	1293	-	+	+
9	2-acetyl-1-pyrroline ^{b*}	nutty	1326	+	+	++
10	3-mercapto-2-pentanone ^{b*}	sulphury, catty	1347	++	++	++
11	4-mercapto-4-methyl-2-pentanone ^{b*}	sulphury, green	1365	++	-	-
12	(Z)-1,5-octadien-3-one ^{b*}	metallic, geranium-like	1367	-	+	+
13	3-methoxy-2,5-dimethylpyrazine ^{b*}	mouldy, earthy	1418	+	+	+
14	1-nonen-3-one ^{b*}	mushroom-like	1444	-	-	+
15	methional ^{a*}	cooked potato	1448	++	++	++
16	2-sec-butyl-3-methoxypyrazine ^{b*}	earthy	1483	+	++	-
17	(Z)-2-nonenal ^{b*}	cardboard-like	1487	++	-	+++
18	2-isobutyl-3-methoxypyrazine ^{b*}	bell-pepper-like	1516	++	-	-
19	(E)-2-nonenal ^b	cardboard-like	1515	+	+	++
20	linalool ^a	flowery, bergamot-like	1553	++	-	-
21	butanoic acid ^a	cheese	1619	-	+	+
22	phenylacetaldehyde ^a	flowery	1634	+	+	-
23	unknown	blackcurrant-like	1644	+	+	+
24	(E,E)-2,4-nonadienal ^b	fatty	1698	+	+	++
25	3-methyl-2,4-nonandione ^{b*}	hay, fruity	1710	+	+	-
26	(E,E,Z)-2,4-nonatrienal ^{b*}	oat flakes-like	1873	++	++	++
27	unknown	fruity, flowery	1912	+	+	+
28	trans-4,5-epoxy-(E)-2-decenal ^{b*}	metallic	2000	+	+	+
29	unknown	fruity, spicy	2060	+	+	++
30	ethyl 3-phenyl-(E)-2-propenoate ^{b*}	cinnamon-like	2130	+	-	++
31	sotolone ^{b*}	seasoning	2200	-	+	+
32	unknown	fruity, spicy	2417	+	-	-
33	unknown	sweet	2530	+	-	-

RI-FFAP: retention index on FFAP; +++ odorant perceivable in very high intensity; ++ odorant perceivable in high intensity; + perceivable odorant; - odorant was not perceivable; criteria of identification: a) odorant was identified by retention index on FFAP, MS-spectrum and comparison with reference substance concerning the before-mentioned criteria and the odour quality perceived during GC-O analysis; b) odorant was tentatively identified by retention index on FFAP and compared with the reference substance concerning its retention index on FFAP and the odour quality perceived during GC-O analysis; compounds marked with * were analysed for the first time in *Cannabis sativa* flowers.

Among the terpenes, α -pinene, myrcene, 1,8-cineol, β -phellandrene and linalool were analysed as odour-active constituents during GC-O analysis. Myrcene showed the highest odour intensity, especially in KC Virtus and Felina flowers. Similar trends were also observable for the odour-active terpenes such as α -pinene, 1,8-cineole and linalool, which were detected in KC Virtus and Felina with higher intensities. This observation corresponds well with the overall odour impression of these hemp cultivars, which could be described as fresh and citric. In contrast to this, Santhica showed somewhat higher intensities of the compounds, perceivable with fatty (no. 6, 17, 19 and 24), nutty (no. 9) and cinnamon (no. 30) odour notes, corresponding with the observation that the overall odour impression of this hemp cultivar was perceived as fatty, spicy and balsamic. Interestingly, this study indicates that the overall odour impression of the flowers of different hemp cultivars is not only composed of terpenes but also of odour-active compounds from other substance classes.

In addition to the GC-O analysis, the main terpene compounds were identified and quantified as previously reported [8]. The following terpenes, as presented in Figure 1, were identified as the most abundant compounds in the volatile constitution of the flowers of the analysed hemp strains. The results of the quantitative analysis of these major terpenes are displayed in Figure 1.



n=3; standard deviations $\leq \pm 10\%$; * compound detected as odour-active during GC-O analysis (see Table 1)

Figure 1: Major terpenes and their quantities in flowers of different hemp strains.

Higher amounts for almost all analysed terpenes could be detected for the hemp cultivars KC Virtus and Felina. In contrast to that, the concentrations of the quantified terpenes were drastically lower in Santhica. Interestingly, linalool was only detectable in KC Virtus, and γ -terpinene only in Felina.

To investigate if the harvest period had an influence on the terpene profile, the major terpenes were analysed in flowers of KC Virtus cultivar at different points of time. Figure 2 presents the evolution of the monoterpenes, the sesquiterpenes and the total terpene content during plant growth, as previously reported [8].

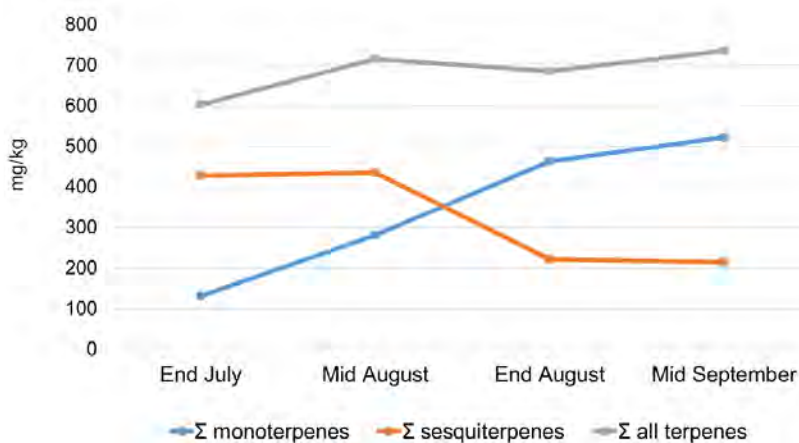


Figure 2: Terpene evolution during plant growth in flowers of KC Virtus.

Overall, our analysis revealed that the total amount of the terpene compounds increased during plant growth. It was observable that the monoterpene content was lower than the sesquiterpene content at the early flowering stages and increased during the cultivation period. In contrast to that, the sesquiterpenes decreased during the cultivation period.

Conclusion

Our study shows that the odour-active constitution of different varieties of industrial hemp flowers is not only composed of terpenes but also other key odorants of different substance classes, such as lipid degradation products, methoxypyrazines, sulphur compounds, one ester and even one pyrrole. Nevertheless, the terpenes constitute the main part of the volatile fraction, whereby the monoterpenes α -pinene, myrcene, β -phellandrene, 1,8-cineole and linalool could be analysed as odour-active constituents during GC-O analysis. In contrast to that, the sesquiterpenes β -caryophyllene, humulene and α -bisabolol were not perceivable during GC-O, indicating that these components are less important for the odour profiles of the analysed hemp flowers. Furthermore, species-related differences could be perceived in the odour constitution of the flowers of different hemp cultivars, and an alternation of the terpene composition was observable in the flowers during plant growth. However, the compounds potentially identified as odour-active by GC-O analysis will have to be verified by further quantitation experiments and the calculation of their odour activity values. It should be noted that possible changes in the odour constitution related to the drying process have to be kept in mind and should be analysed in subsequent investigations.

Overall, the findings of the study show that flowers of industrial hemp varieties, as a side product of hemp fibres and the oil production, can be regarded as a valuable source of aroma compounds, to be valorised in the development of future food and beverage applications.

References

1. Piluzza G, Delogu A, Cabras A, Marceddu S, Bullita S. Differentiation between fiber and drug types of hemp (*Cannabis sativa* L.) from a collection of wild and domesticated accessions G. *Genet Resour Crop Evol.* 2019;60:2331–2342.
2. Appendino G, Chianese G, Tagliatalata-Scafati O. Cannaboids: Occurrence and Medicinal Chemistry. *Curr Med Chem.* 2011;18(7):1085-1099.
3. Leizer B, Ribnicky D, Poulev A, Dushenkov S, Raskin I. The Composition of Hemp Seed Oil and Its Potential as an Important Source of Nutrition, *Journal of Nutraceuticals, Functional & Medical Foods.* 2000;2(4):35-53.
4. Pellati F, Brighenti V, Sperlea J, Marchetti L, Bertelli D, Benvenuti S. New Methods for the Comprehensive Analysis of Bioactive Compounds in *Cannabis sativa* L. (hemp). *Molecules.* 2018;23:2639.
5. Andre C, Hausman J-F, Guerriero G. *Canabis sativa*: The Plant of the Thousand and One Molecules. *Front. Plant Sci.* 2016;7:19.
6. Bertoli A, Tozzi S, Pistelli L, Angelini L. Fibre hemp inflorescences: From corp-residues to essential oil production. *Industrial Corps and Products.* 2010.32(3):329-337.
7. Mudge E, Brown P, Murch S. The Terroir of Cannabis: Terpene Metabolomics as a tool to understand *Canabis sativa* selections. *Planta Med.* 2019;85(09/10):781-796.
8. André A, Leupin M, Kneubühl M, Pedan V, Chetschik I. Evolution of the polyphenol and terpene contents, antioxidant activity and plant morphology of eight different fiber-type cultivars of *Cannabis sativa* L. cultivated at three sowing densities. *Plants.* 2020;9(12):1740.
9. Engel W, Bahr W, Schieberle P. Solvent assisted flavour evaporation, a new and versatile technique for the careful and direct isolation of aroma compounds from complex food matrices. *Eur. Food Res. Technol.* 1999;209:237-241.
10. Chetschik I, Pedan V, Chatelain K, Kneubühl M, Hühn T. Characterization of the flavor properties of dark chocolates produced by a novel technological approach and comparison with traditionally produced dark chocolates. *J. Agric. Food Chem.* 2019;67(14):3991-4001.

Using the Check-All-That-Apply (CATA) methodology to evaluate the flavour of foreign global and domestic Chinese coffee products

YAN PING CHEN¹, Xiayidan Julaiti¹, Chenyang Guo¹, Imre Blank², Disheng Zhou¹, Lingxiao Yu¹ and Yuan Liu¹

¹ Department of Food Science & Technology, School of Agriculture & Biology, Shanghai Jiao Tong University, 200240 Shanghai, China, catherinechenyp@sjtu.edu.cn

² Zurich University of Applied Sciences (ZHAW), Coffee Excellence Center, 8820 Waedenswil, Switzerland

Abstract

The Chinese coffee consumption is growing with the domestic market mainly dominated by imported coffee beans and coffee brands. In this study, the check-all-that-apply (CATA) method was used to evaluate two groups of coffee products. One group was consisting of commercial samples containing four foreign and four domestic brands. The other group comprised lab-roasted samples using raw coffee beans grown in China, in the Yunnan province. The hedonic scores of each sample were collected to present subjects' liking intensities. The results showed that Chinese young subjects participating in this study preferred coffee with cocoa, caramel, nutty aroma, and a distinct mouthfeel. They also prefer coffee with milder bitter and less sour taste. Over-roasting Yunnan coffee beans may cause undesired musty sensation, while mild thermal processing tend to result in lower roasted notes. This study provided an efficient way to obtain sensory profiles of coffee samples using CATA. Different from the traditional consumer survey, this method presents clues for the coffee industry to optimise their products, which resonate with Chinese consumers' sensory preference.

Keywords: the Chinese coffee, check-all-that-apply (CATA), consumer preference, principal coordinate analysis

Introduction

The check-all-that-apply (CATA) is a relatively low cost and time saving method allowing a quick response from consumers when compared to quantitative descriptive analysis (QDA). A CATA question consists of a list of attributes (words or phrases) from which reviewers should select all the attributes they deem appropriate to describe a product and examine the best attributes in the list to classify the product [1]. Evaluators can check as many properties as they want and spend as much time as they need. These attributes are not limited by sensory aspects and may also be related to hedonic and emotional aspects, product use or conceptual fit [2]. There is also a hedonic scale to obtain a rough description of the product. Because the CATA method could gather the intuitive feedback from consumers, many consumer tests use it for analysis and evaluation, such as for example fruit-flavoured powders, ice creams and tea drinks [3], and different parts of the Chinese blanched chicken [4]. Coffee flavour is the liking driver of consumers, and it is also an important criterion to judge the quality. The flavour of coffee varies according to the bean variety, origin, blend, processing method, and roasting conditions. China is one of the largest emerging coffee consuming countries in the world. Some of the Yunnan coffee have already won reputations outside China for their flavour quality, but the foreign brands hold a monopoly position in the Chinese coffee market. The aim of this paper is to (1) understand the coffee consumption trends of the young consumers in China, and (2) understand the main reasons why domestic coffee is less competitive than imported coffee. This investigation could provide advice to improving the competitiveness of domestic coffee in the Chinese market, especially in the young consumers' segment.

Experimental

Materials

Three foreign brands of commercial roasted coffee beans (ST, PA, and CO), and the instant coffee powder (NI) were bought from Shanghai local supermarket. The other four domestic brands of roasted coffee beans (YN, HN, XH, and NK) were provided by the China Coffee Engineering Research Center. All commercial roasted coffee beans were *Arabica* at moderate roasting degree.

The domestic raw coffee beans used for roasting, called "Katim AA Green Beans", were bought from Gaosheng Manor Coffee (Yunnan, China). The lab-roasted coffee beans (SA-L, SB-L, SC-L, and SD-L) were prepared at four different levels of heat load using an electrically heated coffee roaster (TK-200 electric roaster, Stubborn Coffee, Shandong, China). All lab-roasted samples were first roasted to 220°C within 6.5 minutes. In addition, sample SA-L was roasted for another 3 min to reach the final temperature of 195 °C. Sample SB-L was roasted

for another 4 min to reach the final temperature of 195 °C. Sample SC-L was roasted for another 3 min to reach the final temperature of 228 °C. Sample SD-L was roasted for another 4 min to reach the final temperature of 238 °C.

Check-all-that-apply (CATA)

Samples were served in a random design. For each cup of coffee, the subjects were asked to fill the three-digit number on the cup into the CATA questionnaire at first. They then opened the lid and sniffed the aroma for 1-2 s. After sniffing, they took a mouthful brew to evaluate the taste and flavour after swallowing. In the meantime, they first scored the overall liking intensity on a 9 points hedonic scales. Secondly, they used the CATA method to tick the sensory terms that could be used to best describe the coffee sample. The sensory descriptors appear in random order in the questionnaire to reduce bias. The subjects were instructed to rinse their mouth with water after tasting one coffee sample and rest for 0.5 minutes to evaluate the next coffee sample.

Data processing and analysis

CATA was analysed by XLSTAT 2016 (New York, USA). Frequency of use of each CATA term was determined by counting the number of consumers that used the term to describe the sensory descriptors. Cochran's Q test was used to identify significant differences among samples for each of the sensory descriptor. Pairwise comparisons were performed using sign test. Correspondence analysis (CA) performed using chi-square distances was used to get a bi-dimensional representation of the samples based on the frequency of sensory descriptors [5].

Results and discussion

Figure 1a shows the relationship among commercial coffee brews by correspondence analysis (CA). The results showed that PA-F was associated with cocoa, green, and mouthfeel attributes, ST-F was associated with bitter attribute, CO-F was associated with caramel aroma, and NT-F made from instant commercial coffee powder was associated with roasted attribute (Figure 1a). The remaining four coffee brews made from domestic coffee beans were located at the opposite of the foreign brands (except NH-D), showing distinct sensory relationships (Figure 1a). YN-D, HN-D, and XH-D were associated with musty attribute, which contributed to the undesirable perception noted by subjects. In addition, YN-D was associated with astringency and sourness, while XH-D was associated with sour and fermented (Figure 1a). Combining with Table 1, the results show YN-D, HN-D, and XH-D received lower liking scores (4.2, 4.2, and 3.5) from subjects. But NH-D, located close to fruity and floral, but far away from musty, received higher liking scores (4.5) than the other three samples (Table 1 and Figure 1a).

Figure 1b shows the relationship among lab-roasted coffee brews by correspondence analysis (CA). The results show that all samples were located far from floral, fruity, and fermented aroma (Figure 1b). SC-L were ticked with high frequencies for roasted sensation. Its liking score was the highest (5.8), even higher than the commercial samples (Table 1). SB-L is associated with cocoa and sweet attributes (Figure 1b), but its roasting level is lower than SD-L. The low roasting aroma and mouthfeel attributes could be one reason of the lower hedonic score (5.5) of SB-L (Table 2). SD-L got more thermal energy due to the longer roasting time, and it is located close to bitter, mouthfeel, and astringency sensation. On the contrary, SA-L is located far away from roasted aroma. The hedonic scores show both SD-L and SA-L have low liking scores (5.1 and 4.8) (Table 2). This phenomenon may suggest that subjects preferred coffee with an appropriate level of roasted aroma. Lacking this attribute would result in very low subjects' preference, and they would think the product have not enough coffee flavour. However, over-roasting the raw coffee bean could induce undesirable sensation, which could also reduce subjects' preference as shown for SD-L. As a result, SC-L with just the right roasting level, though not rich in the floral, cocoa, and fruity aroma profiles, was preferably selected by subjects.

Table 1 The hedonic scores from subjects towards commercial coffee samples

Samples	NT-F	PA-F	ST-F	CO-F	HN-D	NH-D	XH-D	YN-D
Hedonic scores [†]	4.5±2.1	5.0±2.0	4.4±2.1	4.3±2.2	4.2±1.7	4.5±2.1	3.5±1.8	4.2±2.1

[†] Hedonic scores rated on a 9-point scale were showed as average ± SD (n=59).

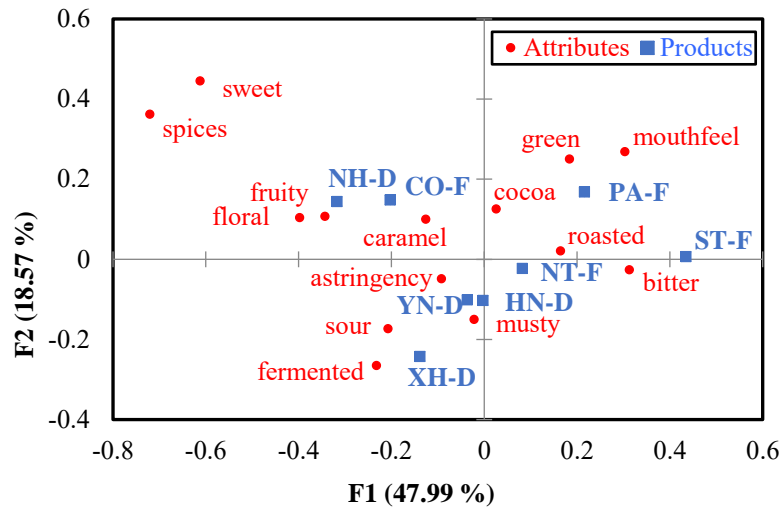
Table 2 The hedonic scores from subjects towards lab-roasted coffee samples

Samples	SA-L	SB-L	SC-L	SD-L
Hedonic scores [†]	4.8±1.7	5.5±1.5	5.8±1.6	5.1±1.7

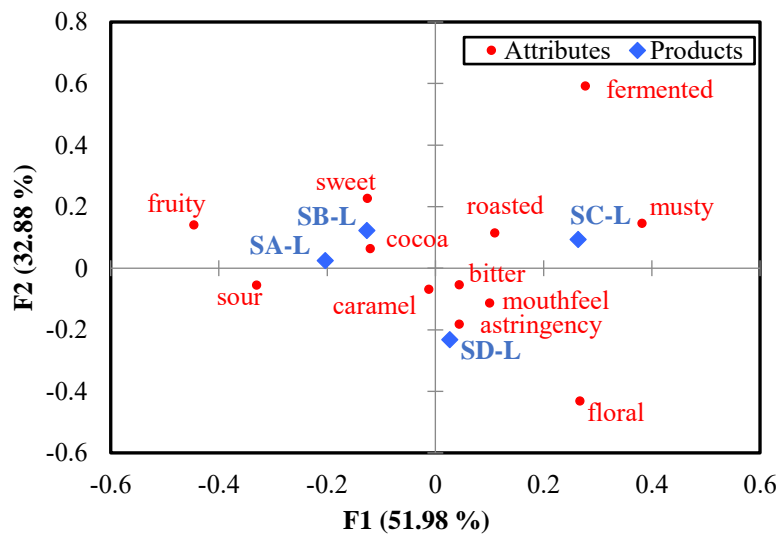
[†] Hedonic scores rated on a 9-point scale were showed as average ± SD (n=31).

Figure 2a shows subjects' liking tendency towards commercial coffee products. The Principal Coordinate Analysis (PCoA) graphically represented the attributes in a space, which is similar to the Principal component

analysis (PCA). But PCoA is applied to the matrix of Euclidean distances between attributes, based on the calculation of standardised columns using unbiased standard deviation. In Figure 2a, liking is more positively associated with the attributes cocoa (0.282) and caramel aroma (0.263) and mouthfeel (0.326), being less associated or negatively associated with other attributes, such as bitter (0.021), sour (-0.227), astringency (-0.204), and musty (-0.180). Figure 2b showed subjects' liking tendency towards lab-roasted coffee products. To attract subjects' preference and balance the sour and bitter taste, sugar was added to coffee brews of the lab-roasted sample. The results showed that subjects preferred sweet taste (Figure 2b). Furthermore, liking is positively associated with caramel (0.340), cocoa (0.384), and sweet (0.219), but less associated or negatively associated with bitter (0.101), astringency (0.080), and musty (-0.219).



(a)



(b)

Figure 1: Check-all-that-apply (CATA) results showing the relationship among sensory descriptors with eight coffee brews made from commercial samples (a) and lab-roasted coffee beans (b) by correspondence analysis. The blue colour represents coffee brews, the red colour represents sensory descriptors. The distance between the row points in the symmetric plot (respectively column points) approximate the inter-row (respectively inter-column) chi-square distance. PC1 and PC2 account for 66.56% variances in commercial samples (a), and 84.86% variances in lab-roasted samples (b).

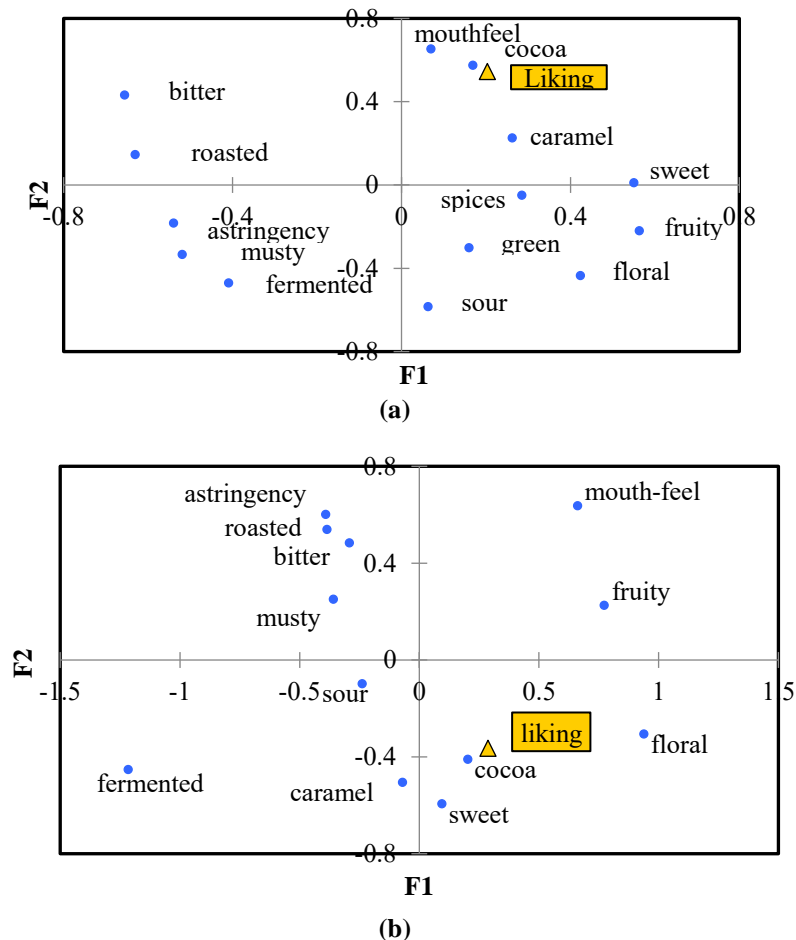


Figure 2: Principal Coordinate Analysis (PCoA) results for commercial coffee brews (a) and lab-roasted coffee brews (b).

Conclusion

The results showed that the subjects involved in this test do not like coffee brews with high sour and bitter taste, astringency, and musty flavour. They favoured coffee brews with caramel and cocoa aroma, sweet taste and mouthfeel. Compared with the commercial samples, the lab-roasted coffee brews made from domestic coffee bean lacked in subjects preferred sensory attributes. Over-roasting domestic coffee beans could generate undesired musty flavour. Not enough thermal processing could make coffee beans lacking the typical roasted flavour. Adding the appropriate content of sugar into coffee brew could improve their hedonic scores. In the future, possible cultivation and manufacturing methods could be applied to improve the flavour precursor composition that could generate sensory attributes during the roasting process that are preferred by subjects. This investigation resulted in clues for improving the flavour quality of domestic coffee products. It gave hints for optimising coffee products that could be appreciated by the Chinese consumers.

References

1. Jaeger S R, Cadena R S, Torres-Moreno M, Antúnez L, Vidal L, Giménez A, et al. Comparison of check-all-that-apply and forced-choice Yes/No question formats for sensory characterisation. *Food Qual Prefer.* 2014;35:32–40.
2. Fabien L, Véronique C, Evelyne V, Amaury L, Mostafa Q E. A new approach for the analysis of data and the clustering of subjects in a CATA experiment. *Food Qual Prefer.* 2018;72:31-39.
3. Piqueras-Fiszman B, Ares G, Alcaide-Marzal J, Diego-Más J A. Comparing older and younger users' perceptions of mobile phones and watches using CATA questions and preference mapping on the design characteristics. *J Sens Stud.* 2010;26(1):1-12.
4. Xu Y, Chen Y P, Deng S, Li C, Xu X, Zhou G, et al. Application of sensory evaluation, GC-ToF-MS, and E-nose to discriminate the flavor differences among five distinct parts of the Chinese blanched chicken. *Food Res Int.* 2020;137:109669.
5. Meyners M, Castura J C, Carr B T. Existing and new approaches for the analysis of CATA data. *Food Qual Prefer.* 2013;30(2):309-319.

Correlation between volatile aroma compounds and sensory changes during storage of heat processed beef flavour

ZEYU ZHANG¹, Bei Wang¹, Imre Blank² and Yanping Cao¹

¹Beijing Advanced Innovation Centre for Food Nutrition and Human Health (BTBU), School of Food and health, Beijing Higher Institution Engineering Research Centre of Food Additives and Ingredients, Beijing Technology & Business University (BTBU), Beijing, China, zhangzeyubtu@163.com

²Zhejiang Yiming Food Co., Yiming Industrial Park, Pingyang County, Wenzhou 325400, China

Abstract

Heat processed beef flavour (HPBF) is deteriorated by the storage environment, which is an urgent problem to be solved. This study aimed to explore the flavour quality change of HPBF based on both aroma compounds and sensory characteristics. The volatile compounds of HPBF were investigated with gas chromatography-olfactometry-mass spectrometry (GC-O-MS) using the aroma extract dilution analysis (AEDA) giving access to flavour dilution factor (FD), and odour activity values (OAV). Twenty key aroma active compounds of HPBF with $\text{Log}_3\text{FD} \geq 3$ and $\text{OAV} > 1$ were identified and followed during a 6-months storage. A total of 13 HPBF samples representing different storage time could be divided into four groups by hierarchical cluster analysis (CA) based on the changing of the 20 key aroma compounds. The sensory intensity of burnt and sauce-like notes gradually increased with time, while the characteristic beef aroma became weaker. Based on principal component analysis (PCA) and partial least squares regressions (PLSR) analysis, 2-methyl-3-furanthiol, 2-furfurylthiol, bis-(2-furfuryl) disulphide and others were correlated to the characteristic beef aroma in the early stage. Moreover, 2-methylbutanal and 2-ethyl-3,5-dimethylpyrazine could be correlated with the decrease of the characteristic beef aroma ($p < 0.05$) and increase of the sauce-like note ($p < 0.05$), enhancing the burnt character with time. Dimethyl disulphide and dimethyl trisulphide had significant effects on the formation of burnt and sauce-like notes modifying the spice intensity in HPBF during storage. The correlation between flavour profiles and sensory characteristics have been clearly explained and demonstrated.

Keywords: beef flavour, heat processing, storage, aroma-active compound, sensory

Introduction

Heat processed beef flavour (HPBF) is a very important raw material for preparing beef flavour. During the process of transportation or storage, the flavour quality of HPBF was greatly affected by the environment effects. The components of HPBF changed gradually, which directly impacted the quality of the flavour profile.

This study aimed to explore the flavour quality change of HPBF based on both aroma compounds selected by GC-O-MS and sensory characteristics at the accelerated experiment (50 °C) during the 6 months storage. The contribution of aroma-active compounds of different storage times and the correlation between aroma-active compounds and sensory characteristics were further studied by PCA and PLSR analyses. The study of flavour quality variation of HPBF could provide technical guidance and a theoretical basis for HPBF applications.

Experimental

HPBF sample preparation

Fresh beef lean meat was hydrolysed by protease, mixed with bovine bone, yeast extract, amino acids were placed in a steam sterilization pot with fresh onion, garlic and some spice (fennel, cloves, nutmeg) at 115 °C for 60 min. After degreasing and filtering, the HPBF samples were packed separately, sealed and stored for 168 days in a sterile environment at 50 °C. The relevant indexes were determined with different analysis time: 1, 14, 28, 42, 56, 70, 84, 98, 112, 126, 140, 154, and 168 days. Each analysis was triplicated in the 13 sets.

Data collection

The volatile compounds of HPBF were analysed with headspace solid-phase microextraction (HS-SPME) GC-MS (Agilent 7890B GC, Agilent 5977A MS) coupled with a sniffing port ODP-3 from Gerstel. The GC-O (AEDA) of HPBF was performed according to Ozkara et al. [1], with the dilutions of 1/3, 1/9, 1/27, 1/81, 1/243 and so on, corresponding to FD values 1, 3, 9, 27, and 81, respectively. OAVs were calculated as the ratio of concentrations to odour thresholds in water generally taken from the literature (Table 1).

Sensory evaluation was carried out by a panel of 10 sensory-trained members at every analysis time. Five sensory attributes, characteristic beef aroma, burnt, sauce, sour, and spice were used to describe the aroma of HPBF, the evaluation of which was based on the 10 panellists' consensus for each attribute, and also for

discriminability and replicability of all the samples. The odour attributes were estimated on a scale from 1 (extremely weak) to 9 (extremely strong), and the average values were calculated.

Statistical analysis

PLSR was used to analyse the correlation between aroma compounds and sensory properties using The Unscrambler, Version 9.7 (CAMO Software Inc., Woodbridge). SIMCA-P version 14.1 (Umetrics Inc., Umea, Sweden) was used for PCA and hierarchical cluster analysis (CA) to analyse the changing of aroma compounds during storage. Other experiments dates were analysed by single-factor analysis of variance (ANOVA) using SPSS (version 22.0, IBM Corp., Armonk, NY, USA).

Results and discussion

The relative aroma contribution of each compound could be evaluated by AEDA and odour description in GC-O. Twenty volatile aroma-active compounds including 2-methyl-butanal, 2-methyl-3-furanthiol, 2-furfurylthiol and 2-[(methylthio)methyl]-furan were selected ($\text{Log}_3\text{FD} \geq 3$, $\text{OAV} > 1$) as key volatiles of HPBF during the 6-months storage (Table 1). Most of the OAV values of the 20 aroma-active compounds decreased with storage time, except for 2-methylbutanal, dimethyl disulphide and dimethyl trisulphide which gradually increased with time.

Table 1: Aroma-active components ($\text{Log}_3\text{FD} \geq 3$, $\text{OAV} > 1$) identified by SPME/GC-O-MS in HPBF stored for 168 days (d).

No ^a	Odour thresholds ^b	OAV					No ^a	Odour thresholds ^b	OAV				
		1 d	42 d	84 d	126 d	168 d			1 d	42 d	84 d	126 d	168 d
1	1 ^A	-	122	116	84	95	11	80 ^A	2	0	0	0	-
2	1.1 ^A	-	6	12	12	15	12	6 ^A	28	12	9	5	8
3	0.3 ^B	124	-	-	-	-	13	16 ^A	55	24	23	13	27
4	0.587 ^A	1	3	5	-	-	14	20 ^F	28	12	10	7	7
5	0.007 ^A	322	103	151	91	-	15	0.04 ^E	2768	1046	953	620	1345
6	0.1 ^A	-	-	-	35	59	16	21.8 ^A	234	150	118	65	125
7	0.13 ^D	142	64	53	28	46	17	22.3 ^A	2	0	0	0	-
8	1.1 ^A	4	2	3	-	-	18	2.5 ^A	306	121	90	51	83
9	0.08 ^A	1345	69	63	20	-	19	100 ^A	1	1	0	0	0
10	0.04 ^A	-	76	58	21	73	20	1 ^F	54	15	10	6	7

^a The 20 key aroma compounds are numerically represented: No. 1: 2-Methylbutanal; No. 2: Dimethyl disulphide; No. 3: Methyl 2-propenyl; No. 4: Octanal; No. 5: 2-Methyl-3-furanthiol; No. 6: Dimethyl trisulphide; No. 7: Dipropyl disulphide; No. 8: Nonanal; No. 9: 2-Furfurylthiol; No. 10: 2-ethyl-3,5-dimethyl-pyrazine; No. 11: Diallyl disulphide; No. 12: Linalool; No. 13: Estragole; No. 14: 2,2,4,4,6,6-hexamethyl-1,3,5-trithiane; No. 15: 2-[(methylthio)methyl]-furan; No. 16: Anethole; No. 17: Furaneol; No. 18: Eugenol; No. 19: 4-methyl-5-thiazoleethanol; No. 20: Bis-(2-furfuryl)-disulphide.

^b Odour threshold value in water (ng/mL): ^A value from van Gemert [2]. ^B value from Abe et al. [3]. ^C value from Schiffman et al. [4]. ^D value from Tian et al. [5]. ^E value from Mottram and Mottram [6]. ^F Odour thresholds value in water were self-determined by the authors.

CA allowed to divide HPBF samples into four groups during the storage process, which were shown with different colours in Figure 1. HPBF with high similarity of volatiles were classified as one group as shown in Figure 1.

PCA was employed to analyse the changing of key aroma compounds of HPBF samples during different storage steps (Figure 2). HPBF could be divided into four groups, shown with different colours, along the PC1 axis, result that was consistent with the result of CA (Figure 1). The number of key aroma compounds gradually decreased with storage time indicating that the flavour quality of HPBF was affected by the storage time.

Based on Figure 2, 2-methyl-3-furanthiol, 2-furfurylthiol, bis-(2-furfuryl)-disulphide and others located on the negative axis of PC1 were close to the 1st day HPBF that contributed to the formation of the overall flavour of the samples on early storage time. Octanal was close to the point of 14 and 28 days indicating that fatty acids are gradually oxidised [7]. 2-Methylbutanal, dimethyl disulphide, dimethyl trisulphide and 2-ethyl-3,5-dimethyl-pyrazine were located on the positive PC1 axis. They were close to the points of 42, 56, up to 168 days, which might be the dominant aroma compounds in the later storage phase.

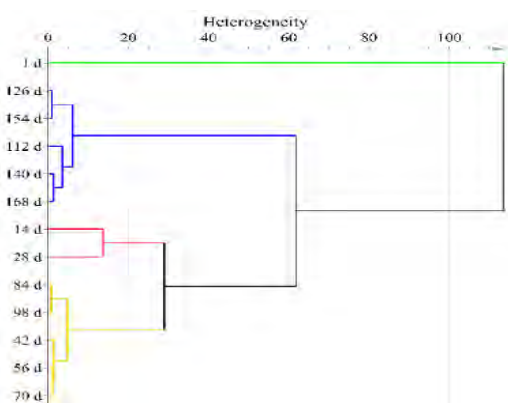


Figure 1: Dendrogram of hierarchical cluster analysis of HPBF at different storage time points based on 20 key aroma compounds.

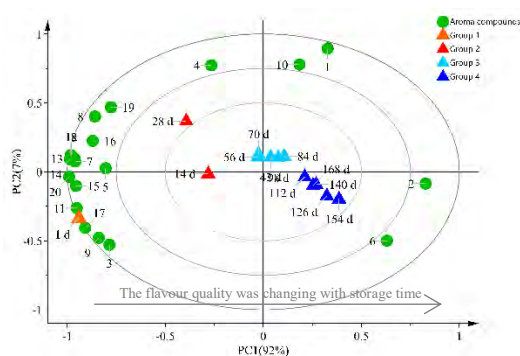


Figure 2: PCA of 20 key aroma compounds of HPBF at the various storage time points (1st to 168th day).

The flavour profiles of HPBF during the 6-months storage are shown in Figure 3. The intensity of characteristic beef aroma gradually became weaker with time, while the intensity of burnt and sauce-like notes of HPBF were increasing with time. The spice intensity measured in HPBF showed no clear trend. The content changes of aroma-active compounds with characteristic beef aroma indirectly reflect the variation trend of flavour profile of HPBF during the storage, a result consistent with the result of PCA (Figure 2).

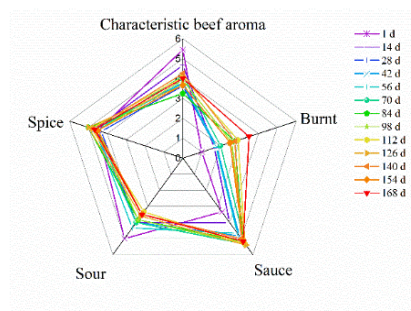


Figure 3: Evaluation of sensory attributes of HPBF for 168-days storage.

PLSR analysis was undertaken to evaluate the relationship between the 20 key aroma-active compounds and sensory attributes. PC1-PC2 model could explain these variables more accurately based on PLSR correlation loading plot shown on Figure 4.

It showed that 2-methyl-3-furanthiol, 2-furfurylthiol, diallyl disulphide, bis (2-furfuryl) disulphide and other compounds in the lower right part were correlated with the characteristic beef aroma and sour taste, which was consistent with the results of Sun and co-workers [8]. 2-Methylbutanal, dimethyl disulphide, dimethyl trisulphide and 2-ethyl-3,5-dimethyl-pyrazine on the PC1 positive axis were highly correlated with spice, burnt and sauce-like notes as shown in Figure 4. Combined with the result of sensory attributes evaluation, the above four compounds might be the dominant aroma components of HPBF leading to obvious burnt and sauce-like notes upon storage.

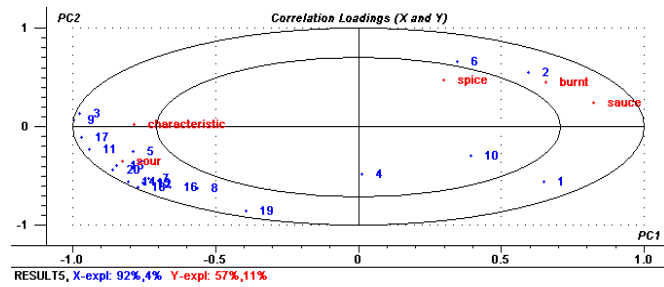


Figure 4: PLSR correlation loading plot for 20 key aroma compounds of HPBF. The blue plots represent the 20 key aroma active compounds. The red plots represent sensory attributes.

To explore the significant influence and correlation of aroma compounds to each sensory attribute, the OAV values of the 20 aroma-active compounds and sensory attributes were respectively taken as X and Y variables for PLS analysis. It can be seen from the Figure 5 that 2,2,4,4,6,6-hexamethyl-1,3,5-trithiane could contribute to the characteristic beef aroma ($p < 0.05$) and mitigate the intensity of the burnt note of HPBF during storage. It was interesting that 2-methyl-3-furanthiol, an intense meaty aroma compound, with a higher FD value and a lower threshold had a significant ($p < 0.05$) and positive effect on the sauce-like note of HPBF, instead of the characteristic beef aroma. 4-Methyl-5-thiazoleethanol derived from thiamine (Vitamin B1) just had a few positive effects on the characteristic beef aroma. In addition, anethole with anise smelling ($2 \leq \text{Log}_3\text{FD} \leq 8$) had a low positive correlation with the characteristic beef aroma and a significant effect on the sour and spice notes.

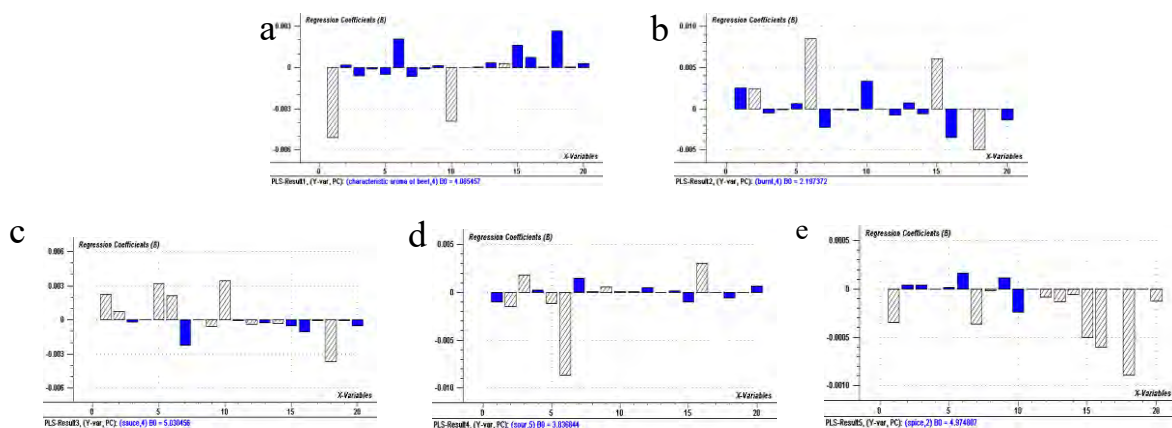


Figure 5: PLS correlation analysis and significance indications (streaked bars) between 20 key aroma compounds and sensory attributes of HPBF samples stored at 50 °C for 168 days, a: the characteristic beef aroma; b: burnt; c: sauce; d: sour; e: spice.

Conclusion

It was found that 20 aroma-active compounds were selected as key volatiles ($\text{Log}_3\text{FD} \geq 3$, $\text{OAV} > 1$) for HPBF stored for 168 days. Based on the changing of these 20 key aroma-active compounds during the storage period, HPBF samples could be divided into four groups by CA and PCA. The number of key aroma compounds gradually decreased, which had a negative effect on the flavour quality of HPBF during storage. 2-Methyl-3-furanthiol, 2-furfurylthiol, bis-(2-furfuryl)-disulphide and other compounds contributed to the characteristic beef aroma and sour note in the early stage of storage. The intensity of the characteristic beef aroma gradually became weaker with time. During the later storage period, 2-methylbutanal, dimethyl disulphide, dimethyl trisulphide and 2-ethyl-3,5-dimethyl-pyrazine contributed to intensity increase of the spice, burnt and sauce-like notes. In the future, adjusting the dynamic balance between aroma-active compounds could be a useful method to mitigate burnt and sauce-like notes and to improve the characteristic beef aroma note of HPBF during storage.

References

1. Ozkara KT, Amanpour A, Guclu G, Kelebek H, Selli S. GC-MS-Olfactometric Differentiation of Aroma-Active Compounds in Turkish Heat-Treated Sausages by Application of Aroma Extract Dilution Analysis. *Food Analytical Methods*. 2018;12(3):729-41.
2. van Gemert LJ. Odour thresholds. *Compilations of Odour Threshold Values in Air, Water and Other Media* (second enlarged and revised edition). Utrecht (The Netherlands): Oliemans, Punter & Partners BV; 2011.
3. Abe K, Hori Y, Myoda T. Characterization of key aroma compounds in aged garlic extract. *Food chemistry*. 2020;312:126081.
4. Schiffman SS, Bennett JL, Raymer JH. Quantification of odors and odorants from swine operations in North Carolina. *Agricultural and Forest Meteorology*. 2001;108(3):213-40.
5. Tian P, Zhan P, Tian H, Wang P, Lu C, Zhao Y, et al. Analysis of volatile compound changes in fried shallot (*Allium cepa* L. var. *aggregatum*) oil at different frying temperatures by GC-MS, OAV, and multivariate analysis. *Food chemistry*. 2021;345:128748.
6. Mottram DS, Mottram HR. An overview of the contribution of sulfur-containing compounds to the aroma in heated foods. In: Reineccius GA, Reineccius TA, editors. *Heteroatomic Aroma Compounds*. ACS Symposium Series. 826. Washington: Amer Chemical Soc; 2002. p. 81-100.
7. Frank D, Hughes J, Piyasiri U, Zhang Y, Kaur M, Li Y, et al. Volatile and non-volatile metabolite changes in 140-day stored vacuum packaged chilled beef and potential shelf life markers. *Meat science*. 2020;161:108016.
8. Sun Y, Zhang Y, Song H. Variation of aroma components during frozen storage of cooked beef balls by SPME and SAFE coupled with GC-O-MS. *Journal of Food Processing and Preservation*. 2021;45(1):e15036.

Investigation of the amino acid derivatives and small peptides profile in culinary bases

BENEDIKT STIGLBAUER¹, David Komarek², Maria Monteiro de Araújo Silva²,
Timo D. Stark¹ and Thomas Hofmann¹

¹ Food Chemistry and Molecular Sensory Science, Technical University of Munich, Freising, Germany, benedikt.stiglbauer@tum.de

² Nestlé Product Technology Centre Food, Singen, Germany

Abstract

Taste is an important aspect affecting the palatability of food. As such, it is essential to determine responsible compounds influencing taste perception. In the savoury area, monosodium glutamate (MSG) and sodium chloride (NaCl) are the predominant compounds responsible for taste attributes “umami” and “salty”, respectively, but both ingredients are sometimes avoided by consumers for various reasons. Although numerous alternative compounds are reported in literature as having taste modulating activity, identification and quantification is often restricted to only specific food products and compound classes. Data on concentration of described taste modulating substances in a wide range of raw materials is limited and a systematic correlation with the taste perception of the final products is lacking. Therefore, this study was conducted to 1) gain a first insight into the role of previously described compounds with umami, salty or kokumi activity in savoury applications and 2) to establish their potential to increase the taste complexity beyond MSG and NaCl. To fulfil this demand, an LC-qTOF-MS method was developed allowing the simultaneous quantification of various small peptides and amino acid derivatives known to have taste modulating activity in the savoury area. The method was validated as a semi-quantitative screening method for a large number of compounds and the selected components were quantified in several food ingredients commonly used in savoury applications.

Keywords: taste, savoury food, small peptides, amino acid derivatives, LC-qTOF-MS

Introduction

There is growing interest to discover new compounds that improve savoury taste quality besides L-glutamate and sodium chloride and, especially, find natural sources containing these components. Many have already been reported in literature including umami tasting as well as umami and salty increasing compounds. Additionally, another taste modulating activity, kokumi, has gained more attention and several responsible compounds with this activity have been identified. These molecules are reported to increase mouthfulness, thickness, complexity, and taste continuity [1-3]. Compounds that can impact the savoury taste belong to various chemical classes, seven of which are displayed in Figure 1. However, quantitative data on these numerous compounds in foods is limited. Therefore, in this work a Liquid Chromatography-Quadrupole Time-of-Flight-Mass Spectrometry (LC-qTOF-MS) multi-method was developed to move towards establishing the potential of these molecules to increase taste complexity as well as enable their in-situ generation.

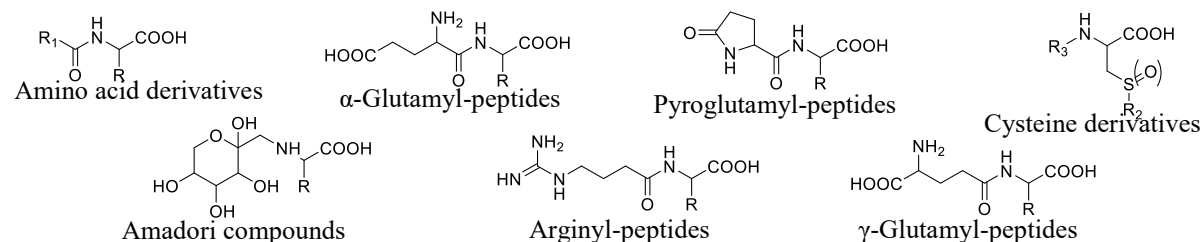


Figure 1: Compound classes that are reported to influence savoury taste and were analysed in the developed multi-method.

Experimental

Samples

The analysed samples were ingredients commonly used in savoury applications including commercial yeast extracts, kitchen-scale cooking bases, lab-scale hydrolysed vegetable mixtures and mushrooms, lab-scale wheat gluten hydrolysates and fermented wheat gluten. Vegetable, mushroom, and wheat gluten hydrolysates were prepared by hydrolysis using different peptidases.

Sensory evaluation

Hydrolysed and fermented wheat gluten samples were comparatively evaluated to a binary mixture of NaCl and MSG by a trained sensory panel with and without nose-clip. For the comparative analysis, NaCl and MSG concentrations of samples and references were adjusted to the same level in two sets, Set 1 and Set 2 (low and high MSG concentration).

Sample Extraction

Samples were extracted with an aqueous formic acid solution (0.1 %) for 30 min at 25 °C. The resulting mixture was centrifuged, the supernatant filtered through a membrane filter and diluted 1:1 with acetonitrile. After another centrifugation step, the supernatant was analysed by sequential window acquisition of all theoretical fragment ion–mass spectrometry (SWATH-MS).

LC-ESI⁺-SWATH-MS analysis

The extracted samples were analysed on a Sciex TripleTOF 5600+ System. Liquid chromatographic separation was achieved on an Agilent 1260 Infinity system with a Waters ACQUITY UPLC BEH Amide Column (130Å, 1.7 µm, 2.1 mm x 150 mm) using mobile phases A (H₂O/ACN-90/10; 20 mM ammonium formate, pH 2.8) and B (H₂O/ACN-10/90; 20 mM ammonium formate, pH 2.8) by applying gradient elution. MS analysis was done in SWATH mode with a TOF survey scan (*m/z* 50-1250, 80 ms) followed by 10 product ion scans with variable Q1 isolation windows from *m/z* 50 to 1250 with an overlap of 1 Da. Product ion spectra were accumulated in high-sensitivity mode for 70 ms using DP of 70 V, CE of 35 V, and CES of 15 V. Quantification was achieved by the standard addition method.

Amino acid and ribonucleotide analysis

The content of free amino acids and ribonucleotides of the five wheat gluten samples evaluated by a sensory panel were determined by LC-UV analysis.

Results and discussion

Reported compounds with savoury taste influencing activity belong to various chemical classes (see Figure 1) and can therefore represent a challenge for simultaneous analysis in a multi-method. Despite gaining selectivity by applying high-resolution mass spectrometry with a qTOF-MS, many of the analytes have the same molecular weight and needed to be chromatographically separated. The optimized method enabled good separation of most analytes to satisfy selective quantification (chromatogram see Figure 2).

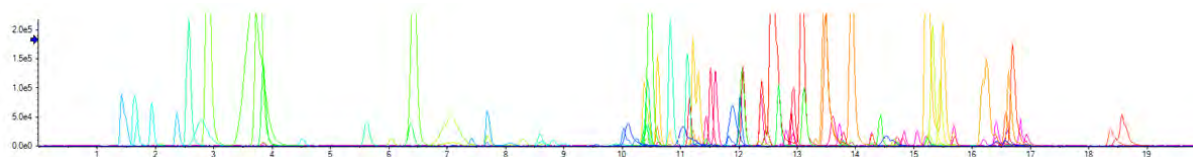


Figure 2: LC-chromatogram of a standard solution containing all analytes.

A good LC separation along with SWATH-MS analysis and High-Resolution (HR)-MS of the TOF scan allowed to obtain HR-MS/MS spectra for all detected compounds (13 amino acid derivatives, 15 α -glutamyl-peptides, 18 γ -glutamyl-peptides, 13 arginyl-peptides, five cysteine derivatives, 15 Amadori compounds and 16 pyroglutamyl-peptides). In the very complex food matrices evaluated interferences in the TOF scan could often be observed which hamper secure identification and quantification. SWATH-MS analysis using MS or MS/MS acquisition for quantification enabled the determination of the whole range of analysed compounds.

The developed method was validated with two representative matrices, vegetable mixture (VM) and hydrolysed wheat gluten (WG). Limit of quantification was determined as the concentration for which signal-to-noise ratios were above 10. They varied per compound group, were predominantly lower than 0.1 µg/mL and below known taste thresholds for the respective compounds. Recovery and precision of the method for the analysed compounds are summarised in Figure 3 and showed recovery values between 70 and 120 % and precision values predominantly below 20 %. The linearity range was also applicable to the concentrations quantified in the analysed samples.

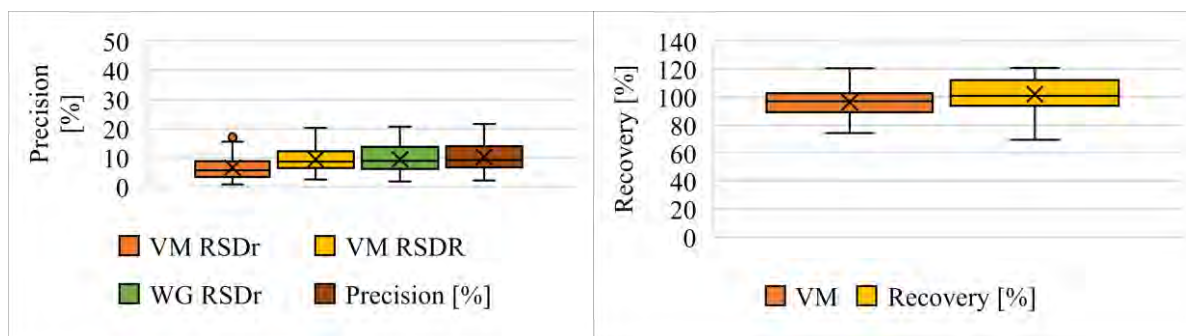


Figure 3: Box-Plots for recovery and precision values for vegetable mixture (VM) and hydrolysed wheat gluten (WG) samples of all analysed compounds (RSDr: intra-day precision; RSDR: inter-day precision).

Subsequently, the developed method was applied to a range of different samples and determined quantities of the various compounds are summarised as a heatmap in Figure 4. It could be observed that amino acid derivatives were only present in fermented wheat gluten as well as yeast extracts, in line with their reported generation during fermentation [3]. Yeast extracts generally showed a relatively high quantity of small peptides compared to the other samples. Mushroom samples showed high amounts of α -glutamyl-peptides compared to the other hydrolysates investigated. It could be observed that different enzyme preparations displayed a varied peptide profile even though the same substrate (wheat gluten) was used. Enzyme preparation 1 (Enz 1) showed a significant increase of γ -glutamyl-peptides, whereas with enzyme preparation 2 (Enz 2) almost none could be detected. This observation suggests a side activity to peptide hydrolysis that generates γ -glutamyl-peptides in Enz 1. Pyroglutamyl peptides are present in high amounts in wheat gluten samples. This could be explained by the high concentration of glutamine in wheat gluten, as pyroglutamyl peptides can also be formed from glutaminyl peptides [3]. Further optimization of the food process based on these observations can be performed as clearly sample discrimination was achieved.

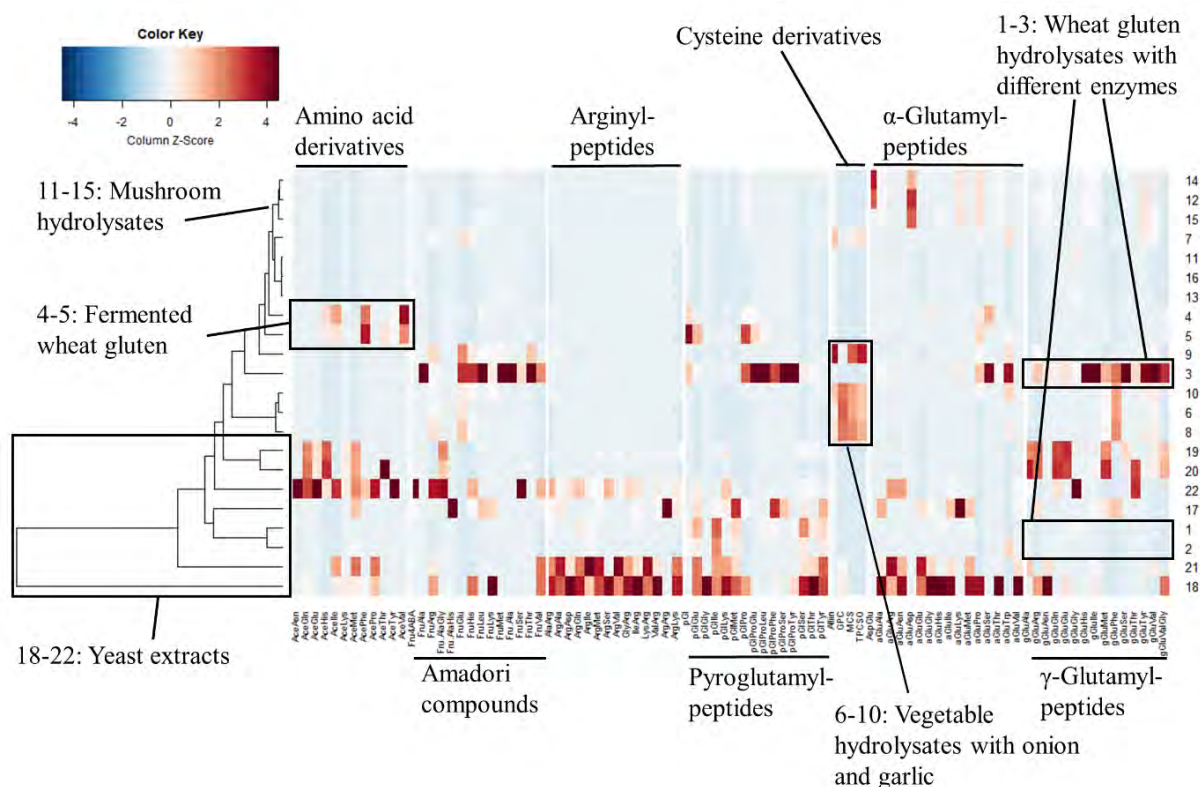


Figure 4: Hierarchical cluster analysis and heat map visualization of samples (rows) and display of the quantified compounds (columns).

Wheat gluten samples were evaluated by a sensory panel with and without nose-clip, the former to focus primarily on taste. In order to gain a first insight into the taste profile that extends beyond MSG and NaCl, their corresponding concentrations were determined and adjusted in all samples to the same value in Set 1 and Set 2

with low and high MSG concentration, respectively. In a comparative analysis, it was observed that all the samples showed a significant increase in umami and/or salty taste perception compared to the reference (Figure 5). Therefore, sensory analysis indicated further compounds present in the samples that influence (additive, synergistic and/or enhancing effects) taste perception. Specifically, an increase of umami and salty tastes as well as an increase in umami aftertaste and in total time-intensity of taste perception were observed. This effect was still perceivable even at a higher concentration of MSG (Set 2). The lack of ribonucleotides in these samples can exclude their contribution to the observed increase in taste perception, which suggest other responsible compounds to be present [1]. Further sensory and analytical experiments are needed to determine which compound(s) are responsible for the increase in the mentioned taste profiles.



Figure 5: Comparative taste profile analyses on a scale of 0-10 against reference which was set to a value of 0. Only significant differences to the reference are shown. FL: Flavour determined with nose-clip; AF: Aftertaste – intensity after set time with nose-clip; Time-intensity: Taste-intensity after set time with nose-clip; MF: Mouthfeel; Salivation: Increased salivation; *MF values determined without nose-clip.

Conclusion

An LC-SWATH-MS multi-method was developed to simultaneously quantify a total of 95 compounds belonging to the chemical classes of small peptides and amino acid derivatives that have been reported to influence the savoury taste perception. The method was successfully applied to various culinary bases that are commonly used in savoury applications, and, therefore fulfilled its role as a semi-quantitative screening multi-method for seven different compound classes with the possibility to easily include a higher number of compounds. This analytical tool can be used to move towards determining the full profile of taste compounds in complex samples in a fast and simple manner. Generated data could be used for a more data-driven recipe generation process and selection of ingredients to achieve the desired taste profile. Sensory analysis confirmed the possibility to increase taste complexity beyond salt and MSG. Furthermore, this method can also offer the opportunity to monitor process optimization for the generation of reported taste influencing compounds in the savoury area. Therefore, the developed LC-qTOF-MS multi-method represents a versatile tool for taste improvement.

References

- Behrens M, Meyerhof W, Hellfritsch C, Hofmann T. Sweet and Umami Taste: Natural Products, Their Chemosensory Targets, and Beyond. *Angew Chem Int Ed.* 2011;50(10):2220-42.
- Schindler A, Dunkel A, Stähler F, Backes M, Ley J, Meyerhof W, Hofmann T. Discovery of Salt Taste Enhancing Arginyl Dipeptides in Protein Digests and Fermented Fish Sauces by Means of a Sensomics Approach. *J Agric Food Chem.* 2011;59(23):12578-88.
- Zhao CJ, Schieber A, Gänzle MG. Formation of taste-active amino acids, amino acid derivatives and peptides in food fermentations – A review. *Food Res Int.* 2016;89:39-47.

Understanding sweetness of dry wines: First evidence of Astilbin isomers in red wines and quantitation in a one-century range of vintages

MARIE LE SCANFF, Syntia Fayad and Axel Marchal

Unité de recherche Œnologie, EA 4577, USC 1366 INRAE, ISVV, Université de Bordeaux, F33882 Villenave d'Ornon, France, marie.le-scanff@u-bordeaux.fr

Abstract

Astilbin (2*R*, 3*R*) was recently reported to contribute to wine sweetness [1]. As its aglycon contains two stereogenic centres, three other stereoisomers may be present: neoastilbin (2*S*, 3*R*), isoastilbin (2*R*, 3*S*), and neoastilbin (2*S*, 3*S*). These compounds have already been observed in natural products, but never in wine. This work aimed at assaying their presence for the first time in wines as well as their taste properties. The isomers were synthesised from astilbin and purified by semi-preparative HPLC. Sensory analysis highlighted the sweet taste of these stereoisomers whose intensity varied according to their configuration. Their content was assayed by developing a UHPLC-Q-Exactive quantification method. After validation, this method was applied to screen astilbin and isomers in various wines, especially in different vintages from the same estate. While young wines contained higher concentrations of astilbin than the old ones, the concentrations of the other isomers, mainly neoastilbin, were higher in the old wines, suggesting their formation over time.

Keywords: Sweetness, sensory analysis, taste, isomers, wines

Introduction

The gustatory balance of wines relies on sweetness, bitterness and sourness. In dry wines, sweetness does not result from the presence of residual sugars as in sweet wines, but is due to other non-volatile compounds. Natural sweet compounds released by oak wood [2, 3] or yeast lees [4] have been identified by taste-guided purification. Recently, such an approach allowed the isolation of two compounds from grapes that might contribute to the sweetness of dry wines: epi-DPA-G and astilbin [5, 6].

Astilbin, or (2*R*,3*R*)-3,3',4',5,7-pentahydroxyflavanon-3- α -L-rhamnopyranoside, is a dihydroflavonol rhamnoside found in many plants and plant-derived products, such as rhizoma of *Smilax glabra* [7], grape and wine [5,8,9]. The aglycon of astilbin is dihydroquercetin, also named taxifolin. It contains two stereogenic centres: carbons C-2 and C-3. Depending on the configuration of these carbons, astilbin (2*R*, 3*R*) has three other stereoisomers, i.e. neoastilbin (2*S*, 3*R*), isoastilbin (2*R*, 3*S*), and neoastilbin (2*S*, 3*S*), as shown in Figure 1 [10]. Astilbin was identified in wine for the first time by Trousdale and Singleton [8] within a concentration range of 0.10-2 mg/L. The sweet taste of astilbin has been recently described [5] and an LC-HRMS method has been developed to quantify it in dry wines [1]. However, the presence of astilbin isomers has never been reported in wine.

The present work investigated the presence of astilbin isomers in red wines. First, neoastilbin, isoastilbin, and neoastilbin were synthesised from astilbin and their sensory properties were assessed. Their presence was sought in commercial red wines by LC-HRMS targeted screening. A quantitative method was then applied to screen astilbin and its isomers in various commercial wines, especially in different vintages from the same estate, to analyse their evolution over time [11].

Experimental

Chemicals and commercial wines

Astilbin (LC-MS purity \geq 95 %) was isolated from vine stems by centrifugal partition chromatography and semi-preparative high performance liquid chromatography (HPLC) according to the procedure described by Cretin [5]. Samples of 63 commercial red wines were used for isomers identification and quantitation. The wines were from various regions (39 from Bordeaux, 16 from Burgundy, 6 from Beaujolais, 1 from Roussillon and 1 from Germany) with vintages varying from 1918 to 2017. Among them, a series of different vintages from the same winery in Burgundy was analysed, i.e. 16 wines from 1918 to 2017.

Astilbin isomerisation

An aliquot of 340 mg of astilbin was dissolved in 300 mL of hydro-ethanolic solution (12 % v/v EtOH in ultrapure water) and pH was adjusted to 5 with formic acid. This value had been chosen after preliminary tests at various pHs. The mixture was heated at 60 °C for 7 days. After five liquid-liquid extractions with 50 mL of butanol saturated with water, the combined organic layers were evaporated to dryness, suspended in water and freeze-dried to obtain 323 mg of pale orange powder.

Purification by semi-preparative liquid chromatography

Semi-preparative HPLC analyses were performed using a Waters Prep 150 LC including a 2545 Quaternary Gradient Module, a 2489 UV/ Visible detector, and a 2424 ELSD detector (Waters, Guyancourt, France). An Atlantis T3 OBD prep column (19 × 250 mm, 5 µm, Waters, Guyancourt, France) was used. The mobile phase was a mixture of ultrapure water containing 0.1 % of formic acid (Eluent A) and acetonitrile with 0.1 % of formic acid (Eluent B). The flow rate was set to 20 mL/min. The gradient was 0 min, 10 % (B); 2.46 min, 10 % (B); 4.91 min, 20 % (B) 14.73 min, 20 % (B); 24.56 min, 25 % (B); 34.38 min, 50 % (B); 39.29, 98 % (B); 44.20 min, 98 % (B); 44.70, 10 % (B). Aliquots (around 40 mg) of powder were dissolved in 200 µL of methanol and in 200 µL of ultrapure water, 0.45 µm-filtered and successively introduced manually into the system. A total of 320 mg were injected. UV detection was carried out at 254 and 280 nm and chromatographic peaks were collected manually in tubes just after the detector. Samples obtained were pooled, evaporated *in vacuo* to remove acetonitrile, and freeze-dried to obtain white powders. Thus, 59 mg of astilbin, 29 mg of neoastilbin, 10.80 mg of isoastilbin and 25.40 mg of neoisoastilbin were obtained.

Sensory analysis

The sensory analysis took place in a specific room air-conditioned at 20 °C and equipped with individual booths. The compounds were dissolved at 5 mg/L in a non-oaked white wine (Bordeaux, 2013, 100 % Sauvignon blanc, 13 % vol. alc.). Samples were tasted in clear IAO wine glasses by five experts in wine-tasting (four women, one man, aged from 24 to 54 years old). The tasters were informed of the nature and risks of the present study and were asked for their written consent to participate. They were asked to describe the gustatory perception of each compound using the vocabulary of wine-tasting. Sweetness and acidity intensity were evaluated on a scale from 0 (not detectable) to 5 (strongly detectable) and compared to a blank solution. Even though the compounds were observed in wines, the panellists were advised not to swallow but to spit out the samples after tasting.

Liquid chromatography – High Resolution Mass Spectrometry (LC-HRMS)

Chromatographic separation was achieved using a Vanquish Flex system (Thermo Fisher Scientific, Les Ulis, France) consisting in a binary pump, an autosampler and a heated column compartment. MS detection was performed using a Q-Exactive mass spectrometer equipped with a heated electrospray ionization (HESI II) probe (both from Thermo Fisher Scientific, Les Ulis, France). A C18 column is used, High Silica Strength (HSST3; 100 mm x 2.1 mm, 1.8 µm) from Waters. The flow rate was set at 400 µL/min. The injection volume was 5 µL and the eluents were (A) 0.1 % formic acid in water and (B) 0.1 % formic acid in acetonitrile. For the optimized gradient, eluent B varied as follows: 0 min, 10 %; 1 min, 20 %; 3 min, 20 %; 5 min, 25 %; 7 min, 50 %; 8 min, 98 %; 10 min, 98 %; 10.1 min, 10 %; 12 min, 10 %. The column and sample temperatures were 25 °C and 10 °C, respectively.

Results and discussion

Synthesis and Sensory Characterisation of Astilbin Stereoisomers

In a recent study, the analysis of a red wine by LC-HRMS revealed different signals in the extracted ion chromatogram (XIC) corresponding to m/z ions characteristic of the empirical formula of astilbin [1]. These results might suggest the presence of astilbin isomers in wine. Previous studies reported the isomerisation of astilbin and the mechanism of this reaction has been clearly established for taxifolin using quantum chemistry calculation and circular dichroism [11]. The same mechanism was proposed for the rhamnosyl derivatives [12]. The interconversion between astilbin (2R, 3R) and its stereoisomers involved a ring opening leading to a quinone methide. This compound can lead to neoisoastilbin (2S, 3R) by recyclization. The quinone methide can also epimerize by the formation of an α -hydroxychalcone to give isoastilbin (2R, 3S) and neoastilbin (2S, 3S) by recyclization (Figure 1). Preliminary tests guided the choice of a pH suited for isomerisation and avoiding hydrolysis of the glycoside moiety. Mild acidic conditions (pH 5) were subsequently chosen to stay close to the composition of wine. From a solution of pure astilbin, a mixture of four main compounds was obtained after 7 days at 60 °C. LC-HRMS confirmed that these compounds had the same m/z ions. After extraction with butan-1-ol, the reaction mixture was submitted to semi-preparative HPLC to purify the four isomers.

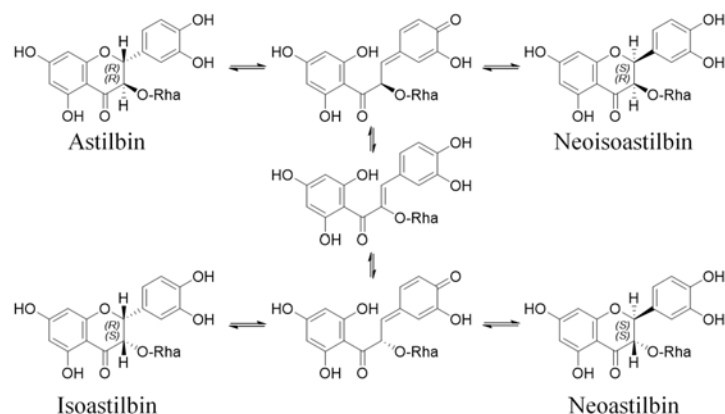


Figure 1: Interconversion of astilbin and its isomers neoastilbin, isoastilbin and neoisoastilbin.

The sensory properties of the four stereoisomers purified were then investigated. Five experts in wine-tasting evaluated the taste characteristics of a white non-oaked wine spiked individually with the compounds. They rated the intensity of sweetness, bitterness, and sourness on a scale from 0 to 5. The non-spiked wine used as a reference was evaluated as 1/5 for bitterness and sweetness, and 5/5 for acidity. An increase in sweetness was perceived for the modalities added with astilbin and isoastilbin (3/5 both). The taste of neoastilbin and neoisoastilbin was evaluated as sweeter (4/5 both). For all compounds, a decrease in acidity was also observed (3/5 for astilbin and neoisoastilbin, 4/5 for isoastilbin and neoastilbin). No impact on bitterness was detected. These results highlighted the sweetness of the four isomers, which confirmed and supplemented previous studies. Indeed, Kasai et al. [13] had extracted astilbin and its isomers from *Engelhardtia chrysolepis* leaves. Only neoastilbin was reported as sweet but the tasting conditions were not described [14]. The sweetness intensity of the isomers seemed to be influenced by their stereochemistry. Interestingly, for the sweetest compounds, neoisoastilbin and neoastilbin, the stereogenic centre C2 had an S absolute configuration.

Identification and quantitation of astilbin stereoisomers in red wines

A LC-HRMS method was developed to search for the presence of astilbin isomers in red wine. For each sample of wine analysed, extracted ion chromatograms (XIC) was built in a 5-ppm window around m/z 449.10681, which corresponded to the theoretical m/z of the deprotonated $[M-H]^-$ ion of astilbin. In most samples, five main peaks were observed in the XIC. Considering the mass measurement accuracy, four peaks suggested the presence of astilbin isomers. Spiking wine samples with standards led to a perfect co-elution and an increase in peak areas. To confirm this hypothesis, MS2 spectra were recorded for the five peaks. Their spectra were similar to that of astilbin and showed main fragment ions at m/z 303 and 285. These results confirmed the presence of neoastilbin, isoastilbin and neoisoastilbin in red wine. For the other peak, the MS2 spectra of $[M-H]^-$ ion showed different fragments at m/z 287 and 269, this compound might be dihydrokaempferol-3-O-glucoside. Analysis of pure standards would be necessary to identify its chemical structure unambiguously.

The method developed for targeted screening was also used for absolute quantitation of astilbin isomers in 63 commercial wines from different regions and different vintages. In all wines, astilbin was the most abundant stereoisomer. The average concentration of astilbin was 9.10 mg/L with a minimum value of 0.60 mg/L and a maximum value of 41.10 mg/L. Regarding isomers, the mean values of neoastilbin, neoisoastilbin and isoastilbin were 1.08, 0.70 and 1.03 mg/L respectively. The maximum concentrations of neoastilbin, neoisoastilbin and isoastilbin were 5.94, 2.73 and 4.45 mg/L respectively. All isomers were shown to increase the sweetness perception of a wine at 5 mg/L, so the quantitative results suggested the sensory potential of these flavanonols for some wines.

In the set of samples analysed in this work, there were a series of vintages from the same winery in Burgundy. Even if weather conditions and, to a lesser extent, winemaking techniques may differ from one vintage to another, such series could be useful for comparing the concentrations of astilbin stereoisomers in old or recent vintages. Figure 2 shows that young wines contained higher concentrations of astilbin than old ones, while the concentrations of the isomers, mainly neoastilbin, were higher in old wines. The difference in concentrations between astilbin and neoastilbin appeared to decrease over time. By plotting the vintage and the concentration, inverse correlations were observed for neoastilbin ($r^2 = 0.62$) and astilbin ($r^2 = 0.31$) (Figure 2). These results suggest that neoastilbin was formed over time, maybe through isomerisation of astilbin. The levels of isoastilbin and neoisoastilbin, albeit slightly higher in old wines, seemed less affected by the age of the wine.

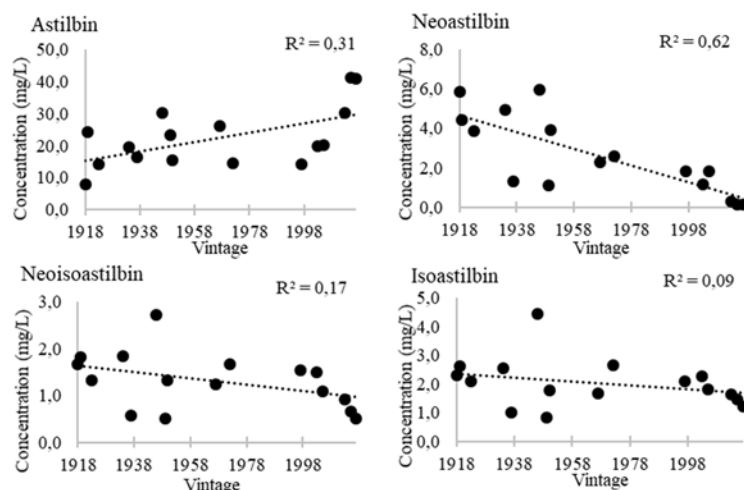


Figure 2: Relationship between concentration of compounds and ageing in Pinot noir wines from a Burgundian winery.

Conclusion

This study reports the first identification of astilbin stereoisomers in wines. Isoastilbin, neoastilbin and neoisostilbin were synthesised to allow the study of their sensory properties. Their addition to a wine modified the taste balance by increasing the perceived sweetness, whose intensity varied according to the stereochemistry. Neoastilbin and neoisostilbin were the most active compounds. Their content was assayed by developing a UHPLC-Q-Exactive quantification method. After validation, this method was applied to screen astilbin and isomers in various wines, especially in different vintages from the same estate. While young wines contained higher concentrations of astilbin than the old ones, the concentrations of the other isomers, mainly neoastilbin, were higher in the old wines, suggesting their formation over time. These results highlight the contribution of astilbin isomers in wine sweetness. More generally, this study brings new insights to understand the chemical origin of wine taste.

References

- Fayad, S.; Cretin, B.N.; Marchal, A. Development and Validation of an LC–FTMS Method for Quantifying Natural Sweeteners in Wine. *Food Chem.* 2019;125881.
- Gammacurta, M.; Waffo-Teguo, P.; Winstel, D.; Cretin, B.N.; Sindt, L.; Dubourdiou, D.; Marchal, A. Triterpenoids from *Quercus Petraea*: Identification in Wines and Spirits and Sensory Assessment. *J Nat Prod.* 2019;82:265–275.
- Marchal, A.; Waffo-Téguo, P.; Génin, E.; Méryllon, J.-M.; Dubourdiou, D. Identification of New Natural Sweet Compounds in Wine Using Centrifugal Partition Chromatography–Gustatometry and Fourier Transform Mass Spectrometry. *Anal Chem.* 2011;83:9629–9637.
- Marchal, A.; Marullo, P.; Moine, V.; Dubourdiou, D. Influence of Yeast Macromolecules on Sweetness in Dry Wines: Role of the *Saccharomyces Cerevisiae* Protein Hsp12. *J Agric Food Chem.* 2011;59:2004–2010.
- Cretin, B. Recherches Sur Les Déterminants Moléculaires Contribuant à l'équilibre Gustatif Des Vins Secs. PhD Thesis, Université de Bordeaux, 2016.
- Cretin, B.N.; Waffo-Teguo, P.; Dubourdiou, D.; Marchal, A. Taste-Guided Isolation of Sweet-Tasting Compounds from Grape Seeds, Structural Elucidation and Identification in Wines. *Food Chem.* 2019;272:388–395.
- Zheng, D.; Zhang, L.; Zhang, Q.-F. Isomerization of Astilbin and Its Application for Preparation of the Four Stereoisomers from *Rhizoma Smilacis Glabrae*. *J Pharm Biomed Anal.* 2018;155:202–209.
- Trousdale, K.; Singleton, L. ASTILBIN AND ENGELETIN IN GRAPES AND WINE. 1983, 2.
- Landrault, N.; Larronde, F.; Delaunay, J.-C.; Castagnino, C.; Vercauteren, J.; Merillon, J.-M.; Gasc, F.; Cros, G.; Teissedre, P.-L. Levels of Stilbene Oligomers and Astilbin in French Varietal Wines and in Grapes during Noble Rot Development. *J Agric Food Chem.* 2002;50:2046–2052.
- Gaffield, W.; Waiss, A.C.; Tominaga, T. Structural Relations and Interconversions of Isomeric Astilbins. *J Org Chem.* 1975;40:1057–1061.
- Fayad, S.; Le Scanff, M.; Waffo-Teguo, P.; Marchal, A. Understanding Sweetness of Dry Wines: First Evidence of Astilbin Isomers in Red Wines and Quantitation in a One-Century Range of Vintages. *Food Chem.* 2021;352:129293.
- Elsinghorst, P.W.; Cavlar, T.; Müller, A.; Braune, A.; Blaut, M.; Gütschow, M. The Thermal and Enzymatic Taxifolin–Alphitonin Rearrangement. *J Nat Prod.* 2011;74:2243–2249.
- Kasai, R.; Hirono, S.; Chou, W.-H.; Tanaka, O.; Chen, F.-H. Sweet Dihydroflavonol Rhamnoside from Leaves of *Engelhardtia chrysolepis*, a Chinese Folk Medicine, Hung-Qi. *Chem Pharm Bull.* 1988;36:4167–4170.
- Zhang, Q.-F.; Fu, Y.-J.; Huang, Z.-W.; Shanguang, X.-C.; Guo, Y.-X. Aqueous Stability of Astilbin: Effects of PH, Temperature, and Solvent. *J Agric Food Chem.* 2013;61:12085–12091.

Gluten-free breads: a response to a technological challenge

Lidwine Grosmaire ¹, Lan Lin ^{1,2} and ISABELLE MARAVAL ^{1,2}

¹ Qualisud, Univ Montpellier, CIRAD, Montpellier SupAgro, Univ d'Avignon, Univ de La Réunion, Montpellier, France

² CIRAD, UMR Qualisud, F-34398 Montpellier, France
isabelle.maraval@cirad.fr

Abstract

The market of gluten-free foods has exploded in recent years and this growth can be essentially put down to an increasing incidence in celiac disease (about 1% in the world), or other allergic reactions to gluten consumption. The replacement of gluten presents a major technological challenge, as it is a very important component in relation to the overall quality and structure of baked products and this is particularly the case for bread. To date, few studies are published on gluten-free breads, which reflects the difficulty of the technological challenge and explain that most of gluten-free products on the market are poor quality and taste. Hence, the gluten-free sector needs to lose the image of being “better than nothing”, and offers a range of products that choice, taste and quality are improved to satisfy the growing demand. For this purpose, three gluten-free formulation and two baking processes have been defined. These formulations contain a mixture of starches and flours (rice, corn, cassava, potato and chestnut) combined with hydrocolloid and dairy ingredients to produce a gluten-free bread of similar quality than wheat bread. The aim of this work was to assess the effect of these formulations and baking processes on texture and sensory properties of GF breads. Physical properties were carried out on GF breads, textural and sensory analyses were also achieved on crust and crumb. Results showed that formulation and process play a key role on bread textural and sensory evaluation. Increasing amount of starch improved both crust and crumb properties. The crust texture was essentially affected by the baking process and the crumb sensory and textural attributes was more depending on the formulation.

Keywords: gluten free, bread texture, sensory analysis

Introduction

Gluten plays a major role in the overall quality and texture of baked products, especially bread. Gluten has unique viscoelastic properties and is the main structure-forming protein in flour which contributes to the good bread making ability of wheat dough. However, gluten is responsible for serious diseases like celiac disease (CD) or wheat allergy and gluten sensitivity [1]. In recent years, gluten-free (GF) market exploded due to the increasing incidence of these pathologies [2]. To date, a large number of bread-like GF products appears on the market claiming to look like traditional French bread. However, replacement of gluten presents a major technological challenge which explains that most of GF products are of poor quality and taste.

In this study, two baking processes and three formulations based on a mixture of flours and starches with xanthan gum were performed. Textural and sensory analyses were also achieved on crust and crumb of GF breads. The aim of this work was to assess the effect of these formulations and baking processes on texture and sensory properties of GF breads and to establish a correlation between texture parameters and sensory attributes of the final products.

Experimental

Bread making process and bread formulation

Firstly, dry ingredients were blended with oil, vinegar and egg white in a mixer (5KSM150PS, KitchenAid, St Joseph, MI, USA) during 1 minute. In the same time, yeast and sugar were dissolved in warm water (35 °C) and regenerated in the oven (Emeraude Prestige, HMI Thirode, Mitry-Mory, France) at 35 °C during 15 min. This suspension was added to the premixed ingredients. Subsequently, mixing was carried out at medium speed during 3 minutes. The resultant batter was placed in a rectangular pan for 30 minutes at 35 °C in the oven. Following this fermentation, the bread was baked in the oven. All baking was performed in two subsequent steps: (i) under moisture condition (steam 10%) at T1 (°C) during t1 (min), necessary stage creating a smooth and crispy crust and (ii) under dry condition at T2 (°C) during t2 (min) for the evaporation of water. After baking, the bread was allowed to cool down for 60 minutes at 25 °C. Fresh loaves were tested for textural and sensory evaluations. Table 1 summarised the different baking processes used and the three gluten-free formulations.

Table 1: Formulations and baking conditions.

Samples codes	Ingredients (wt. %)													Moisture condition		Dry condition	
	Water	Sugar	Dry yeast	Fermented cassava flour	Rice flour	Corn starch	Potato starch	Chestnut flour	Xanthan gum	Olive oil	Egg white	Salt	Vinegar	T1 (°C)	t1 (min)	T2 (°C)	t2 (min)
1S1P	44	0.6	1.2	2.6	20.9	0	11.4	9.6	1.1	2.1	4.7	0.8	1	140	30	185	75
1S2P														170	15		60
2S1P	44	0.6	1.2	2.6	12.4	12.4	11.4	5.7	1.2	2.1	4.6	0.8	1	140	30	185	75
2S2P														170	15		60
6C1P	44	0.6	1.2	8.8	12.4	6.2	11.4	5.7	1.2	2.1	4.6	0.8	1	140	30	185	75
6C2P														170	15		60

Texture of bread

The puncture test (PT) was carried out with a TA-XT plus texturometer (Stable Micro Systems, Godalming, United Kingdom) with a 5 kg load cell, to evaluate the texture of crust by punching the sample at 3 different levels of the crust isolated from the crumb of 3 slices of cold bread, with a cylindrical probe of 2 mm-diameter at 2 mm.s⁻¹ cross-speed. The compression used was 80% with a trigger force of 5 g. The failure force, calculated as the peak force, and the failure deformation, defined as the deformation at the peak point, were determined according to studies by Jackman and Stanley [3]. The average value was calculated for each bread.

Crumb texture profile analysis (TPA) was performed using the same device. A 2 cm-thick slice was compressed in dual cycle using a 25 mm cylinder probe with the maximum compression of 40% with a trigger force of 5 g at a crosshead speed of 2 mm.s⁻¹ and the waiting time between the first and second compression cycle was 5 s. Hardness, cohesiveness, springiness, adhesiveness, resilience and chewiness were calculated from the TPA curve [4]. Each sample was assessed 6 times at different points and mean response for the crumb properties recorded.

Sensory quantitative descriptive analysis (QDA)

Then, descriptive analysis was conducted in the sensory laboratory of UMR Qualisud (CIRAD, Montpellier, FRANCE). 13 trained panellists (3 males and 10 females including 3 celiac people) were selected for their sensory ability and availability for the study. Training was conducted with 4 different breads on 2 sessions. The first one was to define an appropriate descriptive vocabulary to characterise the crust and the crumb. Finally, 7 quantitative attributes were selected for the crust and 7 different for the crumb (Table 2) and in the same time, each term should be given a definition by consensus. The second one was to score on a structured discrete scale (0-10) with “low intensity” corresponding to 0 and “high intensity” to 10, each attribute previously selected.

Descriptive analysis was conducted on 6 breads cooked with different formulations and processes. The samples (crust and crumb separately) were cut into 1 cm slices, served monadically according to Williams’ Latin square designs and were coded with random numbers. The analyses were realised in duplicate. The room was temperature and humidity controlled (22 °C and 45% respectively) and white light was used.

Table 2: List of sensory attributes.

Sense	Attribute	
	Crust	Crumb
Appearance	Brownness	
	Thickness	Alveolate
	Heterogeneity	
Odor	Bread	Bread
		Cereal
Mouth feel	Crispy	Soft
		Wet
		Stickiness
Aroma	Cereal	Cereal
	Grilled	

Experimental design and statistical analysis were established using XLSTAT software (2019, Addinsoft, USA).

Results and discussion

For the crust texture, the failure force, related to the crust hardness, was significantly affected by the formulation and the process (Table 3). Significant crust softening was observed when decreasing the corn starch content. Furthermore, the 1P process significantly increased the crust hardness: temperature and duration of the first step of the baking process were relevant for the crust formation. For the failure deformation, low values were associated to firmer and elastic crust, while high values suggesting soft and plastic-like crust. When the 1P process was used, no significant ($p \leq 0.05$) difference was observed among the three formulations. However, regarding the 2P process, a significant reduction of the failure deformation was noticed when decreasing the corn starch content.

Table 3: Textural parameters of bread crust and crumb.

Sample code	Puncture test parameters of crust			Texture profile analysis parameters of crumb				
	Failure force (N)	Failure deformation (mm)	Hardness (N)	Adhesiveness (N.s)	Springiness ¹	Cohesiveness ¹	Chewiness (N)	Resilience ¹
1S1P	10.02(4.39) ^b	3.32(0.93) ^{ab}	4.56(0.73) ^b	-0.31(0.08) ^b	0.61(0.07) ^{bc}	0.74(0.02) ^{bc}	2.06(0.48) ^b	0.31(0.02) ^{bcd}
2S1P	13.84(3.23) ^a	3.44(0.87) ^{ab}	2.14(0.32) ^c	-0.06(0.07) ^a	0.61(0.03) ^{abc}	0.81(0.03) ^a	1.06(0.18) ^c	0.38(0.03) ^a
6C1P	10.92(2.41) ^{ab}	3.55(0.59) ^{ab}	4.65(0.89) ^b	-0.35(0.11) ^b	0.69(0.03) ^a	0.74(0.02) ^{bc}	2.36(0.45) ^{ab}	0.29(0.02) ^{cd}
1S2P	4.36(2.02) ^c	3.79(1.13) ^a	5.92(0.85) ^a	-0.39(0.06) ^b	0.66(0.07) ^{ab}	0.70(0.03) ^c	2.77(0.59) ^a	0.28(0.02) ^d
2S2P	7.45(2.13) ^{bc}	1.67(0.49) ^c	2.75(1.45) ^c	-0.046(0.05) ^a	0.63(0.09) ^{ab}	0.79(0.07) ^a	1.38(0.71) ^c	0.34(0.05) ^{ab}
6C2P	5.88(1.79) ^c	2.54(0.72) ^{bc}	2.92(1.46) ^c	-0.12(0.09) ^a	0.55(0.08) ^c	0.79(0.05) ^{ab}	1.21(0.59) ^c	0.34(0.05) ^{bc}

For each parameter values followed by the same letter are not significantly different at $p \leq 0.05$. Standard deviations are given within brackets. ¹Dimensionless terms

The sample 1S2P, which contains less starch and is defined by an overall shorter cooking duration and a higher temperature of the first stage, presented higher mean of crumb hardness and was statistically ($p \leq 0.05$) different from the others. The adhesiveness was separated into two significant different groups depending on the quantity of corn starch in the formulation: a reduction of this latter resulted in a significant decrease in adhesiveness. The springiness is an indicator of crumb elasticity and hence of fresh bread quality. This parameter appeared to be influenced both by the process and the formulation (cassava flour content) as the sample 6C1P presented higher mean of springiness and was statistically ($p \leq 0.05$) different from the others. The cohesiveness reflects the internal cohesion of the material and, therefore, is an indicator of bread quality. High cohesiveness is desirable because the crumb disintegrates less during mastication. The sample with higher starch content (2S), regardless the process, presented higher mean of cohesiveness and was statistically ($p \leq 0.05$) different from the others. The chewiness is related to the energy required to masticate a solid food product to a state ready for swallowing [4]. Chewiness is consequently an indicator of bread quality: an increase of this parameter is associated to a decline of crumb properties. This parameter appeared to be influenced both by the process and the formulation. The resilience, like springiness, is commonly related to the loss of crumb elasticity and the decline of crumb properties of breads [5]. The sample 2S1P presented the highest mean of resilience and was statistically ($p \leq 0.05$) different from the others. A reduction of this parameter was observed when decreasing the corn starch content in the formulation.

Increasing concentration of starch improved both crust and crumb properties. Starch plays a key role on the bread texture, through its gelatinization and gel-forming properties. Starch gives to dough adequate viscosity to retain gas bubbles and a sufficient elasticity to allow the bubbles to expand during baking. On the other hand, the baking process could also have a negative effect on the bread texture. The findings suggested that the impact of the process was enhanced when the formulation contains high amount of cassava flour (6C).

For the sensory analysis, the panel's performance was assessed and was good in terms of agreement, reliability and repeatability for all the attributes. ANOVA results showed sensory descriptors that could statistically discriminate 6 different breads samples.

The correlation of instrumental parameters with sensory attributes was performed by a Principal Component Analysis (PCA). The PCA of the crust (Figure 1) represents 93.53% of the variance carried by 7 sensory attributes. Figure 2 shows the PCA for the crumb which represent 80.24% of the total variation.

For the crust (Figure 1), instrumental attributes "PT_Failure deformation" and "PT_Failure force" were well correlated ($p \leq 5\%$) with the sensory attributes "Ar_Grilled", "Ap_Brownness" and "Ap_Thickness", "M_Crispy", respectively. PC1 was positively correlated to "Ar_Grilled", "Ap_Brownness" and "PT_Failure deformation" (and negatively with "Ap_Heterogeneity"). The score plot shows that these qualities predominated for 1S formulations. Indeed, these formulations contain (i) lower starch that could explain a high failure force deformation by the softening of the crust and (ii) higher chestnut contents giving darker color and grilled taste of the crust. The second dimension of the PCA was positively correlated with "Ap_Thickness", "M_Crispy" and "PT_Failure force" (and negatively with "Ar_Cereal"). These characteristics are related to the 1P process: a longer primary cooking time at a lower temperature improved crust texture by increasing crust hardness and thickness. Also, a shorter second cooking time at higher temperature gave a more intense cereal aroma.

For the crumb (Figure 2), the first dimension of the PCA correlates the instrumental attributes "TPA_Adhesiveness", "TPA_Cohesiveness", "TPA_Resilience" with the sensory attributes "Ap_Alveolate". On

the opposite, this first dimension also correlates “TPA_Chewiness”, “TPA_Hardness” with “M_Stickyness” and “M_Wet”. So, the crumb sensory and textural attributes were more depending on the formulation: corn starch improved crumb characteristics and fermented cassava flour has an incidence on crumb taste. The overall quality was rating for the bread and no significant difference were observed, between 6.02 (6C2P) and 6.79 (2S1P).

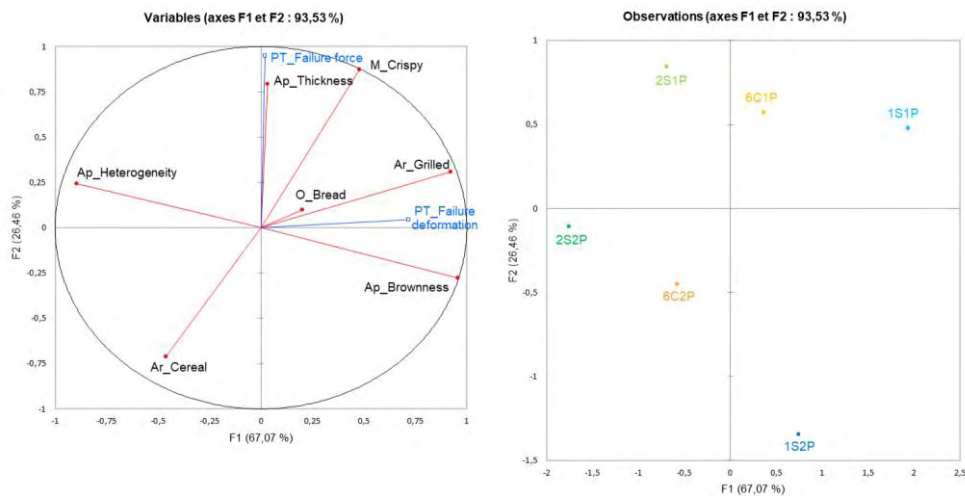


Figure 1: Principal Component Analysis (PCA) biplot of the 7 sensory attributes (in dark) and the 2 instrumental parameters (supplementary variable in blue) on the crust.

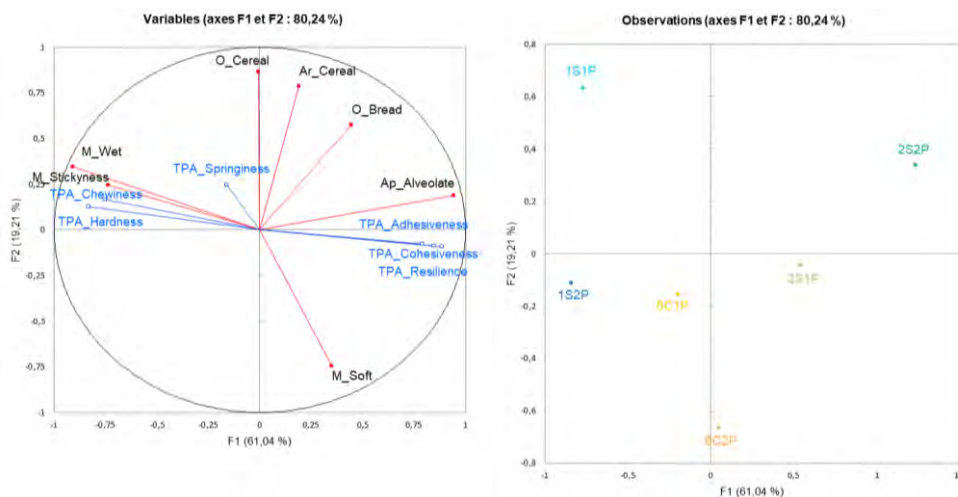


Figure 2: Principal Component Analysis (PCA) biplot of the 7 sensory attributes (in dark) and the 2 instrumental parameters (supplementary variable in blue) on the crumb.

Conclusion

The textural and sensory results showed that formulation and process play a key role on bread textural and sensory evaluation. The substitution of gluten is possible and results show that GF breads obtained from these formulations and processes have a good overall quality. Based on these results, new formulations and processes for GF bread have potential in new recipes to improve the quality of GF market products.

References

1. Rosell C-M, Barro F, Sousa C, Mena MC. Cereals for developing gluten-free products and analytical tools for gluten detection. *J Cereal Sci.* 2014;59:354-364.
2. Lamacchia C, Camarca A, Picascia S, Di Luccia A, Gianfrani C. Cereal-based gluten-free food: how to reconcile nutritional and technological properties of wheat proteins with safety for celiac disease patients. *Nutrients.* 2014;6:575-590.
3. Jackman R-L, Stanley D-W. Area and perimeter dependent properties and failure of mature green and ripe tomato pericarp tissue. *J Texture Stud.* 1992;23:461-474.
4. Bourne MC. Principles of objective texture measurement. In M. C. Bourne (Ed.), *Food texture and viscosity: Concept and measurement* (San Diego, USA). 2002:107–188.
5. Onyango C, Mutungi C, Unbehnd G, Lindhauer M-G. Modification of gluten-free sorghum batter and bread using maize, potato, cassava or rice starch. *LWT-Food Sci Technol.* 2011;44:681-686.

Oral astringency: effect of ageing and role of saliva

MEI WANG, Chantal Septier, H el ene Brignot, Christophe Martin, Francis Canon and Gilles Feron

Centre des Sciences du Go t et de l'Alimentation, AgroSup Dijon, CNRS, INRAE, Universit  Bourgogne Franche-Comt , Dijon, France, mei.wang@inrae.fr

Abstract

Oral astringency is an important sensory characteristic of food and beverages containing polyphenols. However, while polyphenols enriched diet are recommended especially for elderly, astringency perception in elderly people is not documented. The aim of the present work was to evaluate sensitivity to astringency in function of age and saliva (flow and composition). Fifty-four panellists including 30 elderly people (age=75±4.2) and 24 young people (age=29.4±3.8) participated in this study. Astringency was evaluated by 2-Alternative Forced Choice procedure using four tannic acid solutions (from 0.02 g/l to 0.574 g/l). Whole unstimulated saliva was collected for 5 min before and after sensory tests. Each 2-AFC test was done 3 times and evaluation was performed 3 times in three different sessions. Results showed that there was a significant difference in astringency threshold between young group and elderly group (elderly=0.41 g/l ± 0.23, young=0.29g/l ± 0.26; p=0.011). There were no significant differences in unstimulated salivary flow either at the beginning (p=0.56) or the end (p=0.1) of the session between young and elderly. Moreover, correlation between unstimulated salivary flow and threshold was significant only for young group (r=-0.44, p=0.029).

Keywords: elderly, young, astringency, flow rate, threshold

Introduction

Dietary polyphenols are a class of compounds present in some foods and beverages such as vegetables, nuts, unripe fruits, wine and tea [1]. They are of great interest for the food industry because of their potential beneficial effects on health in particular for the ageing population [2]. In food and beverages, polyphenols, especially tannins, can elicit astringency that is perceived as a quality parameter and desired in balanced levels [3]. On the contrary, above a certain intensity, astringency is usually described as a non-pleasant oral sensation [4], limiting the use and promotion of polyphenols at moderate level in food despite their benefits for health [5]. Several mechanisms have been proposed for the astringency onset but recent results indicate that it most probably relies on the interactions of tannins with the mucosal pellicle [4], causing the aggregation of this thin layer of salivary proteins anchored at the surface of oral mucosa via their interaction with MUC1, a transmembrane protein [6]. This aggregation has been correlated to an increase of the friction forces at the surface of the epithelial cell. This observation indicates that the mucosal pellicle loses its lubricating properties during the aggregation process. In this hypothesis, astringency can be modulated by the presence in saliva of proline-rich proteins (PRPs). Indeed, PRPs, which are secreted by the parotid glands, bind and scavenge tannins [7], giving them the ability to protect the mucosal pellicle toward tannin aggregation.

When it comes to the effect of ageing on astringency perception, the literature is quite scarce, despite that ageing is a common main factor that affects flavour perception [8]. Therefore, the main objective of this study is to investigate the sensitivity to astringency in function of age and salivary flow. On this purpose, a 2-AFC methodology was applied to estimate astringency sensitivity in young and elderly panels while evaluating salivary flow. Relationships between salivary flow and sensitivity in function of age are discussed.

Experimental

All materials (pectin, bicarbonate, Evian water, sodium chloride, leucine, sucrose, glutamate, lactic acid, tannic acid) used in this experiment were food grade.

Sensory evaluation

Fifty-four panellists including 30 elderly (O) people and 24 young (Y) people were recruited to participate in sensory sessions. Training session was conducted before testing session. First, subjects were asked to evaluate tasting samples (salty, bitter, sweet, umami, sour, astringency) in a fixed order at room temperature in plastic cups coded with random number. Second, subjects were trained for the 2-Alternative Forced Choice (2-AFC) procedure using astringency stimulus to understand perfectly the procedure of the sensory test.

At the beginning of each testing session, panellists were asked to taste model tannic acid solution of 1.76 g/L to be well aware of astringency. Astringency threshold was evaluated by a 2-AFC procedure with ascending concentrations (0.02, 0.062, 0.188, 0.574 mg/mL) of tannic acid as described above in material section. In each

2-AFC presentation, two samples were presented: one is aimed sample, one is control. Each 2-AFC test was done 3 times and evaluation was performed 3 times in three different sessions. The testing procedure started from the lowest concentration. Panellists were given the reference or stimulus sample. They were asked to put the samples into their mouth, swirled it gently around the mouth for 30s then spit it. They rinsed mouth with pectin and waited for 1 min before evaluating the second sample. After one additional minute, the panellists were asked to indicate which sample was perceived as astringent. Then, panellists rinsed their mouth with pectin, bicarbonate and Evian water before performing another 2-AFC test.

The sensitivity level is reached when three correct answers from the same concentration are achieved. The best estimate threshold for each subject was evaluated as the geometric mean of the three correct answered concentration and the previous lower concentration. When subjects identified correctly the lowest concentration (0.02 g/l), the geometric mean was calculated between this concentration and the theoretical concentration below, i.e. $0.02/3.05=0.0065$ g/l. On the opposite, when subjects did not identify correctly the highest concentration (0.574 g/l), the geometric mean was calculated between this concentration and the theoretical concentration above, i.e. $0.574*3.05=1.75$ g/l.

Saliva collection

Whole saliva was collected after panellists had rinsed their mouths with pectin 0.1%, bicarbonate 1% and water for 5 min at the start (SFStart) and at the end (SFEnd) of the session. After collection, the tubes were weighted and then stored at -80 °C. Flow rates were determined gravimetrically and expressed as gram per minute (ml/min).

Statistical analysis

Non-parametric analyses were conducted. Mann-Whitney U tests were performed to evaluate differences between Y and O subjects regarding sensory and salivary parameters. Wilcoxon test were performed to evaluate differences between SFStart and SFEnd. Friedman Anova analysis was conducted on threshold and salivary flux measurements to evaluate differences between the three sessions. Spearman rank order correlations were performed for the whole group and within each group (Y and O) to evaluate relationships between salivary and sensory parameters. The significance was set at $p < 0.05$. These tests were done using Statistica® version 13.5.0.17, 1984-2018 TIBCO Software Inc.

Results and discussion

No significant differences were observed between sessions regarding SFStart and SFEnd for both groups, Y (SFStart: Friedman $\chi^2=0.75$, $p=0.68$; SFEnd: Friedman $\chi^2=0.75$, $p=0.68$) and O (SFStart: Friedman $\chi^2=5.2$, $p=0.07$; SFEnd: Friedman $\chi^2=1.3$, $p=0.53$). For this reason, we decided to merge both variables in a unique variable, i.e. mean salivary flow (SF). With regard to the comparison of salivary flow rate, there was no significant difference in SF between Y and O groups ($Z = 1.66$, $p=0.09$) (Table 1).

Table 1: Characteristics of the young and elderly panels

	Y (n=24)				O (n=30)			
	Mean	Median	Range	SD	Mean	Median	Range	SD
Age (years)	29.4	30	24-35	3.8	75	73.5	70-87	4.23
SFStart (ml/min)	0.47	0.47	0.26-0.73	0.14	0.44	0.36	0.23-1	0.24
SFEnd (ml/min)	0.51	0.45	0.23-1.03	0.21	0.41	0.33	0.19-0.91	0.23
SF (ml/min)	0.49	0.47	0.27-0.82	0.16	0.42	0.35	0.11-0.92	0.23
Threshold (g/l)	0.29	0.2	0.04-1.00	0.26	0.41	0.35	0.06-0.78	0.24

No significant differences were observed between the three sessions regarding astringency thresholds for both groups, Y (Friedman $\chi^2=1.13$, $p=0.56$) and O (Friedman $\chi^2=1.14$, $p=0.56$).

A significant difference was observed between Y and O groups ($Z=-2.5$, $P=0.0110$), the O group showing a higher mean astringency threshold than the Y group (Table 1, Figure 1).

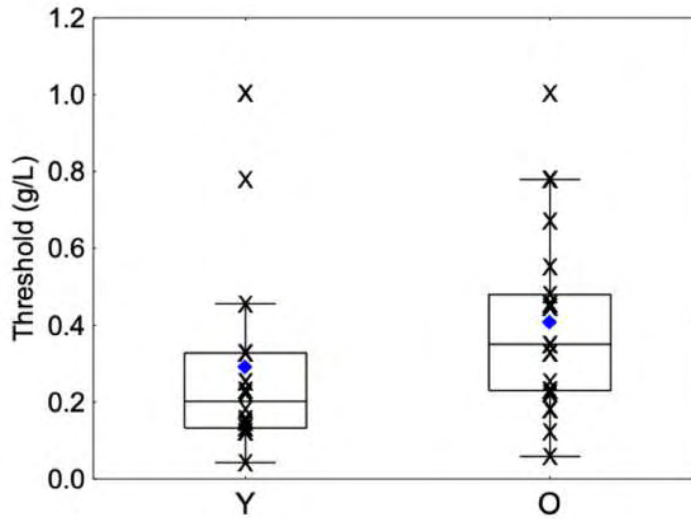


Figure 1: Box-plot distributions of threshold values in function of age category (young (Y) and elderly (O)) are shown. The bottom and top of the box correspond to the 25th and 75th percentile, respectively. The horizontal band and the blue diamond correspond to the median and the mean, respectively. The ends of the whiskers represent non-outlier range. X cross correspond to individual data.

Spearman correlation was not significant in whole ($r=-0.16$, $p=0.242$) and O ($r=0.14$, $p=0.47$) group. However, a significant and negative correlation was observed in young (Y) group ($r=-0.44$, $p=0.029$), higher is the salivary flow, lower is the threshold (Figure 2).

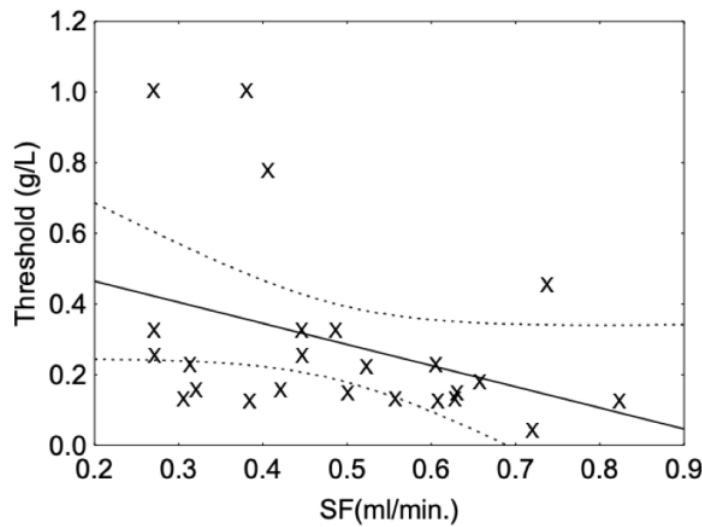


Figure 2: correlation between astringency threshold and whole salivary flux observed in the group of young panellists. Plain line corresponds to fitted data. Dotted line corresponds to confidence interval at 95%. X cross correspond to individual data.

Astringency is a complex group of sensations involving drying, roughing and puckering of oral surface, mucosa and muscles around the mouth. To the best of our knowledge, very few researches have investigated sensitivity to astringency in function of age. In this study, it was observed for the first time that astringency threshold was significantly higher in elderly participants than in young participants. In other words, young adults are more sensitive to astringency than elderly adults are. Differences in salivary properties can explain differences regarding taste sensitivity and in particular the flux. Indeed, saliva is present in the oral cavity and constantly bathes the taste buds on the tongue where it can interact with sensory stimulants and play a role in

taste, smell, and chemo-sensation [9]. When it comes to astringency, salivary flow rate has been reported to modulate its perception [10], i.e. subjects with low salivary flow rated astringency higher and recorded longer duration of astringent aftertaste than subjects with high salivary flow. Horne et al. (2002) [11] proposed that there is a negative correlation between resting salivary flow and astringency perceived intensity. Fischer et al. (1994) [12] indicated that the subject group with high salivary flow rate perceived astringency intensity at a significantly lower level than the low flow rate group.

In the present study, this negative relationship was observed significantly for young panel only which is in accordance with studies mentioned previously. However, we did not observe such relationships in the elderly group as well as a difference in salivary flow between Y and O groups, which should explain difference in sensitivity between the two groups. These observations suggest that the role of saliva in astringency sensitivity in function of age should be linked to other salivary parameters, such as its protein composition and, in particular, the level of PRPs.

Conclusion

In summary, the present experiment highlighted the sensory analysis of astringency perception sensitivity in function of age and saliva from a panel formed by 30 elderly people and 24 young people using 2-AFC method with four tannic acid concentrations. This work has demonstrated for the first time that astringency threshold was higher in elderly group than in young group. Concerning salivary flow rate, there were no significant differences between young and elderly groups. However, correlation between salivary flow and threshold was observed only for young individuals suggesting that salivary properties, which influence astringency sensitivity in elderly, are different.

References

1. Troilo M, Difonzo G, Paradiso VM, Summo C, Caponio F. Bioactive Compounds from Vine Shoots, Grape Stalks, and Wine Lees: Their Potential Use in Agro-Food Chains. *Foods*. 2021;10(2):342.
2. Serino A, Salazar G. Protective Role of Polyphenols against Vascular Inflammation, Aging and Cardiovascular Disease. *Nutrients*. 2019;11(1):53.
3. Soares S, Garcia-Estevez I, Ferrer-Galego R, Bras NF, Brandao E, Silva M, et al. Study of human salivary proline-rich proteins interaction with food tannins. *Food Chem*. 2018;243:175-85.
4. Ployon S, Morzel M, Belloir C, Bonnotte A, Bourillot E, Briand L, et al. Mechanisms of astringency: Structural alteration of the oral mucosal pellicle by dietary tannins and protective effect of bPRPs. *Food Chem*. 2018;253:79-87.
5. Pires MA, Pastrana LM, Fucinos P, Abreu CS, Oliveira SM. Sensorial Perception of Astringency: Oral Mechanisms and Current Analysis Methods. *Foods*. 2020;9:1124.
6. Aybeke EN, Ployon S, Brule M, De Fonseca B, Bourillot E, Morzel M, et al. Nanoscale Mapping of the Physical Surface Properties of Human Buccal Cells and Changes Induced by Saliva. *Langmuir*. 2019;35(39):12647-55.
7. Canon F, Ployon S, Mazauric J-P, Sarni-Manchado P, Réfrégiers M, Giuliani A, et al. Binding site of different tannins on a human salivary proline-rich protein evidenced by dissociative photoionization tandem mass spectrometry. *Tetrahedron*. 2015;71(20):3039-44.
8. Mojet J, Heidema J, Christ-Hazelhof E. Taste perception with age: Generic or specific losses in supra-threshold intensities of five taste qualities? *Chem. Senses*. 2003;28(5):397-413.
9. Feron G. Unstimulated saliva: background noise in taste molecules. *Journal of texture studies*. 2018.
10. Ishikawa T, Noble AC. TEMPORAL PERCEPTION OF ASTRINGENCY AND SWEETNESS IN RED WINE. *Food Qual. Prefer*. 1995;6:27-33.
11. Horne J, Hayes J, Lawless HT. Turbidity as a measure of salivary protein reactions with astringent substances. *Chem. Senses*. 2002;27(7):653-9.
12. Fischer U, Boulton RB, Noble AC. Physiological factors contributing to the variability of sensory assessments: relationship between salivary flow rate and temporal perception of gustatory stimuli. *Food Qual. Prefer*. 1994;5:55-64.

Impact of ingredient composition on sensory properties of powdered cocoa malted beverage

RUO XIN CHAN^{1,2}, Yi-Xin Seow³, Florian Viton³ and Weibiao Zhou¹

¹ Department of Food Science & Technology, National University of Singapore, Singapore

² Nestlé R&D Centre (Pte) Ltd, Singapore

³ Previous affiliation: Nestlé R&D Centre (Pte) Ltd, Singapore; Present affiliation: CJ CheilJedang Blossom Park, Food Research Institute, South Korea
ruoxin.chan@rdsg.nestle.com

Abstract

Powdered cocoa malted beverage (PCMB) is a multi-component beverage where various taste and aroma interactions may occur to affect its final sensory properties. Constrained mixture designs were generated to quantify relative taste impact of PCMB ingredients. Sugar-containing ingredients like sucrose, malt extract and skimmed milk provided different magnitudes of sweetness enhancement to PCMB while cocoa suppressed sweetness of PCMB through its strong bitterness. Cocoa aroma was perceived most frequently in PCMB but did not significantly affect taste. Non-sugar constituents in malt extract and skimmed milk enhanced and suppressed the sweetness of their sugar constituents respectively. Further sensory characterization of ingredients should be conducted for better control of PCMB flavour.

Keywords: cocoa malted beverage, mixture design, taste, aroma, interaction

Introduction

Cocoa- and dairy-based beverages are widely consumed around the world, with powdered cocoa malted beverage (PCMB) being one of the popular varieties containing cocoa, malt extract, skimmed milk, sucrose and palm oil. With rising demand for sugar reduction in beverages, it is important to understand how ingredient composition affects sensory properties of beverages. While sensory properties of individual PCMB ingredients have been characterised previously, their relative impact on overall sensory properties of PCMB may be affected by interactions between various tastes and aromas [1, 2]. This study aimed to quantify the relative impact of each ingredient on the taste of PCMB and to identify potential ingredients for modulating the sweetness of PCMB. Since multiple ingredients are mixed in different proportions among various PCMB products, constrained mixture designs [3] were used to generate sample sets that represented the wide ranges of ingredient composition present in PCMB products.

Experimental

PCMB samples

For Part 1 and 2 which aimed to quantify taste impact of PCMB ingredients, samples were prepared daily by weighing the 5 main ingredients of PCMB into separate containers according to mixture designs generated with the constraints shown in Table 1. The constraints were determined by a preliminary survey on ingredient composition of more than 20 commercial beverages containing at least 3 of the 5 main ingredients. Samples were reconstituted with 25 °C water to form 15 %w/v solutions, then poured and sealed in individual cups of 15 mL portions. Samples were incubated at 40 ± 1 °C then served to panellists in randomised and counter-balanced orders.

Table 1: Ingredient composition range of PCMB samples.

Study	% in PCMB					No. of Samples Served
	Sucrose	Cocoa	Malt Extract	Skimmed Milk	Palm Oil	
1	0, 15, 30	0 – 40	0 – 60	0 – 60	0 – 15	24 ¹
2	0 – 30	5 – 25	15 – 60	10 – 50	0 – 15	16

¹ Three groups of 8 samples each containing same level of sucrose (0, 15 or 30 %) but different levels of other ingredients.

Part 1

Twelve panellists aged 18 – 30 were recruited and trained to rate sweetness on a 15 cm unstructured line scale with 1, 5 and 9 %w/v sucrose representing weak, moderate and strong sweetness respectively. Subsequently, panellists rated the sweetness of 24 different PCMB samples in triplicates while wearing nose clip to remove any influence of odour.

Part 2

Fourteen panellists aged 18 – 30 were recruited and trained to rate sweetness and bitterness, which were the 2 dominant tastes detected in PCMB, on a 15 cm unstructured line scale. For training, 0.75, 3.75 and 6.75 %w/v sucrose represented weak, moderate and strong sweetness respectively, while 0.02, 0.1, 0.18 %w/v caffeine represented weak, moderate and strong bitterness respectively. Subsequently, panellists rated the sweetness and bitterness of 16 different PCMB samples in at least duplicates under 2 conditions: wearing nose clip and without nose clip, to compare the influence of odour on taste ratings. Panellists also completed a check-all-that-apply (CATA) questionnaire when tasting sample without nose clip to indicate which PCMB-related aroma attribute (i.e. cocoa, milky, malty, and oily) was detected.

Part 3

For Part 3 which aimed to investigate the sweetness of malt extract and skimmed milk, 76 untrained participants aged 18 – 50 were recruited to taste samples in pairs as shown in Table 2 and select which sample they perceived to be sweeter. Samples were prepared by weighing ingredients into separate containers and reconstituting with 25 °C water. Samples were incubated to 40 ± 1 °C before serving.

Table 2: Samples for pairwise comparison.

Sample	1	2	Nose clip worn
Pair 1	9 %w/v skimmed milk	Equivalent %w/v lactose	Yes
Pair 2	9 %w/v malt extract	Equivalent %w/v glucose + maltose	Yes
Pair 3	0 % sucrose PCMB with 60 % milk	0 % sucrose PCMB with 60 % malt	No

Data Analysis

Markings on sweetness and bitterness line scales were converted to quantitative values of 0.0 – 10.0 based on distance from origin. Average and standard deviation (SD) of panel means across replicate sessions were reported. One-way analysis of variance (ANOVA) at 95 % confidence interval with Tukey post-hoc test was conducted to determine if taste ratings significantly differed between samples. A two sample t-test was conducted to determine if aroma perception significantly affected taste ratings for each sample. Mixture regression models were fitted to sweetness and bitterness ratings to quantify the impact of each ingredient on each taste. All statistical analyses were conducted with Minitab 18 (Minitab LLC, USA).

Results and discussion

Sucrose is commonly used in various beverages due to its desirable sweetness. For Part 1, sweetness of PCMB samples generally increased with sucrose content but samples with the same sucrose content had significantly different sweetness, which confirmed that other ingredients could affect sweetness (Figure 1). A mixture regression model was fitted to the sweetness ratings to quantify the impact of each ingredient as follow:

$$\text{Sweetness} = 15.7 \times \% \text{sucrose} - 4.5 \times \% \text{cocoa} + 4.3 \times \% \text{malt extract} + 4.2 \times \% \text{skimmed milk} + 0.6 \times \% \text{palm oil}$$

The model had an adjusted R^2 of 0.979 and root mean square error (RMSE) of 0.3 on a sweetness scale of 0.0 – 10.0 where samples had a pooled standard deviation of 0.3. This indicates a good fit for predicting sweetness of PCMB for any ingredient composition within the constraints tested in Table 1. Quadratic terms were not added to the model to avoid over-fitting. The model coefficients show that sweetness of PCMB was determined mainly by sucrose (+15.7), while malt extract (+4.3) and skimmed milk (+4.2) also contributed to sweetness. Cocoa reduced sweetness of PCMB (−4.5) while palm oil had negligible impact. The lack of quadratic terms suggests that there was no significant synergism or antagonism between ingredients influencing sweetness of PCMB.

Part 2 was conducted to evaluate sweetness and bitterness of PCMB simultaneously (Figure 2). Mixture regression models were fitted to the sweetness and bitterness ratings of PCMB tasted while wearing nose clip as follow:

$$\begin{aligned} \text{Sweetness} &= 22.4 \times \% \text{sucrose} - 5.3 \times \% \text{cocoa} + 4.0 \times \% \text{malt extract} + 4.1 \times \% \text{skimmed milk} - 2.3 \times \% \text{palm oil} \\ \text{Bitterness} &= -1.2 \times \% \text{sucrose} + 24.3 \times \% \text{cocoa} - 0.7 \times \% \text{malt extract} - 1.2 \times \% \text{skimmed milk} + 2.5 \times \% \text{palm oil} \end{aligned}$$

Both models appear to be good fits, with the sweetness model possessing an adjusted R^2 of 0.976 and RMSE of 0.3, while the bitterness model had an adjusted R^2 of 0.912 and RMSE of 0.5. The sweetness model in Study 2 was similar to that of Study 1 in terms of the enhancing or suppressing impact of individual ingredients, with changes in magnitude of coefficients due to different concentration of sucrose solutions used as standards. For the bitterness model, it was observed that cocoa was the main contributor to bitterness while all other ingredients had

minimal impact. In addition, there was mostly no significant difference in sweetness and bitterness ratings when panellists tasted PCMB with and without nose clip (Figure 2).

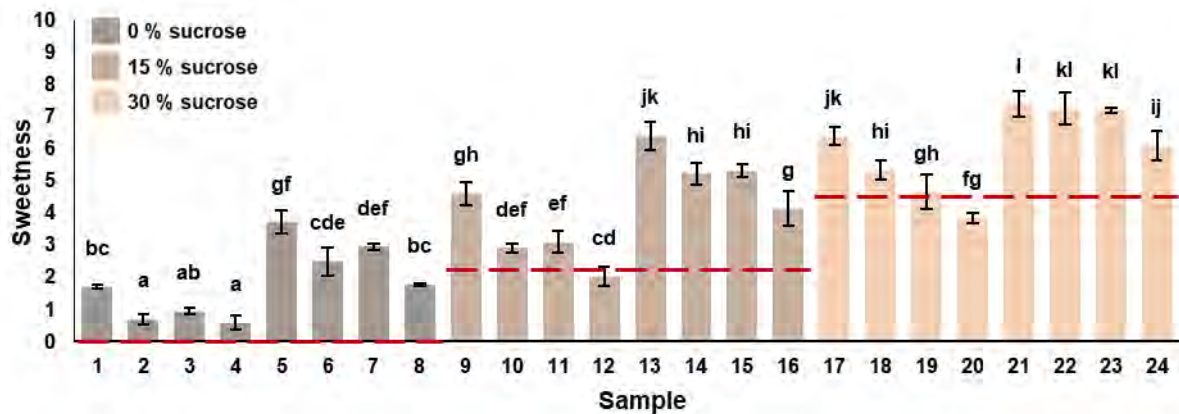


Figure 1: Mean \pm SD of sweetness ratings for 24 PCMB samples in Part 1. Samples that do not share a letter are significantly different ($p < 0.05$). Dashed lines represent expected sweetness from sucrose for each sample group.

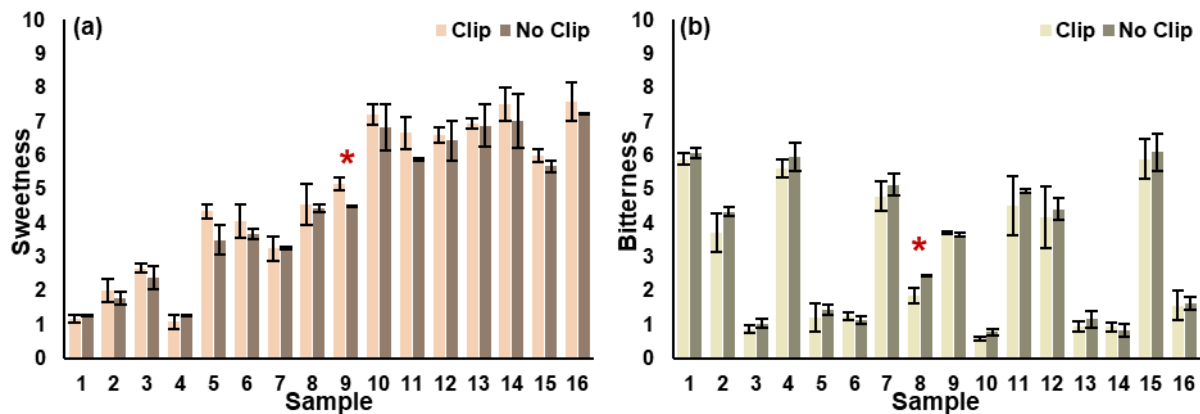


Figure 2: Mean \pm SD of (a) sweetness ratings and (b) bitterness ratings for 16 PCMB samples in Part 2. * represents significant difference between ratings with and without nose clip ($p < 0.05$).

Among all the natural sugars, sucrose is known to elicit a strong sweet taste and thus is used as the main sweetener in most beverages. Malt extract and skimmed milk contained 35 % and 51 % sugars respectively, which was why they could also increase sweetness of PCMB. Substituting sucrose with these ingredients could facilitate sugar reduction in PCMB, but they would be unable to maintain the same sweetness in PCMB. This is because malt extract contained glucose and maltose while skimmed milk contained lactose, which are sugars with lower sweetness than sucrose [4].

Cocoa is the only PCMB ingredient known to contain various bitter and sour compounds, which corresponds to its strong impact on bitterness [5]. The bitter taste of cocoa likely suppressed sweetness due to taste-taste interactions. Part 2 was conducted to determine if encouraging panellists to adopt an analytical strategy for taste rating would remove the influence of cocoa bitterness on sweetness ratings. It was observed that sweetness continued to be suppressed by cocoa while bitterness was barely suppressed by sweet-tasting ingredients, in contrast to previous study that showed predominance of sweetness in equi-intense taste mixtures [6]. This suggests that sweetness in PCMB was generally weaker than bitterness and that the taste interactions might not be occurring only at the cognitive level.

Other than taste-taste interaction, aroma-taste interaction was also explored in Part 2 by asking panellists to rate sweetness and bitterness with and without nose clip. CATA was conducted to determine which aroma attributes were perceived in PCMB samples (Figure 3). The aroma attribute “cocoa” could be detected in most samples by most panellists, while “milky” and “malty” could not be detected as frequently despite malt extract and skimmed milk being used at higher proportions than cocoa (Figure 3). It was hypothesised that cocoa aroma would enhance bitterness and suppress sweetness of PCMB due to taste-aroma congruency [7]. However, aroma perception did not significantly affect taste ratings, which could be caused by PCMB ingredients having

insufficient strong aroma intensity or interactions between various aromas and tastes that led to negligible net effect.

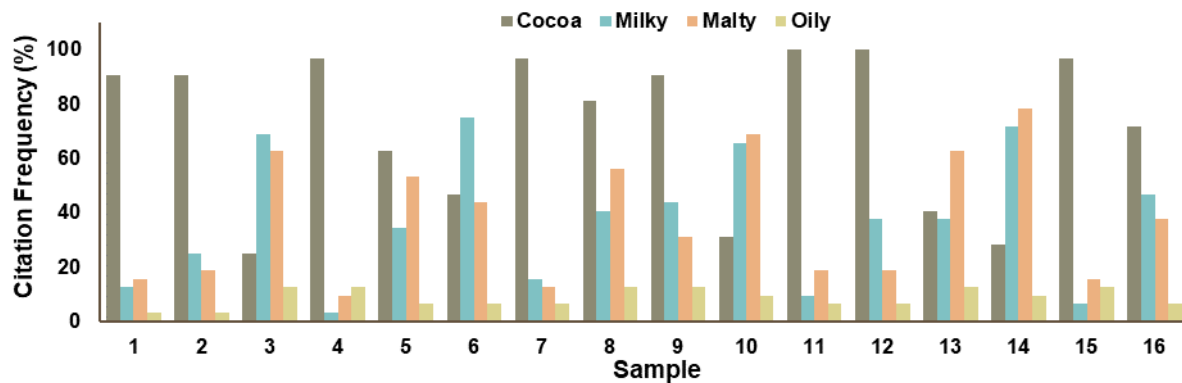


Figure 3: Citation frequency of aroma attributes detected in 16 PCMB samples in Part 2.

Part 3 was conducted to investigate the sweetness of skimmed milk and malt extract (Figure 4). Skimmed milk was less sweet than its lactose constituent (34 % vs 61 %), meaning that other constituents like milk proteins and mineral salts might have suppressed the sweetness of lactose. Meanwhile, malt extract was perceived to be sweeter than its glucose and maltose constituents (74 % vs 13 %), suggesting that other constituents such as oligosaccharides, amino acids and peptides might have enhanced its sweetness. Despite similar impact on the sweetness of PCMB as seen in Part 1 and 2, a sucrose-free PCMB containing 60 % malt extract was perceived to be sweeter than a sucrose-free PCMB containing 60 % skimmed milk when compared directly (67 % vs 25 %). This suggests that malt extract has better potential to be used as an alternative sweetener in PCMB than skimmed milk which had a higher sugar content. More study should be done to characterise the taste impact of non-sugar constituents in malt extracts.

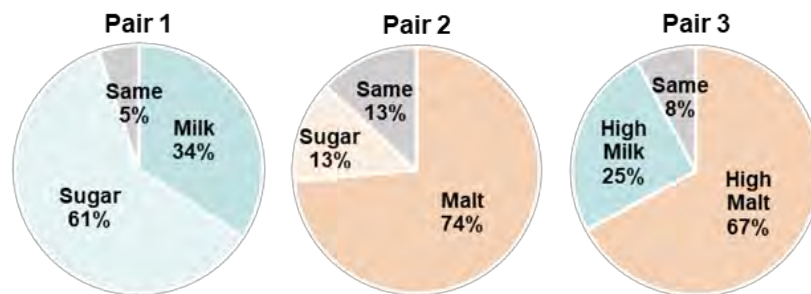


Figure 4: Percentage of sample selected to be sweeter by 76 general consumers (aged 18 – 50) in pairwise comparison tests in Part 3.

Conclusion

This study revealed the usefulness of mixture design for quantifying ingredient impact on tastes of multi-component beverages, as important taste modulators in PCMB was identified. PCMB sweetness was more easily influenced by bitterness than vice versa, but both were not affected by aroma perception. Sweetness of PCMB ingredients like skimmed milk and malt extract did not depend only on their sugar contents, which suggests that composition of individual PCMB ingredients should be further explored for better control of beverage flavour.

References

1. Keast R.S.J., Breslin P.A.S. An overview of binary taste–taste interactions. *Food Qual. Prefer.* 2003;14(2):111-124.
2. Auvray M., Spence C. The multisensory perception of flavor. *Conscious Cogn.* 2008;17(3):1016-1031.
3. Ryzt A., Moser M., Lepage M., Mokdad C., Perrot M., Antille N., Pineau N. Using fractional factorial designs with mixture constraints to improve nutritional value and sensory properties of processed food. *Food Qual Prefer.* 2017;58:71-75.
4. Mao Y., Tian S., Qin Y., Han J. A new sensory sweetness definition and sweetness conversion method of five natural sugars, based on the Weber-Fechner Law. *Food Chem.* 2019;281:78-84.
5. Stark T., Bareuther S., Hofmann T. Molecular Definition of the Taste of Roasted Cocoa Nibs (*Theobroma cacao*) by Means of Quantitative Studies and Sensory Experiments. *J Agric Food Chem.* 2006;54:5530-5539.
6. Green B.G., Lim J., Osterhoff F., Blacher K., Nachtigal D. Taste mixture interactions: Suppression, additivity, and the predominance of sweetness. *Physiol Behav.* 2010;101:731-737.
7. Labbe D., Damevin L., Vaccher C., Morgenege C., Martin N. Modulation of perceived taste by olfaction in familiar and unfamiliar beverages. *Food Qual Prefer.* 2006;17:582-589.

Section 4

Flavour generation

Furfuryl alcohol confirmed as key intermediate for furfurylthiol in coffee

CHRISTOPH CERNY, Hedwig Schlichtherle-Cerny, Romelo Gibe and Yuan Yuan

Firmenich Aromatics, Shanghai, China, cerny1093@gmail.com

Abstract

Furfurylthiol (FFT) is a key odorant and largely determines the aroma of fresh roasted coffee. Earlier studies showed formation of FFT from furfuryl alcohol (FFA) and glutathione in aqueous model reactions. It was suggested that FFA and coffee proteins are precursors for sulphur odorants in coffee. The present study investigated the role of FFA in the formation of FFT during coffee roasting by “in-bean” experiments. Green coffee beans were soaked with FFA and freeze-dried. After roasting FFT was quantified by stable isotope dilution analysis. Spiking with FFA increased the FFT level in roasted coffee. In another experiment beans were spiked with deuterium labelled d_2 -FFA. After roasting the isotopologue distribution of FFT was determined. Beans spiked with labelled d_2 -FFA generated labelled d_2 -FFT and unlabelled furfural. These results unambiguously confirmed FFA as key intermediate for FFT in coffee. On the other hand, furfural, which does not originate from FFA, seems not related to FFT formation. The suggested formation pathway comprises formation of furfuryl cation from FFA, which reacts with protein-bound cysteine, and subsequent elimination of FFT from the protein-bound S-furfurylcysteine.

Keywords: coffee, aroma precursor, furfuryl alcohol, furfurylthiol, in-bean approach, stable isotope dilution analysis

Introduction

Coffee, after water and tea, is the third most popular beverage worldwide. It has little nutritional value and is mainly consumed for its stimulating character and delicious flavour. The aroma of brewed coffee is caused by around 22 key odorants [1]. The most important aroma compound is 2-furfurylthiol (FFT), which has a concentration of 1.1 mg/kg in roasted coffee and 19 μ g/L in a coffee brew; this exceeds 1900-times its odour threshold [1].

The formation pathway to FFT in coffee is still unclear. Various studies have tested potential precursors in model reactions. Aqueous reactions at 200 °C for 1 min between cysteine and various sugars as well as furfuryl alcohol (FFA) and furfural revealed furfural as the most potent precursor, followed by arabinose and FFA [2]. Consequently, the authors suggested furfural as an immediate precursor of FFT. Other experiments reacted solutions of FFA with various sulphur precursors such as cysteine, N-acetylcysteine and glutathione under reflux [3]. While cysteine was virtually ineffective, glutathione proved to be efficient as sulphur precursor. The author suggests protein-bound cysteine and FFA as precursors of FFT. The level of FFA generated during coffee roasting reaches up to 500 mg/kg [4]. This amount of FFA makes FFT a good precursor candidate to be investigated. However, it is still unclear how FFA will react under roasting conditions.

Roasting experiments with water-extracted green coffee beans surprisingly produced 60% more FFT than regular coffee beans [5] suggesting that FFT precursors in coffee are water-insoluble. Therefore, green coffee constituents like free cysteine, sucrose and other free sugars seem unlikely FFT precursors.

The “in-bean” approach, which was first proposed in 2001 [6] allowed to study coffee precursors under real roasting conditions. Green beans were spiked with potential precursors prior to roasting. Analyses of the roasted beans revealed higher formation of ethylated pyrazines after spiking with alanine [5]. In contrast, FFT formation was not favoured after spiking with arabinose. Furthermore, spiking with 13 C-labelled arabinose did not produce 13 C-labelled FFT. These findings support the hypothesis that FFT precursors are not water-soluble.

The present study investigated the role of FFA as potential intermediate of FFT during coffee roasting using the in-bean approach. Green beans were spiked with FFA, and the resulting FFT was measured in the roasted beans. After spiking with deuterium labelled d_2 -FFA the resulting FFT mass spectrum and isotopologue distribution in the roasted coffee was investigated.

Experimental

Materials

Green coffee (washed Arabica) was from Yunnan (China). The chemicals L-cysteine, LiAlD₄ and diethyl ether were from TCI (Tokyo, Japan). FFA was from Firmenich and d_2 -FFT from Aromalab (Planegg, Germany). Deuterium labelled d_2 -FFA was synthesised according to a slightly modified procedure of Sen and Grosch [8].

Spiking of coffee with precursors

Green coffee beans (50 g) were mixed with aqueous precursor solutions (20 g) and soaked at 50 °C during 4 h using a rotary evaporator. Then water (8 g) was added, and soaking was continued for another hour at 50 °C. The soaked beans were freeze-dried. Precursor solutions contained:

- FFA (50 mg)
- FFA (100 mg)
- FFA (150 mg)
- L-Cysteine (150 mg)
- L-Cysteine (150 mg) + FFA (50 mg)
- d₂-FFA (50 mg)
- d₂-FFA (100 mg)
- d₂-FFA (100 mg)

Coffee preparation

Dried coffee beans were roasted at small scale (17 g) in an IKAWA coffee roaster (Ikawa Ltd., London, England) at a temperature profile from 150 °C to 200 °C during 5 min. The roasted beans were immediately ground in an electric burr grinder (Baratza Encore, Bellevue, Washington, USA) at espresso grade. Freshly ground coffee powder (7 g) was used to produce approximately 35 ml espresso with a DeLonghi EC 680 espresso machine (Treviso, Italy). Coffee brews were immediately cooled in an ice bath prior to analysis.

Coffee analysis

Espresso brews (4 ml) were immediately analysed by solid-phase microextraction coupled to gas chromatography/mass spectrometry (SPME-GC-MS) in a 20 ml headspace vial. After conditioning at 40 °C for 10 min (250 rpm agitation), the headspace of the brew was extracted by a 75 µm DVB/CAR/PDMS fibre (2 cm length) at 40 °C for 30 min. Desorption was at 250 °C for 1 min in the GC injection port (splitless mode). GC analysis was on a DB-WAX column (30 m × 0.25 mm, i.d. 0.25 µm) with helium as carrier gas. The temperature was 45 °C isotherm for 5 min, then increased at 5 °C/min to 150 °C, followed by heating at 10 °C/min to 250 °C. Mass spectrometry was in EI mode (*m/z* 29-300).

Quantifications were by stable isotope dilution analysis [7]. For FFA quantification, samples were diluted 12.5-times with water prior to addition of the internal standard d₂-FFA. Ions *m/z* 81 and *m/z* 83 were used for quantification. For FFT quantification, cysteine (200 mg) was added in order to avoid oxidation and binding to the coffee matrix. Then the internal standard d₂-FFT was added. The ions *m/z* 114 and *m/z* 116 were used for quantification. Analyses were done in duplicate. Results are expressed as quantity of FFT per gram of green beans.

For the isotopologue study, green beans were spiked with deuterium labelled d₂-FFA. No standards were added prior to analysis.

Results and discussion

Spiking green coffee with FFA and/or cysteine

Coffee beans were spiked with either FFA (1-3 mg/g), cysteine (3 mg/g) or both FFA and cysteine (1+3 mg/g). The resulting concentrations of FFT are illustrated in Figure 1. FFT concentrations were determined in espresso brews and are expressed per gram of green beans. Spiking with FFA generated higher FFT concentrations than with unloaded beans. Adding 3 mg/g FFA resulted in 390 ng/g FFT in the roasted beans compared to 246 ng/g in the unloaded reference.

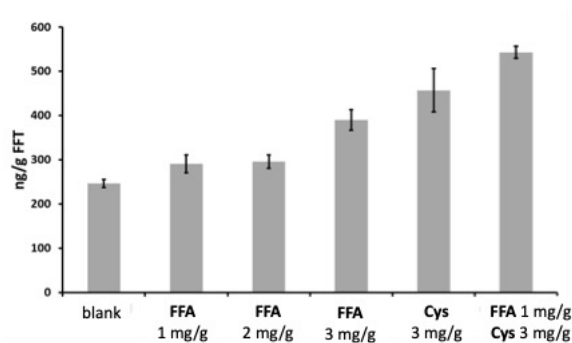


Figure 1: FFT formed during roasting of coffee beans spiked with FFA and/or cysteine.

The highest FFT level was obtained when beans were spiked with both cysteine (3 mg/g) and FFA (1 mg/g). Because FFA boosts FFT generation during coffee roasting it is suggested as key intermediate to FFT under coffee roasting conditions.

Spiking green coffee with deuterium labelled d₂-FFA

Next, green coffee was spiked with deuterium labelled d₂-FFA. The resulting mass spectra of FFT, furfural and furfuryl methyl sulphide (Figure 2) indicate to which extent deuterium labelled and unlabelled isotopologues are formed upon roasting. The mass spectrum of FFT (Figure 2A) was composed of the mass spectra of unlabelled FFT and labelled d₂-FFT. Analysis of the indicator ions *m/z* 114 and *m/z* 116 points to a portion of 41% labelled d₂-FFT. Indeed d₂-FFT forms from d₂-FFA added to the beans. Presumably, FFA from endogenous precursors was also converted to FFT during roasting.

Figure 2B shows the mass spectrum of furfural, which is exclusively unlabelled. Singly labelled d-furfural would be expected if formed from d₂-FFA. As this was not the case, although furfural was formed during roasting, it did not stem from FFA. Furfuryl methyl sulphide (Figure 2C) was a mixture of d₂-labelled and unlabelled compound. This points to FFA as precursor, as in the case of FFT.

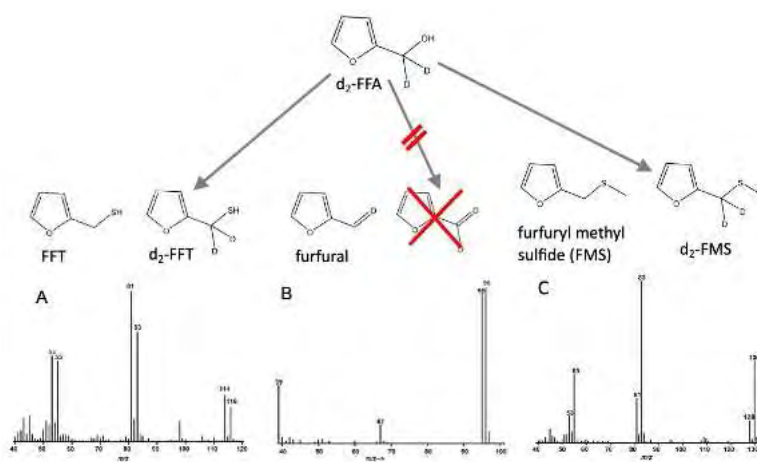


Figure 2: Mass spectra of compounds formed during roasting coffee beans spiked with d₂-FFA.

The ratio of labelled to unlabelled FFA and FFT during coffee roasting changed during the roasting process. During the first 2 min unlabelled FFA was not detected (Figure 3, left). Only after 3 min unlabelled FFA from endogenous precursors appears, proportionally increasing until 5 min. Both unlabelled and labelled d₂-FFT appeared only after 3 min roasting. The portion of unlabelled FFT dominated and increased until the end of roasting. Labelled d₂-FFT formed from labelled d₂-FFA, while unlabelled FFT seems to be formed from the unlabelled intermediate FFA and possibly other precursors.

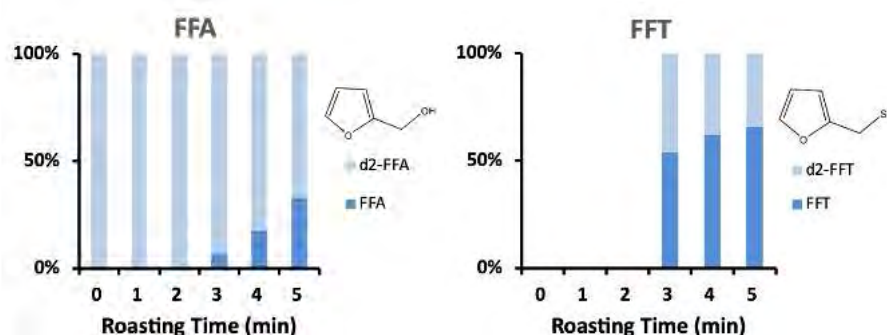


Figure 3: Proportion of d₂-labelled versus unlabelled FFA and FFT, respectively in roasted coffee (150 to 200 °C, 5 min), spiked with d₂-FFA (2 mg/g) prior to roasting.

When green coffee was spiked with increasing amounts of d₂-FFA (0-3 mg/g) the proportion of labelled d₂-FFT to labelled FFT increased as indicated by the ratios of *m/z* ions 114 to 116 in Table 1, which shows the relative percentage of ions in the mass spectra of FFT. Detection of *m/z* 116 is not only due to d₂-FFT but also to a small extent of undeuterated FFT that carries the natural sulphur isotope ³⁴S (natural abundance 4.2%), the value for *m/z* 116 needs to be corrected.

The fact that increasing amounts of labelled d_2 -FFA lead to proportionally more labelled FFT in the roasted beans further substantiates the role of FFA as key intermediate to FFT in coffee.

Table 1: Influence of the quantity of spiked d_2 -FFA in coffee beans on the ratio of FFT m/z ions after roasting.

m/z	d_2 -FFA (mg/g)			
	0	1	2	3
114	89%	70%	60%	50%
115	6%	6%	6%	6%
116	5%	21%	31%	39%
117		2%	2%	3%
118		1%	1%	2%

Formation pathway from FFA to FFT during coffee roasting

Our results revealed that FFA was not converted into furfural during coffee roasting. Furthermore, earlier studies showed that furfural is not converted into FFT during roasting neither [5]. Therefore, a formation pathway from FFA to FFT without furfural is suggested.

Kreppenhofer and co-workers had suggested a formation pathway to substituted catechol during coffee roasting that involves the formation of furfuryl cation from FFA [9]. The furfuryl cation then binds in an electrophilic attack to catechol, formed from chlorogenic acid during roasting, resulting in 4-furfurylcatechol.

A similar pathway is suggested for the formation of FFT, which also starts with the formation of furfuryl cation from FFA. As illustrated in Figure 4, the furfuryl cation attacks the thiol group of protein-bound cysteine resulting in the intermediate protein-bound S-furfurylcysteine. Subsequent elimination releases FFT and leaves protein-bound dehydroalanine.

The suggested formation pathway is in agreement with our experimental findings and backed by literature that suggests that FFT precursors are water insoluble.

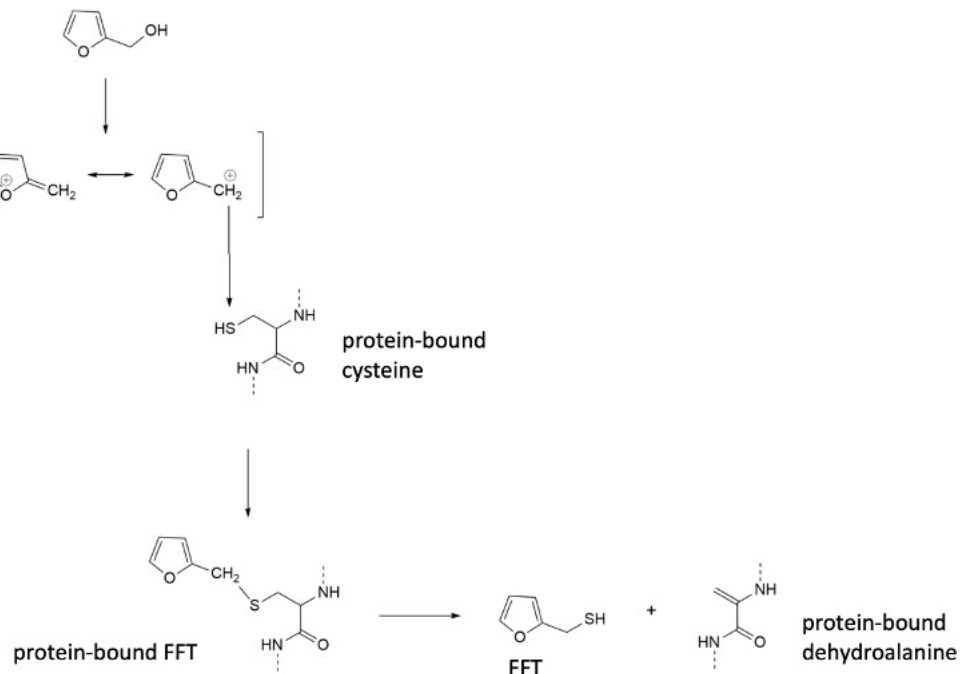


Figure 4: Suggested pathway from FFA to FFT during coffee roasting.

Conclusion

The study showed that coffee beans spiked with FFA increased the FFT level after roasting and thus, substantiating the role of FFA as FFT precursor. Spiking with labelled d_2 -FFA generated labelled d_2 -FFT. On the other hand, only unlabelled furfural was found. These findings further corroborate the central role of FFA in FFT formation confirming it as key intermediate to FFT in roasted coffee. Furfural, in contrast, apparently plays no major role as FFT intermediate. On this basis, a pathway to FFT is suggested that involves the reaction of FFA with protein-bound cysteine.

References

1. Semmelroch P, Grosch W. Studies on character impact odorants of coffee brews. *J Agric Food Chem.* 1996;44:537-543.
2. Parliment TH, Stahl HD. Formation of furfuryl mercaptan in coffee model systems. In: Charalambous G, editor. *Food Flavors: Generation, Analysis and Process Influence.* Amsterdam (Netherlands). Elsevier; 1995; pp 805-813.
3. Rizzi GP. Formation of sulfur-containing volatiles under coffee roasting conditions. In: Parliment TH, Ho CT, Schieberle P, editors. *Caffeinated Beverages: Health Benefits, Physiological Effects, and Chemistry.* Washington DC (USA). American Chemical Society; 2000; pp 210-215.
4. Alabouchi A, Murkovic M. Formation kinetics of furfuryl alcohol in a coffee model system. *Food Chem.* 2018;243:91-95.
5. Poisson L, Schmalzried F, Davidek T, Blank I, Kerler J. Study on the role of precursors in coffee flavor formation using in-bean experiment. *J Agric Food Chem.* 2009;57:9923-9931.
6. Milo C, Badoud R, Fumeaux R, Bobillot S, Fleury Y, Huynh-Ba T. Coffee flavour precursors: contribution of water non-extractable green bean components to roasted coffee flavour. In: *Proceedings of the 19th International Scientific Colloquium on Coffee, Trieste (Italy).* Paris (France). ASIC; 2001; pp 87-96.
7. Schieberle P, Grosch W. Quantitative analysis of aroma compounds in wheat and rye bread crusts using a stable isotope dilution assay. *J Agric Food Chem.* 1987;35:252-257.
8. Sen A, Grosch W. Synthesis of six deuterated sulfur containing odorants to be used as internal standards in quantification assays. *Z Lebensm Unters Forsch.* 1991;192:541-547.
9. Kreppenhofer S, Frank O, Hofmann T. Identification of (furan-2-yl)methylated benzene diols and triols as a novel class of bitter compounds in roasted coffee. *Food Chem.* 2011;126:441-449.

Odour compounds in thermo-mechanically processed food based on pulse ingredients

SVENJA KRAUSE, Anahita Hashemi, Séverine Keller, Catherine Bonazzi and Barbara Rega

Université Paris-Saclay, INRAE, AgroParisTech, UMR SayFood, 91300 Massy, France
svenja.krause@agroparistech.fr

Abstract

This study investigates the effect of pulse flours (chickpea, lentil, lupin, yellow and green pea) on the formation of key volatiles with likely impact on the odour of sponge cakes compared to a wheat reference. Twenty molecules with an odour activity value of five or higher were determined from a wide variety of volatile compounds identified using headspace-solid phase microextraction/gas chromatography-mass spectrometry (HS-SPME/GC-MS) and quantified by internal isotope standards. While the majority of these originated from lipid oxidation, the remaining compounds were generated through Maillard reaction. Principle component analysis revealed that the lipoxidation-derived volatiles typically possessing green, fatty odours were mainly related to cakes made with lentil, chickpea, yellow and especially green pea flour. Among these, hexanal was assumed to be of substantial sensory importance based on its outstanding odour activity values. 3-Methylbutanal (malty, chocolate notes) was identified as most odour-active compound in all formulations and might have contributed to the overall flavour, in particular in wheat, green pea and yellow pea cakes. Moreover, lentil formulas were associated with 2-ethyl-3,5-dimethylpyrazine, which is known to be responsible for an earthy aroma. From these results it can be concluded that the raw material determines the potential to generate odour-active compounds during product development and mastering the reactions likely to occur might offer an opportunity to tailor the global flavour quality of food.

Keywords: lipid oxidation, Maillard reaction, odour activity, reactivity, cake

Introduction

The increasing interest for sustainable and plant-based eating practices has prompted the incorporation of pulses into the human diet. Owing to their high protein content and attractive nutritional value, pulses are emerging ingredients in baked goods, particularly in gluten-free or healthy food design applications. The substitution of traditional ingredients, such as wheat flour, by novel constituents might, however, alter the chemical reactivity during food processing due to a modified profile of nutrients with diverging susceptibilities to oxidative and thermal degradation. This can further be accompanied by the formation of volatile compounds, which in turn might affect the aroma quality of the final bakery products.

Therefore, this study aimed at identifying key volatile compounds with high probability to contribute to the aroma of sponge cakes made with different pulse flours (lentil, chickpea, lupin, green and yellow pea) in comparison to a wheat reference. Accordingly, the molecules identified using headspace-solid phase microextraction/gas chromatography-mass spectrometry (HS-SPME/GC-MS) and quantified by internal isotope standards were associated with their odour activity value and submitted to multivariate data analysis to estimate the potent odours in the different pulse-based applications.

Experimental

Sponge cake elaboration and characterization

Wheat and pulse cakes were elaborated as reported by Krause [1] from 45% (w/w) pasteurized liquid whole eggs, 25% (w/w) sucrose, 25% (w/w) wheat or pulse flour and 5% (w/w) sunflower oil. Twenty-one cakes were generated per cakes recipe, applying the three-step development process described by Cepeda-Vázquez [2], comprising (1) whipping of sugar and eggs, (2) addition of flour and oil and (3) batter baking at 170 °C for 25 min. In the pulse-based formulations, wheat flour (T55, Grands Moulins de Paris, France) was completely replaced by certified organic flours from lentils (Celnat, France), chickpeas (Celnat, France), lupins (Moulin Meckert-Diemer, France), green peas (Moulin Meckert-Diemer, France) and yellow peas (Improve, France). Immediately after baking, samples were deep-frozen at -20 °C in hermetically closed glass vessels until chemical analysis.

For each recipe, composite sampling was performed on ten cakes randomly chosen and ground in frozen state to a similar particle size distribution (d₅₀ ~250 μm). Reproducibility and repeatability of processing conditions were assessed at each step of cake development by means of classic physical and chemical measurements, including dry matter content, pH value, density and colour, as well as HS-SPME/GC-MS analysis [1].

Identification and quantification of volatile organic compounds

Gas chromatography (GC) analysis of volatile compounds was carried out as described by Krause [1]. Samples (2 g) were weighed in triplicates, spiked with 100 μ L aqueous solution of deuterated internal standards (411 mg/L hexanal-d₁₂, 15 mg/L furfural-d₄ and 3 mg/L 2-methylpyrazine-d₆), hermetically sealed in 20 mL headspace vials with PTFE-coated silicon septa and stored overnight at 4 °C.

Headspace Solid Phase Microextraction (HS-SPME) was performed by applying the following parameters: DVB/CAR/PDMS fibre (50/30 μ m, 2 cm, Supelco); incubation (18 min) and extraction (42 min) at 50 °C. Analyses were carried out using a TRACE GC Ultra gas chromatograph (Thermo Fisher Scientific) equipped with a ZB-wax capillary column (30 m \times 0.25 mm \times 0.5 μ m). Compounds were thermally desorbed at 250 °C during 2 min and separated using the oven temperature program from 40 °C with an isotherm of 5 min to 240 °C at a rate of 4 °C/min. Helium carrier gas was used at a flow rate of 1.2 mL/min.

For detection, an ISQ single quadrupole mass spectrometer (Thermo Fisher Scientific) was operated in the EI mode at 70 eV, scanning masses from m/z 33 to 300 and in SIM mode for selected molecules. Compounds were identified through mass spectra libraries search (NIST 08, Wiley 8) and by comparing their experimental retention indices obtained using a series of *n*-alkanes (C5-C21) with those from the NIST database. Hexanal, furfural and 2-methylpyrazine were quantified using their deuterated internal standards by isotopic dilution method. In addition, relative quantification of other specific classes of compounds was performed using 2-methylpyrazine-d₆ for nitrogenous-containing heterocycles, furfural-d₄ for furanic compounds and hexanal-d₁₂ for the remaining compounds (aldehydes, ketones, alcohols).

Determination of odour activity values

Odour activity values of the extracted compounds were determined as the ratio of compound concentration to its odour threshold in water described in literature. Nonetheless, sponge cakes are complex food systems, for which reason the utilization of odour threshold values in water can only give an idea of the most powerful odorants in cakes. Odour thresholds in matrices similar to cakes, such as starch, would give better insights into the odour activity values of individual compounds. However, this information is only available for a limited number of molecules in literature, for instance in simple starch models, which, however, are still far from the realistic cake matrix. Consequently, in order to take this uncertainty into account, only odour activity values ≥ 5 were considered for multivariate data analysis. Moreover, this value helped to select and hierarchize those compounds with probably the highest contribution to the odour of the final products.

Statistical analysis

One-way analyses of variance (ANOVA) were performed on determined concentrations of volatile compounds and significant differences evaluated by Tukey's test at $p < 0.05$, using SAS studio version 3.8 (SAS Institute Inc., Cary, NC, USA). Principal component analysis (PCA) was conducted on both concentration and odour activity values of extracted volatiles using XLSTAT version 2020.1 (Addinsoft, Paris, France).

Results and discussion

Complex profiles of volatile organic compounds were detected in the wheat and different pulse-based cakes, which mainly belonged to the chemical classes of alcohols, aldehydes, ketones, pyrazines and furans. In order to identify the compounds that are likely to affect the odour of the individual cakes, the odour activity values of all the 59 identified volatiles were calculated and those with an odour activity value of 5 or higher were selected.

As shown in Table 1, a total of 20 odour-active molecules was found with an odour activity value of 5 or higher. Among these, the majority of components were identified as typical markers of lipid oxidation, denoting the degradation of unsaturated fatty acids in the presence of oxygen, which can be either catalysed by endogenous lipoxygenase or triggered by heat, light and metals [3, 4]. In the case of sponge cakes, lipid oxidation is assumed to be initiated during batter beating, attributable to the entrapment of atmospheric oxygen while mixing the ingredients into a foam, and persists during baking due to heat-induced autoxidation [1, 5]. In the course of this reaction, hydrogen atoms are abstracted from the unsaturated fatty acids, thereby yielding hydroperoxides, which in turn can be converted into volatile compounds *via* subsequent reactions such as β -scission [6]. The odour-active molecules generated through such pathway and extracted from the diverse cakes were mainly deriving from linoleic acid (C18:2). Typical representatives included pentanal, hexanal, heptanal, octanal, 2-heptenal, 2-octenal and 2,4-decadienal as well as 1-octen-3-ol and 2-pentylfuran (Table 1) [6-8]. However, hexanal and 2-heptenal are likewise known as possible oxidation products of linolenic acid (C18:3), whereas heptanal and octanal could have alternatively originated from oleic acid (C18:1) [6, 7]. Both oleic and linolenic acid might have also been the precursors of the aldehydes nonanal and 2-hexenal, respectively [6, 7].

Apart from these lipoxidation markers, the remaining odour-active components were associated with the thermal-induced breakdown of sugars and amino acids mainly *via* Maillard reaction occurring during batter baking.

These included Strecker aldehydes (2-methylpropanal, 2-methylbutanal, 3-methylbutanal, acetaldehyde, phenylacetaldehyde), 2,3-butanedione, 2,3-pentanedione and 2-ethyl-3,5-dimethylpyrazine (Table 1). Maillard reaction involves the condensation of amino acids and reducing sugars at elevated temperatures to produce aminoketoses (Amadori compounds) or aminoaldoses (Heyns compounds) [6]. In subsequent steps, these constituents are degraded through enolization, dehydration and hydrolysis into 1-deoxyosones or 3-deoxyosones [6]. Owing to their high reactivity, these α -dicarbonyl compounds are likely to undergo further reactions, resulting in the release of a wide variety of molecules. Among these, Strecker aldehydes are commonly found, deriving from the reaction of α -dicarbonyl compounds with amino acids [6]. In the present study, multiple Strecker aldehydes were identified as key odour-active compounds in the diverse cake formulations, comprising 2-methylpropanal, 2-methylbutanal, 3-methylbutanal, acetaldehyde and phenylacetaldehyde, which originated from valine, isoleucine, leucine, alanine and phenylalanine, respectively [6]. In addition to Strecker aldehydes, the nitrogen-containing compound 2-ethyl-3,5-dimethylpyrazine was present, being characterized by a very low odour threshold (Table 1). This heterocyclic molecule may have been formed from α -aminocarbonyls obtained next to the Strecker aldehydes in the condensation reaction of α -dicarbonyl compounds and amino acids. It is generally supposed that two α -aminocarbonyls react under formation of dihydropyrazine, which in turn can be substituted to create alkylpyrazines [9]. In this context, the generation pathway of 2-ethyl-3,5-dimethylpyrazine is postulated to involve the incorporation of acetaldehyde into the corresponding dihydropyrazine carbanion [10]. Acetaldehyde could not only emerge from Strecker degradation as previously discussed, but likewise from oxidation of ethanol [10], an alcohol that was largely present in the diverse batters and cakes (data not shown). Moreover, two further compounds with pronounced odour activity value were determined, namely 2,3-butanedione and 2,3-pentanedione (Table 1), which have been reported to likewise originate from Maillard reaction [11]. According to Yaylayan and Keyhani [11, 12], the former structure might be either directly formed from glucose upon dehydration and retroaldol cleavage or from the α -dicarbonyl compound 3-deoxyosone *via* pyruvaldehyde, followed by chain elongation by one carbon atom coming from amino acids like glycine. The latter pathway can be similarly applied to describe the production of 2,3-pentanedione, however requiring the incorporation of two carbon units into pyruvaldehyde, which, for instance, could be donated by alanine [11]. The authors further underlined that both structures could be considered precursors for Strecker degradation [13].

Table 1: Odour activity values, odour thresholds in water (OT) and odour descriptors of volatiles identified in sponge cakes made with wheat (WC), lupin (LUC), chickpea (CPC), green pea (GPC), lentil (LEC) or yellow pea flour (YPC). Only key compounds with odour activity values ≥ 5 are shown.

Compound	Odour activity value						OT [$\mu\text{g/L}$]	Odour descriptor
	WC	LUC	CPC	GPC	LEC	YPC		
3-Methylbutanal	10264	8163	8963	10570	5802	11600	0.2 ^d	Malty, roasty, chocolate ^{a,b,g}
Hexanal	327	183	2641	5266	2675	3502	4.5 ^d	Green, grassy, tallow ^{a,b}
2,4-Decadienal			1174	1991	1209	1256	0.07 ^d	Deep fat fried ^b
2-Ethyl-3,5-dimethylpyrazine	352	535	786	781	1207	869	0.04 ^d	Earthy ^b
2-Methylbutanal	557	468	606	652	353	742	3 ^d	Almond, malty ^b
2-Methylpropanal	108		523		271		1 ^f	Malty ^b
Pentanal	19	14	162	248	100	215	12 ^e	Pungent, strong acrid ^b
Nonanal	34	49	161	204	168	147	1 ^d	Citrus, soapy ^{a,b}
1-Octen-3-ol	15		132	289	142	179	1 ^d	Mushroom, vegetable ^{b,c}
Octanal	23	28	133	151	112	119	0.7 ^d	Citrus, flowery ^{a,b}
Heptanal	25	17	122	140	117	120	3 ^d	Green, fatty, rancid ^{a,c}
2-Octenal			33	72	33	43	3 ^d	Fatty, nutty, roasted ^b
2-Pentylfuran	10	5	57	36	48	38	6 ^d	Green, floral, fruity ^a
Phenylacetaldehyde	16	28					4 ^d	Honey-like, sweet ^{a,b}
2,3-Butanedione	27						3 ^d	Buttery, caramel ^{a,b}
2,3-Pentanedione	11	13	12	7	13	13	20 ^d	Buttery ^b
Acetaldehyde	8	8	10	17		14	15 ^e	Fruity ^b
Butanal			8	13	10	13	9 ^d	Malty ^b
2-Heptenal			5	13	5	6	13 ^d	Green, fatty ^b
2-Hexenal				5	5		17 ^d	Green, fatty ^b

^a from Birch [14].

^b from Pico [15].

^c from Murat [3].

^d from Buttery and Ling [16].

^e from Buttery [17].

^f from Belitz [6].

^g from Rega [18].

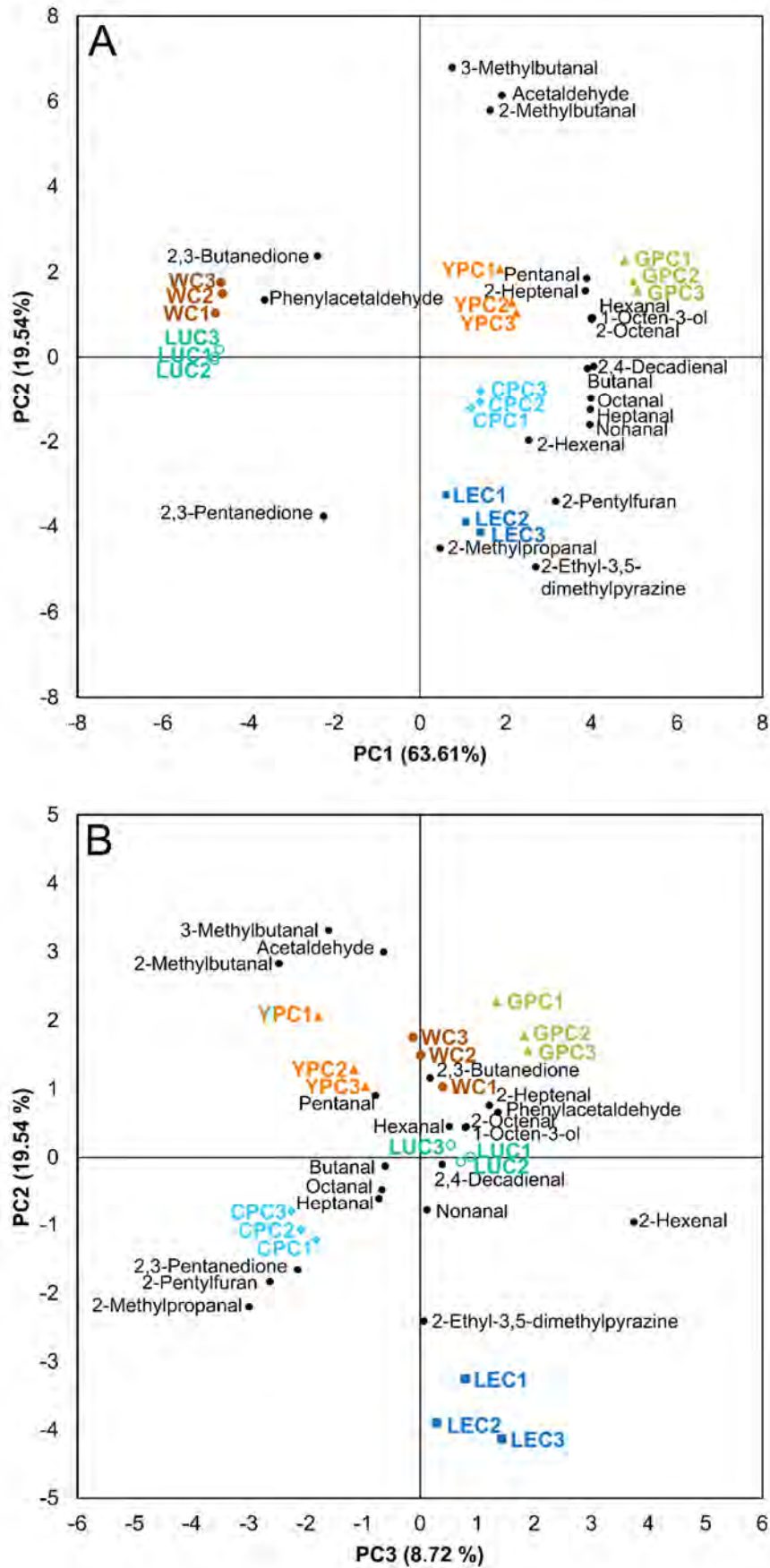


Figure 1: Biplots of (A) PC1 and PC2 and (B) PC2 and PC3 on odour-active compounds in sponge cakes made with wheat (WC), lupin (LUC), chickpea (CPC), green pea (GPC), lentil (LEC) or yellow pea flour (YPC).

The twenty odour-active compounds listed in Table 1 were subsequently subjected to principle component analysis in order to visualize how they drive the discrimination of the wheat and pulse cakes.

As depicted in Figure 1, PC1, PC2 and PC3 accounted for 63.61%, 19.54% and 8.72% of total variability. Along PC1, two groups of highly correlated cakes were distinguished. While wheat cakes (WC) and lupin cakes (LUC) clustered in the negative part of PC1, positive loadings were associated with cakes made from lentil (LEC), chickpea (CPC) green pea (GPC) and yellow pea (YPC). This differentiation was mainly driven by lipoxidation markers, which were characterized by positive signs, and thus, were directly linked to the second group of cakes. From these findings, it could be concluded that the unsaturated fatty acids contained in the associated flours possessed higher susceptibility towards oxidative degradation, hence promoting the generation of lipoxidation-derived volatiles. According to Krause [1], chickpea, lentil, yellow pea and green pea flours were not only significantly enriched in oleic, linoleic and linolenic acid compared to wheat and lupin, but concurrently comprised lipoxygenase with considerably higher activity, thus accelerating fatty acid oxidation. Following the general consensus of literature, the thereby released volatiles are typically responsible for a green, citrus and fatty odour (Table 1) [3, 14, 15]. Owing to its outstanding odour activity values among all lipoxidation markers identified, ranging from 183 to 5266, hexanal was assumed to be of substantial sensory importance. Interestingly, green pea cakes were characterized by the highest odour activity values of almost all lipoxidation markers. From this it was inferred that the associated green notes will probably be strongly perceived in this product. Lupin and wheat cakes, on the other hand, were correlated in the negative part of PC1 with phenylacetaldehyde, 2,3-butanedione and 2,3-pentanedione, probably emerging from Maillard reaction. These molecules are generally described to impart sweet, buttery and caramel-like odours [14, 15], however, they had only low odour activity values (7-28) (Table 1).

Further distinction of the individual cakes was obtained by consideration of PC2. As visible from both PC1 vs PC2 and PC3 vs PC2 biplots, the yellow and green pea products as well as the wheat cakes were spotted in the positive part of PC2, hence being associated with 3-methylbutanal, 2-methylbutanal and acetaldehyde formed during Strecker degradation (Figure 1). Of all odour-active compounds observed, 3-methylbutanal appeared to have the highest odour activity values in all products, varying from 5802 to 11600 (Table 1). This molecule is known to cause a malty, roasty and chocolate odour [14, 15, 18], which is likely to be easily perceived in the various cakes and could have been a key odorant especially in cakes made with wheat, yellow and green pea flours. In these products, the malty odour might have been intensified by 2-methylbutanal, although the correlated odour activity values were relatively lower. From the PC3 vs PC2 biplot, it further emerged that chickpea and lentil cakes were linked to 2-methylpropanal likewise reported to possess a malty but also almond-like aroma [15], however having similar odour activity values as 2-methylbutanal (Table 1). Consequently, it could be concluded that Strecker degradation was an important chemical reaction occurring in all products, yielding substances with similar flavour despite different amino acid precursors.

Lentil cakes further differed from the other cakes in the clear correlation with 2-ethyl-3,5-dimethylpyrazine (earthy notes) linked with negative loadings on PC2. Table 1 indicates a very low odour threshold for this heterocycle [15], for which reason it was supposed to be a strong contributor to the aroma especially of lentil cakes. Krause [1] assigned the higher ability of lentil flour to form pyrazines during sponge cake development to the exclusive presence of specific amino acids known to favour pyrazine production.

Interestingly, the discussed discrimination of the cakes based on the odour activities of relevant volatiles was comparable to that based on the concentrations of all extracted volatiles as reported by Krause [1]. This indicated that the selection of key odour-active compounds did not distort the global positioning of cakes on the PCA biplots and thus seemed to be an adequate approach to describe principle differences between the products.

In general, it needs to be considered that the overall odour of food is affected by a complex mixture of many odour-active compounds occurring at specific proportions. Consistently, the results presented in this study are primarily helping to understand and predict major differences between thermo-mechanically treated products prepared from diverse raw materials. Further techniques should thus be applied to gain deeper insight into the sensory discrimination of bakery products, such as cakes.

Conclusion

Total replacement of wheat by pulse flours seemed to considerably change the profile of volatile compounds with potent odour in sponge cakes. The volatile compounds were extracted from the individual bakery products by means of HS-SPME/GC-MS and quantified using isotopic dilution of internal standards. Odour activity values of all analysed components were determined on the basis of their calculated concentrations and known odour threshold values. Those molecules with an odour activity value greater than or equal to five were selected as main odour contributors and submitted to principle component analysis in order to evaluate their role in the discrimination of the diverse cakes. The majority of the twenty aroma-active compounds appeared to originate from the oxidative degradation of unsaturated fatty acids, while the remaining components were assigned to the thermally induced breakdown of sugars and amino acids mainly *via* Maillard reaction. This implied that different chemical reactions took place during sponge cake making, through which diverse compounds were released with interesting odour characteristics.

Multivariate data analysis disclosed that the pulse-based cakes mainly differed from the wheat cakes in being strongly correlated with lipoxidation markers usually possessing green, fatty odours. Among these pulse products, lupin represented an exception as it was rather related to Maillard-derived compounds with known buttery, sweet notes, which were concurrently associated with the wheat cakes. Nonetheless, Maillard reaction also seemed to play a non-negligible role in the pulse-containing products. In the course of this reaction, Strecker aldehydes seemed to be released with probable sensory importance (typically malty odours) in all samples examined, particularly in wheat, yellow pea and green pea cakes. In addition, lentil cake could be further discriminated by its association with 2-ethyl-3,5-dimethylpyrazine, which was suggested to be responsible for an earthy aroma.

These results highlight that diverse odour-active volatile compounds can be produced during development of baked goods dependent on the raw material used. Therefore, the right choice of ingredient type is crucial in processing food with designed sensory attributes.

Acknowledgement

This research was financially supported by the European Union's Horizon 2020 Research and Innovation Program under the Marie Skłodowska Curie Training Network FOODENGINE (Grant Agreement No. 765415).

References

1. Krause S, Keller S, Hashemi A, Descharles N, Bonazzi C, Rega B. From flours to cakes: Reactivity potential of pulse ingredients to generate volatile compounds impacting the quality of processed food. [Submitted for publication]. 2021.
2. Cepeda-Vázquez M, Rega B, Descharles N, Camel V. How ingredients influence furan and aroma generation in sponge cake. *Food Chemistry*. 2018;245:1025-33.
3. Murat C, Bard M-H, Dhalleine C, Cayot N. Characterisation of odour active compounds along extraction process from pea flour to pea protein extract. *Food Research International*. 2013;53(1):31-41.
4. Rackis JJ, Sessa DJ, Honig DH. Flavor problems of vegetable food proteins. *Journal of the American Oil Chemists' Society*. 1979;56(3Part2):262-71.
5. Maire M, Rega B, Cuvelier M-E, Soto P, Giampaoli P. Lipid oxidation in baked products: Impact of formula and process on the generation of volatile compounds. *Food Chemistry*. 2013;141(4):3510-8.
6. Belitz H-D, Grosch W, Schieberle P. *Food Chemistry*. 4th ed: Springer-Verlag Berlin Heidelberg; 2009.
7. Murray KE, Shipton J, Whitfield FB, Last JH. The volatiles of off-flavoured unblanched green peas (*Pisum sativum*). *Journal of the Science of Food and Agriculture*. 1976;27(12):1093-107.
8. Adams A, Bouckaert C, Van Lancker F, De Meulenaer B, De Kimpe N. Amino Acid Catalysis of 2-Alkylfuran Formation from Lipid Oxidation-Derived α,β -Unsaturated Aldehydes. *Journal of Agricultural and Food Chemistry*. 2011;59(20):11058-62.
9. Adams A, Polizzi V, van Boekel M, De Kimpe N. Formation of Pyrazines and a Novel Pyrrole in Maillard Model Systems of 1,3-Dihydroxyacetone and 2-Oxopropanal. *Journal of Agricultural and Food Chemistry*. 2008;56(6):2147-53.
10. Shibamoto T, Akiyama T, Sakaguchi M, Enomoto Y, Masuda H. A study of pyrazine formation. *Journal of Agricultural and Food Chemistry*. 1979;27(5):1027-31.
11. Yaylayan VA, Keyhani A. Origin of Carbohydrate Degradation Products in L-Alanine/D- ^{13}C Glucose Model Systems. *Journal of Agricultural and Food Chemistry*. 2000;48(6):2415-9.
12. Yaylayan VA, Keyhani A. Origin of 2,3-Pentanedione and 2,3-Butanedione in D-Glucose/L-Alanine Maillard Model Systems. *Journal of Agricultural and Food Chemistry*. 1999;47(8):3280-4.
13. Keyhani A, Yaylayan VA. Elucidation of the Mechanism of Pyrazinone Formation in Glycine Model Systems Using Labeled Sugars and Amino Acids. *Journal of Agricultural and Food Chemistry*. 1996;44(9):2511-6.
14. Birch AN, Petersen MA, Arneborg N, Hansen ÅS. Influence of commercial baker's yeasts on bread aroma profiles. *Food Research International*. 2013;52(1):160-6.
15. Pico J, Bernal J, Gómez M. Wheat bread aroma compounds in crumb and crust: A review. *Food Research International*. 2015;75:200-15.
16. Buttery RG, Ling LC. Additional Studies on Flavor Components of Corn Tortilla Chips. *Journal of Agricultural and Food Chemistry*. 1998;46(7):2764-9.
17. Buttery RG, Turnbaugh JG, Ling LC. Contribution of volatiles to rice aroma. *Journal of Agricultural and Food Chemistry*. 1988;36(5):1006-9.
18. Rega B, Guerard A, Delarue J, Maire M, Giampaoli P. On-line dynamic HS-SPME for monitoring endogenous aroma compounds released during the baking of a model cake. *Food Chemistry*. 2009;112:9-17.

Methods for predicting and assessing flavour evolution during white wine ageing

JOSH HIXSON^{1,2}, Lisa Pisaniello¹, Mango Parker^{1,2}, Yevgeniya Grebneva^{1,3}, Eleanor Bilogrevic¹, Robin Stegmann⁴ and Leigh Francis^{1,2}

¹ The Australian Wine Research Institute, Adelaide, Australia, josh.hixson@awri.com.au

² The University of South Australia, Adelaide, Australia

³ Hochschule Geisenheim, Geisenheim, Germany

⁴ Technische Universität Dresden, Dresden, Germany

Abstract

Estimating future flavour evolution in wine generally requires quantitative analysis of a known precursor compound or forcible production using elevated temperature and/or lower pH with analysis of the produced volatiles. While it is understood that these methods are not always accurate, they can provide an indicative assessment of the magnitude of evolving species. However, due to the complex pathways by which some key odorants are formed, these predictive measures may not provide a compositionally relevant outcome, and do not provide any indication of future flavour evolution. Here, extracts derived from the winemaking by-product, grape marc, rich in monoterpene glycosides have been analysed by 'predictive' methods and also added to wine to provide a correlation with real-world evolution profiles. While analysis of a precursor molecule, geraniol glucoside, and acid-catalysed hydrolytic assessment of the extracts both provided good correlations with total flavour production in wine, neither were good predictors for final monoterpene composition in wines. Additionally, a single extract was monitored over 36 months in two different base wines and at two different concentrations to gain a better understanding of hydrolysis kinetics, which was also explored computationally. The generation of first-order rate curves provided a mechanism to determine reaction half-lives for the hydrolysis of geraniol glucoside and related to the monoterpene composition in wines.

Keywords: white wine, monoterpenes, glycoside hydrolysis, shelf-life, computational

Introduction

Wine is an inherently unstable product that is continually changing with time, with additional complexity surrounding the fact that the time from production to consumption is highly varied and can be at the inclination of the consumer. Winemakers hold a wealth of experience in determining the optimum window of time for a certain wine to be consumed, but what happens when the ability to interpolate specific outcomes is replaced by the need to extrapolate?

Throughout the world, grape-growing regions are experiencing climatic extremes and shifts in growing season temperatures that can push grape and wine composition outside that previously experienced, with respect to flavour compounds and the matrix they exist in [1, 2]. Additionally, the growing trend for no- or low-alcohol products [3], can be satisfied by removal of excess alcohol or by supplementation of base grape or wine components into a different matrix [3, 4]. These scenarios equate to a situation where grape or wine components are taken out of their usual context and result in the need for better understanding of flavour evolution to be able to extrapolate known flavour generation pathways into new matrices.

The evolution of monoterpenes has been widely studied due to their ubiquity. In wines, it is well understood that acid-catalysed hydrolysis of a structurally diverse group of saccharide-bound analogues yield the free, odoriferous monoterpenes [5]. Quantitation of the monoterpene potential in grapes can be achieved by either direct analysis of the saccharide-bound monoterpenes, or via catalytic release of the volatiles and subsequent GC-MS analysis [5]. While both methods can provide information as to the magnitude of future monoterpene production, little can be gained about the speed of hydrolysis reactions as it relates to wine ageing and the evolution of monoterpenes, let alone the ability to extrapolate outcomes into different matrices.

Recently, we outlined the use of monoterpene-rich extracts from the winemaking by-product, grape marc, as a latent flavour enhancer when added into wines, giving rise to monoterpenes over the six-month experiment [6]. Here, the storage of grape marc extracts in two different wines described previously has been monitored for 36 months with respect to geraniol glucoside hydrolysis and monoterpene evolution. Additionally, a selection of grape varieties has been accessed to generate similar extracts and investigate their potential as latent flavour additives. The aims were to better understand the role of grape marc-derived extracts in the generation of flavour via 1) specifically investigating mechanistic and kinetic factors of glucoside hydrolysis under different pH conditions; 2) assess the role of extract characterisation methods on predicting flavour generation.

Experimental

Grapes, wines and marc extraction

Long-term glycoside extract storage trials in Chardonnay and Riesling wines were initiated as previously described [6], with analysis progressing past the initial six-months to include 18- and 36-month time points. In short, 300 kg of Gewürztraminer grape marc obtained in vintage 2016 was extracted with water followed by purification of the extract on FPX66 resin. The resultant ethanolic extract was dried by low-pressure distillation to yield a brown powder rich in monoterpene glycosides. The extract was added in duplicate to two different wines (Chardonnay, pH 3.40 or Riesling, pH 3.10) at either 0.4 g/L or 0.8 g/L of extract, at pre- and post-fermentation. Here, duplicates at the same concentration but added at different times have been grouped into quadruplicates for simplicity.

Additionally, short-term glycoside storage trials were performed from grape marc extracts isolated from ten different grape varieties collected across South Australia during vintages 2017 or 2018. Isolation and extraction of extracts was performed as described above, but on a laboratory-scale starting with approximately 10 kg of grapes that were hand-pressed to yield approximately 5 kg of marc which was stored at -20 °C until used for isolation of monoterpene glycoside-rich extract. For all short-term trials, each extract was added to 1.2 L of commercially available Chardonnay wine (pH 3.40) at 0.4 g/L, and the wine was then bottled in triplicate (375 mL screwcap sealed glass bottles) and stored at 15 °C for six months prior to volatile analysis by gas chromatography-mass spectrometry (GC-MS). All wine handling was performed under anaerobic conditions using solid CO₂ in vessels, with transfers and bottling performed with laboratory grade nitrogen gas.

Marc extracts and research wine analysis

For quantitation of geraniol glucoside by liquid chromatography (LC)-MS/MS as previously recorded [6], wines were analysed neat and grape marc extracts were dissolved in water, followed by the addition of the internal standard (d₂-geraniol glucoside) prior to instrumental analysis. Hydrolysis of grape marc extracts was performed as per Grebneva (2019) [7], where a weighed amount was dissolved in water, acidified to pH 1 and heated at 100 °C for an hour before the hydrolysate was cooled prior to volatiles analysis. Volatiles were quantified from extract hydrolysates or wine samples for a range of monoterpenes and norisoprenoids by SIDA SPME (solid phase microextraction)-GC-MS, as previously described [6].

Computational chemistry

Structures were drawn in Avogadro (version 1.2.0) [8], then optimised (UFF) and systematic rotor conformer search performed, with the resulting geometry used to create initial input files for GAMESS (Linux distribution, version 2019 R2, University of Iowa, USA) [9] running on the University of South Australia's High Performance Compute Cluster. Calculations were first performed for molecules in the gas phase (RHF/3-21G) to provide starting geometries which were then used as the input for density functional theory (B3LYP/6-311G(d)) equilibrium geometry calculations in water (SMD solvent model). Local minima were confirmed by vibrational analysis and the presence of all real frequencies, and all structural outcomes visualised using MacMolPlt (v7.7) [10]. Each calculation was performed in parallel across eight cores.

Data, graphing and calculations

Data handling was performed in R [11], and graphs produced using the package ggplot2 [12]. Rate-order graphs (Figure 2) provided rate constants (k , in months⁻¹) from the negative slope of regression lines, estimated initial geraniol glucoside concentration from the y-intercept ($e^{y\text{-intercept}}$), and reaction half-lives ($t_{1/2}$, in months) from the natural logarithm of 2 divided by the rate constant, k ($\log_e(2)/k$). The monoterpene concentration values were converted to geraniol glucoside equivalents using the mass proportion of the monoterpenes in geraniol glucoside (48.735%). Odour activity values were determined using the aroma detection thresholds of 30 µg/L for geraniol, 25 µg/L for linalool and 250 µg/L for α -terpineol [13, 14].

Results and discussion

Grape marc-derived extracts from ten different varieties were analysed for their geraniol glucoside concentration, and following acid-catalysed hydrolysis as a marker for potential future flavour evolution, and were subsequently stored in a commercial Chardonnay wine for six months followed by quantitation of the evolved odorants. The concentration of the glucosidic monoterpene precursor and the analysis of extract hydrolysates were compared with the measured monoterpene evolution in wine as a benchmarking of predictive methods. The hydrolytic release and measurement of monoterpenes from the extract correlated well with the monoterpene concentration values after six months of storage ($R^2 = 0.99$, $p < 0.0001$). However, the monoterpenes quantified in the extract hydrolysates did not provide a monoterpene profile or yield concentrations that were predictive of that evolved during wine storage after six months. Instead of wine-like monoterpene profiles, hydrolytic release yielded

decreased proportions of geraniol and preferentially promoted subsequent rearrangement to α -terpineol. Similarly, the amount of geraniol glucoside added correlated with the quantity of monoterpenes present in wine after six months of storage ($R^2 = 0.84$, $p < 0.0001$), but again only enabled the ranking of extracts in total magnitude of monoterpene production.

While both methods of estimating future flavour evolution from marc-derived extracts in wine were adequate for ranking the extracts in terms of the relative magnitude, neither provided realistic results in terms of their total monoterpene quantity or profile. Additionally, they provided limited information regarding the extract performance under different conditions and failed to provide an understanding of shelf-life with respect to the evolved volatiles. As such, additional work was undertaken to investigate mechanisms to better predict the speed of flavour evolution, by extending storage trials that have previously been reported [6] to 36 months (Figure 1).

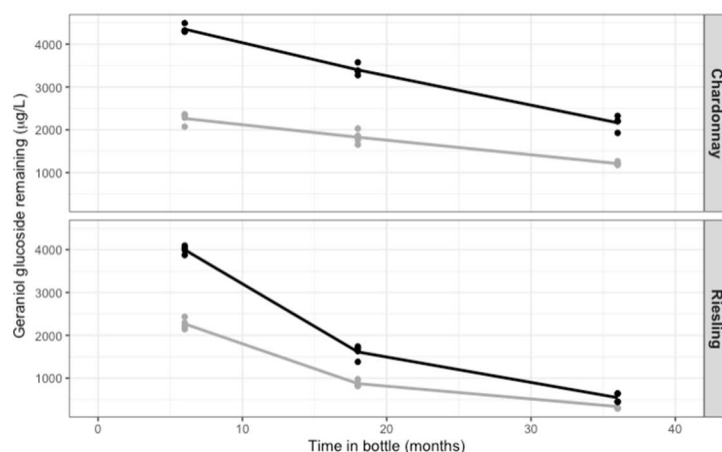


Figure 1: Concentration of geraniol glucoside remaining in Chardonnay (pH 3.40) and Riesling wines (pH 3.10) with 0.4 g/L (grey lines/points) or 0.8 g/L (black lines/points) of Gewürztraminer marc extract across 36 months of storage. Points represent individual samples; lines represent mean at each time point ($n = 4$).

The wines exhibited expected decreases in geraniol glucoside, which was more rapid for the Riesling wine with a lower pH (3.10) compared with the Chardonnay wine (pH 3.40) [15], albeit with different hydrolysis profiles between the varieties. While the lower pH Riesling wine showed initially rapid decreases which slowed, the Chardonnay wine displayed a linear decrease with time. As expected, the linear relationship of the natural logarithm of the geraniol glucoside concentration against time supported a first-order reaction (Figure 2), in alignment with reported glycoside hydrolysis reaction kinetics [16]. However, the mean rate constant (k) determined across both addition rates for each pH (3.10, $0.0649 \text{ months}^{-1}$; 3.40, $0.0222 \text{ months}^{-1}$) differed, suggesting a pH effect which could not be accounted for by a single-step first-order hydrolysis reaction alone.

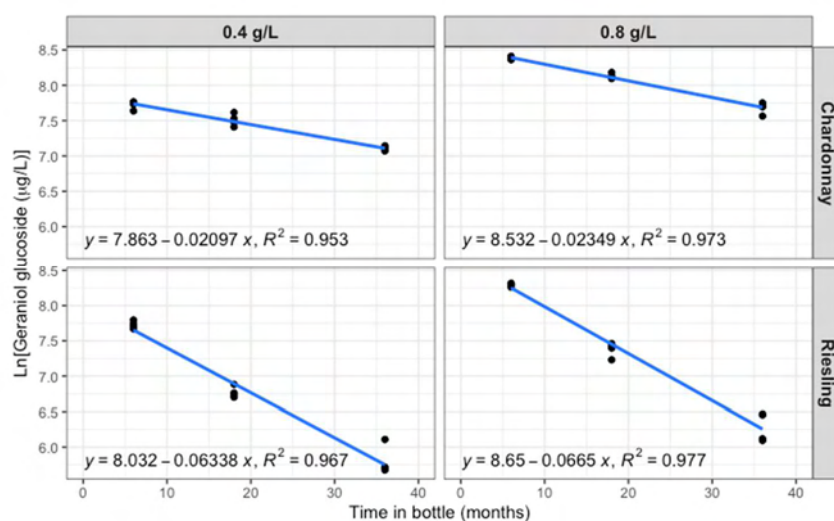


Figure 2: Natural logarithm of geraniol glucoside concentration in Chardonnay or Riesling wines ($n = 4$ at each point), showing regression (blue line) representing the hydrolysis of geraniol glucoside as a first-order reaction.

The concerted geraniol glucoside hydrolysis mechanism proposed previously [17], explains the over representative formation of linalool from geraniol glucoside [17, 18], via the cationic species, linalyl cation [19] (compound **3**, Figure 3). However, here it failed to explain the changes in hydrolysis with concentration and pH, or a hydrolysis rate that solely relies on the concentration of geraniol glucoside. Additionally, many of the possible acid-catalysed mechanisms proposed for general glucoside hydrolysis involve the aglycone retaining the glycosidic ether oxygen [20], which would fail to yield linalyl cation and would lead to the generation of geraniol only from geraniol glucoside hydrolysis. As such, the findings here can only be explained by hydrolysis involving the initial protonation of the glucoside oxygen (as shown in Figure 3, **1** to **2**) [20], which then proceeds via cleavage of the glycosidic bond to yield **3** [17].

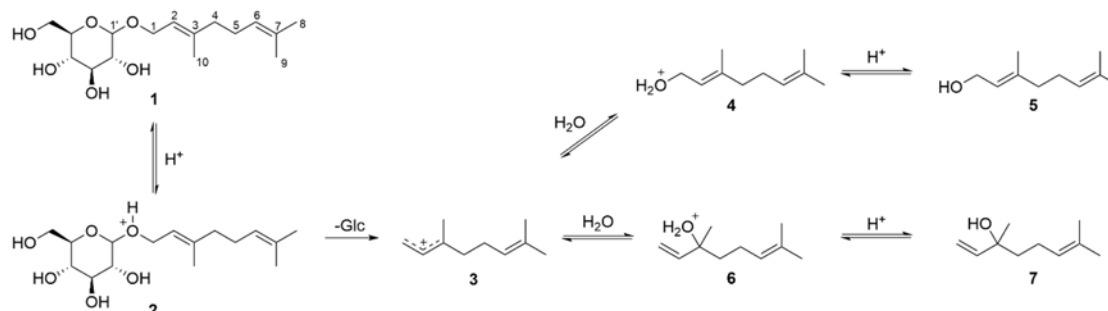


Figure 3: Indicative formation of free monoterpenes (**5** and **7**) from non-volatile geraniol glucoside (**1**) via formation of protonated glucoside (**2**) and linalyl cation (**3**), including interchange between geraniol (**5**) and linalool (**7**) via cationic species (**3**, **4** and **6**).

In the event of a two-step hydrolysis of **1** via the protonated geraniol glucoside (**2**), the cation formed must be stable for the mechanism to be viable. To investigate this, all compounds shown in Figure 3 were studied computationally to determine stability, and to re-confirm previous findings on the transition between geraniol and linalool [19]. The key atomic charges and bond lengths are shown below in Table 1.

Table 1: Key atom and bond properties of energy minimised structures following equilibrium geometry optimisation using B3LYP/6-311G(d) in water.

Structure	Atomic charges (a.u.)					Bonds, length in Å (order)			
	C ₁	C ₂	C ₃	O [#]	H [^]	C _{1/3} -O [#]	C ₁ -C ₂	C ₂ -C ₃	O-H
1	-0.22	-0.26	0.07	-0.41	N/A	1.45 (0.88)	1.50 (1.00)	1.34 (1.89)	N/A
2	-0.21	-0.31	0.13	-0.50	0.49	1.58 (0.57)	1.47 (1.04)	1.35 (1.78)	0.99 (0.65)
3*	-0.27	-0.19	0.21	N/A	N/A	N/A	1.36 (1.64)	1.42 (1.27)	N/A
4	-0.17	-0.35	0.15	-0.66	0.54	1.55 (0.54)	1.47 (1.07)	1.35 (1.77)	0.98 (0.67)
5	-0.18	-0.30	0.09	-0.64	0.42	1.45 (0.91)	1.50 (1.00)	1.34 (1.86)	0.93 (0.78)
6	-0.38	-0.19	0.12	-0.71	0.55	1.64 (0.44)	1.33 (1.91)	1.50 (1.05)	0.97 (0.67)
7	-0.45	-0.19	0.18	-0.65	0.41	1.44 (0.88)	1.33 (1.94)	1.52 (1.00)	0.97 (0.78)

*optimisation via both geraniol (**5**) and linalool (**7**) gave the same structure. [^]refers to the newly installed hydrogen for protonated species (**2**, **4** and **6**) and only hydrogen for neutral species (**5** and **7**). [#]refers to the oxygen attached to C₁ for geranyl species (**4** and **5**) and C₃ for linalyl species (**6** and **7**).

Firstly, the generation of **3** via either **5** or **7** yielded structures that align closely with experimental outcomes with respect to the preferential re-production of **7** from **3** over **5** [19], given the greater positive charge on C₃ over C₁ due to the stability of the tertiary carbocation. For the generation of **2** from **1**, the formation of a stable intermediate supported the two-step mechanism, and the structural changes were consistent with cleavage of the glucoside between the ether oxygen and C₁ of the aglycone, given the increase in bond length between C₁-O, and decrease in bond order. As such, the computational structural investigation supported the proposal of an initial protonation of geraniol glucoside, and then cleavage to yield the linalyl cation, which is consistent with previous findings [17,18]. Furthermore, it explains the pH-related change in geraniol glucoside hydrolysis rate. The greater extent of protonation of **1** at the lower pH provides a greater proportion of the hydrolysis reactant, **2**. In essence, the hydrolysis curves showing the removal of **1** (Figure 1) provide a pH-dependant proxy for the actual reactant, **2**.

While the generation of a universal rate constant for the hydrolysis of geraniol glucoside will ultimately rely on determining the pH-dependent equilibrium constant between **1** and **2**, the rate constants estimated above still allowed for the generation of reaction half-lives at each pH. Half-lives of geraniol glucoside hydrolysis of approximately 11 months or 31 months at pH 3.10 or 3.40, respectively, provided an indication of the production of volatiles over time, and information into shelf-life of wines. Shown below (Figure 4) are the key monoterpenes

generated in the Chardonnay and Riesling wines via hydrolysis of geraniol glucoside and subsequent rearrangement, with an indication of the geraniol glucoside half-life.

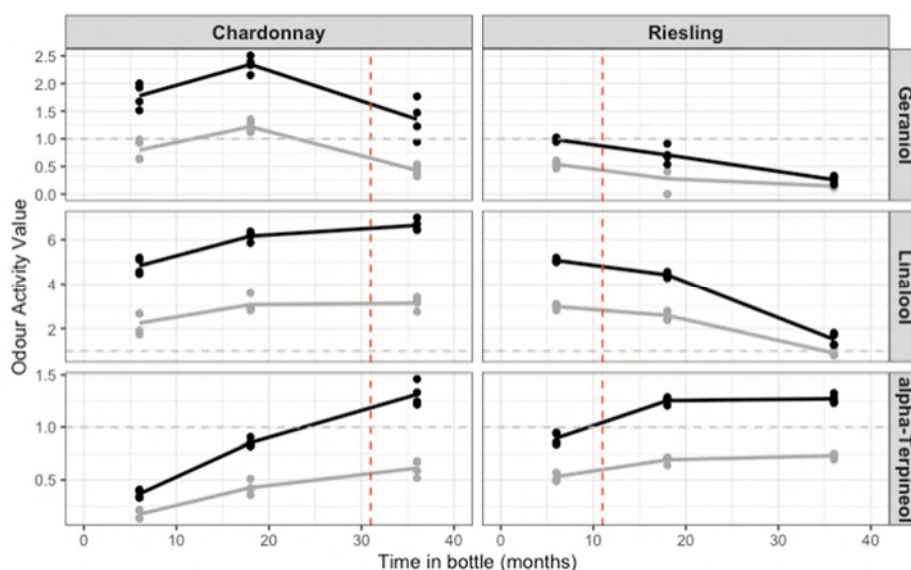


Figure 4: Concentration, expressed as odour activity value, of key monoterpenes in Chardonnay and Riesling wines with 0.4 g/L (grey lines/points) or 0.8 g/L (black lines/points) of Gewürztraminer marc extract across 36 months of storage, with red dashed vertical lines indicating the established pH-dependent half-lives of geraniol glucoside in each wine. Horizontal grey dashed lines signify odour activity value of 1. Points represent individual samples; lines represent mean at each time point ($n = 4$).

Interestingly, at the half-life of geraniol glucoside hydrolysis, each wine possessed a similar monoterpene concentration and profile, especially when comparing between the 0.4 g/L additions at each pH (grey lines). The formation of linalool, and to some extent geraniol, then rearrangement to α -terpineol (via nerol), and the equilibria that exist between these compounds [19], appear largely dependent only on the hydrolysis of geraniol glucoside. This suggests that determination of a rate constant for a single key step may allow for better shelf-life estimations, which can only be improved by better understanding the formation of protonated species under different conditions (pH and matrix). Importantly, the hydrolysis of geraniol glucoside has not been completely isolated in this experiment with preceding reactions also taking place to yield additional geraniol glucoside as the storage progressed. As such, future investigation will need to be conducted into other significant precursors that yielded geraniol glucoside in these experiments. While non-targeted LC-MS/MS experiments have been conducted on the initial extract that was used, the ability to identify another significant precursor is dependent on correlations between the ‘missing’ portions and the abundance of mass spectral features. To provide information on the quantity of precursor currently unaccounted for, two different methods were conducted (Table 2).

Table 2: Estimation of total geraniol glucoside pool including that present in higher precursor forms, using either the sum of free monoterpenes (MTs) and geraniol glucoside (Ger-glc) present at six months of ageing, or using the first-order rate curves.

Variety	Extract addition (g/L)	Mean value at 6 months in bottle ($\mu\text{g/L}$)			From rate curves		
		Sum MTs*	MTs in Ger-Glc equivs [^]	Ger-glc remaining	Estimated starting concentration	y-intercept	Ger-glc ($\mu\text{g/L}$)
Chardonnay	0.4	127	260	2265	2525	7.863	2599
	0.8	278	570	4351	4921	8.532	5075
Riesling	0.4	226	464	2268	2732	8.032	3078
	0.8	385	790	3998	4788	8.650	5710

*Geraniol, linalool, nerol and α -terpineol. [^]converted using mass proportion factor of 0.48735.

Firstly, the concentration of evolved monoterpenes after six-months of storage has been summed and converted to the equivalent concentration if derived from geraniol glucoside. This value was added to the concentration of remaining geraniol glucoside at six-months to give an estimated starting concentration considering formation from

other sources. However, from our analysis of model experiments, the recovery of geraniol glucoside and the four main evolved monoterpenes is not complete (data not shown), so this method is expected to provide an underestimate. Secondly, the rate-order curves (Figure 2) provided a theoretical estimation of geraniol glucoside starting concentration from the y-intercept, albeit inherently over-estimated. Future efforts will investigate the 'missing' portion of geraniol glucoside and any higher precursors that yield geraniol glucoside as a way of better predicting future flavour evolution from marc-derived extracts.

Conclusion

Evolution of monoterpenes from winemaking by-product-derived extracts has been followed over 36 months of storage in wines at two different pH values. While the hydrolysis of geraniol glucoside was not an isolated reaction, this system has allowed a deeper understanding of the mechanism and kinetics of hydrolysis. The reaction appears to proceed via a pH-driven protonation, followed by a first-order cleavage, for which the former step requires further investigation. A computational investigation of the proposed intermediates supported the hypothesis and aligns with previous experimental reports.

The chemical investigation into the hydrolysis of geraniol glucoside in wine from odourless extracts has provided an improved understanding of the hydrolysis kinetics, and the estimated rates have proven useful in characterising the flavour generation from these extracts. Additionally, the rate curves provide additional information as to the magnitude of flavour precursors that are currently un-quantitated which will prove useful in further interrogation of non-targeted experimental data.

Acknowledgements This project was supported by Australia's grapegrowers and winemakers through their investment body Wine Australia, with matching funds from the Australian Government. The AWRI is a member of the Wine Innovation Cluster in Adelaide.

References

1. Mira de Orduña R. Climate change associated effects on grape and wine quality and production. *Food Res Internat.* 2010;43(7):1844-55.
2. van Leeuwen C, Darriet P. The Impact of Climate Change on Viticulture and Wine Quality. *Journal of Wine Economics* 2016;11(1):150-67.
3. Liguori L, Russo P, Albanese D, Di Matteo M. Production of Low-Alcohol Beverages: Current Status and Perspectives. *Food Processing for Increased Quality and Consumption* 2018. p. 347-82.
4. Varela C, Dry PR, Kutyna DR, Francis IL, Henschke PA, Curtin CD, et al. Strategies for reducing alcohol concentration in wine. *Aust J Grape Wine Res.* 2015;21:670-9.
5. Black CA, Parker M, Siebert TE, Capone DL, Francis IL. Terpenoids and their role in wine flavour: recent advances. *Aust J Grape Wine Res.* 2015;21:582-600.
6. Parker M, Barker A, Black CA, Hixson J, Williamson P, Francis IL. Don't miss the marc: phenolic-free glycosides from white grape marc increase flavour of wine. *Aust J Grape Wine Res.* 2019;25(2):212-23.
7. Grebneva Y, Bellon JR, Herderich MJ, Rauhut D, Stoll M, Hixson JL. Understanding Yeast Impact on 1,1,6-Trimethyl-1,2-dihydronaphthalene Formation in Riesling Wine through a Formation-Pathway-Informed Hydrolytic Assay. *J Agric Food Chem.* 2019;67(49):13487-95.
8. Hanwell MD, Curtis DE, Lonie DC, Vandermeersch T, Zurek E, Hutchison GR. Avogadro: an advanced semantic chemical editor, visualization, and analysis platform. *J Cheminform.* 2012;4(1):17.
9. Barca GMJ, Bertoni C, Carrington L, Datta D, De Silva N, Deustua JE, et al. Recent developments in the general atomic and molecular electronic structure system. *J Chem Phys.* 2020;152(15):154102.
10. Bode BM, Gordon MS. MacMolPlt: a graphical user interface for GAMESS. *J Mol Graph Model.* 1998;16(3):133-8, 64.
11. R Core Team. R: A Language and Environment for Statistical Computing. Vienna, Austria: R Foundation for Statistical Computing; 2017.
12. Wickham H. *ggplot2: Elegant Graphics for Data Analysis*: Springer-Verlag New York; 2009.
13. Guth H. Quantitation and Sensory Studies of Character Impact Odorants of Different White Wine Varieties. *J Agric Food Chem.* 1997;45(8):3027-32.
14. Ferreira V, Lopez R, Cacho JF. Quantitative determination of the odorants of young red wines from different grape varieties. *J Sci Food Agric.* 2000;80(11):1659-67.
15. Mateo JJ, Jiménez M. Monoterpenes in grape juice and wines. *J Chromatogr A.* 2000;881(1-2):557-67.
16. BeMiller JN. Acid-Catalyzed Hydrolysis of Glycosides. *Advances in Carbohydrate Chemistry* 1967. p. 25-108.
17. Skouroumounis GK, Sefton MA. Acid-catalyzed hydrolysis of alcohols and their β -D-glucopyranosides. *J Agric Food Chem.* 2000;48(6):2033-9.
18. Pedersen DS, Capone DL, Skouroumounis GK, Pollnitz AP, Sefton MA. Quantitative analysis of geraniol, nerol, linalool, and alpha-terpineol in wine. *Anal Bioanal Chem.* 2003;375(4):517-22.
19. Cori O, Chayet L, Perez LM, Bunton CA, Hachey D. Rearrangement of Linalool, Geraniol, and Nerol and Their Derivatives. *J Org Chem.* 1986;51(8):1310-6.
20. Vernon CA. The mechanisms of hydrolysis of glycosides and their relevance to enzyme-catalysed reactions. *Proc R Soc Lond B Biol Sci.* 1967;167(1009):389-401.

Genetic bases of fruity notes (fresh and dried) of the Nacional cocoa variety

KELLY COLONGES^{1,2,3}, Juan-Carlos Jimenez⁴, Alejandra Saltos⁴, Edward Seguin⁵, Rey Gastón Loor Solorzano⁴, Olivier Fouet¹, Xavier Argout¹, Sophie Assemat^{2,3}, Fabrice Davrieux^{2,3}, Eduardo Morillo⁴, Renaud Boulanger^{2,3}, Emile Cros^{2,3}, Claire Lanaud¹

¹ CIRAD, UMR AGAP, F-34398 Montpellier, France. AGAP, Univ Montpellier, CIRAD, INRAE, Institut Agro, Montpellier, France. Kelly.colonges@cirad.fr

² CIRAD, UMR QUALISUD, Montpellier, France. QualiSud, Univ Montpellier, CIRAD, Montpellier SupAgro, Univ Avignon, Univ Réunion, Montpellier, France.

³ Qualisud, Univ Montpellier, Avignon Université, Cirad, Institut Agro, IRD, Université de La Réunion, Montpellier, France.

⁴ Instituto Nacional de Investigación Agropecuarias, INIAP, Ecuador

⁵ Guittard, United-States

Abstract

Theobroma cacao is the only source of cocoa. Cocoa is classified into two types of products: bulk cocoa and fine flavour cocoa. Contrary to bulk cocoa, fine aromatic cocoa is characterized by its floral and fruity aromas [1]. In order to understand the genetic determinism of the formation of these aromas in cocoa beans, a genetic study using the Genetic Wide Association Study (GWAS) method was undertaken. It was carried out on 158 clones belonging to a population of Nacional tree type cultivated in Ecuador, whose volatile compound concentrations and sensory profiles were characterized for its diversity. This study revealed areas of correlation between, on the one hand, the genetic diversity of this population, revealed by molecular marker alleles and the volatile compounds detected in the different clones, and on the other hand, between this same genetic diversity and their sensory profiles. These correlation zones, also called associations, are therefore linked to one of these traits, but also in some cases to both types of traits. Thanks to these associations, which correspond to a restricted area of the cocoa genome, and the knowledge of its complete sequence [2], candidate genes have been brought to light. Some of them are known and identified in biosynthesis pathways of volatile compounds, which are themselves known to have a fruity note. In a preliminary study, a difference in the expression of these genes was identified between four genotypes (two floral and two fruity genotypes) during different stages of development and fermentation of the beans. The results showed that the candidate genes tended to be activated during fermentation and not during the maturation stages of the pods.

Keywords: cocoa, fruity aroma, genetics

Introduction

There are two types of cocoa: "Standard or bulk" cocoa, which has a strong cocoa taste, and aromatic fine cocoa, which is characterised by floral and fruity notes [1]. The Nacional variety of cocoa is classified as a fine variety, characterised by floral and spicy notes [3] known as the "ARRIBA" flavour. At present, the trees grown as Nacional (called Nacional modern in this study) are the result of several generations of crosses between the ancestral Nacional and Trinitarios (themselves hybrids between the Criollo and Amelonado varieties)[4]. Criollo is also a fine aromatic cocoa variety characterised by fruity notes [5]. While Amelonado is known for its strong cocoa aroma. The floral aroma of Nacional has been studied and two main biosynthetic pathways have been identified as responsible for this aroma: the terpene biosynthetic pathway and the L-phenylalanine degradation pathway [6, 7]. In this study, part of the deciphering of the fruity flavour in cocoa from trees of the Nacional modern variety will be presented. A GWAS (Genome Wide Association Study) was conducted to find out which areas of the genome are responsible for this fruity flavour. The GWAS study was carried out using phenotyping data including the determination of volatile compounds related to the fruity taste as well as sensory analyses. To further investigate the genomic determinants of the fruity aroma of Nacional modern, candidate genes in the biosynthetic pathways of the identified fruity compounds were searched for in the identified association areas.

Experimental

Plant material

The plant material used for these experiments was composed of a collection of 151 cocoa trees from Ecuador conserved in the Pichilingue experimental station of the "Instituto Nacional de Investigaciones Agropecuarias" (INIAP) and the "Colección de Cacao de Aroma Tenguel" (CCAT) of Tenguel. This population represents the Nacional variety currently grown in Ecuador and has been described by Loor *et al* [8].

Biochemical analysis

Cocoa beans samples were all fermented and dried with the same method and in the same place of Pichilingue. A part of cocoa beans samples was also roasted. Volatile compounds analysis was carried out on dried fermented beans and roasted beans. The SPME extraction fibre and GC/MS analysis were conducted according to the conditions described by Assi Clair *et al* [9] with Agilent 6890N gas chromatography-mass spectrometer (GC-MS) equipped with a Hewlett Packard capillary column DBWAX, 60 m length \times 0.25 mm internal diameter \times 0.25 μ m film thickness (Palo Alto, CA, USA).

Sensory analysis

146 individuals were characterized by sensory analyses based on blind tastings carried out on 3 repetitions per sample. The tastings were carried out on cocoa liquor. Thirteen fruity notes were judged with a score ranging from zero (no fruity notes detected) to ten. We used the average of the three replicates for the phenotype used to carry out GWAS.

Genetic analysis

GWAS was performed with SNP and SSR markers associated with biochemical (146 accessions \times 5195 markers) and sensory (144 accessions \times 5195 markers) traits using TASSEL v5. Two models were used: mixed linear model (MLM) and a fixed effect model (GLM). In both cases, a structure matrix was determined by running a PCA. Candidate genes were identified through association zones and their annotated function in the cocoa genome.

Expression analysis

The expression of four genes (two coding for alpha-beta hydrolases, one for carboxylesterase and one for GDSL esterase/lipase) was studied during pod ripening at 18, 20 and 22 weeks of development as well as 24 hours after the start of fermentation. These studies were conducted on four different clones, known for their fine flavour, characterised by a fruity and floral aroma: EET103, EET19, EET575 and EET62.

Results and discussion

GWAS analyses are used to statistically determine which areas of the genome are linked to the traits being tested.

Sensory traits

Thanks to this genetic analysis method, 22 areas of associations related to sensory data were detected. Of the 13 fruit sensory categories, associations were detected for 3 of them: "Fruity-Dark Tree Fruit", "Fruity-Dried fruit" and "Fruity-Berries". The strongest areas of association were detected for the note "Fruity-Dark Tree Fruit" on chromosome 1 (Figure 1).

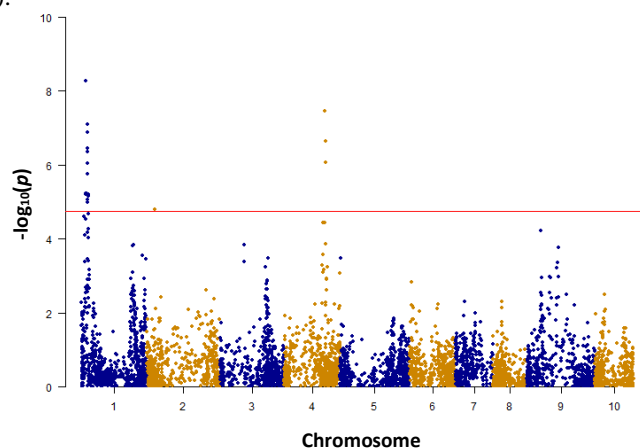


Figure 1: Manhattan plot representing all markers tested along the 10 cocoa chromosomes for associations with the Fruity Dark tree fruit note.

Biochemical traits

The GWAS analysis allowed the detection of 480 areas of associations related to the concentrations of volatile compounds. These association zones were detected in relation to 3 acids, 12 alcohols, 7 aldehydes, 22 esters, 8 ketones, 1 lactone, 11 pyrazines and 5 terpenes. According to these results, five biosynthetic pathways appear to

play a role in the synthesis of fruity aroma in cocoa: the monoterpene biosynthetic pathway, the L-phenylalanine degradation pathway, the simple sugar degradation pathway, the fatty acid degradation pathway and the pyrazine biosynthetic pathway. The study of associations related to the monoterpene biosynthetic pathway and the L-phenylalanine degradation pathway have been extensively studied previously [7].

Areas of common associations between sensory and biochemical traits were first sought. These areas have a higher probability to explain the fruity aroma of cocoa. Six co-locations between associations related to pyrazines and those related to sensory traits were identified. Four of them are present on chromosome 1, one on chromosome 4 and one on chromosome 10. Eight areas of co-locations between associations related to sensory traits and compounds involved in the degradation pathways of fatty acids and simple sugars were observed: four co-locations are on chromosome 1, two on chromosome 2, one on chromosome 4 and one on chromosome 10.

Candidate genes

In all the areas of association detected, candidate genes were sought. A first search was carried out by looking for genes coding for proteins with essential enzymatic functions for the different biosynthesis pathways identified.

In cocoa, it is well known that pyrazines are synthesized through the Maillard reaction [10]. It is a set of chemical reactions that take place during the process. In cocoa processing, the Maillard reaction occurs mainly during roasting, but it can also occur during drying. The Maillard reaction allows the synthesis of pyrazine by combining free amino acids and reducing sugars. In this study, we therefore looked for genes coding for enzymes involved in protein degradation or in the synthesis of reducing sugars.

In the 277 association areas related to pyrazines, 213 candidate genes involved in the production of precursors of the Maillard reaction were identified. These genes have mainly peptidase or protease functions.

Preliminary expression studies of some of these genes were conducted. The expression of two genes coding for alpha-beta hydrolases was studied. The two genotypes EET103 and EET19 express alpha-beta hydrolase 1 equally or more during fermentation. The EET575 genotype expresses it more at 18 weeks of maturity and the EET62 genotype expresses it more at 18 and 20 weeks of maturity. Alpha-beta hydrolase 2 is most expressed at 20 weeks of pod development for genotype EET103, at 22 weeks of development for genotypes EET19 and EET575, at 18 and 20 weeks of development for genotype EET62 (Figure 2). Some genotypes appear to express more alpha-beta hydrolase 1 during fermentation than during pod maturity. It is at this time that alpha-beta hydrolases would break down proteins into amino acids through their peptidase functions. Cocoa beans would then be richer in amino acids, which would allow more pyrazine synthesis through the Maillard reaction during drying and roasting. Reineccius (2006) observed a higher concentration of pyrazine in well-fermented beans [11]. The expression of alpha-beta hydrolase 2 seems to be more intense during pod maturation than during the fermentation. Pod ripening also seems to play a role in aroma synthesis.

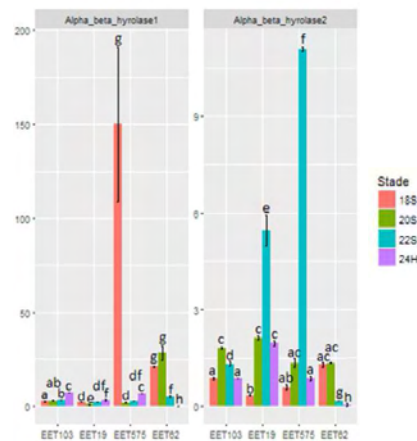


Figure 2: Histogram of the expression profile of the genes coding for Alpha-Beta Hydrolase at different stages of bean maturity and during fermentation. Histograms with the same letter are not significantly different at the 1% threshold.

Acids, alcohols, ketones and esters are mainly synthesised as a result of the degradation of fatty acids and/or simple sugars. Candidate genes encoding enzymes involved in these degradation pathways were searched for in all association zones of all volatile compounds.

In the 480 association areas related to compounds involved in simple sugars degradation, 125 candidate genes were identified. These genes have mainly hydrolase or esterase functions. In the association areas related to compounds involved in fatty acid degradation, 217 candidate genes were identified. These genes have mainly lipase or esterase functions. There are common candidate genes between these simple sugar degradation pathway and fatty acid degradation pathway.

Preliminary expression studies of some of these genes were conducted. The first one coding for a carboxylesterase and the second for a GDSL esterase/lipase. The carboxylesterase gene is more expressed during fermentation in genotypes EET19 and EET575, more expressed after 20 weeks of seed development in genotype EET103 and similarly expressed at 18 and 22 weeks of seed development in genotype EET62. The GDSL esterase lipase gene is more expressed during fermentation in all genotypes except EET103. In EET103, it is more expressed at 20 weeks of development (Figure 3).

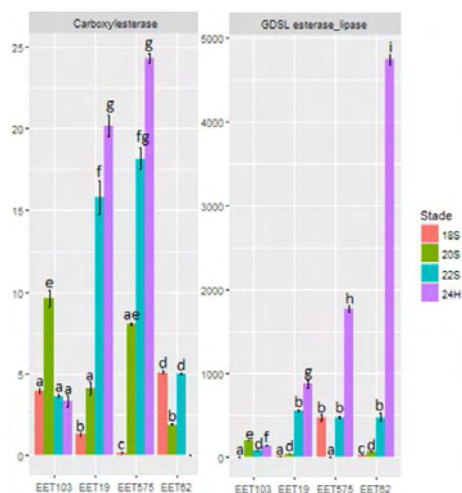


Figure 3: Histogram of the expression profile of the genes coding for Carboxylesterase and GDSL esterase/lipase at different stages of bean maturity and during fermentation. Histograms with the same letter are not significantly different at the 1% threshold.

In most cases, the genes seem to be more strongly expressed during fermentation. During this processing stage, cocoa beans are exposed to fermenting micro-organisms. These exponentially growing micro-organisms are detected by the beans, which then set up a defence system. A large number of volatile compounds have been identified as being used by plants to defend themselves against micro-organism attacks [12–14].

Of the 67 volatile compounds, association zones could not be detected for 13 of them. These compounds belong to different chemical families (two acids, three alcohols, one aldehyde, five esters and two ketones). As most of these different compounds do not seem to be genetically related to the cocoa trees in this population, it is very likely that they were synthesised by the microorganisms present during the fermentation [15–17]. In addition, it is possible that the microorganisms present during fermentation synthesise some intermediate compounds. The biosynthesis of these compounds could be a synergy between the enzymatic actions of the fermenting microorganisms and the cocoa tree.

The Nacional fruity aroma could also include compounds belonging to the L-phenylalanine degradation pathway, such as benzaldehyde, benzyl alcohol and 1-phenylethyl acetate. Associations have been detected for these three compounds and reported in a previous study [7]. These compounds are also precursors of compounds known to have floral tastes. The enzymatic activity allowing the degradation of benzoic acid into benzaldehyde or benzyl alcohol is one of the keys to the increased presence of compounds with fruity tastes (Figure 4).

Conclusion

The study of aroma determinism is complex. Flavours depend on different factors such as genetics, growing environment and processing. In this study, the objective was to investigate the genetic part of the fruity notes of cocoa (fresh and dry). Using GWAS, we were able to begin to determine how the fruit notes were synthesised by the cocoa beans. Two types of fruity notes were observed: fresh fruity notes, which are mainly, composed of esters and terpene compounds. In this case, three metabolic pathways seem to be involved: the degradation of fatty acids, the degradation of simple sugars and the monoterpene biosynthetic pathway. Similarly, dried fruit aromas were observed, mainly composed of pyrazines. Pyrazines were synthesised by the Maillard reaction during the drying or roasting process. The concentration of pyrazine depends on the synthesis of the Maillard precursors: amino acids and reducing sugars.

A large number of genes potentially involved in the synthesis of fruity aromas have been identified. Preliminary study of the expression of candidate genes shows that the synthesis of enzymes responsible for the production of certain volatile compounds takes place during bean development but also during fermentation, before the death of

the embryo. The hypothesis is that cocoa beans detect fermenting microorganisms and trigger defence mechanisms.

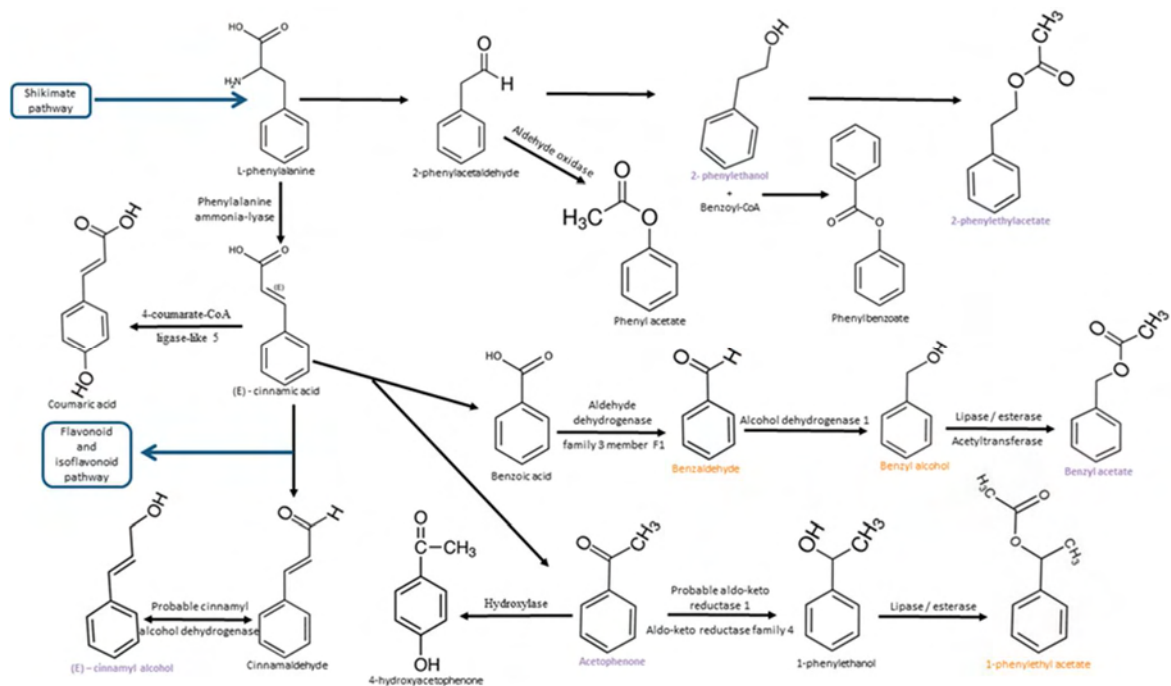


Figure 4: Degradation pathway of L-phenylalanine identified in cocoa. Compounds known to have a floral taste are noted in purple and compounds known to have a fruity taste are noted in orange.

The exact role of these candidate genes in this synthesis is still difficult to determine. A study of the enzymatic activity of the different enzymes encoded by these candidate genes could complement this study. This could also help to identify more precisely the roles of each enzyme.

A complementary analysis, made by Gas-Chromatography-Olfactometry (GCO), comparing fruity, floral and standard genotypes of cocoa, would allow identifying key compounds of the fruity aroma of cocoa.

References

1. Sukha DA, Butler DR, Umaharan P, Boulton E. The use of an optimised organoleptic assessment protocol to describe and quantify different flavour attributes of cocoa liquors made from Ghana and Trinitario beans. *Eur Food Res Technol.* 2008;226(3):405-13.
2. Argout X, Martin G, Droc G, Fouet O, Labadie K, Rivals E, et al. The cacao Criollo genome v2.0: an improved version of the genome for genetic and functional genomic studies. *BMC Genomics.* 2017;18:730.
3. Luna F, Cruzillat D, Cirou L, Bucheli P. Chemical composition and flavor of Ecuadorian cocoa liquor. *J Agric Food Chem.* 2002;50(12):3527-32.
4. Llorca RG, Risterucci AM, Courtois B, Fouet O, Jeanneau M, Rosenquist E, et al. Tracing the native ancestors of the modern *Theobroma cacao* L. population in Ecuador. *Tree Genet Genomes.* 2009;5(3):421-33.
5. Lachenaud P, Motamayor JC. The Criollo cacao tree (*Theobroma cacao* L.): a review. *Genet Resour Crop Evol.* 2017;64(8):1807-20.
6. Ziegler G. Linalool contents as characteristic of some flavor grade cocoas. *Z Lebensm-Unters Forsch.* 1990;191(4-5):306-9.
7. Colonges K, Jimenez JC, Saltos A, Seguine E, Solorzano RL, Fouet O, et al. Two main biosynthesis pathways involved in the synthesis of the floral aroma of the Nacional cocoa variety. *Front Plant Sci.* 2021; Submitted.
8. Llorca S. RG. Contribution à l'étude de la domestication de la variété de cacaoyer Nacional d'Equateur : recherche de la variété native et de ses ancêtres sauvages. INIAP Archivo Historico; 2007. 406 p.
9. Assi-Clair BJ, Koné MK, Kouamé K, Lahon MC, Berthiot L, Durand N, et al. Effect of aroma potential of *Saccharomyces cerevisiae* fermentation on the volatile profile of raw cocoa and sensory attributes of chocolate produced thereof. *Eur Food Res Technol.* 2019;245(7):1459-71.
10. Afoakwa EO, Paterson A, Fowler M, Ryan A. Flavor Formation and Character in Cocoa and Chocolate: A Critical Review. *Crit Rev Food Sci Nutr.* 2008;48(9):840-57.

11. Reineccius GA. Flavor Chemistry and Technology [Internet]. CRC Press; 2006 [cited 19 March 2021]. Available at: <https://www.taylorfrancis.com/books/flavor-chemistry-technology-gary-reineccius/10.1201/9780203485347>.
12. Pichersky E, Lewinsohn E, Croteau R. Purification and Characterization of S-Linalool Synthase, an Enzyme Involved in the Production of Floral Scent in *Clarkia breweri*. *Arch Biochem Biophys*. 1995;316(2):803-7.
13. Parent GJ, Giguère I, Mageroy M, Bohlmann J, MacKay JJ. Evolution of the biosynthesis of two hydroxyacetophenones in plants. *Plant Cell Environ*. 2018;41(3):620-9.
14. Palmqvist E, Almeida JS, Hahn-Hägerdal B. Influence of furfural on anaerobic glycolytic kinetics of *Saccharomyces cerevisiae* in batch culture. *Biotechnol Bioeng*. 1999;62(4):447-54.
15. Soles RM, Ough CS, Kunkee RE. Ester Concentration Differences in Wine Fermented by Various Species and Strains of Yeasts. *Am J Enol Vitic*. 1982;33(2):94-8.
16. Abbas CA. Production of Antioxidants, Aromas, Colours, Flavours, and Vitamins by Yeasts. In: *Yeasts in Food and Beverages* [Internet]. Springer, Berlin, Heidelberg; 2006. p. 285-334. Available at: https://link.springer.com/chapter/10.1007/978-3-540-28398-0_10.
17. Ho VTT, Zhao J, Fleet G. Yeasts are essential for cocoa bean fermentation. *Int J Food Microbiol*. 2014;174:72-87.

Generation of bitter blocker Maillard-dietary phenolic compound reaction products

ADELINE BONNEAU, Edison Tello and Devin G. Peterson

Flavor Research and Education Center (FREC), Ohio State University (OSU), Columbus, Ohio, USA

Abstract

Bitterness is a well-known aversive taste that can negatively impact consumer's acceptance. The aim of this study was to investigate the generation of bitter blocker compounds derived from the bitter dietary phenolic compound epigallocatechin gallate (EGCg) through the Maillard reaction. Reaction models were investigated using different reaction variables (temperature, time, moisture, nature of sugars and amino acids, and reactants molar ratio) to obtain different phenolic-Maillard reaction products. Isotope labelling experiments using carbon labelled sugars were performed to identify the reaction products and compare the different reaction models. The main resulting reaction products were further isolated and purified for sensory analysis and accurate identification purposes to discover bitter blockers. A total of fourteen isolated reaction products were identified by accurate mass spectrometry analysis (HRMS) and nuclear magnetic resonance (NMR). Those reaction products were evaluated by sensory analysis through 2-AFC test comparisons and bitterness intensity ratings to determine their bitterness modulation properties. Two reaction products were found to significantly decrease the bitterness perception of caffeine bitter samples. The optimised Maillard reaction conditions to produce those bitter blockers were further described to provide new knowledge and insight regarding the generation of bitter blocker compounds during food processing.

Keywords: Bitterness, Bitterness Modulation, Maillard Reaction, Reaction Products, Bitter Blocker Compounds.

Introduction

Despite health recommendations, many healthy and natural food products (vegetables, whole cereals, vegetable proteins, etc.), as well as functional foods (enriched in vitamins, phytonutrients, fish oils, etc.), are often poorly consumed due to their bitter attributes [1, 2]. The reduction of bitterness by the addition of salts, sweeteners, strong flavours, or a debittering process remains challenging for the food industry because these methods affect the food quality and remove health-promoting bitter compounds [2, 3]. Thus, the advancement of food technology aimed to mask bitterness perception is needed.

This work focused on a food-based strategy by using dietary phenolic compounds and Maillard reaction models to generate reaction products able to modulate the bitterness perception and act as bitter blockers. Bitter compounds and bitter blocker compounds have been reported in the literature to possess similar chemical structures that are competitive towards the different bitter receptors hTAS2Rs [4]. Thus, a strategy to generate bitter blocker compounds would be designed by the derivatisation of original bitter compounds into bitter blocker structures. In that way, the dietary phenolic compound epigallocatechin gallate (EGCg) was chosen as a potential bitter blocker compound precursor due to its low bitterness threshold in sensory analysis [5] and its activity toward the human bitter receptors hTAS2Rs [6, 7]. The Maillard reaction, which is accelerated during thermal food processing and has been previously reported to generate phenolic-reaction products [8], was chosen to derivatise the phenolic EGCg into potential bitter blocker products. Maillard reaction models were investigated using different reaction variables (temperature, time, moisture, nature of sugars and amino acids, and reactants molar ratio) with the phenolic EGCg. The main resulting EGCg-Maillard reaction products highlighted by isotope labelling experiments were further evaluated through sensory analyses to discover bitter blocker compounds.

Experimental

Maillard reaction models were performed using the phenolic compound epigallocatechin gallate (EGCg) and different reaction variables with different sugars (glucose, galactose, fructose), amino acids (glycine, alanine, proline, cysteine, tyrosine, serine, phenylalanine, asparagine), reactants molar ratios EGCg:amino acid:sugar (equimolar (1:1:1), or counterbalanced (1:1:2)), reaction temperatures (80-200°C), reaction times (5-20 min), and moistures (8-60%). Meanwhile, isotope labelling experiments were also performed using labelled sugars (e.g. mixture of D-glucose/[U-¹³C₆]-D-glucose) to identify different reaction products and compare the Maillard reaction model mixtures. The main reaction products obtained were further isolated and purified by sample preparation (ultrafiltration, solid-phase extraction), and multidimensional liquid chromatography-mass spectrometry preparative fractionation (Prep-LC/MS). For sensory analysis purposes, the Maillard reactions and purification steps were performed with food-grade reactants and solvents with high purity. All experimental steps were followed by UPLC-QToF-HRMS analysis to compare the Maillard reaction models, and to determine the accurate

chemical formula as well as the purity of each reaction product. Mono- and bi-dimensional Nuclear Magnetic Resonance (NMR) experiments were performed to obtain the accurate chemical structure of each isolated reaction product.

To evaluate the bitterness modulation properties of the isolated reaction products, eight trained sensory panellists evaluated bitter samples using a series of 2-alternative forced choice (2-AFC) difference tests followed by bitterness intensity ratings (IRB protocol 2020B0310). Each pair of samples was prepared using a bitter control of caffeine at 1.36 mM vs. a bitter mixture of caffeine at 1.36 mM with the addition of one reaction product (or the phenolic precursor EGCg) at 0.136 mM to reach a molar ratio of 1:10 against caffeine. 3 mL of each sample was presented in 1-oz black cups labelled with 3-digit blinding codes. While wearing nose clips, the panellists were asked to select the bitterest sample, and then rate the bitterness intensity perceived in each sample using a 10-point caffeine bitterness scale. Samples were presented in randomised order and were evaluated in triplicate over three independent sessions, for a total of 24 evaluation points per sample.

The most relevant reaction products which showed bitterness modulation activities were further tracked in Maillard reaction models by response surface methodology (RSM) to highlight the optimised reaction conditions to enhance the generation of those specific compounds. The RSM analysis was conducted with the MINITAB 18 Statistical Software.

Results and discussion

Maillard reaction models were performed using the phenolic EGCg under different reaction conditions consisting of various sugars and amino acids, and alteration of the reaction time, temperature, moisture content, and ratio of reactants (Figure 1). The isotope labelling experiments allowed the identification of the reaction products (RP) resulting in the condensation of the initial phenolic structure EGCg with labelled and unlabelled sugars ($^{13}\text{C}/^{12}\text{C}$). The reaction products observed in UPLC-QToF-MS analysis showed one or two sugar adducts on the EGCg phenolic structure resulting in numerous isotopomers (Figure 2). The main isomer reaction products observed (based on peak area) were further isolated and purified by multidimensional Prep-LC/MS fractionation. Through the different Maillard reaction models a total of fourteen phenolic-Maillard reaction products were obtained and their accurate chemical formula and structures were elucidated using high-resolution mass spectrometry analysis (HRMS) and NMR experiments. The results showed that C-sugar adducts in position 6 or/and 8 of the phenolic structure, in alpha or beta configuration, as well as in pyranose or furanose or spiro configuration could explain the large diversity of the isomer reaction products obtained.

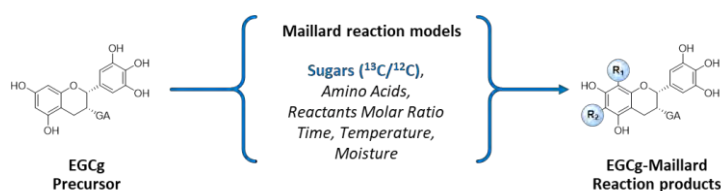


Figure 1: Derivatisation of the phenolic EGCg into EGCg-Maillard reaction products.

The fourteen isolated compounds were further evaluated by sensory analysis with eight trained panellists to determine their potential bitterness modulation activities against caffeine. Based on the 2AFC comparison tests and bitterness intensity rating tests, two of the fourteen reaction products RP10 (ESI-, [M-H]⁻; m/z_781) and RP4 (ESI-, [M-H]⁻; m/z_763) were able to significantly decrease the bitterness intensity of the caffeine solutions (P-values of 0.025 and 0.066 respectively). Further investigation of the reaction product structures indicated the C-sugar adducts to the original phenolic structure influenced the sensory properties of the reaction products, indicating the chemical motifs were critical to obtain the bitter blocker structure.

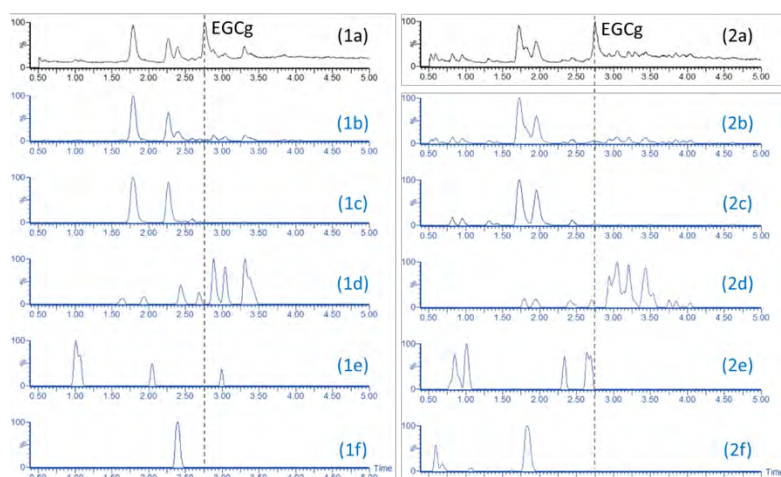


Figure 2: UPLC-QToF-MS analysis (ESI-) of EGCg-Maillard reaction models with the labelled sugars glucose (1a-f, $^{13}\text{C}_6/^{12}\text{C}_6$ -D-glucose) and galactose (2a-f, $^{13}\text{C}_6/^{12}\text{C}_6$ -D-galactose): extraction of the overall isotomers (1b-2b); isotomers with one sugar adduct $m/z_{619/625}$ (1c-2c) and $m/z_{601/607}$ (1d-2d); isotomers with two sugar adducts $m/z_{763/769/775}$ (1e-2e) and $m/z_{781/787/793}$ (1f-2f).

Finally, response surface methodology (RSM) analyses were performed to determine the reaction conditions that generated the highest yield of the bitter blocker RP10 and RP4. The temperature, the ratio of sugars, and the moisture content were the most significant parameters (P -values < 0.05 , $R^2 = 0.93$) to enhance the production of those compounds (Figure 3). Thus, the reported significant impact of the Maillard reaction models suggests strategies to optimise the production in-situ of bitter blockers in foodstuffs during food processing.

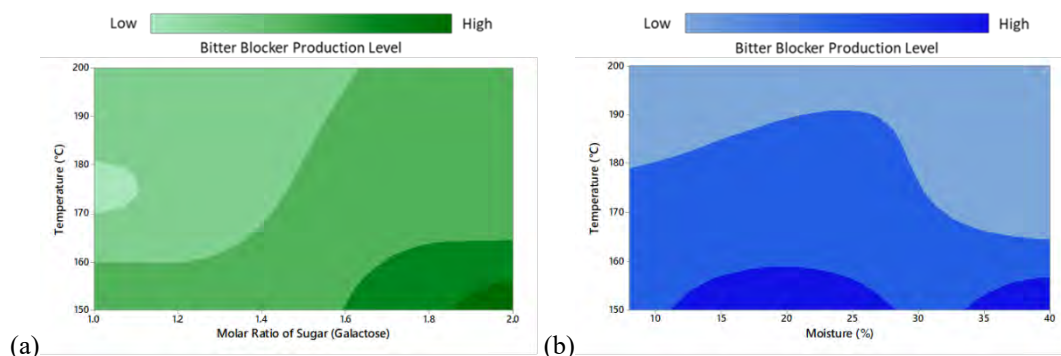


Figure 3: Response surface analysis of the production of the bitter blocker RP10 through Maillard reaction models: Contour Plot Temperature vs. Sugar Ratio (a), Contour Plot Temperature vs. Moisture (b).

Conclusion

The bitter phenolic compound EGCg was derivatised through Maillard reaction models and generated different reaction products which were investigated for bitter blocker activity. Two reaction products (RP10 and RP4) were found to decrease the bitterness of caffeine solutions and acted as bitter blocker compounds. The choice of the bitter blocker precursor EGCg, as well as the Maillard reaction models performed, appeared to be decisive key points in the generation of bitter blocker compounds. Overall this study provided new knowledge and insight regarding the chemistry and fate of bitter phenolic compounds, indicating they can be transformed into bitter blockers through reactions that occurred during food processing, as well as provided improved understanding of the possible chemical motifs critical for a bitter blocker activity.

References

1. Drownowski A, Gomez-Carneros C. Bitter taste, phytonutrients, and the consumer: A review. *Am J Clin Nutr.* 2000;72(6):1424–1435.
2. Ley JP. Masking Bitter Taste by Molecules. *Chemosens Percept.* 2008;1(1):58–77.
3. Gaudette NJ, Pickering GJ. Modifying Bitterness in Functional Food Systems. *Crit Rev Food Sci Nutr.* 2013;53(5):464–481.

4. Roland WSU, Gouka RJ, Gruppen H, Driesse M, van Buren L, Smit G, et al. 6-Methoxyflavanones as Bitter Taste Receptor Blockers for hTAS2R39. *PLoS One*. 2014;9(4):e94451.
5. Soares S, Kohl S, Thalmann S, Mateus N, Meyerhof W, De Freitas V. Different phenolic compounds activate distinct human bitter taste receptors. *J Agric Food Chem*. 2013;61(7):1525–1533.
6. Roland WSU, Van Buren L, Gruppen H, Driesse M, Gouka RJ, Smit G, et al. Bitter taste receptor activation by flavonoids and isoflavonoids: Modeled structural requirements for activation of hTAS2R14 and hTAS2R39. *J Agric Food Chem*. 2013;61(44):10454–10466.
7. Scharbert S, Hofmann T. Molecular definition of black tea taste by means of quantitative studies, taste reconstitution, and omission experiments. *J Agric Food Chem*. 2005;53(13):5377–5384.
8. Zhang L, Xia Y, Peterson DG. Identification of bitter modulating maillard-catechin reaction products. *J Agric Food Chem*. 2014;62(33):8470–8477.

Occurrence of (suspected) genotoxic flavouring substances in Belgian alcohol-free beers

ALEXANDRE DUSART¹, Birgit Mertens¹, Els Van Hoeck¹, Margaux Simon²,
Séverine Gosciny¹ and Sonia Collin²

¹ Department of Chemical and Physical Health Risks, Sciensano, Rue Juliette Wytsman 14, 1050 Ixelles, Belgium, Alexandre.Dusart@sciensano.be

² Unité de Brasserie et des Industries Alimentaires, Louvain Institute of Biomolecular Science and Technology (LIBST), Faculté des Bioingénieurs, Université catholique de Louvain, Croix du Sud 2, Box L7.05.07, 1348 Louvain-la-Neuve, Belgium

Abstract

The regulatory landscape of flavourings is evolving, thereby putting pressure on control laboratories to develop analytical methods for a wide range of compounds in various types of food (including drinks). In order to improve the monitoring of flavouring substances, a versatile and accurate analytical method using the solvent-assisted flavour evaporation (SAFE) technique coupled to gas chromatography-mass spectrometry in selected ion monitoring mode GC-MS (SIM) was developed and validated. Focus was put on authorised flavouring substances requiring specific attention due to a genotoxic concern based on information available in European risks assessment reports. Thirty-seven (suspected) genotoxic flavouring substances were analysed in a selection of ten alcohol-free beers. Five suspected genotoxic compounds (i.e. 1-(2-furyl)propan-2-one, 2-acetylfuran, 2-acetyl-5-methylfuran, 2-acetyl-3,5-dimethylfuran, hex-2-eno-1,4-lactone) as well as two confirmed genotoxic flavouring substances (*p*-mentha-1,8-dien-7-al, pentan-2,4-dione) were identified and quantified among the selected samples. The relatively low concentrations and natural occurrences of the identified compounds suggested that these were not added as such but rather originated from heat-treatments or from plant-based extracts.

Keywords: Flavouring substances, Genotoxicity, SAFE, GC-MS, Alcohol-free beers

Introduction

Nowadays, thousands of chemically defined flavouring substances exist and are added to a wide variety of food and drinks to impart or modify odour and/or taste. In Europe, Regulation (EC) No 1334/2008 lays down the general provisions on the use of flavourings in food. This includes restrictions of use such as maximum levels of certain substances for certain food categories, conditions of use for some source materials, as well as substances which shall not be added as such to food. In parallel, over the past twenty years, the European Food Safety Authority (EFSA) has assessed the risks of flavouring substances. While a few compounds have already been confirmed genotoxic and are prohibited to be added as such to food, others are under evaluation due to genotoxic concern although being authorised on the market. Although different analytical methods for the analysis of flavouring substances already exist, a general lack of analytical methodology in the context of law enforcement was reported in Europe [1]. Here, the solvent-assisted flavour evaporation (SAFE) technique was used and validated for the analysis of multiple (suspected) genotoxic flavouring substances in a selection of Belgian alcohol-free beers.

Experimental

Selection of compounds

According to Regulation (EC) No 1334/2008 (consolidation of 21st of May 2019), 302 compounds were under evaluation. However, as this regulation was not consolidated each time a new EFSA opinion was available, all relevant opinions were reviewed to select only compound for which an evaluation was effectively still pending.

Alcohol-free beer samples

Ten popular commercial Belgian AFBs (A, B, C, D, E, F, G, H, I, J) were selected and analysed. Beers G, H, I and J were specifically selected because of the presence of citrus spp. (citrus, orange, bergamot) in the ingredients, a known source of *p*-mentha-1,8-diene-7-al (perillaldehyde) [2]. Samples were purchased in September 2020 and stored in the dark at 20°C until analysis.

Characterisation of the samples

The beers were characterised by their ethanol content, colour, bitterness and pH following Analytica EBC methods 9.2.6, 9.6, 9.8, 9.35 respectively [3]. Density was also measured using a density meter (DM4500, Anton Paar GmbH, Graz, Austria).

Isolation of the volatiles

Degassed samples (50 mL) were spiked with 150 μ L of 2-acetylthiophene solution (8 mg/L) as internal standard (IST). Samples were then extracted with bidistilled dichloromethane (1 x 75 mL) during 20 min. After centrifugation (20 min at 2264g) of the resulting emulsion, the aqueous phase was discarded and the remaining organic phase was dried over anhydrous sodium sulphate. Non-volatile compounds were then separated by high-vacuum distillation using the SAFE system (Glasblaeserei Bahr, Manching, Germany)[4]. The conditions for the SAFE analyses were: the water bath temperature was set to 40 °C, the pressure was kept below 10⁻³ Pa and the apparatus body was at 30 °C. The distillate was recovered in a liquid nitrogen cooled flask for 15 min distillation, followed by an extraction with distilled water (3 x 25 mL) to remove any residual alcohol. The extract was dried over anhydrous sodium sulphate. To measure absolute recoveries, 25 μ L of decane solution (250 mg/L) was spiked as an external standard (EST) before concentration to 500 μ L in a Kuderna-Danish apparatus at 45 °C. Extracts were stored at -80 °C until analysis by gas chromatography-electron ionisation mass spectrometry.

Gas chromatography - mass spectrometry (GC-MS)

SAFE extracts were analysed with a wall-coated open tubular apolar capillary column (CP-Sil 5 CB, 50 m \times 0.32 mm i.d., 1.2 μ m film thickness) on an Agilent 7890B gas chromatograph. Injections (1 μ L) were carried out at 250 °C in splitless mode. The carrier gas was helium and the pressure was set at 65 kPa. The oven temperature was programmed to rise from 36 °C to 85 °C at 20 °C/min, then to 145 °C at 1 °C/min, and finally to 250 °C (held for 30 min) at 3 °C/min. The column was connected to a single quadrupole mass spectrometer (Agilent 5977B MSD) operating in selected ion monitoring (SIM) mode with electron ionisation at 70 eV. Full-scan (FS) chromatograms (40 – 380 m/z) were also recorded on separate runs for possible qualitative retro-analysis. Data was recorded and analysed with the Agilent OpenLab software (version 2.1).

Quantification of the flavouring substances

Standard addition technique was used to quantify analytes. A mix containing analytical standards in dichloromethane was prepared and used to spike four times the sample (10; 25; 50; 75 μ g/L). The IST (2-acetylthiophene) was spiked in the sample at a constant concentration (24 μ g/L). The concentration of an analyte X in the sample was obtained using the following equation: X concentration (in μ g/L) = IST concentration (in μ g/L) \times (X area / IST area) \times (IST response coefficient / X response coefficient) \times (IST absolute recovery / X absolute recovery).

Because standard addition was a time consuming experiment, it was performed on three different samples. For each compound, standard addition slopes values were statistically compared (t-test, 95% confidence) to determine if matrix effects were similar between samples.

Validation of the method

The developed method was validated in house in terms of linearity, matrix effects, intra- and interday repeatability, limit of detection (LOD) and quantification (LOQ), selectivity and apparent recoveries. "Beer A" was used as the matrix for validation. The spiked levels were chosen in accordance with the expected flavouring substances concentrations in the targeted matrix. Coefficient of variation on the intraday repeatability ($CV_{intra-r}$) and interday repeatability ($CV_{inter-r}$) were evaluated using Horwitz statistical analysis, based on triplicate experiments, performed three times on different days. The measurement of uncertainties (MU) was assessed through $CV_{inter-r}$ [5].

Results and discussion

Selection of compounds

Recent EFSA opinions (up to June 2020), showed that only 53 out of 302 flavouring substances were still under evaluation due to a genotoxic concern. For these 53 substances, it was verified whether they could be analysed by GC-MS by collecting additional information on commercial availability of the analytical standards, retention time and mass fragmentation. This revealed that 34 substances could be analysed by GC-MS. In addition, 3 confirmed genotoxic flavouring substances that were no longer authorised to be added as such to food in Europe were also included in this study: *p*-mentha-1,8-diene-7-al (perillaldehyde), pentan-2,4-dione and 3-acetyl-2,5-dimethylthiophene. In total, 37 compounds were included in this method:

2-ethyl-5-methylfuran (1); 2-octylfuran (2); 1-(2-furyl)-propan-2-one (3); for 2-acetylfuran (4); 2-pentylfuran (5); 3-acetyl-2,5-dimethylfuran (6); 2-heptylfuran (7); 2-hexanoylfuran (8); 2-acetyl-5-methylfuran (9); 2-acetyl-3,5-dimethylfuran (10); 2-butylfuran (11); 2-butyrylfuran (12); 1-(2-furyl)butan-3-one (13); 3-methyl-2(3-methylbut-2-enyl)furan (14); 2-pentanoylfuran (15); 2-(sec-butyl)-4,5-dimethyl-3-thiazoline (16); 4,5-dimethyl-2-ethyl-3-thiazoline (17); 4,5-dimethyl-2-isobutyl-3-thiazoline (18); 4-methyl-5-vinylthiazole (19); 1-(4-methoxyphenyl)pent-1-en-3-one (20); vanillylidene acetone (21); 1-(4-methoxyphenyl)-4-methylpent-1-en-3-one (22); 2-phenylcrotonaldehyde (23); 5-methyl-2-phenylhex-2-enal (24); 4-methyl-2-phenylpent-2-enal (25); 2-phenylpent-2-enal (26); 5,6,7,7a-tetrahydro-3,6-dimethylbenzofuran-2(4H)-one (27); hex-2-eno-1,4-lactone (28); 3-(2-furyl)acrylaldehyde (29); 4-(2-Furyl)but-3-en-2-one (30); 3-(2-furyl)-2-methylprop-2-enal (31); 3-(5-methyl-2-furyl)prop-2-enal (32); *delta*-damascone (33); *alpha*-damascone (34); *p*-mentha-1,8dien-7-al (35); pentan-2,4-dione (36) and 3-acetyl-2,5-dimethylthiophene (37).

Method development

Liquid samples like alcohol-free beers could be extracted with an organic solvent before or after the SAFE [4, 6-7]. Both approaches were tested and compared. Absolute recoveries were above 80% for most of the compounds when performing the SAFE directly on beers. However, some substances were not recovered at all including 2-pentylfuran (5), 2-heptylfuran (7), 2-butylfuran (11) and thiazolines 16, 17, 18. Instead, when the samples were extracted with dichloromethane before the SAFE, similar recoveries were obtained, but substances that were not extracted with the previous approach, were also extracted this time. In addition, the vacuum distillation of the organic extract was much faster than that carried out directly on aqueous samples (15 min vs 60 min). Nonetheless, recoveries of ethone (20) and vanillylidene acetone (21), two very apolar compounds, remained low.

Validation

External calibration curves at 6 concentration levels (i.e. 0.25; 2.5; 5; 7.5; 10 and 15 mg/L) were submitted a Mandel's Fitting test ($R^2 > 0.99$) and were linear. Standard addition inherently took into account matrix effects. Performed on three different samples (A, B, D), it showed similar relative standard addition slopes for most of the compounds (at 95% confidence level). This indicated that matrix effects were similar between samples so that the relative standard addition slopes from a reference sample (A) could be used for the other AFBs. However, substances 5,7,11 and 16,17,18 showed non-linear responses. No clear explanation could be found on their difficulty of analysis. Additionally, despite linear responses of compounds 20 and 21, relative standard addition slopes differed from sample-to-sample. These compounds could therefore only be semi-quantitatively analysed.

For each compound, the peak from the smallest standard addition spike was used to determine the limits of detection (LOD) with $S/N = 3$, and limits of quantification (LOQ) with $S/N=10$. Low LOD and LOQ were obtained, in average 0.01 $\mu\text{g/L}$ and 0.05 $\mu\text{g/L}$.

Coefficients of variation on intra- and interday repeatability were respectively below 10 % and 13%. The measurement of uncertainties was comprised between 6-26%. Apparent recoveries, comprised between 101-123%, were calculated based on spiked samples of triplicate analysis performed three times on different days.

Sample analysis

Among the ten Belgian AFBs, 5 different suspected genotoxic flavouring substances were identified as well as 2 genotoxic flavouring substances (Table 1). Unsurprisingly for products containing heat-treated ingredients, malts here, furan-substituted compounds were identified. 2-Acetylfuran content did not significantly differ between dealcoholized beer and beers brewed with special yeasts ($p = 0.44$), and was always much below its 10 mg/L odour threshold[2]. No correlation was found between colour and 2-acetylfuran content.

Table 1: Concentrations ($\mu\text{g/L}$) of suspected and confirmed* genotoxic flavouring substances among 10 Belgian alcohol-free beers.

N°	Compound	A	B	C	D	E	F	G	H	I	J
3	1-(2-Furyl)-propan-2-one	–	–	–	–	n.q.	–	–	–	–	n.q.
4	2-Acetylfuran	8.1 ± 1.4	5.7 ± 1.0	7.6 ± 1.4	6.6 ± 1.2	23.3 ± 4.2	6.8 ± 1.2	8.1 ± 1.4	6.4 ± 1.1	9.1 ± 1.6	8.0 ± 1.4
9	2-Acetyl-5-methylfuran	–	–	–	–	0.9 \pm 0.1	–	–	–	–	–
10	2-Acetyl-3,5-dimethylfuran	0.08 \pm 0.01 ^a	–	–	–	–	–	–	–	–	–
28	Hex-2-eno-1,4-lactone	–	–	1.3 ± 0.2	–	5.6 ± 0.7	1.3 ± 0.2	2.3 ± 0.3	–	–	2.5 ± 0.3
35	<i>p</i> -Mentha-1,8-dien-7-al*	–	–	–	–	–	–	45.4 \pm 6.7	23.2 \pm 3.4	–	–
36	Pentan-2,4-dione*	–	–	–	–	6.3 ± 1.3	–	–	–	1.3 ± 0.3	2.4 ± 0.5

– = not detected (mean LOD = 0.01 $\mu\text{g/L}$); n.q. = not quantifiable (mean LOQ = 0.05 $\mu\text{g/L}$); ^a= LOQ of compound 10 is 0.02 $\mu\text{g/L}$

As anticipated for products containing citrus-related ingredients (G and H, both with strong citrus aroma), the genotoxic compound *p*-mentha-1,8-diene-7-al (perillaldehyde) was found (45 and 23 µg/L in G and H respectively). The higher concentration of perillaldehyde in beer G is in line with its higher content of citrus-related ingredients. Perillaldehyde levels were in the range of its odour threshold (30-62 µg/L) [2]. Interestingly, perillaldehyde was not found in beer I which contained raspberry juice, raspberry aroma, coriander and orange peel. Neither was it found in beer J containing fresh bergamot, another source of perillaldehyde [2].

Finally, the genotoxic active methylene compound pentan-2,4-dione was found in samples E, I and J, at concentrations of 6, 1 and 2 µg/L respectively, below its odour threshold of 10 µg/L [8]. These concentrations were below levels already found in roasted chicken and mango, up to 70 and 90 µg/kg respectively [9, 10].

Conclusion

A versatile and accurate extraction procedure using SAFE was optimised and validated for the analysis of 29 (suspected) genotoxic flavouring substances in alcohol-free beers. The SAFE technique, usually used without an appropriate validation, showed here the importance of the validation procedure to guaranty accurate results. Seven flavouring substances of interest were identified and quantified in alcohol-free beers. Based on the origins of the samples ingredients and the fact that their concentrations were below or equal to their odour threshold, it can reasonably be assumed that all the identified flavouring substances were not individually added as such. They probably originated from heat-treatment processes or from plant-based extracts. No significant differences of levels of furan-substituted compounds were observed between dealcoholized beers and beers brewed with special yeasts.

The majority of the (suspected) genotoxic compounds were not identified in the analysed samples. Analysis of upcoming new AFBs brewed with darker malt would provide relevant information on heat-formed flavouring substances levels, certainly higher than in current AFBs.

Further monitoring of flavouring substances in drinks and food is advised to broaden the occurrence assessment of these compounds. Besides alcohol-free beers, a special focus should be put for products more likely to be consumed by sensitive people such as children or pregnant women. Food and drinks containing citrus-related ingredients (e.g. juices, lemonades) should be assigned high priority because of the ubiquitous presence of perillaldehyde in such products.

References

1. European Court of Auditors. Chemical hazards in our food: EU food safety policy protects us but faces challenges. 2019;65.
2. Burdock GA, Fenaroli G. Fenaroli's handbook of flavor ingredients. 6th ed. Boca Raton: CRC Press/Taylor & Francis Group; 2010. 2135 p.
3. Brewers of Europe. The Analytica EBC. 2020.
4. Engel W, Bahr W, Schieberle P. Solvent assisted flavour evaporation - a new and versatile technique for the careful and direct isolation of aroma compounds from complex food matrices. *Eur Food Res Technol.* 1999;209(3-4):237-41.
5. ISO. ISO/IEC GUIDE 98-3:2008 Uncertainty of measurement — Part 3: Guide to the expression of uncertainty in measurement (GUM:1995). 2008.
6. Piornos JA, Balagiannis DP, Methven L, Koussissi E, Brouwer E, Parker JK. Elucidating the Odor-Active Aroma Compounds in Alcohol-Free Beer and Their Contribution to the Warty Flavor. *J Agric Food Chem.* 2020;68(37):10088-96.
7. Uselmann V, Schieberle P. Decoding the Combinatorial Aroma Code of a Commercial Cognac by Application of the Sensomics Concept and First Insights into Differences from a German Brandy. *J Agric Food Chem.* 2015;63(7):1948-56.
8. Pubchem [Internet]. Available from: <https://pubchem.ncbi.nlm.nih.gov/>
9. EFSA. Opinion of the Scientific Panel on food additives, flavourings, processing aids and materials in contact with food (AFC) related to Flavouring Group Evaluation 11 (FGE.11): Aliphatic dialcohols, diketones, and hydroxyketones from chemical group 10 (Commission Regulation (EC) No 1565/2000 of 18 July 2000). *EFSA J* [Internet]. 2004 [cited 2020 Dec 6];(EFSA Journal). Available from: <https://data.europa.eu/doi/10.2903/j.efsa.2005.166>.
10. Pino JA, Mesa J, Muñoz Y, Martí MP, Marbot R. Volatile Components from Mango (*Mangifera indica* L.) Cultivars. *J Agric Food Chem.* 2005;53(6):2213-23.

Supplemental study on acetals in food flavourings

JÁN PEŤKA and Johann Leitner

Austria Juice GmbH, Kröllendorf 45, 3365 Allhartsberg, Austria, jan.petka@austriajuce.com

Abstract

Acetals are reaction products between aldehydes or ketones on the one hand and alcohols on the other. Acetals are preferably formed under acidic conditions and low water content. These conditions are common with food flavourings. Acetals make it difficult to accurately identify the ingredients of food flavourings because many acetals are missing from commercial MS databases. In this work, we present additional data to the study, which was first presented on the XV Weurman Symposium [1], where the reactivity of 32 carbonyls with propylene glycol and ethanol was investigated. We supplemented the study with reactions with methanol and seventeen additional carbonyl compounds were included too. The novel mass spectra is presented in the form of the most common ions, and AMDIS database from the complete study is available upon request from the first author.

Keywords: acetal, flavouring, synthesis

Introduction

Food flavourings are ingredients that are added to food or beverages to give the product a certain flavour profile or modify the current one. They are used in comparatively small amounts, so consumer exposure is relatively low [1]. Since aroma compounds are principally hydrophobic, various solvents are used to increase their solubility in hydrophilic media such as food or beverage. The most common solvents used to produce food flavourings, propylene glycol and ethanol, form acetals with aldehydes and ketals with ketones, respectively, under acidic conditions. In this study, we completed the previous study [2] with additional compounds and methanol as an alcohol. The source of methanol in food flavouring are fruit essences.

Experimental

Chemicals

Additional compounds in this study, were purchased from Sigma-Aldrich (Munich, D) : (2E,4E)-deca-2,4-dienal, 3-phenylpropanal, (Z)-dec-4-enal, 5-(hydroxymethyl)furan-2-carbaldehyde (HMF), 5-methyl-2-phenylhex-2-enal, 3-hydroxybutan-2-one (Acetoin), (Z)-non-6-enal, 2,6-dimethylhept-5-enal (Melonal), 3-methylsulfanylpropanal (Methional), (2E,6Z)-nona-2,6-dienal, 3-(2-methoxyphenyl)prop-2-enal (o-Methoxycinnamaldehyde), 2-oxopropanal (Pyruvaldehyde), (E)-non-2-enal, pentanal, 3,4-dimethoxybenzaldehyde (Veratraldehyde). Alpha-Sinensal and (E)-tetradec-2-enal were purchased from R.C.Treant (Bury St. Edmunds, UK).

Preparation of acetals

100 μ L of carbonyl compound, 890 μ L of solvent, 10 μ L of acetic or formic acid, 2 days at 37°C.

Gas chromatography-Mass spectrometry

Gas chromatograph Agilent 7890B equipped with autosampler Gerstel Robotic and mass detector Agilent 5977B, operated at 70eV (all Gerstel, Mühlheim a.d. Ruhr, Germany), S/SL injector, injection volume 0.5 μ L, split ratio 200:1, injector temperature: 230°C, column: Restek Vms 20m x 0.8mm x 1 μ m (Restek GmbH, Bad Homburg, Germany), carrier gas: helium, constant flow = 1 mL/min, acquisition mode: Scan, 26-250 amu, oven program: 50°C(3min), 10°C/min, 250°C (6min), retention indices: C7-C20.

Results and discussion

Table 1 shows the overview of reactivity of carbonyl compounds with studied solvents. Same phenomena as discussed in the previous study [1] – differences in the electrophilicity of C=O group – applies here too. Methanol, in comparison with Ethanol, shows ambivalent susceptibility to form acetals. In the following cases Methanol was

Table 1. Reactivity of carbonyl compounds with Ethanol (EtOH), Methanol (MeOH) and Propylene glycol (PG). Red colour signifies no reactivity, green colour reaction under the presence of acetic acid, yellow reactivity under the presence of formic acid.

CAS number	Name	EtOH	MeOH	PG
620-02-0	5-Methylfurfural	Green	Green	Green
75-07-0	Acetaldehyde	Green	Green	Green
513-86-0	Acetoin	Red	Green	Red
100-52-7	Benzaldehyde	Green	Green	Green
472-66-2	beta-Homocyclocitral	Green	Green	Yellow
123-72-8	Butyraldehyde	Green	Green	Red
104-55-2	Cinnamaldehyde	Green	Green	Green
78-84-2	2-Methylpropanal	Green	Green	Yellow
123-11-5	Anisaldehyde	Green	Green	Green
17909-77-2	alpha-Sinensal	Red	Red	Red
2363-88-4	(E,E)-2,4-Decadienal	Green	Red	Red
30390-50-2	4-Decenal	Green	Green	Green
4411-89-6	2-Phenyl-2-butenal	Red	Red	Red
67-47-0	5-HMF	Red	Red	Green
104-53-0	3-Phenyl-1-propanal	Green	Yellow	Green
122-40-7	alpha-Amylcinnamaldehyde	Green	Red	Green
2277-19-2	(Z)-6-Nonenal	Green	Green	Green
21834-92-4	5-Methyl-2-phenyl-2-hexenal	Red	Red	Red
5392-40-5	Citral	Yellow	Red	Green
106-23-0	Citronellal	Green	Red	Green
112-31-2	Decanal	Green	Green	Green
121-32-4	Ethylvanillin	Red	Red	Green
98-01-1	Furfural	Green	Green	Green
111-71-7	Heptanal	Green	Green	Green

CAS number	Name	EtOH	MeOH	PG
66-25-1	Hexanal	Green	Green	Green
2111-75-3	Perillaldehyde	Red	Red	Green
590-86-3	Isovaleraldehyde	Green	Green	Green
124-19-6	Nonanal	Green	Green	Green
124-13-0	Octanal	Green	Green	Green
122-78-1	Phenylacetaldehyde	Green	Green	Green
106-72-9	Melonal	Green	Green	Green
3268-49-3	Methional	Green	Green	Green
1504-74-1	o-Methoxycinnamaldehyde	Green	Green	Red
557-48-2	(E,Z)-2,6-Nonadienal	Red	Yellow	Red
120-57-0	Piperonal	Green	Green	Green
123-86-6	Propionaldehyde	Green	Green	Green
78-98-8	Pyruvaldehyde	Red	Yellow	Yellow
116-26-7	Safranal	Yellow	Green	Green
104-87-0	p-Tolualdehyde	Green	Green	Green
6728-26-3	(E)-2-Hexenal	Green	Red	Green
467-03-0	Tiglaldehyde	Red	Green	Yellow
3913-81-3	(E)-2-Decanal	Red	Red	Green
51534-36-2	(E)-2-Tetradecenal	Red	Red	Red
112-44-7	Undecanal	Green	Green	Green
110-62-3	Valeraldehyd	Green	Green	Green
121-33-5	Vanillin	Red	Red	Green
120-14-9	Veratraldehyde	Yellow	Yellow	Green
18829-56-6	(E)-2-Nonenal	Red	Yellow	Red

Table 2. Mass spectra of selected acetals

Aldehyde	Alcohol	Ret. index	Mass spectra: m/z (Abundance)
5-Methylfurfural	Methanol	1125	109 (1000), 110 (951), 156 (934), 126 (742), 43 (310), 81 (185), 53 (171), 75 (164), 95 (134), 51 (116)
Acetoin	Methanol	1208	145 (1000), 72 (479), 159 (165), 57 (108), 146 (78), 115 (41), 114 (34), 113 (28), 61 (9), 46 (2)
(E)-2-Decenal	Propylenglycol	1587	113 (1000), 127 (448), 69 (275), 55 (253), 41 (191), 169 (261), 87 (215), 83 (102), 59 (97), 100 (71)
4-Decenal	Methanol	1406	75 (1000), 97 (533), 69 (217), 55 (147), 41 (124), 81 (124), 67 (101), 71 (94), 54 (84), 45 (71)
4-Decenal	Ethanol	1496	57 (1000), 103 (946), 85 (803), 110 (744), 75 (725), 47 (642), 81 (560), 67 (492), 55 (419), 95 (430)
4-Decenal	Propylenglycol	1517	87 (1000), 113 (762), 59 (448), 41 (257), 55 (216), 100 (212), 169 (207), 69 (157), 67 (112), 155 (116)
Melonal	Methanol	1263	75 (1000), 82 (698), 72 (374), 67 (228), 123 (220), 41 (212), 115 (166), 69 (140), 85 (137), 154 (135)
Melonal	Propylenglycol	1379	87 (1000), 127 (627), 59 (517), 41 (312), 69 (287), 58 (282), 82 (183), 198 (156), 67 (121), 55 (97)
Methional	Methanol	1165	75 (1000), 61 (890), 71 (782), 118 (689), 119 (330), 47 (252), 103 (180), 150 (171), 45 (133), 41 (115)
Methional	Ethanol	1271	85 (1000), 61 (997), 75 (659), 47 (600), 103 (505), 57 (397), 133 (388), 29 (170), 86 (110), 48 (109)
Methional	Propylenglycol	1291	87 (1000), 114 (751), 59 (650), 61 (587), 162 (452), 56 (336), 41 (270), 75 (236), 31 (165), 57 (138)
(E)-2-Nonenal	Methanol	1331	71 (1000), 155 (971), 101 (771), 75 (391), 115 (258), 81 (231), 41 (219), 97 (171), 67 (163), 55 (149)
(Z)-6-Nonenal	Ethanol	1415	103 (1000), 75 (565), 47 (346), 81 (302), 67 (221), 123 (207), 85 (195), 57 (186), 93 (183), 41 (172)
3-Phenyl-1-propanal	Propylenglycol	1559	114 (1000), 105 (558), 117 (466), 92 (405), 77 (315), 118 (312), 65 (297), 115 (277), 78 (248), 79 (157)
Safranal	Ethanol	1574	109 (1000), 107 (771), 137 (740), 81 (527), 152 (491), 91 (461), 135 (404), 95 (341), 79 (325), 123 (323)
Undecanal	Methanol	1524	185 (1000), 71 (817), 97 (547), 41 (537), 83 (441), 43 (349), 69 (346), 47 (336), 76 (292), 58 (271)

more reactive than Ethanol: Acetoin, (2E,6Z)-nona-2,6-dienal, Pyruvaldehyde, Safranal, (E)-2-Methyl-2-butenal, (E)-non-2-enal. Ethanol was more reactive than Methanol in these cases: (2E,4E)-deca-2,4-dienal, 3-Phenyl-1-propanal, alpha-Amylcinnamaldehyde, Citral, Citronellal, (E)-hex-2-enal. We have currently no explanation for these differences.

Selection of some newly reported mass spectra is shown in the Table 2. The full list of mass spectra is available in an AMDIS database upon request via e-mail.

Conclusion

The counter-typing of food flavourings that contain carbonyl compounds is made more difficult by the formation of acetals. In this work we tried to decipher some of them systematically. The next step will be the investigation of lactic acid, which is a common and abundant component of food flavourings and which causes the formation of numerous now unknown volatile compounds.

References

1. <https://effa.eu/library/guidance-documents>
2. Peřka J, Leitner J, Bueno JM, Szolcsányi P. Acetals in Food Flavourings. In: Siegmund B, Leitner E, editors. Flavour Science: Proceedings of the XV Weurman Flavour Research Symposium (522 pages). Graz (Austria): Verlag der Technischen Universität Graz; 2018. p. 313-18.

Investigating the flavour development of scab-resistant Crimson Crisp apples

NIKLAS PONTESEGGER¹, Thomas Rühmer² and Barbara Siegmund¹

¹ Graz University of Technology, Institute of Analytical Chemistry and Food Chemistry, Austria, pontesegger@tugraz.at

² Research Centre for Fruit Growing & Viticulture, Graz-Haidegg, Austria

Abstract

Apple scab is the most important apple disease in terms of economic aspects worldwide. Prevention is crucial, however, chemical or biological control are often uneconomic and time-consuming. To save resources, more and more scab-resistant varieties are bred, especially for cultivation in organic orchards. Fruit flavour is one of the most important properties for consumers. However, many scab resistant varieties lack pronounced apple flavour. The variety *Crimson Crisp* is reportedly on the same level or even higher when it comes to aroma, compared to traditional varieties. Nevertheless, to fully understand the aroma profile of this apple variety, an in-depth aroma profile analysis is needed. We investigated the formation of primary aroma compounds during on-tree maturation and ripening via headspace SPME-GC-MS measurements. In this contribution, we analyse its aroma profile and demonstrate the importance of long on-tree ripening of this promising scab-resistant apple variety. This will support the investigation of the optimal harvest conditions for *Crimson Crisp* and improve marketability of this highly ecological apple variety.

Keywords: apple, aroma, scab-resistant, Crimson Crisp, harvest

Introduction

According to the Food and Agricultural Organization of the United Nations apples are among the top three produced fruits worldwide, taking an overall share of 10 % of the total fruit production quantity for the year 2019 [1]. While banana and watermelon production are higher in overall quantities, apple production takes the top spot in Europe and North America. The versatility of the apple fruit is an essential factor for its popularity, as apples can be consumed raw, served as juices and smoothies as well as a part of sweet and salty meals.

Apples are produced in almost all parts of the world. However, the globalization of this industry also leads to problems. Apple scab is a common disease among the rose family (*Rosaceae*), which has been studied for more than 100 years. The disease, caused by the fungus *Venturia inaequalis*, is reported in almost all apple-producing areas. In terms of economic cost of control, apple scab is considered the most important apple disease worldwide [2].

The disease attacks both leaves and fruits [3]. Leaves may develop yellow to green spots on the upside and darker, sometimes velvety, spots on the lower surface. In more severe cases, the leaves also become twisted or wrinkled and might even drop in early summer. The symptoms on fruits are similar to those on leaves (Figure 1). Dark apple scab spots are deepened and may feature velvety spores in the centre. As these spores become bigger, the spots turn corky and fruits get deformed and have a risk of developing cracks on their surface. Severely infected fruits might drop at an early stage of their growing period.



Figure 1: Apples affected by apple scab.

Traditionally, the prevention of apple scab is a combination of sensible fungicide application as well as plant sanitation [4]. In recent years, producing apples labelled *certified organic*, *pesticide free*, or *integrated pest management* has been identified as a competitive advantage. Thus, the use of scab-resistant apple varieties is becoming more popular, particularly in organic orchards [5]. In 1943, a gene linked to apple scab resistance was discovered, the V_f gene. Although V_f has been described as the most abundant among apple scab resistant varieties in the last decades, nowadays more resistance genes and even more resistant varieties are known [6].

However, when it comes to breeding for new varieties, things are hardly ever straightforward. The target plant with the desired resistance gene often lacks palatable fruits. For example, the source of the V_f gene in *Crimson Crisp* dates five generations back [7]. This shows how much effort is necessary to meet consumer standards and to make farming and selling profitable.

The first seedling of *Crimson Crisp* (or *Coop 39*) was screened for scab-resistance in 1971 and the first fruits were observed in 1979 as part of a cooperative breeding program based in Illinois and New Jersey [7].

These midseason fruits are red, the texture, as the name already indicates, is very crisp. A consumer study in 2010 affirmed the very good flavour compared to both traditional and other scab resistant varieties [5]. However, to the best of our knowledge, an in-depth investigation of the aroma profile in Crimson Crisp apples has not been reported yet. On top, we follow the formation of the volatile aroma compounds from unripe fruits until early stages of senescence. We aim to evaluate the current harvest regimes on the basis of flavour development, since this variety is a rather new, but promising entry in Austrian organic orchards.

Experimental

Apple sampling

Crimson Crisp apples were handpicked in weekly intervals from apple plantations of the Research Centre for Fruit Growing & Viticulture, Graz-Haidegg, Austria. Sampling started on August 5th 2020, exactly 15 weeks after full blossom (wafb) (April 23rd 2020). Due to logistic reasons, the last two samples were taken in a 14-days interval, ending 27 wafb. After sampling, all apples were stored at room temperature in the dark over night until they were further processed. Primary aroma compounds were analysed from an enzyme inhibiting and antioxidant mixture containing approximately 75 g freshly cut and peeled apple pulp from 8-10 fruits, 75 mL deionised water, 30 g NaCl, 250 mg citric acid and 250 mg ascorbic acid. The resulting mixture was mixed in a commercial blender with a glass container to a purée and small amounts (ca. 4 mL) were frozen in glass vials at -25°C until further use.

Gas Chromatography-Mass Spectrometry (GC-MS) sample preparation and measurement

Aliquots of the homogenised samples (250 mg of purée) were transferred into headspace (HS) vials; 2-octanol was used as internal standard (30 ng absolute). Two replicates of each sample were prepared and analysed. After enrichment of the volatiles by HS-SPME (40°C , 20 min, 50/30 μm DVB/CAR/PDMS fibre, 2 cm stable flex fibre) analyses were performed with 1-dimensional GC-MS (Shimadzu GCMS-QP 2010 Plus, Shimadzu Europa GmbH, Rxi[®] 5 ms, 30 m \times 0.25 mm \times 1 μm , Restek Corporation, USA, 35–350 amu, EI (70 eV)). Identification of the compounds was based on the comparison of the obtained mass spectra to those from MS libraries or authentic reference compounds as well as on retention indices (RI). Linear-temperature programmed RI were calculated using *n*-alkanes (C5-C26) and compared to data from authentic reference compounds and data from literature.

Data treatment

Data deconvolution was performed with PARADISE, based on the PARAFAC2 model [8]. The statistical analysis was performed with the MS Excel add-in XLSTAT. For the identification of significant differences between the samples and their ripening stages one-way analysis of variance (ANOVA) was performed ($p=0.05$). If statistically significant differences were observed within the data sets, the ANOVA was followed by post-hoc pairwise comparison using Tukey's Honestly Significant Difference (HSD) test control ($p < 0.05$) to check for differences between single samples. Correlations were analysed conducting a principal component analysis (PCA) using the Pearson correlation.

Results and discussion

In this study, we evaluated the flavour formation and, consequently, the current harvest recommendations for the scab resistant apple variety Crimson Crisp *via* HS-SPME-GC-MS aroma compound analysis. Since Crimson Crisp is primarily sold and consumed as fresh apple, we focused on the analysis of primary flavour compounds. In total, we identified 84 primary volatile compounds (33 esters, 25 carbonyl compounds, 17 alcohols, 9 others). All of these compounds have been described as part of the apple volatilome before. A total of 47 identified volatiles show a clear dependence of their concentrations on the ripening time on the tree. To demonstrate the development of the concentrations of the compound classes during on-tree ripening, six representative examples were selected and their concentrations are plotted in weekly intervals. For this purpose, two alcohols (2-methylbutanol, hexanol), two esters (2-methyl butylacetate, hexyl acetate) and two carbonyl compounds (pentanal and (*E*)-2-octenal) were selected (Figure 2). All these volatiles show odour activity values (OAV) higher than 1 (for alcohols and esters increasing values $20 < \text{OAV} < 150$, for aldehydes decreasing values between $0,5 < \text{OAV} < 5$). This demonstrates the relevance of these volatiles to the overall aroma of Crimson Crisp.

The current recommendations for the optimum harvest period of Crimson Crisp lay between the early to late middle of September [9]. This corresponds to 19-21 wafb in the agricultural area under investigation. However, following the development of the apple volatiles, the formation of compounds that are relevant for the apple flavour is clearly not at its maximum during this period. We observed an increase of 30 volatiles throughout 20-22 wafb, all of these compounds show a similar behaviour as the selected alcohols and esters (Figure 2). Many of these compounds are perceived as fruity, apple or floral notes and are well-known to contribute to the desirable overall flavour of apples. While alcohols and esters showed rising concentrations in 19-21 wafb, a maximum in concentrations was reached in 22-23 wafb for the observed alcohols; at that point the formation of the observed

esters was still not completed. In a previous study, a comparable behaviour was observed, showing that the delayed ester formation during on-tree ripening is primarily due to enhanced availability of alcohols as precursors compounds for esters, rather than enhanced AAT activities upon ripening [10]. On the contrary, aldehydes and ketones showed a steady concentration decrease during the observed period, which is demonstrated with the examples of pentanal and (*E*)-2-octenal (Figure 2). This decrease in concentration of carbonyl compounds is in accordance with findings described previously [10] where a steady decrease of LOX and HPL activities was observed during on-tree ripening in a comparable ripening period leading to lower amounts of LOX products in the fruits. Most aldehydes that were identified in Crimson Crisp apples are associated with green notes – consequently, their loss leads to a decrease of green flavour with a parallel increase of fruity, apple-like properties caused by the reported formation of esters and alcohols.

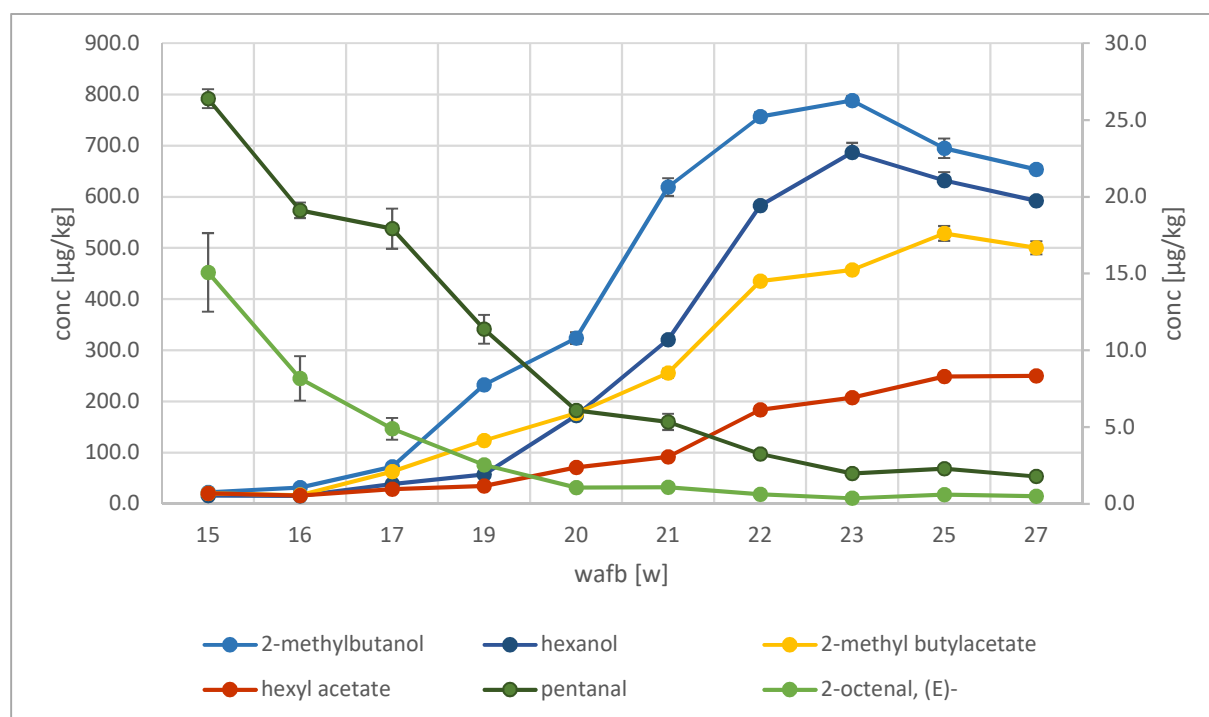


Figure 2: The concentrations [$\mu\text{g}/\text{kg}$] of six representative volatiles in Crimson Crisp pulp over the course of maturation and ripening on the tree in weeks after full blossom (wafb) [w]; concentration of alcohols and esters refer to the left-hand side y-axis, those of aldehydes to the right-hand side y-axis.

Principal component analysis (PCA) was applied to better visualise the correlations between the concentrations of the apple volatiles and the harvest date of the Crimson Crisp fruits (Figure 3). For this purpose, volatile compounds, which did not show concentration dependence on the on-tree development of the fruits were not included in the principal component analysis in order to facilitate interpretation and to keep the focus on compounds related to the on-tree ripening process. Forty-seven volatiles (55 % of the total volatilome) were included. The biplot given in Figure 3 shows 180° counter-clockwise behaviour of the on-tree ripening times from the border of quadrants II and III to the border between quadrants I and IV. The unripe fruits harvested after 15-17 wafb are closely correlated to volatiles with green, grassy unripe sensory attributes (mainly aldehydes, green dots in Figure 3) as well as ketones with mushroom-like and metallic attributes such as for example 1-octen-3-one. On the other hand, apples harvested 22-27 wafb are highly correlated with a large group of esters and several alcohols.

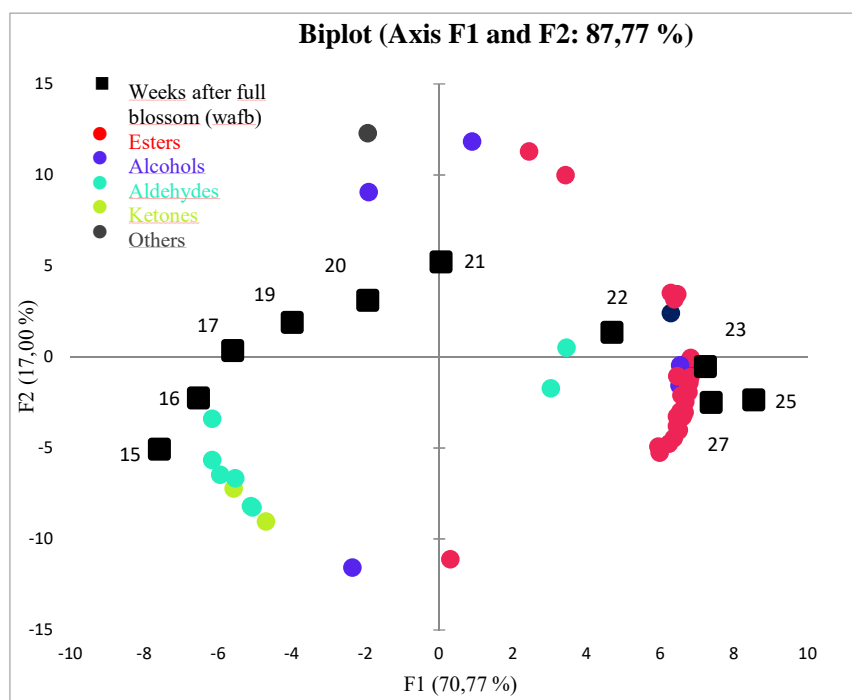


Figure 3: Biplot of the principal component analysis (PCA) based on 47 volatiles in Crimson Crisp apples and the harvest dates. Weeks after full blossom (wafb) (black squares), esters (red dots), alcohols (purple dots), aldehydes (green dots), ketones (yellow dots) and others (grey dots).

Conclusion

Our findings demonstrate that Crimson Crisp apples show strong flavour formation upon on-tree ripening. According to the current harvest recommendations, the apples are harvested long before the maximum formation of compounds that are relevant for the flavour formation. Based on our finding, we propose a shift of the recommended harvest period from 19-21 wafb to 22-25 wafb, to fully develop the flavour of Crimson Crisp apples. Although this leads to storage of fruits with an unusually high starch degradation index of > 8.0. Early experiments show good storage stability of Crimson Crisp apples harvested 23 wafb. With these results, we demonstrate the importance of flavour analysis for agricultural purposes for the optimisation of flavour properties of domestic agricultural crop.

Declaration of Competing Interest

The authors declare that they have no known competing financial interests or personal relationships that could have appeared to influence the work reported in this paper.

References

1. FAO. FAOSTAT. Crops. Latest Update December 22, 2020. Accessed March 12 2021;
2. Carisse O, Bernier J. Effect of environmental factors on growth, pycnidial production and spore germination of *Microsphaeropsis* isolates with biocontrol potential against apple scab. *Mycol Res.* 2002;106(12):1455–1462.
3. Jha G, Thakur K, Thakur P. The *Venturia* apple pathosystem: pathogenicity mechanisms and plant defense responses. *J Biomed Biotechnol.* 2009;2009:680160.
4. Bowen J K, Mesarich C H, Bus V G, Beresford R M, Plummer K M, Templeton M D. *Venturia inaequalis*: the causal agent of apple scab. *Mol Plant Pathol.* 2011;12(2):105–122.
5. Kelley K, Hyde J, Travis J, Crassweller R. Assessing Consumer Preferences of Scab-resistant Apples: A Sensory Evaluation. *Hortte.* 2010;20(5):885–891.
6. Carisse O, Dewdney M. A review of non-fungicidal approaches for the control of apple scab. *Phytoprotection.* 2002;83(1):1–29.
7. Janick J, Goffreda J C, Korban S S. 'Co-op 39' (CrimsonCrisp™) Apple. *Hortscience.* 2006;41(2):465–466.
8. Petersen M A, Bro R. PARADISE - a ground-breaking tool to treat complex GC-MS datasets. ; Verlag der Technischen Universität Graz, 2018.
9. Lafer G. Lagerungsversuch bei Crimson Crisp. *Haidegger Perspektiven.* 2012(4):7–9.
10. Ortiz A, Graell J, Lara I. Volatile ester-synthesising capacity throughout on-tree maturation of 'Golden Reinders' apples. *Sci Hortic.* 2011;131:6–14.

Enzymatic release of flavour compounds from Heritage apple varieties

Valerie Ruppert¹, Georg Innerhofer², Jörg Voit³, Peter Hiden³ and BARBARA SIEGMUND¹

¹ Graz University of Technology, Institute of Analytical Chemistry and Food Chemistry, Austria

² School for Fruit Growing & Viticulture, Silberberg, Austria

³ Research Centre for Fruit Growing & Viticulture, Graz-Haidegg, Austria
barbara.siegmund@tugraz.at

Abstract

Heritage apple varieties such as *Ilzer Rose*, which is domestic to the southern area of Austria, are often used as a raw material for the production of apple wines due to their pleasant flavour properties. In this study, we investigated if the concentrations of terpenes that had been identified in the skin of this variety might be increased upon modification of the fermentation strategy by the addition of pectolytic enzyme with pronounced β -glucosidase activity. Furthermore, the impact of prolonged juice maceration as well as mash fermentation were investigated regarding a potential release of terpenes from glycosides. These strategies led to a significant increase of the investigated compounds in apple wine; however, the resulting concentrations were still below their odour threshold values in the matrix apple wine. Nevertheless, the modified fermentation management resulted in interesting products that will be in the centre of future investigations.

Keywords: apple wine, heritage apple varieties, terpenes, glycosides, odour threshold

Introduction

With the recent trend to increase the consumption of local and regional foods, heritage apple varieties have regained popularity in Austria. Several hundreds of apple varieties are domestic to meadow orchards; some of them have also been cultivated in plantations during the last decade. Many of these heritage varieties are characterised by excellent sensory properties and are, thus, of high interest especially for the production of apple wine and cider. In a recent study, we showed that a large number of interesting terpenes is present in the skin of the heritage apple variety *Ilzer Rose*, an apple variety that is known for its floral, rose-like flavour [1]. We assume that these terpenes contribute to the floral properties of *Ilzer Rose* wine.

Oenology has been tackling glycosylated aroma compounds for years to enhance the flavour profile of certain wines. Approximately 90 % of monoterpenes were found in their glycosylated form in Muscat wines [2]. Glycosides are built by an aglycone linked to at least one sugar molecule as glycone. Hydrolysis of the glycosidic bonds then leads to the release of the aglycone and the glycone. If the released aglycone is an aroma active compound, the flavour profile of the resulting wine can be affected. Some members of the class of monoterpenes are important representatives for aroma compounds with floral and 'sweet' characteristics. Especially, in grape varieties of aromatic wines such as Gewürztraminer, Muskateller or Riesling these monoterpenes are essential. However, these compounds mainly occur as glycosides in grapes meaning that they are odourless and most likely transported to the vacuoles, where they are stored as potential flavour precursors [3]. However, the odour-active terpenes may be released from these precursors by the activity of certain glucosidases, which are added during the vinification of aromatic white wines.

In this study, we transported this concept to the production of apple wines. We investigated if the concentrations of terpenes and sesquiterpenes in apples wines from *Ilzer Rose* apples were increased upon enzymatic treatment during apple wine production, whereas we followed two different strategies, (i) maceration of the juice, and (ii) mash fermentation over several days. The assumed release of terpenes from their glycosides during the fermentation similar to their release from specific grape varieties could boost the flavour of *Ilzer Rose* wines and make them even more attractive to consumers.

Experimental

Material

A total of 157 kg *Ilzer Rose* apples was harvested from an apple orchard at their commercial ripeness in October 2018. After the harvest, the apples were stored for further two weeks under cooled conditions to promote postharvest ripening and flavour development. Juice preparation and the subsequent apple wine (AW) production was carried out in special micro fermentation devices. Figure 1 gives a summary about the processing steps for the five apples wines. AW1 was produced as a reference product without maceration; the mash was pressed

immediately after milling of the apples; pectinase (Enzym MS flüssig, Preziso, 5 ‰) was added to the juice for AW1. A pectolytic enzyme with β -glucosidase activity (Trenolin® Bouquet PLUS, Erbslöh, Germany) was added to the mashes of the apple wines AW2-5. For the production of AW2 and AW4, the juice was let to macerate for 8 hours prior to fermentation. For the production of AW4 and AW5, the fining agent Gerbinol® CF (Erbslöh, Germany; 2 ‰) was added to the mash with the purpose to bind unbalanced tannins and for clarification. Mash fermentation for AW3 and AW5 was performed for 10 days with subsequent fermentation after pressing of the mash. *Saccharomyces cerevisiae* var. *bayanus* (LALVIN® EC-1118; Lallemand Inc.; Canada; 250 mg/L) was added to all approaches to initiate the fermentation. Fermentation was controlled for AW1, AW2 and AW4 (FC, temperature control (15.5 °C); addition of thiamine and diammonium phosphate (Vitamon Liquid; Erbslöh; Germany) as nutrients during the fermentation; addition of bentonite 2.5 g/L); for AW3 and AW5 neither temperature was not controlled nor nutrient was added (NFC).

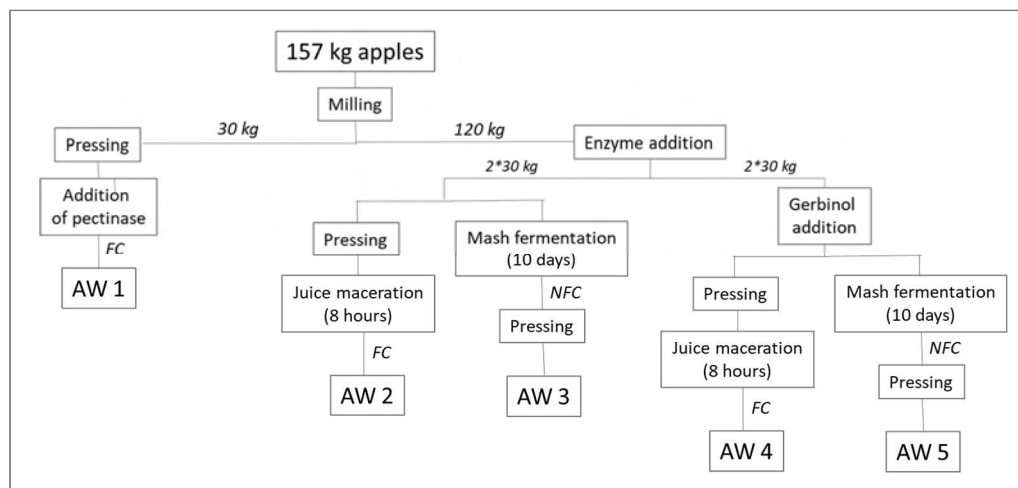


Figure 1: Survey about the fermentation strategies, AW apple wine, FC fermentation control, NFC no fermentation control.

Gas chromatography-mass spectrometry (GC-MS) of the volatile compounds

An aliquot of 50 μ L of apple wine was transferred into 20 mL headspace vials with the addition of 50 mg NaCl. 2-Octanol was added as an internal standard (10 ng absolute). The extraction/enrichment of the volatiles was performed by headspace solid-phase-microextraction (HS-SPME; 2cm stable flex fibre, 50/30 μ m DVB/Car/PDMS fibre) for 20 minutes at 40°C. Samples were stirred thoroughly during the enrichment process. The GC-MS analysis was conducted on a non-polar column (Rxi-5ms 30 m \times 0.25 mm \times 1 μ m) and as well a as polar column (ZB-Wax 20 m \times 0.18 mm \times 0.18 μ m), GC-MS chromatograms were recorded on Shimadzu GC-2010 Plus, MS QP 2020 (Shimadzu Europa GmbH; EI 70 eV, scan range 35-350 amu). The samples were analysed in fourfold in randomized order. The identification of the volatiles was based on probability-based matching of their mass spectra with those from MS libraries, authentic reference compounds and linear temperature-programmed retention indices. Retention indices were calculated by measuring the homologous series of *n*-alkanes (C6-C26) using the same GC-MS conditions as for the samples. Data deconvolution and integration was done with the PARADISE software, based on the PARAFAC2 model [4]. Semi-quantification was done via the internal standard (2-octanol) assuming a response factor of 1 for all compounds.

Threshold Determination

The determination of odour thresholds (detection as well as recognition thresholds) of selected compounds with floral, rose-like odour (i.e. linalool, rose oxide, 2-phenylethanol) was performed according to the ASTM method E679-04 [5]. Threshold values were calculated as the 'best estimate thresholds' (BET) from the geometric means of individual thresholds. The thresholds were determined in water and in a neutral apple wine that was produced from apples poor in aroma. Sensory experiments were performed with a well-trained expert panel (n=12) under standardized conditions in the sensory laboratory.

Statistical evaluation of the results

Statistical analysis was performed using one-way analysis of variance (ANOVA) to identify statistically significant differences between the samples. For statistical analysis, the MS excel add-in XLSTAT was used (Addinsoft 2020, Long Island, NY, USA).

Results and discussion

Floral and rose-like odour is part of the pleasant flavour of apple wines making the product attractive to consumers. Apples from the heritage apple variety *Ilzer Rose* which is domestic to the southern regions of Austria express a pronounced floral, rose-like aroma. In this work, we investigated if this specific floral and rose-like aroma might be intensified by technological measures. A large variety of terpenes was identified recently in the skin of *Ilzer Rose* apples [1]. In accordance to oenological practices, we applied different fermentation regimes to *Ilzer Rose* apple juice by adding enzymes with pronounced β -glucosidase activity. Maceration of the juices as well as mash fermentation – two common oenological practices leading to increased exposure time of the flash or the apple skin, respectively, to the enzymes – were investigated with respect to the concentration of terpenes, as we hypothesized an enzymatic release of terpenes from their glycosides.

Table 1 shows the concentrations of the selected compounds of interest in the different apple wines. For the terpenes under investigation that show floral and rose-like sensory properties (i.e., linalool, linalool oxide, α -farnesene) as well as for 2-phenylethanol we observed significant, however, low increases in concentrations when comparing the reference apple wine (AW1) to the apple wines AW2-AW5 where a pectolytic enzyme with β -glucosidase activity had been added and different fermentation regimes had been applied. For all compounds, the maceration of the juice or mash fermentation led to an increase in concentration of these volatiles, however, no clear trend is visible depending on the fermentation strategy. In comparison to the apple juice as starting material, we noticed a decrease in concentration by a factor 2 to 10 (data not shown) for the terpenes. 2-Phenylethanol, which also shows expressed floral sensory notes, is significantly higher in overall concentrations in the apple wines compared to terpenes; again, no clear trend can be observed in dependence of the fermentation strategy. However, 2-phenylethanol – which is most likely formed as a metabolite of the amino acid phenylalanine by *Saccharomyces* via the Ehrlich pathway – shows a 300-fold increase in concentration upon the fermentation process.

Table 1: Concentrations of terpenes in apple wine produced with different fermentation approaches; concentrations are given in average concentrations $\mu\text{g/L}$ (n=4); letters indicate significant differences between compound concentrations in the different wines ($p < 0.05$).

	linalool [$\mu\text{g/L}$]	linalool oxide* [$\mu\text{g/L}$]	α-farnesene [$\mu\text{g/L}$]	2-phenyl-ethanol [$\mu\text{g/L}$]
AW1	$3.61 \pm 14.5\%$ ^d	$5.91 \pm 2.3\%$ ^c	$1.98 \pm 20.3\%$ ^c	$629 \pm 8.9\%$ ^{ab}
AW2	$5.45 \pm 2.8\%$ ^a	$9.04 \pm 6.1\%$ ^a	$7.29 \pm 7.3\%$ ^{ab}	$727 \pm 8.8\%$ ^a
AW3	$4.75 \pm 3.2\%$ ^{bc}	$9.18 \pm 5.9\%$ ^a	$9.15 \pm 22.7\%$ ^a	$618 \pm 3.2\%$ ^b
AW4	$5.06 \pm 3.0\%$ ^{ab}	$7.37 \pm 0.7\%$ ^b	$6.32 \pm 8.1\%$ ^b	$612 \pm 7.4\%$ ^b
AW5	$4.42 \pm 4.6\%$ ^c	$8.06 \pm 2.2\%$ ^b	$8.06 \pm 14.7\%$ ^{ab}	$558 \pm 4.3\%$ ^b

* furanoid form; enantiomer not identified

It is well known that odour thresholds of odour-active compounds are highly matrix dependent. In the literature, most values for odour thresholds can be found for the matrices water and oil. In the context of our investigation, we wanted to receive detailed information on the how an apple wine matrix with an average ethanol content of 5% would impact the perception of selected aroma compounds with pronounced floral and rose-like aroma. As a matrix, we chose an apple wine that only showed weak, and especially not rose-like flavour; the investigated volatiles could also not be detected in this apple wine. As it was not possible to receive an α -farnesene-free apple wine, we did not determine the odour thresholds for this compound. Table 2 gives the results from the odour threshold experiments. The results demonstrate that the matrix shows significant impact on the odour thresholds of linalool. Even though the recognition and detection thresholds are close to one another, significantly higher concentrations are required for the sensory detection in the apple wine matrix compared to water. These results are in good accordance with previously reported odour thresholds for linalool in orange juice as matrix [6]. Interestingly, the odour thresholds for rose oxide as well as 2-phenylethanol are affected by the matrix apple wine, but to a far lesser extent than for linalool.

Table 2: Odour thresholds for selected compounds of interest given in water and apple wine in terms of the group BET in µg/L (n=12); group BET was calculated as geometric means of individual BET values.

	Detection threshold [§] [µg/L]		Recognition threshold [§] [µg/L]	
	water	apple wine	water	apple wine
Linalool	4.9	90	5.1	330
Rose oxide [%]	0.02	0.3	0.1	1.0
2-phenylethanol	0.01	3.60	0.5	4.8

[§] The value for the detection threshold is the level at which the differing sample is selected correctly without being able to describe the sensory properties of the compound; [§] The value for the recognition threshold is the level at which the differing sample is selected correctly and the sensory properties could be described.

[%] Rose oxide was incorporated to the study due its odour properties and the structure similarities to linalool oxide.

While setting the odour thresholds in relation to the observed concentrations of the compounds of interest, it is obvious that the investigated terpenes do not play an important role for the rose-like flavour of *Ilzer Rose* apple wine, independently of the way the fermentation is carried out. Obviously, in contrast to aroma-rich grape varieties, terpenes are present mainly in the apple skin, but mostly in their free form and not as glycosides. On the other hand, 2-phenylethanol must be considered an important contributor to the floral aroma of *Ilzer Rose* wines. The formation of 2-phenylethanol via the Ehrlich pathway is highly dependent on the yeast strain. Thus, the selection of a different from the applied *Saccharomyces* strain might be an option to further increase its concentration and to influence the floral aroma of the resulting apple wines.

Conclusion

The results of this study confirmed our initial hypothesis assuming that the treatment of *Ilzer Rose* juice with enzymes showing pronounced β-glucosidase activity would increase the concentration of terpenes due to their release from the corresponding glycosides. However, unfortunately observed concentration increases were too small for a significant impact on the flavour of the apple wines. We assume that the rose-like flavour is more likely attributed to the presence of 2-phenylethanol than to the investigated terpenes. However, the resulting apple wines showed completely different and nonetheless interesting flavour properties in comparison to the reference product. As a consequence, the detailed investigation of the flavour compounds in these apple wines will be subject of future investigations. Refashioning the technology by integrating oenological measures into the production of fruit wines and enhancing flavour release/formation from heritage apple varieties such as *Ilzer Rose* may help develop new flavour attributes in addition to the well-known apple wine properties.

References

1. Tauber I, Innerhofer G, Leitner E, Siegmund B. Characterisation of the Flavour of the old Austrian Apple variety 'Ilzer Rose'. In: *Flavour Science: Proceedings of the XV Weurman Flavour Research Symposium*; Siegmund B, Leitner E (eds.); Verlag der Technischen Universität Graz. 2018;p.135-138.
2. Hjelmeland K, Ebeler SE. Glycosidically Bound Volatile Aroma Compounds in Grapes and Wine: A Review. *Am J Enol Vitic.* 2015;66(1):1-11.
3. Schwab W, Wüst M. Understanding the Constitutive and Induced Biosynthesis of Mono- and Sesquiterpenes in Grapes (*Vitis vinifera*): A Key to Unlocking the Biochemical Secrets of Unique Grape Aroma Profiles. *J Agric Food Chem.* 2015;63(49):10591-10603.
4. Johnsen LG, Skou PB, Khakimov B, Bro R. Gas chromatography - mass spectrometry data processing made easy. *J Chromatogr A.* 2017;1503: 57–64
5. ASTM E679-04 - Standard Practice for Determination of Odor and Taste Threshold By a Forced-Choice Ascending Concentration Series Method of Limits. In ASTM Standards. ASTM International, West Conshohocken, PA, 2011.
6. Plotto A, Margaria CA, Goodner KL, Goodrich R, Baldwin EA. Odour and Flavour thresholds for key aroma components in an orange juice matrix: terpenes and aldehydes. *Flavour Frag J.* 2004:491-498.

Lactic acid bacteria used to produce natural flavour compounds from whey and castor oil

ALEJANDRO ÁLVAREZ^{1,2}, Alejandra Gutiérrez^{1,2}, Frank Cuenca¹, Cristina Ramírez² and Germán Bolívar²

¹ La Tour S.A., Cali, Colombia, jalvarez@la-tour.com

² MIBIA, Universidad del Valle, Cali, Colombia

Abstract

Whey and castor oil are economic raw materials and can be used as nutrients to produce molecules of interest by fermentation with lactic acid bacteria. In this study, aromatic compounds produced by the bacteria *Lactobacillus plantarum* A6 and *Lactococcus lactis cremoris* were investigated in the fermentation of whey with two concentrations of castor oil (3 % and 6 %), using gas chromatography-mass spectrometry (GC-MS) with solid-phase microextraction (SPME). The results showed the production of aromatic compounds, mainly: Hydroxyacetone, Acetic acid, Formic acid, γ -Butyrolactone, 2(5H)-furanone, Furanol, Furfural, Furfuryl alcohol, Dihydroxyacetone and Pentanal. Both microorganisms managed to metabolize the fatty acids from castor oil; however, the concentration of castor oil did not have a significant effect on the production of flavours ($p > 0.05$). On the other hand, significant differences were found according to the type of microorganism ($p < 0.05$), obtaining a different aromatic profile for each lactic acid bacteria. Finally, the flavour profile was described as pungent, sharp, fruity, creamy, buttery, sweet, alcoholic, and fermented, thus achieving an interesting aromatic base to be used in natural flavours.

Keywords: lactic acid bacteria, whey, castor oil, fermentation, natural flavour

Introduction

Whey is considered a by-product of the dairy industry and is classified as a water and soil pollutant, due to its high chemical and biochemical oxygen demand [1]. Both whey and castor oil are economic raw materials and can be used as nutrients to produce molecules of interest by fermentation with lactic acid bacteria, which are known to produce aromatic compounds in different foods [2, 3]. Fermentation has emerged as a promising technology for producing natural molecules for use in flavours, creating the need to search for new strains and substrates to produce natural aromatic compounds. Consequently, the objective of this study was to investigate and characterize the aromatic compounds produced by fermentation of whey and castor oil (CO) with the bacteria *Lactobacillus plantarum* A6 (Lp) and *Lactococcus lactis cremoris* (Ll). For this, a liquid fermentation was carried out, the aromatic compounds were analysed using gas chromatography-mass spectrometry (GC-MS) and the treatments were discriminated against through a principal component analysis (PCA), evidencing the aromatic molecules generated.

Experimental

The microorganisms used were obtained from the laboratory of microbiology and applied biotechnology (MIBIA) Cali - Colombia, were reactivated and cultivated in medium MRS until use. Analysis of fermented assays was carried out using gas chromatography (Agilent Technologies, GC 7890B) with mass spectrometry (Agilent Technologies, 5977A) (GC-MS), the tests were sampled by SPME (Solid Phase Microextraction) with a DVB/CAR/PDMS fibre. The column used was a Thermo TG-1MS (30 m x 0.25 mm internal diameter, 1 μ m film thickness). The injection port was maintained at 250 °C for a 6 min desorption time. The GC oven was programmed from 60 °C to 280 °C with a temperature ramp of 4 °C/min. The injection mode was split (5:1), high purity helium was used as carrier gas at a flow of 1.5 mL/min. The quadrupole MS detector was maintained at 230 °C with an ionisation energy of 70 eV. Mass spectra were compared with the NIST library using the Agilent MassHunter Unknowns Analysis program, and the peak area of each volatile was obtained and calculated using the normalization technique.

Fermentation

The fermentation was carried out in Erlenmeyer flasks with 100 mL culture medium, which consisted of 11.4 % whey, 3 % or 6 % castor oil, 10 % bacteria inoculum with 24 h of previous incubation in MRS medium, and water (72.6 – 75.6 %). The assays were fermented for 48 h at 35 °C. The trials were performed triplicate for each treatment. After the fermentation, 300 μ L were sampled and analysed by GC-MS.

Statistical design and analysis

A two-factor design was performed with three levels; microorganism type: without microorganism (control), *Lactobacillus plantarum* A6 (Lp) and *Lactococcus lactis cremoris* (LI); and amount of castor oil: oil-free (CO0), 3% (CO3), and 6% (CO6). A heat map was made to visualize the aromatic production of each treatment and a Principal component analysis (PCA) was performed to discriminate the molecules produced for each treatment, the analysis was carried out in the XLSTAT statistic program. The factorial design was carried out with the MINITAB 2018 program, to analyse the effects of the factors for each aromatic molecule. Analyses were performed with a significance level of $\alpha = 0.05$.

Results and discussion

Changes in the aromatic profile according to the treatment evaluated during fermentation can be seen in Figure 1. Regarding the control without fermentation, a natural increase in the production of acetic acid, formic acid, and furfuryl alcohol, all molecules characteristic of the metabolism of lactic acid bacteria, can be seen for both Lp and LI. In addition, it is observed that the control has a profile of fatty acids and molecules from castor oil, which were not found in fermented treatments, indicating the metabolization and transformation of the above-mentioned compounds.

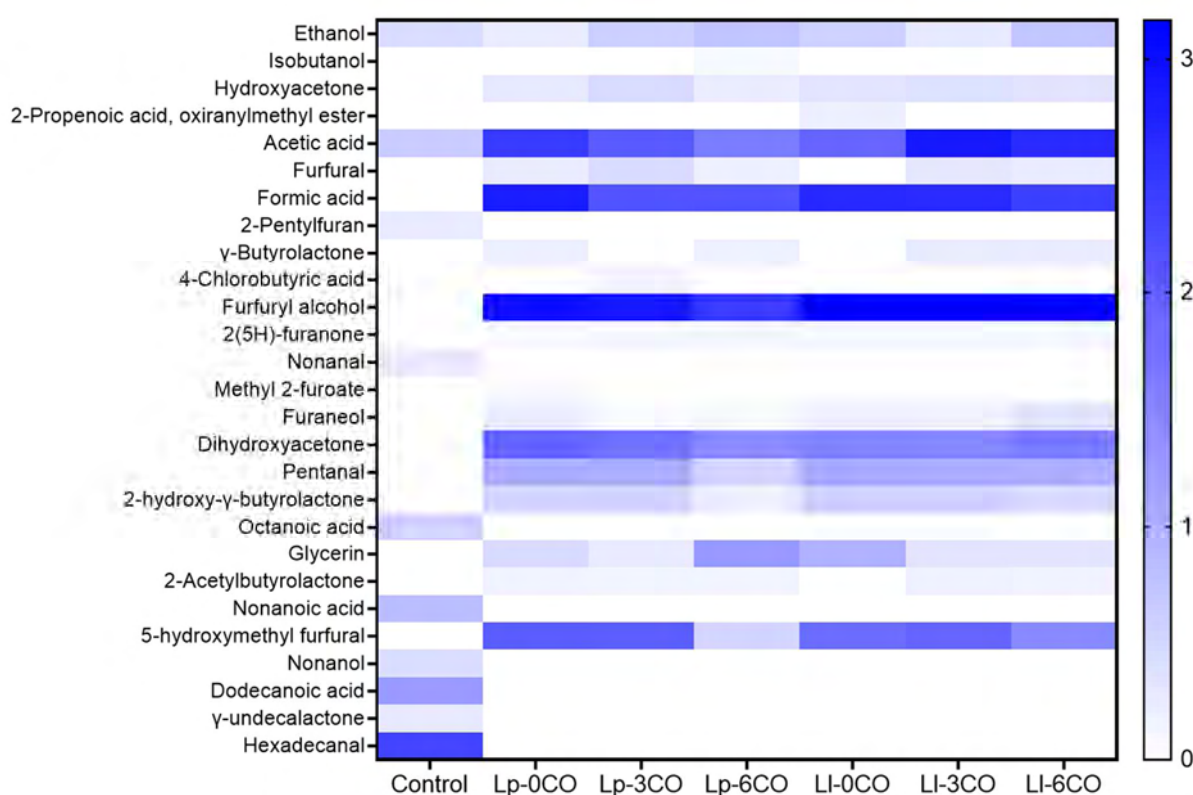


Figure 1: Heatmap representing the production of different aromatic molecules analysed by GC-MS. The horizontal axis shows the different treatments with *L. plantarum* (Lp), *L. lactis* (LI), and control without microorganism, with different amounts of castor oil 0 % (0CO), 3 % (3CO), and 6 % (6CO). The colour bar represents the relative percentage of peak areas obtained by SPME.

For some molecules (furfuryl alcohol, 2-pentylfuran, 2(5H)-furanone, pentanal, and methyl 2-furoate), the concentration of castor oil did not have a significant effect ($p > 0.05$), therefore, the generation of those molecules is not related to the transformation of the oil, and are probably generated by the action of the whey consumption. The main molecules produced were furfuryl alcohol, acetic acid, formic acid, 5-hydroxymethyl furfural, and dihydroxyacetone. Also, some molecules with less concentration were detected, such as hydroxyacetone, γ -butyrolactone, furaneol, pentanal, and 2-pentylfuran. The aromatic profile of the produced compounds was described as pungent, sharp, fruity, creamy, buttery, sweet, alcoholic, and fermented, so it can be used to formulate flavours with these characteristics.

As shown in Figure 2, principal component analysis allows to classify the treatments for both microorganisms. With both microorganisms, the treatments were assorted by the production of aromatic molecules, with two main components representing 96.9 % of the data for the treatments. Mainly, it is observed that both microorganisms

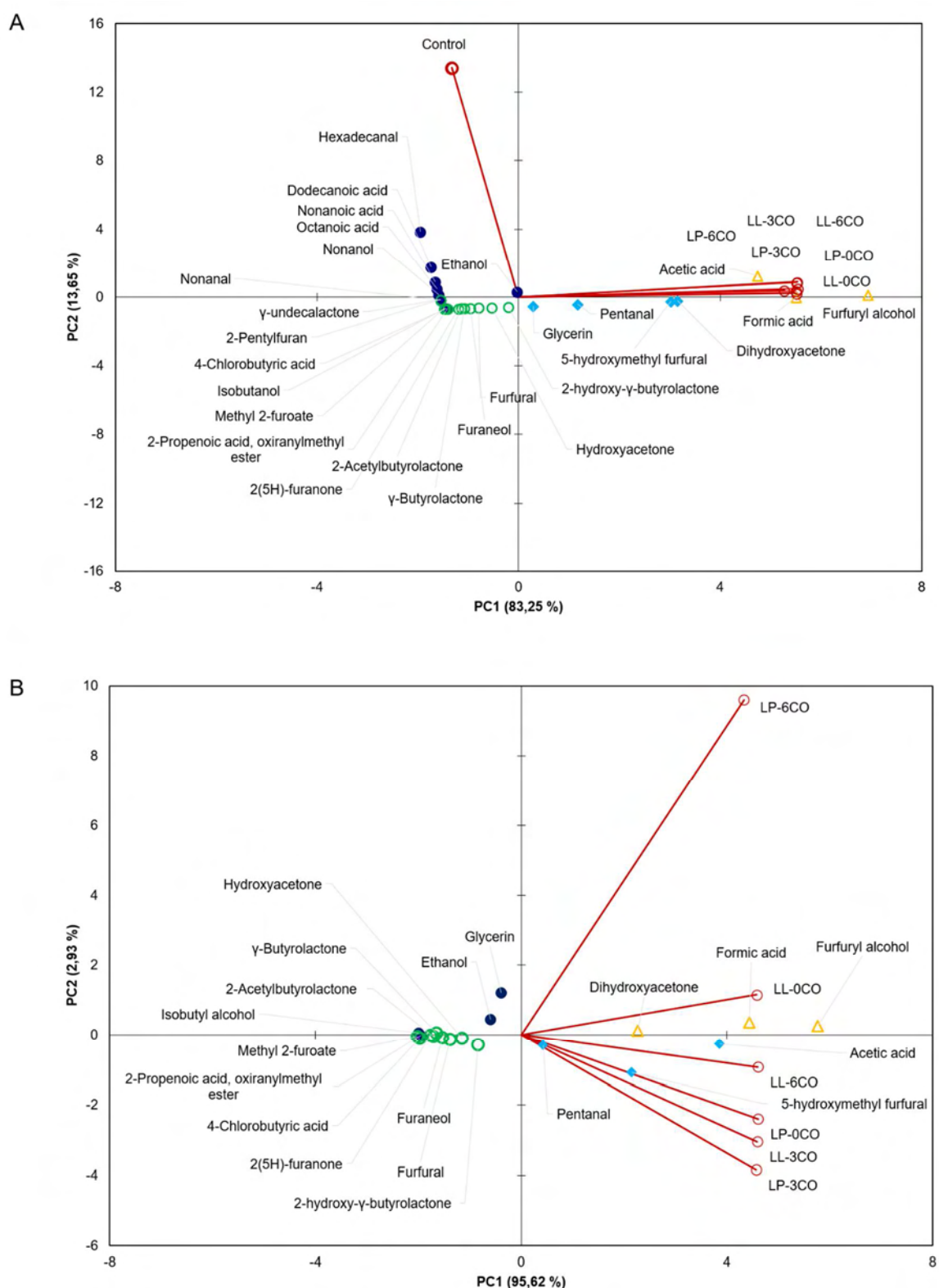


Figure 2: Principal component analysis (PCA) discriminating the molecules produced for each fermentation treatment used, A) with the control treatment, and B) with only the fermentation treatments. Components represent A) 96.9 % and B) 98.55 % of the analysed data. LL represents the treatments with *L. lactis* and LP with *L. plantarum*. 0CO, 3CO, and 6CO, represent the castor oil (CO) concentrations (0%, 3%, and 6%), and control treatment represents the unfermented treatment. Molecules are discriminated in quadrants representing their chemical origin (triangles for quadrant one primary metabolites, filled circles for quadrant two secondary metabolites, empty circles in quadrant three, and rhombus for quadrant four).

managed to produce similar molecules, and all the castor oil concentration treatments had no effect on the generation of differences in the aromatic profile. However, the control was discriminated against with molecules with a fat profile, because of the oil present in the unfermented treatment

Figure 2B, representing 98.55 % of the data, shows the discriminative analysis of treatments without the inclusion of the unfermented control. Variability are well represented in the analysis, where the first component PC1 represents 95.62 % of the total variance of data. In this analysis it can be seen that primary molecules of major metabolites, such as acetic acid and formic acid, are discriminated in quadrant one, the treatments were discriminated between microorganisms, and it can be observed that the concentration of castor oil had a significant effect at 6 % with the strain *L. plantarum*. This effect is not so significant in the treatments with *L. lactis*. It can also be seen that secondary metabolites are classified in the quadrant opposite to treatments, showing that there is no direct relationship in their production, regardless of the type of microorganism and the amount of substrate, and may be favoured by fermentation conditions.

Fermentations can be subjected to optimization of biotechnological parameters, to increase the generation of certain molecules using different substrates, or even new strains of lactic acid bacteria. This study managed to demonstrate the possibility of using whey as a raw material for biotechnological processes, and in this way, reduce its negative effect on the environment through its fermentation and use to generate added value.

Conclusion

Fermentation of whey and castor oil with the use of lactic acid bacteria proved to be a promising treatment to produce aromatic compounds. The analysis using gas chromatography-mass spectrometry (GC-MS) with solid-phase microextraction (SPME) was able to identify the production of several compounds, and the principal component analysis (PCA) allowed to discriminate the treatments, and observe the effect of fermentation in the generation of some compounds. Finally, this work is a contribution to the investigation in the use of new sources of substrates to generate flavour compounds, which implies the need to continue this type of studies, to achieve interesting aromatic bases to be used in natural flavours.

References

1. Parashar, A.; Jin, Y.; Mason, B.; Chae, M.; Bressler, D.C. Incorporation of whey permeate, a dairy effluent, in ethanol fermentation to provide a zero waste solution for the dairy industry. *J. Dairy Sci.* 2016;99(1):1859–1867.
2. Mukisa, I.M.; Byaruhanga, Y.B.; Muyanja, C.M.B.K.; Langsrud, T.; Narvhus, J.A. Production of organic flavor compounds by dominant lactic acid bacteria and yeasts from Obushera, a traditional sorghum malt fermented beverage. *Food Sci. Nutr.* 2017;5(1):702–712.
3. Chen, C.; Lu, Y.; Yu, H.; Chen, Z.; Tian, H. Influence of 4 lactic acid bacteria on the flavor profile of fermented apple juice. *Influence of 4 lactic acid bacteria.* *Food Biosci.* 2019;27(1):30–36.

Flavour enhancement of beer and related beverages by increasing flavour precursors in raw materials by enzymes

CLAIRE LIN LIN^{1,2}, Mikael Agerlin Petersen¹, and Andrea Gottlieb²

¹ Department of Food Science, University of Copenhagen, Copenhagen, Denmark

² Brewing AR 345, Novozymes A/S, Lyngby, Denmark

linlin@food.ku.dk

Abstract

In the past two decades, the brewing industry has witnessed the growing consumer demands for new beer types. Meanwhile, responsible drinking and health concern fuel the non-alcoholic and low-alcohol beer market. Towards this end, a plethora of literature has been dedicated to fermentation by non-conventional yeast strains, producing fruity flavours in beer and related beverages [1]. In parallel with this, it is feasible to achieve flavour improvement by using raw material to its fullness. This approach focuses on releasing more flavour precursor amino acids – leucine, isoleucine, valine, and phenylalanine – by enzymes during the beer manufacturing process. These branched-chain and aromatic amino acids participate in the Ehrlich pathway in yeast cells during fermentation, which accounts for the characteristic higher alcohols and their ester derivatives in beer [2]. Lab scale lager beer production was performed to demonstrate this method. GC-MS with stir bar sorptive extraction (Twisters) was applied to characterise the resulting products.

Keywords: beer, enzymes, flavour, non-alcoholic and low-alcohol beer

Introduction

In recent decades, health concern and responsible drinking propel new consumers to pursue non-alcoholic and low-alcohol (NABLAB) beer [1]. There are two main methods to produce this beer type: the physical method involving dealcoholisation and the biological method employing limited fermentation or non-*Saccharomyces* yeast strains. Nonetheless, NABLAB usually associates with taste deficiency compared to related normal strength beer [3]. Dealcoholisation compromises aroma compounds while evaporating alcohol or filtering through a membrane. Limited fermentation results in worty off flavour. Non-*Saccharomyces* yeasts oftentimes introduce novel fruity or floral aromas that can stand as a new beer category, as opposed to the low-alcohol version of the more conventional lager [1, 3]. In order to fulfil the criterion of NABLAB being ‘as close as possible’ to regular lager beer [4], the present study probes the possibility of using proteases to boost the yeast production of higher alcohols and esters relating to conventional lager. These volatiles are mainly from the Ehrlich amino acid degradation pathway. The compounds of interest are 2-methylpropyl alcohol and acetate from valine (Val), 2-methylbutyl alcohol and acetate from isoleucine (Ile), 3-methylbutyl alcohol and acetate from leucine (Leu), and 2-phenylethyl alcohol and acetate from phenylalanine (Phe). In brewing practice, free amino acids come from proteolysis during malting and mashing [5]. Here, we first compared the aforementioned higher alcohols and acetate esters between NABLAB and the related regular lager beer; and then studied the evolution of these compounds in fermentation of wort with added amino acids Val, Ile, Leu, and Phe. Finally, we tested the possibility to apply proteases in mashing to produce more flavoursome lager beer.

Experimental

Reagents and materials

Two commercial alcoholic beer and their corresponding non-alcoholic beer from two Danish manufacturers were used for gas chromatography-mass spectrometry (GC-MS) comparison. All amino acids were purchased from Sigma-Aldrich (St. Louis, MO, USA), and the amino acid stock solutions were sterile filtered before use. Pilsner malt from 2-row spring barley (Sophus Fuglsang Maltfabrik ApS, Haderslev, Denmark) was used in all mashing experiments. All enzymes were obtained from Novozymes A/S (Kongens Lyngby, Denmark).

Mashing and fermentation

High gravity mashing using a liquor/grist ratio of 3 was conducted in a mashing device LB12 (Lochner, Berching, Germany) to imitate industrial process. An infusion mashing program was employed: 45 °C (30 min) → 63 °C (30 min) → 72 °C (20 min) → 78 °C (10 min). Two serine proteases (SP1 and SP2) and two metalloproteases (MP1 and MP2) were added respectively at the beginning of the mashing experiment. Each mashing experiment was carried out in duplicate. At the end of the experiment, wort was obtained by gravity

filtration. A portion of wort (2.000 ± 0.020 mL) was measured by the alpha-amino nitrogen *O*-phthaldialdehyde (NOPA) method for free amino nitrogen content in a photometric analyser Gallery™ Plus Beermaster Discrete Analyzer (Thermo Scientific, Waltham, MA, USA). This resulting wort was boiled in 100 °C water bath for 60 min and sterile filtered before subsequent fermentation. A commercial lager yeast strain (Saflager-34/70, Fermentis, FR) was pitched at 1.5×10^6 viable cells/mL and fermentation was carried out with 14 °Plato wort at 14 °C for 7 days.

GC-MS analysis

The polydimethylsiloxane coated stirring bars, Twister® of 10 mm length and 0.5 mm film thickness (Gerstel, Mülheim an der Ruhr, Germany) were used for sorptive extraction sampling. Volatile compounds were thermally desorbed and analysed using an Agilent 5977B GC/MSD single quadrupole system (Agilent Technologies, Santa Clara, CA, USA). The evolution of volatiles from fermentation of wort containing spiked-in amino acids, was studied using dynamic headspace sampling. The samples were purged with nitrogen and volatiles were trapped on Tenax-TA before thermally desorbed and analysed using an Agilent 5975C GC/MSD Triple-Axis Detector system (Agilent Technologies, Santa Clara, CA, USA).

Results and discussion

In general, the volatiles derived from the Ehrlich amino acid degradation pathway appeared less in NABLAB (F1 and F2, Figure 1) compared to the corresponding regular strength lager beer (B1 and B2, Figure 1). This confirmed the aroma deficiency issue in NABLAB, and thus the shift of focus to the generation of these higher alcohols and acetate esters with amino acid addition. Higher alcohols and acetate esters are produced by yeasts via a three-step catabolic pathway [2]. After amino acid uptake, transamination leads to an α -ketoacid intermediate; an irreversible decarboxylation of this intermediate results in an aldehyde that undergoes reduction to the corresponding alcohol. Further, the alcohol couples with an acetyl coenzyme A to produce the acetate ester. Examination of higher alcohols and acetates evolution with spiking samples at Day 2, Day 4, and Day 6 confirmed such metabolism. For instance, aldehyde intermediates detected in spiking trials in Figure 2 reached maxima at Day 2. This was due to the incomplete reduction of this intermediate at an early fermentation stage. This may partially contribute to aldehyde off-flavours in NABLAB produced by limited fermentation, besides the aldehydes from enzymatic reaction – lipid oxidation, and biochemical reaction – Strecker degradation of amino acids, during malting and mashing. Higher alcohols, on the other hand, increased over the first 4 days and either reached a plateau or decreased afterwards, which could be caused by esterification consuming these higher alcohols. Again, esterification was evidenced by the increase of acetate esters at the end of fermentation in Figure 2. In summary, spiking in these chosen amino acids led to the increase of corresponding higher alcohols and acetates from controls.

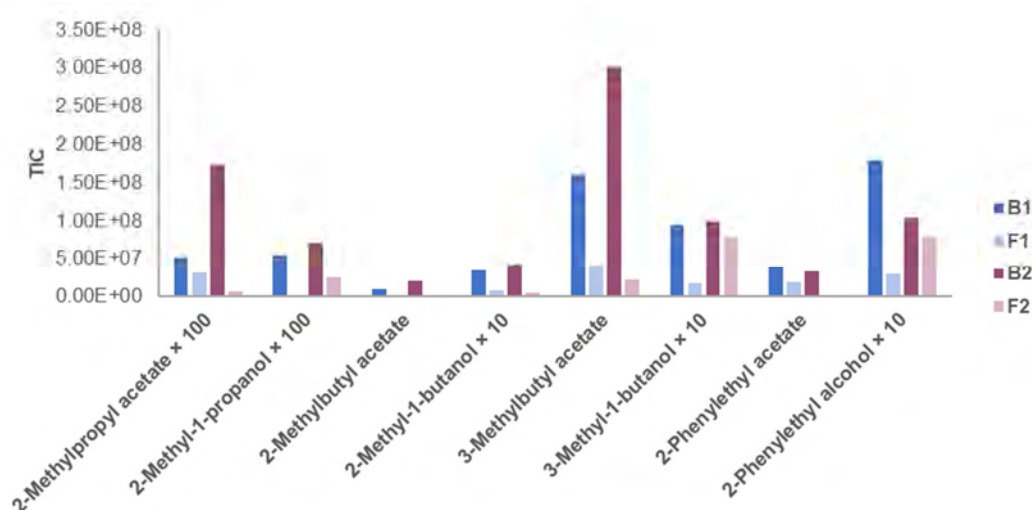


Figure 1: Higher alcohols and corresponding acetate esters in NABLAB (F1 and F2) vs. normal strength beer (B1 and B2). Some volatiles are multiplied by 10 or 100 to improve visibility.

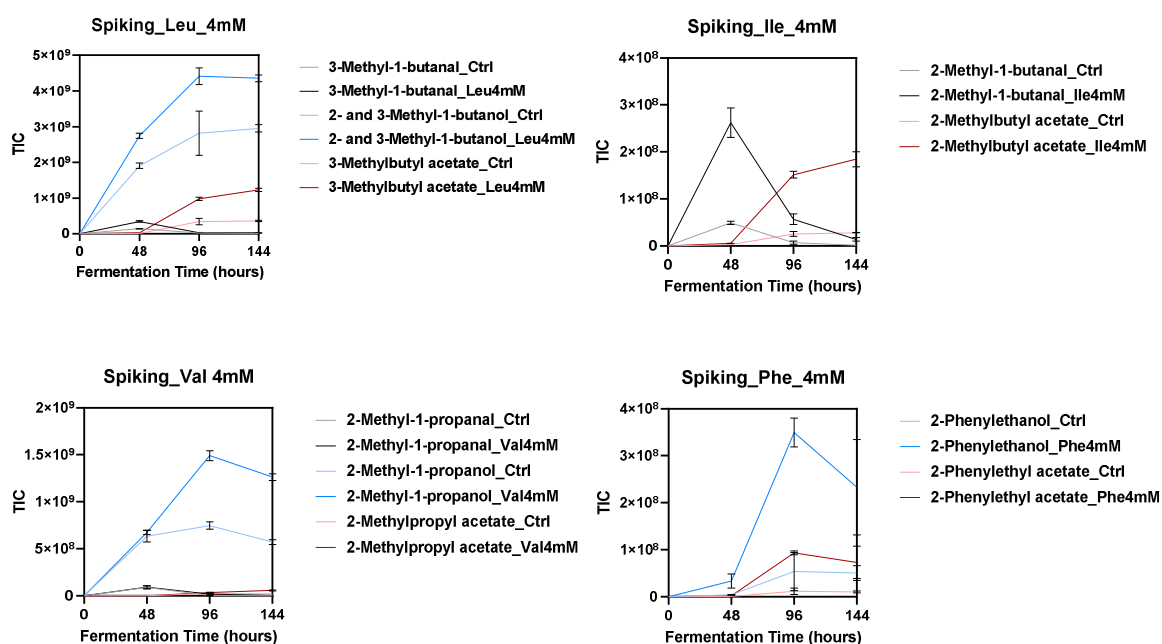


Figure 2: Fermentation of 14 °Plato wort with spiked-in Leu 4mM (upper left), Ile 4mM (upper right), Val 4mM (lower left), and Phe 4mM (lower right). It was noted that 2- and 3-methylbutanol from Ile and Leu respectively, could not be separated.

With these observations in hand, fermentation was conducted with wort derived from protease-treated mash to examine the impact of protease on amino acids (Val, Ile, Leu, and Phe) in wort, and relevant higher alcohols and acetates after fermentation. Figure 3 shows that wort from SP1, MP1, and MP2-treated mashing led to more acetate esters, i.e. 2-methylpropyl acetate from Val, 2- and 3-methylbutyl acetates respectively from Ile and Leu, and 2-phenylethyl acetate from Phe. On the other hand, higher alcohol productions varied. Fermentation following protease-treatment appeared at similar or even lower levels of 2-methylpropyl alcohol, 2-methylbutyl alcohol, and 3-methylbutyl alcohol, compared to control; but 2-phenylethyl alcohol was higher after enzyme treatment. This could be explained by esterification consuming these higher alcohols. It might be that these four higher alcohols were increased to different extent after fermentation (of wort derived from enzyme-treated mash), with 2-phenylethyl alcohol being higher than the rest. Esterification led to lower concentrations of higher alcohols but higher concentrations of acetates. A high 2-phenylethyl alcohol level resulted in more 2-phenylethyl acetate but also retained more starting material afterwards, which was observed in Figure 3.

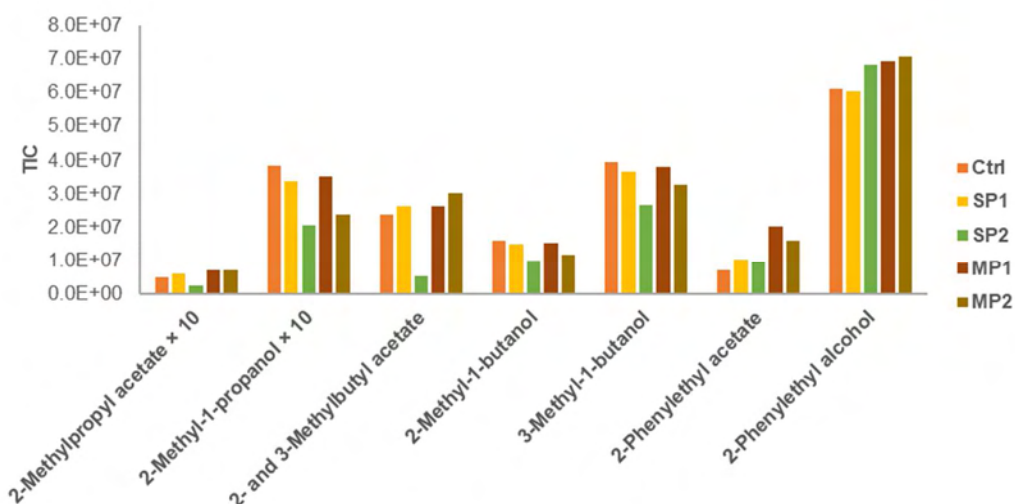


Figure 3: Volatiles from the Ehrlich amino acid degradation pathway after fermentation of wort derived from protease-treated mash vs. control. Some volatiles are multiplied by 10 to improve visibility.

Application of proteases usually result in more free amino nitrogen (FAN) that comprise of free amino acids and peptides, which was the case in this mashing experiment (Figure 4). Nonetheless, the increase of FAN did not necessarily correlate to the increase of these higher alcohols or acetates after fermentation, as was shown by the results from SP2. SP2 produced similar level of FAN as that by SP1 (Figure 4), and yet 2-methylpropyl alcohol and acetate, 2-methylbutyl alcohol and acetate, and 3-methylbutyl alcohol and acetate after fermentation of wort from SP2-treated mash differed from those from SP1 (Figure 3). Further quantification of free amino acid composition in the wort can better elucidate the impact of protease on the generation of these higher alcohols and acetates.

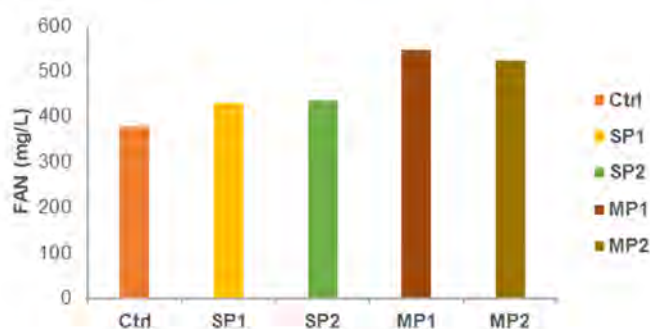


Figure 4: Free amino nitrogen after mashing.

Conclusion

This work focused on aromas derived from the Ehrlich pathway in yeasts. GC-MS comparison of NABLAB and related regular lager beer confirmed the aroma deficiency in the former beer type. Further investigation in aroma evolution from Val, Ile, Leu, and Phe in the spiking trials confirmed the effects of these amino acids on the formation of their corresponding higher alcohols and acetate esters. Finally, increases in acetate esters were observed in protease-treatment and showcased the potential of this method to increase aromas via the Ehrlich pathway.

References

1. Bellut K, Michel M, Zarnkow M, Hutzler M, Jacob F, De Schutter DP, et al. Application of Non-Saccharomyces Yeasts Isolated from Kombucha in the Production of Alcohol-Free Beer. *Fermentation-Basel*. 2018;4(3):19.
2. Pires EJ, Teixeira JA, Branyik T, Vicente AA. Yeast: the soul of beer's aroma—a review of flavour-active esters and higher alcohols produced by the brewing yeast. *Appl Microbiol Biotechnol*. 2014;98(5):1937.
3. Bellut K, Arendt EK. Chance and Challenge: non-Saccharomyces yeasts in nonalcoholic and low alcohol beer brewing—a review. *J Am Soc Brew Chem*. 2019;77(2):77.
4. Blanco CA, Andres-Iglesias C, Montero O. Low-alcohol Beers: flavor compounds, defects, and improvement strategies. *Crit Rev Food Sci Nutr*. 2016;56(8):1379.
5. Aldred P, Kanauchi M, Bamforth CW. An Investigation into Proteolysis in Mashing. *J Inst Brew*. 2021;127(1):21.

Evaluation of methodology to follow volatile composition over time

LENA CHARLOTTE STRÖHLA and Mikael Agerlin Petersen

Department of Food Science, University of Copenhagen, Rolighedsvej 30, DK-1958 Frederiksberg C, Denmark, lcs@food.ku.dk

Abstract

This study aims to evaluate the effect of freezing on the aroma profile of cooked Great Northern beans during storage and whether the method to follow volatiles over a long period can be improved by the use of an external control solution. The use of external control solution shall correct instrumental drifts and allow valid quantifications. Therefore, Great Northern beans (*Phaseolus vulgaris* L., thermally processed, in plastic pouches) were stored at 42 °C for five weeks. The study was conducted as groundwork for a 12 months shelf-life evaluation to observe the flavour evolution of Great Northern beans at different storage conditions. Since the effect of freezing on the volatile composition of Great Northern beans is unknown and could introduce a systematic error, the analysis of the volatile composition was performed both on fresh samples immediately after takeout and on samples taken out and stored frozen until the end of the study. The volatile composition was measured by dynamic headspace sampling combined with gas chromatography-mass spectrometry (GC-MS). All samples were analysed together with a solution containing several external standards to monitor and correct for instrumental drift over time. In this study, only two compounds were selected as external standards and belong to different chemical groups found in the sample. Each external standard showed a different response over time. By calculating the relative response factor of each standard, the concentration of the volatiles belonging to the same chemical group was corrected. Most compounds showed higher levels in the frozen samples than fresh. After 14 days, the impact of freezing increased for benzaldehyde and furfural. In terms of long storage experiments, this could have a significant effect on the result. The difference due to freezing could be explained by several hypotheses. The freezing and thawing could induce degradation of pre-formed volatiles or degradation could take place due to oxidation processes. Also, the freezing process and the crystallisation could damage and modify the structure/microstructure and thus facilitate diffusion out of the sample during headspace sampling. Further research is needed to understand the mechanism behind the changes and to gain insight in the effect of freezing on the overall aroma and sensory quality of the beans.

Keywords: flavour, shelf-life, Great Northern bean, time-resolved analysis, accelerated storage

Introduction

Across shelf-life, the quality of a food product can change as a result of various reactions leading to sensory changes with a possibly negative impact on the consumer's food experience [1]. As shelf-life studies can take up to several months or years, it is crucial to standardise and control the instrumental analysis. A time-resolved analysis is often hard to conduct, especially over a long period due to instrumental drifts. A common method is to freeze the samples until the end of the study and analyse them collectively at once, which has many advantages. The analytical conditions are constant and logistics are simple under the assumption that freezing has no effect on the aroma.

Another method is the additional analysis of standards to increase the robustness and validity over time [2]. Internal standards correct individual sampling inaccuracies and instrumental drift and hence constitute quality control of each individual sample. External standards are directed to the instrumental performance as a quality control of the instrument. As a tool to monitor and correct instrumental drifts over time, a control solution containing external standard compounds can be measured with every analysis of the samples. The compounds of the control solution are selected based on the chemical groups present in the samples to be analysed. A variety of compounds gives a more accurate knowledge about the response of the mass spectrometer detector (MS) to each chemical group. It gives control over the sensitivity and allows a more precise quantification for each group. Therefore, the relative response factor (RRF) between the internal and each external standard of the control solution is calculated. The RRF is defined as the ratio between the response factors of two compounds. The response factor of the analysed compound is described as the ratio between its concentration and the response of the detector to the compound. The response is expressed as the peak area and is influenced by variations of the gas chromatography system (GC) and method. To eliminate those variations, the RRF can be used to ensure a precise quantification.

This study concerns Great Northern beans (*Phaseolus vulgaris* L.) which belong to the group of pulses, which are high in protein and nutrients with a low environmental footprint [3]. The application possibilities of pulses are diverse, but still restricted by difficulties with off-flavours constituting a barrier to mainstream consumption [4]. The impact of freezing and accelerated storage on the volatile composition of cooked Great Northern beans has

not been investigated in past studies. As groundwork for a 12 months shelf-life study on the flavour evolution of Great Northern beans, the volatile profile of cooked Great Northern beans was followed throughout an accelerated storage in this study. It was investigated if 1) freezing is an appropriate way of stabilizing samples from a shelf-life experiment and if 2) monitoring of volatiles can be improved by adding the analysis of an external control solution.

Material and methods

Samples

Dry Great Northern beans (*Phaseolus Vulgaris L.*) were processed at Greenyard (Bree, Belgium). The dry beans were soaked overnight in water, drained and filled into white plastic pouches. Each pouch was filled with 100 g beans and 150 g water, sealed and heat treated for 20 min at 160 °C. After cooling, pouches were packed and shipped to the University of Copenhagen (Copenhagen, Denmark). Upon arrival, the storage of the samples started at 42 °C for five weeks. Samples were taken out weekly. The analyses were performed on fresh samples immediately after take out and on thawed samples which were stored frozen until the end of the study. The frozen samples were thawed overnight at room temperature. For the analysis, the beans were drained, rinsed and blended with water (1:1).

External control solution

The control solution was measured in triplicates with every GC run of the samples. It contained two compounds as external standard and one internal standard (4-methyl-1-pentanol, 0.12 ppm). The two compounds of the control solution were nonanal (0.048 ppm) and 2-pentylfuran (0.019 ppm) representing aldehydes and furans. The pure compounds were first diluted with dipropylene glycol, and then with water.

The relative response factor (RRF) was calculated for each compound (X) in the control solution by the following equation (c = concentration; Area = peak area; ISTD = internal standard):

$$\text{Relative response factor RRF} = \frac{c_{X,\text{control solution}} * \text{Area}_{\text{ISTD,control solution}}}{c_{\text{ISTD,control solution}} * \text{Area}_{X,\text{control solution}}}$$

The concentration of each volatile compound (A) found in the sample was corrected by the following equation using the RRF of the compound belonging to the same chemical group:

$$c_{\text{compound A}} = \frac{\text{Area}_{\text{compound A,sample}} * c_{\text{ISTD,sample}}}{\text{Area}_{\text{ISTD,sample}}} * \text{RRF}$$

Dynamic headspace GC-MS analysis

The volatile composition was analysed by using GC-MS with dynamic headspace sampling (DHS). The samples were analysed in triplicates. For each measurement, 20 g of the bean blend and 0.5 mL of internal standard (4-methyl-1-pentanol in water, 5ppm) were added to the DHS flask. The volatiles were captured by a trap containing 200 mg Tenax TA. The flask was placed in a water bath at 37 °C. The purge time was 20 min with a nitrogen flow of 200 mL/min and stirring rate of 200 rpm. The trap was dry-purged for 10 min with the same flow. The volatiles were released from the trap through an automated two-stage thermal desorption unit (TurboMatrix 350, Perkin Elmer, Shelton, USA) into the GC-MS system (GC-MS, 7890A GC-system interfaced with a 5975C VL MSD with Triple-Axis detector from Agilent Technologies, Palo Alto, California) as described by Alstrup [5].

Data analysis

The peak areas, mass spectra and retention times were extracted from the chromatograms by using PARADISE (University of Copenhagen, Denmark). The software is based on PARAFAC2 modelling. The match factor of NIST databank and the retention index was used to identify the volatile compounds. Statistical analyses were performed with JMP (14.0, SAS).

Results and discussion

External control solution

The relative response factor (RRF) for each compound over time was visualised in a control chart (Figure 1) as a tool to monitor the instrumental performance. Each data point in the graph represents the average RRF of three replicates of the same control solution on the given day (in one GC sequence). The control solutions 'Frozen (1) – (4)' were analysed together with the frozen samples in the same GC sequences. The green centre line (μ_0) represents the average measurement from the first 12 weeks of the experiment. The red lines are the control limits (upper and lower, UCL and LCL) which are +/- three times the standard deviation. The control limits are used as

a tool to monitor the stability of the signal. If a measurement is outside the limits, it indicates a lack of stability [2].

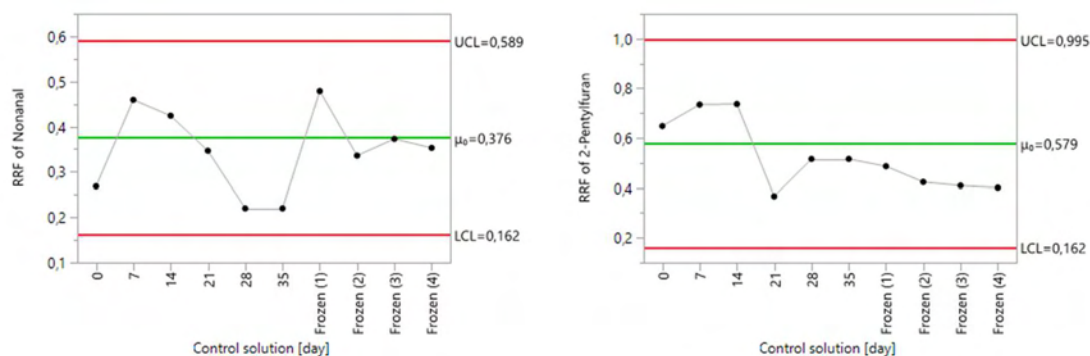


Figure 1: Control chart of nonanal (left) and 2-pentylfuran (right). Control solutions of day 0 – 35 were measured with fresh samples and Frozen (1) – (4) were measured with the frozen samples.

All measurements were within the control limits. Nevertheless, the control charts visualise that the instrumental signal responses change over time and the different external standards do not change in the same way. Based on this observation, the application of the RRF for each chemical group of compounds is necessary to eliminate the instrumental drift.

Application of response factor on selected compounds in sample

The RRF of nonanal and 2-pentylfuran was applied to a selection of aldehydes and furans found in the samples. The changes over time of the concentration of nonanal, benzaldehyde, 2-pentylfuran and furfural in the sample are shown in Figures 2 and 3. The concentrations differ between fresh and frozen samples. Frozen samples show higher levels of benzaldehyde, 2-pentylfuran and furfural, whereas nonanal reaches the highest values in the fresh samples. After 14 days, the difference between the fresh and frozen samples becomes more significant for benzaldehyde and furfural.

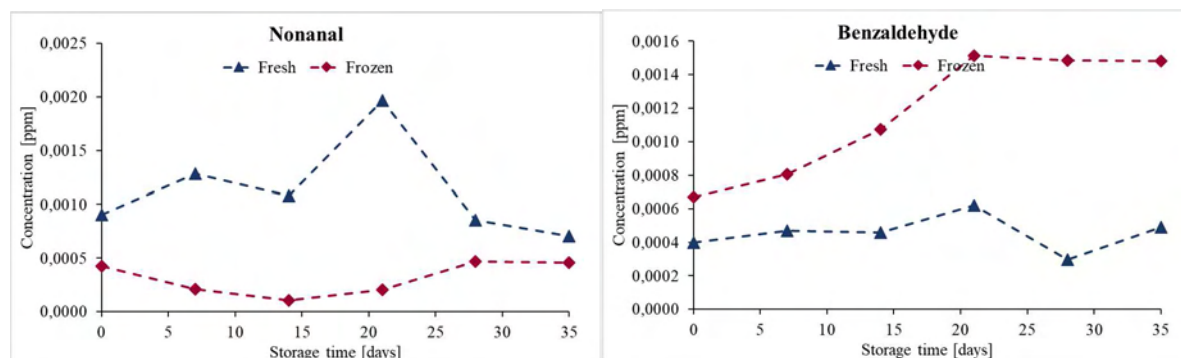


Figure 2: Concentration of nonanal (left) and benzaldehyde (right) in fresh (blue) and frozen (red) samples across accelerated storage.

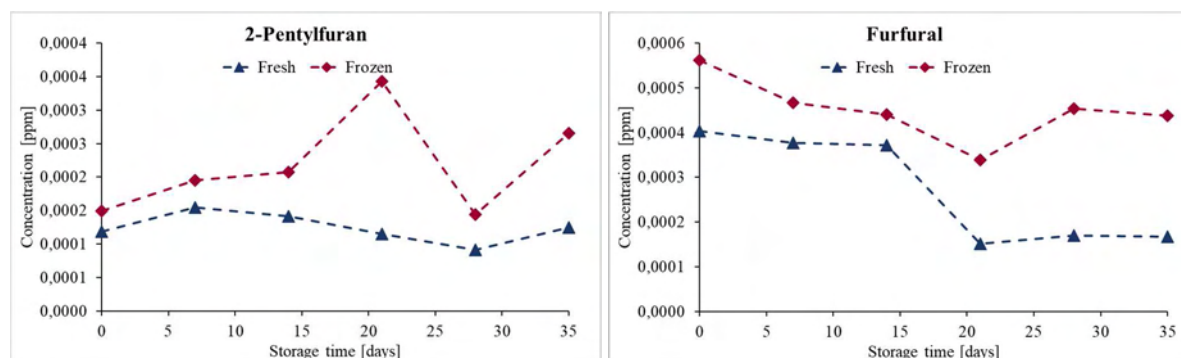


Figure 3: Concentration of 2-pentylfuran (left) and furfural (right) in fresh (blue) and frozen (red) samples across accelerated storage.

Discussion

If the difference between fresh and frozen samples increases over time as shown for benzaldehyde and furfural, it could affect the result of long storage experiments (up to one year) more significantly. Assuming that the correction with the response factors gives accurate results, the levels of benzaldehyde and furfural in the fresh samples did not significantly change over time. Consequently, the freezing process or frozen storage must have affected the volatile concentration of benzaldehyde and furfural in the frozen samples. In other studies about the effect of freezing, the time of the frozen storage played an important role for aroma. Iglesias et al. [6] found that frozen storage of gilthead sea bream fish lead to an increase of volatiles which correlated with oxidation markers. Another study on the aroma of black truffles showed a major change in volatiles, which were identified as possible freezing markers, after 20 and 40 days of frozen storage [7]. Based on those studies, the volatile composition of the bean samples could be affected by the accelerated as well as the frozen storage. In terms of the frozen bean samples, the level of benzaldehyde significantly increased after 14 days of accelerated storage. Those samples were stored frozen for a shorter time than the samples with a lower level of benzaldehyde before day 14. It could be discussed if frozen storage lead to a decrease of benzaldehyde assuming that the level should not change over time as observed in the fresh samples. However, it would still result in a significant difference between fresh and frozen samples. It shows that the two approaches of monitoring volatiles over time could result in different conclusions. Nevertheless, further research is needed to include all important chemical groups in the external standard solution to get a more complete overview.

Conclusion

This study presents an evaluation of two approaches to follow the volatile composition over time. The analysis of an external control solution showed that instrumental signal responses change over time. The change of response is not the same for each analysed compound, so that it is necessary to correct the volatile compounds in the sample by the relative response factor. By comparing the analysis of fresh and frozen samples, it shows that freezing of the samples affects the concentration of selected volatiles. Most compounds showed higher levels in frozen than in fresh samples. To get a more complete overview of the changes and the impact of freezing, all important chemical groups need to be included as external standards. The difference due to freezing could be explained by several hypotheses. The freezing and thawing could induce degradation of pre-formed volatiles and oxidation processes. The freezing process and the crystallisation could damage and modify the structure/microstructure and thus facilitate diffusion out of the sample during headspace sampling. As there is no available literature on the influence of freezing on the aroma of Great Northern beans, further research is needed to comprehend the underlying mechanism of the changes to gain insight in the effect of freezing on the overall aroma and sensory quality of the beans.

References

1. R. Marsili, *Sensory-Directed Flavor Analysis*. 2006, CRC Press.
2. M. Bueno, V. C. Resconi, M. M. Campo, V. Ferreira, and A. Escudero. Development of a robust HS-SPME-GC-MS method for the analysis of solid food samples. Analysis of volatile compounds in fresh raw beef of differing lipid oxidation degrees. *Food Chem.* 2019;281:49-56. doi: 10.1016/j.foodchem.2018.12.082.
3. Z. Ma, J. I. Boye, B. K. Simpson, S. O. Prasher, D. Monpetit, and L. Malcolmson. Thermal processing effects on the functional properties and microstructure of lentil, chickpea, and pea flours. *Food Res Internat.* 2011;44(8):2534-2544. doi: 10.1016/j.foodres.2010.12.017.
4. W. S. U. Roland, L. Pouvreau, J. Curran, F. van de Velde, and P. M. T. de Kok. Flavor Aspects of Pulse Ingredients. *Cereal Chem.* 2017;94(1):58-65. doi: 10.1094/cchem-06-16-0161-fi.
5. J. Alstrup, M. A. Petersen, F. H. Larsen, and M. Münchow. The Effect of Roast Development Time Modulations on the Sensory Profile and Chemical Composition of the Coffee Brew as Measured by NMR and DHS-GC-MS. *Beverages* 2020;6(4):70. Available: <https://www.mdpi.com/2306-5710/6/4/70>.
6. J. Iglesias, I. Medina, F. Bianchi, M. Careri, A. Mangia, and M. Musci. Study of the volatile compounds useful for the characterisation of fresh and frozen-thawed cultured gilthead sea bream fish by solid-phase microextraction gas chromatography–mass spectrometry. *Food Chem.* 2009;115(4):1473-1478. doi: 10.1016/j.foodchem.2009.01.076.
7. L. Cullere, V. Ferreira, M. E. Venturini, P. Marco, and D. Blanco. Chemical and sensory effects of the freezing process on the aroma profile of black truffles (*Tuber melanosporum*). *Food Chem.* 2013;136(2):518-25. doi: 10.1016/j.foodchem.2012.08.030.

Generation of meaty flavour compounds from Maillard origin under mild conditions simulating the dry curing process

Lei Li, Carmela Belloch and MÓNICA FLORES

Instituto de Agroquímica y Tecnología de Alimentos (IATA-CSIC), Avda. Agustín Escardino 7, 46980 Paterna, Valencia, SPAIN, mlflores@iata.csic.es

Abstract

The flavour of dry cured meat products is generated under mild temperatures at long ripening periods. In these conditions, the generation of dry cured aroma compounds from Maillard reactions is unknown. The aim of this study was to evaluate the generation of volatile compounds under mild curing conditions simulating the drying process of fermented sausages. Three model systems labelled initial (I), 1st drying (1D) and 2nd drying (2D) containing different concentrations of amino acids and curing additives, as well as different pH and a_w values, were incubated at different temperatures. The flavour profile was investigated by SPME-GC-MS and the amino acid content was measured by GC-FID. Four compounds detected, dimethyl disulphide, 3-(methylthio)propanal, thiazole and methylpyrazine, were the source of meaty-roasted aromas among seventeen volatile compounds identified in the model systems. The production of dimethyl disulphide and 3-(methylthio)propanal was related to the Strecker degradation of methionine. Thiazole and methylpyrazine increased significantly during the incubation time, although this increase was significantly higher when the model systems were incubated at 37 °C. The presence of methylpyrazine was favoured by presence of lysine and high pH values. This research demonstrates that at mild curing conditions volatile compounds are generated via Maillard reactions from free amino acids. The a_w of model systems resembling the 1st and 2nd drying stages together with the presence of free amino acids was essential for the formation of meaty flavour compounds.

Keywords: Maillard, meat, dry curing, water activity, amino acid

Introduction

Meat flavour formation in dry cured meat products is still a challenge, despite the numerous efforts to describe many savoury aromas [1]. The nitrogen-containing and sulphur-containing compounds are essential for development of meaty aroma in these products. However, the participation of the Maillard reaction (MR) in the formation of dry cured meat flavour is not well known [2, 3]. The mechanisms involved in the formation of meaty flavour compounds in dry fermented sausages and the influence of the physicochemical conditions such as pH and low temperature are poorly comprehended. For this reason, generation of aroma compounds from three model systems containing amino acids and additives (NaCl, nitrate/nitrite, ascorbate, glucose) in composition similar to dry sausages [4] were investigated under the physicochemical conditions (pH, a_w and temperature) simulating the initial, first drying and second drying stages of the sausage manufacture [5]. The model systems were incubated at 25 °C and 37 °C and the meaty aromas formed from the degradation of methionine, lysine and glycine were examined during 35 days of incubation. This study examines the generation of meaty aroma compounds in model systems resembling dry fermented sausages under mild curing conditions.

Experimental

Three different model systems (Table 1) were prepared according to the concentration of additives and free amino acids at the initial (I), 1st drying (1D) and 2nd drying (2D) stages of the process [6]. Phosphate buffer at 0.2 mM was used to adjust the pH, while glycerol was used to adjust the a_w at the different processing stages. Sterilization was done by filtration using a 0.2 µm filter (Sartorius, Göttingen, Germany), and incubation was performed at 25 and 37 °C. Samples from each media and temperature were taken at different times (0, 5, 11, 15, 20, 25, 29 and 35 days) for volatile and amino acid analyses.

Analysis of Volatile Compounds

The analysis of volatile compounds generated during the incubation of models was carried out in a gas chromatograph with a quadrupole mass spectrometer detector GC-MS (GC 7890 series II, MS 5975C, Agilent Palo Alto, CA, USA). For volatile extraction, 5 mL of the model system was placed into a headspace vial and extracted using an automatic sampler Gerstel MPS2 (Gerstel, Germany) by headspace (HS) solid-phase microextraction (SPME) with a 85 µm carboxen/polydimethylsiloxane (CAR/PDMS) fibre (Supelco, Bellefonte, PA, USA).

Before extraction vials were equilibrated at 37 °C for 30 min and then, volatile compounds were adsorbed into the fibre for 60 min at 30 °C and desorbed in the injection port of the GC–MS for 5 min at 240 °C in splitless mode. The volatile compounds were separated using a DB-624 capillary column (30 m, 0.25 mm i.d., film thickness 1.4 µm (J&W Scientific, Agilent Technologies, Palo Alto, CA, USA) using the conditions described by Corral et al. [7]. The MS interface temperature was set to 240 °C. The compounds were identified in full scan mode and by comparison with mass spectra from the library database (Nist'05), with linear retention indices [8] and using authentic standards. The quantitation was performed in SCAN mode using total ion current (TIC) and expressed as abundance units (AU) × 10⁶.

Table 1: Composition of model systems resembling the dry curing stages.

Dry curing stages	Initial stage (I)	1 st drying stage (1D)	2 nd drying stage (2D)
pH	5.45	4.38	4.6
Aw	0.968	0.944	0.895
NaCl (mg/ml)	27	27	27
NaNO ₂ (mg/ml)	0.15	0	0
NaNO ₃ (mg/ml)	0.15	0.1	0.075
Sodium ascorbate (mg/ml)	0.5	0.5	0.5
Glucose (mg/ml)	20	5	5
Glycine (mg/100ml)	10.94	33.06	42.58
Methionine (mg/100ml)	2	33.99	36.27
Lysine (mg/100ml)	6.82	77.55	120.9

Analysis of Amino Acids

The analysis of free amino acids was performed using the EZ-Faast kit (Phenomenex, Torrance, CA, USA). Model system samples were diluted with distilled water at ratio 1:5 (v/v) for I stage, and 1:25 (v/v) for 1D and 2D stages previously to derivatisation and norvaline was added as the internal standard. The derivatised amino acids were analysed using a gas chromatograph with a flame ionization detector (GC-FID) (GC 7890B, Agilent, Palo Alto, CA, USA) equipped with a liquid autosampler (G4513A, Agilent Palo Alto, CA, USA) and a ZB-AAA column (10 m× 0.25mm) (Phenomenex, Torrance, CA, USA). The analysis was done using the conditions described by Li et al., 2021 [6]. Identification and quantification were based on retention time and peak area integration of the reference amino acids. Calibration curves for each amino acid were obtained with the standard amino acids solutions (Phenomenex). Results were expressed in milligrams per 100 mL of model system.

Statistical analyses

The effect of incubation time on volatile compounds and amino acid content was studied by analysis of variance (ANOVA) using the statistic software XLSTAT2018 (Addinsoft, Barcelona, Spain). Principal component analysis (PCA) was plotted to evaluate the relationships between volatile compounds and amino acids in the different models and incubation temperatures.

Results and discussion

Among the volatile compounds detected [6], four compounds, dimethyl disulphide, 3-(methylthio)propanal, thiazole, and methylpyrazine produced meaty-roasted aromas of great impact in dry sausage flavour [1]. The concentration of the amino acids precursors of these volatiles in the model systems (met, gly and lys) were determined, revealing that only met concentration showed a significant decreased during incubation (Figure 1). The highest production of these four aroma compounds was observed in 1D and 2D model systems incubated at 37°C (Figure 2). The high glucose content of the Initial model (I) is not essential for the generation of these volatile compounds, as none of them were produced in high abundances in the I model.

Furthermore, the Strecker degradation of met was related to the production of dimethyl disulphide and 3-(methylthio)propanal. Regarding pH and a_w conditions, model 1D with lower pH and higher a_w than 2D favoured the formation of dimethyl disulfide and 3-(methylthio)propanal. The evolution of 3-(methylthio)propanal was different from the other volatile compounds as it increased with the incubation time until 10 to 15 d, and then it decreased specially in 1D model. Thiazole and methylpyrazine increased significantly during incubation in 1D and 2D models, especially at 10 days of incubation at 37 °C, while at 25°C this increase was detected at longer

incubation times (25 or 30 days). The presence of lys and gly and the low pH values in the models favoured the presence of methylpyrazine, although other factors seem to affect its generation.

In order to examine the relationship between amino acids and flavour compounds generated in the 1D and 2D models a principal component analysis (PCA) was performed (Figure 3). Two principal components were able to explain the 86.47% of the total variability. PC1 accounted for 59.28% of the variability and was strongly related with the incubation time and temperature. Long incubation times and high temperature were located on the left quadrant, while short incubation times and low temperature were on the right. PC2 accounts for 27.20% of the variability and distinguishes samples by model systems and variables (volatile compounds and amino acids). The model systems 2D and variables (dimethyl disulphide, thiazole, methylpyrazine and gly and lys) were on the upper quadrant while on the low quadrant were 1D model and variables (3-(methylthio)propanal and met). It is important to see that 3-(methylthio)propanal is opposite to met while methylpyrazine is opposite to gly and lys. This means that degradation of these amino acids is related with the formation of these compounds as observed for met (Figure 1).

The mild conditions applied were enough to generate aroma compounds in the model systems as observed in other media [9]. However, in dry meat products, as seen in 1D and 2D models, the limiting factor to produce volatile compounds from Maillard reactions is the amino acid content as well as temperature and a_w conditions, while the content of saccharides seems to be no essential.

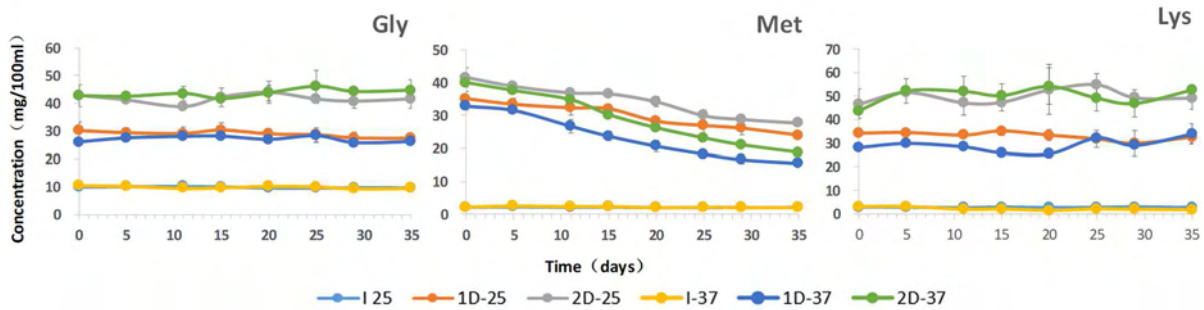


Figure 1: Amino acid concentration in the model systems (mg/100 mL) during incubation at 25 °C or 37 °C and classified according to the dry curing stages (I-Initial stage, 1D-1st drying stage, 2D-2nd drying stage).

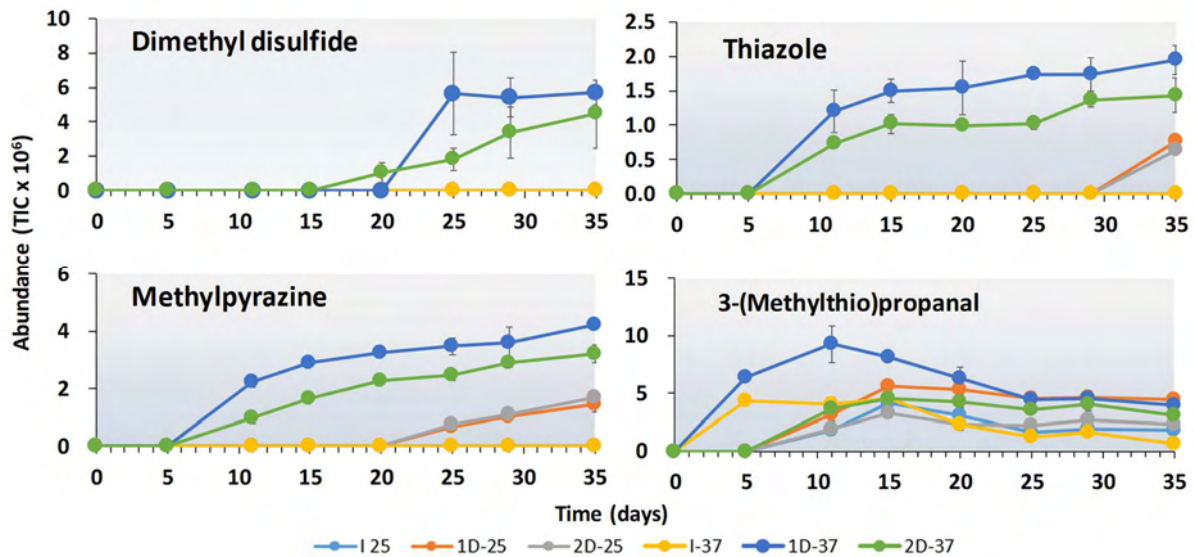


Figure 2: Abundance of volatile compounds in the dry cured model systems (I-Initial stage, 1D-1st drying stage, 2D-2nd drying stage) incubated at different temperatures 25 °C and 37 °C.

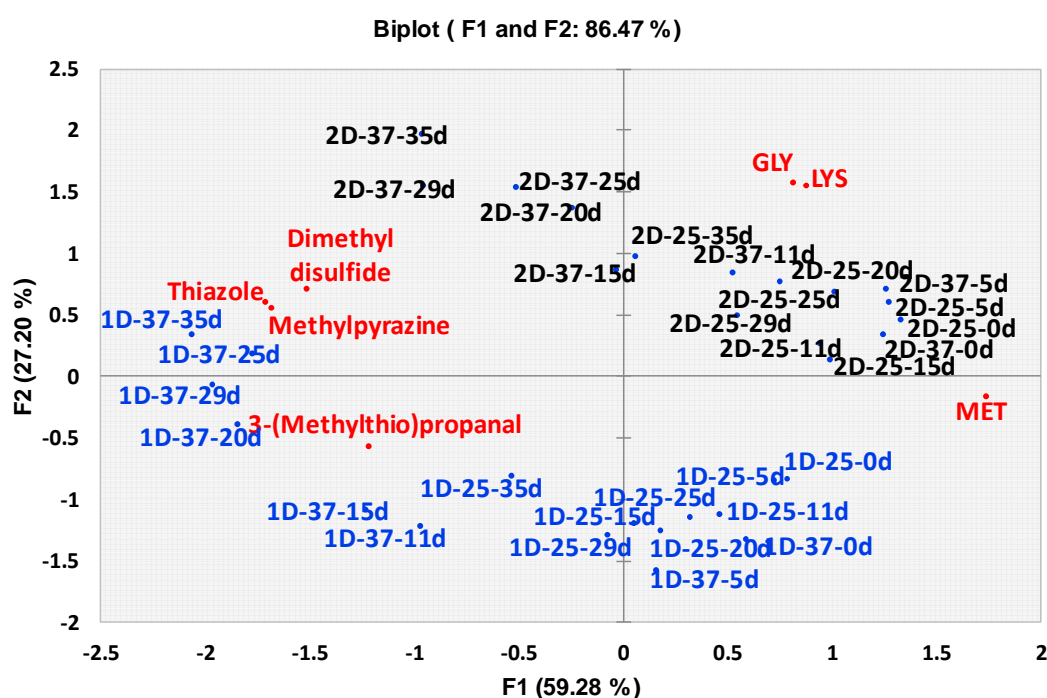


Figure 3: Loadings of the first two principal components (PC1-PC2) of model systems simulating the dry curing stages (1D-1st drying stage, 2D-2nd drying stage) and variables (volatile compounds and amino acids).

Conclusion

Generation of meaty flavour compounds under mild conditions has been demonstrated in model systems simulating the dry curing process in terms of amino acid content, pH, a_w and additives. This experiment proved that free amino acids participate in the generation of volatile compounds via the Maillard reaction in addition to the microbial activity in dry fermented meat products. Moreover, the low water activity of models resembling the 1st and 2nd drying stages together with the presence of free amino acids are essential for the formation of meaty aroma compounds in a dry fermented sausage model under mild conditions of processing.

References

1. Flores M. Understanding the implications of current health trends on the aroma of wet and dry cured meat products. *Meat Sci.* 2018;144:53–61.
2. Van Boekel M.A.J.S. Formation of flavour compounds in the Maillard reaction. *Biotechnol. Adv.* 2006;24:230–233.
3. Modi V.K, Linforth R, Taylor A.J. Effect of pH and water activity in generation of selected meaty aroma compounds in a meat model system. *Am. J. Food Technol.* 2008;3:68–78.
4. Corral S, Leitner E, Siegmund B, Flores M. Determination of sulfur and nitrogen compounds during the processing of dry fermented sausages and their relation to amino acid generation. *Food Chem.* 2016;190:657–664.
5. Olivares A, Navarro J.L, Salvador A, Flores M. Sensory acceptability of slow fermented sausages based on fat content and ripening time. *Meat Sci.* 2010;86:251–257.
6. Li L, Belloch C, Flores M. The Maillard Reaction as Source of Meat Flavor Compounds in Dry Cured Meat Model Systems under Mild Temperature Conditions. *Molecules.* 2021;26(1):223.
7. Corral, S.; Salvador, A.; Belloch, C.; Flores, M. Improvement the aroma of reduced fat and salt fermented sausages by *Debaromyces hansenii* inoculation. *Food Control.* 2015;47:526–535.
8. van Den Dool, H.; Dec. Kratz, P. A generalization of the retention index system including linear temperature programmed gas-liquid partition chromatography. *J. Chromatogr. A* 1963;11:463–471.
9. Pripri-Nicolau, L.; De Revel, G.; Bertrand, A.; Maujean, A. Formation of flavor components by the reaction of amino acid and carbonyl compounds in mild conditions. *J. Agric. Food Chem.* 2000;48(9):3761–3766.

How do oxidoreduction conditions affect the balance of volatile compounds produced by lactic acid bacteria in a curd-based medium?

SOLANGE BUCHIN, Sabrina Jeannin, Céline Arnould, Romain Palme, Franck Dufrene, and Eric Beuvier

INRAE, URTAL, Poligny, France
solange.buchin@inrae.fr

Abstract

The oxidoreduction potential (E_h) of cheeses may affect the balance of volatile compounds that determine their flavour, but few studies are available on this topic. We explored the effect of E_h on the production of volatile compounds by lactic acid bacteria in cheese-like conditions. A strain of *Lactococcus lactis* subsp. *lactis* (Lc) and a strain of *Lactiplantibacillus plantarum* (Lb) were inoculated individually in a curd-based medium, either in the presence of O₂ (O2), or in the presence of N₂ (N2), and incubated at 26°C until 26 days. Microbial numeration and volatile compounds composition were analysed each 7 days and E_h and pH were monitored all over the incubation. Lc was inoculated at 10⁷ ufc.mL⁻¹ and Lb at 10⁶ ufc.mL⁻¹. Numbers were higher in N2 samples for Lc all over the incubation and in O2 ones for Lb, except at 7 and 26 days. E_{h7} (E_h corrected with pH) kinetics differed between N2 and O2 samples with minima at -200 mV and -250 mV respectively after 7-32 h, values turning positive afterwards for Lc and remaining negative for Lb. pH remained constant all over the incubation. Forty-eight and fifty volatile compounds were extracted for Lc and Lb respectively. For Lc, 15 compounds were higher with O2 (8 aldehydes, 4 ketones, 2 oxidized sulphur compounds, 1 furan) and 3 with N2 (1 volatile acid, 2 alcohols); for Lb, 12 compounds were higher with O2 (4 aldehydes, 1 alcohol, 3 ketones, 2 oxidized sulphur compounds, 2 furans) and 3 with N2 (2 alcohols, 1 reduced sulphur compound). This study revealed a significant effect of O2/N2 on volatile compounds, similar for Lc and Lb despite different kinetics in microbial counts, E_h values and volatile compounds production.

Keywords: oxidoreduction, *Lactococcus*, *Lactiplantibacillus*, volatile compounds, curd-based medium

Introduction

The oxidoreduction potential (E_h) of cheeses may affect the balance of volatile compounds that determines their flavour, *via* an effect on the cheese microbiota. However, only few studies are available on this topic, in particular the effect of E_h on the production of volatile compounds by lactic acid bacteria (LAB). Addition of reducing or oxidizing agents was used by Kieronczyk *et al.* [1] with lactococci in a synthetic medium based on amino-acids, by Martin *et al.* [2] in non-fat yoghurt, by Caldeo *et al.* [3] in Cheddar. Ricciardi *et al.* [4] studied *Lactocaseibacillus casei* under anaerobic or respiratory conditions in whey permeate. We explored the effect of oxidoreduction conditions on the production of volatile compounds by two types of LAB *via* incubation in the presence of O₂ or N₂ in a medium and during a time that mimicked cheese during ripening.

Experimental

We inoculated individually a strain of *Lactococcus lactis* subsp. *lactis* (Lc) at 10⁷ ufc.mL⁻¹ and a strain of *Lactiplantibacillus plantarum* (Lb) at 10⁶ ufc.mL⁻¹ in a curd-based medium made of 20h-semi-hard cheese curd ground in ultrapure water containing 18g.L⁻¹ NaCl, 1.2g.L⁻¹ peptone and lactose (1:2 w:w), sterilized 15 min at 110°C [5]. Two oxidoreduction conditions were applied for each strain: one inoculation in the presence of atmospheric O₂ (O2), the other one in an anaerobic chamber filled with N₂ (N2). For each strain and oxidoreduction condition, 70 mL of culture were distributed as follows: 3 mL in fifteen 10mL-SPME-vials, 1 mL in ten 10 mL-SPME-vials and 15 mL in one 40 mL-vial. Vials were incubated at 26°C until 26 days. Each 7 days, 1/5^o of SPME-vials were removed then analysed for microbial counts (one vial of 3 mL) and volatile compounds composition (two vials of 3 mL for neutral compounds and two vials of 1 mL for volatile fatty acids VFAs). Lc were numerated on M17 medium incubated 2 days at 20°C in aerobiosis and Lb on MRS medium incubated 3 days at 30°C in anaerobiosis. Neutral volatile compounds (or VFA) were analysed by SPME on CAR/PDMS 85µm (or 75 µm) fibre (Supelco, L'Isle d'Abeau, France) under agitation (or without agitation but with addition of H₂SO₄) at 40°C (or 60°C), 30 min (or 12 min) equilibration and 40 min (or 20 min) contact. GC/MS was performed with a 6890/5973 Agilent (Les Ulis, France), He at 73 kPa (or 43 kPa), a 60m/0.32mm/1µm RTX-5MS Restek (Lisses, France) column (or 30m/0.32 mm/0.5µm DB-Wax Agilent), 40°C-8 min (or 120°C-1 min) / 6°C.min⁻¹ until 145°C (or 180°C) / 20°C.min⁻¹ (or 10°C.min⁻¹) until 250°C (or 230°C). E_h and pH were monitored all over the incubation into vials of 15 mL with a combined electrode (InPro 3250i/SG/120, Mettler Toledo, Viroflay, France) and iCinac

software (AMS Alliance, Frépillon, France). E_{h7} was calculated to remove the effect of pH variations. The reduction rate $V_m = dE_{h7}.dt^{-1}$, T_m the time at which V_m occurred, and E_{h7m} the E_{h7} at which V_m occurred, were determined [6]. For each strain, the effect of time and O2/N2 on volatile compounds was studied by a 2-factor-ANOVA (XLSTAT software, Addinsoft, Paris, France). Compounds significantly affected at 5% were used to perform a principal component analysis (PCA), with a non-inoculated medium taken as reference.

Results and discussion

Microbial dynamics

Lc was inoculated at 10^7 ufc.mL⁻¹ and Lb at 10^6 ufc.mL⁻¹ (Figure 1). Numbers decreased all over the incubation period until 10^2 ufc.mL⁻¹ for Lc, but were at 10^6 ufc.mL⁻¹ at the end for Lb, after reaching a maximum of 10^7 ufc.mL⁻¹ between 7 (N2) and 14 (O2) days. Numbers were higher in N2 samples for Lc all over the incubation and in O2 ones for Lb, except at 7 and 26 days.

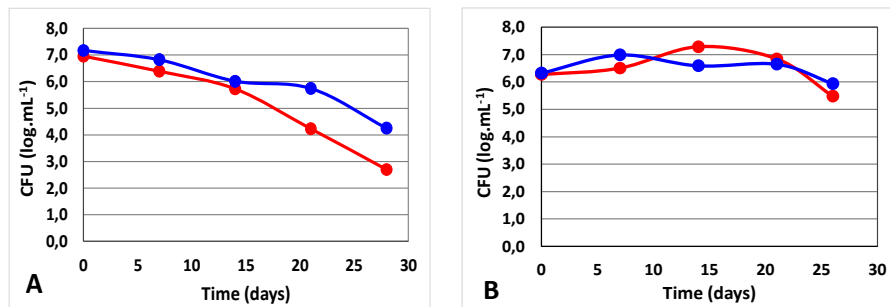


Figure 1: Counts of Lc (A) and Lb (B) in log (colony forming units.mL⁻¹) during the 26 days incubation in curd-based medium, according to O2 (in red) and N2 (in blue) conditions.

pH and oxidoreduction potential E_{h7}

The pH remained constant all over the incubation (Figure 2), which means that all lactose was exhausted in the curd at 20h. Despite a difference of inoculation level, kinetics of E_{h7} decrease were very similar between Lc and Lb (Figure 2). Brasca *et al.* [7] already observed similar minimal values of E_{h7} for *Lc. lactis* and *Lb. plantarum* inoculated in skimmed milk, but a faster decrease for the first. Conversely, E_{h7} kinetics differed between N2 and O2 samples, with minima at -200 mV and -250 mV after 7 and 32 h respectively. For Lc, with O2 and N2 respectively, V_m values were -358 and -260 mV/h, T_m values were 2.6 and 2.3 h, E_{h7m} values were 238 and 70 mV. For Lb with O2, V_m was -332 mV/h, T_m was 8.7 h, E_{h7m} was 63 mV, whereas with N2, values couldn't be calculated. Hence, Lc reached their maximum reduction rate before Lb (2.5 vs 8.7 h), in accordance with values of Brasca *et al.* [7], whereas Lc and Lb showed similar V_m and E_{h7m} values in similar O2 conditions. E_{h7} values became positive afterwards for Lc but remained negative for Lb. N2- E_{h7} values were lower than O2- E_{h7} values for Lc during most incubation, N2 values turning negative at the end. For Lb, the higher N2- E_{h7} than O2- E_{h7} values may result from a dysfunction of the N2 electrode, and so were the values of pH that may be similar to O2 values. This was consistent with the aberrant curve found for the calculation of kinetics parameters with the same electrode. This illustrates how the calibration of such electrodes is a difficult task [8].

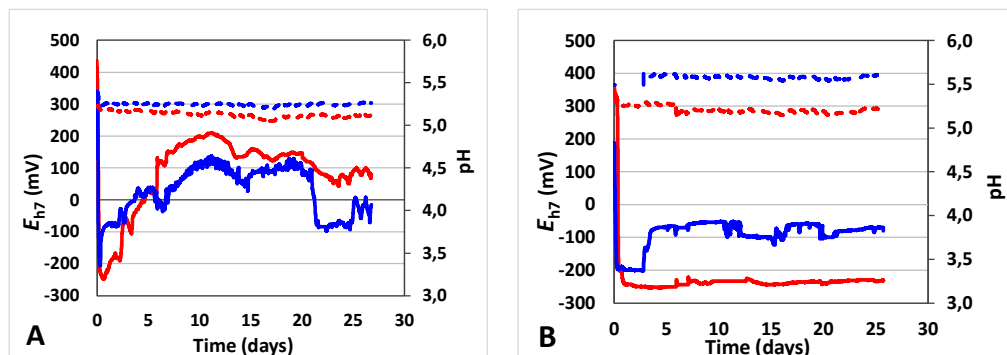


Figure 2: pH (dotted lines) and E_{h7} (plain lines) kinetics for Lc (A) and Lb (B) during the 26 days incubation in curd-based medium, according to O2 (in red) and N2 (in blue) conditions.

Volatile compounds

For Lc (Lb), forty-eight (fifty) volatile compounds were extracted: 12(12) aldehydes, 11(11) ketones, 7(10) alcohols, 7(6) VFAs, 5(5) sulphur compounds, 4(4) esters, 2(2) furans. For Lc, only 2 ketones significantly decreased from 0 to 26 days, whereas 3 alcohols, 2 furans, one aldehyde, one VFA and one ester increased; for Lb, 5 aldehydes and 3 ketones decreased from 0 to 26 days, whereas 7 alcohols, 3 VFAs, 2 furans and one aldehyde increased. A similar evolution according to chemical classes of compounds has already been observed in cheeses [9]. It appears a large evolution from 0 to 7 days incubation, then a switch from 14 to 21 days for Lc and from 21 to 26 days for Lb (Figure 3). This switch was mainly related to alcohols increase and also VFAs for Lb and an ester for Lc. Concerning O₂/N₂ effect, for Lc, 3 compounds were significantly higher with N₂ (1 VFA, 2 alcohols) and 15 with O₂ (8 aldehydes, 4 ketones, 2 sulphur compounds in an oxidized form, 1 furan); for Lb, 3 compounds were higher with N₂ (2 alcohols, 1 sulphur compounds in a reduced form) and 12 with O₂ (4 aldehydes, 1 alcohol, 3 ketones, 2 sulphur compounds in an oxidized form, 2 furans).

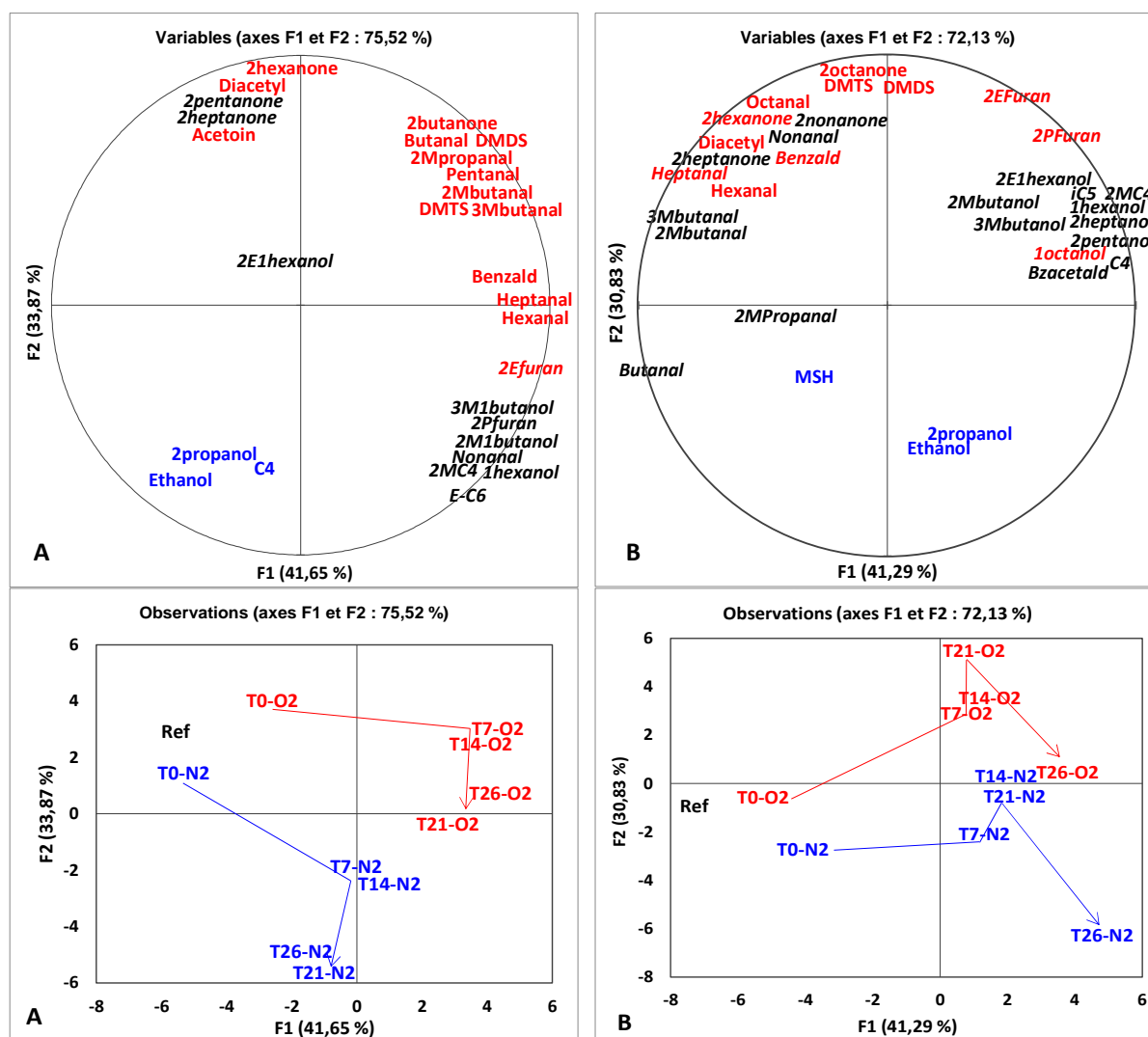


Figure 3: Principal Component Analysis (PCA) made from volatile compounds significantly affected by inoculation time (*italics*) and O₂/N₂ (compounds increased by O₂ in red, by N₂ in blue) at 5% according to ANOVA. A: Lc, B: Lb. M=methyl, E=ethyl, P=penyl, C₄=butyric acid, C₆=caproic acid, iC₅=isovaleric acid, E-C₆=ethyl hexanoate, MSH=methanethiol, DMDS=dimethylsulphide, DMTS=dimethyltrisulphide, Benzald=Benzaldehyde, Bzacetald=Benzenacetald T₀,7,14,21,26=incubation times of 0, 7, 14, 21, 26 days, Ref= medium without inoculation.

Despite different levels of incubation, different effects of O₂/N₂ on kinetics of counts and E_{h7} and different kinetics of volatile compounds production, very similar patterns of volatile compounds distribution according to O₂/N₂ were observed for Lc and for Lb. O₂ presence was favourable for many volatile compounds.

The metabolic way of production of diacetyl and acetoin from pyruvate is favoured by aerobiosis, and was already observed by Ricciardi *et al.* [4] with Lc in a whey permeate medium. Our results were also consistent with the oxidised / reduced form of compounds, the first being enhanced by aerobiosis, the second by anaerobiosis.

Aldehydes (butanal, pentanal, hexanal, heptanal, octanal, 2-methyl-propanal, 2-methyl-butanal, 3-methyl-butanal, benzaldehyde) and methyl-ketones (2-butanone, 2-hexanone, 2-octanone) are the oxidized form of corresponding alcohols (represented here by ethanol and 2-propanol). Similarly, dimethyldisulphide and dimethyltrisulphide, enhanced by O₂, are sulphur compounds in an oxidized form, whereas methanethiol, favoured by N₂, is a reduced sulphur compound. Lastly, furans may originate from the oxidation of fatty acids. Such a balance of aldehydes, ketones and alcohols was not observed by Ricciardi *et al.* [4]. This may be related to the time of incubation, only 48 h in their study, *i.e.* during the exponential and stationary phases of growth, whereas our incubation time reflected the period of cheese ripening. Kieronczyk *et al.* [1] observed a similar pattern than our results for aldehydes, sulphur compounds and acids for Lc in a synthetic amino acids-based medium, and Martin *et al.* [2] for sulphur compounds in yoghurt. Compared to these authors, the present study in a curd-based medium revealed an additional effect on alcohols, ketones and furans. Lastly, in 2-months Cheddar, Caldeo *et al.* [3] found the same trends for aldehydes, but the opposite for sulphur compounds, which emphasizes the importance of the studied medium.

In our study, a 20h-curd-based medium was chosen to mimic cheese conditions, *i.e.* the medium in which the secondary microbiota develops after the activity of starters, particularly lactose depletion. Moreover, a 26 days incubation may mimic the ripening phase. This choice is relevant to study the behaviour of microbiota during the cheese ripening, as evidenced by the different results obtained by other authors in different medium and time conditions.

Conclusion

This study showed that the O₂ or N₂ incubation of LAB in conditions mimicking cheese ripening (a curd-based medium, during 26 days) affects E_h kinetics and the balance of volatile compounds. Whatever the LAB species and the inoculation level, a similar effect on volatile compounds balance was observed. However, the variability between strains into a same or between other species needs to be further studied.

Acknowledgements

This work was funded by the Bourgogne Franche-Comté region.

References

1. Kieronczyk A, Cachon R, Feron G, Yvon M. Addition of oxidizing or reducing agents to the reaction medium influences amino acid conversion to aroma compounds by *Lactococcus lactis*. *J. Appl. Microbiol.* 2006;101:1114–1122.
2. Martin F, Cachon R, Pernin K, De Coninck J, Gervais P, Guichard E, Cayot N. Effect of oxidoreduction potential on aroma biosynthesis by lactic acid bacteria in nonfat yogurt. *J. Dairy Sci.* 2011;94:614–622.
3. Caldeo V, Hannon J-A, Hickey D-K, Waldron D, Wilkinson M-G, Beresford T-P, McSweeney P-L-H. Control of oxidation-reduction potential during Cheddar cheese ripening and its effect on the production of volatile flavour compounds. *J. Dairy Res.* 2016;83:479–486.
4. Ricciardi A, Zotta T, Ianniello R-G, Boscaino F, Matera A, Parente E. Effect of Respiratory Growth on the Metabolite Production and Stress Robustness of *Lactobacillus casei* N87 Cultivated in Cheese Whey Permeate Medium. *Front. Microbiol.* 2019;10:851.
5. Pogacic T, Maillard M-B, Leclerc A, Hervé C, Chuat V, Alyson L, Yee A-L, Valence F, Thierry A. A methodological approach to screen diverse cheese-related bacteria for their ability to produce aroma compounds. *Food Microbiol.* 2015;46:145e153.
6. Cachon R, Jeanson S, Aldarf M, Divies C. Characterisation of lactic starters based on acidification and reduction activities. *Lait* 2002;82:281–288.
7. Brasca M, Morandi S, Lodi R, Tamburini A. Redox potential to discriminate among species of lactic acid bacteria. *J. Appl. Microbiol.* 2007;103:1516–1524.
8. Abraham S, Cachon R, Jeanson S, Ebel B, Michelon D, Aubert C, Rojas C, Feron G, Beuvier E, Gervais P, De Coninck J. A procedure for reproducible measurement of redox potential (E_h) in dairy processes. *Dairy Sci. Technol.* 2013;93:675-690.
9. Buchin S, Duboz G, Salmon J-C. *Lactobacillus delbrueckii* subsp. *lactis* as a starter culture significantly affects the dynamics of volatile compound profiles of hard cooked cheeses. *Eur. Food Res. Technol.* 2017;243:1943–1955.

The role of diketopiperazines in cooked cheese flavour

ROSA C. SULLIVAN^{1,2}, Colette Fagan¹, Maria Oruna-Concha¹ and Jane K. Parker¹

¹ Department of Food and Nutritional Sciences, University of Reading, RG6 6DZ, UK.

r.s.cullivan@pgr.reading.ac.uk

² Synergy Flavours, Hillbottom Road, High Wycombe, HP12 4HJ, UK

Abstract

Diketopiperazines are cyclic dipeptides which impart bitterness and metallic flavour. They have previously been reported at subthreshold levels in raw cheese, but not studied in cooked cheese. Four diketopiperazines (cyclo-Pro-Pro, cyclo-Val-Pro, cyclo-Ala-Pro and cyclo-Leu-Pro) were detected in seven cooked cheeses (parmesan, mozzarella, and five different cheddars). Diketopiperazines were present in substantially higher concentrations in the cooked cheeses than their raw counterparts and were above bitter and metallic thresholds in some cooked samples. Diketopiperazine formation during cooking was higher in mature cheeses than in young cheeses, suggesting that aging cheeses produces precursors to diketopiperazine formation in the raw cheese.

Keywords: Diketopiperazine, cyclic peptide, bitterness, cheese

Introduction

Cheese is a major commodity produced by the dairy industry across Europe and globally. Mintel [1] estimates the UK market value for cheese to be £3.2 billion in 2020. Cheese is commonly used as an ingredient in cooked dishes (e.g. in fondue, as toppings to pizza or pasta, or grilled) with over 50% of cheese consumers reporting purchasing cheese for that purpose [2]. Despite the importance of ensuring good cheese flavour in cooked applications, most previous literature has only addressed raw cheese flavour.

Bitterness is typically regarded as a defect in cheese and, when detected in raw cheese, is thought to be a result of bitter peptides formed during proteolysis. Diketopiperazines (DKPs) are cyclic dipeptides which form in foods during fermentation and cooking. DKPs have been shown to contribute to bitter and metallic flavour [3]. While they have been reported previously in raw cheese, their concentrations were found to be subthreshold [4]. DKPs have also been reported in a number of cooked foods, including bread [5], chicken [6], cocoa [3] and coffee [7]. The aim of this work was to determine whether DKPs are formed in a range of cheeses during cooking, and whether the concentration of DKPs in cooked cheese is above bitter thresholds. Seven cheeses; mozzarella, parmesan and five cheddars were selected for this study to represent a range of cheeses typically used in cooked applications in the UK.

Experimental

Cheeses

Table: 1 List of cheeses used during the study.

Cheese	Abbreviation	Source	Aging period
Mozzarella	Mozz	Commercial *	<1 month **
Parmesan	Parm	Commercial *	> 2 years **
Mature cheddar	Ched	Commercial *	> 18 months **
High fat mild cheddar	HF	Reading pilot plant	3 months
Medium fat mild cheddar	MF	Reading pilot plant	3 months
Low fat mild cheddar	LF	Reading pilot plant	3 months
High fat 24 month aged cheddar	HF24	Reading pilot plant	24 months

* Commercially sourced (Sainsbury's supermarket, High Wycombe, UK). ** Typical aging period for this cheese variety

Cheese making

Milk was obtained from the University of Reading dairy herd of Holstein Friesians cows. Their diet (expressed per cow per day) comprised concentrate blend (9.5 kg), hay (1.0 kg), grass silage (19.0 kg), maize silage (24.0 kg), Trafford Gold (cow feed produced from wheat by-product) (4.0 kg), fat (0.1 kg), salt (0.1 kg), limestone flour (0.1 kg), minerals (0.03 kg). The milk was pasteurised at 73 °C for 15 s and skimmed. The resulting skimmed milk and cream were then recombined to produce 100 L each of low-fat milk (0.10 % fat), medium fat milk (2.7 % fat) and

high fat milk (3.9 % fat). The batches of milk were heated in cheese making vats at an initial pH of 6.75 to 30 °C, when 0.1 g/L starter culture R604 (Chr. Hansen, Hungerford UK) was added. Once the pH had dropped to 6.65, Chymosin, (CHYMAX, Chr. Hansen, Hungerford UK) was added to coagulate the milk. After 60 min the coagulum was cut at a pH of 6.60, after which the temperature was raised to 38 °C and held during the scalding phase, (approximately 90 min). Following the scalding, the whey was drained, and the curd was cheddared (sliced into small cubes to facilitate draining of the whey, before being stacked) for approximately 60 min at 38 °C until the pH reached 5.30. The curd was milled and salt added (2% w/w), then pressed in moulds for 24 h. The three curds were rested at 8 °C for 3 months, to give three mild cheddars. Additionally, a portion of the HF cheddar was ripened further to 24 months in total. The cheese was cut into approximately 250 g pieces, vacuum packed and stored at -20 °C until use. The final weights of high, medium and low-fat cheeses were 10.2, 8.8 and 6.2 kg respectively.

Cooking Procedure

Grated cheese (50 g) was spread evenly on a glass petri dish (90 mm diameter x 10 mm depth) and baked in a gas chromatograph oven (Hewlett Packard 5890 Series II) at 180 °C for 20 min. It was then cooled to room temperature, immersed in liquid nitrogen, and ground in a coffee grinder (Quest, Liverpool UK) to obtain a fine powder (30 s).

Extraction Method

Cheese (raw or cooked) (~50 g) was cut into 1cm³ pieces, immersed in liquid nitrogen, and ground in a coffee grinder (Quest, Liverpool UK) to obtain a fine powder. A portion of cheese (5 ± 0.1 g) was spiked with internal standard solution (50 µL 5-methyl-2-hexanone 0.500 % in isopropyl alcohol) and vortexed vigorously with 25 mL HPLC grade water for 60 min. The slurry was then centrifuged for 3 min at 2038 g and 15 °C. The supernatant underwent solid phase extraction using solid phase extraction (SPE) cartridges (Strata-X 33 µm polymeric reversed phase giga tube, Phenomenex, UK). The SPE cartridge was conditioned using 5 mL ethanol followed by 5 mL HPLC grade water. The sample was loaded slowly onto the cartridge and rinsed with a further 5 mL water and then dried by passing air through the cartridge for 30 s. The sample was then eluted from the cartridge slowly with 5 mL methyl acetate. All cooked cheeses were extracted in triplicate, while the raw cheeses were extracted once.

Gas chromatography-mass spectrometry (GC-MS) parameters

Analyses were performed on an Agilent 7890-5977A GC-MS system (Agilent, Stockport, UK) equipped with an autosampler (Agilent, Stockport, UK). Each liquid extract (1 µL) was injected in splitless mode onto a DB-FFAP polar column (30 m 0.25 mm I.D., 0.25 mm film thickness), (Phenomenex, Macclesfield, UK). The oven temperature was 45 °C initially, rising by 4 °C/min to 220 °C, and held for 45 min. Helium was used as the carrier gas at 1.2 mL/min. The mass spectrometer was operated in EI mode with a source temperature of 230 °C, an ionising voltage of 70 eV, and a scan range from m/z 40 to m/z 300 at 5.3 scans/s. The data were acquired and analysed using Masshunter software (Version 4.5, Agilent, UK). Compounds were identified by comparing their mass spectra and linear retention indices with those of authentic standards (Bachem, Bubendorf, Switzerland).

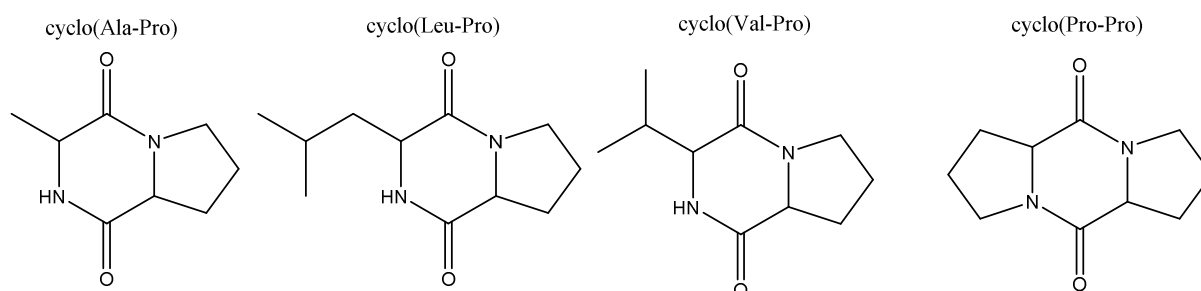


Figure 1: Structures of four proline-containing DKPs detected in cooked cheese.

Results and discussion

Four DKPs were detected in cooked cheese. Their structures (shown in Figure 1) each included a proline moiety (cyclo(Val-Pro), cyclo(Leu-Pro), cyclo(Ala-Pro), cyclo(Pro-Pro)). Proline-containing DKPs are the most common category contributing approximately 90% of DKPs reported in foods [8, 9].

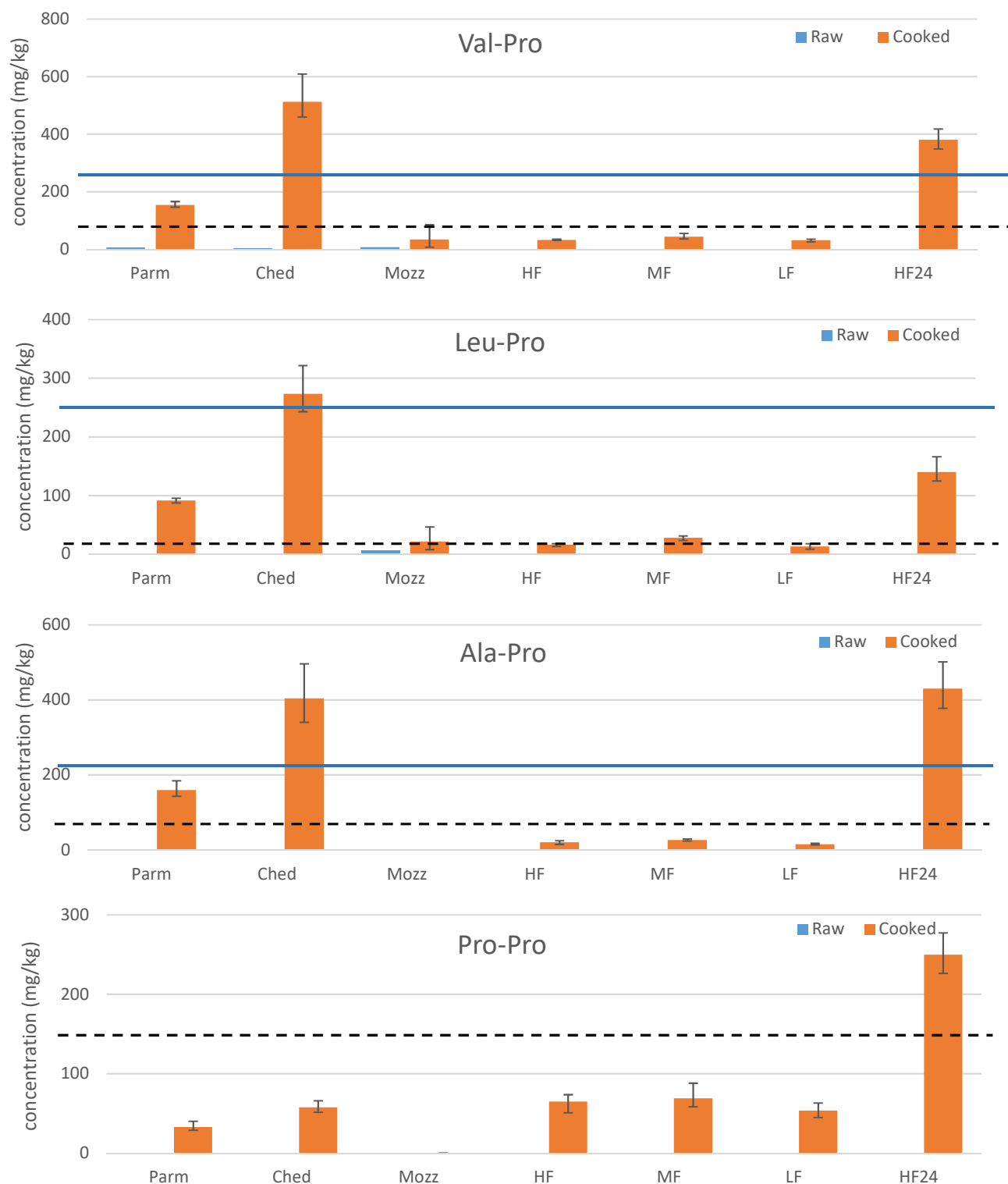


Figure 2: Concentration of four proline-containing DKPs in cooked and raw cheeses. Abbreviations: Parm (parmesan), Ched (mature cheddar), Mozz (mozzarella), HF (high fat mild cheddar), MF (medium fat mild cheddar), LF (low fat mild cheddar), HF24 (portion of HF which underwent 24 month aging). Metallic taste threshold represented by dashed line [3] and bitter taste threshold represented by a solid blue line [3]. Error bars show minimum and maximum range values.

DKP formation has been shown to occur from small peptides during cooking [8]. Otsuka et al [9] reported that when proline is one of the moieties in the precursor peptide, the two reacting atoms in DKP formation have a more favourable interatomic distance. This leads to more rapid formation of proline-containing DKPs than those containing other amino acids. Figure 2 shows the concentration of each DKP in the cooked and raw cheeses, along

with their metallic and bitter taste thresholds [3]. All DKPs detected were subthreshold in the raw cheeses. This agrees with previous analysis of raw Comte, which showed that DKPs were present at subthreshold concentrations in raw cheese and do not contribute to bitter taste [4].

The concentrations of DKPs increased substantially during cooking. Three DKPs were present above their bitter taste thresholds in the Ched and HF24 samples, and above their metallic thresholds in Parmesan. The DKP concentrations were similar between the HF, MF and LF cooked cheddar, demonstrating that the fat concentration in cheese did not influence the formation of DKPs when cooked.

In general, DKP concentration in cooked cheeses was higher in the matured cheeses than the milder cheeses. Comparison of HF and HF24 (the same cheese, differing only in maturation times of 3 and 24 months respectively) showed much higher concentrations of DKPs in cooked HF24 than HF, demonstrating that increased maturation time was associated with higher DKP concentration when cooked. As DKPs were not detected in either raw HF or HF24, this suggests that precursors to DKPs rather than DKPs themselves formed during cheese ripening.

Proline-containing-DKPs were recently found to form rapidly from di-and-tripeptides with proline in the second position from the N-terminal during heating [9]. This position favours rapid formation of DKPs compared to other similar peptides due to reduced steric hindrance around the atoms involved in the reaction. The process of proteolysis during cheese ripening generates small chain peptides and amino acids from cheese proteins [10]. It is likely that formation of proline containing di-and-tri peptides which are precursors to DKPs occurs during cheese ripening.

Conclusion

We report for the first time that DKPs are formed when cheese is cooked, and present at concentrations above taste thresholds in some cooked cheeses. Furthermore, DKP concentration in cooked (but not raw) cheeses increased with the duration of maturation. The process of proteolysis during cheese ripening is the most likely cause for this observation, as small chain peptides are DKP precursors. Future work in this area could look to confirm the sensory impact of DKP presence on cooked cheese flavour, and to determine whether the bitter and metallic thresholds differ for a high-fat matrix such as cheese to those previously reported for DKPs in water.

References

1. Mintel. Cheese: inc impact of Covid-19 - UK - October 2020. 2020. (Accessed: 13 March 2021). Available at: <https://libraryfaqs.worc.ac.uk/faq/164516>.
2. Mintel. Cheese - UK - October 2019. 2019. (Accessed: 1 April 2021). Available at: <https://reports.mintel.com/display/920242/?fromSearch=%3Ffreetext%3Dcheese>.
3. Stark, T., Hofmann, T. Structures, sensory activity, and dose/response functions of 2,5-diketopiperazines in roasted cocoa nibs (Theobroma cacao). *J Agric Food Chem.* 2005; 53:7222-7231.
4. Roudot-Algaron, F., Le Bars, D., Einhorn, J., Adda, J. and Gripon, J. Flavor Constituents of aqueous fraction extracted from comte cheese by liquid carbon dioxide. *J Food Sci.*1993;58:1005-1009.
5. Ryan, L.A. , Dal Bello, F. , Arendt, E. K., Koehler, P. Detection and quantitation of 2,5-diketopiperazines in wheat sourdough and bread. *J Agric Food Chem* 2009;57:9563-8.
6. Chen, Y.H., Liou, S.E. and Chen, C.C. Two-step mass spectrometric approach for the identification of diketopiperazines in chicken essence. *Eur Food Res Technol.* 2004;218:589-597.
7. Ginz M., Engelhardt U.H. Identification of proline-based diketopiperazines in roasted coffee. *J Agric Food Chem.* 2000; 48: 3528-32.
8. Borthwick, A.D. and Da Costa, N.C. 2,5-diketopiperazines in food and beverages: taste and bioactivity. *Crit Rev Food Sci Nutr.* 2017;57:718-742.
9. Otsuka, Y., Arita, H., Sakaji, M., Yamamoto, K., Kashiwagi, T., Shimamura, T. and Ukeda, H. Investigation of the formation mechanism of proline-containing cyclic dipeptide from the linear peptide. *Biosci Biotechnol Biochem.* 2019;83:2355-2363.
10. Murtaza, M.A., Ur-Rehman, S., Anjum, F.M., Huma, N. and Hafiz, I. Cheddar cheese ripening and flavor characterization: A Review, *Crit Rev Food Sci Nutr.* 2004;54:1309-1321.

Identification of key volatiles in boiled chicken aroma

H.Q. YEO¹, D.P. Balagiannis¹, J.H. Koek² and J.K. Parker¹

¹ Department of Food and Nutritional Sciences, University of Reading, Whiteknights, Reading, UK,
h.yeo@pgr.reading.ac.uk

² Unilever, Wageningen University & Research, Bronland 14, Wageningen, Netherlands

Abstract

In this study, we used Likens Nickerson simultaneous distillation extraction to simulate the boiling of chicken in a closed system, such as might be used when preparing a casserole, stew or stock. In the boiled chicken (BC), most of the volatiles identified using Gas Chromatography-Olfactometry (GC-O) were sulphur-containing compounds, which are derived from the Maillard reaction. Families of oxazoles, thiazoles and thiazolines were also found in the extracts by Gas Chromatography-Mass Spectrometry (GC-MS), and novel thiazolines such as 2,4,5-trimethylthiazoline (roasted onion) and 2,4-dimethylthiazoline (meaty) were identified by GC-O. Despite their occurrence at low concentrations, their low odour thresholds make them important contributors to the aroma of boiled chicken. Meanwhile, lipid oxidation resulted in the formation of unsaturated aldehydes such as (E)-2-nonenal, (E,E)-2,4-nonadienal and (E,E)-2,4-decadienal.

Keywords: chicken, beef, Likens-Nickerson, Maillard, lipid

Introduction

The rapid growth in vegan, vegetarian and flexitarian diets has led to renewed interest in the development of process flavourings with authentic flavour profiles. The wealth of literature on meat aroma dates back to decades ago and the topic has been comprehensively reviewed [1-3]. Recent research has found interest in unique species with desirable organoleptic qualities, such as the poulet de Bresse from France, or distinct parts of the bird such as the fat, skin and juice, which led to the discovery of new aroma molecules such as (E)-3-(5-ethylcyclopent-1-enyl)acrylaldehyde, (8E/Z)-8-tetradecen-5-olide, (6E)-6-tetradecen-5-olide and 4-methyl-2-pentylpyridine [4]. The oriental Beijing Youji from China was also touted to have a richer fragrance than commercial broilers and this was attributed to the presence of 32 more odorants identified in the former, including 2-furfurylthiol, (E)-2-heptenal, 2-methyl-3-(methylthio)furan and bis(2-methyl-3-furyl)disulphide with odour activity values ≥ 1 [5]. This latter study also employed Solvent Assisted Flavour Extraction (SAFE), which is a relatively modern and advanced technique as compared to Simultaneous Distillation Extraction (SDE). However, SDE is still widely adopted in the extraction of meat aroma [4, 6, 7] and one of its untapped advantages is the possibility of in-situ cooking and extraction to prevent the inevitable aroma loss during sample transfer.

Thus, the aim of this work was to obtain aroma extracts of boiled chicken for the identification of key volatiles contributing to cooked meat aroma and species-specific character using SDE. This will be useful in the creation and modification of process flavourings in products such as soups, bouillons and plant-based meat analogues.

Experimental

Likens-Nickerson simultaneous distillation extraction (LN-SDE)

Fresh chicken breast from a local retailer was minced and added to a round bottom flask with distilled water (1:1 w/w). The sample was boiled at 100 °C in a heating mantle for 30 min. Likens-Nickerson SDE was performed using 30 mL of redistilled pentane/diethyl ether (9:1 v/v) for 2 h. The extract was concentrated to 0.5 mL using a Vigreux column and stored at -80 °C prior to analysis.

Gas Chromatography-Olfactometry (GC-O)

The analyses were performed on a HP 5890 Series II GC (Hewlett Packard, Palo Alto, CA, USA) equipped with a flame ionisation detector (FID) and an ODO II sniffing port (SGE, Ringwood, Victoria, Australia). The extracts (2 μ L) were injected in manual mode. Chromatographic separation was achieved on two columns of different polarities. For the non-polar Rxi-5 Sil MS column (30 m x 0.25 mm i.d., 1 μ m film thickness, from Restek, Bellefonte, PA, USA), the oven temperature was programmed from 35 °C (held for 10 min) to 200 °C at 6 °C min⁻¹ and finally to 320 °C at 15 °C min⁻¹ (held for 10 min). For the polar ZB-Wax column (30 m x 0.25 mm i.d., 0.25 μ m film thickness, from Zebron, Phenomenex, Torrance, CA, USA), the oven temperature was programmed from 35 °C (held for 10 min) to 200 °C at 6 °C min⁻¹ and finally to 250 °C at 15 °C min⁻¹ (held for

10 min). Helium was used as the carrier gas at a constant flow rate of 2 mL min⁻¹. The column effluent was split equally between the FID and sniffing port, where the odours of the eluting components were evaluated. The samples were analysed in triplicates (twice on DB-5, once on ZB-Wax) by 3 trained assessors, who provided descriptions and intensity scores on a scale of 1 (very weak) to 10 (very strong) for the odours detected.

Gas Chromatography-Mass Spectrometry (GC-MS)

The analyses were performed on an Agilent 7890-5975C GC-MS (Agilent Technologies, Santa Clara, CA, USA). An aliquot of extract (2 µL) was injected in splitless mode. Chromatographic separation was achieved on two columns of different polarities. For the non-polar HP-5 MS column (30 m x 0.25 mm i.d., 1 µm film thickness, from Agilent J&W Scientific, Santa Clara, CA, USA), the oven temperature was programmed from 35 °C (held for 10 min) to 200 °C at 6 °C min⁻¹ and finally to 320 °C at 15 °C min⁻¹ (held for 10 min). For the polar ZB-Wax column (60 m x 0.25 mm i.d., 0.25 µm film thickness, from Zebron, Phenomenex, Torrance, CA, USA), the oven temperature was programmed from 35 °C (held for 10 min) to 200 °C at 6 °C min⁻¹ and finally to 250 °C at 15 °C min⁻¹ (held for 10 min). The carrier gas was helium at a constant pressure of 18 psi. The MS was operated in electron impact mode with a source temperature of 250 °C, an ionising voltage of 70 eV and a scan range from *m/z* 29 to *m/z* 500.

Results and discussion

Table 1 lists the top 25 odour active compounds found in BC. The majority of the compounds with the highest odour intensity scores and detection frequencies were sulphur-containing compounds, such as 2-methyl-3-furanthiol (cooked meat), 2-furfurylthiol (meat) and 3-(methylthio)propanal (potato), which were among the primary odorants identified in chicken broth [8]. Sulphur compounds play a major role in meat aroma as they usually have low odour threshold values. The routes involved in their formation are likely to be the interaction of H₂S with hydroxycarbonyls, dicarbonyls, furanones and furfurals to give thiols and mercaptoketones, which could form a mixture of disulphides upon oxidation [2].

Carbonyl compounds derived from the oxidative degradation of unsaturated fatty acids were also identified in the extract, but they scored lower in odour intensities. (E,E)-2,4-Decadienal, (E)-2-nonenal, 1-octen-3-one and (E,E)-2,4-nonadienal could be formed from the autoxidation of ω-6 fatty acids such as linoleate and arachidonate. Meanwhile, aldehydes such as octanal and nonanal could originate from the autoxidation of ω-9 fatty acids such as oleate. Although none of these identified carbonyl compounds possessed aroma characteristics resembling the complete spectrum of cooked chicken [9], it was reported that the removal of carbonyl compounds from the volatile fraction resulted in a loss of chicken odour and an intensification of meaty odour [10]. However, it was also demonstrated that the omission of (E,E)-2,4-decadienal alone did not result in a significant aroma change [7]. Thus, it is likely that it is the delicate balance of the group of carbonyl compounds, in addition to the potent sulphur compounds, which contribute to the overall aroma rather than a single aroma compound alone.

Besides these known compounds, families of thiazoles and thiazolines were also found in the extracts. These compounds were reported to possess meat-like odours and could be formed from the reaction of α-hydroxyketones or α-dicarbonyls with H₂S and NH₃ in the presence of aliphatic aldehydes [11]. In addition to the α-hydroxyketones and α-dicarbonyls, the presence of mercaptoketones, which are intermediates in the mechanism, could also result in the formation of thiazolines and thiazoles. Since these precursors were identified in the GC-MS and GC-O, the formation of thiazolines and thiazoles in the extract could be possible.

Novel thiazolines were identified in this work. 2,4,5-Trimethylthiazoline, which was described as having a roasted onion character, could be derived from acetaldehyde and 3-mercapto-2-butanone, both of which were present in the extracts. Meanwhile, 2,4-dimethylthiazoline, which had a meaty character, could be derived from acetaldehyde and pyruvaldehyde, which is a highly reactive intermediate formed during the Maillard reaction. Given the high odour intensity scores of these compounds, they could also be important contributors to meat aromas.

Table 1. 25 most odour active compounds in the boiled chicken (BC) extract.

Odour description ^a	Compound ^b	LRI ^c		Odour intensity score ^d
		DB-5	ZB-Wax	
Raw onion, catty	2-Methyl-2-thiazoline	877	1391	45
Sweaty, raw rotting onions	1-Methylthiopropene	765	1256	43
Onion, roasted	2-Propanethiol	<500	<500	43
Raw onion, pickled onion, petroleum	1-(Methylthio)ethanethiol	846	1222	40
Cooked rice, pandan	2-Acetyl-1-pyrroline	920	1340	39
Lamb fat, potato	(Z)-4-Heptenal	898	1249	38
Roasting pan, onion, burnt, meat	2-Furfurylthiol [#]	909	1438	34
	2-Mercapto-3-pentanone [#]	909	nd	34
Boiled potato	3-(Methylthio)propanal	905	1443	33
Fresh grass, green	Hexanal	799	1070	32
Cooked meat, roasty, nutty	2-Methyl-3-furanthiol	869	1330	32
Malty, cocoa	3-Methylbutanal	644	906	29
Poo, rotting chicken, diarrhea	Hydrogen sulfide	<500	<800	28
Meat stew	2,4-Dimethylthiazoline [*]	916	1287	27
Beer headspace, weed	3-Methyl-2-butene-1-thiol	823	nd	26
Cardboard, pyrazine, medicinal	Tetramethylpyrazine	1092	1439	26
Sweaty, onion, cat's pee	3-Mercapto-2-pentanone	900	1353	25
Roasted/ overcooked meat	2,4-Dimethyl-5-ethylthiazole	928	nd	24
Basmati	2-Acetylthiazole	1020	nd	24
Rotten egg, cabbage, poo	Methanethiol	<500	<800	24
Savoury, sulphur, onion	Mercaptopropanone	805	1353	22
Butter	2,3-Butanedione	586	985	21
Floral, perfume	Benzeneacetaldehyde	1051	1650	20
Savoury, grilled meat, fatty, juicy	2,4-Dimethyl-5-ethylthiazoline [*]	1098	1453	20
Popcorn, rice cracker, roasted	2-Acetyl-3,4,5,6-tetrahydropyridine	1142	1583	20

^a Odour perceived at the sniffing port of the GC-O

^b Compounds were identified by comparison of their mass spectra with authentic standards and/or NIST 14 Mass Spectral Database

^c Linear retention index (LRI) was calculated using the retention times of a series of C₅ – C₂₅ *n*-alkanes and compared with authentic compounds where available or with NIST Chemistry WebBook

^d Odour intensity scores were calculated from duplicate assessments by 3 trained assessors (max score = 60)

[#] Co-eluting compounds

^{*} Thiazolines reported for the first time in BC

Conclusion

Besides the known compounds which have been widely reported in literature, novel thiazolines (4-dimethylthiazoline and 2,4-dimethyl-5-ethylthiazoline) are reported to be odour-active in BC in this work and these compounds could be formed from precursors present in the extracts.

References

1. Wilson RA, Katz I. Review of literature on chicken flavor and report of isolation of several new chicken flavor components from aqueous cooked chicken broth. *J Agric Food Chem.* 1972;20(4):741-747.
2. Mottram DS. Flavour formation in meat and meat products: a review. *Food Chem.* 1998;62(4):415-24.
3. Jayasena DD, Ahn DU, Nam KC, Jo C. Flavour chemistry of chicken meat: a review. *Asian-australas J Anim Sci.* 2013;26(5):732-742.
4. Delort E, Velluz A, Frérot E, Rubin M, Jaquier A, Linder S, Eidman KF, MacDougall BS. Identification and synthesis of new volatile molecules found in extracts obtained from distinct parts of cooked chicken. *J Agric Food Chem.* 2011;59(21):11752-11763.
5. Fan M, Xiao Q, Xie J, Cheng J, Sun B, Du W, Wang Y, Wang, T. Aroma compounds in chicken broths of Beijing Youji and commercial broilers. *J Agric Food Chem.* 2018;66(39):10242-10251.
6. Takakura Y, Mizushima M, Hayashi K, Masuzawa T, Nishimura T. Characterization of the key aroma compounds in chicken soup stock using aroma extract dilution analysis. *Food Sci Technol Res.* 2014;20(1):109-113.
7. Feng Y, Cai Y, Fu X, Zheng L, Xiao Z, Zhao M. Comparison of aroma-active compounds in broiler broth and native chicken broth by aroma extract dilution analysis (AEDA), odor activity value (OAV) and omission experiment. *Food Chem.* 2018;265:274-80.
8. Gasser U, Grosch W. Primary odorants of chicken broth. *Z Lebensm Unters Forsch.* 1990;190(1):3-8.
9. Phippen EL, Nonaka M. Volatile carbonyl compounds of cooked chicken. II. Compounds volatilized with steam during cooking. *J Food Sci.* 1960;25(6):764-9.
10. Minor LJ, Pearson AM, Dawson LE, Schweigert BS. Separation and identification of carbonyl and sulfur compounds in volatile fraction of cooked chicken. *J Agric Food Chem.* 1965;13(4):298-300.
11. Elmore JS, Mottram DS. Investigation of the reaction between ammonium sulfide, aldehydes, and α -hydroxyketones or α -dicarbonyls to form some lipid-Maillard interaction products found in cooked beef. *J Agric Food Chem.* 1997;45(9):3595-602.

Identification of a key odorant contributing to Muscat aroma of Darjeeling black tea

YASUHIRO FUKUI, Shunsuke Konishi, Kazuya Kawabata, Kenji Haraguchi,
Yuichiro Ohmori, Akira Nakanishi, and Susumu Ishizaki

R & D Center, T. Hasegawa Co., Ltd., Kariyado, Nakahara-ku, Kawasaki-shi. 211-0022, Japan,
yasuhiro_fukui@t-hasegawa.co.jp

Abstract

The aroma of Darjeeling black tea was investigated. An unknown odorant reminiscent of Muscat grape was detected with multidimensional gas chromatography–mass spectrometry/olfactometry, and the chemical structure of the unknown component was successfully identified as 4-methylene-2-(2-methylprop-1-enyl)oxane (i.e. dehydrorose oxide or DHRO), which has Muscat-like and floral notes on its own. The present study is the first to detect DHRO as an odorant in Darjeeling black tea. The odour threshold of DHRO was calculated to be 0.20 µg/kg in water, and a stable isotope dilution assay showed that the amount of DHRO in a Darjeeling black tea infusion was 0.028 µg/kg. The odour activity value (OAV) of DHRO in the Darjeeling black tea infusion was 0.14. A sensory evaluation was conducted to obtain the orthonasal aroma profiles of black tea aroma model solutions and revealed the effect of DHRO in Darjeeling black tea. DHRO was found to contribute to the characteristic attributes such as Muscat-like, floral, fruity and green aroma of Darjeeling black tea, although the OAV was less than 1.

Keywords: Darjeeling black tea, 4-methylene-2-(2-methylprop-1-enyl)oxane, stable isotope dilution assay, Muscat aroma, sensory evaluation

Introduction

Darjeeling black tea is known for a unique aroma reminiscent of the Muscat grape. Several studies have focused on the aroma of black tea [1-4], however, it remains difficult to recombine this characteristic aroma with known odorants. Therefore, there may be unknown odorants that contribute to this aroma. This work aimed to determine and evaluate the key odorants that contribute to the Muscat-like aroma of Darjeeling black tea.

Experimental

Darjeeling black tea sample

Darjeeling black tea (Goomtee Muscatel Valley, FTGFOP1, 2016-DJ19) was purchased from a local shop (Lupicia, Tokyo, Japan).

Preparation of the volatile concentrate of Darjeeling black tea

Boiling hot water (500 mL) was added to the tea leaves (10 g), and the mixture was allowed to stand still for 3 min. After extraction, the leaves were separated with a strainer, and the infusion was immediately cooled to approximately 25 °C in an ice bath. The obtained infusion (420 g) was distilled at 40 °C using the solvent assisted flavour evaporation (SAFE) method [5]. Sodium chloride (63 g) was added to the distillate, which was then extracted with diethyl ether (1 × 60 mL, 2 × 30 mL) followed by dichloromethane (1 × 60 mL, 2 × 30 mL). The organic phases were individually dried over anhydrous sodium sulphate. The dichloromethane solution was first concentrated to approximately 1 mL by distilling it off the solvent at 48 °C; then, it was added to the diethyl ether solution. The combined organic phase was concentrated at 43 °C to yield 2.3 mg of the volatile concentrate.

Identification of an unknown odorant in Darjeeling black tea

Gas chromatography–mass spectrometry/olfactometry (GC-MS/O) and multidimensional (MD) GC-MS/O were applied to identify the volatile compounds in the concentrate. MDGC-MS/O was also used to analyse DHRO, which was synthesised in our laboratory.

Quantification of DHRO in the Darjeeling black tea infusion

A stable isotope dilution assay (SIDA) was conducted by preparing 0.5 mL of a diluted solution of [*d*₆]-DHRO in dichloromethane and adding it to 200 g of the Darjeeling black tea infusion. The tea infusion was stirred for 10 min. Then, the volatile concentrate was prepared with the SAFE method and solvent extraction as described

above. The calibration curve obtained for the standard solution with MDGC-MS/O was used to quantify DHRO in the Darjeeling black tea infusion.

Sensory evaluation

Sensory evaluation was conducted using a descriptive analysis to elucidate the effect of DHRO in aroma recombinant of Darjeeling black tea. A recombinant model solution was prepared by mixing the key odorants of Darjeeling black tea at quantified values according to published data [3]. The solution was orthonasally compared with another solution to which was added the model solution with DHRO at a concentration quantified via SIDA.

Results and discussion

Detection of the Muscat-like aroma from a volatile concentrate of Darjeeling black tea

A volatile concentrate of Darjeeling black tea infusion was prepared by the SAFE method and solvent extraction using diethyl ether and dichloromethane. GC-MS/O was applied to the concentrate. A characteristic Muscat-like aroma was successfully detected at a retention index (RI) of 1390 on a polar column. However, the mass spectrum of the target odorant was not observed.

Elucidation of the Muscat-like aroma component

MDGC-MS/O was used to elucidate the chemical structure of the unknown component with the Muscat-like aroma. At the retention time when the Muscat-like aroma was detected in the first polar column, the effluent was introduced to the second non-polar column and sniffed. The mass spectrum of the unknown component was obtained successfully in the second column. However, this mass spectrum did not match the data from the libraries. Hence, the chemical structure of the unknown component needed to be estimated from analytical data. The RI, odour quality and mass spectrum of *trans*-rose oxide (*t*RO) were conducive to revealing the chemical structure of the unknown component. The RIs of both columns and the odour quality of the unknown component were quite similar to those of *t*RO (Table 1). Thus, the chemical structure of the unknown component was concluded to resemble that of *t*RO. Additionally, when the mass spectra of the two components were compared, the molecular mass (m/z 152) of the unknown component was less than that of *t*RO by 2 (Figure 1). The same applied to m/z 137 of the unknown component. Thus, the chemical structure of the unknown component was proposed to be dehydrogenated *t*RO.

Table 1: Comparison between the RIs and odour qualities of the two components.

	RI		odour quality
	polar column	non-polar column	
unknown component	1390	1096	Muscat-like, floral
<i>trans</i> -rose oxide (<i>t</i> RO)	1372	1117	Muscat-like, floral

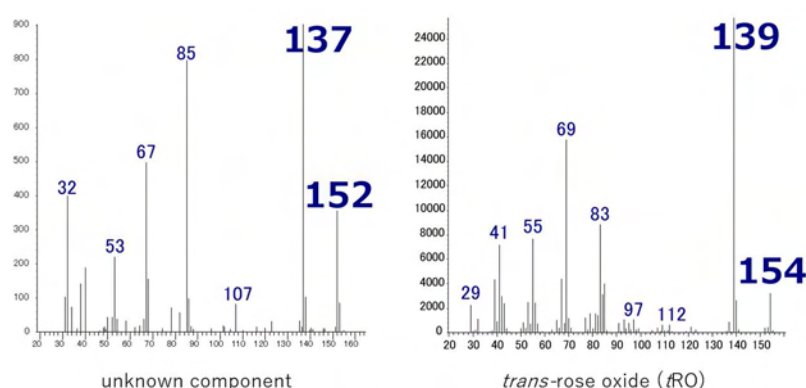


Figure 1: Comparison between mass spectra of the two components.

The candidate compounds were synthesised and analysed. Among the compounds, the RI, mass spectrum and odour quality of DHRO (Figure 2) showed good agreement with those of the unknown component detected from the volatile concentrate of the Darjeeling black tea infusion.

DHRO

Brunke *et al.* detected DHRO as one of the volatile components in *Achillea wilhelmsii*, although they did not refer to its aroma [6]. Königsmann *et al.* filed a patent regarding the utilisation of DHRO as a synthetic intermediate of rose oxide [7]. Ohloff *et al.* described the odour qualities of its enantiomers as floral notes [8]. However, the detection of DHRO in Darjeeling black tea is novel. When orthonasal recognition test was conducted, the odour threshold of DHRO was 0.20 µg/kg in water, and the panellists described the aroma as Muscat-like, floral, lychee-like, rosy and green.

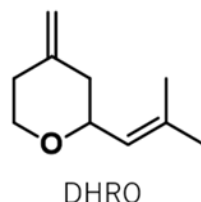


Figure 2: Chemical structure of the Muscat-like odorant newly identified in the Darjeeling black tea infusion.

Quantification of DHRO by SIDA

SIDA was conducted to quantify the amount of DHRO in the Darjeeling black tea infusion. Figure 3 shows 4-methylene-2-(2-(methyl- d_3)-prop-1-enyl-3,3,3- d_3)oxane ($[d_6]$ -DHRO), which was synthesised as the stable isotope internal standard. The concentration of DHRO in the tea infusion was found to be 0.028 µg/kg. The odour activity value (OAV) was calculated as 0.14 from the concentration and odour threshold.

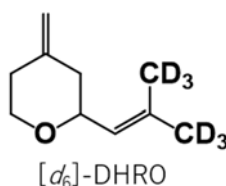


Figure 3: Chemical structure of $[d_6]$ -DHRO.

Sensory evaluation

Although the OAV suggests that DHRO does not contribute to the aroma of Darjeeling black tea, the aroma characteristics of DHRO were extremely interesting because they were similar to the unique Muscat-like aroma of Darjeeling black tea. Additionally, the effect of DHRO in Darjeeling black tea was unknown because it was the odorant identified in the Darjeeling black tea infusion for the first time. Hence, a sensory evaluation was conducted to obtain the orthonasal aroma profiles of two black tea aroma model solutions. Twelve panellists were asked to examine the effect of DHRO in Darjeeling black tea via descriptive analysis. Figure 4 shows the aroma profiles of the two model solutions. DHRO was confirmed to contribute to the aroma of Darjeeling black tea because it enhanced the Muscat-like, floral, fruity and green aroma of Darjeeling black tea, although the amount of DHRO in the infusion was less than the odour threshold.

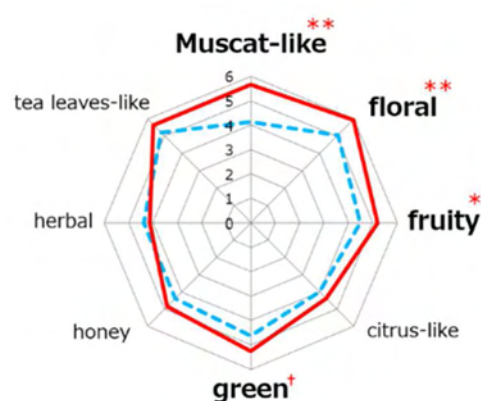


Figure 4: Orthonasal aroma profiles of the recombinant model solution (dotted line) and the solution with added DHRO at the quantified amount (solid line); $n = 12$, t -test, $**p < 0.01$, $*p < 0.05$, $†p < 0.1$.

Conclusion

To elucidate the unknown odorant contributing to the Muscat-like aroma in Darjeeling black tea, a volatile concentrate was prepared and analysed with MDGC-MS/O. DHRO, which has a Muscat-like aroma on its own, was identified in the Darjeeling black tea infusion. This is the first study to detect DHRO in Darjeeling black tea. A sensory evaluation showed that DHRO contributed to the characteristic attributes of Darjeeling black tea, although the OAV of DHRO in the tea infusion was less than 1. Our further examination detected DHRO in other foods such as coffee, lychees and hops (data not shown). It is thought that DHRO widely exists in natural products and may affect their aroma.

References

1. Nakatani, Y., Sato, S., Yamanishi, T. 3S-(+)-3,7-Dimethyl-1,5,7-octatriene-3-ol in the Essential Oil of Black Tea. *Agric Biol Chem.* 1969;33(6):967-968.
2. Imayoshi, Y., Xu, D. Z., Iwabuchi, H. Study on the Volatiles of Black Tea. *The Koryo.* 2003;217:145-150.
3. Schuh, C., Schieberle, P. Characterization of the Key Aroma Compounds in the Beverage Prepared from Darjeeling Black Tea: Quantitative Differences between Tea Leaves and Infusion. *J Agric Food Chem.* 2006;54:916-924.
4. Baba, R., Nakamura, M., Kumazawa, K. Identification of the Odourants Contributing to the Characteristic Aroma of Darjeeling Black Tea Infusion. *Jpn Soc Food Sci Technol.* 2017;64(6),294-301.
5. Engel, W., Bahr, W., Schieberle, P. Solvent assisted flavour evaporation – a new and versatile technique for the careful and direct isolation of aroma compounds from complex food matrices. *Eur Food Res Technol.* 1999;209,237-241.
6. Brunke, E. J., Hammerschmidt, F. J., Aboutabl, E. A. Volatile constituents of *Achillea wilhelmsii* C. Koch (syn. A. *Santolina* auct. Mult.) from Egypt and Turkey. *Prog Essent Oil Res.* 1986;16:85-92.
7. Königsmann, L., Schubert, J., Walch, A., Gottwald, G., Kamasz, M., Schwab, E., Pfaff, K., Slany, M. (BASF SE). Method for producing cis-rose oxide. WO 2009077550 A1, Dec. 17, 2008.
8. Ohloff, G., Giersch, W., Schulte-Elte, K. H., Enggist, P., Demole, E. Synthesis of (*R*)- and (*S*)-4-Methyl-6-2'-methylprop-1'-enyl-5,6-dihydro-2*H*-pyran (Nerol oxide) and Natural Occurrence of its Racemate. *Helv Chim Acta.* 1980;63(6):1582-1588.

Meaty flavour tonalities by Maillard reaction

JAN H. KOEK¹ and Cathy De Sousa Ferreira²

¹ Unilever Research & Development, Wageningen, The Netherlands; jan.koek@unilever.com

² AgroSupDijon, Dijon, France

Abstract

Existing studies reveal that meat flavours from different animal species, although different in tonality, have many aroma molecules in common. Accordingly, we found that from a limited set of starting materials, it is possible to obtain different tonalities of flavour by using different ratios of the materials. Moreover, by changing reaction conditions like pH, time, and temperature one can tune to chicken direction applying a lower temperature. At higher temperature, a beef direction could only be found at a narrower pH interval, around 6.0. Presently this understanding is used to develop natural meaty flavourings based on non-meat foodstuff.

Keywords: Maillard, model reaction, chicken, beef, roast

Introduction

To increase sustainability, meat consumption should be reduced by use of vegetable-based meat replacers with similar nutritional value like Vegetarian Butcher products. These meat replacers however lack the specific precursors for the Maillard reaction responsible for meaty aromas and flavours and need to be flavoured to give the full meat impression. To avoid the use of meat based ingredients, the most efficient applied meaty flavours should be based on Maillard reactions of non-meat ingredients only. These flavours are made on an industrial scale but getting high quality natural vegan flavours remains a challenge. Formation of specific meat flavours of different tonalities should reflect chicken / beef / pork identity and cooking process like boiling / oven / roasting. A natural flavouring preparation should be based on foodstuff ingredients only and traditional processing as laid down in EU regulation [1]. For better understanding to get these meat flavourings tonalities from natural sourced ingredients, reactions with pure substances were evaluated on potential to get different meat tonalities.

Fresh raw meat has a very bland flavour. Only upon cooking the meat, the flavours related to specific animal species (chicken / beef / pork etc.) as well as those reflecting the cooking process (boiling / oven / roasting etc.) are formed. These Maillard reaction flavours originate from a similar set of reducing sugars ribose, glucose and amino acids *e.g.* glycine, cysteine for most animal species. Most of the aroma molecules are formed from Maillard intermediates from amino acid and reducing sugars reaction resulting in reactive semi transient species as diketosugars (oxosones). These react further in sugar degradation products like acetoin, but reaction with amino acids gives also ammoniac and hydrogen sulphide resulting in a complex mixture with Strecker aldehydes *e.g.* isobutyraldehydes, heterocyclic compounds *e.g.* furans, thiophenes and pyrazines besides some thiols and polymeric substances like melanoidins [2].

A meaty flavouring by Maillard reaction was reported by reaction of cysteine with a reducing sugar source [3] also in combination with thiamine [4] and / or fat [5], and more recently in a complex multistep method [6].

Mechanistic work with ¹³C labelled precursors demonstrated that some of the important meaty volatiles are formed from especially the combination of cysteine, thiamine and xylose, but 2-methyl-3-furanthiol and 3-mercapto-2-pentanone can also be derived from thiamine itself, while for others thiamine did not play a role as precursor [7]. Common understanding is that release of H₂S is key for meat flavour formation in the Maillard reaction [8, 9]. Levels of cysteine as H₂S source are much higher in non-meat sources (*e.g.* cabbage, onion with about 1000 ppm) than levels of thiamine (peas and soy with about 1 ppm) [10, 11]. Hence, we focussed on model studies to produce different meat tonalities formed by cysteine (or other sulphur source) with reducing sugars as starting point and observed effect of thiamine and amino acid addition.

The Xylose / Cysteine system was chosen as model to prepare meaty flavours [12]. The work from Gasser and Grosch [13] indicates the same flavour molecules in both chicken and beef extracts to be present although in different ratios, *e.g.* 2-methylfuranthiol is much more abundant in chicken bouillon than in beef, while others were reported to have similar concentrations like furfurylthiol. Impact on the tonality of the flavours was studied by addition of other amino acids, thiamine, and sugars to the reaction mixture: *e.g.* β-alanine was reported to enhance the intensity of chicken and beef taste [14].

The type and intensity of volatiles formed in the Maillard reaction are strongly dependent on reaction conditions: pH, reaction time and temperature [15, 16]. Hence the obtained meat tonality from the model reaction was studied as a function of these parameters.

Experimental

The reaction ingredients β -alanine, cysteine.HCl, glycine, glucose, xylose, lactic acid and thiamine were purchased from SigmaAldrich. The model reaction mixtures was prepared by addition of 1 g xylose, 1 g of cysteine.HCl and 0.2 g lactic acid to 40 ml of water As indicated in Figure 1, optionally were added to the 40 ml reaction mixture: 1 g of glycine, 0.1 g of β -alanine, 0.2 g of thiamine and 1 g of glucose. By addition of 0.1 M of NaOH solution the pH was adjusted to pH = 6 for constant reaction conditions and pH 5, 6 and 7 upon variation of reaction conditions. The temperature was set to 95 °C with 4 hr reaction time for constant reaction conditions and varied from 75 °C to 95 °C with the reaction times between 4 and 8 hours as indicated in Table 1.

The mixture was placed in a 100 ml Duran glass bottle and heated in a hot air circulated oven. After cooling, sensory evaluation was done. Most reactions mixtures were found to be colourless except those prepared with β -alanine (Figure 2). Smell and taste were evaluated by 10x dilution into a 0.35% salt / 0.1% monosodium glutamate solution.

Results and discussion

Influence of amino acids and sugars

In Figure 1 experiments with several additions and ratios of amino acids and sugars are presented. A good meaty taste, *i.e.* pork-like, was observed when xylose and cysteine were combined and heated. Use of glycine addition enhanced the general meaty character. Upon trying several ratios and addition of glucose and β -alanine now clear chicken notes were obtained. Another ratio of ingredients and supplementing with a little thiamine on top gave more beefy notes. Hence it was confirmed that by variation of almost the same set of precursors, quite different flavours are formed by choosing different ratios, possibly giving similar flavour compounds, but at different ratios.

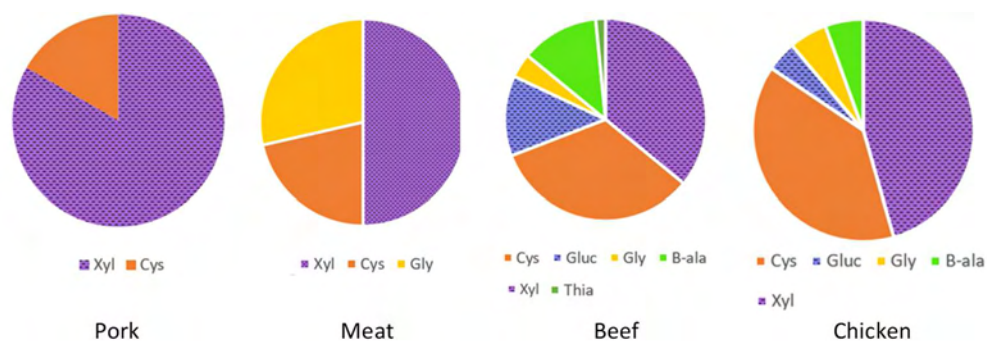


Figure 1: Different meaty profiles from different amino acids with xylose.

As shown in Figure 2 it was noticed that by addition of β -alanine colouring was much more intense. This can be explained from the higher reactivity of the amino acid group now in *beta* position and hence more remote from the carboxylate group. However, we found that this was not a determining factor to get more chicken or more beef type flavour.

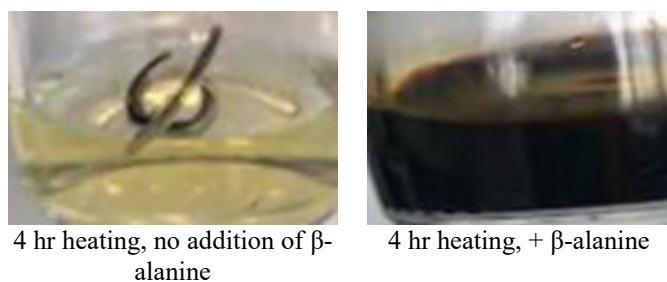


Figure 2: A much darker colour is observed with addition of β -alanine.

Influence of pH, time and temperature in a statistical design of experiments (DOE)

To study the influence of reaction parameters as time, temperature and pH, a simple model system consisting of xylose and cysteine was used. Lactic acid, reported to be present in meat and contributing to taste, was used as acid. By choosing 3 levels of the three parameters, a full factorial design would have required 27 experiments (3 x 3 x 3) while the statistical screening design as shown in Table 1 allows for conclusions on the three parameters with only 9 experiments.

Table 1: Sensory results from reaction of Xylose, Cysteine and Lactic acid upon variation of reaction conditions pH, time and temperature.

Exp.N°	pH	Time (hr)	Temp (°C)	Smell	Taste
01	6	4	75	Sulphury	Chicken
02	7	8	75	No	Chicken
03	6	6	85	Sweet	Beef
04	6	8	95	Roast	Beef
05	5	4	95	No	No
06	5	6	75	Sulphury	Chicken
07	7	6	95	Sweet	Weak
08	7	4	85	No	No
09	5	8	85	Sweet	Sweet

From Table 1 the influence of Maillard reaction efficiency can be clearly observed. In Exp N° 03 and 04 a beef flavour is formed at high temperatures at pH 6. Chicken flavour could be observed at lower temperature (75°C) with no real dependence on pH or reaction time. For beef longer time at higher temperature in Exp N° 04 gave also more roast smell. The pH 6 seems critical at high temperature as at lower or higher pH no meat flavour is formed.

Conclusion

From a limited set of simple starting materials, it is possible to obtain different tonalities of meat flavour by using different ratios of the materials. Moreover, by changing reaction conditions like pH, time and temperature one can tune to chicken direction, but at higher temperature a beef direction seems only to be reached at a narrower pH interval, around 6.0. Presently this understanding is used to develop natural meaty flavourings based on non-meat foodstuff.

References

1. REGULATION (EC) No 1334/2008 OF THE EUROPEAN PARLIAMENT AND OF THE COUNCIL of 16 December 2008 on flavorings and certain food ingredients with flavoring properties for use in and on foods and amending Council Regulation (EEC) No 1601/91, Regulations (EC) No 2232/96 and (EC) No 110/2008 and Directive 2000/13/EC.
2. Mathias K. Sucan and Deepthi K. Weerasinghe. Process and Reaction Flavors. In: ACS Symposium Series 905, Chapter 1, 1-13. ACS: Washington, DC 2005.
3. Morton I.D. Flavoring substances and their preparation. US2934437, 1960.
4. Bidmead D.S. Roasted meat flavor and process for producing same. US3394016, 1968.
5. Soeters, C.J. Process for preparing a savory meat flavoring. US3493395, 1970.
6. Blank I., Davidek T., Hofmann T., Schieberle P. Flavor active composition. US9005689 example 6, 2015.
7. Cerny C. Origin of carbons in sulfur-containing aroma compounds from the Maillard reaction of xylose, cysteine and thiamine. LWT - Food Sci Technol. 2007;40(8):1309-1315.
8. Kerler J. et al, Basic chemistry and process conditions for reaction flavors with particular focus on Maillard-type reactions. In: Food Flavor Technology: p 51, 2nd ed. 2010 Blackwell, Ed. Taylor & Linforth.
9. Jayasena D.D., Ahn D.U., Nam K.C., Jo C. Flavor Chemistry of Chicken Meat: A Review. Asian-Australas J Anim Sci. 2013;26(5):732-742.
10. Zurbruggen B.D. Onion and garlic biohydrolysates and their use as natural flavorings. WO01/30179,2001.
11. Walhqvist M. and Briggs. Water soluble vitamins, Chapter 16 Vitamin B-1 Food Charts Vegetables. In: on-line book Food Facts, : <http://apjcn.nhri.org.tw/server/info/books-phds/books/foodfacts/html> (by Visionary Voyager).
12. Cerny C. and Davidek T. Formation of Aroma Compounds from Ribose and Cysteine during the Maillard Reaction. J Agric Food Chem. 2003;51:2714-272.
13. Gasser U. and Grosch W. Primary odorants of chicken broth. A comparative study with meat broths from cow and ox. Z Lebensm Unters Forsch 1990;190:3-8.
14. Chen Y. and Ho C.T. Effects of Carnosine on Volatile Generation from Maillard Reaction of Ribose and Cysteine. J Agric Food Chem. 2002;50:2372.

15. Meynier A. and Mottram D.S. The effect of pH on the formation of volatile compounds in meat-related model systems. *Food Chem.* 1995;52:361-366.
16. Kwong G.Y., Hong, J.H., Kim Y.S., Lee S.M. and Kim K.O. Sensory characteristics and consumer acceptability of beef stock containing glutathione Maillard reaction products prepared at various conditions. *J. Food Sci.* 2011;76:51-57.

Effect of malt kilning temperature on the concentration of (*E*)- β -damascenone in malt, mashing and wort boiling in the brewing process

JOSÉ A. PIORNOS¹, Jean-Philippe Kanter¹, Dimitrios P. Balagiannis¹, Elisabeth Koussissi^{2, †}, August Bekkers², Johan Vissenaekens³, Bert-Jan Grootes³, Eric Brouwer² and Jane K. Parker¹

¹ Department of Food and Nutritional Sciences, University of Reading, RG6 6DZ, UK. j.piornos@reading.ac.uk

² Heineken Supply Chain BV, Burgemeester Smeetsweg, 1, 2382 PH Zoeterwoude, The Netherlands.

³ Mouterij Albert, Kanaaldijk, 2870 Ruisbroek-Sint-Amands, Belgium.

[†] Current address: Department of Wine, Vine and Beverage Sciences, University of West Attica, Ag. Spyridona Str., 12,210 Athens, Greece.

Abstract

(*E*)- β -Damascenone (bDam) is one of the most important aroma compounds in foods and in both regular and alcohol-free beers. In the present study, the effect of the curing temperature during kilning on the concentration of bDam in malt was monitored, as well as during mashing and wort boiling. Two different varieties of malt (spring and winter) were compared. The results showed different trends during malt kilning, with an increase in the levels of the aroma compound over time at 78 and 90 °C. During mashing and wort boiling, bDam was formed following different trends, this attributed to a balance between formation and evaporation. Moreover, malts and worts from winter barley contained more bDam than spring barley. Further research is required in order to identify and monitor the precursors of this potent aroma compound.

Keywords: damascenone, malting, wort boiling, brewing.

Introduction

(*E*)- β -Damascenone (bDam) is widely known in flavour science because of its extremely low orthonasal detection threshold of 0.004 $\mu\text{g/L}$ in water [1] or even 0.00075 $\mu\text{g/L}$ in water [2]. Despite being present at very low concentrations, it has been demonstrated that it plays a key role in the aroma of several foods as varied as rape honey [3], Syrah wine [4] and blackberries [5], where this compound imparts their characteristic pleasant, fruity aroma. In beers, fruity aroma has been traditionally related to the presence of esters and alcohols. However, the role of bDam must not be underestimated. In Bavarian wheat beers, this compound was reported to have the highest OAV besides ethanol [1]. In pale lager and Pilsner, its concentration was 1.6 $\mu\text{g/L}$ [6] and 2.3 $\mu\text{g/L}$ [7], respectively and bDam has been previously reported in unhopped wort [8]. However, hops have also been reported as one possible source of bDam, where the presence of its precursor, the β -D-glucoside of 3-hydroxy- β -damascone, has been previously identified [9]. However, bDam has also been found in barley malt [10].

bDam in wort was detected at extremely high level (450 $\mu\text{g/kg}$ wort) [11]. Nonetheless, its concentration decreased remarkably after fermentation (7 days at 20 °C), thus leading to a non-detectable final concentration in fresh beer in the cited study. However, in the case of alcohol-free beers produced following a cold contact fermentation (CCF) procedure, the low fermentation temperature (close to 0 °C) not only limited the formation of ethanol, but also limited the reduction of the level of bDam. In our previous study, the concentration of bDam in an alcohol-free beer brewed by CCF was 10.4 $\mu\text{g/L}$, well above its orthonasal detection threshold 0.23 $\mu\text{g/L}$ [12].

Because of the high contribution of this compound to the overall aroma of beer, it is essential to understand the factors affecting its formation throughout the brewing process. Since it was demonstrated that bDam was formed during thermal processes [13], the hypothesis of this study was that the concentration of bDam in malt is affected by the kilning temperature, and that kilning at different temperature has an impact on the worts prepared from these malts. Consequently, the objectives of the present research were to study the formation of this compound during the curing stage of malt kilning from two varieties of barley, as well as to determine its levels at different stages of mashing and wort boiling prepared with malts cured at different temperatures.

Experimental

Briefly, the green malt from two different varieties (spring variety “Planet” and winter “Etincel”) were kilned in a pilot scale micro-malting equipment from Nordon & Cie. (Nancy, France). The samples (650 g) were kilned following a temperature gradient: initial temperature of 25 °C, raised to 55 °C over 10 min, then increased to 64 °C over 45 min, kept for 4 hours and 50 min and then increased to 65 °C over 3 hours and 15 min. After this stage (drying stage), the malt was cured isothermally at 65, 78 or 90 °C for 8.4 h. Samples were collected at the beginning

of the curing stage, after 4.8 h and at the end of curing. After collection from the micro-malting equipment, the rootlets of the grains were removed by manual rubbing, sieved off and the malt stored at $-30\text{ }^{\circ}\text{C}$.

For the preparation of mash and wort, the final malt samples, i.e., those cured for 8.4 h, were coarsely ground using a coffee grinder and sieved through a $355\text{-}\mu\text{m}$ mesh size sieve in order to remove undesired fine particles. The ground malt (40 g) was added to 120 mL deionised water at $55\text{ }^{\circ}\text{C}$ (mash). The mash was kept at this temperature for 15 min with constant magnetic stirring. Then, the temperature was increased to $63\text{ }^{\circ}\text{C}$, kept for 40 min, then raised to $72\text{ }^{\circ}\text{C}$ and kept for another 15 min, and a final step of $78\text{ }^{\circ}\text{C}$ for 20 min. The wort obtained this way was filtered through a 1-mm mesh sieve and then boiled for 30 min in an open beaker. Samples were taken at the beginning of the $63\text{ }^{\circ}\text{C}$ -step, at the end of the $72\text{ }^{\circ}\text{C}$ -step and after wort boiling.

Quantification of (*E*)- β -damascenone

Malt samples (5 g) were extracted with 25 mL of deionised water at room temperature for 60 min under stirring. The malt extracts, as well as the mash and wort, were centrifuged at $5500\times g$ for 15 min at $4\text{ }^{\circ}\text{C}$. The pH was adjusted to 3.0 using 1 M HCl. Aliquots (5 mL) were poured into 20-ml SPME vials containing 1.3 g NaCl. α -Ionone (5 μL at 5 mg/L in ethanol) was used as internal standard. The vials were incubated at $60\text{ }^{\circ}\text{C}$ for 10 min, and then a DVB/Carboxen®/PDMS SPME fibre ($65\text{ }\mu\text{m}$, 2 cm) from Supelco (Bellefonte, PA, USA) was exposed for 45 min. The fibre was desorbed in the injection port of the GC in splitless mode at $250\text{ }^{\circ}\text{C}$ for 20 min. The instrument used was a 7890A gas chromatograph coupled to a 5975C inert XL EI/CI MSD triple axis mass spectroscopy detector from Agilent Technologies (Santa Clara, CA, USA). The carrier gas was helium at 3 mL/min. A non-polar ZB-5MSi column (30 m, 0.25 mm i.d. , $1.0\text{ }\mu\text{m df}$) from Phenomenex (Torrance, CA, USA) was used. Data acquisition was performed in SIM mode, using the ions (first ion for quantification) 121 and 190 for bDam, and 121 and 192 for α -ionone. Mass spectra were recorded in the EI mode at an ionisation voltage of 70 eV and source temperature of $230\text{ }^{\circ}\text{C}$. The experiments were performed in duplicate, and the results were expressed in relation to the concentration of the internal standard.

Statistical analysis

Duncan's test for multiple comparisons was applied at a significance level $\alpha=0.95$ by using the software InfoStat 2017, developed by the National University of Córdoba (Córdoba, Argentina).

Results and discussion

The effect of curing time on the level of bDam in barley malt at different kilning temperatures (isothermally) was studied. Figure 1 shows the concentration of this compound in terms of the ratio of the peak areas of bDam and the internal standard. The results show an increase in the amount of bDam in malts kilned at 78 and $90\text{ }^{\circ}\text{C}$ over time. At $78\text{ }^{\circ}\text{C}$ the maximum level was reached after 8.4 h curing, whereas at $90\text{ }^{\circ}\text{C}$ the levels stabilised at the maximum after 4.8 h, this being not significantly different to the samples kilned for longer time (8.4 h).

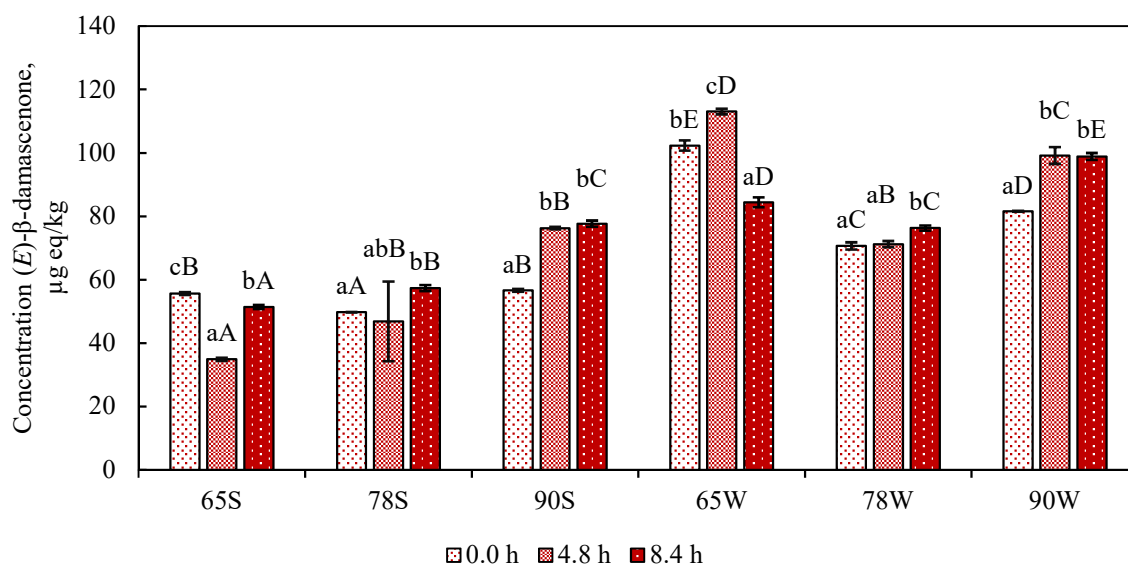


Figure 1: Effect of curing time and temperature (65, 78 and $90\text{ }^{\circ}\text{C}$) on the formation of (*E*)- β -damascenone during malt kilning for spring (S) and winter (W) barley. Results expressed as μg equivalent of α -ionone per kg malt. Significant differences ($p < 0.05$) between curing time within experiments and between experiments at the same curing time are represented by lower and uppercase letters, respectively.

The results showed a certain degree of variability, especially those samples kilned at 65 °C. The reason behind this might be the variability associated with real food matrices. The green malt samples were collected from industrial germination boxes and kilned using a pilot-scale oven. Heating in this kind of pilot-scale ovens is not completely homogenous and also the hot air employed to process the malt may not be spread equally across the samples. The processed malts were placed in aeriated boxes in the oven in different positions, this possibly leading to uneven air flow.

The malts prepared for the first part of this study were used for mashing and the preparation of wort. The mixture of malt grains steeped in water is known as mash, whereas the wort is the liquid extract after filtration. In order to understand the behaviour of bDam during mashing and wort boiling, different samples were collected at the beginning of the mashing process, i.e., before the step at 63 °C, at the end of mashing and at the end of wort boiling. Figure 2 shows the levels of bDam throughout the mashing and wort boiling processes. The data showed different trends dependent on the variety of barley used. Spring barley malts kilned at 65 and 78 °C showed an increasing trend during mashing and wort boiling. However, bDam decreased slightly during mashing and increased after wort boiling when using malts kilned at 90 °C. Similar behaviour was observed in malts from winter barley, but the differences were larger. For these malts, the concentration after mashing decreased significantly and increased to their highest values after wort boiling. These results suggested a balance of loss and formation of bDam: this compound was lost during mashing due to evaporation and its formation was not enough to result in an overall accumulation. However, the higher temperature applied during wort boiling might lead to a formation rate higher than the loss, and also the evaporation of water during boiling could have contributed to an increase in the final concentration of bDam.

With respect to the varieties of barley used in this study, a higher average amount of bDam was found in winter barley than in the spring variety. The differences were significant ($p < 0.05$) for both the malts, as well as in the worts prepared from those malts. Malts from barley winter contained 57% more bDam than spring barley, on average. In the case of the wort, the difference was smaller, around 33% higher.

bDam is an aroma compound present in a huge variety of foods, mainly of plant origin. It is widely accepted that this compound can be formed from the hydrolytic degradation of the carotenoid neoxanthin [14, 15]. These authors proposed a formation mechanism via the so-called “grasshopper ketone”. However, this formation route in barley has not been confirmed yet, despite neoxanthin being found in barley grains [16, 17]. Little is known regarding the role of cultivar on the content of carotenoids in barley grain. Carotenoid content in wheat was found to be lower in spring varieties, but this was not proven in barley [18]. Other studies proved that this compound can be formed from the enzymatic hydrolysis of the β -D-glucosides of 5-megastigmen-7-yne-3,9-diol and 3-hydroxy- β -damascone [19]. These precursors have been identified in fruit juice but not in barley. Nonetheless, the theory of a glycoside precursor has been supported by results showing an increase in the concentration of bDam in beers after the addition of β -glucosidase [11].

The formation of bDam in malt and wort was favoured at higher temperatures. This has been observed in other foods after heat treatment. For instance, a considerable increase in the concentration of bDam (13.5 times higher) has been reported in black tea infusions after sterilisation by heat treatment (121 °C for 10 min) [13]. It is of great

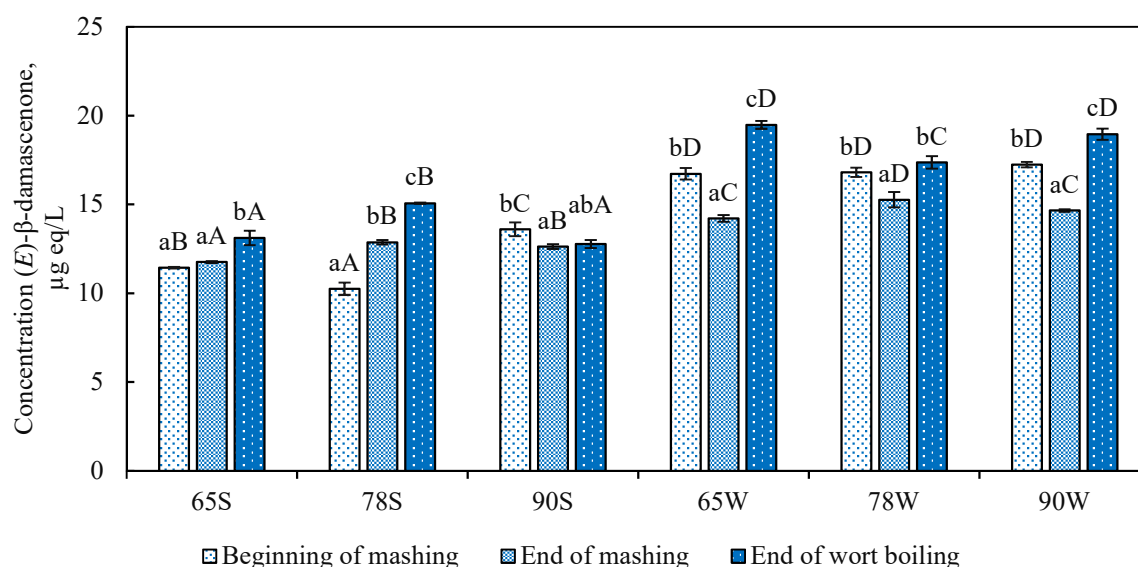


Figure 2: Levels of (*E*)- β -damascenone during mashing and wort boiling for spring (S) and winter (W) malts kilned at different temperatures (65, 78 and 90 °C). Results expressed as μ g equivalent of α -ionone per L wort. Significant differences ($p < 0.05$) between samples within experiments and between experiments at the same sampling stage are represented by lower and uppercase letters, respectively.

importance to understand how process conditions, like temperature, affect the formation of bDam in malt and wort. This is even more critical when brewing alcohol-free beers by fermentation at very low temperature (such is the case of CCF). The formation of bDam was proven to occur during the thermal degradation of 9'-*cis*-neoxanthin in a model system containing peroxyacetic acid at temperatures from 60 to 90 °C [20]. Moreover, identification of precursors and monitoring of their behaviour throughout processing are required in order to elucidate the chemical mechanism and the factors that affect its rate of formation. This would help control the amount of bDam in malts and beers by monitoring and possibly manipulation of the concentrations of the precursors in the raw materials.

Conclusion

bDam was monitored during the curing stage of malt kilning as well as during mashing and wort boiling. During curing in kilning, the level of bDam increased over time at the highest curing temperatures (78 and 90 °C), with maxima reached after 8.4 h curing at 90 °C. These results demonstrated the great importance of temperature and time during malt kilning. The temperature of the malt curing did not have a significant impact on the levels of bDam formed in the subsequent mashing and boiling steps, with different trends for winter and spring barleys. On average, malts and worts from winter barley presented significantly higher amounts of bDam than those from spring barley ($p < 0.05$). Further research could provide better understanding of the differences related to variety, and thus be able to better control the concentration of this powerful aroma compound in the beer.

References

- Langos D, Granvogel M, Schieberle P. Characterization of the key aroma compounds in two Bavarian wheat beers by means of the sensomics approach. *J Agric Food Chem*. 2013;61(47):11303–11.
- Semmelroch P, Laskawy G, Blank I, Grosch W. Determination of potent odourants in roasted coffee by stable isotope dilution assays. *Flavour Fragr J*. 1995;10(1):1–7.
- Ruisinger B, Schieberle P. Characterization of the key aroma compounds in rape honey by means of the molecular sensory science concept. *J Agric Food Chem*. 2012;60(17):4186–94.
- Zhao P, Gao J, Qian M, Li H. Characterization of the key aroma compounds in Chinese syrah wine by gas chromatography-Olfactometry-Mass spectrometry and Aroma reconstitution studies. *Molecules*. 2017;22(7):1045.
- Klesk K, Qian M. Aroma extract dilution analysis of Cv. Marion (*Rubus spp. hyb*) and Cv. Evergreen (*R. laciniatus L.*) blackberries. *J Agric Food Chem*. 2003;51(11):3436–41.
- Schieberle P. Primary odorants of pale lager beer - Differences to other beers and changes during storage. *Z Lebensm Unters Forsch*. 1991;193(6):558–65.
- Fritsch HT, Schieberle P. Identification based on quantitative measurements and aroma recombination of the character impact odorants in a Bavarian Pilsner-type beer. *J Agric Food Chem*. 2005;53(19):7544–51.
- De Schutter DP, Saison D, Delvaux F, Derdelinckx G, Rock J-M, Neven H, et al. Characterization of volatiles in unhopped wort. *J Agric Food Chem*. 2008;56(1):246–54.
- Kollmannsberger H, Biendl M, Nitz S. Occurrence of glycosidically bound flavour compounds in hops, hop products and beer. *Monatsschrift für Brauwiss*. 2006;59(5–6):83–9.
- Fickert B, Schieberle P. Identification of the key odorants in barley malt (caramalt) using GC/MS techniques and odour dilution analyses. *Nahrung / Food*. 1998;42(6):371–5.
- Chevance F, Guyot-Declerck C, Dupont J, Collin S. Investigation of the β -damascenone level in fresh and aged commercial beers. *J Agric Food Chem*. 2002;50(13):3818–21.
- Piornos JA, Balagiannis DP, Methven L, Koussissi E, Brouwer E, Parker JK. Elucidating the odor-active aroma compounds in alcohol-free beer and their contribution to the warty flavor. *J Agric Food Chem*. 2020;68(37):10088–96.
- Kumazawa K, Masuda H. Change in the flavor of black tea drink during heat processing. *J Agric Food Chem*. 2001;49(7):3304–9.
- Isoe S, Katsumura S, Sakan T. The Synthesis of Damascenone and β -Damascone and The Possible Mechanism of Their Formation from Carotenoids. *Helv Chim Acta*. 1973;56(5):1514–6.
- Puglisi CJ, Eelsey GM, Prager RH, Skouroumounis GK, Sefton MA. Identification of a precursor to naturally occurring β -damascenone. *Tetrahedron Lett*. 2001;42:6937–9.
- Sreenivasulu N, Radchuk V, Alawady A, Borisjuk L, Weier D, Staroske N, et al. De-regulation of abscisic acid contents causes abnormal endosperm development in the barley mutant *seg8*. *Plant J*. 2010;64(4):589–603.
- Jaleel CA, Manivannan P, Wahid A, Farooq M, Al-Juburi HJ, Somasundaram R, et al. Drought Stress in Plants: A Review on Morphological Characteristics and Pigments Composition. *Int J Agric Biol*. 2009;11(1):100–5.
- Konopka I, Czaplicki S, Rotkiewicz D. Differences in content and composition of free lipids and carotenoids in flour of spring and winter wheat cultivated in Poland. *Food Chem*. 2006;95(2):290–300.
- Skouroumounis GK, Massy-Westropp RA, Sefton MA, Williams PJ. Precursors of damascenone in fruit juices. *Tetrahedron Lett*. 1992;33(24):3533–6.
- Bezman Y, Bilkis I, Winterhalter P, Fleischmann P, Rouseff RL, Baldermann S, et al. Thermal oxidation of 9'-*cis*-neoxanthin in a model system containing peroxyacetic acid leads to the potent odorant β -damascenone. *J Agric Food Chem*. 2005;53(23):9199–206.

Section 5

Flavour perception/modelling

Effects of fat and coffee concentration on aroma compounds and their intensity in formulated iced-coffee beverages

M M CHAYAN MAHMUD, Russell Keast, Robert A Shellie

CASS Food Research Centre, School of Exercise and Nutrition Sciences, Deakin University, 221 Burwood Highway, Burwood 3125, Australia, mmmahmud@deakin.edu.au and mahmudchayan@gmail.com

Abstract

Nine iced-coffee beverages were formulated: low fat - low coffee (LF-LC); medium fat - low coffee (MF-LC); high fat - low coffee (HF-LC); low fat - medium coffee (LF-MC); medium fat - medium coffee (MF-MC); high fat - medium coffee (HF-MC); low fat - high coffee (LF-HC); medium fat - high coffee (MF-HC); and high fat - high coffee (HF-HC). Aroma compounds were extracted by Head Space Solid Phase Micro-Extraction (HS-SPME) and analysed by Gas Chromatography-Mass Spectrometry Olfactometry (GC-MSO) using Modified Frequency (MF) approach. Fifty-two aroma compounds were detected including one acid, two alcohols, five aldehydes, one aromatic hydrocarbon, two bases, one ester, five furans, four phenols, eight pyrazines, two pyrroles, eight ketones, five sulphurs, and eight others. Five compounds namely '2, 3-butanedione' '2, 5-dimethyl pyrazine' 'furfuryl methyl sulphide' '2-methoxyphenol' and '2, 3-diethyl-5-methyl pyrazine' were commonly identified in all samples. Thirty-one aroma-compounds (MF % \geq 50) were considered as important aroma-active compounds. The total number of aroma compounds and their intensity were affected by fat and coffee concentration. For example, the number of aroma compounds and intensity (sum of modified frequency MF values) for LF-HC were 42 and 2292 while it was 13 and 470 for HF-LC, respectively.

Keywords: iced-coffee beverages, HS-SPME, GC-MSO, aroma

Introduction

The aroma or aroma active compounds of coffee are important for coffee flavour and quality coffee beverages. The effect of coffee variety, growing conditions (e.g., altitude, climate, soil type, topography), farming practice, processing, roasting, grinding, and brewing (e.g., water and coffee ratio) on coffee aroma and flavour are well investigated. However, there is very limited published research on iced-coffee beverages aroma profile, and there is no published research showing the effect of fat and coffee interaction on iced-coffee aroma.

Iced-coffee is a type of coffee beverage served chilled. Iced-coffee can be cold brew or normal brewed (hot) prior to adding the coffee into cold milk. Iced-coffee can be formulated with instant coffee using milk and/or fat. Studying iced-coffee has important implications for the beverage industry. The diversification of coffee drinkers and the popularity of "café culture" has brought iced-coffee to the centre stage of the global market. According to the Fortune Business Insights 2020 [1], the global iced coffee beverages market will reach a valuation of US\$ 42.36 billion by the end of 2027. Therefore, global brands are eyeing this lucrative space and trying to develop and launch premium ready to drink coffee which not only fetch higher margins but also provide a more connecting and enchanting coffee-drinking experience [1].

The addition of fat to coffee will have effects on aroma profile and their intensity. For example, the perceived aroma quality of coffee will change with fat concentration. Further, the release of lipophilic compounds decreases with the increase of fat content [2, 3]. Therefore, the aim of this study was to understand the combined effects of varying concentration of fat and coffee on iced-coffee beverages aroma profile and their intensity.

Experimental

Iced-coffee beverages formulation

Nine iced-coffee beverages were formulated with varying fat and coffee concentrations (Table 1). A constant amount (5 g/100mL) of sucrose (100 % crystal cane sugar, CSR, Australia) was added to all the samples. In brief, components for all iced-coffees were added together and homogenized at 5500 rpm (Silverson L4RT-A homogenizer, Triad Scientific, U.S.) for 10 min. The samples were prepared on the same day and stored in a refrigerator at 4 °C until used for extraction and instrumental analysis.

Extraction of volatile compounds

Head-Space Solid-Phase Micro-Extraction (HS-SPME) was used for the extraction of volatile compounds. Three phases (DVB/CAR/PDMS, grey, 50/30 μ m, Merck, North Ryde, Australia) SPME fibres were considered for the extraction of volatile compounds. From formulated iced-coffee, 5 mL of aliquot was taken into 20 mL headspace

vial and sealed with 18 mm Teflon lined magnetic cap (Agilent, Mulgrave, Australia). SPME fibre was exposed to the headspace of the glass vial for 30 min at 35 °C for 20 min. After the extraction process the fibre was injected into the GC inlet for desorption for 5 min at 250 °C, followed by oven temperature program described in the below section.

Table 1: Iced-coffee beverages formulation.

Sample	Cream (g/100 mL)	Coffee (g/100 mL)	Total fat from cream (approx.) (g/100 mL)
LF-HC	0	6.00	0.00
MF-HC	10.50	6.00	3.70
HF-HC	21.20	6.00	7.40
LF-MC	0.00	2.00	0.00
MF-MC	10.50	2.00	3.70
HF-MC	21.20	2.00	7.40
LF-LC	0.00	0.66	0.00
MF-LC	10.50	0.66	3.70
HF-LC	21.20	0.66	7.40

Note: The volume was adjusted by adding skim milk (Devondale, Murray Goulburn Co-operative Co. Ltd, Australia) to make up the volume to 100 mL (Coffee: Nescafé blend 43, Nestlé, Australia; Cream: Bulla thickened cream, Bulla Dairy Foods Pty. Ltd., Australia). LF-LC = low fat - low coffee; MF-LC = medium fat - low coffee; HF-LC = high fat - low coffee; LF-MC = low fat - medium coffee; MF-MC = medium fat -medium coffee; HF-MC = high fat - medium coffee; LF-HC = low fat - high coffee; MF-HC = medium fat - high coffee; and HF-HC = high fat - high coffee.

Analysis of volatile compounds

The analysis was carried out using an Agilent 7890B gas chromatograph equipped with Agilent 7790B Mass Selective Detector (Agilent, Mulgrave, Australia) and Gerstel ODP-3 Olfactory Detector Port (Gerstel, Lasersan Australasia, Tanunda, Australia). The separation was conducted using a BP-5MS, 30 m × 0.25 mm × 0.25 µm (Trajan Scientific and Medical, Ringwood, Australia) capillary column. A splitless SPME liner (i.d. 0.75mm, PN. 5190-4048, Agilent, USA) was used in the inlet. The inlet was split/splitless using Merlin Microseal (Merck, North Ryde, Australia), and the injection mode was splitless. The inlet temperature was maintained at 250 °C. Research grade He (99.999%) was used as carrier gas under a constant flow of 1.4 mL/min. The column oven temperature started at 40 °C with a 4 min hold time and increased to 200 °C at a rate of 8.6 °C/min with an 8 min hold time. Total analysis time was 30.6 min. MS conditions were: scan range 35 - 450 m. u., solvent cut time 0 min, electron impact mode at 70 eV, MS source 230 °C and MS quad 150 °C.

For ODP, the column was connected with a splitter and the effluent was split 1:1 into two neutral capillary fused silica columns (1.43 m × 0.10 mm i.d. and 0.57 m × 0.10 mm i.d., respectively, Trajan Scientific and Medical, Australia) leading to the MS detector and sniffing port. The auxiliary temperature was maintained at 250 °C and the makeup gas was nitrogen.

GC-O data collection method

Modified Frequency (MF) method was used for GC-O data collection as proposed by Dravnieks 1985 [4]. A panel composed of six trained sniffers (3 female and 3 male) was used to carry out the analyses. Each sniffer smelt each extract once. Each sniffer carried out one session per day, and each session was around 25 min. Panellists were asked to describe and score the intensity of each aroma compounds while sniffing the effluent from ODP. The computer recorded the retention time and sniffing time of each aroma compounds. The aroma-intensity was evaluated using a 6-point scale (1=very weak, 2=weak, 3=clear, 4=very clear, 5=intense, and 6=very intense).

Retention index

An Alkane solution C7 – C40 (49452 U, Supelco, USA) 1000 µg/mL in hexane was employed to calculate the Linear Retention Index (LRI) of each analyte on the BP-5MS column.

HS-SPME, GC-MS-O performance and Retention Time (RT) stability evaluation

The consistent performance of HS-SPME and GC-MS-O were evaluated by monitoring the total peak area of a Quality Control (QC) sample. The coefficient of variation (CV) of the total peak area of QC sample was 9.4% throughout the study. The stability of RT was monitored by n-alkane. The CV % of n-alkane's RT was 0.008.

Statistics

The Modified Frequency (MF) value of each detected aroma compound was calculated using the below formula:

$$MF (\%) = \sqrt{F (\%) \times I (\%)} \quad (\text{Eq 1})$$

Where F (%) is the detection frequency of an aromatic attribute expressed as a percentage ($\frac{\text{number of detections}}{6} \times 100$ %) and I (%) is the average intensity expressed as a percentage of the maximum intensity ($\frac{\text{sum of intensities from 6 sniffers}}{30} \times 100$ %). MF (%) represents the importance of the aroma compound in a sample. The effects of different level of fat and coffee interaction on total intensity or total MF value of different samples and chemical groups was visualised using Excel 2016.

Results and discussion

A total of fifty-two aroma compounds were detected by GC-O analysis, as shown in Table 2, including 1 acid, 2 alcohols, 5 aldehydes, 1 aromatic hydrocarbon, 2 bases, 1 ester, 5 furans, 4 phenols, 8 pyrazines, 2 pyrroles, 8 ketones, 5 sulphurs, and 8 others. For the sake of confirmation or simplicity, those aroma compounds not reaching a minimum GC-O intensity of 25 % (maximum =100 %) and not perceived by three sniffers (maximum = six sniffers) in any of the nine formulated iced-coffee samples were eliminated and considered as noise. Therefore, the absence of a specific aroma compound in some of the samples means that the MF score didn't reach 25 % and the perceived frequency was below three, it still might occur in the sample but the aroma intensity was under the threshold level for the GC-O panellists [5, 6]. The highest number (n=42) of aroma-compounds were identified in LF-HC and the lowest number (n=13) of aroma-compounds were identified in HF-LC. Five aroma compounds namely Butane-2,3-dione, 2,5-Dimethylpyrazine, 2-(Methylsulfanylmethyl)furan, 2-Methoxyphenol and 2,3-Diethyl-5-methylpyrazine were commonly identified in all nine samples.

Among fifty-two aroma compounds, thirty-one presented the highest aroma activities (MF % \geq 50) such as 2, 3-butanedione, 2-butanone, 2-methylbutanal, 2, 3-pentanedione, 4-methylthiazole, methyl pyrazine, furfural and so on. LF-HC contained highest number of intense aroma compounds (n=25) followed by HF-HC (n=23), LF-MC (n=21), MF-HC (n=19), MF-MC (n=17), HF-MC (n=13), LF-LC (n=10), MF-LC (n=7), and HF-LC (n=2). Previous studies reported that aroma compounds such as 2-methylbutanal, furfural, 2,3-diethyl-5-methyl pyrazine, 2,3-butanedione, 2-methoxyphenol, 2,3-pentanedione, 2-butanone, 1-(2-furanyl)ethanone, ethyl pyrazine and 2-furanmethanol [7-9] are important aroma compounds in roasted or brewed coffee. In the current study, based on MF value, thirty-one compounds can be considered as important compounds that could have potential impact on iced-coffee beverages' aroma. Other compounds may be important for overall iced-coffee flavour, but they are not strongly intense, therefore, less important to the iced-coffee beverage aroma.

The MF value of all aroma compounds and major chemical groups were summarised and presented in Figure 1. Overall, the total intensity (sum of MF values) of each sample and different chemical groups' aroma-intensity were affected by fat and coffee ratio. The changes in intensity can be caused by different factors. For example, fat retains most volatiles, while dairy products also contain protein and carbohydrate that can interact by adsorption, entrapment, and encapsulation [10]. Therefore, a simple correlation between fat level and aroma release cannot be established. However, in all samples, high fat content had more negative impact on aroma intensity compared to the zero fat. Contrary, small effect was observed on aroma intensity between medium and high coffee concentration. The possible reason could be the complex matrices effect of volatiles e.g. low aroma intense compounds suppressed by the high intense compounds [11].

Conclusion

Fat and coffee ratio is important to the volatile aroma compounds release and their intensity. Overall, volatile release and/or the intensity of aroma compounds decreased with the increase of fat concentration while it was opposite with coffee concentration. For example, lower number of aroma compounds identified in low coffee concentration. This study suggested that too low coffee concentration is not ideal for the desirable coffee flavour or to maintain the characteristic coffee flavour. Similarly, too much fat in coffee affects the release of the volatiles and their intensity. Therefore, adding too much fat alter the coffee flavour. We used three different levels of fat and coffee concentration and noticed MF-MC is an appropriate ratio to maintain the characteristic coffee aroma. Future study could narrow the range of fat and coffee around the most liked concentrations used in this study to find out the fine-tuning concentrations to maximise the coffee like flavour and consumer acceptance. The result of this study can be utilised to reformulate the iced-coffee with desirable coffee aroma.

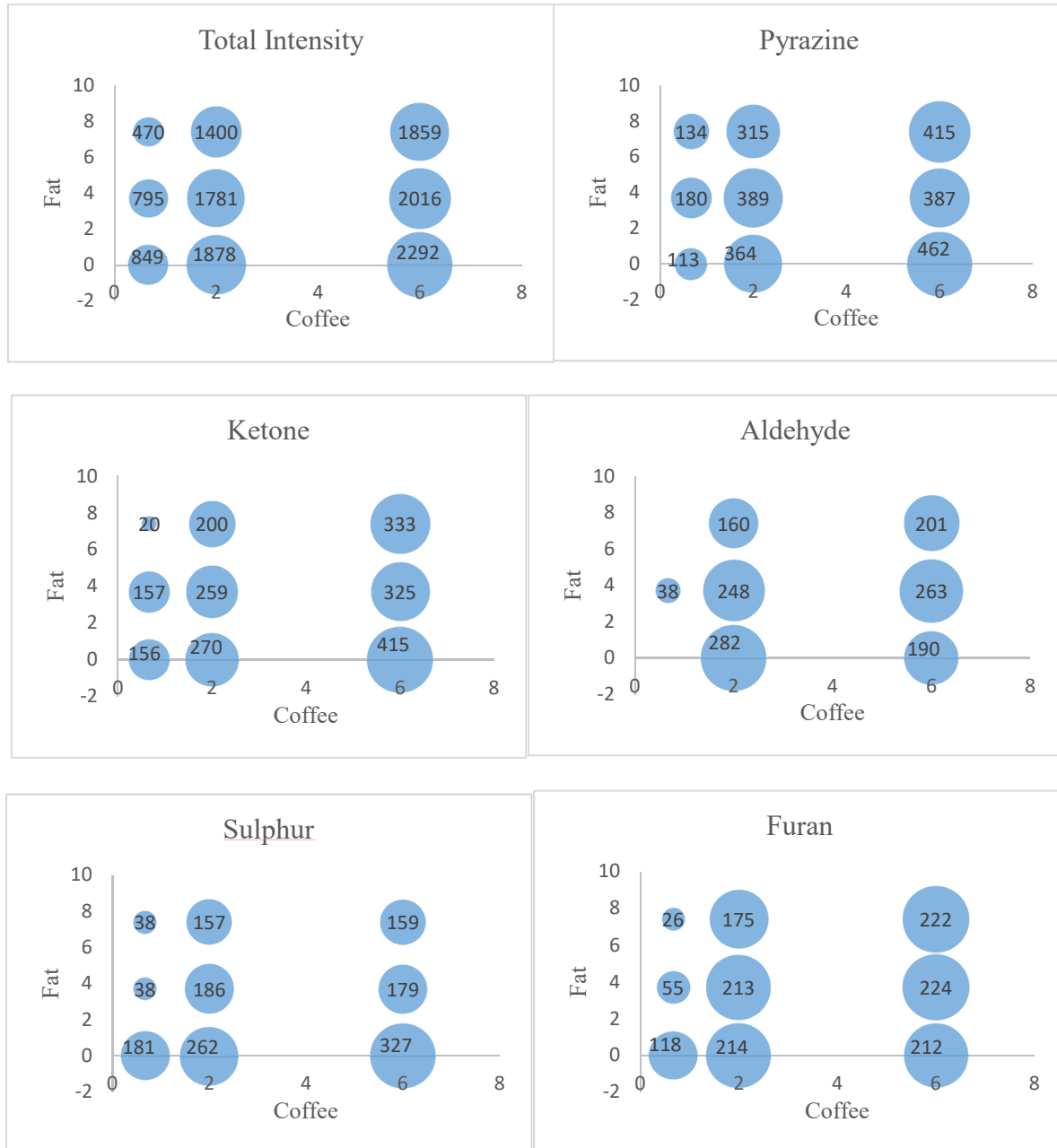


Figure 1: Effects of fat and coffee concentration on the total intensity (sum of MF values) of iced-coffee sample and different chemical groups.

References

1. Fortune Business Insights. Ready to Drink (RTD) coffee market size, share, and COVID-19 impact analysis, by packaging material (glass and PET bottles, cans, and others), distribution channel (supermarket/hypermarkets, convenience stores, and online retail) and regional forecast, 2020-2017. 2020. Report ID: FBI100285. <https://www.fortunebusinessinsights.com/industry-reports/ready-to-drink-rtd-coffee-market-100285>
2. Frank D, Appelqvist I, Piyasiri U, Delahunty C. In vitro measurement of volatile release in model lipid emulsions using proton transfer reaction mass spectrometry. *J Agric Food Chem.* 2012;60(9):2264-2273.
3. Frank D, Appelqvist I, Piyasiri U, Wooster T J, Delahunty C. Proton transfer reaction mass spectrometry and time intensity perceptual measurement of flavor release from lipid emulsions using trained human subjects. *J Agric Food Chem.* 2011;59(9):4891-4903.
4. Dravnieks A. Atlas of Odor Character Profiles, ASTM: Philadelphia. 1985.
5. Bueno M, Resconi V C, Campo M M, Cacho J, Ferreira V, Escudero A. Gas chromatographic-olfactometric characterisation of headspace and mouthspace key aroma compounds in fresh and frozen lamb meat. *Food Chem.* 2011;129(4):1909-1918.

6. Kortensniemi M, Rosensvald S, Laaksonen O, Vanag A, Ollikka T, Vene K, et al. Sensory and chemical profiles of Finnish honeys of different botanical origins and consumer preferences. *Food Chem.* 2018;246:351-359.
7. Blank I, Sen A, Grosch W. Potent odorants of the roasted powder and brew of Arabica coffee. *Z Lebensm Unters Forsch.* 1992;195(3):239-245.
8. Czerny M, Mayer F, Grosch W. Sensory study on the character impact odorants of roasted Arabica coffee. *J Agric Food Chem.* 1999; 47(2): 695-699.
9. Flament I. Coffee Flavour Chemistry. In: Chichester: John Wiley and Sons LTD. 2002.
10. Kinsella J E. Flavor Perception and Binding. *Inform.* 1990;1(3):215-227.
11. Bult J H, Schifferstein H N, Roozen J P, Boronat E D, Voragen A G, Kroeze J H. Sensory evaluation of character impact components in an apple model mixture. *Chem Senses.* 2002;27(6):485-494.

Table 2: List of aroma compounds and their Modified Frequency (MF) values as detected using GC-MS-O. Important aroma compounds (MF %≥ 50) in relation to flavour.

#	Compounds	Aroma descriptions	LRI ¹ (Cal.)	LRI ² (Ref.)	Chemical group	MF values									Identification method ³
						LF-HC	MF-HC	HF-HC	LF-MC	MF-MC	HF-MC	LF-LC	MF-MC	HF-MC	
1	2-Methylpropan-1-ol	caramel, cocoa, green, malt, nut	-	-	Aldehyde	30	29	26	36	30	0	0	0	0	AD, MS
2	Butane-2,3-dione	butter, caramel, fruit, sweet, yogurt	-	-	Ketone	38	31	51	31	45	38	38	47	26	AD, MS
3	Butan-2-one	ether, fragrant, fruit, pleasant, sweet	-	-	Ketone	59	59	65	47	43	57	0	0	0	AD, MS
4	2-Methylbutanal	acid, almond, cocoa, malt, pungent, fermented	660	654	Aldehyde	66	78	68	78	75	50	0	0	0	AD, LRI, MS, ST
5	Pentane-2,3-dione	bitter, butter, caramel, fruit, sweet	697	699	Ketone	41	49	59	0	30	29	0	0	0	AD, LRI, MS, ST
6	2-Methylthiophene	Sulphur	768	771	Sulphur	46	29	0	0	0	0	0	0	0	AD, LRI, MS, ST
7	Methyl 3-methylbutanoate	apple, fruit, pineapple	775	773	Esters	0	0	0	0	36	38	0	0	0	AD, LRI, MS
8	Hexanal	grass, green	797	801	Aldehyde	41	38	0	45	26	0	0	0	0	AD, LRI, MS, ST
9	1-Ethylpyrrole	chemical, roast	809	810	Pyrrole	35	0	0	33	0	0	0	0	0	AD, LRI, MS
10	4-Methyl-1,3-thiazole	green, nut, roasted meat	812	814	Sulphur	57	0	0	57	0	0	0	0	0	AD, LRI, MS
11	2-Methylpyrazine	cocoa, green, hazelnut, popcorn, roasted	819	821	Pyrazine	61	43	45	56	35	45	0	0	0	AD, LRI, MS
12	Furan-2-carbaldehyde	almond, baked potatoes, bread, candy, floral	828	835	Furan	0	38	59	0	33	31	0	0	0	AD, LRI, MS, ST
13	2,4,5- Trimethyl-1,3-oxazole	dairy, butter, aged cheeses, yogurt, caramel	844	848	Oxazol(in)es	37	59	78	45	45	26	0	0	29	AD, LRI, MS
14	Furan-2-ylmethanol	burnt, caramel, cooked, solvent	853	854	Furan	65	45	0	61	0	33	55	55	0	AD, LRI, MS, ST
15	Heptan-2-ol	citrus, coconut, fried, mushroom, oil	899	899	Alcohol	71	66	70	75	63	51	0	45	0	AD, LRI, MS, ST
16	1-(Furan-2-yl) ethenone	cocoa, coffee, smoke, tobacco	904	913	Furan	51	82	85	65	80	78	63	0	0	AD, LRI, MS, ST

Effects of fat and coffee concentration on aroma compounds intensity in formulated iced-coffee beverages

17	2,5-Dimethylpyrazine	burnt plastic, cocoa, medicine, nutty	907	914	Pyrazine	65	78	90	80	82	80	35	78	29	AD, LRI, MS, ST
18	2-Ethylpyrazine	green, iron scorch, must, peanut butter, roasted	911	915	Pyrazine	65	59	68	47	65	59	0	31	38	AD, LRI, MS, ST
19	5-Methylfuran-2-carbaldehyde	almond, caramel, cooked, roasted garlic, spice	957	961	Furan	53	33	45	57	57	33	0	0	26	AD, LRI, MS
20	(Methyltrisulfanyl)methane	cabbage, fish, onion, sulphur, sweat	968	968	Sulphur	75	36	38	71	55	55	53	0	0	AD, LRI, MS, ST
21	Phenol	medicine, phenol, sharp, smoke, spice	978	984	Phenol	0	31	0	0	0	0	0	0	0	AD, LRI, MS
22	Furan-2-ylmethyl acetate	roast, fruity, sweet	988	990	Furan	43	26	33	31	43	0	0	0	0	AD, LRI, MS, ST
23	2-Ethyl-6-methylpyrazine	green, nut, roasted	994	997	Pyrazine	39	0	0	0	0	0	0	0	0	AD, LRI, MS, ST
24	2-(Methylsulfanylmethyl) furan	coffee	996	995	Sulphur	76	73	82	63	78	71	57	38	38	AD, LRI, MS
25	2-Ethyl-3-methylpyrazine	green, must, nut, potato, roasted	998	999	Pyrazine	65	63	76	45	73	35	0	0	0	AD, LRI, MS
26	3-Methylcyclopentane-1,2-dione	coffee, burnt, sugar	1030	1030	Ketone	55	60	76	69	47	0	35	57	0	AD, LRI, MS, ST
27	2-Phenylacetaldehyde	pungent, fermented, earthy	1037	1038	Aldehyde	53	53	53	66	54	59	0	0	0	AD, LRI, MS, ST
28	1-Ethylpyrrole-2-carbaldehyde	burnt, roasted, smoky	1045	1046	Bases	65	75	68	55	35	35	48	33	0	AD, LRI, MS
29	1-(1H-pyrrol-2-yl) ethenone	bread, cocoa, hazelnut, walnut	1059	1063	Ketone	53	0	0	0	0	0	0	0	0	AD, LRI, MS
30	Unknown	musty, bread	1062	-	-	41	0	0	0	0	0	0	0	0	-
31	3-Ethyl-2,5-dimethylpyrazine	broth, earth, potato, roast	1076	1079	Pyrazine	47	75	83	76	67	55	0	0	0	AD, LRI, MS
32	2-Methoxyphenol	bacon, medicine, phenol, smoke, wood, vanilla	1084	1089	Phenol	68	78	58	61	47	65	66	78	61	AD, LRI, MS
33	Nonan-2-one	pleasant, hot milk, fragrant, fruit, green	1087	1090	Ketone	71	78	82	68	51	47	83	53	0	AD, LRI, MS, ST
34	Unknown	cereal, nutty, musty, roasted	1088	-	-	59	49	59	37	35	49	0	0	0	

35	Nonanal	citrus, fat, green, paint, pungent	1101	1104	Aldehyde	0	65	54	57	63	51	0	38	0	AD, LRI, MS, ST
36	Unknown	roast, earth, garden	1128	-	-	0	43	37	0	41	0	0	0	0	-
37	2,3-Diethyl-5-methylpyrazine	earth, meat, potato, roast	1149	1151	Pyrazine	73	69	53	60	67	41	78	71	67	AD, LRI, MS, ST
38	3,5-Diethyl-2-methylpyrazine	baked, cocoa, roast, rum, sweet	1153	1155	Pyrazine	47	0	0	0	0	0	0	0	0	AD, LRI, MS
39	Octanoic acid	fat, cheese, rancid	1171	1174	Acid	73	54	63	76	57	29	80	76	0	AD, LRI, MS, ST
40	1-(Furan-2-ylmethyl) pyrrole	cocoa, green, roast	1176	1182	Pyrrole	82	62	51	69	56	71	87	0	0	AD, LRI, MS, ST
41	2-[(Methylsulfonyl)methyl] furan	Smoke	1213	1222	Sulphur	73	41	39	71	53	31	71	0	0	AD, LRI, MS
42	Unknown	cocoa, green, mint	1239	-	-	0	39	0	0	26	29	0	33	0	-
43	4-Ethyl-2-methoxyphenol	medicine, smoke, woody	1274	1282	Phenol	38	0	0	0	0	0	0	0	0	AD, LRI, MS, ST
44	Undecan-2-one	fatty, cheese, butter, nut, fruit, floral	1289	1295	Ketone	38	0	0	0	0	0	0	0	0	AD, LRI, MS
45	4-Ethenyl-2-methoxyphenol	clove, curry, smoke, spice	1309	1317	Phenol	37	45	45	35	45	0	0	0	31	AD, LRI, MS, ST
46	Unknown	roasted, smoke, nutty	1333	-	-	34	0	0	0	0	0	0	0	0	-
47	Unknown	dairy, milky, cheese, pleasant	1345	-	-	0	37	0	0	0	0	0	29	31	-
48	1-(2,6,6-Trimethylcyclohexa-1,3-dien-1-yl) but-2-en-1-one	boiled apple, floral, fruit, grape, tea	1385	1388	Ketone	60	48	0	55	43	29	0	0	0	AD, LRI, MS
49	Unknown	roast, smoky	1453	-	-	46	0	0	0	0	0	0	0	0	-
50	3,3,7-Trimethyl-8-methylidenetricyclo [5.4.0.0 ^{2,9}] undecane	sweet, woody, rose, vegetable, flower	1461	1451	Aromatic Hydrocarbon	0	0	0	0	0	0	0	0	35	AD, LRI, MS
51	Dodecan-1-ol	fat, wax	1475	1473	Alcohol	0	0	0	0	0	0	0	33	29	AD, LRI, MS, ST
52	Unknown	fruity, sweet	1596	-	-	0	0	0	0	0	0	0	0	36	-

Note: ¹ LRI in BP-5MS column; ² LRI in DB-5MS column; ³ Identification method: MS = matching mass spectra of GC-MS analysis with those from the NIST 2017 library (library match: ≥ 70 %); AD = coincidence of Aroma Description (AD) reported in online data base (<http://www.odour.org.uk>; <http://flavornet.org>; and <http://www.thegoodscentscompany.com/>) or literature; LRI = coincidence of Linear Retention Index (LRI) reported in online data base (e.g. <https://pubchem.ncbi.nlm.nih.gov/> and <https://www.pherobase.com/>) or literature; ST = coincidence of LRI with authentic standard.

The bitter taste of vitamins is mediated by human TAS2R activation

THOMAS DELOMPRÉ, Christine Belloir, Christian Salles and Loïc Briand

Centre des Sciences du Goût et de l'Alimentation (CSGA), AgroSup Dijon, CNRS, INRAE, Université de Bourgogne Franche-Comté, Dijon, France, loic.briand@inrae.fr

Abstract

Vitamins play an important role in maintaining normal physiologic and metabolic functions. Vitamins are known to generate bitterness, which may contribute to the off-taste of nutritional supplements. This negative sensation may decrease product acceptability and patient compliance. Few studies have examined taste thresholds and sensory sensing mechanisms at the origin of vitamin taste detection. To better understand vitamin bitterness perception, we combined human sensory analysis and taste receptor functional assays. We measured the aqueous taste detection threshold of four B vitamins using sensory difference tests. Challenging the 25 human bitter taste 2 receptors (TAS2Rs), we found that three vitamins stimulated one or more receptors. For each positive molecule-TAS2R combination, we measured the half-maximum effective concentrations (EC₅₀). Thus, we found that the combination of sensory and biological data can provide useful explanations for the bitter detection of vitamins.

Keywords: vitamins, bitter, bitter taste threshold, cellular assay, sensory studies

Introduction

Many bitter molecules present in food have beneficial effects on health, such as polyphenols, amino acids, minerals, and vitamins. Although vitamins supply no energy, they are essential for correct human body function. The current classification system, based on physicochemical, storage and excretion properties, divides the thirteen known vitamins into two groups called water-soluble and fat-soluble vitamins. These nutrients are involved in various physiological and biochemical processes that are essential for the proper functioning of the human body [1]. The human body is able to synthesise two vitamins (phyloquinone and calciferol); the others must be provided by a healthy and varied diet. During certain pathologies and/or difficult access to healthy food, vitamin deficiencies may occur in some people. To prevent these deficiencies, vitamin intake in the form of nutritional supplements or supplemented foods is strongly recommended. When taken in the mouth, vitamins can be perceived with a bitter off-taste, leading to a decrease in product acceptability and patient compliance [2]. Although their use in medicine is common, little is known about the taste threshold and sensory sensing mechanism involved in vitamin bitter taste detection. In humans, bitter taste is detected through the activation of 25 bitter taste receptors (TAS2Rs) belonging to the class A subfamily of G protein-coupled receptors (GPCRs) [3]. A previous study demonstrated that thiamine hydrochloride (a vitamin B1 analogue) is able to activate two TAS2Rs (TAS2R1 and TAS2R39) [4]. However, no information is available on other vitamins.

To better understand the mechanisms involved in bitterness perception, we combined taste receptor functional assays and human sensory analysis. First, we challenged the 25 human TAS2Rs with eleven vitamins. For each positive molecule-receptor combination, we measured the half-maximum effective concentrations (EC₅₀). We then determined the bitter taste recognition threshold of four native or analogue vitamins in aqueous solution (thiamine hydrochloride, riboflavin phosphate, niacinamide, pyridoxine hydrochloride) that exhibit a strong bitter taste.

Experimental

Chemicals

Thirteen native or analogue vitamins were provided by Bayer SAS (Global Innovation Centre, Gaillard, France): thiamine hydrochloride (B1); riboflavin phosphate (B2), niacinamide (B3), calcium pantothenate (B5), pyridoxine hydrochloride (B6), biotin (B8), folic acid (B9), cobalamin (B12), ascorbic acid (C), retinal (A), calciferol (D), phyloquinone (K), and α -tocopherol acetate (E).

Receptor Functional Assay

HEK293T-Ga16gust44 cells were seeded on poly-D-lysine-coated 96-well black microplates. After overnight growth, the cells were transiently transfected with the 25 TAS2R expression plasmids using Lipofectamine 2000TM (Life Technologies). Twenty hours later, the cells were loaded with Fluo4-AM for 1 hour. The fluorescence signal was recorded at 510 nm after excitation at 488 nm using the fluorescence microplate reader FlexStation 3

(Molecular Devices). Given that some compounds studied could interfere with cellular viability and calcium assays, they were tested on mock-transfected cells. All vitamins were tested except riboflavin phosphate and niacinamide, which possess intrinsic fluorescence, making them incompatible with the assay. Vitamins were prepared in adapted buffer and tested at different concentrations between 1 μ M and 30 mM. The ratio between maximum variations in fluorescence after ligand addition and initial fluorescence before addition ($\Delta F/F$) was calculated for each well to generate a dose-response curve. The dose-response data were fitted, and EC_{50} values were calculated using a four-parameter logistic equation (SigmaPlot, Systat Software, San Jose, CA).

Human Sensory Analysis

To evaluate the bitterness of vitamins that have not been included in the cell-based assay and to compare *in vitro* and *in vivo* results, we conducted human sensory experiments. The bitter taste detection thresholds of four vitamins (thiamine hydrochloride, riboflavin phosphate, niacinamide, and pyridoxine hydrochloride) were determined by 32 panellists using a discriminative sensory test called three-alternative forced choice (3-AFC) [5]. Samples are presented in black glasses and under red light. Evaluation was conducted with a nose clip, and four repetitions were performed per subject for each tested vitamin. The best estimate threshold method was used to calculate the bitter taste detection threshold of each compound [6]. The vitamin concentrations used were determined according to the daily reference intake, quantities present in the nutritional supplements and toxicity thresholds. The compounds were diluted in water (Evian water, France). This sensory experiment was approved by an ethical committee (Personal Protection Committee 2018-A01342-53).

Results and discussion

To identify the bitter taste receptors activated by the tested vitamins, 25 human TAS2Rs were transiently expressed in HEK293T cells stably expressing the chimeric G protein $G\alpha 16gust44$. Calcium imaging experiments showed that two vitamins activated only one TAS2R. Therefore, calciferol (vitamin D) and retinal (vitamin A) activate TAS2R10 and TAS2R38, respectively. We observed that pyridoxine hydrochloride (the vitamin B6 analogue) activates two TAS2RS proteins, namely, TAS2R7 and TAS2R14. We determined dose-response curves by stimulating transfected cells with increasing concentrations of bitter vitamins (Figure 1), yielding EC_{50} values of 250 and 300 μ M for the TAS2R10-calciferol and TAS2R38-retinal pairs, respectively. Concerning pyridoxine hydrochloride, we measured similar EC_{50} values (10.25 and 25.52 mM) for the two activated receptors, TAS2R7 and TAS2R14, respectively. Comparing the EC_{50} values of each vitamin-receptor pair (Figure 1), we observed that the two fat-soluble vitamins activated bitter taste receptors at lower concentrations than water-soluble vitamins.

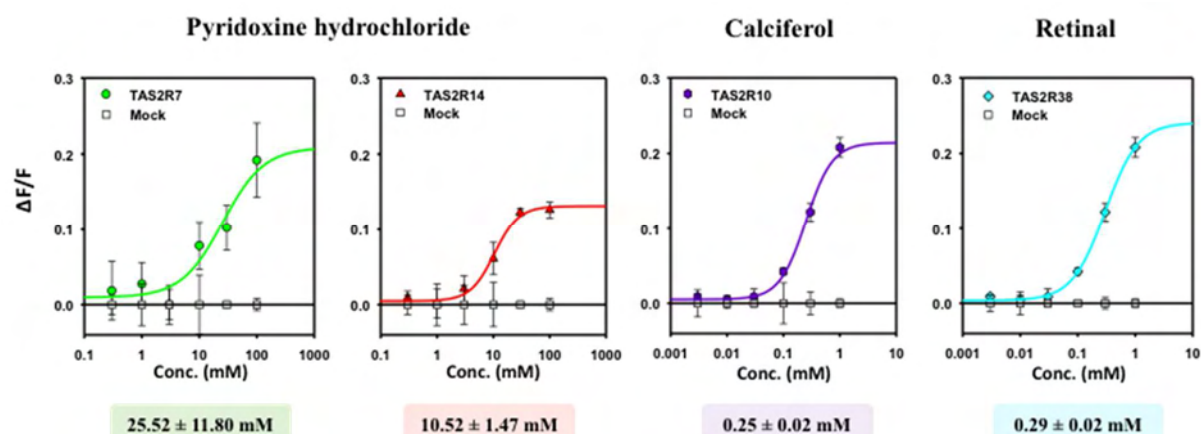


Figure 1: Dose-response curve and EC_{50} value of cell lines transiently expressed TAS2Rs stimulated by three vitamins: pyridoxine hydrochloride, retinal and calciferol.

Our cellular assay detects the cellular response to bitter compounds using a calcium-sensitive fluorescent dye [4]. Therefore, this method cannot be applied to fluorescent vitamins, such as riboflavin phosphate and niacinamide. To evaluate their potential bitterness, we performed human sensory experiments. In addition, to compare *in vitro* and *in vivo* results, two other vitamins previously identified as bitter were included in the sensory analysis. We measured the bitter taste detection threshold of these four vitamins (Figure 2). With a cut-off value between 1.1 and 5.5 mM, we found that thiamine hydrochloride, niacinamide and pyridoxine hydrochloride had a

lower activation potency than riboflavin phosphate (0.65 mM). These sensory experiments confirmed the bitterness of two other vitamins not tested in the cellular assay, riboflavin phosphate and niacinamide.

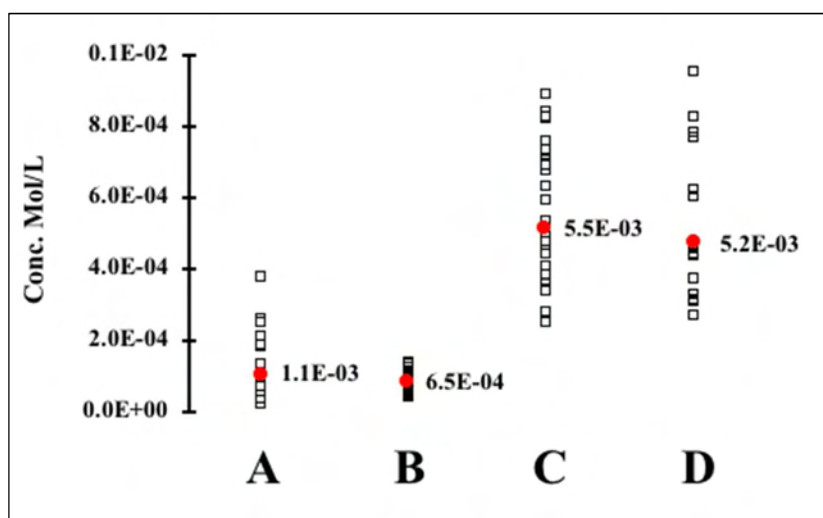


Figure 2: Human bitter taste recognition threshold (mol/L) of four water-soluble vitamins: (A) thiamine hydrochloride, (B) riboflavin phosphate, (C) niacinamide, and (D) pyridoxine hydrochloride

As observed in some studies, the data collected relative to the cellular assay are not in perfect agreement with human bitterness perception [7, 8]. Table 1 summarises the bitter taste threshold of some vitamins (from cell-based assay and/or sensory analysis) and their calculated molar concentration in standard nutritional supplements (based on the recommendations of pharmaceutical companies and consumer habits). Comparing the data obtained, we observed that the bitter taste threshold measured using the cellular-based assay was lower than the bitter taste threshold determined by the 32 assessors. For example, the bitter taste threshold for thiamine hydrochloride differs by a factor of ~10 between *in vivo* and *in vitro* experiments. The same observation was done for pyridoxine hydrochloride (a factor of ~5). Our data demonstrated a slight difference between human bitter vitamin perception and TAS2R activation in a taste receptor functional assay. This difference can have different origins at both peripheral and central levels.

Table 1: Comparison between human bitter detection threshold, cellular bitter detection threshold and concentration in nutritional supplement studied for six bitter vitamins.

Vitamin	Cellular bitter detection threshold (mM)	Human bitter detection threshold (mM)	* Concentration in nutritional supplement (mM)
Thiamine hydrochloride	0.10	1.10	0.44
Riboflavin phosphate	ND	0.65	0.40
Niacinamide	ND	5.50	4.06
Pyridoxine hydrochloride	1	5.20	0.73
Retinal	0.05	ND	0.03
Calciferol	0.05	ND	0.01x10 ⁻⁰⁵

Cellular taste threshold refers to the minimum concentration of vitamin able to activate TAS2R.

* Calculated concentration for a nutritional supplement (Berocca©, Bayer France) dissolved in 100 mL of water. ND, not determined.

Conclusion

Combining cellular assays and psychometric data, we identified vitamins with bitter taste with different threshold values resulting from *in vivo* and *in vitro* experiments. These differences may be due to absorption by the oral epithelium or/and the interaction of bitter compounds with salivary proteins as previously suggested [7, 8]. However, our study revealed that the vitamin concentrations present in the nutritional supplements cannot contribute to their off-taste or bitter taste (Table 1). This observation could be linked to the presence of other nutrients, such as minerals, which have a strong bitter taste [2], and/or additive effects between bitter compounds [7]. Thus, our data provide information on bitter vitamin concentrations that should not be exceeded to develop a nutritional supplement with better organoleptic qualities and consumer acceptability.

References

1. Bender, D-A. The vitamins. Introduction to human nutrition 2009, 2, 132-187.
2. Delompré T, Guichard E, Briand L, Salles C. Taste perception of nutrients found in nutritional supplements: a review. *Nutrients*. 2019;11:2050.
3. Chandrashekar J, Mueller K-L, Hoon M-A, Adler E, Feng L, Guo W, Zuker C-S, Ryba N-J. T2Rs function as bitter taste receptors. *Cell*. 2000;100:703-711.
4. Meyerhof W, Batram C, Kuhn C, Brockhoff A, Chudoba E, Bufe B, Appendino G, Behrens M. The molecular receptive ranges of human TAS2R bitter taste receptors. *Chem Senses*. 2010;35:157-170.
5. Meilgaard M-C, Carr B-T, Civille G-V. Sensory evaluation techniques. CRC press, 2006.
6. Harvey, L.O. Efficient estimation of sensory thresholds. *Behav Res Methods*. 1986;18:623-632.
7. Intelmann D, Batram C, Kuhn C, Haseleu G, Meyerhof W, Hofmann T. Three TAS2R bitter taste receptors mediate the psychophysical responses to bitter compounds of hops (*Humulus lupulus* L.) and beer. *Chemosens Percept*. 2009;2(3):118-32.
8. Soares S, Silva M-S, Garcia-Estevez I, Großmann P, Brás N, Brandão E, Mateus N, de Freitas V, Behrens M, Meyerhof W. Human bitter taste receptors are activated by different classes of polyphenols. *J Agric Food Chem*. 2018;66(33):8814-23.

Sensory analysis, aroma compounds and flavour modulation of rapeseed oil: A review

YOUFENG ZHANG^{1,2}, Yuqi Wu¹, Sirui Chen¹, Binbin Yang¹, Hui Zhang¹, Xingguo Wang¹, Michael Granvogl² and Qingzhe Jin¹

¹ International Joint Research Laboratory for Lipid Nutrition and Safety, State Key Lab of Food Science and Technology, Collaborative Innovation Center of Food Safety and Quality Control in Jiangsu Province, School of Food Science and Technology, Jiangnan University, Wuxi, 214122, China

² Department of Food Chemistry and Analytical Chemistry (170a), Institute of Food Chemistry, University of Hohenheim, Garbenstrasse 28, 70599 Stuttgart, Germany; zhangyoufengwuxi@163.com

Abstract

Rapeseed oil, one of the world's three major vegetable oils, is appreciated for its characteristic flavour and high nutritional value. Flavour is an important determinant of oil quality and consumer acceptance. This review systematically evaluates and discusses recent advances and knowledge on the sensory analysis and aroma compounds of rapeseed oil. One hundred and ninety-nine aroma compounds in rapeseed oil were found in literature. They mainly contribute to the roasty, fatty, cheese-like, green, fruity, pungent, sweaty, sweet, spicy, flowery, nutty, earthy, and sulphury flavour. Among them, one hundred and fourteen substances have been reported to be odorants in rapeseed oil only once before in the literature, which require further validation via aroma reconstitution and omission test. The processes (storage, dehulling, thermal treatment, flavouring with herbs, and refining) affecting the flavour of rapeseed oil from sensory and molecule perspectives were also summarized. Studies to elucidate the formation mechanisms of aroma compounds in rapeseed oil by different processes are needed, which will contribute to get a deeper understanding of factors leading to the variations of flavour and to produce rapeseed oil products with a desired aroma and a higher consumer acceptance.

Keywords: rapeseed oil, flavour, sensory analysis, aroma compounds, flavour modulation

Introduction

Rapeseed oil is one of the world's most consumed edible oils. Due to its characteristic flavour, rapeseed oil is very popular in Europe and China which are the world's first and second producers and consumers, respectively. In Europe, e.g., Austria, Denmark, Germany, and Switzerland, virgin rapeseed oil obtained by cold pressing gains massive popularity due to its mild and fresh taste and cabbage-like aroma [1, 2]. In China, hot-pressed rapeseed oil is popular because of its strong roasted, caramel, and pungent flavour [3]. Flavour is one of the most critical criteria for consumers to choose a certain edible oil. During the past decade, more and more attention has been paid to the flavour of rapeseed oil, odorants in particular. To the best of our knowledge, there is no systematic review on summarizing, comparing, and critiquing the literature regarding the flavour of rapeseed oil. Thus, this review systematically evaluates and discusses recent advances and knowledge on the sensory analysis and aroma compounds of rapeseed oil and summarizes the effects of manufacturing processes (storage, dehulling, thermal treatment, flavouring with herbs, and refining) on rapeseed oil flavour from sensory and molecule perspectives.

Results and discussion

The literature search yielded 20 publications reporting on sensory analysis of rapeseed oil, 13 from Europe, 6 from China, and 1 from the US [1, 2, 4-21]. The number of entities the sensory attributes appeared in the sensory analysis of European and Chinese rapeseed oils is shown in Figure 1. For both European and Chinese rapeseed oils, green, nutty, burnt, roasty, and seed-like sensory attributes were reported. The main difference is the pungent flavour of Chinese rapeseed oil, which might be due to their higher amounts of aroma-active glucosinolate degradation products.

The effects of different approaches on the flavour of rapeseed oil are shown in Figure 3. Rapeseed oil sealed and stored at low temperature without light helps to slow the formation of undesired off-flavours, such as oxidized, rancid, and musty flavours. Previous studies about the influence of dehulling on the flavour of rapeseed oil showed inconsistent results (e.g., Zhou et al. [24] found that dehulling could decrease the pungent flavour while Gracka et al. [25] reported that the whole seed oil and dehulled seed oil revealed similar sensory aspects), which need to be further investigated. Moderate roasting of rapeseeds helps to enhance the aroma of the final oil. However, new thermal treatment technology with higher heat transfer rates and more accurate temperature control are needed to be further explored. During the manufacturing process, the overall flavour of the flavoured rapeseed oils is often tightly related to that of the corresponding spices or herbs. Moderate refining is proposed to guarantee the safety, nutritional value, and desired sensory attributes of rapeseed oil products. High-oleic rapeseed oil was reported to be an excellent alternative to other commonly used edible oils used for cooking at high temperatures. It has better storage and thermal stability compared to widely used normal rapeseed oils due to its higher oleic acid content.

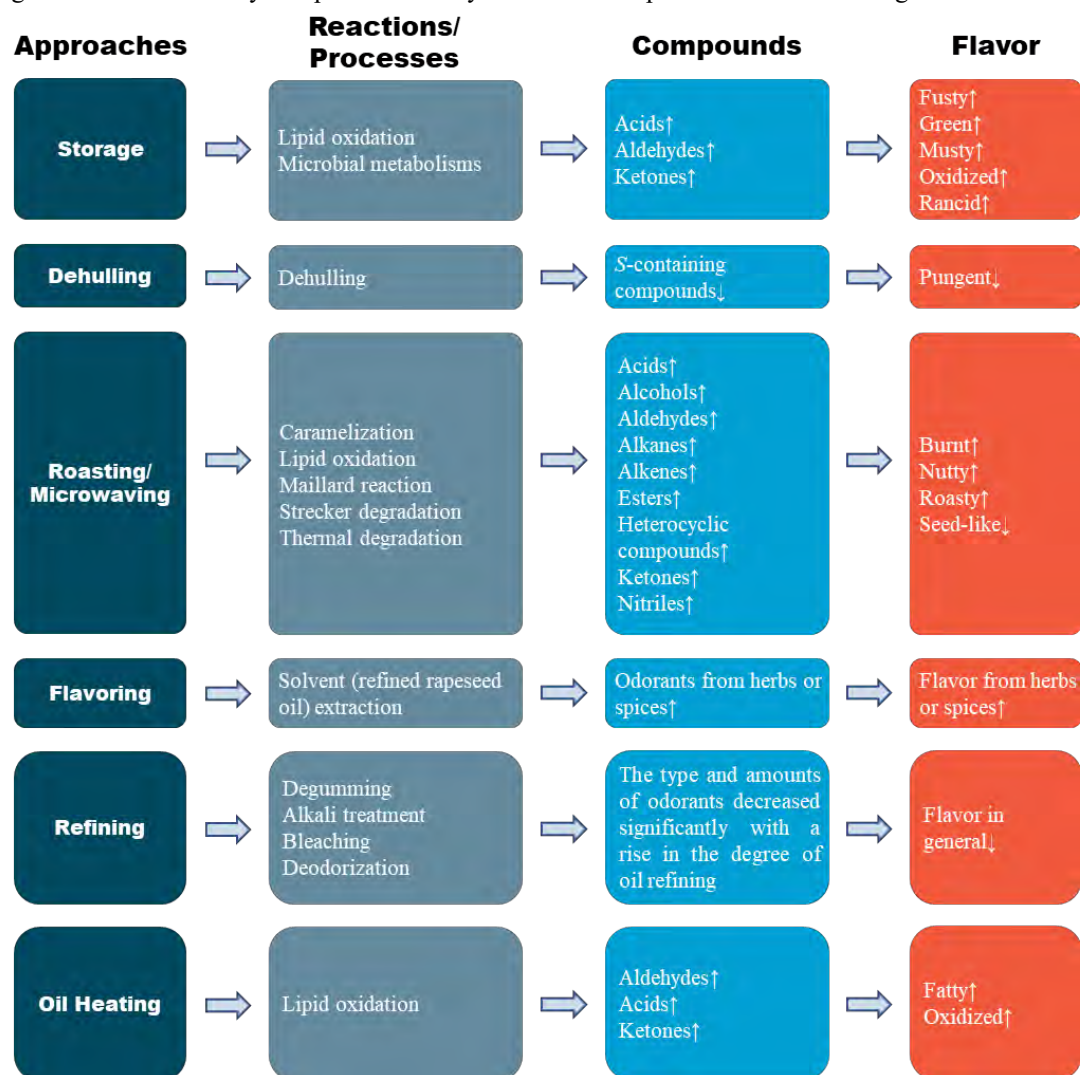


Figure 3: Approaches to modulate the flavour of rapeseed oil.

Conclusion

One hundred and ninety-nine aroma compounds in rapeseed oil were found in a literature survey, contributing to the roasty, fatty, cheese-like, green, fruity, pungent, sweaty, sweet, spicy, flowery, nutty, earthy, and sulphury flavour. One hundred and fourteen of them have only been found once in rapeseed oil; thus, further validation of these odorants is desirable. The main difference between European and Chinese rapeseed oil is the pungent sensory attribute, which can be related to the higher amounts of aroma-active glucosinolate degradation products in Chinese rapeseed oils. The mechanisms by which different treatment affects odorants of rapeseed oil need to be studied further to get a deeper insight how to influence the overall flavour during the production chain and fulfil the expectations by consumers for a well pronounced aroma. This is even more important because consumers of different regions in the world have different prospects regarding a desirable aroma.

References

1. Brühl L, Matthäus B. Sensory assessment of virgin rapeseed oils. *Eur J Lipid Sci Technol.* 2008;110(7):608-610.
2. Matheis K, Granvogl M. Characterisation of the key aroma compounds in commercial native cold-pressed rapeseed oil by means of the Sensomics approach. *Eur Food Res Technol.* 2016;242(9):1565-1575.
3. Zhang Y, Wu G, Chang C, Lv Y, Lai W, Zhang H et al. Determination of origin of commercial flavored rapeseed oil by the pattern of volatile compounds obtained via GC-MS and flash GC electronic nose. *Eur J Lipid Sci Technol.* 2020;122(3):1900332.
4. Wang M, Zhang J, Chen J, Jing B, Zhang L, Yu X. Characterization of differences in flavor in virgin rapeseed oils by using gas chromatography-mass spectrometry, electronic nose, and sensory analysis. *Eur J Lipid Sci Technol.* 2020;122(3):1900205.
5. Mao X, Zhao X, Huyan Z, Liu T, Yu X. Relationship of glucosinolate thermal degradation and roasted rapeseed oil volatile odor. *J Agric Food Chem.* 2019;67(40):11187-11197.
6. Jia X, Wang L, Zheng C, Yang Y, Wang X, Hui J et al. Key odorant differences in fragrant *Brassica napus* and *Brassica juncea* oils revealed by gas chromatography-olfactometry, odor activity values, and aroma recombination. *J Agric Food Chem.* 2020;68(50):14950-14960.
7. Zhou Q, Jia X, Yao Y-Z, Wang B, Wei C-Q, Zhang M et al. Characterization of the aroma-active compounds in commercial fragrant rapeseed oils via monolithic material sorptive extraction. *J Agric Food Chem.* 2019;67(41):11454-11463.
8. Zhou Q, Tang H, Jia X, Zheng C, Huang F, Zhang M. Distribution of glucosinolate and pungent odors in rapeseed oils from raw and microwaved seeds. *Int J Food Prop.* 2018;21(1):2296-2308.
9. Matheis K, Granvogl M. Unraveling of the fishy off-flavor in steam-treated rapeseed oil using the sensomics concept. *J Agric Food Chem.* 2019;67(5):1484-1494.
10. Matheis K, Granvogl M. Characterization of key odorants causing a fusty/musty off-flavor in native cold-pressed rapeseed oil by means of the sensomics approach. *J Agric Food Chem.* 2016;64(43):8168-8178.
11. Kraljić K, Stjepanović T, Obranović M, Pospišil M, Balbino S, Škevin D. Influence of conditioning temperature on the quality, nutritional properties and volatile profile of virgin rapeseed oil. *Food Technol Biotechnol.* 2018;56(4):562-572.
12. Pollner G, Schieberle P. Characterization of the key odorants in commercial cold-pressed oils from unpeeled and peeled rapeseeds by the sensomics approach. *J Agric Food Chem.* 2016;64(3):627-636.
13. Ortner E, Granvogl M, Schieberle P. Elucidation of thermally induced changes in key odorants of white mustard seeds (*Sinapis alba* L.) and rapeseeds (*Brassica napus* L.) using molecular sensory science. *J Agric Food Chem.* 2016;64(43):8179-8190.
14. Gracka A, Jeleń HH, Majcher M, Siger A, Kaczmarek A. Flavoromics approach in monitoring changes in volatile compounds of virgin rapeseed oil caused by seed roasting. *J Chromatogr A.* 2016;1428:292-304.
15. Rekas A, Wroniak M, Rusinek R. Influence of roasting pretreatment on high-oleic rapeseed oil quality evaluated by analytical and sensory approaches. *Int J Food Sci Technol* 2015;50(10):2208-2214.
16. Wei F, Yang M, Zhou Q, Zheng C, Peng J-H, Liu C-S et al. Varietal and processing effects on the volatile profile of rapeseed oils. *LWT-Food Sci Technol.* 2012;48(2):323-329.
17. Tynek M, Pawłowicz R, Gromadzka J, Tylingo R, Wardencki W, Karlovits G. Virgin rapeseed oils obtained from different rape varieties by cold pressed method - their characteristics, properties, and differences. *Eur J Lipid Sci Technol.* 2012;114(3):357-366.
18. Matthäus B, Brühl L. Why is it so difficult to produce high-quality virgin rapeseed oil for human consumption? *Eur J Lipid Sci Technol.* 2008;110(7):611-617.
19. Jeleń HH, Mildner-Szkudlarz S, Jasińska I, Wąsowicz E. A headspace-SPME-MS method for monitoring rapeseed oil autoxidation. *J Am Oil Chem Soc.* 2007;84(6):509-517.
20. Shen N, Moizuddin S, Wilson L, Duvick S, White P, Pollak L. Relationship of electronic nose analyses and sensory evaluation of vegetable oils during storage. *J Amer Oil Chem Soc.* 2001;78(9):937-940.
21. Jeleń HH, Obuchowska M, Zawirska-Wojtasiak R, Wasowicz E. Headspace solid-phase microextraction use for the characterization of volatile compounds in vegetable oils of different sensory quality. *J Agric Food Chem.* 2000;48(6):2360-2367.
22. Su X, Liu X, Huang Y, Guo F. Characteristic flavor compounds in fragrant rapeseed oil by gas chromatography-mass spectrometry and chromatography-olfactometry. *Sci Technol Food Industry.* 2019;40:239-245.
23. Bonte A, Brühl L, Vosmann K, Matthäus B. A chemometric approach for the differentiation of sensory good and bad (musty/fusty) virgin rapeseed oils on basis of selected volatile compounds analyzed by dynamic headspace GC-MS. *Eur J Lipid Sci Technol.* 2017;119(4):1600259.
24. Zhou Q, Yang M, Huang F, Zheng C, Deng Q. Effect of pretreatment with dehulling and microwaving on the flavor characteristics of cold-pressed rapeseed oil by GC-MS-PCA and electronic nose discrimination. *J Food Sci.* 2013;78(7):C961-970.
25. Gracka A, Raczyk M, Hradecký J, Hajslova J, Jeziorski S, Karlovits G et al. Volatile compounds and other indicators of quality for cold-pressed rapeseed oils obtained from peeled, whole, flaked and roasted seeds. *Eur J Lipid Sci Technol.* 2017;119(10):1600328.

3D live cell imaging: study of inter- and intracellular signalling induced by bitter molecules in tongue cell spheroids

Elena von Molitor¹, Elina Nürnberg¹, Torsten Fauth², Paul Scholz², Katja Riedel², Michael Krohn², Mathias Hafner¹, Rüdiger Rudolf¹ and TIZIANA CESETTI¹

¹ Institute of Molecular and Cell Biology, Hochschule Mannheim, Mannheim, Germany

² BRAIN AG, Zwingenberg, Germany

t.cesetti@hs-mannheim.de

Abstract

Tissue complexity is not well represented in a flat 2D environment. In particular, proliferation rates and cellular phenotypes are altered, intercellular communication is lost or severely affected and signalling molecules do not have to diffuse through several cell layers to reach their target. Spheroids allow to investigate cell signalling in a 3D structure with intact cell-to-cell communication. However, there are challenges hampering 3D live-cell imaging including: (i) the stabilization of spheroids under perfusion conditions, (ii) the recording of many z-planes at high spatio-temporal resolution, and (iii) the complexity of data analysis.

Here, we addressed these issues using spheroids made with human-papillae derived tongue cells (HTC-8), immortalized and engineered to express a green-fluorescent genetically-encoded Ca²⁺ (G-GECO) sensors. By confocal and Light Sheet Fluorescence Microscopy (LSFM) we measured quantitatively intracellular Ca²⁺ changes upon acute application of gustatory bitter substances. We developed a simple and robust live-cell imaging perfusion setup for confocal as well as LSFM that granted spheroid stabilization and high-resolution microscopy in many z-planes at high spatio-temporal resolution.

With this approach we could show that Ca²⁺ transients induced by saccharin appeared in the whole spheroid and required extracellular Ca²⁺. However, the responses differed between the border and the centre of the spheroids, with larger and faster response in the outer region. Furthermore, ATP-mediated intercellular communication was found to play a major role in the generation of compound-evoked Ca²⁺ transients, suggesting the presence of an ATP-mediated positive autocrine/paracrine communication in HTC-8 spheroids.

In summary, the presented approach permits the study of fast inter- and intracellular signalling in 3D spheroid cultures upon compounds perfusion.

Keywords: taste, signalling, calcium imaging, optical biosensors, 3D spheroids

Introduction

Sweet and bitter compounds present in food are sensed by specialized differentiated taste cells, called “receptor cells”. They are located in taste buds, onion-like structures present in tongue papillae, receiving afferent innervation. Activation of sweet and bitter receptors in receptor cells induces intracellular Ca²⁺ signals that lead at the end to ATP release, necessary to communicate with afferent nerve terminals and also with other taste bud cells. Measurement of Ca²⁺ responses in taste cells is, therefore, a widely used read-out to evaluate gustatory responses and allows to determine the potency of receptor ligands. However, so far Ca²⁺ responses have been measured either in rodent or recombinant cells [1], which pose limitations wherefore results cannot be necessarily transferred to human. Thus, our aim was to develop a new approach to study gustatory human responses *in vitro*. For this purpose, a stably proliferating cell line (HTC-8) derived from human fungiform papillae [2], was engineered to stably express a genetically encoded Ca²⁺ sensor (G-GECO) and used to produce spheroids by a liquid overlay technique. These spherical cell-aggregates, of about 300 µm in diameter, were then used for live-cell imaging experiments with confocal and light-sheet microscopy. The challenge of stabilizing them during acute dynamic perfusion was addressed with cheap and easy set-up configurations, which allowed time-course recording of fluorescence changes with stability and high spatial resolution. The analysis took in account spatial differences in the response, showing that bitter-induced Ca²⁺ transients are faster and stronger in the outer spheroid region, and require ATP-mediated intercellular communication.

Experimental

HTC-8 cells expressing G-GECO were generated by lentiviral transduction of pLV-Ubic-G-GECO-Puro vector, and cultured as described previously [1, 3]. For spheroid generation, 5000 cells/well were plated and centrifuged in 96-well ULA plates (Greiner). HTC-8-G-GECO spheroids were used for live cell imaging at 5-7 days of *in vitro* culture. For confocal microscopy 3 spheroids/well were placed in µ-Slide III 3D perfusion chamber (Ibidi) in imaging control buffer [1, 3]. Gelatine nonwoven CL130 Scaffoldene pads (Freudenberg) were cut and

placed on spheroids for stabilisation. Once closed, the slides were connected to a gravity-driven custom-made perfusion system. Exchange of solution in the μ -well required 5-15 s. Spheroids were imaged using an inverted Leica TCS SP8 confocal microscope equipped with a water immersion 20x/0.75 objective. A single z-plane, at about 20-40 μ m spheroid depth, was acquired every 5 s upon excitation at 488 nm, and detection at 500-550 nm. For LSM, spheroids were mounted with 0.5 % low melting agarose in a U-shaped glass capillary (Hilgenberg), fixed in a glass bottom dish (Ibidi). Exchange of the buffer occurred in 3.5-5 min. LSM imaging used a Leica TCS SP8 DLS vertical turn light-sheet microscope equipped with Leica HC APO L 10x/0.3 W objective. Spheroids were optically sectioned over 80-90 μ m depth at 3.7 μ m z-steps distance. Sodium saccharin (Sigma), ATP disodium salt (Roche) and Suramin sodium salt (Sigma) were dissolved in control buffer, and osmolarity was adjusted.

Ca^{2+} responses were analysed with ImageJ. The ImageJ erosion function was applied to obtain four concentric rings (R1-R4 from border to centre). The change in fluorescence (ΔF) was normalized to the value before stimulation (F_0) as followed $\Delta F/F_0 = (F - F_0)/F_0$, and plotted as a function of time. The peak intensity was the maximum $\Delta F/F_0$ within the stimulation window. Peak amplitudes were plotted versus the log of saccharin concentrations to obtain a dose-response curve. T_{Peak} and T_{Slope} defined respectively the time interval from the stimulation to the time of the peak or to the onset of the response. $T_{\text{Slope-Peak}}$ was defined as the interval from the onset to the maximum intensity. Bar graphs show mean \pm standard error of the mean (SEM). Statistics were performed using one-way ANOVA or Student t-test. For details, see [3].

Results and discussion

HTP-8 cells were previously shown to express TAS2R8, R31 and R43, encoding the membrane-located bitter receptors for saccharin [1]. Therefore, we investigated saccharin-induced Ca^{2+} response in HTC-8-G-GECO spheroids. Stabilization of the spheroids within the μ -well of the perfusion chamber was achieved by covering them with a collagen-mash (Scaffolene) that gets transparent when wet and is soft, allowing optimal stabilization without hampering diffusion or spheroid structure. Confocal live-cell imaging revealed that saccharin elicited Ca^{2+} responses that required extracellular Ca^{2+} (data not shown) [3]. We observed that the evoked Ca^{2+} transients were not uniform since their amplitudes and kinetics differed between the spheroid border and the inner regions. Analysing the Ca^{2+} changes in four concentric regions of interest, named “rings”, (Figure 1. A-B) confirmed that

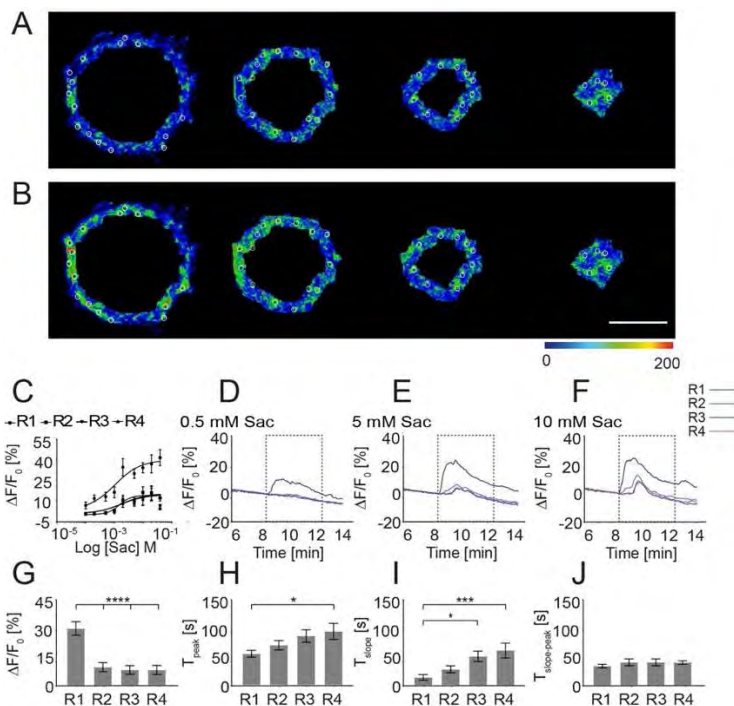


Figure 1: Saccharin response in HTC-8-G-GECO spheroids. Representative confocal experiment of a HTC-8-G-GECO spheroid perfused first with control solution (A) and then with saccharin 5 mM (B). Color code represents fluorescence intensity. Image depth 30 μ m. Scale bar: 100 μ m (C) Dose-response curves were measured in the four concentric rings (R1-R4). EC_{50} : R1=1.06 mM, R2=1.50 mM, R3=1.67 mM and R4=1.46 mM. (D-F) Mean time-course traces responses to saccharin 0.5-5-10 mM in the four rings. Quantitative fluorescence analysis of Peak Intensity (G), Time to Peak (H), Time to Slope (i), and Time Slope to Peak (J) for responses elicited by saccharin (5 mM) stimulation in the four rings. Mean \pm SEM ($n \geq 5$ spheroids). ANOVA.

at all the concentrations tested, the Ca^{2+} transients started earlier, reached a larger peak in a shorter time in the outer ring (R1) (Figure 1 D-I). Consistently, dose-response curves measured in the four rings (R1-R4), showed decreasing sensitivity and potency when moving from the border toward the centre (Figure 1 C). Since the time from the onset to the peak was comparable in all rings, likely these differences are not due to diverse intracellular mechanisms of Ca^{2+} signal generation (Figure 1 J). Furthermore, such differences are evident even at single-cell level and do not depend on a reduced concentration of saccharin in the spheroid core due to diffusion (for data, see [3]).

Since ATP is the major neurotransmitters within the taste bud, we investigated whether HTP-8-G-GECO cells respond to it and whether ATP could play a paracrine/autocrine role in the spheroid. Indeed, ATP at a saturating concentration (1 mM), evoked Ca^{2+} transients with an amplitude comparable to that of saccharin (20 mM) (Figure 2 A, D), and the regional differences were evident as well. Nevertheless, the kinetic differed between the two compounds, as ATP-responses had a much shorter onset (Figure 2 E). Saccharin responses were largely reduced by co-application of the purinergic antagonist Suramin (Figure 2 C, F) suggesting that ATP released by HTC-8-G-GECO cells contributed to amplify bitter-induced Ca^{2+} signals. This effect seemed to be comparable in all spheroid regions, since the reduction of fluorescence was homogeneous (Figure 2 G).

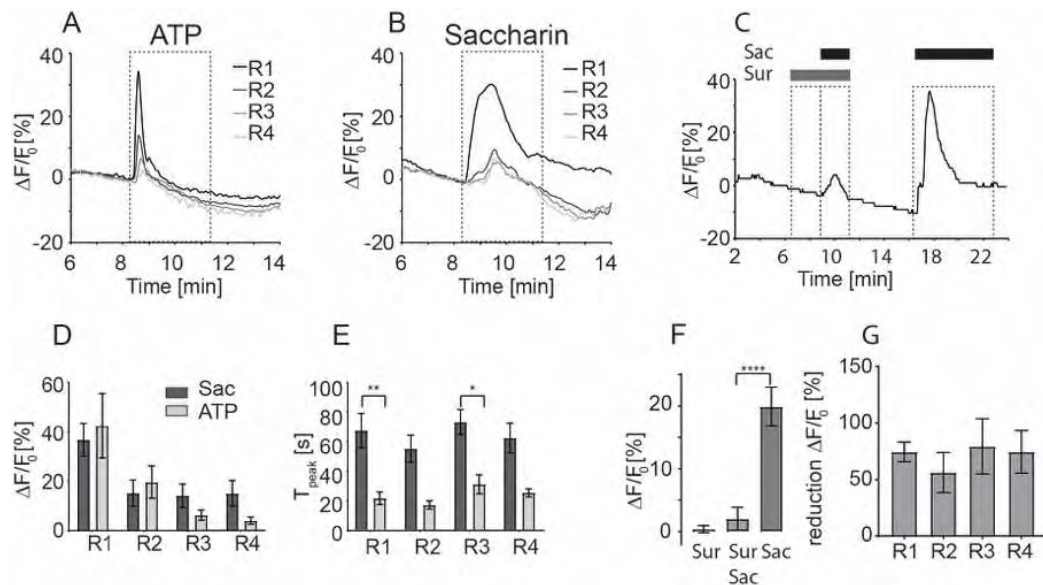


Figure 2: Purinergic signaling is involved in the saccharin response. Mean fluorescence changes over time, in the 4 rings, with ATP (1 mM) (A) or saccharin (20 mM) stimulation (B). (C) Plot of fluorescence changes over time upon perfusion of saccharin (10 mM) alone or in the presence of the purinergic antagonist Suramin (100 μ M). Comparison of the responses between ATP and saccharin for (D) Peak Intensity and (E) Time to Peak. (F) Whole-spheroid mean fluorescence changes upon perfusion as indicated in the x-axis. (G) Percentage of fluorescence reduction induced by Suramin. Data are normalised to saccharin response. Mean \pm SEM ($n \geq 5$ spheroids). ANOVA and Student's *t*-test.

Since confocal live-imaging limited the acquisition to only one z-plane due to poor time resolution, we took advantage of LSFM, which allowed to scan, within the same time frame (4-5 sec), 30 z-planes over a 100 μ m depth, without losing fluorescence intensity with increasing depth [3]. For experiments with acute stimulation, the perfusion set-up needed to be adapted, since the samples had to be positioned between two mirrors, which are submerged in the recording solution. Therefore, the spheroids were embedded with agarose in an open U-shaped glass capillary, which was positioned in a glass-bottom plate, where tubes for in- and out-flow were also fixed. Perfusion with ATP (1 mM) elicited an increase in fluorescence, similarly to what observed with confocal microscopy. The advantage was that we could observe the time-course changes in multiple planes instead of only one. The Ca^{2+} changes were measured in each plane and were plotted over time and spheroid depth (Figure 3 A, B). The analysis confirmed what we observed already with confocal microscopy: ATP-induced Ca^{2+} transients were larger in the outer z-planes, and decreased progressively with increasing depth (Figure 3 B). The peak response was however delayed compared to the confocal experiments, likely due to the larger volume of the recording chamber (ml, instead of μ l).

Live-imaging with LSFM, which allow to scan 3D cell cultures at high speed maintaining cellular resolution and optimal signal-to-noise-ratio even in the deeper planes, may be particularly advantageous in case of irregular

structures, cocultures and focal stimulation. However, the analysis of this large amount of data, not only with quantitative but also with spatial and time information, will require further development.

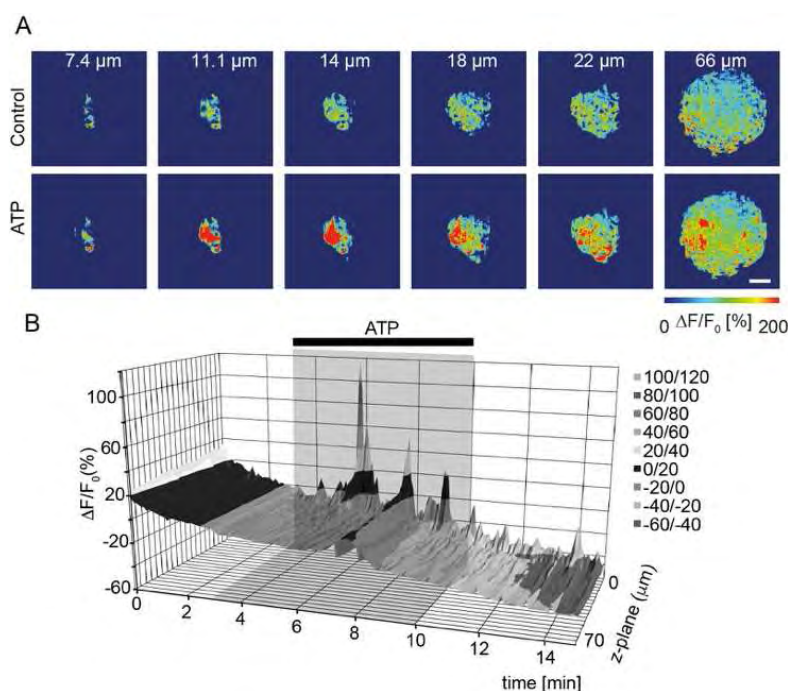


Figure 3: Time course of ATP response acquired by LSFM. (A) Images of a representative HTC-8 G-GECO spheroid at different z-depth, in control buffer and upon stimulation with ATP (1 mM). Scale bar, 50 μm . (B) The fluorescence change was plotted over time and depth (z-plane), for the experiment as in A-B. The mean fluorescence was normalised to the signal before stimulation.

Conclusion

In summary, we showed that the HTC-8-G-GECO cell line, derived from human tongue papillae cells and engineered to express a genetically encoded Ca^{2+} sensor, could be used to produce spheroids that respond to the taste compounds. As read-out, we used live-cell Ca^{2+} imaging. In this three-dimensional structure, the cells find a more physiological environment, as shown by the regional differences in Ca^{2+} response, and the involvement of endogenous ATP in the generation of bitter-induced Ca^{2+} signals. These effects would be neglected in 2D cultures and with static drug application. Furthermore, we showed that it is possible to study by LSFM Ca^{2+} dynamics in the whole spheroid without losing time- and spatial-resolution even in acute perfusion condition. Our approach thus opens new possibilities to study gustatory responses in human-derived cells that, grown in a 3D structure, retain cell-cell interaction. Additionally, the spheroids mimic a native tissue in that the compounds have to diffuse through multiple cell layers to reach their target. While confocal and LSFM allowed to study Ca^{2+} signals with single-cell resolution [3], HTC-8-G-GECO spheroids may also be applied to develop high-throughput gustatory screenings, since they are easy and cheap to be produced.

References

1. Hochheimer A, Krohn M, Rudert K, Riedel K, Becker S, Thirion C, et al. Endogenous gustatory responses and gene expression profile of stably proliferating human taste cells isolated from fungiform papillae. *Chem Senses*. 2014;39:359–377.
2. von Molitor E, Riedel K, Hafner M, Rudolf R, Cesetti T. Sensing senses: Optical biosensors to study gustation. *Sensors (Switzerland)*. 2020;20: 1–42.
3. von Molitor E, Nürnberg E, Ertongur-Fauth T, Scholz P, Riedel K, Hafner M, et al. Analysis of calcium signaling in live human Tongue cell 3D-Cultures upon tastant perfusion. *Cell Calcium*. 2020;87.

A receptor-based assay to study the bitterness masking effect of yeast extracts

CHRISTINE BELLOIR¹, Antoine Thomas², Rudy Menin², Loïc Briand¹

¹ Centre des Sciences du Goût et de l'Alimentation, AgroSup Dijon, CNRS, INRAE, Université de Bourgogne Franche-Comté, 21000 Dijon, France, loic.briand@inrae.fr

² Biospringer by Lesaffre, 94700 Maisons-Alfort, France

Abstract

Yeast extracts (YEs) are widely used by the food industry for the formulation of foods and beverages, as they bring a natural combination of flavour molecules, including aroma-active and non-volatile compounds (taste-active compounds). Adding a touch of umami, some richness or a typical flavour signature, YEs are used as ingredients to mask the bitterness of some food products. In the present work, using functional calcium mobilization assays, we demonstrated the ability of two different YEs (YE1 and YE2) and the ribonucleotide adenosine 5' monophosphate (AMP) to stimulate heterologously expressed human bitter taste receptors named TAS2Rs. We then observed that YE1 inhibits the response of two TAS2Rs stimulated by control agonists. Our data demonstrate that the bitterness masking effect of YEs is a molecular mechanism occurring at the receptor level.

Keywords: yeast extract, bitter taste, GPCR, bitter taste receptor TAS2R, inhibition

Introduction

Yeast extracts (YEs) are valuable ingredients commonly used for their wide variety of powerful taste properties in many food and beverage applications. Derived from fermentation, the molecular composition of YEs is very complex and provides flavours in different ways. YEs are an important source of taste-active compounds generated upon breakdown of polymeric molecules (polysaccharides, proteins, nucleic acids, etc.). Among them, the 5' purine ribonucleotides guanosine 5'-monophosphate (GMP) and inosine 5'-monophosphate (IMP) are known to synergize with glutamic acid and elicit umami taste on their own [1]. YEs also contain adenosine 5' monophosphate (AMP), which has been identified as a bitter taste inhibitor by sensory experiments conducted in humans [2, 3]. Bitter taste perception is one of the five basic taste qualities, generally causing aversion to avoid ingestion of potentially toxic compounds. Bitter compounds are detected by a specific subset of taste receptor cells localized in the mouth and characterized by the expression of the TASTE 2 receptor (TAS2R) gene family. TAS2Rs belong to the family of class A G protein-coupled receptors (GPCRs). They all possess a heptahelical transmembrane domain (TMD) connected by three extracellular loops (ECLs) and three intracellular loops (ICLs), with a short extracellular N-terminus and an intracellular C-terminus [5-7]. The human genome contains 25 genes coding TAS2Rs, which are able to detect thousands of chemically diverse compounds. AMP has been demonstrated to block taste receptor transduction activated by bitter tastants [8]. In addition, some bitter blockers have been identified to act at the TAS2R level to reduce the bitterness intensity of a number of food products [5]. In this study, to further investigate the mechanism of the bitterness masking effect of two YEs (YE1, high content in AMP and GMP; YE2, high content in IMP and GMP) and AMP, we functionally expressed 25 human TAS2Rs using an *in vitro* mammalian expression system coupled to calcium imaging analysis.

Experimental

All experiments were conducted *in vitro* using HEK293T cells stably expressing the chimeric G protein G α 16gust44, which harbours 44 gustducin-specific sequences at its C terminus [9]. Combining functional expression of TAS2Rs and calcium mobilization assays, we followed two different approaches. First, we examined the direct interaction of YEs and AMP with the 25 human TAS2Rs. Next, we measured the potential bitterness masking effect of YE1 towards two specific TAS2Rs stimulated by control agonists.

YE samples and chemicals

The two YEs were supplied by Biospringer by Lesaffre (Maisons-Alfort, France). The first one, YE1, is characterized by high contents of AMP and GMP, while the second one, YE2, derived from YE1 by enzymatic conversion of AMP to IMP, contains high amounts of IMP and GMP. Other chemical compounds, such as AMP, MgSO₄, and aristolochic acid, were purchased from Sigma-Aldrich (Saint-Quentin Fallavier, France). The compounds were dissolved in buffer C1 (130 mM NaCl, 5 mM KCl, 10 mM HEPES, 2 mM CaCl₂, 10 mM glucose, pH 7.4). Dulbecco's modified Eagle's medium (DMEM) and all tissue culture media components were purchased

from Life Technologies (St Aubin, France). The Fluo4-AM calcium indicator was obtained from Molecular Probes (St Aubin, France).

Generation of human TAS2R expression vectors

The amino acid sequence of human TAS2Rs were obtained from the online NCBI Protein database. The synthetic DNAs encoding TAS2Rs were codon optimized for humans (GeneWiz) and subcloned into the pcDNA4/myc-HisA plasmid (Invitrogen) between the *EcoRI* and *NotI* restriction sites. To improve protein expression in mammalian cells, the QBI SP163 translational enhancer sequence (MAX) was added before the start codon. Membrane targeting was increased using the first 45 amino acid residues of rat somatostatin receptor 3 (SST3) located in the receptor N-terminus. Finally, the FLAG epitope was added to the C-terminus to detect the expression and subcellular localization of TAS2Rs by immunocytochemical techniques.

Functional heterologous expression assays

HEK293-G α 16-gust44 cells were seeded at a density of 35,000 cells per well on clear bottom poly-D-lysine-coated 96-well microtiter black plates in DMEM supplemented with 2 mM GlutaMAX, 10% dialysed foetal bovine serum, penicillin/streptomycin and G418 (400 μ g/mL) at 37°C, 6.3% CO₂, and 100% air humidity. After overnight growth, the cells were transiently transfected with each of the TAS2R expression plasmids using Lipofectamine 2000™ (Life Technologies) according to the manufacturer's protocol. For the negative control, cells were transfected with empty pcDNA4/mycHisA vector. Twenty-four hours later, the cells were loaded with the calcium-sensitive dye Fluo4-AM in the presence of 2.5 mM probenecid for 1 hour and washed twice with C1 solution. Calcium responses of cells were recorded after application of test substances in a Fluorometric Imaging Plate Reader, FLIPR (Molecular Devices) after excitation at 488 nm and emission recorded at 510 nm. For direct application, YE1 and YE2 were tested at different concentrations between zero and 1000 μ g/ml (1000 ppm) and from zero to 100 μ M (347 ppm) for AMP. For the pre-treatment experiment, washed cells were bathed in YE1 solutions ranging from zero to 3000 μ g/mL for ten minutes, rinsed once with C1 buffer and subjected to calcium imaging measurements after automatic injection of the control agonist.

Data were collected from at least two independent experiments carried out in duplicate. For the calculation of dose-response curves, signals of wells receiving the same concentration of test substances were averaged. The fluorescence changes of the corresponding mock-transfected cells were subtracted and normalized to background fluorescence. Dose-response relationships and EC₅₀ values were calculated in SigmaPlot (Systat Software) by nonlinear regression using the function $f(x) = \min + (\max - \min)/(1 + (x/EC_{50})^{-Hillslope})$.

Results and discussion

To identify human bitter taste receptors activated by YEs or AMP, we transiently transfected the cDNAs of TAS2Rs in HEK293-G α 16-gust44 cells. Transfected cells were loaded with a calcium-sensitive dye and then subjected to bath application of YEs or AMP, while changes in cytosolic calcium levels were recorded in a fluorometric imaging plate reader. The response profile of TAS2Rs shows that YEs and AMP are able to activate nine TAS2Rs (Table 1). Among them, we confirmed the activation by all compounds of TAS2R10 and TAS2R14, which are known to be broadly tuned receptors. Interestingly, YE1, which contains AMP, and AMP alone activate the same subset of TAS2Rs, except for TAS2R30, TAS2R43 (known for their intermediate agonist spectra) and TAS2R50 (narrowly tuned TAS2R). We confirmed that YE1 and AMP increase the calcium response of TAS2R16 and TAS2R38, which were identified as taste receptors specifically recognizing a distinct class of chemicals (β -glucopyranosides and isothiocyanates, respectively). Interestingly, these two TAS2Rs are associated with variability in taste detection linked to gene polymorphisms. Conversely, for YE2, a restricted response profile and the highest EC₅₀ values were measured for TAS2R10 and TAS2R14, suggesting that this IMP-enriched YE (instead of AMP) contains weaker bitter agonists than YE1.

Table 1: Response profile of 25 TAS2Rs stimulated with YEs and AMP. EC₅₀ values are indicated.

	Receptor	Alias	Compound		
			YE1	YE2	AMP
1	TAS2R1		—	—	—
2	TAS2R3		—	—	—
3	TAS2R4		186 µg/mL	—	254 µM
4	TAS2R5		—	—	—
5	TAS2R7		153 µg/mL	—	213 µM
6	TAS2R8		—	—	—
7	TAS2R9		—	—	—
8	TAS2R10		392 µg/mL	907 µg/mL	109 µM
9	TAS2R13		—	—	—
10	TAS2R14		32 µg/mL	> 1000 µg/mL	69 µM
11	TAS2R16		32 µg/mL	—	79 µM
12	TAS2R19*	TAS2R48	—	—	—
13	TAS2R20	TAS2R49	—	—	—
14	TAS2R30	TAS2R47	108 µg/mL	—	—
15	TAS2R31	TAS2R44	—	—	—
16	TAS2R38		37 µg/mL	—	16 µM
17	TAS2R39		—	—	—
18	TAS2R40		—	—	—
19	TAS2R41*		—	—	—
20	TAS2R42*		—	—	—
21	TAS2R43		—	—	30 µM
22	TAS2R45*		—	—	—
23	TAS2R46		—	—	—
24	TAS2R50		232 µg/mL	—	—
25	TAS2R60*		—	—	—

* receptors remaining orphan; —, no response

To investigate the bitter masking effect of YEs in greater detail, we focused our experiment on YE1, which shows more interactions with TAS2Rs. We asked whether YE1 could inhibit the activation of two receptors (TAS2R7 and TAS2R14) stimulated by their agonist controls. For this purpose, we challenged TAS2R7- and TAS2R14-expressing HEK293-Gα16-gust44 cells with several pre-treatment concentrations of YE1 followed by injection of increasing concentrations of MgSO₄ and aristolochic acid, respectively (Figure 1). The ten-minute pre-treatment of HEK293-Gα16-gust44 cells with the highest YE1 concentration of 3000 µg/mL led to both a right shift of the dose-response curves, corresponding to a decrease in half-maximal response (EC₅₀ value), and a reduction of maximal signal amplitude for the two tested receptors. These results suggest a loss of potency/affinity and a decrease in efficacy, revealing competitive and non-competitive binding mechanisms of YE1 towards receptor and agonist interactions. Compared to TAS2R14, we observed that TAS2R7 is more sensitive to YE1 application, as this shift is clearly visible at a concentration of 300 µg/mL.

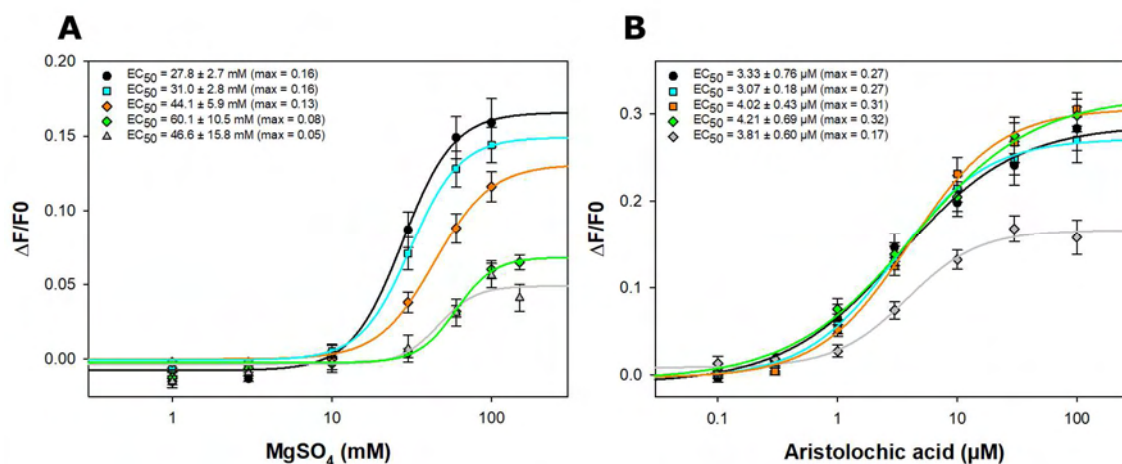


Figure 1: Dose-response curves of TAS2R7 and TAS2R14 with YE1 inhibition of agonist controls. HEK293T-Gα16gust44 cells were transfected with TAS2R7 (A) or TAS2R14 (B). After transfection, cells were treated for ten minutes with increasing concentrations of YE1 diluted in C1 buffer: without YE1 (dark rows) or with 90 µg/mL (cyan rows), 300 µg/mL (orange rows), 900 µg/mL (green rows) and 3000 µg/mL (grey rows) YE1. Then, agonist controls (MgSO₄ and aristolochic acid for TAS2R7 and TAS2R14, respectively) were applied to the cells, and fluorescence changes were monitored for calcium imaging analyses using an automated plate reader. Changes in fluorescence (ΔF/F0) were plotted semi logarithmically upon agonist application (mean ± SEM). Experiments (n = 2) were performed in triplicate.

Conclusion

Using transient expression of human bitter taste receptors in a mammalian expression system, we demonstrated that YEs and AMP stimulate distinct sets of human TAS2Rs. We then tested YE1, a YE rich in AMP, for its ability to inhibit bitter taste receptors and observed a specific inhibition for two of them: TAS2R7, which has been implicated in metal ion detection, and TAS2R14, a broadly tuned bitter taste receptor.

Interestingly, we found that activation of the bitter taste receptor by YE1 occurred at low concentrations, while inhibition required higher concentrations, suggesting complex mechanisms of molecular interactions probably linked to the mixture of constituents present in the extract. Taken together, our findings are relevant to determine the concentration of YEs used in formulations and open the way to better understand the masking of bitter off-taste by YEs.

References

1. Laffitte A, Neiers F, Briand L. Characterization of taste compounds: chemical structures and sensory properties. *Flavor : From Food to Perception*. 2016; 154-191.
2. Keast R, & Breslin P. Modifying the bitterness of selected oral pharmaceuticals with cation and anion series of salts. *Pharm. Res.* 2002; 19 (7), 1019-1026.
3. Keast R, Canty T, Breslin P. Oral zinc sulfate solutions inhibit sweet taste perception. *Chem. Senses.* 2004; 29, 513-521.
4. Ley J. Masking bitter taste by molecules. *Chem. Percept.* 2008; 1, 58-77.
5. Montmayeur JP, Matsunami H. Receptors for bitter and sweet taste. *Curr. Opin. Neurobiol.* 2002; 12, 366-371.
6. Alder E, Hoon M, Mueller K, Chandrashekar J, Ryba N, Zuker C. A novel family of mammalian taste receptors. *Cell.* 2000; 100, 693-702.
7. Chandrashekar J, Mueller K, Hoon M, Alder E, Feng L, Guo W, Zuker C, Ryba N. T2Rs function as bitter taste receptors. *Cell.* 2005; 100, 703-711.
8. Ming D, Ninomiya Y, Margolskee R. Blocking taste receptor activation of gustducin inhibits gustatory responses to bitter compounds. *Proc. Natl. Acad. Sci.* 1999; 96, 9903-9908.
9. Ueda T, Ugawa S, Shimada S. Functional interaction between TAS2R receptors and G-protein α subunits expressed in taste receptor cells. *Chem.Senses.* 2005; 30, suppl 1: i16.

Impact of ageing on pea protein volatile compounds and correlation with odour

ESTELLE FISCHER, Rémy Cachon and Nathalie Cayot

UMR PAM, AgroSup DIJON, estelle.fischer@agrosupdijon.fr

Abstract

The positive effects of plant-based protein consumption are widely reported; nonetheless, several disadvantages such as “grassy” or “beany” off-flavours are encountered [1]. Moreover, the impact of the storage conditions, or ageing, on the evolution of the off-flavour is not well-known [2]. This study aimed to investigate the evolution of the volatile compounds and of the odour during one year using two different ageing processes. The volatile compounds were determined by HS-SPME-GC-MS and the odour by smelling the products at each time of sampling. The mechanisms involved [3-6] and the most impacting factor on the evolution of the volatile compounds were determined. Furthermore, because there is a great challenge to link instrumental data to the odour, a tentative correlation was proposed in order to be able to use instrumental data for early detection of off-flavour and to study the neo-formed compounds during storage.

Keywords: pea protein, ageing, HS-SPME-GC-MS, beany

Introduction

The consumption of plant-based protein is increasing due to their numerous positive effects. However, the consumption is limited by the “beany” off-flavour¹. Numerous works are now dealing with the off-flavour characterization, and the impact of different processes on the volatile compounds. The “beany” off-flavour is generated during the early stages of the production process of protein isolate but it can also evolve during the storage. This work is therefore threefold: - First, to investigate the evolution of the volatile compounds and odour during two ageing processes, close to usual storage conditions of vegetable proteins. - Secondly, to identify the mechanisms involved in this evolution and the most important factor. - And finally, to see if it possible to predict the evolution of the odour using data on volatile compounds.

Experimental

Two ageing processes were applied on a pea protein isolate (PPI) during 12 months. PPI was placed flat in plastic bags at 20°C exposed to light (treatment A) or at 30°C in the dark. PPI was sampled at 0, 3, 6, 9 and 12 months. At each sampling time, the odour was determined by direct sniffing of the product in a glass vial, by three experts. The volatile compounds were also analysed using headspace-solid phase microextraction-gas chromatography-mass spectrometry (HS-SPME-GC-MS). A 0.2 g PPI sample was weighed directly in a clear 20 mL vial. Distilled water was added to obtain a 2 mL suspension at 10% (w/v) and a liquid/gas ratio of 2/18 (v/v). For SPME, equilibrium step and extraction step were conducted both at 40 °C under stirring at 350 rpm in the dark. The equilibrium time was 30 min and the extraction time was 60 min with a DVB/CAR/PDMS fibre. An HP 6890 Series Gas Chromatograph equipped with an HP 5973 Mass Selective Detector was used with a DB-WAX column to analyse the compounds of interest. The SPME fibre was desorbed and maintained in the injection port at 250 °C for 5 min. The programmed temperature was isothermal at 40 °C for 3 min, raised to 100 °C at a rate of 3 °C/min, and then raised to 230 °C. 100 at a rate of 5 °C/min and held for 10 min. The total run time was 59 min.

Results and discussion

Figure 1 is presenting the evolution of the profile of volatile compounds in total chromatographic area per gram of sample, sorted by chemical family, during the ageing and Table 1 is presenting the odour evolution during ageing.

Treatment A (Light – 20°C) had a strong impact on the volatile compounds: high increase of volatile compounds from 0 to 6 months, followed by a small decrease at 9 months and an equilibrium. This was linked to the odour deterioration. An increase in the aldehydes, alcohols and ketones could be observed, with the development of new compounds. The photo-oxidation due to light could be added to the other phenomena presented in Figure 2, playing a crucial role to the formation of volatile compounds.

Treatment B (Dark – 30°C) had a slighter impact on the volatile compounds, with mainly an increase at 12 months [2], as well as a very slight odour change. An increase in aldehydes and furans could be observed, that could be attributed to the Maillard reaction.

Within the range of temperatures we studied, corresponding to the usual storage of a product, the light had a higher impact on the product than the temperature.

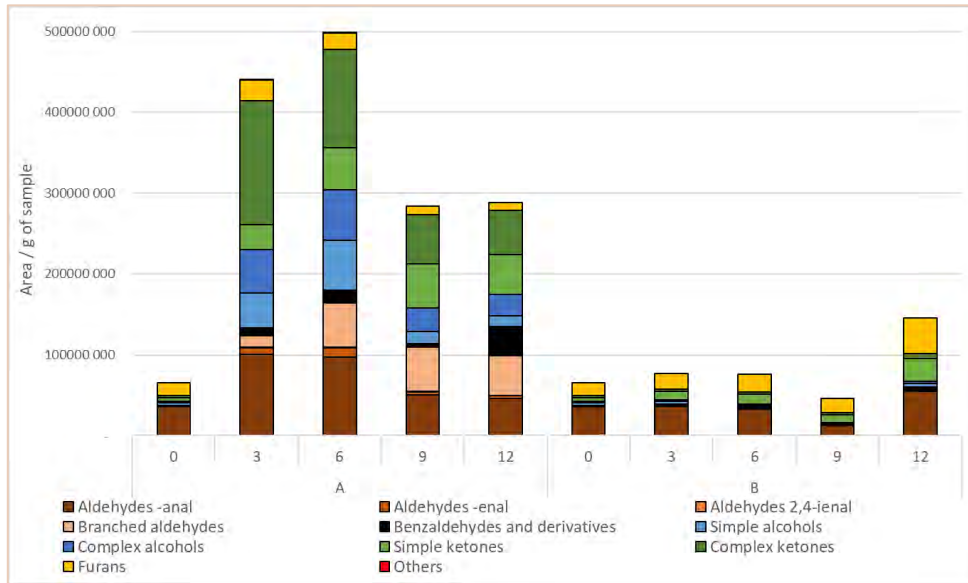


Figure 1: Profile of volatile compounds by chemical family during the ageing.

Table 1: Odour evolution during the ageing.

	0 months	3 months	6 months	9 months	12 months
Treatment A	Beany	Beany, sharp, earthy	Beany+, sharp, earthy	Beany+, sharp, earthy, rancid	Beany+, sharp, earthy, rancid
Treatment B		Light beany, roasted	Light beany, roasted	Light beany, roasted, earthy	Beany, earthy

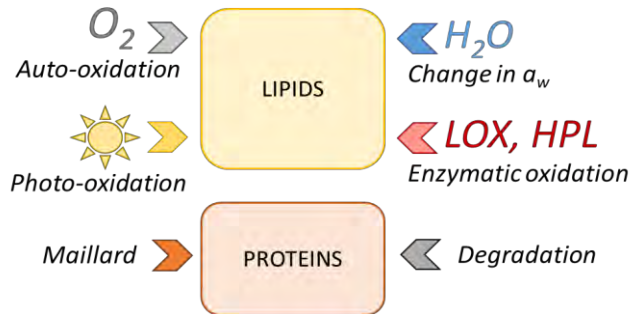


Figure 2: Reactions involved during the ageing [3-6].

The odour evolution of the PPI was linked to an increase in the content of its volatile compounds. To see if it was possible to predict the odour evolution using analytical data, the results used for Figure 1 were sorted by sensory descriptors and were presented in ratios in the global profile to build Figure 3. For each compound, the sensory descriptors were looked up [7] and the compounds were classified into different attribute families like “green” or “earthy”. As the flavour investigated here was “beany”, a focus was made around the “beany” attributes, like the different types of “green”. A given descriptor was then represented as the ratio of the percentage of the cumulative amount of the volatile compounds responsible for the descriptor, to the total amount of all volatile compounds.

With this representation, it was possible to see some links between analytical data and the odour. For example, at 3 months in treatment A, an “earthy” off-flavour was smelled, as presented in Table 1, and this was linked to an increase in the proportion of volatile responsible for “earthy” notes, as presented in Figure 3.

The same way, for 3 and 6 months in treatment B, little to no changes in the odour were smelled and no big changes were seen in the ratio of compounds responsible for the off-flavour.

To conclude, an odour change was linked to a change in the ratios of compounds and the perception of a new off-flavour was linked to an increase in the ratio of compounds responsible for that attribute.

However, there is a limit to these conclusions. This representation (Figure 3) is not sufficient to describe the global sensory profile of a product and this may not work with all attributes. For example, the increase in the proportion of compounds related to “fruity” or “floral” notes in treatment A at 9 months was not perceived.

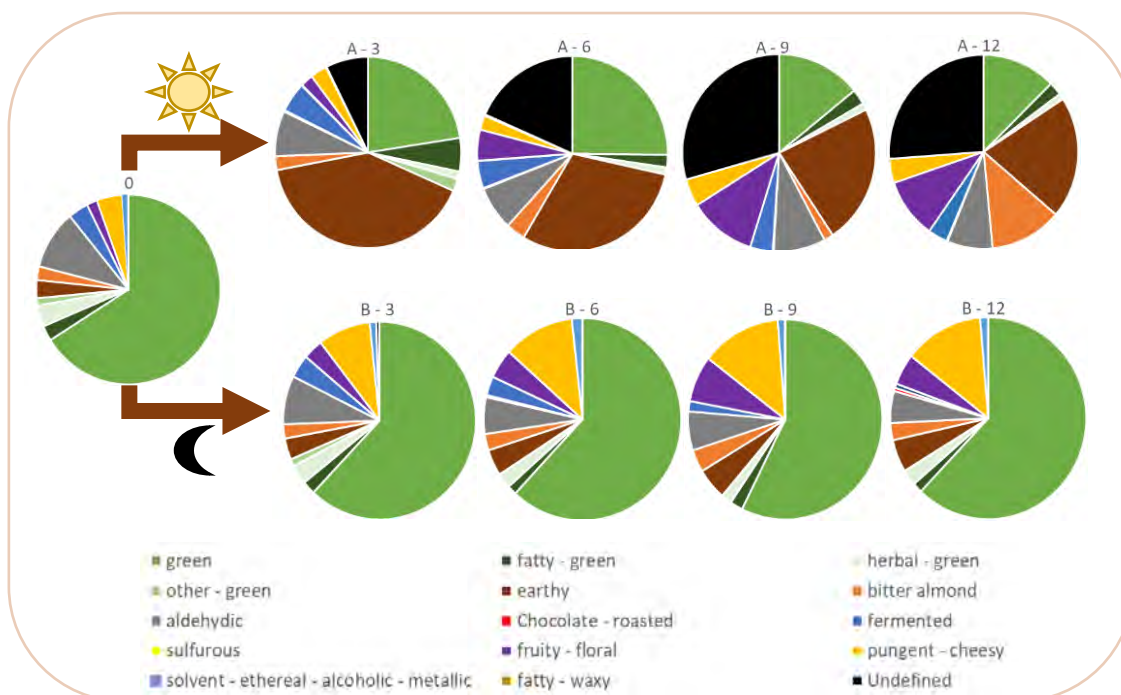


Figure 3: Profile of volatile compounds by sensor descriptors during the ageing (in ratios).

Conclusion

To conclude, the storage conditions of a product have a strong impact on the volatile compounds and odour. An evolution and deterioration of odour during time can be observed and among the conditions we checked, light had the biggest impact. It can be advised to store vegetable protein in the dark to prevent the photo-oxidation.

When presenting analytical data by sensory descriptors, it is possible to predict how compounds responsible for the different attributes are evolving. It can be used for early detection of an odour change, by detecting a change in the ratios of compounds responsible for the different attributes. It is however different from the overall odour perception. Depending on the product and the flavour or off-flavour of interest, it is important to choose and follow compounds that are correlated with that attribute.

References

1. Rackis J.J., Sessa D.J. and Honig D.H. Flavor Problems of Vegetable Food Proteins. *J Am Oil Chem Soc.* 1979;56:262-271.
2. Schindler S., Zelena K., Krings U., Bez J., Eisner P. and Berger R.G. Improvement of the Aroma of Pea (*Pisum sativum*) Protein Extracts by Lactic Acid Fermentation. *Food Biotechnol.* 2012;26(1):58-74.
3. Labuza T.P. and Dungan L.R. Kinetics of lipid oxidation in foods. *C R C Crit Rev Food Technol.* 1971;2(3):355-405.
4. Pripis-Nicolau L., de Revel G., Bertrand A. and Maujean A. Formation of Flavor Components by the Reaction of Amino Acid and Carbonyl Compounds in Mild Conditions. *J Agric Food Chem.* 2000;48(9):3761-3766.
5. Limacher A., Kerler J., Davidek T., Schmalzried F and Blank I. Formation of Furan and Methylfuran by Maillard-Type Reactions in Model Systems and Food. *J Agric Food Chem.* 2008;56(10):3639-3647.
6. Marilley L. and Casey M. G. Flavours of cheese products: metabolic pathways, analytical tools and identification of producing strains. *Int J Food Microbiol.* 2004;90(2):139-159.
7. TGSC The Good Scent Company. Sear Page Available online : <http://www.thegoodscentcompany.com/> (accessed online 15.12.2021)

Fat-salty sensory interactions in model cheeses: multivariate analysis of a compilation of data from different projects organised in the BaGaTeL database

ELISABETH GUICHARD¹, Thierry Thomas-Danguin¹, Hervé Guillemain^{2,3}, Bruno Perret^{2,4}, Solange Buchin³, Caroline Pénicaud⁴ and Christian Salles¹

¹ Centre des Sciences du Goût et de l'Alimentation, AgroSupDijon, CNRS, INRAE, Université Bourgogne Franche-Comté, Dijon, France

² PLASTIC Platform, INRAE, Thiverval-Grignon, France

³ URTAL, INRAE, Poligny, France

⁴ Université Paris-Saclay, INRAE, AgroParisTech, UMR SayFood, Thiverval-Grignon, France
elisabeth.guichard@inrae.fr

Abstract

The food industry needs to develop new strategies to formulate well-balanced products in terms of nutritional and environmental requirements and sensory acceptability by consumers. The BaGaTeL database has been built, guided by a process and observation ontology in food science, PO² ontology, to integrate data on dairy foods composition process, nutritional and sensory properties, using a consensual model and a shared structured vocabulary. We searched the database, using specific queries, for samples for which data of composition, rheological properties and sensory profile analysis were available. However, the composition and structure of the dairy products and the measured variables are often very different, which do not allow a direct comparison of the data. Thus, we made a selection of 68 model cheeses from 6 different projects made with different compositions (fat, protein, minerals, and water). A principal component analysis (PCA) performed on this set of samples revealed that the sensory hardness was better explained by a low moisture-in-non-fat-content than by a high protein content as was often suggested and that the intensity of salty taste was not only linked to salt content but was also modulated by cheese composition. Considering a subgroup of 22 samples from 3 projects, in which fat perception was also measured, a partial least square analysis revealed that fat perception was not only explained by fat content but was also highly influenced by salty taste, and that salty taste was more correlated with fat perception than with sodium ions content, highlighting sensory fat-salty interactions.

Keywords: database, dairy product, rheological properties, sensory analysis, statistical analyses.

Introduction

The food processing sector is facing sustainability challenges of growing complexity, such as climate change, increase of overweight, obesity or population aging. These problems make it necessary for the food industry to develop new strategies to formulate well-balanced products in terms of nutritional and environmental requirements and sensory acceptability by consumers. To tackle this challenge, the BaGaTeL database has been built, guided by a process and observation ontology in food science, PO² ontology [1]. BaGaTeL aims to integrate data in the field of reformulation of dairy products taking into account their nutritional and sensory properties, using a consensual model and a shared structured vocabulary. Our data organization allows gathering information from different projects performed on different samples more or less comparable. The aim of the present paper is to demonstrate that a common analysis of data obtained on samples from different projects could help to generalize the hypotheses from the initial projects and even find new relationships. We restricted our analyses to model hard cheeses as they represent 22% of the samples in BaGaTeL, and focused on the links between cheese composition, structure and sensory properties.

Experimental

Data from 65 different projects (693 samples) have been imported in BaGaTeL, with their associated metadata (project title, coordinator, abstract, references, material, method, unit, description) [2, 3]. In BaGaTeL, 488 samples have data on rheological properties, 524 have data on sensory description but only 252 samples have data on composition, rheological properties and sensory profile analysis. However, the food structures of these samples are very different, from yogurt to hard cheese and the rheological methods are different. We thus restricted our search to model hard cheeses, analysed by uniaxial compression and found 68 samples from six projects.

The statistical analyses (PCA and PLS) were performed with XLStat (Addinsoft, Paris, France). The whole set of data is available on the DataINRAE open access repository in the BaGaTeL dataverse [4]. The data are described

(scatter plots) in Guichard et al. [5], with the correlation matrices for the different sets of samples (Table S1 for PCA, Table S6 for PLS).

Results and discussion

Principal component analysis (PCA) on the whole set of 68 samples

The composition in lipid, protein, NaCl and water of the samples in the different projects is given in Table 1.

Table 1: Short description of the samples from the six selected projects.

Project	Number of samples	Lipid content (g/kg)	Protein content (g/kg)	Added NaCl (g/kg)	Water (g/kg)	Melting salts (g/kg)	Ref.	pH
Adi	8	80 / 160	204 to 310	4.94 / 14.94	600	0	[6]	5 / 6.2
Boisard	6	200 to 280	170 to 240	0 / 10	454 to 467	6,2	[7]	6.67 / 6.85
Lawrence	18	74 to 176	236 to 375	5 to 15	537 to 616	0	[8]	6.2
Tarrega	8	160 to 240	240 to 320	10	479	0	[9]	5.4
PraSel	24	173 to 290	228 to 297	7 to 25	419 to 542	0	np	4.96 / 5.35
Phan	4	197 / 297	283	0	383 / 483	31,2	[10]	5.4

np: non published results (personal communication).

A principal component analysis (PCA) was done on the 68 cheeses and 11 variables: 5 from the initial composition extracted from BaGaTeL, water, lipid, protein, sodium ions content (Na^+), 2 rheological parameters, YM (Young's modulus) and FS (fracture stress) and 2 sensory descriptors, hard/firm and salty. In addition to the variables of composition used in the different projects, three variables were calculated: (i) MNFS (moisture-in-non-fat-substances) is a useful variable in cheese manufacturing, and accounts for the available water, (ii) Lipid/DM (dry matter) better represents the impact of lipids in the lipid/protein network and (iii) Na^+ /water is more relevant to represent the concentration in sodium ions available for the taste receptors. These variables were not taken into account in the initial projects.

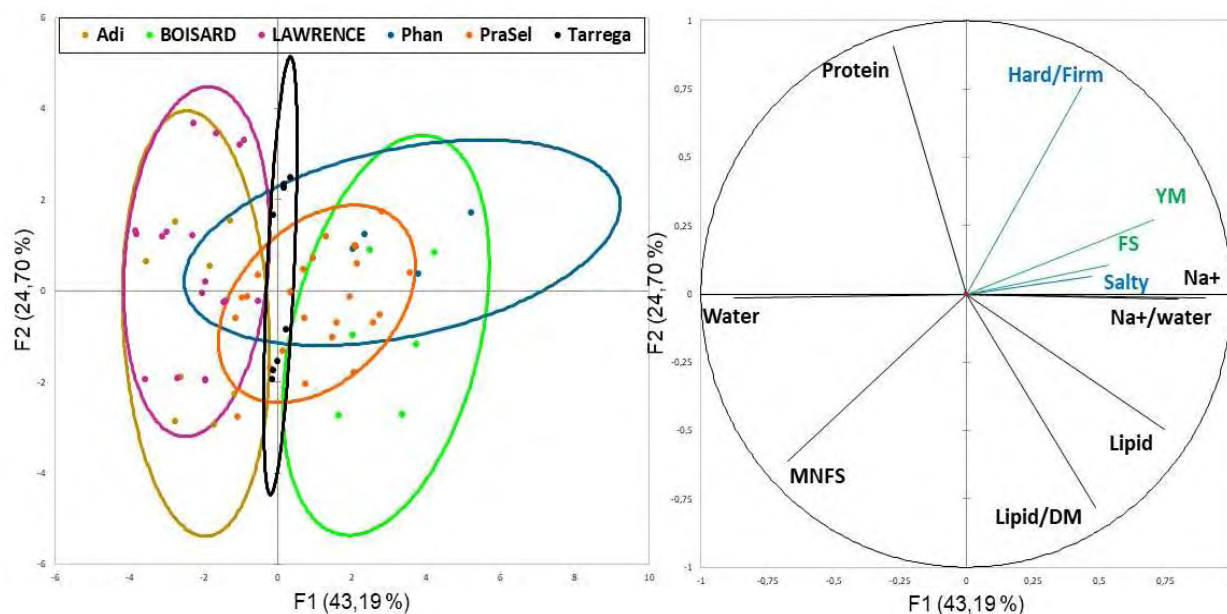


Figure 1: Principal Component Analysis (PCA). Left: representation of the 68 cheese samples in the plane 1-2. Right: representation of the 11 variables in the plane 1-2.

Figure 1 shows that there is a good overlap of the samples from the different projects in the principal plane (Axes 1-2), which accounts for 67.9% of the information. The sensory descriptor hard/firm is explained by a high protein content ($R^2 = 0.542$) and high YM ($R^2 = 0.629$), as was also suggested in the initial projects, however the highest correlation (negative) is with MNFS ($R^2 = -0.723$). The plot of hard/firm versus MNFS is shown in Figure 2.

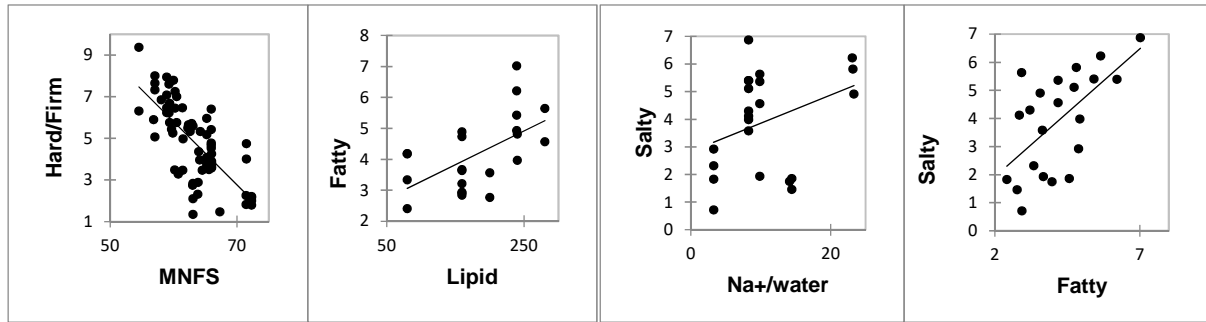


Figure 2: Relationships between hard/firm and MNFS ($R^2=-0.723$) in the set of 68 samples; fatty and lipid ($R^2=0.578$), salty and Na+/water ($R^2=0.348$), salty and fatty ($R^2=0.613$) in the set of 22 samples.

Our results confirm the impact of the protein network on sensory hardness but also emphasize the negative role of the amount of water in the non-fat phase. Our analysis also confirmed that salty taste was not only explained by Na⁺ and Na⁺/water, but also by the Young's modulus and fracture stress. This means that a more resistant cheese will favour the release of sodium ions in saliva and thus increase salty taste. In the individual projects, salty taste was influenced by the lipid content but the effects differed according to the projects. Phan et al., [10] found that salty taste was higher in cheeses with a low lipid content and Boisard et al., [7] found that salty taste was higher in cheeses with a higher lipid/protein ratio, which cannot allow to generalise the effect. Moreover, the impact of lipid, protein and water content was shown to vary according to the salt content, as detailed in Guichard et al., [11].

As some authors suggested the existence of sensory interactions between salty and fatty perception, we selected the samples in which fatty perception was measured, in order to test this hypothesis.

Partial least square (PLS) analysis on a subset of 22 samples

A partial least square (PLS) analysis was done on 22 cheeses with the sensory descriptor fatty, to explain the sensory perception (salty, fatty, hard/firm, crumbly, sticky, and springy) by data on composition and rheology.

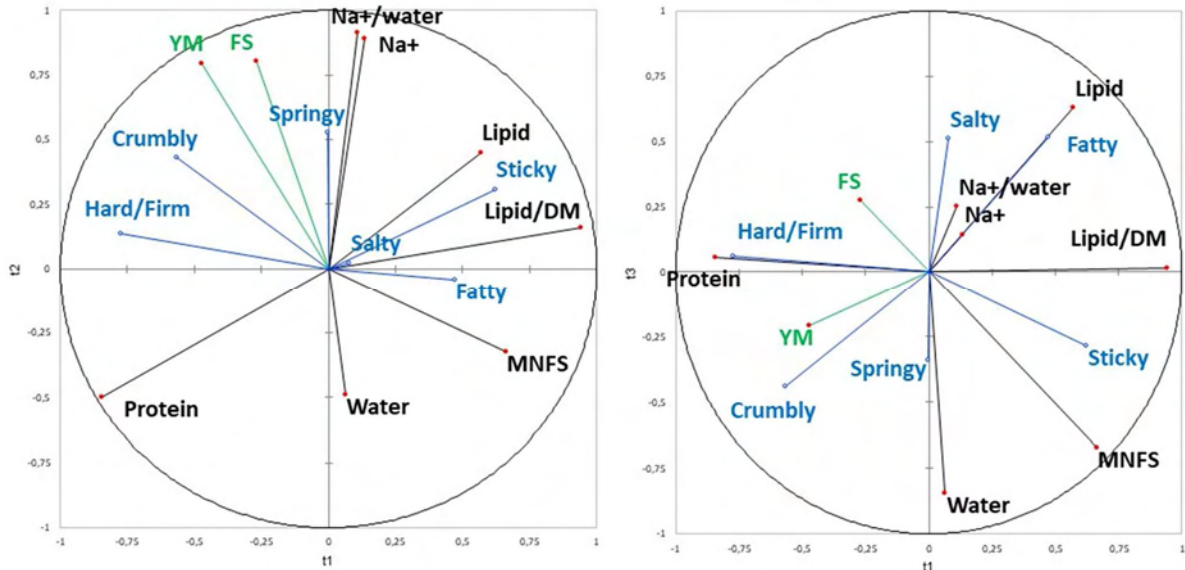


Figure 3: Partial least square (PLS) analysis on 22 samples from Adi, Boisard and Tarrega projects. Left: representation of the variables in the plane 1-2. Right: representation of the variables in the plane 1-3.

The representation on axes 1-2 and 1-3 (Figure 3) shows that the sensory hardness (hard/firm) is positively explained by the protein content ($R^2=0.620$) and negatively by the MNFS ($R^2=-0.606$), as already found in the PCA on 68 samples. A negative correlation was also found between hard/firm and lipid/DM ($R^2=-0.607$). Stickiness is better explained by the lipid/DM content ($R^2=0.479$) than by the lipid content ($R^2=0.299$), suggesting that it is more impacted by the lipid/protein network. Fatty perception is logically explained by the lipid content in the plane 1-3 ($R^2=0.578$), but the correlation is not very strong. In fact, fat perception is a multimodal perception involving olfactory, gustatory and tactile modalities [12]. However, salty taste is not as well explained neither by Na⁺ ($R^2=0.358$) nor by Na⁺/water ($R^2=0.348$). In the literature, the relationship between salty taste and cheese

composition differs strongly depending on the projects, varying according to the salt content and also to the lipid content. The most interesting result is the strong correlation between salty and fatty taste ($R^2=0.613$), which suggests perceptual interactions between these perceptions in cheese. The plot of salty taste versus fatty taste supports this hypothesis (Figure 2). The impact of fatty perception on salty taste is higher for the highest values of fat perception.

Conclusion

BaGaTel database allows gathering with a same structuration, data obtained in different projects. It is thus possible to find relationships between different sets of data, composition, structure and quality, obtained on a wider range of foods, covering a variety of compositions.

This compilation of data from different projects allowed finding more general trends to explain sensory perception by cheese composition and rheological properties. The moisture-in-non-fat-substances variable was shown to be a relevant parameter to explain cheese sensory hardness. The contradictory results on the impact of lipid content on salty taste found in the literature could be explained by salty-fatty sensory interactions, suggesting that salty taste is more impacted by fatty perception than by sodium ions content and lipid composition.

Such a database is thus of tremendous support to uncover the mechanisms driving food perception but also to propose new formulations of well-balanced products in terms of nutritional and/or environmental requirements and sensory acceptability by consumers.

Acknowledgements

This work was supported by the Qualiment Carnot Institute from French National Research Agency through the NutriSensAI project (grant number 16CARN002601) and by French National Research Agency through the DataSusFood project (grant number ANR-19-DATA-0016).

References

1. Ibanescu, L., Dibie, J., Dervaux, S., Guichard, E. & Raad, J. PO² a process and observation ontology in food science. Application to dairy gels. In (Ed.), *Metadata and Semantics Research (10th International Conference, MTSR 2016, Göttingen, Germany, November 22-25, 2016, Proceedings)*. Springer. doi.org/10.1007/978-3-319-49157-8_13
2. ANR-IC-Qualiment-NutriSensAI (<http://plasticnet.grignon.inra.fr/Portailbagatel/>).
3. Pénicaud, C., Ibanescu, L., Allard, T., Fonseca, F., Dervaux, S., Perret, B., Guillemin, H., Buchin, S., Salles, C., Dibie, J. & Guichard, E. Relating transformation process, eco-design, composition and sensory quality in cheeses using PO2 ontology. *Int. Dairy J.* 2019;92:1. doi.org/10.1016/j.idairyj.2019.01.003.
4. Guichard, E., Thomas-Danguin, T., Buchin, S., Perret, B., Guillemin, H., Salles, C. (2020). "Dataset on model cheeses composition, rheological and sensory properties, from six different projects exported from BaGaTel database". *Portail Data INRAE, BaGaTel dataverse, V3*. doi.org/10.15454/F40EXP.
5. Guichard, E., Thomas-Danguin, T., Buchin, S., Perret, B., Guillemin, H., Salles, C. (2021). Compilation of data on model cheeses composition, rheological and sensory properties, from six research projects exported from the BaGaTel database. *Data-in-Brief*, (36), June 2021, 106971, doi.org/10.1016/j.dib.2021.106971.
6. Syarifuddin, A., Septier, C., Salles, C. & Thomas-Danguin, T. Reducing salt and fat while maintaining taste: An approach on a model food system. *Food Qual. Prefer.* 2016;48:59. doi.org/10.1016/j.foodqual.2015.08.009.
7. Boisard, L., Andriot, I., Martin, C., Septier, C., Boissard, V., Salles, C. & Guichard, E. The salt and lipid composition of model cheeses modifies in-mouth flavour release and perception related to the free sodium ion content. *Food Chem.* 2014;145:437. doi.org/10.1016/j.foodchem.2013.08.049
8. Lawrence, G., Buchin, S., Achilleos, C., Berodier, F., Septier, C., Courcoux, P. & Salles, C. In vivo sodium release and saltiness perception in solid lipoprotein matrices. 1. Effect of composition and texture. *J. Agric. Food Chem.* 2012;60:5287. doi.org/10.1021/jf204434t.
9. Tarrega, A., Yven, C., Semon, E. & Salles, C. Aroma release and chewing activity during eating different model cheeses. *Int. Dairy J.* 2008;18:849. doi.org/10.1016/j.idairyj.2007.09.008.
10. Phan, V. A., Yven, C., Lawrence, G., Chabanet, C., Reparet, J.-M. & Salles, C. In vivo sodium release related to salty perception during eating model cheeses of different textures. *Int. Dairy J.* 2008;18:956. doi.org/10.1016/j.idairyj.2008.03.015.
11. Guichard, E., Thomas-Danguin, T., Buchin, S., Perret, B., Guillemin, H., Pénicaud, C. & Salles, C. Relationships between cheese composition, rheological and sensory properties highlighted using the BaGaTel database. *Int. Dairy J.* 2021;118:105039. doi.org/10.1016/j.idairyj.2021.105039.
12. Guichard, E., Galindo-Cuspinera, V. & Feron, G. Physiological mechanisms explaining human differences in fat perception and liking in food spreads-a review. *Trends Food Sci. Technol.* 2018;74:46. doi.org/10.1016/j.tifs.2018.01.010.

Is there a role for salivary detoxification enzymes in taste perception?

MATHIEU SCHWARTZ¹, H  l  ne Brignot¹, Evelyne Chavanne¹, Gilles Feron¹, Thomas Hummel², Yunmeng Zhu², Dorothee von Koskull², Jean-Marie Heydel¹, Loic Briand¹, Francis Canon¹ and Fabrice Neiers¹

¹ Centre for Taste and Feeding Behaviour (CSGA), Dijon, France, mathieu.schwartz@inrae.fr

² Smell & Taste Clinic, Department of Otorhinolaryngology, Dresden, Germany

Abstract

Flavour perception results from the interactions of many molecules in mouth, including the ones that occur between oral enzymes and odorants or tastants, which are released upon food mastication. Taste perception results from the activation of taste receptors present in the taste buds, which are bathed in saliva. As a result, molecules eliciting the taste modality have to be dissolved in saliva to reach the taste receptors and interact with salivary proteins. Some of these salivary proteins have a carrier role or a metabolization role via their enzymatic activity. Among these proteins are found some enzymes involved in the detoxification process. Interestingly, they can potentially recognize a large panel of molecules including taste molecules. The aim of this work was to characterise the presence of such enzymes in saliva, their ability to bind taste compounds and consequently to discuss their possible role in taste modulation.

Keywords: saliva, taste, detoxification, enzymes, glutathione transferases

Introduction

Taste perception results from the activation of taste receptors located in the taste buds on the tongue. These receptors bath in the saliva, which is involved in many processes including the solubilisation of taste molecules. Saliva contains many proteins among which some can interact with flavour molecules (e.g. lipocalins with fatty acids and hydrophobic molecules, proline-rich proteins with polyphenols, etc...) [1]. Using salivary proteomic analysis, differences in protein expression were correlated with cohorts of individuals differing in taste perception (e.g. carbonic anhydrases, cystatins) [2]. These observations support a direct or indirect link of these salivary proteins to taste perception and consequently their potential role in interindividual perception.

Among the 3000 salivary proteins identified [3], numerous enzymes were identified including enzymes ensuring the neutralization or detoxification of the reactive compounds. These enzymes include cytochrome P450, aldehyde and alcohol dehydrogenases and glutathione (GSH) transferases. Among the salivary glutathione transferases, the glutathione transferase GSTP1 seems the most expressed in saliva [4]. Diets rich in coffee or broccoli increase the salivary glutathione transferase activity, suggesting increased expression of this enzyme family [5].

In this study, we have identified two major detoxifying enzymes in the saliva of 32 people, namely glutathione transferases (GST) isoforms GSTA1 and GSTP1. In order to gain a deeper understanding of their binding potential, they were heterologously produced and purified. Then, we measured by an enzymatic screening assay their binding abilities toward taste compounds. Some bitter compounds strongly interacting with these enzymes were identified. To further characterise the molecular interactions, one X-ray structure of GSTA1 in complex with a bitter molecule was solved. These results shed light on the potential modulation of taste perception by glutathione transferases in saliva.

Experimental

Saliva collection and GST titration by ELISA

For this study, a cohort of 32 people participated to saliva collection. Among the people, information about birth date and gender were collected. Saliva was collected by stimulation. People were asked to chew a piece of Parafilm® laboratory film (American National Can, Chicago, IL, USA) during 5 min and to spit out saliva regularly before storage at -80°C until analysis. Before biochemical analysis, saliva samples were thawed and then centrifuged 15 min at 15 000 g. Analysis of all samples were done simultaneously. GSTA1 and GSTP1 were titrated following an ELISA protocol by using commercial kits (Abbeva, Cambridge, UK).

GST production, purification and enzymatic screening conditions

GSTA1 and GSTP1 genes were subcloned in pET22b vector (Novagen, Darmstadt, Germany) by gene synthesis and used for transformation of *E. coli* BL21 (DE3) strain (Novagen). Protein expression was performed as previously described [6] and purified on glutathione-sepharose affinity columns. For enzymatic tests, GSTs were dialyzed in potassium phosphate buffer 0.1 M pH 7.4. GSH-transferase reaction was followed spectrophotometrically at 340 nm by monitoring the absorbance of the glutathione conjugation product of chloro-dinitrobenzene (CDNB). In brief, a typical measurement consisted in 50 nM GST, 1 mM GSH, 1 mM CDNB and 10 μ M of pure bitter compound in 0.1 M potassium phosphate buffer pH 7.4.

X-ray crystallography

In order to obtain a high-resolution structure of GSTA1 in complex with a bitter compound, an X-ray crystallography approach was carried out. GSTA1 was crystallized by the hanging-drop method as previously described [6] and complex crystals were obtained by soaking preformed crystals with 10 mM hexyl-isothiocyanate and 10 mM GSH. Crystals were diffracted to 2.03 angstroms resolution on the beamline PX1 at the SOLEIL synchrotron (St-Aubin, France). Data processing was made following a procedure previously described [6].

Results and discussion

Evaluation of the level of glutathione transferases GSTA1 and GSTP1 in the saliva of 32 people

In a previous study, it was shown that glutathione transferase activity was present in human saliva [5] but the isoform inter-individual concentrations remain to be investigated. GSTs conjugate the glutathione (GSH) group to hydrophobic substrates but can also have a role of small molecule transporter. In this study, our objective was to investigate the inter-individual concentration of two glutathione transferases isoforms, GSTA1 and GSTP1, in a larger cohort of individuals. GSTA1 and GSTP1 concentrations were measured by ELISA assay on each saliva. A direct enzymatic measure was excluded due to the quick inactivation of GSTs activity on saliva samples due to the salivary hypothiocyanite [4]. The results show the presence of the two GSTs in all subjects. The mean concentrations are 10 ng/ml and 5 ng/ml of saliva for GSTP1 and GSTA1, respectively (Figure 1). Interindividual expression variations were observed, in particular for GSTP1 (one saliva contained up to 50 ng/ml of GSTP1).

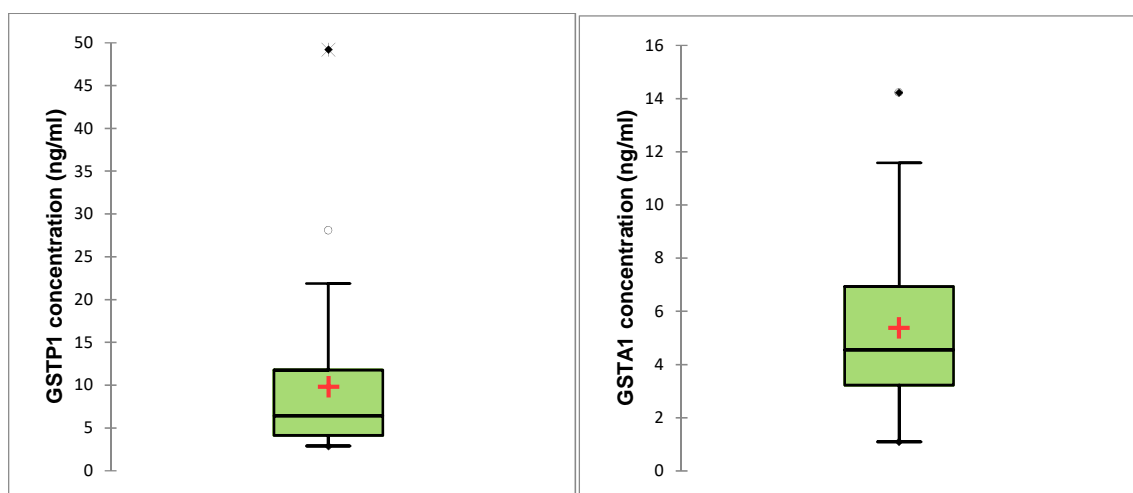


Figure 1: Titration of salivary glutathione transferases GSTP1 (left box-plot) and GSTA1 (right box-plot) in the saliva of 32 people. Boxes represent interquartile range, middle horizontal lines represent medians, errors bars represent 1.5 times the interquartile range, red crosses represent mean values, black diamonds represent minimum and maximum values. Extreme values are indicated by empty circles and asterisks.

Screening of flavour compounds interacting with salivary GSTs

For *in vitro* molecular studies, GSTA1 and GSTP1 were heterologously overexpressed in *Escherichia coli*. High levels of pure proteins were obtained after purification. Previously an increase of salivary GSTs following specific diets such as rich in coffee or broccolis was observed [5]. These foods contain bitter tasting compounds. Thus, we settled a library of molecules with bitter taste properties. This library was screened by using an enzymatic inhibition test. For this test we used chloro-dinitrobenzene (CDNB), a substrate conjugated with glutathione (GSH) upon the transfer reaction catalysed by GSTs. Absorbance of the product GS-DNB at 340 nm enables to monitor the enzymatic reaction. Each flavour compound was added to the reaction mixture at 10 or 100 μ M, allowing to

assess its inhibition potential. The enzymatic inhibition resulting from the addition of the flavour molecule corresponds to the binding in the active site as a substrate, or to the binding in the active site, or in the ligandin site as a non-substrate binder. A good inhibitor means that strong interaction occurs with the GSTs, slowing down the conjugation reaction between GSH and CDNB. By using this method, we screened a library of about 40 bitter compounds of different chemical families namely flavonoids, isothiocyanates, heterosides, alkaloids and N-heterocycles (Figure 2). Two families of compounds showed good inhibition potential: flavonoids and isothiocyanates. This last family contains compounds that are known to be conjugated with GSH by GSTA1 and GSTP1. Hexyl-isothiocyanate inhibits near 50% of the GSH-transfer reaction of GSTA1. In order to have a three-dimensional view of the binding of hexyl-isothiocyanate to GSTA1, we used X-ray crystallography.

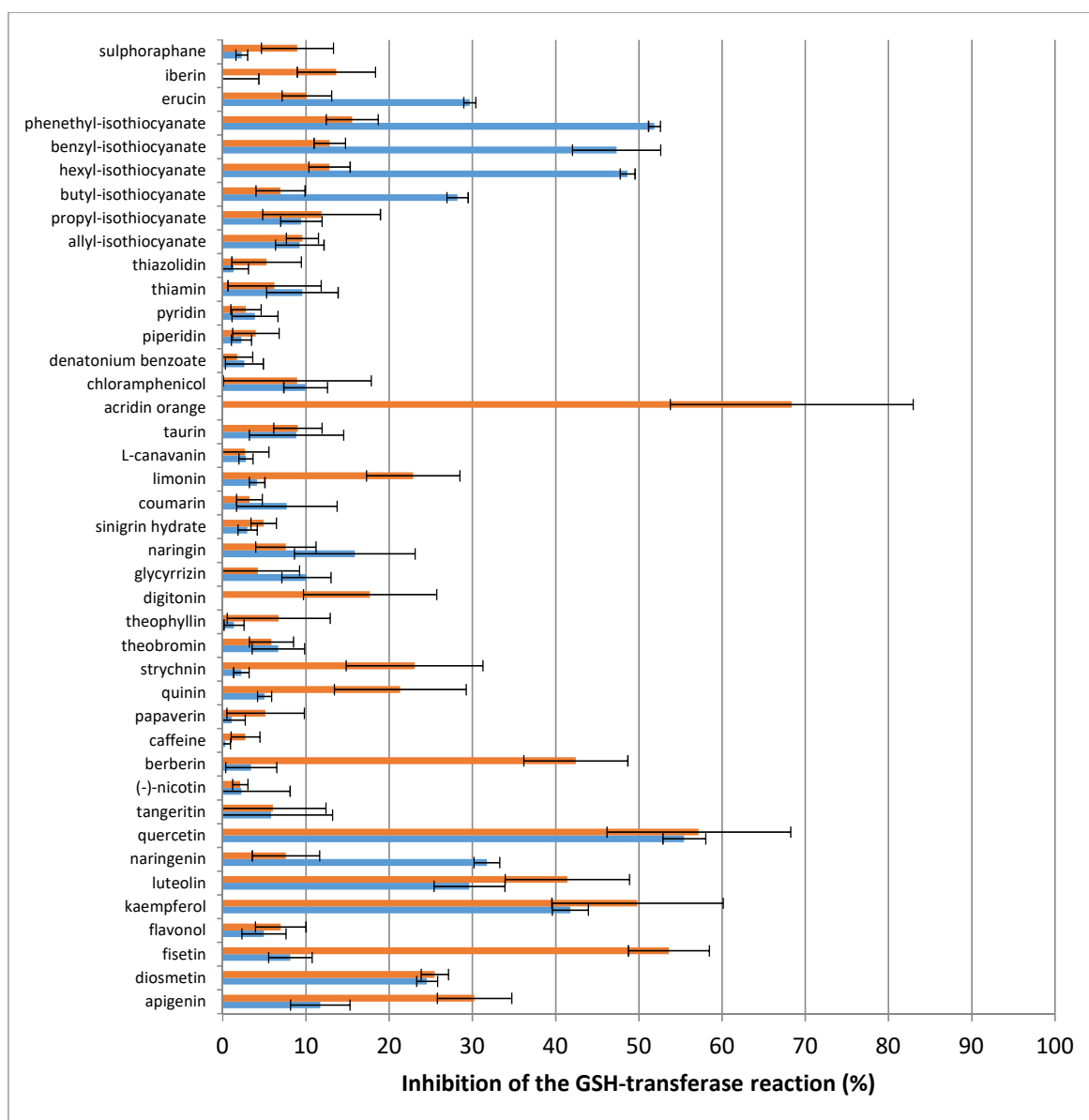


Figure 2: Bitter compounds screen using the inhibition test with CDNB as substrate. Compounds were screened at 10 μ M (blue bars, GSTA1; orange bars, GSTP1). CDNB and glutathione were used at 1 mM in 100 mM potassium phosphate buffer pH 7.0. Results are the mean of three independent measurements.

Interaction of hexyl-isothiocyanate with GSTA1 studied by X-ray crystallography

For the crystallographic study, we choose to deepen the interactions involving isothiocyanates as they were among the best inhibitors. Worth is to mention that isothiocyanates are inducer of glutathione transferases and also their substrates conjugated to glutathione upon catalysis. Crystals of complexes between GSTA1 and hexyl-isothiocyanate were prepared by the soaking method. X-ray diffraction images were collected at the SOLEIL synchrotron. Structural analysis revealed that hexyl-isothiocyanate is conjugated to glutathione and binds to GSTA1 active site (Figure 3). Both active sites of the GSTA1 dimer are occupied by the glutathione/hexyl-

isothiocyanate conjugates. Residues from the glutathione binding site interact with the glutathionyl group whereas residues from the helical domain that form the hydrophobic site interact with the hexyl-isothiocyanate group. Our results show that GSTA1 efficiently and tightly binds hexyl-isothiocyanate, enabling its conjugation to GSH. This process is likely quick in a physiological context such as saliva.

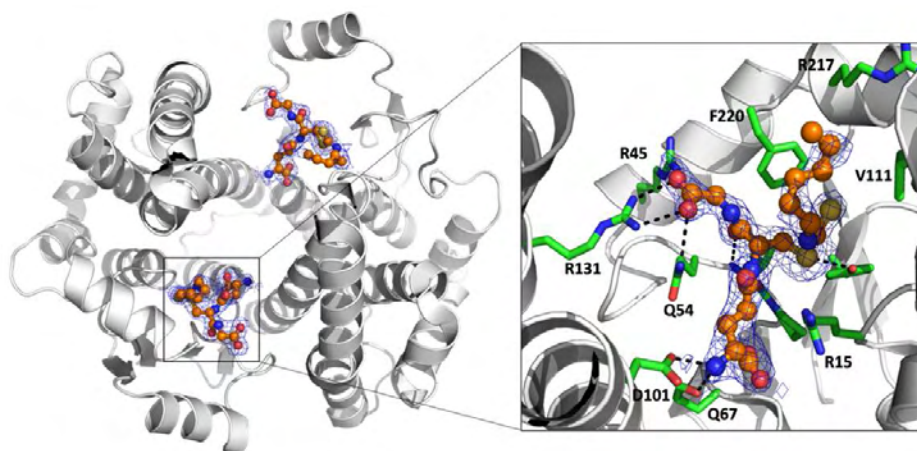


Figure 3: Structural view of hexyl-isothiocyanate metabolised by glutathione transferase GSTA1 deciphered by X-ray crystallography. Enzyme is shown as white cartoon, interacting residues are shown as green sticks, and hexyl-isothiocyanate is shown as orange sticks and spheres.

Conclusion

In this study we have quantified the presence of two detoxification enzymes namely GSTA1 and GSTP1 in the saliva of 32 people. Our results showed that GSTA1 and GSTP1 are recurrent enzymes of the salivary enzymatic arsenal of most people. By using an *in vitro* approach, we have shown that GSTA1 and GSTP1 are able to interact with numerous bitter compounds. Two families of compounds significantly inhibit the GSH-transferase activity, namely flavonoids and isothiocyanates. By using X-ray crystallography, we have shown that hexyl-isothiocyanate is metabolised by GSTA1 due to an active site efficiently adapted for the hydrophobic part of isothiocyanates. Isothiocyanates and flavonoids, as many other bitter compounds, are found in many plant foods and participate to the plant defence mechanisms. It is therefore not surprising that salivary detoxification enzymes act directly in saliva to reduce the toxicity of these exogenous molecules. Previously it was shown that specific diet rich in plant-derived foods such as coffee or broccoli increase the salivary GST activity, suggesting that the oral detoxification system is able to dynamically adapt to specific diet [5]. In two other studies, it was shown that GSTs participate to the termination of the odorant signal [7], and that several odorant molecules are metabolised by GSTs [6]. Salivary GSTs could have a similar role at the oral level by modulating the quantity of taste compounds reaching the taste receptors. In the future, studies aiming at detecting the levels of salivary GSTs in link with specific plant-based diets and in link with the taste perception thresholds of individuals for molecules specifically interacting with these enzymes should be addressed.

References

1. Canon F, Neiers F, Guichard E. Saliva and Flavor Perception: Perspectives. *J Agric Food Chem.* 2018;66(30):7873-9.
2. Dsamou M, Palicki O, Septier C, Chabanet C, Lucchi G, Ducoroy P, et al. Salivary protein profiles and sensitivity to the bitter taste of caffeine. *Chem Senses.* 2012;37(1):87-95.
3. Amado FM, Ferreira RP, Vitorino R. One decade of salivary proteomics: current approaches and outstanding challenges. *Clin Biochem.* 2013;46(6):506-17.
4. Fabrini R, Bocedi A, Camerini S, Fusetti M, Ottaviani F, Passali FM, et al. Inactivation of Human Salivary Glutathione Transferase PI-1 by Hypothiocyanite: A Post-Translational Control System in Search of a Role. *PLOS ONE.* 2014;9(11):e112797.
5. Sreerama L, Hedge M, Sladek N. Identification of a class 3 aldehyde dehydrogenase in human saliva and increased levels of this enzyme, glutathione S-transferases, and DT-diaphorase in the saliva of subjects who continually ingest large quantities of coffee or broccoli. *Clinical cancer research : an official journal of the American Association for Cancer Research.* 1995;1:1153-63.
6. Schwartz M, Menetrier F, Heydel J-M, Chavanne E, Faure P, Labrousse M, et al. Interactions Between Odorants and Glutathione Transferases in the Human Olfactory Cleft. *Chem Senses.* 2020.
7. Robert-Hazotte A, Faure P, Neiers F, Potin C, Artur Y, Coureaud G, et al. Nasal mucus glutathione transferase activity and impact on olfactory perception and neonatal behavior. *Sci Rep.* 2019;9(1):3104.

Oxidation markers of premature ageing in Chardonnay wine: Combined use of GC-MS/MS, GC-O/Olfactoscan and sensory analysis for their characterisation

MARIE SIMON¹, Amandine Vessot², Jérôme Mallard¹, Rémy Romanet³, Noëlle Béno¹, Markus Lübke², Jordi Ballester¹, Maria Nikolantonaki³, Régis Gougeon³, Thierry Thomas-Danguin¹ and Yves Le Fur¹

¹ Centre for Taste, Smell and Feeding Behaviour (CSGA), INRAE, CNRS, AgroSup Dijon, University of Bourgogne Franche-Comté, F-21000, Dijon, France, marie.simon@inrae.fr

² Aromalyse, 3 rue des Ciseaux, F-21800, Quetigny, France

³ Univ. Bourgogne Franche-Comté, AgroSup Dijon, PAM UMR A 02.102, Institut Universitaire de la Vigne et du Vin – Jules Guyot, F-21000 Dijon, France

Abstract

The phenomenon called “premature ageing”, which is characterised by uncontrolled and unwanted ageing of wines, can even impact fairly young wines. The aim of the present study was to determine the chemical nature and the relative importance of oxidation markers in Chardonnay wines through a combined approach of sensory analysis, GC-O & Olfactoscan (OLF) and GC-MS/MS (Chardonnay+ project). We systematically compared a control wine (non-oxidised Chardonnay wine, 2019-vintage) with the same wine artificially oxidised to simulate premature oxidation. On the one hand, a sensory analysis was conducted with a trained panel to characterise the sensory consequences of oxidation in the wine. Then, volatile compounds from the oxidised wine were extracted by Solid-Phase Extraction (SPE) and analysed by GC-O and Olfactoscan. Thereby, the volatile compounds were submitted to a GC/O analysis while at the olfactory port a background odour of the control wine is delivered by an olfactometer. Thus, we could identify the compounds that are responsible for the odour of oxidation within the wine aroma buffer. Finally, volatile compounds of both control and oxidised wines were analysed by GC-MS/MS after two extraction methods: Solid Phase Micro Extraction (SPME) and liquid/liquid extraction. This approach allowed pointing out the modifications in volatile compounds concentration induced by the oxidation process in Chardonnay wine.

Keywords: White wine, Key odorant, Odour mixture, Trained panel, Sensory profile

Introduction

Olfactory markers that are formed during “premature wine ageing” include aldehydes such as methional, phenylacetaldehyde, and benzaldehyde, responsible respectively for the smell of boiled vegetables, wilted rose or bitter almond, which negatively affect consumer liking. In this context, the Chardonnay+ project was conducted following 2 axes. The first one, which is not presented here, aims to develop an accelerated ageing test sensorially validated on multiple wines. The objective of the second axis was to carry out sensory analysis and to identify molecular markers of wine oxidation, taking into account markers identified in a previous work [1]. Through those axes, the aim of the project was to determine the chemical nature and the relative importance of oxidation markers in young Chardonnay wines through a combined approach of sensory analysis, gas chromatography-olfactometry (GC-O) & Olfactoscan and GC-tandem mass spectrometry (MS/MS), comparing non-oxidised and accelerated oxidised wines.

Experimental

Wines samples

Three Chardonnay dry white wines from Burgundy wine producers were selected for this study: Bourgogne Hautes Côtes de Nuits 2019 (HCN), Bourgogne Chitry 2018 (Chitry) and Chablis 1er Cru Côte de Jouan 2018 (Chablis Jouan). The three wines were submitted to accelerated ageing. Non-oxidised (NOW) and oxidised wines (OW) were used in this study.

Experiment 1: Sensory analysis

Sensory sessions took place between November 2018 and March 2020. Two sensory panels were formed successively during this period, composed of oenology students and staff members from the oenology school of Dijon (IUVV - France). After a training period, 11 participants for the first panel and 21 for the second were convened to perform a monadic assessment of the samples. The sessions took place in a sensory room with

individual booths. All samples were evaluated in duplicate. Samples (20 mL) were presented at room temperature in standardised black glasses coded by 3-digits numbers following a William's Latin square design. For each sample, the panellists were first asked to rate the intensity of oxidation–reduction with a continuous REDOX scale orthonasally, using the protocol proposed by Ballester *et al.* (2018) [2]. The scale was structured from –5 (strong reduction), to +5 (strong oxidation), and zero (neither reduced nor oxidised) in the midpoint. Then, panellists performed an odour description of the samples using a Rate All That Apply (RATA) method with a list of 28 attributes related to Chardonnay wines, oxidation and reduction notes and other wine faults.

Experiment 2: GC-O & Olfactoscan

A panel of 13 subjects was formed on the basis of selection tests (ETOC, Bourdon and odour description). Each selected subject was trained to GC-O within 2 training sessions: one with selected odorants in a wine and the other with an SPE [3] extract of wine to simulate a real GC-O run. Both NOW and OW for each wine were extracted by SPE [3] and the extracts were analysed with GC-O and Olfactoscan (OLF). GC-O without background odour was carried out with a HP 6890A GC + FID equipped with a sniffing port. The chromatographic column was a DB-WAX (30 m, 0.32 mm, 0.5 μ m) and 1 μ L of extract was injected. The Olfactoscan technique [4] consists in the combination of the GC-O and an olfactometer (Burghart OM4/b), which allows to add a constant odour of wine as a background. Following this technique, odour compounds from the OW extract that are separated owing to the GC were mixed with odorants from the NOW odour as a background, which allowed to evaluate if the compounds are still perceived in the wine odour and/or if they modulate the wine odour. In both experiments, responses were collected at the sniffing port during 40 minutes with a Gerstel ODP recorder® and the odour zones were identified using the detection frequency method [5].

Experiment 3: GC-MS/MS

Analyses were carried out using two different methods. Liquid/liquid extraction with dichloromethane was performed after adding a known amount of internal standard (4-octanol) to 40 ml of wine. After concentration in a Kuderna–Danish apparatus, extracts were separated on a Restek Stabilwax column (30 m \times 0.32 mm id \times 0.25 μ m film thickness) and 2 μ L were injected. SPME was carried out after adding 7 ml of wine to a 20 ml vial and spiking with a known amount of internal standard (4-octanol). Extraction was performed in headspace mode under stirring with a DVB/Carboxen/PDMS SPME fibre (40 $^{\circ}$ C, 30 min). Separations were done on a Supelco SPB-1 analytical column (30 m \times 0.32 mm id \times 4.0 μ m film thickness).

For both extraction methods, GC-MS/MS analyses were performed using a Shimadzu 2010+ gas chromatograph coupled to a Triple Quadrupole mass spectrometer Shimadzu TQ8050, operated in the electron impact ionization mode (70 eV), and a Shimadzu AOC-5000+ autosampler. GC injector, ion source and transfer line temperatures were maintained at 250, 200 and 250 $^{\circ}$ C, respectively. Non-targeted analysis was used in order to identify compounds which are affected by oxidation. The detection was set to Q3 scan from 29 to 350. For targeted analysis of relevant molecules, Multiple Reactions Monitoring was used. The analytes were positively identified by comparison of spectra and retention times to those of authentic standards.

Results and discussion

Differences in REDOX odour scores were tested statistically using analysis of variance (ANOVA) with $\alpha=5$ %, followed by a Newman-Keuls' test ($\alpha=5$ %) when a significant effect was found. Table 1 shows average redox scores for each wine and reveals a significant effect of redox level. OW showed significantly higher sensory oxidation than NOW, which confirmed that the oxidation has been perceived.

Table 1: Average scores for odour redox assessment of the three wines for NOW and OW, followed by Newman-Keuls' tests ($\alpha=5$ %). Samples associated with the same letter were not significantly different.

Sample Name	Average Redox score	
	NOW	OW
Chitry	0,53 b	2,93 a
Chablis Jouan	0,44 b	2,75 a
HCN	0,14 b	2,44 a

For descriptive analysis of samples, an ANOVA was carried out to determine which attributes were significantly different among the wines ($p < 0.05$). Then, principal component analysis (PCA) was used to visualise the relationships between the wines and the significant sensory attributes.

The results are presented in Figure 1 which shows different aromatic profiles between the 6 samples (3 NOW and 3 OW). Regarding NOW, HCN was correlated to reduction notes (stagnant water, cabbage/truffle/maize) whereas Chitry and Chablis Jouan were correlated to fruity and floral notes. In contrast, oxidation notes were detected in OW as cooked vegetables for oxidised HCN and bruised apple, walnut/curry for oxidised Chitry and Chablis Jouan. These results suggest a matrix effect related to oxidation phenomenon.

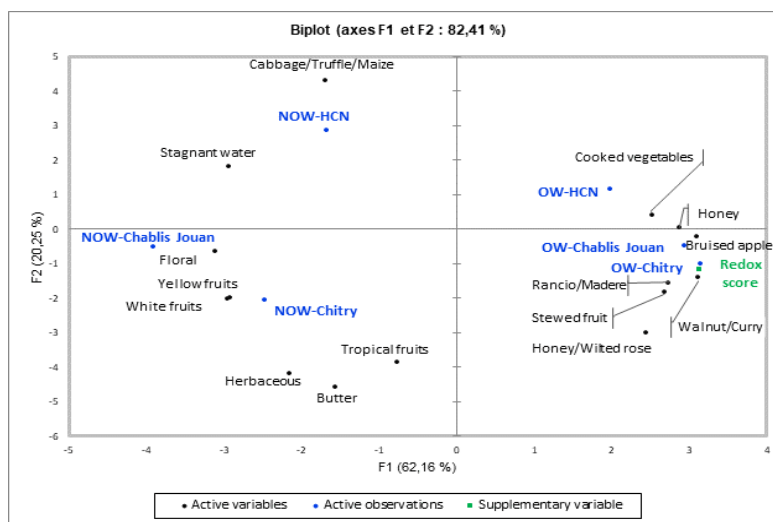


Figure 1: Principal Component Analysis of a sensory description of samples (only significant attributes after ANOVA are showed ($p < 0.05$)).

The results of experiment 2 (GC-O & Olfactoscan) and 3 (GC-MS/MS) are summarised in Table 2, which reported for several selected compounds in each NOW and OW the LRI on DB-WAX, the descriptors given by the panellists in GC-O, the estimated concentration and the perceptual category the odorants belong to. Indeed, 7 perceptual categories were defined according to the sensory effect that produce a compound when added to the background wine odour within the Olfactoscan run (OLF). For example, sotolon had a LRI of 2202 and was described with a “background odour” and “alcohol” notes. This odorant was present at 31.1 $\mu\text{g/L}$ and 74 $\mu\text{g/L}$ respectively in NOW and OW for the HCN wine. Comparing the GC-O & Olfactoscan results for the HCN wine, sotolon was only detected in the Olfactoscan run, suggesting a synergy with molecules in the NOW background odour. Although the descriptors used for sotolon (“background odour” and “alcohol”) were different from those usually reported in the literature (for example “nut” and “spices” for sotolon [6]) the combined results obtained in experiments 2 and 3 allowed to ascertain the compound identification. Such approach was found necessary for several compounds.

Moreover, GC-MS/MS data were found to be highly complementary for the interpretation of the perceptual categories drawn from experiment 2. For example, the concentration of furfural that increased in OW compared to NOW was not reflected with GC-O in OW or masked by the wine odour with OLF. In the case of tryptophol, it was not sensorially detected and at low concentration in NOW but was detected and at high concentration in OW and still detected with OLF, which suggested that it is a key odorant marker of oxidation since it is perceived in OW and maintained within the wine background odour (OLF). Therefore, GC-MS/MS results validated perceptual categories of odorants related to oxidation by showing variation in odorants concentration. At last, this combination of approaches showed that some odorants such as 4-vinylguaicol had a lower concentration in OW but benefit from perceptual synergy by the wine aromatic buffer.

Finally, the integration of the results of the 3 experiments allowed to highlight several points. Sotolon, known for its “curry/burnt” notes [7], was identified in experiments 2 with “background odour” and “alcohol” descriptors and in experiment 3 with an increased concentration in OW, and thus might be responsible for the “walnut/curry” notes related to oxidation found in experiment 1. The fact that the descriptors are different from usual ones for this compound could be explained by the fact that sotolon is coeluted with 4-vinylguaicol that has “smoky/phenolic” notes [7]. Usually known for its “honey/floral” notes [7], phenylacetaldehyde (LRI = 1629) that could be responsible for the “honey/wilted rose” odours in experiment 1, was found in experiment 3 but not in 2. Once again, that could be explained by the fact that phenylacetaldehyde is eluted at a LRI near isovaleric acid that has really strong “cheese/mould” notes. As 5-hydroxymethylfurfural and tryptophol both increased in OW and have respectively “nut/spices” and “cooked/honey” notes, they also could be related to oxidation descriptors found in experiment 1. However, further experiments are still needed to confirm those results.

Table 2: A list of key odorants for wine oxidation common to both experiments 2 and 3, their LRI, descriptors, categories and concentration in NOW and OW. (* SPME quantification).

Molecule	LRI DB-WAX	Descriptors	Concentration (µg/L) NOW/OW		
			HCN	Chitry	Chablis-Jouan
Ethyl butyrate*	1034	strawberry, raspberry	291/267	726/804	570/380
Isoamyl acetate	1118	alcohol	1160/1040	216/167	163/159
Methional	1454	toast, smoke	0.103/0.184	0.146/0.277	0.07/0.98
Furfural	1463	starch, potato, burnt, hot	4.68/9.67	39.3/52.2	12.9/55.7
5-Methylfurfural	1566	vegetal, wood, citrus, sweet	0.05/0.07	0.52/0.59	0.38/0.56
Isovaleric acid	1674	mould, sewage, cheese	108/111	137/128	105/8.4
2-Hexenoic acid	1994	alcohol, flower, red fruits	7.37/7.46	18.7/17.3	17.3/24.5
4-Vinylguaiaicol	2200	Background odour, alcohol	85.2/43.5	229/102	360/115
Sotolon	2202	Background odour, alcohol	31.1/74	2.68/4.08	1.86/7.14
5-Hydroxymethyl furfural	2505	nut, starchy, spices	0.39/0.82	3.83/7.44	1.36/3.86
Tryptophol	2812	cooked, honey, fruit	1.3/312	125/242	3.95/194

Odorants detected in NOW, absent in OW and Olfactoscan (OLF)
Odorants detected in NOW and OW, absent in OLF → not well extracted and masked by background odour
Odorants detected in NOW, OW and OLF
Key odorants detected in OW and masked by OLF
Key odorants detected in OW and maintained within OLF
Key odorants detected only in OLF → synergy with background odour
Absence of odorants in NOW, OW and OLF

Conclusion

Combining instrumental and olfactory/sensory methods permits to draw up a non-exhaustive but consistent list of odour-active compounds identified as key odorants in the oxidation process of Chardonnay wines. Sensory analysis revealed different aromatic profiles between the control and the oxidised wine that could lead to a predictive sensory profile of Chardonnay wine through ageing. Some of the key odorants identified with instrumental/olfactory methods could explain the molecular basis of the odour notes related to oxidation found in the sensory approach but further experiments are needed to confirm these results. Finally, our results represent a step forward in the comprehension of wine oxidation phenomenon and may open up possibilities to control and/or predict a wine's ability to resist oxidation.

Acknowledgements

Amandine Vessot and Markus Lubke acknowledge financial support from the European Union through FEDER/FSE Bourgogne 2014/2020 (Synergie BG0014501) and from BPIFrance Financement (DOS0063324/00). This publication solely reflects the authors' view and does not engage the responsibility of EU, Regional Council or BPIFrance. Amandine Vessot would like to thank Gwenaëlle Steyaert for technical assistance. The Chardonnay+ project was supported by financial grants from the Region Bourgogne Franche-Comté and the "Fonds Européen de Développement Régional (FEDER)".

References

1. Naudot M.C, Alinc J.B, Meurgues O, Gervais J.P, Jaffré J, Le Fur Y. Oxidized Burgundy Chardonnay wines: sensory space boundaries, and identification of volatile target compounds. Wine Active Compounds 2008 International Conference, Oenoplurimédia. 2008;117:119.
2. Ballester J, Magne M, Julien P, Noret L, Nikolantonaki M, Coelho C, Gougeon R. Sensory impact of polyphenolic composition on the oxidative notes of Chardonnay wines. Beverages. 2018;4:19.
3. Ma Y, Tang K, Xu Y, Li J.M. Characterization of the Key Aroma Compounds in Chinese Vidal Icewine by Gas Chromatography–Olfactometry, Quantitative Measurements, Aroma Recombination, and Omission Tests. J Agric Food Chem. 2017;65:394-401.
4. Bursegh K, de Jong C. Application of the Olfactoscan method to study the ability of saturated aldehydes in masking the odor of methional. J Agric Food Chem. 2009;57:9086-9090.
5. Pollien P, Ott A, Montigon F, Baumgartner M, Muñoz-Box R, Chaintreau A. Hyphenated headspace-gas chromatography-sniffing technique: screening of impact odorants and quantitative aromagram comparisons. J Agric Food Chem. 1997; 45:2630-2637.
6. Silva Ferreira A. C, Barbe J.C, Bertrand A. 3-Hydroxy-4,5-dimethyl-2(5H)-furanone: A Key Odorant of the Typical Aroma of Oxidative Aged Port Wine. J Agric Food Chem. 2003;51:4356-4363.
7. Gambetta J.M, Bastian S.E.P, Cozzolino D, Jeffery D.W. Factors influencing the aroma composition of Chardonnay Wines. J Agric Food Chem. 2014;62:6512-6534.

Exploring the odorant and molecular characteristics of molecules sharing the odour notes of an aroma blending mixture

ANNE TROMELIN¹, Florian Koensgen¹, Marylène Rugard², Karine Audouze²,
Thierry Thomas Danguin¹ and Elisabeth Guichard¹

¹UMR CSGA: INRAE, CNRS, Institut Agro, Université de Bourgogne Franche-Comté, 21000 Dijon, France

²Université de Paris, INSERM UMR-S1124, F-75006 Paris, France

anne.tromelin@inrae.fr

Abstract

The human olfactory system allows to perceive and identify a huge number of odours from few hundreds ORs involved in an olfactory coding whereby one olfactory receptor (OR) recognises multiple odorants while one odorant activates different combinations of ORs. Odours perceived in our environment are mainly the result of mixtures of odorants, but the specific mechanisms involved in their processing remain poorly understood. In previous studies performed at INRAE-CSGA, the perception of a binary mixture of ethyl isobutyrate (Et-iB, strawberry-like odour, STR) and ethyl maltol (Et-M, caramel-like odour, CAR) was investigated in comparison with a reference (allyl hexanoate, Al-H, pineapple-like odour, PNA). In humans, the binary specific mixture of Et-iB and Et-M was judged as more typical of a pineapple odour than the individual components, and similar to those of allyl hexanoate. The analysis of the network of odours sharing by 293 molecules described with at least one of the odours STR, CAR or PNA revealed peculiar links between odours, and led to identify 9 STR-CAR and 4 STR-PNA molecules. We investigated the molecular features of these molecules by performing pharmacophore generations using the STR-CAR, STR-PNA sets, both separately and putting together the 13 molecules. Comparing the distances between features of the three models revealed a common distance close to 8 Å between the centres of at least one HY and one HBA. Additionally, the pharmacophore comparison of the three models showed a satisfactory mapping of the features. These results support the hypothesis wherewith molecules sharing the odours involved in a blending mixture could recognise a common set of ORs.

Keywords: odour notes, aroma blending mixture, pharmacophore

Introduction

The perception of the odours begins at the peripheral olfactory system by the interactions of odorants with olfactory receptors (ORs) in the nose [1]. The perception and discrimination of a huge number of odours from few hundreds ORs involves an olfactory scheme whereby one OR recognises multiple odorants while one odorant activates different combinations of ORs [2]. Nevertheless, in spite of advances in the knowledge of olfactory perception, the pathway(s) involved in the odours perception remains poorly understood [3, 4]. It is especially challenging in the case of mixtures of odorants [5, 6], while odours perceived in our environment essentially stem from mixtures of odorants [7]. In some cases, the olfactory processing of a mixture of odorants produces a homogeneous percept in which a single odour is perceived from the mixture thanks to a configural process [5, 7]. Odour blending occurs if a mixture of molecules A and B carrying different odours is perceived to have a specific new odour AB, distinct from the odours of each component A and B [8]. Thus, a blending mixture percept can be represented as $AB \neq A+B$.

Currently, target approaches that concern the interactions of odorants at the OR level are most often undertaken [9-11]. However, in our own study, we focused on a ligand approach that is complementary to the target approach. In the context of aroma blending, we considered a set of odorants, whose selection was based on an aroma blending previously carefully investigated in several studies performed with animals [12, 13] and humans [14-16]. These studies constantly revealed that the perception of a mixture of ethyl isobutyrate (Et-iB), which has a strawberry-like odour (STR), and ethyl maltol (Et-M), which has a caramel-like odour (CAR) is configurally processed by the olfactory system. The binary specific mixture of Et-iB + Et-M was investigated in humans in comparison with allyl hexanoate (Al-H), which has a pineapple-like odour (PNA) and was chosen as reference to evoke an odour close to the one expected in the mixture. It was established that the mixture has an odour close to this reference. Moreover, the binary mixture was judged as having an odour more typical of pineapple than of the individual components [14].

To explore the key features of this aroma blend we built a dataset of 293 molecules by selecting in a large flavour database [17, 18] the odorants having at least one of the odours STR, CAR or PNA. In a recent study [19], we have analysed through a network the co-occurrences of the odour notes in the descriptions of the odorants. The

odours network revealed peculiar links between odours, especially this analysis led to identify 9 STR-CAR and 4 STR-PNA molecules.

Recognising that molecules sharing analogous odour qualities could possess common structural molecular properties, and that combinations of activated ORs encode odour qualities [20, 21], we hypothesised that molecules sharing the common STR odour note should have some common structural features.

With the aim to investigate the structural features of these molecules, we developed an *in silico* approach using pharmacophores study. The pharmacophore generations [22] were performed using the STR-CAR, STR-PNA and STR-CAR+STR-PNA subsets. Comparing the inter-features distances and testing the mapping of the pharmacophore models allowed to put forwards the common as well as the peculiar characteristics of each subset.

Experimental

Data Preparation

The molecules STR-CAR and STR-PNA were extracted on the basis of their odour notes from the large database [18] designed from the 9th version of Flavor-Base [17]. The three subsets STR-CAR, STR-PNA and STR-CAR+STR-PNA encompass respectively 9, 4 and 13 odorants.

Computational Chemistry

The computational analyses were conducted using Discovery Studio 2021, BIOVIA [23] running on Windows 10 for PC. The pharmacophores were generated using the HipHop/Catalyst protocol implemented as the “Common Feature Pharmacophore Generation” protocol in Discovery Studio 2021[22]. A maximum of 250 conformers were generated in a range of 0-20 kcal/mol [24]. The maximum number of generated hypotheses for each run was set to 10. We considered the following pharmacophoric features: hydrogen bond acceptors (HBA features), lipid hydrogen bond acceptors (HBA-lip features), hydrophobic regions (Hy features) and hydrophobic aliphatic regions (Hy-al features). Because the size of the odorants ($74 < MW < 260$), the parameter “Minimum Interfeature Distance” was decreased from to 0.5 Å. The minimum number of feature points were set to 2. All the molecules were regarded as “Active”. The maximum omitted features parameter (“MaxOmitFeat”) that specifies how many features the generated pharmacophore is allowed to miss for each molecule was set to 0 for all molecules (means that all features must map to this molecule).

The pharmacophores were compared using the “Pharmacophore Comparison” protocol, which allows the mapping and alignment of two pharmacophores; an RMSD value is reported for the matching pharmacophore features. The “Best Mapping Only” parameter was used for the comparisons. The terms “pharmacophore [model]” and “hypothesis” refer interchangeably to the assemblage of features required for the biological activity of the ligands oriented in 3D space [22].

Results and discussion

Most of the subsets are characterised by a specific number of acyclic or cyclic structures. The STR-PNA molecules are acyclic esters with saturated, branched and/or unsaturated chains of 7 or 8 carbons, except for ethyl cis-4-decenoate ($C_{12}H_{22}O_2$), which is larger than the other compounds. Conversely, all the STR-CAR molecules except one (2-Methyl-2-pentenoic-acid) have monocyclic structures derived from maltol or furan. It should be noted that four molecules in the STR-CAR subset are artificial maltol derivatives. Thus, the majority of STR-CAR odorants are furan derivatives. The list of STR-CAR and STR-PNA odorants is reported in Table 1.

Table 1. List of the 13 odorants STR-CAR and STR-PNA.

Odorant name	cas_no	nature	subset odor
Dimethylethoxyfuranone	65330-49-6	Nature identical	STR-CAR
Furaneol butyrate	114099-96-6	Nature identical	STR-CAR
Hydroxymethylfuranone	19322-27-1	Nature Identical	STR-CAR
Maltol	118-71-8	Nature Identical	STR-CAR
2-Methyl-2-pentenoic acid	3142-72-1	Nature Identical	STR-CAR
Ethyl maltol isobutyrate	852997-28-5	Artificial	STR-CAR
Ethyl maltol propionate		Artificial	STR-CAR
Maltol Propionate	68555-63-5	Artificial	STR-CAR
Maltyl 2-methylpropanoate	65416-14-0	Artificial	STR-CAR
Ethyl cis-4-decenoate	7367-84-2	Nature Identical	STR-PNA
Ethyl hexanoate	123-66-0	Nature Identical	STR-PNA
Isopropyl butyrate	638-11-9	Nature Identical	STR-PNA
Ethyl 2-methyl-3-pentenoate	1617-23-8	Artificial	STR-PNA

To examine the critical common features present in these subsets of odorants, we performed a pharmacophore approach using the HipHop/Catalyst protocol implemented in Biovia Discovery Studio [23]. Our study was carried out on the following training sets: STR-CAR (9 odorants), STR-PNA (4 odorants) and STR-CAR+STR-PNA (13 odorants).

All the models generated from the three subsets are made up of 2 HBA-lip features. However, STR-PNA model is the only one that has two Hydrophobic feature (HY) while there is only one for STR-CAR and STR-CAR+STR-PNA models.

The inter-features distances and the alignments of odorants of each subset on the corresponding generated pharmacophore and are displayed in Figure 1.

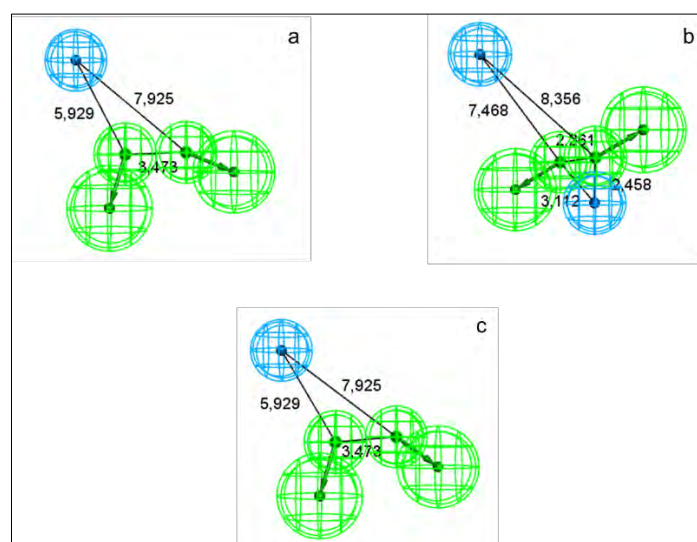


Figure 1: Inter-features distances in Å for the pharmacophores *Hypos_01* generated from the corresponding subsets: (a) STR-CAR; (b) STR-PNA; (c) STR-CAR+STR-PNA.

The distances between the features of *Hypo_01* generated from the STR-CAR and STR-CAR+STR-PNA are the same, and the two models are identical (RMSD=0).

Comparing the distances between features of the two models generated by STR-CAR and STR-PNA revealed a common distance close to 8 Å between the centres of at least one HY and one HBA. The pharmacophore comparison (Figure 2) reveals a satisfactory mapping of the two models (RMSD= 1.189394 Å).

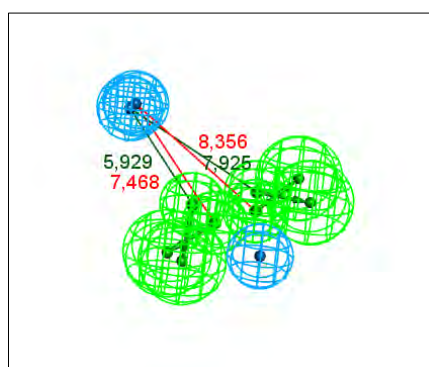


Figure 2: Pharmacophore mapping by pairs of the two pharmacophores models *Hypos_01*: STR-CAR and *Hypo1_STR-PNA*. The distances between *Hypo1_STR-CAR* features are shown in dark green and the distances between *Hypo1_STR-PNA* features are shown in red.

Conclusion

Despite the diversity of molecular structures of molecules STR-CAR and STR-PNA, the generated pharmacophores possess some common characteristics, especially a common distance close to 8 Å between the centres of at least one HY and one HBA, which allows a satisfactory overlap among the models.

These obtained results agree with the scheme of olfactory coding and with the assumption whereby molecules sharing the odours sharing a common odour note could recognise a common pattern of ORs.

This research was funded by Agence Nationale de la Recherche, ANR-18-CE21-0006 MULTIMIX, and INRAE-TRANSFORM department (ANS CAMELIA).

References

1. Buck L, Axel R. A Novel Multigene Family May Encode Odorant Receptors: A Molecular Basis for Odor Recognition. *Cell*. 1991;65(1):175-87.
2. Malnic B, Hirono J, Sato T, Buck LB. Combinatorial receptor codes for odors. *Cell*. 1999;96(5):713-23.
3. Block E. Molecular Basis of Mammalian Odor Discrimination: A Status Report. *J Agric Food Chem*. 2018;66(51):13346-66.
4. Genva M, Kemene TK, Deleu M, Lins L, Fauconnier ML. Is It Possible to Predict the Odor of a Molecule on the Basis of its Structure? *Int J Mol Sci*. 2019;20(12):3018.
5. Berglund B, Berglund U, Lindvall T. Psychological processing of odor mixtures. *Psychol Rev*. 1976;83(6): 432-41.
6. Singh V, Murphy NR, Balasubramanian V, Mainland JD. Competitive binding predicts nonlinear responses of olfactory receptors to complex mixtures. *Proc Natl Acad Sci U S A*. 2019;116(19):9598-603.
7. Thomas-Danguin T, Sinding C, Romagny S, El Mountassir F, Atanasova B, Le Berre E, et al. The perception of odor objects in everyday life: a review on the processing of odor mixtures. *Front Psychol*. 2014;5:504.
8. Wiltrout C, Dogra S, Linster C. Configurational and nonconfigurational interactions between odorants in binary mixtures. *Behav Neurosci*. 2003;117(2):236-45.
9. Pfister P, Smith BC, Evans BJ, Brann JH, Trimmer C, Sheikh M, et al. Odorant Receptor Inhibition Is Fundamental to Odor Encoding. *Curr Biol*. 2020;30(13):2574-87.
10. Xu L, Li WZ, Voleti V, Zou DJ, Hillman EMC, Firestein S. Widespread receptor-driven modulation in peripheral olfactory coding. *Science*. 2020;368(6487):eaaz5390.
11. McClintock TS, Wang Q, Sengoku T, Titlow WB, Breheny P. Mixture and Concentration Effects on Odorant Receptor Response Patterns In Vivo. *Chem Senses*. 2020;45(6):429-38.
12. Coureaud G, Thomas-Danguin T, Le Berre E, Schaal B. Perception of odor blending mixtures in the newborn rabbit. *Physiol Behav*. 2008;95(1-2):194-9.
13. Coureaud G, Thomas-Danguin T, Wilson DA, Ferreira G. Neonatal representation of odour objects: distinct memories of the whole and its parts. *Proc R Soc B-Biol Sci*. 2014;281(1789):20133319.
14. Le Berre E, Thomas-Danguin T, Beno N, Coureaud G, Etievant P, Prescott J. Perceptual processing strategy and exposure influence the perception of odor mixtures. *Chem Senses*. 2008;33(2):193-9.
15. Barkat S, Le Berre E, Coureaud G, Sicard G, Thomas-Danguin T. Perceptual Blending in Odor Mixtures Depends on the Nature of Odorants and Human Olfactory Expertise. *Chem Senses*. 2012;37(2):159-66.
16. Sinding C, Coureaud G, Bervialle B, Martin C, Schaal B, Thomas-Danguin T. Experience shapes our odor perception but depends on the initial perceptual processing of the stimulus. *Atten Percept Psychophys*. 2015;77(5):1794-806.
17. Leffingwell. *Flavor-Base* 9th Ed. 2013.
18. Tromelin A, Chabanet C, Audouze K, Koensgen F, Guichard E. Multivariate statistical analysis of a large odorants database aimed at revealing similarities and links between odorants and odors. *Flavour Frag J*. 2018;33(1):106-26.
19. Tromelin A, Koensgen F, Audouze K, Guichard E, Thomas-Danguin T. Exploring the Characteristics of an Aroma-Blending Mixture by Investigating the Network of Shared Odors and the Molecular Features of Their Related Odorants. *Molecules*. 2020;25(13):3032.
20. Furudono Y, Sone Y, Takizawa K, Hirono J, Sato T. Relationship between Peripheral Receptor Code and Perceived Odor Quality. *Chem Senses*. 2009;34(2):151-8.
21. Saito H, Chi Q, Zhuang H, Matsunami H, Mainland JD. Odor coding by a Mammalian receptor repertoire. *Sci Signal*. 2009;2(60):1-14.
22. Clement OO, Mehl A. HipHop: Pharmacophore Based on Multiple Common-Feature Alignments. In: Güner OF, editor. *Pharmacophore perception, Development and Use in Drug Design*. IUL Biotechnology Series. La Jolla: International University Line; 2000. p. 69-84.
23. Discovery Studio 2021, Dassault Systèmes Biovia Corp.
24. Smellie A, Teig SL, Tobwin P. Poling: Promoting Conformational Variation. *J Comput Chem*. 1995;16(2):171-87.

SketchOscent: towards a knowledge-based model and interactive visualisation of the odour space

ANGELIQUE VILLIÈRE¹, Catherine Fillonneau¹, Carole Prost¹ and Fabrice Guillet²

¹ ONIRIS - College of Veterinary Medicine and Food Science, GEPEA UMR CNRS 6144 MAPS2, Flavour group, Nantes, France; angelique.villiere@oniris-nantes.fr

² Polytech Nantes, graduate school of engineering of the University of Nantes, LS2N CNRS 6004, Nantes, France

Abstract

The representation of an odour space is a challenging issue for scientists and professionals working in odour-related activities. Many food and non-food sectors have created their own classification system and representations of the odorant space to manage objective communication about odours. More generally, many representations of the odorant space have been proposed. These initiatives turn the odorant space into easy-to-digest representations classifying hierarchically a restricted set of odorants in specific categories that provide a common frame of reference to professionals or sensory analysis judges. Nevertheless, the odour set is often restricted and these representations do not reflect the continuum of current odours which are not frozen in single section but on the contrary closely overlap. Thus, the related visualisations face with difficulties to represent such odour relationships.

This work based on knowledge graphs from semantic web aims to propose a readable, interactive and publicly available representation of the aroma space, dedicated to olfactory and sensory practices. This representation relies on a large set of odours and takes into account overlapping categories.

The knowledge-based model thus produced includes about 380 odours which are distributed in 20 main categories, which are decomposed into 117 subcategories. Seventy-seven odours and 26 categories obviously belong to multiple categories depending either on the multidimensional perception they are suggesting or on a conceptual positioning. The odour space is fully encoded into an rdf/owl Knowledge Graph, a semantic web standard language, which can be easily edited, stored, shared and requested. A hierarchical visual representation is derived to get a friendly and readable representation. The flexibility introduced by this representation enables to easily find out the relevant term(s) needed to describe an odorant perception. This approach, applied to food application, can be expanded to non-food sectors such as odour environment for example. *SketchOscent* is freely and publicly available at <https://oniris-polytech.univ-nantes.io/sketchoscent>.

Keywords: odour space representation, human knowledge-based model, semantic representation, interactive visualisation, olfaction.

Introduction

The representation of an odour space is a challenging issue for scientists and professionals working in odour-related activities. Many food sectors such as coffee, whisky, tea or honey have created their own aroma wheels to exchange and communicate easily about odours.

Many representations of the odorant space have been tempted through the 20th century, mainly based on 3 approaches that rely on features of 1) the sensory organ, 2) the sensory stimulus and 3) the sensory percept [1, 2]. Considering the 320 odour receptor types discovered in humans, the first approach has been largely discarded to establish a simple odour classification based on relations between odour classes and receptor types. Similarly, if the chemical structure of an odorant strongly determines its perceived quality, all single measures have failed to predict or explain its odour perception. Thus, structure-odour relationships approaches failed to propose basic classifications. From the first model based on olfactory percepts proposed by Henning in 1916, many models have followed this approach, assuming that odours can be located in a n-dimensional space where their relative position reflects their similarity [1, 2]. However, the methods of analysis used to exploit the data sets are often inadequate to achieve a comprehensive and faithful projection of the odour space. As supposed by Chastrette [1], the olfactory space has probably a weak structure, a high dimensionality (with a signification of that dimensions that remains unclear), with classes of odours not sharply delineated. These outcomes should be linked to the subjective character of the data handled through the perception of the odorants, their conceptualisation and verbalisation [2]. Thus, none of the different models proposed elicit unanimity and the related visualisations face with difficulties to represent such odour relationships and fail to deserve more general fields of sensory practises.

Some works dealing with representation of the odour space, address the challenging issue of the visualisation of this odour space and of its categorisation/classification structure.

In their seminal work about the Field of Odour [3], Jaubert et al. (1995) proposed a visualisation map into a *half wheel* of 52 odours among 12 categories without hierarchy, resulting from the analysis of 1400 aroma

compounds. In the context of urban odours, *SensoryMap* [4] by McLean (2014) organised the odours into a bipartite graph with 2 wheels/rings: the inner ring enumerates 47 categories without hierarchy grouped into 4 families, and the outer ring 355 odours. Another wheel-based visualisation, *Flavor Network* [5], is introduced by Ahn et al. (2011) in order to achieve food pairing for cooking recipes. The visualisation is a single ring of 936 odours grouped into 34 categories without hierarchy. A pairwise relationship between odours is available from co-occurrence on the same compounds. The visualisation is interactive: when clicking on one odour in the ring, the edges with all the co-occurring odours are drawn. In the frame of perfume industry, Baud (2019) designed *ScentTree* [6], a tree like zooming visualisation composed of a hierarchy of 86 categories organised into 6 depth layers starting from 16 main categories, where 552 raw materials used in perfumery are categorised in tree leaves. The category hierarchy was built by a group of experts in fragrance. The visualisation is available online on the web but it offers a limited interactivity by zooming. Liu et al. (2019) visualise a hierarchy for odours with a *circular dendrogram* resulting from an AHC [7]. They limit the representation to 100 odours, and they show 9 main clusters for candidate categories to be identified.

Most of these visualisations are data based and use wheels of odours, where the odour set is restricted and without a detailed hierarchy, restricted to a single layer of categories. They are resulting from a data analysis for classification or clustering, and consist in static map drawings without interaction abilities, and their readability strongly decreases with the increasing of the number of odours. ScentTree approach is the most interesting for a meaningful odour space representation, because it delivers a hierarchical organisation of the odours into categories from the most general to the most specific based on human expertise, and it is available online on webpage interface. Unfortunately, it is very specific to perfume industry, the number of odours is restricted, it shows a readability issue due to a “lost in maze” effect when zooming in, and the interactivity is limited to zooming in/out.

In this context, this work aimed to propose *SketchOscent*, a new visual and interactive representation of the food-related odour space, dedicated to olfactory and sensory practices, relying on a large set of odours, that takes into account the continuous and overlapping nature of the odour space and in which odours can be described by different levels of accuracy and related to several odour categories considering either a perceptual or a conceptual approach. On the contrary of existing representations for classification/categorisation of odours which are mainly *data-based*, our approach proposes both a novel *human knowledge-based* representation in a *Knowledge Graph* delivered by domain expert working in odour-related field, and an adapted visualisation which is readable, interactive and publicly available.

Experimental

Data sources

Data from different sources were extracted and gathered to set up a list of odorant descriptors.

Among the numerous sources that catalogued description of odorant materials, we referred to the olfactory description of molecules referenced on “The good scents company” [8] and “Flavornet” [9] websites databases. These databases were selected owing to the accessibility of the data, their food or natural constituents relative content and a sufficiently high number of descriptors (872 and 197 respectively) referring to a large number of odorants (2360 and 660 respectively), which enable to consider a large spectrum of the food-related odour space. Quality description of odorants is obtained from the published literature on odorants detected by quantitative GC-O for the Flavornet dataset while it results from expert’s description for that found on The Good Scents Company dataset.

Modelling and conceptualisation

The process was challenged by domain experts in olfactive description and olfactometry. Their tasks consisted in firstly modelling a semantic hierarchy of categories/classes of odours (a partial order for generalisation/specialisation relationships between categories which are odorant descriptors as well), secondly the classification/categorisation of the odorant descriptors into the correct categories. These tasks were facilitated both by the list of all available odorant descriptors (vocabulary) and by a set of questionnaires for odour pairing to check the hierarchy and the overlapping of odours. These tasks resulted in a *Knowledge Graph* representation where the vertices are odorant descriptors and the arcs are the categorisation relationships between odorant descriptors. Technically, the representation is implemented in RDF semantic web language which can be easily edited, stored, requested and shared as linked open data.

Interactive visualisation

The representation of the odour space is based on 6 principles: (1) *completeness* - large amount of odours and relationships; (2) *meaningfulness* - human semantic map; (3) *structuration* - hierarchy of categories, odour pairwise relationships, (4) *readability* - wheel-based and hierarchical graph layout, mental map preservation, (5)

selecting and focusing on the partial subgraph of the hierarchical neighbourhood of one vertex/odour; and (5) Information for delivering more details about an odour/vertex such as more general odours, more specific ones, and a link toward the odours and raw materials in “The Good Scent Company” website. In all cases the global layout of the vertices is kept in order to preserve mental map of the user.

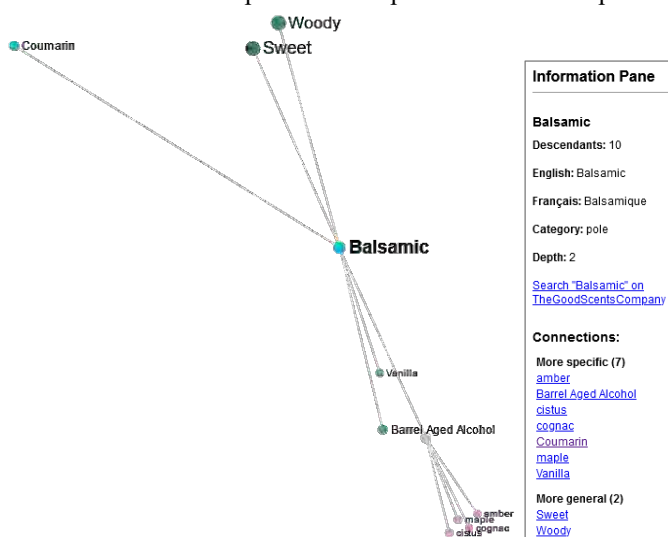


Figure 2: Local view of neighbourhood after clicking on the Balsamic vertex.

Conclusion

SketchOscent implements an original visual, interactive and hierarchical Knowledge Graph of the odour space founded on human domain knowledge. It meets the expectations of users for understanding and reasoning about odours and stretches boundaries of existing representations in terms of completeness, meaningfulness, structuration, readability, interactivity and availability. The flexibility introduced by this representation enables to easily find out the relevant term(s) needed to describe an odorant perception.

Perspectives for SketchOscent improvement consist in the possibility to extract partial subgraphs for food aroma subdomains (wine, cheese, meat, vegetables...), to change the colour assignment to show the root category belongings, mixtures and the overlapping of odours, or to display the relationships for co-occurrence of odours on same odorant materials.

This approach, applied to food application, can be expanded to non-food sectors such as odour environment for example.

SketchOscent is available at <https://oniris-polytech.univ-nantes.io/sketchoscent>

The authors gratefully acknowledge the Polytech Nantes students who actively participated in the SketchOscent implementation, especially Linaël Batard Paboïs, Paul Blanloeil, Lucie Cherigny, Hugo Ricarrere, Efflam Simon, Emilien Simon.

References

1. Chastrette M. Classification of Odors and Structure–OdorRelationships. In: Olfaction, Taste, and Cognition. Cambridge University Press; 2002. p. 100-16.
2. Kaeppler K, Mueller F. Odor Classification: A Review of Factors Influencing Perception-Based Odor Arrangements. Chem Senses. 2013;38(3):189-209.
3. Jaubert J-N, Tapiero C, Dore J-C. The Field of Odors: Toward a Universal Language for Odor Relationships. Perfum Flavorist. 1995;20:1-16.
4. Comparative Smell Vocabularies:| Sensory Maps. <https://sensorymaps.com/portfolio/comparative-smell-vocabularies/>
5. Ahn Y-Y, Ahnert SE, Bagrow JP, Barabási A-L. Flavor network and the principles of food pairing. Sci Rep. 2011;1(1):196.
6. Baud M. ScenTree - Classification innovante des ingrédients parfum. <https://www.scentree.co/>
7. Liu C, Shang L, Hayashi K. Co-occurrence-based clustering of odor descriptors for predicting structure-odor relationship. In: 2019 IEEE International Symposium on Olfaction and Electronic Nose (ISOEN). 2019. p. 1-4.
8. The Good Scents Company - Flavor, Fragrance, Food and Cosmetics Ingredients information. The Good Scents Company. <http://www.thegoodscentscompany.com/>
9. Arn H., Acree T. E. Flavornet: a database of aroma compounds based on odor potency in natural products. Developments in food science 40; 1998.p. 27-28.

Coffee sensory properties: a complementary data fusion to simulate odour and taste integration by instrumental approach. Possibilities and limits

GIULIA STROCCHI¹, Erica Liberto¹, Gloria Pellegrino², Manuela R. Ruosi² and Carlo Bicchi¹

¹ *Dipartimento di Scienza e Tecnologia del Farmaco, Università degli Studi di Torino, Italy, giulia.strocchi@edu.unito.it*

² *Luigi Lavazza S.p.A., Strada Settimo 410, Torino, Italy*

Abstract

Coffee cupping includes both aroma and taste, and its evaluation considers several different attributes simultaneously to define flavour quality therefore requiring complementary data from aroma and taste. This study investigates the potential and limits of a data-driven approach to describe the sensory quality of coffee using complementary analytical techniques usually available in routinely quality control laboratory. Coffee flavour chemical data from 155 samples were obtained by analysing volatile (HS-SPME-GC-MS), and non-volatile (LC-UV/DAD) fractions, as well as from sensory data. Chemometric tools were used to explore the data sets, select relevant features, predict sensory scores and investigate the networks between features. A comparison of the Q model parameter and RMSEP highlights the variable influence that the non-volatile fraction has on prediction, showing that it has a higher impact on describing Acid, Bitter and Woody notes than on Flowery and Fruity. The data fusion emphasised the aroma contribution to driving sensory perceptions, although the correlative networks highlighted from the volatile and non-volatile data deserves a thorough investigation to verify the potential of odour-taste integration.

Keywords: coffee, LC-UV, HS-SPME-GC-MS, chemometrics, sensory data

Introduction

The characteristics and sensory properties of coffee flavour are unique and of high appeal for consumers [1]. The pleasure system includes different brain areas that are linked to emotional, memory-related, motivational and linguistic aspects of food evaluation that are, in turn, mediated by several sensory modalities and sub-modalities that contribute to flavour perception. The sensory panel therefore plays a fundamental role in this respect. The cupping protocol is however time-consuming, requires properly trained and aligned professional panellists, and may suffer from subjectivity. The ever-increasing consumption of coffee means that there is a need for analytical techniques to support the sensory panel in routine quality controls (QC) or formulation and design of new blends. Several analytical approaches and/or integrated strategies attempted, over the years, to combine the chemical composition of a product with its flavour profile [2, 3]; however, to date, they have not replaced a sensory panel evaluation, especially in regulatory contexts where sensory quality concurs to define labelling (e.g., extra-virgin olive oil) or a commercial value (e.g., coffee).

Issues related to their applicability might therefore be related to the attempt of reducing the extremely complex phenomenon of sensory perception, triggered by multiple ligands (volatiles and non-volatiles) and modulated by their cross-modal interactions, to a few correlations (e.g., reductionist approach) or to the adoption of spectroscopic/spectrometric technologies that have limited or not univocal “molecular resolution” [3]. Many research provides proof-of-evidence on the potential of applying omics workflows and concepts to identify “features patterns” (i.e. patterns of potential informative components) with high correlation to a biological output [2]. Moreover, machine learning applied to fingerprinting and/or profiling technologies highlighted strong relationships and networking between aroma and flavour. In this complex and intriguing scenario, starting by preliminary results obtained by applying omics principles to the modelling of specific coffee aroma notes, this study is a step forward in evaluating chromatographic fingerprints of volatile and non-volatile components as diagnostic signatures with strong correlation with selected taste and aroma attributes, i.e. bitterness, acidity, flowery, fruity, woody, and spicy. Moreover, fingerprinting is combined to machine learning, by partial least squares (PLS) algorithms, and extended to a comprehensive data matrix obtained by combining together peak features information deriving from volatiles and non-volatiles. PLS drives features selection toward those informative patterns capable of predicting sensory attributes and explaining correlations between them.

Experimental

Samples, consisting of roasted and ground coffees to suit a coffee-filter machine, were kindly supplied over a period of 24 months by Lavazza Spa (Turin, Italy). Mono-origin coffees from different countries were selected for

their distinctive and peculiar sensory notes, they accounted for a total of 155 samples belonging to *Coffea arabica* L. and *Coffea canephora* Pierre ex- A. Froehner species. Roasting degree was set at 55°Nh to be in line with the international standardization protocol for cupping (SCA protocol). The coffee brew for cupping and analysis was prepared from 18 g of coffee powder and 300 mL of water at 88-94°C with a commercially available coffee filter machine Xlong TSK-197A (Lavazza Spa, Turin, Italy).

Volatile fingerprints: HS-SPME GC-MS set up

Volatile fraction was evaluated by sampling 1.50 g of coffee powder by HS-SPME with a Polydimethylsiloxane/Divinylbenzene (PDMS/DVB) fibre of df 65 µm and 1 cm length from Merck (Bellefonte, PA, USA) at 50°C for 40 minutes, shaken at a constant speed. The internal standard was pre-loaded onto the fiber by sampling 5 µL of a 1000 mg/L solution of n-C13 in dibutylphthalate (DBP) at 50°C for 20 min a constant speed. Analysis was performed with a Shimadzu QP2010 GC-MS system equipped with Shimadzu GC-MS Solution 2.51 software (Shimadzu, Milan, Italy). Chromatographic conditions: T inj.: 250°C; inj. mode: splitless; carrier gas: helium at a flow rate of 1 mL/min. Capillary column: SGE SolGelwax (100% polyethylene glycol) 30 m x 0.25 mm dc x 0.25 µm df (Trajan Scientific and Medical, Melbourne, Australia). Temp. program, from 40°C (1 min) to 200°C at 3°C/min, then to 250°C (5 min) at 10°C/min. MS conditions: ionization mode: EI (70 eV); ion source: 200°C; transfer line: 250°C. Scan range: 35-350 m/z; scan speed 666 amu/sec.

Non-volatile fingerprints: LC-UV/DAD settings

Two millilitres of brew were filtered using a 0.2 µm 13 mm nylon membrane syringe filter (Agilent, Little Falls, DE, USA) and 20 µL were directly injected for LC-UV/DAD analysis. The non-volatile fraction was profiled by Agilent (model 1200), equipped with a Spectra System UV Diode Array Detector 1100 series (Agilent, Little Falls, DE, USA). Data acquisition were performed on Chemstation LC 3D software Rev 3.03 01-SR1 (Agilent, Little Falls, USA). The LC column was a Platinum EPS C18 (250×4.6 mm, 80A, 4 µm) (Alltech, Deerfield, USA).

Operation conditions: injection volume 20 µL; detection wavelength 325 nm for cinnamic and chlorogenic acids (monomers and dimers) and 276 nm for caffeine and trigonelline; mobile phase: A: water/formic acid (999:1, v/v) B: acetonitrile/formic acid (999:1, v/v); flow rate, 1.0 mL/min. The gradient program was as follows: 15% B for 7 min, 15-55% B in 20 min, 55-100% B in 25 min, 100% B for 2 min. Before re-injection, the LC system was stabilised for at least 5 min. Compounds identification, or tentative identification, was carried out on a LC-MS/MS Shimadzu Nexera X2 system equipped with a photodiode detector SPD-M20A connected, in series, to a triple quadrupole Shimadzu LCMS-8040 system equipped with an electrospray ionization (ESI) source (Shimadzu, Dusseldorf Germany).

Sensory analysis

Coffee sensory properties were evaluated by an external trained panel of six assessors both by sniffing the powder and the brew obtained using the filter method, and by tasting aspiring the beverage into the mouth. This multistep protocol allows panellists to evaluate different attributes, with some being more closely linked to aroma (odour notes like *flowery*, *fruity*, *woody* and *spicy*) and others more closely to taste (*acidity* and *bitterness*). The intensities of each attribute were evaluated simultaneously on a scale from 0 to 10.

Data elaboration

Data sets (Sensory scores, GC-MS and LC-UV/DAD fingerprints) were explored by Principal Component Analysis (PCA) followed by Multiple Factorial Analysis (MFA). Features selection for each data set, related to the sensory note, was performed using VIP>1 (variable importance in projection) from Partial Least Square-Discriminant Analysis (PLS-DA) on samples that were suitable to minimise and maximise the sensory notes expression. PLS regression was carried out on single perception modalities (i.e., aroma or taste) or flavour in toto by combining the two data set (i.e., volatiles and non-volatiles fingerprints). Data elaboration was performed using XLSTAT (version 2020.1.3 - copyright Addinsoft 2020). Raw analytical data representing the chromatographic fingerprints of volatiles and non-volatiles were pre-processed, as shown in the work-flow of (Figure 1A), via the temporal alignment of chromatograms and background noise subtraction. This pre-processing was made with Pirouette software ver. 4.5 (Infometrix, Inc., Bothell, WA, USA).

Results and discussion

Data exploration was, at first, performed using PCA on volatiles and non-volatile fingerprint features, treated independently. MFA was then used to compare the three different data matrices: chemical fingerprints (volatiles and non-volatiles) and the sensory data related to the sensory notes considered (Figure 1B) which shows how volatiles and non-volatiles for the different samples have quite similar branches, in a filtered group of samples (by origins) for better visualization, suggesting that there is a possible relationship between the different data matrices.

Bitter and acid notes are typically perceived as taste attributes. Bitter was here chosen as model note to explore how the volatile, non-volatile fraction or combined data, might correctly describe the bitter-score in prediction.

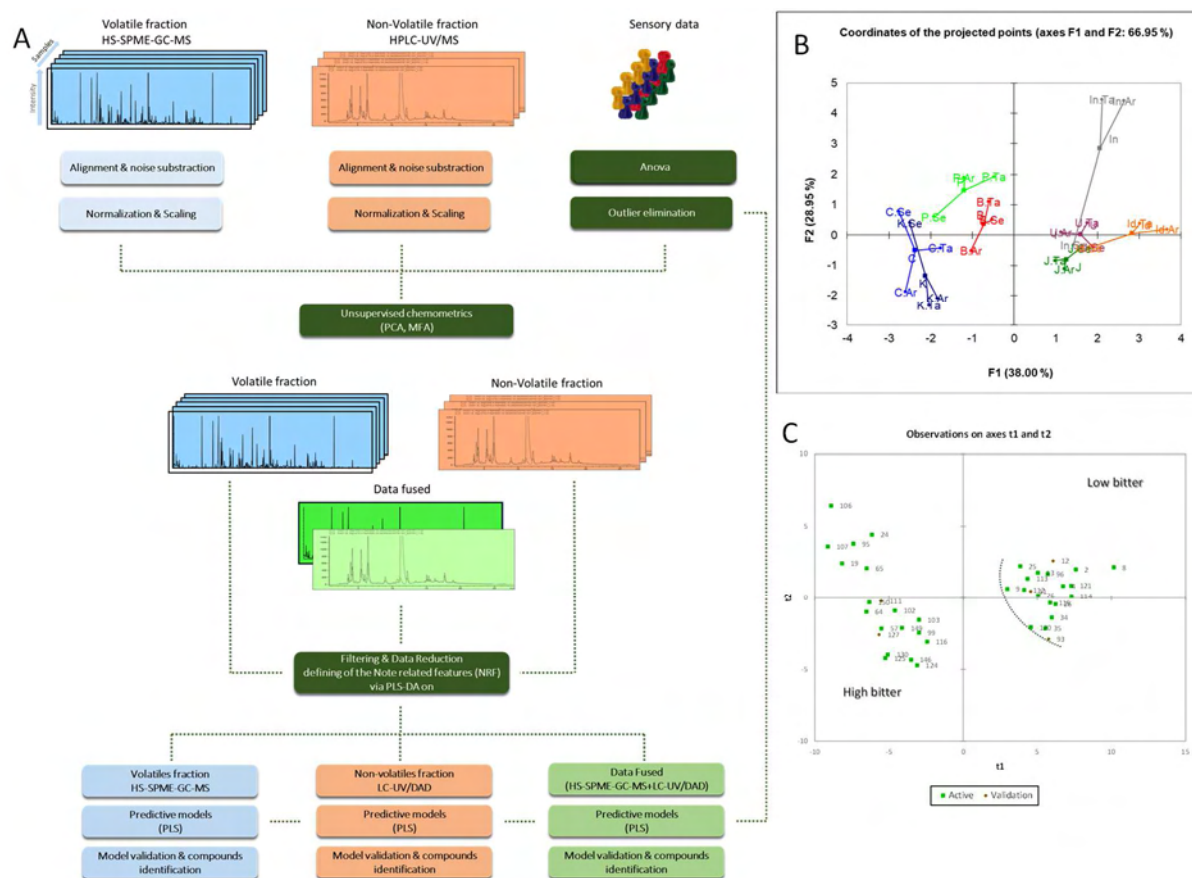


Figure 1: A) Instrumental and sensory data elaboration Work-flows, B) Coordinates of projection points from MFA. Legend: B, C, J, U, In, Id, K, P indicate coffee origins; Se: sensory data; Ar: aroma data (volatile fraction by HS-SPME-GC-MS); Ta: taste data (non-volatile fraction by LC-UV/DAD). C) PLS-DA for bitter feature selection.

The objective is to understand whether a traditional taste attribute can be (more) correctly described by combining chemical data from both taste-active and odour-active features. The Bitter note was also taken as a test bench because of its relevance in the hedonic profile of the coffee brew. The adopted strategy was then also applied to all other sensory notes considered. The features that were highly correlated to the expression of high and low Bitter notes were first selected by PLS-DA. This step was applied to volatile and non-volatile data sets separately, and later, to the fused data matrix. The values for the Variable Impact on Projections (VIP) were used as a filter parameter, cut-off of 1 and a non-zero standard deviation (SD) were used to select features (Figure 1 C).

The prediction models were then developed by applying a PLS regression algorithm to the selected Bitter-related features. 138 samples were used to build up the regression model, 20 of them were randomly employed as a validation set and 13 were excluded from the training set and adopted as an external test set.

Our hypothesis was that the information carried by the different analytical instrumentations was complementary, the predictive performance of the model would have improved. Performance data reported in the histogram suggest that the inclusion of the taste data to those obtained from the volatile fraction does not provide a relevant enhancement of the performances as we can see from the average error (SDEC in fitting and SDEP prediction) on the modelled response. A comparison of the Q2 model parameter within the other sensory notes under investigation highlights a different contribution of this taste fraction in their description; more important in the case of Acid, Bitter, Woody notes that for flowery and fruity notes.

The volatile fraction provides information that is useful in characterising the bitter-note signature in the analysed samples. Further MS investigation into Bitter-related features has led to the identification of several aroma-active compounds, some of them are key-aroma coffee compounds. Interestingly, these compounds are described as earthy, roasty, burnt and phenolic, but none of them is directly related to bitterness. Some researchers observed a relationship between Bitter taste perception and a pattern of non-Bitter-eliciting odorants, such as:

ethyl-2-methyl- and 2-ethylbutanoate, γ -decalactone, furfural and pentanoic acid, stating that odorants that enhance a target-taste perception may be exploited to modulate the overall taste perception in foods and beverages [4, 5].

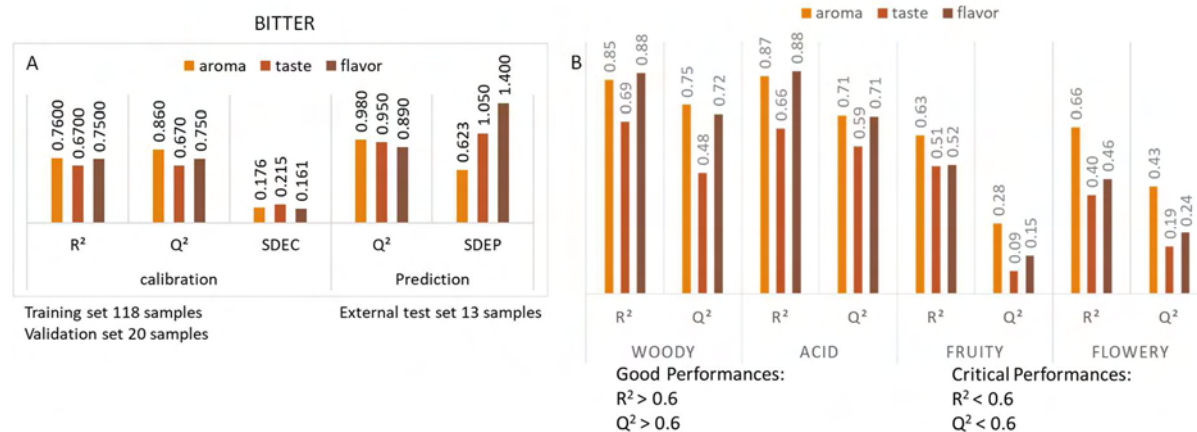


Figure 2: A) PLS-regression models parameter for bitter, in validation and prediction, that were obtained using aroma and taste, singularly, and data fusion (flavour: volatiles + non-volatiles), B) comparison of the PLS parameters for four of the investigated notes. Models are built with specific selected features that were derived from PLS-DA analysis carried out on each sensory attribute.

Moreover, although to a different extent, in this work most of the identified tastants are positively correlated with volatiles related to *Bitter*. As flavour perception derives from the interaction between aroma and taste, the combination of the information provided by the two different fractions was expected to increase the performance of the predictive model.

The performance of the fused data matrix regression model was in line with those obtained using fingerprint data from volatile and non-volatile models. However, data fusion did not improve the overall prediction quality of the model (Q^2 figure 2A). Although the coffee non-volatile fraction analysed is not fully representative, nevertheless the considered non-volatile markers are well-established sensory quality marker in routine controls. The volatile fraction possibly has an actual influence in driving the description of this sensory attribute. This possibility, together with the correlation pathways between volatiles and non-volatiles, deserves much more in-depth investigation.

Conclusion

One major barrier to accurate predictions of flavour is due to the multi-dimensionality of the chemical stimuli involved in flavour perception. The fact of considering as many compounds as possible in the models takes care of possible correlations within and across stimuli, generally not accounted for by traditional research methods. There is an actual contribution to the multi-modal description for several attributes but the power in the definition of the sensory notes is negligible.

These observations, together with the good results obtained in the definition of *Bitter* and *Acid* notes (considered as “typical taste notes”) from the volatile data, make it possible to hypothesise that the analysis of the volatile fraction may be sufficiently representative to delineate coffee flavour, and provide reliable chemical fingerprints that can be associated to some sensory notes, including those typical of taste. Moreover, the correlative results highlighted from the volatile – non-volatile fused data deserves a thorough investigation to verify the potential of odour-taste integration.

References

1. Prescott J. Multisensory Processes in Flavour Perception and Their Influence on Food Choice. *Curr Opin Food Sci.* 2015;3:47-52.
2. Charve J. et al. Evaluation of instrumental methods for the untargeted analysis of chemical stimuli of orange juice flavor. *Flavour Fragr J.* 2011;26:429-440.
3. Lindinger C. et al. When Machine Tastes Coffee: Instrumental Approach To Predict the Sensory Profile of Espresso Coffee *Anal Chem.* 2008;80:1574-1581.
4. Thomas-Danguin, T.; et al. Cross-Modal Interactions as a Strategy to Enhance Salty Taste and to Maintain Liking of Low-Salt Food: A Review. *Food Funct.* 2019;10:5269.
5. Guichard, E. et al.. Multivariate Statistical Analysis and Odor-Taste Network To Reveal Odor-Taste Associations. *J Agric Food Chem.* 2020;68(38):10318-10328.

Flavour profiling and sensory acceptance of *Premna cordifolia* Roxb. functional drink: comparison of different sample preparation methods

Farah Nini Liyana Mohamad Zuhaidi and NURUL HANISAH JUHARI

Department of Food Service and Management, Faculty of Food Science and Technology, Universiti Putra Malaysia, 43400 UPM Serdang, Selangor, Malaysia. n_hanisah@upm.edu.my

Abstract

Premna cordifolia Roxb. is one of the popular herbs consumed by the Malaysian community. This herb is cherished for its phytochemicals and antioxidant contents that contribute to many health benefits. The aroma compounds responsible for this *P. cordifolia* functional drink were evaluated by solid-phase micro-extraction (SPME). In contrast, a hedonic test was carried out to assess the sensory acceptability towards the drink. Results revealed that *P. cordifolia* functional drink prepared using WF_2 was the most accepted by consumers. Overall, volatile analysis exhibited 35 compounds. Specifically, for WF_2 *P. cordifolia* functional drink contained higher alcohol compounds comprising (*E*)-3-hexen-1-ol, 1-hexanol, 1-octen-3-ol, 2-ethyl-1-hexanol, and 1-nonanol. These compounds contributed to green, herbal, fresh, and earthy odour notes. Besides colour, aroma, and texture, panellists preferred *P. cordifolia* functional drink prepared by WF_2 and gave a high mean score in taste, bitterness, aftertaste, and overall acceptability. Therefore, it was concluded that WF_2 was the most appropriate sample preparation to produce *P. cordifolia* functional drink.

Keywords: Functional drink, *Premna cordifolia*, sensory acceptability, SPME, volatiles

Introduction

World tea production reached almost 4.68 million metric tons of tea in 2002 [1]. It is the second most common beverage globally. It constitutes a rich source of polyphenolic flavonoids and is consumed mainly in East and Southeast Asia, especially China, Japan, and Taiwan. The beneficial health properties of teas have raised their popularity as a functional food or beverage [2]. Various herbs can be used to produce tea or a functional drink. One of them is *Premna cordifolia* Roxb, locally known as ‘ulam bebuas’ in Malaysia, an edible plant, and is typically eaten raw or as one ingredient in cooking [3]. *P. cordifolia* functional drink production process is not as complicated as other tea products, but finding a proper standard to brew it is challenging. It affects the taste, aroma, and acceptability of the drink prepared. In addition, there is no established form of sample preparation available to produce *P. cordifolia* functional drink. Therefore, this study aims to determine the effects of functional drinks prepared from *P. cordifolia* leaves using different sample preparation methods followed by the determination of flavour profiling and sensory acceptance towards the drink. To our knowledge, volatile compounds present in functional drinks of *P. cordifolia* need still to be characterised.

Experimental

Fresh *P. cordifolia* (obtained from the Traditional Vegetables Garden, MARDI Herbarium Serdang, Selangor, Malaysia) was chosen for the study. Samples used were harvested at a fully mature stage, and characterisation of the accessions of the specimens was verified with MARDI Herbarium Serdang, Selangor, Malaysia.

Sample preparation

Functional drinks were prepared by six different methods based on the standard procedure of herbal tea preparation by the Small Medium Enterprise (SME) industry in Malaysia and analysed in duplicate as below:

1% of whole fresh leaves (WF_1): 10g of whole fresh leaves were boiled in 1L of boiling water for 5 min, cooled, and sampled by SPME.

2% of whole fresh leaves (WF_2): 20g of whole fresh leaves were boiled in 1L of boiling water for 5 min, cooled, and sampled by SPME.

1% of fresh ground leaves (FG_1): 10g of milled fresh leaves were boiled in 1L of boiling water for 5 min, cooled, and sampled by SPME.

2% of fresh ground leaves (FG_2): 20g of milled fresh leaves were boiled in 1L of boiling water for 5 min, cooled, and sampled by SPME.

1% of sun-dried ground leaves (DG_1): 10g of milled sun-dried (<40°C for 20-24 h until moisture content 8%) leaves were boiled in 1L of boiling water for 5 min, cooled and sampled by SPME.

2% of sun-dried ground leaves (DG_2): 20g of milled sun-dried (<40°C for 20-24 h until moisture content 8%) leaves were boiled in 1L of boiling water for 5 min, cooled and sampled by SPME.

Solid-phase micro-extraction (SPME) and gas chromatography-mass spectrometry (GC-MS)

A sample (3 ml) of *P. cordifolia* was placed in a 20 ml vial. NaCl (26%) was added to the sample matrix to decrease the solubility of volatile compounds in the water phase and give the salting-out effect. The sample vials were sealed by an air-tight Teflon septum and an aluminium cap and incubated at 40 °C for 60 min in a water bath using a magnetic stirrer (Advantec TBS181SB). The SPME fibre, coated with 2 cm 50/30 µm divinylbenzene (DVB)/carboxen/polydimethylsiloxane (PDMS), was manually inserted into the headspace of the sample vial for 60 min. Desorption was finally performed by exposing the fibre for 10 min in the injection port of the gas chromatograph. The extraction process was conducted in duplicate for each sample with a gap of fibre condition between each consecutive sample. Volatiles were determined as described by Farag *et al.* [4]. Volatile components were identified by probability-based matching of their mass spectra with those of a commercial database (NIST 17.L and WILEY library database). The software program, MSDChemstation (Version E.02 GC-MSD 5975C, Agilent Technologies, Palo Alto, California), was used for data analysis. The results from the volatile analysis are presented as peak area. Retention indices were calculated after analysis under the same conditions of a n-alkane series (C8-C20 and C21-C40).

Sensory analyses

Fifty untrained panellists carried out a sensory evaluation in duplicate sessions. An aliquot of 20 ml of each warm drink was served in the black colour cups one at a time. All samples were labelled with a three-digit random number. The drinks were evaluated for their colour of infusion, aroma, texture (concentrated/diluted), taste, bitterness, astringency, aftertaste, and overall acceptability. The panellists were asked to rank each attribute of functional drinks based on 9- points hedonic scale given with '9' for like extremely and '1' for dislike extremely.

Statistical analysis

All the data obtained from analyses were analysed using one-way Analysis of Variance (ANOVA) using Minitab 14 software. Tukey's HSD test was used for multiple comparisons as carried out to determine the sources of variations.

Results and discussion

A total of 35 compounds were identified, including acids (4), alcohols (8), aldehydes (6), esters (2), terpenes (3), ketones (7), phenols (2), and others (3). The total number of volatile compounds for each class found is shown in Figure 1.

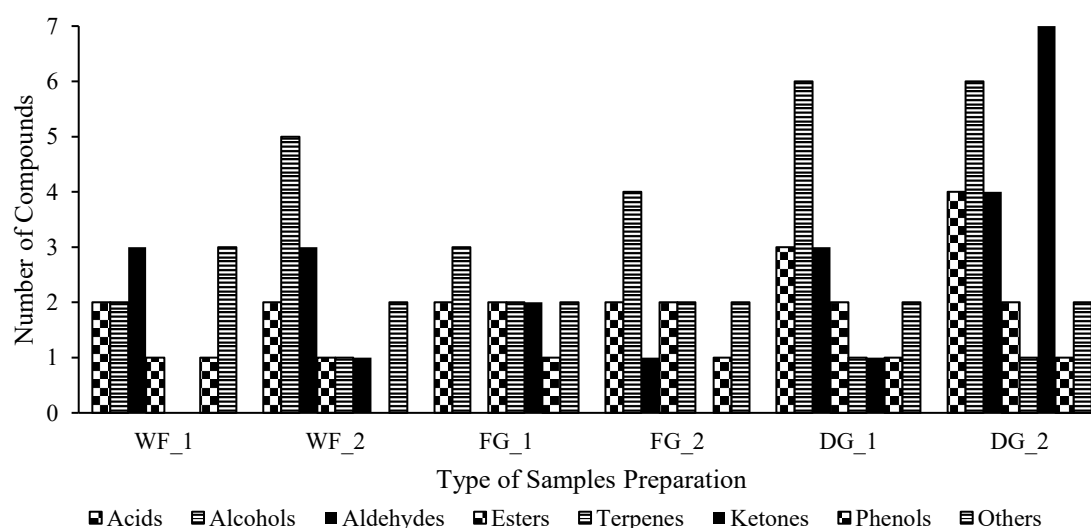


Figure 1: Class of volatile compounds in *P. cordifolia* functional drinks sampled by SPME and GC-MS.

Volatiles are vital contributors to tea aroma. Each type of tea has its typical aroma; it has specific aroma-active volatiles. The differences among six *P. cordifolia* functional drinks were observed (Figure 1). This might result from different sample preparation techniques used to produce the drink, whole fresh, fresh ground and sun-dried ground. In this study, four acids were detected in six *P. cordifolia* functional drinks: nonanoic acid, dodecanoic acid, tetradecanoic acid, and n-hexadecanoic acid. Nonanoic acid, dodecanoic acid, tetradecanoic acid have previously been reported in green tea [5-6]. Acids are responsible for fatty, sweaty and waxy odour. Eight alcohols

were identified, including (*Z*)-3-hexen-1-ol, (*E*)-3-hexen-1-ol, 1-hexanol, 1-octen-3-ol, 2-ethyl-1-hexanol, benzyl alcohol, phenylethyl alcohol and 1-nonanol. Most of these compounds have been detected in various type of tea [5-7]. 1-Octen-3-ol is the most abundant alcohol identified in all six *P. cordifolia* functional drink, which imparts mushroom, earthy, green and herbal notes. Among all WF_2, DG_1 and DG_2 contain a higher number of alcohol compounds.

The third highest class of compounds in *P. cordifolia* functional drinks is aldehydes, consisting of hexanal, benzaldehyde, nonanal, decanal, β -cyclocitral and *p*-anisaldehyde. However, the only hexanal, benzaldehyde and nonanal have been reported previously in green tea infusion [5], brewed green teas [6] and black tea produced in Turkey [7]. Hexanal gives a green, fresh and grassy odour, while benzaldehyde possesses almond, burnt sugar and fruity odour. Nonanal responsible for fatty, citrus and green in green tea. These aldehydes are considered as lipid autoxidation products during manufacture [8], which involved some processes such as milling, boiling and also sun-drying. FG_1 did not contain any aldehyde, whereas DG_2 contained four aldehydic compounds (Figure 1). Two esters, namely methyl salicylate and 2,2,4-Trimethyl-1,3-pentanediol diisobutyrate were detected in *P. cordifolia* functional drinks. Methyl salicylate exhibited minty, peppermint-like and sweet notes. Three terpenes were identified, among which linalool has previously been identified in other types of tea with floral, sweet and flowery odour [5-7]. In the present study, seven ketones (i.e., 2-undecanone, α -ionone, *trans*-geranyl acetone, *trans*- β -ionone, benzophenone, 2-pentadecanone, and 7,9-di-tert-butyl-1-oxaspiro(4,5)deca-6,9-diene-2,8-dione) were detected. WF_1 contained neither terpene nor ketone compounds, whereas DG_2 contained the highest number of ketones among others. It is assumed that the sun-drying process contributes to the formation of ketones. However, Alasavar et al. [7] also supported that ketones may be produced by thermal oxidation/degradation of polyunsaturated fatty acids, amino acid degradation, or microbial spoilage. Two phenolic compounds were found in *P. cordifolia* functional drinks, for instance, eugenol (clove, spicy, woody, sweet odour) and 2,4-di-tert-butylphenol (phenolic odour).

Figure 2 shows the mean score of sensory acceptability of *P. cordifolia* functional drinks prepared from different sample preparation technique. A drink made from DG_2 had the highest ($p > 0.05$) mean score for colour acceptability (6.05 ± 0.33), while a drink made from WF_1 obtained the lowest score for colour acceptability (4.67 ± 1.01). The drinks made from the whole fresh leaves (WF_1 and WF_2) were the lightest, followed by sun-dried ground leaves (DG_1 and DG_2) and fresh ground leaves (FG_1 and FG_2) were most to dark green colour. A similar result was observed in a study on tea bioactivity and therapeutic potential [9]. They also reported chlorophyll A (green) and B (yellow-green) as the main contributing factors to the green tea colour. In terms of aroma attribute, drink from DG_2 had the highest ($p > 0.05$) score (5.28 ± 0.11), whereas FG_2 had the lowest score (4.56 ± 0.14). The different aroma acceptability by panellists may be affected by the different volatile releases, as shown in Figure 1. DG_2 functional drink had the greatest number of alcohols (i.e., 3-hexen-1-ol, (*E*), 1-hexanol, 1-octen-3-ol, benzyl alcohol, phenylethyl alcohol, and 1-nonanol) and ketones (i.e., 2-undecanone, α -ionone, *trans*-geranyl acetone, *trans*- β -ionone, benzophenone, 2-pentadecanone, and 7,9-di-tert-butyl-1-oxaspiro(4,5)deca-6,9-diene-2,8-dione). Similar results to colour and aroma attribute, a functional drink made from DG_2 had the highest ($p > 0.05$) mean score for texture acceptability (6.10 ± 0.23), while FG_1 had the lowest score (5.51 ± 0.25). The mean score of taste acceptability of *P. cordifolia* functional drink was from 3.51 (FG_2) to 4.76 (WF_2) (Figure 2). Generally, this indicated that the acceptability of colour, aroma, texture, and taste was not affected by different sample preparation. On the other hand, it can be seen that bitterness, astringency, aftertaste, and overall acceptability was significantly ($p < 0.05$) influenced by different sample preparation. *P. cordifolia* functional drink prepared by WF_2 exhibited the highest ($p < 0.05$) bitterness score (4.98 ± 0.62). In comparison, sample FG_2 exhibited the lowest bitterness ones (3.41 ± 0.27). This could be because, in WF_2, there is no phenolic compound detected. Besides that, catechin (the main polyphenol in tea) is the primary compound responsible for the bitter and astringent flavour notes [10]. The astringency level of *P. cordifolia* functional drink is highly accepted in WF_1 (5.04 ± 0.14) compared to FG_2 (3.72 ± 0.17). Panellists gave both aftertastes, and overall acceptability attributes the highest score for WF_2 (5.26 ± 0.42) and (5.12 ± 0.62), respectively. On the contrary, panellists gave both aftertastes and overall acceptability attributes the lowest score for FG_2 (3.65 ± 0.24) and (3.73 ± 0.14), respectively.

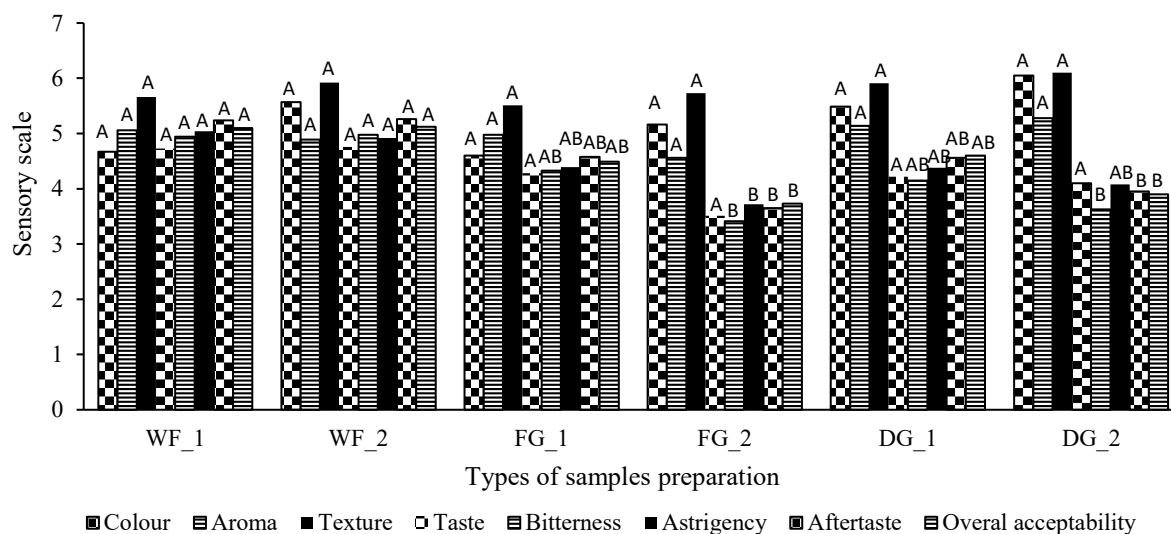


Figure 2: Results from the sensory acceptability of *P. cordifolia* functional drinks.

Conclusion

This study has shown that the WF_2 would be the preferred sample preparation technique for *P. cordifolia* functional drinks, followed by WF_1, FG_1, DG_1, DG_2, and the most unacceptable is FG_2. A volatile analysis led to the identification of 35 compounds, and these odourants exhibited an array of odour notes such as green, fresh, herbal, woody, waxy, earthy, sweet, and fruity. Thus, different sample preparation significantly affects the flavour and sensory acceptance of *P. cordifolia* functional drinks. This information constitutes a vital standpoint for market growth and is expected to ensure consumer acceptance towards healthier and natural consumption of functional drinks that have a good potential for commercialisation.

References

1. Statista, The statistics portal. Available from World Wide Web: <http://www.statista.com/statistics/264188/production-of-tea-by-main-producing-countries-since-2006/>. 2013.
2. Graham, H. N. Green tea composition, consumption, and polyphenol chemistry. *Prev Med.* 1992;21:334-350.
3. Nabihah, S., Dzulsuhaimi, D., Noorain, H. Comparative effects of *Cosmos caudatus*, *Piper sarmentosum* and *Premna cordifolia* ethanolic extracts on mice (*Mus musculus*) sperm parameters. *UiTM. J Pharm Adv Res.* 2017;1(7):346-351.
4. Farag, M. A., Fahmy, S., Choucry, M. A., Wahdan, M. O., Fahmi, M. Analysis metabolites profiling reveals for antimicrobial compositional differences and action mechanism in the toothbrushing stick " miswak " *Salvadora persica*. *J Pharm Biomed Anal.* 2017;133:32-40.
5. Shimoda, M., Shigematsu, H., Shiratsuchi, H., Osajima, Y. Comparison of the odor concentrates by SDE and Adsorptive Column Method from green tea infusion. *J Agric Food Chem.* 1995;43:1616-1620.
6. Lee, J., Chambers, D. H., Chambers IV, E., Adhikari, K. Yoon, Y. Volatile aroma compounds in various brewed green teas. *Molecules.* 2013;18:10024-10041.
7. Alasalvar, C., Topal, B., Serpen, A., Bahar, B. Pelvan, E., Gökmen, V. Flavor characteristics of seven grades of black tea produced in Turkey. *J Agric Food Chem.* 2012;60:6323-6332.
8. Ravichandran, R., Parthiban, R. Lipid occurrence, distribution and degradation to flavour volatiles during tea processing. *Food Chem.* 2000;68:7-13.
9. Chen, Z. M., Wang, H. F., You, X. Q., Xu, N. Non-volatile chemistry. In: Zhen YS, Chen ZM, Cheng SJ, Chen ML. *Tea bioactivity and therapeutic potential*. New York, NY, USA: Taylor & Francis. 2002.p 57-88
10. Chen, Z., Zhu, Q. Y., Tsang, D., Huang, Y. Degradation of green tea catechins in tea drinks. *J Agric Food Chem.* 2001;49:477-482.

Minutes of the Workshop

‘Perceptual interactions in flavour perception’

Workshop 4: Perceptual interactions in flavour perception

Charlotte Sinding¹, Vicente Ferreira², Janina Seubert³, Barry C. Smith⁴, Thierry Thomas-Danguin¹

¹ Centre des Sciences du Goût et de l'Alimentation, AgroSup Dijon, CNRS, INRAE, Université Bourgogne Franche-Comté, F-21000 Dijon, France.

² Laboratorio de Análisis del Aroma y Enología (LAAE), Department of Analytical Chemistry, Faculty of Science, Universidad de Zaragoza, Instituto Agroalimentario de Aragón (IA2) (UNIZAR-CITA), 50009 Zaragoza, Spain.

³ Karolinska Institute, Department of Clinical Neuroscience, Psychology Division, Nobels väg 9, 17 177 Stockholm, Sweden

⁴ Centre for the Study of the Senses, Institute of Philosophy, School of Advanced Study, University of London, Senate House, Malet Street, London WC1E 7HU.

Abstract

This chapter sums up the discussion arising from workshop 4 of the 16th Weurman Flavour Research Symposium about perceptual interactions in flavour perception. In the first part, we defined flavour and flavour perception by presenting the definitions of three leading researchers in the domains of food chemistry, neurosciences, and philosophy. The second part of this chapter presents the questions and answers around flavour. The third part details future challenges as proposed by the speakers.

Keywords: odour, taste, trigeminal, configural, definition

Introduction

Sensory and food scientists, flavourists, neuroscientists, and philosophers are confronted with the difficulty of defining flavour. This lack of definition is symptomatic of the complexity of the properties, the systems, and the phenomenon involved. Part of the flavour mystery comes from the interactions within the food matrix, at the periphery of chemosensory systems, within the brain, and from our poor ability to understand the relationship between the food itself and its perception.

This chapter is a summary of the discussion issued from workshop 4 of the 16th Weurman Flavour Research Symposium about perceptual interactions in flavour perception. In the first part, we defined flavour and flavour perception by integrating the definitions of three leading researchers in the domains of food chemistry, neurosciences and philosophy, represented respectively by Prof Vicente Ferreira, Dr. Janina Seubert, and Prof Barry C Smith. The second part of these minutes sums up the questions and answers around flavour. The third part details future challenges as proposed by the speakers.

Speakers

Vicente Ferreira (VF) is a Professor of Analytical Chemistry and Director of the LAAE, the Lab for Flavour Analysis and Oenology, at the University of Zaragoza. His work consists in understanding the chemical bases of aromatic and gustatory perception. He is a specialist in the identification, quantification, characterisation of flavour compounds, and numerical modelling of the sensory response.

Janina Seubert (JS) is a cognitive neuroscientist leading the Nutritional Neuroscience group at Karolinska Institute, in Stockholm. She investigates the perceptual experiences associated with eating, among which the experience of odour and taste during anticipation and consumption of food, their effects on memory and learning as well as emotion and motivation, and their regulation by metabolic feedback.

Barry C Smith (BCS) is a Professor of philosophy and director of the Institute of Philosophy at the University of London's School of Advanced Study. He is the founder of the Centre for the Study of the Senses, which pioneers collaborative research between philosophers, psychologists, and neuroscientists. His current research is on multisensory perception, focusing on taste, smell, and flavour.

Organisers

Thierry Thomas-Danguin (TTD) is a research director at INRAE, leading the Flavour, Food Oral Processing, and Perception team at the Centre for Taste, Smell and Feeding Behaviour in Dijon. Through a transdisciplinary approach, he aims at understanding the role of perceptual interactions, induced by odour mixtures processing and cross-modal integration, in odour objects and food flavour coding and perception. The objective is to unravel the chemical and biological mechanisms of food flavour construction and perception to develop a healthier diet, but tasty, which may be better appreciated by consumers and therefore contribute to their health and wellness sustainably.

Charlotte Sinding (CS) is a researcher in the Neurosciences of food perception at the Centre for Taste, Smell and Feeding Behaviour in Dijon. She aims at highlighting and understanding the brain mechanisms of flavour perception. She is investigating odour-taste interactions in obese and normal-weight people. She developed an EEG lab dedicated to flavour perception and is developing dedicated methods for fMRI investigations of odour-induced taste perception.

Flavour Definitions

Food Chemistry (VF):

As a **perception, the flavour** is the complex cerebral response, involving variable levels of consciousness and emotion, to the majorly (but not exclusively) chemical stimuli released during the consumption of food and impacting different senses, mainly olfaction and taste. As a **food property, the flavour** is the group of material properties and material constituents of the food able to induce in humans the set of measurable sensory descriptors, which we can reasonably expect, will be elicited during its consumption.

Neurosciences (JS):

Flavour perception is a mental representation of food, resulting from the integration of, at least, taste and odour perceptions. **Flavour** is a holistic percept of a single integrated quality- it arises from at least odour and taste through perceptual binding. Flavour binding has distinct perceptual indicators (odour mouth referral, odour-induced taste enhancement) and is modulated by experience (familiarity) which builds congruency between odour and taste. The contributing sensory modalities are stimulated separately in the periphery, each by distinct perceptual features of the food (e.g. volatile and water-soluble chemicals) which are only merged at higher stages of cortical processing, giving rise to a meaningful integrated percept. As such, the cognitive neuroscience viewpoint is that flavour exclusively exists as a perceptual construct that arises inside the brain, rather than as an inherent property of the food itself.

Philosophy (BCS):

Flavours are configurations of sapid, odorous, tactile properties of foods and liquids, including their temperature that have the power to stimulate our senses of taste, touch, smell, trigeminal nerve endings, and mechanoreceptors. It is important to distinguish **flavour** and **flavour perception**.

There are flavours in foods and liquids. **Flavours** are emergent properties that supervene or depend on the underlying chemistry but are not reducible to it. And we should not confuse flavours with our perceptions of them. Perceiving those flavours can be difficult. Individual perceptions are variable. They are snapshots at a time, of the flavours of, say, wines that can evolve in the glass or the bottle. It is best to talk of the *flavour profile* of the wine over time, and the skill of a good taster is to predict how the wine will taste over time, and when warmer or cooler. This is best modelled by theories of predictive coding. When eating or drinking, we are predicting and tracking properties of food or wines over time. We need to study the relationship between individual variable perceptions and something more stable, something more linked to the wine chemistry, the wine's flavour profile.

Questions and Answers

What are the necessary steps to recreate wine flavour stimuli?

VF: One of the most important learnings in the study of wine flavour is that to recreate it, it is completely essential not to miss any of the relevant “aroma vectors” taking part in the perception. Here, aroma vector refers to a qualitative perceptual unit, which can be composed either by a single molecule or by a large pool of molecules

displaying some similarity in their odour properties. Surprisingly, the relevance of the aroma vector is not only related to its intensity, but to the uniqueness of its odour in relationship to the overall mixture.

These facts show that to recreate any complex flavour stimuli it is necessary to have a clear idea of the number of “qualitative perceptual units” contained in the mixture. For this, screening by gas chromatography-olfactometry is necessary, but the attention has to be directed to, both, the most intense odorants in the mixture, and to those others of small intensity but present in relatively large numbers. There are several series of complex aroma vectors in the wines of this type.

How important is the odour in the flavour perception in comparison to taste?

VF: Of course, both are important and essential, since perception integrates everything into a whole, but odour carries far more qualitative information than taste. In fact, for many modest sensory applications in wine, only orthonasal evaluation is carried out.

The peri-receptor mechanisms also play a role in perception: how long is a receptor activated by compounds before being taken in charge by enzymes or scavengers? Do we know, for example in wine how much the perception is modified by metabolites?

VF: We do not know much about the temporal sequence of receptors activation in complex mixtures, such as wine, in which the influx of volatiles is extremely rich, with high levels of ethanol and higher alcohols, and changes during time. On the other hand, there are several reported cases of aroma precursors which are hydrolysed by salivary enzymes, contributing to wine aftertaste. These perceptions can last up to 30 seconds.

A set of peri-receptor mechanisms that to me is particularly important in wine perception is the presence of small trigeminal fibres in the taste buds or near the olfactory receptors that may modulate taste and olfactory perceptions. This refers to the activation of the trigeminal nerve endings by volatiles (in the nostrils) or non-volatiles (in the mouth). Ethanol and other alcohols play a very important role, providing a burning sensation that has to be compensated by aroma compounds or by volatiles displaying cooling or refreshing effects. Acetaldehyde and other aldehydes at much smaller levels also contribute to the burning effect.

Why superadditivity is necessary for flavour perception to occur? Or is superadditivity a way to measure flavour integration? In other words, could it be that flavour perception arises in the brain without superadditivity?

JS: In multisensory perception research, “integration” is usually experimentally defined as a process which results in a perceptual advantage of some sort that would be unexpected if no integration were to occur. As such, simultaneous processing of odour and taste is just that, processing that occurs in parallel. As soon as we experience sensations that exceed the prediction of the sensory experience of odour by itself plus the sensory experience of taste by itself, we conclude that special processing resources have been activated and we call this specific form of processing that exclusively arises to shared stimuli “Flavour”. This is just one way in which sensory integration can be defined, another more conservative criterion is that of “enhancement”, where activation that is higher than that to one of the stimuli alone already qualifies as sensory integration.

How may flavour facilitate emotional experience? How to measure that?

JS: There is strong evidence that combined stimulation with all parts of a flavour facilitates emotional experience relative to the components alone, in the sense that stimuli that contain a familiar flavour consisting of both smell and taste are perceived as more pleasant than either of those sensory stimuli by themselves. A classic task would present people with stimuli containing parts of a flavour either in separation or in combination and overtly ask the participant to rate them for some form of emotional assessment (liking) or their motivational features (wanting). Implicit tasks may study the effect of flavours on a third, unrelated task known to be facilitated by emotional experience to avoid an intentional bias of the study participant. How exactly facilitation works is more difficult to study and may to some extent rely on results of functional neuroimaging studies where we might find that flavours selectively activate specific brain regions linked to emotional and memory processing. Candidate areas that are discussed in the literature include, for example, the insular cortex, frontal operculum, orbitofrontal cortex, and limbic areas involved in memory, emotion and reward.

Do you think that the anticipatory effect of an odour or a visual scene can promote signals’ integration?

JS: Visual and olfactory signals, perceived prior to insertion of food in the mouth, are appetitive cues which stimulate the reward network and create cravings for the specific rewards that they indicate. As such, they might sensitize for detection of specific macronutrients and lower perceptual thresholds. I am not aware of any research indicating that specifically integration during consumption is facilitated by prior visual/olfactory stimulation, but I think that this would be an interesting study to do.

CS: Priming studies looking at taste primers on odour perception have shown that the late brain processing (linked to higher cognitive processing) occurred earlier when a congruent odour matched the taste (e.g.: a sweet

dispenser was placed in the mouth of participants and when vanilla was presented, the brain activity increased, while it did not change when the participant was primed with sour taste (Welge-Lussen et al. 2009).

Prof. Markus Stieger showed that when mayonnaise was used in conjunction with eating a product, the physical release of compounds may increase (due to the effect of mastication hence inducing an improved release) but the sensory intensity of these compounds decreased. This must be a cognitive effect of integration of the food experience with the mayo. Would you be able to suggest a mechanism? Why do people do not eat mayo and French fries separately which would increase intensity perception?

JS: I think this example illustrates that maximisation of physical release of sensory compounds (odorants and tastants) is not the only criterion driving food pleasantness, or even subjective experience of intensity. There are many examples of compounds where a high sensory intensity is in fact undesirable and perceived as unpleasant, amyl acetate being one of them, for example. In that sense, maximisation of intensity perception may not be something to strive for, and the complexity that is experienced when two flavours merge may be more important here as a factor leading to a pleasant percept. In addition, in the specific case of mayonnaise and fries, texture pleasantness might be relevant, where a certain viscousness in combination with crunchiness might enhance the overall mouth feel of a food item and thus its perceived flavour pleasantness.

If flavour stimuli form a configuration in the external world, how are odorants and tastants bonded together? Can we even talk of binding there since there is not always a physical binding? What are the boundaries of flavour stimuli in the external world?

VF: Integration is an essential part of perception, with no need for physical binding. The single requisite is co-occurrence in time, not even in space. This has been demonstrated by the strong interaction of astringency and aroma in the perception of the green character of wines, for instance, or for the relevance of fruity aroma in the taste perception of white wines.

BCS: Part of the binding problem is which things do we bind together? Trigeminal, taste, odour, somatosensory sensations can occur, but which inputs get bound together? Which senses do we need to perceive a food's flavour? The answer is that it depends on the food. Flavour perceptions do not require that inputs from the same senses must always be bound together: not all foods contain trigeminal stimulants. We use the senses we need to track the flavours there are in foods and liquids. Certain configurations of odorants and tastants are found together in some foods but not in others. The multisensory integration of inputs into unified flavour percepts, occurs when those combinations track the configurations of odorants and tastants found together in our foods and drinks. We should start with the objective flavours our senses try to track rather than trying to settle the binding challenge about which sensory inputs contribute to and settle the boundaries of flavour perception. The ingredients in foods and configurations of odorants, tastants and textures dictate which sensory inputs need to be integrated to perceive and track their flavours.

How could you imagine an experiment manipulating the level of novelty? Could an accurate level of novelty be key for new product acceptance meaning behaviour change?

BCS: Neuroscientists say that you rarely smell a new odour. Novelty is often harder to achieve than we think. Things are often on a continuum with what we already know. So a totally novel product in terms of its taste, touch and smell may be very hard to achieve. It's only when you get these surprising recombinations of familiar taste and odours, or textures that you get novelty, and this is what good blending does. Blending is an art and science and it results in a blend of physical ingredients that produce novel sensory blending. It is very interesting that people who suffer from post-covid parosmia, tend to say that the usual flavours they enjoy (roasted meat for example, or coffee) tend to smell and taste completely new and off-putting. That suggests that it may take the replacement and regeneration of olfactory receptors to get these novel combinations. That is something that was not anticipated before.

JS: I agree with Barry that most "novel" food items fall on a deviation continuum from a familiar odour. I would add that when we are confronted with an item that deviates from our earlier experiences, evolutionarily, there is a competition going on between two competing instincts: generalisation (highlighting commonalities with a slightly different familiar item and thus, prioritising energy intake to promote survival through consumption of calories over the potential risk of intoxication) and segregation (highlighting differences to familiar items to avoid accidental consumption of toxins, and thus promote survival over the potential risk of starvation). The more different, the more likely segregation wins over, of course, but the boundaries between the two are not always clear and, depending on the nature of the compounds, involved as well the internal state and external context. As such, I would agree that an appropriate level of novelty is likely key to promoting acceptance, but that this level might be variable between different people and over time, and as such, difficult to define experimentally. Recently, a number of studies have come out that employ gradual variation paradigms and I think those are key to promoting understanding of the rules underlying the formation of an approach/avoidance decision boundary when it comes to food flavour perception.

Do you think that the predictive coding theory of flavour perception works for any individual, in everyday life, or more specifically flavour experts, such as wine tasters, oenologists, chefs,...?

BCS: Chefs and oenologists will be better predictors than others of the flavour perceptions that certain arrangements of ingredients or compounds will give rise to because they have had so many trials of tasting different combinations. Similarly, experienced wine makers and wine tasters will be better at predicting how a wine will behave when it ages, when it's a degree cooler, or warmer when it opens up in the glass. This is due to experience and practice that establishes reliable priors.

Are there any results comparing tasting in the total dark compared to usual tasting conditions and "laboratory" conditions?

BCS: There are restaurants that offer diners the chance to taste in the dark. Many believe that when one of our senses is missing the others compensate and that diners will experience a more intense tasting of the food than they usually would. It's an interesting real-world experiment but the results are not clear. It takes time for other senses to compensate when one sensory input is missing. Also, there is a difference between early blind and late blind individuals in terms of how their sense of smell and taste are affected. Research on the congenitally blind reveals greater perceived odour intensity but also more neophobia about foods. When eating in the dark, we can be uncertain and uneasy about what we are eating. For most of us, it's not a normal perceptual experience and people often report that they cannot even distinguish lamb and chicken when eating in these restaurants. When tasting under these circumstances we may be less accurate than when we taste in normal conditions or even than when we taste under unusual laboratory conditions.

What is your opinion on the salt perception that modifies tactile sensations (hotness/coldness)? Would it affect the flavour perception? Can you give an example of how temperature plays a role in flavour perception?

BCS: Salt is said to modify our perception of the heat of capsaicin as a trigeminal irritation giving rise to a burning sensation. This would be a cross-modal effect of the working of one sensory input on the reception of the input of another sense. There is experimental evidence of this effect but others are still testing this effect, especially in the Covid group of patients who have lost their sense of smell but still have intact gustation and trigeminal sensitivity. Temperature plays an important and often hidden role in flavour perception. When coffee gets cold it often tastes bitterer, so coldness enhances bitterness and acidity; warmth enhances sweetness. Also, around 25% of the population are thought to be Thermal Tasters for whom ice cubes taste salty or sour, and warm spoons taste sweet.

TTD: In an experiment we performed, using cottage cheese served at either 7°C or 15°C, we observed that the increase in tasting temperature induced a decrease in aroma (retronasal odour) detection threshold that might be explained by the higher release of odorants from the matrix at higher temperatures. Nevertheless, the tasting temperature did not impact taste, supra-threshold aroma, or astringency, while perceived texture (thickness) was strongly modified by tasting temperature.

Future challenges

We just start to understand when and how the multifaceted flavour is formed, and we are now facing many future challenges to go deeper in these investigations and to integrate this knowledge into the thematic of food choices, diets, rewards, emotions... One of these challenges concerns what is classified as a familiar or unfamiliar flavour experience. Most of the studies have been done on very familiar or very unfamiliar foods but that poorly reflects on the actual tasks that we experience in everyday life, where most foods are slightly familiar but not entirely similar to the food experienced before. These slight differences in familiarity seem to activate dedicated brain areas (prefrontal cortex) and therefore might modulate food decision making. Therefore, it would be interesting to know how much flavour novelty is too much? How does the context influence tolerance for flavour novelty? Finally, it would require more careful modulation of stimulus sets and novel techniques analysis.

Another challenge is to connect the flavour stimuli and the flavour perception. However, we should not try to connect chemistry, wine chemistry for example, to individual perceptions. Flavour is something in between wine chemistry and flavour perception, from there we can make progress on how we tackle the issues we are interested in, of connecting things up. We should think of flavour not as a static thing synchronically but think of a flavour profile. From there we have got two challenges, instead of one. We are not trying to connect wine chemistry to what perceivers experience. Instead, we have two tasks: 1) how are perceivers able to recognise the flavour profiles of wine over time at a single moment of tasting, how do perceivers improve their skills of tasting and recognising what the extended flavour profile of a wine is; 2) how do we understand the relationship between changes in the underlying wine chemistry and the evolving flavour profile, what by-products of fermentation or ageing give rise to changes in the flavour profile of the wine? When thinking in terms of dynamic flavour, predictive coding is of

interest. It allows us to make predictions of how the wine will evolve under certain conditions and later as we taste under these conditions we can confirm whether we were right or not, or whether we get an error signal from the sensory information. We are trying to predict and track the properties of wine and we are looking at that relationship between individual perceptions and something more stable more rooted in wine chemistry. Because in the end, we are trying to get accurate perceptions of what exists there to be perceived.

In the chemical part, there is a number of challenges, all of them related to the way in which information about the number and nature of odorants and tastants is obtained and, of course, also about the way in which such information is integrated. Regarding the gathering of information, there are good perspectives about the recent introduction of ultra-high resolution mass spectrometers coupled to gas chromatographs, which should make it possible to expand the number and range of molecules targeted. At present, we need four different powerful instruments and different methodologies to do the task. A big challenge also remains in the part of understanding chemesthesis and touch in the mouth. Regarding the integration of information, it is compulsory to understand how similar have to be different odours to be processed together; it is also compulsory to understand how to relate the intensities (concentrations) of the odorants composing an aroma vector to the overall intensity of the vector; and it is finally necessary to develop mathematical models able to deal with the discontinuities or anomalies observed in complex mixtures, related to those specific profiles in which a new odour concept emerges.

References

Welge-Lüssen, A, Husner, A, Wolfensberger, M, Hummel, T, Influence of simultaneous gustatory stimuli on orthonasal and retronasal olfaction, *Neurosci. Lett.* 454 (2009) 124–128.



**16th Weurman
Online
May 4-6, 2021**

Since 1975, the Weurman Flavour Research Symposia held every three years in different European countries have been unique opportunities for scientists from academia and industry, from different disciplines, and from all over the World, to discuss trends and new paradigms in the field of flavour research. This e-book 'Progress in Flavour Research 2021' constitutes the Proceedings of the 16th edition held online from 4th to 6th May, 2021.

INRAE



ISBN: 978-2-7592-3622-0